OKLAHOMA GEOLOGICAL SURVEY

CIRCULAR 109

# Evaporite Karst and Engineering/Environmental Problems in the United States

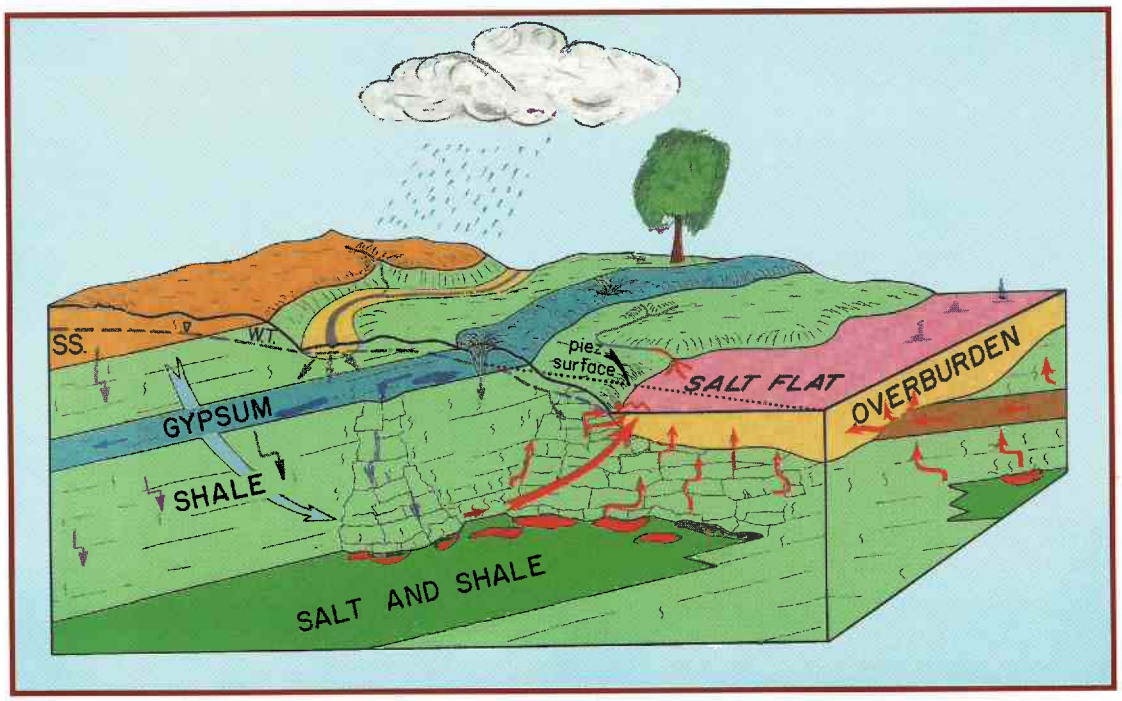


**Kenneth S. Johnson and James T. Neal**
***Editors***

**2003**

*Published in cooperation with:*
United States Geological Survey
and
National Cave and Karst Research Institute—
National Park Service

USGS science for a changing world

NATIONAL PARK SERVICE

Oklahoma Geological Survey
Charles J. Mankin, *Director*

**Circular 109**
ISSN 0078-4397

# Evaporite Karst and Engineering/Environmental Problems in the United States

KENNETH S. JOHNSON AND JAMES T. NEAL, *Editors*

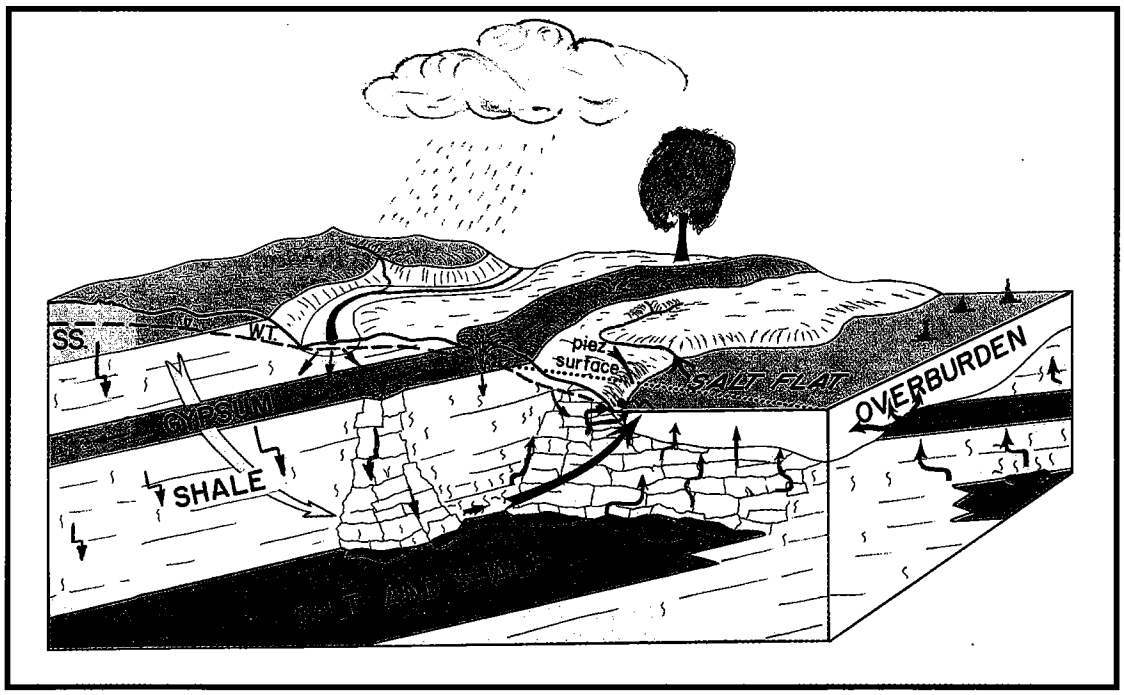


*Published in cooperation with:*
United States Geological Survey
and
National Cave and Karst Research Institute—
National Park Service

**The University of Oklahoma**
**Norman**
**2003**

## OKLAHOMA GEOLOGICAL SURVEY

CHARLES J. MANKIN, *Director*

### SURVEY STAFF

JAMES H. ANDERSON, *Manager of Cartography*
RICHARD D. ANDREWS, *Geologist IV*
BETTY D. BELLIS, *Word-Processing Operator II / Technical Typist*
MITZI G. BLACKMON, *Clerk-Typist I*
DAN T. BOYD, *Geologist III*
JERLENE A. BRIGHT, *Technical Project Specialist*
RAYMON L. BROWN, *Geophysicist III*
RUTH E. BROWN, *Assistant to the Director*
JOCK A. CAMPBELL, *Geologist IV*
BRIAN J. CARDOTT, *Geologist IV*
JAMES R. CHAPLIN, *Geologist IV*
JANISE L. COLEMAN, *Office Assistant IV*
CHRISTIE L. COOPER, *Managing Editor*
TAMMIE K. CREEL-WILLIAMS, *Secretary II*
JIMMY G. DENTON, *Manager, Oklahoma Petroleum Information Center*
CHARLES R. DYER III, *Drilling Technician*
ROBERT O. FAY, *Geologist IV*
AMIE R. FRIEND, *Research Specialist I*
JAMES W. KING, *Research Specialist II*
STANLEY T. KRUKOWSKI, *Geologist III*
EUGENE V. KULLMANN, *X-Ray / Imaging Technician*
JAMES E. LAWSON, JR., *Chief Geophysicist*
LAURIE A. LOLLIS, *Cartographic Technician II*
KENNETH V. LUZA, *Geologist IV*
MICHAEL J. MERCER, *Manager, Log Library*
GALEN W. MILLER, *Research Associate*
RICHARD G. MURRAY, *Copy Center Operator*
SUE M. PALMER, *Office Assistant II*
DAVID O. PENNINGTON, *Operations Assistant II*
CONNIE G. SMITH, *Promotion and Information Specialist*
PAUL E. SMITH, *Supervisor, Offset Press Copy Center*
G. RUSSELL STANDRIDGE, *Information Tech Analyst I*
THOMAS M. STANLEY, *Geologist III*
LLOYD N. START, *Assistant Drilling Technician*
JOYCE A. STIEHLER, *Chief Clerk*
MICHELLE J. SUMMERS, *Technical Project Coordinator*
NEIL H. SUNESON, *Assistant Director, Geological Programs*
JANE L. WEBER, *Publication and Database Coordinator*

### Cover Picture

Schematic diagram of intrastratal salt karst in western Oklahoma.
This is a colored version of the figure on p. 3 of this volume.

This publication, printed by the Oklahoma Geological Survey, is issued by the Oklahoma Geological Survey as authorized by Title 70, Oklahoma Statutes, 1981, Sections 231–238. 1,050 copies have been prepared for distribution at a cost of $15,563 to the taxpayers of the State of Oklahoma. Copies have been deposited with the Publications Clearinghouse of the Oklahoma Department of Libraries.

# PREFACE

Evaporite rocks, mainly gypsum (or anhydrite) and salt (halite), are the most soluble of common rocks. They are dissolved readily to form caves, sinkholes, disappearing streams, and other karst features typically associated with carbonate rocks (limestone and dolomite). Evaporites underlie about 35–40% of the contiguous United States, and are present in 32 of the 48 states. Evaporite karst (EK) is known to be present at least locally (and sometimes quite extensively) in almost all areas underlain by evaporites, and is much more widespread than is commonly suspected. The principal difference between evaporite and carbonate karst is that EK features can form rapidly, in a matter of days, weeks, or years, whereas carbonate-karst features typically take years, decades, or centuries to form.

EK can result from natural processes, wherein precipitation or ground water circulates through, and dissolves, an evaporite deposit. EK also can result from human activities, such as: construction upon, or directing water into or above, outcropping or shallow evaporites; and the drilling of boreholes, or making excavations, into or through subsurface salt deposits. Because evaporite dissolution is so rapid, EK features can quickly produce engineering or environmental problems that are hazards to humans and property; under some conditions, these problems can arise within a matter of several months or years. These hazards can include damage to, and/or collapse of, homes, buildings, civil projects (such as dams, bridges, and highways), and farmlands. Such hazards can cause great economic hardship, disruption of lives, and even loss of life.

This symposium volume is based upon a half-day theme session on EK that was held on October 28, 2002, in Denver, Colorado, as part of the annual meeting of the Geological Society of America (GSA). The session was organized and chaired by us, and was co-sponsored by the Engineering Geology, Hydrogeology, and Quaternary Geology and Geomorphology Divisions of GSA. We thank GSA and the three Divisions for their support in sponsoring the theme session. The EK session was held because of the growing awareness of karst problems in evaporite rocks. Although evaporite deposits and their associated karst problems are widespread in the United States, they have received scant attention from most geologists.

Co-sponsorship in the publication of this symposium volume has been provided by the United States Geological Survey and the National Cave and Karst Research Institute—National Park Service. Both these agencies are actively investigating karst and cave features throughout the nation, and we appreciate very much their participation in this project.

A total of 16 talks and posters were presented at the GSA meeting, and we then invited another 17 papers to be prepared especially for this volume. The 33 papers are grouped into *Introductory and General Papers*, and then into a series of geographic areas, based upon states. Each of the papers provides insight into significant engineering and/or environmental problems related to EK.

Technical editing, layout, and production of this volume were done by William D. Rose and Virginia Rose, of Rose Perspectives, Frederick, Maryland; coordination of editing and publication management was carried out by Christie Cooper, Oklahoma Geological Survey.

We hope that the GSA session and this symposium volume will heighten awareness in the geologic and engineering communities to the processes and potential engineering and environmental problems of EK. And we welcome contact from others interested in EK so that we can include them in plans for future sessions on this important subject.

KENNETH S. JOHNSON
Oklahoma Geological Survey
100 East Boyd, Room N–131
Norman, OK 73019
Phone: 405/329-4150
E-mail: ksjohnson@ou.edu

JAMES T. NEAL
Sharlot Hall Museum
415 W. Gurley St.
Prescott, AZ 86305
Phone: 928/771-2307
E-mail: hjneal@commspeed.net

# CONTENTS

iii **Preface to the Symposium**

*INTRODUCTORY AND GENERAL PAPERS*

1 **Evaporite-Karst Problems in the United States**
Kenneth S. Johnson

21 **The Need for a National Evaporite-Karst Map**
Jack B. Epstein and Kenneth S. Johnson

31 **Effects of Karst Processes on Gypsum Mining**
Roger D. Sharpe

*OKLAHOMA*

41 **Evaporite Karst in the Permian Blaine Formation and Associated Strata of Western Oklahoma**
Kenneth S. Johnson

57 **Exploration of Western Oklahoma Gypsum Caves**
John Bozeman

65 **Correlating the Location of a Cave Passage in Gypsum Karst to a Highway Right-of-Way Using a Cave Radio**
Scott Christenson, Curtis Hayes, Earl Hancock, and John McLean

71 **Laser Positioning and Three-Dimensional Digital Mapping of Gypsum Karst, Western Oklahoma**
Galen Miller, Thomas Dewers, and Aondover Tarhule

77 **Integrated Subsurface-Imaging Techniques for Detecting Cavities in the Gypsum Karst of Oklahoma**
Aondover Tarhule, Thomas Dewers, Roger Young, Alan Witten, and Todd Halihan

85 **Gypsum Karst and Abandonment of the Upper Mangum Damsite in Southwestern Oklahoma**
Kenneth S. Johnson

95 **Gypsum Karst As a Major Factor in the Design of the Proposed Lower Mangum Dam in Southwestern Oklahoma**
Kenneth S. Johnson

113 **Regional Mapping of Karst Terrains in Oklahoma for Avoidance of Engineering and Environmental Problems**
Kenneth S. Johnson

*KANSAS*

119 **Evaluation of the Role of Evaporite Karst in the Hutchinson, Kansas, Gas Explosions, January 17 and 18, 2001**
W. Lynn Watney, Susan E. Nissen, Saibal Bhattacharya, and David Young

149 **Subsidence on Interstate 70 in Russell County, Kansas, Related to Salt Dissolution—A History**
Neil M. Croxton

157 **High-Resolution Seismic-Reflection Investigation of a Subsidence Feature on U.S. Highway 50 near Hutchinson, Kansas**
Richard D. Miller

169 **High-Resolution Magnetic Survey Used in Searching for Buried Brine Wells in Hutchinson, Kansas**
Jianghai Xia and Stephen L. Williams

177 **Evaporite Karst and Ground-Water Flow, Discharge, and Quality in the Crystal Spring Catchment Area in the Central Flint Hills of Kansas**
P. Allen Macfarlane and Margaret A. Townsend

*TEXAS AND NEW MEXICO*

183 **Sinkholes and Land Subsidence Owing to Salt Dissolution Near Wink, West Texas, and Other Sites in Western Texas and New Mexico**
Kenneth S. Johnson, Edward W. Collins, and Steven J. Seni

197 **Intrastratal Karst at the Waste Isolation Pilot Plant Site, Southeastern New Mexico**
Carol A. Hill

211 **Geological Factors Related to the Transmissivity of the Culebra Dolomite Member, Permian Rustler Formation, Delaware Basin, Southeastern New Mexico**
Dennis W. Powers, Robert M. Holt, Richard L. Beauheim, and Sean A. McKenna

219 **Jal Sinkhole in Southeastern New Mexico: Evaporite Dissolution, Drill Holes, and the Potential for Sinkhole Development**
Dennis W. Powers

227 **Evaporite Karst and Regional Ground-Water Circulation in the Lower Pecos Valley of Southeastern New Mexico**
Lewis A. Land

233 **Field Survey of Evaporite Karst along New Mexico Highway 128 Realignment Routes**
Dennis W. Powers and David Owsley

*WYOMING AND SOUTH DAKOTA*

241 **Gypsum Karst in the Black Hills, South Dakota–Wyoming: Geomorphic Development, Hazards, and Hydrology**
Jack B. Epstein

255 **Engineering Problems of Gypsum Karst along the Interstate 90 Development Corridor in the Black Hills of South Dakota**
Arden D. Davis, Frank W. Beaver, and Larry D. Stetler

263 **A Stinking Lake and Perpetual Potholes: Living with Gypsum Karst in Laramie, Wyoming**
Todd Jarvis and Peter Huntoon

271 **The Money Pit: Karst Failure of Anchor Dam, Wyoming**
Todd Jarvis

*COLORADO, UTAH, AND ARIZONA*

279 **Engineering and Environmental Aspects of Evaporite Karst in West-Central Colorado**
R. M. Kirkham, J. L. White, M. A. Sares, R. G. Mock, and D. J. Lidke

293 **Gypsum Karst in Southwestern Utah: Failure and Reconstruction of Quail Creek Dike**
C. Charles Payton and Michael N. Hansen

305 **A Compound Breccia Pipe in Evaporite Karst: McCauley Sinks, Arizona**
James T. Neal and Kenneth S. Johnson

*EASTERN UNITED STATES*

315 **Evaporite Karst in Michigan**
Tyrone J. Black

321 **Mechanism of Sinkhole Formation in Glacial Sediments above the Retsof Salt Mine, Western New York**
Samuel W. Gowan and Steven M. Trader

337 **Development History and Subsidence Resulting from Salt Extraction at Saltville, Virginia**
Charles S. Bartlett

347 **Sinkholes above the U.S. Strategic Petroleum Reserve Storage Site at Weeks Island Salt Dome, Louisiana: Recognition, Diagnostics, and Remediation**
James T. Neal

# Evaporite-Karst Problems in the United States

***Kenneth S. Johnson***
Oklahoma Geological Survey
Norman, Oklahoma

**ABSTRACT.**—Evaporites, including gypsum (or anhydrite) and salt (halite), are the most soluble of common rocks; they are dissolved readily to form caves, sinkholes, disappearing streams, and other karst features that typically are found in limestones and dolomites. The four basic requirements for evaporite karst to develop are (1) a deposit of gypsum or salt; (2) water, unsaturated with $CaSO_4$ or NaCl; (3) an outlet for escape of dissolving water; and (4) energy to cause water to flow through the system. Evaporites are present in 32 of the 48 contiguous states, and they underlie ~35–40% of the land area; they are reported in rocks of every geologic system from the Precambrian through the Quaternary. Evaporite karst is known at least locally (and sometimes quite extensively) in almost all areas underlain by evaporites. The most widespread and pronounced examples of problems in both gypsum and salt karst are in the Permian Basin of the southwestern United States, but many other areas also have significant problems. Human activities have caused some evaporite-karst development, primarily in salt deposits. Boreholes may enable (either intentionally or inadvertently) unsaturated water to flow through or against salt deposits, thus allowing development of small to large dissolution cavities. If the dissolution cavity is large enough and shallow enough, successive roof failures above the cavity can cause land subsidence or catastrophic collapse.

## INTRODUCTION

Evaporite deposits are those sediments that form as a result of precipitation of various salts out of evaporating water, mainly seawater. Principal evaporite rocks are gypsum (or anhydrite) and salt (halite), although potash salts and other, rarer salts also are locally important. With continued replenishment of the water from which these salts originally were precipitated, it is possible for evaporite layers to accumulate to considerable thicknesses, even tens to hundreds of meters thick. These evaporites are widely distributed in the United States, and they contain evidence of karst in most areas (Fig. 1).

Evaporite rocks are the most soluble of the common rocks throughout the world. Gypsum and salt are dissolved readily to form the same types of karst features and problems that typically are found in limestones and dolomites. The principal difference is that evaporite-karst features can form rapidly, in a matter of days, weeks, or years, whereas carbonate-karst features typically take years, decades, or centuries to form.

The current report provides an overview and summary of the general characteristics and distribution of gypsum karst and salt karst in the United States, and examples of engineering and environmental problems associated with this karst. Most of this report is reprinted from an earlier article published in *Carbonates and Evaporites* (Johnson, 1997), but those data are modified and updated to incorporate new information from Johnson (2001, in press) and from other articles in this volume, *Evaporite Karst and Engineering/Environmental Problems in the United States*.

Principal earlier studies were by Johnson and Gonzales (1978) and Dean and Johnson (1989), and review papers were prepared by Quinlan and others (1986), Johnson (1996, 1997, 1998, 2001, in press), and Martinez and others (1998). Other comprehensive studies of gypsum and/or salt in the United States were published by Withington and Jaster (1960), Pierce and Rich (1962), Withington (1962), Lefond (1969), Smith and others (1973), and Ege (1985). In addition, numerous local or regional studies deal with karst development in the various evaporite deposits: contact with the appropriate state geological surveys, the U.S. Geological Survey, and local cave-exploration groups is usually the best way to begin a search for such published or unpublished data.

Hundreds of areas or districts in the United States contain karst features that have developed in evaporite rocks, but it is beyond the scope of this summary report to document them all. Therefore, I will discuss the following: (1) the general characteristics of evaporite-karst processes; (2) the general distribution of natural evaporite karst, and cite several examples of problems that have been well documented; and (3) the occurrence of human-induced evaporite karst that causes collapse structures associated with solution mining, petroleum activities, or dry mining in salt.

Johnson, K. S., 2003, Evaporite-karst problems in the United States, *in* Johnson, K. S.; and Neal, J. T. (eds.), Evaporite karst and engineering/environmental problems in the United States: Oklahoma Geological Survey Circular 109, p. 1–20.

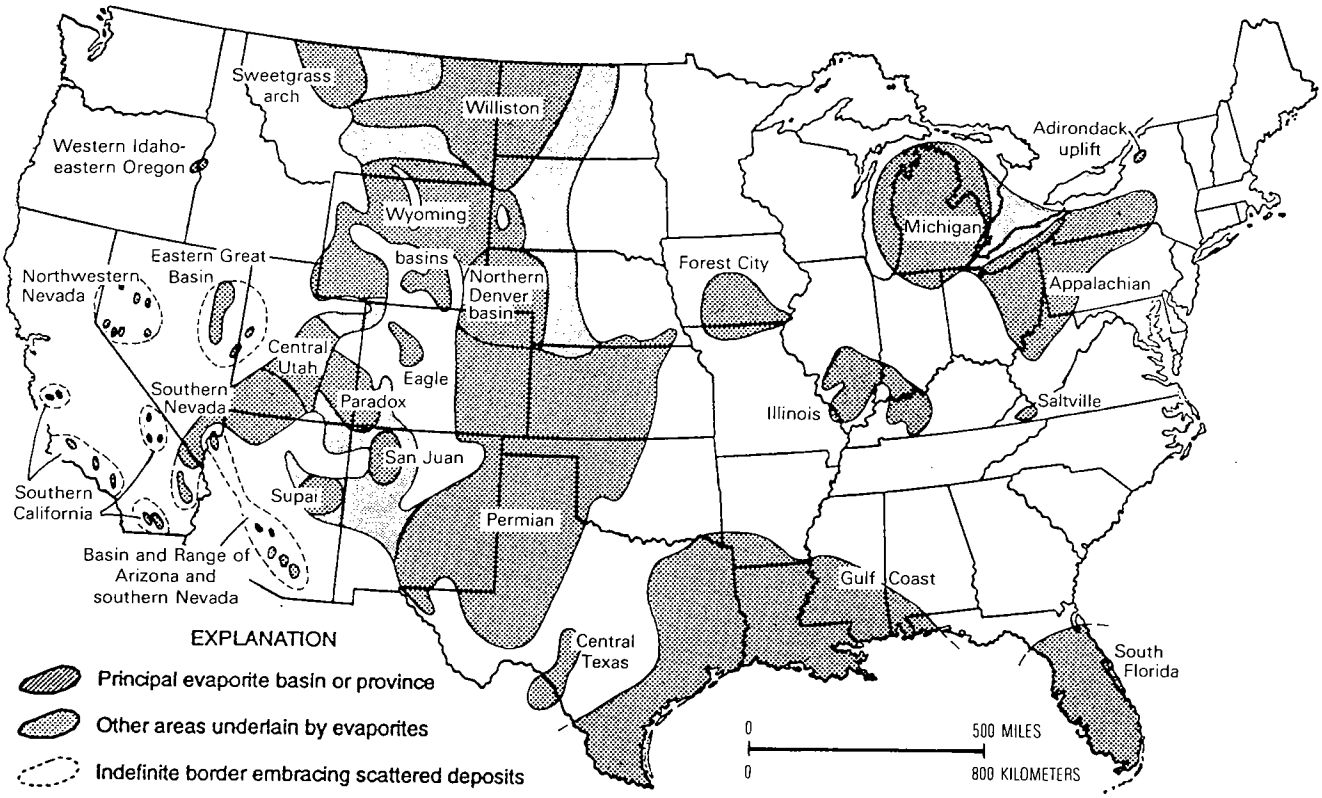


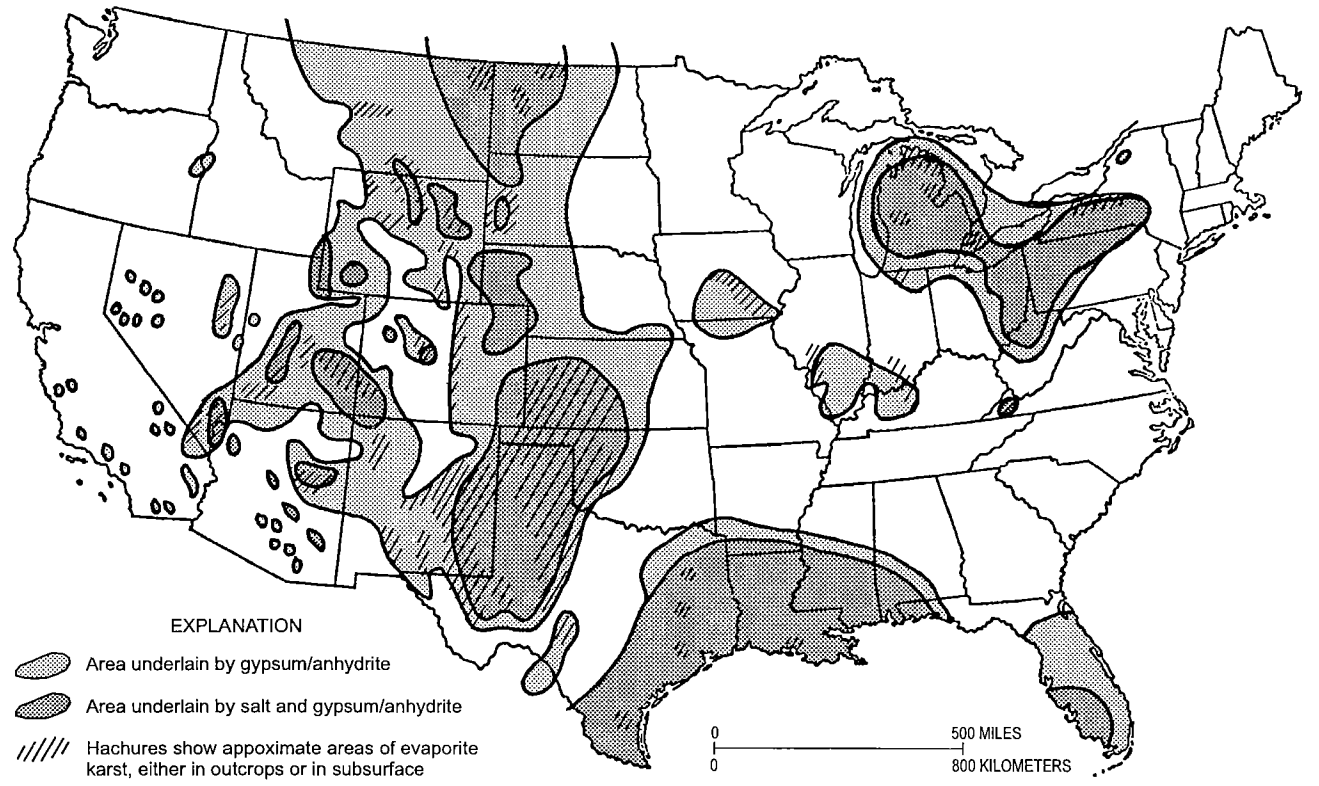


Figure 1. Maps of the conterminous United States; from Johnson (1997), based on Johnson and Gonzales (1978) and Dean and Johnson (1989). Upper map shows evaporite basins and districts; lower map shows distribution of gypsum/anhydrite and salt deposits, and areas of evaporite karst.

## EVAPORITE-KARST PROCESSES

The processes for development of karst features in evaporite rocks are identical to those that form karst features in limestone and dolomite, except that the processes are much more rapid. Water percolates over or through gypsum or salt and dissolves the highly soluble rock; typically, this causes formation of a series of sinkholes, caves, natural bridges, disappearing streams, and springs. Once a through-flowing passage is created in the evaporite rock, enlargement results from further dissolution and from abrasion as water-borne particles are transported through the cavity.

The process for dissolution of evaporites was described earlier by Johnson (1981), with particular reference to salt; but it clearly applies to dissolution of gypsum as well. He pointed out that ground water in contact with an evaporite deposit will dissolve some of the rock (Fig. 2), providing the water is not already saturated with $CaSO_4$ (or NaCl). For extensive dissolution to occur, it is necessary for the aqueous solution (or brine) thus formed to be removed from the evaporite deposit; otherwise, the water becomes saturated, and the process of dissolution stops. The four basic requirements for dissolution of gypsum (or salt) are (1) a deposit of gypsum (or salt) against which, or through which, water can flow; (2) a supply of water unsaturated with $CaSO_4$ (or NaCl); (3) an outlet whereby the resulting solution (or brine) can escape; and (4) energy (such as a hydrostatic head or density gradient) to cause the flow of water through the system. When all four of these requirements are met, dissolution of gypsum (or salt) can be quite rapid, in terms of geologic time.

Evaporite karst is rarely seen at the land surface in the eastern United States, but gypsum karst is fairly common in outcrops in the semiarid to arid regions of the West. Owing to rapid dissolution of gypsum and (especially) salt, most would-be outcrops in the East are quickly destroyed, and the rock and its dissolution features are observable only in excavations, mines, tunnels, and boreholes. Abrupt thinning or termination of an evaporite unit, particularly where overlying strata are brecciated, commonly marks a dissolution front (either ancient or modern) where karst processes are, or have been, occurring.

### Gypsum-Karst Processes

Gypsum karst develops rapidly, because gypsum is highly soluble in water. The solubility of $CaSO_4 \cdot 2H_2O$ ranges from about 2,200 to 2,600 ppm in the temperature range of 0–40°C (Hardie, 1967; Blount and Dickson, 1973). Gypsum-karst development can even be accelerated when accompanied by dedolomitization (Raines and Dewers, 1997). Karst features may be present in gypsum deposits in all parts of the United States, whether the gypsum crops out or is in the deep subsurface; the karst may result from climatic and hydrologic conditions of today, or it may be a relict from an earlier, wetter climate and/or hydrogeologic regime of the Pleistocene or pre-Pleistocene epochs.

In the eastern United States, where average annual precipitation commonly is >75 cm, gypsum deposits generally are eroded or dissolved to depths of at least several meters or tens of meters below the land surface. In the West, however, in areas where the average annual precipitation commonly is less than ~75 cm, gypsum tends to resist erosion and typically caps ridges, mesas, and buttes; in spite of its resistance to erosion in the West, gypsum commonly contains karst features, such as cavities, caves, and sinkholes, attesting the importance of ground-water movement, even in low-rainfall areas.

Evidence of gypsum karst includes surface and shallow-subsurface features, such as caves, sinkholes (dolines), karren, disappearing streams (swallow holes), springs, collapse structures, and the dropping

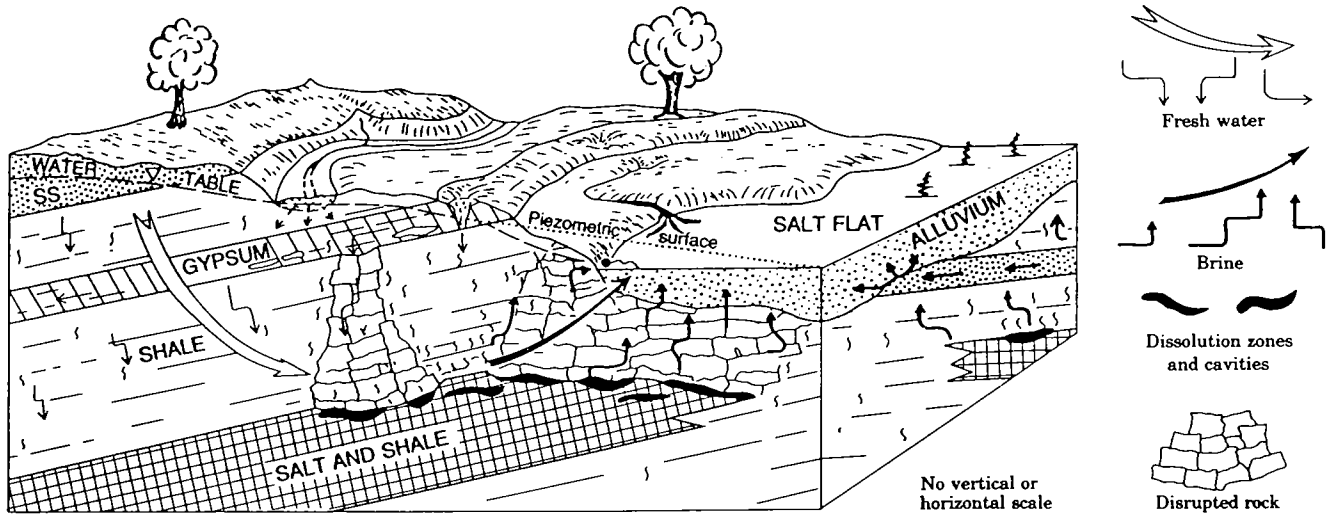


Figure 2. Schematic block diagram of intrastratal salt karst in western Oklahoma (from Johnson, 1981). The horizontal dimension is 1–15 km; the vertical dimension is 30–300 m.

of drill bits and/or loss of drilling fluids while drilling through gypsum beds. All these karst features, and many more, are identical in character and genesis to those found in carbonate rocks, with dissolution typically developing first along joints and bedding planes (Fig. 3). In fact, paleokarst, brecciated zones, and other karst features found in some carbonates may have been initiated by earlier dissolution and karst development in gypsum that is interbedded with the carbonates; Sando (1988), Palmer and Palmer (1995), and Friedman (1997) provide examples and a summary of this sulfate/carbonate karst relationship. Gypsum-karst features commonly have a linear orientation, and these appear to be controlled by joints or fractures in the rock (Fig. 3); however, some karst features have a seemingly random orientation, wherein the controls are not understood.

### Salt-Karst Processes

Salt is extremely soluble in ground water. Halite solubility in water is 35.5% by weight at 25°C, and it increases at higher temperatures (White, 1988). Salt-karst features can be present in all parts of the United States that are underlain by salt. The mechanisms for salt dissolution and development of intrastratal karst are described by Johnson (1981) and illustrated in Figure 2. Fresh ground water can be recharged through sandstone, gypsum, carbonates, alluvium, or other permeable and/or karstic units at or near the land surface (Fig. 2). This water migrates downward and/or laterally to the salt beds and dissolves the salt to form a brine. The resulting brine can then be forced through, and away from, the salt to make room for additional unsaturated ground water. Brine can migrate into an aquifer, or it can be forced back to the land surface in brine springs or salt flats. These mechanisms involve the four basic requirements for the dissolution of salt, as described above.

Salt is so soluble that it survives at the land surface only in arid areas. The two sites in the United States with salt recently at the surface are Sevier Valley, Utah (where salt outcrops were quarried), and Virgin Valley, in Nevada and Arizona (where the salt outcrops are now inundated by Lake Mead). Elsewhere, salt has been dissolved to depths ranging from tens to hundreds of meters below the present land surface, locally causing collapse and brecciation of overlying rocks and development of sediment-filled dissolution troughs (Fig. 4). In many places it is not easy (or possible) to distinguish between modern dissolution/karst and paleodissolution/paleokarst: some of the salt karst may be remnant from an earlier hydrogeologic regime (perhaps as early as shortly after original deposition of the salt unit).

Evidence of salt karst includes collapse structures, sinkholes, subsidence features, brine springs, salt flats, brecciated zones (in salt beds and overlying rocks), and the dropping of drill bits and loss of drilling fluids while drilling through salt beds. Many salt-karst features are similar to those in carbonate rocks, but there are only a few places in the world with extensive salt outcrops (e.g., Mount Sedom in the Dead Sea Depression of Israel, and Forrat Mico near Cardona in eastern Spain) where typical karst features, such as caves, sinkholes, shafts, and karren, can be documented (White, 1988; Frumkin and Raz, 2001; Gutiérrez and others, 2002).

## DISTRIBUTION OF NATURAL EVAPORITE KARST

Gypsum and salt are present in 32 of the 48 contiguous states, and they underlie ~35–40% of the land area (Fig. 1). These evaporites occur in 24 separate structural basins or geographic districts in the United States, and are reported in rocks of every geologic system from the Precambrian through the Quaternary. Local or extensive evaporite karst is known in almost all of these basins or districts. Below is a discussion of the distribution and selected examples of gypsum karst and salt karst.

### Natural Gypsum Karst

Gypsum deposits are more widespread than salt and are a significant part of all evaporite deposits in the United States (Fig. 1). Gypsum crops out or is in the subsurface in 32 of the 48 contiguous states. Generally, in areas where gypsum crops out, or is <30 m below the land surface, karst features are present (at least locally). The most widespread and pronounced examples of gypsum karst are in the Permian Basin of the southwestern United States. Other significant examples are in the Illinois Basin, Michigan Basin, Forest City Basin, the Black Hills area of South Dakota, and parts of Texas, Wyoming, and other western states.

The Permian Basin contains a thick sequence of Permian evaporites and red beds that extend from West Texas and southeastern New Mexico into western Oklahoma, western Kansas, and southeastern Colorado (Fig. 1). Individual gypsum beds typically are 3–10 m thick in most Permian Basin formations but are 20–200 m thick in the Castile Formation of

Figure 3. Karst development in the Permian Cloud Chief Gypsum in western Oklahoma. Dissolution is most pronounced along joints and bedding planes.

the Delaware Basin part of the Permian Basin (Dean and Johnson, 1989). Low rainfall in the region permits extensive outcrops of gypsum, particularly in the Delaware Basin, to the south, and along the Permian Basin's west flank (eastern New Mexico) and east flank (north-central Texas and western Oklahoma). In these areas, typical gypsum-karst features abound, and are described by Olive (1957), McGregor and others (1963), Fischer and Hackman (1964), Myers and others (1969), Kelley (1971), Quinlan (1978), Johnson (1986, 1990, 1996, 1997, 2003a,b,c), Bozeman (1987, 2003), Sares and Wells (1987), Belski (1992), Hill (1996), Forbes and Nance (1997), Christenson and others (2003), Miller and others (2003), Tarhule and others (2003), and Powers and Owsley (2003). Quinlan and others (1986) report more than 500 gypsum caves in the United States, most of them being in the Permian Basin; most of the literature on these caves has been published by local cave-exploration groups.

The Delaware Basin of West Texas and southeastern New Mexico, in the southwestern part of the Permian Basin, contains one of the greatest accumulations of evaporites in the United States (Dean and Johnson, 1989). Evaporites (gypsum/anhydrite and salt) of the Upper Permian Castile, Salado, and Rustler Formations typically are 500 m to >1,500 m thick within the Delaware Basin (Fig. 4), and are >450 m thick where these deposits extend north and east of the basin. Outcrops of these three formations constitute the most extensive examples of gypsum karst in the nation. The area referred to as the Gypsum Plain comprises about 2,600 km$^2$ of outcropping gypsum of the Castile and Salado Formations (Kirkland and Evans, 1980), and additional gypsum outcrops are present just to the east in the Rustler Hills and into Reeves County, Texas.

The Delaware Basin gypsum deposits contain abundant sinkholes, caves, closed depressions, collapse

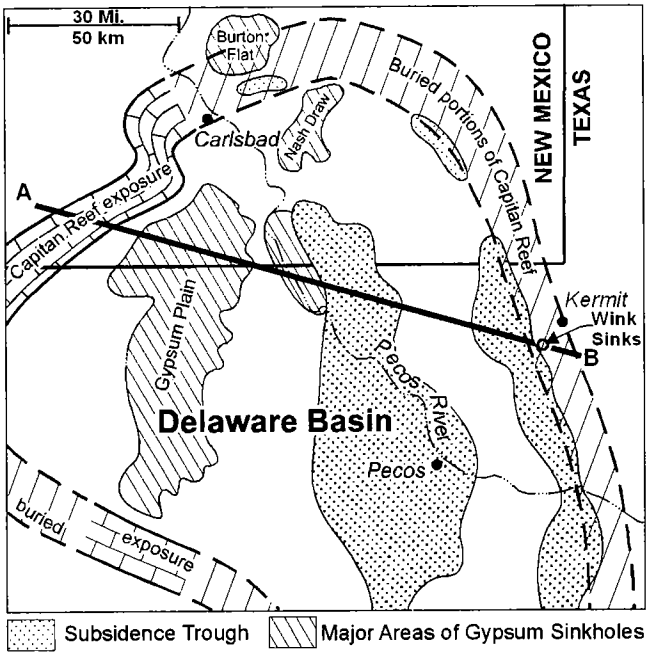


Figure 4. Map and cross section showing salt dissolution, subsidence troughs, and areas of gypsum sinkholes in the Delaware Basin of West Texas and southeastern New Mexico (modified from Martinez and others, 1998). Deep, sediment-filled subsidence troughs result from natural dissolution of salt by unsaturated ground water and resultant collapse of overlying strata. Asterisks (***) show where preexisting salt layers have been dissolved and now are marked by collapsed, brecciated, or karstic masses of anhydrite or gypsum. Wink Sinks are shown at east end of cross section.

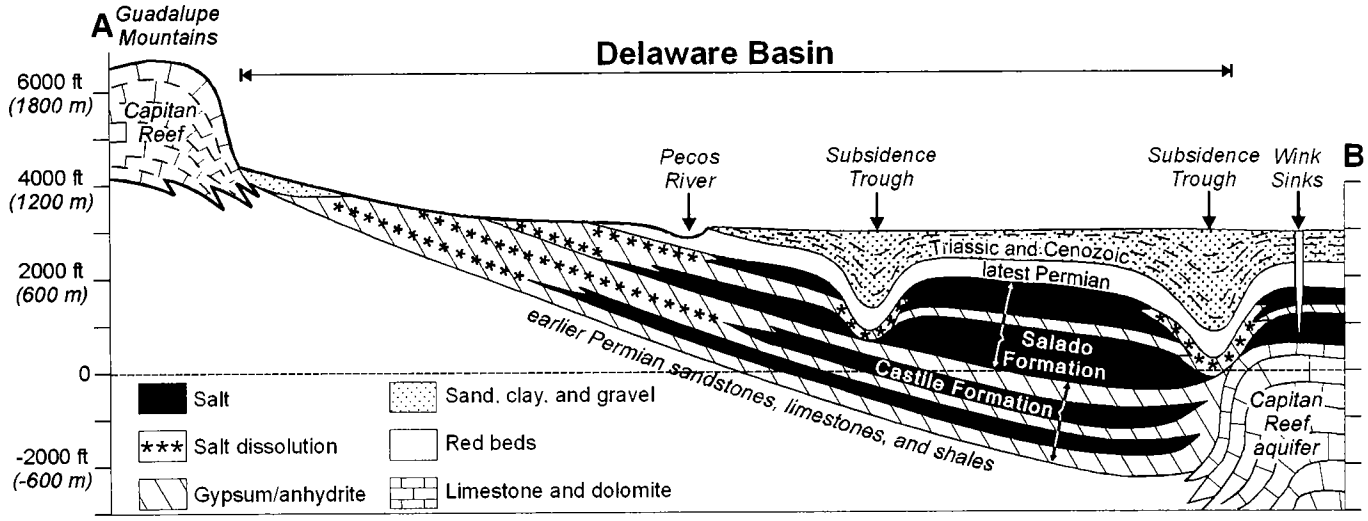

sinks, and underground drainage; an excellent summary is provided by Hill (1996). Much of the area has been affected by subsurface dissolution of some of the salt layers, and most of the outcrops consist of massive beds of gypsum (Fig. 4). Four principal areas of gypsum karst in the area are the Gypsum Plain, Nash Draw, Burton Flat, and the Pecos River Valley (Hill, 1996). Sinkholes, a few meters to 100 m across, are active collapse features in all four areas, and generally they are related to shallow underground caverns <100 m deep. One sinkhole, formed during a storm in 1918, collapsed suddenly to form a gaping hole ~25 m across and 20 m deep (Hill, 1996). Caves are prominent and abundant on the Gypsum Plain and Burton Flat (Sares and Wells, 1987; Belski, 1992), and gypsum karst is having an adverse impact on the alignment of New Mexico Highway 128 in parts of Nash Draw (Powers and Owsley, 2003).

Along the west flank of the Permian Basin, in eastern New Mexico, gypsum crops out extensively along parts of the Pecos River Valley. Various gypsum and carbonate units are present in the Permian Artesia Group and San Andres Formation, and they contain a large number of sinkholes, caves, and other karst features in the Vaughn–Roswell area (Fischer and Hackman, 1964; Kelley, 1971; Forbes and Nance, 1997; Land, 2003). Several of the caves in this area are >3.2 km long, and the deepest has a vertical extent of >120 m (Forbes and Nance, 1997). Subsurface evaporite dissolution and collapse of overlying gypsum and mudstone units have created the well-known Bottomless Lakes State Park just east of Roswell (Land, 2003).

Another major gypsum-karst area of the Permian Basin is along its east flank, in north-central Texas and western Oklahoma. Principal gypsum units are the Permian Blaine and Cloud Chief Formations, with gypsum beds 3–30 m thick. Among the more important gypsum-karst features of the region are two well-known caves and a major freshwater aquifer, all developed in the Blaine Formation; these three gypsum-karst phenomena are beneficial, rather than being problems. The D. C. Jester Cave of southwestern Oklahoma (Fig. 5) was surveyed between 1983 and 1987 (Bozeman, 1987; Johnson, 2003a); the main passage is 2,413 m long, but, along with the side passages, the total length is 10,065 m, making it the longest reported gypsum cave in the western world. The cave has passageways that typically are 1–5 m in diameter, and locally are up to 20 m wide. Alabaster Cavern of northwestern Oklahoma (Fig. 5), now developed as a state park and tourist cave, has a main passage ~700 m long; it has a maximum width of 18 m and a maximum

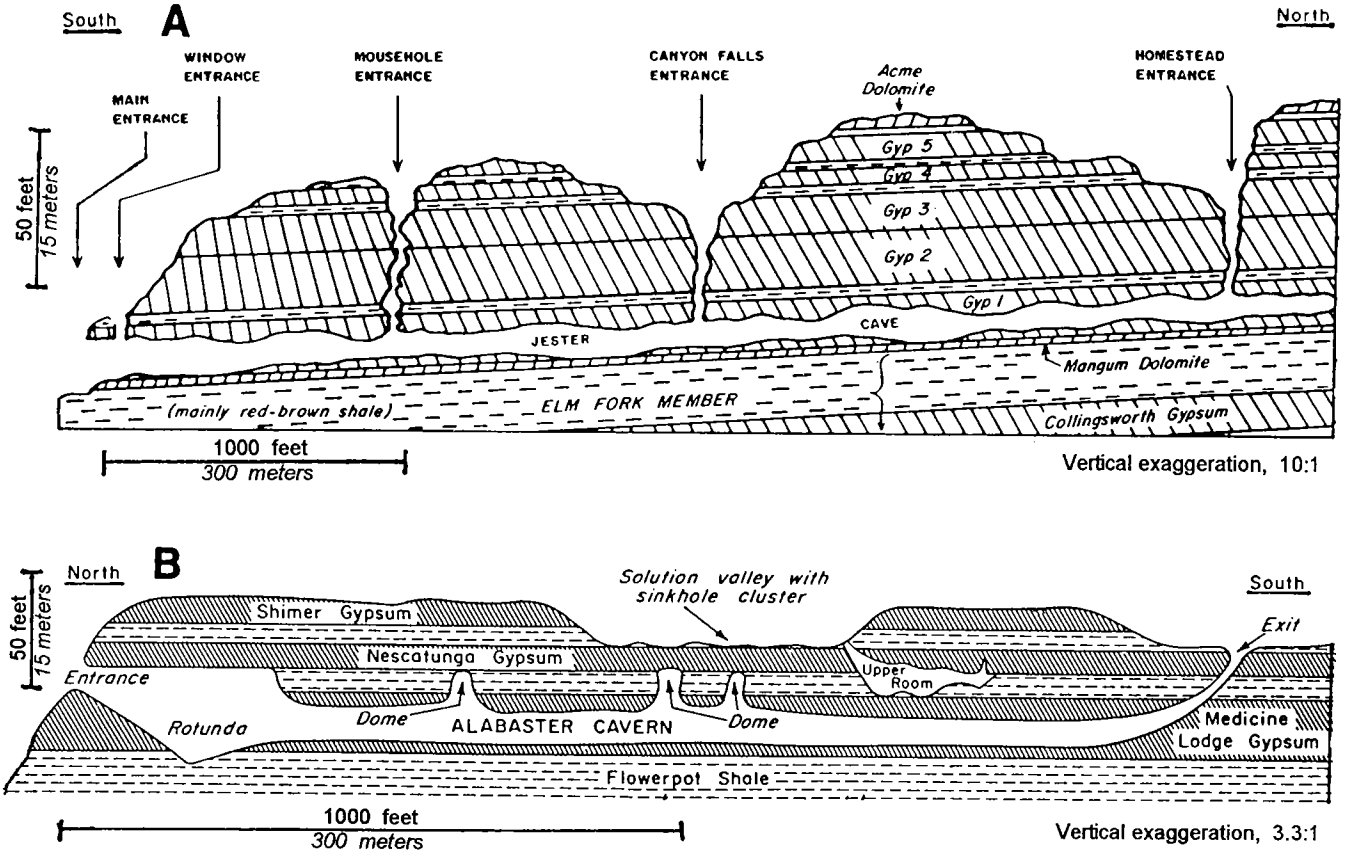


Figure 5. Schematic cross sections through major gypsum caves in the Permian Blaine Formation of western Oklahoma; from Johnson (1997), based on Myers and others (1969), Bozeman (1987), and Johnson (2003a). At top (A) is D. C. Jester Cave; at bottom (B) is Alabaster Cavern.

height of 15 m (Myers and others, 1969; Johnson, 2003a). A major freshwater aquifer is developed in the Blaine Formation of southwestern Oklahoma and north-central Texas (Runkle and Johnson, 1988; Johnson, 1990, 2003a). Water is produced from the karstic and cavernous gypsum and dolomite beds of the Blaine aquifer. The aquifer is 50–65 m thick and consists of nine thick gypsum beds (each 3–8 m thick) interbedded with thinner dolomite beds (0.1–1.5 m thick) and shale beds (0.3–8.0 m thick). Irrigation wells typically are 15–100 m deep and commonly yield 1,000–8,000 L/min. The water is a calcium sulfate type; total dissolved solids average ~3,100 mg/L (of which ~90% is $CaSO_4$), and the water is suitable for irrigation but generally is unsuitable for drinking.

Exploration and speleology of gypsum caves in the Blaine and Cloud Chief Formations of western Oklahoma have been described by Bozeman and Bozeman (2002) and Bozeman (2003). Special studies also have been made of the Nescatunga Cave and the Vickery Cave System in the Blaine of northwestern Oklahoma: U.S. Highway 412 is being widened above these caves, and there is concern about possible adverse impacts on the highway as well as the need to preserve an important cave fauna (Christenson and others, 2003; Miller and others, 2003; Tarhule and others, 2003).

Problems associated with gypsum karst in southwestern Oklahoma affected the siting of the Upper and Lower Mangum Damsites (Johnson, 2003b,c). After ~60 years of study to find a suitable damsite for the Upper Mangum Dam in the thick Blaine gypsum beds, the search was abandoned because of extensive karst in the abutments and in the impoundment area (Johnson, 2003b). An alternative site, the Lower Mangum Damsite, has been examined and found capable of containing water; however, gypsum karst in the Blaine Formation in the upper parts of the reservoir will limit the elevation of the lake level and the amount of water that can be stored (Johnson, 2003c).

Dams built in other areas where gypsum karst has caused problems recently are the Anchor Dam in northwestern Wyoming, the Quail Creek Dike in southwestern Utah, and the Horsetooth and Carter Lake Reservoirs in northern Colorado. Sinkholes in the Anchor Dam reservoir area allow drainage of lake water into underlying karstic gypsum and limestone units (Jarvis, 2003). The dam, constructed ~60 km west of Thermopolis in 1960, has not met expectations, and only a small amount of water has been held in the reservoir.

The Quail Creek Dike, an earth-fill embankment near St. George, Utah, was constructed above a zone of gypsum karst (Fig. 6) (Catanach and others, 1989; Payton and Hansen, 2003). Strata beneath the dike were thinly bedded layers of dolomite, gypsiferous siltstone, gypsum, and sandstone in the upper part of the Triassic Moenkopi Formation: these strata were jointed, karstic, and dipped at angles of 15–25°. Preconstruction investigation did not detect the extent of the joint-related karst system, or the potential for seepage problems (Catanach and others, 1989). Upon completion of the dike, lake water flowed through the joints and karst features, opened or enlarged the passageways in the gypsum, undercut the dike, and caused its collapse and failure on January 1, 1989 (Fig. 6). Fortunately, there was no loss of life, but there was considerable damage downstream from the dike. A concrete dike was successfully rebuilt on the site in 1990, at a cost of about $12 million, with a deep cutoff trench excavated down through the gypsum-karst zone.

Horsetooth Reservoir and Carter Lake Reservoir, just west of Fort Collins and Loveland, Colorado, respectively, were built in the 1940s above the Permian/Triassic Lykins Formation (Pearson, 2002). The Lykins here consists of interbedded siltstone, shale, limestone, and gypsum (anhydrite at depth), with cavities, intrastratal breccias, paleo-collapse chimneys, and other karstic features locally present. During the late 1980s and 1990s, sinkholes formed at the south end of Horsetooth Reservoir, and seepage from the lake increased dramatically (Pearson, 2002). In 2000, a sinkhole formed at the upstream toe of the dam. At Carter Lake Dam, seepage that exits downstream from the dam is >100 L/s, and some of this water is nearly saturated with dissolved gypsum (Pearson, 2002). Water loss at both reservoirs is due to karst features in the Lykins Formation, at least in part, and current investigations are aimed at controlling this water loss.

Gypsum karst is indicated, indirectly, along the east and west sides of the Illinois Basin in Illinois, Indiana, and Kentucky. The St. Louis Limestone (Upper Mississippian) contains several gypsum/anhydrite beds, 1–15 m thick, in the subsurface (McGregor, 1954; Saxby and Lamar, 1957; McGrain and Helton, 1964). Gypsum does not crop out in Indiana and Kentucky, however, because intrastratal karstification is dissolv-

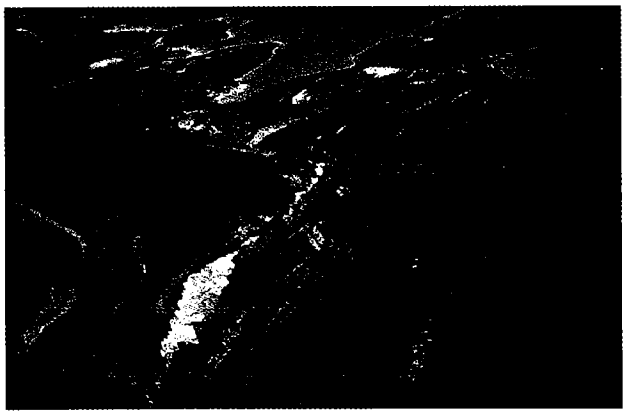

Figure 6. Aerial view of Quail Creek Dike failure in southwestern Utah (photo courtesy of Utah Division of Water Resources, Ben Everitt). The central part of the earth-fill embankment, built over a zone of gypsum karst, collapsed and washed away in 1989 (center of photo). Partially drained reservoir at top of photo; water flowed to the southwest (lower left).

ing the evaporites and producing ground water with a high concentration of dissolved sulfates along the eastern boundary of the subsurface gypsum deposits (George, 1977). Chemical analyses of springs and well water show a sulfate concentration of up to 1,350 mg/L, and a low chloride concentration, usually <30 mg/L. Westward (downdip) advance of the gypsum-dissolution front in this region generates the sulfate-rich water and collapse of overlying carbonate rocks into cavities. George (1977) cites an example of the collapsed carbonates in Squire Boone Caverns, Harrison County, Indiana. Jorgensen and Carr (1973) show an abrupt lateral thinning of gypsum (from ~4 m thick to <0.5 m thick, within a distance of 150 m) in the St. Louis Limestone near Shoals, Indiana; those authors, along with French and Rooney (1969), ascribe this thinning to dissolution along the eastern, updip limit of the gypsum. Saxby and Lamar (1957) also recorded the presence of breccia and the absence of gypsum in outcrops of St. Louis Limestone on the west (Illinois) side of the Illinois Basin, and they felt this may have resulted from dissolution of the gypsum.

The Michigan Basin contains gypsum karst in the Mississippian Michigan Formation in the central part of the State (Elowski and Ostrander, 1977). The Michigan Formation contains a series of gypsum beds, 1–10 m thick, interbedded with sandstone and shale; these strata crop out locally or are mantled by glacial drift on the east and west sides of the basin. Gypsum caves, sinkholes, and collapse features are described in the Grand Rapids area of Kent County (in the west), and also in parts of Iosco and Arenac Counties (in the east) (Elowski and Ostrander, 1977). Black (2003) provides a recent overview of gypsum and salt karst in Michigan.

The Forest City Basin area of Iowa contains evidence of gypsum karst in Devonian and Jurassic strata. The Devonian Wapsipinicon and Cedar Valley Groups contain numerous gypsum/anhydrite beds in central and southern Iowa (Witzke and others, 1988). Devonian gypsum does not crop out in Iowa, and it is thought that the present limits of some of the evaporite units are dissolutional; some of the breccia beds (i.e., the Devonian Davenport breccias) are interpreted as having formed by gypsum dissolution and collapse shortly after evaporite deposition (Witzke and others, 1988). The Fort Dodge Formation is an outlier of Jurassic gypsum present in ~40 km$^2$ of Webster County, central Iowa. The gypsum is as thick as 10 m, but the upper surface is irregular owing to partial dissolution before deposition of an overlying Pleistocene till (Cody and others, 1996; Sharpe, 2003). This till commonly is 10–30 m thick, but gypsum is exposed locally in stream cuts and quarry faces. The principal karst features are joint-controlled dissolution channels, ~1 m wide and 1–3 m deep, incised into the upper surface of the Fort Dodge gypsum.

Other examples of gypsum karst are noted in central Texas, South Dakota, and Wyoming. The Cretaceous Kirschberg Evaporite Member of the Terrett Formation contains 10 m of gypsum in a quarry near Fredericksburg, Texas (Warren and others, 1990). Vertical pipes, caves, and collapse breccia are well exposed, and gypsum and calcite speleothems (mainly in the form of popcorn and flowstone) were deposited in the pipes and caves. In the Black Hills area of South Dakota, gypsum in the Triassic Spearfish Formation locally contains sinkholes and caves that have caused environmental problems (Rahn and Davis, 1996; Davis and Rahn, 1997; Davis and others, 2003; Epstein, 2003). Gypsum beds up to 5 m thick contain sinkholes and caves, and the karst has resulted in general ground subsidence, foundation cracking and seepage in houses, failure of a sewage lagoon, and problems with a proposed mine-tailings facility and a golf-course reservoir. Gypsum karst and sinkhole development in several other formations in the Black Hills have shown the need to consider gypsum karst in land-use planning (Epstein, 2003). In Wyoming, Sando (1988) describes widespread paleokarst in the Madison Limestone of Mississippian age. He notes that dissolution of gypsum beds within the predominantly limestone sequence during Late Mississippian–Early Pennsylvanian time enhanced contemporaneous development of sinkholes, caves, dissolution-enlarged joints, and breccia zones. In Laramie, Wyoming, gypsite (an earthy form of gypsum) has been dissolved locally to produce collapse of roads and soil instability under streets, gutters, sidewalks, and foundations (Jarvis and Huntoon, 2003).

Mining of gypsum can be impacted adversely by natural dissolution and karst features (Sharpe, 2003). Dissolution can create an irregular surface or boundary of a gypsum unit, and solution-enlarged fractures may be filled with soil or mud that degrades the quality of the stone. Karst features in an underground gypsum mine can lead to a potentially hazardous influx of ground water into the mine. However, on the positive side, circulation of ground water near and within preexisting anhydrite beds causes hydration of the rock to gypsum.

## Natural Salt Karst

Salt deposits underlie a part of 25 of the 48 contiguous states (Fig. 1). Some of the deposits are extensive, such as the Salina Group salts of the Michigan and Appalachian Basins, the Permian salts of the Permian Basin, and the Louann Salt and salt domes of the Gulf Coast Basin. These deposits rank among the greatest salt deposits of the world. Data on salt deposits of the United States were compiled by Pierce and Rich (1962), Lefond (1969), and Johnson and Gonzales (1978). Evidence of modern natural dissolution or paleodissolution of salt has been found in almost every one of the states and districts, and therefore salt karst is a much more widespread phenomenon than commonly suspected.

The Delaware Basin area of West Texas and south-

eastern New Mexico contains a great thickness of Permian salts in the Castile and Salado Formations (Fig. 4). Castile salt beds have been dissolved from the western half of the basin, and hence their stratigraphic position is marked by brecciated zones of anhydrite that result from collapse and lowering of overlying units (Fig. 4) (Anderson and others, 1972, 1978; Anderson, 1982). Salt dissolution, resulting in subsidence and increased basin-fill sedimentation, has been observed in various parts of the Delaware Basin; most of the dissolution and subsidence occurred during the Cenozoic Era (Maley and Huffington, 1953; Bachman, 1976, 1984; Lambert, 1983), but some of the dissolution occurred during or shortly after deposition of the Permian salts (Powers and Hassinger, 1985; Johnson, 1993). Salt dissolution is still going on in the Delaware Basin area, as attested by the presence of saline seeps along Malaga Bend of the Pecos River in southeastern New Mexico. Hill (1996, 2003) has provided a summary of salt-dissolution processes in the Delaware Basin, along with discussion of lateral and vertical dissolution features, subsidence troughs, breccia pipes, sinks, and other disturbed zones related to salt karst. Powers and others (2003) provide evidence that salt dissolution has increased the transmissivity of the Rustler Formation in southeastern New Mexico.

Permian salt beds are being dissolved at shallow to moderate depths in western Oklahoma, western Kansas, and the Texas Panhandle (Fig. 2). Conspicuous results of this process are collapse and subsidence features that reach to the land surface; for example, the High Plains Escarpment coincides with, and is above, the salt-dissolution front that is advancing westward beneath the Texas Panhandle (Gustavson and others, 1980, 1982). Salt dissolution in the area is also accompanied by sediment-filled subsidence basins and fractured rock at the surface (Irwin and Morton, 1969; Simpkins and others, 1981; Gustavson and Finley, 1985; Johnson, 1989). Salt dissolution has also caused formation of a series of breccia pipes in the Lake Meredith area of the Texas Panhandle (Eck and Redfield, 1965). Hovorka (1983) conducted petrographic studies of the deep-seated evaporites in the area and recognized criteria for post-Permian dissolution of the salt beds. Another result of modern salt dissolution is the presence of large, salt-encrusted salt plains that form where high-salinity brines are emitted at the surface (Baker, 1977; Johnson, 1981, 2003a); emission of these NaCl-rich brines attests ongoing salt dissolution and karst development. Near Hutchinson, Kansas, an active sinkhole, probably of natural origin, is subsiding along U.S. Highway 50 at a rate of 0.3 m per year (Miller, 2003): at this site the Hutchinson salt is ~40 m thick and 125 m deep.

The Holbrook Basin (formerly Supai Basin) of northeastern Arizona is the site of >500 sinkholes, fissures, depressions, and other karst features that result from ongoing dissolution of salt in the Permian Schnebly Hill Formation (Fig. 7) (Neal and others, 1998). Sinkholes and collapse structures related to this natural salt dissolution would be potentially catastrophic if they were to occur in densely populated areas. Salt dissolution on the southwest side of the basin, in the vicinity of the Holbrook anticline, has been recognized for many years (Bahr, 1962; Johnson and Gonzales, 1978; Neal, 1995; Martinez and others, 1998; Rauzi, 2000), and the relationship of the dissolution front to the surface karst features is now well documented (Fig. 7). The salt-dissolution front is migrating downdip to the northeast, and collapse of overlying strata has enabled karst to develop in such areas as The Sinks, Dry Lake Valley, and McCauley Sinks (Neal and others, 1998). Evaporite-karst development at other sites in the Holbrook Basin is reported by Neal and Colpitts (1997), Rauzi (2000), and Neal and Johnson (2003).

Salt deposits of central and southeastern Utah have undergone diapiric movement and dissolution. In the Paradox Basin of southeastern Utah and adjacent southwestern Colorado, thick salts of the Pennsylvanian Paradox Member of the Hermosa Formation have flowed into a series of long and narrow salt anticlines (Hite and Lohman, 1973; Doelling, 1988). Past and/or present dissolution of salt in the Paradox Basin apparently is limited to the western and southeastern edges of the salt basin and to the crestal areas of the salt anticlines (Hite and Lohman, 1973). Hite and Lohman (1973) point out that rivers draining the Paradox Basin increase their load of dissolved sodium chloride by ~610 metric tons per day: they also estimate

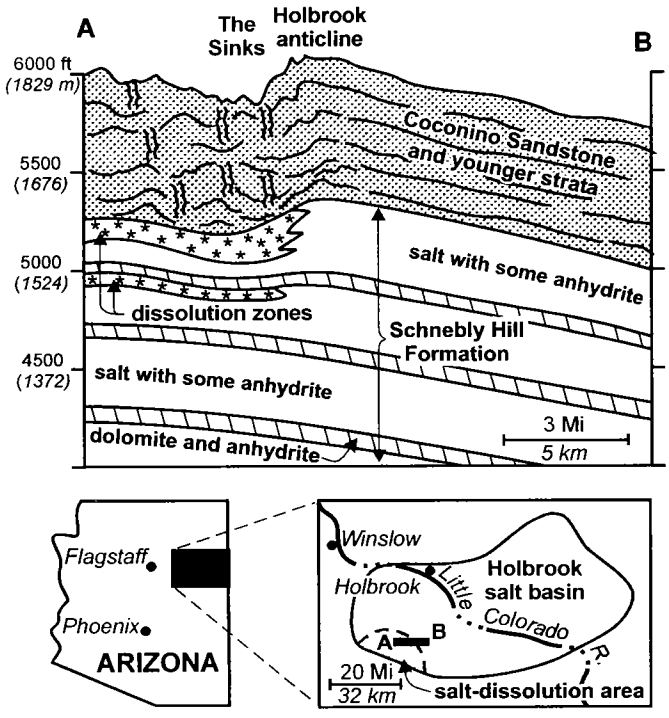


Figure 7. East–west cross section showing natural salt dissolution and collapse on the southwest side of the Holbrook Basin, Arizona. Modified from Neal and others (1998) and Martinez and others (1998).

that the present-day, 33-m-thick cap rock in the anticlines represents the residue formed by dissolution of ~900 m of halite-bearing rock from the central cores of the anticlines. In central Utah, the Jurassic Arapien Shale and its thick interbeds of salt have flowed into several major salt-cored anticlines similar to those of the Paradox Basin (Willis, 1986; Witkind, 1994); these anticlines also are believed to have undergone episodes of salt dissolution and collapse. Exposed rock salt was surface mined in several small areas of the Sevier River Valley along the Sevier–Sanpete county line.

Major evaporite-karst features in west-central Colorado are the result of dissolution and flow of the Pennsylvanian Eagle Evaporites (Kirkham and others, 2002, 2003). Regional subsidence has occurred in the Carbondale and Eagle collapse centers, an area of at least 3,600 $km^2$. Dissolution, mainly of salt and also of some gypsum, caused vertical settlement of up to 1,200 m, mostly in the past 3 million years. Karst features are still forming in both centers, as attested by active sinkhole development and by contribution of large amounts of dissolved evaporites into the Colorado River from the collapse areas.

Salt dissolution has been documented at several places in the Wyoming basins and the Williston Basin. Parker (1967) described dissolution of salt beds of Middle Devonian and Permian age in the deep subsurface of Wyoming, North Dakota, and Montana. Salt removal caused overlying rocks to subside and collapse into the depressions thus formed, with subsidence having occurred at various times between the Late Devonian and Late Jurassic. Orchard (1987) showed that beds of salt in the Mississippian Charles Formation pinch out abruptly over the Poplar Dome, at a depth of 1,700 m in northeastern Montana; salt dissolution probably occurred during the Tertiary, and salt removal was a major factor in creation of the large oil field at Poplar Dome. Rasmussen and Bean (1984) described salt dissolution and subsidence of overlying strata in the Powder River Basin of Wyoming; Late Permian salts of the Goose Egg Formation (Ervay Member) were dissolved mainly during the Late Jurassic and Early Cretaceous, and the dissolution zone now is ~3,000 m below the surface.

The Michigan Basin contains several examples of salt karst. Dissolution of salts in the Salina Group (Silurian) and Detroit River Group (Devonian) across the northern edge of the Michigan Basin by Middle Devonian time created a broad area of collapsed rocks, referred to as the Mackinac Breccia (Landes, 1959; Black, 1984, 2003). In addition, Black (1983, 1984, 1997, 2003) has shown that a number of modern sinks in the area, and subsurface zones where drilling fluids are lost, are due to paleodissolution and ongoing dissolution of the Detroit River Group salts by ground water circulating in open fault systems.

The Gulf Coast Basin is one of the most significant salt-dome provinces in the world (Halbouty, 1967; Lefond, 1969; Johnson and Gonzales, 1978; Martinez, 1991). The Jurassic Louann Salt has flowed (and continues to move) into diapiric structures; more than 260 domes are either known or inferred in the onshore portion of this region. The processes by which salt-dome cap rock forms is a special type of intrastratal salt karst; as salt rises in diapirs, ground water dissolves the upper surface of the salt, forming an accumulation of residual, relatively insoluble anhydrite and calcite as the cap rock (Walker, 1974; Kreitler and Dutton, 1983). About half of the known domes have a cap rock, and thus attest salt dissolution.

## HUMAN-INDUCED EVAPORITE KARST

Human activities can play a special role in inducing or enhancing karst processes in evaporite rocks, and the results can be catastrophic. Owing to the rapid dissolution of gypsum, and the extremely rapid dissolution of salt, small to large dissolution cavities can be developed in subsurface evaporites by allowing unsaturated water to flow through or against the rock. Human activity that can cause such cavity development typically involves (1) construction upon, or directing water into or above, outcropping or shallow gypsum or salt deposits; or (2) the drilling of boreholes into or through subsurface salt deposits. Human-induced karst problems in gypsum areas are very much like those that are well known in carbonate-karst areas, and I will cite only a couple of studies on this problem; but human-induced salt karst is not as widely understood, and its problems can be highly significant.

### Human-Induced Gypsum Karst

Gypsum karst can be accelerated by human activity. Gypsum-karst problems are caused by the same activities that cause problems in carbonate-karst terranes: (1) building structures that induce differential compaction of soils above an irregular gypsum-bedrock surface; (2) building structures directly upon gypsum-collapse features; and (3) impounding water above, or directing water into, a gypsum unit where soil piping can divert water (and soil) into underground gypsum cavities. These human activities can cause land subsidence, or can cause new or concealed sinkholes and cave systems to open up; and this can result in settling or catastrophic collapse of the ground.

Specific human activities that have accelerated gypsum karst in the Black Hills area of South Dakota include the following examples: (1) sewage lagoons, built on alluvium above a karstic gypsum layer, began leaking badly within 1 year, and then failed with partially treated sewage escaping the site; and (2) directing runoff into buried gypsum karst caused several houses to settle and crack, and produced sinkholes in urban/suburban areas (Rahn and Davis, 1996; Davis and Rahn, 1997; Davis and others, 2003; Epstein, 2003). Cooper (1995) also pointed out that (because gypsum dissolution is so rapid) pumping large volumes of gypsiferous water from wells means that

subsurface gypsum will be dissolved at an accelerated rate, and this can cause increased subsidence and possible collapse.

Human activities in areas of natural gypsum karst can result in creating major problems in the siting, construction, and/or water-retention capacity of dams and reservoirs, such as those in Oklahoma, Wyoming, and Utah (these are discussed above, under "Natural Gypsum Karst"). Gypsum-karst features can make it impossible for water retention in an impoundment area, or it is possible for impounded water to force open preexisting, sediment-filled solution passages (Fig. 6).

## Human-Induced Salt Karst

Human-induced salt dissolution can have catastrophic effects locally (Walters, 1978, 1991; Dunrud and Nevins, 1981; Ege, 1984; Coates and others, 1985; Johnson, 1987, 1997, 1998, in press; Johnson and others, 2003). The drilling of boreholes into or through the salt can enable (either intentionally or inadvertently) unsaturated water to enter the borehole and dissolve the salt. If the dissolution cavity is large enough and shallow enough, successive roof failures can cause the water-filled void to migrate upward; this can result in land subsidence or catastrophic collapse (Fig. 8).

Human activities that can contribute to salt-karst problems include solution mining of salt, petroleum activity, and dry mining of salt.

### *Problems Caused by Solution Mining*

Solution mining is the process of extracting soluble minerals, such as salt or potash, by (1) introducing a dissolving fluid (i.e., water) into the subsurface, (2) dissolving the mineral (or rock) and forming a brine, (3) recovering the brine, and (4) extracting the mineral from the brine (usually by evaporation) (Johnson, 1997, 1998). Solution mining typically entails creating one or several large underground cavities that are filled with brine; the cavities may be in bedded salts, salt domes, or salt anticlines. Cavities typically are 10–100 m in diameter and are 10–600 m high, both dimensions based largely on the thickness of the salt and the depth to the top of the cavity. At some sites, unfortunately, the cavity becomes too large, and the roof collapses. Dunrud and Nevins (1981) reported 10 areas of solution mining and collapse in the United States. Most solution-mining collapses result from cavities formed 50–100 years ago, before modern-day engineering safeguards were developed. Proper, modern design has virtually eliminated this problem in new facilities.

Four well-documented subsidence/collapse features resulting from solution mining are Cargill Sink (Kansas), Grand Saline Sink (Texas), Grosse Ile (Michigan), and Tully Valley (New York). Examples of the explosive escape of gaseous hydrocarbons related to man-made, solution-mined storage caverns in salt are the Elk City blowout (Oklahoma) and the Hutchinson natural-gas explosion (Kansas).

The Cargill Sink formed in 1974 as a result of solution mining for salt by Cargill, Inc., near Hutchinson, Kansas (Fig. 9) (Walters, 1978; Johnson, 1998, in press). The surface crater reached a diameter of 60 m within 4 hours and stabilized with a diameter of 90 m and a maximum depth of ~15 m (Fig. 10); the volume of the crater was calculated to be ~70,000 $m^3$. Salt had been solution mined in the area since 1888. The Permian Hutchinson salt is ~105 m thick and occurs at a depth of ~130 m. The sink developed in an active brine field that included both operating and abandoned wells. Embraced within the sinkhole was a brine well that was drilled in 1908 and abandoned in 1929.

Grand Saline Sink developed in the city of Grand Saline, Texas, in 1976 (Fig. 9) (Dunrud and Nevins, 1981; Johnson, 1998, in press). The sink occurred at the site of a brine well that penetrated the top of the Grand Saline salt dome at a depth of 60 m and had produced brine from 1924 through 1949. The sink eventually grew to a diameter >15 m, and a total of 8,500 $m^3$ of silt and clay was displaced into the underground cavity.

On Grosse Ile, in the Detroit River near Detroit, Michigan, several sinkholes developed in 1971 as a result of 30 years of solution mining the Silurian Salina Group salts at a depth of 325 m below the surface (Nieto-Pescetto and Hendron, 1977; Ege, 1984). Dunrud and Nevins (1981) estimated that the area affected by subsidence was 37,000 $m^2$ and the volume of subsidence, 1,200,000 $m^3$.

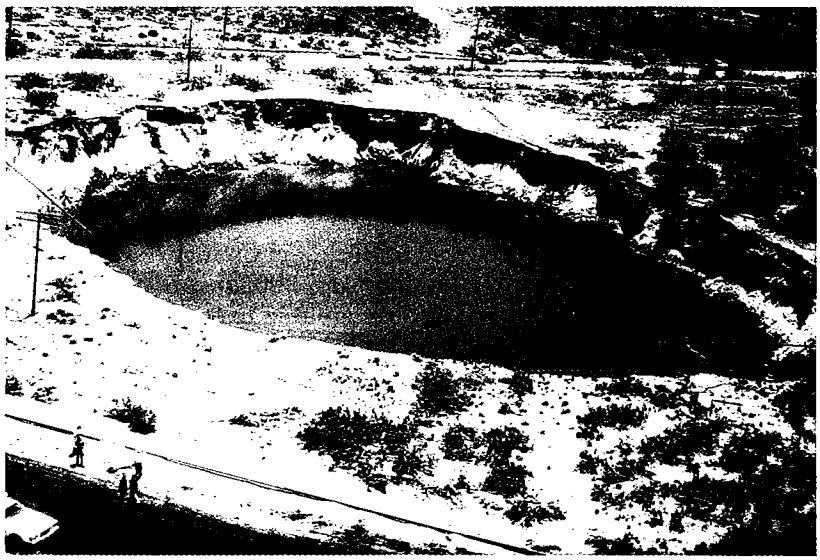

Figure 8. Aerial view of Wink Sink no. 1 in West Texas, shortly after its collapse in 1980 (photo courtesy of R. W. Baumgardner, Jr.). The sink, with a diameter of 110 m, formed at the site of an abandoned oil well.

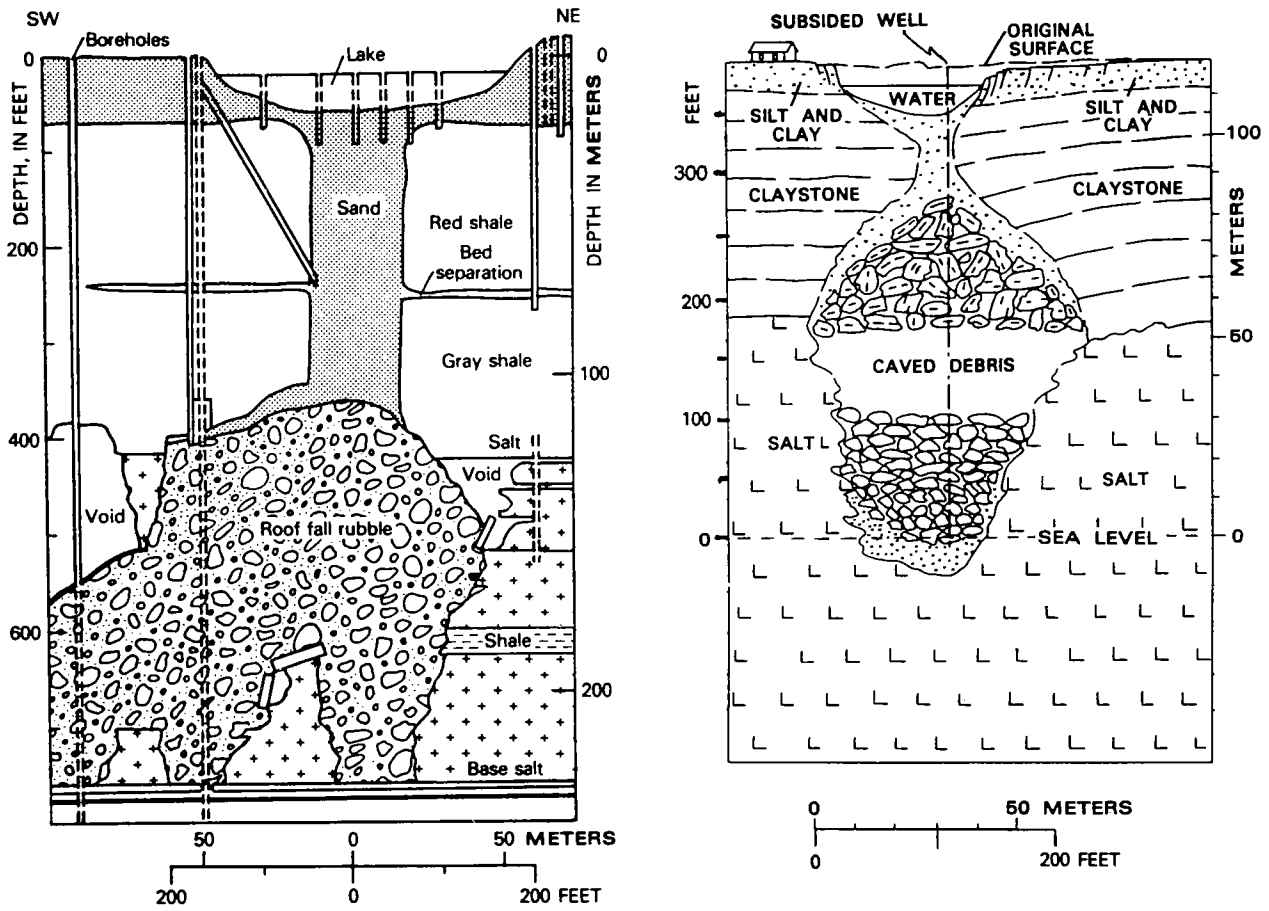


Figure 9. Collapse and sinkholes resulting from solution mining in salt. On left is cross section through Cargill Sink, Kansas (modified from Walters, 1978); cavity shape is hypothetical. On right is cross section through Grand Saline Sink in Grand Saline salt dome, Texas (modified from Dunrud and Nevins, 1981).

In Tully Valley of central New York, the top of the Silurian Salina Group salt ranges from 335 to 485 m below the surface. The Salina comprises ~300 m of interbedded shale, dolomite, halite, and gypsum/anhydrite; salt has a cumulative thickness ranging from ~8 to 100 m (Getchell, 1995). These salts had been solution mined from the late 1800s until the mid 1980s, and removal of the salt has resulted in land-subsidence features that generally are closed depressions with vertical displacements of 10–20 m and diameters >60 m (Getchell, 1995).

The Elk City blowout occurred in Beckham County, Oklahoma, in 1973 (Fay, 1973; Johnson, 2003a). An underground salt-dissolution cavern, created to store propane in the Permian Blaine Formation, leaked small amounts of hydrocarbons over a long period of time. Escaped propane accumulated in a shallow, permeable siltstone, and it migrated laterally (about 700 m) away from the cavern borehole until it burst to the surface along natural joint patterns. The blowout was explosive: it made a large crater, 6 m deep, and disrupted rock slabs that weighed up to 30 metric tons. It was in rural pastureland, and there were no injuries.

In the central Kansas town of Hutchinson, in Reno County, natural gas exploded to the surface through abandoned boreholes in January 2001, killing two people, destroying two downtown businesses, and causing evacuation of hundreds of residences (Watney and others, 2003). The source of the gas was a casing leak at an underground salt-dissolution storage cavern created in the Permian Hutchinson salt near Yaggy, ~11 km northwest of Hutchinson. The failure occurred above the salt unit in one of the wells at the Yaggy facility; this allowed high-pressure gas to escape, apparently migrating in the subsurface to Hutchinson within 2 days, and coming to the surface through a number of abandoned wells that had been drilled for solution mining or water supply. The gas-migration path from Yaggy to Hutchinson was in fractured dolomites that apparently were, in part, fractured when the underlying Hutchinson salt was partly dissolved, and overlying strata (including the dolomites) subsided (Watney and others, 2003). Upon discovery of the leak at Yaggy, the cavern was emptied, and the supply of natural gas was cut off.

### *Problems Caused by Petroleum Activity*

Petroleum-industry activities that can produce unintentional dissolution cavities include the drilling of exploration, production, or disposal boreholes into, or

through, subsurface salt units (Johnson, 1998, in press). Unintentional dissolution of the salt can create a cavity that is as large and shallow as those created in solution-mining activities. And if the cavity becomes too large for the roof to be self-supporting, successive roof failures may cause the collapse to migrate upward and perhaps reach the land surface (Fig. 8). Most collapses related to petroleum activity involve boreholes drilled long ago, before development of proper engineering safeguards pertaining to drilling-mud design, casing placement, and salt-tolerant cements.

Three well-documented subsidence/collapse features resulting from petroleum activities are the Wink Sinks (Texas), Panning Sink (Kansas), and the Gorham oil field (Kansas).

Several large sinkholes and subsidence features have formed since 1980 in the giant Hendrick oil field near the town of Wink, in Winkler County, West Texas (Fig. 11) (Baumgardner and others, 1982; Johnson, 1987, 1998; Collins, 2000; Johnson and others, 2003). Wink Sink no. 1 formed in 1980 (Fig. 8); it reached a maximum diameter of 110 m, a depth of 34 m, and an estimated volume of 159,000 $m^3$ (Baumgardner and others, 1982). One abandoned well that produced oil from 1928 to 1951 was incorporated within the sink itself. This suspect well, the No. 10-A Hendrick, was drilled through 260 m of salt in the Permian Salado Formation, with the top of the salt ~400 m deep. Johnson (1987, 1998) described the various drilling and well-completion activities that probably led to eventual collapse around the suspect well (Fig. 12): (1) fresh ground water unintentionally reached the salt and created a large dissolution cavity around the well; (2) collapse of the non-salt roof into the cavity; and (3) by successive roof failures, the cavity migrated upward until it finally reached the land surface to create Wink Sink no. 1.

A second sink, Wink Sink no. 2, developed 1.6 km south of Wink Sink no. 1 in May 2002 (Fig. 11). It formed around, and thus incorporated, a water-supply well drilled through the Salado salts and into the underlying Capitan Reef aquifer. By March 2003, Wink Sink no. 2 was ~238 m long, 186 m wide, and had an estimated volume of 1.33 million $m^3$ (Johnson and others, 2003). Also near Wink, broad subsidence features and earth fissures were first noticed at the land surface ~300–900 m from Wink Sink no. 2 in 1999 (Fig. 11) (Collins, 2000; Johnson and others, 2003). The land surface had sagged as much as 7 and 8.5 m between 1970 and 1999 in two separate areas that contained several producing or abandoned oil wells and a water-supply well, all of which had been drilled to depths below the Salado salts. The outlines of areas A and B (Fig. 11) are approximate and indicate the probable maximum extent of subsidence and earth fissures. It appears that the sinkholes and subsidence features near Wink resulted from collapse or settling into underground dissolution cavities developed in salt

Figure 10. Aerial view of Cargill Sink, formed by collapse of a solution mine in salt near Hutchinson, Kansas (photo courtesy of Deming Studio). Sudden collapse left the railroad tracks suspended 6 m in the air, with the sink reaching a diameter of ~90 m.

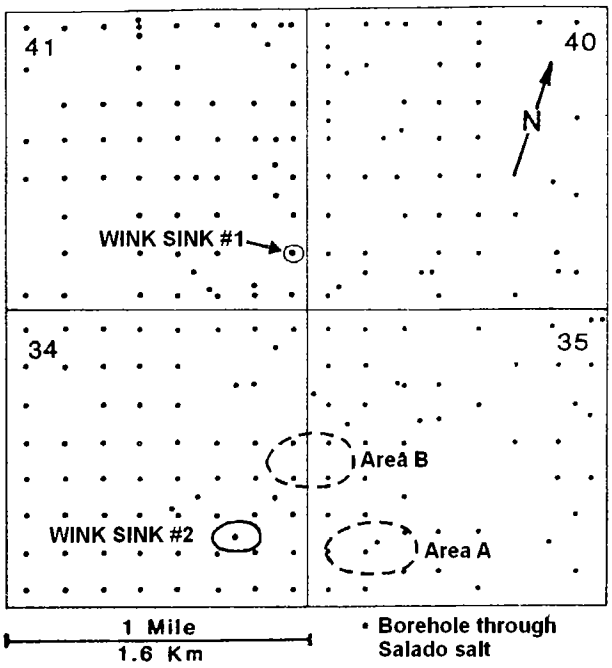


Figure 11. Location of Wink Sinks nos. 1 and 2, and approximate outlines of two broad subsidence features (areas *A* and *B*), just northeast of the town of Wink, in Winkler County, Texas; modified from Johnson (1987) and Johnson and others (2003). Map area is in Block B-5, Public School Land Survey.

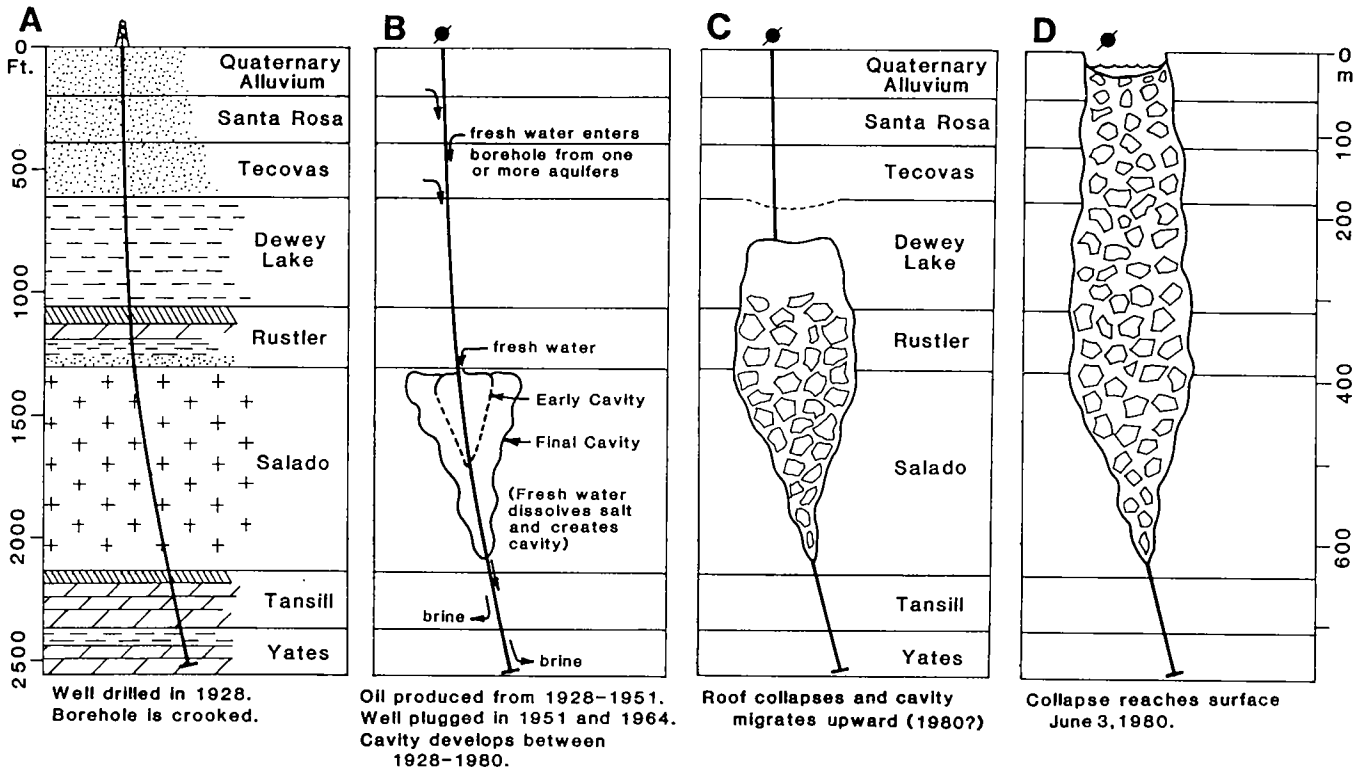


Figure 12. Cross section through the No. 10-A Hendrick well, showing possible relationship of well to salt dissolution and development of Wink Sink no. 1. From Johnson (1987) and Johnson and others (2003).

beds of the Salado Formation, and that cavity development apparently resulted from, or was accelerated by, local oil-field activity (Johnson and others, 2003).

Panning Sink was formed in 1959 by subsidence and collapse around a salt-water-disposal (SWD) well on the Panning lease in Barton County, Kansas (Fig. 13) (Walters, 1978; Johnson, 1998, in press). The sinkhole reached a diameter of 90 m and was at least 18 m deep. The suspect well, drilled originally as a producing oil well in 1938, penetrated 91 m of Permian Hutchinson salt at a depth of 298 m. Freshwater drilling fluids dissolved the salt in the borehole to an excessive diameter (1.4 m), and this washed-out zone was not cemented behind the 15.2-cm-diameter casing. Conversion of the borehole to a SWD well from 1946 to 1958 caused a large quantity of unsaturated oil-field brines (about 28,000 ppm NaCl) to be pumped into the well and inadvertently encounter, and further dissolve, the salt. A large cavern was formed, and with successive roof falls the water-filled void migrated upward to cause surface subsidence, tilting of an oil-field derrick, and eventual collapse.

Gorham oil field, in Russell County, Kansas, is the site of slow subsidence of a major highway (Interstate 70) above salt-dissolution zones in the Permian Hutchinson salt (Walters, 1991; Croxton, 2003). A series of oil wells, drilled on 4-hectare spacing in 1936–37, penetrated 75 m of salt at a depth of 390 m. The wells are now plugged and abandoned, but some of them contain corroded casing that was left in the boreholes above, within, and below the salt unit. As a result, unsaturated water probably has flowed down some of the boreholes and dissolved large volumes of the salt. Subsidence of the I-70 pavement has occurred at rates of <0.3 m/year, but cumulative subsidence through 1987 in two "sinks" is ~4 m, and in a third "sink" is ~0.3 m; this has required rebuilding parts of I-70 in 1971 and again in 1986 (Walters, 1991; Croxton, 2003).

### *Problems Related to Dry Salt Mines*

Sinkholes may form at the surface above underground mines of all kinds as a result of the collapse of overburden into subsurface voids, especially where the mines are shallow and overburden is poorly supported because of large roof spans. Dry (room-and-pillar) salt mines create special problems in this regard, when abundant ground water enters the mined-out voids; the salt can be dissolved quite rapidly. With introduction of large volumes of water, mined-out rooms can fill with salt-dissolving water, and the facility then behaves like a solution mine in salt. Uncontrolled dissolution can enlarge the rooms, remove salt pillars that support the roof, dissolve salt that remains in the roof, induce collapse of the overburden, and thus create small to large sinkholes.

Two dry salt mines that have been invaded by water and have developed overlying sinkholes are Jefferson Island mine (Louisiana) and Retsof mine (New York). Both mines are flooded and are now

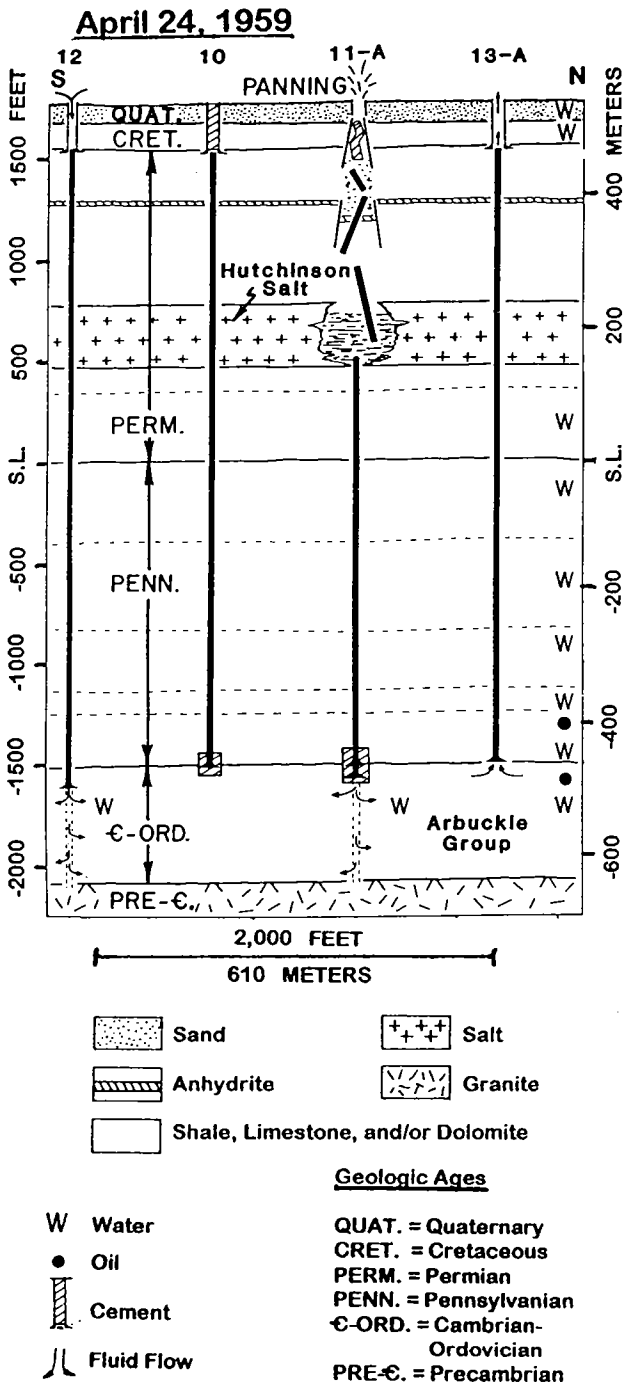


Figure 13. North–south cross section through the No. 11-A Panning salt-water-disposal well, showing the result of unplanned dissolution of the Hutchinson salt and development of the Panning Sink in Kansas (modified from Walters, 1978).

closed. The following discussion is modified and updated from earlier reports by Martinez and others (1998) and Johnson (in press).

Jefferson Island salt dome, just west of New Iberia, Louisiana, was the site of a catastrophic sink that developed in 1980 (Autin, 1982; Martinez, 1991). This huge sinkhole formed when an oil rig drilled into a chamber of the Jefferson Island salt mine, some 400 m below shallow Lake Peigneur. Lake water began leaking through the borehole into the underground room-and-pillar mine. The flow of water became a torrent, and soon the entire lake was drained; more water was then drawn through a canal that connected the lake to the Gulf of Mexico. The $5 million drilling rig vanished into the giant sink, along with barges, a tugboat, and 4 hectares of land. Although more than 50 workers were in the mine and on the lake at the time of the accident, there was no loss of life—a miracle, owing to well-planned evacuation and escape procedures established for just such an emergency.

The Retsof salt mine, located in western New York near the town of Cuylerville, just west of Geneseo, had a roof failure in March 1994, and this led to a large inflow of ground water from overlying strata (Nieto and Young, 1998; Gowan and Trader, 2000, 2003; Yager and others, 2001). The Retsof mine opened in 1885 and was the world's largest salt mine, underlying some 26 km$^2$. It was an underground room-and-pillar mine developed in Upper Silurian Salina Group salts. Collapse occurred where the mine was ~340 m below the land surface, and rooms in the salt mine were ~3.5 m high. Mine-roof collapse opened hydraulic pathways through newly created fractures in overlying rocks; ground water could now percolate down through, and partly dissolve, a series of salt layers above the mine and eventually enter the salt mine itself.

About 4 weeks after the initial collapse, dissolution of salt pillars in the Retsof mine (and parts of overlying salt beds), along with downward slump or piping of thick, near-surface unconsolidated sediments, caused subsidence of the land above the mine, resulting in three large sinkholes—the largest, some 200 m across and ~20 m deep. Flooding of the mine, at a flow rate that eventually exceeded 60,000 L/min, could not be controlled by in-mine grouting (the normal practice), and the entire mine was flooded. Adverse impacts in the area include disruption of land, damage to houses (some as far as 1.5 km from the sinkholes), loss of a major highway and bridge, loss of water wells, prohibition of public access to the collapse area, and economic disruption to the community.

## SUMMARY AND CONCLUSIONS

This report provides a brief overview of the processes and distribution of evaporite karst in the United States. Caves, sinkholes, disappearing streams, and other features typical of karst terranes are present in evaporite deposits throughout the nation. Evaporites are present in 32 of the 48 contiguous states, and karst is known at least locally in almost all of these areas. Evaporite karst is, in most respects, identical to karst in carbonate rocks, except that the process is much more rapid. It is much more widespread than is commonly believed.

Gypsum karst is most conspicuous in outcrops of gypsum, but also it is likely to be found in many areas

where the gypsum is as much as 30 m below the land surface. The most pronounced areas of gypsum karst are in the Permian Basin of the southwestern United States, although other important areas include the Michigan, Forest City, and Illinois Basins, and parts of Texas, South Dakota, Wyoming, and other western States.

Salt karst is almost entirely a subsurface feature, owing to the extremely high solubility of salt and the virtual lack of salt outcrops in the United States. Salt karst is most conspicuous and widespread in the Permian Basin region; several major salt units have been extensively dissolved here to produce collapse features and sediment-filled subsidence troughs. Other areas of significant salt karst are the Holbrook, Paradox, Michigan, and Gulf Coast Basins, and west-central Colorado.

Human-induced karst results chiefly from mining of, or drilling into, subsurface evaporite deposits. The most conspicuous problems have developed in salt deposits as a result of solution mining, petroleum activity, or dry mining of salt. Deep-seated dissolution cavities can result in land subsidence or catastrophic collapse, with surface sinks commonly being 90–270 m wide and tens of meters deep.

## REFERENCES CITED


Anderson, R. Y., 1982, Deformation–dissolution potential of bedded salt, waste isolation pilot plant site, Delaware Basin, New Mexico, *in* Lutze, W. (ed.), Scientific basis for waste management: Elsevier, Amsterdam, p. 449–458.

Anderson, R. Y.; Dean, W. E., Jr.; Kirkland, D. W.; and Snider, H. I., 1972, Permian Castile varved evaporite sequence, West Texas and New Mexico: Geological Society of America Bulletin, v. 83, p. 59–87.

Anderson, R. Y.; Kietzke, K. K.; and Rhodes, D. J., 1978, Development of dissolution breccias, northern Delaware Basin, New Mexico and Texas, *in* Austin, G. S. (compiler), Geology and mineral deposits of Ochoan rocks in Delaware Basin and adjacent areas: New Mexico Bureau of Mines and Mineral Resources Circular 159, p. 47–52.

Autin, W. J., 1982, Engineering geology of the Jefferson Island event, November 20, 1980: Louisiana Geological Survey Guidebook Series 1, 30 p.

Bachman, G. O., 1976, Cenozoic deposits of southeastern New Mexico and an outline of the history of evaporite dissolution: U.S. Geological Survey Journal of Research, v. 4, no. 2, p. 135–149.

_____1984, Regional geology of Ochoan evaporites, northern part of the Delaware Basin: New Mexico Bureau of Mines and Mineral Resources Circular 184, 22 p.

Bahr, C. W., 1962, The Holbrook anticline, Navajo County, Arizona, *in* Guidebook of the Mogollon Rim region, east-central Arizona: New Mexico Geological Society, 13th Field Conference, p. 118–122.

Baker, R. C., 1977, Hydrogeology of karst features in evaporite deposits of the Upper Permian in Texas, *in* Dilamarter, R. R.; and Csallany, S. C. (eds.), Hydrologic problems in karst regions: Western Kentucky University, Bowling Green, p. 333–339.

Baumgardner, R. W., Jr.; Hoadley, A. D.; and Goldstein, A. G., 1982, Formation of the Wink Sink, a salt dissolution and collapse feature, Winkler County, Texas: University of Texas at Austin, Bureau of Economic Geology, Report of Investigations 114, 38 p.

Belski, D. S. (ed.), 1992, GYPKAP report, no. 2, 1988–1991: National Speleological Society, Southwest Region, 56 p.

Black, T. J., 1983, Tectonics, structure, and karst in northern Lower Michigan: Michigan Basin Geological Society 1983 Field Conference, 139 p.

_____1984, Tectonics and geology in karst development of northern Lower Michigan, *in* Beck, B. F. (ed.), Sinkholes: their geology, engineering and environmental impact; proceedings of the first multidisciplinary conference on sinkholes: Balkema, Rotterdam, p. 87–91.

_____1997, Evaporite karst of the northern Lower Peninsula of Michigan: Carbonates and Evaporites, v. 12, no. 1, p. 81–92.

_____2003, Evaporite karst in Michigan, *in* Johnson, K. S.; and Neal, J. T. (eds.), Evaporite karst and engineering/environmental problems in the United States: Oklahoma Geological Survey Circular 109 [this volume], p. 315–320.

Blount, C. W.; and Dickson, F. W., 1973, Gypsum–anhydrite equilibria in systems $CaSO_4$–$H_2O$ and $CaCO_3$–NaCl–$H_2O$: American Mineralogist, v. 58, p. 323–331.

Bozeman, John, 2003, Exploration of western Oklahoma gypsum caves, *in* Johnson, K. S.; and Neal, J. T. (eds.), Evaporite karst and engineering/environmental problems in the United States: Oklahoma Geological Survey Circular 109 [this volume], p. 57–64.

Bozeman, J.; and Bozeman, S., 2002, Speleology of gypsum caves in Oklahoma: Carbonates and Evaporites, v. 17, no. 2, p. 107–113.

Bozeman, S. (ed.), 1987, The D. C. Jester Cave system: Central Oklahoma Grotto, Oklahoma Underground, v. 14, 56 p.

Catanach, R. B.; James, R. L.; O'Neill, A. L.; and Von Thun, J. L., 1989, Investigation of the cause of Quail Creek Dike failure; report of independent review team, March 7, 1989 (unpublished document).

Christenson, Scott; Hayes, Curtis; Hancock, Earl; and McLean, John, 2003, Correlating the location of a cave passage in gypsum karst to a highway right-of-way using a cave radio, *in* Johnson, K. S.; and Neal, J. T. (eds.), Evaporite karst and engineering/environmental problems in the United States: Oklahoma Geological Survey Circular 109 [this volume], p. 65–70.

Coates, G. K.; Lee, C. A.; McClain, W. C.; and Senseny, P. E., 1985, Closure and collapse of man-made cavities in salt, *in* Schreiber, B. C.; and Harner, H. L. (eds.), Sixth international symposium on salt: The Salt Institute, Alexandria, Virginia, v. 2, p. 139–157.

Cody, R. D.; Anderson, R. R.; and McKay, R. M., 1996, Geology of the Fort Dodge Formation (Upper Jurassic), Webster County, Iowa: Iowa Geological Survey Bureau Guidebook Series 19, 74 p.

Collins, E. W., 2000, Reconnaissance investigation of active subsidence and recent formation of earth fissures near the 1980 Wink Sink in the Hendrick oil field, Winkler County, Texas [abstract]: Geological Society of America Abstracts with Programs, v. 32, no. 3, p. 6.

Cooper, A. H., 1995, Subsidence hazards due to the dissolution of Permian gypsum in England: investigation and remediation, *in* Beck, B. F. (ed.), Karst geohazards; proceedings of 5th multidisciplinary conference on sinkholes: Balkema, Rotterdam, p. 23–29.

Croxton, N. M., 2003, Subsidence on Interstate 70 in Russell County, Kansas, related to salt dissolution—a history, *in* Johnson, K. S.; and Neal, J. T. (eds.), Evaporite karst and engineering/environmental problems in the United States: Oklahoma Geological Survey Circular 109 [this volume], p. 149–155.

Davis, A. D.; and Rahn, P. H., 1997, Karstic gypsum prob-

lems at wastewater stabilization sites in the Black Hills of South Dakota: Carbonates and Evaporites, v. 12, no. 1, p. 73–80.

Davis, A. D.; Beaver, F. W.; and Stetler, L. D., 2003, Engineering problems of gypsum karst along the Interstate 90 development corridor in the Black Hills of South Dakota, *in* Johnson, K. S.; and Neal, J. T. (eds.), Evaporite karst and engineering/environmental problems in the United States: Oklahoma Geological Survey Circular 109 [this volume], p. 255–261.

Dean, W. E.; and Johnson, K. S. (eds.), 1989, Anhydrite deposits of the United States and characteristics of anhydrite important for storage of radioactive wastes: U.S. Geological Survey Bulletin 1794, 132 p.

Doelling, H. H., 1988, Geology of Salt Valley anticline and Arches National Park, Grand County, Utah: Utah Geological and Mineral Survey Bulletin 122, 58 p.

Dunrud, C. R.; and Nevins, B. B., 1981, Solution mining and subsidence in evaporite rocks in the United States: U.S. Geological Survey Miscellaneous Investigation Series Map I-1298, 2 sheets.

Eck, W.; and Redfield, R. C., 1965, Engineering geology problems at Sanford Dam, Borger, Texas: Engineering Geology, v. 2, no. 1, p. 15–25.

Ege, J. R., 1984, Mechanisms of surface subsidence resulting from solution extraction of salt, *in* Holzer, T. L. (ed.), Man-induced land subsidence: Geological Society of America, Reviews in Engineering Geology, v. 6, p. 203–221.

_____1985, Maps showing distribution, thickness, and depth to salt deposits of the United States: U.S. Geological Survey Open-File Report 85-28, 11 p., 4 pls.

Elowski, R. C.; and Ostrander, A. C., 1977, Gypsum karst and related features in the Michigan Basin, *in* Official 1977 guidebook, Alpena, Michigan: National Speleological Society, p. 31–41.

Epstein, J. B., 2003, Gypsum karst in the Black Hills, South Dakota–Wyoming: geomorphic development, hazards, and hydrology, *in* Johnson, K. S.; and Neal, J. T. (eds.), Evaporite karst and engineering/environmental problems in the United States: Oklahoma Geological Survey Circular 109 [this volume], p. 241–254.

Fay, R. O., 1973, The Elk City blowout—a chronology and analysis: Oklahoma Geology Notes, v. 30, p. 135–151.

Fischer, W. A.; and Hackman, R. J., 1964, Geologic map of the Torrance Station 4 NE quadrangle, Lincoln County, New Mexico: U.S. Geological Survey Miscellaneous Geologic Investigations Map 1-400, 4 p.

Forbes, J.; and Nance, R., 1997, Stratigraphy, sedimentology, and structural geology of gypsum caves in southeast New Mexico: Carbonates and Evaporites, v. 12, no. 1, p. 64–72.

French, R. R.; and Rooney, L. F., 1969, Gypsum resources of Indiana: Indiana Geological Survey Bulletin 42-A, 34 p.

Friedman, G. M., 1997, Solution-collapse breccias and paleokarst resulting from dissolution of evaporite rocks, especially sulfates: Carbonates and Evaporites, v. 12, no. 1, p. 53–63.

Frumkin, A.; and Raz, E., 2001, Sinkholes initiated by salt dissolution, Dead Sea Basin, Israel: Carbonates and Evaporites, v. 16, no. 2, p. 117–130.

George, A. I., 1977, Evaluation of sulfate water quality in north-central Kentucky karst, *in* Dilamarter, R. R.; and Csallany, S. C. (eds.), Hydrologic problems in karst regions: Western Kentucky University, Bowling Green, p. 340–356.

Getchell, F. J., 1995, Subsidence and related features in the Tully Valley, central New York, *in* Beck, B. F. (ed.), Karst geohazards: proceedings of the 5th multidisci-plinary conference on sinkholes: Balkema, Rotterdam, p. 31–42.

Gowan, S. W.; and Trader, S. M., 2000, Mine failure associated with a pressurized brine horizon: Retsof salt mine, western New York: Environmental and Engineering Geoscience, v. 6, no. 1, p. 57–70.

_____2003, Mechanism of sinkhole formation in glacial sediments above the Retsof Salt Mine, western New York, *in* Johnson, K. S.; and Neal, J. T. (eds.), Evaporite karst and engineering/environmental problems in the United States: Oklahoma Geological Survey Circular 109 [this volume], p. 321–336.

Gustavson, T. C.; and Finley, R. J., 1985, Late Cenozoic geomorphic evolution of the Texas Panhandle and northeastern New Mexico—case studies of structural controls on regional drainage development: University of Texas at Austin, Bureau of Economic Geology, Report of Investigations 148, 42 p.

Gustavson, T. C.; Finley, R. J.; and McGillis, K. A., 1980, Regional dissolution of Permian salt in the Anadarko, Dalhart, and Palo Duro Basins of the Texas Panhandle: University of Texas at Austin, Bureau of Economic Geology, Report of Investigations 106, 40 p.

Gustavson, T. C.; Simpkins, W. W.; Alhades, A.; and Hoadley, A., 1982, Evaporite dissolution and development of karst features on the Rolling Plains of the Texas Panhandle: Earth Surface Processes and Landforms, v. 7, p. 545–563.

Gutiérrez, F.; Ortí, F.; Gutiérrez, M.; Pérez-González, A.; Benito, G.; Gracia, F. J.; and Durán, J. J., 2002, Paleosubsidence and active subsidence due to evaporite dissolution in Spain: Carbonates and Evaporites, v. 17, no. 2, p. 121–133.

Halbouty, M. T., 1967, Salt domes, Gulf region, United States and Mexico: Gulf Publishing Co., Houston, 425 p.

Hardie, L. A., 1967, The gypsum–anhydrite equilibrium at one atmosphere pressure: American Mineralogist, v. 52, p. 171–200.

Hill, C. A., 1996, Geology of the Delaware Basin, Guadalupe, Apache, and Glass Mountains, New Mexico and West Texas: Permian Basin Section–SEPM Publication 96-39, 480 p.

_____2003, Intrastratal karst at the Waste Isolation Pilot Plant site, southeastern New Mexico, *in* Johnson, K. S.; and Neal, J. T. (eds.), Evaporite karst and engineering/environmental problems in the United States: Oklahoma Geological Survey Circular 109 [this volume], p. 197–209.

Hite, R. J.; and Lohman, S. W., 1973, Geologic appraisal of Paradox Basin salt deposits for waste emplacement: U.S. Geological Survey Open-File Report 4339-6, 75 p.

Hovorka, S. D., 1983, Petrographic criteria for recognizing post-Permian dissolution of evaporites, Donley County, Texas: University of Texas at Austin, Bureau of Economic Geology, Geological Circular 83-4, p. 66–74.

Irwin, J. H.; and Morton, R. B., 1969, Hydrogeologic information on the Glorieta Sandstone and the Ogallala Formation in the Oklahoma Panhandle and adjoining areas as related to underground waste disposal: U.S. Geological Survey Circular 630, 26 p.

Jarvis, Todd, 2003, The money pit: karst failure of Anchor Dam, Wyoming, *in* Johnson, K. S.; and Neal, J. T. (eds.), Evaporite karst and engineering/environmental problems in the United States: Oklahoma Geological Survey Circular 109 [this volume], p. 271–278.

Jarvis, Todd; and Huntoon, Peter, 2003, A stinking lake and perpetual potholes: living with gypsite karst in Laramie, Wyoming, *in* Johnson, K. S.; and Neal, J. T. (eds.), Evaporite karst and engineering/environmental problems in the United States: Oklahoma Geological Survey Circular 109 [this volume], p. 263–269.

Johnson, K. S., 1981, Dissolution of salt on the east flank of the Permian Basin in the southwestern USA: Journal of Hydrology, v. 54, p. 75–93.

_____1986, Hydrogeology and recharge of a gypsum–dolomite karst aquifer in southwestern Oklahoma, USA, *in* Gunay, G.; and Johnson, I. V. (eds.), Karst water resources; proceedings of the international symposium on karst water resources, Ankara, Turkey, July 7–19, 1985: International Association of Hydrological Sciences Publication 161, p. 343–357.

_____1987, Development of the Wink sink in West Texas due to salt dissolution and collapse, *in* Beck, B. F.; and Wilson, W. L. (eds.), Karst hydrogeology; proceedings of 2nd multidisciplinary conference on sinkholes: Balkema, Rotterdam, p. 127–136. (Also published in 1989, Environmental Geology and Water Science, v. 14, p. 81–92.)

_____1989, Salt dissolution, interstratal karst, and ground subsidence in the northern part of the Texas Panhandle, *in* Beck, B. F. (ed.), Proceedings of the 3rd multidisciplinary conference on sinkholes: Balkema, Rotterdam, p. 115–121.

_____1990, Hydrogeology of the Blaine gypsum–dolomite karst aquifer, southwestern Oklahoma: Oklahoma Geological Survey Special Publication 90-5, 31 p.

_____1993, Dissolution of Permian Salado salt during Salado time in the Wink area, Winkler County, Texas, *in* Love, D. W. (ed.), Carlsbad region, New Mexico and West Texas: New Mexico Geological Society 44th Field Conference, p. 211–218.

_____1996, Gypsum karst in the United States, *in* Klimchouk, A., and others (eds.), Gypsum karst of the World: International Journal of Speleology, v. 25, nos. 3–4, p. 183–193.

_____1997, Evaporite karst in the United States: Carbonates and Evaporites, v. 12, no. 1, p. 2-14.

_____1998, Land subsidence above man-made salt-dissolution cavities, *in* Borchers, J. W. (ed.), Land subsidence; case studies and current research; proceedings of the Dr. Joseph F. Poland symposium on land subsidence: Association of Engineering Geologists Special Publication 8, p. 385–392.

_____2001, Karst in evaporite rocks of the United States, *in* Gunay, G.; Johnson, K. S.; Ford, D.; and Johnson, A. I. (eds.), Present state and future trends of karst studies; proceedings of the 6th international symposium and field seminar, Marmaris, Turkey, September 17–26, 2000: Published by UNESCO, IHP-V, Technical Documents in Hydrology, no. 49, v. 1, p. 3–12. (Also published in 2002, Carbonates and Evaporites, v. 17, no. 2, p. 90–97.)

_____2003a, Evaporite karst in the Permian Blaine Formation and associated strata of western Oklahoma, *in* Johnson, K. S.; and Neal, J. T. (eds.), Evaporite karst and engineering/environmental problems in the United States: Oklahoma Geological Survey Circular 109 [this volume], p. 41–55.

_____2003b, Gypsum karst and abandonment of the Upper Mangum Damsite in southwestern Oklahoma, *in* Johnson, K. S.; and Neal, J. T. (eds.), Evaporite karst and engineering/environmental problems in the United States: Oklahoma Geological Survey Circular 109 [this volume], p. 85–94.

_____2003c, Gypsum karst as a major factor in the design of the proposed Lower Mangum Dam in southwestern Oklahoma, *in* Johnson, K. S.; and Neal, J. T. (eds.), Evaporite karst and engineering/environmental problems in the United States: Oklahoma Geological Survey Circular 109 [this volume], p. 95–111.

_____[in press], Salt dissolution and subsidence or collapse due to human activities, *in* Ehlen, J.; Haneberg, W. C.; and Larson, R. A. (eds.), Humans as geologic agents: Geological Society of America, Reviews in Engineering Geology.

Johnson, K. S.; and Gonzales, S., 1978, Salt deposits in the United States and regional geologic characteristics important for storage of radioactive waste: Prepared for Union Carbide Corporation, Nuclear Division, Office of Waste Isolation, Y/OWI/SUB–7414/1, 188 p.

Johnson, K. S.; Collins, E. W.; and Seni, S. J., 2003, Sinkholes and land subsidence owing to salt dissolution near Wink, West Texas, and other sites in western Texas and New Mexico, *in* Johnson, K. S.; and Neal, J. T. (eds.), Evaporite karst and engineering/environmental problems in the United States: Oklahoma Geological Survey Circular 109 [this volume], p. 183–195.

Jorgensen, D. B.; and Carr, D. D., 1973, Influence of cyclic deposition, structural features, and hydrologic controls on evaporite deposits in the St. Louis Limestone in southwestern Indiana, *in* Proceedings of 8th forum on geology of industrial minerals: Iowa Geological Survey Public Information Circular 5, p. 43–65.

Kelley, V. C., 1971, Geology of the Pecos country, southeastern New Mexico: New Mexico Bureau of Mines and Mineral Resources Memoir 24, 69 p.

Kirkham, R. M.; Scott, R. B.; and Judkins, T. W. (eds.), 2002, Late Cenozoic evaporite tectonism and volcanism in west-central Colorado: Geological Society of America Special Paper 366, 234 p.

Kirkham, R. M.; White, J. L.; Sares, M. A.; Mock, R. G.; and Lidke, D. J., 2003, Engineering and environmental aspects of evaporite karst in west-central Colorado, *in* Johnson, K. S.; and Neal, J. T. (eds.), Evaporite karst and engineering/environmental problems in the United States: Oklahoma Geological Survey Circular 109 [this volume], p. 279–292.

Kirkland, D. W.; and Evans, R., 1980, Origin of castiles on Gypsum Plain of Texas and New Mexico, *in* Dickerson, P. W.; and Hoffer, J. M. (eds.), Trans-Pecos region, southeastern New Mexico and West Texas: New Mexico Geological Society 31st Field Conference, p. 173–178.

Kreitler, C. W.; and Dutton, S. P., 1983, Origin and diagenesis of cap rock, Gyp Hill and Oakwood salt domes, Texas: University of Texas at Austin, Bureau of Economic Geology, Report of Investigations 131, 58 p.

Lambert, S. J., 1983, Dissolution and evaporites in and around the Delaware Basin, southeastern New Mexico and West Texas: Sandia National Laboratories, Albuquerque, New Mexico, SAND82–0461.

Land, L. A., 2003, Evaporite karst and regional groundwater circulation in the lower Pecos Valley of southeastern New Mexico, *in* Johnson, K. S.; and Neal, J. T. (eds.), Evaporite karst and engineering/environmental problems in the United States: Oklahoma Geological Survey Circular 109 [this volume], p. 227–232.

Landes, K. K., 1959, The Mackinac breccia, *in* Geology of Mackinac Island and Lower and Middle Devonian south of the Straits of Mackinac: Michigan Basin Geological Society, Annual Geological Excursion Guidebook, p. 19–24.

Lefond, S. J., 1969, Handbook of world salt resources: Plenum Press, New York, 384 p.

Maley, V. L.; and Huffington, R. M., 1953, Cenozoic fill and evaporite solution in the Delaware Basin, Texas and New Mexico: Geological Society of America Bulletin, v. 64, p. 539–546.

Martinez, J. D., 1991, Salt domes: American Scientist, v. 79, p. 420–431.

Martinez, J. D.; Johnson, K. S.; and Neal, J. T., 1998, Sink-

holes in evaporite rocks: American Scientist, v. 86, no. 1, p. 38–51.
McGrain, Preston; and Helton, W. L., 1964, Gypsum and anhydrite in the St. Louis Limestone in northwestern Kentucky: Kentucky Geological Survey, Series X, Information Circular 13, 26 p.
McGregor, D. J., 1954, Gypsum and anhydrite deposits in southwestern Indiana: Indiana Geological Survey Report of Progress 8, 24 p.
McGregor, D. R.; Pendry, E. C.; and McGregor, D. L., 1963, Solution caves in gypsum, north-central Texas: Journal of Geology, v. 71, p. 108–115.
Miller, Galen; Dewers, Thomas; and Tarhule, Aondover, 2003, Laser positioning and three-dimensional digital mapping of gypsum karst, western Oklahoma, *in* Johnson, K. S.; and Neal, J. T. (eds.), Evaporite karst and engineering/environmental problems in the United States: Oklahoma Geological Survey Circular 109 [this volume], p. 71–75.
Miller, R. D., 2003, High-resolution seismic-reflection investigation of a subsidence feature on U.S. Highway 50 near Hutchinson, Kansas, *in* Johnson, K. S.; and Neal, J. T. (eds.), Evaporite karst and engineering/environmental problems in the United States: Oklahoma Geological Survey Circular 109 [this volume], p. 157–167.
Myers, A. J.; Gibson, A. M.; Glass, B. P.; and Patrick, C. R., 1969, Guide to Alabaster Cavern and Woodward County, Oklahoma: Oklahoma Geological Survey Guidebook 15, 38 p.
Neal, J. T., 1995, Supai salt karst features: Holbrook Basin, Arizona, *in* Beck, B. F. (ed.), Karst geohazards; proceedings of 5th multidisciplinary conference on sinkholes: Balkema, Rotterdam, p. 53–59.
Neal, J. T.; and Colpitts, R. M., 1997, Richard Lake, an evaporite-karst depression in the Holbrook Basin, Arizona: Carbonates and Evaporites, v. 12, no. 1, p. 91–98.
Neal, J. T.; and Johnson, K. S., 2003, A compound breccia pipe in evaporite karst: McCauley Sinks, Arizona, *in* Johnson, K. S.; and Neal, J. T. (eds.), Evaporite karst and engineering/environmental problems in the United States: Oklahoma Geological Survey Circular 109 [this volume], p. 305–314.
Neal, J. T.; Colpitts, R. M.; and Johnson, K. S., 1998, Evaporite karst in the Holbrook Basin, Arizona, *in* Borchers, J. W. (ed.), Land subsidence; case studies and current research; proceedings of the Dr. Joseph F. Poland symposium on land subsidence: Association of Engineering Geologists Special Publication 8, p. 373–384.
Nieto, A. S.; and Young, R. A., 1998, Retsof salt mine collapse and aquifer dewatering, Genesee Valley, Livingston County, New York, *in* Borchers, J. W. (ed.), Land subsidence; case studies and current research; proceedings of the Dr. Joseph F. Poland symposium on land subsidence: Association of Engineering Geologists Special Publication 8, p. 309–325.
Nieto-Pescetto, A. S.; and Hendron, A. J., Jr., 1977, Study of sinkholes related to salt production in the area of Detroit, Michigan: Solution Mining Research Institute Open-File Report, Woodstock, Illinois, 49 p.
Olive, W. W., 1957, Solution-subsidence troughs, Castile Formation of Gypsum Plain, Texas and New Mexico: Geological Society of America Bulletin, v. 68, p. 351–358.
Orchard, D. M., 1987, Structural history of Poplar dome and the dissolution of Charles Formation salt, Roosevelt County, Montana, *in* Carlson, C. G.; and Christopher, J. E. (eds.), Fifth international Williston Basin symposium: Saskatchewan Geological Society Special Publication 9, p. 169–177.
Palmer, A. N.; and Palmer, M. V., 1995, The Kaskaskia paleokarst of the northern Rocky Mountains and Black Hills, northwestern U.S.A.: Carbonates and Evaporites, v. 10, no. 2, p. 148–160.
Parker, J. M., 1967, Salt solution and subsidence structures, Wyoming, North Dakota, and Montana: American Association of Petroleum Geologists Bulletin, v. 51, p. 1929–1947.
Payton, C. C.; and Hansen, M. N., 2003, Gypsum karst in southwestern Utah: failure and reconstruction of Quail Creek Dike, *in* Johnson, K. S.; and Neal, J. T. (eds.), Evaporite karst and engineering/environmental problems in the United States: Oklahoma Geological Survey Circular 109 [this volume], p. 293–303.
Pearson, R. M., 2002, Gypsum karst of the Lykins Formation and effects for Colorado Front Range water projects; Horsetooth and Carter Lake Reservoirs [abstract]: Geological Society of America Abstracts with Programs, v. 34, no. 6, p. 216.
Pierce, W. G.; and Rich, E. I., 1962, Summary of rock salt deposits in the United States as possible storage sites for radioactive waste materials: U.S. Geological Survey Bulletin 1148, 91 p.
Powers, D. W.; and Hassinger, B. W., 1985, Synsedimentary dissolution pits in halite of the Permian Salado Formation, southeastern New Mexico: Journal of Sedimentary Petrology, v. 55, p. 769–773.
Powers, D. W.; and Owsley, David, 2003, Field survey of evaporite karst along New Mexico Highway 128 realignment routes, *in* Johnson, K. S.; and Neal, J. T. (eds.), Evaporite karst and engineering/environmental problems in the United States: Oklahoma Geological Survey Circular 109 [this volume], p. 233–240.
Powers, D. W.; Holt, R. M.; Beauheim, R. L.; and McKenna, S. A., 2003, Geological factors related to the transmissivity of the Culebra Dolomite Member, Permian Rustler Formation, Delaware Basin, southeastern New Mexico, *in* Johnson, K. S.; and Neal, J. T. (eds.), Evaporite karst and engineering/environmental problems in the United States: Oklahoma Geological Survey Circular 109 [this volume], p. 211–218.
Quinlan, J. F., 1978, Types of karst, with emphasis on cover beds in their classification and development: University of Texas at Austin unpublished Ph.D. dissertation, 325 p. (Published in 1987 by Texas Memorial Museum.)
Quinlan, J. F.; Smith, R. A.; and Johnson, K. S., 1986, Gypsum karst and salt karst of the United States of America, *in* Atti symposio international sul carsismo nelle evaporiti (proceedings, international symposium on karst in evaporites, Palermo, Italy, October 27–30, 1985): Le Grotte d'Italia, Series 4, v. 13, p. 73–92.
Rahn, P. H.; and Davis, A. D., 1996, Gypsum foundation problems in the Black Hills area, South Dakota: Environmental and Engineering Geoscience, v. 2, p. 213–223.
Raines, M. A.; and Dewers, T. A., 1997, Dedolomitization as a driving mechanism for karst generation: Carbonates and Evaporites, v. 12, no. 1, p. 24–31.
Rasmussen, D. L.; and Bean, D. W., 1984, Dissolution of Permian salt and Mesozoic syndepositional trends, central Powder River Basin, Wyoming, *in* Goolsby, J.; and Morton, D. (eds.), The Permian and Pennsylvanian geology of Wyoming: Wyoming Geological Association 35th Annual Field Conference Guidebook, p. 281–294.
Rauzi, S. L., 2000, Permian salt in the Holbrook Basin, Arizona: Arizona Geological Survey Open-File Report 00-03, 20 p.
Runkle, D. L.; and Johnson, K. S., 1988, Hydrogeologic study of a gypsum–dolomite karst aquifer in southwestern

Oklahoma and adjacent parts of Texas, U.S.A., *in* Karst hydrogeology and karst environment protection: Geological Publishing House, Beijing, China, Proceedings of the IAH 21st Congress, held in Guilin, China, October 10–15, 1988, v. 21, pt. 1, p. 400–405.

Sando, W. J., 1988, Madison Limestone (Mississippian) paleokarst: a geologic synthesis, *in* James, N. P.; and Choquette, P. W. (eds.), Paleokarst: Springer-Verlag, New York, p. 256–277.

Sares, S. W.; and Wells, S. G., 1987, Geomorphic and hydrogeologic development of the Gypsum Plain karst, Delaware Basin, New Mexico, *in* Powers, D. W.; and James, W. C. (eds.), Geology of the western Delaware Basin, West Texas and southeastern New Mexico: El Paso Geological Society Guidebook 18, p. 98–117.

Saxby, D. B.; and Lamar, J. E., 1957, Gypsum and anhydrite in Illinois: Illinois State Geological Survey Circular 226, 26 p.

Sharpe, R. D., 2003, Effects of karst processes on gypsum mining, *in* Johnson, K. S.; and Neal, J. T. (eds.), Evaporite karst and engineering/environmental problems in the United States: Oklahoma Geological Survey Circular 109 [this volume], p. 31–40.

Simpkins, W. W.; Gustavson, T. C.; Alhades, A. B.; and Hoadley, A. D., 1981, Impact of evaporite dissolution and collapse on highways and other cultural features in the Texas Panhandle and eastern New Mexico: University of Texas at Austin, Bureau of Economic Geology, Circular 81-4, 23 p.

Smith, G. I.; Jones, C. L.; Culbertson, W. C.; Ericksen, G. E.; and Dyni, J. R., 1973, Evaporites and brines, *in* Brobst, D. A.; and Pratt, W. D. (eds.), United States mineral resources: U.S. Geological Survey Professional Paper 820, p. 197–216.

Tarhule, Aondover; Dewers, Thomas; Young, Roger; Witten, Alan; and Halihan, Todd, 2003, Integrated subsurface-imaging techniques for detecting cavities in the gypsum karst of Oklahoma, *in* Johnson, K. S.; and Neal, J. T. (eds.), Evaporite karst and engineering/environmental problems in the United States: Oklahoma Geological Survey Circular 109 [this volume], p. 77–84.

Walker, C. W., 1974, Nature and origin of cap rock overlying Gulf Coast salt domes, *in* Coogan, A. H. (ed.), Fourth symposium on salt: Northern Ohio Geological Society, Cleveland, v. 1, p. 169–195.

Walters, R. F., 1978, Land subsidence in central Kansas related to salt dissolution: Kansas Geological Survey Bulletin 214, 82 p.

_____1991, Gorham oil field, Russell County, Kansas: Kansas Geological Survey Bulletin 228, 111 p.

Warren, J. K.; Havholm, K. G.; Rosen, M. R.; and Parsley, M. J., 1990, Evolution of gypsum karst in the Kirschberg Evaporite Member near Fredericksburg, Texas: Journal of Sedimentary Petrology, v. 60, p. 721–734.

Watney, W. L.; Nissen, S. E.; Bhattacharya, Saibal; and Young, David, 2003, Evaluation of the role of evaporite karst in the Hutchinson, Kansas, gas explosions, January 17 and 18, 2001, *in* Johnson, K. S.; and Neal, J. T. (eds.), Evaporite karst and engineering/environmental problems in the United States: Oklahoma Geological Survey Circular 109 [this volume], p. 119–147.

White, W. B., 1988, Geomorphology and hydrology of karst terrains: Oxford University Press, New York, 464 p.

Willis, G. C., 1986, Geologic map of the Salina quadrangle, Sevier County, Utah: Utah Geological and Mineral Survey Map 83.

Withington, C. F., 1962, Gypsum and anhydrite in the United States, exclusive of Alaska and Hawaii: U.S. Geological Survey Mineral Investigations Resource Map MR-33.

Withington, C. F.; and Jaster, M. C., 1960, Selected annotated bibliography of gypsum and anhydrite in the United States and Puerto Rico: U.S. Geological Survey Bulletin 1105, 126 p.

Witkind, I. J., 1994, The role of salt in the structural development of central Utah: U.S. Geological Survey Professional Paper 1528, 145 p.

Witzke, B. J.; Bunker, B. J.; and Rogers, F. S., 1988, Eifelian through lower Frasnian stratigraphy and deposition in the Iowa area, central Midcontinent, U.S.A., *in* McMillan, N. J.; Embry, A. F.; and Glass, D. J. (eds.), Devonian of the world: Canadian Society of Petroleum Geologists, v. 1, p. 221–250.

Yager, R. M.; Miller, T. S.; and Kappel, W. M., 2001, Simulated effects of salt-mine collapse on ground-water flow and land subsidence in a glacial aquifer system, Livingston County, New York: U.S. Geological Survey Professional Paper, Report P-1611, 85 p.

# The Need for a National Evaporite-Karst Map

***Jack B. Epstein***
U.S. Geological Survey
Reston, Virginia

***Kenneth S. Johnson***
Oklahoma Geological Survey
Norman, Oklahoma

**ABSTRACT.**—The U.S. Geological Survey, in cooperation with state geological surveys, other federal agencies, and academia, is preparing a digitized map showing the distribution of karst in the conterminous United States. The present *Engineering Aspects of Karst* (Davies and others, 1984) will be revised to better display surficial-karst features. The digital map will be maintained by the National Cave and Karst Research Institute and will serve as a source for more detailed information at the state level. Evaporite rocks will be more adequately shown than on the original map. Among the many areas of evaporite karst not shown on the Davies and others map, the Holbrook Basin, Arizona, and the Black Hills, South Dakota, are herein used as examples of how data can be presented on the new map. The variety of karstic features that are produced by dissolution of the host evaporites, as well as by collapse in overlying strata, include intrastratal collapse breccia, breccia pipes, and sinkholes in overlying non-soluble rocks. The differences between karst in carbonate and evaporite rocks in the humid eastern United States, and those in the semiarid to arid western United States are delimited approximately by a zone of mean annual precipitation of 32 in.

## INTRODUCTION

During the energy crisis in the 1970s, the U.S. Geological Survey (USGS), in collaboration with other federal, state, and local agencies, universities, and the private sector, developed programs to enhance the understanding of earth systems and their mutual interactions that might affect exploitation of the nation's energy resources. One aspect of this endeavor was to educate the public on natural geologic hazards so that earth-science information could be intertwined with public policy. Maps showing the distribution of geologic hazards were an integral part of this effort.

In 1975, the Environmental Aspects of Energy Program was initiated in the USGS to study geologic influences on the development of coal and nuclear-energy resources, and the effects of energy development on the geologic environment. One aspect of that program was the development of a National Atlas (maps at a scale of 1:7,500,000) showing the distribution of geologic events and processes that affect or are affected by energy-resource extraction and utilization. The maps included such hazards as swelling soils, volcanic eruptions, earthquakes, and landslides.

Another map, *Engineering Aspects of Karst,* was published by Davies and others (1984) that depicted areas of karstic rocks (limestone, dolomite, and evaporites), and "pseudokarst" areas, classified as to their engineering and geologic characteristics (size and depth of voids, depth of overburden, rock/soil–interface conditions, and geologic structure). This generalized map has been the only synopsis of karstic conditions in the country (Fig. 1). However, federal, state, and local government agencies, the speleological community, and academia have

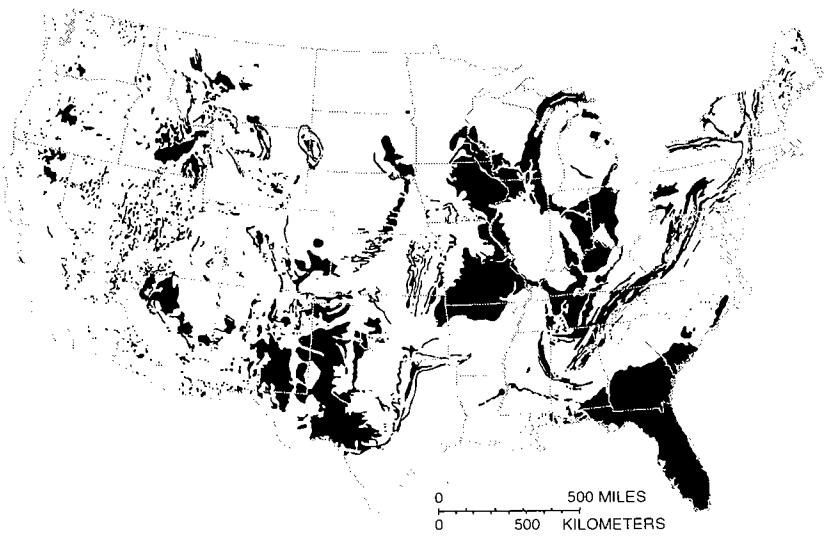


Figure 1. Map showing all types of karst, and features analogous to karst, in the United States (modified from Davies and others, 1984).

Epstein. J. B.; and Johnson, K. S., 2003, The need for a national evaporite-karst map, *in* Johnson, K. S.; and Neal, J. T. (eds.), Evaporite karst and engineering/environmental problems in the United States: Oklahoma Geological Survey Circular 109, p. 21–30.

repeatedly expressed the need for a more accurate and detailed national map to give a better understanding of the distribution of soluble rocks in the United States. Maps at a variety of scales are needed for the following: to educate the public and legislators about karst issues; to provide a basis for cave and karst research; and to aid federal, state, and local land-use managers in managing karst resources.

During the past 3 years, a diverse group of karst experts strategized a long-term plan for karst mapping on a national scale. The resultant goal is to produce a national karst map in digital form, derived primarily from maps prepared by the individual states, and to link that national map on a web-based network to state- and local-scale maps and related data. The newly formed National Cave and Karst Research Institute (NCKRI; http://www2.nature.nps.gov/nckri/index.htm) will establish a web-based network of karst information that will be used to build the national map. The digital map will reside on the NCKRI web site and be linked to individual states and speleological organizations showing individual state karst maps, detailed information about karst, annotated bibliographies, and outreach products.

The USGS will facilitate compilation of the national map by cooperating with state geological surveys to update or produce state karst maps and to establish standards and consistent digital products. Methods for presentation of data on karst maps vary considerably, and boundaries of karst areas between some adjacent states do not match. Some states have a digitized geologic map from which a karst map could be prepared. Outlines of known karst areas, caves and sinkholes, depth of burial of karstic rocks, and areas of "pseudokarst" of several types are among the types of data shown on some maps. The new national map will consider the distribution of carbonate and evaporite units, intrastratal karst, karst beneath surficial overburden, and the percentages of areas covered by karst.

## NATIONAL EVAPORITE-KARST MAP

The occurrence of karst in carbonate rocks (limestone and dolomite) in the United States is fairly well known, as shown by Davies and others' (1984) map. However, the widespread distribution of evaporite karst, including both gypsum (and/or anhydrite) karst and salt karst, in the United States is not as well appreciated. Evaporites underlie about one-third of the country but are not necessarily exposed at the surface. Karst features may be present in gypsum deposits in all parts of the United States, whether the gypsum crops out or is in the deep subsurface; the karst may result from climatic and hydrologic conditions of today, or it may be a relict from an earlier, wetter climate and/or a hydrogeologic regime of the Pleistocene or pre-Pleistocene epochs.

In the eastern United States, where average annual precipitation commonly is greater than 75 cm, gypsum deposits generally are eroded or dissolved to depths of at least several meters or tens of meters below the land surface. So, although gypsum in the East may locally be karstic, the lack of exposures makes it difficult to prove this without subsurface study of the gypsum and its dissolution features. In the semiarid western part of the United States, however, in areas where the average annual precipitation commonly is less than about 75 cm, gypsum tends to resist erosion and typically caps ridges, mesas, and buttes. In spite of its resistance to erosion in the West, gypsum commonly contains visible karst features, such as cavities, caves, and sinkholes, attesting the importance of ground-water movement, even in low-rainfall areas.

Salt karst is commonly more difficult to identify at the earth's surface than is gypsum karst. Salt is so soluble that it survives at the land surface only in arid areas. The two sites in the United States with salt recently at the surface are Sevier Valley, Utah (where salt has been quarried), and Virgin Valley, in Nevada and Arizona (where the salt outcrops are now inundated by Lake Mead). Elsewhere, salt has been dissolved to depths ranging from tens to hundreds of meters below the present land surface. In many places it is not easy (or possible) to distinguish between modern dissolution/karst and paleodissolution/paleokarst: some of the salt karst may be a remnant from an earlier hydrogeologic regime (perhaps as early as shortly after original deposition of the salt unit).

Whereas the distribution of carbonate karst on Davies and others' map is generally adequate, his map only depicts gypsum karst in a few areas (Fig. 2). In an extensive text on the back of the map, Davies men-

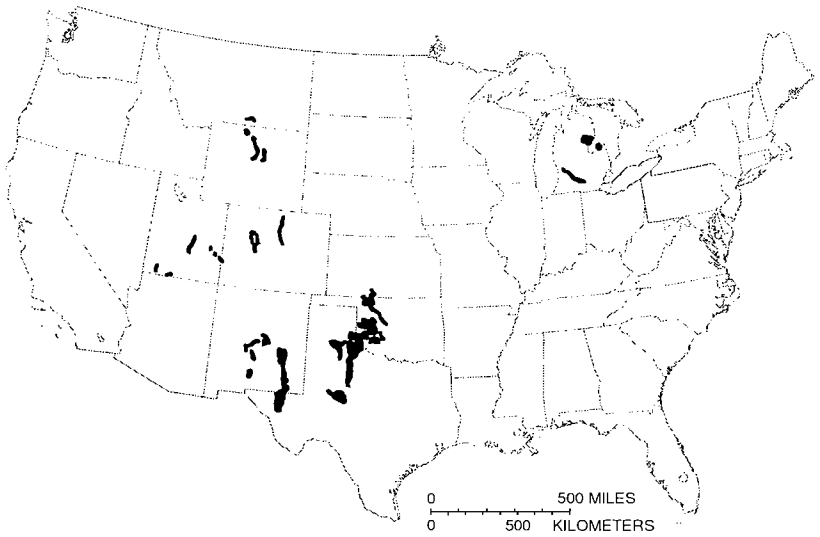


Figure 2. Map showing areas of evaporite karst in the United States, as depicted by Davies and others (1984).

tions caves and fissures in gypsum in western Oklahoma and the eastern part of the Texas Panhandle. His map does not show the distribution of salt or salt karst, however, even though his text mentions natural subsidence and man-induced subsidence as a result of solution mining in salt beds in south-central and southwestern Kansas.

A more accurate delineation of evaporite karst than that presented by the Davies and others map is required at the national, state, and local scale to better understand subsidence hazards, surface- and groundwater-contamination potential, and cave resources, and also to serve as a guide to topical research in these rocks. Such a map would also be useful to educate land-use managers, politicians, and the public on issues related to karst, both in carbonate rocks and evaporites.

Several national maps of evaporite deposits were prepared earlier than the one of Davies and others (1984). The first was a map by Adams and others (1904) that showed several mines in gypsum throughout the United States, supplemented with a few detailed regional maps of gypsum-bearing formations. A similar map, with additional localities, was produced by Stone and others (1920). Krumbein (1951) depicted the subsurface and outcrop distribution of evaporites in a variety of lithologic associations and by individual geologic periods or systems. He showed that these rocks are much more widespread than was generally realized. Figure 3 is a compilation of his 10 systemic maps. Withington (1962) prepared an annotated bibliography of gypsum and anhydrite deposits, categorized by age.

The distribution of rock-salt (halite) deposits was mapped by Pierce and Rich (1962), and this was upgraded by Johnson and Gonzales (1978) and by Ege (1985). The precursor of the 1984 Davies and others map was one prepared earlier (Davies and LeGrand, 1972) that was based on Davies' extensive knowledge of karst systems in the country. The present-day understanding of the widespread distribution of marine evaporites in the United States was presented by Smith and others (1973). They showed four categories of deposits, in combinations of gypsum, anhydrite, halite, polyhalite, sylvite, and carnallite. Modifications of earlier national anhydrite maps were prepared by Dean and Johnson (1989) and Johnson (1996); and finally the map of Johnson (1997) showed generalized areas of evaporite karst throughout the United States.

Figure 4 combines the information of Ege (1985) and Johnson and others (1989), showing the present perception of evaporite distribution in the United States. Figure 5 includes the various gypsum/anhydrite and halite basins of that map, and incorporates the rather limited areas of evaporite karst depicted by Davies and others (1984) compared to the larger areas of the same shown by Johnson (1997, 2003). Collapse as a result of human activities, such as solution mining, is also shown as well as a line of mean annual precipitation (32 in.) that we suggest approximates

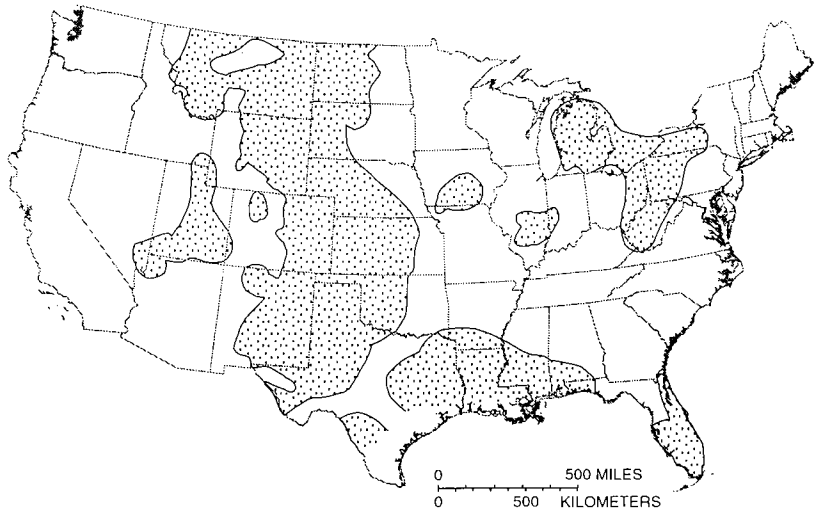


Figure 3. Map showing distribution of evaporite deposits in the United States (modified from Krumbein, 1951).

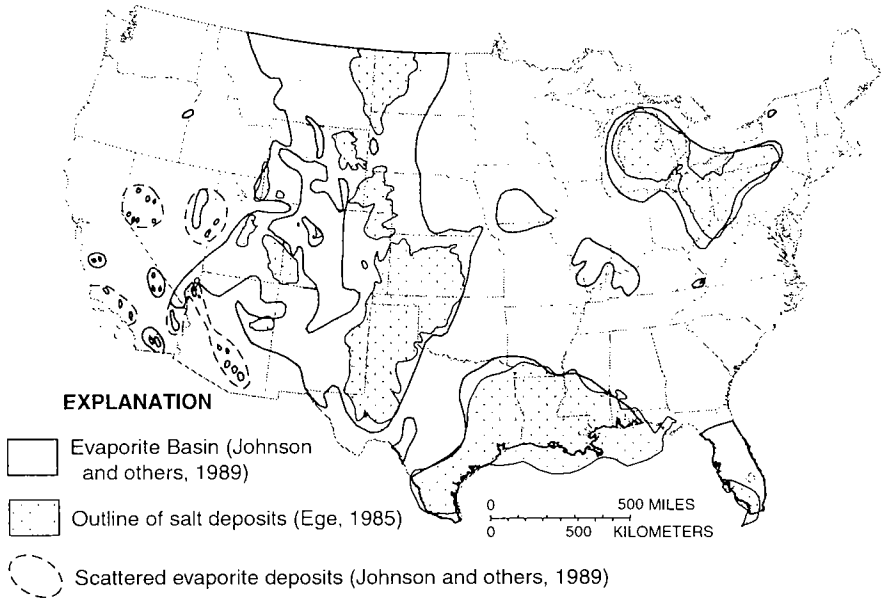


Figure 4. Map showing distribution of outcropping and subsurface evaporite rocks in the United States.

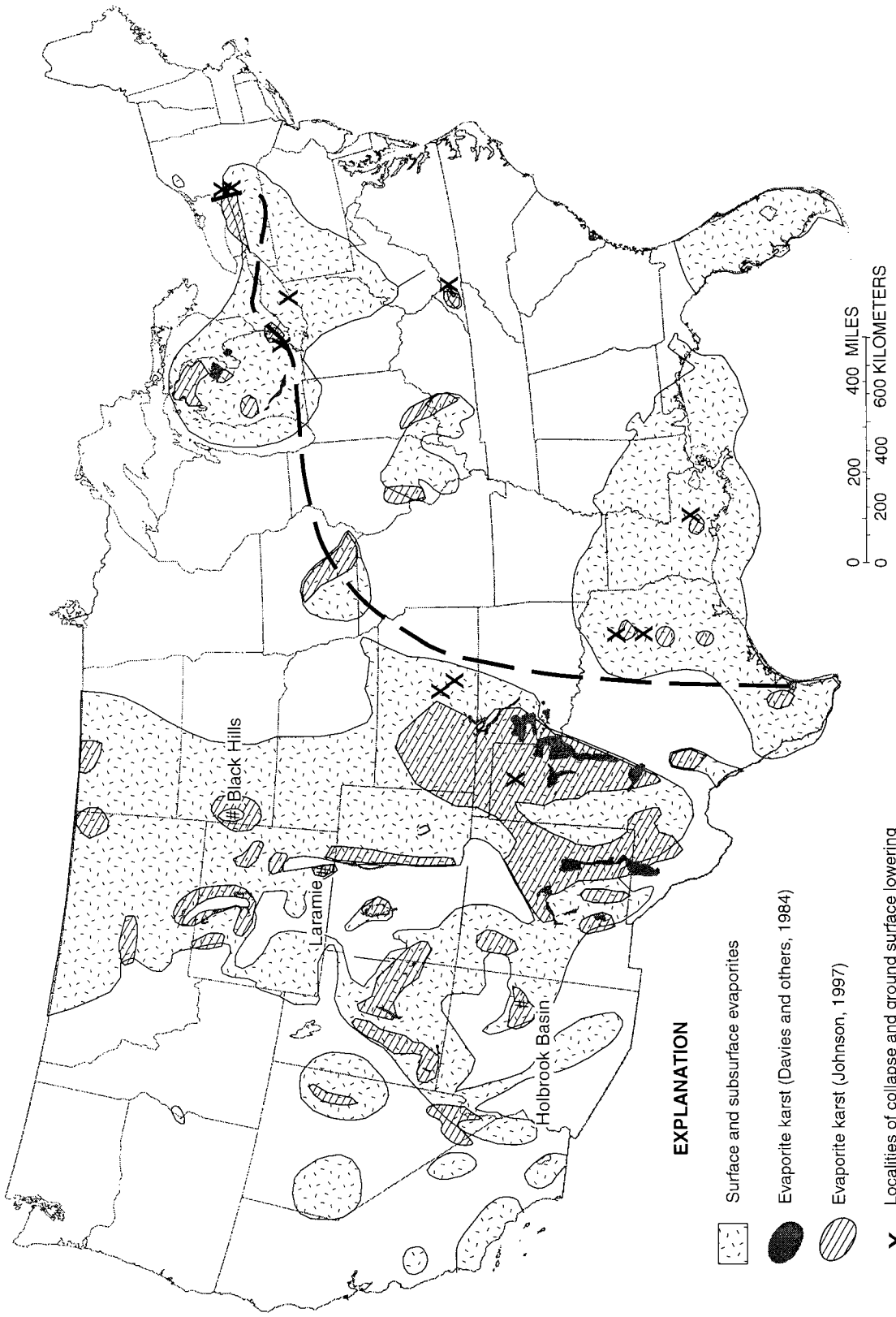


Figure 5. Map showing distribution of outcropping and subsurface evaporite rocks in the United States (from Fig. 4) and areas of reported evaporite karst. The 32.5-in. mean-annual-precipitation line approximates a diffuse boundary between eastern and western karst.

the boundary between distinctively different karst characteristics, both carbonate and evaporite karst, between the humid eastern United States and the semiarid West. Also shown are two localities for which we briefly describe a variety of surface and subsurface evaporite-karst features in areas not shown on the national Davies and others map; these areas are the Holbrook Basin in Arizona and the Black Hills of South Dakota.

### Holbrook Basin, Arizona

The map by Davies and others (1984) shows areas of carbonate rocks in Arizona, but no evaporites. Several workers have reported a variety of evaporite- and carbonate-karst features that are not found on this map. Figure 6A shows some of these features and suggests possible types of information that could be displayed on a state and national karst map for Arizona. The anhydrite basins shown are similar to the ones depicted in Figure 4. Subsurface halite deposits were mapped by Eaton and others (1972), Johnson and Gonzales (1978), Ege (1985), and Neal and others (1998); more detailed mapping of salt deposits in the Holbrook Basin was done by Peirce and Gerrard (1966) and Rauzi (2000). An area of breccia pipes was delimited in northwest Arizona by Harris (2002); they were probably the result of collapse over carbonate rocks, but evaporite collapse could not be ruled out. Scattered gypsum and anhydrite localities were shown by Withington (1962). Comparing this composite map with the one by Davies and others (Fig. 6B) shows that many types of karstic features could be depicted for both evaporite and carbonate rocks in Arizona.

The Holbrook Basin in east-central Arizona is interesting because it demonstrates that dissolution of deeply buried evaporites can cause subsidence of over-

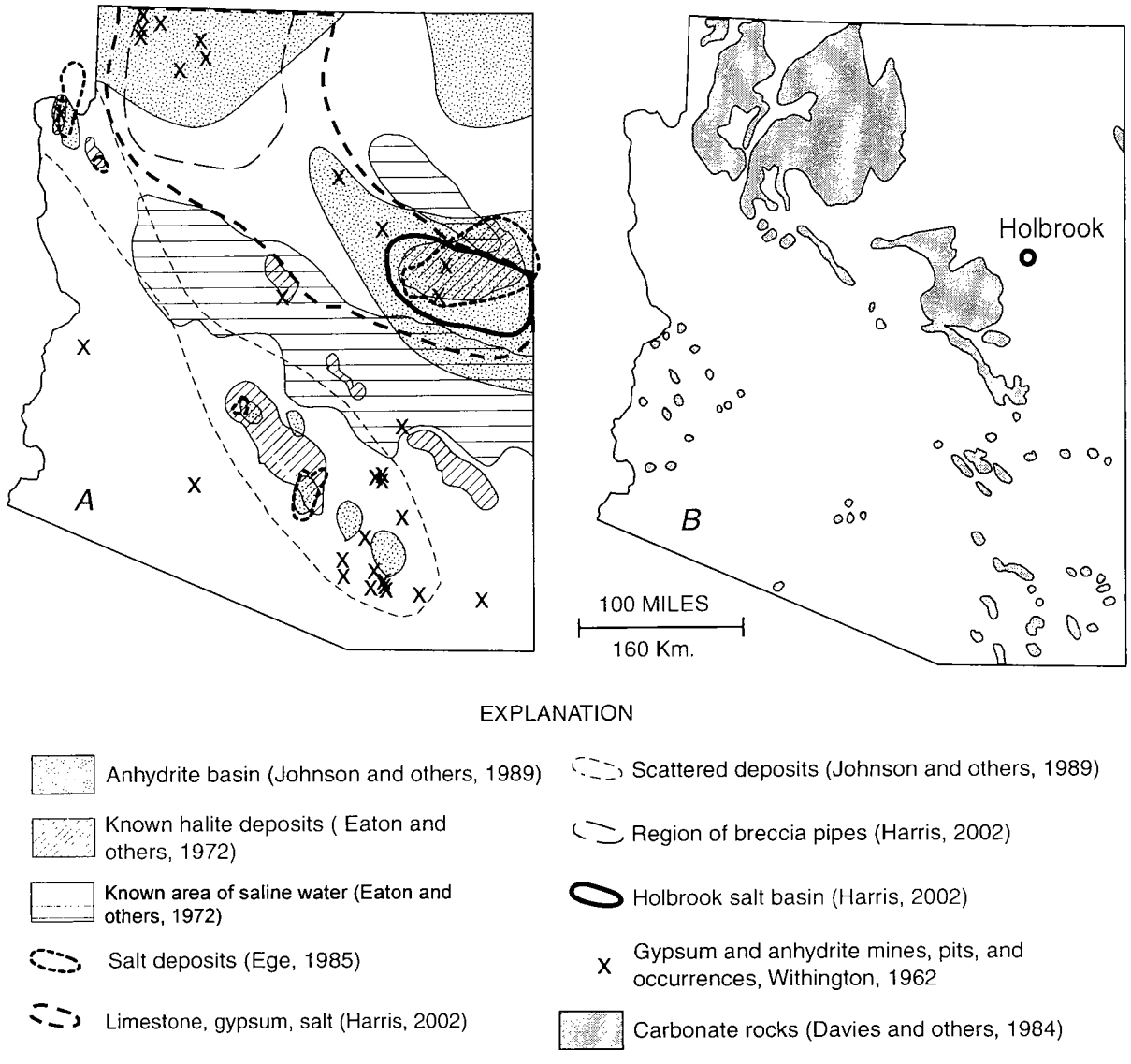


Figure 6. Maps comparing types and distribution of karst features in Arizona. (A) Distribution of evaporite and carbonate karst, as presented by various authors. (B) Distribution of carbonate karst (with no evaporite karst), as presented by Davies and others (1984).

lying non-soluble rocks. The basin is >100 mi wide and contains an aggregate of ~1,000 ft of salt, anhydrite, and sylvite interbedded with clastic red beds in the Permian Sedona Group (formerly Supai Group) (Peirce and Gerrard, 1966; Neal and others, 1998; Rauzi, 2000). The top of the salt is between 600 and 2,500 ft below the surface (Mytton, 1973). These workers describe the removal of evaporites at depth along a northeast-migrating dissolution front, causing the development of presently active collapse structures in the overlying Coconino Sandstone and Moenkopi Formation.

For example, in the area ~10 mi northwest of Snowflake, Arizona, the Coconino and other rocks dip monoclinally southward along the Holbrook "anticline" (actually a monocline) toward a large depression enclosing a dry lake. The depression is the result of subsidence caused by evaporite removal. Collapse extends upward from the salt, forming a network of spectacular sinkholes in the overlying Coconino Sandstone (Neal and others, 1998; Harris, 2002) (Fig. 7A). Draping of the Coconino has caused the opening of extensive tension fissures, some of which are many tens of feet deep (Neal and others, 1998; Harris, 2002) (Fig. 7B). If the definition of *karst* is allowed to include subsidence structures from the dissolution and removal of soluble rocks below and extending upward into non-soluble rocks, then a separate map category may be needed to delineate these rocks. Thus, the proposed national karst map must show non-soluble rocks whose collapse structures are the result of dissolution of evaporite rocks below. A somewhat similar situation prevails in the Black Hills of South Dakota and Wyoming.

### Black Hills, South Dakota and Wyoming

In the semiarid western part of the United States, such as in the Black Hills of South Dakota and Wyoming, gypsum and, to a lesser extent, anhydrite are exposed at the surface (Fig. 8A). As discussed by Epstein (2003), the outcrop pattern of sedimentary units in the Black Hills is controlled by erosion on an irregular domal uplift ~130 mi long and 60 mi wide. A central core of Precambrian rocks is surrounded by four zones of rock with contrasting lithologies and differing karstic features. These are, from the center (and oldest) outward: (1) The limestone plateau, made up of Cambrian to Pennsylvanian limestone, dolomite, and siliciclastic rocks, and containing world-class caves, such as Wind and Jewel Caves in the Mississippian Madison (Pahasapa) Limestone. Overlying these limestones, within the plateau, is the Minnelusa Formation, which contains as much as 235 ft of anhydrite in its upper half in the subsurface. This anhydrite has been dissolved at depth, producing a variety of dissolution structures (Fig. 8B). (2) The Red Valley, predominantly underlain by red beds of the Spearfish Formation of Triassic age and containing several gypsum beds totaling >75 ft thick in places (Fig. 8A) and shown areally by Darton (1904). Dissolution of these evaporites, and those in underlying rocks, has produced sinkholes, some of which are >50 ft deep (Fig. 8C). The surficial expression of such collapse is also indicated by many shallow depressions as much as 400 ft in diameter. Fresh scarps within the Spearfish are evidence of ongoing subsidence. The Jurassic Gypsum Spring Formation, which overlies the Spearfish, contains a respectable gypsum unit that has developed abundant sinkholes in places. (3) The "Dakota" hogback, held up by resistant sandstone of the Inyan Kara Group of Cretaceous age, and underlain by shales and sandstones of the Sundance and Morrison Formations of Jurassic age. Collapse structures, such as breccia pipes and sinkholes, extend up through some of these rocks from underlying soluble rocks, probably in the Minnelusa Formation (Fig. 8D). (4) Limestone

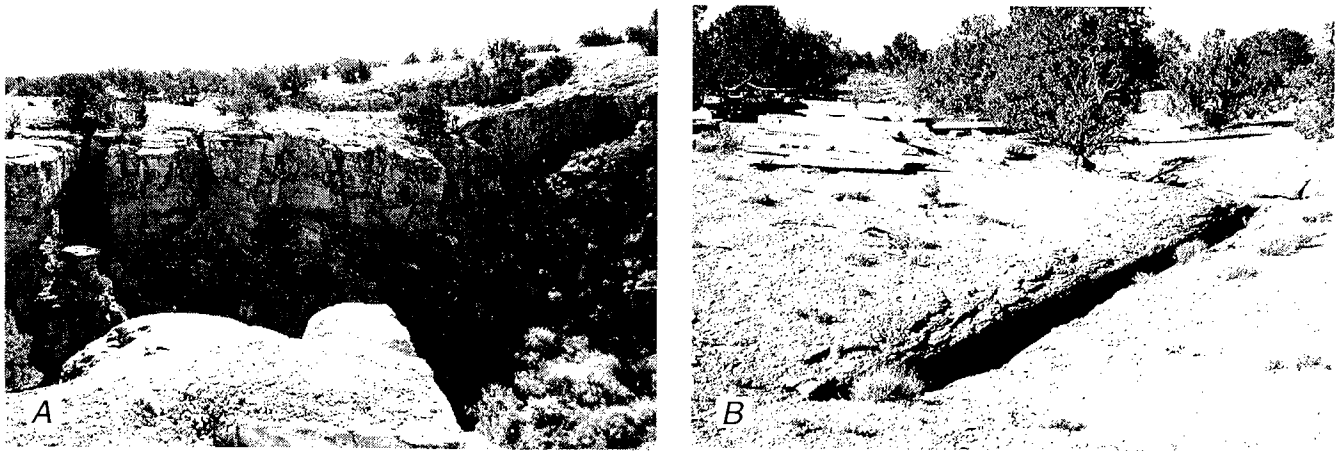


Figure 7. Collapse structures in clastic rocks overlying the salt-bearing Sedona Group in the Holbrook Basin, 8–10 mi northwest of Snowflake, Arizona. (A) Steep-sided sinkhole in a hole-pocked area called "The Sinks," developed in the Coconino Sandstone. Note the variable amount of subsidence along major joints. (B) Open tension fractures in the Moenkopi Formation caused by flexure of the Holbrook "anticline" (actually a monocline) caused by dissolution of salt at depth. Also see figures in Harris (2002).

and shale extending outward beyond the hogback, some of which are shown as karstic units on Davies and others' (1984) map.

Figure 9 compares the map of limestone outcrops shown by Davies and others (1984) for the Black Hills of South Dakota with the more detailed categories that we propose, including both carbonate and evaporite karst, intrastratal karst, and non-soluble rocks with collapse features caused by dissolution of other rock units at depth. This characterization may also be suitable for other areas of the western United States.

Discernment of the surface and subsurface karstic features in the Black Hills by state and local governments is necessary for understanding aquifer characteristics and the potential for ground-water contamination and susceptibility to surface subsidence. This is especially important in the Red Valley because of increased urban development (Davis and Rahn, 1997; Davis and others, 2003). The city of Spearfish, South Dakota, is an example of the very rapid growth in this part of the western United States, although it is small in comparison to the growth of other, major cities.

Anhydrite in the Minnelusa is generally not seen in surface outcrops. It has been, and continues to be, dissolved at depth, forming collapse breccias, breccia pipes, and collapse sinkholes that extend upward >1,000 ft into overlying units. Mapping this intrastratal karst is fairly easy, because the outcrop distribution of the Minnelusa is well known. At depth, brecciation of the upper part of the Minnelusa has developed significant porosity, resulting in an important aquifer. Ground water migrates along breccia pipes that extend upward through overlying formations.

Removal of anhydrite in the rocks of the Black Hills

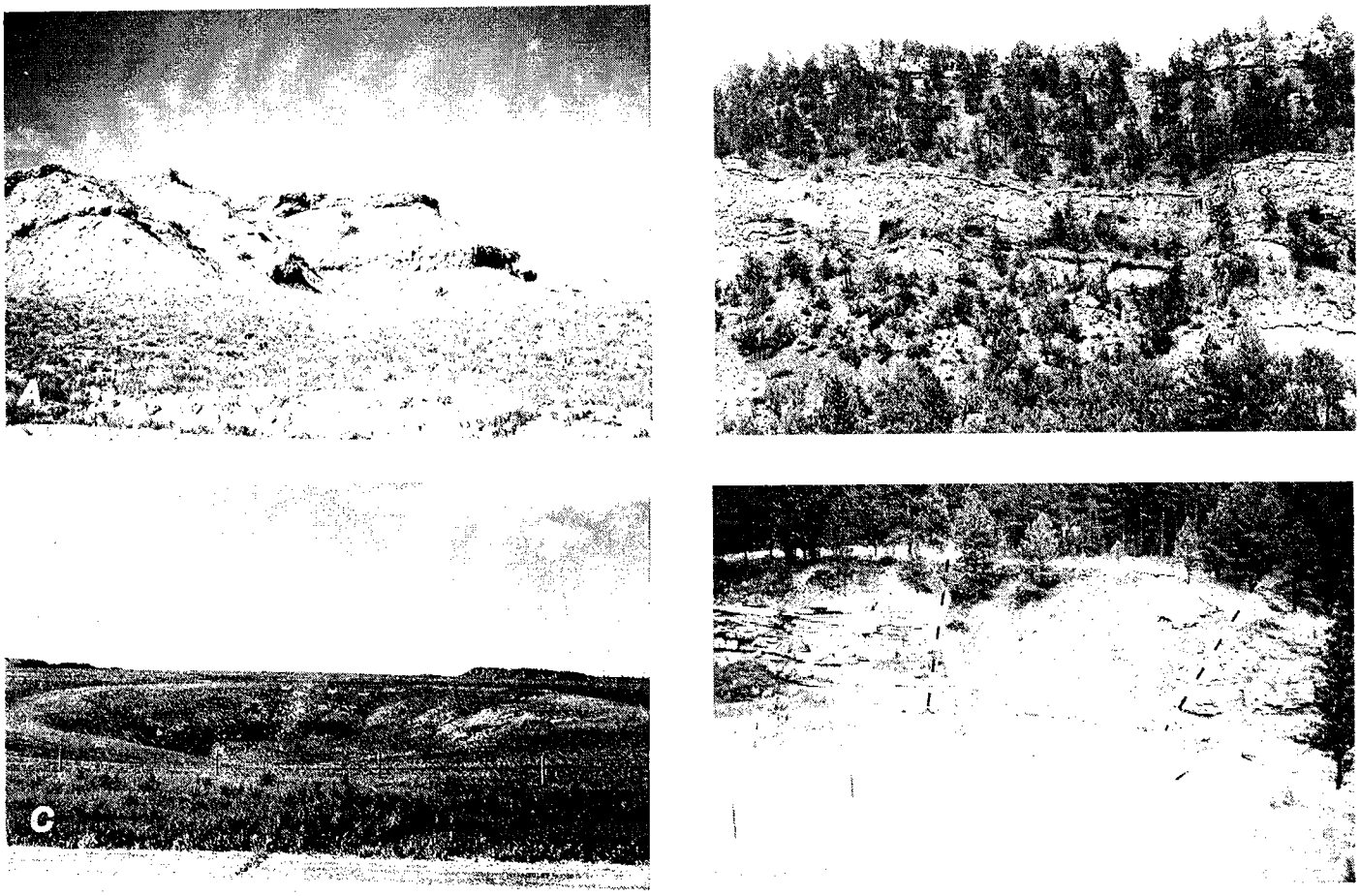


Figure 8. Karstic features in the Black Hills, Wyoming and South Dakota. (A) Typical exposure of gypsum interbedded with red beds in the Spearfish Formation, ~10 mi southeast of Newcastle, Wyoming. (B) Disrupted bedding and breccia pipes in the upper part of the Minnelusa Formation, Hot Brook Canyon, 3 mi west of Hot Springs, South Dakota. The Opeche shale forms the pine-covered slope above the Minnelusa, with the Minnekahta Limestone forming the top. Regional collapse from anhydrite dissolution in the Minnelusa has caused undulations in the Minnekahta. (C) Sinkhole in the lower part of the Spearfish Formation, north of I-90, 4 mi west of Beulah, Wyoming. A larger sinkhole nearby is 1,000 ft in diameter, and another steep-sided hole was used by the plains Indians as a "buffalo jump," whereby bison were driven over the rim to their slaughter. (D) Sinkhole in the Sundance Formation, west of U.S. 85, 8 mi north of Newcastle, Wyoming. Below the Sundance are interbedded gypsums, aggregating as much as 100 ft, in the Gypsum Spring and Spearfish Formations, and still farther down, as much as 200 ft of anhydrite and some salt in the Minnelusa Formation, to a total depth of ~1,500 ft, below which are carbonate rocks of the Mississippian Madison Limestone. The Minnelusa is favored as the focus of subsidence.

probably began soon after the Black Hills were uplifted in the early Tertiary. Dissolution and collapse continue today, as evidenced by recently formed sinkholes, collapse features in springs and water wells, fresh scarps, and calcium sulfate issuing from many springs. Considering all the information regarding dissolution of anhydrite and gypsum in the Minnelusa, Epstein (2003) describes a transition zone or "dissolution front" that is present in the subsurface where dissolution of anhydrite is currently taking place, similar to the situation reported for the Holbrook Basin in Arizona.

Subsidence caused by calcium sulfate dissolution has resulted in collapse of houses, unstable and unsuitable sewage-lagoon sites, and draining of retention ponds (Davis and Rahn, 1997). Outcropping gypsum beds form level terraces in some places, and such sites are considered by some to be suitable for building houses in the Black Hills area. However, because of the potential for karst and collapse, the siting of houses upon these gypsum deposits poses engineering and environmental problems (Fig. 10).

### Humid versus Semiarid Karst

Comparing the known locations of surface evaporite karst with a map showing annual average rainfall shows a striking relationship between precipitation and the occurrence of evaporite karst (Fig. 5). Most occurrences of surficial karst in gypsum, shown in Figure 5, lie west of a zone with annual precipitation of ~32 in. (represented by the 32.5-in. mean-annual-precipitation line). Many of the karst areas shown in Figure 5 are due to dissolution at depth. In Michigan, earlier studies suggest that the karstic collapse features there were formed soon after deposition of the Devonian evaporites (Landes and others, 1945), but Black (1997) showed that sinkhole development occurred after the most recent glaciation.

The degree to which soluble rocks are dissolved depends, in part, on the amount of rainfall and the

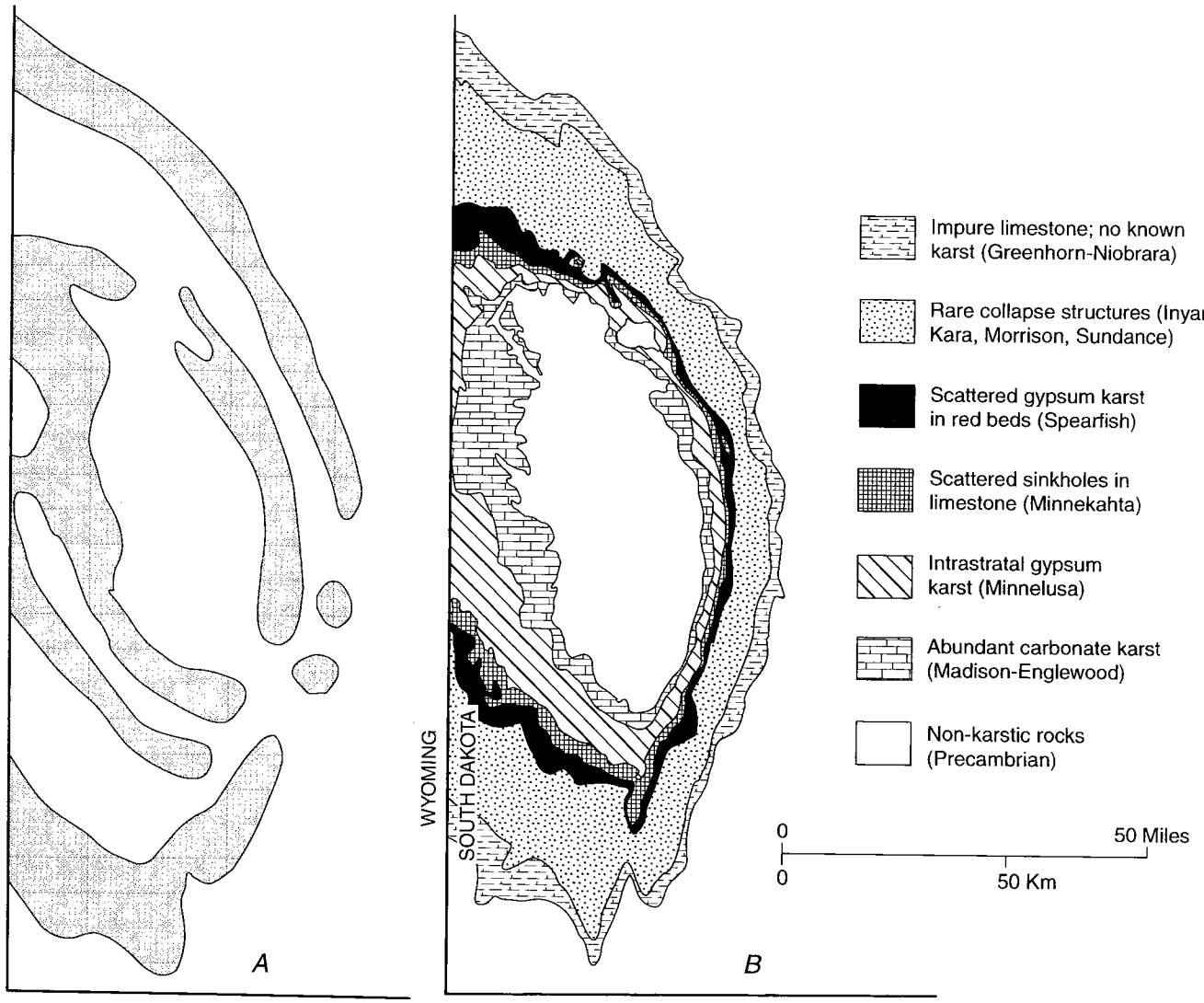


Figure 9. Maps comparing depiction of karst areas in the Black Hills of South Dakota. (A) Carbonate-karst units as presented by Davies and others (1984). (B) Carbonate- and evaporite-karst units, as herein proposed for a new national karst map.

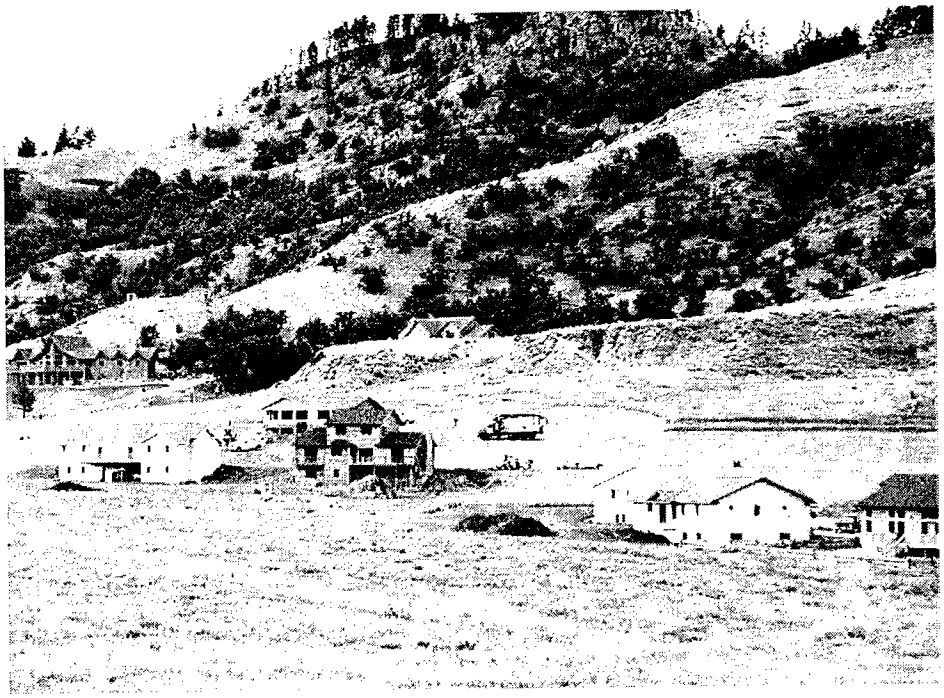

Figure 10. Lookout Peak, at the top of the photograph, overlooks the City of Spearfish, South Dakota, and offers scenic views of the surrounding hills. Lower down, the bench formed on a 20-ft-thick gypsum bed in the Gypsum Spring Formation (arrow) offers what seems to be an attractive building site. However, this same gypsum bed has developed numerous sinkholes elsewhere in the area, and similar sinks here would be a hazard to any construction.

solubility of the rock. Sulfate-bearing rocks—gypsum and anhydrite—are perhaps 10–30 times more soluble in water than carbonate rocks (Klimchouk, 1996). Both carbonates and sulfates behave differently in the humid eastern United States and the semiarid to arid West. Low ground-water tables and decreased ground-water circulation in the West do not favor rapid carbonate dissolution and development of karst. In contrast, sulfate rocks are dissolved much more readily and actively than carbonate rocks, even under semiarid to arid conditions. The presence of extensive karst in carbonates in the West probably dates to a more humid history. Additionally, the generally thicker soils in humid climates provide the carbonic acid that enhances carbonate dissolution. Gypsum and anhydrite, in contrast, are more readily soluble in water that lacks organic acids. This relationship suggests an interesting area for future study.

### Human-Induced Karst

It is well known that subsidence in karstic rocks can be exacerbated by human activities. Lowering of the water table by well pumping or by draining of quarries can reduce support of soils overlying sinkholes, thus causing their collapse. Subsurface mining of salt and other evaporites may eventually cause collapse of overlying rocks, such as at the Retsof mine in Livingston County, New York (Nieto and Young, 1998; Gowan and Trader, 2003). Localities of subsidence resulting from solution mining were mapped by Dunrud and Nevins (1981) and are shown in Figure 5. Ege's (1979) bibliographic list of ground subsidence from evaporite dissolution contains many instances where such subsidence was due to human activities. Knowing the location of shallow and deep mines is important to local officials in order to understand the potential for such subsidence. For example, abandoned gypsum mines in western New York are abundant, and recent settlement of many houses near Buffalo, New York, partly may be the result of subsidence over these mines. This possibility is currently under investigation.

## REFERENCES CITED

Adams, G. I., and others, 1904, Gypsum deposits in the United States: U.S. Geological Survey Bulletin 223, 129 p.

Black, T. J., 1997, Evaporite karst of northern lower Michigan: Carbonates and Evaporites, v. 12, p. 81–83.

Daly, Chris; and Taylor, George, 2000, United States average annual precipitation, 1961–1990: Spatial Climate Analysis Service, Oregon State University; USDA–NRCS National Cartography and Geospatial Center, Fort Worth, Texas; online linkage: http://www.ftw.nrcs.usda.gov/prismdata.html.

Darton, N. H., 1904, Gypsum deposits in South Dakota, *in* Stone, R. W., and others, 1920, Gypsum deposits of the United States: U.S. Geological Survey Bulletin 163, p. 76–78.

Davies, W. E.; and LeGrand, H. E., 1972, Karst of the United States, *in* Karst regions of the Northern Hemisphere: Elsevier, Amsterdam, p. 467–505.

Davies, W. E.; Simpson, J. H.; Ohlmacher, G. C.; Kirk, W. S.; and Newton, E. G., 1984, Map showing engineering aspects of karst in the United States: U.S. Geological Survey National Atlas of the United States of America, Reston, Virginia, scale 1:7,500,000.

Davis, A. D.; and Rahn, P. H., 1997, Karstic stabilization problems at wastewater stabilization sites in the Black Hills of South Dakota: Carbonates and Evaporites, v. 12, p. 73–80.

Davis, A. D.; Beaver, F. W.; and Stetler, L. D., 2003, Engineering problems of gypsum karst along the Interstate 90 development corridor in the Black Hills of South Dakota, *in* Johnson, K. S.; and Neal, J. T. (eds.), Evaporite

karst and engineering/environmental problems in the United States: Oklahoma Geological Survey Circular 109 [this volume], p. 255–261.

Dean, W. E.; and Johnson, K. S. (eds.), 1989, Anhydrite deposits of the United States and characteristics of anhydrite important for storage of radioactive wastes: U.S. Geological Survey Professional Paper 1794, 132 p.

Dunrud, C. R.; and Nevins, B. B., 1981, Solution mining and subsidence in evaporite rocks in the United States: U.S. Geological Survey Miscellaneous Investigation Series Map I-1298, 2 sheets.

Eaton, G. P.; Peterson, D. L.; and Schumann, H. H., 1972, Geophysical, geohydrological, and geochemical reconnaissance of the Luke salt body, central Arizona: U.S. Geological Survey Professional Paper 753, 28 p.

Ege, J. R., 1979, Selected bibliography on ground subsidence caused by dissolution and removal of salt and other soluble evaporites: U.S. Geological Survey Open-File Report 79-1133, 28 p.

_____1985, Maps showing distribution, thickness, and depth to salt deposits of the United States: U.S. Geological Survey Open-File Report 85-28, 11 p.

Epstein, J. B., 2003, Gypsum karst in the Black Hills, South Dakota–Wyoming: geomorphic development, hazards, and hydrology, *in* Johnson, K. S.; and Neal, J. T. (eds.), Evaporite karst and engineering/environmental problems in the United States: Oklahoma Geological Survey Circular 109 [this volume], p. 241–254.

Gowan, S. W.; and Trader, S. M., 2000, Mine failure associated with a pressurized brine horizon: Retsof salt mine, western New York: Environmental and Engineering Geoscience, v. 6, no. 1, p. 57–70.

_____2003, Mechanism of sinkhole formation in glacial sediments above the Retsof Salt Mine, western New York, *in* Johnson, K. S.; and Neal, J. T. (eds.), Evaporite karst and engineering/environmental problems in the United States: Oklahoma Geological Survey Circular 109 [this volume], p. 321–336.

Harris, R. C., 2002, A review and bibliography of karst features of the Colorado Plateau, Arizona: Arizona Geological Survey Open-File Report 02-07, 43 p.

Johnson, K. S., 1996, Gypsum karst in the United States of America, *in* Klimchouk, A.; Lowe, D.; Cooper, A.; and Sauro, U. (eds.), Gypsum karst of the World: International Journal of Speleology, v. 25, p. 183–193.

_____1997, Evaporite karst in the United States: Carbonates and Evaporites, v. 12, p. 2–14.

_____2003, Evaporite-karst problems in the United States, *in* Johnson, K. S.; and Neal, J. T. (eds.), Evaporite karst and engineering/environmental problems in the United States: Oklahoma Geological Survey Circular 109 [this volume], p. 1–20.

Johnson, K. S.; and Gonzales, S., 1978, Salt deposits in the United States and regional geologic characteristics important for storage of radioactive waste: Prepared for Union Carbide Corporation, Nuclear Division, Office of Waste Isolation, Y/OWI/SUB–7414/1, 188 p.

Johnson, K. S.; Gonzales, S.; and Dean, W. E., 1989, Distribution and geologic characteristics of anhydrite deposits in the United States, *in* Dean, W. E.; and Johnson, K. S. (eds.), Anhydrite deposits of the United States and characteristics of anhydrite important for storage of radioactive wastes: U.S. Geological Survey Professional Paper 1794, p. 9–90.

Klimchouk, Alexander, 1996, The dissolution and conversion of gypsum and anhydrite, *in* Klimchouk, Alexander; Lowe, David; Cooper, Anthony; and Sauro, Ugo (eds.), Gypsum karst of the World: International Journal of Speleology, v. 25, nos. 3–4, p. 21–36.

Krumbein, W. C., 1951, Occurrence and lithologic associations of evaporites in the United States: Journal of Sedimentary Petrology, v. 21, no. 2, p. 63–81.

Landes, K. K., 1945, The Mackinac Breccia: Michigan Geological Survey Publication 44, p. 121–154.

Mytton, J. W., 1973, Two salt structures in Arizona—the Supai salt basin and the Luke salt body: U.S. Geological Survey Open-File report, 40 p.

Neal, J. T.; Colpitts, R.; and Johnson, K. S., 1998, Evaporite karst in the Holbrook Basin, Arizona, *in* Borchers, J. W. (ed.), Land subsidence case studies and current research; Proceedings of the Dr. Joseph F. Poland Symposium on Land Subsidence: Association of Engineering Geologists Special Publication 8, p. 373–384.

Nieto, A. S.; and Young, R. A., 1998, Retsof salt mine collapse and aquifer dewatering, Genesee Valley, Livingston County, New York, *in* Borchers, J. W. (ed.), Land subsidence case studies and current research; Proceedings of the Dr. Joseph F. Poland Symposium on Land Subsidence: Association of Engineering Geologists Special Publication 8, p. 309–325.

Peirce, H. W.; and Gerrard, T. A., 1966, Evaporite deposits of the Permian Holbrook Basin, Arizona, *in* Rau, J. L. (ed.), Second symposium on salt: Northern Ohio Geological Society, Cleveland, v. 1, p. 1–10.

Pierce, W. G.; and Rich, E. I., 1962, Summary of rock salt deposits in the United States as possible storage sites for radioactive waste materials: U.S. Geological Survey Bulletin 1148, 91 p.

Rauzi, S. L., 2000, Permian salt in the Holbrook Basin, Arizona: Arizona Geological Survey Open-File Report 00-03, 20 p.

Smith, G. I.; Jones, C. L.; Cuberttson, W. C.; Ericksen, G. E.; and Dyni, J. R., 1973, Evaporites and brines, *in* Brobst, D. A.; and Pratt, W. D. (eds.), United States mineral resources: U.S. Geological Survey Professional Paper 820, p. 197–216.

Stone, R. W., and others, 1920, Gypsum deposits of the United States: U.S. Geological Survey Bulletin 163, 151 p.

Withington, C. F., 1962, Gypsum and anhydrite in the United States, exclusive of Alaska and Hawaii: U.S. Geological Survey Mineral Investigations Resource Map MR-33.

# Effects of Karst Processes on Gypsum Mining

***Roger D. Sharpe***
United States Gypsum Company
Chicago, Illinois

**ABSTRACT.**—The minability of a gypsum deposit is highly dependent upon the presence or absence of ground water and karst processes. The hydration of anhydrite to gypsum is related to structural and stratigraphic factors as well as to the availability of ground water. Infiltration of water affects the quality, quantity, and minability of the gypsum. If the permeability is low, a deposit may contain a significant proportion of anhydrite that may not be used to produce valuable products. If the permeability and availability of ground water are high, the deposit may have been fully hydrated and subjected to karst processes that significantly affect the recoverability of gypsum reserves.

In surface mining, the minability of gypsum may be affected by solution, erosion, and staining. An irregular bedrock surface, varying from hummocks to cutter-and-pinnacles to erosional cutouts may be formed. Solution-enlarged fractures may be filled by soil, mud, or organic material. The gypsum may be heavily stained by mud and/or iron and manganese oxides. Any of these conditions may significantly reduce the recoverable gypsum reserves.

In underground mining, the hydration pattern, mining geometry, accessibility of mining equipment, and potential for significant water inflows may be affected. In shallow underground gypsum mines the workings may intersect solution-enlarged fractures, allowing direct pathways for surface-water inflows. This may lead to soil piping, the formation of surface sinkholes, or poor mine-roof conditions.

In deeper mines, ground water may travel from remote recharge zones through a combination of fractures and porous strata. Where the ground-water-infiltration rate has been low, a gypsum deposit may contain significant areas of reserves that are contaminated by anhydrite. Where ground water is abundant, the gypsum interval may thin quickly to an unminable thickness or be completely dissolved in the updip direction. Zones of solution-collapse breccia may occur within the gypsum seam, reducing reserves, and they are potential zones of poor roof conditions and/or water inflows. Changes in mine geometry to avoid such zones may result in the disruption of the location of haulageways, conveyor beltlines, ventilation, or other mining utilities, as well as the loss of gypsum reserves.

## INTRODUCTION

There are two hydrologic states in the geology and mining of gypsum deposits: too little water and too much water. There has rarely been just enough ground water available to produce a fully hydrated gypsum deposit without detrimental effects. Structural or hydrologic conditions may have limited the infiltration of ground water, resulting in gypsum containing significant impurities of anhydrite or soluble salts. Conversely, when surface and ground water are readily available, the gypsum may have significant solution or erosional features. In either case, the result may be a decrease in the amount of recoverable gypsum reserves and an increase in the cost of mining.

Many papers deal with geotechnical engineering problems, such as the location and construction of dams, associated with gypsiferous rocks. However, this paper describes the interaction of surface and ground water with gypsum and anhydrite and the effects on the minability of gypsum. Examples are given for several of United States Gypsum Company's (USG) underground- and surface-mining operations.

Although usually considered detrimental because of gypsum's high solubility, the interaction of water with gypsum and anhydrite ultimately determines the extent, minability, and quality of gypsum deposits. In many cases the effects of karst processes on gypsum mining are manageable if the geologic, hydrologic, and topographic factors are understood and integrated into the mining plan.

The conversion of anhydrite to produce gypsum is a reversible chemical reaction and occurs over a wide range of temperature and pressure conditions:

$$CaSO_4 + 2H_2O \leftrightarrow CaSO_4 \cdot 2H_2O.$$

Gypsum is formed from several primary and secondary geological processes. Primary gypsum and anhydrite may simultaneously precipitate from sea-

Sharpe, R. D., 2003, Effects of karst processes on gypsum mining, *in* Johnson, K. S.; and Neal, J. T. (eds.), Evaporite karst and engineering/environmental problems in the United States: Oklahoma Geological Survey Circular 109, p. 31–40.

water in a lagoonal environment or from pore water in a tidal-flat (sabkha) environment. Gypsite, an impure gypsum crust, forms as a crust on playa lakes in arid climates. Minor amounts of gypsum occur as exhalative deposits associated with deep-sea volcanic vents (black smokers). Satin spar and selenite varieties of gypsum are generally secondary in origin. These forms may be derived from hydrothermal fluids or from the solution and reprecipitation of gypsum along fractures, fault zones, and vugs.

Gypsum and anhydrite may be converted to one another, regardless of their origin. For example, primary gypsum may be converted to anhydrite after burial in sedimentary basins. At depths greater than about 2,000 ft, gypsum can easily dehydrate to form anhydrite. Anhydrite will react with ground water to form gypsum because of uplift, development of joints and fractures, and the removal of overlying strata as a result of tectonic activity or erosion. In some cases, a gypsum deposit may contain evidence of multiple phases of dehydration and hydration.

The effects of karst processes range from serious to potentially catastrophic events, such as flooding of underground mine workings to "nuisance" problems affecting surface-mining conditions and the quality of the gypsum.

## FLOODING

The most serious effect of karst processes on gypsum mining is an encounter with a water-filled cavity system either adjacent to or hydraulically connected to the mine workings. The USG Shoals, Indiana, underground gypsum mine experienced total flooding in 1960 and 1965. In 1960, flooding occurred when development headings encountered a substantial solution-cavity system in the gypsum seam and overlying carbonate rocks. Extensive grouting from the surface and construction of a bulkhead eventually stemmed the inflow of water. In 1965, ground water worked around and breached the 1960 grout plug and bulkhead. The mine was shut down and production was interrupted for about 6 months following each episode of flooding. All of the mobile equipment and electrical facilities were subjected to hydrogen sulfide–laden ground water and required extensive refurbishing or replacement.

### Geological Background

Gypsum occurs near the town of Shoals in Martin County in southwestern Indiana. The gypsum occurs near the top of the St. Louis Limestone (Mississippian) and was deposited in a broad sabkha (tidal-flat) environment. The United States Gypsum Company and the Gold Bond Products Division of National Gypsum Company operate underground room and pillar mines near Shoals. The mines are ~450 ft deep, and the mining seam is ~12 ft thick.

The St. Louis Limestone dips ~35 ft/mi to the southwest into the Illinois Basin. The mine is about 11–15 mi downdip of the outcrop area of the formation, which is known as the Mitchell Karst Plain. The karst plain extends over an area of several hundred square miles and forms a large recharge area with abundant caves and subterranean drainages. Traces of nodular gypsum and breccia zones have been observed in the outcrop area, suggesting the widespread solution of a more extensive gypsum deposit (French and Rooney, 1969).

### Hydrology

Solution of the gypsum at Shoals is related to the migration of ground water downdip from the Mitchell Karst Plain to the east and the percolation of ground water through the overlying strata. Ground water flows down gradient through the St. Louis Limestone from the karst-plain outcrop area and actively dissolves the updip fringe of the gypsum seam. Ground water also percolates through the overlying strata through fractures into the mining seam. A paleo-erosional surface developed at the top of the overlying Ste. Genevieve and Paoli Limestones (Mississippian). Sand channels in the overlying fluvio-deltaic Bethel Sandstone (Mississippian) also provide reservoirs of ground water that migrate through fractures into the underlying limestone strata. As the gypsum dissolves, the ground water becomes laden with hydrogen sulfide ($H_2S$), often called "pluto water."

The hydrologic system in the Shoals area is complex. Under normal conditions, ground water traverses through a fracture system extending almost 300 ft above the gypsum seam to resurge in the Indian and Trinity Springs area, 7–8 mi north-northeast of the USG mine. Features such as Sulphur Springs and Sulphur Creek are also indicative of the resurgence of hydrogen sulfide–laden water. Indian Creek flows into Indian Spring during flooding conditions or when the static water level in the cavity system declines. Monitoring of pressure gauges installed into holes drilled into the cavity system from mine workings indicates that the hydrostatic head varies from nearly the mining seam elevation to 230 ft above the mining seam. Fluctuations of the water level in the cavity system correlate relatively well to flow conditions in Indian Creek and the White River.

Production blasting in 1960 encountered a significant cavity system in the updip direction of the gypsum seam. Widely spaced diamond-core holes had encountered solution rubble along the eastern (updip) margin during exploration for and delineation of the deposit. The subsequent water inflow was estimated at 25,000 gallons per minute. The hoist operator discovered the flooding while performing the daily preshift inspection. The man cage encountered resistance when lowered to the bottom of the hoisting shaft. Water continued to flow into the mine until the static water level stabilized at ~315 ft above the elevation of the mining seam.

A grout plug was created to stem the water inflow by drilling numerous holes from the surface and with

the introduction of sand and grout. Extensive drilling from the surface was carried out to locate the cavity system just ahead of the development heading for the injection of sand and cement grout. Some of the drill holes encountered a cavity system at the top of the mining seam. Most of the injected cement grout flowed into the mine workings rather than into the cavity system.

Dewatering of the USG mine took ~18 days at a pumping rate of 7,500 gallons per minute. During dewatering of the mine the flow from nearby springs declined or ceased. Hydrogen sulfide has been present in the resurgent springs.

The mine was compartmentalized, and concrete and steel flood-control doors and air vents were constructed through continuous pillars. Mining in the area near the flood-inflow point and along the northeastern margin of the mine was terminated. A concrete arch-shaped bulkhead was constructed in the development heading that originally encountered the cavity system. The bulkhead was hitched into rib abutments in the gypsum pillars.

By 1965, ground water had developed pathways in, through, and/or around the cement grout plug and concrete bulkhead. Initially, the inflow was ~300 gallons per minute. As solution channels were enlarged, ground-water inflows >10,000 gallons per minute occurred. The mine was totally inundated again, with subsequent loss of production, and had to be completely rehabilitated. The flood-prevention measures constructed after the 1960 flood were relatively ineffective.

A massive concrete friction-plug bulkhead was constructed in 1976. Sulfate-resistant cement grout was injected into about 200 drill holes to seal the fractured rock adjacent to the plug and shrinkage cracks in the plug. Chemical grout was also used at various times since the construction of the bulkhead to stem minor inflows of ground water.

In 1985, fluorescein dye that was injected during the 1970s began to appear in minor roof "drippers" near the bulkhead. The appearance of dyed water near the bulkhead indicated the ongoing interaction of fresh ground water with the gypsum seam. A new concrete bulkhead was constructed in front of the other two bulkheads, and an extensive grouting program was carried out in 1987.

Lessons learned from the flooding of the Shoals mine have been applied to other company underground mines. Four out of five of USG's underground mines have solution zones at the updip edge of the gypsum seam. However, the Shoals mine is the only mine to have encountered complete flooding. The updip edge–active solution zone has been generally outlined by surface diamond-drill holes. The proximity of the solution zone is determined during normal mining operations by (1) test drilling of roof strata with a face drill, (2) thinning of the height of the mining seam, and (3) the occurrence of poor or wet roof conditions.

### Paleokarst Features

The USG Shoals underground mine contains solution breccia pipes or sinkholes that partially or completely penetrate the gypsum seam and are locally termed "brown tornadoes" (Fig. 1). The brown tornadoes consist of blocks of carbonate rocks from the overlying strata that are indurated with clay. Although the brown tornadoes generally do not produce significant ground-water inflow, they represent a loss of recoverable reserves. The areas may have poor mine-roof conditions and dilute the purity of the gypsum recovered.

The USG Sigurd quarry, in Sevier County, Utah, has a unique problem associated with old solution features. Solution-enlarged fractures that extend deep into the complexly folded gypsum strata contain mouse middens and fecal material. The organic material is a contaminant in the quarried gypsum, which, upon calcination to form calcium sulfate hemihydrate, acts as a natural retarder for the recrystallization to gypsum during the wallboard-manufacturing process.

## SUBSIDENCE

The USG Fort Dodge operation is in Webster County, Iowa. Gypsum has been mined in this area since the 1870s. Underground mining of gypsum by USG took place from the 1880s until 1927. Surface mining of gypsum in the Fort Dodge area is currently carried out by USG, National Gypsum Company, BPB, and Georgia-Pacific. All of the companies operated underground mines during their early history, but all mining is currently done by surface methods. The areas of underground mining contain hundreds of oval to circular, water-filled sinkholes (Fig. 2), which have formed by soil piping along solution-enlarged joints. A sinkhole occurred beneath a building at the USG plant in early 2002 (Fig. 3). An investigation of the

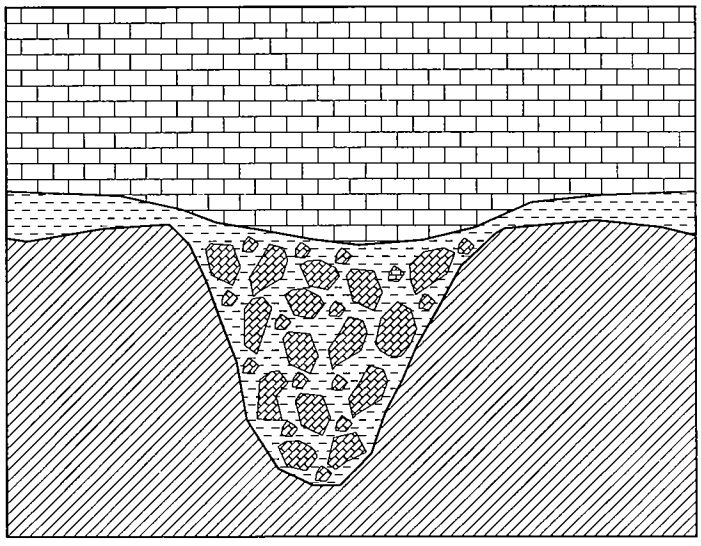

Figure 1. Development of paleo-sinkhole or "black tornado" at Shoals, Indiana.

underground-mine workings discovered candy bars from vending machines in the sloughed mud-glacial till. Figure 4 shows a cross section of the underground workings, including an enlarged fracture and incipient soil piping that have been exposed in a quarry face. Although the sinkholes are generally of small diameter (10–30 ft), there are also areas of extensive subsidence that developed over areas of very high extraction in the Georgia-Pacific mine. Figure 5 shows areas of underground mining with abundant sinkholes adjacent to the USG wallboard plant.

Figure 2. Typical circular, water-filled sinkhole overlying underground-mine workings at Fort Dodge, Iowa.

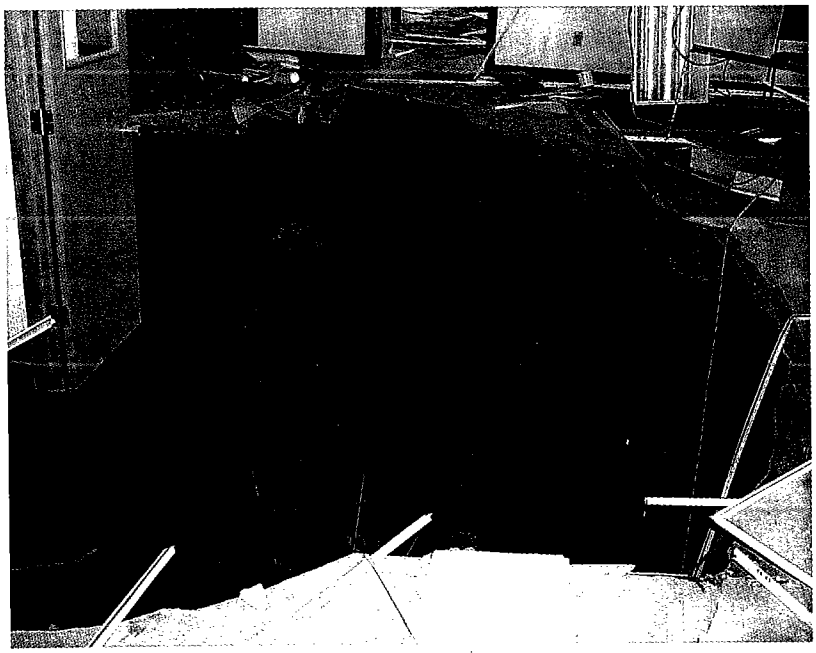

Figure 3. Development of a sinkhole inside a building at the USG Fort Dodge, Iowa, plant in early 2002.

## Geological Background

Gypsum occurs in the Fort Dodge Formation (Jurassic) and crops out discontinuously over an area of ~15 mi$^2$ in the vicinity of Fort Dodge. Although originally deposited in a single evaporite basin, gypsum occurs as discontinuous masses with a maximum thickness of ~30 ft. The gypsum was deposited on an erosional surface that truncates the underlying Pennsylvanian and Mississippian strata. The gypsum has been subjected to dissolution and erosion from glacial and fluvial processes. Pleistocene glacial till covers the gypsum everywhere except in ravines near the Des Moines River. These areas were the first to be mined by underground methods in the late 1800s. In some areas the gypsum is directly overlain by the "Soldier Creek beds," an informal stratigraphic unit that protected the gypsum from dissolution and erosion. These beds consist of calcareous siltstone and sandstone and shale, as thick as 50 ft, that overlie the gypsum (Cody and others, 1996).

Solution enlargement of joints and fractures occurred prior to Pleistocene glaciation, according to Cody and others (1996). However, Hayes (1986) attributes the fracture orientations to the effects of the deposition of gypsum on a disconformable topographic surface and differential compaction of the strata underlying the gypsum during glacial advances. A deep paleo-stream channel was observed by the author in the USG Carbon Quarry during the early 1990s. The bell-shaped channel cut downward through almost the total thickness of the gypsum seam. Scouring by coarse gravel and boulders carried in the bed load resulted in smooth, undercut channel walls. The undercut channel contained stratified gravels when it was exposed during quarrying.

## Underground Mining

Underground mining began in the Fort Dodge area during the 1870s and continued until the 1940s. Enlarged solution channels that were developed along joints were commonly encountered during underground mining. The solution channels are termed *slips* and are up to 3 ft wide, and they extend partially to completely through the gypsum seam. Most slips are filled with clay. However, some slips are filled with sand or clayey sand. If there had been no ground-water infiltration, the slips were lagged and timbered to provide support. Internal friction of the relatively dry sand grains assists in holding the sand in place. An examination of the underground workings in 2002 showed some slips that were still intact 75 years after mining had ceased (Fig. 6). Although the wooden lagging has almost completely decayed, the sand fill is intact.

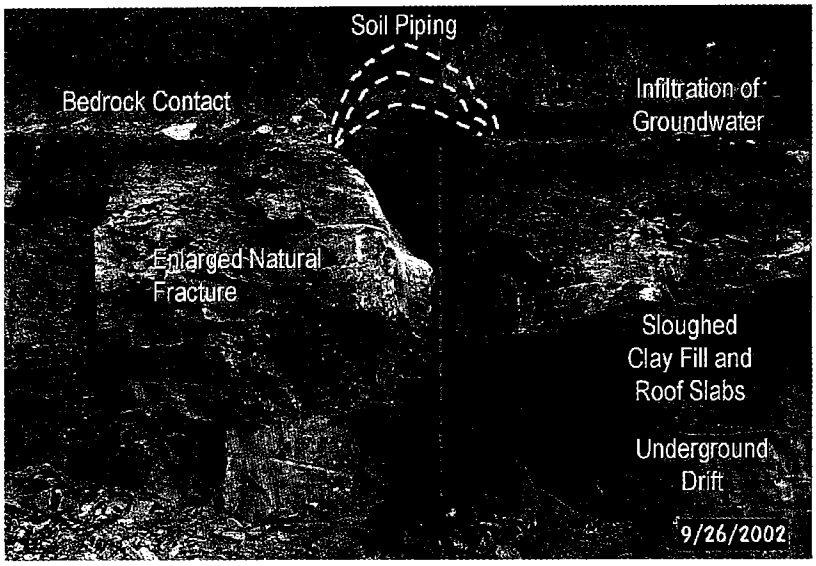


Figure 4. Anatomy of a sinkhole that developed along a solution-enlarged fracture at Fort Dodge, Iowa. Underground workings are now exposed in a quarry face.

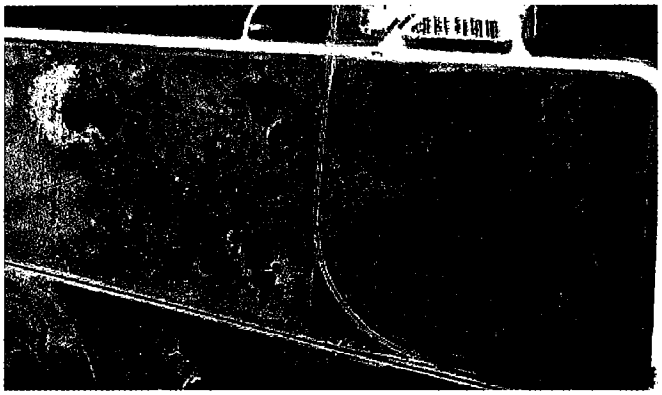

Figure 5. Sinkholes formed over underground-mine workings at Fort Dodge, Iowa. Aerial photograph.

Most of the solution-enlarged slips are effective conduits for ground-water inflow into the underground-mine workings. Saturated clayey fracture filling and the overlying glacial till often flowed into the mine when mine headings encountered slips (Fig. 7). The downward movement of the fracture fill and till resulted in soil piping and ultimately the formation of sinkholes at the surface.

## INCOMPLETE HYDRATION OF THE MINING SEAM

The thickness and composition of the strata overlying the gypsum and the presence of pathways for ground-water infiltration are the predominant controls for the conversion of anhydrite to economic gypsum deposits. The effects of topography on the hydration of gypsum deposits are evident in both underground- and surface-mining operations.

### Underground Mining

The USG Sperry underground gypsum mine is in southeastern Iowa. The wallboard-manufacturing facility and mine are in Des Moines County, ~12 mi north of the town of Burlington. A large deposit of gypsum occurs at a depth of ~600 ft and has been mined by USG since 1962. The mine currently covers an area of ~820 acres.

The main impurities in the Sperry deposit are anhydrite and dolomite. The thickness of anhydrite is highly variable in the middle to lower part of the mining seam (Fig. 8). The anhydrite thickness may vary significantly over short distances as the mining-face line advances. Maintaining a constant head grade at the mine for manufacturing wallboard begins with the blending of numerous mine faces. Daily production planning involves the measurement of the thickness of anhydrite in the mining seam and selection of available faces within the active parts of the face line for blending. Areas of significant anhydrite must be mined along with the higher purity faces to keep the face line relatively smooth and

Figure 6. Stull and lagging support in an open, sand-filled fracture in underground-mine workings at Fort Dodge, Iowa. Supports have been in place for >75 years.

well formed to facilitate ventilation and development activities. The face line in the active part of the mine currently extends >2 mi.

Anhydrite is screened from the mine-run production after processing through the secondary crusher and screening circuit. Most of the anhydrite is removed from the raw-material feed to the calcining plant by removing the +0.5-in. to –2-in. fraction. About 25% of the total production is screened, stockpiled, and shipped to portland-cement plants for use in the manufacture of cement.

### *Geological Setting*

Gypsum occurs in carbonate and evaporite rocks of the Spring Grove Member of the Wapsipinicon Formation (Devonian). The deposit lies on the western flank of the Mississippi Arch between two large depositional basins, the Forest City Basin to the west and the Illinois Basin to the east. The general dip of the strata is ~40–50 ft/mi toward the west. The originally deposited evaporites were buried by several thousand feet of sediments, converting the originally deposited gypsum to anhydrite. Subsequent regional uplift and erosion of the sediments, followed by subsidence and burial, have resulted in several periods of hydration and dehydration.

The surface topography in the Sperry area is relatively flat and consists of glacially deposited loess and till having a total thickness of 75 ft to ~300 ft. The surface topography masks a subcrop terrain of glacially gouged stream and river channels and highlands with topographic relief of >200 ft. The buried highlands are capped by the Burlington Limestone (Mississippian), which overlies the Maple Mill Shale (Devonian). Most of the mine underlies a glacial river channel ~1 mi wide that extends to a depth of ~300 ft in the Maple Mill Shale.

Figure 7. Mud flow from enlarged solution fracture into underground-mine workings at Fort Dodge, Iowa.

Figure 8. Anhydrite in the mining seam in the Sperry, Iowa, underground gypsum mine.

The Spring Grove Member contains three gypsum sequences, locally named the no. 1, no. 2, and no. 3 seams, in descending order. The no. 1 seam is 2–5 ft thick and thickens in the downdip direction. The no. 2 seam varies in thickness from zero in the updip direction to a maximum of ~16 ft. The no. 3 seam lies ~3–4 ft below the base of the no. 2 seam and is ~5 ft thick.

The no. 1 seam consists of friable, porous, recrystallized calcite. This is residue from the solution of an originally thicker gypsum interval. A distinct collapse breccia of sublithographic limestone is present directly above the no. 1 seam in many drill cores. The seam occurs 15–20 ft above the no. 2 seam. The no. 1 seam forms a tabular aquifer between lower permeability carbonate units. Ground water may take indirect pathways into the anhydrite/gypsum strata by infiltration through joints or fractures in the overlying carbonate strata, traveling downdip through the no. 1 seam and then entering the mining seam or mine workings upon encountering other fractures.

The no. 2 seam consists of (1) an upper zone of 10–11 ft of nodular gypsum and anhydrite with dolomite impurities, (2) gypsiferous dolomite with a thickness of 1–2 ft, and (3) a lower zone of dolomitic gypsum 2–3 ft thick. Only the upper zone of the no. 2 seam is

mined by USG. The updip limit of the no. 2 seam is a solution-cavity system. The limestone strata above the gypsum crops out several miles to the east near the Mississippi River flood plain. The downdip mining limit occurs where the no. 2 seam is deeper and consists almost entirely of anhydrite.

Although gently dipping westward, the strata are deformed into a series of gentle, northeast-oriented, open anticlinal and synclinal folds. The folds have a wavelength of ~800 ft with an amplitude of only a few feet. Delineation of the folding is not readily evident in widely spaced diamond-drill holes. Instead, the folding has been mapped by level surveys of the mine floor and roof elevations. There are also prominent northeast-oriented joints and fractures and less well developed northwest-oriented discontinuities.

The northeast-oriented joints formed along the crests and troughs of the folds. The origin of the folding is unclear, but there are two contributing factors: (1) lithostatic unloading during formation of the overlying buried river channel, and (2) volumetric expansion during the conversion of anhydrite to gypsum. Glacial gouging of the channel removed at least 300 ft of overlying strata and cut significantly downward into the underlying Maple Mill Shale. Beneath the highlands, the Maple Mill Shale is ~480 ft thick and acts as an aquitard. The hydration of anhydrite to gypsum results in a volumetric expansion of ~26% (Fig. 9).

### *Mining Conditions*

The minable part of the gypsum seam varies in thickness from 9 to 12 ft. The gypsum is mined by room and pillar techniques and currently covers >820 acres. The spatial distribution of anhydrite within the mining seam is the predominant quality factor in the development of the mine. Anhydrite is commonly present in the middle and lower parts of the mining seam. The eastern mining limit is defined by the thinning of the gypsum seam as the updip solution zone is approached. The minimum mining height is 9 ft, based upon equipment height restrictions and past experiences with poor roof conditions associated with gypsum solution. Solution cavities occur at the top of the mining seam as the eastern mining limit is approached (Fig. 10). Drill holes farther to the east of the mine encountered cavities and collapse breccias. The predominance of anhydrite determines the westward limit of mining. Between these constraints the no. 2 seam contains a highly variable thickness of anhydrite, varying from zero to almost the full mining height. As a mine heading advances, anhydrite initially appears as a thin wedge in the middle part of the gypsum seam and increases abruptly into the lower part of the seam. Most of the hydration took place from the top down. However, the wedge-shaped appearance of gypsum in the middle part of the mining seam also indicates lateral migration of ground water. Anhydrite thickness is highly variable over short distances, such as opposite walls of a mine room (27–38 ft apart) or within the width of one to two pillars (~70–90 ft).

Attempts to model and predict the distribution of anhydrite within the mined part of the seam, as well as into undeveloped areas, have not been successful. A data set of more than 10,000 anhydrite-thickness measurements was subjected to rigorous geostatistical techniques. The thickness of anhydrite forms "text-

Figure 9. Enterolithic fold in gypsum resulting from expansion of anhydrite to gypsum near Sperry, Iowa.

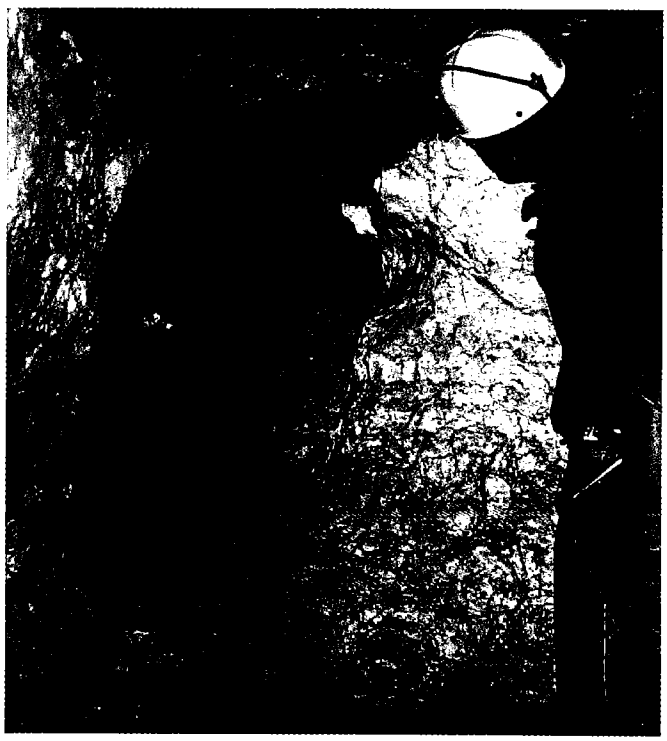

Figure 10. Solution cavity at the top of the gypsum seam, Sperry, Iowa.

book" spherical variograms in which the range, sill, and nugget values were used in kriging to predict the distribution of anhydrite over short distances into the unmined areas. The kriging tests incorporated the anhydrite thicknesses in mine pillars as well as from nearby drill-hole information.

## Surface Mining—Sweetwater, Texas

Gypsum has been mined by USG at Sweetwater, Nolan County, Texas, since the early 1920s. Multiple beds of gypsum crop out along a highly dissected erosional escarpment with a topographic relief of ~100 ft. The topography and overburden thickness are highly correlative with the occurrence of anhydrite in the underlying gypsum seams.

### *Geological Setting*

The gypsum occurs in the Eskota Member of the Peacock Formation (Permian). Four distinct beds of gypsum are mined, and they are named, in descending order, the top vein (17 ft), middle vein (3–4 ft), thin vein (0–18 in.), and bottom vein (8–10 ft). The top vein is overlain by sandy-clay overburden. Some of the overburden is relatively well indurated. Lenses of weakly indurated sandstone occur in the lower part of the overburden where the sandy clay is >25 ft thick. The strata strike approximately north and dip toward the west at ~45 ft/mi. The gypsum "veins" are separated by shaly interburden varying in thickness from 3 to 9 ft.

The topographic surface is dissected by a trellis drainage system developed along northwest-oriented fractures. Stream erosion has cut headward along fractures, forming deep ravines. Solution activity has resulted in disappearing streams that reappear near the bottom of the gypsum outcrop or quarry faces.

Gypsum outcrops along the low escarpment have been subjected to considerable solution and erosion. The gypsum is overlain by residual material, such as clay and fragments of weathered gypsum and colluvium from downslope wash of the overburden.

The tops of the gypsum seams vary from smooth and regular to hummocky and ultimately erosional cutouts (Fig. 11). In the updip direction, the top and bottom veins may be significantly thinned, representing a significant loss of recoverable gypsum reserves.

### *Quarrying Conditions*

The effects of ground-water solution and erosion significantly impact the productivity of the Sweetwater operation. Considerable effort is expended in the preparation of the upper surface of the gypsum. The USG Sweetwater plant produces a variety of construction and industrial plaster products in addition to Sheetrock® brand gypsum panels. High-purity gypsum is required for the manufacture of the plaster products. Most of the overburden is removed by draglines. Near the upper contact of the gypsum the surface is cleaned by either a smooth-lipped dragline bucket (Fig. 12) or by ripping and pushing by a dozer. The surface of the gypsum varies from relatively smooth and unaffected to hummocky to highly eroded. The rough gypsum surface provides some difficulty of access to the blasthole drill. Where highly eroded, the remnants of the gypsum seam may be completely directed to waste, representing a loss of recoverable reserves.

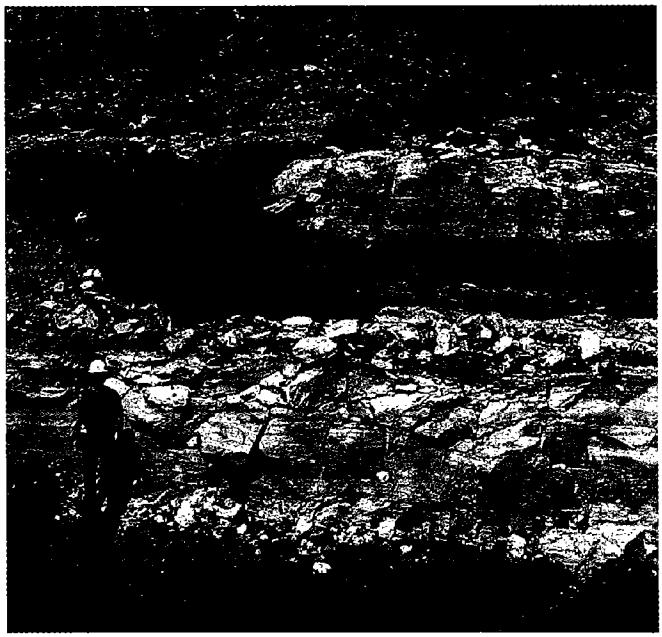

Figure 11. Erosional cutout of gypsum seam at Sweetwater, Texas.

Figure 12. Cleaning of hummocky bedrock surface of gypsum by dragline at Sweetwater, Texas.

Anhydrite appears in three of the four gypsum seams as mining progresses downdip. The thin vein, generally <18 in. thick, is fully hydrated. The occurrence of anhydrite is staggered toward the outcrop of each gypsum seam, so that the combination of overburden plus anhydrite plus interburden in the overlying strata has a cumulative effect on the availability of ground water in the lower seams. The appearance of anhydrite in the top vein generally occurs where the overburden thickness is 35–40 ft. Anhydrite initially appears in the middle part of the gypsum in the top vein and thickens downward, similar to the anhydrite at the Sperry underground mine. However, anhydrite occurs in the lower parts of the middle and bottom veins and forms the floor of the quarry pits in these seams. There is generally no recoverable gypsum in a seam underlying an upper seam that contains anhydrite.

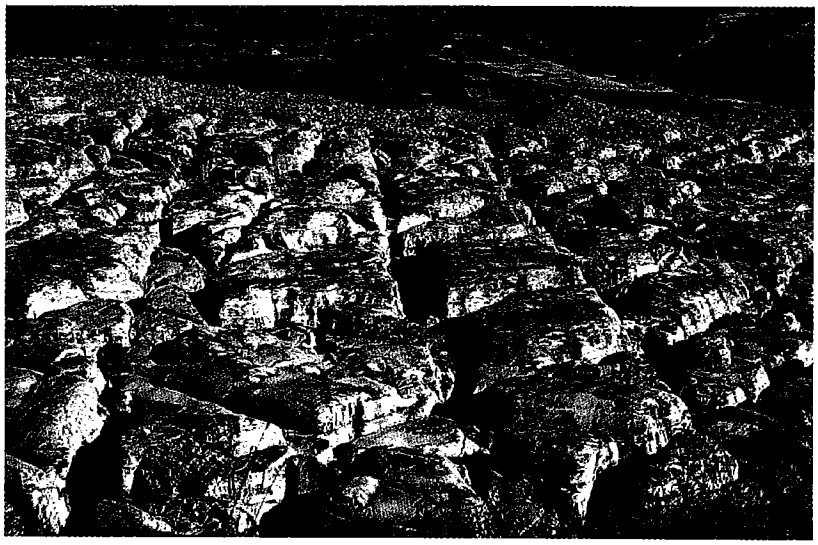

Figure 13. Pattern of solution-enlarged, intersecting joints at Fort Dodge, Iowa.

## Surface Mining—Fort Dodge, Iowa

The geological conditions at Fort Dodge, Iowa, were described in detail in an earlier section. Since the late 1920s, all mining at the USG Fort Dodge operation have been by surface methods. Glacial-till overburden is stripped by pan scraper and disposed of in earlier quarried areas. The top of the gypsum seam is highly dissected by solution-enlarged fractures. The Fort Dodge plant produces high-value-added products, such as specialty plasters and cement products. Therefore, the quarry needs to provide the calcining mill with pure gypsum.

### *Quarrying Conditions*

The top of the gypsum commonly forms a relatively level surface that has been highly dissected into lozenge-shaped blocks by intersecting fractures (Fig. 13). Stripping of the overburden progresses to within a few feet of the gypsum contact. The remaining overburden is scraped off by a hydraulic excavator. Mud-filled, solution-enlarged fractures are cleaned with "dental" precision by Gradall articulated excavators using successively narrower buckets down to 8 in. wide (Fig. 14). Almost all of the mud, clay, and surface-stained gypsum rock are removed by these methods.

The spaces between the blocks of gypsum have to be backfilled with broken gypsum in order to provide a relatively level working surface for a blasthole drill. Because the gypsum is highly dissected, considerable attention is paid to the drilling pattern to ensure efficient breakage of the gypsum.

Gypsum is also recovered in areas that were previously mined underground. Several feet of gypsum was left in the roof of the mine to provide stable underground-mining conditions. The gypsum is currently being recovered in some areas of past underground mining. The bedrock surface of the gypsum is very rough, owing to glacial scouring and proximity to a prominent sand-filled paleo-stream channel. Sinkholes into the underlying underground mine are common at the intersection of enlarged fractures (Fig. 15).

## Pinnacle Terrain

In humid environments the rate of solution and erosion may exceed the rate of hydration of anhydrite to gypsum. The resulting terrain consists of steep pinnacles or "heads" of gypsum or anhydrite alternating with deep pockets filled with mud, clay, and organic material.

Two subsidiaries of USG operate large gypsum quarries in Nova Scotia, Canada. Fundy Gypsum Company operates near Windsor, Hants County. Little Narrows Gypsum Company, Ltd., operates near Baddeck, Victoria County, on Cape Breton Island.

Figure 14. Final surface preparation by cleaning clay from solution-enlarged fractures at Fort Dodge, Iowa.

### *Geological Setting*

The major deposits of gypsum in Nova Scotia occur in the Mississippian Windsor Group. The Windsor Group consists of 2,500 ft of interbedded marine evaporites and nonmarine sediments that were deposited in a large, complex intracontinental basin. The Windsor Group is divided into five subzones representing transgressive–regressive depositional cycles. Economic gypsum and anhydrite deposits occur in the two lowest subzones of the Windsor Group. The earliest cycle (A subzone) represents a single rapid marine transgression and slow regression. The next cycle (B subzone) represents numerous transgressive–regressive pulses with extensive deposition of sulfates. The A subzone consists of as much as 1,000 ft of anhydrite with a variable thickness of near-surface gypsum. The depth of hydration varies from 0 to 250 ft. The B subzone consists of ~1,300 ft of sulfates interbedded with dolomite, limestone, and siltstone. Gypsum occurs to a maximum depth of 330 ft.

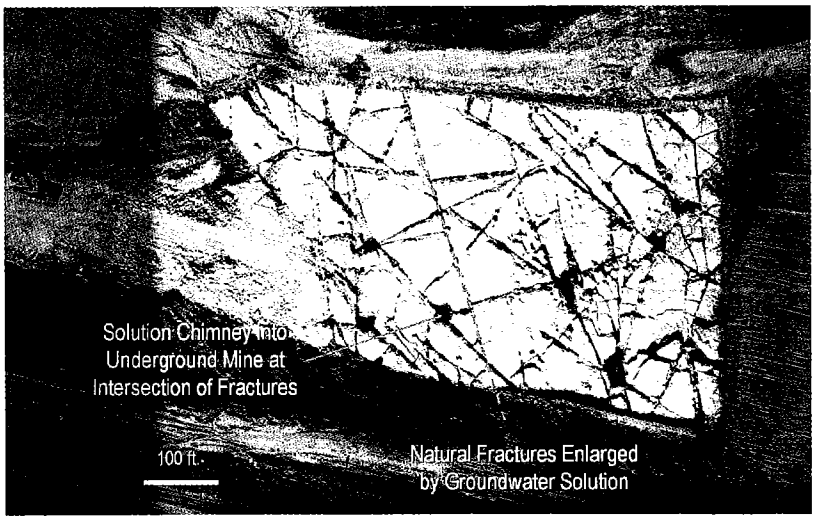


Figure 15. Vertical aerial view of active quarrying over an underground mined area at Fort Dodge, Iowa.

The gypsum and interbedded waste units have been complexly folded and faulted into a series of anticlines and synclines. The folding is complex and varies from upright to recumbent. The folds have been refolded and truncated by normal and reverse faults.

### *Quarrying Conditions*

The surface topography varies from relatively flat, where covered by glacial till, to a deeply incised karst terrain in which gypsum and anhydrite are exposed in outcrop. Solution pits as deep as 60 ft occur between pinnacles of gypsum and anhydrite.

Figure 16 shows sharp, steep outcrops of gypsum, with considerable vegetation growing in the deep intervening pockets. The preparation of quarry workings requires the excavation of the mud and organic material from the deep pits with hydraulic excavators. The initial surface of the gypsum in a newly developed area is extremely rough and requires considerable effort to form a workable surface for blasthole drills, loading, and haulage (Fig. 17).

Figure 16. Pinnacles of gypsum with deep pockets of mud, peat, and vegetation at Little Narrows, Nova Scotia, Canada.

Figure 17. Recently developed quarry area in pinnacle terrain at Little Narrows, Nova Scotia, Canada (see Wilson and Sharpe, 1994).

## REFERENCES CITED

Cody, R. D.; Anderson, R. R.; and McKay, R. M., 1996, Geology of the Fort Dodge Formation (Upper Jurassic), Webster County, Iowa: Iowa Geological Survey Bureau Guidebook Series 19, 74 p.

French, R. R.; and Rooney, L. F., 1969, Gypsum resources of Indiana: Indiana Department of Natural Resources, Geological Survey Bulletin 42-A, 34 p.

Hayes, D. T., 1986, Origin of fracture patterns and insoluble minerals in the Fort Dodge Gypsum, Webster County, Iowa: Iowa State University, Ames, unpublished M.S. thesis, 76 p.

Wilson, G. A.; and Sharpe, R. D., 1994, Quarrying operations of the Little Narrows Gypsum Company, Victoria County, Cape Breton Island, Nova Scotia, Canada: Proceedings of 30th Forum on Geology of Industrial Minerals, Halifax, p. 22–31.

# Evaporite Karst in the Permian Blaine Formation and Associated Strata of Western Oklahoma

***Kenneth S. Johnson***
Oklahoma Geological Survey
Norman, Oklahoma

**ABSTRACT.**—Bedded evaporites (gypsum and salt) of Permian age have been dissolved naturally by ground water to form a major evaporite-karst region in western Oklahoma. The Blaine Formation and associated evaporites comprise 30–250 m of strata that dip gently into broad structural and depositional basins. Fresh ground water has circulated down to the evaporites in the Blaine Formation and associated strata at various times in the past, thus creating the karstic features seen in the evaporites. Ground-water circulation and karst development are ongoing processes in the region, inasmuch as both gypsum and salt deposits are currently being dissolved. Outcropping gypsum, dolomite, and red-bed shales of the Blaine display typical karstic features, such as sinkholes, caves, disappearing streams, and springs. These karst features locally produce the normal problems associated with karst, such as sinkholes and collapse structures. Large caves, such as Jester Cave and Alabaster Cavern, are developed in gypsum beds 3–8 m thick. In southwestern Oklahoma the Blaine aquifer is a major gypsum/dolomite karst unit that provides irrigation water to a large region, and gypsum karst is a major factor in the siting of the Mangum Dam.

Salt karst is present beneath much of western Oklahoma, where salt layers above, within, and below the Blaine Formation have been partly dissolved at depths of 10–250 m below the land surface. Salt dissolution causes development of brine-filled cavities, into which overlying strata collapse. Salt-water brine is emitted at the land surface at nine large salt plains and salt springs in the State, and the brine degrades the quality of water downstream from the emission sites.

Natural-gas blowouts near Elk City and Freedom are both related to natural or man-made dissolution cavities in the Blaine Formation and associated strata.

## INTRODUCTION

Evaporites, including gypsum (or anhydrite) and salt, underlie about 35–40% of the contiguous 48 states of the United States, and they underlie nearly 30% of Oklahoma (all in the western part of the State; Fig. 1). In areas where the evaporites crop out, or are less than 250 m deep, they may be partly or wholly dissolved by unsaturated water to form karst features identical to those formed in carbonates. The present report summarizes the processes, geologic setting, characteristics, and associated problems of a major evaporite-karst region in western Oklahoma, and is modified and updated from an earlier report by Johnson (1992). The study region consists mainly of rural grasslands currently being used for agriculture or ranching; it has a subhumid (nearly semiarid) climate, with precipitation averaging 55–70 cm/year.

Four major evaporite sequences are present in the Permian of western Oklahoma: these include, in ascending order, the Wellington, Cimarron, Beckham, and Cloud Chief evaporites (Jordan and Vosburg, 1963). The current report deals only with the Blaine Formation and associated strata (in the Beckham evaporites), because they contain the most conspicuous, widespread, and problematic karst features in the State.

Overviews of evaporite karst and evaporite-karst processes in the United States are given by Quinlan and others (1986), Johnson (1997, 2001, 2003a), and Martinez and others (1998). Studies dealing with evaporite-karst features in western Oklahoma and adjacent Texas include those of Jordan and Vosburg (1963), McGregor and others (1963), Myers and others (1969), Johnson (1972, 1981, 1986, 1990a,b, 1992, 2003b,c), Gustavson and others (1982), Bozeman (1987), Runkle and Johnson (1988), Hovorka and Granger (1988), Bozeman and Bozeman (2001), Bozeman (2003), Christenson and others (2003), Miller and others (2003), and Tarhule and others (2003). Also, White (1988) provides a good, brief overview of karst processes in evaporite rocks.

## DEVELOPMENT OF EVAPORITE KARST

Whereas most karst features in the world are developed in carbonate rocks, evaporite rocks are much

Johnson, K. S., 2003, Evaporite karst in the Permian Blaine Formation and associated strata of western Oklahoma, *in* Johnson, K. S.; and Neal, J. T. (eds.), Evaporite karst and engineering/environmental problems in the United States: Oklahoma Geological Survey Circular 109, p. 41–55.

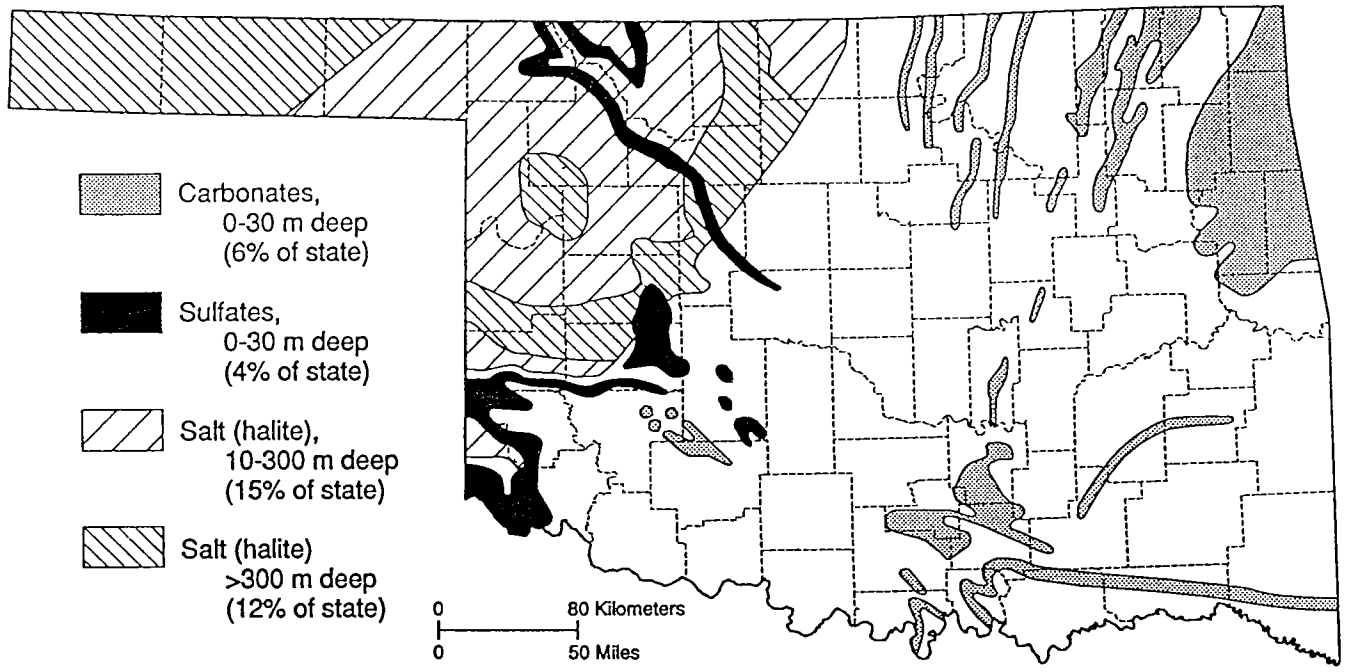


Figure 1. Map of Oklahoma showing generalized distribution of outcropping sulfates (gypsum and anhydrite) and carbonates (limestone and dolomite), and subsurface distribution of bedded rock salt (from Johnson and Quinlan, 1995). These areas represent the general distribution of karst terranes in the State. Outcrops of the Blaine Formation gypsum are those in northwestern and southwestern Oklahoma.

more soluble than carbonates, and they can be sculpted into similar karst features. Karst features develop at a much faster rate in evaporites than in carbonates, and evaporite karst is found at and near the land surface mainly in arid to semiarid areas of the world, where rock-dissolving precipitation and seepage from streams are minimal. The Permian Basin of the southwestern United States, including West Texas, the Texas Panhandle, eastern New Mexico, western Oklahoma, western Kansas, and southeastern Colorado, constitutes the greatest area of evaporite karst in the United States. Principal among the karstic units in western Oklahoma is the Permian Blaine Formation, which, in outcrops, consists of 30–75 m of interbedded gypsum (or anhydrite), dolomite, and shale (Fig. 1). In subsurface, the directly overlying and underlying formations contain interbedded salt and shale, and thus the entire sequence of bedded evaporites locally is as thick as 250 m.

Evaporite-karst features in western Oklahoma are mostly covered by a mantle of overlying soil, sediment, or rocks, but in many areas the gypsum karst is exposed. The term *interstratal karst* (Quinlan and others, 1986; White, 1988) is used for dissolution beneath a covering layer of younger, non-karstic rocks. This term applies to all the salt karst and much of the gypsum karst in western Oklahoma. Fresh water percolates down through overlying rocks and dissolves the salt or gypsum, forming a system of cavities (Fig. 2). As a cavity enlarges, and the roof can no longer be supported, overlying rocks settle or collapse; this disruption of the overlying rocks increases their permeability and allows more fresh water to percolate down to the evaporite rocks (Johnson, 1981).

Gypsum karst is exposed at many places along the outcrop belt of the Blaine Formation. Although gypsum is much more soluble than carbonate rocks, the low rainfall in western Oklahoma inhibits the complete dissolution or erosion of gypsum in most outcrops, and thus the gypsum stands as a resistant and conspicuous caprock on escarpments, buttes, and hills throughout the area. In such areas, the dissolution of gypsum has created a series of sinkholes, caves, and other karst features that are well exposed.

## GEOLOGIC SETTING FOR BLAINE EVAPORITES

The Blaine Formation and associated strata involved in the current evaporite-karst studies in western Oklahoma are of early Guadalupian (Permian) age. They make up a thick sequence of red beds and evaporites deposited in and near a broad, shallow, inland sea that extended north and northeast of the marine-carbonate platform that bordered the Midland Basin (Fig. 3) (Johnson, 1981, 1990b). Evaporites, mainly gypsum (or anhydrite) and salt (halite), were precipitated from evaporating seawater as sedimentary layers on the sea floor, or grew as coalescing crystals and nodules within the mud just below the depositional surface. Thick clastic units, such as red-bed shales, siltstones, and sandstones, were deposited around the perimeter of the evaporite basin, and some of these also extended as blanket deposits across the

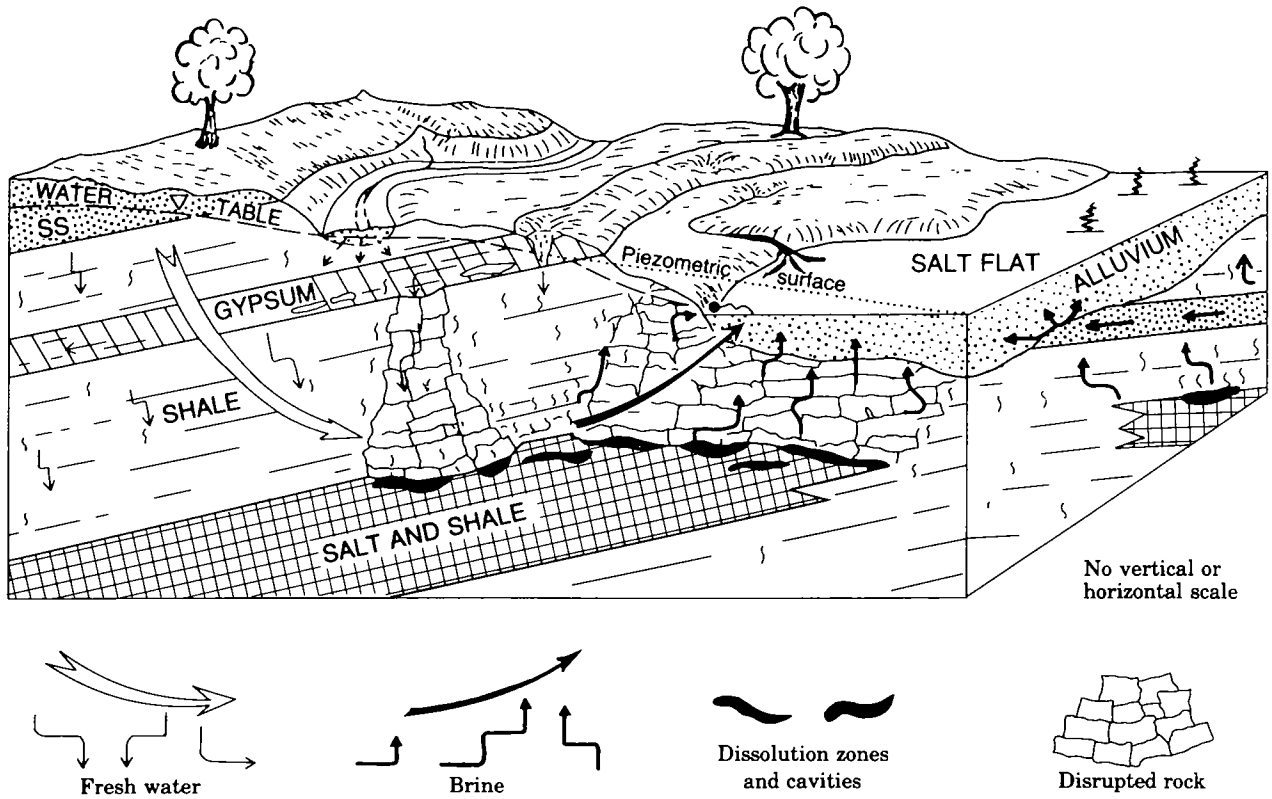


Figure 2. Schematic block diagram of interstratal karst, showing circulation of fresh water and brine in areas of salt dissolution in western Oklahoma (from Johnson, 1981). No scale for diagram, but length may be 1–15 km, and height 30–300 m.

basin. Many thin red-bed clastic units are interbedded with the evaporites.

Evaporites deposited in the inland sea during Permian time now occur in several thick rock sequences that underlie a vast area extending across western Oklahoma and adjacent states (Fig. 4). Principal stratigraphic units studied for this report are (in ascending order) the Flowerpot Shale, Blaine Formation, and Dog Creek Shale (Fig. 5).

In outcrops the Flowerpot typically is 60–100 m thick and consists mainly of reddish-brown shale with thin layers of greenish-gray shale, gypsum, and dolomite. Salt is present in the upper and middle parts of the Flowerpot at shallow to moderate depths, just back from the outcrop in many areas of western Oklahoma and adjacent states (Fig. 5). The total thickness of the Flowerpot salt (the sequence of salt-bearing strata in the upper part of the Flowerpot Shale) generally is 30–90 m (Jordan and Vosburg, 1963). The salt unit consists of reddish-brown shale containing layers, crystals, and veins of transparent, translucent, or opaque salt. Commonly the salt is reddish, owing to red-brown-shale impurities, and in many layers it is intimately intermixed with shale. Individual salt beds typically are 0.5–3.0 m thick, and halite appears to make up about half of the entire Flowerpot salt unit.

Outcrops of the Blaine Formation consist of gypsum beds, typically 2–10 m thick, separated by red-brown shales 2–8 m thick; each gypsum bed is underlain by a dolomite bed that commonly is 0.05–2.0 m thick. Anhydrite, instead of gypsum, normally is present in the Blaine where the unit is >10–60 m below the land surface, and anhydrite also is present in some outcrops. The total thickness of the Blaine ranges from ~30 m in northwestern Oklahoma to 60–75 m in southwestern Oklahoma and nearby parts of Texas. In the deep subsurface of the Anadarko Basin, and farther west in the Texas Panhandle, the Blaine Formation contains several salt interbeds that are each 2–6 m thick.

The Dog Creek Shale consists of 15–60 m of red-bed shales in outcrops, although several gypsum and dolomite beds 0.1–5.0 m thick are present in the lower half of the formation in southwestern Oklahoma and in Texas. The formation also contains 50–100 m of salt interbeds (called the Yelton salt by Jordan and Vosburg, 1963) in the deep Anadarko Basin and in parts of the Texas Panhandle (Fig. 5). The Yelton salt is lithologically similar to the Flowerpot salt.

## GYPSUM KARST

Gypsum and dolomite make up a major karstic unit that crops out and is at shallow depths in southwestern and northwestern Oklahoma. The formation is 30–75 m thick and consists of a sequence of laterally persistent gypsum, dolomite, and shale interbeds. Surface and near-surface Permian strata are essentially structurally undisturbed in western Oklahoma: strata typically dip gently toward the central part of either

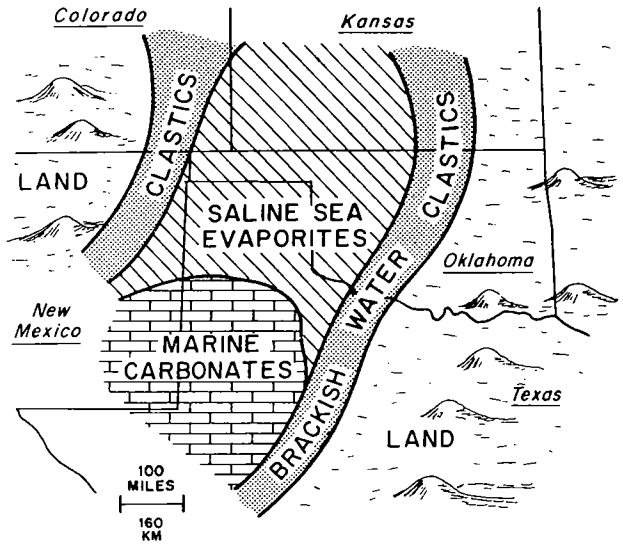


Figure 3. Permian paleogeography and principal facies in southwestern United States during deposition of evaporites in the Blaine Formation and associated strata (from Johnson, 1981).

the Hollis Basin or the Anadarko Basin (Fig. 5) at rates of 2–6 m/km (0.1°–0.3°).

Outcropping and near-surface gypsum and dolomite beds of the Blaine have been partly dissolved by circulating ground water, thus locally creating a cavernous and karstic system. Karst features include sinkholes, caves, disappearing streams, springs, and underground water courses, and in some areas the Blaine is a major aquifer. These features are most common in areas where the Blaine consists predominantly of thick gypsum beds and thin shale interbeds.

The development of porosity, and eventually of the open conduits through which water flows, initially occurs most commonly in the dolomite layers and in the lower part of each of the overlying gypsum beds. Dolomite porosity locally is due to early dissolution of fossils (mainly pelecypod shells), of cement around oolites and pellets, or of small nodules of gypsum; in other places it is intercrystalline porosity. In many places the development of porosity is so advanced that the dolomite beds have a honeycombed appearance, with only a skeletal framework of rock supporting a system of voids.

The early flow of water through the dolomite beds causes concentration of gypsum dissolution at the base of the gypsum beds. Therefore, cavities and caverns most commonly are at and near the contact between gypsum and dolomite layers. Locally, the caverns have been developed along joints and bedding planes in the gypsum, but no preferential orientation of the dissolution features is known yet.

Caverns generally have a height and width that range from a few centimeters to ~3 m, although locally they are up to 18 m wide. Enlargement of individual cavities and caverns occurs from dissolution and also from abrasion by gravel, sand, and silt carried by through-flowing waters. The sediment carried by ground water is deposited locally in the underground caverns, and it partly or totally fills some of the openings, thus forming clay-filled (or sediment-filled) cavities.

In some areas the caverns have become so wide that their roofs have collapsed to partly close the caverns. The collapse structures and resultant fractured rocks thus enable vertical movement of water in many parts of the karst system. Such enhancement of vertical flow of water through fractures and collapse structure accelerates dissolution of all affected strata, thus increasing the amount of karst features in those areas. Dissolution and resultant collapse also can create many problems in the local correlation of strata making up the Blaine: in some boreholes, one or more of the individual gypsum beds have been completely removed by dissolution, and overlying strata have collapsed, apparently occupying the stratigraphic position of the dissolved strata.

Karst features are generally sparse to nonexistent in those areas where the Blaine is buried at depths >20–60 m below the surface. In these areas there has been little or no hydration of massive beds of anhydrite to gypsum, and the pathways for ground-water movement appear to be limited to the dolomite beds.

## Southwestern Oklahoma

Three major karstic aspects of the Blaine Formation have been examined in southwestern Oklahoma: the Blaine aquifer, which provides large quantities of irrigation water in the Hollis Basin area; the D. C. Jester Cave system, the longest known cave system in Oklahoma and, reportedly, the longest gypsum cave in the western world; and the Mangum Dam, a project that for many years was planned in a gypsum-karst area.

### *Blaine Aquifer*

The Blaine aquifer is a major karst aquifer that is providing irrigation water in 2,500 km$^2$ of the Hollis Basin (Fig. 6) in southwestern Oklahoma (Johnson, 1986, 1990a; Runkle and Johnson, 1988). The aquifer typically is 50–65 m thick in the basin and consists of nine thick gypsum units (each 3–8 m thick), interbedded with thin dolomite beds (0.1–1.5 thick) and shale beds (0.3–8.0 m thick) (Fig. 6A).

The Blaine Formation is divided into the Van Vacter Member (above) and the Elm Fork Member (below) (Fig. 6A). The Van Vacter is ~30 m thick and is made up of six evaporite/clastic sequences. In some areas, water moving through the Van Vacter Member has dissolved and removed the gypsum and eroded the thin shales, thus developing a good hydraulic connection among gypsum beds. The Elm Fork Member is ~35 m thick and consists of three evaporite/clastic sequences. Shale beds, which tend to impede the vertical movement of water, are two to five times thicker in the Elm Fork Member than in the Van Vacter Member.

In areas where depths to the top of the Blaine aquifer are greater than 30 m, anhydrite, or a combina-

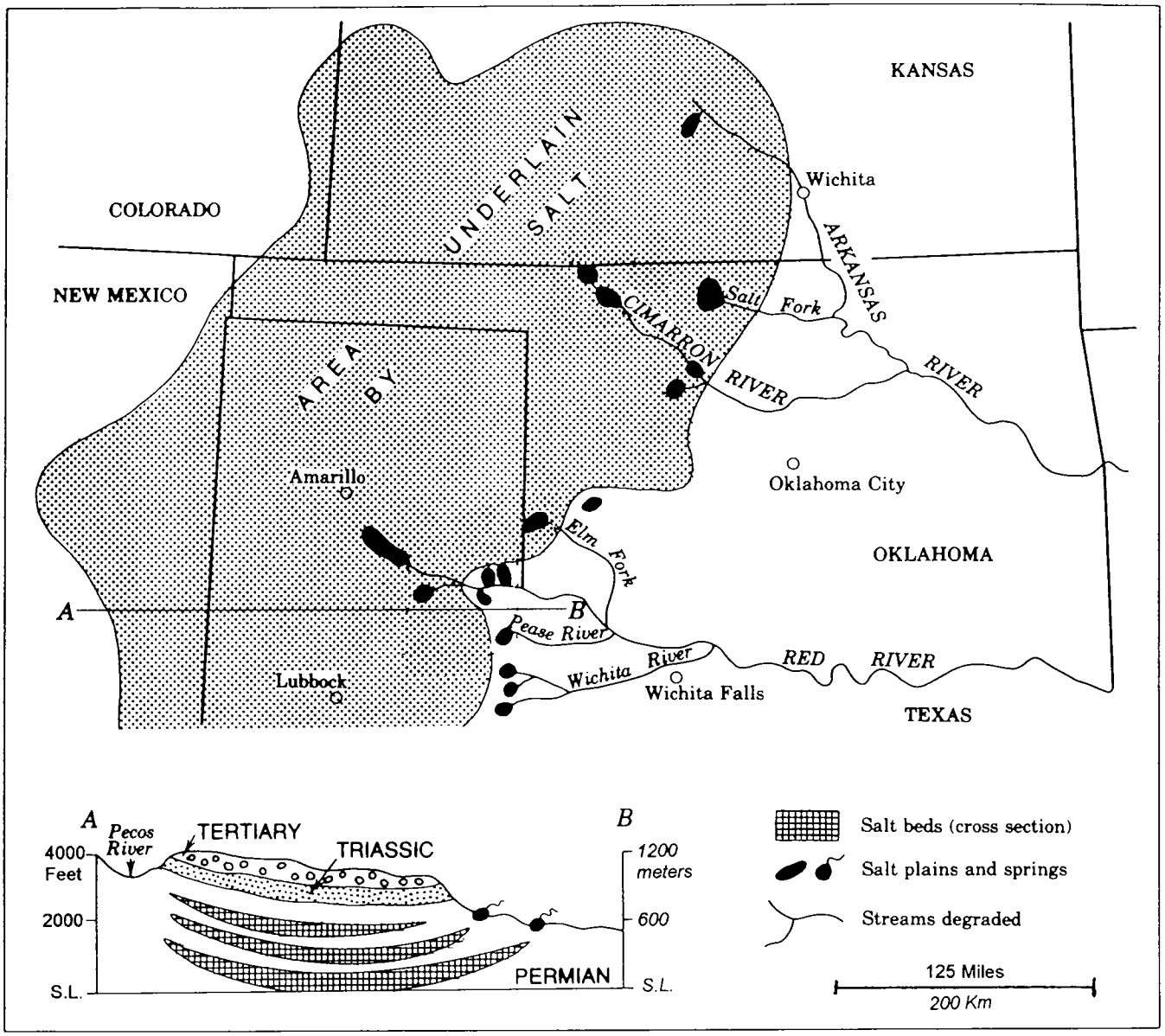


Figure 4. Map and schematic cross section showing distribution of Permian salt, salt plains, and salt springs in western Oklahoma and adjacent areas (from Johnson, 1981).

tion of anhydrite and some gypsum, is present (Fig. 6C). The presence of anhydrite suggests that only small quantities of slow-moving water may have infiltrated the aquifer. Because of the relatively limited contact with fresh water, anhydrite at these depths generally has not been converted to gypsum, and the small amount of gypsum that is present has not been dissolved away. In these areas the permeability of the Blaine aquifer is low (Fig. 6B).

In the western part of the study area the Blaine aquifer is overlain by 15–60 m of Dog Creek Shale, consisting of reddish-brown shale with three notable gypsum and dolomite beds in the lower 20 m (Fig. 6). Where >30 m thick, the Dog Creek Shale generally acts as a confining unit; where it has been eroded to a thickness <30 m, the Dog Creek Shale typically is a leaky confining unit.

The Blaine aquifer is recharged naturally in the following areas (Fig. 6C): (1) mostly where karstic gypsum beds of the Blaine crop out; (2) where the Blaine aquifer is overlain by less than about 30 m of the Dog Creek Shale, which is a leaky confining unit; and (3) where the Blaine aquifer is overlain by alluvium or terrace deposits. The Blaine aquifer typically is an unconfined aquifer, except where overlain by at least 30 m of Dog Creek Shale.

Surface-water recharge to the ground-water system enhances the conversion of anhydrite to gypsum and the dissolution of gypsum, thereby increasing the permeability of the Blaine aquifer (Fig. 6B,C). In many areas less than 5 km from the streams, gypsum and dolomite beds have been largely or totally dissolved, thus creating extensive conduits that allow large quan-

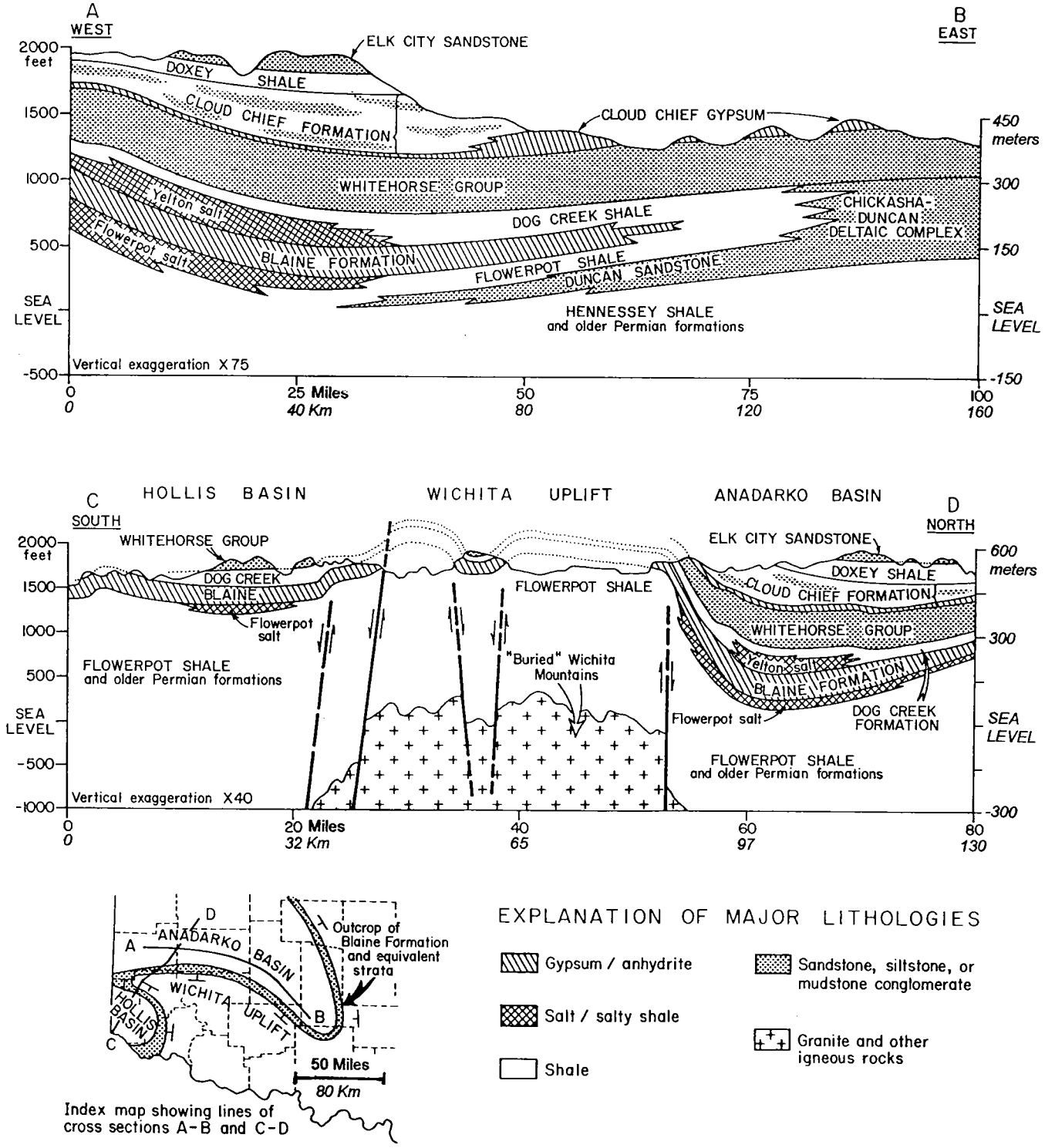


Figure 5. North–south and east–west cross sections, showing stratigraphy and structure of Permian evaporites and other rocks in southwestern Oklahoma (modified from Johnson and Denison, 1973).

tities of water to move rapidly through the aquifer. Steele and Barclay (1965) estimated the following properties for the Blaine aquifer: the transmissivity ranges from ~1,500 to ~5,700 $m^2$/day, with an average of ~3,250 $m^2$/day; and the storage coefficient ranges from ~0.0004 to ~0.03, with an average of ~0.016. The average annual runoff in the study area is estimated at 1.3–3.1 cm, and the average annual evapotranspiration is estimated to be 60 cm (Pettyjohn, 1983).

Irrigation wells completed in the Blaine aquifer are typically 15–100 m deep and commonly yield 1,000–8,000 L/min. The depth to water in the Blaine com-

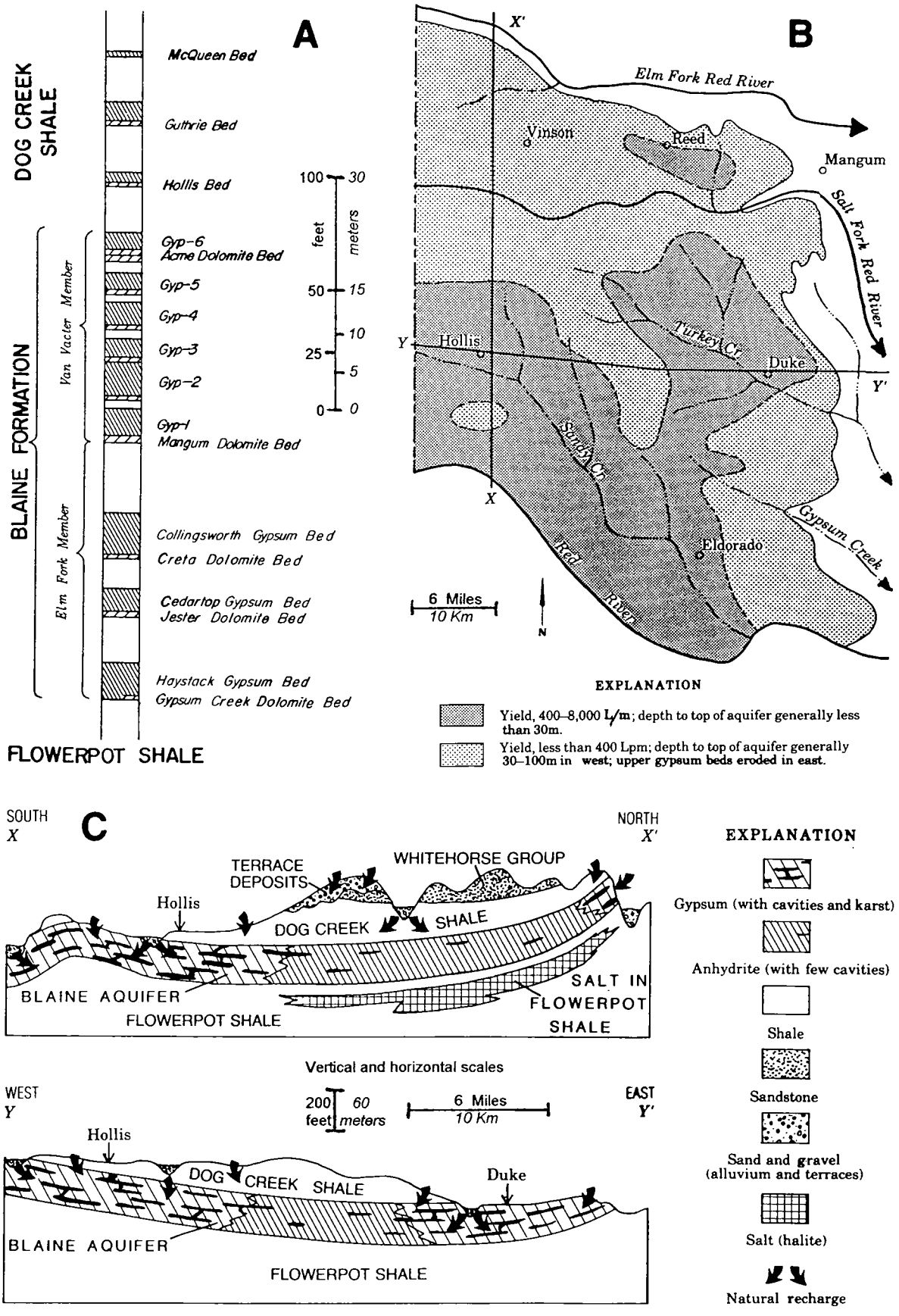


Figure 6. Hydrogeology of the Blaine aquifer in the Hollis Basin of southwestern Oklahoma (from Johnson, 1986, 1990a). (A) Standard stratigraphic column. (B) Map showing ground-water yields and depth to the aquifer. (C) Two cross sections through the irrigation district; lines of sections shown in map B.

monly is ~1.5–25 m below land surface. The water is a calcium sulfate type; the average dissolved-solids concentration is ~3,100 mg/L, which is suitable for irrigation but generally is unsuitable for drinking. At a few localities, sodium and chloride concentrations are high enough to kill irrigated crops, but in general there has been no harmful buildup of other salts in soils that have been irrigated for more than 50 years.

### *D. C. Jester Cave*

The D. C. Jester Cave system was surveyed between 1983 and 1987 (Bozeman, 1987; Johnson, 1990a; Bozeman and Bozeman, 2001). The surveyed length of the main passage is 2,413 m, but, along with side passages, the total length is 10,065 m, making Jester Cave the longest cave in Oklahoma and the longest gypsum cave reported in the western world (Bozeman, 1987). The cave follows a sinuous course, with the passageways generally 1–3 m in diameter. It is a dry cave except during and after periods of moderate rainfall.

Most parts of the Jester Cave system are developed in a 5-m-thick bed of white gypsum (gypsum bed 1) near the base of the Van Vacter Member of the Blaine Formation (Fig. 7A). This gypsum directly overlies 0.5 m of resistant Mangum Dolomite that forms the floor of the main cave in many areas. In addition to the main cave, many tributary branches are present in the cave system. There are also many sinkholes and other entrances to the cave system from the land surface (Fig. 7A).

The local structure of the Jester Cave area consists of Blaine strata dipping toward the west and southwest at ~10 m/km (~0.5°). A cursory examination of the alignment of various segments of the cave system suggests that they may be controlled by several sets of joints or fractures in the rock. If subtle joint patterns do control the cave system, then ground water has dissolved the rock and moved along the principal joint system until it intersected a cross-cutting joint; the water then followed that cross-cutting joint for a short distance until it again encountered another solutionally enlarged fracture in the principal joint system.

### *Mangum Dam*

Recent engineering-geology assessment of a proposed damsite in an area of gypsum karst in southwestern Oklahoma has shown that the site is unsuitable and should be abandoned, and that an alterna-

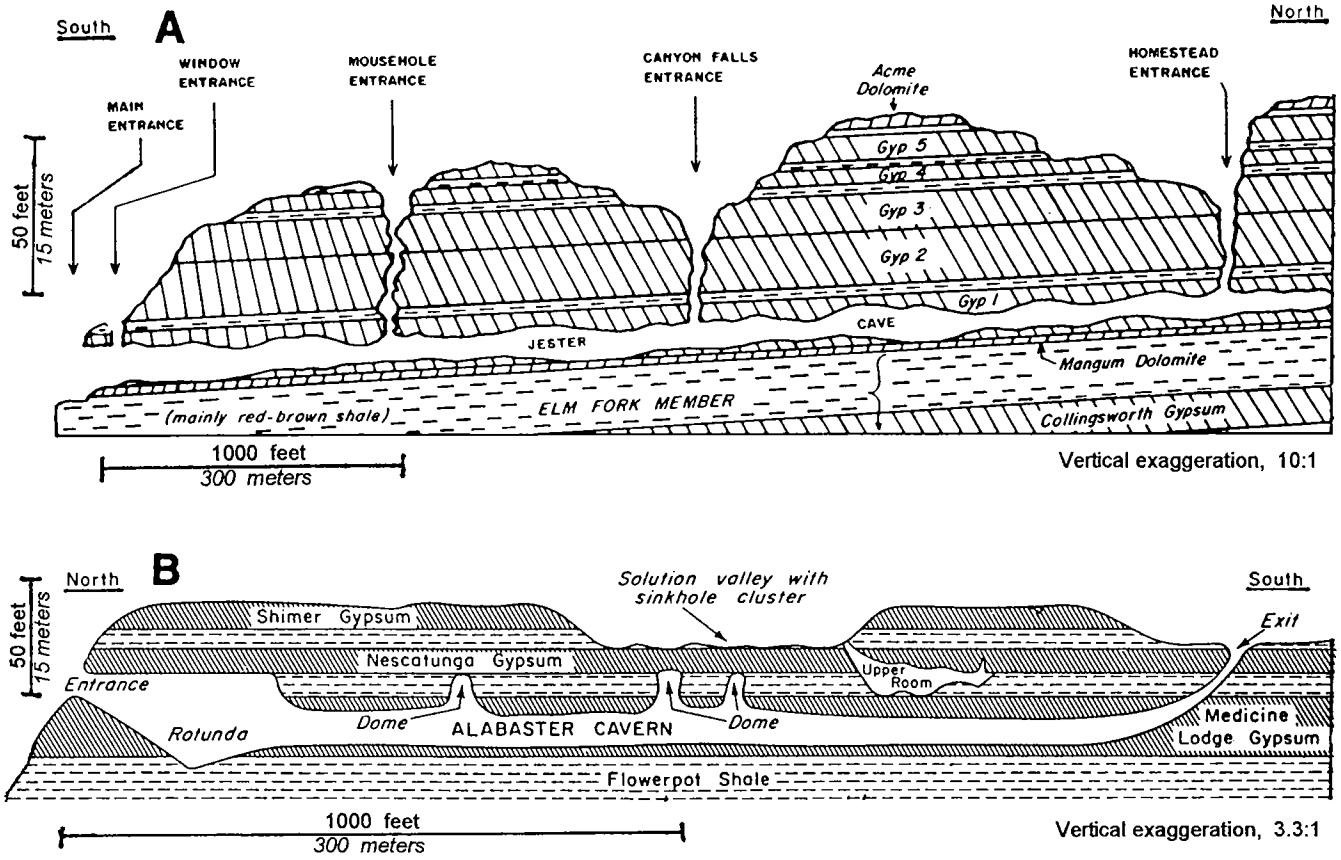


Figure 7. Schematic cross sections through major gypsum caves in the Blaine Formation of western Oklahoma. (A) D. C. Jester Cave, developed in gypsum bed 1 near the base of the Van Vacter Member in southwestern Oklahoma (from Bozeman, 1987; Johnson, 1990a). (B) Alabaster Cavern, developed mainly in the Medicine Lodge Gypsum in northwestern Oklahoma (from Myers and others, 1969).

tive site would be more acceptable. The proposed Mangum Damsite has been investigated and evaluated since 1937 as a potential site for a compacted, earth-fill dam, about 33 m high, that would provide for irrigation water, flood control, and recreation. The initial site, the Upper Mangum Damsite, is ~14 km west of Mangum on the Salt Fork of Red River (Fig. 8). The original approval of this site was based only upon its favorable topography; both proposed abutments are high and are separated by a narrow water gap. This decision did not adequately consider the geology, foundation conditions, or water-impoundment capabilities of the site. Abutments would be in the Blaine Formation, here consisting of 60 m of gypsum with thin interbeds of dolomite and shale (Fig. 8). The Blaine Formation locally has abundant gypsum-karst features, such as caves, sinkholes, disappearing streams, and springs. Efforts since 1937 focused on finding a suitable location for the Upper Mangum Damsite, where karst problems would be minimal within the flat-lying Blaine Formation.

In 1999, a final assessment was made of the surface geology and the results of coring and pressure testing of five boreholes (each 40–46 m deep) along the proposed dam alignment (Johnson, 2003b). The assessment showed that open cavities, clay-filled cavities, and other karst features are abundant in and near the abutments (Fig. 8); and fluid losses (in each 3-m interval that was tested) ranged from 60 to 250 L/min in most borehole pressure tests, and in one borehole all losses were 1,600–5,300 L/min. Engineering measures needed to remediate karstic-foundation condi-

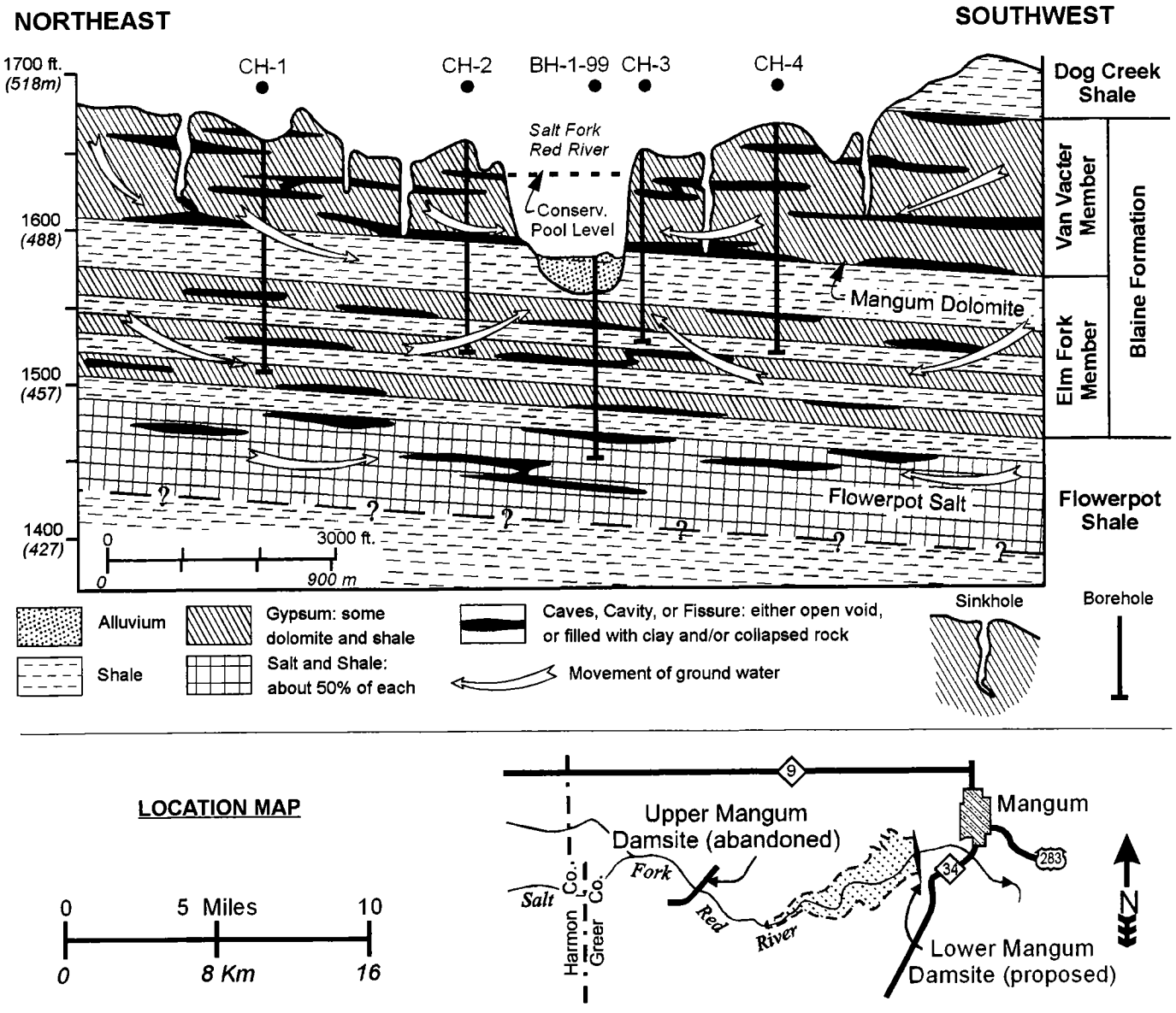


Figure 8. Schematic cross section along alignment of proposed Upper Mangum Dam, looking downstream (from Johnson, 2003b). Although the topography was favorable at this site, extensive karst features (caves, cavities, fissures, and sinkholes) in gypsum, dolomite, and salt led to its abandonment.

tions here would add greatly to the cost of construction and still would not assure tightness of the reservoir or integrity of the dam. It was therefore recommended that further examination of the Upper Mangum Damsite be abandoned (Johnson, 2003b).

As a result, the first site was abandoned, and a study of the Lower Mangum Damsite was initiated in 2002 (Johnson, 2003c). This newly proposed damsite is 11 km farther downstream on the Salt Fork of Red River, just 3 km west of Mangum (location map in Fig. 8). The foundation and abutments here would be below the Blaine gypsums, in the thick Flowerpot Shale. On the basis of geologic and hydrogeologic field studies, along with core study, pressure tests, and laboratory tests of cores, the foundation conditions at this damsite appear favorable (Johnson 2003c). However, owing to the presence of the karstic Blaine Formation in upper reaches of the proposed Lower Mangum impoundment area, there will be limitations on the lake level, size, and storage capacity at the new location. If the reservoir level here is too high, it may cause excess water to escape from the lake in the upper reaches; the water then will enter a subsurface gypsum-karst conduit in the Blaine Formation, and flow as ground water out of the reservoir and into a different watershed. Investigations at the Upper and Lower Mangum Damsites demonstrate the importance of hydrogeological studies in areas of evaporite karst for planning the location and size of potential dams and reservoirs.

### Northwestern Oklahoma

Northwestern Oklahoma contains a number of gypsum-karst features. The speleology of caves in the region is discussed by Bozeman and Bozeman (2001), and the Nescatunga Cave is described elsewhere in this volume (Christenson and others, 2003; Miller and others, 2003; Tarhule and others, 2003). But the best known and most visited karst site in the region is the Alabaster Cavern area of Woodward County.

#### *Alabaster Cavern*

Alabaster Cavern was discovered by settlers in the late 1800s and was first explored in 1898; but tourism at the cave was not seriously encouraged until the mid-1950s (Myers and others, 1969). The main cave, as well as four other known smaller caves, are now included in the Alabaster Caverns State Park, one of the finest tourist attractions in northwestern Oklahoma. The following description is based mainly upon the study by Myers and others (1969).

Alabaster Cavern is almost wholly developed within the Medicine Lodge Gypsum Bed, near the base of the Blaine Formation (Fig. 7B). The accessible part of the cave is about 700 m long and has a maximum width of 18 m and a maximum height of 15 m. Although there are many branches from the main chamber, most lateral openings are small and have not been explored. A second, smaller cave, called the Upper Room, has developed in the Nescatunga Gypsum and its underlying shale (Fig. 7B). The Upper Room has a single known opening through a sinkhole. Although no large opening has been found connecting the Upper Room to Alabaster Cavern, there are probably small, open crevices or tubular connections.

Alabaster Cavern consists of three main sections, each of nearly equal length: a collapse section near the entrance, a middle section with domes in the roof, and a channel section at the end. In the collapse section, the cavern floor is a mass of gypsum, shale, and selenite boulders that have fallen from the roof. In the Rotunda, the first and largest room, the roof is the base of the Nescatunga Gypsum, and the floor is part of the Flowerpot Shale: thus, the entire Medicine Lodge Gypsum has been dissolved here, and parts of the underlying and overlying shales are also eroded.

The ceiling of the middle section is characterized by many domes. The land surface above the dome section is a dissolution valley with a cluster of sinkholes that recharge the perennial stream flowing through the cave. The abrasive action of the underground stream that helped form the cavern is best seen in the channel section, where the gypsum roof, walls, and floor are smooth and polished.

Rock layers at Alabaster Cavern are essentially flat-lying: they dip no more than 1–2 m/km (<0.1°). The strata are not faulted or noticeably jointed, and there is no conspicuous alignment to various segments of the cave system or drainage features. The control for development of the cave system is not clear, but most likely it is the result of faint and irregular fractures in the rock that have established slightly preferential zones of ground-water dissolution; and these fissures then were widened by through-flowing waters, once the underground stream system was developed. Myers and others (1969) believe that Alabaster Cavern probably began to develop in the latter part of the Pleistocene Epoch, when the nearby major river and its tributaries cut down to elevations below the Blaine gypsums.

## SALT KARST

Salt (halite) beds in the Flowerpot, Blaine, and Dog Creek Formations (Fig. 5) are being dissolved naturally at shallow to moderate depths in western Oklahoma. They are the shallowest salt beds in most areas underlain by salt (Fig. 1), and these strata constitute a significant interstratal karstic unit in the region. The most conspicuous surface manifestations of natural salt-karst processes are the large and barren, salt-encrusted salt plains that have formed in a number of stream and river courses where the high-salinity brines are being emitted (Figs. 2, 4). Data on natural salt karst in this region are mainly from Johnson (1981). In addition, human activities in the Elk City and the Freedom areas of western Oklahoma have triggered problems related to salt dissolution and salt karst.

Fresh ground water is recharged generally to the west of the salt plains, in upland areas where uncon-

solidated sands, sandstone, gypsum, dolomite, alluvium, or terrace deposits are at the surface (Fig. 2). This water migrates downward and laterally (eastward) to salt beds that are 10–250 m below the surface, and dissolves the salt to form brine. The resulting brine is then forced laterally and upward by hydrostatic pressure through aquifers or through fractures in aquitards until it is discharged at the surface (Fig. 2). Fresh water and the brines can flow laterally in the subsurface through aquifers, such as sandstone or cavernous gypsum, dolomite, or salt, and the water also can move vertically through fractures, sinkholes, and collapse features.

A total of nine significant salt plains and salt springs are present in western Oklahoma (Fig. 4; three of the salt plains on Elm Fork, in the southwest, are shown together on the map). Several of the salt plains are only 2–10 hectares in size, whereas the two largest are 16 and 64 $km^2$. Individual salt plains release brines with concentrations of 20–340 g NaCl/L, and each contributes 100–3,000 metric tons of NaCl per day that degrades the quality of water flowing in the Arkansas and Red River systems.

Salt is highly soluble, more soluble than any other rock in the Permian sequence of western Oklahoma and nearby areas. Ground water in contact with salt will dissolve some of the salt, providing the water is not already saturated with NaCl. For extensive dissolution to occur, it is necessary for the brine thus formed to be removed from the salt deposit; otherwise the brine becomes saturated, and the process of dissolution stops.

Four basic requirements are necessary for salt dissolution to occur here, or in other evaporite basins (Johnson, 1981): (1) a deposit of salt against which or through which water can flow, (2) a supply of water unsaturated with NaCl, (3) an outlet whereby the resulting brine can escape, and (4) energy (such as a hydrostatic head or density gradient) to cause the flow of water through the system. When all four of these requirements are met, salt dissolution and brine transport can be quite rapid, in terms of geologic time.

There are four principal ways whereby fresh ground water is recharged in the region (Fig. 2): (1) water seeps into the ground through permeable rocks and soils, such as in areas where sands or sandstones are at the surface; (2) water enters the bedrock through highly permeable alluvium and terrace deposits along and near the major streams and rivers; (3) water enters the ground through sinkholes, caverns, and other karstic features, in areas where gypsum, dolomite, or limestone is at the surface; and (4) water enters the ground through joints and fractures in the rocks, particularly where underlying salt beds are partly dissolved and the rock is more fractured owing to collapse.

After the water has dissolved some of the salt and has become brine, there are six principal ways whereby the brine moves underground and is eventually discharged (Fig. 2): (1) brine moves through dissolution cavities in the salt or other soluble rocks; (2) brine moves vertically and/or laterally through joints and fractures, particularly where the rock is disrupted over dissolution cavities; (3) brine moves laterally through aquifers consisting of sandstone, siltstone, or other permeable rocks; (4) brine may be discharged at a point source as a saline spring; (5) brine may be discharged along the course of a stream bed and become part of the surface flow; and (6) brine may enter the base of an alluvial deposit, where it can be forced upward under hydrostatic pressure and then drawn upward by capillary action as the brine is evaporated; a thin crust of salt then is precipitated on the land surface as water is evaporated from the brine.

In all cases cited above, the energy needed to cause flow of the water is the hydrostatic head created in the recharge areas. The brine moves laterally and upward toward the piezometric surface (Fig. 2).

The process of salt dissolution produces cavities, normally at the updip limit or at the top of the salt unit, into which overlying rocks can settle or collapse chaotically (Fig. 2). Disrupted rock helps to make salt dissolution a somewhat self-perpetuating process, inasmuch as cavern development, followed by collapse and fracturing of the rock, will cause a greater vertical permeability, and this allows further access of fresh water to the salt. In most areas, strata overlying a salt-dissolution zone are mildly to intensely folded, faulted, jointed, or fractured where they have collapsed and subsided into the dissolution cavities. It is possible that collapse of overlying rock into the cavity can ultimately reach up to the land surface as a sinkhole or subsidence feature, and this can be a danger to humans, livestock, or property.

Boreholes drilled in and around the salt plains commonly encounter artesian flows of brine. Solution cavities or zones of lost circulation 0.1–1.0 m thick are also common at or near the top of the salt unit, but these features generally are absent within the salt unit (Fig. 2). Such cavities represent the zones at which dissolution is most actively taking place, and the pathways whereby high-salinity brine is escaping from the salt beds. The thin, somewhat cavernous zone at the top of the salt typically is an artesian aquifer, wherein the piezometric surface locally is at, or just above, the elevation of the surface of the salt plains (Fig. 2).

## Salt-Dissolution Problems Associated with Human Activities

Human activities have caused evaporite-karst problems at various places in the United States, particularly in salt deposits (Johnson, 2003a), and some of these problems also have occurred in Oklahoma. Boreholes have been drilled into salt deposits to create underground solution caverns in the State (Jordan and Vosburg, 1963), and one of these caverns (near Elk City) ultimately developed a leak that caused a catastrophic blowout at the land surface. Also, a petro-

leum test that was drilled through a zone of natural salt karst apparently allowed natural gas to escape from the well, migrate 16 km laterally through solution cavities, and emerge in blown-out craters near Freedom in northwestern Oklahoma.

### *Elk City Blowout*

In February 1973 a landowner in rural Beckham County, western Oklahoma, reported that a creek bed on his land was blown out and uplifted 1.5–6 m or more (Fay, 1973a,b). The blowout site consisted of (1) a central crater 9 m wide, 15 m long, and 6 m deep; (2) pressure cracks (with 1.5–3 m of uplift) radiating as much as 50 m from the crater; (3) tension zones with cracks up to 0.3 m wide and 2.5 m deep; and (4) ejecta, consisting of 0.3-m blocks of rock weighing up to 33 kg, thrown as much as 23 m from the crater (Fay, 1973b). Monoliths thrown up around the main crater were up to 1 m thick, 3 m wide, and 6 m high, and weighed an estimated 30 metric tons; once-horizontal slabs of bedrock were tilted 28° to 78° from the horizontal (Fig. 9).

The Elk City blowout occurred in the NE¼ sec. 22, T. 10 N., R. 21 W., ~10 km south of Elk City. This site also is close to the Shell Oil Company natural-gas-processing plant, where LPG (liquefied petroleum gas), mostly propane, was being stored in an underground cavern formed by intentionally dissolving salt in the Van Vacter Member of the Blaine Formation (Jordan, 1959; Jordan and Vosburg, 1963). The storage cavern, completed in 1954, was at a depth of 415–430 m in the Shell No. 1-LPG Yelton well, in the SE¼ sec. 15, ~700 m north of the blowout. The cavern is in the Blaine Formation, in the deep part of the Anadarko Basin (see Fig. 5, cross section C–D).

Fay (1973b) concluded, on the basis of information from cooperative Shell Oil Company officials and various State and federal agencies, that long-term undetected leakage of small amounts of propane through near-surface casing in the No. 1-LPG Yelton well had occurred. Propane evidently accumulated in a shallow, permeable siltstone (a "thief" zone) and migrated laterally away from the well until it burst to the surface along natural joint patterns. The blowout was an explosive event that caused no injuries, and it was not heard or observed. On March 12, 1973, the blowout site was bulldozed and restored to its normal appearance.

### *Freedom Gas Blowout*

On January 31, 1980, natural gas erupted at a number of sites in the flood plain and valley of Cimarron River, about 6 km northwest of the town of Freedom, in northwestern Oklahoma (Fig. 10; Preston, 1980a,b). The rural site, along the Woods-Woodward county line, is ~5 km west of the crossroads at Camp Houston, and ~45 km north-northeast of Woodward. Surficial deposits in the Cimarron River Valley are Quaternary alluvium and terrace deposits that mantle the Flowerpot Shale, which is the bedrock in the valley.

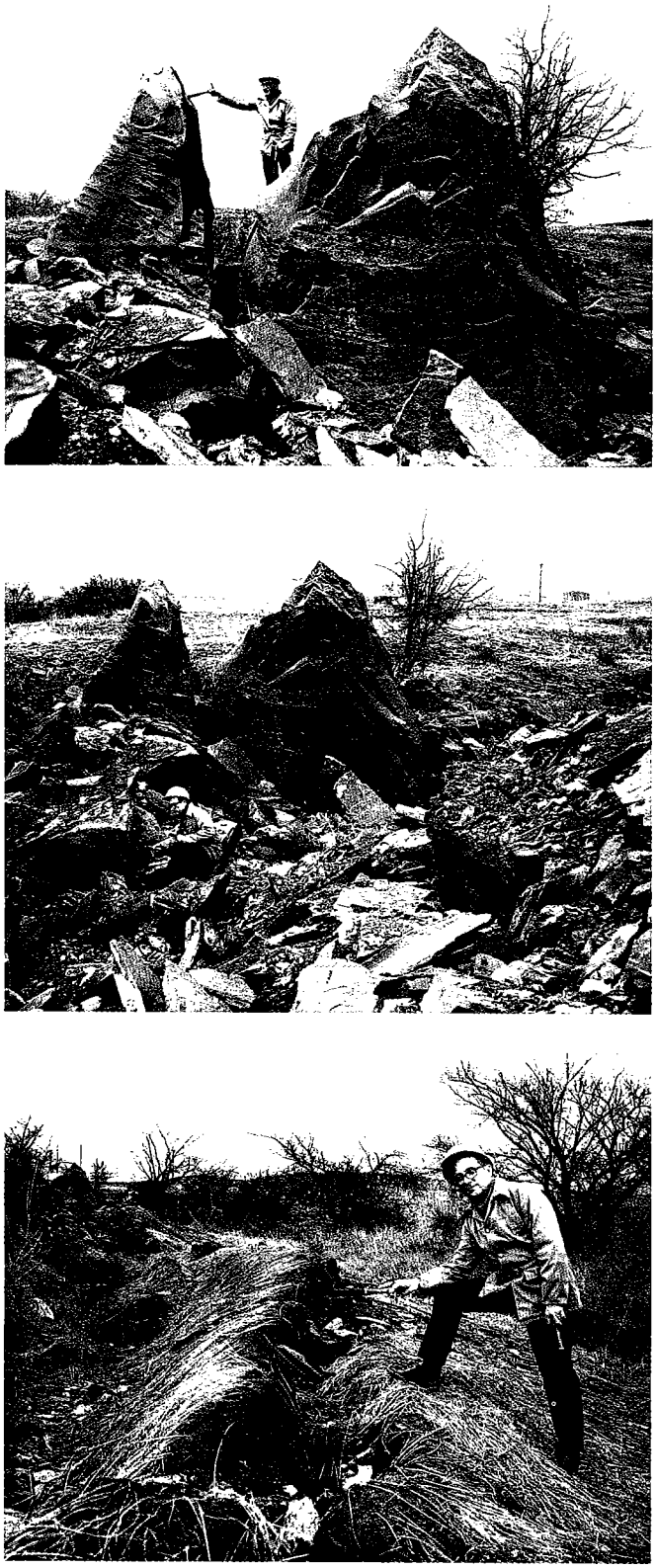

Figure 9. Views of Elk City blowout, with Robert O. Fay for scale. *Top,* large uplifted vertical blocks of siltstone stand 6 m high and weigh 30 metric tons. *Middle,* view of same uplifted blocks, with Shell Oil Company natural-gas-processing plant in right background. *Bottom,* pressure cracks up to 50 m long raised the ground about 1.5–3 m.

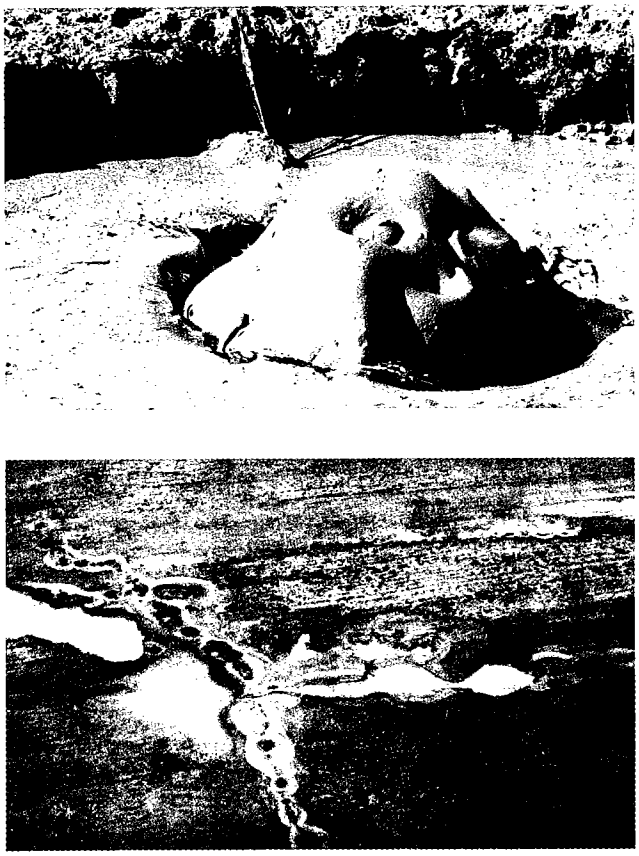

Figure 10. Views of Freedom gas blowout in northwestern Oklahoma (from Preston, 1980). *Top,* a gas bubble rises about 0.5 m in one of the larger mud craters. *Bottom,* gas vents and craters in the Cimarron River flood plain reflect fracture orientations in the underlying Flowerpot Formation.

Just 3 km west of the blowout area is the Big Salt Plain, an area well known for natural dissolution and intrastratal karst in the Flowerpot salt, and the natural emission of salt-saturated brines onto this salt plain on Cimarron River (Johnson, 1970, 1972, 1981; Joachims, 1999). In the blowout area the depth to the top of the karstic Flowerpot salt is ~60 m, and the depth to the top of the Cimarron salts is ~150 m.

Initial venting occurred along a county road (SW¼ sec. 19, T. 27 N., R. 18 W.), creating a 6-m-wide crater from which viscous mud was ejected to a height of more than 15 m (Preston, 1980b). Other craters in the area were up to 9 m wide and 3.7 m deep. More than 50 separate vents were mapped in an area ~1.5 km by 2.5 km, although there were also many more small craters, collapsed fissures, and violently boiling bubble trains in local stock ponds. Within 2 days, many large fish and much of the other aquatic life in the ponds began to die. Preston (1980a,b) estimated that the total gas emitted from the larger vents alone was about 20 million cubic feet per day; but he felt this was a highly conservative estimate for the total emissions, because it did not include gas from the smaller vents or the general effusion of gas through the sandy soils.

Initially, a mechanical failure in one of the several nearby gas-producing wells was suspected as the source of the gas. However, all these wells were checked and found to be intact. Comparison of analyses of the escaping gases with wellhead samples in the area showed that these gases were probably coming from the Mississippian Chester/Oswego interval, at depths of ~1,700 m in the area. A temperature log run on a nearby well disclosed a temperature anomaly in the Cimarron evaporites at a depth of 180–200 m. Preston (1980a,b) presumed that this anomaly resulted from natural gas entering the wellbore at this depth, between the wall rock and the production casing.

Although the origin of the gas has not been proven, the Oklahoma Corporation Commission, which regulates oil and gas activities in the State, finally concluded that the gas probably came from a well ~16 km southwest of the blowout (Vanderwater, 1980). The well, the National Cooperative Refining Association No. 1-31 Selman (SE¼ sec. 31, T. 26 N., R. 19 W.), was spudded on January 2, 1980, and casing was set and cemented at a depth of 305 m in the Cimarron anhydrite. The overlying Upper Cimarron salt appears to be absent in this hole (apparently due to salt dissolution), and the Lower Cimarron salt is present just 26 m below the Cimarron anhydrite. The hole was finally drilled to a depth of 2,449 m. Following a drillstem test at the bottom of the hole, high-pressure natural gas in the well caused a blowout just 4 days prior to the initial gas eruptions near Freedom. During drilling of the NCRA well, a lost-circulation zone was encountered at a depth of 54 m, a depth that is within the Flowerpot salt (known for its salt-karst features in the region).

Commission officials concluded (Vanderwater, 1980) "that the same pressure that caused the blowout at the NCRA well fractured the underground rock. That let natural gas below the well's casing [set at 305 m] enter caverns which honeycomb the area, building up pressure there and eventually erupting through weak surface points like cracks and under ponds." If that analysis is correct, then high-pressure gas escaping from the NCRA well may have (1) entered the intrastratal karst system in the Cimarron and/or Flowerpot salt; (2) migrated laterally for 16 km to the northeast, through salt-dissolution cavities; and (3) then (within 4 days) reached the land surface through the fractured Flowerpot Shale, which overlies the salts.

So, if these events did occur, salt karst was instrumental in allowing fugitive, high-pressure natural gas to travel a long distance in a short period of time, thus creating a potentially hazardous condition at a site far removed from the site of the initial well blowout.

## SUMMARY AND CONCLUSIONS

The Blaine Formation and associated strata constitute a major evaporite-karst unit in western Oklahoma and adjacent areas. Gypsum, dolomite, and shale interbeds, with an aggregate thickness of 30–75 m in outcrops, contain a well-developed suite of karstic fea-

tures, such as caves, sinkholes, disappearing streams, and springs. Where these same strata are in the shallow subsurface, they locally are a major karst aquifer used beneficially as a source of irrigation water. But elsewhere, gypsum karst can create problems, such as difficulty in the siting of a dam in the Mangum area of southwestern Oklahoma.

Where salt is interbedded with red-bed shale, gypsum (or anhydrite), and dolomite in the deeper subsurface, the evaporite unit typically is 100–250 m thick. Salt at depths of 10–250 m below the surface locally is being dissolved by ground water to form a karst system typified by brine-filled cavities, collapse structures (in overlying strata), salt plains, and salt springs. Salt-rich brine emitted at the land surface degrades the quality of water in several of the major rivers and streams of Oklahoma. Also, human activities in salt-karst areas may trigger problems such as those associated with the storage of LPG in an underground salt-dissolution cavern near Elk City, and drilling through natural salt-dissolution cavities in the vicinity of Freedom.

## REFERENCES CITED


Bozeman, John, 2003, Exploration of western Oklahoma gypsum caves, *in* Johnson, K. S.; and Neal, J. T. (eds.), Evaporite karst and engineering/environmental problems in the United States: Oklahoma Geological Survey Circular 109 [this volume], p. 57–64.

Bozeman, J.; and Bozeman, S., 2001, Speleology of gypsum caves in Oklahoma, *in* Gunay, G.; Johnson, K. S.; Ford, D.; and Johnson, A. I. (eds.), Present state and future trends of karst studies; Proceedings of the 6th International Symposium and Field Seminar, Marmaris, Turkey, September 17–26, 2000: UNESCO, IHP-V, Technical Documents in Hydrology, no. 49, v. 1, p. 155–163. (Reprinted in 2002 in Carbonates and Evaporites, v. 17, no. 2, p. 107–113.)

Bozeman, S. (ed.), 1987, The D. C. Jester Cave system: Central Oklahoma Grotto, Oklahoma Underground, v. 14, 56 p.

Christenson, Scott; Hayes, Curtis; Hancock, Earl; and McLean, John, 2003, Correlating the location of a cave passage in gypsum karst to a highway right-of-way using a cave radio, *in* Johnson, K. S.; and Neal, J. T. (eds.), Evaporite karst and engineering/environmental problems in the United States: Oklahoma Geological Survey Circular 109 [this volume], p. 65–70.

Fay, R. O., 1973a, The Elk City blowout: Oklahoma Geology Notes, v. 33, p. 29–30.

_____1973b, The Elk City blowout—a chronology and analysis: Oklahoma Geology Notes, v. 33, p. 135–151.

Gustavson, T. C.; Simpkins, W. W.; Alhades, A.; and Hoadley, A., 1982, Evaporite dissolution and development of karst features in the Rolling Plains of the Texas Panhandle: Earth Surface Process and Landforms, v. 7, p. 545–563.

Hovorka, S. D.; and Granger, P. A., 1988, Subsurface to surface correlation of Permian evaporites—San Andres–Blaine–Flowerpot relationships, Texas Panhandle, *in* Morgan, W. A.; and Babcock, J. A. (eds.), Permian rocks of the Midcontinent: Midcontinent SEPM Special Publication 1, p. 137–159.

Joachims, G., 1999, Solar-salt production in northwest Oklahoma, *in* Johnson, K. S. (ed.), Proceedings of the 34th Forum on the Geology of Industrial Minerals, 1998: Oklahoma Geological Survey Circular 102, p. 69–71.

Johnson, K. S., 1970, Salt produced by solar evaporation on Big Salt Plain, Woods County, Oklahoma: Oklahoma Geology Notes, v. 30, p. 47–54.

_____1972, Northwest Oklahoma, *book II of* Guidebook for geologic field trips in Oklahoma: Oklahoma Geological Survey Educational Publication 3, 42 p.

_____1981, Dissolution of salt on the east flank of the Permian Basin in the southwestern USA: Journal of Hydrology, v. 54, p. 75–93.

_____1986, Hydrogeology and recharge of a gypsum-dolomite karst aquifer in southwestern Oklahoma, USA, *in* Gunay, G.; and Johnson, I. V. (eds.), Karst water resources; Proceedings of the International Symposium on Karst Water Resources, Ankara, Turkey, July 7–19, 1985: International Association of Hydrological Sciences Publication 161, p. 343–357.

_____1990a, Hydrogeology and karst of the Blaine gypsum–dolomite aquifer, southwestern Oklahoma (guidebook for field trip no. 15, Geological Society of America annual meeting, 1990): Oklahoma Geological Survey Special Publication 90-5, 31 p.

_____1990b, Standard outcrop section of the Blaine Formation and associated strata in southwestern Oklahoma: Oklahoma Geology Notes, v. 50, p. 144–168.

_____1992, Evaporite karst in the Permian Blaine Formation and associated strata in western Oklahoma, U.S.A., *in* Back, W.; Herman, J. S.; and Paloc, H. (eds.), Hydrogeology of selected karst regions: International Association of Hydrogeologists, International Contributions to Hydrogeology, v. 13, p. 405–420.

_____1997, Evaporite karst in the United States: Carbonates and Evaporites, v. 12, no. 1, p. 2–14.

_____2001, Karst in evaporite rocks of the United States, *in* Gunay, G.; Johnson, K. S.; Ford, D.; and Johnson, A. I. (eds.), Present state and future trends of karst studies; Proceedings of the 6th International Symposium and Field Seminar, Marmaris, Turkey, September 17–26, 2000: UNESCO, IHP-V, Technical Documents in Hydrology, no. 49, v. 1, p. 3–12. (Reprinted in 2002 in Carbonates and Evaporites, v. 17, no. 2, p. 90–97.)

_____2003a, Evaporite-karst problems in the United States, *in* Johnson, K. S.; and Neal, J. T. (eds.), Evaporite karst and engineering/environmental problems in the United States: Oklahoma Geological Survey Circular 109 [this volume], p. 1–20.

_____2003b, Gypsum karst and abandonment of the Upper Mangum Damsite in southwestern Oklahoma, *in* Johnson, K. S.; and Neal, J. T. (eds.), Evaporite karst and engineering/environmental problems in the United States: Oklahoma Geological Survey Circular 109 [this volume], p. 85–94.

_____2003c, Gypsum karst as a major factor in the design of the proposed Lower Mangum Dam in southwestern Oklahoma, *in* Johnson, K. S.; and Neal, J. T. (eds.), Evaporite karst and engineering/environmental problems in the United States: Oklahoma Geological Survey Circular 109 [this volume], p. 95–111.

Johnson, K. S.; and Denison, R. E., 1973, Igneous geology of the Wichita Mountains and economic geology of Permian rocks in southwest Oklahoma (guidebook for field trip no. 6, Geological Society of America annual meeting, 1973): Oklahoma Geological Survey Special Publication 73-2, 33 p.

Johnson, K. S.; and Quinlan, J. F., 1995, Regional mapping of karst terrains in order to avoid potential environmental problems: Cave and Karst Science, Transactions of British Cave Research Association, v. 21, no. 2, p. 37–39.

(Reprinted in 1996 in Swindler, D. L.; and Williams, C. P. [compilers], Transactions of the 1995 AAPG Mid-Continent Section meeting, Tulsa, Oklahoma: Tulsa Geological Society, p. 295–298.)

Jordan, Louise, 1959, Underground storage in salt, Elk City field: Oklahoma Geology Notes, v. 19, p. 32–34.

Jordan, L.; and Vosburg, D. L., 1963, Permian salt and associated evaporites in the Anadarko basin of the western Oklahoma–Texas Panhandle region: Oklahoma Geological Survey Bulletin 102, 76 p.

Martinez, J. D.; Johnson, K. S.; and Neal, J. T., 1998, Sinkholes in evaporite rocks: American Scientist, v. 86, p. 38–51.

McGregor, D. R.; Pendry, E. C.; and McGregor, D. L., 1963, Solution caves in gypsum, north-central Texas: Journal of Geology, v. 71, p. 108–115.

Miller, Galen; Dewers, Thomas; and Tarhule, Aondover, 2003, Laser positioning and three-dimensional digital mapping of gypsum karst, western Oklahoma, *in* Johnson, K. S.; and Neal, J. T. (eds.), Evaporite karst and engineering/environmental problems in the United States: Oklahoma Geological Survey Circular 109 [this volume], p. 71–75.

Myers, A. J.; Gibson, A. M.; Glass, B. P.; and Patrick, C. R., 1969, Guide to Alabaster Cavern and Woodward County, Oklahoma: Oklahoma Geological Survey Guidebook 15, 38 p.

Pettyjohn, W. A., 1983, Water atlas of Oklahoma: University Center for Water Research, Oklahoma State University, Stillwater, 72 p.

Preston, D. A., 1980a, Bursting natural-gas bubble, Woods County, Oklahoma: Oklahoma Geology Notes, v. 40, p. 1–2.

_____1980b, Gas eruptions taper off: Geotimes, v. 25, no. 10, p. 18–20.

Quinlan, J. F.; Smith, R. A.; and Johnson, K. S., 1986, Gypsum karst and salt karst of the United States of America, *in* Atti symposio internationale sul carsismo nelle evaporiti (Proceedings, International Symposium on Karst in Evaporites, Palermo, Italy, October 27–30, 1985): Le Grotte d'Italia, Series 4, v. 13, p. 73–92.

Runkle, D. L.; and Johnson, K. S., 1988, Hydrogeologic study of a gypsum–dolomite karst aquifer in southwestern Oklahoma and adjacent parts of Texas, USA, *in* Karst hydrogeology and karst environment protection (Proceedings of the IAH 21st Congress, Guilin, China, October 10–15, 1988): Geological Publishing House, Beijing, China, v. 21, part 1, p. 400–405.

Steele, C. E.; and Barclay, J. E., 1965, Ground-water resources of Harmon County and adjacent parts of Greer and Jackson Counties, Oklahoma: Oklahoma Water Resources Board Bulletin 29, 96 p.

Tarhule, Aondover; Dewers, Thomas; Young, Roger; Witten, Alan; and Halihan, Todd, 2003, Integrated subsurface-imaging techniques for detecting cavities in the gypsum karst of Oklahoma, *in* Johnson, K. S.; and Neal, J. T. (eds.), Evaporite karst and engineering/environmental problems in the united States: Oklahoma Geological Survey Circular 109 [this volume], p. 77–84.

Vanderwater, B., 1980, Re-entry slated in suspect well: The Daily Oklahoman [newspaper], Wednesday, August 27, p. 23.

White, W. B., 1988, Geomorphology and hydrology of karst terrains: Oxford University Press, New York, 464 p.

# Exploration of Western Oklahoma Gypsum Caves

***John Bozeman***
Central Oklahoma Grotto, National Speleological Society
Oklahoma City, Oklahoma

**ABSTRACT.**—The gypsum karst of western Oklahoma, comprising three separate geomorphic provinces variously referred to as "gypsum hills," contains an abundance of gypsum caves. Caves of the Cimarron Gypsum Hills (northwest) and the Mangum Gypsum Hills (southwest) are developed in the Permian Blaine Formation with its alternating dolomite, gypsum/anhydrite, and shale beds. Caves of the Weatherford Gypsum Hills (west central) are formed in the Permian Cloud Chief Formation, which contains lenticular gypsum bodies within a series of interbedded shale, sandstone, and thin dolomite units. The caves and associated karst features, such as natural bridges, solution pans, solution valleys, sinkholes, and disappearing streams, attest to the high solubility of gypsum and its susceptibility to erosion. The processes of dissolution and passage enlargement found in limestone caves also take place in gypsum caves, but the development and evolution of gypsum caves proceed at a much more rapid rate. Entrances and passages have collapsed in the recent past, and conditions are currently evolving at rates measured in decades rather than millennia, as in limestone.

Because the rates of chemical and mechanical modification of gypsum caves and karst are so high, monitoring them is especially important, allowing for adequate response to those engineering, environmental, and agricultural considerations common for all karst terrains. Many of the gypsum-karst features can be monitored through surface mapping and aerial-photography techniques. Currently, however, the physical and hydrological complexities of western Oklahoma gypsum caves and karst features can be documented best through active cave exploration and survey. Such efforts illustrate how internal collapses and other ongoing modifications within the cave environment exert influences on surface processes and help in predicting them and their consequences.

## INTRODUCTION

Organized groups of cavers, such as the Central Oklahoma Grotto (COG), a chapter of the National Speleological Society (NSS), have been locating, exploring, mapping, and otherwise documenting western Oklahoma gypsum caves from the 1950s through the present. The locations of ~280 gypsum caves have been verified, and evidence of many more awaits investigation. Exploration and mapping of the various caves is an ongoing process. The results of most of those efforts, along with personal observations of the cavers providing the details of exploration and mapping, have been documented in the monthly COG newsletter, *C.O.G.nizance*, and in *Oklahoma Underground*, the journal of the Central Oklahoma Grotto. Observations have dealt with surface phenomena as well as subterranean ones. The most important service provided (in return for the pleasure of exploration) by cavers to cave owners, whether public or private, is this documentation process. Trip reports, maps, photographs, and the like, over the last forty-odd years, have done much to illustrate the rapid changes common in gypsum caves and karst.

Cavers are usually amateurs rather than professionals, in that most pursue caving on a recreational basis. Nevertheless, their accumulated observations on the speleology, geology, zoology, and environmental ecology of western Oklahoma's caves and karst are resources that should be utilized. Methods used by cavers have evolved over the years; therefore, as in all human efforts, the information is variable in its utility, but it is nonetheless valuable in any synthesis of gypsum caves generally, and Oklahoma gypsum caves specifically. The current report is an attempt to characterize some of those observations, focusing on those concerned with geology and karst geomorphology, and through them a variety of the pleasures and the problems associated with exploration of western Oklahoma gypsum caves. Other observations and findings such as ones dealing with zoology, biology, archaeology, anthropology, and other aspects would best be characterized elsewhere.

## GYPSUM CAVES IN WESTERN OKLAHOMA

All of the known gypsum caves of western Oklahoma are formed in the Permian red beds of three

Bozeman, John, 2003, Exploration of western Oklahoma gypsum caves, *in* Johnson, K. S.; and Neal, J. T. (eds.), Evaporite karst and engineering/environmental problems in the United States: Oklahoma Geological Survey Circular 109, p. 57–64.

separate geomorphic provinces (Fig. 1). In the Cimarron Gypsum Hills of northwestern Oklahoma and the Mangum Gypsum Hills of southwestern Oklahoma, the caves are found in the Blaine Formation and have significant similarities. The Blaine Formation of northwestern and southwestern Oklahoma is stratigraphically and lithologically similar, for in both areas it is composed of cyclical rock units of (in ascending order) dolomite, gypsum, gypsiferous red-brown shale, and argillaceous green-gray shale. These two areas are stratigraphically dissimilar in that the Blaine in the northwest, which varies from 40 to 100 ft in thickness (Fay, 1964), normally contains three cyclical rock units, and the Blaine in the southwest, which averages ~200 ft in thickness, contains nine cyclical rock units (Fig. 2).

The gypsum caves of the Blaine Formation, with its relatively thin beds, commonly have collapsed entrances and large rooms filled with breakdown. The various collapses result from the inability of the thin gypsum beds and the thinner dolomite beds to support wide ceiling expanses. Passage segments in gypsum and dolomite members are usually relatively narrow (2–15-ft) solutional tubes or canyons, but the segments through shale members are usually wider (20–50 ft), with flat ceilings formed by the next dolomite or gypsum above. Whereas dissolution plays the major role in passage enlargement in the gypsum and dolomite beds, corrasion is dominant in the shale beds. The large, sediment-laden water flows of major rain events are extremely effective in passage widening. Episodically, downstream passage constrictions cause backflooding, resulting in undercutting in the shale intervals (Fig. 3). Eventually, the ceilings of these ever-widening rooms collapse. Such collapses may extend upward through the overlying cyclical rock units, resulting in collapse sinks, or breakdown rooms, often with ceilings only a few feet or inches from the surface and, therefore, very unstable.

In the Weatherford Gypsum Hills, the caves occur in the Permian Cloud Chief Formation, which contains lenticular gypsum bodies within a series of interbedded shale, sandstone, and thin dolomites. In cavernous areas the Cloud Chief gypsum is 60–100 ft thick and has a sandy to chalky texture with thin laminations (S. Bozeman and others, 1979). The caves formed in the more massively bedded Cloud Chief gypsum typically have rather narrow (2–10-ft) passages (Fig. 4) with vadose channels in the floors. This gypsum is less crystalline than the gypsum members of the Blaine and seems softer and more susceptible to both solution and corrasion. The caves are more segmented, and large rooms are rare, because the Cloud Chief does not exhibit the shale interbeds and undercutting relationships found in the Blaine. Hence, breakdown constrictions are also extremely rare. Recognition of the stratigraphic influences on speleogenesis and cave modification is critical to any appreciation or anticipation of problems to be encountered during exploration and mapping. A more detailed report on the speleology of

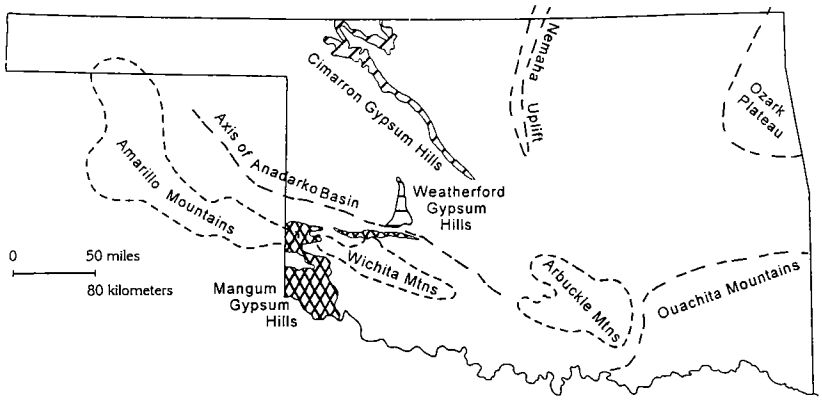


Figure 1. Schematic map showing areas of gypsum outcrops (hatched) of western Oklahoma in relation to other regional features (modified from Fay, 1964, and Curtis and Ham, 1972).

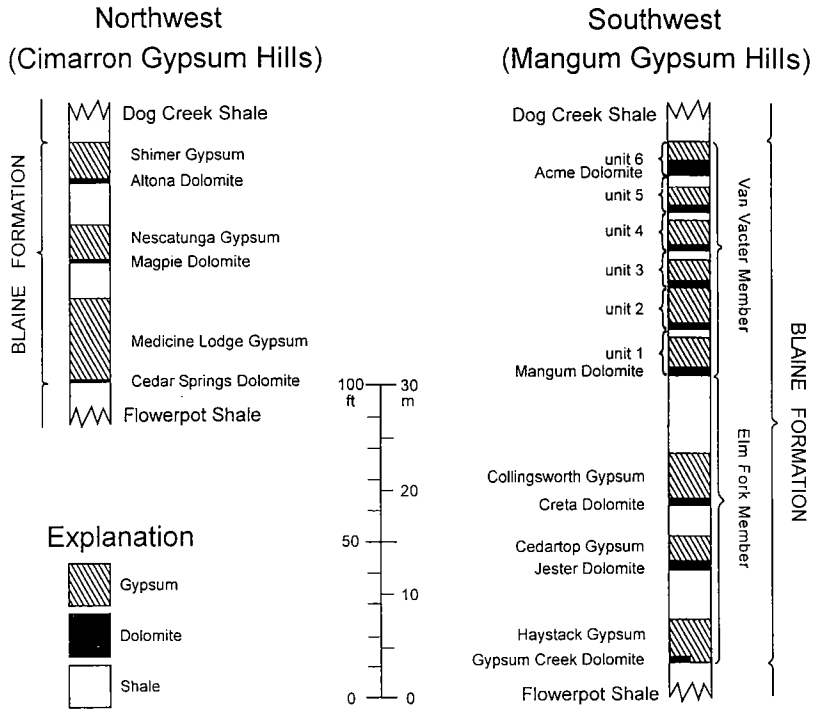


Figure 2. Generalized geologic sections showing the Permian Blaine Formation as encountered in the gypsum karst of northwestern Oklahoma (modified from Fay, 1964, 1965; Myers and others, 1969) and southwestern Oklahoma (modified from Johnson, 1990).

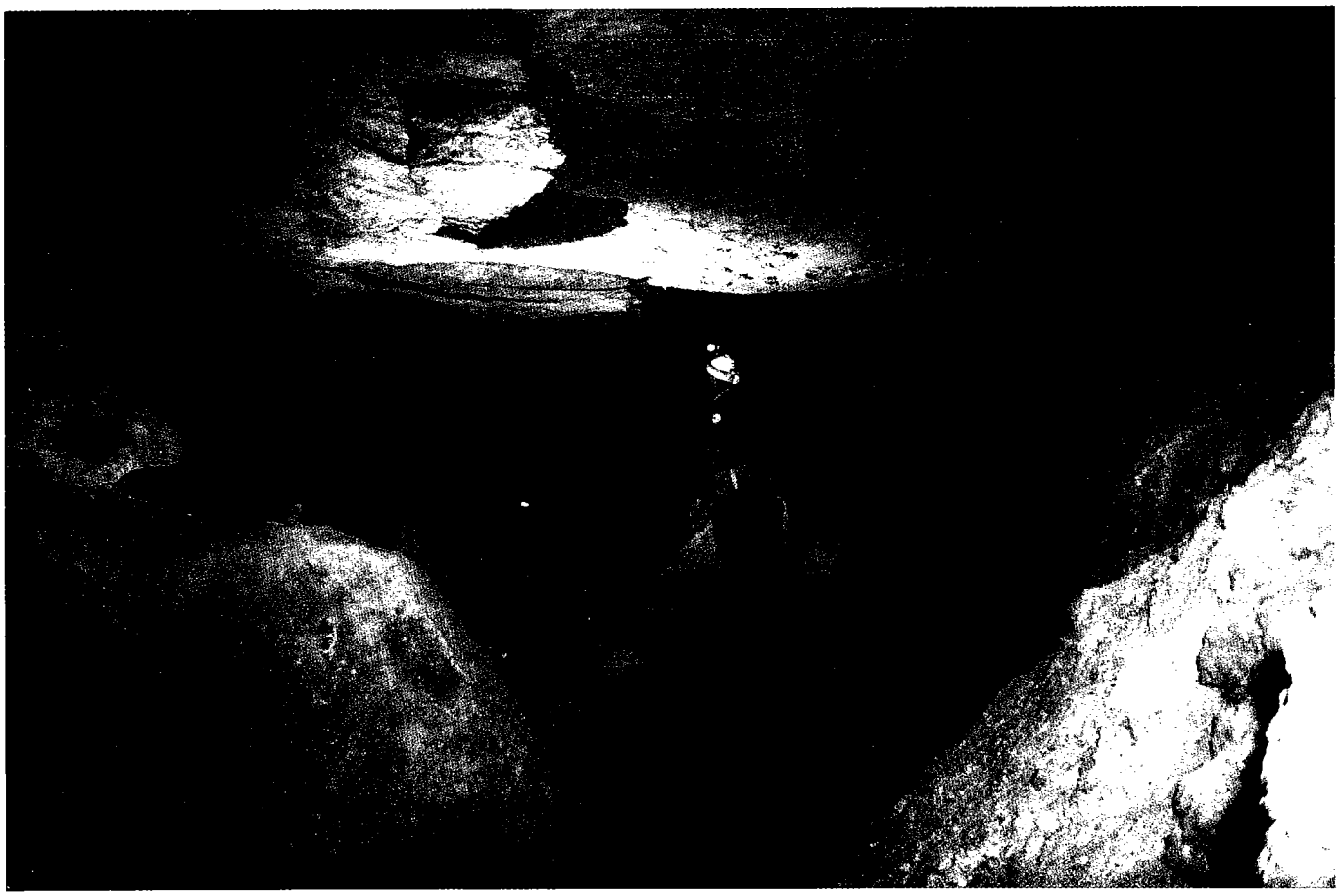

Figure 3. View of cave-passage section, showing passage widening common in shale members. The Nescatunga Gypsum/Magpie Dolomite ceiling has a narrow, meandering canyon channel, and a similar channel is incised in the Medicine Lodge Gypsum floor (obstructed from view). The large breakdown boulders are also Nescatunga Gypsum/Magpie Dolomite. (Photo by Susan Bozeman.)

Oklahoma gypsum caves can be found in Bozeman and Bozeman (2002).

## Locating Caves

Over the years, organized cavers have been led to western Oklahoma gypsum caves through rumors, landowner referrals, fortuitous encounters, newspaper articles, literature searches of historical archives, and surface reconnaissance. More recently other, more dependable, data sources—such as aerial photographs, topographic-quadrangle maps (first, 15-min. maps, and later, 7.5-min. maps), digital orthophotoquads, and satellite imagery—have become generally available. The exposure of the gypsum karst (Fig. 5), and the relative lack of vegetative cover of the typically semiarid terrain of western Oklahoma, present an almost totally unobscured view of sinkholes, pits, and other cave-entrance types. The few trees and other dense vegetation are associated with cave entrances or with entrenched streams of which the caves are usually tributaries.

An indispensable part of the cave-location effort is obtaining permission to explore the caves, the majority of which are privately owned. Conversations with landowners, ranch hands, farm workers, oil-field workers, and others have provided a wealth of anecdotal material on the gypsum caves and some of the problems associated with them. Much of this falls into the realm of local folklore, but a significant portion is helpful. In the folklore portion of anecdotes are included matters such as cave size ("big enough to drive a wagon through"), cave length ("it comes out at Carlsbad Caverns"), and, of course, Jesse James, but other accounts have the ring of authenticity. Members of the COG have been told of drilling rigs that required "skidding" because of washouts beneath well pads; the use of a cave as a "reserve pit" during drilling operations; sudden appearances of new sinkholes; the loss of horses and cattle in the caves; or livestock killed through falls into cave-pit entrances or over cliff faces into a cave entrance below. This personal contact with people familiar with the land and its history is as important as the physical survey of the caves and is a crucial, and rewarding, component of the documentation process.

## Cave Exploration and Documentation

After a cave has been located, and permission to explore it has been secured, the process of mapping is

Figure 4. View of a narrow cave passage in a Weatherford Gypsum Hills cave formed in the Cloud Chief Formation. This passage configuration, showing vadose modification, is common in gypsum members. (Photo by Marcus Barker.)

controlled by the physical proportions of the cave and the personal attributes of the cavers. A cave survey can take from just hours or weeks, to months or years, for successful completion. The mapping of 6.25-mi-long Jester Cave, in the Mangum Gypsum Hills, and the longest gypsum cave in the United States (Collins, 1968, 1969; S. Bozeman, 1987), took ~5 years. After a survey is initiated by the COG, the group makes an effort to conduct at least one survey trip per month. Typical survey parties are made up of three to four people: one person to take survey notes and sketch (both plan and cross-sectional views), two people on tape for distance measurements (the one closest to the note taker is the primary instrument person, and the other establishes each survey station and is the secondary [back-sighting] instrument person), and optionally a scout—passage dimensions permitting. Often two or three separate crews may be simultaneously at work in different parts of the subject cave.

The cave surveys are conducted using fiberglass tape, compass (either a pocket transit [Brunton™ type] or a direct-sighting compass), and clinometer (either direct sighting or the one on the pocket transit). These types of instruments have proven to be the most suitable and versatile in the sometimes harsh subterranean conditions. In gypsum caves, a typical survey traverse may include commodious passage segments; narrow, tortuously meandering canyon segments; crawlways; unstable breakdown; bedding-plane segments; and complex multilevel mazes. Those conditions, along with the generally high humidity of the caves, muddy conditions associated with cave streams, partial to almost complete immersion, and various situations entailing high-angle survey shots, require the use of sturdy, easily manipulated instruments. Back-sighting of survey shots is normally done to reduce instrument-reading errors, but in particularly awkward sections back-sighting is often difficult to impossible to accomplish. Errors, of course, are introduced in those circumstances but are usually of acceptable magnitude. Generally, re-surveys are done whenever closure errors exceed ±1%. Most of the cave maps have been hand drafted, but more recently computers have been utilized in the data-storage and -reduction phases, as well as in the final drafting phase. The map of the Selman Cave System (Fig. 6), published in 2002, is an example of the maps being produced.

Figure 5. This view of a part of the Cimarron Gypsum Hills shows the exposed karst development of the Permian Blaine Formation. A cave entrance is visible in the middle right foreground, and the Cimarron River flood plain is visible in the background. (Photo by David Jagnow.)

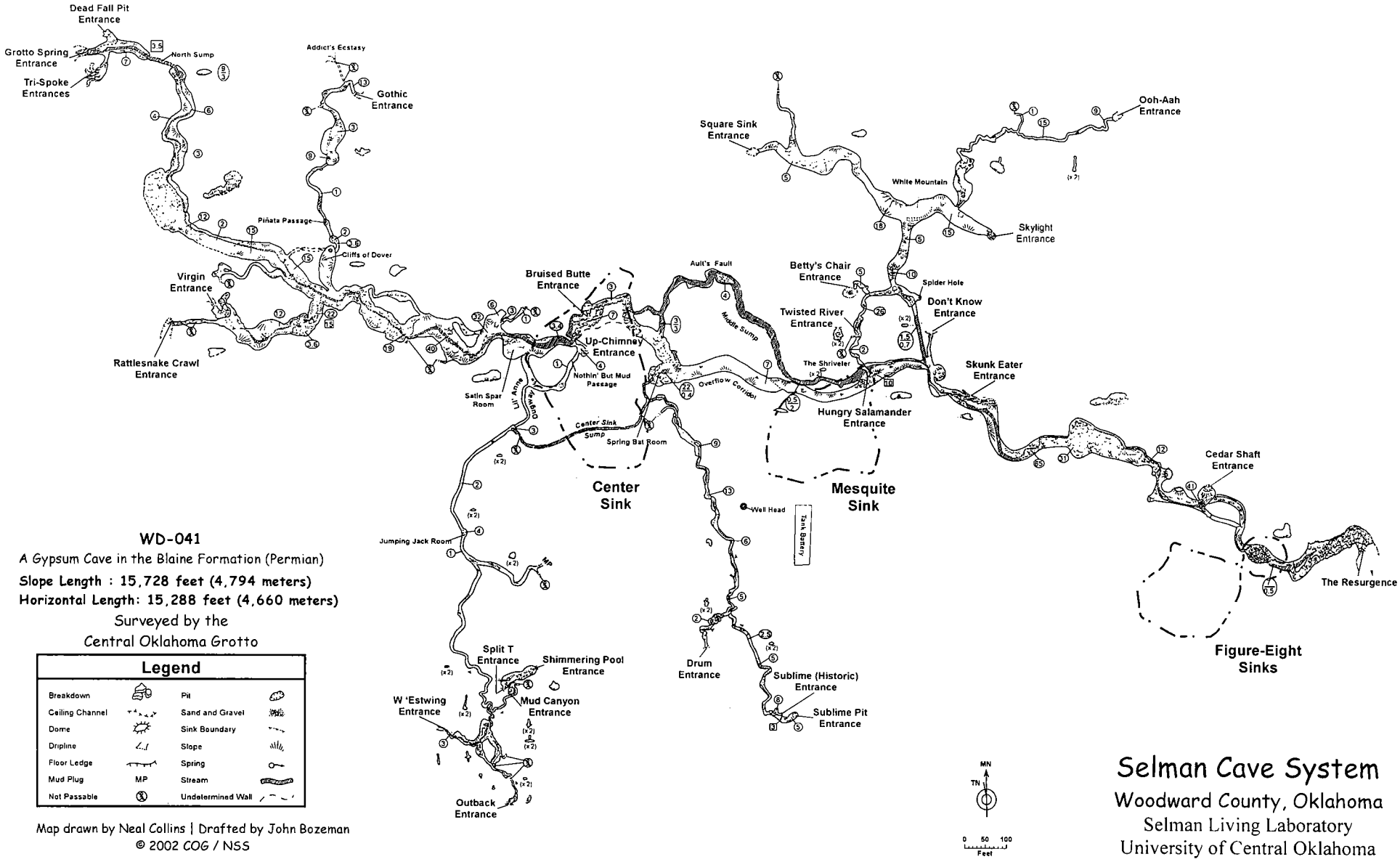


Figure 6. Selman Cave System map (modified from S. Bozeman, 2002). Located in the Cimarron Gypsum Hills, the cave is part of the Selman Living Laboratory (SLL), a field station administered by the Department of Biology at the University of Central Oklahoma.

Ultimately, the purpose of the maps is to resolve the relationships of the subterranean components of the local karst to the visible surface components (e.g., Selman Cave has >25 entrances, and Jester Cave has >70 entrances). The resultant maps delineate hydrologic connections, which are often much more complex than would at first be supposed based solely upon examination of surface features. The moderately dendritic patterns, obvious on most maps of large gypsum caves, mask their complex dissolutional histories. Passages are often oriented along ceiling fractures (Fig. 7), and many dead-end cross-passages are enlarged along cracks. Other passages are free of fractures, whereas some areas of complex passage interconnections are associated with bedding-plane anastomoses, most of which terminate in mud plugs. These anastomosed passages, whether joint related or not, point to an earlier phreatic phase of interstratal dissolution that predated stream entrenchment and the current vadose regime. Examples of phreatic dissolution, which have escaped vadose modification, are occasionally found in upstream sections or in remnant higher level passages.

Figure 7. Cave-passage view, illustrating the influence of ceiling fracture on passage development in Cascade Spring Cave (J. Bozeman, 1994) in the Mangum Gypsum Hills.

During the exploration and mapping of a cave or system, beyond the survey itself, cavers document other observations concerning the zoology, paleontology, archaeology, geology, and any other aspect of the cave considered germane. The completeness of the observations is determined by the makeup of the exploring group. In most caving groups (grottos), the membership is in constant flux and is composed of those with a desire to explore caves rather than those trained in any particular discipline. Since both experience and necessity are often good teachers, most committed cavers tend to develop a broad general knowledge of the multidisciplinary science of speleology.

Historical graffiti (from the late 1800s and early 1900s) are in degraded condition and illustrate rapid dissolution. Some of the areas of graffiti have fallen to the cave floor as breakdown blocks (S. Bozeman, 1987, 1996). In some cases, dissolution has erased deep carvings in under a decade. Cave entrances, both inflows and resurgences, have collapsed in the period from the 1950s to the present, and others have altered sufficiently to pose a present danger of collapse. Canyons, along which landslides (Fig. 8) are common, are also features of western Oklahoma gypsum karst, and commonly result from such progressive collapses. Within a number of the gypsum caves, large breakdown blocks of several tons have fallen, and ceiling collapses have also been documented. The high solubility of gypsum and its susceptibility to corrasion have resulted in high rates of dissolution and passage collapses, leading to ephemeral karst development on a human scale. Another indicator of the short-lived nature of western Oklahoma gypsum caves is zoological: no cave-adapted biota has thus far been found associated with them.

Exploration in gypsum caves is potentially dangerous, as is all caving. However, proper training in an organized grotto, with members familiar with gypsum karst and its caves, helps to effectively reduce the likelihood of accident or injury. Attention to the cave environment and proper regard for personal and group safety are vitally important in cave exploration and are required in any successful exploration effort.

The maps and sketches produced in the 1950s, 1960s, and early 1970s by organized Oklahoma cavers were done more casually than is now the case. Many of the older maps in the COG files are pace maps—really no more than rough sketches. Others were made using tapes and military-style lensatic compasses, without the benefit of a clinometer for vertical control.

## Gypsum Caves and Human Impact

Human impact—past and present—is one of those aspects requiring inclusion in trip reports and narratives of survey histories. Evidently, humans have used sinkholes and pits as handy disposal sites—"trash sinks" associated with old homesteads (Fig. 9). Evidence of earlier, aboriginal use of gypsum caves and sinkholes is relatively rare and is, presumably, due to lower environmental impact, coupled with rapid evo-

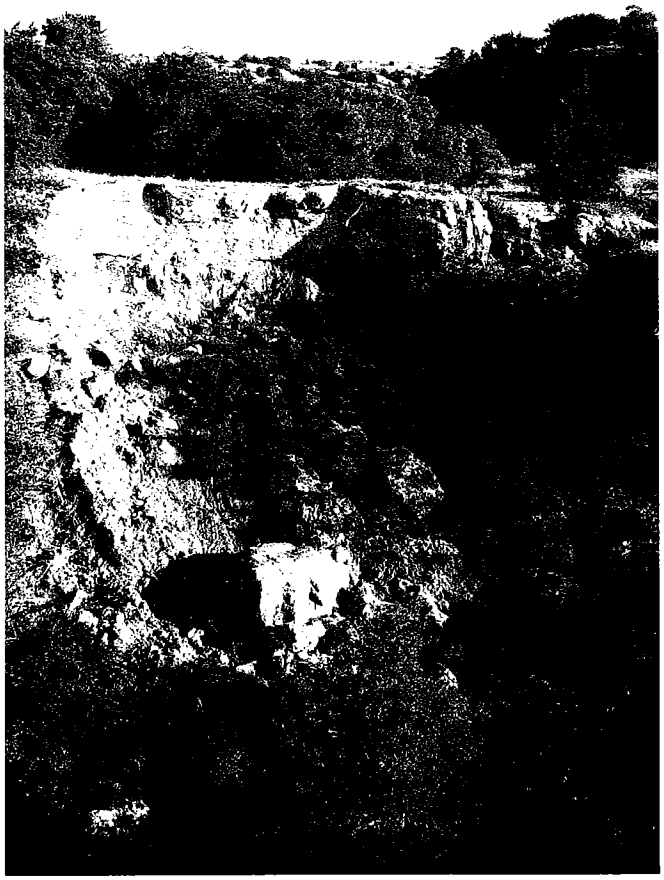

Figure 8. View of a canyon landslide downstream of the resurgence entrance of Vickery Bat Cave (Beaty, 1969). The canyon was developed, and is evolving, through progressive headward collapses of the cave-entrance ceiling.

Figure 9. View along a series of sinkholes associated with Swimminghole Cave (S. Bozeman, 1999), in the Mangum Gypsum Hills. The small sinkhole in the foreground has been used as a "trash sink." The middle sink exceeds 60 ft in depth.

lution of the gypsum-karst terrain. More recent trash, usually beer cans and the like, discarded by trespassers, is routinely collected and removed by cavers. However, much older debris have been found cemented into travertine dams and pavements or partially buried in cave fills.

Cave maps have been used to illustrate the subterranean interconnectedness of the surface sinks, alerting current cave owners to the danger to livestock posed by the dumping of any pollutants into the sinks. This information is especially important in western Oklahoma because the gypsum caves drain plateaus or other high areas, collecting meteoric waters and/or perennial stream flows, shunting them through to resurgences as karst springs or free-flowing streams near the level of the nearest entrenched streams and thereby extending the scope of any detrimental effects.

Information sharing is an ongoing effort and, if done correctly, helps cave owners to appreciate the subsurface component of their properties; and most seem to respond positively. In one situation, the COG was requested to "check out" the proposed path of a salt-water-disposal pipeline across a karsted area in northwestern Oklahoma. In another instance, because gypsum is used locally to surface and repair ranch and section-line roads, COG cavers were consulted concerning the safety of a proposed surface-mining site before any gypsum was removed. Such inquiries indicate that the efforts of the cavers have had some success.

Grotto maps and observations have been used, at least on one occasion, to alert county officials of a dangerous situation in which a cave passage lay beneath a section-line road (Kowalski, 1990). The distance from the cave ceiling to the roadbed was estimated to be <2 ft. The county road was regularly used by heavy vehicles, such as petroleum tank trucks, and has subsequently been diverted to avoid the cave. Fortunately, the examples of caves crossing beneath public roadways—with such dangerous potential—are few in Oklahoma's gypsum karst. However, roads need not be public to warrant concern, and cave surveys and caver observations have been used to warn ranchers of "thin spots" on their land with a view to avoiding any surprise, catastrophic sinkhole appearances.

Finally, cave maps and the knowledge of experienced gypsum cavers have been useful in rescue situations in western Oklahoma. Although a rarity, grotto members have been contacted for assistance in rescues (of humans and animals), and, happily, those rescues have been successful. The most recent incident was a Christmas Eve call for help in removing a yearling that had fallen into a pit. The large calf was suc-

cessfully, and somewhat comically, liberated in good condition—perfectly healthy and assured of its date with a meatpacker.

## CONCLUSIONS

Cave location, exploration, and survey amid western Oklahoma's gypsum-karst areas bring some light of knowledge to the subsurface complexities of gypsum karst. Admittedly, cavers are driven by personal considerations, and the exploration and mapping efforts are not altruistically conducted. Curiosity about "how it all fits together" and the desire to find something "no one else has seen" are paramount. The process of producing the cave maps linking surface geomorphologic expressions—mesa, canyon, solution valley, sinkhole, and stream—to intricate subsurface geomorphologic expressions—slot canyon, bedding-plane crawlway, breakdown chamber, and phreatic maze—is, at once, the pursuit and the pleasure of organized groups of cavers.

The relative speed with which chemical and mechanical alterations in western Oklahoma gypsum karst occur suggests that those alterations should be monitored on a continuous basis in order to properly, and in a timely fashion, respond to them. The work done by organized groups of cavers in the past, and their future efforts, have the potential to be of significant use in any such process. Certainly, professional efforts are vital for a more complete knowledge and appreciation of western Oklahoma gypsum caves and karst. However, the dangers and discomforts experienced in cave exploration are usually not ones most researchers relish or are prepared to endure. Indeed, one researcher, who was also a member of the COG, was heard to proclaim that "biologists don't crawl!" Accordingly, the ongoing efforts of organized groups of cavers, such as the Central Oklahoma Grotto, can go far in helping to assure that knowledge of Oklahoma's gypsum karst is not merely superficial.

## REFERENCES CITED

Beaty, B., 1969, Vickery Bat Cave: Central Oklahoma Grotto, Oklahoma City, Oklahoma Underground, v. 2, no. 2, p. 12–15.

Bozeman, J., 1994, Cascade Spring Cave: Central Oklahoma Grotto, Oklahoma City, Oklahoma Underground, v. 17, p. 27–35.

Bozeman, J.; and Bozeman, S., 2002, Speleology of gypsum caves in Oklahoma: Carbonates and Evaporites, v. 17, no. 2, p. 107–113.

Bozeman, S. (ed.), 1987, The D. C. Jester Cave System: Central Oklahoma Grotto, Oklahoma City, Oklahoma Underground, v. 14, 56 p.

_____1996, Horseshoe Valley Cave: Central Oklahoma Grotto, Oklahoma City, Oklahoma Underground, v. 18, p. 17–26.

_____1999, Swimminghole Cave: Central Oklahoma Grotto, Oklahoma City, Oklahoma Underground, v. 19, p. 33–38.

_____ (ed.), 2002, The Selman Cave System: Central Oklahoma Grotto, Oklahoma City, Oklahoma Underground, v. 20, 44 p.

Bozeman, S.; Bozeman, J.; and Barker, M., 1979, Gyp Falls karst system: Central Oklahoma Grotto, Oklahoma City, Oklahoma Underground, v. 8, p. 3–9.

Collins, M., 1968, Exploring a legend—Jester Cave: Central Oklahoma Grotto, Oklahoma City, Oklahoma Underground, v. 1, no. 2, p. 46–48.

_____1969, Exploring a legend—Jester Cave II: Central Oklahoma Grotto, Oklahoma City, Oklahoma Underground, v. 2, no. 1, p. 8–11.

Curtis, N. M., Jr.; and Ham, W. E., 1972, Geomorphic provinces of Oklahoma, *in* Johnson, K. S., and others, Geology and earth resources of Oklahoma—an atlas of maps and cross sections: Oklahoma Geological Survey Educational Publication 1, p. 3.

Fay, R. O., 1964, The Blaine and related formations of northwestern Oklahoma and southern Kansas: Oklahoma Geological Survey Bulletin 98, 238 p.

_____1965, Geology and mineral resources of Woods County, Oklahoma: Oklahoma Geological Survey Bulletin 106, 189 p.

Johnson, K. S., 1990, Standard outcrop section of the Blaine Formation and associated strata in southwestern Oklahoma: Oklahoma Geology Notes, v. 50, p. 144–168.

Kowalski, D., 1990, Falls River Cave and Tunnel: Central Oklahoma Grotto, Oklahoma City, Oklahoma Underground, v. 16, p. 32.

Myers, A. J.; Gibson, A. M.; Glass, B. P.; and Patrick, C. R., 1969, Guide to Alabaster Cavern and Woodward County, Oklahoma: Oklahoma Geological Survey Guidebook 15, 38 p.

# Correlating the Location of a Cave Passage in Gypsum Karst to a Highway Right-of-Way Using a Cave Radio

***Scott Christenson***
1721 Seminole Drive
Edmond, Oklahoma

***Curtis Hayes***
1809 Edgewood Drive
Edmond, Oklahoma

***Earl Hancock***
6016 North Lakeside Drive
House Springs, Missouri

***John McLean***
11151 East Grant Road
Franktown, Colorado

**ABSTRACT.**—The Oklahoma Department of Transportation (ODOT) plans to widen U.S. Highway 412 in western Oklahoma in an area underlain by the Permian Blaine Formation. The project would widen the highway from a two-lane to a four-lane divided highway and decrease the existing grades. One area of particular concern was in Major County where Nescatunga Cave passes under the highway at a relatively shallow (<65-ft) depth, but the location of the cave passage relative to the highway was not known. The preliminary plans for the highway-widening project specified lowering the grade by removing overburden in the vicinity of Nescatunga Cave.

Concern regarding possible roadbed failure caused the ODOT to seek methods to determine the location of Nescatunga Cave relative to the highway-widening project. Volunteers from the National Speleological Society used low-frequency-radio direction-finding equipment, commonly referred to as a cave radio, and a tape-and-compass survey to depict the position and dimensions of the Nescatunga Cave passages relative to the highway-widening project. A transmitter was placed sequentially at seven stations in the cave passage, and a radio direction-finding receiver was used to identify and mark points at the surface directly above the transmitter stations.

Subsequent core drilling by the ODOT at three of the survey sites intercepted the cave passage at all three locations. Knowledge of the depth and location of the cave passages allowed the ODOT to minimize drilling costs. The ODOT is considering design changes for the highway-widening project to maintain more overburden above the cave passage.

## INTRODUCTION

The Oklahoma Department of Transportation (ODOT) plans to widen U.S. Highway 412 in western Oklahoma, including an area underlain by the Permian Blaine Formation (Fig. 1). The Blaine Formation contains evaporite karst and numerous large caves. The ODOT's project would widen the highway from a two-lane to a four-lane divided highway and decrease the existing grades.

One area of particular concern was in Major County where Nescatunga Cave passes under the highway at a relatively shallow (<65-ft) depth, but the precise location of the cave passage relative to the highway was not known (Fig. 2). The preliminary plans for the highway-widening project specified lowering the grade by removing overburden in the vicinity of Nescatunga Cave. Concern regarding possible roadbed failure caused the ODOT to seek methods for determining the location of Nescatunga Cave relative to the highway.

Members of the Tulsa Regional Oklahoma Grotto, the Meramec Valley Grotto, and the Boston Mountain Grotto chapters of the National Speleological Society volunteered to assist the ODOT in locating Nescatunga Cave's position relative to the existing highway and the proposed widened highway. They used a device commonly referred to as a cave radio (a low-frequency-radio direction-finding system) and a tape-and-compass survey in Nescatunga Cave to determine the location of the cave relative to the highway.

## GEOLOGIC SETTING

U.S. Highway 412 crosses the Blaine Formation in western Oklahoma in an area with well-developed evaporite karst (Fig. 1). Nescatunga Cave was developed in the Medicine Lodge Gypsum Member of the Blaine Formation, with some of the larger rooms possibly extending upward to the Nescatunga Gypsum Member (Fig. 3). The Blaine Formation in northwest-

Christenson, Scott; Hayes, Curtis; Hancock, Earl; and McLean, John, 2003, Correlating the location of a cave passage in gypsum karst to a highway right-of-way using a cave radio, *in* Johnson, K. S.; and Neal, J. T. (eds.), Evaporite karst and engineering/environmental problems in the United States: Oklahoma Geological Survey Circular 109, p. 65–70.

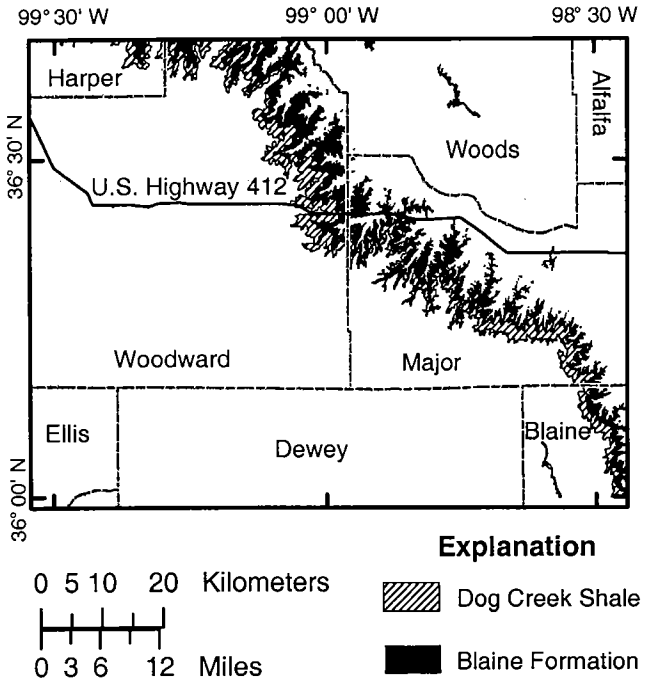


Figure 1. Map showing U.S. Highway 412, the Blaine Formation, and the overlying Dog Creek Shale.

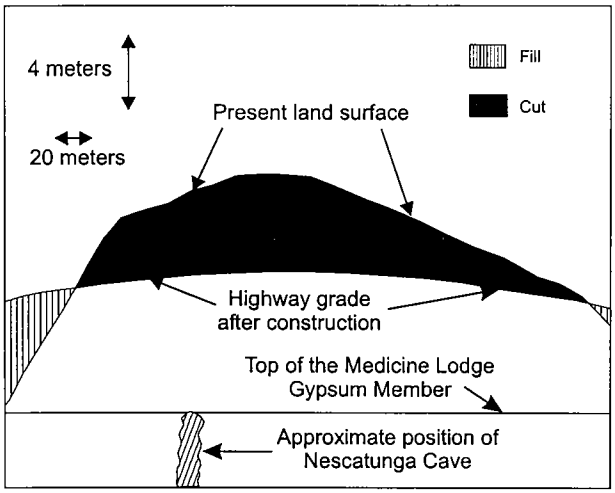


Figure 2. Cross section along U.S. Highway 412 where it passes over Nescatunga Cave.

ern Oklahoma is as thick as 90 ft and consists of an alternating cyclic sequence of three or four named massive gypsum beds with red-brown shale layers, generally with a dolomite at the base of each gypsum layer, and a greenish-gray shale layer at the base of each dolomite layer (Morton, 1981). The gypsum members are, from top to bottom, Shimer, Nescatunga, Kingfisher Creek (not shown in Fig. 3), and Medicine Lodge (Fay, 1964).

Stratigraphically, the Dog Creek Shale is above the Blaine Formation (Fig. 3). The lower section of the Dog Creek is found at the top of the hill above Nescatunga Cave. The Dog Creek Shale ranges in

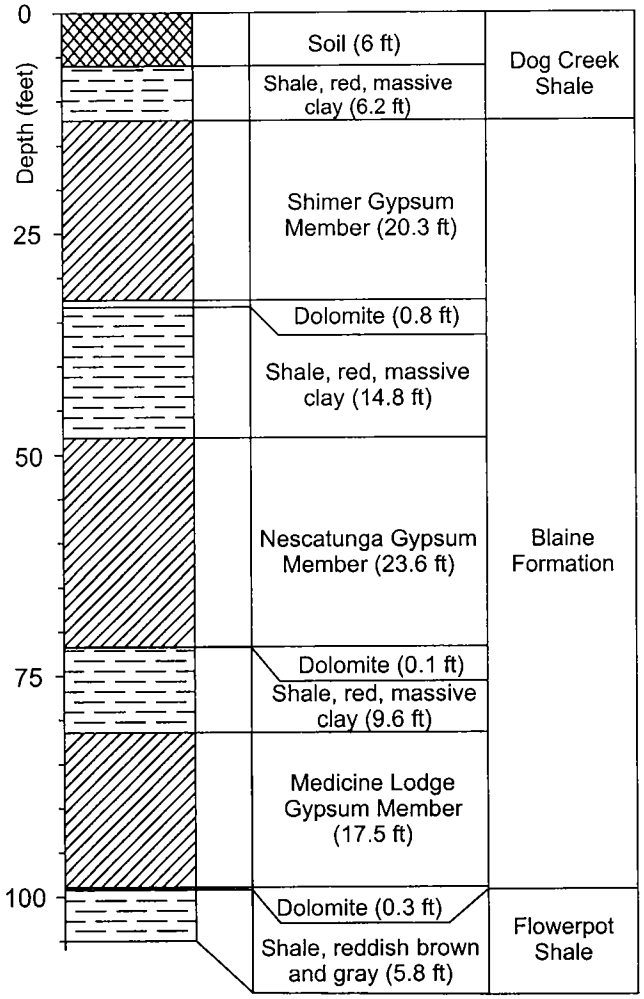


Figure 3. Lithology and stratigraphy of a boring near the centerline of the proposed parallel lane of the highway-construction project. The Kingfisher Creek Gypsum Member is absent at this location.

thickness from 30 to 100 ft and consists of red-brown shale and silty shale, with gypsum, dolomite, and orange-brown sandstone layers (Morton, 1981).

Fay (1964) described a measured geologic section in eastern Woodward County a few miles from Nescatunga Cave. Part of the measured section is given in Table 1. A cross section showing the topography and location of Nescatunga Cave is shown in Figure 2.

The ODOT obtained a core drilled through the entire Blaine Formation near the centerline of the proposed parallel lane, 740 ft east and 60 ft north of the extreme west end of the highway-construction project, about 1.25 mi west of the cave. The core provided information on the thickness and character of the entire Blaine Formation underlying the highway-construction project.

At this location the Blaine consists of three gypsum members, with underlying thin dolomites and

**Table 1. — Measured Section along Ewers Creek, Eastern Woodward County, Oklahoma**

| Description | Thickness (feet) |
|---|---|
| *Haskew Gypsum Bed (Dog Creek Shale):* | |
| Gypsum, white, mottled red-brown, fine-grained, wavy bedded, massive; forming ledge | 0.5 |
| Shale, red-brown, silty, well-indurated, crinkly bedded; with much gypsum | 3.7 |
| BLAINE FORMATION (total thickness, 86.5 ft) | |
| *Shimer Gypsum Member:* | |
| Gypsum, white, fine-grained, well-cemented, laminated; with crinkly upper surface | 21.0 |
| *Altona Dolomite Bed:* | |
| Dolomite, light-gray, fine-grained, oolitic, medium-bedded; weathering massive, into boxworks | 1.7 |
| *Unnamed units (Blaine):* | |
| Shale, greenish-gray, weakly indurated, blocky | 0.3 |
| Shale, red-brown, blocky; mottled with greenish-gray spots | 12.5 |
| *Nescatunga Gypsum Member:* | |
| Gypsum, white, fine-grained, massive, weathering coarsely selenitic; forming escarpment | 22.0 |
| *Magpie Dolomite Bed:* | |
| Dolomite, light-gray, oolitic, well-cemented, massive; grading into gypsum at top, weathering into boxworks | 0.5 |
| *Unnamed units (Blaine):* | |
| Shale, greenish-gray, dolomitic, blocky, weakly indurated; grading into argillaceous dolomite | 2.0 |
| Shale, red-brown, blocky | 1.0 |
| *Kingfisher Creek Gypsum Bed:* | |
| Gypsum, greenish-gray and red-brown, argillaceous, well-indurated, thin-bedded, crinkly bedded; forming ledge | 1.2 |
| *Unnamed unit (Blaine):* | |
| Shale, red-brown, blocky; with much selenite | 2.8 |
| *Medicine Lodge Gypsum Member:* | |
| Gypsum, white, mottled light-gray, fine-grained, massive; weathering coarsely selenitic | 17.0 |
| *Cedar Springs Dolomite Bed:* | |
| Dolomite, light-gray to light-brown, fine-grained, oolitic, thin-bedded; grading upward into gypsum | 4.5 |
| FLOWERPOT SHALE | |
| Shale and siltstone, greenish-gray and red-brown, with thin beds of dolomite (exposed thickness, 97.0 ft) | |

Source: Fay (1964).

intervening red clay shales (Fig. 3). The thickness of the gypsum layers in this boring were as follows: Shimer Gypsum Member, 20.3 ft; Nescatunga Gypsum Member, 23.6 ft; and Medicine Lodge Gypsum Member, 17.5 ft. The Kingfisher Creek Gypsum Member is absent at this location. In this boring, the Shimer and Nescatunga Gypsum Members are composed of massive, pure, coarsely crystalline selenite, whereas the Medicine Lodge Gypsum Member contains substantial amounts of anhydrite.

## CAVE-RADIO SURVEY

The cave-radio survey of Nescatunga Cave consisted of three parts: (1) radio soundings using a cave radio, (2) a tape-and-compass survey of the cave, and (3) data reduction and map production.

### Radio Soundings

Radio soundings were performed with a home-built low-frequency (874-Hz) radio transmitter, which was placed in the cave, and a home-built double-quadrature radio receiver at the surface. This specific cave-radio system was constructed by several members of the Meramec Valley Grotto of the National Speleological Society, following plans described in France and Mackin (1991).

The transmitter consists of a square, hand-wound antenna 50 cm in diameter and covered with wood and fiberglass, a small plastic box containing the transmitter electronics, and a battery. The electronics, battery, and antenna are connected, and a switch is closed to begin transmission. In addition to the transmission coils, the antenna contains a single independent coil of wire connected to a resistor and a small incandes-

cent light bulb. The transmission coils generate current in the independent coil sufficient to illuminate the light bulb to verify that the transmitter is operating. The signal pulses two times per second (120 Hz) to provide a distinct signal to the receiver.

The receiver consists of a loop antenna, a double-quadrature radio receiver with an internal battery, and headphones. When the transmitter is operating, the 120-Hz pulsed signal is heard in the receiver headphones.

To conduct a radio sounding, cavers carry the transmitter into the cave in steel ammunition cans, except for the antenna, which is rugged enough to transport unprotected. Once at the site in the cave chosen for transmission, the antenna is leveled (that is, the loop antenna is horizontal) using attached spirit levels. The transmitter and receiver of this particular unit cannot transmit messages (although cave radios can be constructed for voice or data communication), so it was not possible for the in-cave and surface parties to communicate. A schedule for transmission was established prior to carrying the transmitter into the cave.

At the time scheduled for a transmission, the receiver is switched on. The antenna is held vertically and rotated until the signal disappears or "nulls." The transmitter is positioned on the plane of the receiver antenna when the receiver antenna is in the null position. After establishing an initial null plane, the receiver antenna is taken to a new position and a new null plane established. The transmitter is positioned on the vertical line defined by the intersection of the two null planes. In practice, after establishing the two null planes, the receiver operator moves to the approximate position of the intersection of the planes and moves the antenna loop until the spot is found where the signal is nulled regardless of the orientation of the receiver loop antenna. This location is designated *ground zero* and marked as the point directly over the transmitter antenna.

After ground zero is determined, the receiver can be used to get an approximate depth of the transmitter. The receiver is moved some distance from ground zero, the receiver antenna is turned perpendicular to ground zero, and the antenna is tipped until the signal nulls. In this case, because of the shape of the transmitter field, the transmitter is not in the same plane as the receiver antenna.

The approximate depth of the transmitter antenna can be computed by knowing the angle of the antenna from the vertical, the shape of the field, the conductivity of the rock, and the distance from ground zero. This specific receiver has a plumb bob and scale mounted on the side of the antenna that incorporates all these factors except the distance from ground zero, making computation of depth relatively simple.

The cave radio used for this survey is home-built, so there are no manufacturer's specifications. An estimate of the performance of this specific unit is based on field observations for the Nescatunga survey and other applications. The range of the transmitter is ~1,000 ft, and the horizontal repeatability of the location of ground zero during the Nescatunga Cave survey was ~2 in.

Seven radio soundings were performed for the Nescatunga Cave radio survey. The surface crew successfully located six of the seven points. Difficulty in moving the transmitter in the cave caused the in-cave team to deviate from the schedule, so that point D (Fig. 4) was not located by the surface team. The points spanned the width of Highway 412 and the proposed widening project, including two points directly under the existing two-lane highway. A stake was driven into

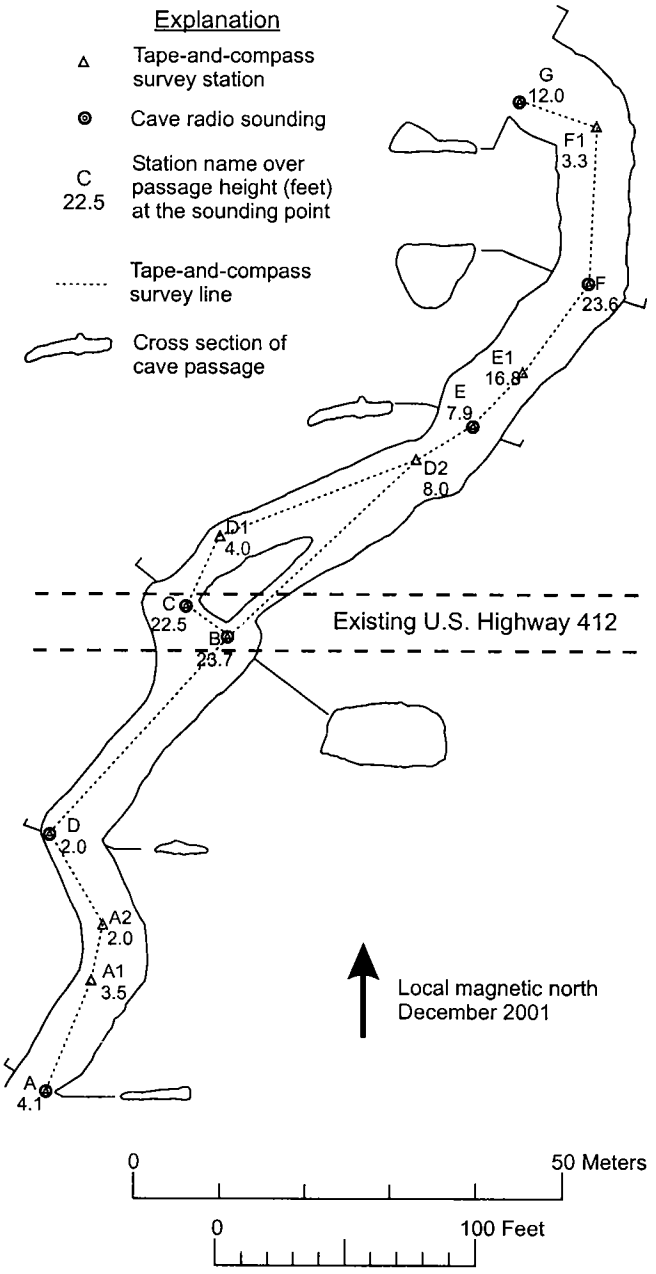


Figure 4. Map of a section of Nescatunga Cave that passes under U.S. Highway 412.

the surface at each radio sounding location, and, for the locations on the pavement, marks were painted on the road surface.

### In-Cave Tape-and-Compass Survey

A tape-and-compass survey also was performed in Nescatunga Cave to show the configuration of the cave passages in the vicinity of Highway 412 and the proposed widening, as well as the relationship between the cave-radio soundings and the cave passages. Tape-and-compass surveying requires establishing a series of points in the cave with line of sight between the points. Compass bearings, clinometer readings, and distance measurements (using a tape measure) are taken between points.

Points are typically rocks in the middle of the passage, or prominent spots on the passage wall, to which a marker with a station number can be attached. Distance, bearing, and vertical angle are recorded in a survey book with waterproof pages by one caver, designated "the bookman." Passage dimensions are recorded at every survey station, and the bookman may draw passage cross sections or profiles at selected sites. The bookman also makes a sketch showing the configuration of passage walls and other prominent features in relation to the survey points, such as details about the floor of the cave passage. Of course, sketches are subjective, and vary between bookmen.

The procedure described in the preceding paragraph for a typical cave survey was modified slightly for the Nescatunga Cave radio survey. Cavers typically extend the distance between stations to the maximum possible for rapid surveying, which often results in survey stations that are close to passage walls. For the Nescatunga survey, the stations were sited near the center of the cave passage for subsequent drilling by the ODOT. Stations in the center of the passage offer the best possibility for drilling into the passage.

Because of the uneven floor of Nescatunga Cave, it was not possible to place all the radio-sounding stations in the passage center. Passage dimensions were measured at every survey point instead of the typical caving practice of estimating dimensions, and cross sections were drawn at every radio sounding. Ceiling heights in the two largest rooms encountered in the survey were determined by triangulation using a laser pointer, a clinometer, and a tape measure, because the ceiling heights were too tall for direct determination with a tape measure. Floor detail was completely omitted from the survey, as it was felt to be irrelevant to the project's objectives.

Tape-and-compass surveys are not especially accurate by modern surveying standards, with an error factor typically on the order of one part per hundred. This level of accuracy is sufficient to meet the needs of most caving applications, which is to show the general extent and configuration of cave passages and for speleologists to travel through the cave without getting lost, but it is not sufficient to meet the needs of the ODOT. The accuracy of the cave-radio soundings and that of the tape-and-compass survey are completely independent of each other.

### Data Reduction and Map Production

The tape-and-compass survey in Nescatunga Cave established 12 stations in the cave and surveyed 627.8 ft of passage (Fig. 4). Measured distances, bearings, inclinations, and passage dimensions were entered into a cave-survey computer program named *Compass* (http://www.fountainware.com/compass/). Compass allows the user to enter cave data, revise the data, generate statistics for the cave, close loops using least-squares methods, view plots from various angles on the screen, and generate plots. Compass generates an ASCII output file of coordinates that was passed to Fortran programs to generate ASCII input files for the Arc/Info Geographic Information System. Arc/Info coverages were created of survey lines and stations.

The underground sketches of passage geometry were scanned and output as TIFF images, then digitized and registered to export the digitized images to Arc/Info. The cave sketches were registered using the coordinates from Compass, then exported to Arc/Info as shape files, and combined with the coverages of survey lines and stations to produce the cave map (Fig. 4). Final annotation of the map was done with the CorelDraw program.

## VERIFICATION BY DRILLING

Subsequent to the cave-radio soundings and tape-and-compass survey, the ODOT conducted a drilling project to verify the location of Nescatunga Cave beneath U.S. Highway 412 and the proposed widening project. The ODOT used a CME-55 drilling rig with a coring system. The drillers raised the mast to the vertical position but did not take extraordinary measures to ensure that the borehole was vertical.

Drill holes were bored at stations D1, F, and G, and all three borings encountered the cave passage. The depths to the roof of the cave passage are as follows:

| *Station* | *Depth* |
|---|---|
| D1 | 62.5 ft |
| F | 65.0 ft |
| G | 76.0 ft |

Cavers associated with this project entered Nescatunga Cave several months after the borings were completed to measure the deviation between the borings and the radio sounding stations in the cave. The boring at station D1 emerged from the cave passage ceiling ~1 ft from the marker in the cave. Considerable shale had fallen from the cave roof at station G, possibly as a result of the drilling, and the marker could not be found in the cave, but a caver familiar with the location of the station estimated that the borehole was ~6.5 ft from the marker. The marker at station F was missing, and no features existed in that part of the cave from which to estimate the original position of the marker. Visual observation of the

base of the boreholes gave the impression that the boreholes were not exactly vertical.

## SUMMARY

The Oklahoma Department of Transportation (ODOT) plans to widen U.S. Highway 412 in western Oklahoma in an area underlain by the Blaine Formation of Permian age. The project would convert the highway from a two-lane to a four-lane divided highway and decrease the existing grades. One area of particular concern was in Major County where Nescatunga Cave passes under the highway at a relatively shallow (<65-ft) depth, but the location of the cave passage relative to the highway was not known. The preliminary plans for the highway-widening project specified lowering the grade by removing overburden in the vicinity of Nescatunga Cave. Concern regarding possible roadbed failure caused the ODOT to seek methods for determining the location of Nescatunga Cave relative to the highway-widening project.

Volunteers from the National Speleological Society used low-frequency-radio direction-finding equipment, commonly referred to as a cave radio, and a tape-and-compass survey to depict the position and dimensions of the Nescatunga Cave passages relative to the highway-widening project. A transmitter was placed sequentially at seven stations in the cave passage, and a radio direction-finding receiver was used to identify and mark points at the surface directly above the transmitter stations. Transmitter stations, as well as the cave-passage position and dimensions, were surveyed using a tape and compass. The surface points were repeatable to within 5 cm.

Subsequent core drilling by the ODOT at three of the survey sites intercepted the cave passage, which ranged in width from 16 to 32 ft, at all three locations. Knowledge of the depth and location of the cave passages allowed the ODOT to minimize drilling costs. The ODOT is considering design changes for the highway-widening project to maintain more overburden above the cave passage.

## ACKNOWLEDGMENTS

The authors would like to extend their gratitude to Mark Whitlaw, owner of the property overlying Nescatunga Cave, and to Gary and Cinda Inman, caretakers of the property, for allowing access to Nescatunga Cave and the land above the cave for this study. Jim Nevels from the Oklahoma Department of Transportation supported the project and assisted with the field work. Special thanks are extended to Chris Cearley, Jeff Fusselman, Ken Lyon, Larry Moritz, and Roger Ryan, members of the National Speleological Society, for their hard work underground in difficult conditions to accomplish the cave-radio soundings and tape-and-compass survey in Nescatunga Cave.

## REFERENCES CITED

Fay, R. O., 1964, The Blaine and related formations of northwestern Oklahoma and southern Kansas: Oklahoma Geological Survey Bulletin 98, 238 p.

France, Stuart; and Mackin, Bob, 1991, Making a simple radiolocation device: Caves & Caving, v. 52, Summer, p. 7–11.

Morton, R. B., 1981, Reconnaissance of the water resources of the Woodward Quadrangle, northwestern Oklahoma: Oklahoma Geological Survey Hydrologic Atlas 8, 4 sheets, scale 1:250,000.

# Laser Positioning and Three-Dimensional Digital Mapping of Gypsum Karst, Western Oklahoma

***Galen Miller***
Oklahoma Geological Survey
Norman, Oklahoma

***Thomas Dewers and Aondover Tarhule***
University of Oklahoma
Norman, Oklahoma

**ABSTRACT.**—Cavern morphology and distribution in two western Oklahoma evaporite-karst systems were mapped using a laser/Global Positioning System (GPS) device. Parts of the Corn Caves and Nescatunga Cave systems, within the gypsiferous Permian Cloud Chief and Blaine Formations, respectively, are being mapped in association with a series of surface geophysical studies to develop a cavern-detection methodology.

To map the caverns digitally, an initial carrier-phase GPS position was first determined directly outside a cavern entrance. By means of laser-range-finder position offsets, transects of position stations were established into and throughout the cave. Three-dimensional (3-D) cavern morphology at select localities was determined by combing the inside of the cavern with laser positions from a single station at a given locality. Data were logged with handheld computers and downloaded into a 3-D geographic information system (GIS). Absolute positioning errors were determined by reoccupying stations and were found to be ~30 cm or less in the horizontal plane. Under optimal conditions, these cave systems can be easily mapped in this manner at a rate of ~100 m per hour.

## INTRODUCTION

The Permian Blaine and Cloud Chief Formations, outcropping in western Oklahoma, contain numerous intricate cavern systems developed in their soluble gypsum members (Johnson, 1990; Bozeman and others, 1987). Many of these cavern systems have been painstakingly mapped by the traditional "tape-and-compass" method (Bozeman and others, 1987), in which directional vectors are determined with a Brunton compass, elevation changes marked with a surveyor's staff, and distances determined with measuring tape. A standard surveying technique for use under bridges, next to tall buildings, and under heavy tree canopies combines Global Positioning System (GPS) receivers with laser range finders. In this method, positions to be mapped—but in locations where sufficient GPS satellite signals are unattainable—are recorded as laser position offsets, or a series of position offsets, from one or more GPS locations with good satellite coverage.

In this study, novel digital mapping of cavern voids makes use of this technology, using a reflectorless laser range finder with an internal inclinometer linked to a digital compass and referenced to GPS receivers positioned outside the cavern entrances. A series of control stations are laser-located along a cavern traverse at roughly 20-m intervals and marked by mounted reflectors. Fifty or so additional laser positions of cavern floors and walls are taken as offsets from each station. In such a manner, a three-dimensional (3-D) digital map of a cavern system can be accurately and relatively rapidly made.

Laser/GPS positioning was used as "ground truth" to test methodology and imaging algorithms of several surface geophysical-imaging techniques. Results are discussed in Tarhule and others (2003) in this volume.

## STUDY AREAS AND GEOLOGIC SETTING

Both of the study areas are in the extensive Permian strata of western Oklahoma that contain cyclic red beds and evaporite units. Regions in which gypsum strata crop out or lie within 30 m of the surface, and thus are susceptible to karstic processes, are shown in Figure 1. In the Nescatunga Cave study area (Looney, 1968), the Blaine Formation consists of two to four massive gypsum beds, each with an underlying dolomite bed. The members of the Blaine Formation (from oldest to youngest) are the Cedar Springs Dolomite, Medicine Lodge Gypsum, unnamed shale, Kingfisher Creek Gypsum, unnamed shale, Magpie

Miller, Galen; Dewers, Thomas; and Tarhule, Aondover, 2003, Laser positioning and three-dimensional digital mapping of gypsum karst, western Oklahoma, *in* Johnson, K. S.; and Neal, J. T. (eds.), Evaporite karst and engineering/environmental problems in the United States: Oklahoma Geological Survey Circular 109, p. 71–75.

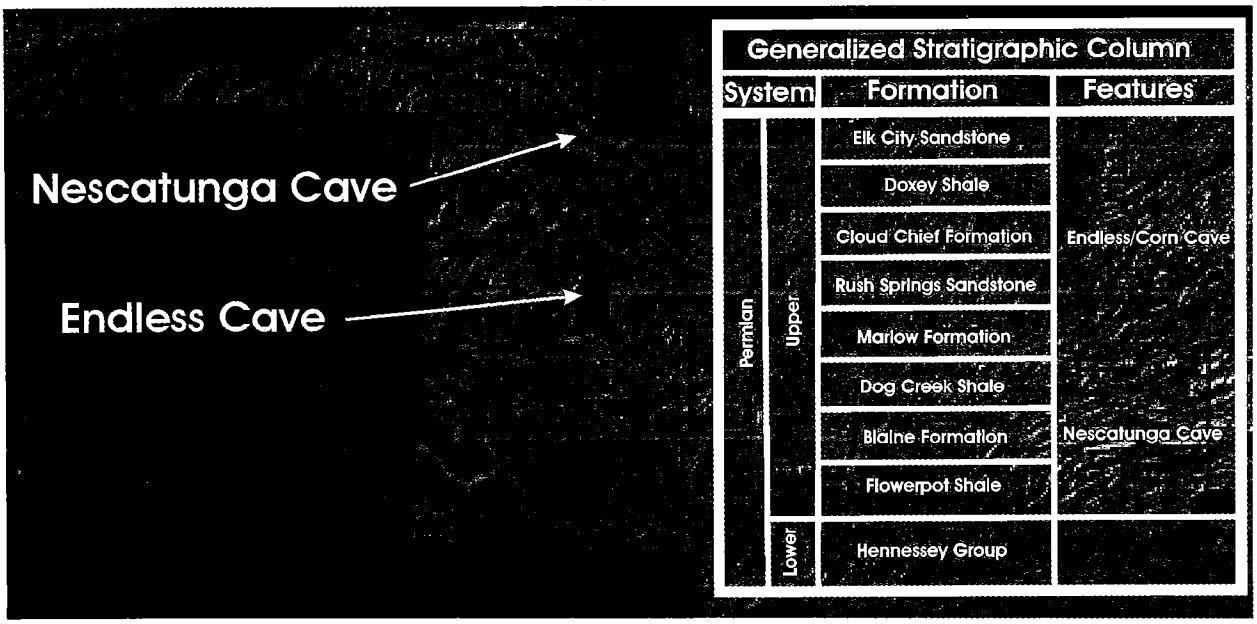


Figure 1. Digital elevation model of Oklahoma, showing areas (darker shaded) underlain by gypsum and susceptible to karst-related collapse and other hazards (after Johnson and Quinlan, 1995). A generalized stratigraphic section shows the gypsum-bearing units in which the surveyed caves have been formed.

Dolomite, Nescatunga Gypsum, unnamed shale, Altona Dolomite, and at the top the Shimer Gypsum (Fay and others, 1962). The Nescatunga Cave was formed in the Medicine Lodge Gypsum. The Blaine Formation is in conformable contact with the underlying Flowerpot Shale and the overlying Dog Creek Shale (Stanley and others, 2002).

Endless Cave, one among several cavern systems in the region known collectively as the Corn Caves (Looney and Bozeman, 1984), was formed in the Permian Cloud Chief Formation (Fig. 1). In the study area the Cloud Chief Formation is ~300 ft thick and consists of (oldest to youngest) an unnamed shale, a Moccasin Creek gypsum/anhydrite unit, and a unit at the top containing alternating sandstone and shale beds. At the type locality of the Cloud Chief Formation near Endless/Corn Caves, the gypsum/anhydrite unit is 100 ft thick (Fay and others, 1962). The Cloud Chief Formation is conformable with the underlying Rush Springs Sandstone and the overlying Doxey Shale.

## EQUIPMENT AND METHODS

The equipment we used in our methodology is relatively mobile and can be easily handled by a single person (Fig. 2). We used a Trimble ProXRS™ system, a LaserTech™ reflectorless range finder, and a MapStar™ digital compass together with a Compaq IPAQ™ running the SOLOField™ data-logging software. Uniform resource locators (URLs) for equipment vendors are found in the Acknowledgments section below.

To map the caves, the ProXRS™ GPS receiver was mounted on a tripod near an entrance to the cavern system being surveyed, along with the reflectorless laser range finder and digital compass. A differential GPS (DGPS) carrier-phase location was established at this initial position. Differential corrections were obtained onsite using the OmniStar™ system and later, via internet resources, using Trimble's Pathfinder™ software. A series of control points or stations were then located within the cavern itself spatially referenced to the DGPS position by a series of offsets using mounted bicycle reflectors (Fig. 2A,B).

The laser was aimed at the reflectors and "fired" in filter mode, which only records a position if sufficient energy is returned to the laser. This was done to ensure that the laser was hitting only the reflector—i.e., only the reflector position was being returned. The mounting height on the tripod of the laser/compass assembly was entered directly into the handheld computer at each location so that each position was automatically referenced to the tripod base on the cavern floor in Universal Transverse Mercator (UTM) northing, easting, and elevation in meters. Beginning at the entrance to the cave, the laser/compass configuration then occupied each of these control stations successively, permitting a survey of the surrounding cavern walls consisting of locations referenced to the control points to be conducted. This was done with the filter mode turned off so that every laser "shot" returned a position. Although positioning error invariably increases with each successive control point occupied within the cavern, we achieved decimeter-scale accuracy in distance and inclination from each control point, and confirmed the accuracy by reoccupying control stations. Other sources of error influencing the precision of the method include errors in the geoid

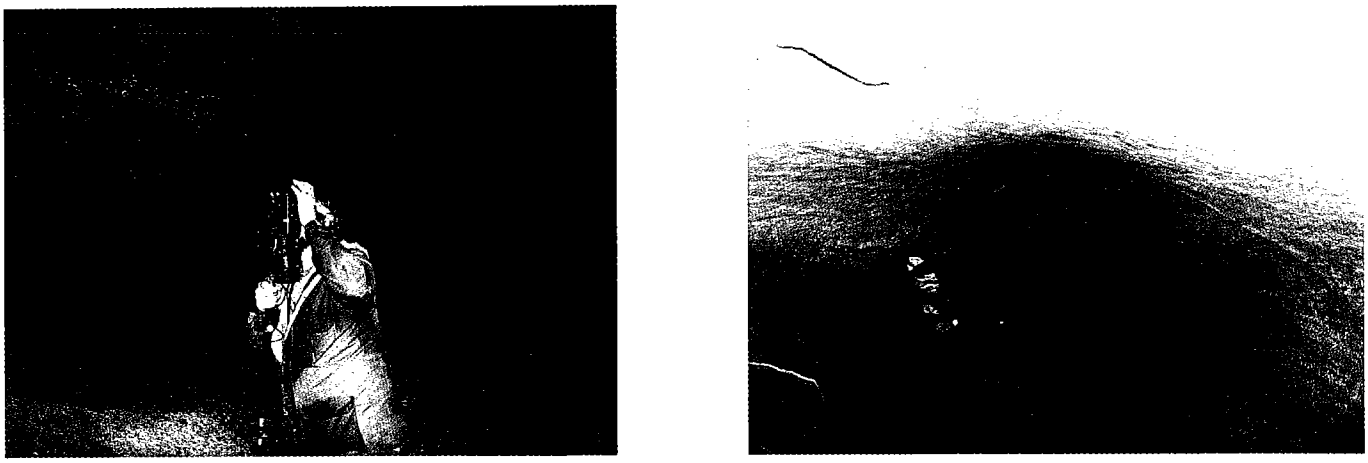

A B

Figure 2. (A) A co-author (GM), showing the digital-mapping method in action, taking a laser position of horizontal distance, vertical distance, and azimuth to a reflector shotpoint. The reflectorless laser range finder, a digital compass, and a handheld computer are all mounted on a monopod/tripod assembly. Cave graffiti seen in the background unfortunately are a common occurrence close to the entrance. (B) The other end of the survey: reflection of camera flash is seen from a bicycle reflector used in laser positioning of cave transects.

model and random errors in the initial DGPS position determination. These are estimated to be a few tens of centimeters in the horizontal plane and roughly twice that in the vertical.

Positioning data were then downloaded from the data logger onto a laptop computer and visualized with GIS and computer-aided-design (CAD) software, enabling a real-time geo-referenced image of cavern shape to be developed. The resulting digital 3-D map of a part of each cavern system investigated was used in interpreting the results of surface geophysical-imaging techniques (Tarhule and others, 2003), both in order to provide "ground truth" for the geophysical surveys and to refine methods for cavern detection in surface-inaccessible sites.

In summary, the steps used in acquiring and utilizing the data are as follows: (1) acquire carrier-phase DGPS position outside the cave entrance; (2) survey a series of offset stations from this position into and through the cave using laser positioning (in filter mode) and reflectors; (3) survey cavern-wall morphology at sites of interest from surveyed offset stations with filter mode off; and (4) export positions to CAD or GIS software for visualization.

## RESULTS

### Corn Caves

The Corn Caves, in Washita County, have long been explored and mapped, largely by the Central Oklahoma and Tulsa Grotto Societies (Looney and Bozeman, 1984). We mapped a small part of Endless Cave (see elegant map on page 39 in Looney and Bozeman, 1984) over about 3 hours in September 2002. In Figure 3, we show the traverse used in a geophysical survey (Tarhule and others, 2003), the initial DGPS position outside the cave, the surveyed stations, and the data points collected to record cavern morphology, at two scales and in two and three dimensions. These are included with various sources of GIS—including digital orthophoto quadrangles (DOQs), a digital raster graph (DRG) of the USGS 7.5-minute Corn, Oklahoma, quadrangle, and a 10-m-resolution digital elevation model (DEM)—and assembled using ESRI's ARCView™ software.

Figure 3A shows the Endless Cave study site on Gyp Creek near the boundary between Washita and Custer Counties. A base map of surface topography was produced by draping a 1-m DOQ over the DEM. In Figure 3B the horizontal locations of the resistivity survey discussed by Tarhule and others (2003) and the cave-survey station transect are given by intersecting white lines. A cluster of points at this intersection denotes more than 50 locations of cave-wall, ceiling, and floor morphology that were used by Tarhule and others (2003) as "ground truth" for the surface geophysical imaging of the cavern in this locality. A three-dimensional portrayal of this data set is shown in Figure 3C, with the DOQ drape rendered transparent. This image is oriented as north-looking; north–south-running section-line roads are visible on the underlying digital raster graph going from the bottom of the image to the horizon at the middle of the image.

### Nescatunga Caves

The Nescatunga Cave system, discussed by Looney (1968, see map on p. 9) and briefly by Elliot (1994), is found in Major County in northwestern Oklahoma, close to Alabaster Caverns and Boiling Springs State Parks, both of which contain gypsum karst. Similar to Endless Cave shown in Figure 3, we show in Figure 4 the two- and three-dimensional GIS of a part of Nescatunga Cave produced in about half a day during

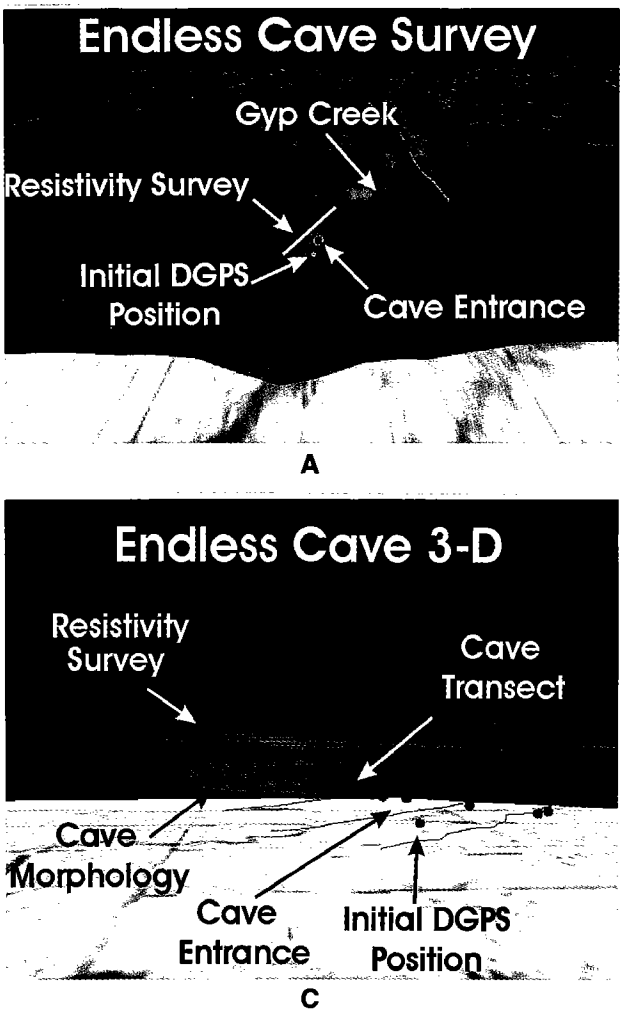


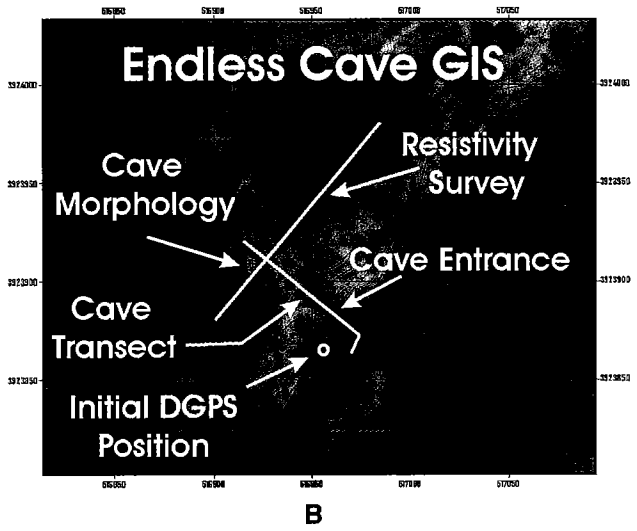


Figure 3. Results of survey at Endless Cave, part of the Corn Caves in Washita County, in September 2002. (A) Study area, viewed from the south on draped DOQ/DEM. (B) Two-D GIS depiction of cave locations, cave morphology, and surface resistivity survey line discussed by Tarhule and others (2003). (C) Three-D GIS depiction of cavern location beneath ground surface. Contour interval is 2 m, and UTM grid shows 50-m spacing for scale.

July 2002. Figure 4A shows the Window study site south of Highway 15, ~20 mi east of Woodward in Major County. Figure 4B shows the horizontal points along the resistivity survey discussed by Tarhule and others (2003), and the cave survey–station transect is shown by intersecting white lines connecting the survey points. A cluster of points at this intersection denotes approximately 100 locations of cave-wall, ceiling, and floor morphology that were used by Tarhule and others (2003) as "ground truth" for the surface geophysical imaging of the cavern. A three-dimensional portrayal of this data set is shown in Figure 4C, with the DOQ drape rendered transparent. The DRG beneath is the 7.5-minute Belva, Oklahoma, quadrangle. The view is looking nearly due east.

## SUMMARY

Herein we introduce a method for three-dimensional digital mapping of cavern systems. The method offers a fast, accurate, and relatively non-intrusive means for mapping cave position and morphology. It provides "(under)ground truth" for geophysical methods used for cavern detection. It is a bit costly, but equipment is rugged and fairly mud-proof. Better accuracy and precision could be obtained with more sophisticated (and expensive) laser and GPS devices currently available. Millimeter-to-centimeter-scale accuracy could be used to ascertain the degree to which such cavern systems evolve over time scales of decades.

## ACKNOWLEDGMENTS

We wish to thank the Oklahoma Department of Transportation, the Oklahoma Department of Environmental Quality, the U.S. Geological Survey, the University of Oklahoma's "Using Technology for the Improvement of Learning" program, and the Oklahoma Geological Survey for financial and logistical support during this study.

The following people are gratefully acknowledged for helpful discussions and help in the field: Ken Johnson, Roos Tarhule, Scott Christenson, Neil Suneson, Joseph Zume, Brent Wilson, Nicole Baylor, and Lori Bryan. John and Sue Bozeman showed us the Corn Cave site and infected us with their energy and enthusiasm for Oklahoma karst. Finally, we acknowledge the wonderful support, cooperation, and hospitality of the cave-site landowners.

No endorsement of this methodology or the equipment used is expressed or implied by the Oklahoma Geological Survey.

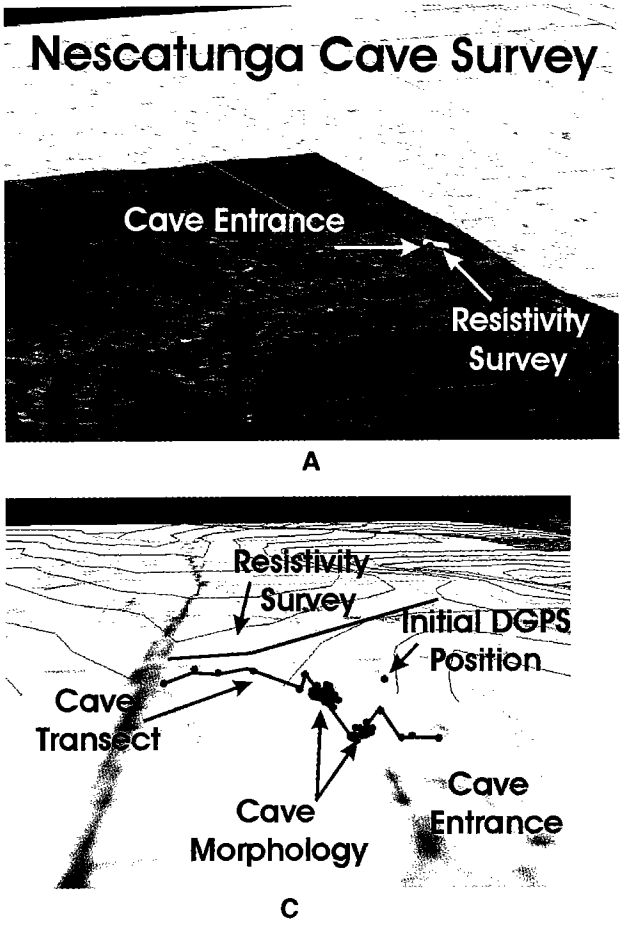


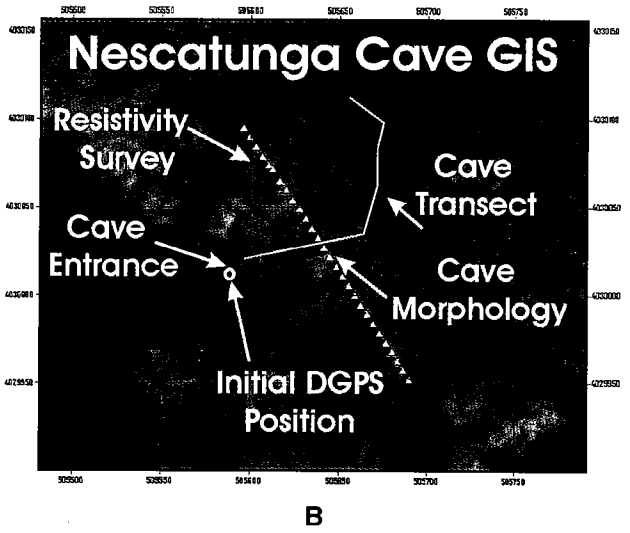


Figure 4. Results of survey at the Window area, Nescatunga Cave, in Major County, in July 2002. (A) Study area, viewed from the southwest on draped DOQ/DEM. (B) Two-D GIS depiction of cave locations, cave morphology, and surface resistivity survey line discussed by Tarhule and others (2003). (C) Three-D GIS depiction of cavern location beneath ground surface. Contour interval is 2 m, and UTM grid shows 50-m spacing.

URLs for equipment used in this study as of this writing are: for the GPS, http://www.trimble.com/pathfinderproxrs.htm; the reflectorless laser range finder and digital compass, http://www.afds.net/lasertech.html#B; the Compaq IPAQ palmtop computer and data-logging software, http://welcome.hp.com/country/us/eng/prodserv/handheld.html and http://tdsway.com; and finally the differential GPS beacon, http://www.omnistar.com/.

## REFERENCES CITED

Bozeman, S.; Johnson, K. S.; Jagnow, B.; Baker, B.; Kowalski, G.; Looney, J.; Ziegler, P.; Dodds, A.; Martinez, S.; and Riley, P., 1987, The D. C. Jester Cave System: Oklahoma Underground, v. 14, p. 1–56.

Elliot, W. R., 1994, Conservation of western Oklahoma bat caves: Oklahoma Underground, v. 27, p. 44–53.

Fay, R. O.; Ham, W. E.; Bado, J. T.; and Jordan, Louise, 1962, Geology and mineral resources of Blaine County, Oklahoma: Oklahoma Geological Survey Bulletin 89, 252 p.

Johnson, K.; and Quinlan, J., 1995, Regional mapping of karst terrains in order to avoid potential environmental problems, *in* Cave and Karst Science, Transactions of the British Cave Research Association, v. 21, no. 2, p. 37–39.

Johnson, K. S., and others, 1990, Hydrogeology of the Blaine gypsum–dolomite karst aquifer, southwestern Oklahoma: Oklahoma Geological Survey Special Publication 90-5, 31 p.

Looney, J.; and Bozeman, S., 1984, Washita County caves—an overview: Oklahoma Underground, v. 11, p. 32–50.

Looney, M., 1968, Editorial: Oklahoma Underground, v. 1, p. 1–11.

Stanley, T. M.; Miller, G. W.; and Suneson, N. H., 2002, Geologic map of the Fairview 30- × 60-minute quadrangle, Blaine, Dewey, Garfield, Kingfisher, Major, and Woods Counties, Oklahoma: Oklahoma Geological Survey Open-File Report 5-2002.

Suneson, N. H.; and Johnson, K. S., 1996, Geology of Red Rock Canyon State Park: Oklahoma Geology Notes, v. 56, p. 88–105.

Tarhule, A.; Halihan, T.; Dewers, T.; Young, R.; and Witten, A., 2003, Integrated subsurface-imaging techniques for detecting cavities in the gypsum karst of Oklahoma, *in* Johnson, K. S.; and Neal, J. T. (eds.), Evaporite karst and engineering/environmental problems in the United States: Oklahoma Geological Survey Circular 109 [this volume], p. 77–84.

# Integrated Subsurface-Imaging Techniques for Detecting Cavities in the Gypsum Karst of Oklahoma

***Aondover Tarhule, Thomas Dewers, Roger Young, and Alan Witten***
University of Oklahoma
Norman, Oklahoma

***Todd Halihan***
Oklahoma State University
Stillwater, Oklahoma

**ABSTRACT.**—Timely detection of karst geohazards could potentially minimize expensive investigations, litigation, or remediation that frequently attends damage to surface structures such as buildings or highways. This paper reports preliminary results from a study that investigated the feasibility of using geophysical subsurface-imaging techniques to detect voids in the gypsum karst of Oklahoma.

Four methods—seismic reflection and refraction, broadband electromagnetic induction (EMI), and electrical-resistivity tomography (ERT)—were used to map the Nescatunga Cave system along U.S. Highway 412, ~20 mi east of Woodward. The following procedure was adopted. First, a coupled Trimble ProXRS® GPS system and LaserTech® reflectorless range finder were used to map the precise location of sections of the cavern. Next, geophysical surveys (using the four methods above) were carried out at the surface to attempt to detect the known caverns. This approach permits evaluation of the relative positional accuracy of cavern detection by the various methods.

The following findings emerged from the study: (1) shot records of seismic reflection did not detect the cavern, but seismic refraction appears to hold some hope for detecting, though not imaging, the cavern; (2) broadband EMI showed some indication of the presence of the cavern, but the image is poorly resolved; (3) ERT successfully detected the cavern, although cavern position was slightly offset.

It is concluded that further investigations of these methods are warranted, especially because of significant cost and time savings that could result from combining rapid, noninvasive surveys with conventional well-drilling programs.

## INTRODUCTION

Undetected subsurface voids and cavities may undermine highways and other surface structures, causing economic damage, insurance claims, litigation, expensive engineering remediation work, and, in some cases, loss of lives (Smith, 1997; Lambert, 1997; Johnson and Quinlan, 1995; Paukstys and others, 1999). The risk of subsidence and/or collapse is especially severe in gypsum karst because of the rapid dynamics of gypsum karstification: gypsum is approximately 150 times more soluble than limestone (Galloway and others, 1999). As a result, gypsum karst can develop on a human/engineering time scale, sometimes in a matter of days to years, particularly when land-use practices induce changes in ground-water-circulation patterns.

Timely detection of voids is therefore desirable—preferably in the preplanning phase of projects—to save time and potentially minimize expensive investigations or remediation owing to structural damage. The problem is that conventional site-characterization techniques, such as drilling and core sampling, downhole geophysical logging, well monitoring, and hydrochemical- and spring-discharge hydrograph analysis, can be expensive and unreliable. Johnson (2001) describes the case of the Mangum dam site, investigated and evaluated since 1937. Coring and borehole-pressure testing conducted in 1999 along the proposed dam alignment revealed open and clay-filled cavities in and near the abutments. Fluid losses ranged from 60 L/min to 5,300 L/min. Engineering measures needed to remediate karstic foundation problems would greatly add to the cost of the dam, and still would not assure tightness of the reservoir or dam integrity. This example illustrates the point that even with close-spaced networks of drilled wells, the risk

Tarhule, Aondover; Dewers, Thomas; Young, Roger; Witten, Alan; and Halihan, Todd, 2003, Integrated subsurface-imaging techniques for detecting cavities in the gypsum karst of Oklahoma, *in* Johnson, K. S.; and Neal, J. T. (eds.), Evaporite karst and engineering/environmental problems in the United States: Oklahoma Geological Survey Circular 109, p. 77–84.

that the discrete well points miss large voids is very high. Additionally, significant uncertainties can arise in interpolating the lateral continuity and true subsurface geometry of voids between wells.

On the other hand, integrating conventional borehole information with continuous subsurface-imaging techniques could significantly improve both stratigraphic resolution and the probability of void detection. In this paper we report preliminary results of a study applying geophysical subsurface-imaging techniques to detect, delineate, and map the karst geohazards around the Nescatunga Cave system along U.S. Highway 412 in Major County, western Oklahoma. Within this large cave system (some chambers measure 25 ft high by 30 ft wide), there is clear evidence of partial collapse beneath U.S. 412, possibly dating to the original construction of the highway. Our approach is to test the effectiveness and reliability of the study methods for detecting known caverns, and then to use the insights and experience gained to map unknown voids, vents, and chambers.

## BACKGROUND AND STUDY AREA

The Oklahoma Department of Transportation (ODOT) proposes to upgrade U.S. 412 from the present two lanes to four lanes. The new engineering designs will lower the grade of the highway above the Nescatunga cavern by about 20 ft, significantly increasing the risk of structural damage to the highway if subsurface karstic features are not detected and properly treated. The geology of the study site consists of Permian soluble gypsum beds and red-shale beds of the Blaine Formation, underlain by the Flowerpot Formation. Four gypsum beds, two dolomites, and intervening clay shales make up the Blaine Formation at this site. The Medicine Lodge Gypsum Member, the lowermost gypsum layer of the Blaine, contains the cavern system. The Medicine Lodge is overlain by shale, dolomite, and then by the Nescatunga Gypsum Member. Red shales overlie the Nescatunga, and topping the red shales is another layer of dolomite. Fay (1964) and Miller and others (2003) provide more extensive descriptions of the geological setting. Successful detection of subsurface karstic features at this site could have wide applications throughout the State of Oklahoma, because soluble rocks underlie significant parts of the State (see Johnson and Quinlan, 1995).

## METHODS

The research approach consisted of a two-step process. First, a new GPS/laser positioning system, which is capable of taking GPS (UTM) coordinates inside a cave was used to map the internal dimensions of sections of the Nescatunga cavern. The system, comprising a Trimble ProXRS® GPS unit and a Laser Tech® reflectorless range finder, established the coordinates and elevations of selected points inside the cave passage. Miller and others (2003) provide detailed descriptions about the procedure. Next, surface surveys, utilizing seismic reflection, seismic refraction, broadband electromagnetic induction (EMI), and electrical-resistivity tomography (ERT), were carried out in an attempt to detect the previously mapped cavern sections. For each method, survey transects were carried out approximately perpendicular to the known cave passage. The Trimble ProXRS® GPS system was again used to obtain GPS coordinates and elevations of selected points along each transect. Superimposing the two transects allowed us to establish the true position and elevation of the cave beneath the surface transect. Miller and others (2003) illustrate the procedure. Finally, the relative accuracy of each method in detecting the cavern was evaluated by comparing the position of the cavern signature detected from the geophysical methods against its true location as determined from the internal cave mapping.

Surveys were carried out along two sections of the cavern, designated *A* and *B* (Fig. 1). The depths to the cave at section A are available from cores drilled by ODOT, which are used as "ground truth" to validate features detected from geophysical surveys. A major collapse at B permits entry into the cave at this point and is sometimes referred to as the "window" entrance. Here, GPS coordinates and elevations of the cave passage were determined for ~300 m, using the combined GPS/laser range-finder system. The following paragraphs describe the surface survey methods.

### Seismic Reflection and Refraction

Seismic experiments were conducted from July 23 to July 24, 2002, to assess the feasibility of using hammer seismic shear-wave surveys in the karst topography of the Nescatunga Cave area. Two surveys were completed: one parallel to and north of U.S. 412, and the second near the window entrance (Fig. 1). A 24-channel EG&G StrataView recorder was used to record shear waves generated by the OU shear source and sensed by 10-Hz horizontal-component geophones. The choice of shear-wave surveys rather than compressional-wave surveys was made to minimize the ground-roll noise frequently observed in shallow seismic recordings. The anticipated geologic structure was a cave of uncertain extent (but estimated to be about 5 m wide by 2 m high and situated ~21 m below ground surface).

### Broadband Electromagnetic Induction

Electromagnetic induction (EMI) exploits the fact that whenever an electrically conductive object is exposed to a time-varying magnetic field, a time-varying electric current is induced in the object (Witten and others, 1997a). The magnitude of this current, referred to as an eddy current, depends on the strength of the magnetic field to which it is exposed and the electrical conductivity of the object. The stronger the field or the greater the electrical conductivity, the stronger the eddy current induced. Since any object

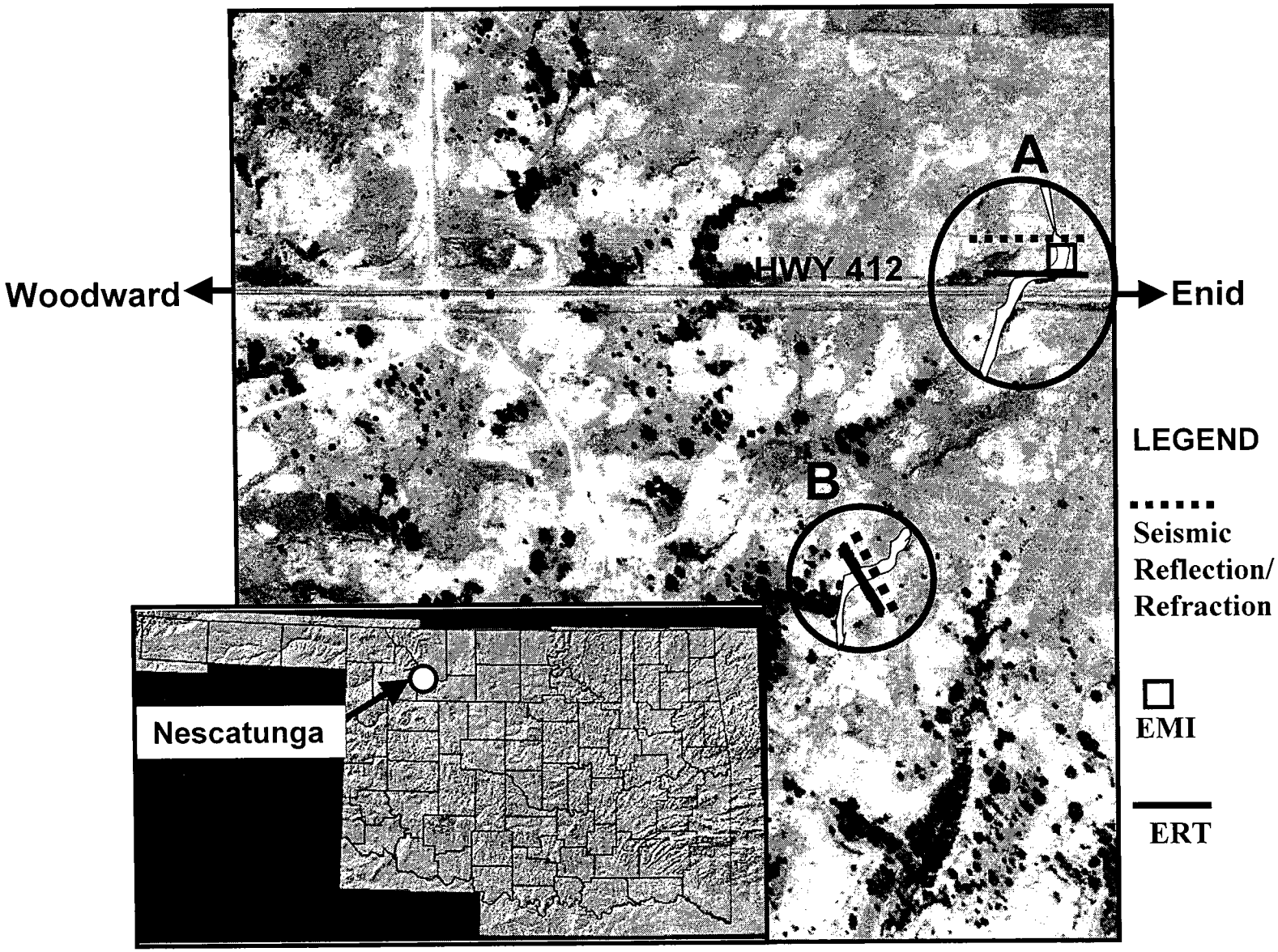


Figure 1. Aerial view of the study area, showing the survey site near U.S. Highway 412 (*A*) and the "window" entrance to the cave (*B*). The aerial photograph was produced by Scott Christenson (U.S. Geological Survey). At both sites the actual location of the cavern passage underneath the ground is shown, as well as the approximate location of survey transects used by each geophysical method. Inset map shows the location of Nescatunga Cave in Oklahoma. EMI = electromagnetic induction; ERT = electrical-resistivity tomography.

conveying a time-varying electrical current will emit a time-varying magnetic field, the conducting object can be detected by monitoring the strength of its emitted secondary field. Depth information can be extracted from EMI measurements by transmitting time-varying magnetic fields that oscillate with different frequencies. Higher frequency magnetic fields are preferentially attenuated by geologic material, so depth sounding can be accomplished by sequentially lowering the transmitted frequency (see Witten and others, 1997b).

We employed the GEM-2, consisting of two coils, one to transmit a time-varying electric field and a second to measure the secondary field. One survey was conducted over a 20-m by 20-m grid at the Nescatunga Cave system. The grid was positioned directly above a cavern chamber 25 m below ground surface. Measurements were made at intervals of 0.66 m (2 ft) along grid lines 0.66 m (2 ft) apart, and the results were plotted in Surfer.

### Electrical-Resistivity Tomography

These ERT methods consist fundamentally of introducing an electrical current of known voltage into the subsurface through two current electrodes, and then using two potential electrodes to measure the potential drop induced by the differential response of various earth materials to the penetrating current. Voids or cavities appear as anomalously low (water-filled) or high (air-filled) areas relative to the background-resistivity field (National Research Council, 2000). The method has been successfully employed to map subsurface cavities and karst in limestone (e.g., Lambert, 1997; Zou and others, 2000; Abdul Nassir and others, 2000).

ERT mapping was accomplished by using a Sting R1-IP resistivity meter (28 electrodes) manufactured by Advanced Geosciences, Inc. (AGI), in Austin, Texas. Surveys utilizing dipole–dipole, Wenner and Wenner-Schlumberger arrays, were carried out between May 28 and May 29, 2002, along the highway (Fig. 1, *A*). Electrode spacing was set at 7 m. A second survey, utilizing the same arrays and with electrode spacing at 5 m, was completed (Fig. 1, *B*) between July 24 and July 25, 2002. The field data were analyzed using RES2DINV (Loke and Barker, 1996).

## RESULTS AND DISCUSSION

### Seismic Reflection and Refraction

Figure 2 shows the very noisy records obtained near the highway. High-frequency noise (240 Hz or higher) swamps most traces. The farther offset traces do exhibit seismic noise, but no reflections are observable. It was surmised that construction work using bulldozers, plus a pumping unit, in the vicinity of the survey might have been the source of the seismic noise. However, high-frequency noise (west end) and seismic noise (east end) were still present during a subsequent survey near the window entrance when no construction activity took place (Fig. 3). It is possible, therefore, that the noise is simply ambient noise amplified by the very high gains (~50 dB) applied. Any reflections present ought to have been detectable at these gains. Hence, it appears that the pursuit of very weak to nonexistent reflections compelled the use of extreme amplification in order to see them. As a result, however, exaggerated noise dominates the profile because the noise is very large relative to the possible reflections.

Figure 3 shows dots marking the traveltime picks for the refraction. Note how the times are linear from traces 1–15, then the time increases, producing a cup-shaped set of picks. Clearly, something has caused the apparent velocity of the refraction to increase and then start to decrease at traces 22–24. The center of the cave is at approximately trace 11. The traveltime increase is seen to the right of the cave. Additionally, both the first-arrival pattern and ground roll changed, possibly suggesting the presence of the cave.

Hence, seismic reflection failed to detect the pres-

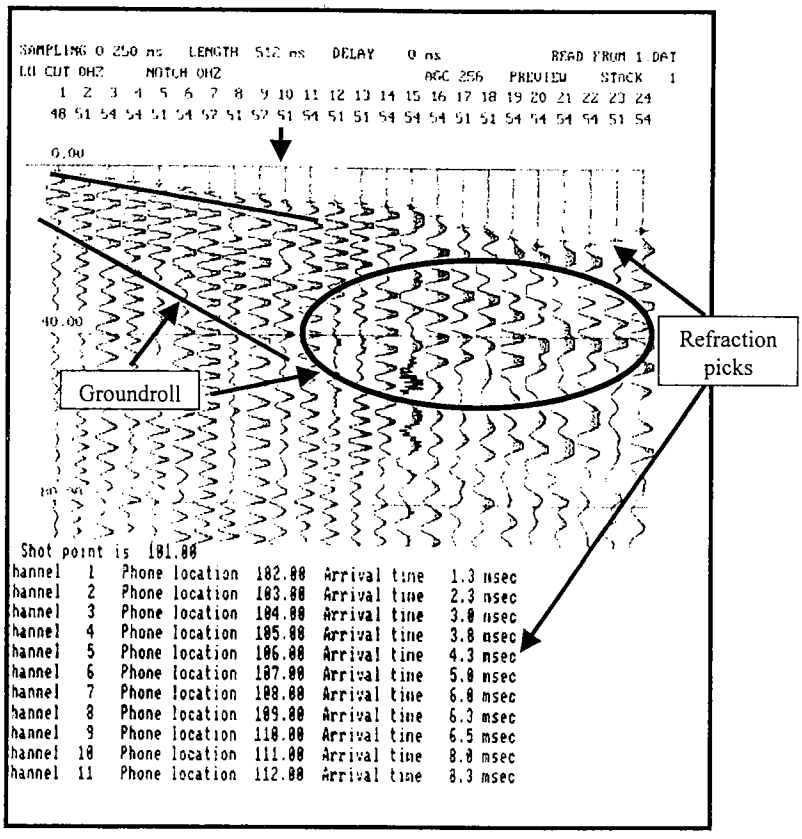


Figure 2. Results of seismic reflection and refraction survey near U.S. Highway 412.

ence of the cave. It is possible that the irregularity of the karst terrain, which is characterized by small to large and irregularly shaped voids plus compositional variation in the gypsum, results in extreme scattering of energy and no specular reflection. On the other hand, the refraction traveltimes (seismic refraction) and the change in appearance of ground roll hold some hope of *detecting,* but not imaging, the cavern.

### Electromagnetic Induction

Figure 4 plots the result of the EMI survey. The cavern extends diagonally across this region from lower right to upper left, and some indication of its presence is evidenced by the relatively low conductivity response displayed in the light shades. Whereas the possible outline of the cave is indicated, it is poorly resolved, most likely because of the significant slope (>7°) in the surface terrain. In general, voids are best resolved with a uniform background. Further studies are therefore needed to improve cavern resolution.

### Electrical-Resistivity Tomography

Figure 5A shows the resistivity cross section near the highway. The plot is based on a dipole–dipole array utilizing 7-m electrode spacing. Electrode 14 was positioned next to an ODOT drill hole (95 m from the start of the survey transect). The depth to the bottom of the cave (measured in the drill hole) is 21 m. The cavern is approximately 5 m high by 10 m wide. This information was used to locate the cave on the resistivity profile. The cave coincides in position with an area of anomalously high resistivity (>22,000 ohm-m), providing definitive proof of this anomaly as a void. However, the resistivity anomaly is slightly offset to the right of the true position of the cave. An examination of the measured resistivity data points revealed two missing measurements at this depth. Missing measurements occur during surveys owing either to a faulty electrode or an inability of the Sting device to obtain usable data at that measurement point. Hence, interpolation over the missing points could have resulted in a shift of the anomaly. Even so, the result is consistent with other investigators (see www.agiusa.com/stingcave.shtml) that have also reported marginal positional offsets to the true locations of caves as detected from resistivity profiles. No other resistivity anomalies are detected on this profile.

Figure 5B is a plot of the resistivity cross section near the window entrance. The survey utilized a Wenner array with 5-m electrode spacing (equipment failure precluded the use of a dipole–dipole array at this site). The plot revealed two anomalies, one in the center of the plot with a resistivity >24,000 ohm-m, and a second to the left of the profile but at the same depth as the first anomaly with a resistivity >11,000 ohm-m. From the results of the GPS/laser-range mapping, it was established that the centroid of the cave passage is at electrode 14 (65 m) and the depth to the bottom of the cave is 10–11 m. The cave itself measured 3 m high by 12 m wide at this point. Superimposing this information on the resistivity profile confirmed that the anomaly in the center of the image is the target cave passage. Such excellent agreement suggests strongly that the second anomaly is also most likely a cavern passage. Although this passage is not mapped, local cavers with whom we spoke mentioned a second cave passage parallel to the main one we surveyed and in the general location of the anomaly identified. The results suggest that ERT is a viable method for detecting subsurface features in the gypsum karst of Oklahoma. Further studies are needed, however, to determine the dimensions and depths at which karst features can be detected reliably and consistently.

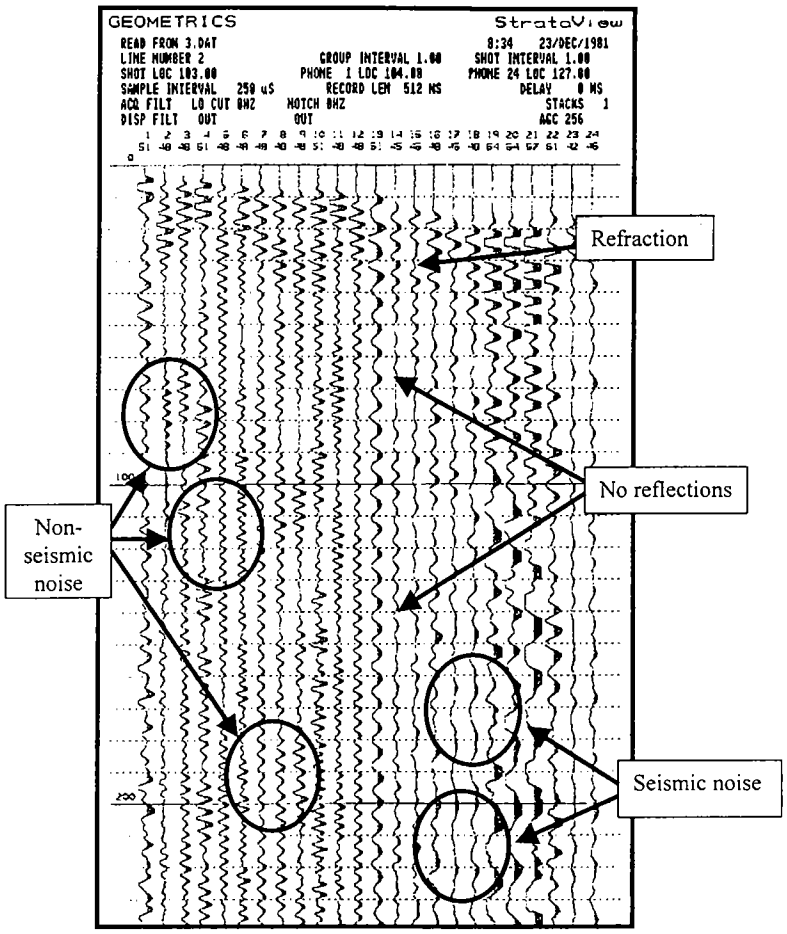


Figure 3. Results of seismic reflection and refraction survey near the window entrance.

## SUMMARY AND CONCLUSIONS

Rapid dissolution of karstic rocks poses serious hazards for land use and surface

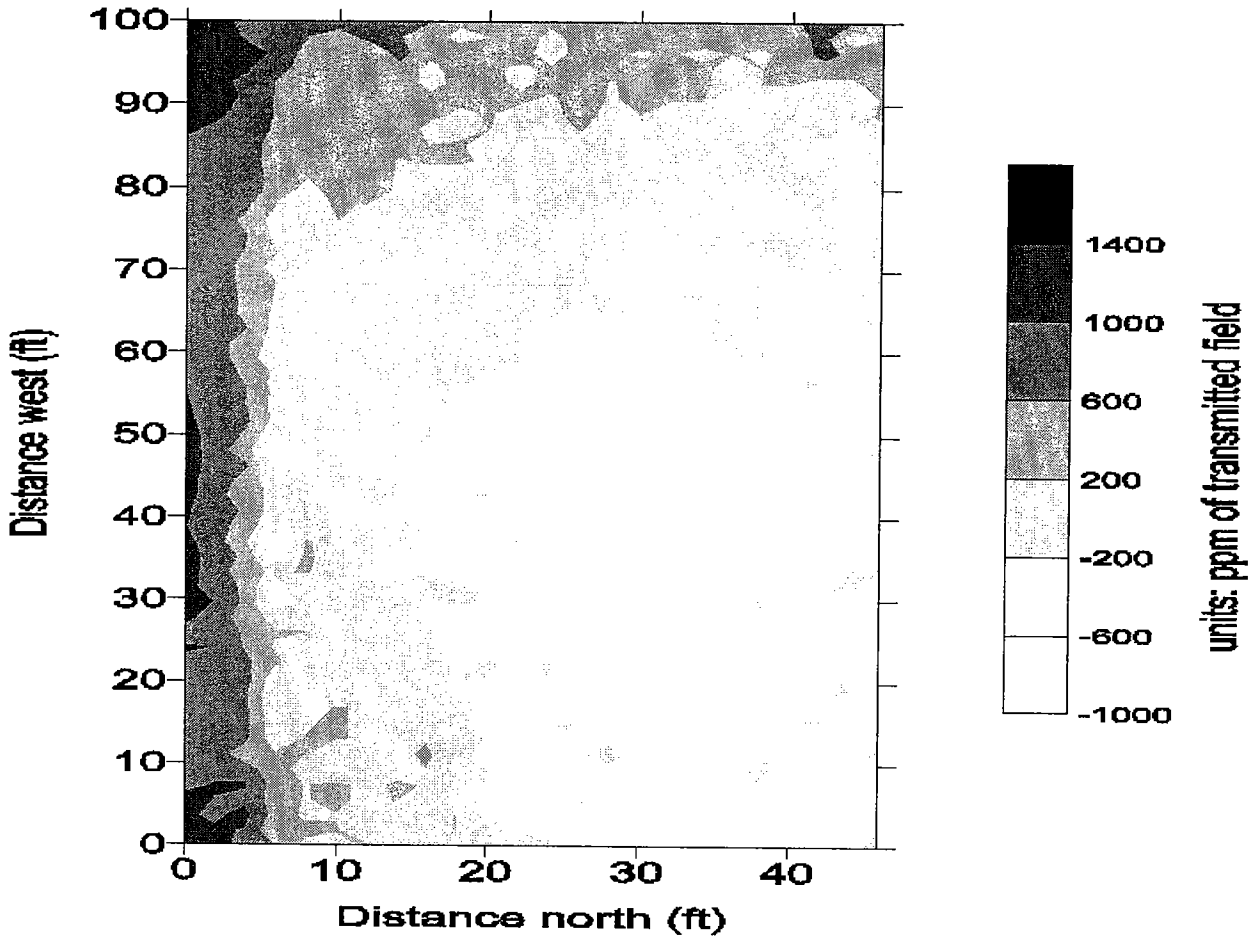


Figure 4. Electromagnetic-induction data near U.S. Highway 412, showing the response to subsurface variations in electrical conductivity. Lower measured values are associated with lower conductivity. The target cavern crosses the image diagonally from upper left (west) to lower right (north).

features including highways. This study investigated the feasibility of using geophysical methods to noninvasively detect and map voids in Oklahoma's gypsum-karst environments. The following preliminary findings emerged from the study.

1. The capability for GPS mapping inside a cave system allowed us to establish the precise location of target voids in an x,y,z coordinate system. This information is used to evaluate the positional accuracy of anomalous features detected from geophysical methods. This approach minimizes uncertainties that may arise concerning the true location of a cavern on modeled plots of geophysical surveys. As a research tool, the method could provide valuable insight about the void-detection potential of different subsurface-imaging methods, permitting refinements to be made prior to surveys in areas with limited or no information about subsurface features.

2. Seismic reflection failed to detect the target voids in the study area. We hypothesize that extreme scattering of energy in the highly irregular karst geology may be responsible for the inability to detect the voids. On the other hand, the refraction traveltimes and the change in appearance of ground roll hold some hope of *detecting*, but not imaging, a cave.

3. Broadband EMI produced a smudged image, suggesting the possible location of the target cave passage. The orientation of the image on the EMI plot is consistent with the known direction of the cave passage, but its resolution is poor, possibly as a result of significant terrain heterogeneity. Further tests in areas with more homogeneous terrain are recommended, as well as methods that incorporate terrain heterogeneity.

4. ERT successfully detected target cavities at both study sites. Resistivity anomalies show excellent agreement with the true position of caverns established from GPS/laser-range mapping and drilled holes. Such "ground truth" provides confidence in the results and suggests that resistivity tomography is a viable method for detecting subsurface voids in Oklahoma's gypsum karst.

## ACKNOWLEDGMENTS

The Oklahoma Transportation Center (OTC) provided major funding for this study, for which we are

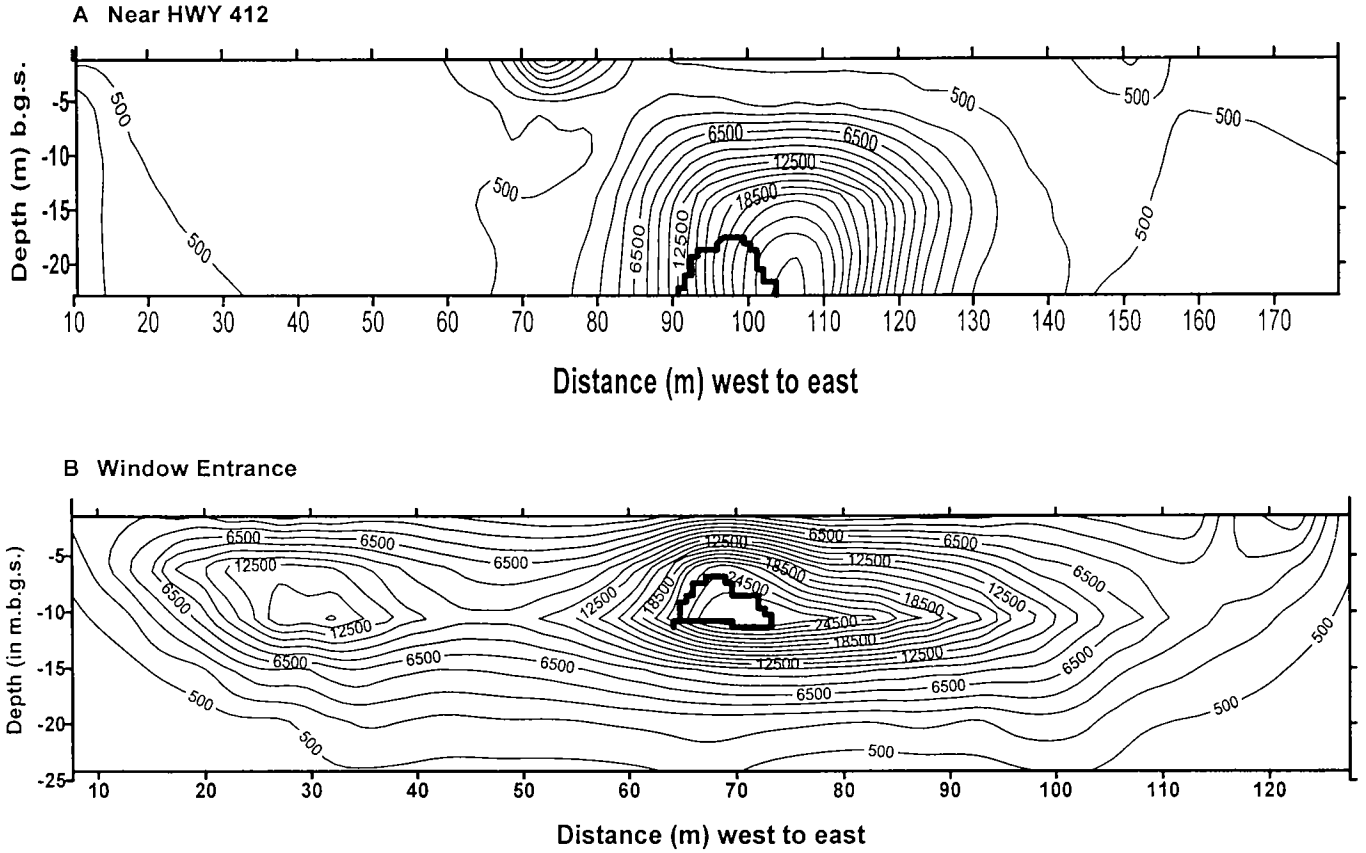


Figure 5. Two-dimensional resistivity cross sections of the subsurface (*A*) near U.S. Highway 412, based on a dipole–dipole array and 7-m electrode spacing, and (*B*) near the window entrance, based on a Wenner array and 5-m electrode spacing. The true location of the cavern is shown on both plots, and contours represent resistivity values in ohm-meters; m.b.g.s. = meters below ground surface.

very grateful. We thank especially Drs. Gorman Gilbert and Thomas Landers for coordinating the research initiatives. The Oklahoma Department of Environmental Quality (ODEQ) and the Oklahoma Water Resources Research Institute (OWRRI) provided additional funding. We acknowledge with gratitude the assistance and cooperation received from the landowners, including the Ingmans, R. Harris, and L. Harms. We thank Scott Christenson (U.S. Geological Survey), Curt Hayes (consulting geologist for ODOT), and Jim Nevels (chief soil scientist, Materials Division, ODOT) for their cooperation and assistance in various aspects of this study. We are grateful to Galen Miller for field assistance and support provided by the Oklahoma Geological Survey. Finally, we are pleased to acknowledge the contribution of our field assistants: Mark Jaeger, Zakari Saley-Bana, Julie Turrentine, Brent Wilson, and Joseph Zume.

## REFERENCES CITED

Abdul Nassir, S. S.; Locke, M. H.; Lee, C. Y.; and Nawawi, M. N., 2000, Salt-water intrusion mapping by geoelectrical imaging surveys: Geophysical Prospecting, v. 48, p. 647–661.

Fay, R. O., 1964, The Blaine and related formations of northwestern Oklahoma and southern Kansas: Oklahoma Geological Survey Bulletin 98, 238 p.

Galloway, D.; Jones, R. J.; and Ingebritsen, S. E., 1999, Land subsidence in the United States: U.S. Geological Survey Circular 1182, 158 p.

Johnson, K. S., 2001, Gypsum karst leads to abandonment of a proposed damsite in Oklahoma [abstract]: Geological Society of America Abstracts with Programs, v. 33, no. 6, p. A-132.

Johnson, K. S.; and Quinlan, J. F., 1995, Regional mapping of karst terrains in order to avoid potential environmental problems: Cave and Karst Science, v. 21, p. 37–39.

Lambert, D. W., 1997, Dipole–dipole D.C. resistivity surveying for exploration of karst features, *in* Beck, B. F.; and Stephenson, Brad (eds.), The engineering geology and hydrogeology of karst terranes: Balkema, Rotterdam, p. 413–418.

Loke, M. H.; and Barker, R. D., 1996, Rapid least-squares inversion of apparent resistivity pseudosections by a quasi-newton method: Geophysical Prospecting, v. 44, p. 131–152.

Miller, Galen; Dewers, Thomas; and Tarhule, Aondover, 2003, Laser positioning and three-dimensional digital mapping of gypsum karst, western Oklahoma, *in* Johnson, K. S.; and Neal, J. T. (eds.) Evaporite karst and engineering/environmental problems in the United States: Oklahoma Geological Survey Circular 109 [this volume], p. 71–75.

National Research Council, 2000, Seeing into the Earth; noninvasive characterization of the shallow subsurface for environmental and engineering applications: National

Academic Press. Washington. D.C., 129 p.
Paukstys, B.; Cooper, A. H.; and Arustiene, J., 1999, Planning for gypsum geohazards in Lithuania and England: Engineering Geology, v. 52, p. 93–103.
Smith, T. J., 1997, Sinkhole damage investigations for the insurance industry, *in* Beck, B. F.; and Stephenson, Brad (eds.), The engineering geology and hydrogeology of karst terranes: Balkema, Rotterdam, p. 299–304.
Witten, A. J.; Won, I. J.; and Norton, S., 1997a, Subsurface imaging with broadband electromagnetic induction: Inverse Problems, v. 13, p. 1621–1639.
_____1997b, Imaging underground structures using broadband electromagnetic induction: Journal of Environmental and Engineering Geophysics, v. 2, p. 105–114.
Zou, W.; Beck, B. F.; and Stephenson, J. B., 2000, Reliability of dipole–dipole electrical resistivity tomography for defining depth to bedrock in covered karst terranes: Environmental Geology, v. 39, p. 760–766.

# Gypsum Karst and Abandonment of the Upper Mangum Damsite in Southwestern Oklahoma

***Kenneth S. Johnson***
Oklahoma Geological Survey
Norman, Oklahoma

**ABSTRACT.**—Recent engineering-geology assessment of the proposed Upper Mangum Damsite, in an area of gypsum karst in southwestern Oklahoma, has shown that the site is unsuitable and should be abandoned. The damsite, on the Salt Fork of Red River near the town of Mangum, has been investigated since 1941, based mainly upon its favorable topography; both proposed abutments are high and form a narrow water gap between them. This decision did not adequately consider the geology, foundation conditions, or water-impoundment capabilities of the site. Abutments would be in the Permian Blaine Formation, here consisting of 200 ft of gypsum with thin interbeds of dolomite and shale. The Blaine Formation locally is characterized by abundant gypsum-karst features, such as caves, sinkholes, disappearing streams, and springs.

In 1999 a final assessment was made of the surface geology, and the results of coring and pressure testing five boreholes (each 130–151 ft deep), along the proposed dam alignment. The assessment showed that open cavities, clay-filled cavities, and other karst features are abundant in and near the abutments; and fluid losses (in each 10-ft interval of rock that was tested) ranged from 15 to 62 gpm in most borehole pressure tests, and in one borehole the losses were 410–1,316 gpm. Engineering measures needed to remediate karstic-foundation conditions here would add greatly to the cost of construction and still would not assure tightness of the reservoir or integrity of the dam. Therefore, it is recommended that this site be abandoned and that future studies be at the Lower Mangum Damsite, a more favorable site 7 mi farther downstream on the Salt Fork of Red River.

## INTRODUCTION

This report presents the results of geotechnical investigations at the proposed Upper Mangum Damsite, on the Salt Fork of Red River in the southwestern part of Greer County, Oklahoma (Fig. 1). The site is ~9 mi west and 2 mi south of the city of Mangum. Investigations consisted of evaluating all previous geologic and hydrogeologic studies bearing on the project, drilling five exploratory core borings, collecting soil samples for laboratory testing, water-pressure testing of completed boreholes, and geologic reconnaissance along the dam axis.

The study was carried out on behalf of the Tulsa District Office of the U.S. Army Corps of Engineers (Corps), the Oklahoma Water Resources Board (OWRB), and the citizens of Mangum. It was done under the Planning Assistance to States Program (Public Law 93-251). This report is a summary of the final study (U.S. Army Corps of Engineers, 1999), which was prepared by the current author.

Appreciation for support and assistance is expressed to the following individuals: Phil Cline, Frank Oler, and Bob Thurman, with the Corps; Mike Mathis and Terri Sparks, with OWRB; and Stephen Scott, Roger Lively, Dale Clayton, and other members of the Mangum Reservoir Project Committee.

## PROJECT HISTORY

A series of reports by the U.S. Bureau of Reclamation (BOR) characterized several potential damsites on the Salt Fork of Red River, upstream from Mangum (Kirchen, 1941; Smith and Nickell, 1941; Current, 1942; U.S. Bureau of Reclamation, 1943, 1963; Darnell, 1954; Redfield, 1960). The earliest reports (Kirchen, 1941; Smith and Nickell, 1941) summarized reconnaissance surveys of five potential sites, and an early decision was made that "the best site at least from a topographic standpoint which we saw on Salt Fork is the Upper Mangum in section 10, T. 4 N., R. 23 W., 6½ miles southwest of Mangum" (Smith and Nickell, 1941, p. 3). That decision was based mainly upon topography at the potential damsite and did not adequately consider the geology, foundation conditions, or water-impoundment capabilities of the site.

Since the 1941 report, all efforts were focused on the search for a possible damsite in that general area,

Johnson, K. S., 2003, Gypsum karst and abandonment of the Upper Mangum Damsite in southwestern Oklahoma, *in* Johnson, K. S.; and Neal, J. T. (eds.), Evaporite karst and engineering/environmental problems in the United States: Oklahoma Geological Survey Circular 109, p. 85–94.

in spite of the extensive gypsum-karst system discovered at all prospective damsites at or near the original Upper Mangum site. Gypsum-karst features identified in the project area, and described in most of the site investigations, include major caves, sinkholes, disappearing streams, springs, and underground water courses; these result from dissolution of relatively soluble gypsum and dolomite rock units that are widespread in the area.

Following a final BOR report on the Upper Mangum project (Jackson, 1991), the Corps was asked to join with the OWRB and local Mangum officials to make a final determination of the viability of the project (U.S. Army Corps of Engineers, 1993). A second Corps report (U.S. Army Corps of Engineers, 1995) focused on characterizing the geology and ground-water conditions at and near the site on the basis of a review of existing data and of new geotechnical investigations conducted at the proposed damsite. The report concluded that (1) the abutments contain extensive amounts of soluble gypsum; (2) core samples and pressure tests show these rock units to be highly permeable; (3) karst features are present at the surface and at depth, particularly near the stream bed; (4) foundation conditions are marginal, at best, and could impact the integrity of the dam foundation and embankment; and (5) defensive measures required to mitigate the adverse impact of these conditions would be extensive, and still may not provide a permanent solution to the problem posed by karst features.

The final Corps report on the project (U.S. Army Corps of Engineers, 1999) incorporates data from the 1995 report, along with new evaluations of the geology, salt deposits, hydrogeology, karst features, foundation conditions, and reservoir tightness at and near the proposed damsite. That report (summarized here) pointed out that almost all geologic, engineering-geology, and hydrogeologic conditions at the site are adverse to building a dam and reservoir that would hold water, and that the Upper Mangum Damsite is unsuitable and should be abandoned. Furthermore, a more suitable site was identified about 7 mi downstream on the Salt Fork of Red River; a preliminary study of this Lower Mangum Damsite is reported by Johnson (2003b).

## GEOLOGY

The proposed Upper Mangum Dam and Reservoir would be situated in the Mangum Gypsum Hills of southwestern Oklahoma (Curtis and Ham, 1972). The area is characterized by a series of low-lying, widely spaced benches or escarpments, capped by resistant layers of gypsum and dolomite in the Permian Blaine Formation. In the vicinity of the damsite the escarpments are well defined and are up to 100 ft high. The Salt Fork of Red River rises in the High Plains of the Texas Panhandle, near the city of Claude, and flows in an east-southeasterly direction, through the Mangum area, to its confluence with Red River near

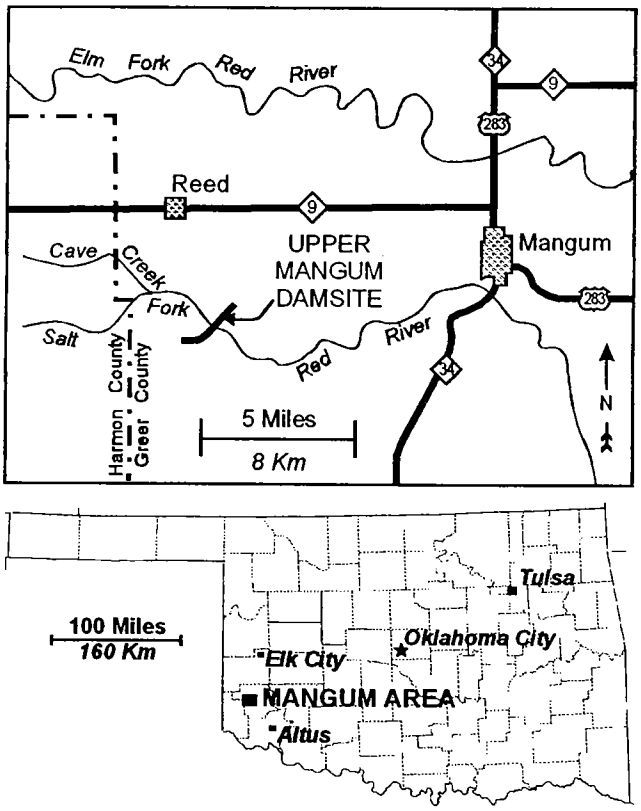


Figure 1. Map showing location of proposed Upper Mangum Damsite in southwestern Oklahoma.

Elmer, Oklahoma. The drainage basin of Salt Fork above the proposed damsite is about 1,313 mi$^2$.

Some of the most striking topographic and geologic features of the area are the dissolution and karst features in outcropping and underlying bedrock strata. Karst features, which are most prevalent along and near major streams, include numerous caves, disappearing streams, springs, fissures, and sinkholes, as well as subsidence basins and locally erratic dips of the underlying rocks (Johnson, 1986, 1990b, 2003a; Jackson, 1991).

### Regional Geology

Rock units in the project area are a thick sequence of Permian sedimentary red beds and evaporites. The red beds are mostly reddish-brown shales, siltstones, and sandstones; the evaporites consist of layers or beds of gypsum, dolomite, and salt that were deposited on the Permian sea floor owing to evaporation of seawater (Fig. 2). The proposed dam is situated in the Hollis Basin, directly south of the Wichita Uplift. The Wichita Uplift, a part of which is now exposed as the Wichita Mountains, separates the deep Anadarko Basin on the north from the Hollis Basin on the south. As a result, bedrock units of the project area dip to the south and southwest into the Hollis Basin at rates of 10–50 ft per mi. Local variations of dip and strike result from karst features, including sinkholes and subsidence basins (Johnson, 1986, 1990b, 2003a; Jackson, 1991).

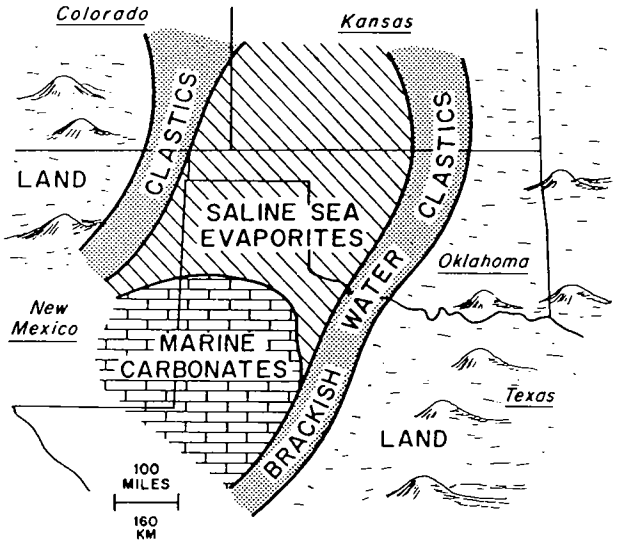


Figure 2. Map showing paleogeography and principal facies in the Permian Basin during deposition of gypsum and other evaporites in the Blaine Formation (from Johnson and Denison, 1973).

## Site Geology

Principal bedrock stratigraphic units at the damsite are Permian in age and include, in descending order, Dog Creek Shale, Blaine Formation, Flowerpot Shale, and Flowerpot Salt (Fig. 3). The Blaine Formation has been subdivided into the Van Vacter Member (above) and the Elm Fork Member (below). A general geologic map is presented in Figure 4. Permian bedrock units are overlain locally by overburden in the form of (1) alluvial (flood-plain) deposits along principal streams, and (2) terrace deposits in uplands away from the streams.

### *Overburden*

Alluvial deposits at the damsite are of Quaternary age and consist predominantly of sand, silt, clay, and minor gravel in the channel of Salt Fork and the adjacent flood plain. The thickness of these deposits is 23 ft in borehole BH-1-99, and they are estimated to be 1–50 ft thick in the area. Terrace deposits mantle some of the upland areas near the proposed reservoir. These loose sediments are Quaternary in age and consist mainly of sand, gravel, silt, and clay; their thickness generally ranges from 5 to 50 ft.

### *Dog Creek Shale*

The Dog Creek Shale consists of ~50–150 ft of red-brown shales in nearby outcrops, with several dolomite and gypsum beds present in the lower half of the formation. The gypsum and dolomite beds are generally 0.3–16 ft thick (Johnson, 1990a,b). Thin remnants of the lower part of the Dog Creek Shale are present in the right abutment (Fig. 4).

### *Blaine Formation*

The Blaine Formation consists of interbedded gypsum, dolomite, and shale, and has a total thickness of ~200 ft (Johnson, 1990a,b). Individual beds of gypsum and dolomite are laterally persistent and have a fairly uniform thickness throughout the project area, except where they are partly or totally removed by dissolution or erosion. The Blaine Formation consists of nine major gypsum beds, each 10–30 ft thick; each gypsum bed typically is underlain by a dolomite bed 0.5–5.0 ft thick (Fig. 3). Where deeply buried (at a depth >85 ft in BH-1-99), the Blaine contains layers and lenses of anhydrite within the gypsum beds.

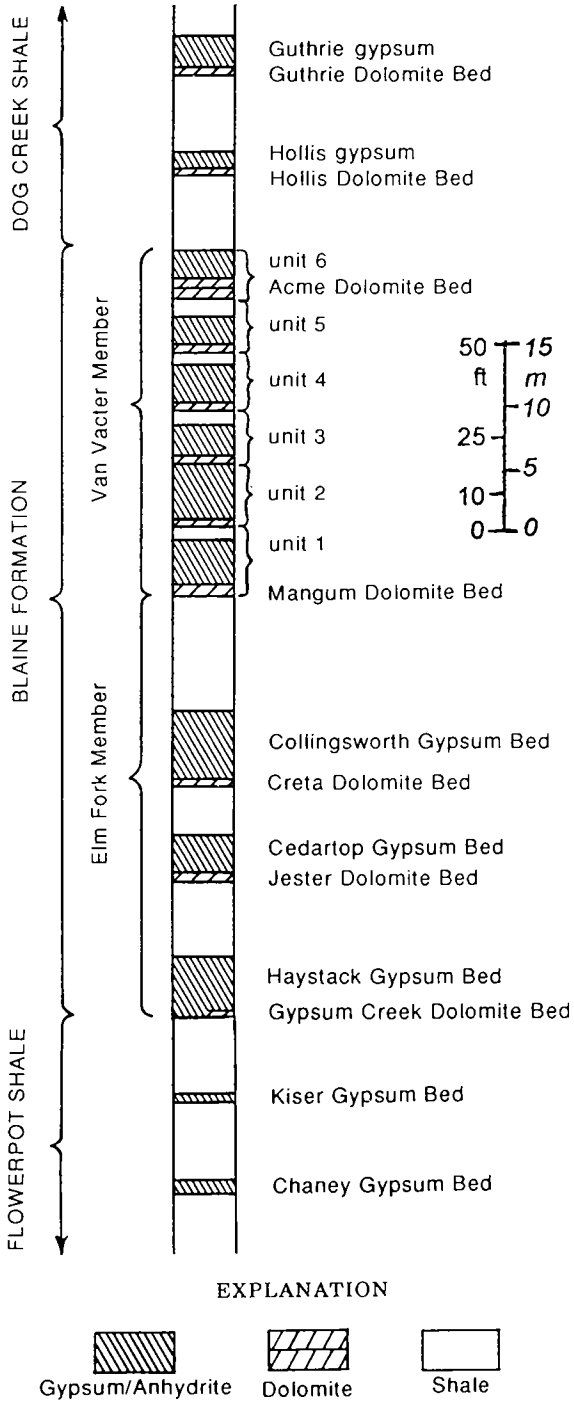


Figure 3. Stratigraphy of the Permian Blaine Formation and associated strata in the Hollis Basin area of southwestern Oklahoma (from Johnson, 1990a).

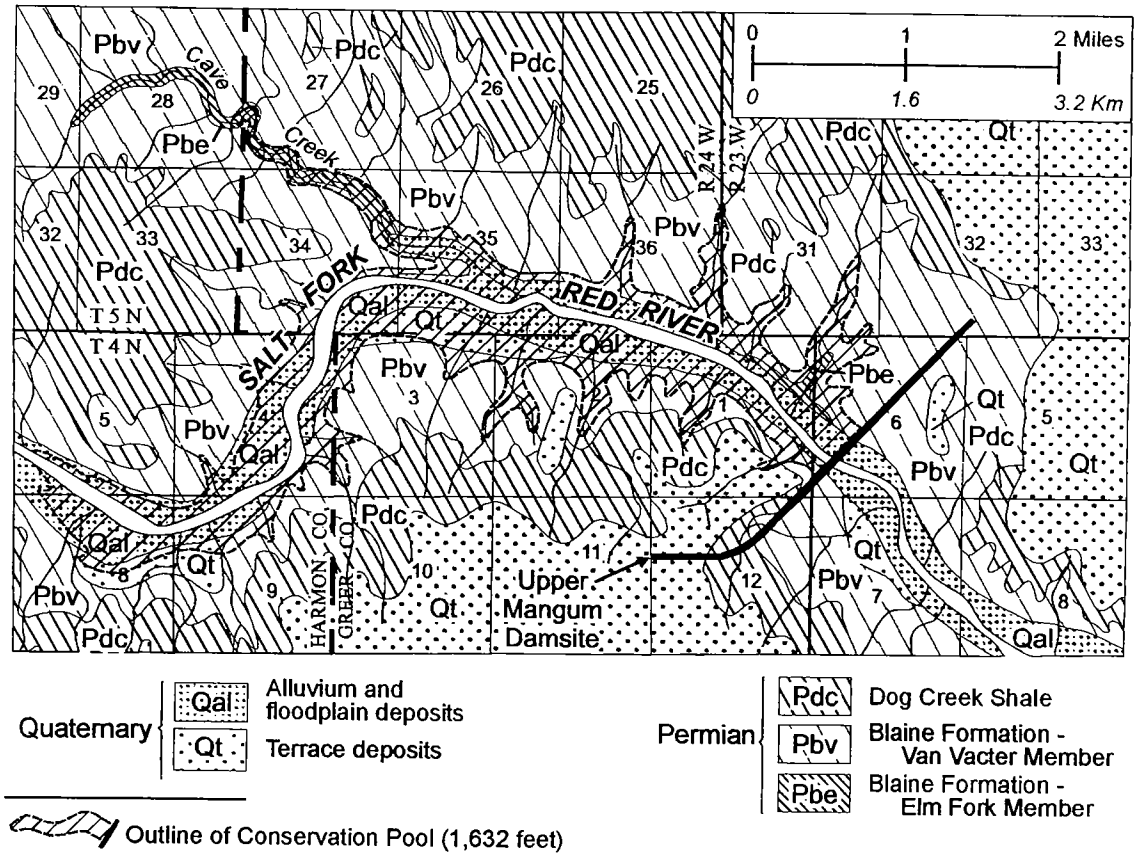


Figure 4. Geologic map of the proposed Upper Mangum Dam and Reservoir area (from Johnson and Ham, undated), and outline of proposed Conservation Pool.

The Blaine Formation is subdivided into two members, the Van Vacter Member above, and the Elm Fork Member below. The Van Vacter Member is ~100 ft thick and consists of six thick gypsum/dolomite units, separated by thin shales (Fig. 3). Gypsum beds in the Van Vacter are informally referred to as gyp-1 through gyp-6, and at the base of the Van Vacter is the widespread Mangum Dolomite Bed, which locally is up to 5 ft thick. The great amount of soluble gypsum and dolomite in the Van Vacter Member (~90% of its total thickness) makes this unit especially vulnerable to natural dissolution and development of karst features. The Van Vacter Member forms the left and right abutments for the proposed dam, and it also forms most of the impoundment area for the proposed reservoir (Fig. 4).

The Elm Fork Member is ~100 ft thick and consists of three thick gypsum/dolomite units, separated by thick shales (Fig. 3). The only Elm Fork outcrops in the project area are shales (just below the Mangum Dolomite) exposed ~0.5 mi upstream of the dam, and also along Cave Creek (Fig. 4). Soluble gypsum and dolomite make up ~50% of the Elm Fork Member, and a number of cavities and solution fractures occur within these units in subsurface.

### *Flowerpot Shale and Salt*

Underlying the Blaine Formation throughout the project area is the Flowerpot Shale. It consists mainly of red-brown shale with thin layers of greenish-gray shale, gypsum, dolomite, and salt (Johnson, 1990a,b). West of the damsite, in northern Harmon County, the Flowerpot contains layers of salt (halite), which is referred to as the Flowerpot Salt. The Flowerpot Salt was not known to be present in the project area until it was encountered in borehole BH-1-99 at a depth of 115 ft, ~14 ft below the top of the Flowerpot Shale. Only the uppermost 15 ft of Flowerpot Salt was cored beneath the damsite; rock salt makes up about half of this cored interval, and layers of shale containing veins of reddish-brown halite make up the remainder. Drilling ceased upon encountering artesian brine water and a flow of gas from the salt beds. The Flowerpot Salt has been partly dissolved in the project area by circulating ground waters, leaving patches of undissolved salt and/or high-salinity brine in the upper part of the Flowerpot Shale and the Flowerpot Salt.

## CORING AND PRESSURE TESTING OF BOREHOLES

Foundation exploration at the final proposed damsite consisted of four core borings, CH-1 through CH-4, drilled in 1995 in the abutments, along the centerline of the proposed dam (Fig. 5). A fifth core boring, BH-1-99, was drilled in March 1999 in the stream bed of Salt Fork along the centerline of the proposed dam. Bedrock units were cored using a 4-in.

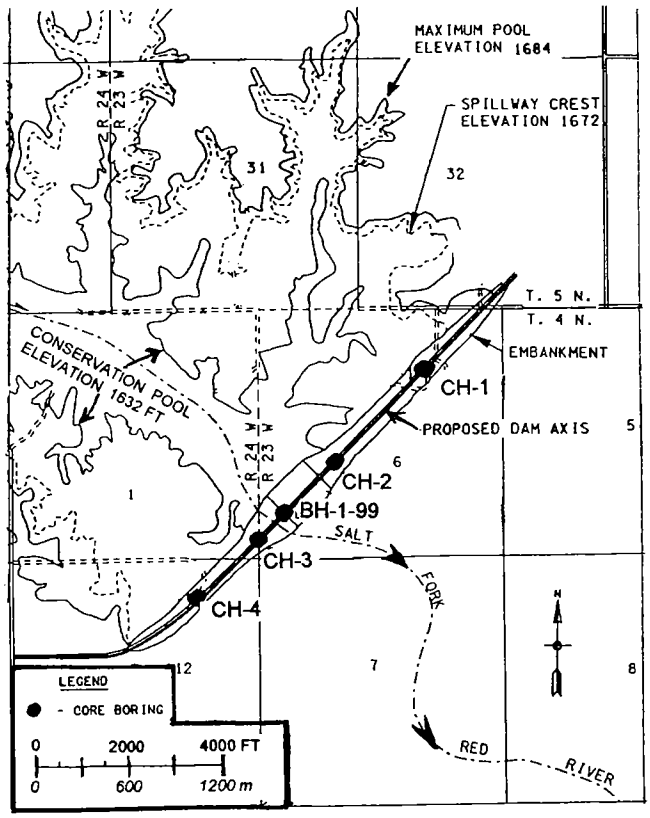


Figure 5. Map of proposed Upper Mangum Dam axis and locations of exploration boreholes.

core barrel equipped with a diamond bit. A geologic log of one of the borings is shown in Figure 6.

The rock most commonly encountered in the boreholes was gypsum, with lesser amounts of dolomite and shale. None of the borings encountered open cavities or caves as large as those exposed in the left abutment, or in the several caves mapped in the area. Some smaller voids were encountered in the boreholes, where the drill bit dropped rapidly during drilling; these voids are a few tenths of a foot to 1.8 ft high. All boreholes encountered vugs and open solution joints in most of the gypsum beds, and the Mangum and Creta Dolomite Beds typically are described as "solutioned, pitted, and broken" on geologic logs. Clay-filled solution cavities, cored in several holes, show that the original dolomite and gypsum have been removed locally by dissolution, and soft clayey rubble has collapsed into the cave or was deposited from through-flowing cave waters.

Borehole BH-1-99, drilled in the stream valley, also encountered solution cavities, solution fractures, and vugs in each of the gypsum and dolomite beds. The drill rig lost circulation of drilling fluid at the 24.5-ft depth, in the upper part of the Collingsworth Gypsum, indicating the presence of a through-going cavity that could accept a large amount of water. In addition, the rig drilled into a 2-ft-high dissolution cavity at the top of the Flowerpot Salt at a depth of 115.2–117.2 ft, and encountered additional vertical and horizontal voids to the total depth of 130 ft. At 128.5 ft the drill bit entered an artesian zone that caused salt water to flow up through the borehole to the land surface. Therefore, karst features are well developed in each of the Blaine gypsum and dolomite beds at the proposed damsite, and also in the underlying Flowerpot Salt.

Pressure tests were conducted in all borings at 10-ft intervals to determine seepage characteristics of the bedrock materials (Table 1). In borings CH-1 through CH-4, zones of high water loss were common. In borings CH-2 and CH-3, which are nearer the stream valley and thus subjected to more dissolution and collapse (as evidenced in the rock cores), zones of high water loss (15–61.7 gpm) typically were present over the entire length of each borehole rather than being confined only to selective intervals.

Pressure testing of BH-1-99 showed a remarkably high water loss from 40 to 120 ft (Table 1). Water loss increased constantly from 410 gpm (at 40–50 ft) to 1,316 gpm (at 100–110 ft), and the average loss for all 11 pressure tests was 682 gpm. Most of these pressure tests involved injection of water into gypsum, dolomite, and/or salt beds, thus showing that karst development is most extreme at, and beneath, the stream valley.

Therefore, the Blaine Formation and Flowerpot Salt are highly permeable, karstic formations at the damsite, as indicated by the following: a lack of drill-water return during coring; a general high loss of water pumped into the ground during borehole pressure testing; and the condition of the bedrock observed in rock cores and outcrops (cavities, voids, and open solution joints). A geologic profile depicting general foundation conditions and inferred karst along the proposed dam axis is shown in Figure 7. Construction at the proposed damsite would require addressing methods of cutting off the flow of water at all levels down to at least 120 ft (and probably to 130 ft or more) beneath the dam in the stream valley.

## HYDROGEOLOGY

### Regional Karst and Hydrogeology

Gypsum and dolomite beds of the Blaine Formation contain extensive caves and sinkholes and make up a major karst aquifer that is providing irrigation water for much of the Hollis Basin (to the south) and the Reed area (just north of the proposed damsite) (Steele and Barclay, 1965; Havens, 1977; Johnson, 1986, 1990b, 2003a; Runkle and McLean, 1995; Runkle and others, 1997; Osborn and others, 1997). The aquifer typically is 160–210 ft thick and generally is unconfined. Gypsum and dolomite have been partly dissolved by circulating ground water, creating a karst system that includes major caves, sinkholes, disappearing streams, springs, and underground water courses. These features are most common in areas where the thick and abundant gypsum beds of the Van Vacter Member are at or near the surface.

Borehole BH-1-99, drilled on March 5–9, 1999. Surface elevation about 1,580 ft *(482 m)*; total depth is 130 ft *(39.6 m)*.

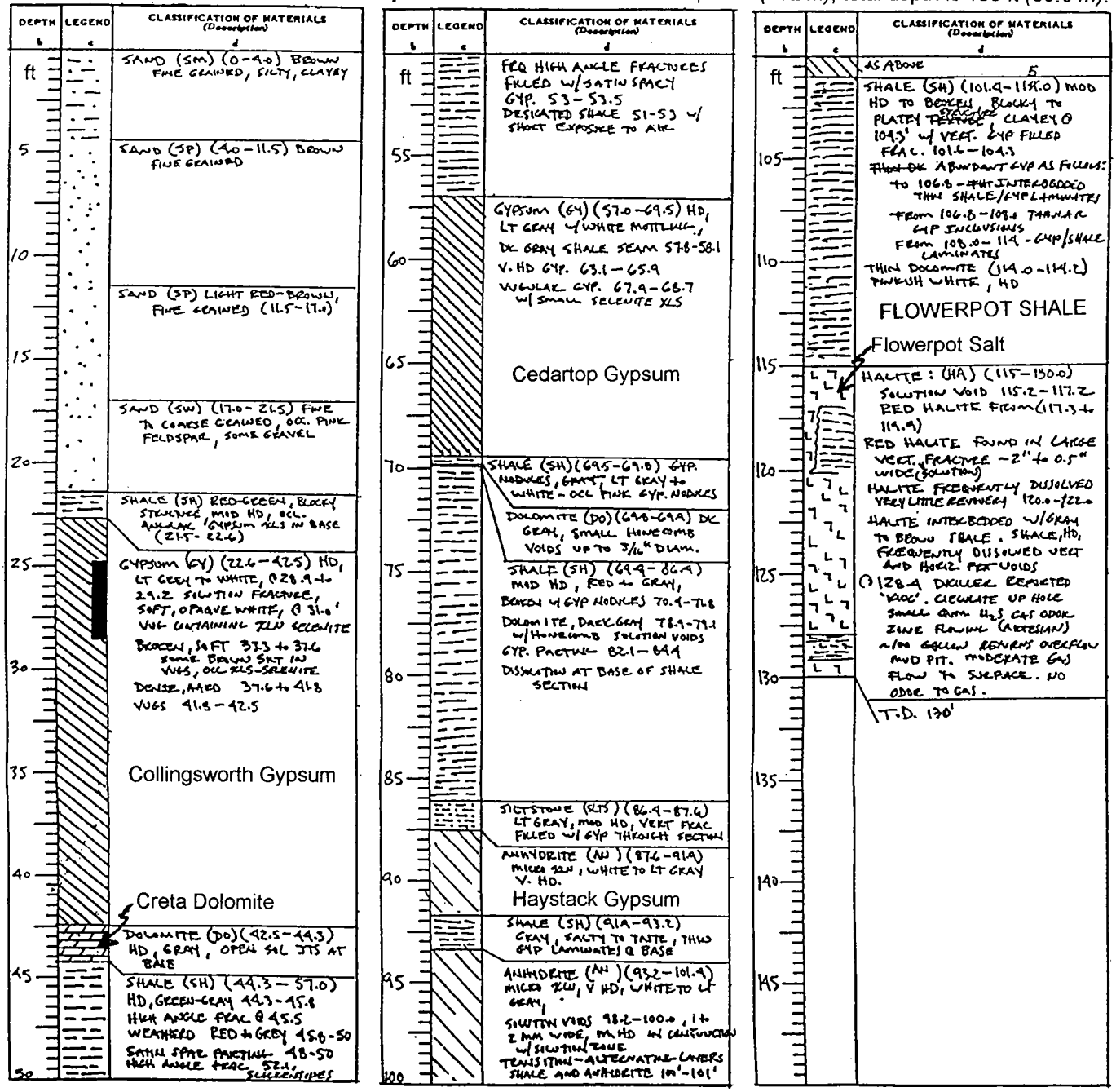


Figure 6. Geologic log of borehole BH-1-99, drilled in the stream valley along the axis of the proposed Upper Mangum Dam.

The development of porosity, and eventually of the open conduits through which water flows, occurs most commonly in the dolomite layers and in the lower part of each of the overlying gypsum beds. Dolomite porosity occurs along bedding planes and cross-cutting fractures. In many places the development of porosity is so advanced that the dolomite beds have a honeycombed appearance, with only a skeletal framework of rock supporting a system of voids. The early flow of water through the dolomite beds causes gypsum dissolution and cavern development to occur most commonly at, and just above, the gypsum–dolomite contact.

Gypsum caverns in the region generally have a height and width that range from several inches to about 10 ft, although some caves reach a width of 50 ft. Enlargement of individual cavities and caverns is due to dissolution of the soluble rock as well as to abrasion of the rock by gravel, sand, and silt carried by through-flowing waters. The sediment carried by ground water is deposited locally in the underground caverns, and it partly or totally fills some of the openings.

**Table 1. — Charts of Pressure Tests in Boreholes Drilled at Proposed Upper Mangum Dam**

| CH-1 | | |
|---|---|---|
| DEPTH | GAUGE PSI | GPM |
| 13.0 - 23.0 | -- | ---- |
| 23.0 - 33.0 | 10 | 31.0 |
| 33.0 - 43.0 | 10 | 60.7 |
| 43.0 - 53.0 | 10 | 48.3 |
| 53.0 - 63.0 | 10 | 2.0 |
| 63.0 - 73.0 | 10 | 2.3 |
| 73.0 - 83.0 | 10 | 60.7 |
| 83.0 - 93.0 | 10 | 60.0 |
| 93.0 - 103.0 | 10 | 3.3 |
| 103.0 - 113.0 | 10 | 2.3 |
| 113.0 - 123.0 | 10 | 1.7 |
| 123.0 - 133.0 | 10 | 2.3 |
| 133.0 - 143.0 | 10 | 46.7 |
| 143.0 - 148.0 | 10 | 0.7 |
| - | | |

| CH-2 | | |
|---|---|---|
| DEPTH | GAUGE PSI | GPM |
| 6.0 - 13.0 | 10 | 16.7 |
| 13.0 - 23.0 | 10 | 27.3 |
| 23.0 - 33.0 | 10 | 10.7 |
| 33.0 - 43.0 | 10 | 36.0 |
| 43.0 - 53.0 | 10 | 37.7 |
| 53.0 - 63.0 | 10 | 37.3 |
| 63.0 - 73.0 | 10 | 61.7 |
| 73.0 - 83.0 | 10 | 57.3 |
| 83.0 - 93.0 | 10 | 51.3 |
| 93.0 - 103.0 | 10 | 50.0 |
| 103.0 - 113.0 | 10 | 2.7 |
| 113.0 - 123.0 | 10 | 6.8 |
| 123.0 - 133.0 | 10 | 0.0 |
| - | | |
| - | | |

| CH-3 | | |
|---|---|---|
| DEPTH | GAUGE PSI | GPM |
| 14.0 - 22.0 | -- | ---- |
| 22.0 - 32.0 | 10 | 30.0 |
| 32.0 - 42.0 | 10 | 22.0 |
| 42.0 - 52.0 | 10 | 1.6 |
| 52.0 - 62.0 | 10 | 18.4 |
| 62.0 - 72.0 | 10 | 44.0 |
| 72.0 - 82.0 | 10 | 46.4 |
| 82.0 - 92.0 | 10 | 36.4 |
| 92.0 - 102.0 | 10 | 33.0 |
| 102.0 - 112.0 | 10 | 21.6 |
| 112.0 - 122.0 | 10 | 15.0 |
| 97.0 - 107.0 | -- | ---- |
| 107.0 - 117.0 | 10 | 31.6 |
| 117.0 - 127.0 | 10 | 19.0 |
| - | | |

| CH-4 | | |
|---|---|---|
| DEPTH | GAUGE PSI | GPM |
| 15.0 - 25.0 | 10 | 30.0 |
| 25.0 - 35.0 | 10 | 1.0 |
| 35.0 - 45.0 | 10 | 26.8 |
| 45.0 - 55.0 | 10 | 2.8 |
| 55.0 - 65.0 | 10 | 2.6 |
| 65.0 - 75.0 | 10 | 2.4 |
| 75.0 - 85.0 | 10 | 0.8 |
| 85.0 - 95.0 | 10 | 1.8 |
| 95.0 - 105.0 | 10 | 1.6 |
| 105.0 - 115.0 | 10 | 15.6 |
| 115.0 - 125.0 | 10 | 3.0 |
| 125.0 - 135.0 | 10 | 0.0 |
| 135.0 - 145.0 | 10 | 0.0 |
| - | | |
| - | | |

| BH-1-99 | | |
|---|---|---|
| DEPTH | GAUGE PSI | GPM |
| 33.8 - 41.8 | 10 | 39 |
| 40.0 - 50.0 | 10 | 410 |
| 50.0 - 60.0 | 10 | 528 |
| 60.0 - 70.0 | 10 | 561 |
| 70.0 - 80.0 | 10 | 707 |
| 80.0 - 90.0 | 10 | 724 |
| 80.0 - 90.0 | 40 | 830 |
| 90.0 - 100.0 | 40 | 1,065 |
| 100.0 - 110.0 | 40 | 1,316 |
| 110.0 - 120.0 | 40 | 554 |
| 110.0 - 120.0 | 55 | 765 |
| 120.0 - 130.0 | | |
| — | | |
| — | | |

In many parts of the region, underground caverns have become so wide that their roofs have collapsed to partly close the caverns. The collapse structures and fractured strata enable vertical movement of water in many parts of the aquifer, thus increasing the amount of karst features in those areas. Dissolution and resultant collapse in some areas have caused one or more of the individual gypsum beds to be completely removed by dissolution, and they have been "replaced" by overlying strata that have dropped to a lower level.

### Karst Features in the Reservoir Area

All of the regional karst features described above are present in the area of the proposed reservoir, and previous reports by the BOR and the Corps all make numerous references to the presence of these karst features. Caves, sinkholes, disappearing streams, springs, and underground water courses have all been observed or reported in the area.

One specific feature in the reservoir area is Horseshoe Valley Cave, just northwest of the center of sec. 35, T. 5 N., R. 24 W. This cave system, just north of the mouth of Cave Creek, was mapped by members of the Central Oklahoma Grotto (S. Bozeman, 1996; J. Bozeman, 1996). About 10,900 ft of passages have been surveyed and mapped, and all these passages are in the lower part of the Van Vacter Member of the Blaine Formation (Johnson, 1990b). The explored portion of Horseshoe Valley Cave consists mainly of sinuous passages 10–40 ft wide and 5–20 ft high. If the reservoir were to rise to the planned Conservation Pool level of 1,632 ft, water would flow into, and flood, much of the Horseshoe Valley Cave system, and presumably it could then completely bypass, or flow under, the dam.

Several other caves in or adjacent to the impoundment area have been mapped or identified by the Central Oklahoma Grotto (Sue Bozeman, personal communication, 1999). These caves are inhabited by three species of bats (*Myotis velifer, Pipistrellus subflavus,* and *Corynorhinus townsendii*), and one of the caves contains an Oklahoma Archaeological Site.

Field examination of the dam abutments revealed several sinkholes and caves in the immediate abutment area. One sinkhole/cave system, ~300 ft upstream of the centerline of the left abutment, appears to be 50–75 ft long and to be several feet high and several feet wide. In addition, several crevices and small openings in gypsum beds exposed in bluffs at and near the right abutment may open into cave systems just back of the outcrop.

A large number of sinkholes, caves, and disappearing streams are visible in Van Vacter strata at other sites adjacent to the Salt Fork of Red River. Although the abundant sinkholes, caves, and disappearing streams are the only visible parts of the karst system, each of these surface features leads down underground into part of an unseen cave passage.

## SIGNIFICANCE OF KARST ON THE PROJECT

The abundance of karst features in the abutments and beneath the foundation (Fig. 7), as well as in the impoundment area, seriously compromises the ability or likelihood that the proposed reservoir would be able to contain and retain water, without extensive and expensive engineering actions (such as deep excavation, deep cutoff trenches, and/or extensive and deep grout curtains). Such defensive measures may not even provide a permanent solution to the karst problem. Furthermore, reservoir impoundment may act as a catalyst for initiating, or further accelerating, dissolution of the evaporites. The hydraulic head of the reservoir also may cause clay-filled cavities in gypsum beds to weaken and fail, thus allowing water to flow through preexisting subsurface solution channels.

Bedrock in almost the entire impoundment area consists of karstic gypsum, dolomite, and shale of the Van Vacter Member of the Blaine Formation (Fig. 4). Beneath the Van Vacter Member are additional karst features in the Elm Fork Member and in the Flowerpot Salt. Thus, the final depth to which excavations, cutoff trenches, and/or grout curtains would need to extend is uncertain, and this makes it difficult even

to estimate the engineering needs and costs for impounding water in the reservoir.

Owing to the extensive karst features in the abutments, beneath the foundation, and throughout the impoundment area, the ability of the proposed dam and impoundment area to hold water is unlikely. A number of remedial engineering steps in the foundation and impoundment area should increase the tightness of the proposed structure, but even then there is no assurance that the results would be acceptable. Karst features already identified include (1) voids, cavities, clay-filled cavities, and caves in the left abutment; (2) voids, cavities, and clay-filled cavities in the right abutment; (3) voids, cavities, clay-filled cavities, bedded salt (with cavities), and artesian flow of salt water beneath the stream valley; and (4) long caves, sinkholes, clay-filled cavities, disappearing streams, and springs at numerous sites in the impoundment area. The full extent of the karst system in subsurface can only be speculated upon at this time.

## CONCLUSIONS

On the basis of evaluation of data from boreholes, laboratory tests, aerial-photography analysis, field studies, geologic mapping, and hydrologic mapping along the proposed dam axis and in the impoundment area, the following is observed:

1. The abutments, and almost all of the impoundment area, are in the Van Vacter Member of the Blaine Formation;

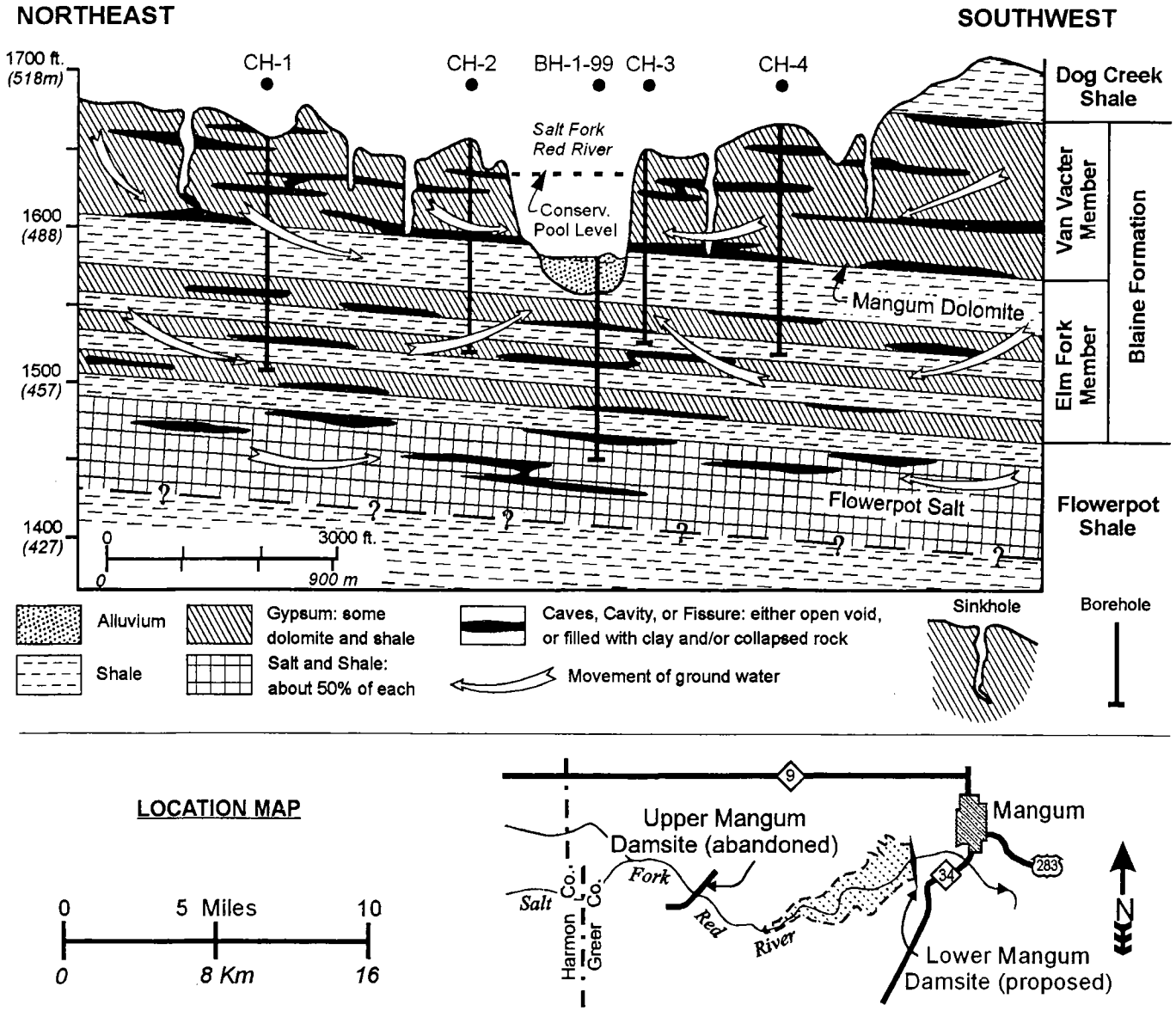


Figure 7. Schematic cross section along proposed Upper Mangum Dam, showing bedrock geology and karst features (caves, cavities, fissures, and sinkholes) in gypsum, dolomite, and salt. Cross section is based upon borehole data and field studies. View looking downstream to the southeast. Proposed Conservation Pool level (1,632 ft) is shown.

2. The Blaine Formation, especially the Van Vacter Member, contains extensive amounts of soluble gypsum and dolomite;

3. Extensive karst features, including caves, sinkholes, disappearing streams, springs, clay-filled cavities, and underground water courses, have all been observed or reported in the area;

4. Karst features are widespread at the surface and at depth, particularly close to and beneath the Salt Fork of Red River;

5. Karst features are also present in the Flowerpot Salt, including a 2-ft-high dissolution cavity at the top, numerous dissolution features throughout its thickness, and an artesian flow of brine that reached to the land surface;

6. Cores and pressure-testing data from along the dam axis show that the foundation materials are highly permeable;

7. A loss of fluids during pressure testing in boreholes generally ranged from 15 to 62 gpm in CH-1 through CH-4, and losses of 410–1,316 gpm occurred in most intervals tested in BH-1-99; and

8. Several known extensive gypsum-cave systems and sinkholes in the impoundment area would be flooded when water reaches the Conservation Pool level of 1,632 ft, and these karst features lead underground into unseen cave passages.

These foundation conditions are marginal at best, and could impact the integrity of the dam foundation and embankment. Engineering (defensive) measures required to mitigate these adverse conditions would be extensive and expensive, and still may not even provide a permanent solution to the problems posed by karst features. Additionally, reservoir impoundment may act as a catalyst for initiating, or further accelerating, dissolution of the gypsum, dolomite, and salt units within and beneath the dam foundation.

Engineering measures that may be needed to address the karstic foundation conditions at the proposed damsite include (1) excavation of the left and right abutments for placement of cutoff trenches; (2) excavation of alluvial and karstic bedrock beneath the stream bed for placement of a cutoff trench; (3) remediation of the karstic condition of the Flowerpot Salt at depths >115 ft beneath the stream bed; (4) grouting the karstic units in the foundation and abutments beneath the cutoff trenches; and (5) grouting the karstic units for 0.5 mi north of the left abutment, and for 2–4 mi west of the right abutment, to prevent impounded water from moving underground and bypassing the dam.

All these engineering steps would add significantly to the cost of construction, and still would not assure the tightness of the reservoir. Further investigation of the proposed Upper Mangum Damsite, or any nearby site that would be mostly within the Van Vacter Member, will not give any greater assurance of its suitability for impoundment.

Owing to the adverse geologic and hydrologic conditions at the proposed Upper Mangum Damsite, and the potential difficulties and high costs in attempting to remediate these conditions, it is herein recommended that this site be abandoned. Also, an alternative damsite, with more favorable geologic and hydrologic characteristics, is herein proposed at a site about 7 mi downstream on the Salt Fork of Red River. Preliminary studies of this new site, the Lower Mangum Damsite, indicate that it appears to be a favorable site (Johnson, 2003b).

## REFERENCES CITED

Bozeman, J., 1996, Geology of Horseshoe Valley Cave and vicinity: Central Oklahoma Grotto, Oklahoma City, Oklahoma Underground, v. 18, p. 27–28.

Bozeman, S., 1996, Horseshoe Valley Cave: Central Oklahoma Grotto, Oklahoma City, Oklahoma Underground, v. 18, p. 17–26.

Current, E. L., 1942, Report of geophysical survey of Upper Mangum investigations: U.S. Bureau of Reclamation unpublished report, dated 1942, 6 p. plus tables and figures (Appendix E in Jackson, 1991).

Curtis, N. M., Jr.; and Ham, W. E., 1972, Geomorphic provinces of Oklahoma, *in* Johnson, K. S., and others, Geology and earth resources of Oklahoma—an atlas of maps and cross sections: Oklahoma Geological Survey Educational Publication 1, p. 3.

Darnell, J. L., 1954, Geological report on the Mangum project, Salt Fork of the Red River, Oklahoma: U.S. Bureau of Reclamation unpublished report, dated September 1954, 5 p. plus photographs and figures (Appendix B in Jackson, 1991).

Havens, J. S., 1977, Reconnaissance of the water resources of the Lawton Quadrangle, southwestern Oklahoma: Oklahoma Geological Survey Hydrologic Atlas 6, 4 sheets, scale 1:250,000.

Jackson, J. L., 1991, Mangum project, Oklahoma, geologic appraisal of damsites: U.S. Bureau of Reclamation unpublished report, dated February 1991, 20 p. (includes Appendixes A–G, which are all the letters and reports prepared previously by U.S. Bureau of Reclamation and cited separately in this list of References Cited).

Johnson, K. S., 1986, Hydrogeology and recharge of a gypsum–dolomite karst aquifer in southwestern Oklahoma, U.S.A.; International Symposium of Karst Water Resources, 1985, Ankara, Turkey: International Association of Hydrological Sciences Publication 161, p. 343–357.

_____1990a, Standard outcrop section of the Blaine Formation and associated strata in southwestern Oklahoma: Oklahoma Geology Notes, v. 50, p. 144–168.

_____1990b, Hydrogeology of the Blaine gypsum–dolomite karst aquifer, southwestern Oklahoma: Oklahoma Geological Survey Special Publication 90-5, 31 p.

_____2003a, Evaporite karst in the Permian Blaine Formation and associated strata in western Oklahoma, *in* Johnson, K. S.; and Neal, J. T. (eds.), Evaporite karst and engineering/environmental problems in the United States: Oklahoma Geological Survey Circular 109 [this volume], p. 41–55.

_____2003b, Gypsum karst as a major factor in the design of the proposed Lower Mangum Dam in southwestern Oklahoma, *in* Johnson, K. S.; and Neal, J. T. (eds.), Evaporite karst and engineering/environmental problems in the United States: Oklahoma Geological Survey Circular 109 [this volume], p. 95–111.

Johnson, K. S.; and Denison, R. E., 1973, Igneous geology of

the Wichita Mountains and economic geology of Permian rocks in southwest Oklahoma: Oklahoma Geological Survey Special Publication 73-2, 33 p.

Johnson, K. S.; and Ham, W. E. [undated], Unpublished geologic maps of the Mangum–Erick area and the Hollis–Duke area, southwestern Oklahoma: Oklahoma Geological Survey, scale 1:63,360.

Kirchen, H. W., 1941, Geological reconnaissance of several dam sites on the Salt Fork of the Red River, Oklahoma: U.S. Bureau of Reclamation, unpublished memorandum to Hydraulic Engineer, dated January 14, 1941, Denver, Colorado, p. 24–28 (Appendix G in Jackson, 1991).

Osborn, N. I.; Eckenstein, E.; and Fabian, R. S., 1997, Demonstration and evaluation of artificial recharge to the Blaine aquifer in southwestern Oklahoma: Oklahoma Water Resources Board Technical Report 97-5, 136 p.

Redfield, R. C., 1960, Mangum project, Oklahoma, geologic report on investigation of Mangum reservoir basin, 1960: U.S. Bureau of Reclamation unpublished report, dated June 1960, 8 p. plus figures (Appendix A in Jackson, 1991).

Runkle, D. L.; and McLean, J. S., 1995, Steady-state simulation of ground-water flow in the Blaine aquifer, southwestern Oklahoma and northwestern Texas: U.S. Geological Survey Open-File Report 94-387, 92 p.

Runkle, D. L.; Bergman, D. L.; and Fabian, R. S., 1997, Hydrogeologic data for the Blaine aquifer and associated units in southwestern Oklahoma and northwestern Texas: U.S. Geological Survey Open-File Report 97-50, 213 p.

Smith, F. F.; and Nickell, F. A., 1941, Mangum project comparison of dam sites on Salt Fork in order to provide storage for land near Altus, Oklahoma: U.S. Bureau of Reclamation, unpublished letter to Chief Engineer, dated May 22, 1941, Denver, Colorado, 5 p. (Appendix F in Jackson, 1991).

Steele, C. E.; and Barclay, J. E., 1965, Ground-water resources of Harmon County and adjacent parts of Greer and Jackson Counties, Oklahoma: Oklahoma Water Resources Board Bulletin 29, 96 p.

U.S. Army Corps of Engineers, 1993, Mangum, Oklahoma, reservoir study: Unpublished report prepared by USACE for Oklahoma Water Resources Board, dated September 1993, 30 p. plus appendixes.

_____1995, Mangum reservoir study, Mangum, Oklahoma, phase II geotechnical investigations, summary report: Unpublished report prepared by USACE for Oklahoma Water Resources Board, dated July 1995, 15 p. plus appendixes.

_____1999, Mangum reservoir study, Mangum, Oklahoma, phase III geotechnical investigations, summary report: Unpublished report prepared by USACE for Oklahoma Water Resources Board, dated December 1999, 45 p. plus appendixes.

U.S. Bureau of Reclamation, 1943, Geologic logs for Upper Mangum dam site: U.S. Bureau of Reclamation, unpublished logs of 20 boreholes, dated February–March–April, 1943 (Appendix D in Jackson, 1991).

_____1963 (revised in 1965), Plan of development for Mangum project, Oklahoma (supplemental water supply for the W. C. Austin project): U.S. Bureau of Reclamation unpublished report to the Commissioner, 63 p. plus appended reports.

# Gypsum Karst As a Major Factor in the Design of the Proposed Lower Mangum Dam in Southwestern Oklahoma

***Kenneth S. Johnson***
Oklahoma Geological Survey
Norman, Oklahoma

**ABSTRACT.**—Foundation conditions at the newly proposed Lower Mangum Damsite, 2 mi southwest of Mangum on the Salt Fork of Red River, appear to be favorable. Studies conducted at and near the damsite indicate that water would be contained behind the dam. Bedrock for the dam foundation, and in most of the impoundment area, would be the thick Permian Flowerpot Shale, which is an impermeable (or low-permeability) aquiclude that would allow little or no loss of water. Overlying the Flowerpot Shale are karstic gypsum, dolomite, and shale beds of the Permian Blaine Formation. These karstic strata would be above the proposed conservation-pool level in all but the uppermost parts of the reservoir, and thus would not affect reservoir tightness in most areas. Karstic strata in the abutments are above conservation-pool level and would be excavated during dam construction.

Complex geology and karst conditions in the uppermost part of the proposed reservoir, near Commissioner bend of Salt Fork, probably will impose limits on the lake level, size, and capacity of the Mangum Reservoir. Impounding water to an elevation above 1,550 ft may cause loss of lake water into karstic rocks at Commissioner bend, and that ground water then may flow south through a karst conduit into the Turkey Creek watershed. However, it may be possible to raise the lake level to as much as 1,560 ft if additional investigations show that no excessive water loss would occur at Commissioner bend.

If the projected surface area, storage volume, and water-supply yield are sufficient to justify further study, then additional investigations are needed to fully evaluate conditions at the damsite and at and near Commissioner bend, where reservoir water is most likely to be lost. With better data on the level to which the lake level can be raised, design of the dam can proceed.

## INTRODUCTION

This report presents the results of geotechnical investigations at the newly proposed Lower Mangum Damsite, which is 2 mi southwest of the city of Mangum, Oklahoma (Fig. 1). The site is on the Salt Fork of Red River in the southwestern part of Greer County. The investigations consist of evaluating all previous geologic and hydrogeologic studies bearing on the project, drilling three exploratory core borings along the proposed-dam alignment, water-pressure testing of completed boreholes, collecting water-well data to determine the elevation and configuration of the regional water table, and geologic reconnaissance along the dam axis and in the reservoir area.

The proposed dam probably would be a compacted, earth-fill embankment that would be 60–80 ft high and about 5,000–6,000 ft long (Fig. 2). Preliminary study indicates that the conservation-pool level should not exceed 1,550 ft (to prevent lake water from inundating a karst area and leaving the reservoir), but later studies may show that the pool level can be as high as 1,560 ft without adverse effects. Water depth directly behind the dam would be 40–50 ft deep. The total storage volume in the reservoir would be 26,080 to 47,043 acre-ft, depending upon whether the conservation-pool level is set at an elevation of 1,550 or 1,560 ft, respectively.

Investigation of the Lower Mangum Damsite was recommended at the conclusion of a long-term study to find a suitable damsite in the vicinity of Mangum (Johnson, 2003b). Studies in the area since 1941 had focused on a potential damsite about 7 mi farther upstream on Salt Fork (the Upper Mangum Damsite), but that site was finally abandoned in 1999 because of extensive gypsum karst in the Blaine Formation in the proposed abutments and impoundment area. The history of the Mangum Dam Project, the importance of gypsum karst at the abandoned Upper Mangum Damsite, and the reason for recommending the Lower Mangum Damsite are presented by Johnson (2003b).

Study of the Lower Mangum Damsite was carried out on behalf of the Tulsa District Office of the U.S. Army Corps of Engineers (Corps), the Oklahoma Water Resources Board (OWRB), and the citizens of

Johnson, K. S., 2003, Gypsum karst as a major factor in the design of the proposed Lower Mangum Dam in southwestern Oklahoma, *in* Johnson, K. S.; and Neal, J. T. (eds.), Evaporite karst and engineering/environmental problems in the United States: Oklahoma Geological Survey Circular 109, p. 95–111.

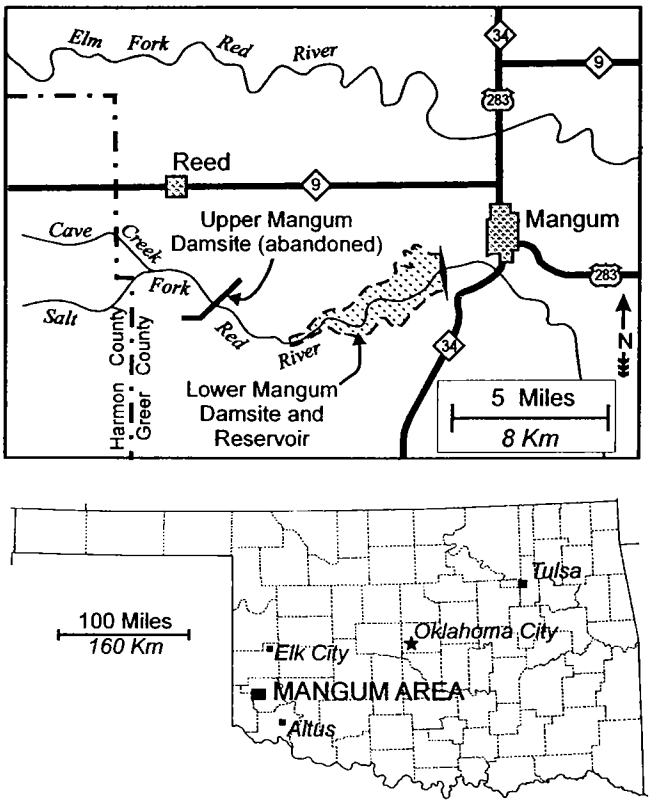


Figure 1 (*at left*). Map showing location of proposed Lower Mangum Damsite and Reservoir in southwestern Oklahoma.

Mangum. It was done under the Planning Assistance to States Program (Public Law 93-251). The current report is a summary of a study done by the current author and released by the Corps (U.S. Army Corps of Engineers, 2002).

Appreciation for support and assistance is expressed to the following individuals: Phil Cline, Frank Oler, and Randy Mead, with the Corps; Mike Mathis and Terri Sparks, with OWRB; Stephen Scott, Roger Lively, Dale Clayton, and other members of the Mangum Reservoir Project Committee; and Charles and Renée Schwabe, J. W. and Phyllis Burns, and Charles and Ronald Greb, local residents who assisted during the field investigations. Supervision of core drilling and pressure testing in boreholes was performed by Traci Thomas and Heather Balven, MACTEC Engineering and Consulting, Inc., Tulsa, Oklahoma.

## GEOLOGY

The proposed dam and reservoir would be situated at the eastern edge of the Mangum Gypsum Hills of southwestern Oklahoma (Curtis and Ham, 1972). The

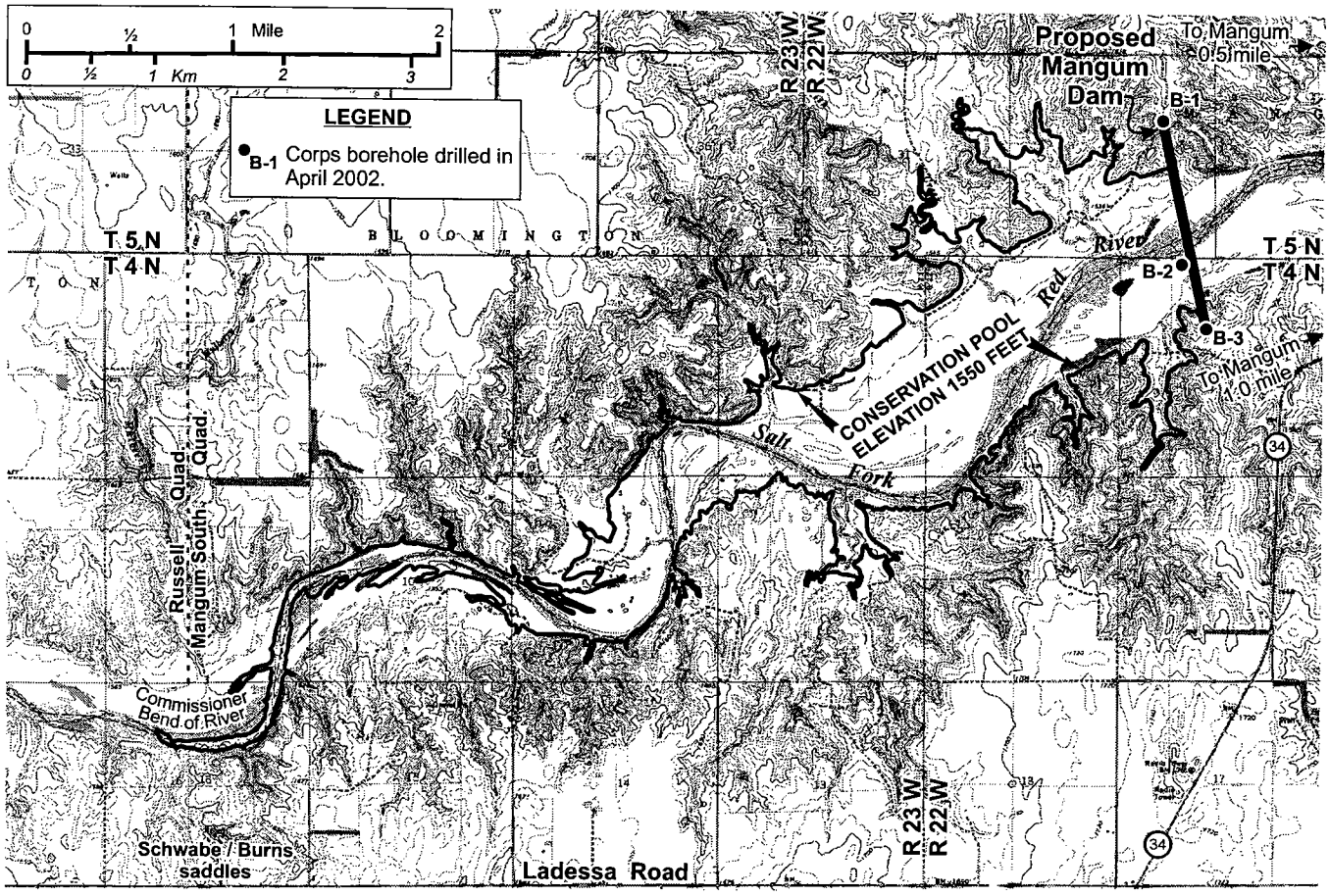


Figure 2. Topographic map showing proposed Lower Mangum Dam and Reservoir, along with boreholes at the damsite and outline of conservation pool (1,550 ft). Base maps: 7.5-minute topographic maps; contour interval is 10 ft (~3 m).

region around the reservoir is characterized by a series of low-lying (10–50-ft high), widely spaced benches or escarpments capped by resistant layers of gypsum and dolomite in the Permian Blaine Formation (Fig. 3). Adjacent to the damsite and reservoir, however, the escarpments are better defined and range up to 100 ft high (7.5-minute topographic maps for the Mangum South and Russell quadrangles). The dam and reservoir would be sited almost entirely in the thick Flowerpot Shale, although the upper reaches of the reservoir would inundate a small area of Blaine Formation gypsum and dolomite outcrops.

The Salt Fork of Red River rises in the High Plains of the Texas Panhandle, near the city of Claude, and generally flows in an east-southeasterly direction, through the Mangum area, to its confluence with Red River near Elmer, Oklahoma. The drainage basin of Salt Fork above the proposed damsite is about 1,356 mi².

Some of the most striking topographic and geologic features near the reservoir are the dissolution and karst features in outcropping and underlying bedrock strata. Karst features, which are most prevalent along and near major streams, include numerous caves, disappearing streams, springs, fissures, and sinkholes, as well as subsidence basins and locally erratic dips of the outcropping rocks (Johnson, 1986, 1990b, 2003a,b; Jackson, 1991). Such karst features should be only minor concerns at the damsite, but are of higher concern in the upper reaches of the reservoir.

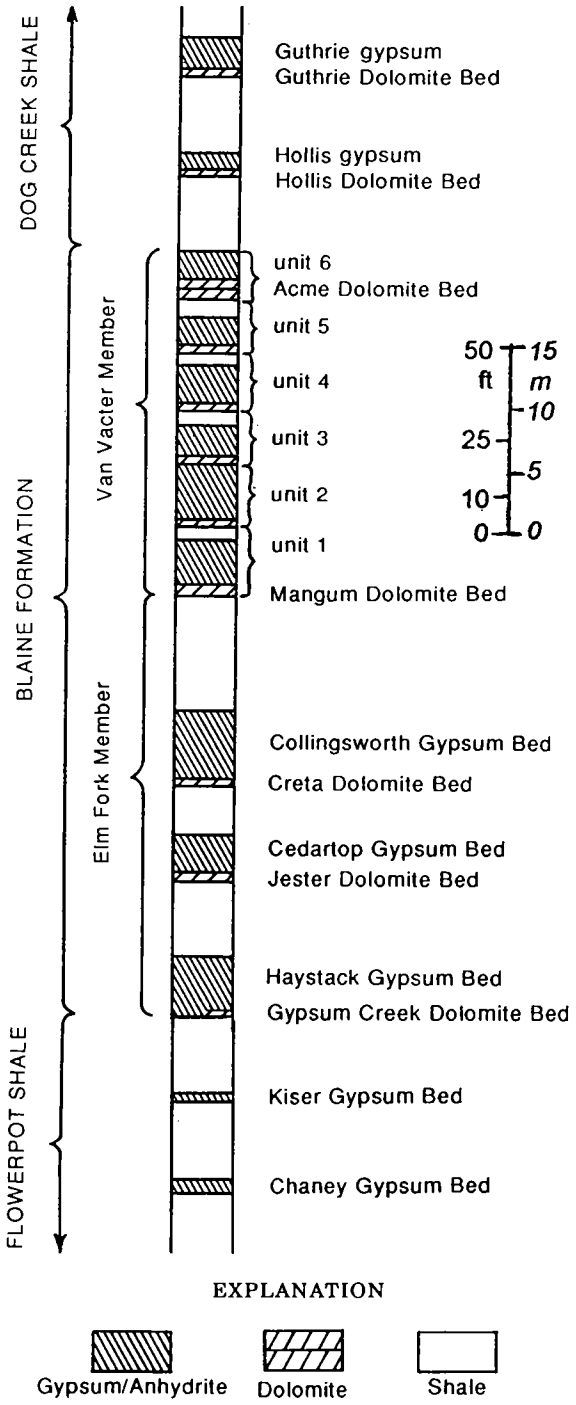


Figure 3. Stratigraphy of the Blaine Formation and associated strata in the Hollis Basin area of southwestern Oklahoma (from Johnson, 1990a).

## Regional Geology

Rock units in the project area consist of a thick sequence of Permian sedimentary red beds and evaporites. The red beds are mostly of reddish-brown shales and siltstones; the evaporites consist of layers or beds of gypsum and dolomite that were deposited on the Permian sea floor owing to evaporation of seawater (Fig. 4). The proposed dam is situated in the Hollis Basin, directly south of the Wichita Uplift. The Wichita Uplift, a part of which is now exposed as the Wichita Mountains, separates the deep Anadarko Basin on the north from the Hollis Basin on the south. As a result, bedrock units of the project area dip gently to the

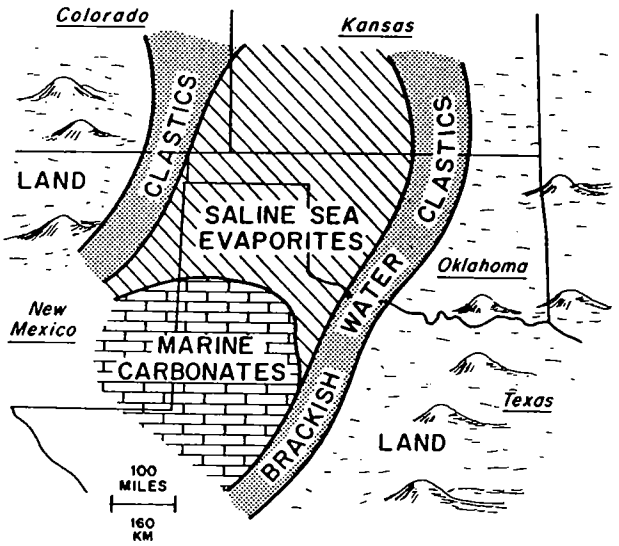


Figure 4. Permian paleogeography and principal facies in southwestern United States during deposition of evaporites in the Blaine Formation and associated strata (from Johnson and Denison, 1973).

southwest. Local variations of dip and strike just outside of the reservoir area result largely from karst features, including sinkholes and subsidence basins (Johnson, 1986, 1990b, 2003a,b; Jackson, 1991). A local system of faults and/or flexures near Commissioner bend, in the upper reaches of the reservoir, is due to post-Permian tectonic movements.

## Site Geology

Principal bedrock units at the damsite and reservoir area are Permian in age and include, in ascending order: Flowerpot Shale, Blaine Formation, and Dog Creek Shale (Fig. 3). The Blaine Formation has been subdivided into the Elm Fork Member (below) and the Van Vacter Member (above). A geologic map of these units in the reservoir area is presented in Figure 5. Permian bedrock units are overlain locally by Quaternary overburden in the form of (1) alluvial (floodplain) deposits of Salt Fork and principal streams, and (2) terrace deposits in uplands away from the streams.

### *Flowerpot Shale*

The major rock unit throughout the project area is the Flowerpot Shale, which is 200–300 ft thick in the region. The uppermost Flowerpot strata make up most of the damsite abutments and are the bedrock unit for almost all of the reservoir-impoundment area. In outcrops and cores, this formation is mainly red-brown shale with thin layers of greenish-gray shale and gypsum. The shale generally is blocky and is non-laminated; it contains varying amounts of silt and sand, and technically could be called a *mudstone*. Shale typically has a very low permeability, and this is the case for the Flowerpot Shale in the project area.

Several thin beds of gypsum are present in the upper part of the Flowerpot Shale (Fig. 3); the most conspicuous is the Chaney Gypsum Bed, ~50 ft below the top of the Flowerpot. The Chaney Bed typically is 2–3 ft of white, massive rock gypsum that locally forms a topographic bench. About 20 ft above the Chaney Bed is the Kiser Bed, which consists of 1–2 ft of impure, greenish-gray gypsum that also locally forms a small topographic bench. Both the Chaney and Kiser Beds are exposed only in the vicinity of the proposed damsite, and along Salt Fork for 1–2 mi upstream from the dam. There is no evidence of karst development in the Chaney or Kiser Bed—probably because these beds are thin gypsums overlain and underlain by thick

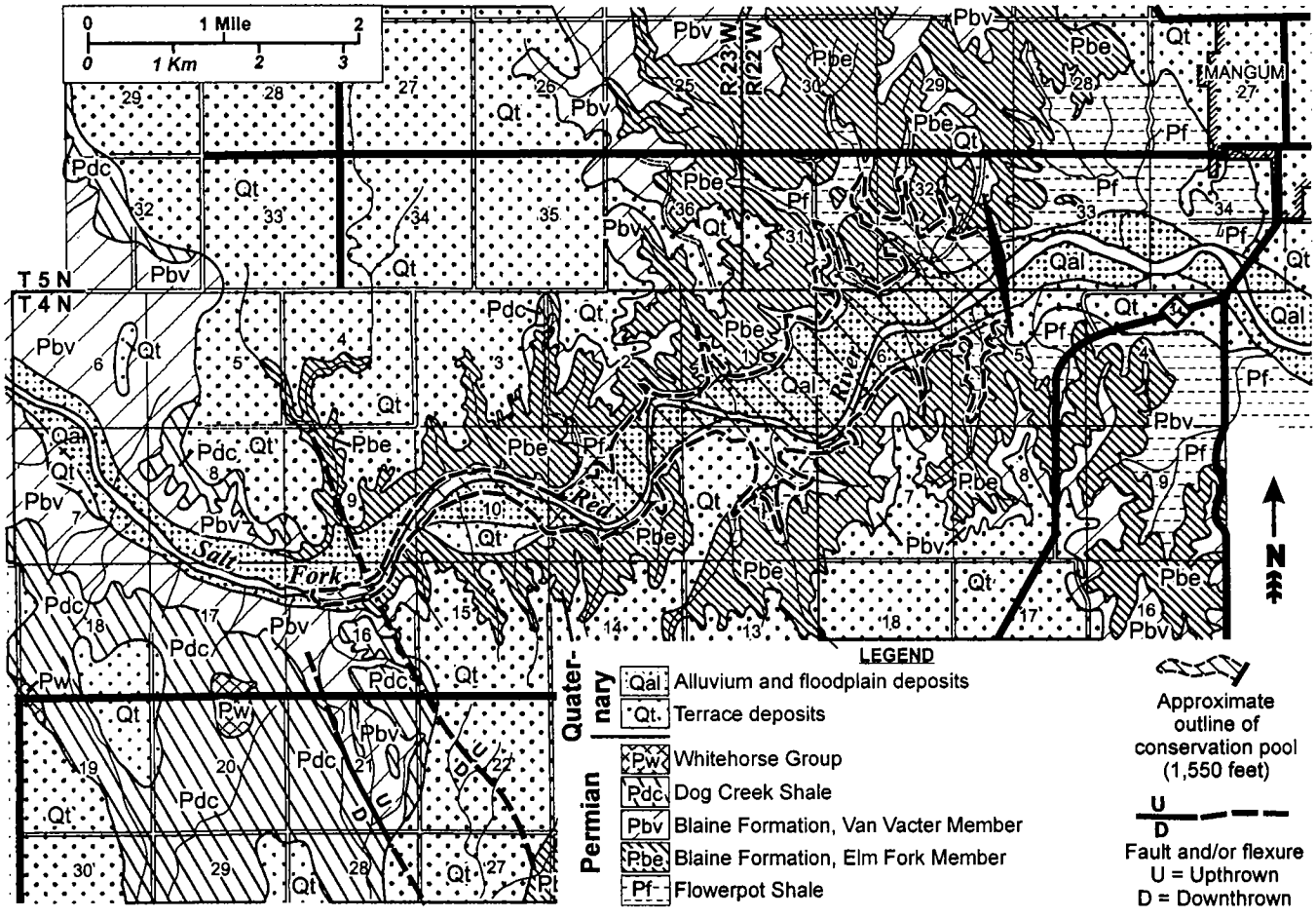


Figure 5. Geologic map of proposed Lower Mangum Damsite and Reservoir area (from Johnson and Ham, undated), and outline of proposed conservation pool (elevation, 1,550 ft).

units of impermeable (or low-permeability) shale, and thus there is little or no known flow of karst-producing ground water through these shales and gypsum beds.

West of the damsite, in northern Harmon County and farther to the west, the Flowerpot contains layers of salt (halite), which are referred to as the Flowerpot Salt. The Flowerpot Salt was encountered beneath the Upper Mangum Damsite (7 mi west of the Lower Mangum Damsite) at a depth of 115 ft, ~14 ft below the top of the Flowerpot Shale (Johnson, 2003b). No evidence of salt is present in outcrops of the top 50–60 ft of Flowerpot strata at and near the proposed Lower Mangum Damsite, or in the three drill holes that cored the uppermost 200 ft of Flowerpot Shale along the proposed dam alignment. The Flowerpot Shale does, however, have a salty taste in a core recovered 140 ft below the top of the formation (at depths below 88 ft in borehole B-2).

#### *Blaine Formation*

The Blaine Formation consists of interbedded gypsum, dolomite, and shale, and has a total thickness of ~200 ft in the study area (Fig. 3). Individual beds of gypsum and dolomite are laterally persistent and have a fairly uniform thickness throughout the project area, except where they are partly or totally removed by dissolution or erosion. The Blaine Formation consists of nine major gypsum beds, each 10–30 ft thick; each gypsum typically is underlain by a dolomite bed that is 0.2–5.0 ft thick (Fig. 3). Where deeply buried (at depths >75–100 ft) the Blaine typically contains layers or lenses of anhydrite within the gypsum beds.

The Blaine Formation is subdivided into the Elm Fork Member below and the Van Vacter Member above. The Elm Fork Member is ~110 ft thick in the project area and consists of three thick gypsum and dolomite units separated by thick shales (Fig. 3). Soluble gypsum and dolomite make up ~50% of the Elm Fork Member, and a number of cavities and other karst features occur within these units in outcrops and in subsurface. The most important unit in the Elm Fork Member for this study is the Haystack Gypsum Bed, at the base of the Blaine Formation, directly above the top of the Flowerpot Shale. (The Gypsum Creek Dolomite Bed, at the base of the Haystack Bed, is thin and is only locally present.) The Haystack is white, massive rock gypsum 10–15 ft thick; it consists of a lower gypsum bed (8–10 ft thick) and an upper gypsum bed (2–4 ft thick), separated by ~1 ft of shale.

The Van Vacter Member is ~85 ft thick in the study area and consists of six thick gypsum and dolomite units, separated by thin shales (Fig. 3). Gypsum beds in the Van Vacter are sometimes informally referred to as gyp-1 through gyp-6, and at the base of the Van Vacter is the widespread Mangum Dolomite Bed that locally is up to 6 ft thick. The great amount of soluble gypsum and dolomite in the Van Vacter Member (~90% of its total thickness) makes this unit especially vulnerable to natural dissolution and development of karst features. Although ground water can flow readily through karst features in any of the gypsum or dolomite beds, the Mangum Dolomite typically is highly porous and commonly is the major water conduit in the Blaine aquifer (Johnson, 1990b).

#### *Dog Creek Shale*

The Dog Creek Shale consists of ~150–200 ft of red-brown shale in outcrops in the Hollis Basin, with several beds of dolomite, gypsum, and green-gray shale in the lower half of the formation. Gypsum and dolomite beds are generally 0.3–16 ft thick in the Hollis Basin (Johnson, 1990a). The Dog Creek Shale crops out ~50–100 ft above the Salt Fork of Red River near Commissioner bend, in the upper reaches of the reservoir (Fig. 5), and includes exposures of the Guthrie Gypsum Bed (5–7 ft thick) and the underlying Guthrie Dolomite Bed (0.5–1.0 ft thick). The Guthrie Beds are ~40 ft above the base of the Dog Creek, although locally they have been dissolved and are missing.

#### *Alluvium and Terrace Deposits*

Alluvium at the damsite is of Quaternary age and consists predominantly of unconsolidated sand, silt, clay, and gravel in the channel of the Salt Fork of Red River and the adjacent flood plain. The thickness of these deposits is 51 ft in borehole B-2 and is estimated to be typically 15–60 ft in the area. Alluvium and terrace deposits are also referred to as "overburden," which rests upon bedrock.

Terrace deposits mantle the bedrock in both the left and right abutments, and also cover some of the upland areas near the proposed reservoir. These sediments are Quaternary in age and consist mainly of unconsolidated sand, gravel, silt, and clay, and their thickness generally ranges from 5 to 50 ft; they are 25 and 39 ft thick, respectively, in boreholes B-1 and B-3, drilled in the abutments.

#### *Structural Geology*

Permian bedrock units are essentially flat lying in all parts of the project area except in the uppermost reaches of the proposed reservoir. Flowerpot and Blaine strata are mostly horizontal, or dip gently to the southwest at rates of 5–10 ft per mile (~0.1°). For example, the elevation of the base of the Haystack Bed (at the base of the Blaine Formation) is 1,569 ft at the proposed damsite, and it ranges from 1,565 to 1,585 ft for 4 mi farther upstream (to the west and southwest). Westward across sec. 10, T. 4 N., R. 23 W., the elevation of the base of the Haystack Bed descends from ~1,565 to 1,545 ft within a distance of 1 mi, and then it dips below Salt Fork river level (Fig. 5) in the vicinity of Commissioner bend of Salt Fork and the Price fault/flexure zone (described below, under the major section "Karst and Hydrogeology").

The Blaine gypsum beds would be above the conservation-pool level of 1,550 ft (or 1,560 ft) in all parts

of the reservoir except in the uppermost reaches (the W½ sec. 10, T. 4 N., R. 23 W., and farther west and southwest). Therefore, karst features in the Blaine gypsums and dolomites would not pose any problem concerning containment of water in the impoundment area except in these uppermost parts of the reservoir.

## GEOTECHNICAL INVESTIGATIONS

Geotechnical studies at the Lower Mangum Damsite and Reservoir area consisted of drilling three core borings, performing pressure tests in those boreholes, aerial-photograph examination, field studies, geologic mapping, and hydrogeologic mapping in and around the proposed impoundment.

### Borehole Investigations

#### *Core Borings*

Three core borings, B-1, B-2, and B-3, were drilled in March and April 2002 along the centerline of the proposed dam. Borehole B-1 is on the left abutment, B-3 is on the right abutment, and B-2 is in the stream bed of Salt Fork (Fig. 2). These boreholes were drilled with a BK-66, truck-mounted drill rig equipped with wireline coring equipment. The holes were advanced using a hollow-stem auger with a 5-in.-diameter drill bit, and were drilled to depths of 149.5 to 150 ft (Table 1).

The boreholes penetrated mostly shale, with minor amounts of gypsum and siltstone (Fig. 6). The thick Flowerpot Shale typically is red brown, blocky shale in the boreholes, with some thin interbeds of green shale, siltstone, gypsum, and anhydrite. Gypsum and anhydrite occur as thin beds, as zones of nodules, and as veins of satin-spar gypsum. The most prominent of these units is the Chaney Gypsum Bed, which is ~2.5 ft thick in B-1 and B-3. There is no evidence of karst development in the Chaney Gypsum or other gypsum units in the Flowerpot, probably because there is little or no circulation of ground water through the thick shales that surround the gypsums.

At several depths in hole B-1, core recovery consisted of loose, sand-sized particles of shale and gypsum (at depths of 85, 114, and 135 ft). The particles are fine to medium, rounded grains of shale (rolled into balls) and of selenite gypsum; they comprise about 85% shale and 15% gypsum. Field studies near B-1 show that such anomalous beds or zones of loose sand-sized material do not exist in outcrops of the upper Flowerpot Shale. Thus it is concluded that the core samples resulted from drilling, crushing, and grinding of blocky gypsiferous shale, which is common in nearby outcrops. It appears that these zones are competent in subsurface and have a low permeability that is typi-

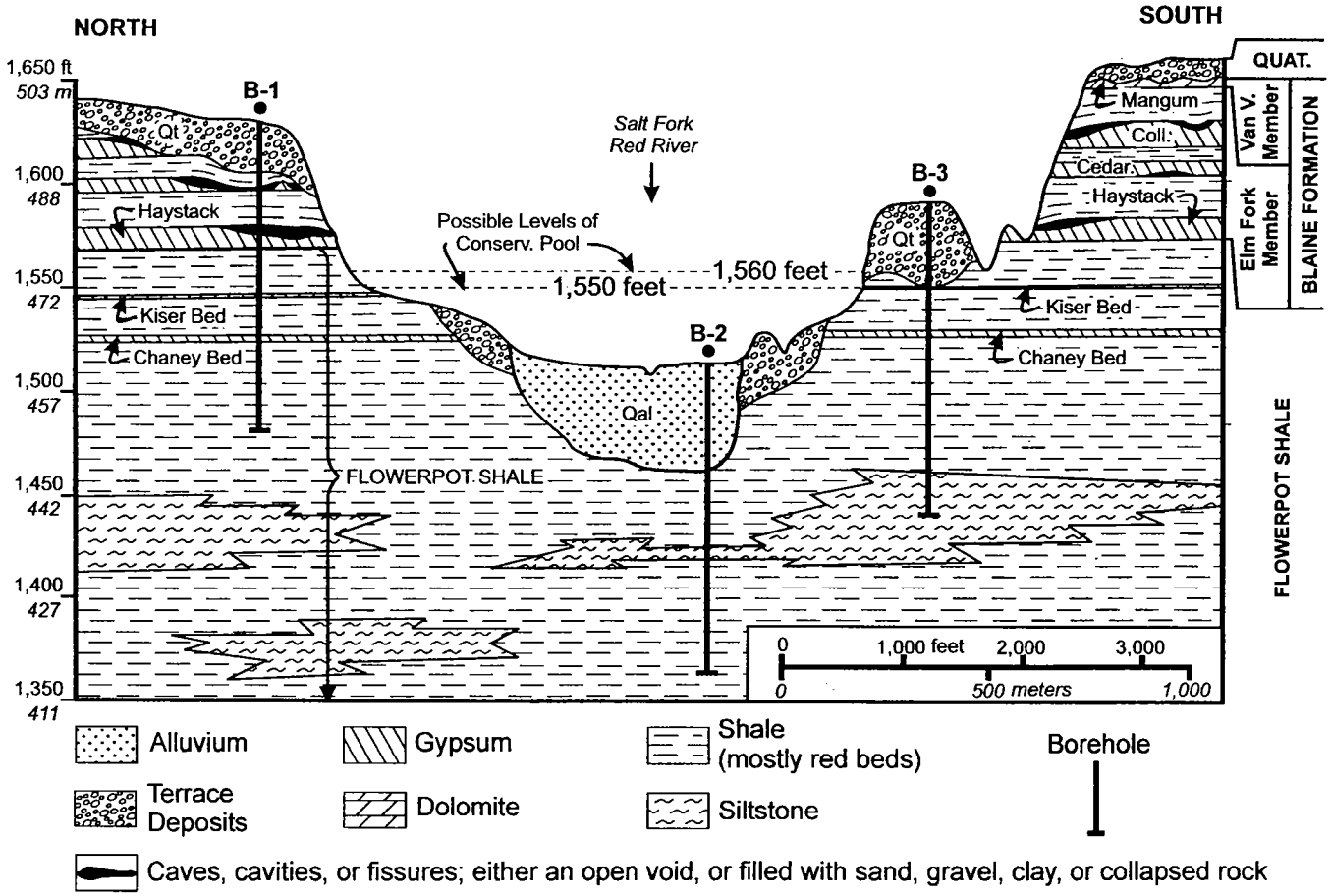


Figure 6. Schematic geologic cross section along proposed Lower Mangum Dam alignment. Cross section based upon borehole data and field studies. View looking downstream. Conservation-pool levels (1,550 or 1,560 ft) are shown.

**Table 1. — Borehole Information for Cores Drilled at Lower Mangum Damsite**

| Borehole no. | Borehole elevation (feet) | Depth of borehole (feet) | Depth to water table (feet) | Elevation of water table (feet) | Depth to top of rock (feet) |
|---|---|---|---|---|---|
| B-1 | 1,630.5 | 150.0 | 58.0 | 1,572.5 | 24 |
| B-2 | 1,515.2 | 149.5 | 2.0 | 1,513.2 | 51 |
| B-3 | 1,592.1 | 150.0 | 46.0 | 1,546.1 | 39 |

cal of shale, as attested by pumping tests in these zones.

The Flowerpot Salt is not present at the Lower Mangum Damsite; the boreholes penetrated 205 ft below the top of the Flowerpot, and no salt was encountered. The only evidence of salt at the damsite is the salty taste of shales in the Flowerpot in B-2 at depths below 88 ft (~140 ft below the top of the Flowerpot). Such a salty taste probably results from incorporation of salty sea water in these Flowerpot sediments at the same time that rock salt was being deposited at the Upper Mangum Damsite and farther to the west.

Gypsum in the lower part of the Blaine Formation was penetrated only in B-1 (Fig. 6). A cavity at the top of the Haystack Gypsum Bed is 2.5 ft thick, and it was an interval of high water loss during pressure tests. Strata drilled above the Haystack Bed in B-1 do not include the overlying gypsum and dolomite beds that normally are present; these soluble strata have been dissolved or eroded, and are replaced by red and green shales. The base of the Haystack Gypsum (base of Blaine Formation) is at an elevation of 1,569 ft in B-1, and if the conservation-pool level is only 1,550 ft (or perhaps 1,560 ft), then reservoir water will not encounter these karst features. Furthermore, the Blaine strata undoubtedly will be excavated and removed during dam construction.

Quaternary alluvium and terrace deposits range from 25 to 51 ft thick in the three boreholes (Fig. 6). Alluvium in B-2 is 51 ft thick and consists of poorly graded loose sand and silt that grades down into coarser sand and gravel. The alluvium is porous and permeable, and will have to be excavated, or removed in a cutoff trench, to establish an impermeable barrier down to unweathered shale in the Flowerpot. Terrace deposits are unconsolidated sand, gravel, silt, and clay that are 25 ft thick (B-1) and 39 ft thick (B-3). These deposits are porous and permeable, and will be excavated down to impermeable zones in the upper part of the Flowerpot Shale.

### *Pressure Testing*

Pressure testing, using an NQ2 wireline double-packer system (operating as a single packer), was performed following completion of each 5 ft of coring. Water was pumped into the borehole for a set amount of time (mostly 15 minutes), and the water loss was measured; these data are summarized in Table 2.

Water loss in almost all parts of the Flowerpot Shale is low to extremely low, typically ranging from 0.1 to 1.0 gpm (gallons per minute) (Table 2). Only in the uppermost layers of the Flowerpot in borehole B-1 (64.5–69.5 ft) is the water loss a moderate 13.8 gpm. This part of the Flowerpot is just below the karst zone of the Haystack Gypsum Bed, and the higher water loss here probably is due to proximity to karst in the overlying gypsum. Furthermore, this part of the Flowerpot Shale probably will be excavated in dam construction and will be replaced by impermeable material.

The average water loss in unweathered Flowerpot strata in each borehole was 1.23 gpm in B-1 (at depths below 69.5 ft), 0.31 gpm in B-2 (below 59.5 ft), and 0.30 gpm in B-3 (below 39.0 ft). The highest water losses in the Flowerpot were 2.5, 3.2, and 4.06 gpm, respectively, in the three 5-ft increments between 89.5 and 104.5 ft in B-1 (Table 2). However, even these values are low, and thus the Flowerpot Shale is characterized by a very low permeability.

The Blaine Formation was cored and pressure tested only in borehole B-1. A moderate water loss of 8.56 gpm was recorded in the upper part of the Haystack Bed (from 49.5 to 54.5 ft), and karst conditions in the Haystack made it impossible to pressure test the interval 54.5–64.5 ft. These karstic strata will be excavated during dam construction and will be replaced by impermeable material.

## Aerial-Photography Analysis

Aerial photographs of the proposed dam and impoundment area were examined to determine (1) the geology of the area, and (2) the presence and character of karst features in the area. Black-and-white photos, at a scale of 1:20,000, provided stereoscopic coverage of the entire reservoir and all lands extending several miles from the reservoir. The results of this study are incorporated in the geologic map (Fig. 5).

## Field Studies

Field studies involved examination of outcropping rocks and overburden in the vicinity of the left and right abutments, and in the impoundment area. Special attention was given to examining karst features —such as caves, sinkholes, springs, disappearing streams, collapse structures, and clay-filled cavities in gypsum or dolomite beds—that might be flooded or covered by the reservoir. The elevation of the base of

**Table 2. — Pressure-Test Data in Boreholes at Lower Mangum Damsite**

| B-1 | | | B-2 | | | B-3 | | |
|---|---|---|---|---|---|---|---|---|
| Depth Range (feet) | Gauge Pressure (psi) | Water Loss (gpm) | Depth Range (feet) | Gauge Pressure (psi) | Water Loss (gpm) | Depth Range (feet) | Gauge Pressure (psi) | Water Loss (gpm) |
| 29.5–39.5 | 10.0 | 0.331 | 59.5–64.5 | 8.0 | 0.180 | 39–44 | 26.5 | 0.0704 |
| 39.5–44.5 | 16.0 | 1.092 | 64.5–69.5 | 13.0 | 0.017 | 39–49 | 15.0 | 0.0088 |
| 44.5–49.5 | 20.0 | 1.377 | 69.5–74.5 | 16.0 | 0.000 | 49–54 | 20.0 | 0.0264 |
| 49.5–54.5 | 6.0 | 8.562 | 74.5–79.5 | 22.0 | 0.159 | 49–59 | 22.0 | 0.1849 |
| 64.5–69.5 | 20.0 | 13.836 | 79.5–84.5 | 25.0 | 0.564 | 59–64 | 27.0 | 0.1744 |
| 69.5–74.5 | 25.0 | 2.164 | 114.5–119.5 | 50.0 | 0.120 | 64–69 | 30.0 | 0.8101 |
| 74.5–79.5 | 27.0 | 0.204 | 119.5–124.5 | 52.0 | 0.120 | 69–74 | 30.0 | 0.0176 |
| 79.5–84.5 | 30.0 | 0.377 | 124.5–129.5 | 56.0 | 0.171 | 74–79 | 40.0 | 0.2201 |
| 84.5–89.5 | 36.0 | 0.963 | 129.5–134.5 | 60.0 | 0.000 | 79–84 | 45.0 | 0.0757 |
| 89.5–94.5 | 40.0 | 2.501 | 84.5–89.5 | 30.0 | 1.770 | 79–89 | 48.0 | 0.3381 |
| 94.5–99.5 | 42.0 | 3.182 | 89.5–94.5 | 35.0 | 0.217 | 89–94 | 50.0 | 0.2606 |
| 99.5–104.5 | 48.0 | 4.063 | 94.5–99.5 | 38.0 | 0.218 | 94–99 | 54.0 | 0.6199 |
| 104.5–109.5 | 38.0 | 1.150 | 99.5–104.5 | 42.0 | 0.238 | 99–104 | 58.0 | 0.3152 |
| 109.5–114.5 | 50.0 | 0.810 | 104.5–109.5 | 46.0 | 0.180 | 104–109 | 60.0 | 0.4579 |
| 114.5–119.5 | 56.0 | 0.652 | 109.5–114.5 | 50.0 | 0.134 | 104–114 | 64.0 | 0.2730 |
| 119.5–124.5 | 60.0 | 0.800 | 134.5–139.5 | 64.0 | 0.315 | 114–119 | 65.0 | 0.2025 |
| 124.5–129.5 | 60.0 | 0.669 | 139.5–144.5 | 70.0 | 0.748 | 119–124 | 68.0 | 0.1796 |
| 129.5–134.5 | 65.0 | 1.127 | 144.5–149.5 | 69.0 | 0.382 | 124–129 | 70.0 | 0.1374 |
| 134.5–139.5 | 66.0 | 0.421 | | | | 129–134 | 70.0 | 1.7030 |
| 139.5–144.5 | 70.0 | 0.491 | | | | 134–139 | 72.0 | 0.3170 |
| 144.5–150 | 80.0 | 0.088 | | | | 139–144 | 75.0 | 0.0528 |
| | | | | | | 144–150 | 78.0 | 0.1814 |

Data compiled by Heather Balven, MACTEC Engineering and Consulting, Inc., Tulsa, Oklahoma.

the Haystack Gypsum Bed adjacent to the impoundment area was determined to ascertain that it would be above the conservation-pool level in all but the uppermost parts of the proposed reservoir.

## Geologic Mapping

The geologic map of the reservoir area (Fig. 5) summarizes the results of field studies, borehole data, and aerial-photo analysis. Superposition of the outline of the proposed conservation pool (1,550 ft) onto the geologic map shows that almost the entire impoundment will be in the Flowerpot Shale, or in alluvium and terrace deposits that overlie the Flowerpot. Only in the uppermost reaches of the reservoir (secs. 9, 10, and 16, T. 4 N., R. 23 W.) do the Blaine gypsum and dolomite beds dip down below the proposed conservation-pool level.

## Hydrogeologic Mapping

Four principal hydrogeologic units are present in the project area: the Flowerpot Shale aquiclude, the Blaine aquifer, the terrace deposits aquifer, and the Salt Fork alluvium aquifer.

### *Flowerpot Shale Aquiclude*

The Flowerpot Shale has a very low permeability and is an *aquiclude*. The low permeability of this aquiclude is attested by the minimal loss of water during pumping tests in the Flowerpot at the proposed damsite (Table 2). Inasmuch as the Flowerpot Shale is the bedrock unit in all but the uppermost part of the impoundment area, there should be little or no loss of reservoir water to the aquiclude, except the water that will go into bank storage. Also, the low permeability of the Flowerpot aquiclude will prevent or inhibit seepage or flow of reservoir water through the dam abutments. The several thin gypsum beds (the Chaney and Kiser Beds) are not known to be karstic, and thus should not be pathways for flow of water through the abutments. However, the potential for karst features and water transmission in the thin gypsum units should be examined in all future boreholes and excavations in the abutments.

### *Blaine Aquifer*

The Blaine gypsum/dolomite karst aquifer is the principal source of irrigation water in the areas around

Hollis, Duke, and Eldorado (to the south), and in the area just east of Reed (to the north). And the Blaine aquifer could be the principal conduit for loss of water from the upper reaches of the Mangum Reservoir if the conservation-pool level is raised too high (above 1,550 or 1,560 ft). Reports on the Blaine aquifer in the region are by Schoff (1948), Steele and Barclay (1965), Havens (1977), Johnson (1986, 1990b, 2003a,b), Runkle and McLean (1995), Osborn and others (1997), and Runkle and others (1997).

The elevation of the water table in the Blaine aquifer and other bedrock units in the project area is presented in Figure 7. Most of the water wells examined for this map are drilled into the unconfined Blaine aquifer; however, several water wells close to Salt Fork, and the three Corps boreholes at the damsite, yield water levels in the Flowerpot aquiclude. Elevations for water levels in the Flowerpot aquiclude and Salt Fork stream bed are usable on this map because the Blaine aquifer is hydrologically connected with the Flowerpot aquiclude and also with the alluvium and streamflow. Ground water, recharged mainly from precipitation in upland areas, moves toward Salt Fork and its tributaries, where it is discharged. The water table slopes down toward Salt Fork from all upland areas (Fig. 7).

A comparison of current water levels (Fig. 7) with data collected in earlier studies (Steele and Barclay, 1965; Jackson, 1991; Runkle and others, 1997) shows a similar configuration of the regional water table from 1949 to the present.

#### *Terrace Deposits Aquifer*

Terrace deposits in the area are highly porous and permeable, and typically they are excellent freshwater aquifers. Commonly, these deposits rest directly upon the Blaine aquifer, and these two units are hydrologically connected. Terrace deposits overlie bedrock in both abutments at the proposed damsite. Owing to their high permeability, terrace deposits on the abutments probably will need to be removed to prevent water loss.

#### *Salt Fork Alluvium Aquifer*

Quaternary alluvium generally is highly porous and permeable, and typically is a good freshwater aquifer. It is in direct contact with the underlying Flowerpot aquiclude in most of the impoundment area, and with the Blaine aquifer in the upper reaches of the proposed reservoir. Alluvium probably will have to be excavated down to unweathered Flowerpot Shale beneath the dam foundation to eliminate flow of water beneath the dam.

## KARST AND HYDROGEOLOGY

### Regional Karst and Hydrogeology

Gypsum and dolomite beds of the Blaine Formation contain extensive caves and sinkholes and make up a major karst aquifer that is providing irrigation water for much of the Hollis Basin and Reed area (Schoff, 1948; Steele and Barclay, 1965; Havens, 1977; Johnson, 1986, 1990b, 2003a,b; Bozeman, 1987; Runkle and McLean, 1995; Osborn and others, 1997; Runkle and others, 1997). The aquifer typically is 160–210 ft thick in southwestern Oklahoma and generally is unconfined. Karst features include caves, sinkholes, disappearing streams, springs, and underground water courses. These features are most common in areas where the thick and abundant gypsum beds of the Van Vacter Member are at or near the surface; the low-permeability shale interbeds in the Van Vacter are quite thin, and they do little to inhibit aquifer development.

Gypsum caverns in the region generally have a height and width that range from several inches to ~10 ft, although some caves reach a width of 50 ft. Enlargement of individual cavities and caverns is due to dissolution of the soluble rock as well as to abrasion of the rock by gravel, sand, and silt carried by through-flowing waters. The sediment carried by ground water is deposited locally in the underground caverns, and it partly or totally fills some of the openings.

In many parts of the region, underground caverns have become so wide that their roofs have collapsed to partly close the caverns. The collapse structures and fractured strata enable vertical movement of water in many parts of the aquifer, thus developing a good hydraulic interconnection among the various gypsum and dolomite beds. Dissolution and resultant collapse in some areas have caused one or more of the individual gypsum beds to be completely removed by dissolution, and they have been replaced by collapsed overlying strata or cave-filling sediments. These cave-filling sediments are not well cemented, and they can be eroded easily if ground water again starts to flow through them.

Ground-water and surface-water interaction near principal streams, such as the Salt Fork of Red River, enhance the dissolution of gypsum, thereby increasing the number and size of karst features and the permeability of the Blaine aquifer. In areas within 2 or 3 mi of these streams, gypsum and dolomite beds are more likely to have been partially or totally dissolved, thus creating conduits that allow large quantities of water to move rapidly through the aquifer.

### Karst Features in the Reservoir Area

All of the regional karst features described above are present in the project area, mostly in the upper reaches of the proposed reservoir. All the earlier reports by the BOR and the Corps make numerous references to the presence of caves, sinkholes, and collapse structures just upstream from the Lower Mangum Reservoir area, and discuss the likelihood that severe leakage would occur if a reservoir had been built at the Upper Mangum Damsite (Johnson, 2003b).

Examination of the dam abutments, and boreholes

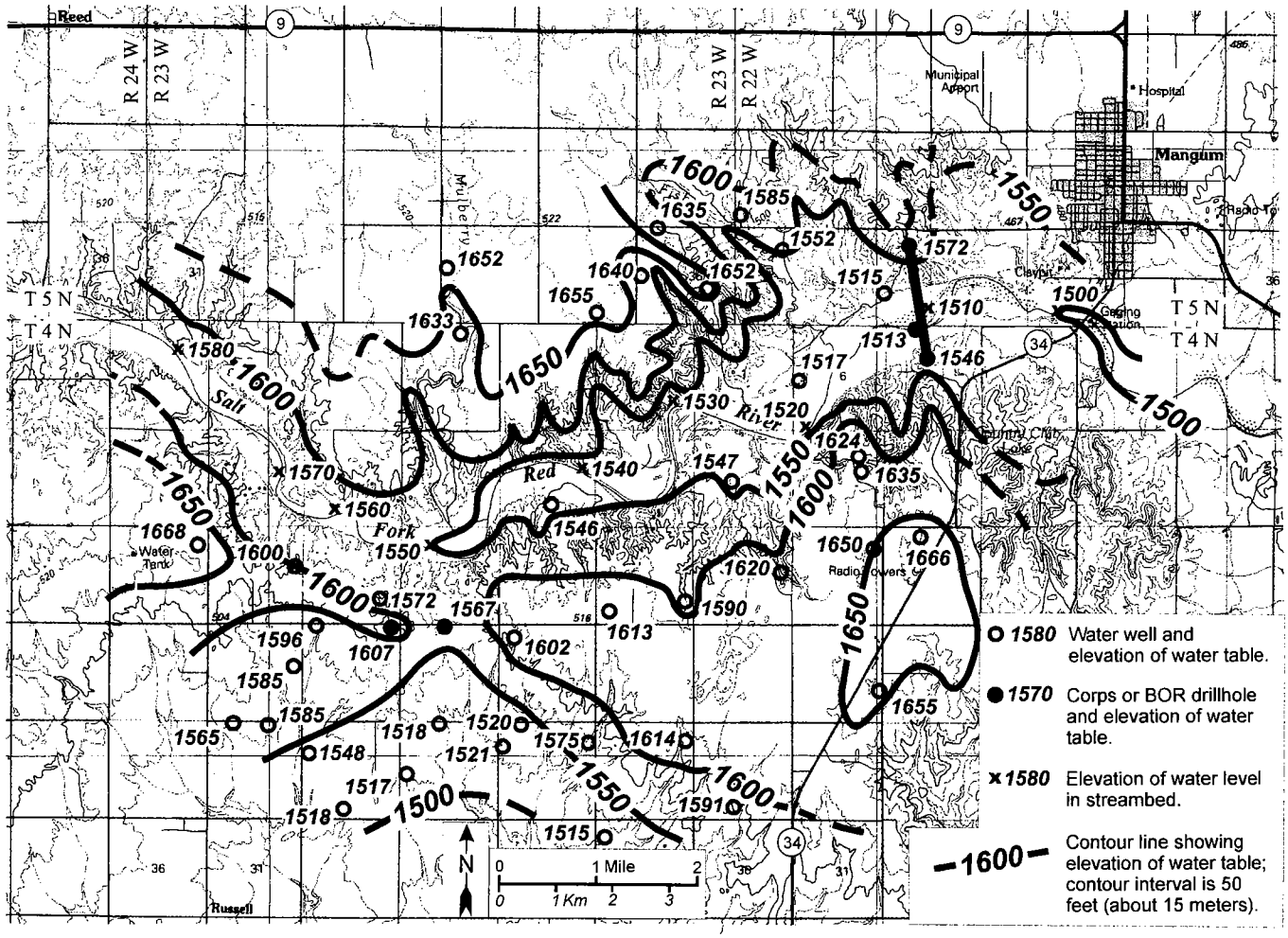


Figure 7. Map showing the regional water table in bedrock units near the proposed Lower Mangum Damsite and Reservoir. Elevations (in feet above sea level) measured April 1–19, 2002. Base map: U.S. Geological Survey, Altus 1:100,000-scale metric topographic map; contour interval of base map is 10 m (~30 ft).

B-1 and B-3 in the abutments, revealed karst features in the Blaine gypsum beds in the immediate damsite area. However, these karst conditions are at elevations above 1,569 ft and would not impact water containment if the conservation pool is maintained at 1,550 or 1,560 ft. Furthermore, karstic zones in the Blaine Formation would probably be excavated along with unconsolidated terrace deposits during dam construction.

The Haystack Gypsum Bed and overlying gypsum and dolomite units of the Blaine Formation contain karst features in many places upstream from the proposed damsite. However, these karstic strata are at elevations greater than 1,565 ft in all but the uppermost part of the reservoir and thus would be above the conservation-pool level of 1,550 or 1,560 ft; therefore, these karst conditions will not affect retaining water in most of the impoundment.

In the uppermost reaches of the reservoir (in secs. 9 and 16, and W½ sec. 10, T. 4 N., R. 23 W.), the Blaine Formation gypsum beds are partly or totally missing owing to dissolution. Most outcrops consist mainly of the intervening shales, interbedded with remnants of partly dissolved or eroded gypsum and/or dolomite beds, and these strata are largely mantled by Quaternary terrace deposits. Where these karstic beds dip below stream level, or below conservation-pool level, they constitute a zone where reservoir water will enter into bank storage and will possibly flow (as ground water) into the Turkey Creek watershed to the south.

Examination of the Chaney and Kiser Gypsum Beds, and other units in the upper Flowerpot Shale, yields no evidence of karst conditions in these thin gypsum beds. Therefore, there appears to be no potential for water loss from the reservoir related to these upper Flowerpot strata. However, future boreholes and excavations in the Flowerpot should be examined for possible evidence of karst.

## Geologic and Karst Features in the Upper Part of the Reservoir

Although the geology at the damsite and in most of the reservoir appears favorable for impounding and holding water, the complex geology and karst condi-

tions near the upper reaches of the proposed reservoir will impose limits on the size and capacity of the reservoir. If lake water rises and covers the Commissioner bend of Salt Fork, there may be a loss of reservoir water southward (to the Turkey Creek watershed) through the complex Price fault/flexure zone. The Price zone coincides with the area where the Burns ground-water saddle can allow ground-water flow beneath the Schwabe topographic saddle. These features are herein named for principal landowners in the area.

### *Commissioner Bend of Salt Fork of Red River*

An important topographic feature in the project area is the Commissioner bend of the Salt Fork of Red River in the N½ sec. 16, T. 4 N., R. 23 W. (Figs. 2, 8); it is herein named because that land is administered by the Oklahoma Commissioner of School Land Office. Commissioner bend is important because (1) it is where the Price fault/flexure zone crosses Salt Fork; (2) it has a stream-level elevation of 1,550 ft, and it would be the upper end of the reservoir if the conservation-pool level is 1,550 ft; (3) it is just north of the Schwabe topographic saddle and the Burns ground-water saddle, through which water may exit the reservoir if the pool level exceeds 1,550 or 1,560 ft; and (4) it is a segment of Salt Fork in which there appears to be a loss of river water into the ground.

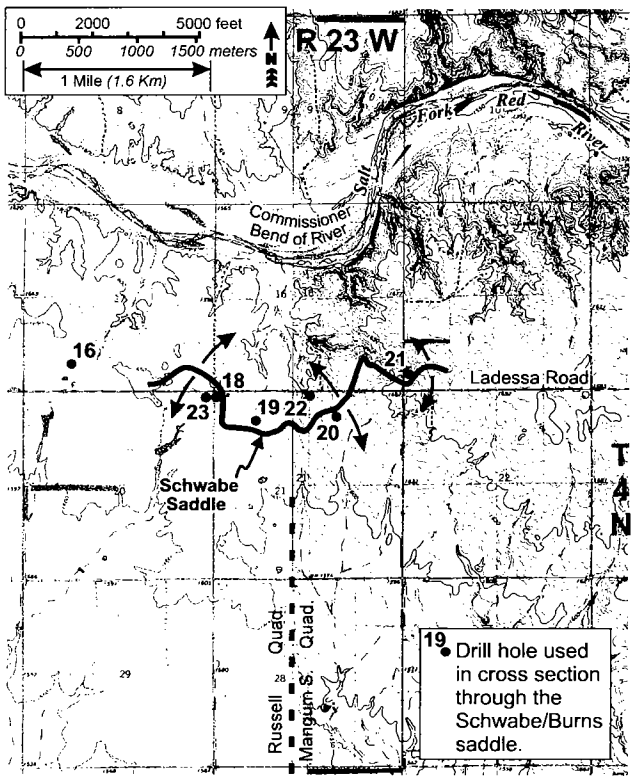


Figure 8. Map showing the Schwabe topographic saddle (along Ladessa Road), and the Commissioner bend of Salt Fork of Red River near the upper part of the proposed Lower Mangum Reservoir. Also shown are boreholes portrayed in Figure 9. Base maps: U.S. Geological Survey, Russell and Mangum South 7.5-minute-quadrangle topographic maps; contour interval of base maps is 10 ft (~3 m).

### *Price Fault/Flexure Zone*

An area of complex structure in the upper reaches of the reservoir is herein named the Price fault/flexure zone; the zone crosses lands owned by Ronald Price in the S½ sec. 16, T. 4 N., R. 23 W. (Fig. 5). The Price zone consists of at least two faults and/or flexures that extend in a N. 30° W. direction across Ladessa Road, and then across the Salt Fork of Red River in the vicinity of the Commissioner bend of the river. The faults and/or flexures are known through field studies and interpretation of data from earlier drilling by BOR along Ladessa Road, in the area of the Schwabe and Burns saddles (Fig. 9). The fault/flexure zone is a tectonic feature of Late Permian or post-Permian age; it is not a collapse structure resulting from karst development in the Blaine gypsum beds.

The Price zone is ~4,000 ft wide, and strata in the Blaine Formation (and overlying and underlying strata) are dropped down ~100–150 ft on the west (Fig. 9). Within this zone the Blaine Formation and associated strata have been faulted, fractured, and strained; this undoubtedly has increased the permeability of these rocks. Therefore, rocks here are more readily subject to weathering and erosion, and the gypsum and dolomite units of the Blaine and Dog Creek Formations are more susceptible to dissolution and karst development. These karst conditions enhance the flow of ground water toward the south from the Commissioner bend of Salt Fork, beneath the Schwabe topographic saddle.

### *Schwabe Topographic Saddle*

The topographic divide between the Salt Fork of Red River (on the north) and the Turkey Creek watershed (on the south) forms a saddle near Ladessa Road, along the north side of sec. 21, T. 4 N., R. 23 W. (Fig. 8). This roughly east–west-trending feature is herein named the Schwabe topographic saddle, after Charles and Renée Schwabe (pronounced "shwa'-bee"), owners of the NE¼ sec. 21.

The lowest elevation on the drainage divide along the Schwabe saddle is about 1,620 ft, which is 70 ft above stream level (1,550 ft) of the nearby Salt Fork at Commissioner bend. There are geologic reasons for the low elevation in this part of the saddle: (1) the Price fault/flexure zone passes through the saddle here, and the faulted, fractured, and strained rock is more readily eroded; (2) the less resistant, more easily eroded Dog Creek Shale is at the land surface in much of the saddle area; and (3) karst development in gypsum and dolomite beds beneath the saddle probably has caused subsidence of some of the land surface in the area.

### *Burns Ground-Water Saddle*

The Burns ground-water saddle is a subsurface hydrologic feature that divides ground-water move-

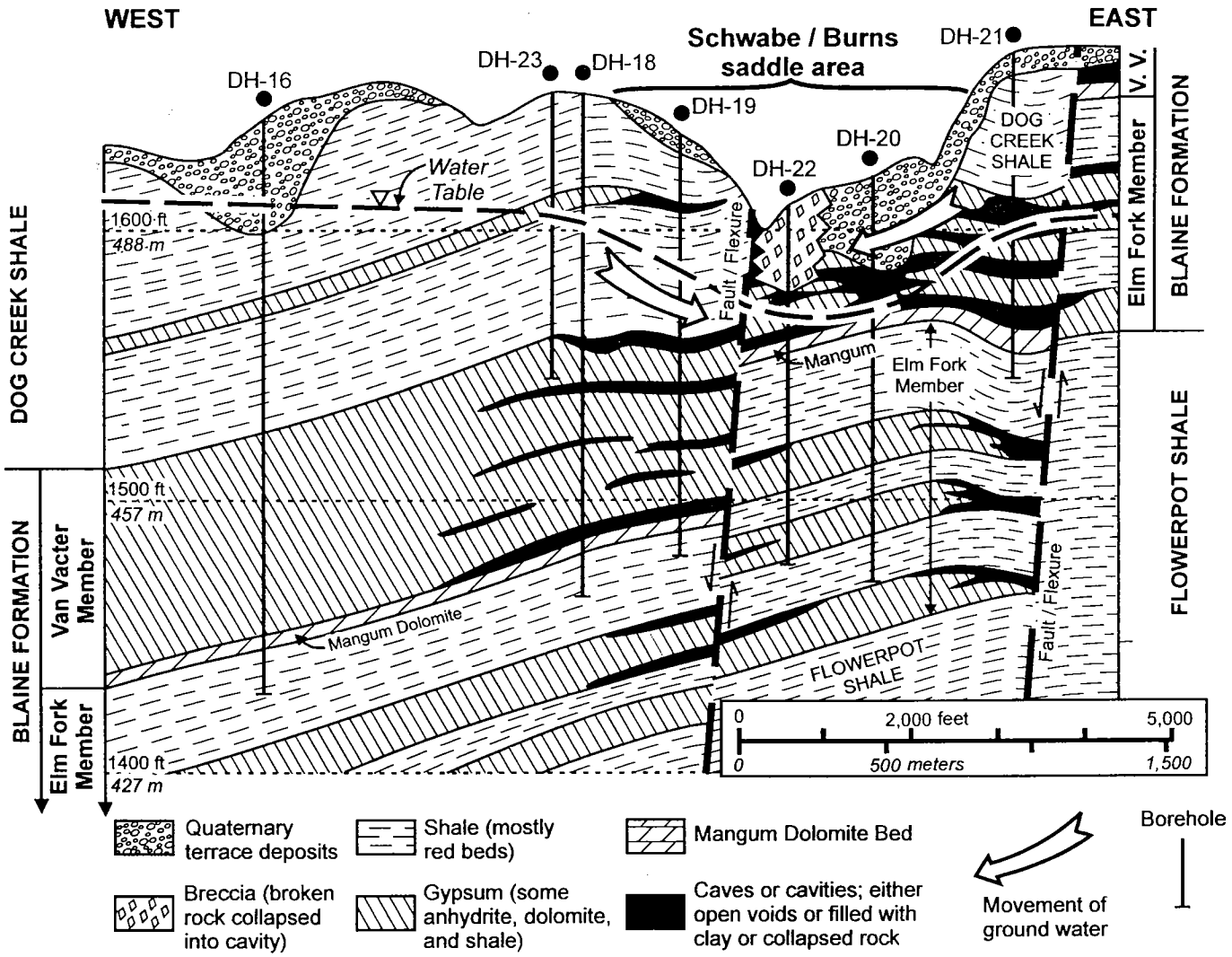


Figure 9. Schematic geologic cross section through the Schwabe and Burns saddle area. This is also the location of the Price fault/flexure zone. Cross section based upon boreholes (shown in Fig. 8) and field studies. Water table measured April 1–19, 2002. View looking to the north.

ment into a northward flow (to Salt Fork of Red River) and a southward flow (to the Turkey Creek watershed) (Fig. 10). The saddle lies along the north side of sec. 21, T. 4 N., R. 23 W., and is named for J. W. and Phyllis Burns, owners of the NW¼ sec. 21. The Burns saddle is within the complex Price fault/flexure zone (Fig. 5) and underlies the Schwabe topographic saddle (Figs. 8, 9).

Gypsum and dolomite beds of the Blaine Formation beneath the Schwabe saddle have been partly to extensively dissolved to form a system of karst features. This is affirmed by examination of BOR cores and of drillers' logs from seismic shot holes in the area, and is readily understood because permeability and karst development would be enhanced by faults, fractures, and strains in the gypsum and dolomite beds in the Price fault/flexure zone. Karst development in this area, particularly in the thick gypsum beds of the Van Vacter Member, undoubtedly has been accompanied by intermittent subsidence or collapse in the past, thus increasing the hydraulic interconnection between the various gypsum and dolomite beds. Raising the level of the reservoir up to or above the karst features may act as a catalyst for initiating, or further accelerating, dissolution of gypsum and dolomite.

Earlier studies of the Upper Mangum Damsite (Darnell, 1954; Redfield, 1960) established the importance of the Schwabe/Burns saddle area to the success of a dam and reservoir that might inundate the Commissioner bend of Salt Fork, and they described the potential for excessive leakage of impounded water through this area. This concern is attested by the significant amount of drilling and collection of water-level data in this area during earlier studies, and those data are presented here in Figure 11.

Currently, the lowest known elevation of the water table along the Burns saddle is 1,567 ft (Fig. 10). However, in earlier studies the lowest measured elevation was 1,563 ft in 1954 and 1,568 ft in 1960 (Fig. 11). Unfortunately, there are not enough data (enough water-level measurements) to define the precise loca-

tion and elevation of the crest and the low point on the Burns saddle. Additional test holes and water-level measurements in the Schwabe/Burns saddles would help establish these parameters.

#### *Loss of Streamflow at Commissioner Bend*

Several observations indicate that there may be a loss of streamflow from the Salt Fork of Red River at Commissioner bend. These include measurements that show loss of streamflow in the vicinity of Commissioner bend, a change in the stream gradient of Salt Fork just above Commissioner bend, and the pronounced flow of ground water just south of Commissioner bend.

Loss of streamflow in the general area is described by Darnell (1954, p. 3). He mentions that streamflow studies show a slight increase in streamflow down to the Upper Mangum Damsite, and a loss of streamflow from there to the Mangum bridge (see locations in Fig. 1). Unfortunately, data are not provided on precise locations where the water loss is suspected, but it appears that they may be in the vicinity of Commissioner bend.

The gradient of Salt Fork changes significantly at, and just above, Commissioner bend. Far above and below this area, the elevation of the stream bed normally drops 20 ft within river distances of 15,000–20,000 ft—a stream gradient of 5–7 ft per mile. However, the elevation of the stream bed drops 20 ft (from 1,570 ft to 1,550 ft) within a river distance of only 11,000 ft just above Commissioner bend (Fig. 7)—a stream gradient of ~9.6 ft per mile. The steeper gradient here indicates that the river is flowing more rapidly and is cutting down more rapidly, and then the water appears to be removed from the river near Commissioner bend. This suggests that there may be a sink or some other feature that is draining water from the river near Commissioner bend, thus causing an increase in the stream's gradient as it approaches the bend.

The location and configuration of the Burns ground-water saddle, and the water table for several miles south of the saddle, indicate that a highly permeable conduit exists for ground-water flow from north to south in the area (Figs. 7, 9, 10, 11). The Burns saddle and this permeable, karstic conduit are directly south of Commissioner bend and probably represent a pathway for some of the surface flow of Salt Fork to exit the river and move southward as ground water into the Turkey Creek watershed.

To determine the quantity and location of streamflow loss, and the potential for loss of reservoir water to ground water in this area, measurements of streamflow in Salt Fork should be made at one or two sites upstream and downstream of Commissioner bend.

### Significance of Karst on the Project

If karst features are present in the abutments and in the impoundment area, these features could compromise the ability of the proposed reservoir to contain water. Furthermore, filling the reservoir to too high a level could act as a catalyst for initiating, or further accelerating, dissolution of the evaporites. The hydraulic head of a reservoir that is too full may also cause clay-filled cavities in gypsum beds to weaken and fail, thus allowing water to flow through preexisting subsurface solution channels.

Fortunately, bedrock in almost all parts of the impoundment area is the thick Flowerpot Shale, which lacks karst features. The abutments do contain karst features in the Haystack Gypsum Bed and overlying strata in the Blaine Formation. However, these karstic strata are at elevations above 1,569 ft, well above the proposed conservation-pool level of 1,550 or 1,560 ft; also, these karstic rocks will be excavated in constructing the dam.

Only in the upper reaches of the reservoir, at the Commissioner bend of Salt Fork and the Schwabe/Burns saddles, are karst features of the Blaine Formation likely to allow reservoir water to escape as ground water and flow south to the Turkey Creek watershed. To prevent, or at least minimize, such a loss of water, the conservation-pool level should not exceed 1,550 ft (stream level in Commissioner bend), or perhaps 1,560 ft (based upon what is learned about water levels and ground-water flow in the Schwabe/Burns saddles).

It is likely that ground water is flowing northward from the Burns ground-water saddle toward Salt Fork at Commissioner bend (in sec. 16), as is indicated by water-level contours (Figs. 10, 11). If so, perhaps the reservoir level could be raised to an elevation approaching the low point on the ground-water divide: to an elevation of about 1,560 ft. Although current data show that the divide may be as low as 1,567 ft (Fig. 10), the data are sparse along the divide and it may locally be lower than 1,567 ft. It is also possible that the 1,567-ft value represents a perched water table, and that karstic features in underlying Blaine gypsum and dolomite beds may be channeling water to the south at a lower elevation, beneath the ground-water divide.

Additional data are needed to answer certain important questions: (1) What is the lowest elevation along the ground-water divide? (2) Is there a perched water table at the Burns ground-water saddle? (3) Is ground water flowing to the south beneath the ground-water divide through karst conduits that are not connected with a shallower (perched) water table? (4) Can the reservoir level be raised above 1,550 ft, with assurance that there would not be excessive loss of water through the Schwabe/Burns saddles? Until these conditions are evaluated, it is uncertain whether the conservation-pool level should be limited to 1,550 ft, or perhaps be raised as high as 1,560 ft. These data are critical in designing the Lower Mangum Dam.

## RESERVOIR TIGHTNESS

The combination of geologic and hydrogeologic field studies, along with core descriptions and pressure tests

on the three boreholes, indicates that the proposed dam and most of the impoundment area are water tight and will hold water behind the dam. Providing that the conservation-pool elevation does not exceed 1,550 ft (or perhaps 1,560 ft), the bedrock unit at the damsite, and in all but the uppermost part of the reservoir, will be the Flowerpot Shale; and Flowerpot strata have such a low permeability that seepage of water should be minimal. The loose, sand-sized particles of shale and gypsum recovered at three levels in borehole B-1 are regarded as an artifact of drilling, and those strata will not be pathways for water loss under the dam. Also, there is no evidence of karst features in the thin Chaney and Kiser Gypsum Beds, or in other gypsiferous zones in the Flowerpot, so they should not be conduits for water loss.

Karst features in the Blaine Formation are potential pathways for water loss if the reservoir level were to rise up to (or above) the elevation of the Haystack Gypsum Bed. At the damsite, the base of the Haystack is 1,569 ft, and excavating the gypsum beds here and replacing them with impermeable material removes the potential for karst problems at the damsite. In most of the reservoir area, the elevation of the base of the Haystack Bed is 1,565–1,585 ft; thus the karst zones of the Blaine Formation will be above the conservation-pool level in all but the uppermost part of the reservoir. Only in the vicinity of Commissioner bend and the Price fault/flexure zone does the base of the Blaine dip to 1,545 ft, and lower, beneath the stream bed of the Salt Fork of Red River.

The elevation of the regional water table slopes down toward the reservoir from all directions (Fig. 7). This assures that lake water will be contained within the impoundment in all but the uppermost part of the reservoir. Some of the lake water will go into bank storage as the reservoir fills up; bank-storage water will seep into currently unsaturated alluvium, terrace deposits, and bedrock units that will be inundated. Once the bank-storage capacity is reached, there should be no additional bank-storage seepage into these rocks and sediments.

One of the limiting factors on reservoir tightness and the capacity of the reservoir is the potential for loss of surface water to the subsurface at Commissioner bend of Salt Fork, in the uppermost parts of the reservoir. In this area, the Blaine Formation is faulted, fractured, and strained in the Price fault/flexure zone, and ground water may flow southward through the Schwabe/Burns saddles to the Turkey Creek watershed. Karstic gypsum and dolomite beds of the Blaine Formation are below river level (below 1,550-ft elevation) in this area (Fig. 9), and thus would be below conservation-pool level. To eliminate loss of surface water at Commissioner bend, where the elevation is 1,550 ft, it may be necessary to limit the conservation-pool level to 1,550 ft; this would assure that there is no more loss of water at this site than is already occurring. However, water-level contours in the Schwabe/Burns saddle area (Fig. 10) indicate that the reservoir level might be raised nearly as high as the low point on the Burns ground-water divide, or to an elevation of about 1,560 ft. Further study will be needed to assess this possibility.

Alluvium and terrace deposits at the proposed damsite are permeable. They consist of loose sand, gravel, and clay, and are potential pathways for water loss beneath the dam. Alluvium underlies much of the valley of the Salt Fork of Red River, and terrace deposits overlie bedrock units on both abutments (Figs. 5, 6). Both alluvium and terrace deposits probably will need to be excavated down to the competent, impermeable (or low-permeability) Flowerpot Shale at the damsite, either by complete excavation of the overburden or by a narrow cutoff trench, backfilled with impermeable material.

## RESERVOIR STORAGE AND WATER-SUPPLY YIELDS

Data on the surface area, reservoir storage, and water-supply yields for several different conservation-

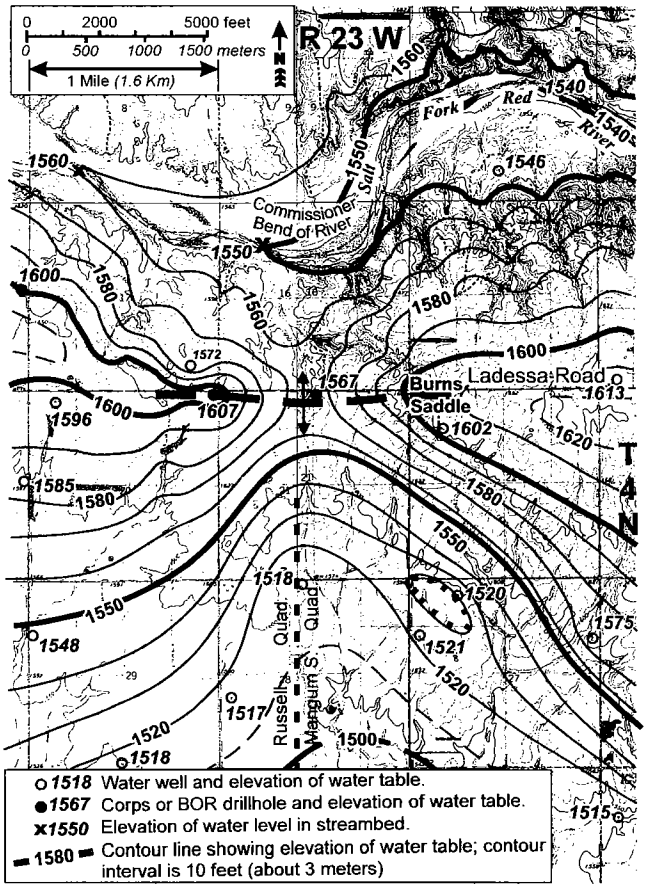


Figure 10. Map showing water-table contours at and near the Burns ground-water saddle in 2002; elevations (in feet above sea level) measured April 1–19, 2002. Base maps: U.S. Geological Survey, Russell and Mangum South 7.5-minute-quadrangle topographic maps; contour interval of base maps is 10 ft (~3 m).

pool elevations of the Lower Mangum Damsite and Reservoir were determined (Tables 3, 4). Streamflows along the Salt Fork of Red River were measured by U.S. Geological Survey stream gages at Wellington, Texas, and Mangum, Oklahoma, for the period of January 1967 through September 1991. Also, the water-supply yields determined here are based on conditions that existed during the period-of-record available at the stream gages used in the analysis.

Current data (Tables 3, 4) for the proposed reservoir are as follows: if the conservation pool is established at 1,550 ft, the lake would have a surface area of 1,863 acres, a total storage volume of 26,080 acre-ft of water, and a water-supply yield of 11.07 mgd (million gallons per day); and if the conservation pool can be set higher, at 1,560 ft, the lake would have a surface area of 2,604 acres, a total storage volume of 47,043 acre-ft of water, and a water-supply yield of 16.51 mgd. Water-supply yields were calculated for conservation storage amounts ranging from 7,314 to 46,993 acre-ft, resulting in yields from 2.67 to 16.51 mgd.

**Table 3. — Elevation–Area–Capacity Data for Lower Mangum Dam and Reservoir**

| Elevation (feet) | Surface area (acres) | Storage volume (acre-feet) |
|---|---|---|
| 1,540 | 1,184 | 12,311 |
| 1,545 | 1,397 | 18,766 |
| 1,550 | 1,863 | 26,080 |
| 1,555 | 2,142 | 35,953 |
| 1,560 | 2,604 | 47,043 |

Data compiled by Russell Wyckoff, U.S. Army Corps of Engineers, Tulsa, Oklahoma.

## SUMMARY AND CONCLUSIONS

Foundation conditions at the proposed damsite appear favorable. The combination of geologic and hydrogeologic field studies, along with core descriptions and pressure tests on the three boreholes drilled at the damsite, indicates that water would be contained behind the dam. The thick Flowerpot Shale will be the bedrock foundation for all parts of the dam and most of the impoundment area. Reservoir tightness is demonstrated by pressure testing in boreholes at the damsite and by the presence of the low-permeability Flowerpot Shale aquiclude as bedrock in almost all parts of the reservoir. Pressure tests show the water loss typically to be only 0.1–1.0 gpm, with some values up to 4.6 gpm. The highest water loss (13.8 gpm) in the Flowerpot is in borehole B-1 at a depth of 64.5–69.5 ft; this interval is at an elevation of 1,566–1,561 ft, and this rock would be excavated with the overlying Blaine strata.

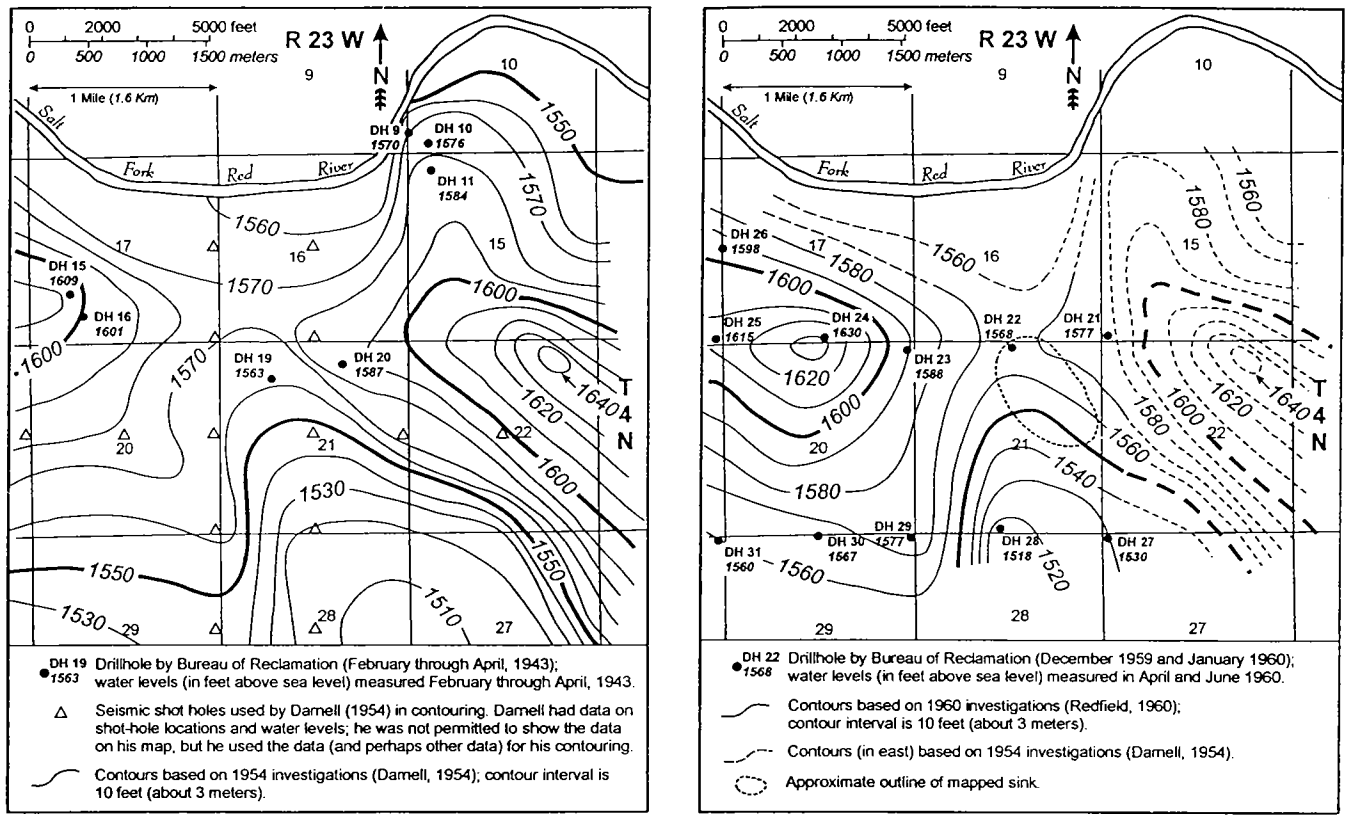


Figure 11. Maps showing water-table contours at and near the Burns ground-water saddle in 1954 (left, modified from Darnell, 1954) and in 1960 (right, modified from Redfield, 1960). Elevations are in feet above sea level.

**Table 4. — Water-Supply and Yield Data for Lower Mangum Dam and Reservoir**

| Runs: | 1 | 2 | 3 | 4 | 5 | 6 | 7 | 8 |
|---|---|---|---|---|---|---|---|---|
| Top conservation pool: | 1,550 | 1,550 | 1,550 | 1,560 | 1,560 | 1,560 | 1,550 | 1,560 |
| Bottom conservation pool: | 1,520 | 1,525 | 1,530 | 1,520 | 1,525 | 1,530 | 1,545 | 1,550 |
| Water-supply storage (ac-ft): | 26,030 | 24,351 | 22,182 | 46,993 | 45,314 | 43,145 | 7,314 | 11,090 |
| Water-supply yield (mgd): | 11.07 | 10.46 | 9.65 | 16.51 | 15.9 | 15.13 | 2.67 | 3.28 |
| Drawdown time: | 4 yr 6 mo | 3 yr 1 mo | 3 yr 1 mo | 8 yr 3 mo | 8 yr 3 mo | 8 yr 3 mo | 2 yr 10 mo | 2 yr 11 mo |

Runs 1, 2, and 3 have acceptable drawdown periods, whereas runs 4, 5, and 6 have excessive drawdown periods. Runs 7 and 8 have minimal drawdowns, but small yields, representing a small pool fluctuation for recreational interests.

Data compiled by Russell Wyckoff, U.S. Army Corps of Engineers, Tulsa, Oklahoma.

The water table for all areas around the reservoir is above the proposed conservation-pool level of 1,550 ft (or 1,560 ft), and it slopes down toward the reservoir from all directions. This assures that lake water will be contained within the impoundment, except perhaps in the uppermost reaches of the reservoir, at the Commissioner bend of Salt Fork and the Schwabe/Burns saddle area.

Karst features are present in the Blaine Formation in areas surrounding the proposed reservoir. However, these karstic units will be excavated at the damsite, or will be above conservation-pool level in all but the uppermost parts of the reservoir. Therefore, these karst conditions will not affect reservoir tightness in most of the impoundment.

The complex geology and karst conditions in the uppermost reaches of the proposed reservoir will impose limits on the lake level, size, and capacity of the Mangum Reservoir. Water impounded up to and above the Commissioner bend of Salt Fork may cause loss of reservoir water southward (to the Turkey Creek watershed) through the Price fault/flexure zone. Rock in this zone is faulted, fractured, and strained, and the karst conditions here may allow ground water to pass through the Burns ground-water saddle, beneath the Schwabe topographic saddle. Also, raising the reservoir level too high may act as a catalyst for initiating, or further accelerating, dissolution of gypsum and dolomite units beneath the Schwabe topographic saddle.

There appears to be a loss of some streamflow from the Salt Fork of Red River at Commissioner bend, and this water then appears to move as ground water to the south through a karstic zone in the Schwabe/Burns saddles. The elevation of the stream bed in Salt Fork at Commissioner bend is 1,550 ft, and it may be necessary to maintain the conservation pool at a maximum of 1,550 ft. Under these conditions, water loss through the Schwabe/Burns saddles would be no more than it is currently. It may be possible to raise the conservation pool to as much as 1,560 ft if subsequent testing shows that the low point of the Burns groundwater saddle is higher than 1,560 ft, and if one can assure that excessive reservoir water will not pass southward (as ground water) into the Turkey Creek watershed.

If the calculated surface area, storage volume, and water-supply yield are sufficient to warrant further study and planning, several activities are necessary to determine limits on the conservation-pool level and reservoir size. These activities include drilling additional boreholes along the dam, determining the quantity and location of streamflow loss at Commissioner bend, and fully assessing the hydrogeologic conditions (and the potential for loss of reservoir water) in the Schwabe/Burns saddle area.

## REFERENCES CITED

Bozeman, S. (ed.), 1987, The D. C. Jester Cave system: Central Oklahoma Grotto, Oklahoma City, Oklahoma Underground, v. 14, 56 p.

Current, E. L., 1942, Report of geophysical survey of Upper Mangum investigations: U.S. Bureau of Reclamation unpublished report, dated 1942, 6 p. plus tables and figures (Appendix E in Jackson, 1991).

Curtis, N. M., Jr.; and Ham, W. E., 1972, Geomorphic provinces of Oklahoma: Oklahoma Geological Survey map, scale 1:2,000,000.

Darnell, J. L., 1954, Geological report on the Mangum project, Salt Fork of the Red River, Oklahoma: U.S. Bureau of Reclamation unpublished report, dated September 1954, 5 p. plus photographs and figures (Appendix B in Jackson, 1991).

Havens, J. S., 1977, Reconnaissance of the water resources of the Lawton Quadrangle, southwestern Oklahoma: Oklahoma Geological Survey Hydrologic Atlas 6, 4 sheets, scale 1:250,000.

Jackson, J. L., 1991, Mangum project, Oklahoma, geologic appraisal of damsites: U.S. Bureau of Reclamation unpublished report, dated February 1991, 20 p. (includes Appendixes A–G, which are all the letters and reports prepared previously by U.S. Bureau of Reclamation).

Johnson, K., S., 1986, Hydrogeology and recharge of a gypsum–dolomite karst aquifer in southwestern Oklahoma, U.S.A.; International Symposium of Karst Water Resources, 1985, Ankara, Turkey: International Association of Hydrological Sciences Publication 161, p. 343–357.

_____1990a, Standard outcrop section of the Blaine Formation and associated strata in southwestern Oklahoma: Oklahoma Geology Notes, v. 50, p. 144–168.

_____1990b, Hydrogeology of the Blaine gypsum–dolomite karst aquifer, southwestern Oklahoma: Oklahoma Geological Survey Special Publication 90-5, 31 p.

_____2003a, Evaporite karst in the Permian Blaine Formation and associated strata in western Oklahoma, *in* Johnson, K. S.; and Neal, J. T. (eds.), Evaporite karst and engineering/environmental problems in the United States: Oklahoma Geological Survey Circular 109 [this volume], p. 41–55.

_____2003b, Gypsum karst and abandonment of the Upper Mangum Damsite in southwestern Oklahoma, *in* Johnson, K. S.; and Neal, J. T. (eds.), Evaporite karst and engineering/environmental problems in the United States: Oklahoma Geological Survey Circular 109 [this volume], p. 85–94.

Johnson, K. S.; and Denison, R. E., 1973, Igneous geology of the Wichita Mountains and economic geology of Permian rocks in southwest Oklahoma: Oklahoma Geological Survey Special Publication 73-2, 33 p.

Johnson, K. S.; and Ham, W. E. [undated], Unpublished geologic maps of the Mangum–Erick area and the Hollis–Duke area, southwestern Oklahoma: Oklahoma Geological Survey, scale 1:63,360.

Kirchen, H. W., 1941, Geological reconnaissance of several dam sites on the Salt Fork of the Red River, Oklahoma: U.S. Bureau of Reclamation unpublished memorandum to Hydraulic Engineer, dated January 14, 1941, Denver, Colorado, p. 24–28 (Appendix G in Jackson, 1991).

Osborn, N. I.; Eckenstein, E.; and Fabian, R. S., 1997, Demonstration and evaluation of artificial recharge to the Blaine aquifer in southwestern Oklahoma: Oklahoma Water Resources Board Technical Report 97-5, 136 p.

Redfield, R. C., 1960, Mangum project, Oklahoma, geologic report on investigation of Mangum reservoir basin, 1960: U.S. Bureau of Reclamation unpublished report, dated June 1960, 8 p. plus figures (Appendix A in Jackson, 1991).

Runkle, D. L.; and McLean, J. S., 1995, Steady-state simulation of ground-water flow in the Blaine aquifer, southwestern Oklahoma and northwestern Texas: U.S. Geological Survey Open-File Report 94-387, 92 p.

Runkle, D. L.; Bergman, D. L.; and Fabian, R. S., 1997, Hydrogeologic data for the Blaine aquifer and associated units in southwestern Oklahoma and northwestern Texas: U.S. Geological Survey Open-File Report 97-50, 213 p.

Schoff, S. L., 1948, Ground-water irrigation in the Duke area, Jackson and Greer Counties, Oklahoma: Oklahoma Geological Survey Mineral Report 18, 10 p.

Smith, F. F.; and Nickell, F. A., 1941, Mangum project comparison of dam sites on Salt Fork in order to provide storage for land near Altus, Oklahoma: U.S. Bureau of Reclamation unpublished letter to Chief Engineer, dated May 22, 1941, Denver, Colorado, 5 p. (Appendix F in Jackson, 1991).

Steele, C. E.; and Barclay, J. E., 1965, Ground-water resources of Harmon County and adjacent parts of Greer and Jackson Counties, Oklahoma: Oklahoma Water Resources Board Bulletin 29, 96 p.

U.S. Army Corps of Engineers, 2002, Final report, Mangum Reservoir study (geotechnical investigations), Mangum, Oklahoma, phase IV: Unpublished report prepared by USACE for the Oklahoma Water Resources Board, dated August 2002, 52 p. plus appendixes.

U.S. Bureau of Reclamation, 1943, Geologic logs for Upper Mangum dam site: U.S. Bureau of Reclamation unpublished logs of 20 boreholes, dated February–March–April, 1943 (Appendix D in Jackson, 1991).

# Regional Mapping of Karst Terrains in Oklahoma for Avoidance of Engineering and Environmental Problems

***Kenneth S. Johnson***
Oklahoma Geological Survey
Norman, Oklahoma

**ABSTRACT.**—The Oklahoma Geological Survey will prepare a map of the State at a scale of 1:500,000 (or possibly 1:750,000) to show potential karst terrains and associated engineering and environmental problems in Oklahoma. Surface and near-surface carbonates (limestone and dolomite) cover ~6% of the surface area of the State, whereas surface and near-surface sulfates (gypsum and anhydrite) cover ~4% of the State. Areas of carbonates and sulfates will be differentiated and mapped separately as two zones: in zone 1 these water-soluble rocks are 0–6 m deep, and in zone 2 they are 6–30 m deep. Areas underlain by bedded salt (halite) within 300 m of the surface extend over 14.6% of the State, and they will be mapped as zone 3. Data on the karst map of Oklahoma will be incorporated into a planned national karst map.

## INTRODUCTION

This brief paper, modified and updated from an earlier report by Johnson and Quinlan (1995), describes plans of the Oklahoma Geological Survey (OGS) for preparing a map and text showing the potential karst terrains and associated engineering and environmental problems in Oklahoma. This will not be a detailed map showing individual caves, sinkholes, or other specific karst features. Instead, the map will show the general distribution of potential karstic areas in the State so that engineering, construction, and ground-water-related projects in those areas can anticipate, and then solve or avoid, problems related to development in karst terrains. The State map and text will not replace the need for site-specific geotechnical and/or hydrogeological investigations for projects that may be impacted by location in or near a karst terrain.

Almost all terrains in which carbonate, sulfate, or chloride rocks crop out, or are in the shallow subsurface, are probably karstic, at least to some extent. In the case of carbonates and sulfates in Oklahoma, it is likely that karst features may cause problems in areas where the soluble rock is 0–6 m below the land surface, and problems may even exist where the soluble rock is 6–30 m deep; for chlorides (halite, or rock salt), karst features may be important where the salt is 0–300 m deep.

The karst map of Oklahoma is part of a larger program of preparing a generalized karst map for the entire United States. This national program, described by Epstein and Johnson (2003), is being carried out by the U.S. Geological Survey (USGS) in cooperation with state geological surveys, other federal agencies, and academia. The digitized national karst map will be maintained by the National Cave and Karst Research Institute (NCKRI). Oklahoma's karst map also is part of an overall OGS program to identify and characterize the State's geologic hazards (Luza and Johnson, 2003).

A related program being carried out by OGS is preparation of an annotated bibliography on caves and karst in Oklahoma. This bibliography is being prepared with support from NCKRI and is available online through the OGS web site (http://www.ogs.ou.edu/).

## GEOLOGIC SETTING

Sedimentary and low-grade metasedimentary rocks make up ~99.5% of the outcrops in Oklahoma (Fig. 1), and Paleozoic strata are as thick as 6,000–9,000 m in the depocenters of the major sedimentary basins (Figs. 1, 2). Carbonates and evaporites make up a significant portion of the outcrops and shallow-subsurface rocks in several of the geologic provinces, and thus the known and potential karst regions of the State are widespread.

Carbonates, mostly limestone and minor dolomite, crop out chiefly in the Arbuckle Mountains, Wichita Mountains, and Ozark Uplift (Figs. 2, 3): in these areas, carbonates occur in units 15–2,000 m thick and are of Late Cambrian through Early Pennsylvanian age. Pennsylvanian and Early Permian limestones, 2–15 m thick, occur in the northern shelf areas; and Cretaceous limestones, ~6 m thick, crop out in the Coastal Plain of southeastern Oklahoma. Permian evaporites (gypsum, anhydrite, and salt) are important in, and

Johnson, K. S., 2003, Regional mapping of karst terrains in Oklahoma for avoidance of engineering and environmental problems, *in* Johnson, K. S.; and Neal, J. T. (eds.), Evaporite karst and engineering/environmental problems in the United States: Oklahoma Geological Survey Circular 109, p. 113–117.

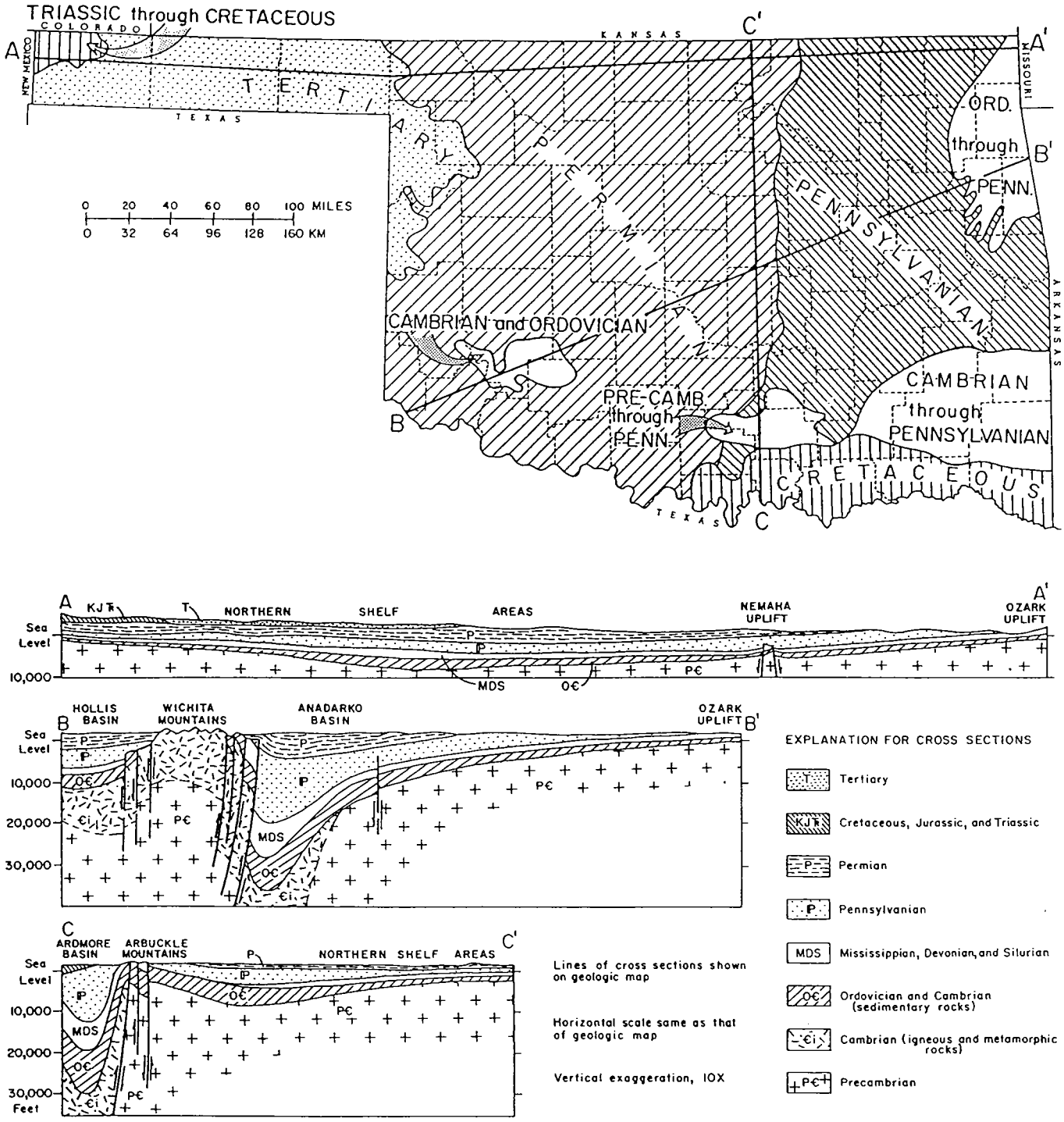


Figure 1. Generalized geologic map and cross sections of Oklahoma.

are restricted to, western Oklahoma (Figs. 1, 3). Outcropping gypsum beds typically are 2–30 m thick, and five major subsurface salt (halite) sequences are each commonly 30–150 m thick and consist of shale interbedded with salt beds that are 1–10 m thick.

Within Oklahoma's area of ~180,000 km$^2$, limestone and dolomite crop out, or are no more than 30 m deep, in ~10,700 km$^2$ (6% of the State) (Fig. 3); gypsum and anhydrite crop out, or are no more than 30 m deep, in ~7,100 km$^2$ (4%); and salt is within 300 m of the land surface in ~26,300 km$^2$ (14.6%).

## MAPPING PROCEDURES

The OGS has been involved for many years in a long-term program of basic geologic mapping, carried out by OGS staff members, university faculty, and supervised graduate students. Field mapping normally is conducted through a coordinated program involv-

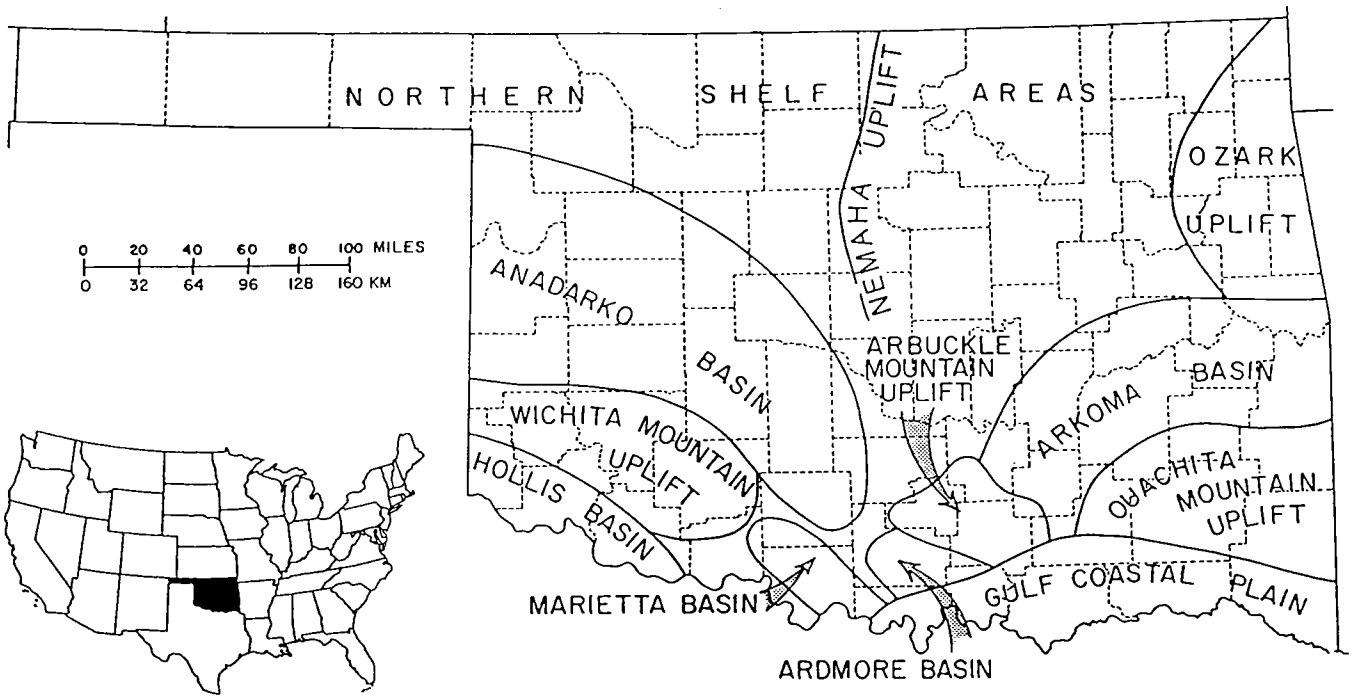


Figure 2. Map showing major geologic provinces of Oklahoma.

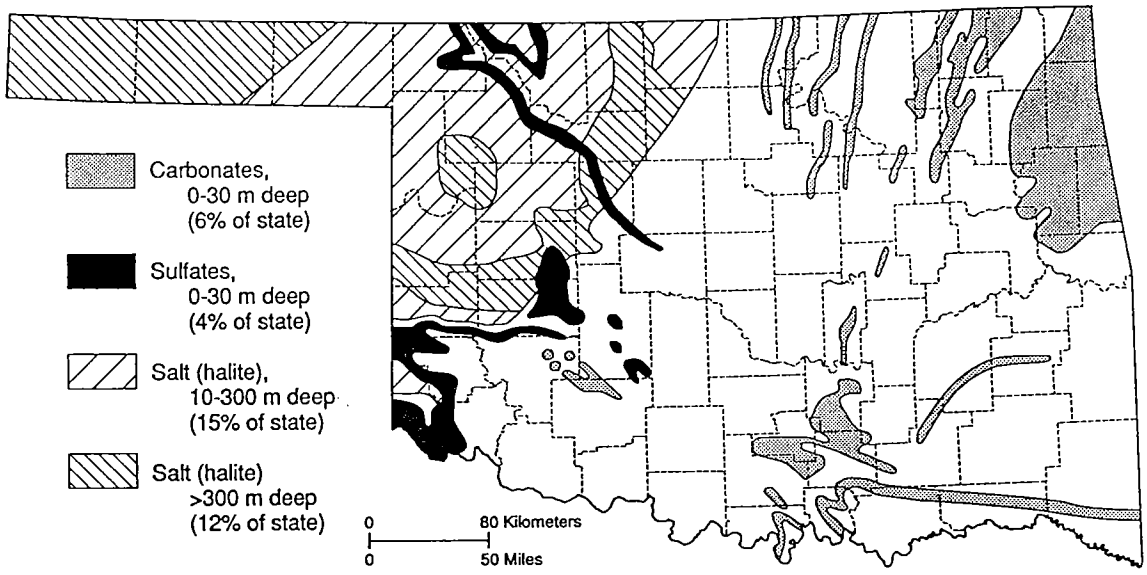


Figure 3. Map showing general distribution of potential karst terrains in Oklahoma (from Johnson and Quinlan, 1995).

ing stereoscopic examination of aerial photos and field study. Carbonate and sulfate rocks in Oklahoma can be mapped somewhat easily; they commonly form conspicuous topographic highs (ridges and escarpments), because the annual precipitation is rather low—ranging from ~50 cm in the west to ~125 cm in the east.

At present, ~40% of Oklahoma's surface geology has been mapped at a scale of 1:62,500, or larger, and this is adequate for delineating areas where potentially karstic rock units crop out or are in the shallow subsurface. Fortunately, most of the counties or regions containing karstic-rock outcrops are among those already mapped, and compilation of reconnaissance-level data for karst areas in unmapped terrain will be carried out by stereoscopic photo examination and field checking.

Using geologic maps and aerial photos, OGS will outline the areas in Oklahoma where carbonates and/or sulfates are at least 1 m thick and are <30 m deep. Furthermore, these areas will be divided into two zones (Fig. 4). In zone 1 the karstic rocks crop out, or are within 6 m of the surface, and in this zone the potential is greatest for karst development and associated engineering and environmental problems. In

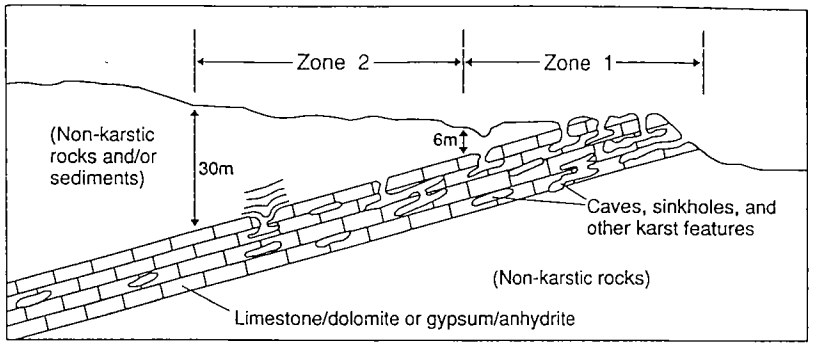


Figure 4. Schematic diagram showing proposed karst zones 1 and 2, which are related to the depth of karstic carbonates and sulfates in Oklahoma (from Johnson and Quinlan, 1995).

zone 2 the top of the karstic rocks is 6–30 m deep, and here there is a somewhat lesser (yet real) potential for karst development and associated problems. These two zones will be shown separately on the final State map, and the areas of carbonates and sulfates will be differentiated (i.e., carbonates, zones 1 and 2; and sulfates, zones 1 and 2).

Depth limits of 6 m and 30 m for zones 1 and 2 are somewhat arbitrary but reasonable. Any significant construction/engineering project in Oklahoma is likely to excavate, and/or deal directly with, bedrock karst units that are present to a depth of 6 m. And karst development in the greater depth range of 6–30 m may be important, locally, and may have an adverse impact on a construction/engineering project. Karst features are also present in Oklahoma carbonates and sulfates at depths greater than 30 m (probably as deep as 50–100 m, locally), but they are much more sporadic and less well developed, and their potential to cause problems is probably quite low.

Areas underlain by shallow salt deposits in western Oklahoma are well known as a result of interpretation of cores, sample logs, and geophysical logs available for a great number of oil and gas tests and other boreholes drilled throughout the State. OGS will delineate those areas where the top of the shallowest salt is within 300 m of the land surface, and show those areas as zone 3 on the karst map. Salt does not crop out in Oklahoma, but it does occur at depths of only 10–15 m in several localities (Big Salt Plain and the northern Harmon County salt plains).

The depth limit of 300 m for zone 3 is also arbitrary but reasonable. Active, natural dissolution of salt in Oklahoma occurs locally at depths of 10–150 m; and human-induced dissolution and consequent collapse, commonly associated with boreholes (drilled for salt-cavern development or in petroleum activity), have occurred at several places in the United States where salt beds are as deep as 300 m below the surface (Johnson, 1998, 2003, in press). I am not aware of any ongoing, natural dissolution of salt in Oklahoma at depths greater than 300 m, although paleodissolution may have occurred in salts that now are at such great depths.

Depth ranges described above for zones 1, 2, and 3 are considered reasonable for karst development in Oklahoma at this stage of the study. OGS will, however, evaluate these depth ranges as work progresses, and will modify them, if warranted. The final map will be prepared at a scale of 1:500,000 (or possibly 1:750,000). The base map probably will show the land grid (townships and ranges), counties, towns, highways, railroads, and principal rivers and lakes. The map will delineate areas of potential limestone/dolomite karst and gypsum/anhydrite karst (zones 1 and 2), and will outline areas of shallow salt deposits (zone 3). An accompanying text will describe the geology and nature of karstic rocks in Oklahoma, and will discuss the known and potential hazards associated with karstic rocks and karstic terrains.

## SUMMARY AND CONCLUSIONS

Owing to the importance of assessing the significance of karst in engineering and environmental problems in Oklahoma, the OGS will prepare a statewide map showing the general distribution of potentially karstic terrains and a description/discussion of known and potential karst-related problems in the State. These data will then be incorporated into the national karst map being prepared by the USGS. The Oklahoma map will be compiled at a scale of 1:500,000 from existing geologic maps and reports, and from stereoscopic aerial-photo examination in areas not yet mapped in detail.

Areas of limestone/dolomite and gypsum/anhydrite will be differentiated, and each will be divided into two zones (0–6 m deep, and 6–30 m deep). Areas where salt is within 300 m of the surface will be mapped as a third zone. Depths for each of these zones are considered reasonable for Oklahoma at this stage of the study, but they will be further evaluated (and perhaps modified) as the work progresses. These data, and the accompanying text, will aid in the planning of engineering, construction, and ground-water-related projects, and should reduce the adverse impact of engineering and environmental problems associated with karstic terrains. Such data will not take the place of site-specific studies, as these detailed studies always will be needed to evaluate the relationship between a proposed project and local karst conditions.

## REFERENCES CITED

Epstein, J. B.; and Johnson, K. S., 2003, The need for a national evaporite-karst map, *in* Johnson, K. S.; and Neal, J. T. (eds.), Evaporite karst and engineering/environmental problems in the United States: Oklahoma Geological Survey Circular 109 [this volume], p. 21–30.

Johnson, K. S., 1998, Land subsidence above man-made salt-dissolution cavities, *in* Borchers, J. W. (ed.), Land subsidence; case studies and current research (Proceedings

of the Dr. Joseph F. Poland symposium on land subsidence): Association of Engineering Geologists Special Publication 8, p. 385–392.

_____2003, Evaporite karst problems in the United States, *in* Johnson, K. S.; and Neal, J. T. (eds.), Evaporite karst and engineering/environmental problems in the United States: Oklahoma Geological Survey Circular 109 [this volume], p. 1–20.

_____[in press], Salt dissolution and subsidence or collapse due to human activities, *in* Ehlen, J.; Haneberg, W. C.; and Larson, R. A. (eds.), Humans as geologic agents: Geological Society of America, Reviews in Engineering Geology.

Johnson, K. S.; and Quinlan, J. F., 1995, Regional mapping of karst terrains in order to avoid potential environmental problems: Cave and Karst Science, Transactions of the British Cave Research Association, v. 21, no. 2, p. 37–39. (Reprinted in 1996 in Swindler, D. L.; and Williams, C. P. [compilers], Transactions of the 1995 AAPG Mid-Continent Section meeting, Tulsa, Oklahoma: Tulsa Geological Society, p. 295–298.)

Luza, K. V.; and Johnson, K. S., 2003, Geologic hazards in Oklahoma: Oklahoma Geology Notes, v. 63, p. 4–22.

# Evaluation of the Role of Evaporite Karst in the Hutchinson, Kansas, Gas Explosions, January 17 and 18, 2001

***W. Lynn Watney, Susan E. Nissen, Saibal Bhattacharya, and David Young***
Kansas Geological Survey
Lawrence, Kansas

**DISCLAIMER**

This study is designed to provide insights into the geology related to the gas transport that culminated in the gas explosions at Hutchinson, Kansas. Multiple scenarios have been invoked regarding the source of gas released and how gas has been transmitted in the subsurface. This paper takes no direct position on this matter.

**ABSTRACT.**—On January 17 and 18, 2001, a series of natural-gas explosions and geysers occurred at widely spaced locations within the City of Hutchinson in central Kansas. A major natural-gas leak, estimated later to have been 143 million cubic feet, was reported at the Yaggy gas-storage field 7 mi northwest of Hutchinson. The Kansas Geological Survey (KGS) was involved from the outset to understand the transmission of natural gas through the subsurface. Subsequent vent and observation wells drilled adjacent to the Yaggy gas-storage field, between Yaggy and Hutchinson, and in the City of Hutchinson, encountered natural gas in shallow dolomite beds referred to as the 3-finger dolomite. The KGS also acquired two seismic lines to image the gas zone. The dolomite-bearing interval is probably equivalent to the Milan Limestone Member, at the top of the Lower Permian Wellington Formation of the Sumner Group. The 3-finger dolomite refers to the three lobes imaged on a gamma-ray log that were used to correlate the gas-bearing zone.

The current investigation into the potential role of evaporite dissolution in the formation of geological pathways for gas migration is focused on interpretation of high-resolution stratigraphic correlation and mapping of 14 intervals within the Permian strata ranging from the upper salt beds in the Hutchinson Salt Member to intervals above the 3-finger dolomite. Well logs used in the analysis represent 116 wells covering 150 $mi^2$ in the area surrounding Hutchinson. Also, detailed interpretations were made of two seismic lines, one crossing a broad, westerly plunging anticline between Yaggy and Hutchinson, and the other at the crest of the anticline on the west side of Hutchinson. General findings indicate that this anticline forms the northern margin of a much larger (~3-mi-wide) northwest-trending structural feature referred to here as the Arkansas River Lineament (ARL) that extends beyond the mapped area and probably between Great Bend and Wichita based on other regional mapping. This northwest-trending lineament is characterized by episodic structural activity that led to recurring minor vertical movements, including development of fractures and minor faults, probably linked to the distinctive southern boundary of the Midcontinent Rift graben. A second major regional structural feature, the Voshell Anticline, imparts a north-northeasterly "grain" to the maps, the crest of the anticline itself controlling the main dissolution front of the Hutchinson Salt Member east of Hutchinson. Fractures paralleling the Voshell Anticline are probably responsible for creating small-scale (~10–15 ft of thinning over a distance of 1 mi), linear northeast-trending paleodissolution margins of salt beds within the uppermost Hutchinson Salt Member within central and eastern Hutchinson.

A set of northwest-trending fractures associated with the ARL apparently episodically acted as conduits for contact between undersaturated ground water and uppermost halite beds that led to an extensive, elongated area of dissolution of an upper salt bed in the Hutchinson Salt Member immediately south of the Yaggy–Hutchinson anticline. Episodes of dissolution include Permian (just after deposition), pre–Equus Beds, and probably during

Watney, W. L.; Nissen, S. E.; Bhattacharya, Saibal; and Young, David, 2003, Evaluation of the role of evaporite karst in the Hutchinson, Kansas, gas explosions, January 17 and 18, 2001, *in* Johnson, K. S.; and Neal, J. T. (eds.), Evaporite karst and engineering/environmental problems in the United States: Oklahoma Geological Survey Circular 109, p. 119–147.

the early Holocene. Early Holocene and younger dissolution may be expressed by isolated areas of surface depressions seen west of Hutchinson along the Arkansas River as inferred from topographic maps. High-resolution isopach mapping reveals paleosubsidence resulting from salt dissolution that probably led to enhanced structural dip of the southern flank of the Yaggy–Hutchinson anticline. In addition, narrow zones (0.25 mi wide) of minor salt dissolution (several feet), interpreted as pre–Equus Beds in age, occurred on either side of the crestal area of the Yaggy–Hutchinson anticline, further accentuating local relief. Small faults are interpreted from the seismic lines at locations corresponding to the edges of these areas of salt dissolution, suggesting a role of fractures in episodic salt dissolution. Faulting is both deep-seated, extending below the Hutchinson Salt Member, and shallow, bottoming out in upper beds of halite that have undergone dissolution in the Hutchinson Salt Member. The narrow northwest–southeast bands of salt dissolution probably reflect the location of a tectonic fracture system that borders the northern edge of the ARL. The linear trend of this dissolved salt may also delimit locations of fractures attributed to either later stage salt dissolution or tectonic origin. North-northeast linear trends of dissolved salt in eastern Hutchinson probably have similar affiliations to fracture systems that parallel the Voshell Anticline trend, as discussed in the paper.

## INTRODUCTION AND BACKGROUND

While the stated objective of this paper is to evaluate the role of evaporite karst in the gas explosions at Hutchinson, the investigation results from the general goal to improve the geologic understanding of apparently subtle geological features associated with the gas explosions and locations of active gas venting and observation wells in the Hutchinson area and adjacent to the Yaggy gas-storage field. The current seismic and geologic study attempts to improve understanding of the formation of the geologic features, particularly structures and lineaments, to better ascertain subsurface gas conduits. The study also attempts to resolve suspected occurrences of salt dissolution, including their timing and distribution, and to evaluate their relation to the geologic setting. Methodologies developed here could be generally useful in characterization of the geology related to gas containment. Color versions of the graphics in this paper are available on the Kansas Geological Survey's Hutchinson Response Project website, http://www.kgs.ku.edu/Hydro/Hutch.

### Gas Explosions in Hutchinson, Kansas

On the morning of January 17, 2001, a gas explosion occurred in downtown Hutchinson, Kansas. Later that day, gas geysers began erupting 2 mi to the east, along the eastern edge of Hutchinson. The following day, a gas explosion at a trailer park near the geysers in eastern Hutchinson led to the death of two people. The outgassing in the city began 2½ days after a major gas leak in a natural-gas-storage well, S-1, at the Yaggy gas-storage facility, 7 mi northwest of Hutchinson (Fig. 1), where natural gas is stored in caverns in the Lower Permian Hutchinson Salt Member of the Wellington Formation of the Sumner Group (Fig. 2). An estimated 143 million standard $ft^3$ of natural gas at high pressure (600+ psi) escaped from a casing leak at a depth of ~600 ft. The casing leak was stratigraphically just below the top of the Hutchinson Salt Member (bedded halite and shale) and 184 ft above the top of the salt cavern in which the natural gas had been stored. The salt-storage cavern itself was not breached nor directly involved in the loss of gas. The Yaggy gas-storage facility was originally developed in the early 1980s to store liquid propane. The wells were later removed from service and in 1989 were plugged by filling the casings with cement on top of bridge plugs. In the early 1990s the cement was drilled out and the wells converted to store high-pressure natural gas. It is believed that the casing in the S-1 well was damaged at the depth of the leak when a metal obstruction was milled during reentry in the cemented well. The metal obstruction in the S-1 well was apparently part of the tubing used in the cement injection above the bridge plug that was not removed, but left in the well. The S-1 had a satisfactory casing-pressure test, as required by the Kansas Department of Health and Environment, demonstrating the integrity of the casing at that time. However, the well at the depth of the leak was never tested to the maximum pressure that would be experienced in service. New Kansas Department of Health and Environment regulations require a much more rigorous well-testing program.

In order to find and vent remaining gas from beneath Hutchinson, a vent-well drilling program commenced. Observation wells near Yaggy encountered gas at a depth of 420 ft, in a stratigraphic interval ~170 ft above the level of the casing leak at the top of the Hutchinson Salt Member. Vent wells drilled in eastern Hutchinson encountered gas as shallow as 240 ft in an equivalent stratigraphic zone, reflecting regional westerly structural dip typical of bedrock in this area of Kansas. With the exception of DDV (deep drill vent) no. 64, gas was confined to a 17–21-ft-thick interval encompassing three thin (2–3-ft) beds of dolomicrite. DDV 64, on the western edge of Hutchinson, is unique in that, on July 7, 2001, it suddenly vented gas measured at 330 psi with an estimated 30–40-ft flare. Gas pressure diminished to 6 psi after 3 days (Allison, 2001a). This gas seems to have originated from a zone 70 ft below the gas interval in the other wells.

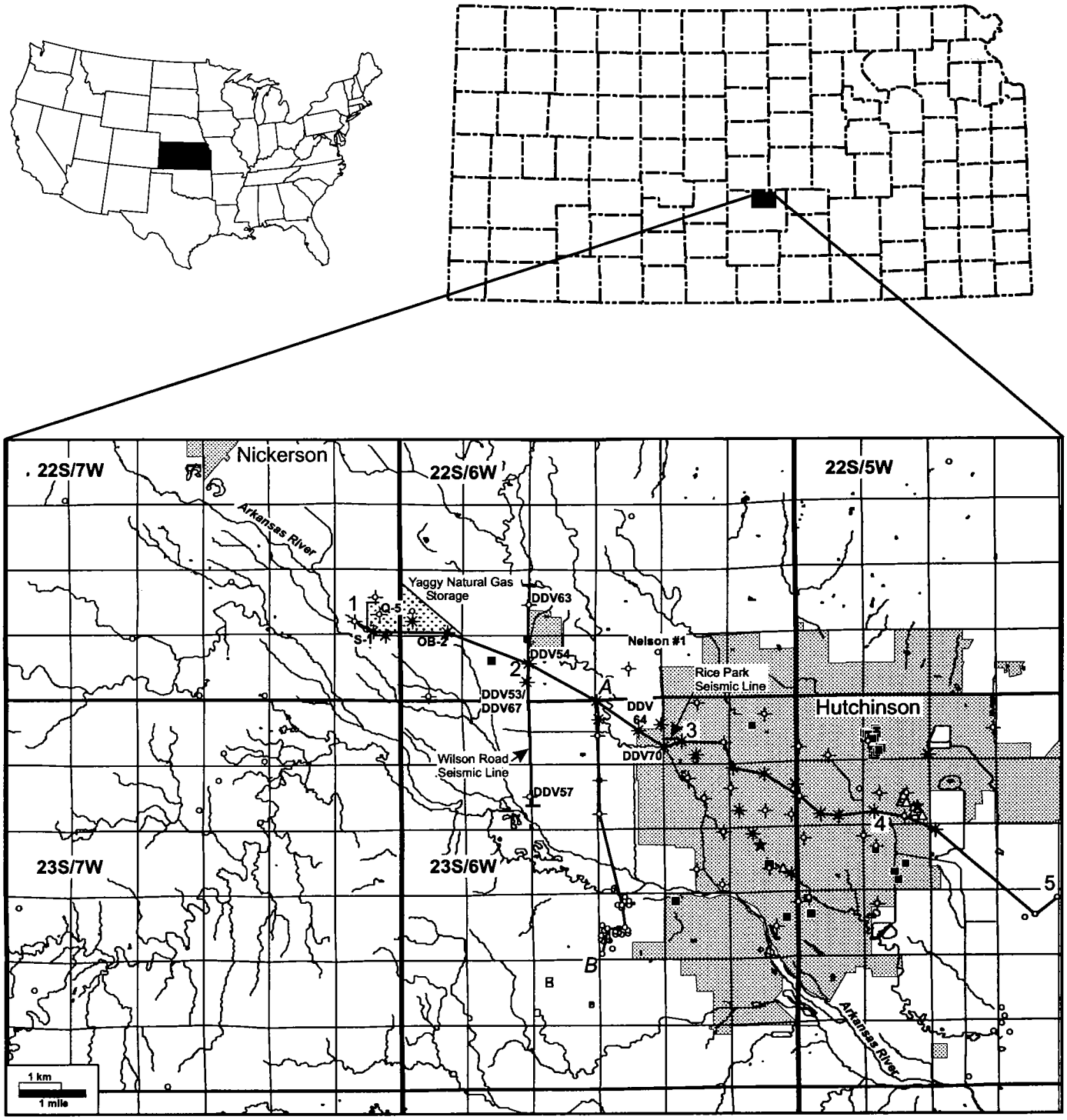


Figure 1. Surface-drainage map of the detailed study area around Hutchinson and the Yaggy natural-gas-storage facility. Locations of gas geysers are shown by white triangles, and explosion sites are shown by black stars. Observation and vent wells that vented natural gas are indicated by black producing-well symbols. Vent wells that did not produce gas are indicated by dry-hole symbols. Additional wells used for log correlations are shown by open circles. Wells discussed in the text are labeled. Locations of log cross sections in Figures 6 and 7 and seismic lines in Figures 8 and 9 are indicated. Known areas of subsidence are shown by black squares.

In general, engineering-test results have noted higher surface shut-in pressures in vent and observation wells closer to Yaggy, forming a linear trend of gas-producing wells on the north side of a broad, westerly dipping asymmetric anticline. Surface shut-in pressures, measured only after the pressures were low enough to shut in the wells safely, beginning in March 2001, have decreased and are now subhydrostatic, with no measureable flow at any of the vent wells currently open. Maps showing bottom-hole pressures in the gas-

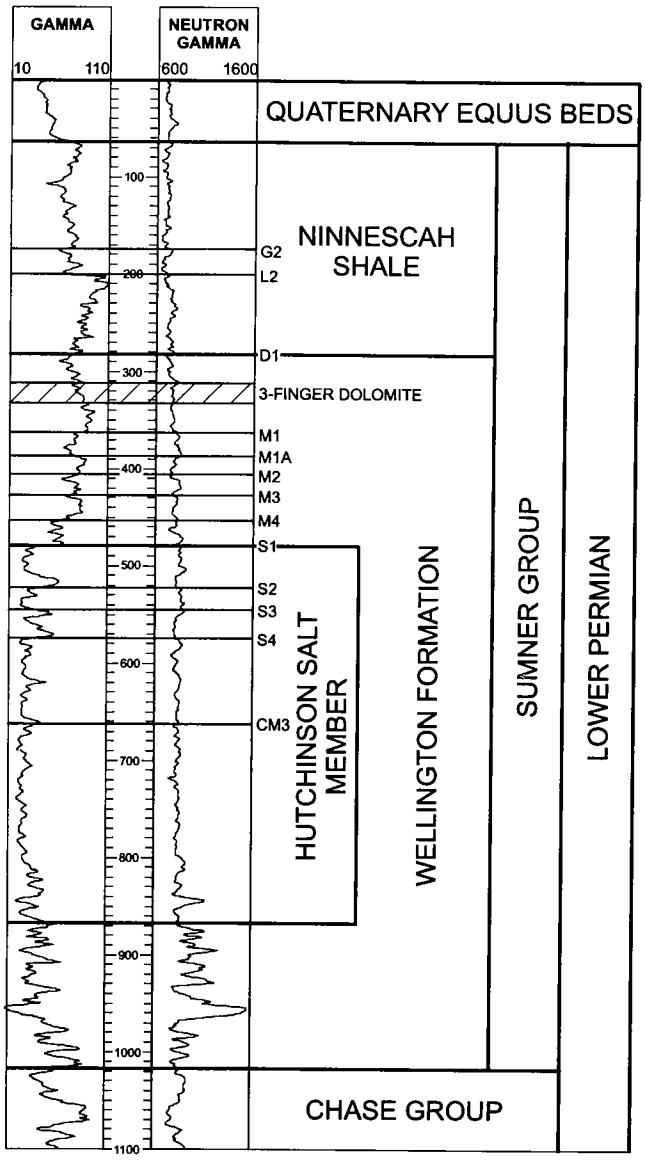


Figure 2. Natural-gamma-ray and unscaled neutron-porosity logs from the No. 1 Nelson well in sec. 34, T. 22 S., R. 6 W., showing distinctive log responses of stratal members significant to the study, including Lower Permian Leonardian Sumner Group containing the Hutchinson Salt Member of the Wellington Formation and the Ninnescah Shale, unconformably overlain by the Quaternary Equus Beds. Closely spaced marker beds G2 to S4 mapped in this study are shown as horizontal lines. The regional CM3 marker bed mapped in Watney and others (1988), which divides the upper and lower Hutchinson Salt Member, is also indicated.

bearing zone under shut-in conditions (March 2001 and July 2002) can be interpreted to indicate apparent continuity of a subsurface region pressurized by gas between producing vent wells in and around Hutchinson. Subsequent maps of pressures from later dates show a slow decline in subsurface (shut-in) pressures at the 3-finger dolomite associated with negligible gas flow at vent wells, indicating reduced permeabilities and perhaps loss of apparent connectivity (Bhattacharya and Watney, 2002). A fracture model was proposed on the basis of linear trends of pressurized subsurface areas, fractures in a borehole-image log from a borehole adjacent to the Yaggy gas-storage facility, and faulting interpreted from seismic data acquired between Yaggy and Hutchinson and at the western edge of Hutchinson. Also, a lack of notable matrix porosity, as obtained from core plugs from vent well DDV 67, in the strata harboring the gas implied possible fracture control. Calculated static bottom-hole pressure of 250 psi at zones at depths of 300–400 ft translate to a pressure gradient that is close to the fracture gradient of the rock (roughly 0.8–1 psi/ft). Initial gas pressure in the gas-producing interval may have, for a limited time, parted preexisting fractures and/or allowed propagation of fractures and lateral gas migration comparable to published models and field data on stress-dependent porosity and permeability and fracture propagation (Settari and others, 1999). With declining gas pressure, the loss of permeability in the vent wells and accompanying negligible gas flow, as now observed in shut-in pressure tests, may be indicative of reduced and closed fracture apertures as a result of decreased pore pressure.

At the vent wells, multiple surveys of tubing-head shut-in pressures (THSPs) and corresponding static fluid columns were carried out, starting in March 2001. The shut-in times in the first survey were short, <30 hours for most wells, owing to safety concerns related to the surface equipment's ability to handle the buildup pressures. Shut-in times in later surveys varied from 72 to 96 hours. Pressure in the 3-finger dolomite was calculated by adding the THSP to the pressure exerted by the fluid column. Figure 3 shows the distribution of subsurface pressures as of March 2001 and July 2002. Automated triangulation gridding was used to generate the subsurface-pressure distribution because of the irregular distribution of data points. The pressure maps indicate that pressurized subsurface areas are aligned along the northern edge of the subtle northwest-trending anticline between Hutchinson and the Yaggy gas-storage facility. Subsurface pressures under the City of Hutchinson have decreased between March 2001 and July 2003. However, pressures as high as 180 psi (though sub-hydrostatic) still prevail in the vicinity of the Yaggy gas-storage facility (at vent well OB 2) as recently as the last series of reported pressure measurements taken in January 2003.

A rough calculation was carried out using estimated data to approximate the average effective permeability necessary for gas to be transmitted laterally over significant distances—i.e., miles. The formulation used for this calculation includes viscous (laminar) gas flow in a homogeneous linear system and is given below and on the next page (Ahmed, 2000).

$$Qsc = \frac{0.003164 T_{sc} A k (P_1^2 - P_2^2)}{P_{sc} T L z \mu_g} \quad (1)$$

Where:

$Qsc$ = gas flow rate at standard conditions, scf/d;

$k$ = permeability, md;
$T$ = temperature, °R;
$\mu_g$ = gas viscosity, cp;
$A$ = cross-sectional area available to gas, ft²;
$L$ = total length of the conduit, ft;
$z$ = gas-compressibility factor.

The preceding formulation assumes constant $z$ and $\mu_g$ over the range of the pressure gradient and is therefore valid for applications where the pressure is below 2,000 psi. It was assumed that the upstream pressure in the flow system was 650 psi (pod pressure at Yaggy).

Along with the gas explosions, a geyser erupted in downtown Hutchinson. Also in the current model, the depth of the 3-finger dolomite under the city is 250–300 ft. Lacking other data, it was assumed that the downstream pressure in the flow conduit was at least 130 psi (using a water gradient of 0.433 psi/ft). A gas gravity of 0.66 was assumed in these flow calculations. The total volume of gas that leaked from the Yaggy facility is estimated at 143 MMscf. Gas surfaced in the city of Hutchinson through abandoned, unplugged brine wells within 2.5 days after the reported leak. Vent wells drilled in and around the city continued to produce measurable quantities of gas for another 3 months. To estimate the average permeability of the gas conduit in this scenario, the gas-flow rate was calculated by assuming that this leaked volume took at least 90 days to bleed off. Also, it is unknown what fraction of the leaked volume would make it to the city. Thus, two cases were modeled: (1) assume that all of the leaked gas came toward the city, and (2) assume that only one-tenth of the leaked volume came toward the city. Using equation (1), a conduit with 460-darcy permeability would be necessary to transmit all of the leaked gas volume from Yaggy storage to Hutchinson's city center. However, if one assumes that only one-tenth of the leaked volume traveled toward the city, the conduit permeability must be in the range of 46 darcies. It is not unreasonable to think that a fracture system could have permeabilities ranging from tens to hundreds of darcies.

New geologic data described in this paper provide further support for several extensive kilometer-scale lineaments and associated fracture systems that could have served as conduits for gas migration in and around Hutchinson. Also, the implication important to the City of Hutchinson is that if fracture continuity were developed between the gas source and its release point, darcy-level permeability could have vented a considerable amount of the pressurized gas in a short period of time (days to months) (Watney and others, 2003). Furthermore, the implication is that certain geological elements, such as fracture systems and lineaments, may present inherent risks for focused lateral migration of gas stored under pressure.

## Geology of the Hutchinson Area

The Quaternary Equus Beds, an extensive unconfined freshwater aquifer, unconformably overlies the Permian strata in the vicinity of Hutchinson, ranging from zero to as much as 100 ft thick (Fig. 2). The Lower Permian Hutchinson Salt Member of the Wellington Formation of the Sumner Group, ~350 ft thick in the area of Hutchinson and the Yaggy gas-storage facility, unconformably underlies the Equus Beds and dips westward at 20 ft/mi beneath the storage facility from the subcrop, a natural, regional salt-dissolution front ~13 mi east of the storage facility and 6 mi east of Hutchinson (Fig. 4). The Hutchinson Salt Member is overlain by ~450 ft of Permian gypsiferous shales that are interbedded with thin (1–3-ft-thick) intervals of gypsum, anhydrite, and dolomite. The Permian section above the Hutchinson Salt Member is divided into the upper Wellington Formation, a gray gypsiferous shale, and the Ninnescah Shale, a reddish, more silty gypsiferous shale.

A 15–20-ft-thick zone of thin interbedded dolomite and shale ~160–170 ft above the top of the Hutchinson Salt Member, informally referred to as the 3-finger dolomite, provided the primary conduit along which natural gas migrated through the area. This unit is probably equivalent to the Milan Limestone Member of the upper Wellington Formation. The 3-finger dolomite refers to three characteristic lobes observed on the gamma-ray log trace, the primary logging tool that was used to define and correlate the interval between vent and observation wells (Fig. 2). The dolomite beds, while approximately less than 3 ft in thickness and variable in shale content, are continuous throughout the immediate study area.

The gypsiferous shales of the upper Wellington Formation contain abundant irregular satin-spar veins/fractures, which probably formed during volume increase that occurred during hydration of anhydrite to gypsum as the overlying strata were removed by erosion, burial depths decreased, and undersaturated water contacted these strata. These fractures may have been involved in movement of high-pressure gas, but no data are available to corroborate this.

## Evaporite Dissolution and Evaporite Karst Near Hutchinson

### *Natural Dissolution*

Dissolution along a part of the eastern margin of the Hutchinson Salt Member in central Kansas has been well documented, most recently using seismic data (Steeples and others, 1984; Anderson and others, 1994; Anderson and others, 1995a,b; Anderson and others, 1998; Miller, 2002). The prominent dissolution front, characterized by abrupt loss of the entire Hutchinson Salt Member over several miles, lies 7.5 mi east of Hutchinson (Fig. 4), where halite beds come to within 200 ft of the surface (Watney and others, 1988). The primary mechanism for dissolution of the shallow salt beds is believed to be contact with meteoric ground water. The area east of the salt-dissolution front near Hutchinson is inferred once to have contained bedded salt, and which now contains col-

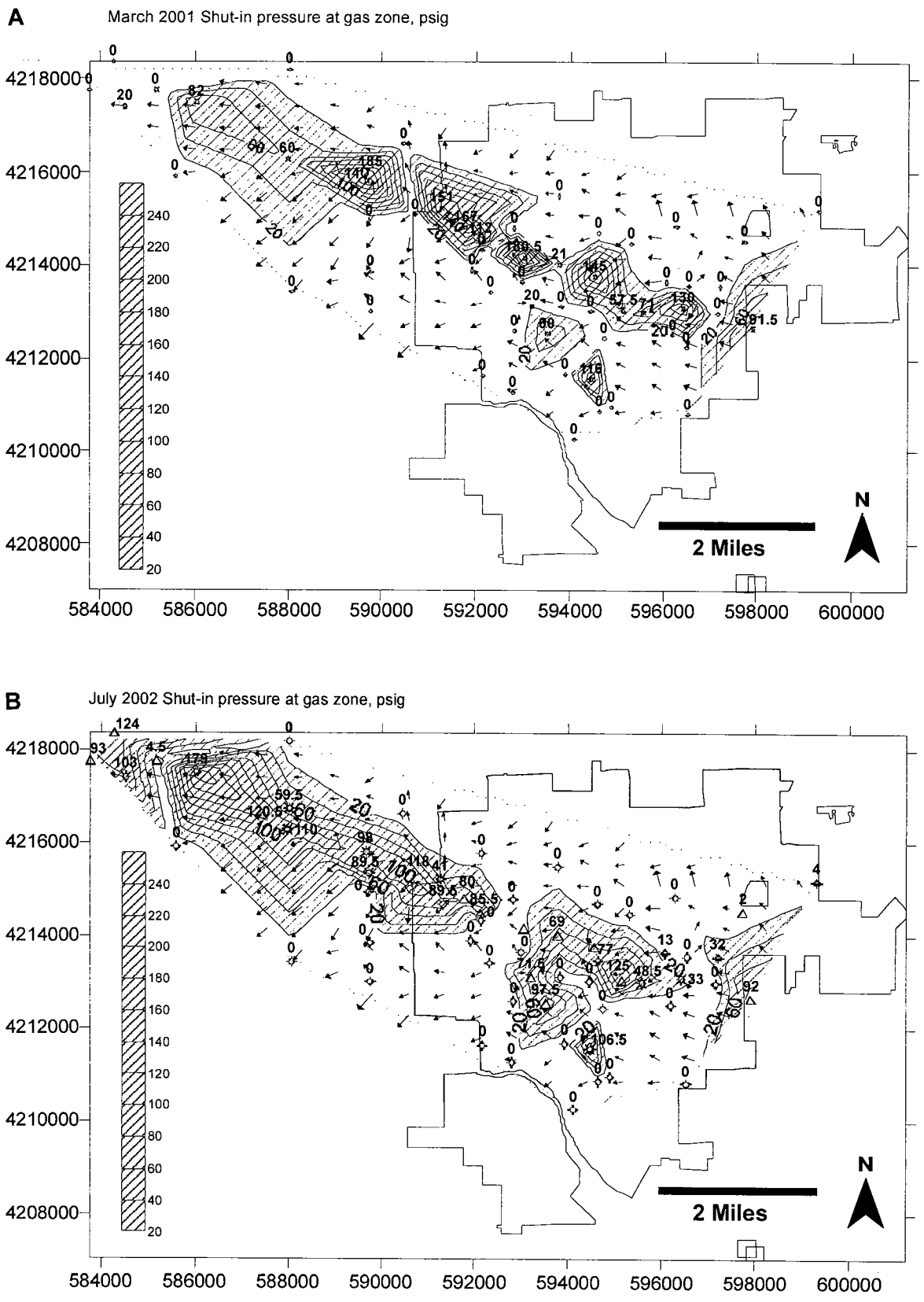


Figure 3. (A) March 2001 shut-in-pressure map gridded by triangulation, showing pressures in psig units. Dip vectors at the top of the 3-finger dolomite are also shown. Shut-in pressures were not taken in several active gas-venting wells owing to excessive pressure and safety concerns. Shut-in pressures are calculated at the 3-finger dolomite using recorded surface pressures and standing fluid columns. (B) July 2002 shut-in pressure calculated at the 3-finger dolomite.

lapsed Permian strata called the Wellington aquifer. Quaternary alluvial sediments, the Equus Beds, were deposited in the surface depression left by the collapse of the upper Wellington Shale resulting from the dissolved halite strata. The Equus Beds in aggregate accumulated as part of large, ancient river systems that drained the Rocky Mountains during wetter interglacial periods, contrasting with today's setting. Upward of 200 ft of salt was dissolved along a corridor between Wichita and McPherson, forming a bedrock low some 50 mi long, covering 300 mi$^2$ (Lane and Miller, 1965).

The uppermost salt beds progressively pinch out eastward at depths shallower than 300 ft below the surface and some 15 mi west of the inferred maximum limit of deposition (Watney and others, 1988; Anderson and others, 1994). A broad stair-stepped salt-dissolution margin was formed. The pinch-outs may have been depositional as halite accumulation came to a close, or the result of later dissolution that led to truncation of the edges of the salt (Miller, 2002).

A regional net-salt map (Fig. 5A) reveals the dominant north-northeast trend of the primary salt front between the cities of Hutchinson and Salina. A prominent salient or embayment of the main dissolution front was formed at the juncture of the dissolution front and the Arkansas River southeast of Hutchinson (Figs. 4, 5A). Local north-northeast-trending secondary salt dissolution behind (west) and parallel to the primary salt front immediately east of Hutchinson is attributed to a fracture zone along the Voshell Anticline (Anderson and others, 1994). The greater McPherson–Voshell Anticline closely corresponds to a deep-seated magnetic lineament in the underlying Precambrian Midcontinent Rift system and is a prominent, ~50-mi-long, faulted anticline affecting Paleozoic strata (Xia and others, 1995a,b; Newell and Hatch, 1999). The southern terminus of this lineament corresponds to the southern end of the sediment-filled portion of the Midcontinent Rift. Lineaments corresponding to the Arkansas River and the Voshell Anticline are also shown on a preliminary State lineament map for Kansas (Gerhard, 2003).

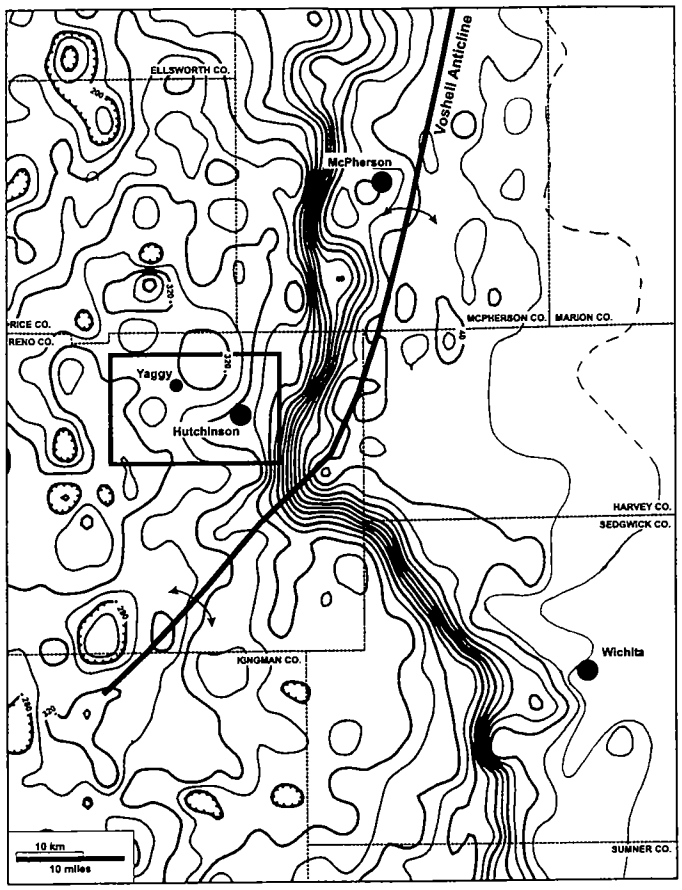


Figure 4. Net-salt isopach map of the Hutchinson area from Watney and Paul (1980). Contour interval = 20 ft. The axis of the Voshell Anticline, believed to be related to north-northeast-trending salt dissolution, is shown. The box outlines the detailed study area in Figure 1.

Recent 2-D-seismic surveys acquired ~6.5 mi southeast of the eastern Hutchinson explosion sites along U.S. Highway 50 in the Arkansas River Valley by Miller (2002) indicate that a moderate-sized (300-ft-diameter) sinkhole developed at the surface along the highway. Miller found that this surface expression is only a small part of a much larger area of subsidence in the subsurface, as much as 1,500 ft wide and elongated west to east, immediately west of the main dissolution front. Sinkhole development probably began in earnest during the late Tertiary during a significant erosion and valley-incision event, prior to deposition of the Equus Beds (Miller, 2002). Widespread ponding of surface waters in this general area within several miles of the solution front suggests recent natural subsidence in addition to that along U.S. Highway 50. Seismic data show that 135 ft of salt remains at the Highway 50 location within 0.5 mi of the salt front, suggesting that some 200 ft of the Hutchinson Salt Member has been removed by dissolution.

The Wellington aquifer, the deformed Permian section that lies above the dissolved Hutchinson Salt Member, closely corresponds to areas of dissolved salt (Gogel, 1981). The younger Quaternary Equus Beds aquifer also occupies space created by dissolution of underlying salt. The Equus Beds locally extend westward beyond the main dissolution front as valley-fill sands, including the Yaggy–Hutchinson area. Modern surface drainage dominated by the northwest-trending Arkansas River Valley closely coincides with the major trunk valley and tributary systems of the Equus Beds, as inferred from the map depicting the configuration of the base of these beds (see Fig. 10A). Based on new seismic data (Miller, 2002), major paleosinkhole development was probably concurrent with the erosion and deposition of the Neogene Equus Beds and was probably related to a greater flux of undersaturated water associated with a wetter climate, elevated stream flow, erosion, and valley incision associated with these deposits (Lane and Miller, 1965). Subsequent sinkhole development also has continued to the

present, including reactivation of earlier subsidence as indicated in recent seismic lines acquired along a surface sinkhole on U.S. Highway 50 southeast of Hutchinson (Miller, 2002).

Surface sinks and closed surface depressions are numerous in areas west of Hutchinson along the greater Arkansas River Valley as seen on 7.5-minute topographic maps. Reported surface sinks, such as in the Yaggy townsite near the Yaggy gas-storage facility, have an unknown origin (Kansas Department of Health and Environment, 2001). Reported surface subsidence and sinks in the Hutchinson area have been annotated on the map in Figure 1. Ver Wiebe (1937) described a surface locality exhibiting faulted and upturned Permian beds in a road cut beneath flat-lying Cretaceous Dakota Sandstone in east-central Ellsworth County ~40 mi north of Hutchinson. He attributed deformation to an early episode of dissolution of the Hutchinson Salt Member that is ~300 ft thick at a depth of 650 ft. This location is ~15 mi west of the main salt-dissolution front.

### *Anthropogenic Dissolution*

Brine-recovery wells are used to dissolve bedded salt at shallow depths near the eastern margin of the Hutchinson Salt Member. Those brine wells, developed prior to the 1960s, typically dissolved the upper salt beds at depths of ~400 ft, some leading to collapse of the relatively weak shales overlying the salt, and occasionally to sinkhole development (Walters, 1978; Miller and others, 1993). Well-documented sinkholes, 300 to 500 ft in diameter, developed in Hutchinson, with both subtle and catastrophic surface subsidence ranging from a few inches to several tens of feet of vertical relief (Young, 1926; Walters, 1978; Miller and others, 1993).

Abandoned brine wells served as the pathways for natural gas to reach the surface at the Hutchinson explosion and geyser sites. Known sinkholes associated with abandoned brine wells did not appear to contribute significant gas migration or gas buildup in the Hutchinson area, a scenario that was considered immediately following the gas explosions. Gas found in vent wells was, with the exception of DDV 64 as noted previously, confined to the 3-finger dolomite interval, with no evidence of gas in known surface sinks. The gas seems to have moved into the unplugged brine

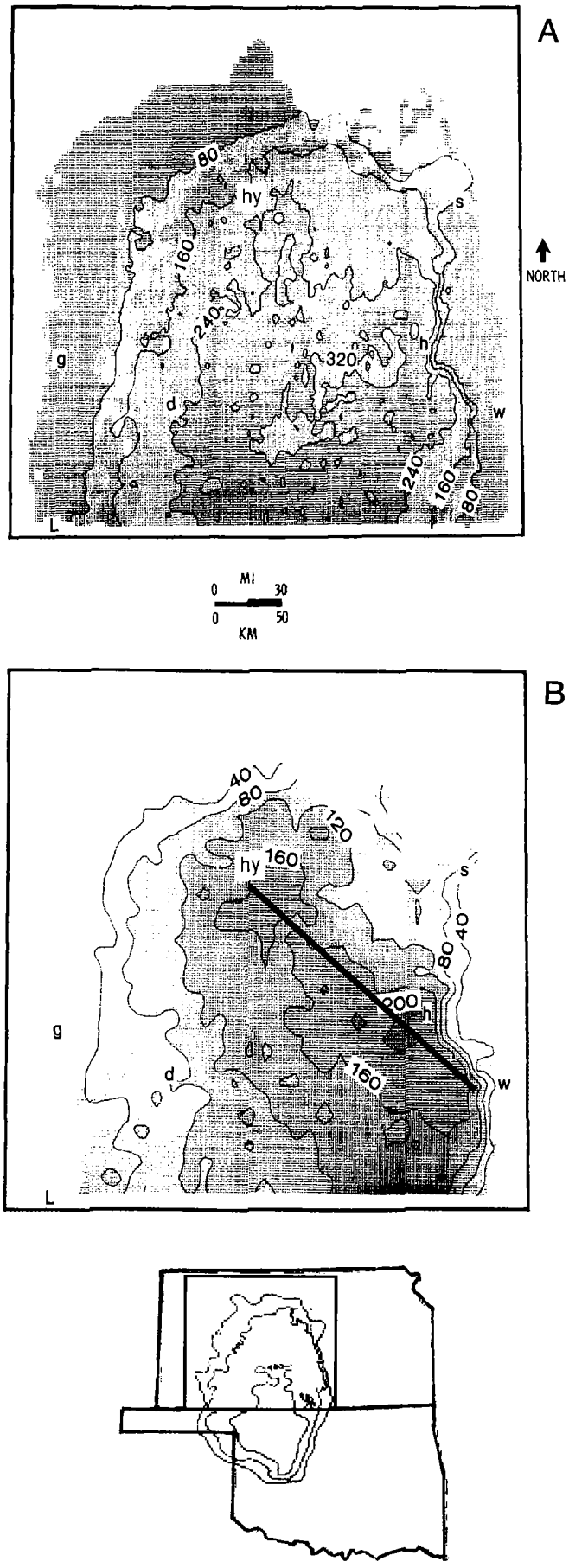


Figure 5 *(right).* (A) Regional total net-halite isopach map of the Hutchinson Salt Member. (B) Regional net-halite isopach map of lower Hutchinson Salt Member below CM3 marker shown in Figure 2. Mapped area covers most of western Kansas, as shown by index map below. Mapped area developed from >3,700 wells, representing sampling of one well per 77 mi². Letters on maps refer to city references: *g,* Garden City; *L,* Liberal; *d,* Dodge City; *hy,* Hayes; *s,* Salina; *h,* Hutchinson; and *w,* Wichita. Contours are in feet. Lineament aligned with Arkansas River shown on lower map. Salt-dissolution front indicated by closely spaced contours along southeastern margin of the salt.

wells at the depth of the 3-finger dolomite and then to the surface. Recently acquired sonar and gamma-ray logs and televiewer photos from 11 unplugged brine wells in Hutchinson indicate that no significant collapse has occurred in solution-mined cavities in the Hutchinson Salt Member (Burns and McDonnell Engineering Company, Inc., 2003).

## METHODOLOGY IN NEW MAPPING AND SEISMIC INTERPRETATION

A regional stratigraphic and sedimentologic database obtained in the 1980s was used to establish the general geologic setting of the salt-bearing strata in the Hutchinson area. Some 3,700 wells are included in the database covering the region underlain by the Hutchinson Salt Member, which encompasses >37,000 $mi^2$ of central and western Kansas (Watney and others, 1988). The stratigraphic interval described in the database extends from the Lower Permian Stone Corral Formation to the top of the Chase Group, including the interval of interest in this current investigation (Fig. 2). A datum ~30 ft above the 3-finger dolomite was mapped in the regional database at the approximate contact between the Wellington Formation and Ninnescah Shale.

Over the course of several months after the initial gas leak and explosions, 57 vent wells and five observation wells were drilled in the vicinity of Yaggy and Hutchinson (Fig. 1). Twenty-four of these wells produced gas. Natural-gamma-ray and temperature logs were acquired from all of the vent wells, and additional logs from several wells. Surface elevations and locations were accurately measured, and logging was done over a span of several months. Most of these wells penetrated the Hutchinson Salt Member, providing new data on the distribution of the upper Hutchinson Salt Member and overlying layers at a high degree of spatial resolution. The gamma-ray logs from these wells, along with gamma-ray logs from nearby oil wells and gas-storage wells, and lithologic logs from KGS Bulletins and water-well completion reports, were used to generate new cross sections and structure and isopach maps of the upper Hutchinson Salt Member and overlying layers for an area of ~150 $mi^2$ around Hutchinson. The new data were used to identify and refine structural and sedimentological features that helped resolve characteristics of potential gas-migration pathways and to define the role of salt dissolution in the formation of these pathways.

In February 2001, the Kansas Geological Survey acquired two high-resolution seismic-reflection surveys in the Hutchinson area. A 0.3-mi-long line was shot in Rice Park on the west side of Hutchinson, adjacent to a gas-producing vent well, DDV 5, and a 3.4-mi-long north–south line was acquired along Wilson Road, midway between the western city limit of Hutchinson and the Yaggy gas-storage facility (Fig. 1). High-resolution reflection data were acquired by a minivib (vibroseis) survey and vertical-component geophones. The source interval was 5 m, and the receiver-group spacing was 2.5 m. A 6-s record with a sample interval of 0.5 ms was recorded. The data were filtered with a trapezoidal band-pass filter with corner frequencies of 61, 122, 250, and 300 Hz. Common-midpoint (CMP) stacked data have folds ranging from 1 to 31 and a CMP spacing of 1.25 m. The fold is 15 or greater for 0.27 mi of the Rice Park seismic line and 3.31 mi of the Wilson Road seismic line. The displays shown in Figures 8 and 9 were scaled using automatic gain control (AGC) over a 200-ms sliding window. The Rice Park line was selected to determine if the gas zone produced a seismic anomaly, and the Wilson Road line was selected to identify potential gas pathways between Yaggy and Hutchinson (Nissen and others, 2002). Two amplitude anomalies at the level of the proposed gas-bearing interval were identified and drilled on the Wilson Road line. Gas was found at both sites (DDV 53 and 54). In March 2001, DDV 67 was drilled ~70 ft southwest of DDV 53 to core the gas zone and obtain density and sonic logs to calibrate the seismic line. Two dry holes (DDV 57 and 63) also were drilled at the northern and southern ends of the Wilson Road line to provide core (DDV 63 only) and sonic and density logs. A sonic log also was acquired in DDV 5 in Rice Park in October 2001. These data were used to correlate the seismic profiles with the stratigraphic units encountered in these wells. Although the Wilson Road and Rice Park seismic lines are spatially limited, they provided information locally on the lateral variation in salt thickness between wells (i.e., gradual versus sharp thickness changes) and allowed for the identification of structural elements such as faults, which may have controlled the gas-migration pathways. Findings from other seismic surveys in the area also were considered to help in the geological and geophysical characterization (Miller, 2002; Anderson and others, 1994; Anderson and others, 1995a; Anderson and others, 1998).

A borehole-imaging log was acquired in observation well OB 2, adjacent to the southeast corner of Yaggy, for fracture characterization.

Core data were examined to characterize the 3-finger dolomite interval and the upper Hutchinson Salt Member. After the Hutchinson incident, two cores were acquired along Wilson Road. One was from a gas-producing well, DDV 67, and the other was from a dry hole, DDV 63. The core from the Q-5 gas-storage well in the Yaggy gas-storage facility was acquired by the facility operator before the Hutchinson incident to characterize the salt-containment system. This core was described for the interval just above and into the top of the Hutchinson Salt Member. A core obtained in 1970 from the Atomic Energy Commission (AEC) no. 1 test hole near Lyons, 20 mi northwest of Hutchinson in Rice County, was used initially to establish the stratigraphy of the interval equivalent to the gas-bearing zone in Hutchinson (Allison, 2001a; Stockstad, 2002). Surface exposures also were used to

help characterize the local character of the thin dolomite beds in the upper Wellington Formation, which are roughly equivalent to the gas-bearing zone.

## RESULTS

### Regional Mapping

Information on formation tops and net halite content for the stratigraphic interval between the top of the Stone Corral Formation to the top of the Chase Group was reviewed to ascertain depositional and stratigraphic trends and the nature of the salt-dissolution front (Watney and others, 1988). Several regional geologic studies also were reviewed to better understand the stratigraphy and structural setting (Swineford, 1955; Bayne, 1956). Swineford (1955) delimited small-scale sedimentary cycles in the outcrop that culminate in thin carbonate or gypsum beds that probably are the basis for the marker beds used here in the high-resolution stratigraphic mapping. Bayne (1956) delineated the extent of the Equus Beds in Reno County.

A structural map depicting the top of the Wellington marker (slightly above the gas-bearing 3-finger dolomite) was originally based on previous regional mapping using approximately five wells per township. This map reveals only gradual, steady westerly dip of ~20 ft/mi between Yaggy and Hutchinson (http://www.kgs.ukans.edu/Hydro/Hutch/StructureMaps/index.html). New mapping of a 10- × 16-mi area surrounding the City of Hutchinson incorporates data from 116 wells (including the 62 new vent and observation wells), allowing the top of the 3-finger dolomite to be mapped in more detail, and revealing features not previously depicted on the regional map of the top of the Wellington marker.

A regional map of the net halite in the Hutchinson Salt Member indicates that thickness slowly decreases from 325 ft of net halite near Yaggy to 250 ft 3 mi east of Hutchinson (gradient of 25 ft/mi) (Fig. 4). These changes in thickness are typical of those along the salt-basin margins and suggest local depositional changes. Alternatively, these minor thickness changes may be indicative of minor dissolution at the top of the salt as observed in all cores that have been examined in the area. East of Hutchinson the net halite decreases dramatically, defining the primary salt-dissolution front, which is characterized by greater changes in salt thickness (83 ft/mi).

Net-halite maps of the Hutchinson Salt Member (Figs. 4, 5A) show several marked changes in the local salt section in the Hutchinson area, including abrupt thinning along the eastern margin, defining the salt-dissolution front, and a local embayment along the salt-dissolution front extending between Hutchinson and Wichita. A much more gradual change in salt thickness (5.3 ft/mi) occurs south of Wichita. This reduced gradient in net halite suggests predominantly depositional thinning south of Wichita, corresponding to the eastern margin of the Hutchinson salt basin. Nevertheless, local halite dissolution in this area still occurs. The net halite in the lower part of the Hutchinson Salt Member (below the CM3 marker, as illustrated in Fig. 5B) reveals a large northwest-trending region of thick halite in the middle part of the salt basin. Its northern border is aligned with an extension of the northwest-trending salt-dissolution margin between Hutchinson and Wichita. This linear trend, some 50 mi in length, extends at least to Great Bend.

Current and past geologic conditions along the northeastern margins of the salt basin are dynamic, reflecting the interaction of deposition, dissolution, hydrologic, and structural processes. More detailed mapping is required to resolve the contribution of these processes in controlling the migration of gas.

### Detailed Mapping Incorporating Observation- and Vent-Well Data

Fifteen closely spaced marker beds were correlated among 116 gamma-ray well logs within a 150-mi$^2$ area encompassing Hutchinson and Yaggy. Ten marker beds (including the top and base of the 3-finger dolomite) were defined and correlated within the Ninnescah and upper Wellington shales (Figs. 2, 6, 7). The M1A marker corresponds to the lower gas zone in DDV 64 and is also a prominent seismic reflector (Figs. 8, 9). Also, the top of the Hutchinson Salt Member (S1) and four marker beds within the upper Hutchinson Salt Member were correlated within the study area. The S2 marker is equivalent to the regional CM5 marker, and the S4 marker is equivalent to the regional CM4 marker of Watney and others (1988). At the eastern edge of the study area the S1, S2, and S3 salt markers are correlative with thinner beds exhibiting higher gamma-ray values (M5, M6, and M7, respectively), suggesting that the uppermost salt in this area may have undergone a lateral facies change associated with the depositional edge of the salt basin (Fig. 6). This regressive stratigraphic framework is supported by Watney and others (1988).

Automated structure and isopach maps of the marker beds were generated using triangulation and a least-squares algorithm to define the shape of the gridded surface. Consistent gridding parameters were used for all maps.

The mapping of structure, thickness, and natural-gamma-ray values of the 3-finger dolomite interval helps explain the occurrence of gas production from vent wells. First, the gas-productive vent wells indicate a northwest-trending line between Yaggy and Hutchinson. A map of the elevation at the top of the upper bed of the 3-finger dolomite interval delimits a broad (1-mi-wide), low-relief (<15-ft), west- to northwest-trending and plunging (20–25 ft/mi) asymmetric anticline (Fig. 10B). The dip along the south flank of the anticline is roughly 15 ft/mi, double that of the north flank. The locations of the gas-producing vent wells closely correspond to the northern edge of the anticline. A ~2.5-mi-wide break in the overall west-

erly stratigraphic dip occurs along the crest of the anticline in western Hutchinson. Regional dip decreases from ~20 ft/mi to 10 ft/mi or less. To the east of this feature, a regional dip of ~20 ft/mi ensues, and the anticline becomes a series of more complex structural undulations at a point where a linear trend of gas-producing wells between Yaggy and Hutchinson separates to follow these various structural undulations. Thus, in eastern Hutchinson two separate trends of gas wells are evident.

Local tectonic stresses along the crest of the anticline could have resulted in oriented fractures/joints that subparallel the anticline axis. Scattered discontinuous fractures observed in the dolomicrite and gypsum-filled veins in the DDV 67 core appear to be unrelated to structure. However, two sets of "partial" fractures, as interpreted on a formation micro-imaging log from observation well OB 2, adjacent to the Yaggy gas-storage facility, are west–east and north–south oriented and at a high angle (50°), occurring in the middle and lower zones of the 3-finger dolomite (Fig. 11). OB 2 has flowed significant amounts of gas and maintained the greatest pressures over the longest period of time (Bhattacharya and Watney, 2002), suggesting that the distinctive fractures in this well may be associated with the anticlinal trend and that they may correlate with the high, sustained shut-in pressures.

Cross sections and detailed structure maps of the marker beds indicate several other features that may have had an impact on gas migration:

1. The anticline along which the gas migrated persists with depth in all of the mapped marker beds between G2 and S4 and is also expressed as a local elevated northwest-trending ridge on the configuration map of the base of the Equus Beds (Fig. 10A). The consistent relief suggests that the anticline includes post-Ninnescah structural deformation. Additionally, the anticline seems to have greater relief above S2 in proportion to the thinning of the uppermost salt (Fig. 10C, D; Fig. 12C), indicating that structural relief was enhanced by salt dissolution along the flanks of the anticline.

2. DDV 64 is located on a closed high along the crest of the anticline at all mapped intervals. This structurally high position apparently made DDV 64 a focus for gas migration and was the only site of gas flow from zone M1A, ~70 ft beneath the 3-finger dolomite.

3. The headward end of a north-northeast-trending secondary (tributary) valley adjacent to the main trunk valley, inferred from the map of the configuration of the base of the Equus Beds and interpreted as a buried erosion surface (Fig. 10A), terminates immediately adjacent to the crest of the ridge near DDV 64. Its position intersects the ridge where the plunge angle of the anticline is notably diminished (i.e., flattened) to the east. This north-northeast-trending valley also corresponds to an apparent local area of salt dissolution as inferred from isopach maps that are discussed below. Local surface drainage and salt dissolution possibly are influenced by the same local structural deformation, in this case paralleling the trend of the Voshell Anticline. Fractures or faults are observed in a nearby seismic line in Rice Park (Fig. 9). The structural features may have been pathways for gas migration.

Isopach maps of the intervals between 15 marker beds were used to establish patterns and trends to aid in interpretation of the succession and interaction of processes including deposition, dissolution, erosion, and structure. One objective was to evaluate the possible role of minor dissolution of upper Hutchinson Salt Member beds in the gas-migration event.

The isopach of the lowermost salt interval mapped (S3–S4) indicates no eastward thinning of the salt, suggesting that salt dissolution has not reached this depth within the study area (Fig. 12A).

The isopach of the S2–S3 salt interval (Fig. 12B) shows little variation over the western three-quarters of the study area. However, in central Hutchinson, there is rather abrupt thinning from west to east, forming a 1-mi-wide, north-northeast-trending wedge. The halite bed thins from a consistent 22–27 ft at Yaggy and western Hutchinson down to 3 ft in central Hutchinson, where a north-northeast-trending linear zone <0.5 mi wide constitutes an isopach of only 3–5 ft in thickness. Eastward over a distance of 1 mi, the layer thickens again to ~10–11 ft before thinning again to 4 ft at the extreme eastern edge of the study area. A facies change from halite to sulfate or carbonate occurs along this eastern edge, suggested by lateral gradation from a low gamma-ray response to intermediate values (Fig. 6). In the area of local thinning of the S2–S3 interval, the overlying S1–S2 isopach thickens by up to 8 ft (Fig. 12C; Fig. 6, DDV 42), suggesting that the accommodation space for the upper salt bed may have been formed by early, interformational dissolution of the underlying layer prior to deposition of the S1–S2 interval. Dissolution and precipitation of halite likely occurred along the edges of the Hutchinson salt basin concurrent with deposition. This is observed in salt mines in deeper halite beds within the salt where halite-dominated cycles are capped by erosion surfaces exhibiting karstic pipes and local scallop-shaped dissolution surfaces. The apparent dissolution event in the S2–S3 interval appears to be unrelated to the natural-gas migration because (1) dissolution was early (syndepositional), (2) dissolution resulted in a thicker S1–S2 interval but did not affect strata above S1 (supporting early dissolution), and (3) a dry well is in the trend. The distinct north-northeast trend suggests a structural control, such as fracturing, that may have at one time facilitated access of water to the salt bed. This trend also parallels the main dissolution front of the salt that follows the axis of the Voshell Anticline.

The uppermost salt interval (S1–S2) (Fig. 12C) also shows an abrupt eastward thinning from 38 to 24 ft over a distance of 0.7 mi in the eastern part of the study area. The north-northeast-trending thinning of

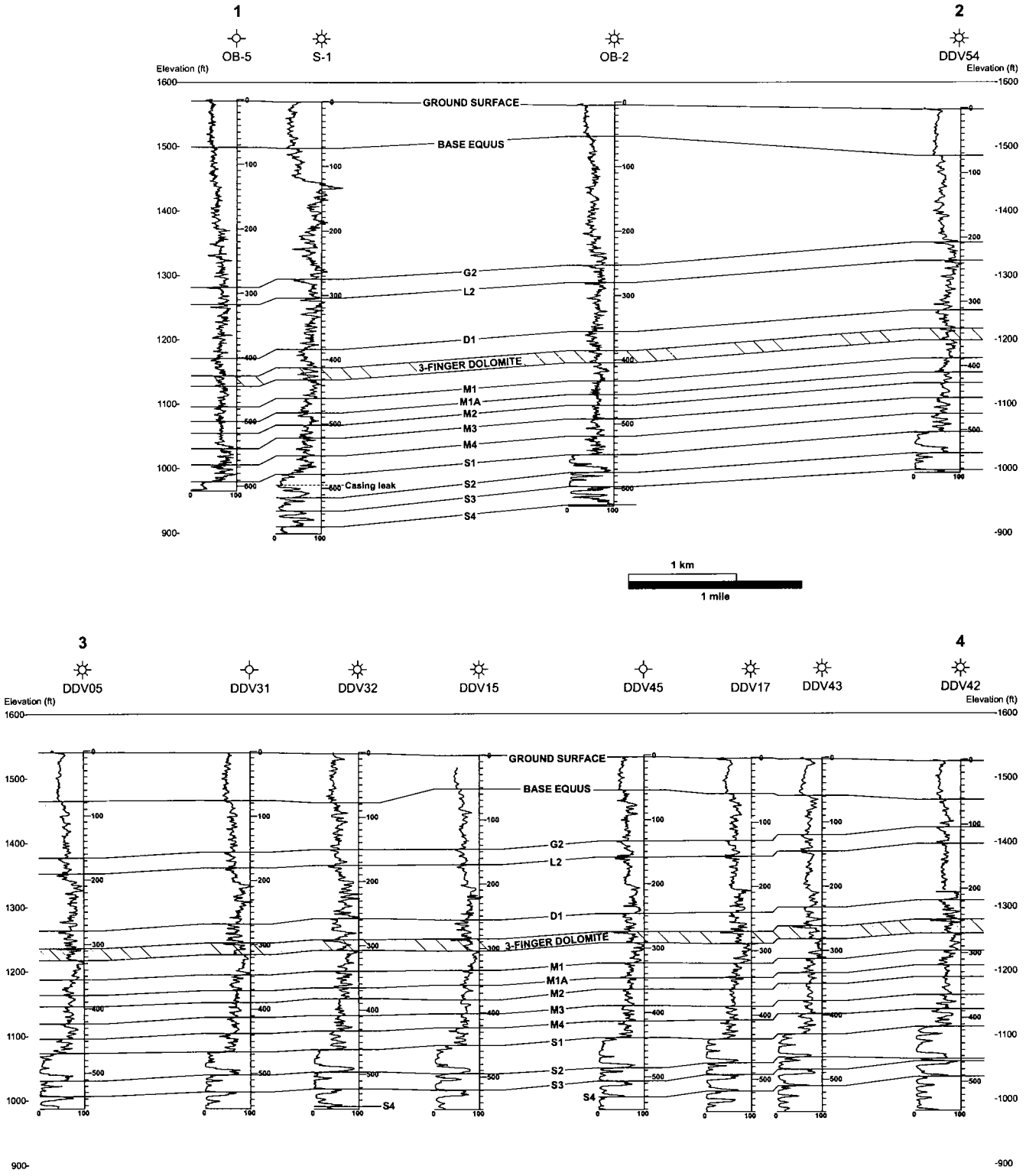


Figure 6 *(above and facing page).* West–east cross section between Yaggy and Hutchinson. Line of section shown in Figure 1. Normalized gamma-ray logs, in which units range from 0 (salt) to 100 (shale), show the log responses of the correlated marker beds.

this uppermost salt layer occurs ~0.7 mi to the east of the thinning in the underlying S2–S3 interval. This thinning may be depositional, corresponding with an apparent facies change in the S1–S2 interval between the eastern edge of Hutchinson and the eastern edge of the study area (Fig. 6), or local dissolution behind and parallel to the main dissolution front, which is ~5 mi to the east.

A broad (1–2-mi-wide) zone of thinning is present in the S1–S2 isopach along the Arkansas River to the

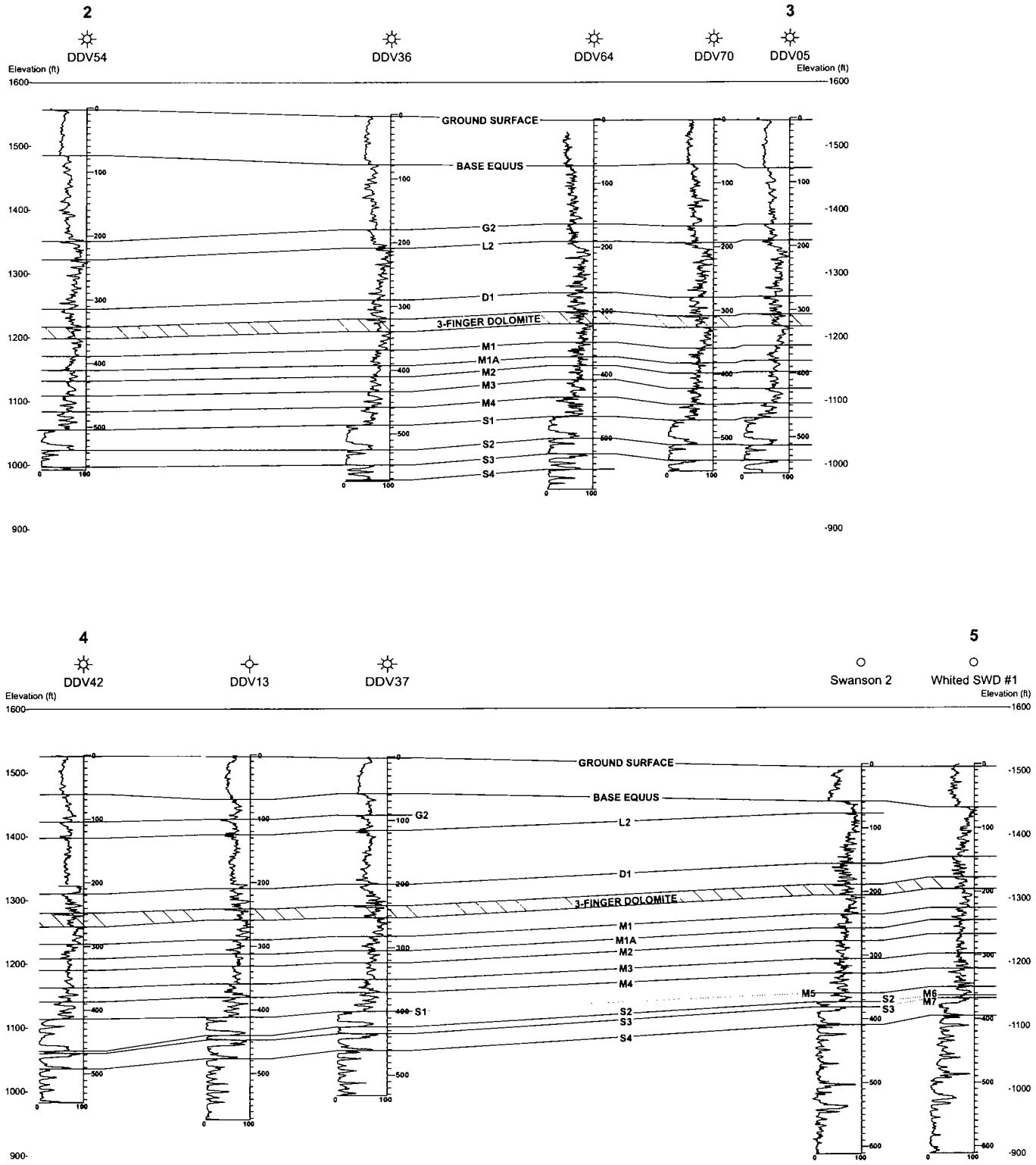


Figure 6.—*Continued.*

south and west of Hutchinson, parallel and adjacent to the Yaggy–Hutchinson anticline. The area of thinning is interpreted as a dissolution reentrant extending west of the main dissolution front. The underlying isopachs show no clear change in thickness along this trend. Focused local thinning by up to 20 ft over a distance of less than 350 ft also occurs approximately 0.9 mi to the south of the Arkansas River. North–south cross sections (Figs. 7, 8) clearly show both regional and local thinning. The presence of local thins in the S1–S2 isopach along the Arkansas River suggests that salt dissolution occurred adjacent to the Arkansas River,

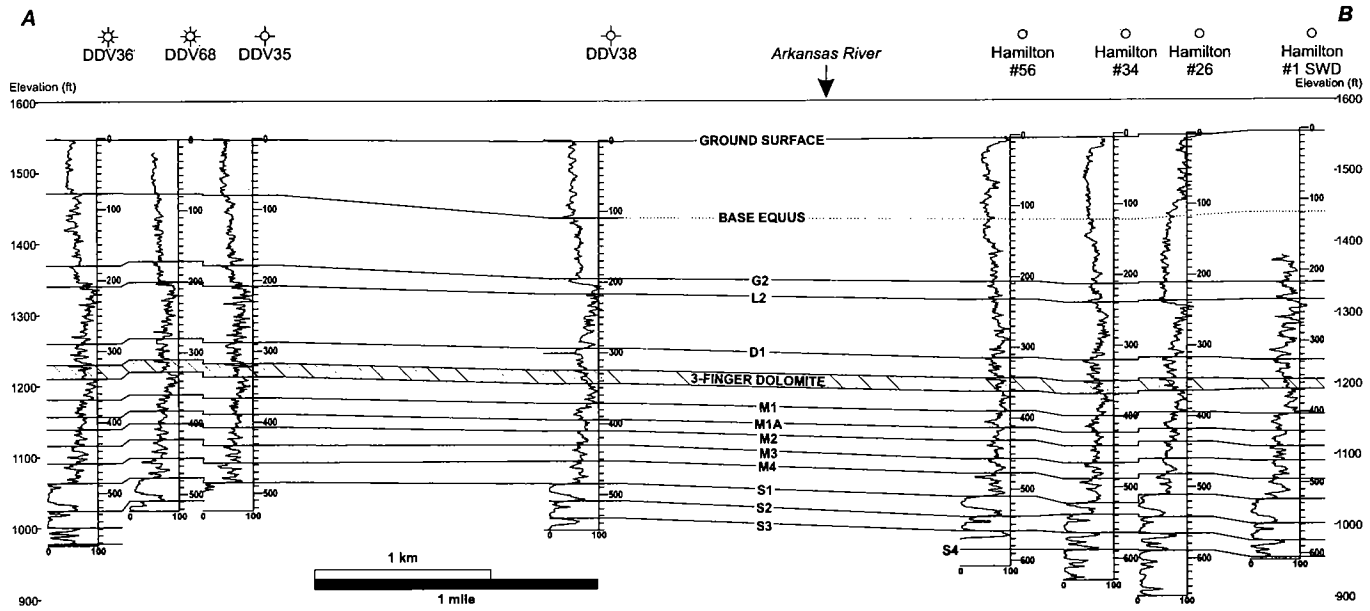


Figure 7. North–south cross section, intersecting the natural-gas pathway from Yaggy to Hutchinson. *A* is north, and *B* is south. Line of section shown in Figure 1. Normalized gamma-ray logs, scaled as in Figure 5, are shown.

resulting from ground water that at one time contacted the upper salt, probably along natural fractures, as inferred from the linearity of the feature (Fig. 13).

North of, and parallel to, the crest of the Yaggy–Hutchinson anticline, another zone of thinning occurs in the S1–S2 isopach. This thinning is much more subtle (<4 ft of local thinning occurs in an area less than a mile wide), but its presence further indicates a structural relationship between the anticline and adjacent zones of salt dissolution. The parallel elongate sets of thicks and thins may be closely linked to previously mapped structure, suggesting possible cause and effect.

Yet another area of thinning in the S1–S2 isopach occurs at the western edge of Hutchinson, coincident with the north-northeast-trending valley in the Equus Beds mentioned above.

In general, the S1–S2 map illustrates distinctive sets of northwest- and northeast-trending lineaments, dominated by the northwest trend (Fig. 13). Moreover, the trend of gas-bearing vent wells between Yaggy and Hutchinson corresponds closely to the subtle northwesterly trends of elongate thinning and thickening of the uppermost salt beds. In Hutchinson, the relationships of gas wells and the S1–S2 isopach are not clearly defined owing to apparent interaction between these nearly orthogonal sets of lineaments.

The M4–S1 isopach (Fig. 12D) shows an elongated area of thickening along the Arkansas River south and west of Hutchinson, closely corresponding to a similar elongated area of thinning in the underlying S1–S2 isopach. This indicates that at least some of the dissolution of the uppermost salt was early, occurring prior to deposition of the overlying M4–S1 clastic-dominated interval. However, only a maximum of 5 ft of local thinning in the S1–S2 isopach along the Arkansas River is compensated by M4–S1 sedimentation, indicating that the remaining 15 ft of local thinning resulted from later dissolution. Overlying isopachs up to G2 (Fig. 12E–H) do not show preferred deposition along the Arkansas River trend, which would be expected if there were episodes of renewed salt dissolution along this trend during the M4 to G2 time interval. This indicates that the majority of the S1–S2 salt dissolution along the Arkansas River was post-Permian. Isopach maps of intervals between M4 and G2 show new patterns of generally northerly trending thicks and thins, suggesting a fundamental shift in depositional pattern. These isopachs represent strata that constitute the uppermost Wellington Formation and the Ninnescah Shale, which from previous studies (Swineford, 1955; Watney and others, 1988) indicate an abrupt change to more continental conditions, reflecting the waning regressive stage of the evapo-

Figure 8 *(facing page). Top:* Correlated well-log cross section along Wilson Road, midway between Hutchinson and the Yaggy gas-storage facility. Line of section shown in Figure 1. Gamma-ray logs, scaled as in Figure 5, are shown. *Middle:* Wilson Road seismic line. Seismic peaks are black; troughs are white. Synthetic seismograms calculated from sonic and density logs in the DDV 57, 67, and 63 wells are shown. The seismic reflections corresponding to the top of the 3-finger dolomite, the M1A marker, and the top of the Hutchinson Salt Member (S1) are highlighted. Heavy black lines are interpreted faults. *Bottom:* Seismic isochron of the uppermost salt layer (S1–S1A). The S1–S1A isopach from well control is shown for comparison. Thickness and time scales are coincident, assuming a seismic velocity of 14,000 ft/s. Locations where the interpreted faults intersect the S1 seismic reflection are highlighted by arrows.

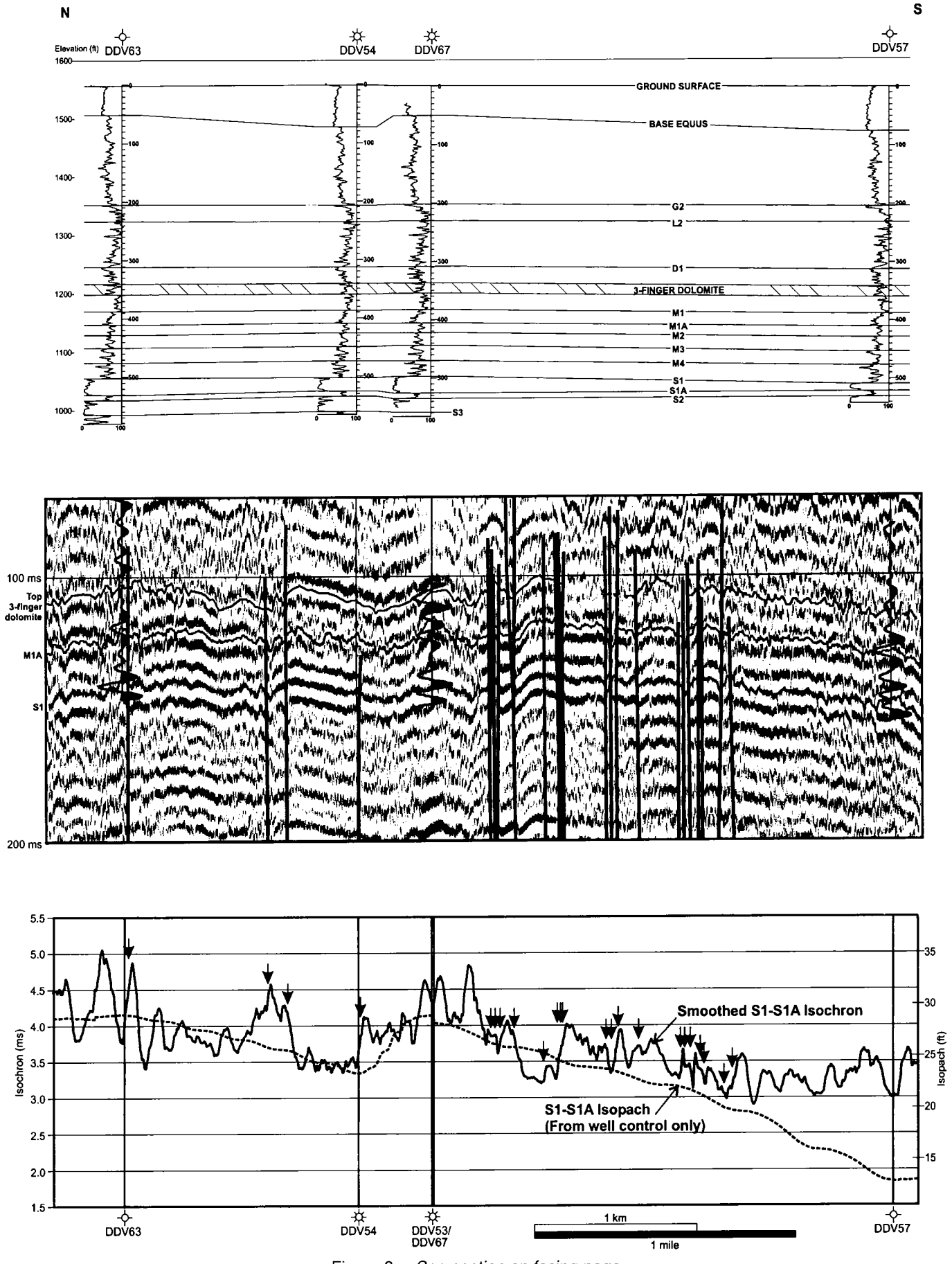


Figure 8.—*See caption on facing page.*

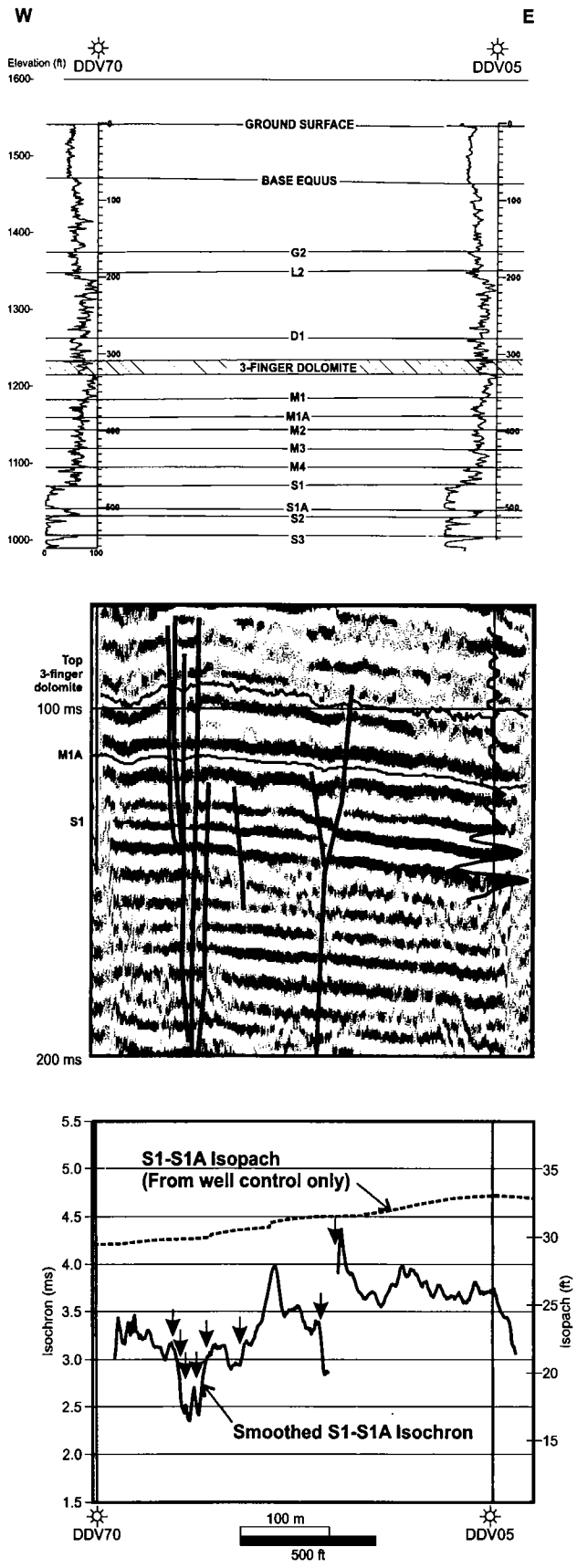


Figure 9. Well-log cross section, seismic line, and S1–S1A seismic isochron for Rice Park. Line of section shown in Figure 1. Instruction is the same as for Figure 8.

rite-filled embayment in which the Hutchinson Salt Member was deposited. The variations in thickness seem simply to reflect local sedimentation, perhaps both continental and marginal marine, along the shrinking basin margin.

Post-Permian dissolution of the S1–S2 salt bed along the Arkansas River trend extends northward to the southern edge of the Yaggy–Hutchinson anticline, which suggests structural linkage between the northwest-trending anticline and the parallel elongate area of salt dissolution.

The Arkansas River dissolution trend corresponds with a valley seen on the map of the configuration of the base of the Equus Beds (Fig. 10A). The configuration of the Equus Beds is believed to reflect patterns of incised valley development. The maximum area of elongated S1–S2 salt dissolution occurs north of the maximum elongated thickness of the Equus Beds, but both trends are closely parallel, as they are to the Yaggy–Hutchinson anticline. The main incised paleovalley in the Equus Beds continues northwestward beyond the mapped area of the current study, closely following the current Arkansas River Valley. The corresponding patterns suggest some common control, possibly a reflection of episodic structural activation along a zone of basement structural weakness.

### *Seismic Data*

Sonic and density logs have been collected for DDV 57, 67, and 63. Synthetic seismograms calculated from these logs indicate that the top of the Hutchinson Salt Member (S1) corresponds to a moderate-amplitude seismic peak for DDV 63 and 67 (Fig. 8, middle panel). For DDV 57, the amplitude of the top salt reflector is significantly lower. This is largely due to a thinner uppermost salt layer (S1–S1A) at this location. At DDV 57, the S1–S1A thickness is 13 ft, compared to 28 ft at DDV 67 and 29 ft at DDV 63. A seismic model (Fig. 14), constructed using average velocities and densities from the logs and a 100-Hz Ricker wavelet, which approximates the seismic source of the Wilson Road and Rice Park seismic lines, shows how the uppermost salt isochron and amplitude vary as the S1–S1A interval thins.

The seismic reflectors corresponding to S1 and S1A (the trough just below the S1 peak) were interpreted on both the Wilson Road and Rice Park seismic lines, and an isochron was extracted (Fig. 8, bottom panel) to see if the thinning of the uppermost salt observed on log cross sections and in the S1–S2 isopach map could be seen in more detail. Because of noise in the seismic data, this isochron was smoothed using a 49-point running average prior to display. On the Wilson Road seismic line, the smoothed isochron varies between 3 and 5 ms. The isochron averages 4 ms on the northern half of the line. However, beginning just south of DDV 67, there is a regional decrease in the isochron toward the south. The average isochron decreases to ~3 ms over a distance of 1 mi. This change

is corroborated by thinning of the S1–S1A isopach between DDV 67 and 57. These results suggest that the thinning of the uppermost salt interval associated with the Arkansas River trend began ~2 mi to the north of the river along Wilson Road and was gradual, in contrast to the apparent abrupt thinning to the south of the river (Fig. 7). Over the southernmost 0.7 mi of the Wilson Road line the isochron flattens at ~3 ms, even though the isopach suggests continued thinning. This apparent discrepancy can be explained by viewing the seismic model, which shows that the temporal resolution of our seismic data is ~3 ms.

The Wilson Road seismic line shows a number of apparent faults, all of which extend below the salt (the base of salt is estimated to be ~40–50 ms below the top of salt). Most of these faults are also apparent in the sedimentary section above the 3-finger dolomite. The pervasive nature and extent of these faults indicate that they are related to a deep-seated structural activity including movement that followed deposition of the 3-finger dolomite. These faults were not produced by salt dissolution, although they may have influenced salt dissolution and provided a possible gas pathway. Indeed, the diffuse southward thinning of the uppermost salt interval along the Wilson Road line is associated with a high concentration of faults. The orientations of the faults are unknown, but they may be hypothesized to parallel other structural lineaments in the area (Fig. 13).

Two local thins in the S1–S1A isochron, bounded by faults, occur on the flanks of the anticline along which gas migrated. DDV 54 sits on the southern edge of the northern thin, which is 0.25 mi wide. The southern thin resides 0.3 mi south of DDV 67 and is 0.2 mi wide. If salt dissolution was responsible for these thins, it also may have caused local enhanced structural relief of the flanks of the anticline and elevated tensional forces along the crest of the anticline. Thus, fractures oriented parallel to the anticlinal crest may have more likely been continuous and prone to opening owing to high-pressure gas.

Two zones of faulting have been identified on the Rice Park seismic line (Fig. 9). At the center of the line two conjugate faults are visible, which markedly offset the S1 reflector and form a depression in the overlying strata. Overlying strata, at least up to the 3-finger dolomite, are affected, although there is no known surface expression of this feature. The S1 reflector is offset by 4 ms (~20 ft) on the east and 2 ms (~10 ft) on the west. The feature is 33 ft wide at S1 and 139 ft wide at the 3-finger dolomite interval. The faults appear to converge at approximately the S2 reflector. A faulted zone seems to extend well below the S2 horizon, but deeper reflectors do not show significant offset along the fault. This suggests that the shallow faults resulted from salt dissolution above S2, focused along a deeper seated structural element.

On the western half of the Rice Park line is an apparent swarm of faults that penetrates from the shallow section to below the Hutchinson Salt Member. Although no major offsets are seen in the S1 horizon at these faults, the S1–S1A isochron shows marked thinning in this zone, and there is apparent sag in overlying reflectors at this location, again suggesting possible salt dissolution associated with deeper seated structural elements.

The proposed salt dissolution on the Rice Park seismic line seems to have occurred over a very localized area, which is too small to be detected by well control alone. The isopach map, constructed using control points at DDV 5 and 70, gives no indication of local thinning of the upper salt in this area but rather shows only 2 ft of thickness variation.

Because the orientations of the faults on the Rice Park seismic line cannot be determined, the structural elements on the Rice Park line may be associated either with the northwest-trending anticline or with the north-northeast-trending structure, which is proposed to have been responsible for a nearby tributary valley in the Equus Beds and local S1–S2 salt dissolution (Fig. 13). Whatever the controlling structural elements, the presence of faults in proximity to the anticline may have provided conduits to both vertical and lateral gas migration, including charging of the lower gas zone in DDV 64.

### *Rock Properties*

Pervasive veins of satin-spar gypsum permeate the upper Wellington Formation shales, as observed in cores available from the Hutchinson and Lyons areas in locations tens of miles west of the salt-dissolution front. The mechanical stress caused by the change in volume of approximately 40% for hydration of anhydrite to gypsum probably led to the emplacement of the veins in the shale through the reaction:

$$CaSO_4 \text{ (anhydrite)} + 2H_2O = CaSO_4 \cdot 2H_2O \text{ (gypsum)}.$$

Sulfate-rich waters probably slowly precipitated in the stress fractures to form the satin spar as observed in core. Shales are gypsiferous in the upper Wellington Formation as calculated from Rhomma-Umma plots from density–neutron–photoelectric logs. Transformation to gypsum probably occurred during the late Tertiary, when the Permian strata were eroded to current depths of burial, under 1,000 ft (300 m), the approximate burial depth for the stability of anhydrite. Water apparently was more readily accessible to drive the sulfate hydration reaction as also evidenced by halite dissolution at the top of the Hutchinson Salt Member that occurred near the same time.

The top of the Hutchinson Salt Member in the Q-5 core at the Yaggy gas-storage facility reveals small, centimeter-scale interformational disrupted bedding, brecciated shale, mud cracks, and veins of red halite. This suggests an early dissolution event that occurred shortly after deposition, a situation not dissimilar to what is observed deeper in the Hutchinson Salt Member at the tops of other halite beds (Watney and oth-

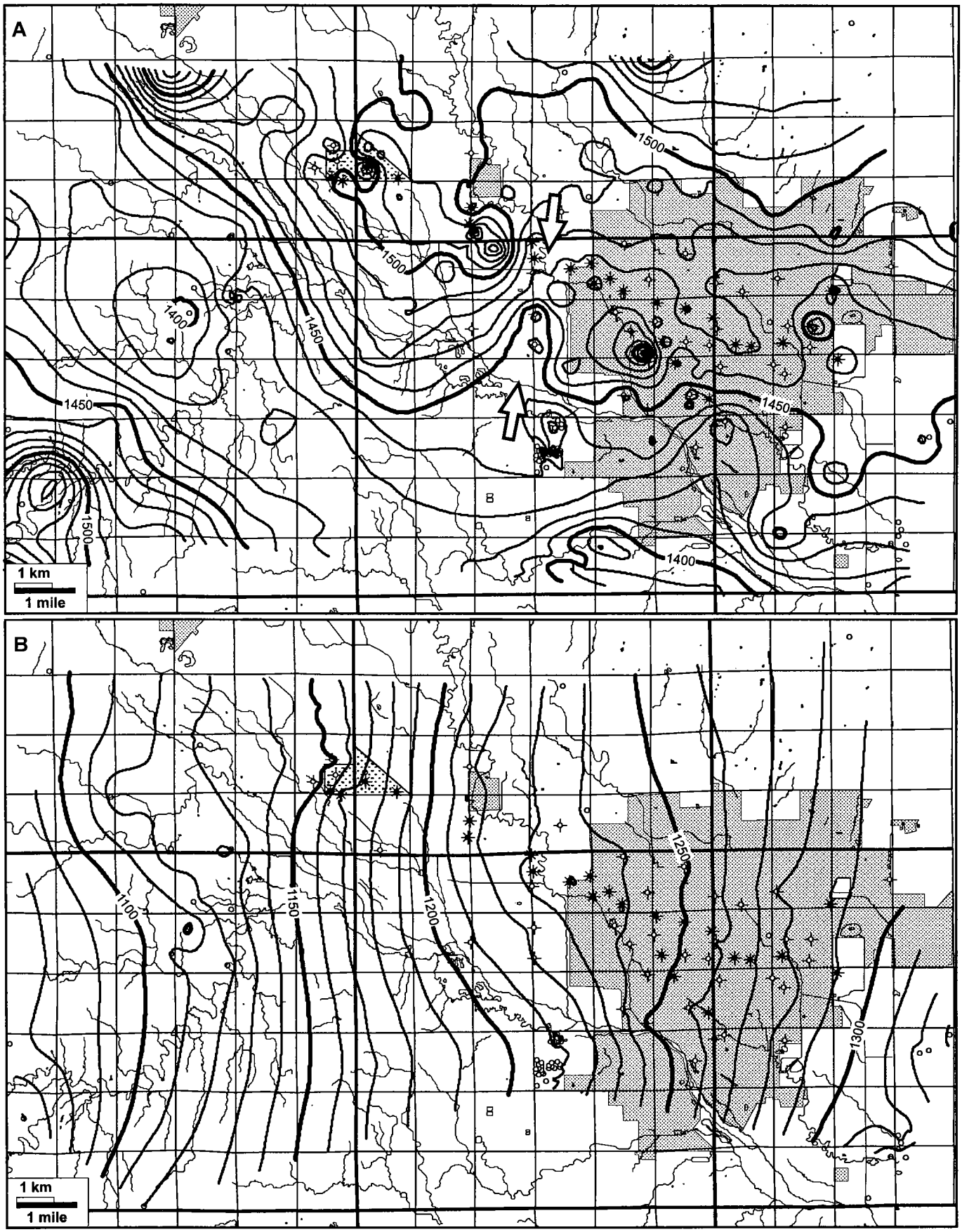


Figure 10 *(above and facing page).* Structure maps of the following horizons for the study area shown in Figure 1: (A) base of Quaternary Equus Beds, (B) top of 3-finger dolomite, (C) top of Hutchinson Salt Member (S1 marker), and (D) S2 marker. Contour interval = 10 ft. Arrows in (A) highlight a north-northeast-trending tributary valley that parallels the Voshell Anticline and overlies an area of subtle thinning in the uppermost salt.

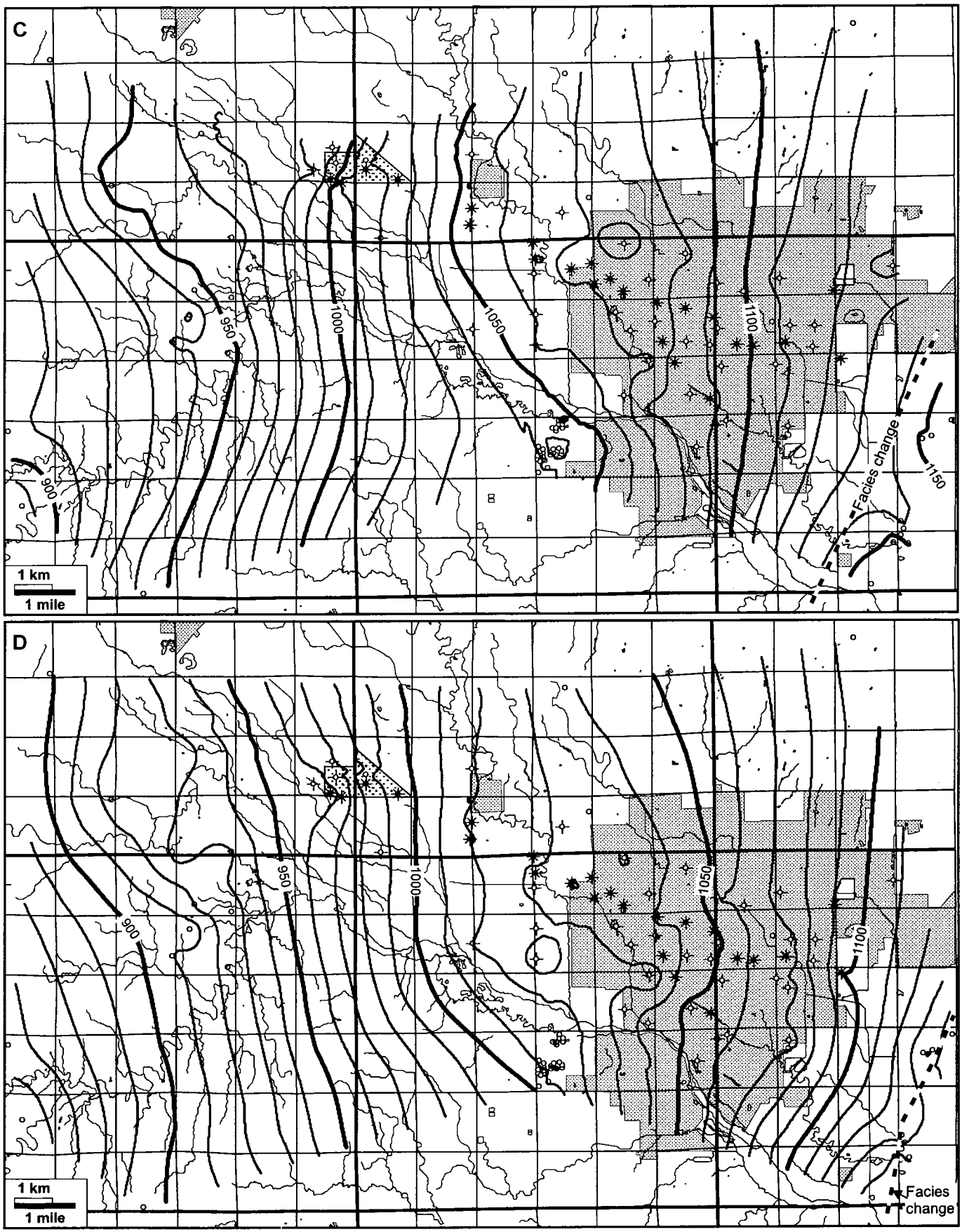


Figure 10.—*Continued.*

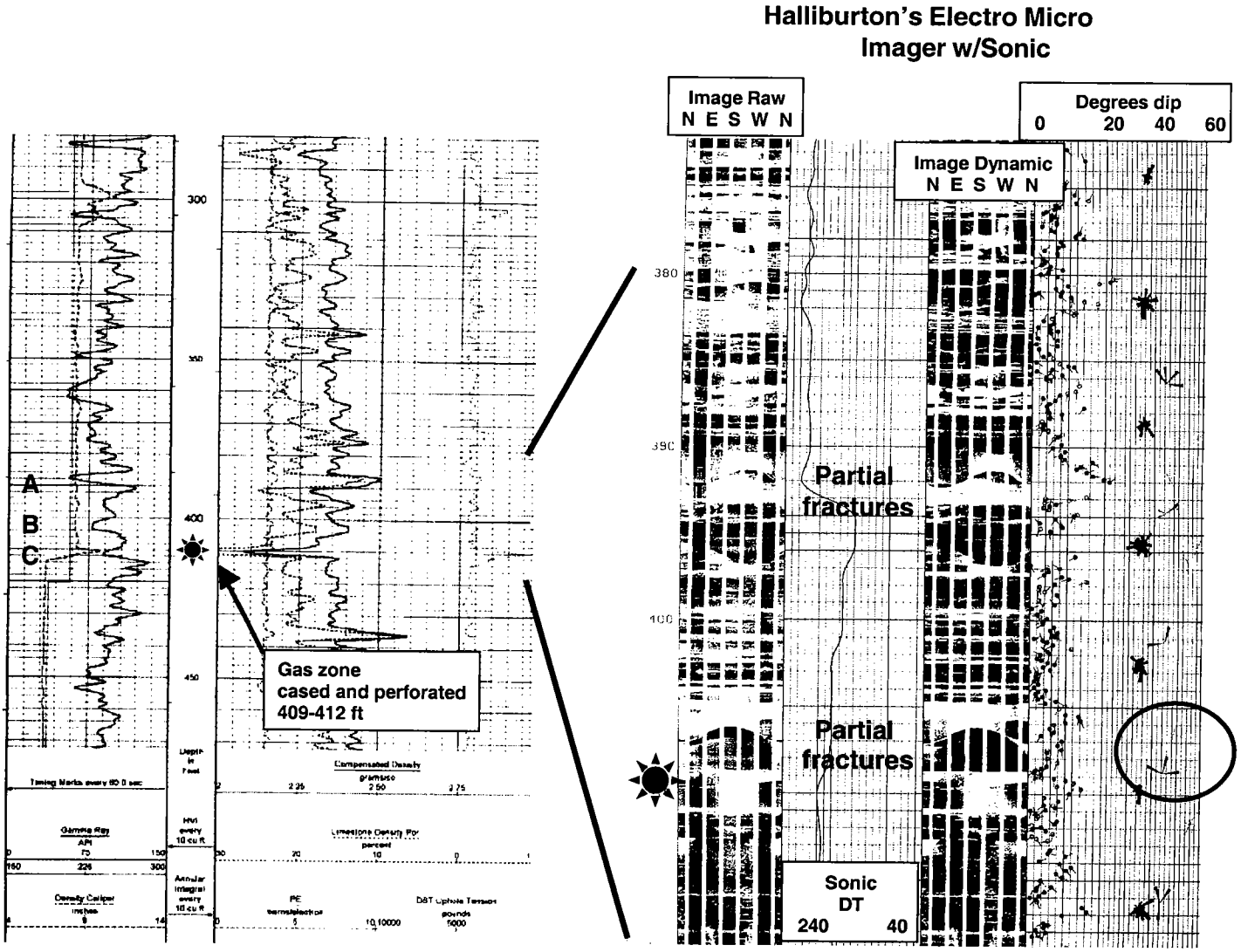


Figure 11. Formation micro-imaging log on right alongside conventional gamma-ray–caliper–neutron–density–photoelectric log on left for observation well OB 2. On left, 3-finger dolomite is labeled with letters *A, B,* and *C.* The C zone is a gas-bearing dolomite interval in this well, exhibiting washout and gas show on drilling. Washout creates anomalously high porosity-log response. Formation micro-imaging log shown on an expanded scale. Lighter parts of image correlate with gypsum and dolomite beds. Scalloped patterns are fractures with dips of ~50°. Orientation of fractures in the gas-bearing C zone are dominated by a west-northwest trend, with a minor north-northeast trend.

ers, 1988). Porosity and permeability in this zone appear to be minor. Examination of core from the AEC no. 1 test well in Rice County (20 mi northwest of Hutchinson) similarly shows centimeter-scale breccia with clasts of shale and halite interbedded with contorted shale and halite at the top of the Hutchinson Salt Member.

Evidence of fracturing was obtained from a borehole micro-imaging log that was run in observation well OB 2, adjacent to the east edge of the Yaggy gas-storage facility. Cavitation of the borehole occurred between 409 and 412 ft, suggesting the interval of gas release, which corresponds with the lowest dolomite layer in the 3-finger dolomite. Fracture sets are observed on the micro-imaging log. Partial fractures in the interval encompassing the gas-bearing interval are oriented east–west, dipping at 50°, while healed fractures occur along north–south axes (Halliburton Energy Services, 2001) (Fig. 11). These fractures parallel the two major lineaments observed in the mapping, including the crest of the proximal anticline. OB 2 had the highest recorded surface shut-in pressure of ~250 psi, with the gas-bearing zone at 410 ft. Shut-in pressures continued to be high (172 psi) in this well in January 2003. A pressure-buildup test in late 2001 indicated low permeability, approximately 2 md. Outcrops of similar thin dolomites in the upper Wellington Formation exhibit oriented joint sets. Also, higher values of the dynamic Young's modulus calculated from dipole sonic and density logs for the equivalent dolomite in eastern Hutchinson indicate greater strength and ability to maintain inherited fractures

from local and regional stress (Joe Ratigan, 2001, personal communication).

Dolomite beds are composed of dolomicrite with negligible matrix porosity and permeability.

## DISCUSSION

### Integrated Geologic Model

Evidence for fracture-controlled gas-bearing conduits include (1) the presence of linear trends of gas-bearing wells that parallel mapped lineaments, (2) elevated pressure in wells along fracture trends, and (3) faults interpreted from seismic data corresponding with mapped lineaments and structural features such as the anticline between Yaggy and Hutchinson. Pressure-induced parting of preexisting fractures in a shallow dolomite seems to be a likely mechanism for directing natural gas to the unplugged brine wells. The fractures may be associated with faulting that extends beneath the Hutchinson Salt Member as interpreted from the Wilson Road and Rice Park seismic profiles. Core, well-log, and seismic data further reveal that episodic dissolution of the uppermost bed of the Hutchinson Salt Member occurred locally along the northern and southern flanks of the anticline along the area between Yaggy and Hutchinson. Mapping also indicates episodic dissolution along northeasterly and northerly trends in eastern and central Hutchinson that parallel the main dissolution front of the Hutchinson Salt Member. Associated preexisting fractures preserved in the dolomite layer may have been opened in the high-pressure-gas event to transmit gas under the city only to be closed once pore pressures declined below the parting pressure. Adjoining shales would less likely be able to mechanically support this organized fracture system and thus not be in a position to transmit the gas.

The southern area of northwest-trending salt dissolution forms an elongated trough ~2–3 mi wide, a feature closely aligned with the Yaggy–Hutchinson anticline (which forms the northern boundary) and the main valley systems of the current Arkansas River and early Neogene Equus channels. Preexisting fractures seem to have provided conduits for water movement beneath the major fluvial drainages of the Equus Beds and Arkansas River, leading to episodic dissolution of parts of the upper beds of Hutchinson salt. Fractures also may have influenced the formation of the distinctive northwest linear trends of the drainages.

This multi-episode, broad-scale salt dissolution, which extends at least 12 mi behind the main dissolution front and beyond the western boundary of the mapped area, increases the dip of the southern flank of the Yaggy–Hutchinson anticline as the upper salt beds thin. The loss of section and increased dip may have contributed to tensional forces focused on the coincident northern edge of salt dissolution and crest of this anticline. Other localized north-northeast trends of salt dissolution could have similarly created tensional forces and oriented fractures.

The regional alignment of these geologic features suggests subtle but episodic activation of a deep-seated basement structure. The area is in general coincident with the southern boundary of the Precambrian Midcontinent Rift, expressed by magnetic, gravity, basement-structure, and compositional patterns. The basement heterogeneity may represent a site of localized crustal stress release spanning a time frame from at least the Late Permian, Neogene, and into the Holocene. Subtle structural activation along deep-seated basement features in a cratonic setting and their impact on local geology are common, and their recognition can provide a template that can unify and strengthen interpretations (e.g., regional Pennsylvanian sedimentation controlled by structural blocks—Watney and others, 1999; Upper Pennsylvanian incised valleys in the Tonganoxie Sandstone Member occupying boundaries between basement blocks—Beaty and others, 1999; a basement lineament controlling Mississippian chert reservoirs corresponding to the southwest extension of a basement feature associated with the Voshell Anticline—Watney and others, 2001).

#### *Structural Controls and Salt Dissolution: A Case for the Voshell and Arkansas River Lineaments*

Episodic activation of the Voshell Anticline was suggested by Anderson and others (1994) to have influenced sites of salt dissolution. Differential activation of basement structure likely served as a template for orthogonal and linear patterns of subsidence, sediment accommodation, local structural deformation, and salt dissolution. Deep-seated, structurally related fractures and faulting appear to have affected the orientation of the primary salt-dissolution front and dissolution trends within the upper salt deposit behind the primary dissolution front. Similar structural controls are suggested for other salt-dissolution fronts including (1) the eastern edge of the Flowerpot Shale in western Kansas (Holdoway, 1978), which corresponds with the Oakley Anticline and the basement structure associated with the Eubank–Pleasant Prairie fields in Haskell County, Kansas; and (2) weak northwesterly and northeasterly trends that define the northeastern dissolution margin of the Upper Permian Cimarron salt member of the Ninnescah Shale in south-central Kansas over the Pratt Anticline and southern Central Kansas Uplift (Martinez and others, 1996). These correlations with basement lineaments support the possible interpretation that intermittent basement activation acted as a control on preserved geometries of other salt bodies in the subsurface, and consequently their expression and impact on the overlying strata and land surface.

The anticline between Hutchinson and Yaggy is a minor expression of an apparently larger scale structural system, the northwest-trending Arkansas River Lineament. The lineament encompasses a 60-mi linear section of the Arkansas River extending at least

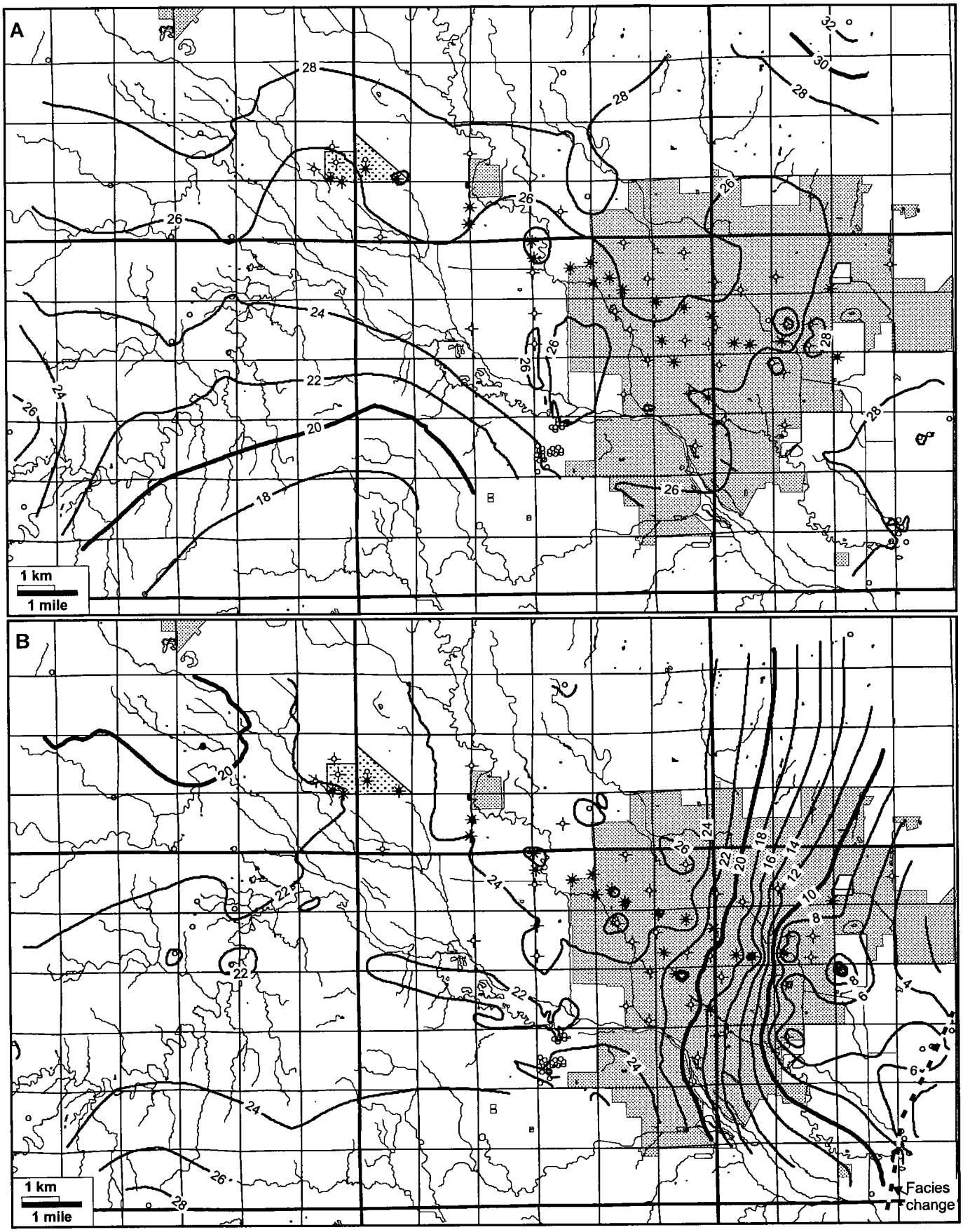


Figure 12 *(above and next three pages).* Isopach maps of the following intervals for the study area shown in Figure 1: (A) S4–S3, (B) S3–S2, (C) S2–S1, (D) M4–S1, (E) M3–M4, (F) top 3-finger–M3, (G) L2–top 3-finger, (H) G2–L2. Contour interval = 2 ft. Arrows in (C) highlight a zone of subtle local thinning in the uppermost salt interval north of, and parallel to, the crest of the Yaggy–Hutchinson anticline.

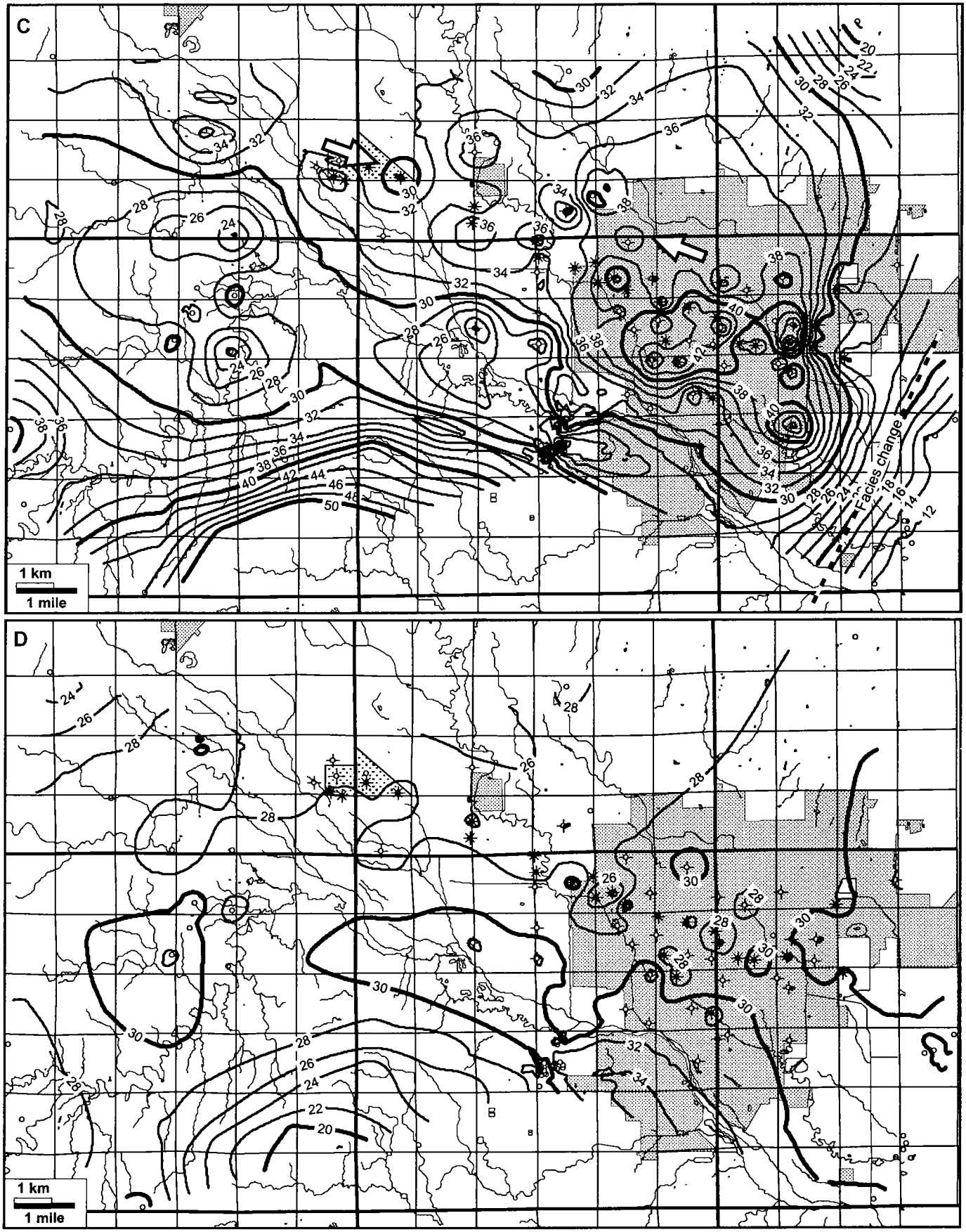


Figure 12.—*Continued above and next two pages.*

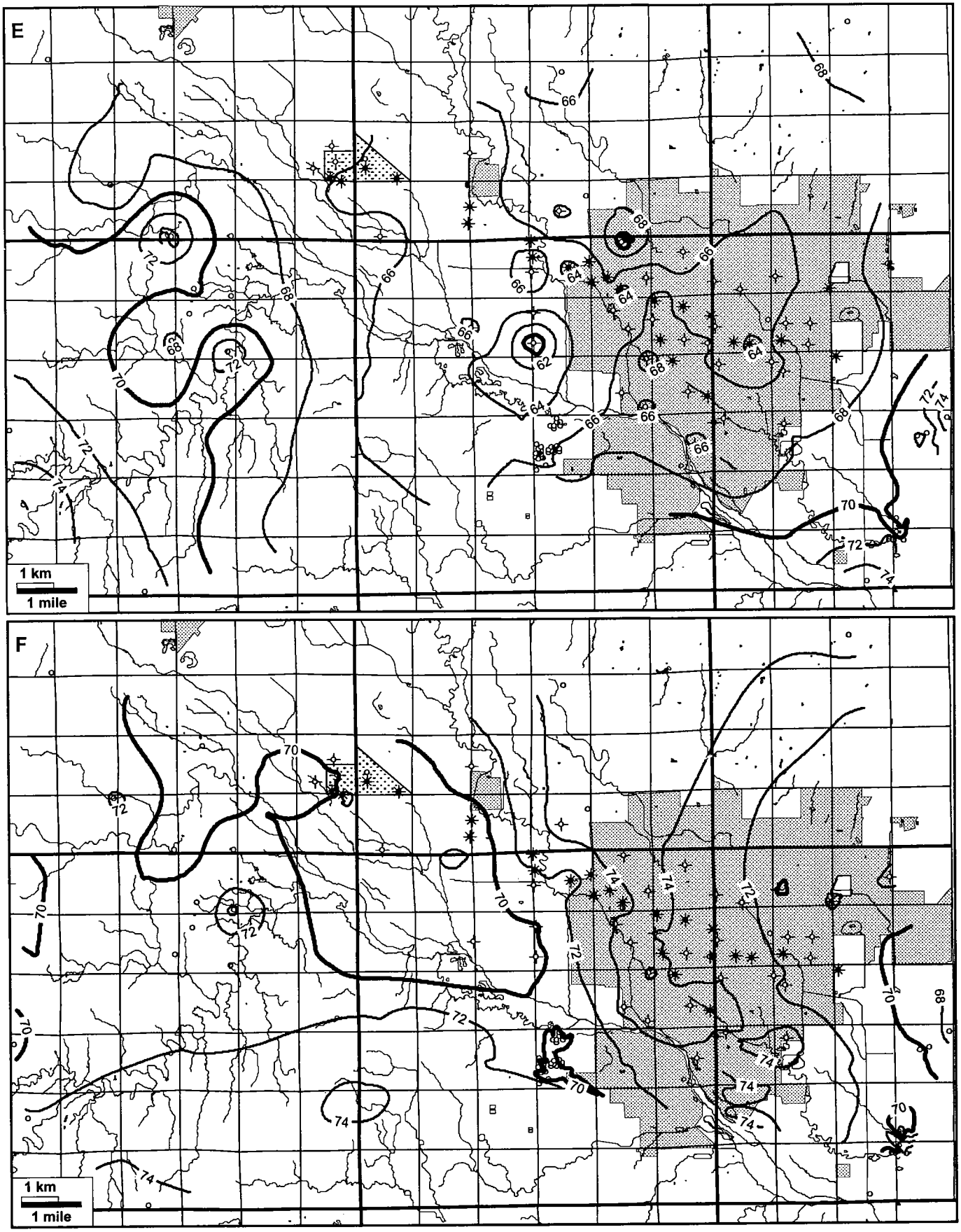


Figure 12.—*Continued above and facing page.*

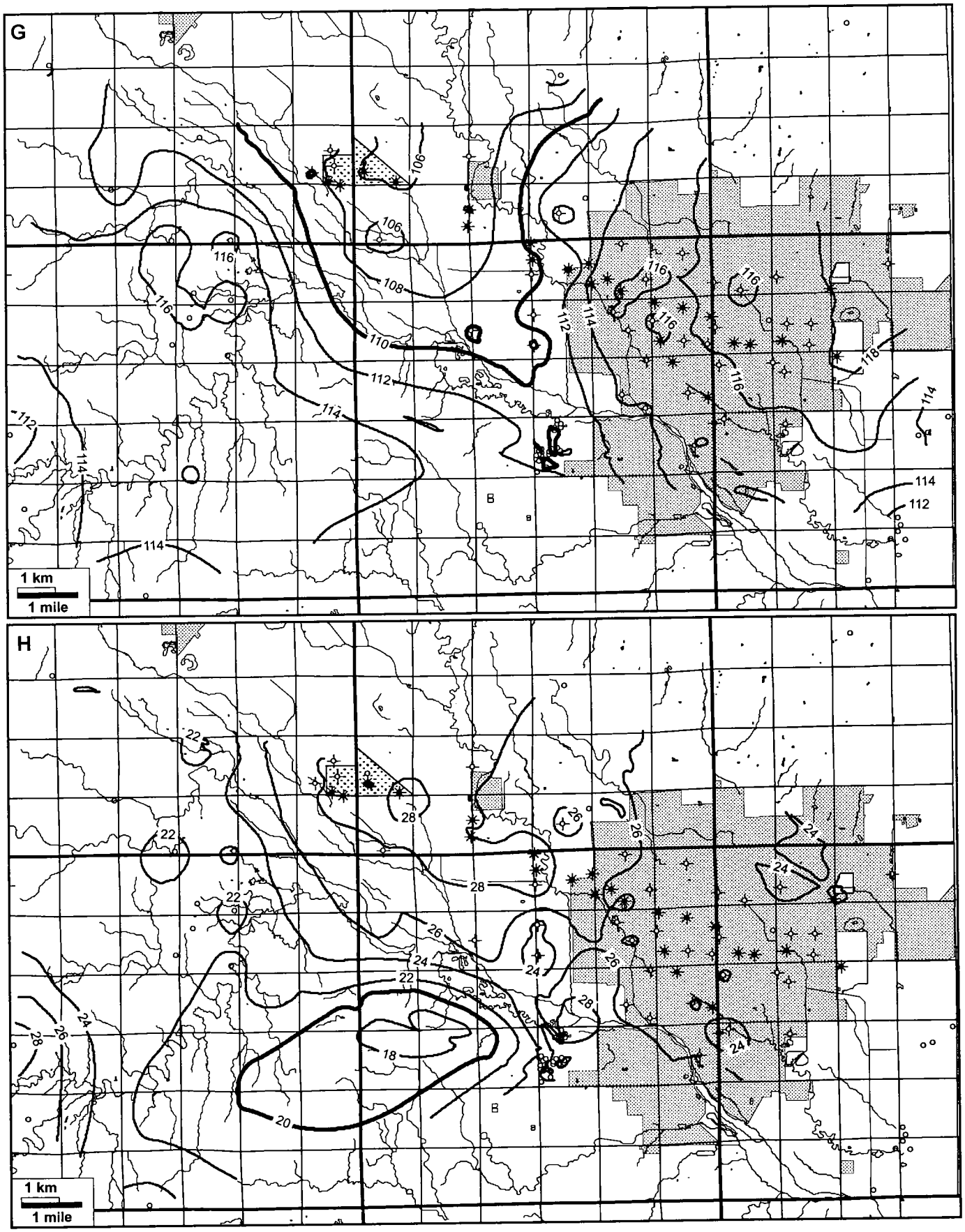


Figure 12.—*Continued.*

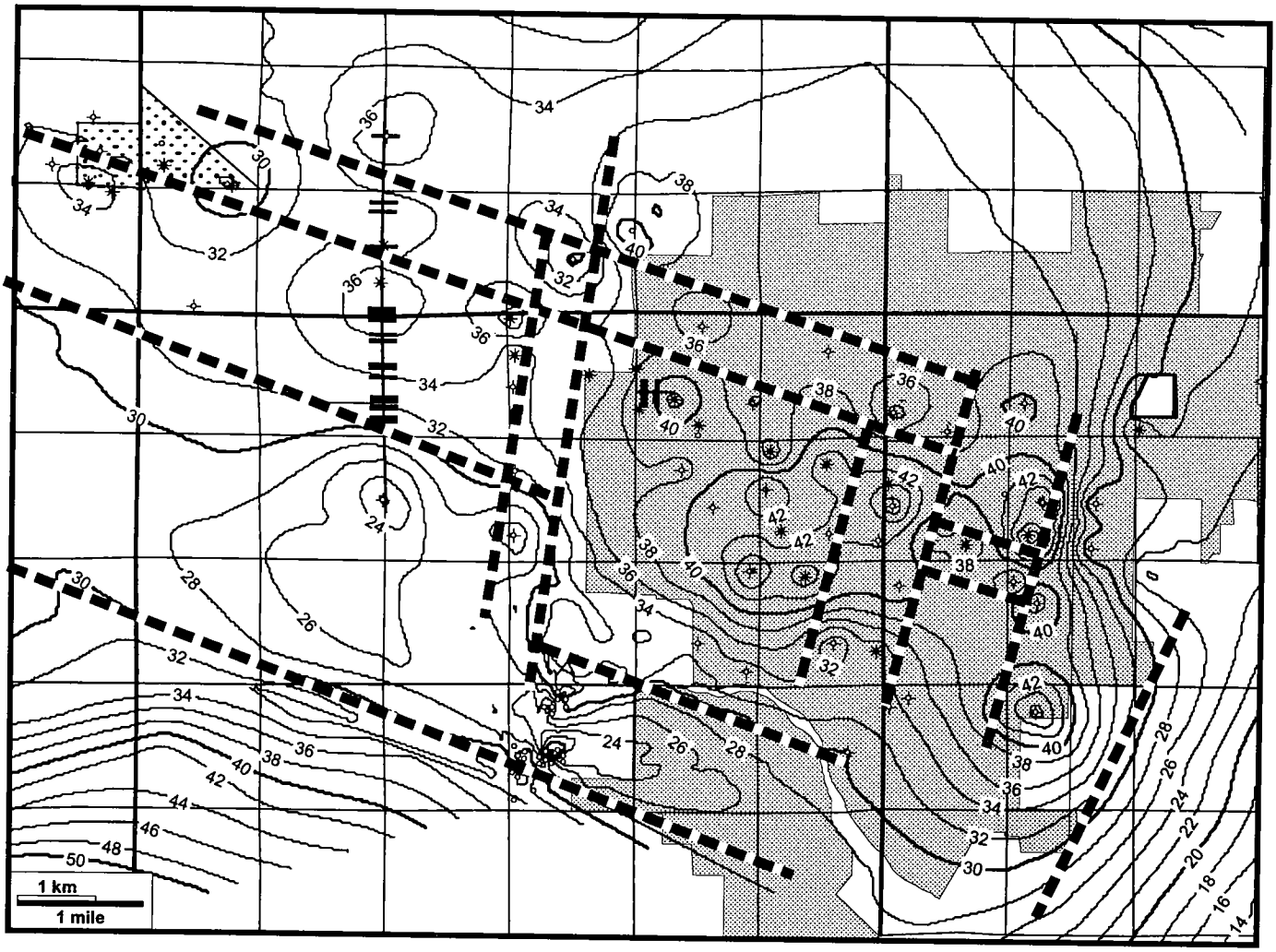


Figure 13. S2–S1 isopach map for the Yaggy–Hutchinson area, with a preliminary interpretation of structural lineaments superimposed (heavy dashed lines). Contour interval = 2 ft. Locations of faults intersecting the S1 horizon, as interpreted from the Wilson Road and Rice Park seismic lines, are shown as short, heavy black lines.

between Wichita and Great Bend to the northwest. The northwesterly trending incised paleovalley mapped at the base of the Pleistocene–Tertiary Equus Beds is closely aligned with this feature (Fig. 15). In addition, the lineament coincides with a regional 125-mi-long linear northern border of the lower part of the Hutchinson Salt Member (Fig. 5B) and is in proximity to the northwest-trending contact between contrasting Precambrian basement terranes—the southern edge of the Precambrian sediment-filled portion of the Midcontinent Rift graben and the northern edge of the rhyolite–granite basement terrane (Van Schmus and others, 1996). The intersection of the Arkansas River with the eastern dissolution margin of the Hutchinson Salt Member forms a 15-mi westward retreat in the salt-dissolution front, which suggests enhanced dissolution activity along this lineament. In addition, documented sinkholes occur within 20 mi on either side of this northwest-trending lineament, including Cheyenne Bottoms, a natural lake possibly related to partial solution of the underlying Hutchinson Salt Member (Bayne, 1977; Anderson and others, 1995a).

## SUMMARY AND CONCLUSIONS

Geologic, geophysical, and engineering evidence supports the existence of extended trends of fractures and episodic salt dissolution along subtle geologic structures, including the northwest-trending anticline between the Yaggy gas-storage facility and Hutchinson as part of the Arkansas River Lineament (ARL). Similar northeast-trending geologic features associated with the Voshell Anticline are also indicated. An expanded subsurface-study area covering 150 mi$^2$ surrounding Hutchinson identified fractures, faults, and a subtle anticline that reside along the northern edge of the larger ARL. Episodic movement along the ARL led to subtle folding, fracturing, and minor faulting along parts of a northwest–southeast-trending 3-mi-wide corridor that extends through the mapped area. Fractures episodically allowed undersaturated water to access Permian salt (halite) beds and led to occa-

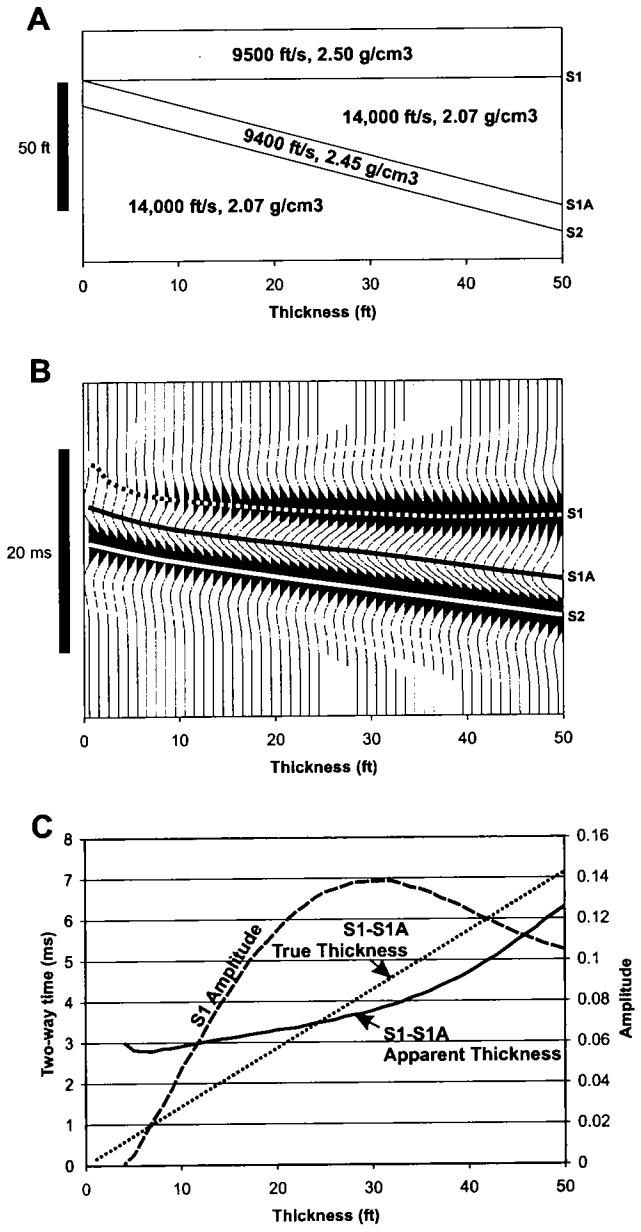


Figure 14. Model showing seismic effects of varying thickness of the uppermost salt (S1–S1A). (A) Depth model in which uppermost salt varies from 0 to 50 ft in thickness. Velocities and densities assigned to each of the modeled layers are shown. (B) Synthetic seismic traces created by convolving a reflectivity series calculated from the velocities and densities in (A) with a 100-Hz Ricker wavelet. (C) Plot of S1 amplitude (dashed line) and S1–S1A apparent time thickness (solid line) extracted from (B), compared to S1–S1A true time thickness.

sional dissolution, albeit subtle (on the order of tens of feet thick, mile or fractions of a mile wide, and apparently miles in length), in mapped areas that lie west of the main dissolution front. Dissolution in the uppermost salt bed of the Hutchinson Salt Member forms an elongate northwest-trending trough following the ARL. While some thinning was very early, shortly after deposition, later dissolution that is post-Permian in age is also indicated. This later dissolution occurred in spite of current burial depths >500 ft. The widespread, predominantly post-Permian salt dissolution along the 3-mi-wide corridor is bordered on the north by the Yaggy–Hutchinson anticline, apparently leading to increased dip of the southern flank of this anticline along the entire structure west of the city. This subsidence enhanced the deep-seated structural deformation. Moreover, a narrow (<1-mi-wide) salt-dissolution-trough zone formed on either side of the crest of the anticline. This dissolution zone is associated with localized deep-seated and salt-based fracturing and faulting, suggesting episodic access of undersaturated water along the faults followed by additional fracturing from salt subsidence. The subsidence probably led to further flexure and probable tensional forces that helped maintain the oriented fractures over this extended distance.

The Voshell Anticline also has exerted a strong influence on the location of the main dissolution front of the Hutchinson Salt Member east of Hutchinson. Associated fractures and faults are inferred to have exerted control on the location of Holocene drainage, in turn creating access of undersaturated water facilitating salt dissolution. The north-northeast-trending grain (anisotropy) of the isopach maps, particularly in central and eastern Hutchinson well behind the main salt-dissolution front, parallels the trend of the Voshell Anticline. Local thinning of mapped intervals follows this trend and has been attributed to additional salt dissolution on the basis of well-log data. North-northeast-trending sets of gas-bearing vent wells in eastern Hutchinson may follow these fracture elements lying oblique to the ARL.

Gas migration apparently followed these inferred fracture systems, based on the correspondence of gas-bearing vent wells with some of these structures. Also, it is possible that anthropogenic salt dissolution may have been involved—e.g., subsidence of strata overlying shallow collapsing salt caverns associated with brine-extraction wells. In particular, a series of interconnected brine wells, caverns, and collapse features could move gas laterally; but gas would have accumulated in caverns, and there is no evidence of this phenomenon to date. However, no gas is known to have escaped through any collapse features with surface expression. Also, recent logging of 11 unplugged brine wells in Hutchinson revealed no significant collapse of the brine caverns.

The timing of salt dissolution ranges from shortly after deposition of the affected uppermost beds of the Hutchinson Salt Member to post-Permian, pre–Equus Beds, and into the Holocene. The post-Permian, pre–Equus Beds activation of the Yaggy–Hutchinson anticline is suggested by the coincidence of an interfluve high mapped on the configuration of the base of the Equus Beds and the crest of the anticline.

Since early Holocene time, local streamflow has led to incised valleys that appear to be influenced by the

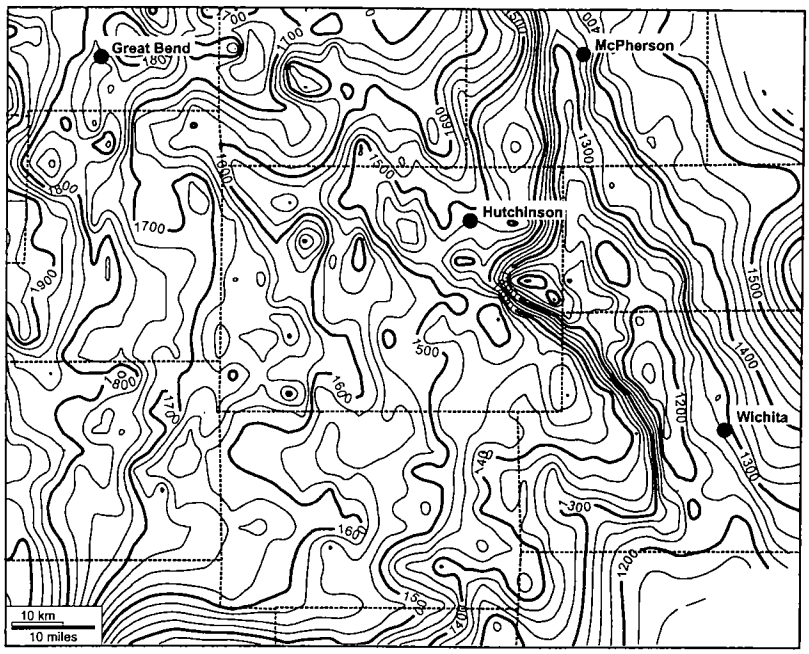


Figure 15. Configuration map of the base of the Equus Beds, showing the northwesterly trending incised paleovalley between Wichita and Great Bend. Contour interval = 25 ft. Dashed lines are county boundaries.

northwest-trending ARL and structures paralleling the Voshell Anticline. Meteoric water supplied by these streams apparently penetrated Permian strata and locally led to salt dissolution. Besides dissolution of clearly defined beds of halite, shale-dominated gypsiferous intervals that have been mapped above the Hutchinson Salt Member may have similarly undergone even more subtle local thinning through dissolution of more dispersed halite or sulfates.

Validation of basement-related lineaments as templates for salt dissolution may add an element of understanding and prediction in assessing salt stability and structural integrity of overlying strata useful in siting underground gas-storage facilities or establishing potential pathways for lateral gas migration. Areas may be more predisposed to dissolution, either natural or man-made, and could help target sites for further geologic investigation. Integrated high-resolution mapping, including subregional-structure, isopach, lithofacies, and engineering-data maps integrated with seismic interpretation, provides useful perspectives of the spatial and temporal geologic history.

## ACKNOWLEDGMENTS

Thanks are given to reviewers of this manuscript, including Alan Byrnes at the Kansas Geological Survey (KGS); Mike Cochran of the Kansas Department of Health and Environment (KDHE); and Roberto Aguilera, Joe Ratigan, and Larry Fisher and his staff at ONEOK, Inc. Marla Adkins-Heljeson is thanked for providing editorial review. Thanks are also given to Alan Byrnes for his insights into fracture systems and to Joe Ratigan for sharing thoughts on underground gas storage. We gratefully acknowledge Rick Miller and his KGS Exploration Services staff, particularly Jianghai Xia for collecting and processing the seismic data. The KDHE and ONEOK, Inc., staff are thanked for sharing information and providing access to wells. Joe Palacioz, City Manager, and Dennis Clennan, Director of Public Works and Engineering, are thanked for their logistical support and encouragement. Thanks are given to Lee Allison for organizing the KGS response to the emergency and to Lee and Rex Buchanan for extensive public-relations activities related to the gas leak conducted on behalf of the University of Kansas and the Kansas Geological Survey. Tim Carr is thanked for general support of contributions from a number of his staff members in the KGS Petroleum Research Section. Larry Skelton is thanked for sharing his expertise of the local geology.

PETRA (GeoPLUS Corporation) was used for well-log correlations and mapping. The Kingdom Suite (Seismic Micro-Technology) was used for seismic modeling and interpretation. Both companies are thanked for providing software for use by the University of Kansas and the Kansas Geological Survey.

## REFERENCES CITED

Ahmed, Tarek, 2000, Reservoir Engineering Handbook: Gulf Publishing, Houston, 863 p.

Allison, M. L., 2001a, Hutchinson, Kansas—a geologic detective story: Geotimes, October, p. 14–18.

_____2001b, The Hutchinson gas explosions: unraveling a geologic mystery: Kansas Bar Association, 26th Annual KBA/KIOGA Oil and Gas Law Conference, v. 1, p. 18.

Anderson, N. L.; Hopkins, J. F.; Martinez, A.; Knapp, R. W.; Macfarlane, P. A.; Watney, W. L.; and Black R. A., 1994, Dissolution of bedded rock salt; a seismic profile across the active eastern margin of the Hutchinson Salt Member, central Kansas: Computers and Geosciences, v. 20, p. 889–903.

Anderson, N. L.; Watney, W. L.; Macfarlane, P. A.; and Knapp, R. W., 1995a, Seismic signature of the Hutchinson Salt Member and associated dissolution features, *in* Anderson, N. L.; Hedke, D. E.; Baars, D. L.; Crouch, M. L.; Miller, W. A.; Mize, F.; and Richardson, L. J. (eds.), Geophysical atlas of selected oil and gas fields in Kansas: Kansas Geological Survey Bulletin 237, p. 57–65.

Anderson, N. L.; Knapp, R. W.; Steeples, D. W.; and Miller, D. D., 1995b, Plastic deformation and dissolution of the Hutchinson Salt Member in Kansas, *in* Anderson, N. L.; Hedke, D. E.; Baars, D. L.; Crouch, M. L.; Miller, W. A.; Mize, F.; and Richardson, L. J. (eds.), Geophysical atlas of selected oil and gas fields in Kansas: Kansas Geological Survey Bulletin 237, p. 66–70.

Anderson, N. L.; Martinez, A.; Hopkins, J. F.; and Carr, T. R., 1998, Salt dissolution and surface subsidence in central Kansas; a seismic investigation of the anthropogenic and natural origin models—case history: Geophysics, v. 63, p. 366–378.

Bayne, C. K., 1956, Geology and ground-water resources of Reno County, Kansas: Kansas Geological Survey Bulletin 120, 130 p.

_____1977, Geology and structure of Cheyenne Bottoms—Barton County, Kansas: Kansas Geological Survey Bulletin 211, pt. 2, 12 p.

Beaty, S.; Watney, W. L.; and Martinez, A., 1999, Analysis of structural controls on the development of the Upper Pennsylvanian Tonganoxie incised paleovalley system of northeast Kansas, *in* Merriam, D. F. (ed.), Transactions: American Association of Petroleum Geologists Midcontinent Meeting, p. 141–151.

Bhattacharya, S.; and Watney, W. L., 2002, Analyses of data from vent wells around Yaggy gas storage facility, Hutchinson, Kansas: Kansas Geological Survey Open-File Report 2002-71.

Burns and McDonnell Engineering Company, Inc., 2003, Brine well abandonment project: Data Summary Report, City of Hutchinson, Kansas, City Improvement Project 2002 C118, Project no. 31747.

Gerhard, L. C., 2003, Preliminary lineament map of Kansas: Kansas Geological Survey Open-File Report 2003-7.

Gogel, T., 1981, Discharge of saltwater from Permian rocks to major stream-aquifer systems in central Kansas: Kansas Geological Survey Chemical Quality Series 9, 60 p.

Halliburton Energy Services, 2001, EMI Interpretation—OB #2, NE/4 Section 30-22s-6w: 4 p.

Holdoway, K. A., 1978, Deposition of evaporites and red beds of the Nippewalla Group, Permian, western Kansas: Kansas Geological Survey Bulletin 215, 43 p.

Kansas Department of Health and Environment, 2001, Locations of salt solution mining operations and methane gas incidents (2/2/01): Unpublished working map.

Lane, C. W.; and Miller, D. E., 1965, Geohydrology of Sedgwick County, Kansas: Kansas Geological Survey Bulletin 176, 100 p.

Martinez, A.; Anderson, N. L.; and Carr, T. R., 1996, Distribution and thickness of the Cimarron salt (Lower Permian) in southern Stafford and northern Pratt Counties, Kansas: Kansas Geological Survey Open-File Report 96-11, http://www.kgs.ku.edu/PRS/publication/OFR96_11/cim1.html.

Miller, R. D., 2002, High resolution seismic reflection investigation of the subsidence feature on U.S. Highway 50 at Victory Road near Hutchinson, Kansas; final report to Kansas Department of Transportation, District 5: Kansas Geological Survey Open-File Report 2002-7, 30 p., 6 pls., 3 appendixes.

Miller, R. D.; Steeples, D. W.; Schulte, L.; and Davenport, J., 1993, Shallow seismic reflection study of a salt dissolution well near Hutchinson, KS: Mining Engineering, v. 45, p. 1291–1296.

Newell, K. D.; and Hatch, J. R., 1999, Petroleum geology and geochemistry of a production trend along the McPherson anticline in central Kansas, with implications for long- and short-distance oil migration, *in* Merriam, D. F. (ed.), Geoscience for the 21st century; transactions of the 1999 American Association of Petroleum Geologists, Midcontinent Section Meeting: Kansas Geological Survey Open-File Report 99-28, p. 22–28.

Nissen, S. E.; Xia-J.; and Watney, W. L., 2002, Seismic detection of shallow natural gas beneath Hutchinson, Kansas: Society of Exploration Geophysicists, International Exposition and 72nd Annual Meeting; SEG Annual Meeting Expanded Technical Program Abstracts with Biographies, no. 72, p. 1547–1550.

Settari, A.; Warren, G. M.; Jacquemont, J.; Bieniawski, P.; and Dussaud, M., 1999, Brine disposal into tight stress-sensitive formations at fracturing conditions: design and field experience: Society of Petroleum Engineers, Reservoir Evaluation and Engineering, v. 2, p. 186–195.

Steeples, D. W.; Knapp, R. W.; and Miller, R. D., 1984, Examination of sinkholes by seismic reflection, *in* Beck, B. F. (ed.), Sinkholes—their geology, engineering, and environmental impact: Balkema, Boston, p. 217–223. (Proceedings of First Multi-disciplinary Conference on Sinkholes.)

Stockstad, E., 2002, Data dilemma—stow it, or kiss it goodbye: Science, v. 297, p. 181–183.

Swineford, A., 1955, Petrography of Upper Permian rocks in south-central Kansas: Kansas Geological Survey Bulletin 111, 179 p.

Van Schmus, W. R.; Bickford, M. E.; and Turek, A., 1996, Proterozoic geology of the east-central Midcontinent basement, *in* van der Pluijm, B. A.; and Catacosinos, P. A. (eds.), Basement and basins of eastern North America: Geological Society of America Special Paper 308, p. 7–32.

Ver Wiebe, W. A., 1937, Cretaceous deformation in Kansas: American Association of Petroleum Geologists Bulletin, v. 21, p. 954–958.

Walters, R. F., 1978, Land subsidence in central Kansas related to salt dissolution: Kansas Geological Survey Bulletin 214, 32 p.

Watney, W. L.; and Paul, S. E., 1980, Maps and cross sections of the Lower Permian Hutchinson Salt Member in Kansas: Kansas Geological Survey Open-File Report 80-7, 11 p., 9 maps, 3 cross sections.

Watney, W. L.; Berg, J. A.; and Paul, S. E., 1988, Origin and distribution of the Hutchinson Salt Member (lower Leonardian) in Kansas, *in* Morgan, W. A.; and Babcock, J. A. (eds.), Permian rocks of the Mid-continent: Society of Economic Paleontologists and Mineralogists, Midcontinent Section, Special Publication 1, p. 113–135.

Watney, W. L.; Kruger, J.; Davis, J. C.; Harff, J.; Olea, R. A.; and Bohling, G. C., 1999, Validation of sediment accumulation regions in Kansas, U.S.A., *in* Harff, J. (ed.), Computerized basin analysis [Proceedings of symposium, Computerized Modeling of Sedimentary Systems]: Springer, New York, p. 341–360.

Watney, W. L.; Guy, W. J.; and Byrnes, A. P., 2001, Characterization of the Mississippian Osage chat in south-central Kansas: American Association of Petroleum Geologists Bulletin, v. 85, p. 85–114.

Watney, W. L.; Byrnes, A.; Bhattacharya, S.; Nissen, S.; and Anderson, A., 2003, Natural gas explosions in Hutchinson, Kansas—geologic factors [abstract]: Geological Society of America Abstracts with Programs, v. 35, no. 2, p. 33.

Xia, J.; Miller, R. D.; and Adkins-Heljeson, D. M., 1995a, Residual bouguer gravity map of Kansas, the second-order regional trend removed: Kansas Geological Survey Map Series 41(E), 1 sheet, scale 1:1,000,000.

_____1995b, Residual aeromagnetic map of Kansas, the second-order regional trend removed: Kansas Geological Survey Map Series 41(F), 1 sheet, scale 1:1,000,000.

Young, C. M., 1926, Subsidence around a salt well: Transactions, American Institute of Mining Engineers, v. 74, p. 810–817.

# Subsidence on Interstate 70 in Russell County, Kansas, Related to Salt Dissolution—A History[1]

***Neil M. Croxton***
Kansas Department of Transportation
Abilene, Kansas

**ABSTRACT.**—A short section of Interstate 70 in Russell County, Kansas, crosses two active sinkholes, the Crawford Sink and the Witt Sink. These sinkholes have slowly and steadily pulled down the driving lanes since the highway was constructed in the mid-1960s. They are the result of dissolution of a thick salt bed >1,300 ft below the surface. Oil-drilling activity has allowed fresh water to pass through the salt, dissolving a considerable volume of salt and causing the overlying strata to sink. Two areas of this highway have been re-graded at significant cost. Efforts were made in 1986 to stop the subsidence at one of the sinkholes, but the lanes continue to drop. Eventually, a nearby bridge will have to be replaced because of the subsidence. The Russell County sinkholes continue to be costly objects of attention to geologists and engineers at the Kansas Department of Transportation.

## DISCOVERY OF THE CRAWFORD SINK

All highway construction in Kansas is preceded by a geological survey. When geology crews began their preliminary studies for this section of Interstate 70 in the early 1960s, there was a large pond along the right-of-way 6 mi west of Russell (Fig. 1). They noticed that the pond appeared rather deep, and although it was situated in a streambed, it apparently had no dam (Fig. 2). Asking around among local residents, Highway Commission geologists were told that the pond had always been there. An 83-year-old woman who had lived in the area all her life reported that there had been a pond in that location ever since she could remember. Little additional thought, therefore, was given to the mysterious origin of the pond. During construction the pond was filled in, and the highway was built, along with a nearby bridge to carry county traffic over the highway. Final grading for the new lanes was finished in the spring of 1966.

But something was wrong. Just east of the new bridge, exactly where the pond had been, the subgrade kept dropping. Since it was a stream crossing and a fill section, Highway Commission officials at first just assumed that the fill dirt was settling. But it was not just the lanes that were sinking. A few quick level runs confirmed the worst: the new interstate, the pride of western Kansas, had been built right over a sinkhole.

The summer of 1966 was a busy one for our geology crews. While the I-70 lanes were being paved on either side, geologists and their technicians scrambled

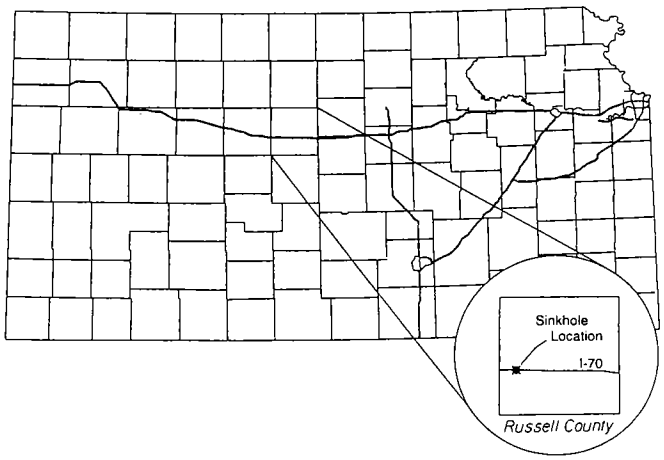


Figure 1. Map of Kansas showing the location of the Crawford sinkhole along Interstate 70.

to find out what was causing the sinking. Someone thought to check some air photographs of the region that were taken in the 1950s. There was no pond. The locals had been wrong—the deep pond with no dam was a relatively new feature. And the State Highway Commission of Kansas had a big problem.

### Cause of the Subsidence

I-70 in this area is aligned through the heart of the Gorham oil field. This is a densely drilled part of the State, and although sinkholes had not caused much trouble at the time, geologists quickly suspected that the subsidence was caused by improper plugging of abandoned wells. Research into oil-field geology and

[1]Reprinted, with modifications, from *The Professional Geologist*, v. 39, no. 8, p. 2–7.

Croxton, N. M., 2003, Subsidence on Interstate 70 in Russell County, Kansas, related to salt dissolution—a history, *in* Johnson, K. S.; and Neal, J. T. (eds.), Evaporite karst and engineering/environmental problems in the United States: Oklahoma Geological Survey Circular 109, p. 149–155.

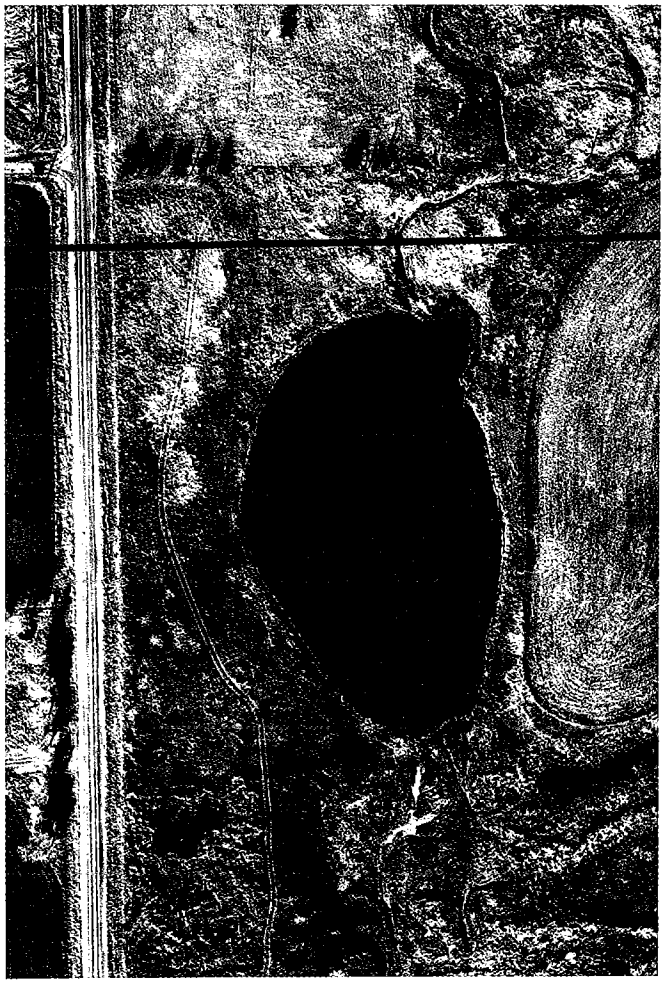

Figure 2. Air photograph taken in the early 1960s, used in the planning for I-70. The large pond (Crawford Sink) was filled during construction. The alignment of the future interstate highway is shown by the black line. North is at top.

deep ground-water movement led the Highway Commission to the cause—dissolution of the Hutchinson Salt Member of the Permian Wellington Formation.

In western Russell County the Hutchinson Salt is 270 ft thick, and its top is 1,300 ft below the surface. Above the salt are three sandstone units—the Dakota Formation and Cheyenne Sandstone of Cretaceous age, and the Cedar Hills Sandstone of Permian age. All three are characterized by considerable flows of fresh or brackish water.

Oil wells in the Gorham field were drilled through the salt to a structural high in strata of the Lansing–Kansas City Group (Pennsylvanian) and the Arbuckle Group (Cambrian–Ordovician). Hundreds of wells were drilled here, beginning in the 1920s; many have since been abandoned. If an abandoned well is not plugged correctly, the fresh water flowing through the overlying sandstones pours down the borehole to replace water taken out of oil-producing layers by nearby active wells. On the way down, the fresh water washes across the salt face, dissolving it. The cavity in the salt grows, and eventually overlying beds sag downward until the depression shows up on the surface.

The sinkhole east of the bridge was named the Crawford Sink, after the Crawford oil lease. Two wells 50 ft apart are at the center of the sink, the No. 12 Crawford and the No. 16 Crawford. Both were drilled in 1937 and abandoned in the early 1940s.

## INVESTIGATION OF THE SINKHOLES

Geologists with the State Highway Commission of Kansas realized that the highway was probably safe as long as the sinking continued. But the I-70 project was too high-profile to take chances with, so during the summer of 1966, before the highway opened, a test hole was drilled and cored in the Crawford Sink to a depth of 240 ft. (This remains the deepest hole ever drilled by our crews.) Only solid bedrock was encountered the entire way. The geologist who logged the hole called the cores "as perfect cores as you could ever find in that section." The crews also drilled and dug down to the Cretaceous Fencepost Limestone, which is close to the surface here. A structural-contour map was drawn that showed the bowl-shaped drop in strata (Fig. 3). Officials were reasonably sure there was not a void under the highway that could suddenly cause a collapse.

At about that time, still before the highway was open, construction crews had more bad news: another section of road was not holding its profile. This area was half a mile west of the Crawford Sink. The oil well responsible was the No. 1 Witt A, just south of the right-of-way. This well was drilled in 1937 and plugged in 1957.

Highway Commission engineers and geologists got together late that summer (1966) to decide how to proceed. There was serious talk of rerouting the highway around the sinkholes, despite the enormous cost and delays. But the Gorham oil field stretches several miles to the north and south. Geologists told officials there was no way to guarantee that a new alignment would not put I-70 over other sinkholes. Because there was no apparent danger to the public, the lanes in the subsidence area were paved that fall. I-70 between Russell and Hays opened on schedule November 16, 1966.

The next summer the Highway Commission contracted with a drilling company to drill a deep exploratory well at the Crawford site. A crew with Rosencrantz-Bemis Drilling, of Great Bend, Kansas, drilled to 100 ft below the base of the Hutchinson Salt to a total depth of 1,670 ft (Fig. 4). Circulation was lost at 250 ft and never regained, which was attributed to washing of loose material at and below the Dakota Formation. Analysis of a gamma-ray–neutron log indicated that the salt itself was washed along its entire thickness and had been replaced by material from above. An anhydrite marker bed 350 ft above the salt had, at that time, already dropped 36 ft (Fig. 5). Most importantly, however, very few voids were found, and

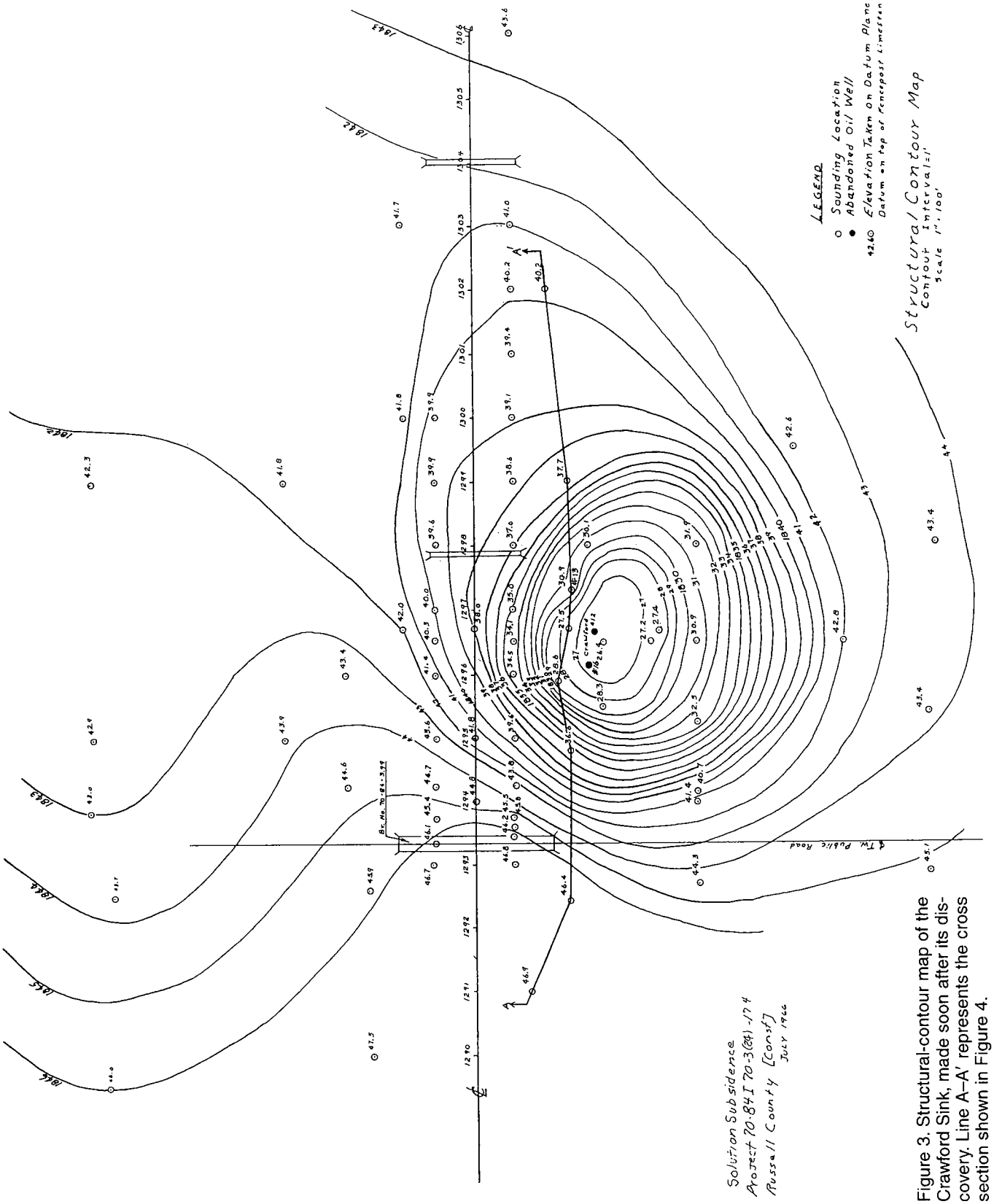


Figure 3. Structural-contour map of the Crawford Sink, made soon after its discovery. Line A–A' represents the cross section shown in Figure 4.

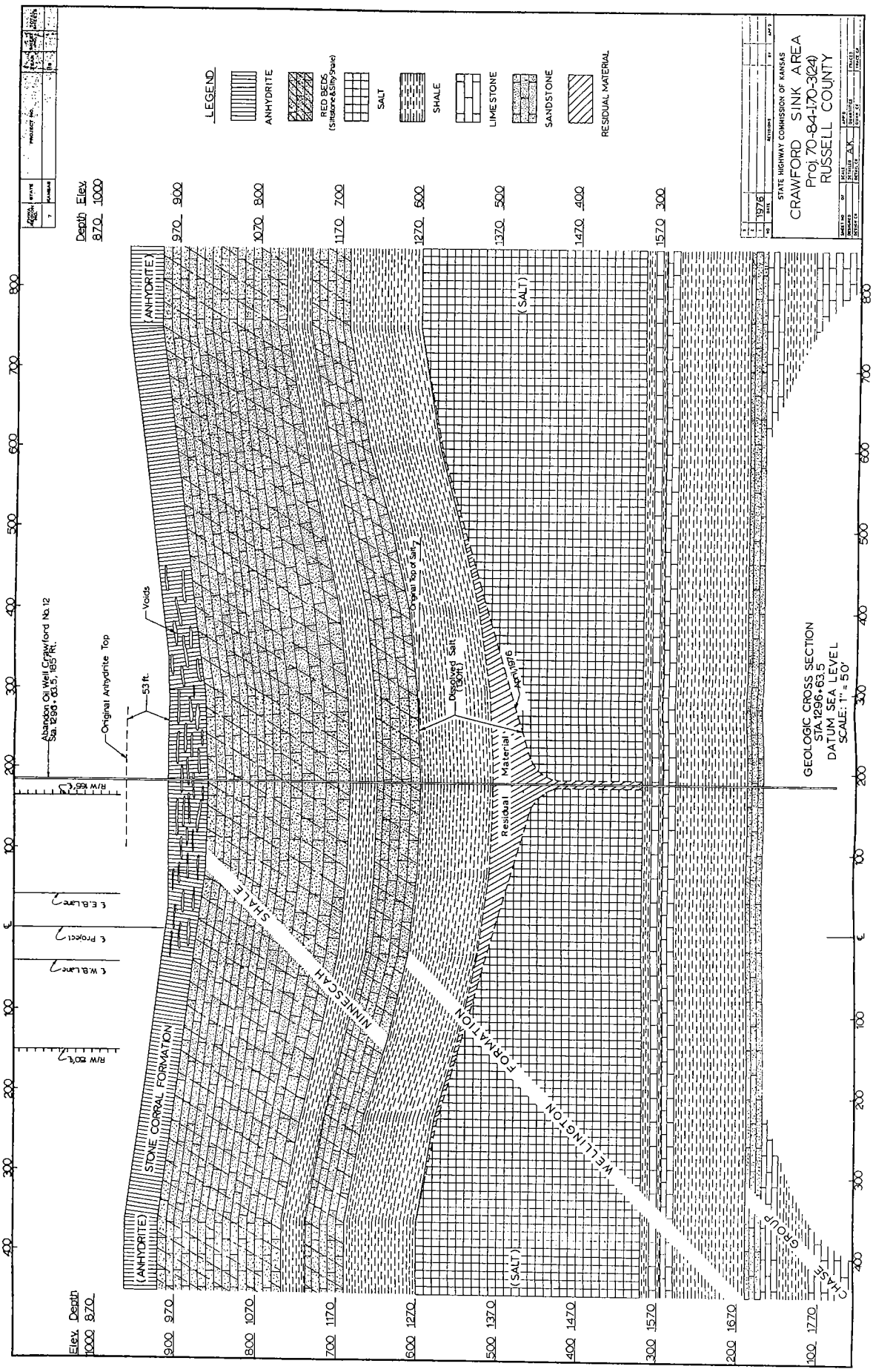


Figure 4. Cross section A–A′ of the strata through and below the Crawford Sink, drawn after the initial deep study in 1967. See Figure 3 for line of section.

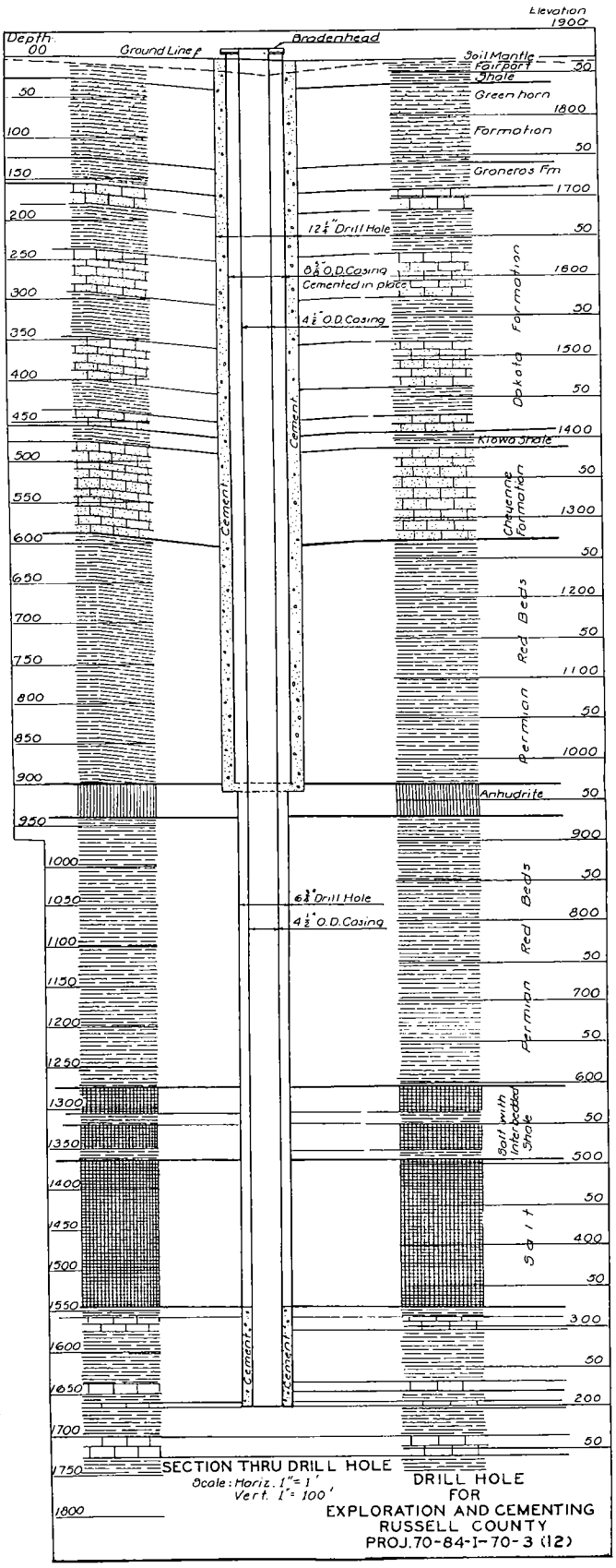


Figure 5. Cross section of strata penetrated by a hole drilled for the first grouting attempt in 1986.

none of these were large or near the surface. Officials told the public that the highway was safe and that the sinkholes would cause only minor damage to the highway.

## THE 1970S

Nothing was done for a few years. The sinkholes continued to get deeper and broader, and the pond at the Crawford site re-formed. The Witt Sink, which formed near the top of a ridge, created a noticeable depression. By 1971, the lanes had dropped so much that they had to be regraded. During the summer of that year, both areas were brought up 5 ft and re-paved at a cost of $220,000. Elevations of the lanes and the bridge were taken every 6 months, making it the most surveyed section of road in the State. The highway continued to drop at almost 6 in. per year. Public relations in the area began to sour when local newspapers figured out that the subsidence showed no sign of stopping. Still, there was no danger, and people gradually got used to sinkholes under I-70. It became old news.

Overnight on May 1 or 2, 1978, however, a huge sinkhole suddenly opened in a field 20 mi northwest of the I-70 sinks. This hole, in northeastern Ellis County, was also centered on an old well. In a few days the hole was 75 ft across and 100 ft deep. The press coverage of the nearby sudden collapse forced the Highway Department, now KDOT, into action once again.

Our geologists were still reasonably sure that the gradual subsidence of the highway was a good indication that nothing catastrophic was going to happen to I-70. But, primarily in response to public pressure, new studies were ordered late that year. The Kansas Department of Health and Environment (KDHE) and the Kansas Geological Survey (KGS) helped this time. Not enough money was available to do any deep drilling, but the KGS ran seismic refraction surveys along both the I-70 sinkholes and near the Ellis County collapse. Again, no near-surface voids were found beneath I-70—only a few deep voids. No satisfactory conclusions were ever drawn, however, as to why the Ellis County sinkhole behaved differently than the I-70 sinks.

In addition, the KDHE took infrared air photographs of the Gorham oil field to try to identify new sinkholes that might be developing. The idea was that shallow surface depressions would hold water after rainfall, and therefore show more lush vegetation. Regular air photos were taken early in the morning and late in the afternoon to try to find new sinks highlighted by shadows cast by the low-angle sunlight. Neither of these endeavors yielded much useful information. The *Hays Daily News* took credit for instigating the investigations; the uproar finally died down.

## ATTEMPT TO STOP SUBSIDENCE AT THE WITT SINK

By August 1984, the lanes at the Witt Sink were back down 8 ft. This drop was starting to cause sight-

distance problems: engineers were afraid that a stalled car at the bottom of the depression would be rear-ended. So this section of highway was again regraded and repaved at a cost of nearly $500,000.

KDOT engineers in that district were beginning to get more and more concerned. There didn't seem to be any end to the subsidence, and public relations in the Hays–Russell area were a serious problem. In January 1986 the State again contracted with a drilling company. The goal this time was to stop subsidence at the Witt sinkhole by shutting off the flow of water across the salt.

A hole was drilled 4 ft west of the old No. 1 Witt A well to a total depth of 1,948 ft (see Fig. 5). This depth is ~400 ft below the base of the salt. Circulation was lost at 157 ft and never regained. A thickness of 124 ft of the salt was dissolved at that time, having been replaced by soft, residual material. No major voids were found during the drilling. Casing was set and cemented.

The casing was perforated between 1,930 and 1,940 ft, in a limestone zone below the Wellington Formation. The limestone was acidized and fractured in an attempt to establish communication with the original No. 1 Witt A hole.

After re-cementing, the casing was again perforated, this time at the base of the salt between 1,538 and 1,548 ft. Fresh water was then pumped at 4–5 gallons a minute in an attempt to wash through the basal salt and reach the old hole. After 400 barrels of water had been used, there was a pressure drop. Then 200 cubic yards of cement with additives was squeezed to try to plug the old well at the base of the salt.

More than 30 cubic yards of cement was pumped down the new hole until pressure built up. Satisfied that the breach below the salt had been sealed, officials resumed their frequent surveys of the lanes. And, in fact, this procedure worked—for a while. For 6 months the lanes did not move. But somehow, water got around the plug, and the highway quickly resumed its subsidence of 5–6 in. a year.

In 1988, more cement was pumped down both holes at the Witt sink. This cement was saturated with salt in the hope that it would bond to the salt face itself. After "lubricating" the hole and cavity with 200 sacks of bentonite, drillers pumped almost 100 cubic yards of the salt-rich cement down the holes. Eventually, pressure built up to 300 psi in both wells at the same time. The voids in the immediate vicinity of the boreholes were filled, and KDOT geologists were again cautiously optimistic. Again, their optimism was short-lived, because water soon ate another hole in the salt and the subsidence continued.

Nothing has been done at the sinkholes since this attempt to stop movement at the Witt Sink. A drilling program of several holes in a circular pattern around each original well would probably give the best chance of stopping the subsidence. No one can guess the quantities of cement or other fill material that would be required to fill the voids at depth. Of course, the tremendous cost of such an undertaking is a concern, especially since there is no guarantee that it would succeed. In the current economic climate, it seems unlikely that another attempt will be made to halt the subsidence in the foreseeable future.

## THE BRIDGE

The highway in the vicinity of the Witt Sink can be regraded as many times as necessary. The Crawford Sink is a different matter. It cannot be regraded any more because of clearance requirements under the nearby bridge; the bridge is sinking, too. One end of the two-pier concrete structure has dropped >6 ft since it was built in 1965. At the south abutment the east curb is now 2 ft higher than the west curb. Strangely, about the only indication that the bridge is under any stress at all is narrow cracks in the curbs just over the piers. Except for its noticeable tilt to the east, the structure looks like any other 35-year-old bridge in Kansas.

## FUTURE OF THE RUSSELL COUNTY SINKS

After more than a decade of inactivity, work is once again planned for I-70 in the vicinity of the sinkholes. The Crawford Sink (Fig. 6) is the biggest concern: either it will finally subside enough to become a sight-distance problem, or water will begin to cover the roadway during storms. A current project proposal calls for removing the bridge over the highway at the Crawford sinkhole and closing the county road. The roadbed—which in addition to dropping has in recent years developed a distinct tilt to the south—can then be brought back to grade. The highway will also be regraded through the Witt area. This reconstruction project was scheduled to start in November 2003.

Meanwhile, traffic continues to go over the sinks at a count of more than 11,000 vehicles a day (Fig. 7). The Witt Sink continues to drop at a rate of 5 in. a year; the Crawford Sink is subsiding at ~4 in. a year (Fig. 8). The Witt and Crawford areas will keep sinking until the Gorham oil field is finally abandoned and water is no longer drawn out of the strata below the salt.

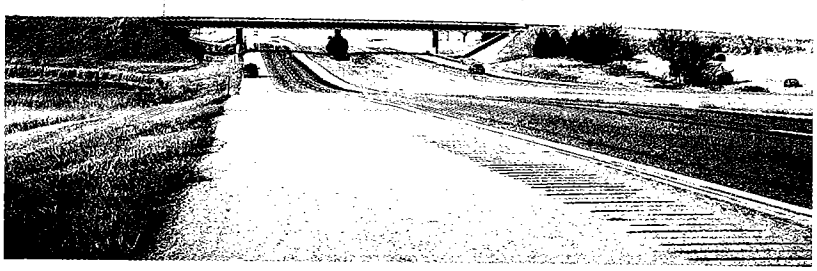

Figure 6. View looking west across the Crawford Sink.

## SUMMARY

Improper plugging of abandoned oil wells in Russell County led to the development of two large salt-related sinkholes beneath Interstate 70. The Kansas Department of Transportation has struggled with costly, embarrassing repairs and a failed attempt at remediation during the 35-year history of the highway. Despite our knowing in detail the cause of the subsidence, an economical solution has eluded us. At present, KDOT plans simply to regrade the lanes for as long as possible. The sinkholes will continue to consume our time and resources well into the 21st century.


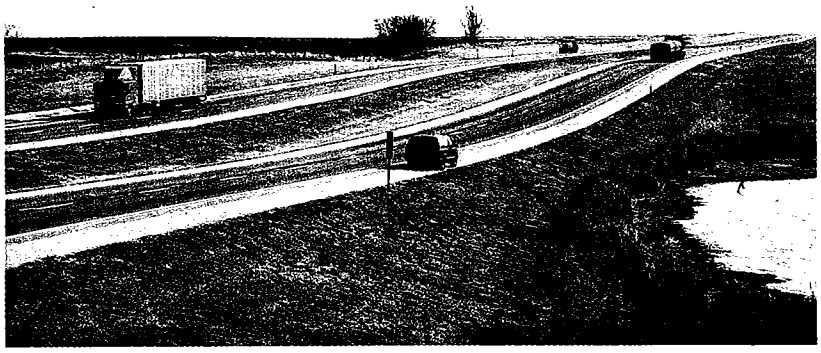

Figure 7. View looking northeast across the Crawford Sink.


## ACKNOWLEDGMENTS

Most of the information presented in this paper was taken from records and reports on file at the KDOT Geology Section in Topeka, Kansas. In addition, the author would like to acknowledge valuable information gained from interviews with the following individuals, all of whom work or have worked for the KDOT: Mr. Wally Taylor, regional geologist, northwest region (retired); Mr. Larry Rockers, chief geologist (retired); Mr. Ron Sherard, area engineer at Hays (retired); and Mr. Wes Moore, district maintenance engineer at Norton. Alex Kotoyantz, regional geologist, northwest region (retired) drew Figures 3 and 4. Recognition is also given to the photo section in Topeka for their assistance in preparing the photographs for this paper, and to Jeff Geist, R. J. Crow, and Lynn Byrne for their help in preparing the diagrams for publication.


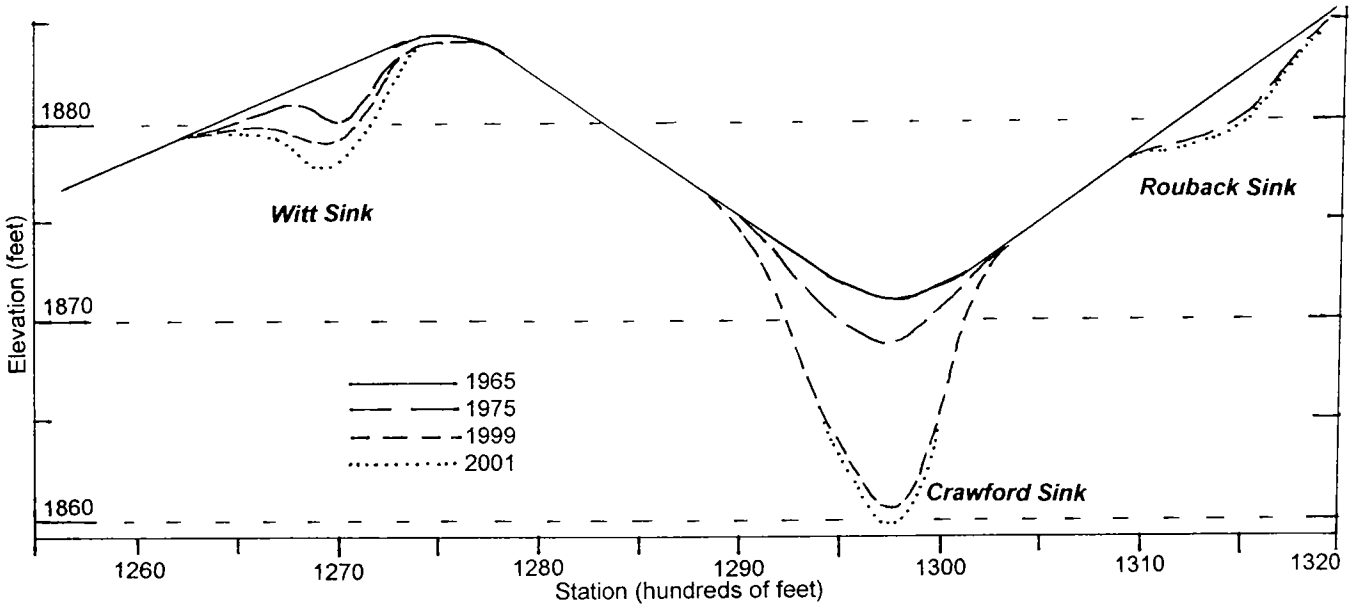


Figure 8. Profile of the eastbound lanes of I-70 in the area, comparing elevations of the original grade (in 1965) and those surveyed in 1975, 1999, and May 2001. The small Rouback Sink to the east moved slightly in the 1970s but has since stabilized. The current shallow nature of the Witt Sink in this profile is due to filling in the sink and regrading the highway two times (in 1971 and 1986).

# High-Resolution Seismic-Reflection Investigation of a Subsidence Feature on U.S. Highway 50 near Hutchinson, Kansas

***Richard D. Miller***
Kansas Geological Survey
Lawrence, Kansas

**ABSTRACT.**—High-resolution seismic reflections were used to map the upper 150 m of the ground surface around and below an actively subsiding sinkhole currently affecting the stability of U.S. Highway 50 in Reno County, Kansas. Primary objectives of this study were to delineate the subsurface expression of this growing sinkhole induced by salt dissolution and appraise its threat to highway stability and the characteristically heavy commercial traffic load. The high signal-to-noise ratio and resolution of these seismic-reflection data allowed detection, delineation, and evaluation of rock failure and associated episodes of material collapse into voids left after periodic and localized leaching of the 125-m-deep, 40-m-thick Hutchinson Salt Member of the Wellington Formation (Permian).

Mechanisms and gross chronology of structural failures as interpretable from stacked seismic sections suggest that initial subsidence and associated bed offset occurred as accumulated stress was rapidly released and was constrained to a tensional dome defined by reverse-fault planes. As the downward movement (settling, relaxation) of sediments slowed with little or no incremental buildup of stress, gradual subsidence continued in the subsurface, advancing as an ever-expanding bowl, geometrically defined by normal-fault planes.

## INTRODUCTION

Sinkholes are common hazards to property and human safety the world over (Beck and others, 1999). Their formation is generally associated with subsurface subsidence that occurs when overburden loads exceed the strength of the roof rock bridging voids or rubble zones formed as a result of dissolution or mining. Understanding sinkhole processes and what controls their formation rate is key to reducing their impact on human activities, and in the case of anthropogenic causes, potentially avoiding their formation altogether. Sinkholes can form naturally or anthropogenically from the dissolution of limestone (karst), gypsum, or rock salt, or from mine/tunnel collapse. With the worldwide abundance of limestone, karst-related sinkholes are by far the most commonly encountered and studied. Both simple and complex sinkholes have formed catastrophically and/or gradually as the result of dissolution of limestone or rock salt, and by natural and man-induced dissolution processes in many parts of Kansas (Merriam and Mann, 1957).

In central Kansas, most sinkholes are the result of leached-out volumes of the Permian Hutchinson Salt Member of the Wellington Formation (Watney and others, 1988). Sinkholes that have formed above salt layers have been studied throughout Kansas (Frye, 1950; Walters, 1978) and the United States (Ege, 1984). Studies of subsidence related to mining of the salt around Hutchinson, Kansas (Walters, 1980), disposal of oil-field brine near Russell, Kansas (Walters, 1991), and natural dissolution through fault/fracture-induced permeability (Frye and Schoff, 1942) have drawn conclusions about the mechanism responsible for subsidence geometries and rates based on surface and/or borehole observations.

Using only surface observations and borehole data, a great number of assumptions and a good deal of geologic/mechanical sense must be drawn on to define and explain these features and their impact. High-resolution seismic-reflection profiling has proven an effective tool in three-dimensional (3-D) mapping of the subsurface expression and predicting future surface deformation associated with dissolution of the Hutchinson Salt in Kansas (Steeples and others, 1986; Miller and others, 1993, 1995, 1997; Anderson and others, 1995a).

Salt-dissolution sinkholes are found in all areas of Kansas where the Hutchinson Salt is present in the subsurface. Sinkholes have been definitely correlated to the failed containment of disposal wells into which oil-field brine was injected. This correlation was determined by means of stem pressure tests and/or seismic-reflection investigations at a variety of sites throughout central Kansas (Steeples and others, 1986; Knapp and others, 1989; Miller and others, 1995, 1997). Sinkholes that have formed by natural dissolu-

Miller, R. D., 2003, High-resolution seismic-reflection investigation of a subsidence feature on U.S. Highway 50 near Hutchinson, Kansas, *in* Johnson, K. S.; and Neal, J. T. (eds.), Evaporite karst and engineering/environmental problems in the United States: Oklahoma Geological Survey Circular 109, p. 157–167.

tion and subsidence processes are most commonly documented at the depositional edges on the west and north and at the erosional boundary on the east of the Hutchinson Salt (Frye and Schoff, 1942; Frye, 1950; Merriam and Mann, 1957; Anderson and others, 1995a). The vast majority of published works studying the source of localized leaching of salt in Kansas directly contradict suggestions that recent land subsidence in Kansas is mostly natural in origin (Anderson and others, 1995a).

Natural dissolution of the Hutchinson Salt is not uncommon in Kansas and has been occurring for millions of years (Ege, 1984). Faults extending up to Pleistocene sediments containing fresh water under hydrostatic pressure are postulated as the conduits that instigated salt dissolution and subsidence along the western boundary of the salt in Kansas (Frye and Schoff, 1942). Paleosinkholes resulting from dissolution of the salt before Pleistocene deposition were discovered previously with high-resolution seismic surveys (Anderson and others, 1998).

Subsidence can occur at rates ranging from gradual to catastrophic. These rates are, to some extent, related to the type of deformation in the salt (ductile or brittle) and the strength of rocks directly above the salt layer. As salt is leached, the resulting pore space provides the differential pressure necessary to support creep (Carter and Hansen, 1983). If this pore space gets large enough to exceed the strength of the roof rock, the unsupported span will fail, and subsidence occurs. Depending on the strength of the roof rock, and therefore the size of the void, characteristics of the failure within and just above the salt will dictate how the void progresses upward until it eventually reaches the ground surface. In general, gradual surface subsidence is associated with ductile deformation that, besides vertically sinking, progresses outward, forming an ever-growing bowl-shaped depression with bed geometries and offsets constrained by normal-fault geometries (Steeples and others, 1986; Anderson and others, 1995b). When rapid to catastrophic subsidence rates are observed, failure within the salt is usually brittle, with the void area migrating to the surface as an ever-narrowing cone with bed offsets and rock failure controlled by reverse-type fault planes (Davies, 1951; Walters 1980; Rokar and Staudtmeister, 1985).

Seismic-reflection data targeting beds altered by dissolution and subsidence in this area have ranged in quality and interpretability from poor (Miller and others, 1995) to outstanding (Miller and others, 1997). Interpretations from poor-quality data have unfortunately been relegated to indirect inference of structural processes and subsurface expression (mainly from interpretations of structural deformation in layers above the salt) owing to low signal-to-noise ratios. However, data with excellent signal-to-noise ratios and resolution have allowed direct detection of structures and geometries that appear characteristic of complex sinkholes. The resolution potential and signal-to-noise ratio of seismic data from this study are superior to those of any studies previously published that have targeted the salt interval. These data provide conclusive images of important structural features and unique characteristics that control sinkhole development.

The sinkhole that is the subject of this study is centered a few tens of meters northwest of the intersection of U.S. Highway 50 and Victory Road in Reno County (Fig. 1). The symmetry and compact nature of the sinkhole, as well as its subsidence rate, are consistent with conceptual models of sinkhole formation when salt is leached by borehole-released fluids (Miller and others, 1997). These similarities in geometry and subsidence rates raise suspicions that this feature might somehow be related to the disposal of oil-field wastewater, even though no records or surface installations exist to support that suggestion. Two seismic-reflection profiles acquired orthogonally, and centered on the intersection of the highway and county road, provided optimal coverage for mapping bed geometries, growth potential, and future surface footprints for identifying structural characteristics that might someday put vehicle traffic at risk.

## GEOLOGIC SETTING

Several major salt basins exist throughout North America (Ege, 1984). The Hutchinson Salt Member of the Wellington Formation is present in central Kansas, northwestern Oklahoma, and the northeastern part of the Texas Panhandle and is prone to, and has an extensive history of, dissolution and formation of sinkholes (Fig. 1). In Kansas the Hutchinson Salt possesses an average net thickness of 76 m and reaches a maximum of >152 m in the southern part of this salt basin. Deposition that occurred during fluctuating sea levels caused numerous halite beds, 0.15 to 3 m thick, to be interbedded with shale, minor anhydrite, and dolomite/magnesite. Individual salt beds may be continuous for only a few miles, despite the remarkable lateral continuity of the salt as a whole (Walters, 1978).

Rock salt under a depositional load is almost incompressible, highly ductile, and easily deformed by creep (Baar, 1977). Plastic deformation of the salt associated with creep is expected naturally to occur in these salts (Anderson and others, 1995b). Thin anhydrite beds within the halite succession have a strong acoustic response. Considering the extreme range of possible strain rates the salt can undergo during creep deformation, some of these thin interbeds possess quite dramatic, high-frequency folds within relatively short distances.

Red-bed evaporites that overlie the Hutchinson Salt are a primary target of any study in Kansas that looks at salt-dissolution sinkhole development and associated risks to the environment and human activity. The failure and subsidence of these evaporite units are responsible for the eventual formation of sinkholes and provide a pathway for ground water to gain access to

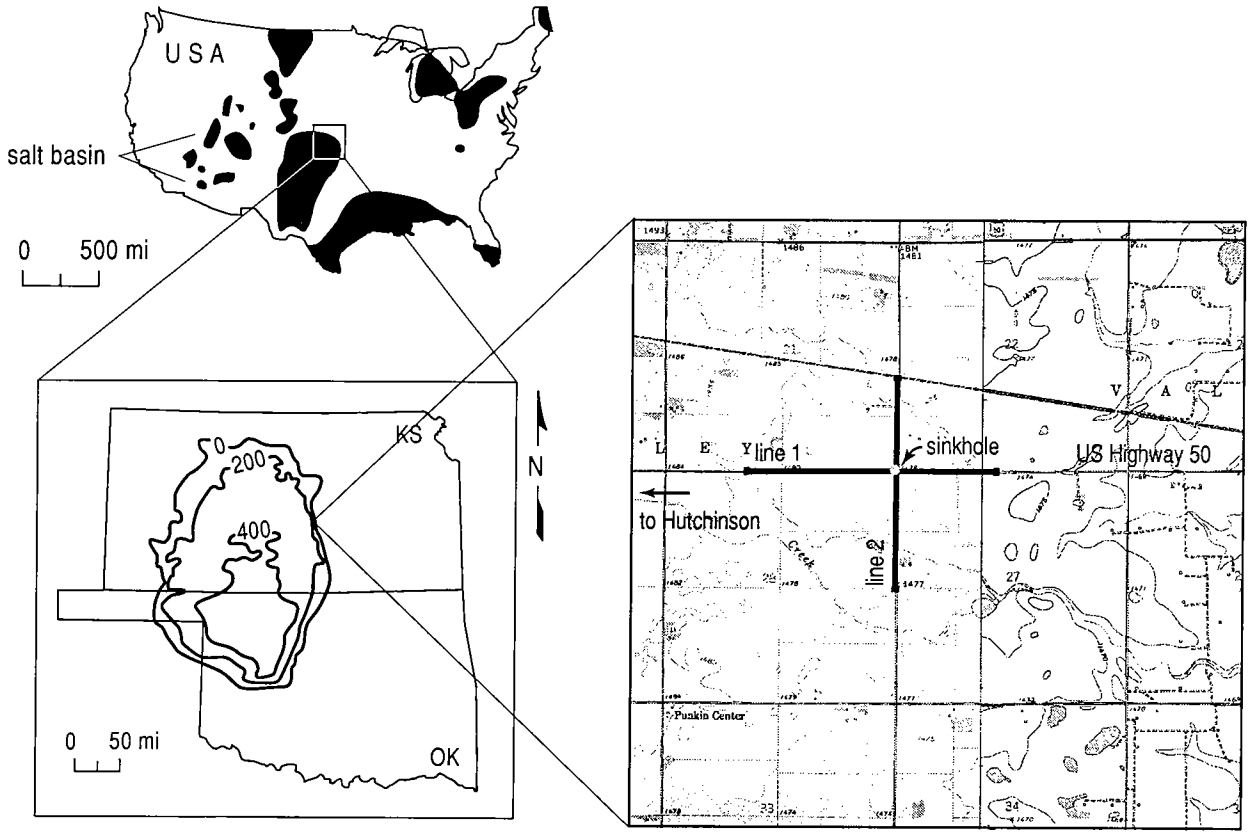


Figure 1. Site map relative to bedded salt deposits. The Hutchinson Salt is a bedded salt deposit extending from central Oklahoma across most of south-central Kansas. Along the eastern extremity of the salt bed is the currently active dissolution front responsible for many natural dissolution features, both sinkholes and paleosubsidence. Two 1.2-km seismic profiles tie at the intersection of U.S. Highway 50 and Victory Road in Reno County, Kansas.

the salt. In proximity to the dissolution front, fractures, faults, and collapse structures compromise the confining properties of the Permian shale bedrock and put the major freshwater aquifer (the Pliocene–Pleistocene Equus Beds) in this part of southern Kansas at risk. Along the eastern boundary (dissolution front), the salt, which ranges from 0 to >100 m thick, is buried beneath ~120 m of Permian red-bed evaporites.

The eastern margin of the salt was exposed during the late Tertiary Period, when erosion and leaching began the 30-km westward progression of the front to its present-day location (Bayne, 1956). The ability of the front to migrate while under as much as 100 m of sediments was a direct consequence of ready access to an abundant supply of ground water (Watney and others, 1988). The subsidence of Permian, Cretaceous, and Tertiary rocks has progressed along the migration front as the salt has been leached away. While this subsidence was going on, Quaternary alluvium was being deposited in volumes consistent with the amount of salt that was being removed. These processes resulted in today's moderate to low surface relief that masks the extremely distorted (faulted and folded but non-tectonic) rock layers within the upper Wellington Formation and the overlying Ninnescah Shale (Anderson and others, 1998). About 30 m of salt is still in place at the U.S. 50–Victory Road site, where a maximum of ~85 to 100 m once existed.

Most of the upper 700 m of rock at this site consists of Permian shales (Merriam, 1963). The currently disputed Permian–Pennsylvanian boundary is ~700 m deep and seismically marked by a strong sequence of cyclic reflecting events. The Chase Group (top at 250 m deep), Lower Wellington shales (top at 175 m deep), Hutchinson Salt (top at 125 m deep), Upper Wellington shales (top at 70 m deep), and Ninnescah Shale (top at 25 m deep) make up the packets of reflecting events easily identifiable and segregated within the Permian portion of the section. Bedrock is defined as the top of the Ninnescah Shale, with the unconsolidated Pliocene–Pleistocene Equus Beds making up most of the upper 30 m of sediment. The thickness of Quaternary alluvium that fills the stream valleys and paleosubsidence features ranges from 0 to as much as 100 m, depending on the dimensions of the features.

## SEISMIC ACQUISITION

To ensure that the entire subsurface "root" of the sinkhole was clearly imaged, the survey was designed with two seismic lines, each possessing at least 1.0 km of full-fold subsurface coverage centered on the sinkhole (Fig. 1). With the sinkhole conveniently lo-

cated at the intersection of U.S. 50 and Victory Road, two orthogonal seismic lines were acquired along the roads where surface materials and coupling were relatively consistent. These data were acquired using a rolling fixed-spread design that eliminated the need for a roll-along switch and extended the range of far offsets available during processing. This survey design provided the wide range of source offsets necessary for detailed velocity analysis, and the close receiver spacing for improved confidence in event identification; and it maximized the range of imageable depths.

Acquisition parameters were defined on the basis of experience and walkaway tests along line 1 (Fig. 1). Twin Mark Products L28E 40-Hz geophones were planted at 2.5-m intervals in approximate 1-m arrays. They were planted into firm to hard soil at the base of the road ditch in small divots left after the top few inches of loose material was removed to ensure good coupling. Four 60-channel Geometrics StrataView seismographs were networked to simultaneously record 240 channels of data. An IVI Minivib using a prototype Atlas valve delivered three 10-s, 25–250-Hz upsweeps at each 5-m spaced shot location. Experiments at this site were consistent with bench tests, which suggested that this new rotary-valve design will produce up to 4 times the peak force of conventional valves at 250 Hz. The pilot was telemetried from the vibrator to the seismograph and recorded as the first trace of each shot record. Each of the three sweeps generated per shot station was individually recorded and stored in an uncorrelated format with the ground-force pilot occupying channel 1.

Reflections can be interpreted on raw, correlated shot records (scaled for display purposes) from ~30 ms to two-way-traveltime depths >500 ms (Fig. 2). Considering the optimum window (Hunter and others, 1984) these data possess, it was imperative to keep a wide range of offsets to ensure that the entire target zone was imaged. Reflections with dominant frequencies of ~200 Hz can be interpreted as deep as 200 ms, whereas the dominant frequency of reflections at 500 ms have dropped to ~100 Hz. Several milliseconds of reflection "chatter" observable between traces in proximity to the sinkhole is indicative of the dramatic localized changes in material velocities associated with rock-layer failure and subsidence. Considering that the dominant frequency of some reflections exceeds 200 Hz, a 2.5-ms static between adjacent traces represents a 180° phase shift and complete cancellation. Therefore, it is critical that these static irregularities be compensated for before the data are CMP (common-midpoint) stacked.

## SEISMIC PROCESSING

The basic CMP processing flow was consistent with 2-D high-resolution seismic-reflection methodologies (Steeples and Miller, 1990). All lines were processed using WinSeis2, beta seismic-data-processing software

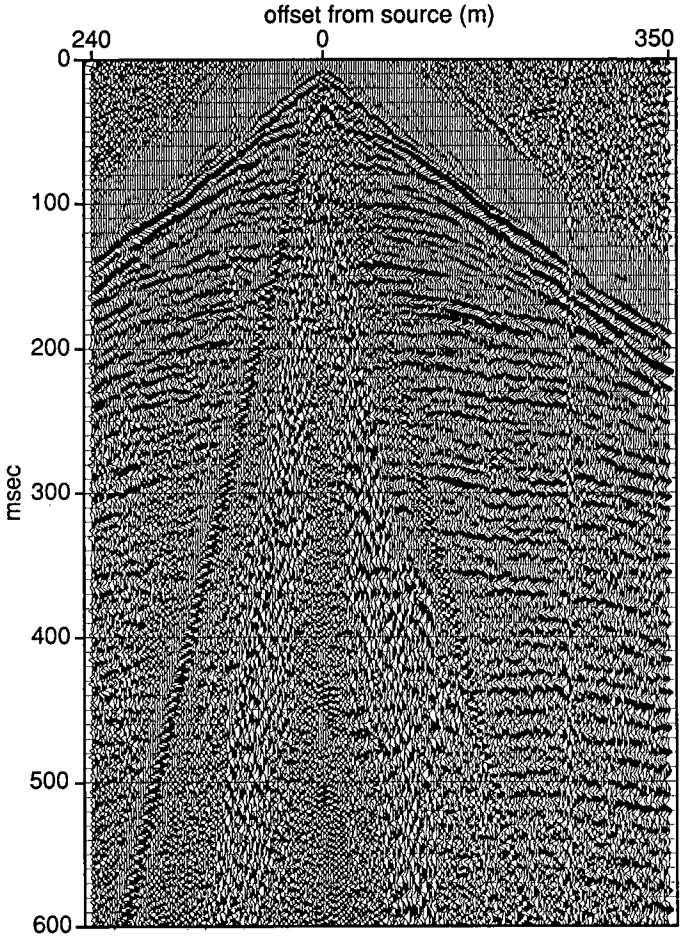


Figure 2. Representative 240-channel shot gather with 2.5-m receiver spacing and IVI Minivib source, scaled for display. Dozens of reflections are interpretable in the upper 600 ms. The top of salt is indicated by the high-amplitude reflection at ~130 ms.

(next generation of WinSeis Turbo) from the Kansas Geological Survey. Any reflection data acquired in this highly disturbed subsurface setting will be plagued with static problems and subject to dramatic swings in NMO (normal-moveout) velocity over relatively short distances; this data set was no exception. For the purposes of this survey the surface topography was flat with the exception of the 1-m-deep low associated with the 100-m-wide sinkhole. Changes in velocity related to differentially compacted fill, anomalous rubble zones, and distorted rock layers produced several millisecond fluctuations in event-arrival times across distances of 5 to 10 m. In extreme cases, shifts of 10 ms can be measured across a span of <10 m.

## SEISMIC INTERPRETATION

The confident interpretation of reflections on shot gathers is essential to optimizing the acquisition, processing, and interpretation of high-resolution seismic-reflection data. Dozens of reflections dominate the average shot gather from this site (Fig. 2). Reflections throughout the primary time–depth target window

(50–200 ms) possess broad spectral bandwidths and sufficient coherency to interpret reflections clearly across several to tens of traces. The irregular seesaw (zigzag) pattern evident in reflections across several traces denotes static related to lateral velocity irregularities. The nonlinear pattern observed in the first arrivals is the result of velocity irregularities, either at or very near the bedrock surface or between bedrock and the ground surface. Reflection events can be traced through the air-coupled wave and just into the ground-roll wedge. To avoid any contamination by the air-coupled wave, all energy after the air wave was removed during processing.

For quality-control reasons, it is important that reflections interpreted at two-way traveltimes <30 ms on CMP stacks can be correlated with equivalent 30-ms reflection hyperbolae on shot gathers. This consistency between shot records and stacked sections can be seen at various places along both lines of this survey (Fig. 3). Identification of these reflections on field files, and tracking them throughout the processing flow, were necessary to ensure that CMP sections were correctly stacked and interpreted. Ultra-shallow reflections (<30 ms) were a critical aspect in discerning the times since the Permian that these sediment-filled sinkholes may have been active. Besides the reflection "chatter" indicative of lateral variations in material velocity, a striking characteristic of these seismic data is the contradictory effects of AVO (amplitude variation with offset), depending on source and receiver orientation (Fig. 3B). Changes in reflection amplitude in this setting could be indicative of changes in acoustic impedance of the reflector itself and/or lateral variations in attenuation owing to rock failure and collapse. True amplitude analysis intended to search for localized changes in material properties, possibly indicative of changes indicating increased loading, does not seem to be an effective first-order tool at this site.

High signal-to-noise ratio and bed-resolution potential of observed reflections on shot and CMP gathers between ~20 and 350 m deep suffer little degradation as a result of horizontal stacking (Figs. 4, 5). Bed resolution on the order of 2 to 4 m, depending on specific reflections, was more than sufficient for confident delineation of rock layers distorted by collapse into voids left after rock salt was leached away. The Permian bedrock surface varies in and around the subsidence features from 25 to as much as 50 m below ground surface with drape in the Equus Beds clearly interpretable within the upper 40 ms beneath station 2400 (Fig. 4). Between the surface of bedrock and the top of salt is a 125-ft-thick sequence of red-bed evaporites comprising mostly shales. The highly plastic nature of these shale units is evident in the conformal nature of the folding that overlies the highly altered beds of the salt unit. Amplitude changes across these folded units are interpreted only in a very general fashion as related to compaction, bridging, and energy scattering. Interpreting migrated data provided only minor improvement in differentiating the subsidence mechanisms and their sequence, but migration did focus much of the energy distortion associated with very localized (30- to 40-m) undulations at the salt–upper Wellington contact (Fig. 4B). Dramatic subsidence structures revealed on CMP-stacked sections allude to a complex chronology of nonlinear interaction between salt leaching and associated roof-rock failure.

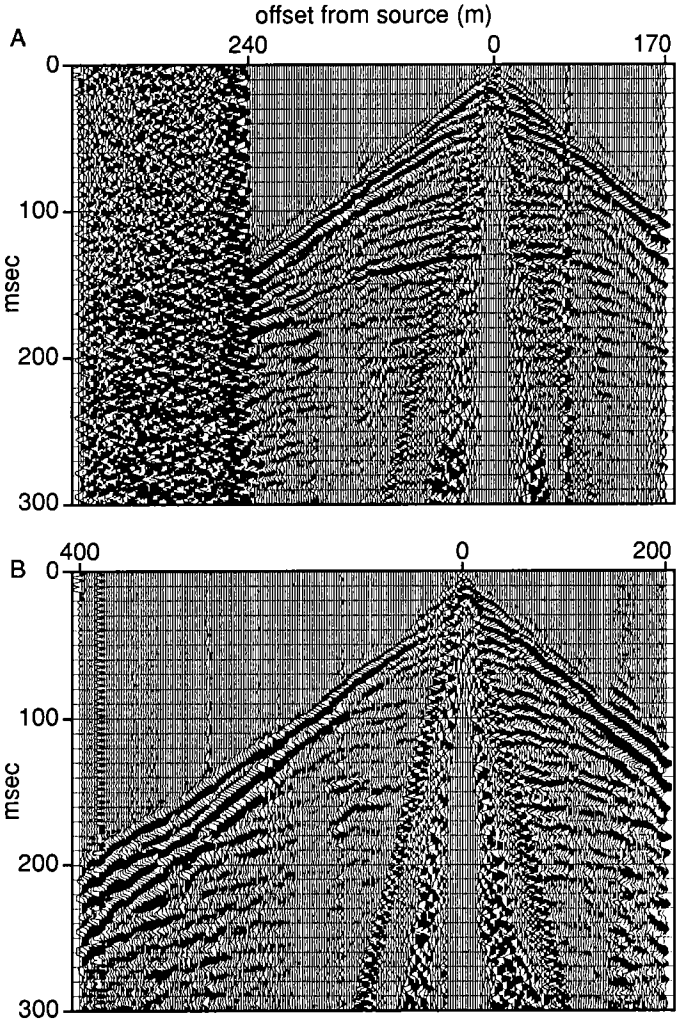


Figure 3. (A) True-amplitude shot gathers (24 dB/s spherical-divergence correction) demonstrate the highly variable reflection waveforms that do not seem to correlate to a single change in physical or seismic characteristics (velocity, attenuation, offset, or density) but more likely represent some complex combination of several. (B) Apparent anisotropic characteristics (in this case, attenuation), pronounced on some shot gathers, are directly related to the near surface in close proximity to the source.

The current sinkhole expression and associated distortion of rock layers are the result of a minor episode of dissolution and subsidence in the history of this site. Rock layers disturbed by subsidence span >350 m along the transect cut by line 1 (Fig. 4). Changes in bed dip across this feature provide the key criteria for deciphering the sequence of dissolution and subsid-

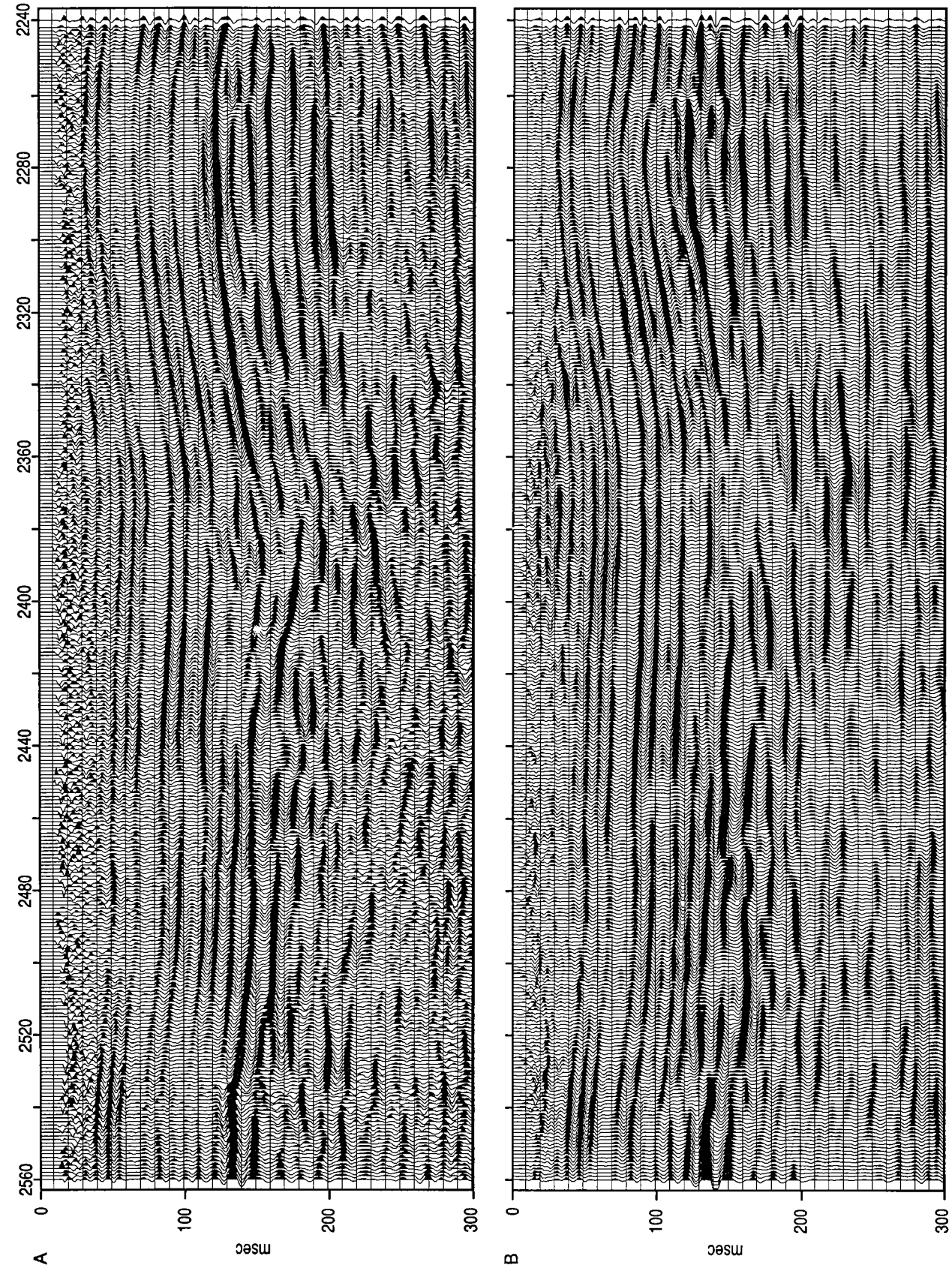


Figure 4. CMP-stacked section from a part of line 1. Bed distortion is exaggerated on this stacked section owing in part to the decrease in average velocity within the disturbed portion of earth (A). The sinkhole is centered around station 2480. Migration corrected for much of the optical distortion that results from dipping beds but reduced the resolution potential a bit (B).

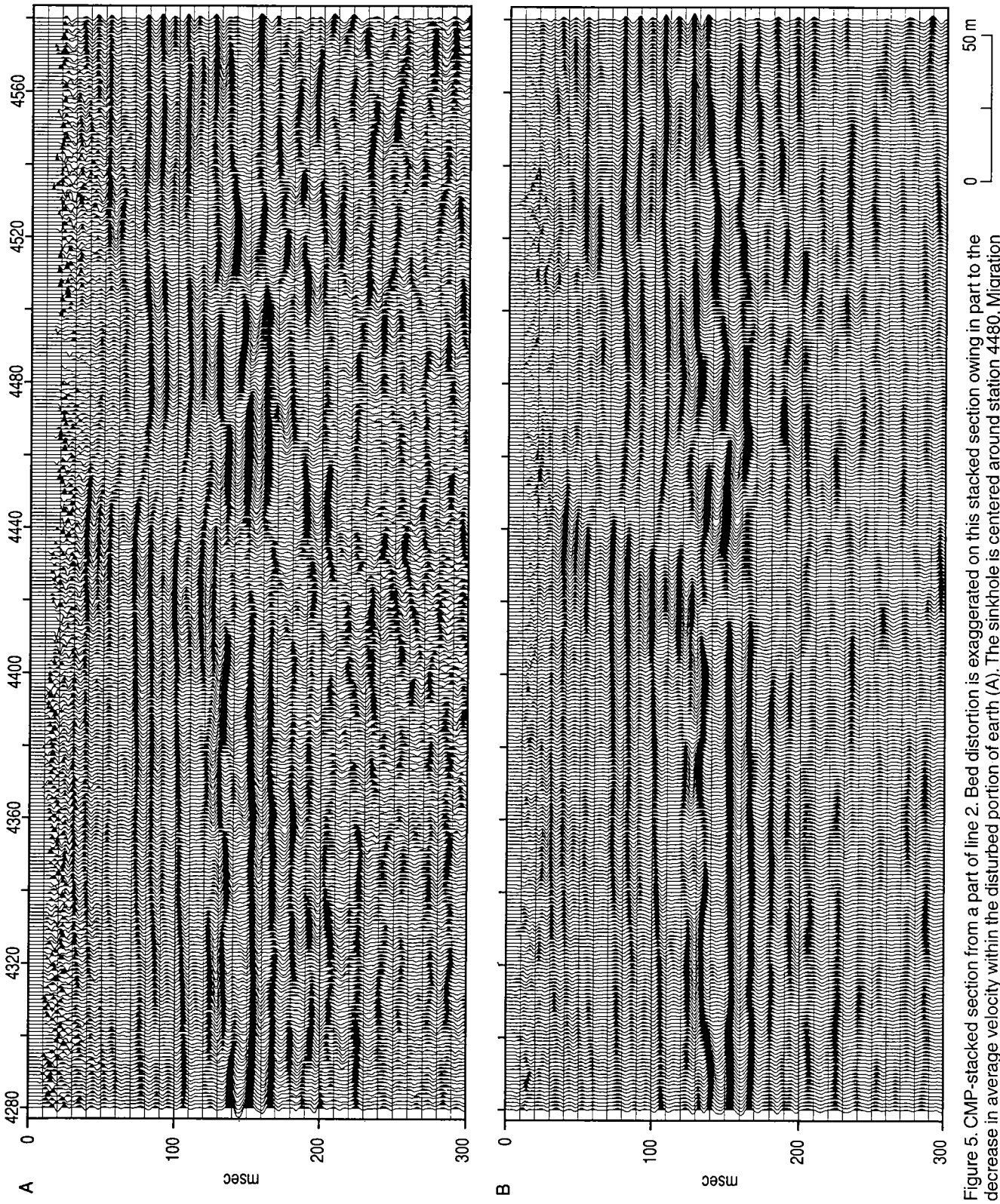


Figure 5. CMP-stacked section from a part of line 2. Bed distortion is exaggerated on this stacked section owing in part to the decrease in average velocity within the disturbed portion of earth (A). The sinkhole is centered around station 4480. Migration corrected for much of the optical distortion that results from dipping beds but reduced the resolution potential a bit (B).

ence events that led to the current sinkhole. The north–south slice through the sinkhole provides a complementary but significantly different picture of the subsurface (Fig. 5). The root of the sinkhole along line 2 is only ~125 m across and appears to be related to two periods of activity. Both the individual features and gross structure of the subsidence along line 2 is consistent with dissolution failures formed after a breach in borehole confinement or overmining. The subsidence structure does not rule out natural dissolution, but the line 2 feature alone more closely fits the anthropogenic model for the instigation of salt leaching. The coincident interpretation of lines 1 and 2 strongly supports natural dissolution.

Several episodes of subsidence are evident in most dissolution-related features (current and paleo) imaged on these two 1-km-long seismic profiles. Current surface subsidence at the intersection of U.S. 50 and Victory Road is probably related to the reactivation of natural salt-dissolution processes, which produced the seismically imaged, 350-m-wide subsidence feature. Focusing on the area likely active at the current time, at least in relationship to the sinkhole, allows an understanding of the current processes (Fig. 6). The original subsidence in proximity to the current sinkhole was likely at the very end of the Tertiary Period or just prior to deposition of the Pliocene–Pleistocene Equus Beds, which appear as the much subdued draping layers within the deepest part of the bedrock low. With this as the backdrop, a well-defined set of faults can be interpreted, which likely defines the formation of the original sinkhole. The westernmost of these faults is about 50 m west of the current sinkhole. After this initial collapse came a period of gradual plastic deformation, when the rock layers were releasing stress in the form of an ever-growing synform defined by faults with normal geometry.

The current sinkhole is one of possibly many minor reactivations of dissolution and subsidence or oscillations between times of high and low stress release. During times of high strain rates, material above the salt subsided along reverse-fault planes, which defined an ever-narrowing cone structure extending to the ground surface. Alternately, the current development

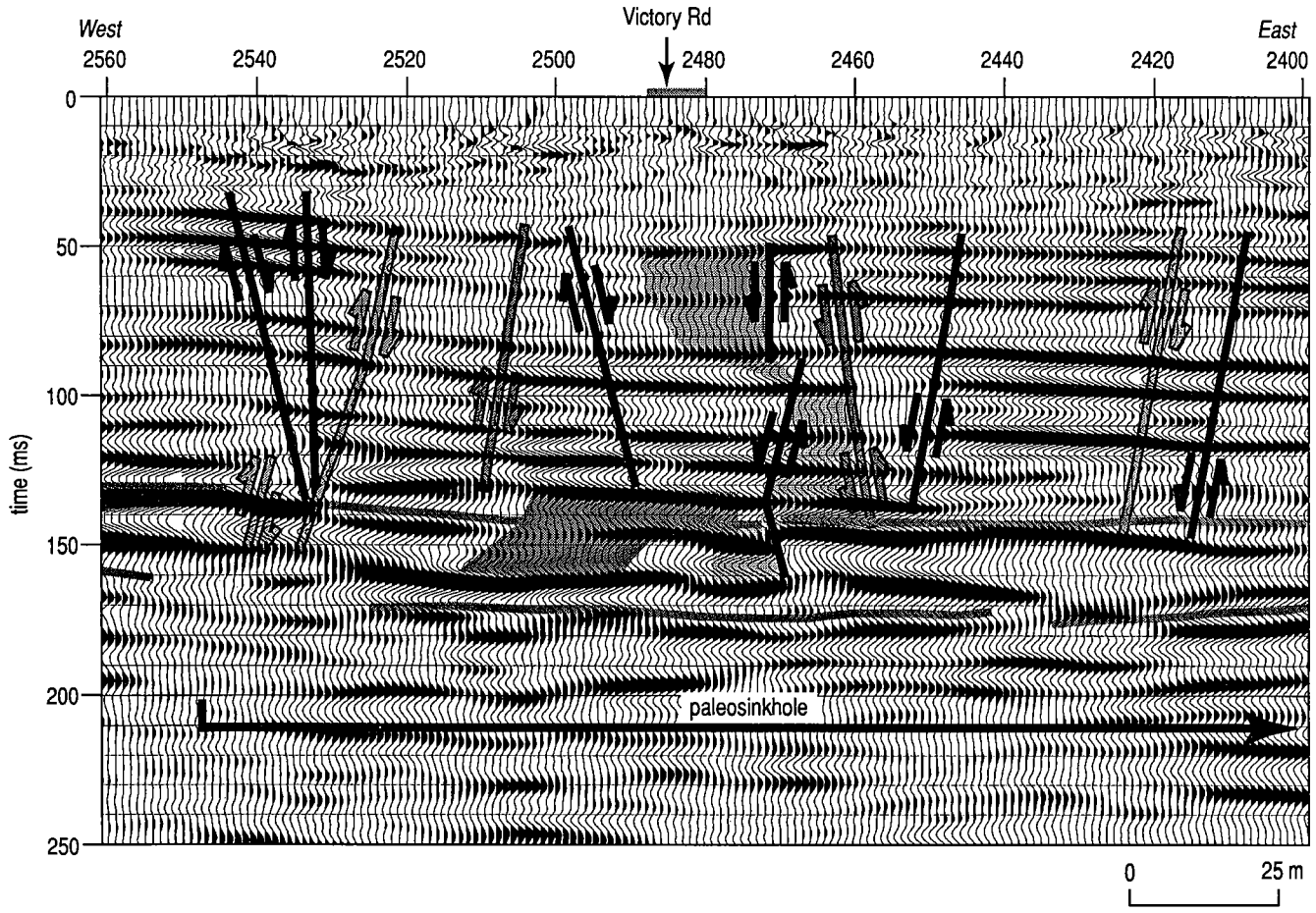


Figure 6. An interpreted part of line 1, showing two different paleosinkhole margins as reverse-oriented faults (light gray) that formed after rapid strain release in a brittle-rupture fashion. This was followed by a low-velocity, low-stress release that formed a synform (bowl-shaped depression) bounded by normal-type faults (black). The most recent subsidence was again the result of rock failure and rapid strain release that formed the tensional dome that caused beds to subside along reverse-fault planes (darker gray, toward center). Lighter shading (above) represents areas currently active, whereas darker shading (below) indicates areas for future concern.

of this sinkhole could be explained as recent failure of Permian rock layers above the salt that had bridged (roof-rock) void or rubble areas that remained following the Tertiary to Quaternary subsidence, as imaged on the seismic sections.

Using changes in amplitude and subtle breaks in rock-layer slopes, the high-angle reverse faults and subsidence cone (volume) can be defined (Fig. 6). Drape in the bedrock beneath station 2480, with a noticeable change in amplitude, is interpreted to define the top of the subsidence cone. The subsidence volume, based on amplitude and synforms, appears to be nonsymmetrical, likely following a path of least strength. Faulting and differential compaction of materials within and above the salt represent a highly unsettled section of earth with a variety of areas indicative of bridging and the upward progression of subsidence. Areas of apparent bridging above the salt within the dissolution zone are good candidates for infilling by collapsing red-bed sediments. With the volume of undercompacted earth (possibly void or rubble) suggested by the seismic section and the proximity of the dissolution front, this area will continue to experience variable rates of subsidence significantly into the future.

The complexity and diversity of subsidence patterns along line 2 are markedly different from those observed across line 1 (Fig. 7). The sinkhole appears symmetrically located within the subsurface subsidence zone and possesses a "root" consistent in size with subsidence features observed on seismic data from other sites that were induced by leaking oil-field brine from injection wells. This subsidence feature appears to have a well-defined zone where salt has been or is being leached, with an associated offset in intra-salt anhydrite or shale units. Reverse faults, which define the cone of disturbed sediments associated with the original subsidence at this site, are well defined by the amplitude zones near the points of greatest offset in the red-bed reflections. This area has undergone at least one period of gradual, low-stress relief, as the normal-fault geometries indicate. Consistent with line 1, the active cone of subsidence is bounded by reverse-fault planes centered on the sinkhole.

Mechanisms and gross chronology of structural failures, as interpreted from stacked seismic sections,

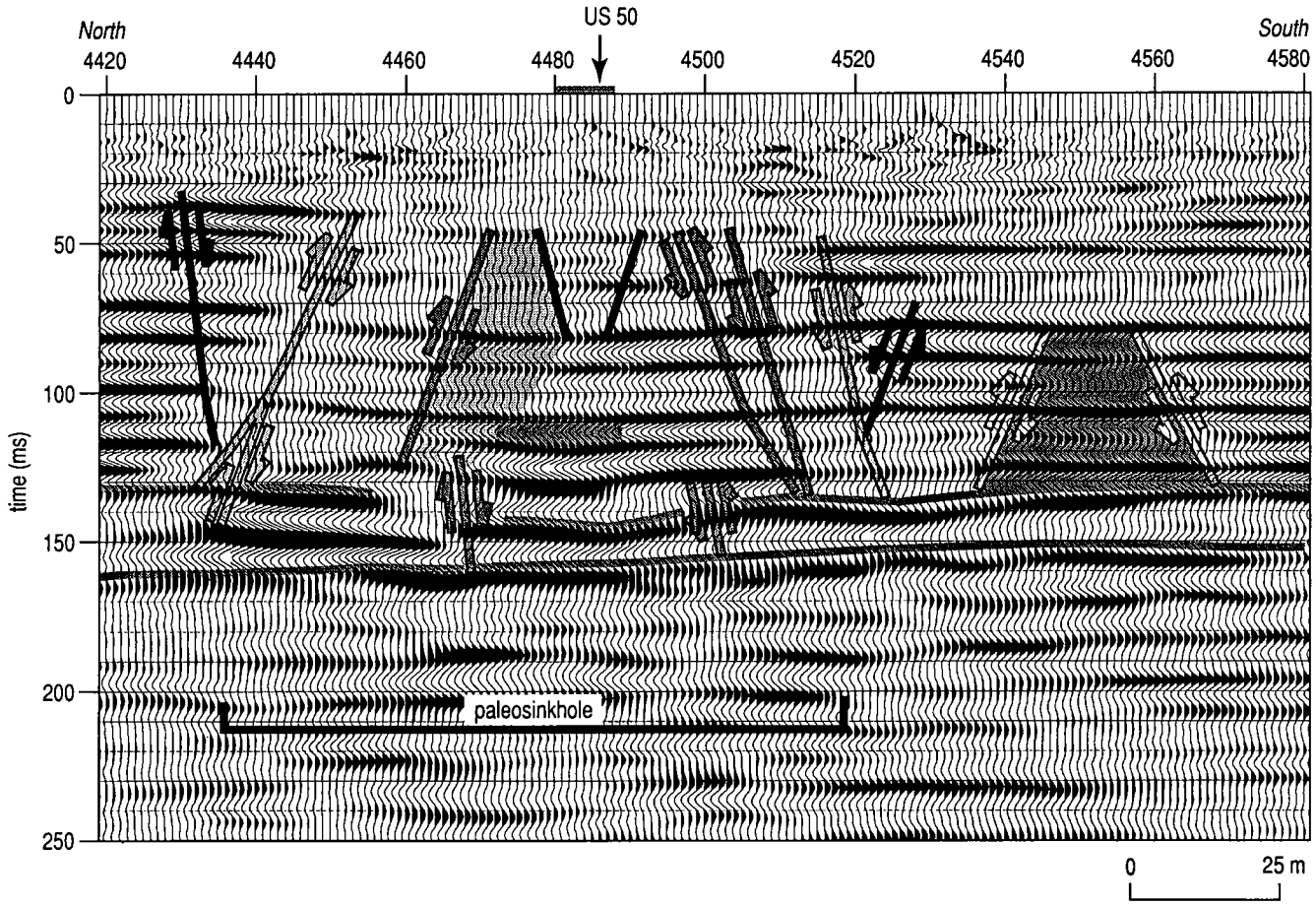


Figure 7. An interpreted part of line 2, with the original sinkhole margins indicated by reverse-oriented faults (light gray), which formed during rapid stress release during brittle-rock failure. This was followed by low-velocity, low-stress release forming a synform (bowl-shaped depression) bounded by normal-type faults (black). The most recent subsidence was again the result of rock failure and rapid stress release that formed the tensional dome that caused beds to subside along reverse-fault planes (darker gray, toward center). Darker shading bounded by white reverse faults indicates an area for future concern.

suggest that initial subsidence and associated bed offset occurred at high strain rates and were confined to a cone defined by reverse-fault planes. This process was active at least twice: once when the current 100-m-wide sinkhole developed, and initially as the 350-m-wide dissolution feature originally formed as a single, relatively continuous event. This 350-m-wide footprint could also be the result of dozens of uniquely segregated events occurring throughout the last million or so years. Separating each of the periods of rapid subsidence was a long period (not necessary represented by uniform or continuous rates) of the downward movement (settling, relaxation) of sediments when little or no stress was building up on rock layers. These episodes of gradual subsidence continued in the subsurface, advancing as an ever-expanding bowl, geometrically defined by normal-fault planes until roof-rock failure above the salt reactivated high stress-relief processes. The rate of destabilization and failure, as well as the load-bearing potential of the rock layers above zones of dissolution, strongly influenced both the original subsidence geometries and dimensions as well as the subsequent reactivation of subsidence along the profiles.

## SUMMARY AND CONCLUSIONS

Several episodes of subsidence are evident in most dissolution-related features (current and paleo) imaged on these two 1-km-long seismic profiles. The rate of destabilization and failure, as well as the load-bearing potential of the rock layers above zones of dissolution strongly influenced both the original subsidence geometries and dimensions as well as the subsequent reactivation of subsidence along the profiles. Current surface subsidence at the intersection of U.S. 50 and Victory Road is probably related to the reactivation of natural salt-dissolution processes that produced the seismically imaged, 300-m-wide subsidence feature interpreted to have been active during Tertiary and/or Quaternary time. Alternately, recent failure of Permian rock layers above the salt-bridging (roof-rock) void or rubble areas that remained after most of the Tertiary to Quaternary subsidence had slowed or stopped could explain the most recent sinkhole development.

With a subsidence history at this site potentially extending as far back as mid-Tertiary time, it is unlikely that subsidence will end within the next millennium. Until the highway started sinking here during 1998, little if any subsidence seems to have been associated with this paleosinkhole throughout late Quaternary time. This long period of inactivity, followed by the localized, rapid subsidence observed at this site, makes it reasonable to expect other small sinkholes to form without warning above this paleofeature or other similar paleofeatures in this area. Considering the interpreted bed geometries, surface subsidence at the current sinkhole site will likely continue gradually along its northern and eastern edges, elongating the sinkhole in those directions. Besides the obvious disruption to the road system, this subsidence feature unfortunately provides a pathway between the fresh waters of the Equus Beds and the more brackish waters of the Permian rocks. Surface subsidence will likely continue at a gradual rate for some time into the future. Sufficient bridging and undercompacted rock layers still exist beneath this sinkhole to sustain the current subsidence rate of ~0.3 m/yr for several years.

The interpretation of reflections from key stratigraphic horizons suggests that plastic deformation of rock layers over dissolution voids was followed by roof-rock failure along reverse-fault planes within an earth volume known as the tension dome. The original tensional dome was centered on the dissolution volume and extended from the base of the salt interval to near the surface. A long period of low strain, evident in layers outside the tensional dome, occurred along normal-fault planes for a significant part of the late Tertiary and early Quaternary. A much smaller tensional dome at the western extremity of the original tensional dome has controlled recent subsidence. Subsidence, associated with failure defined by this most recent dome, has followed a somewhat asymmetric path from salt to surface.

This study evaluated the effectiveness of using high-resolution vibroseis techniques on the shoulder of U.S. 50 when traffic was slowed but not stopped. Previous data collected in this area were acquired 1.5 km south along a quiet, east–west county road using a small recording-channel seismograph and an invasive, low-energy, impulsive-source survey. Equivalent dominant frequencies were recorded on both surveys, but recent efforts resulted in significantly greater energy penetration and a signal-to-noise ratio that resulted in usable data regardless of cultural noise levels. The bed resolution, coherency of bedding within subsidence features, and overall signal-to-noise ratio were greatly improved using minivibroseis-survey techniques.

If salt dissolution—anthropogenic or natural—has begun at this site, it is not possible with these data alone to identify definitively a fluid source or pathway. However, with the superimposition of this modern sinkhole and the mid-Tertiary to early Quaternary subsidence feature, and considering that the nearest disposal well with a history of fluid-containment problems is >2 km away, the sinkhole is likely natural in origin. Unfortunately, considering the long history of oil-field disposal-well-induced dissolution in this area and the proximity of this particular site to the natural dissolution front, neither catalyst can be completely ruled out.

## ACKNOWLEDGMENTS

The author would like to thank Charles Ludders of the Kansas Department of Transportation, Mike Dealy from Groundwater Management District 2, and

Morris Korphage and Doug Lewis from the Kansas Corporation Commission for their support of this project. Also, thanks go to Rex Buchanan of the Kansas Geological Survey, who provided assistance during media coverage, and the field crew on this project: David Laflen, Joe Anderson, Mitchell Fiedler, and Chad Gratton.

## REFERENCES CITED

Anderson, N. L.; Watney, W. L.; Macfarlane, P. A.; and Knapp, R. W., 1995a, Seismic signature of the Hutchinson Salt and associated dissolution features: Kansas Geological Survey Bulletin 237, p. 57–65.

Anderson, N. L.; Knapp, R. W.; Steeples, D. W.; and Miller, R. D., 1995b, Plastic deformation and dissolution of the Hutchinson Salt Member in Kansas: Kansas Geological Survey Bulletin 237, p. 66–70.

Anderson, N. L.; Martinez, A.; and Hopkins, J. F., 1998, Salt dissolution and surface subsidence in central Kansas: a seismic investigation of the anthropogenic and natural origin models: Geophysics, v. 63, p. 366–378.

Baar, C. A., 1977, Applied salt-rock mechanics 1: Elsevier, 294 p.

Bayne, C. K., 1956, Geology and ground-water resources of Reno County, Kansas: Kansas Geological Survey Bulletin 120, 130 p.

Beck, B. F.; Pettit, A. J.; and Herring, J. G. (eds.), 1999, Hydrogeology and engineering geology of sinkholes and karst–1999: Balkema, Rotterdam, 130 p.

Black, R. A.; Steeples, D. W.; and Miller, R. D., 1994, Migration of shallow seismic reflection data: Geophysics, v. 59, p. 402–410.

Carter, N. L.; and Hansen, F. D., 1983, Creep of rock salt: Tectonophysics, v. 92, p. 275–333.

Davies, W. E., 1951, Mechanics of cavern breakdown: National Speleological Society, v. 13, p. 6–43.

Ege, J. R., 1984, Formation of solution-subsidence sinkholes above salt beds: U.S. Geological Survey Circular 897, 11 p.

Frye, J. C., 1950, Origin of Kansas Great Plains depressions: Kansas Geological Survey Bulletin 86, pt. 1, p. 1–20.

Frye, J. C.; and Schoff, S. L., 1942, Deep-seated solution in the Meade Basin and vicinity, Kansas and Oklahoma: American Geophysical Union Transactions, v. 23, pt. 1, p. 35–39.

Hunter, J. A.; Pullan, S. E.; Burns, R. A.; Gagne, R. M.; and Good, R. S., 1984, Shallow seismic-reflection mapping of the overburden–bedrock interface with the engineering seismograph—some simple techniques: Geophysics, v. 49, p. 1381–1385.

Knapp, R. W.; Steeples, D. W.; Miller, R. D.; and McElwee, C. D., 1989, Seismic reflection surveys at sinkholes in central Kansas, *in* Steeples, D. W. (ed.), Geophysics in Kansas: Kansas Geological Survey Bulletin 226, p. 95–116.

Merriam, D. F., 1963, The geologic history of Kansas: Kansas Geological Survey Bulletin 162, 317 p.

Merriam, D. F.; and Mann, C. J., 1957, Sinkholes and related geologic features in Kansas: Transactions of Kansas Academy of Science, v. 60, p. 207–243.

Miller, R. D.; Steeples, D. W.; Schulte, L.; and Davenport, J., 1993, Shallow seismic reflection study of a salt dissolution well field near Hutchinson, Kansas: Mining Engineering, October, p. 1291–1296.

Miller, R. D.; Steeples, D. W.; and Weis, T. V., 1995, Shallow seismic-reflection study of a salt-dissolution subsidence feature in Stafford County, Kansas, *in* Anderson, N. L.; and Hedke, D. E. (eds.), Geophysical atlas of selected oil and gas fields in Kansas: Kansas Geological Survey Bulletin 237, p. 71–76.

Miller, R. D.; Villella, A. C.; and Xia, J., 1997, Shallow high-resolution seismic reflection to delineate upper 400 m around a collapse feature in central Kansas: Environmental Geosciences, v. 4, no. 3, p. 119–126.

Rokar, R. B.; and Staudtmeister, K., 1985, Creep rupture criteria for rock salt, *in* Schreiber, B. C.; and Harner, H. L. (eds.), Sixth International Symposium on Salt: Salt Institute, Inc., Virginia, v. 1, p. 455–462.

Steeples, D. W.; and Miller, R. D., 1990, Seismic reflection methods applied to engineering, environmental, and groundwater problems, *in* Ward, S. (ed.), Geotechnical and environmental geophysics, v. 1: review and tutorial: Society of Exploration Geophysicists, p. 1–30.

Steeples, D. W.; Knapp, R. W.; and McElwee, C. D., 1986, Seismic reflection investigation of sinkholes beneath Interstate Highway 70 in Kansas: Geophysics, v. 51, p. 295-301.

Walters, R. F., 1978, Land subsidence in central Kansas related to salt dissolution: Kansas Geological Survey Bulletin 214, p. 1–32.

_____1980, Solution and collapse features in the salt near Hutchinson, Kansas: Geological Society of America, South-Central Section, Field Trip Notes, 10 p.

_____1991, Gorham oil field: Kansas Geological Survey Bulletin 228, p. 1–112.

Watney, W. L.; Berg, J. A.; and Paul, S., 1988, Origin and distribution of the Hutchinson Salt (lower Leonardian) in Kansas: Society of Economic Paleontologists and Mineralogists, Mid-Continent Section, Special Publication 1, p. 113–135.

# High-Resolution Magnetic Survey Used in Searching for Buried Brine Wells in Hutchinson, Kansas

***Jianghai Xia***
Kansas Geological Survey
Lawrence, Kansas

***Stephen L. Williams***
City of Hutchinson
Hutchinson, Kansas

**ABSTRACT.**—The City of Hutchinson, Kansas, designed seven sites with a total area of 512,000 ft$^2$ to search for buried and abandoned brine wells after the city researched literature of the salt-mining history in the Hutchinson area. A high-resolution magnetic survey was conducted at these seven sites in May 2002. Twenty-three anomalies were verified by excavation with a backhoe, of which five were identified as brine wells, four as suspected brine wells, one as a probable water well, and one as a probable gas pipe. In addition to using the half-width of an anomaly to estimate depth to an anomalous source, a monopole anomaly with >12,000 nanoteslas in amplitude is a basic criterion for identifying a well with 8-in. metal casing. A monopole anomaly with several thousand nanoteslas in amplitude is a basic criterion for identifying a 2.5-in. or 4-in. well. The high-resolution magnetic method with theodolite-defined grids was successful in locating a number of the abandoned wells in the City of Hutchinson. Voids were normally associated with these wells, owing to salt mining. The area around these wells continues to hold potential for future engineering and environmental problems.

## INTRODUCTION

On January 17, 2001, a natural-gas explosion and fire destroyed two downtown businesses in Hutchinson, Kansas. The next day another explosion occurred at a mobile-home park 3 mi away. Two residents died of injuries from the explosion, which forced the evacuation of hundreds of people as gas geysers began erupting in the area. The geysers spewed a mixture of natural gas and salt water. The pathways to the land surface at both explosion sites and the geysers were abandoned brine wells used for solution mining of salt (http://www.kgs.ukans.edu/Hydro/Hutch/Background/index.html, Allison, 2001; Watney and others, 2003).

Locating abandoned brine wells is an objective of the Hutchinson Response Project of the Kansas Geological Survey. Some of the known wells in the mobile-home park consisted of vertical steel-cased pipes that are nominally 400–700 ft long. The feasibility of using various geophysical methods to locate abandoned brine wells was evaluated in terms of their effectiveness and efficiency.

The predicted maximum gravity signal caused by this pipe is only 4–6 μGal (microgals). We also calculated the gravity anomaly caused by a salt cavern with an assumed volume of 100 ft × 100 ft × 100 ft buried at a depth 400 ft, a typical depth of salt voids in the Hutchinson area. The maximum anomaly for this cavern is ~25 μGal, assuming that the cavern is completely empty. In actuality, the maximum anomaly for the cavern will be much less than 25 μGal, because caverns are typically filled with water, soil, and/or rocks, which make a density contrast considerably smaller. To detect this sub-25-μGal anomaly, the sensitivity of the gravity meter and accuracy of elevation measurements are critical. The sensitivity of the most advanced gravity meters available in the market is 1–10 μGal. It takes much longer (normally >15 minutes/station) to acquire microgravity data than for a regular exploration gravity survey to achieve the 1-μGal sensitivity level. Elevation measurements are the other main challenge in the microgravity survey. The error associated with elevation measurements is 5 μGal per inch. To confidently identify a gravity anomaly, the maximum anomaly should be at least 3 times greater than possible errors. Therefore, to detect an anomaly with an amplitude <25 μGal, the sensitivity of the gravity meter should be not less than 4 μGal (in the range of 1–4 μGal), and the accuracy of elevation measurements should be within 1 in. It is very difficult to achieve an elevation survey accurate within a 1-in. range. In addition, for detection of a sub-25-μGal anomaly in an urban area, cultural noise (traffic, running motors, power lines, buildings, etc.) is a serious problem. A microgravity survey, therefore, was ruled out as a means for locating abandoned brine wells.

A three-dimensional (3-D) ground-penetrating-radar (GPR) survey was considered as a means for locating these wells. The ground in this area is debris/

Xia, Jianghai; and Williams, S. L., 2003, High-resolution magnetic survey used in searching for buried brine wells in Hutchinson, Kansas, *in* Johnson, K. S.; and Neal, J. T. (eds.), Evaporite karst and engineering/environmental problems in the United States: Oklahoma Geological Survey Circular 109, p. 169–175.

dirt fill, however, and there could be a lot of reflected/diffracted events caused by objects other than the brine wells. Furthermore, 3-D GPR data acquisition and processing can often take much longer than expected.

The electromagnetic (EM) method was proposed as the method for searching for these wells (Xia, 2001, 2002a). One abandoned brine well at a depth of 5 ft was successfully located, based on EM anomalies at a testing site near 11th and Chemical Streets in Hutchinson. However, uniquely identifying well-generated EM anomalies at historical salt-mining sites remains a challenge. In addition, the effective investigation depth of the EM method is still an active research topic.

In May 2002, a high-resolution magnetic survey was used to locate abandoned brine wells at seven selected sites with a total area of 512,000 ft$^2$ after the city researched literature of the salt-mining history in the Hutchinson area. Much higher relative anomalies could be observed in high-resolution magnetic measurements based on forward calculations. The maximum magnetic signal caused by the well pipe can be higher than 15,000 nanoteslas (nT) in addition to the normal geomagnetic field in Hutchinson. This anomaly is larger than 25% of the normal geomagnetic field. An anomaly this large provides great promise in locating brine wells in the city's noisy environment. Furthermore, the magnetometer's continuous recording ability makes a high-resolution magnetic survey more efficient.

This paper reports the successful results of the high-resolution magnetic survey in locating abandoned brine wells.

## METHODOLOGY

The survey areas were most commonly defined as 100-ft × 100-ft grids using a theodolite (Fig. 1A). The accuracy of the horizontal location within each grid is greater than ±0.5 ft and was verified by a tape mea-

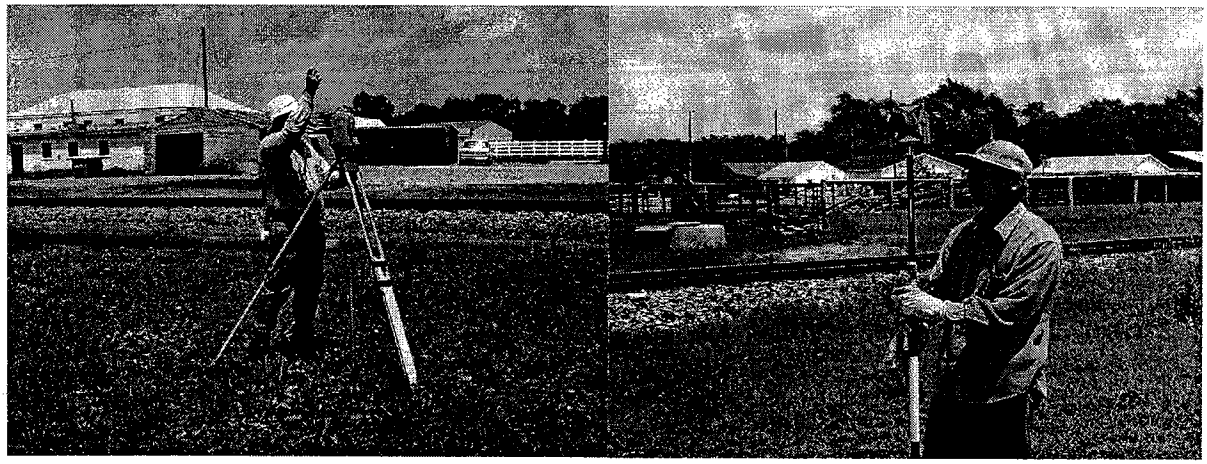

A

B

Figure 1. (A) A theodolite was used to define grids for this high-resolution magnetic survey. David Laflen (left) and Gang Tian (right) were defining grids. (B) A portable cesium G-858 magnetometer was used to continuously measure the total-field component of the geomagnetic field. Xia was performing the magnetic survey. A traffic cone was used as a line guide.

surement. A portable cesium G-858 magnetometer (Fig. 1B) was used to measure the total component of the geomagnetic field. The sensitivity of the meter is 0.01 nT. The overall accuracy of magnetic measurements is on the order of 1 nT. The sensor height is consistently 2.5 ft from the ground surface during the survey. The data density of a high-resolution magnetic survey along a line is 2.3 measurements/ft. Magnetic data were acquired at three sites with known wells (sites C4, C8, and C13) to serve as signatures in locating brine wells. Once the anomaly signature at these known wells was determined, a line spacing of 3 ft was chosen. Approximately 35 mi of data was collected in the 512,000 ft$^2$ survey area.

The normal total-field component of the geomagnetic field in the City of Hutchinson is 53,600 nT. The maximum change of the geomagnetic field in the quiet period (Kp <4) is <15 nT/hour. The Kp index is a 3-hourly planetary geomagnetic index of activity generated in Göttingen, Germany, based on the K index from 12 or 13 stations distributed around the world. The K index is a 3-hourly quasi-logarithmic local index of geomagnetic activity relative to an assumed quiet-day curve for the recording site and can range in value from 0 to 9. The K index measures the deviation of the most disturbed horizontal component (http://www.maj.com/sun/status.html). No drifting correction of the geomagnetic field is necessary, because we completed the survey grid by grid individually during the quiet period of the geomagnetic field. The time for finishing each 10,000 ft$^2$ grid was ~15 minutes, and the amplitude of well anomalies was on the order of several thousand nanoteslas.

Measurements were first assigned field geometry, then corrected for the sensor locations on the basis of shapes of known anomalies by shifting odd-numbered lines by 1.2–2 ft, and finally adjusted for data dropouts that are zero readings owing to extremely high anomalies (>100,000 nT). Processed data were then gridded into 1-ft × 1-ft grids by the kriging method (Surfer®, 1999). Gridded data were correlated with anomalies from known wells. Anomalies were picked on the basis of their amplitudes, shapes, and/or correlation coefficients. Some anomalies were also inverted to find their magnetization and depths to the top of the anomaly source. Processed high-resolution magnetic data were finally displayed using Surfer® in a color scale (gray scale for this paper) to enhance anomalies potentially caused by brine wells.

## MAGNETIC SIGNALS FROM KNOWN WELLS

We acquired high-resolution magnetic data at sites of wells C4, C8, and C13. The survey area at each site is 40 ft × 40 ft with line spacing of 2 ft (Fig. 2). To make sure that the anomaly shape is not related to a line (survey) direction, we acquired data in both the east–west direction and the north–south direction at site C4 (Fig. 3A,B). The monopole anomaly (Breiner, 1973, p. 24) at well C4 is almost perfectly imaged in both directions, which told us that in the production phase we could perform the survey in either the north–south or the east–west direction, depending on field accessibility and efficiency of data acquisition. The monopole anomaly at C13 (Fig. 3C) is as high as 83,000 nT, which is an almost 30,000-nT (≈83,000 – 53,600) anomaly. The reason for this extremely high anomaly is that the wellhead is at the ground surface. Measurements at well C8 (Fig. 3D) showed the same anomaly shape. There are two peaks at the site of well C8. One is related to well C8 at (20, 24), and the other is at (31, 25) but was not excavated owing to a legal accessibility issue. Comparing the anomaly (shape and amplitude) at (31, 25) with anomalies at wells C4 and C13 (Fig. 3A–C), it is likely that the anomaly at (31, 25) is caused by a buried brine well. The centers of the "bull's-eyes" are the locations of the wells. The amplitudes of the anomalies at these wells are >20,000 nT. The half-width, a horizontal distance between the principal maximum (or minimum) of the anomaly and the point where the value is exactly one-half the maximum value (Breiner, 1973, p. 31), is ~7 ft for all these anomalies. The magnetic signatures (shape, amplitude, and half-width) of these wells provided a basis for distinguishing brine-well anomalies from others. These huge anomaly amplitudes also showed promise in searching for abandoned brine wells in areas with high cultural background noise.

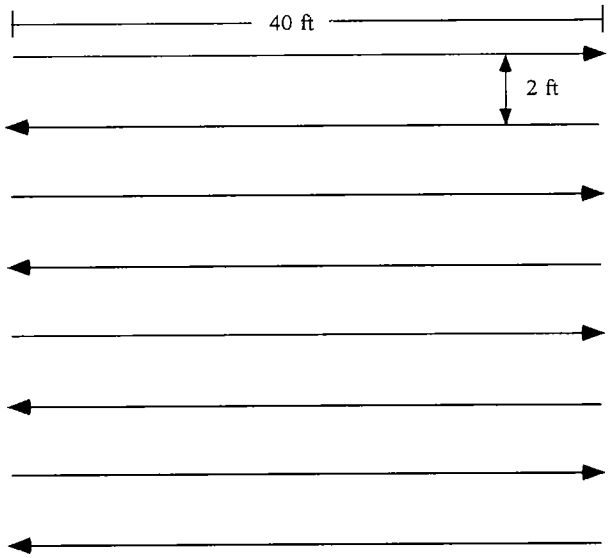


Figure 2. A grid with arrows indicates the walking direction. The 40-ft length of a line was used in the test phase on the known well sites. Grids in the production phase were normally defined by 100-ft-long lines with 3-ft line spacing.

## MAGNETIC SURVEY IN HUTCHINSON

The high-resolution magnetic survey was performed at seven sites chosen by the City of Hutchinson after review of the historical literature on salt mining in the Hutchinson area (Fig. 4). The magnetic data were normally acquired at 100 ft × 100 ft grids with line

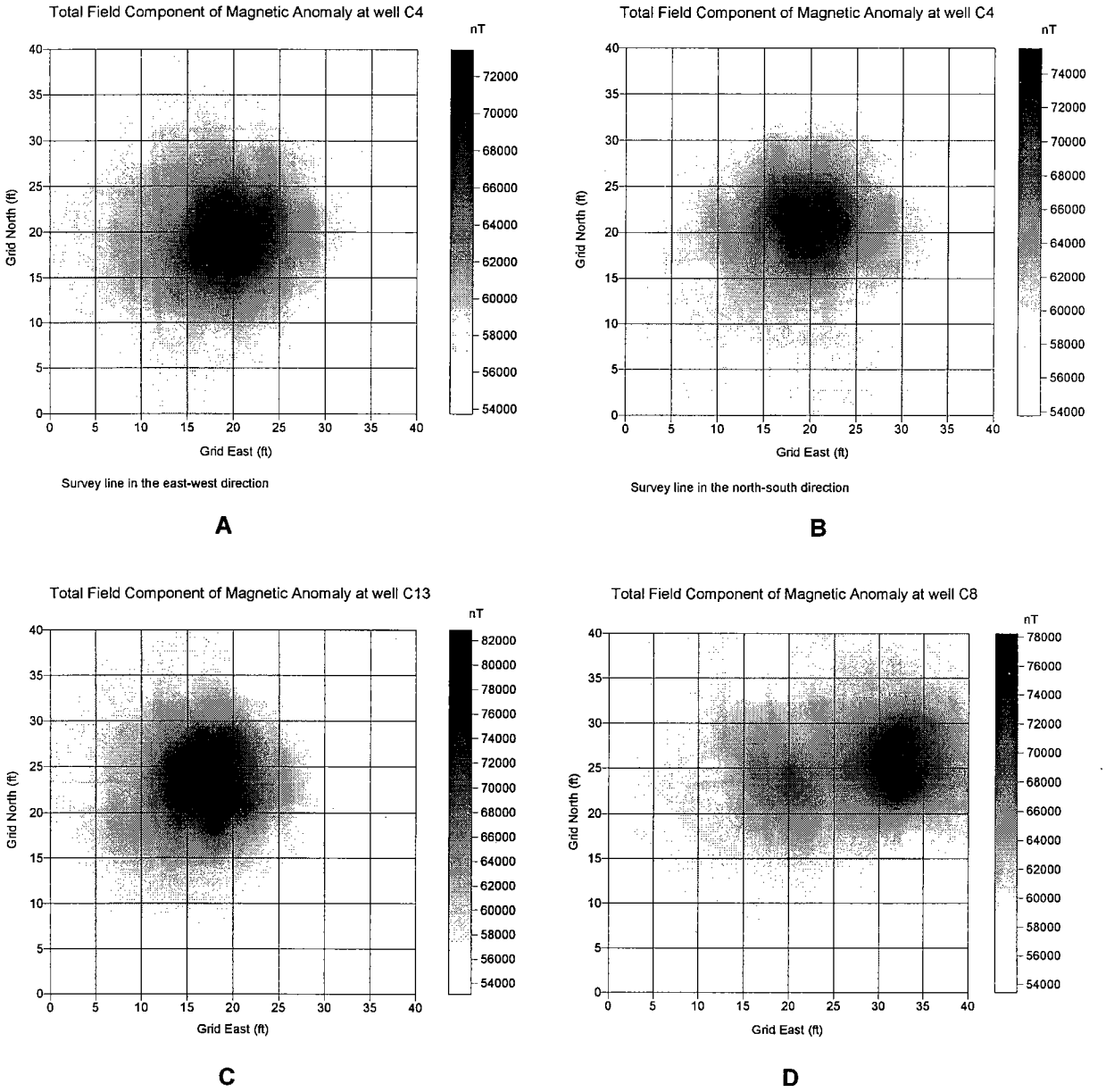


Figure 3. Total-field component of magnetic anomalies at known brine wells C4 (A, B), C13 (C), and C8 (D). The monopole anomaly at well C4 is almost perfectly imaged in both directions. The peaks of anomalies directly indicate the locations of these wells. There are two peaks at the site of well C8. One is related to well C8 at (20, 24). The other is at (31, 25); this site has not been excavated owing to a legal accessibility issue.

spacing of 3 ft. Twenty-three anomalies were verified by excavation with a backhoe. Eleven anomalies were caused by five abandoned brine wells, four suspected brine wells, one probable water well, and one probable gas pipe (Table 1). Here we present only two anomalies excavated at the Union Salt site (Fig. 5). Complete results of the high-resolution magnetic survey can be found in Xia (2002b).

Based on the anomalies of known wells (Fig. 3), the first criterion for interpreting a processed anomaly possibly caused by a brine well is its shape: a monopole. The second is its amplitude. It is easy to interpret anomalies with the monopole shape and amplitudes as high as 20,000 nT to be brine wells with 8-in. metal casing. We interpreted five such anomalies with amplitudes >12,000 nT to denote brine wells. Excavation of these anomalies indicated that all were due to 8-in. brine wells encased in steel. Some were covered by road asphalt, some by soil, and some by concrete. Depths were between 1 and 7 ft (Table 1). For example, anomaly U5_1 (Fig. 6, top) is at (42, 23) of grid U5. The shape of this anomaly is a nearly perfect monopole similar to anomalies of known wells (Fig. 3). The total component of the geomagnetic field is >80,000 nT, which indicates that the anomaly has an amplitude of >26,000 nT (≈80,000–53,600). The half-width

**Table 1. — List of Excavated Brine Wells and Suspected Brine Wells on the Basis of Magnetic Anomalies[a]**

| Anomaly | Source of anomaly |
|---|---|
| *Grids at Union Salt (Avenue C and Walnut St.)* | |
| U1_1 | 8-in. brine well at 1-ft depth |
| U2_1 | Two suspected brine wells (2.5- and 2.875-in.) at 4-ft depth |
| U4_1 | 4-in. probable gas pipe at 1-ft depth |
| U5_1 | 8-in. brine well at 1-ft depth |
| *Grids at Salvation Army Eagle Park (Avenue C and Main St.)* | |
| S2_1 | 8-in. brine well at 7-ft depth |
| S4_2 | 2.5-in. suspected brine well at 2-ft depth |
| *Grids at Ironhorse Equestrian Center (K-96/Nickerson Blvd. and Hendricks St.)* | |
| I9&11_1 | 8-in. brine well at 4.5-ft depth |
| I10_2 | 4-in. suspected brine well at 2-ft depth |
| *Grids at Trailer Park (8th and Grand Sts.)* | |
| T10_1 | 2.5-in. suspected brine well at 1-ft depth |
| *Grids at Chemical and 8th Sts.* | |
| C_1 | 1.5-in. possible water well at 1-ft depth |
| *Grids at Monroe St. and Avenues E and F* | |
| M3_1 | 8-in. brine well at 2-ft depth |

[a]The designation of an anomaly (left column) starts with a letter that indicates the site (see Fig. 4) and is followed by the grid number. The number following the underline (_) is a serial number for one of the anomalies in each grid (see Xia, 2002b, for details).

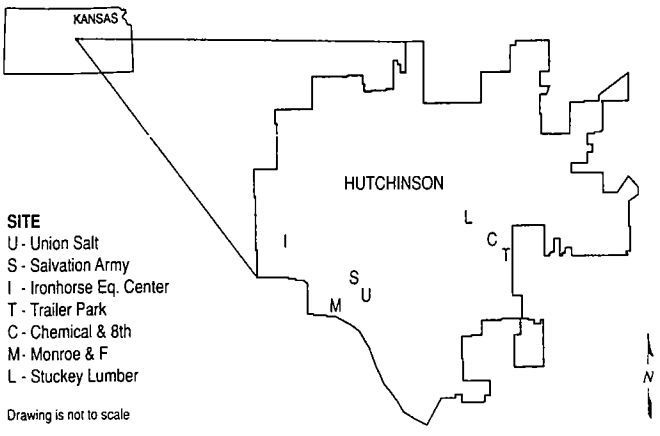


Figure 4. Site map showing the locations of the seven high-resolution magnetic surveys performed in the City of Hutchinson.

of the anomaly is ~7 ft. Excavation proved this anomaly to be an 8-in. brine well at a depth of 1 ft under 6 in. of concrete (Fig. 6, bottom).

Monopole anomalies with amplitudes of several thousand nanoteslas were also verified by excavation. Five anomalies proved to be 2.5-in. or 4-in. vertical pipes. Four of these were suspected brine wells, and one was a probable water well (Table 1). For example, the peak of anomaly U2_1 (Fig. 7, top) is at (75, 56) of grid U2. It is partly due to a 2.5-in. vertical pipe around (74, 56) at a depth of 4 ft (Fig. 7, bottom). The pipe is suspected to be an inner pipe of a brine well. The anomaly elongates slightly in the east–west direction with a peak of 3,900 nT (=57,500–53,600). We thought the elongation was due to errors in line locations until a well-plugging project began in January 2003. Another 2.785-in. vertical well was discovered at (78, 56) at a depth of 4 ft during the surface work in preparation for plugging the well at (74, 56). Discovery of the new well explains the elongation of anomaly U2_1. Because the two wells were so close relative to their depths, the high-resolution magnetic survey could not individually distinguish them. A magnetic vertical-gradient survey has a much greater horizontal resolution than a magnetic survey, so there is some hope of distinguishing objects in close proximity.

## SUMMARY AND CONCLUSIONS

The high-resolution magnetic method has proved successful in locating abandoned brine wells in the City of Hutchinson, Kansas. Five brine wells, four suspected brine wells, one probable water well, and one probable gas pipe were found by magnetic anomalies. The anomalies owing to brine wells with 8-in. steel casing have an almost perfect monopole shape with an amplitude >12,000 nT. Anomalies owing to suspected brine wells with 2.5- or 4-in. pipe also have an almost perfect monopole shape with an amplitude of >2,000 nT. The half-width of these anomalies is approximately 5–7 ft, which roughly correlates with the depth to the top of the wells. A vertical-gradient survey can be used in the future to improve the horizontal resolution of a magnetic survey in the hope of distinguishing wells in close proximity relative to their depths.

## ACKNOWLEDGMENTS

We greatly appreciate Dennis Clennan of the City of Hutchinson for his support of this project. We would like to thank Michael Cochran and Mary Daily of the Kansas Department of Health and Environment for discussion and materials on salt-mining history in Hutchinson. We would like to thank Sihao Xia of the University of Kansas for his assistance in data acquisition and data processing, and also David Laflen and Brett Bennett of the Kansas Geological Survey, and Gang Tian of Jinlin University (PRC), for their assistance in data acquisition. We would also like to thank Reg Jones and his crew at the City of Hutchinson for their help in field operations, and Ross Johnson of Geometrics, Inc., for valuable discussion on the use of the G-858 magnetometer. Finally, we would like to thank Dean Keiswetter of AETC Incorporated and Ken Johnson of the Oklahoma Geological Survey for their constructive suggestions and review, and Mary

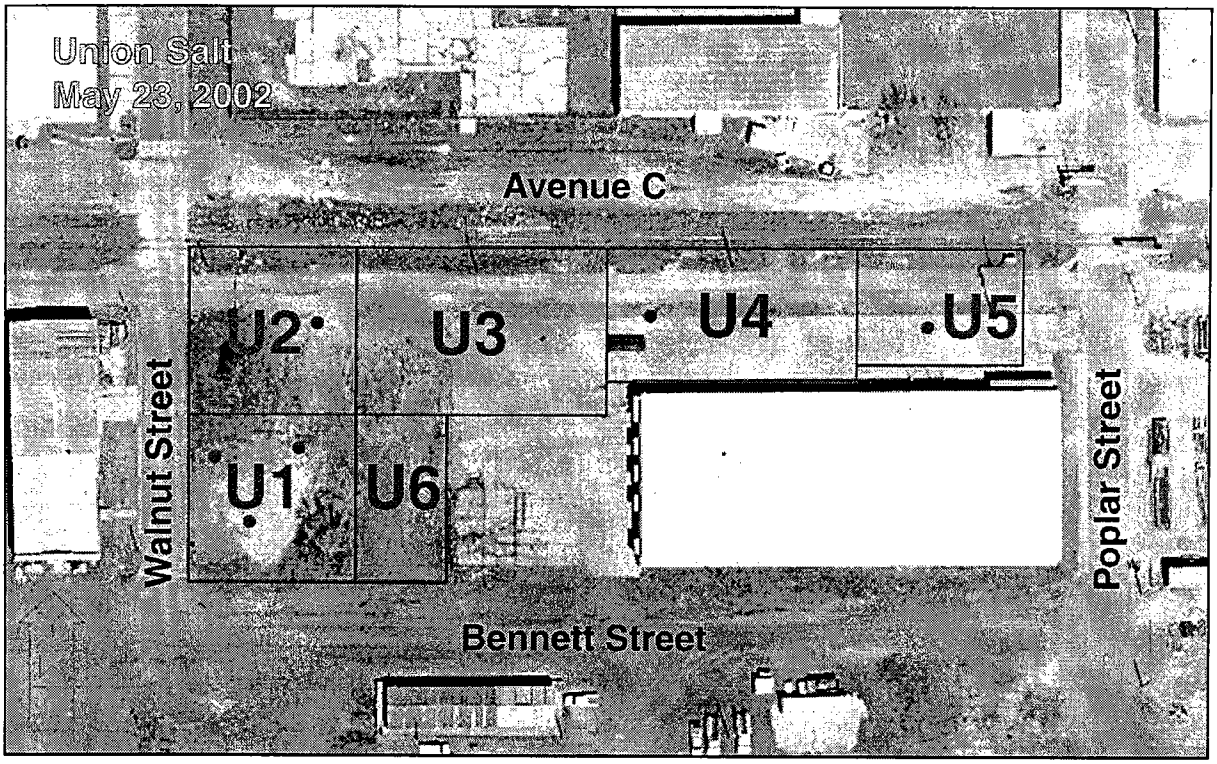


Figure 5. Aerial photograph of the Union Salt site, with grids superimposed. Dots in each grid indicate locations of verified anomalies.

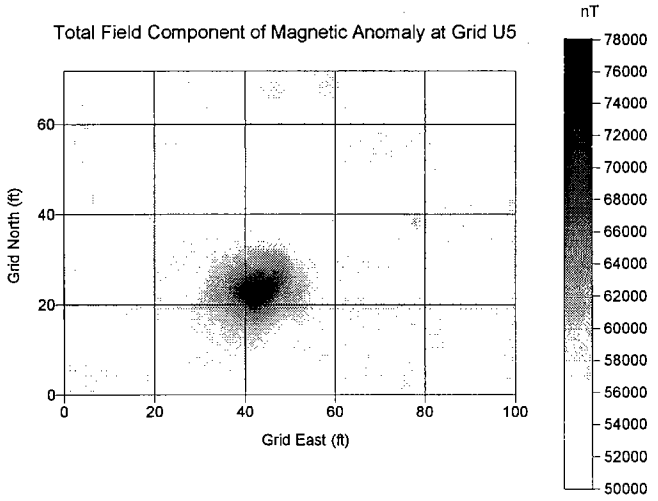


Figure 6. Total-field component of the magnetic anomaly in grid U5 at the Union Salt site (top). The anomaly at (42, 23) is due to a brine well under 6 in. of concrete. Depth to the top of the well is 1 ft (bottom). (Richard Harper of the Kansas Department of Health and Environment was taking a note.)

Brohammer for her efforts in the preparation of this paper.

## REFERENCES CITED

Allison, M. L., 2001, Hutchinson, Kansas: a geologic detective story: Geotimes, v. 46, no. 10, p. 14–18.

Breiner, S., 1973, Application manual for portable magnetometers: Geometrics, Inc., 58 p.

Surfer® 7, 1999, User's guide: Golden Software, Inc., 619 p.

Watney, W. L.; Nissen, S. E.; Bhattacharya, Saibal; and Young, David, 2003, Evlauation of the role of evaporite karst in the Hutchinson, Kansas, gas explosions, January 17 and 18, 2001, *in* Johnson, K. S.; and Neal, J. T. (eds.), Evaporite karst and engineering/environmental problems in the United States: Oklahoma Geological Survey Circular 109 [this volume], p. 119–147.

Xia, Jianghai, 2001, Using electromagnetic methods to locate abandoned brine wells in Hutchinson, Kansas: Kansas Geological Survey Open-File Report 2001-17.

_____2002a, Using electromagnetic methods to locate abandoned brine wells in Hutchinson, Kansas: Symposium on the Application of Geophysics to Engineering and Environmental Problems (SAGEEP), 2002 Annual Meeting of EEGS, Las Vegas, Nevada, February 10–14, 2002, 11 p., available on CD-ROM.

_____2002b, Using the high-resolution magnetic method to locate abandoned brine wells in Hutchinson, Kansas: Kansas Geological Survey Open-File Report 2002-43, 58 p.

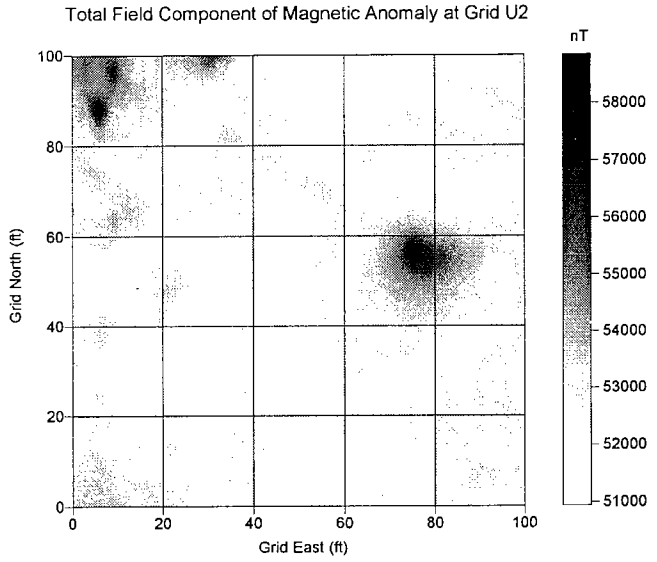


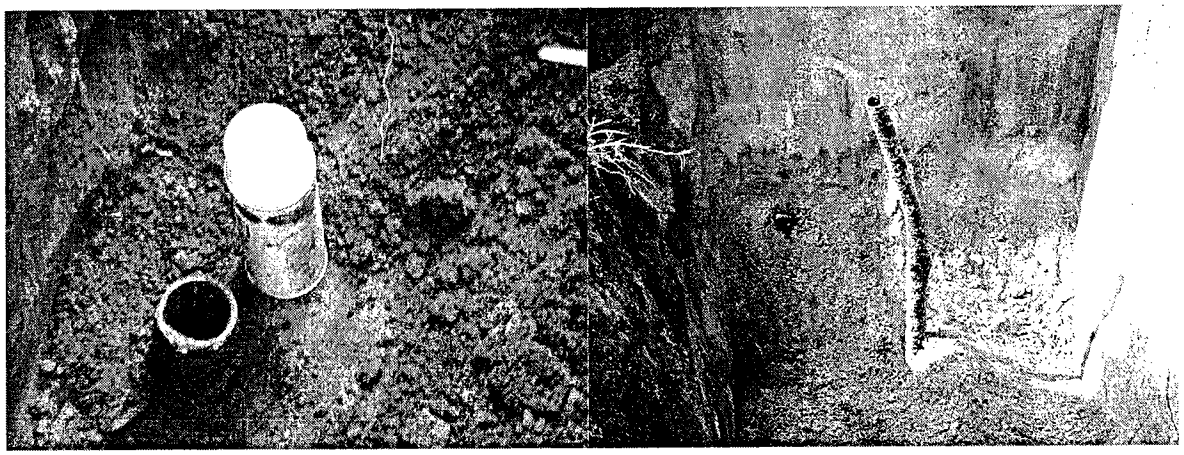

Figure 7. Total-field component of the magnetic anomaly in grid U2 at the Union Salt site (top). The anomaly at (75, 56) is due to two suspected brine wells (one 2.5 in. and the other 2.785 in.) at a depth of 4 ft (bottom, left). These photos show only the 2.5-in. well at (74, 56). A spray-paint can is shown for scale. We dug down 7 ft (bottom, right) to make sure this was not just a junk pipe.

# Evaporite Karst and Ground-Water Flow, Discharge, and Quality in the Crystal Spring Catchment Area in the Central Flint Hills of Kansas

***P. Allen Macfarlane and Margaret A. Townsend***
Kansas Geological Survey
Lawrence, Kansas

**ABSTRACT.**—Crystal spring issues from the Barneston Limestone (Permian) outcrop belt in Marion County, Kansas, and is one of many high-yielding springs in the Flint Hills region. During this study, spring discharge from karstic aquifer zones ranged from 28.3 to >340 L/s. Observations of the Barneston in a nearby quarry and from core descriptions in the literature indicate significant development of interconnected secondary porosity from dissolution of its contained evaporites in the near-surface environment. Geochemical evidence indicates that Crystal spring is fed by ground-water discharge from two sources moving through the Barneston limestones: (1) diffuse recharge from the Barneston outcrop and confined regional flow, and (2) focused recharge through stream-bottom sinkholes within the outcrop. High-amplitude fluctuations in spring discharge are directly tied to precipitation events in the up-gradient Martin Creek drainage basin. Dye-trace studies indicate that sinkholes in Martin Creek and the spring are hydraulically connected by a well-developed conduit system in the limestone aquifer. Water-level data from monitoring wells near the sinkholes show rapid development of a recharge mound in the adjacent aquifer when there is flow in the creek, and the gradual loss of water in storage from the conduit system in the ensuing dry periods. Differences in the fracture/solution–channel conduit system between the upper and lower Barneston provide an explanation for the apparent water-level behavior.

## INTRODUCTION

This study was originally undertaken to assist the Kansas Department of Health and Environment with a source-water assessment (SWAA) of Crystal spring, the sole water supply for the city of Florence in Marion County, Kansas (Fig. 1). A key activity in the Kansas Source Water Assessment Program is the delineation of all public water-supply source-water-assessment areas. Crystal spring is fed by ground-water discharge from a karst aquifer in the Barneston Limestone, and during this study spring discharge ranged from 28.3 to >340 L/s. For public supplies that depend on spring sources, the SWAA includes the ground-water-flow system (catchment area) that supplies water to the spring.

Very little is known of the regional hydrogeology of the Flint Hills region. Springs of varying magnitude in the region have been noted in the literature since the late 1800s (Sawin and others, 1999). O'Connor and Chaffee (1983) identified ground-water sources and took measures of flow and water quality of the springs in Marion County. Sawin and others (1999) assembled historic data on and conducted an inventory of springs within the Flint Hills region.

In keeping with the theme of this symposium volume, the overall purpose of this contribution is to describe the hydrogeologic highlights of our investigation of the catchment for Crystal spring in Marion County with respect to evaporite karst. The impact of these processes on secondary porosity and ground-water storage and movement is discussed in the context of a hydrogeologic model of the Barneston Limestone.

## SETTING

The study area lies in the tallgrass prairie of the central part of the Flint Hills physiographic province, in the eastern part of Marion County, north of the Cottonwood River (Schoewe, 1949; Fig. 1). The Cottonwood River flows along the study area's southern boundary. Martin and Bruno Creeks are tributaries of the Cottonwood; they flow southeastward across the study area and are typically dry for much of the year. Except for where the bedrock crops out at the surface, soils in the study area are excessively to well-drained soils with a silty-clay to silty-clay-loam texture (Horsch and McFall, 1983). The climate is sub-humid continental, and most of the annual 762–889 mm of precipitation occurs in the late spring months (Goodin and others, 1995).

Alternating Lower Permian shale and limestone units belonging to the uppermost Council Grove and

Macfarlane, P. A.; and Townsend, M. A., 2003, Evaporite karst and ground-water flow, discharge, and quality in the Crystal spring catchment area in the central Flint Hills of Kansas, *in* Johnson, K. S.; and Neal, J. T. (eds.), Evaporite karst and engineering/environmental problems in the United States: Oklahoma Geological Survey Circular 109, p. 177–182.

Chase Groups underlie the study area. Confining layers of shaly bedrock units separate karstified aquifers dominated by limestone and cherty limestone. Perennial and wet-weather springs are common along the outcrop of the Barneston.

## BARNESTON LIMESTONE HYDROGEOLOGIC FRAMEWORK

In ascending order, the Barneston Limestone consists of the Florence Limestone, the Oketo Shale, and the Fort Riley Limestone Members (Fig. 2; Zeller, 1968; Mazzulo and others, 1997). The Barneston is well exposed in the Sunflower rock quarry near the southeastern edge of the study area (Figs. 1, 2) and is 25.7 m thick in the quarry.

Secondary porosity is prominent in the Barneston Limestone exposed in the Sunflower quarry and has developed from both evaporite and carbonate dissolution. Vertical planar joints extend across the entire section of the Barneston in the quarry, whereas curvilinear to non-vertical planar joints are confined to the Fort Riley (Fig. 2). Many of the joint surfaces are smooth, are slightly red stained, appear to be solution enlarged, and contain a filling of red clayey-silt residuum. Mazzullo and others (1997) attributed the vuggy nature of the weathered, thin-bedded, shaly limestone in the upper Fort Riley and lower Florence to the dissolution of disseminated evaporite nodules. Downdip of the outcrop belt in Riley County, Kansas, Twiss (1991) reported finding nodules and seams of gypsum in the upper Fort Riley and small inclusions of halite in many thin zones within the Fort Riley and Florence.

Solution-channel segments in the lower Fort Riley range in diameter from <2.5 to 15.2 cm and in length from <10 cm to 2 m. The segments appear to be scalloped, and some contain a filling of red clayey-silt residuum (Fig. 2). The smaller diameter and shorter length sub-vertical pipes may have formed from the dissolution of burrow-filling carbonates (Twiss, 1991). Many of these features intersect the joint planes. However, from observation it is not clear if the distribution of these solution channels is directly related to the jointing in the rocks. This zone of dissolution features occurs 1–3.7 m above the Fort Riley base.

Near the top of the Florence, the remnants of a partially silt-filled cavern were found along one wall of the quarry (Fig. 2). The cavern is ~1.5 m in height and slightly >0.3 m in width, with a layer of stratified clayey silt ~0.5 m thick covering the bottom (Fig. 2). Two vuggy zones, each slightly >0.3 m thick and spaced approximately a meter apart, occur near the bottom of the cherty-limestone interval of the Florence (Fig. 2). Vug sizes range from <2.5 cm to ~0.3 m in diameter. These zones were encountered during the cable-tool drilling of a monitoring well 4 km north of the quarry (Fig. 1). Water-level data collected from the monitoring well indicate that these zones are saturated nearer Martin Creek and are sufficiently continuous to transmit water laterally from the catchment area to Crystal spring.

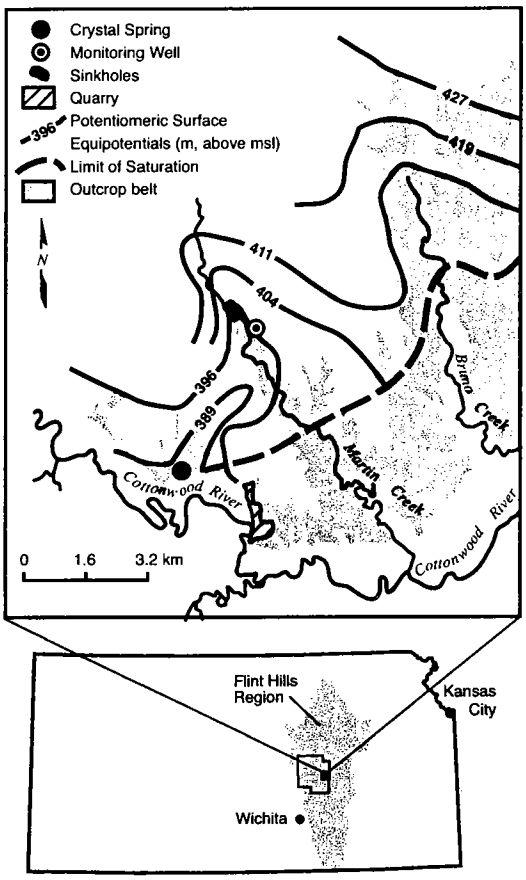


Figure 1. Map showing Crystal spring, surface hydrologic features, the Sunflower rock quarry, and the monitoring well. Superimposed on the map are contours showing the potentiometric surface associated with aquifer zones in the Barneston Limestone.

Approximately 5.6 km north of Crystal spring, the stream bottom of Martin Creek rests on the uppermost Fort Riley, where sinkholes have developed along exposed joint planes that intersect the stream channel (Fig. 1). Each sinkhole is an elliptical depression ~0.6–1.0 m deep with one or more small openings, 5–15 cm in diameter, into the top of the limestone. Pools of water typically remain in these depressions for up to several weeks following a wet period or a heavy rain, slowly draining water into the underlying Fort Riley Limestone.

## GROUND-WATER-FLOW PATTERNS AND DYE TRACES

A potentiometric-surface map (Fig. 1) is based on scattered measurements of the hydraulic head in wells and the elevations of perennial springs that discharge ground water from the Barneston aquifer. The hydraulic-head measurements were collected from domestic and stock wells during November–December 2000, normally a dry period in the region (Fig. 1). Considering the limited number of hydraulic-head measurements and the karstified nature of the aquifer, only

the general direction of ground-water flow can be reasonably interpreted from the map. Taking these limitations into account, the potentiometric surface indicates that ground water flows in a generally southerly direction from areas where the Barneston Limestone is covered by younger rocks, Crystal spring, and the Cottonwood River. The contour map also suggests southwestward ground-water flow along the Barneston outcrop, where it is water saturated.

The sinkholes in the stream bottom of Martin Creek are hydraulically up-gradient and 5.6 km away from Crystal spring (Fig. 1). Two sets of dye-trace experiments were performed to evaluate the hydraulic connection and estimate time of travel between the sinkholes and the spring. The first set of experiments was run in September 2000 and yielded a travel time of <43 hours, when spring discharge was ~73.6 L/s. A second experiment was conducted in October 2002 and yielded a travel time of 55 hours, when the spring was discharging at ~28.3 L/s.

## STREAM–AQUIFER RELATIONS NEAR MARTIN CREEK

In May and early June 2002, a series of storms generated streamflow in Martin Creek. Overall, the monitoring-well hydrograph shows the decline of water levels in the Barneston aquifer at the monitoring well from this wet period through the dry summer and early fall (Fig. 3). During the previous dry winter period, the water level in the monitoring well was 24.4 m below the casing top, and Martin Creek was dry. The high water level in the monitoring well at the beginning of the record is attributed to ground-water-mound formation caused by surface-water inflow into the Fort Riley through the sinkholes and exposed solution-widened fractures in Martin Creek.

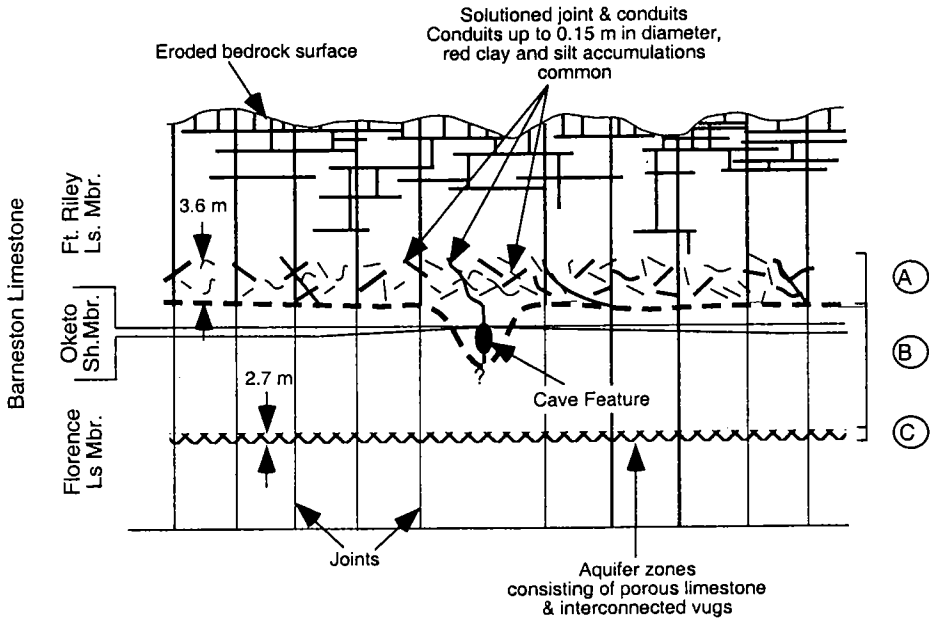


Figure 2. Schematic cross section of the Barneston Limestone secondary-porosity features observed in the Sunflower rock quarry and elsewhere in the study area. Interval A is a secondary porosity consisting of sinuous solution-channel pipes of various diameters and lengths, and solution-enlarged fracture apertures within the lower part of the Fort Riley. Interval B is a secondary porosity consisting primarily of vertical fractures that exhibit some aperture-solution enlargement. Interval C is a secondary porosity consisting of two zones of highly porous and vuggy limestone that appear to extend across the study area.

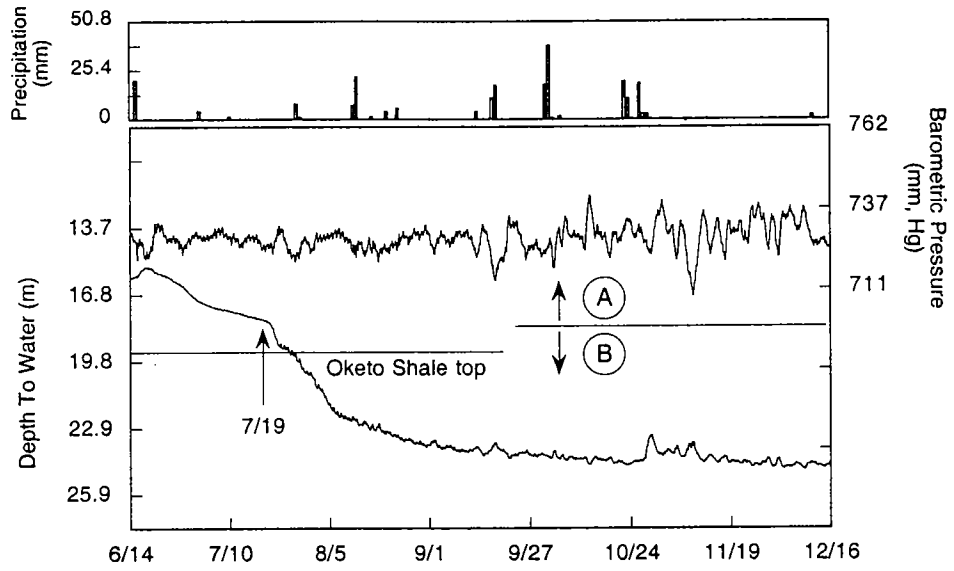


Figure 3. Plot showing water-level recession in the monitoring well near Martin Creek following the Spring 2002 wet period. The beginning of record indicates bank-full conditions in Martin Creek owing to spring storms. The monitoring well is screened in the lower part of the Florence Member. Note the change in the response of the water level to barometric-pressure changes shortly after July 19. *A* and *B* refer to the secondary-porosity zones described in Figure 2.

Changes in the character of the hydrograph over time during the recession provide insight into the nature of the storage in the Fort Riley and the ability of the vertical fractures to transmit water in storage downward into the underlying saturated aquifer zones in the Florence. Ideally, the recession hydrograph following recharge entering an aquifer from an intermittent stream, such as Martin Creek, is typically concave upward in shape (Moench and Kisiel, 1970). In this hydrograph, segments of record follow the concave-upward shape, but the remainder has convex segments. Changes in the shape of the hydrograph are indicative of the variability in the interconnected secondary porosity observed in the Sunflower quarry (Fig. 1). Figure 4 is a hydrogeologic model of the Barneston Limestone that provides one explanation for the observed water-level behavior in the monitoring well following the late spring 2002 wet period.

The early part of the hydrograph (up to about July 19, 2002) shows the slow decline of water levels from the period of recharge, and does not seem to be as affected by fluctuations in barometric pressure as the later part of the hydrograph (Fig. 3). During this time period, water levels were in the lower part of the Fort Riley Limestone, where the secondary porosity consists of solution-enlarged fractures and solution channels (Figs. 2, 4). The pattern of water-level change seems to follow what would be expected for groundwater levels in recession. The damped response of the water level in the monitoring well to atmospheric-pressure changes suggests that the aquifer framework is relatively open to the atmosphere (Figs. 3, 4).

After July 19, the monitoring-well water level dropped rapidly through the lowermost Fort Riley, the Oketo, and into the underlying Florence (Fig. 3). The much greater water-level-decline rate in the lowermost Fort Riley and in the underlying upper Florence was most likely caused by a reduction in the available storage and loss of the solution channel and solution-enlarged fracture permeability (Fig. 4). This leaves only the vertical fractures to transmit ground water vertically to the aquifer zones in the lower part of the Florence, with little storage out in the formation away from the fractures. The increased amplitude of water-level fluctuations in the monitoring well suggests greater isolation and partial confinement of ground water in the Florence (Figs. 3, 4). The cause of this apparent confinement is likely the low secondary porosity and permeability in the lowermost limestone unit in the overlying Fort Riley (Fig. 4). In the Sunflower quarry, only vertical fractures provide secondary porosity and permeability in the basal massive limestone of the Fort Riley. Water levels in the August–September part of the hydrograph seem to follow the normal concave-upward pattern of response to recession from a recharge event in a relatively homogeneous aquifer.

## GROUND-WATER HYDROCHEMISTRY

The overall water type in the area is Ca–$HCO_3$, $SO_4$. Chloride concentrations are generally low (<20 mg/L; Fig. 5). As is typical for ground-water systems, $SO_4$, Cl, and $HCO_3$ are highly correlated ($R^2 = 0.8$) with specific conductance (SPCD; Hem, 1985), and, in the Crystal spring discharge, their concentrations are inversely related to flow rate as reflected by SPCD values (Fig. 6).

Flow to Crystal spring originates from two possible sources: diffuse flow from both regional sources and

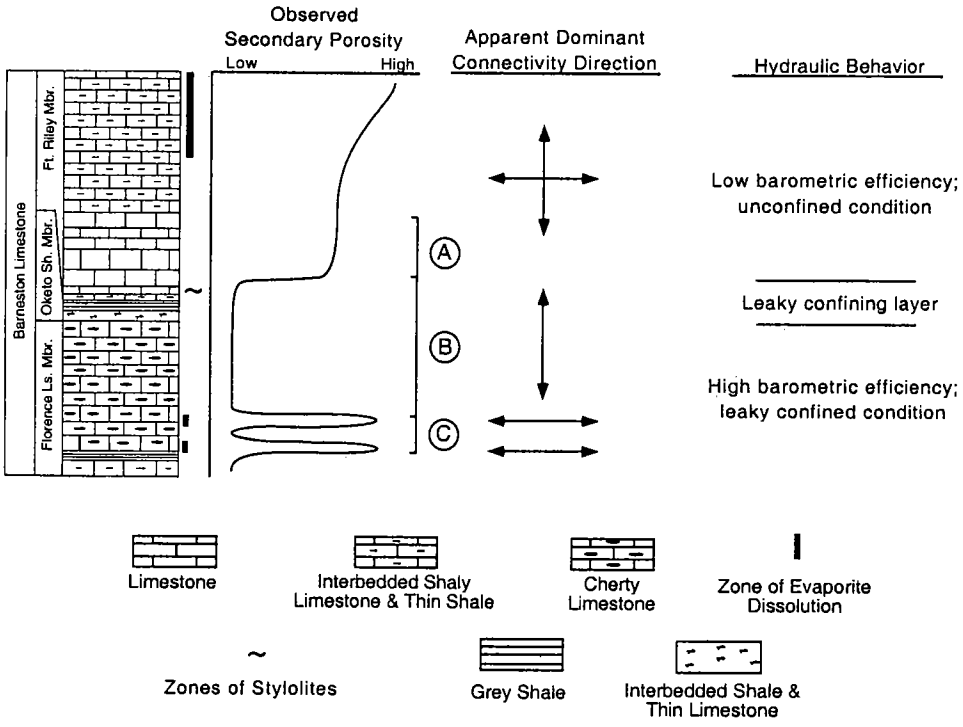


Figure 4. Hydrogeologic model of the Barneston Limestone in the study area, showing the relative development of secondary porosity, apparent degree of hydraulic connectivity laterally and vertically, and hydraulic behavior based on the hydrograph for the monitoring well. Zones of evaporite dissolution are taken from Mazzulo and others (1997). *A*, *B*, and *C* refer to the secondary-porosity zones described in Figure 2.

local flow from the outcrop areas; and focused recharge through sinkholes in the stream bottoms. These flow systems are identified by use of $SO_4$/Cl ratios (Fig. 5) and by dissolved organic carbon (DOC) and SPCD (Fig. 7). Diffuse-flow chemistry is quite variable, depending upon the degree of interconnectedness that is encountered in the rock framework (Figs. 2, 4). The diffuse-flow system tends to have somewhat higher $SO_4$/Cl ratios than the focused-recharge chemistry, perhaps reflecting the longer residence time. In Figure 5 the chemistry of the focused recharge, and the springs that occur along the outcrop belt, have similar $SO_4$/Cl ratios and range of Cl concentrations, suggesting similar sources of water.

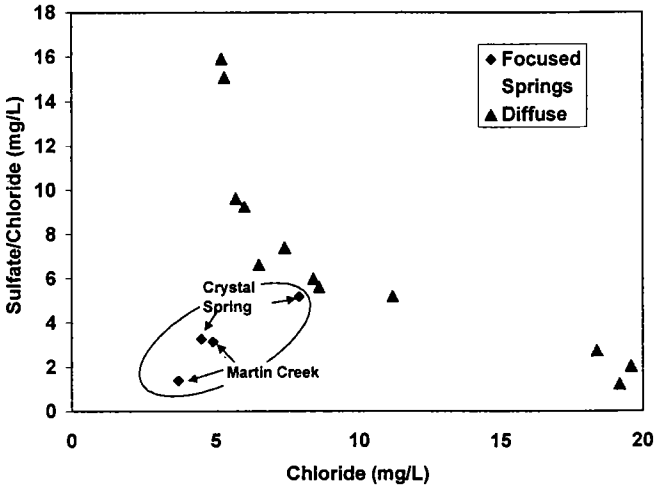


Figure 5. Plot shows delineation of focused and diffuse discharge flow systems, based on $SO_4$/Cl ratios and chloride concentrations. Diffuse sources from regional and local flow systems have higher $SO_4$/Cl ratios and/or chloride values reflecting the increased travel or residence time of the water and the variation in the karst geometry of the flow path. Focused discharge from surface runoff is reflected in lower $SO_4$/Cl ratios and overall lower chloride concentrations than shown by diffuse sources.

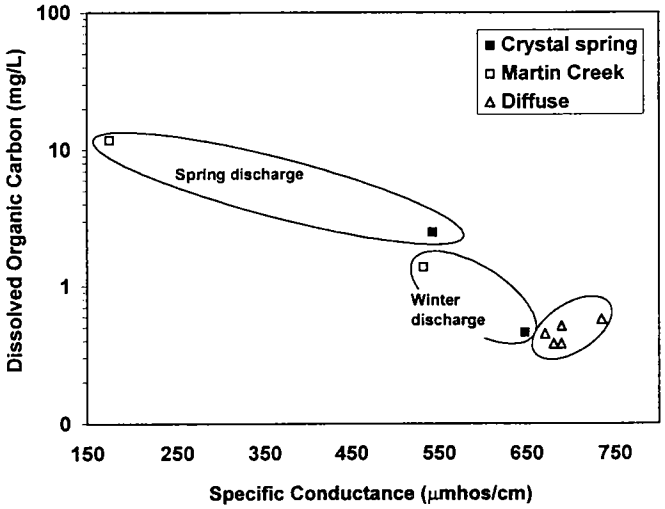


Figure 7. Focused-discharge values for Martin Creek and Crystal spring are higher in the spring than in the winter (see also Fig. 6). Higher DOC and lower SPCD values reflect the higher discharge effects on the water chemistry. Lower DOC and higher SPCD values reflect the lower winter-discharge values. The diffuse-flow sources show a similar DOC and SPCD range that is lower in both spring and winter than the focused-discharge samples.

Figure 6 shows the correspondence of discharge, specific-conductance, and turbidity values at Crystal spring to precipitation events in the watershed. The high discharge has low SPCD and elevated turbidity values. The low discharge (base flow) has elevated SPCD and depressed turbidity values related to diffuse flow sources, whether regional or local in nature. The correspondence of discharge and turbidity values to precipitation events is also well illustrated.

Figure 7 shows the differentiation of sources of recharge based on DOC and SPCD values. The wide variation in DOC values for the focused discharge reflects the impact of surface runoff and the high-volume recharge from sinkholes in Martin Creek. The tight clustering of the diffuse-flow points suggests that storm events have less impact on the quantity of DOC injected into the system. In addition, the higher SPCD values for these points imply a longer residence and travel time for these samples. The similarity of the higher SPCD values with the low-flow chemistry from Crystal spring suggests the possibility that base flow to Crystal spring is fed by diffuse-flow sources.

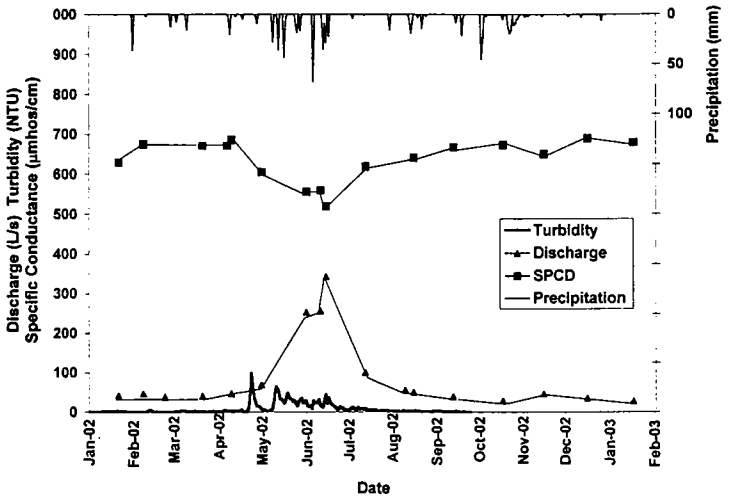


Figure 6. Graph shows the correspondence of precipitation and discharge events at Crystal spring. Increased turbidity and decreased SPCD values show the influence of surface runoff and the impact of focused discharge on the chemistry of the spring. SPCD values reflect the variation in $SO_4$ and Cl concentrations that occur during high- and low-flow conditions at the spring.

## SUMMARY AND CONCLUSIONS

The hydrostratigraphic units that laterally transmit ground water to Crystal

spring from its catchment are the thin aquifer zones in the Florence Limestone Member of the Barneston Limestone. The evidence collected during this investigation suggests that spring discharge originates from (1) diffuse flow from regional, confined ground-water flow and local ground-water flow in the Barneston outcrop belt that has higher chloride and $SO_4$/Cl values and lower DOC values; and (2) focused recharge through sinkholes in the bottom of Martin Creek that has lower $SO_4$/Cl values but higher DOC values. Spring-discharge measurements, the water-level data from the monitoring well, and the water-chemistry fluctuations in the spring indicate that precipitation is a major control on the ground-water-flow system in the catchment, and, consequently, spring discharge. During the dry season, regional ground-water flow from the confined Barneston aquifer is the dominant contributor to spring discharge.

The monitoring-well hydrograph and observations of the Barneston in a nearby quarry suggest that (1) porous zones in the lower part of the Florence Limestone are the primary means by which ground water is transmitted to the spring, and (2) solution features and solution-enlarged fractures in the Fort Riley Limestone locally enhance the water-storage capacity of the Barneston, especially in the vicinity of Martin Creek. Porosity development in the lower Florence and upper Fort Riley is partly due to evaporite and carbonate dissolution. The dye-trace experiments confirm that a well-developed conduit system exists between the sinkholes and the spring, which is 5.6 km to the south.

## REFERENCES CITED

Goodin, D. G.; Mitchell, J. E.; Knapp, M. C.; and Bivens, R. E., 1995, Climate and weather atlas of Kansas: Kansas Geological Survey Educational Series 12, 24 p.

Hem, J. D., 1985, Study and interpretation of the chemical characteristics of natural water: U.S. Geological Survey Water-Supply Paper 2254, 263 p.

Horsch, M. L.; and McFall, G., 1983, Soil survey of Marion County, Kansas: U.S. Department of Agriculture, Soil Conservation Service, 111 p.

Mazzulo, S. J.; Teal, C. S.; and Burtnett, C. A., 1997, Outcrop stratigraphy and depositional facies of the Chase Group (Permian, Wolfcampian) in Kansas and southeastern Nebraska: Kansas Geological Survey Technical Series 6, 210 p.

Moench, A. F.; and Kisiel, C. C., 1970, Application of the convolution relation to estimating recharge from an ephemeral stream: Water Resources Research, v. 6, p. 1087–1094.

O'Connor, H. G.; and Chaffee, P. K., 1983, Geohydrology field trip, Marion County, Kansas, November 18–19, 1983: Kansas Geological Survey Open-File Report 83-25, 42 p.

Sawin, R. S.; Buchanan, R. C.; and Lebsack, W., 1999, Flint Hills springs: Kansas Academy of Science Transactions, v. 102, p. 1–31.

Schoewe, W. H., 1949, The geography of Kansas: Kansas Academy of Science Transactions, v. 52, p. 261–333.

Twiss, P. C., 1991, Chase Group from the near-surface Amoco No. 1 Hargrave core, Riley County, Kansas, *in* Kansas Geological Survey (ed.), Midcontinent core workshop—Integrated Studies of Petroleum Reservoirs in the Midcontinent: American Association of Petroleum Geologists, Midcontinent Section Meeting, Wichita, Kansas, p. 123–141.

Zeller, D. E. (ed.), 1968, The stratigraphic succession in Kansas: Kansas Geological Survey Bulletin 189, 81 p.

# Sinkholes and Land Subsidence Owing to Salt Dissolution near Wink, West Texas, and Other Sites in Western Texas and New Mexico

***Kenneth S. Johnson***
Oklahoma Geological Survey
Norman, Oklahoma

***Edward W. Collins***
Bureau of Economic Geology
The University of Texas
Austin, Texas

***Steven J. Seni***
Railroad Commission of Texas
Austin, Texas

**ABSTRACT.**—Since 1980, several large sinkholes and anomalous subsidence features have formed in the giant Hendrick oil field near the town of Wink, in Winkler County, West Texas. Wink Sink no. 1 (360 ft wide) and Wink Sink no. 2 (780 ft long in March 2003) are catastrophic sinkholes that formed when underground cavities in salt migrated upward by successive roof failures until they breached the land surface. Other anomalous features include earth fissures and several areas of broad ground subsidence that have sagged as much as 28 ft between 1970 and 1999. We infer that underground cavities in the Wink area have formed in the Permian Salado Formation salt beds, which here are about 1,300 ft below the surface. Although natural dissolution of salt has occurred in the region, and also near Wink, it is likely that historic oil-field activities initiated the large dissolution cavities and resultant collapse and subsidence features near Wink by allowing fluids, unsaturated with salt, to contact and dissolve salt beds along unprotected boreholes. Other sinkholes in the region that apparently formed in association with petroleum- or brine-well activity include Jal Sink, in Lea County, New Mexico; McCamey Sinkhole, in Upton County, Texas; and Borger Sinkholes, in Hutchinson County, Texas. To ensure that petroleum boreholes do not cause, or contribute to, development of salt-dissolution sinkholes, the Railroad Commission of Texas requires that drilling, completion, and plugging practices assure integrity of the boreholes and prevent unintended dissolution of subsurface salt deposits.

## INTRODUCTION

A 1-mi$^2$ area near the town of Wink, in Winkler County, Texas (Fig. 1), has developed two catastrophic sinkholes and several broad areas of subsidence and fissures within the past 23 years. All these features occurred in an unpopulated area near the middle of the Hendrick field, a giant oil field discovered in 1926. Wink Sink no. 1 (Fig. 2) formed on June 3, 1980, 2 mi north of Wink, and within 24 hours it was 360 ft wide (Baumgardner and others, 1982). The second catastrophic sinkhole, Wink Sink no. 2, developed on May 21, 2002, ~1 mi south of Wink Sink no. 1. Initially, the sink was ~450 by 300 ft, and by March 2003 it was ~780 by 610 ft. The volume of Wink Sink no. 1 is estimated at 5.6 million cubic ft, and that of Wink Sink no. 2 at 47.6 million cubic ft. Each of the sinkholes incorporated a plugged borehole.

In 1999, Collins (2000) investigated two areas of broad subsidence and earth fissures that are, respectively, ~1,000 ft north and 2,000 ft east of Wink Sink no. 2. The land surface has sagged as much as 23 and 28 ft in two different subsidence areas since 1970, and this has been accompanied by formation of fissures up to 1 ft wide and 6.5 ft deep. The subsidence areas contain several producing or abandoned oil wells. A water-supply well is centered within the eastern subsidence area.

It appears that the sinkholes and subsidence features have resulted from underground dissolution cavities developed in salt beds of the Permian Salado Formation, which is ~850–1,050 ft thick and is ~1,300 ft below ground level. Natural dissolution of Salado salt beds is well known in Winkler County and other areas of West Texas and New Mexico, but dissolution and collapse or subsidence in the Wink area apparently resulted from, or may have been accelerated by, historic oil-field practices.

Whether salt dissolution at any particular site is due to natural causes or oil-field activity, there are four requirements for such dissolution to occur (Johnson, 1981): (1) a deposit of salt through which water can flow, (2) a supply of water unsaturated with respect to NaCl, (3) an outlet whereby the resulting brine can escape, and (4) energy (such as hydrostatic

Johnson, K. S.; Collins, E. W.; and Seni, S. J., 2003, Sinkholes and land subsidence owing to salt dissolution near Wink, West Texas, and other sites in western Texas and New Mexico, *in* Johnson, K. S.; and Neal, J. T. (eds.), Evaporite karst and engineering/environmental problems in the United States: Oklahoma Geological Survey Circular 109, p. 183–195.

head or density gradient) to cause water to flow through the system.

## GEOLOGIC SETTING

The town of Wink, in Winkler County, Texas, lies astride the boundary between the Delaware Basin on the west and the Central Basin Platform on the east (Fig. 1). These major structural provinces are part of the greater Permian Basin of West Texas and southeastern New Mexico, and are characterized by different sequences of Permian strata. The provinces are separated by the Capitan Reef, a massive limestone and dolomite reef that fringed the eastern and northern margins of the Delaware Basin during Guadalupian (Late Permian) time.

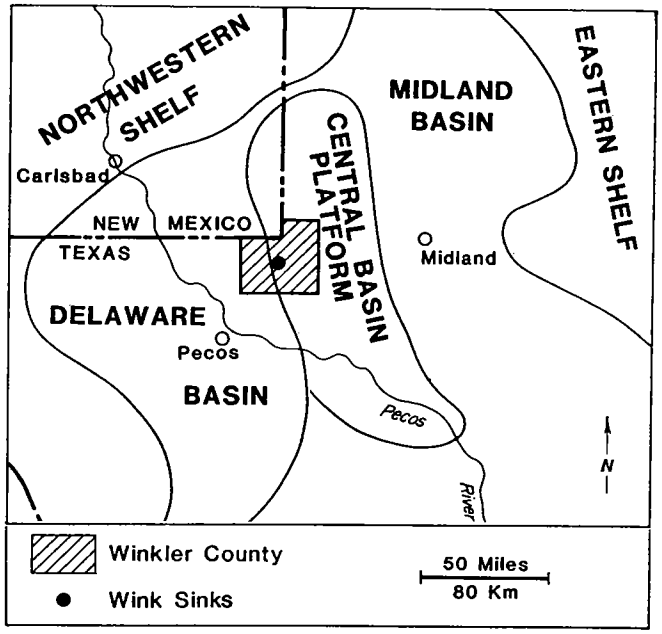


Figure 1. Map of West Texas and southeastern New Mexico, showing major geologic provinces and location of Wink Sinks in Winkler County.

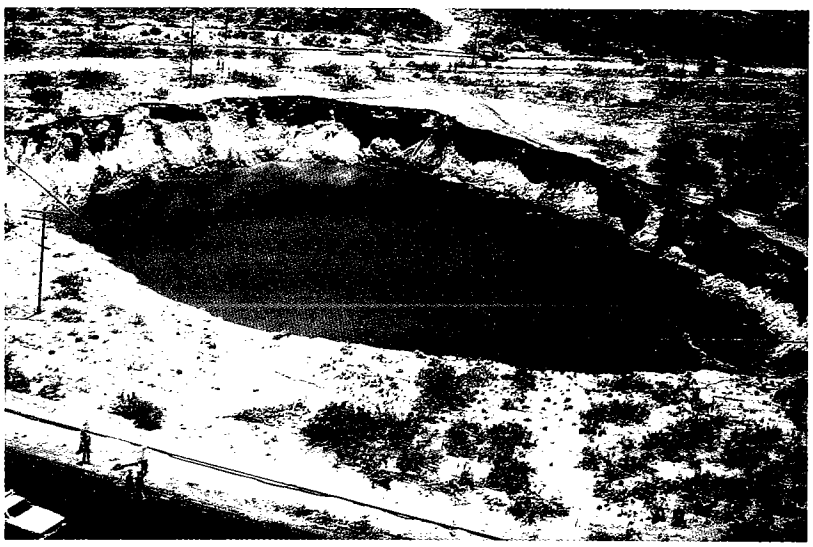

Figure 2. Aerial photograph of Wink Sink no. 1 on June 5, 1980 (photograph by R. W. Baumgardner, Jr.). Sinkhole reached 360 ft wide and 110 ft deep; depth to water surface is ~33 ft.

Rocks of principal concern in the Winkler County area are sedimentary and are of Permian, Triassic, and Cenozoic age (Fig. 3). The Capitan Reef, the oldest Permian unit of interest, is a massive sequence of limestone and dolomite ~1,500–2,000 ft thick and 8–10 mi wide in western Winkler County (Garza and Wesselman, 1959; Hiss, 1975). Carbonate rocks in the Capitan typically have a high porosity and permeability, and they have provided a tremendous volume of water for waterflood operations in West Texas.

Overlying the Capitan Reef are the Yates and Tansill Formations; they consist of dolomite and limestone, with some interbeds of sandstone and shale, and a persistent anhydrite unit at the top of the Tansill (Ackers and others, 1930). In the Wink area the Yates is ~280 ft thick, and the Tansill is ~160 ft thick (Baumgardner and others, 1982). Porosity occurs in the form of irregular solution cavities as much as 2 in. in diameter, and also as interstitial voids in the granular rocks. Solution cavities lined with calcite are common in the oil-producing zones.

Above the Tansill is the Salado Formation, a thick sequence of interbedded salt (halite) and anhydrite. The formation consists of eight salt units, each underlain by an anhydrite bed (Johnson, 1986, 1993); anhydrite units in the area typically are 10–50 ft thick, whereas the intervening salt units commonly are 10–250 ft thick. Salado strata are ~850–1,050 ft thick beneath the Wink sinkholes and subsidence features, but are as thick as 1,300 ft just to the east, and only ~600 ft thick just to the west (Fig. 4). Just another 3–4 mi to the west the Salado Formation lacks salt and is only 300–400 ft thick (Fig. 3). The area where Salado salt is missing is referred to as a *dissolution trough,* because overlying strata thicken into this area of salt removal. Variations in thickness of the Salado Formation and of individual salt units are largely due to dissolution of one or more of the salt units during Salado and post-Salado times. Dissolution of the salts in the Salado has been noted in earlier literature (Ackers and others, 1930; Maley and Huffington, 1953; Anderson and Kirkland, 1980), and later work has shown that dissolution has occurred in each of the Salado salt units in the vicinity of Wink (Baumgardner and others, 1982; Johnson, 1986, 1987, 1993).

Overlying the Salado is the Rustler Formation, which consists of interbedded anhydrite, dolomite, limestone, shale (or mudstone), and sandstone (Ackers and others, 1930; Baumgardner and others, 1982). The Rustler is ~240–280 ft thick

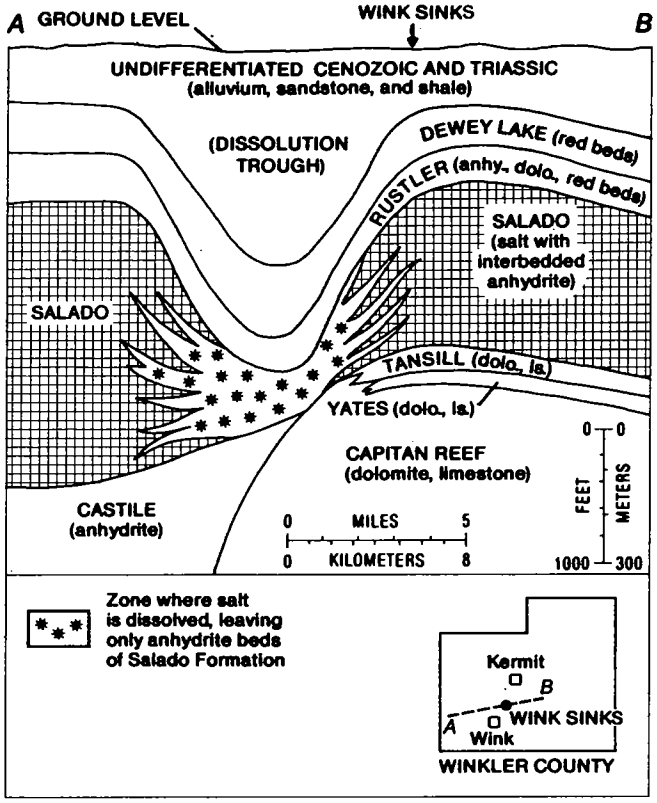


Figure 3. Schematic east–west cross section in Winkler County showing natural dissolution of Salado Formation salts on the east side of the Delaware Basin and location of the Wink Sinks (modified from Baumgardner and others, 1982; Johnson, 1987). All strata below the "Undifferentiated Cenozoic and Triassic" are Permian in age.

near the Wink collapse features (Johnson, 1986) but locally is as thick as 310 ft just to the west, where it thickens owing to dissolution and collapse of the underlying Salado salt units during Rustler deposition (Fig. 3).

The Dewey Lake Formation consists of red-brown shale, sandy shale, and siltstone overlying the Rustler (Ackers and others, 1930; Baumgardner and others, 1982). Dewey Lake strata are 400–460 ft thick beneath the Wink collapse features, but they are much thicker just to the west (Fig. 3) owing to dissolution of Salado salt that occurred during Dewey Lake deposition.

Triassic shales and sandstones unconformably overlie the Dewey Lake Formation. These strata are, in turn, overlain by unconsolidated Cenozoic clastic sediments. Triassic and Cenozoic strata are not readily differentiated in the area, and thus are referred to as "undifferentiated Cenozoic and Triassic." The thickness of these strata increases markedly across the area from ~400 ft on the east to as much as 1,500 ft in the dissolution trough west of Wink (Fig. 3).

Syndepositional thickening of overlying strata in the same area where the salt units are thin helps to determine the timing of salt dissolution (Seni and Jackson, 1984). Abrupt thickening of strata that overlie anomalously thin salt layers in western Winkler County indicates salt dissolution and concurrent basin filling from Permian through Cenozoic time. Natural dissolution of salt beds of the Salado Formation here began during Late Permian time (Baumgardner and others, 1982; Johnson, 1986, 1987, 1993). Abnormal thinning and thickening of individual salt units in the Salado, as well as local thickening of each of the overlying formations of Permian, Triassic, and Cenozoic age, indicate that the process of dissolution and subsidence has occurred intermittently in the Wink area; it began even before the end of Salado deposition (Johnson, 1993) and has continued through the Cenozoic (Fig. 3).

## PETROLEUM ACTIVITY IN THE HENDRICK FIELD

The Hendrick field, which embraces the collapse and subsidence features near Wink, is one of the giant oil fields of Texas. More than 1,400 wells have been drilled in the field since its discovery in 1926, and these wells had yielded a cumulative total of more than 265 million bbl (barrels) of oil by 2000 (Johnson, 1986; Railroad Commission, 2001). Drilling activity and oil production were phenomenally high in the first few years, but by the early 1930s the activity was reduced greatly and has continued to decline to a relatively low level today. One of the major problems in

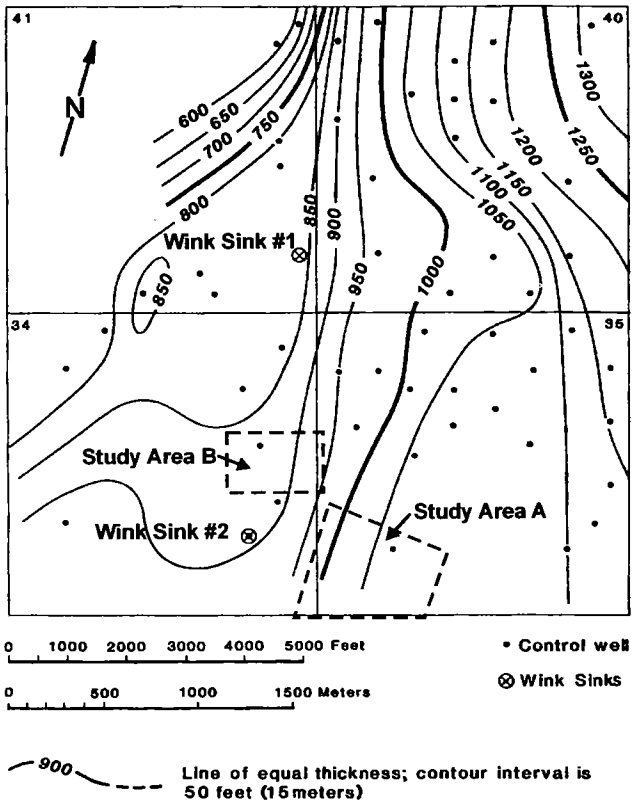


Figure 4. Thickness of the Salado Formation in the Wink area (from Johnson, 1986, 1993). Contour interval is 50 ft. Also shown are locations of Wink Sinks nos. 1 and 2, and outlines of study areas A and B.

the Hendrick field since its beginnings has been the disposal of the great volume of oil-field brine produced along with the oil.

Several articles published during the early boom period of the Hendrick field (Dameron, 1928; Vance, 1928; Bignell, 1929, 1930; Ackers and others, 1930; Heithecker, 1932; Carpenter and Hill, 1936) provide valuable insight into the methods of drilling, well completion, oil production, brine production, and brine disposal used early in the history of field development. Production in the field has been predominantly oil, with small amounts of natural gas; most of the oil has come from the Yates Formation, and some is from the overlying Tansill Formation. Most wells were drilled only 660 ft from neighboring wells, with spacing throughout the field typically being one well per 10 or 20 acres (Fig. 5).

Oil-field brines produced in the Hendrick field are unsaturated with respect to salt; they generally contain 5,000–48,000 ppm (parts per million) dissolved solids (saturated brines would contain >300,000 ppm dissolved solids) (Ackers and others, 1930; Carpenter and Hill, 1936; Garza and Wesselman, 1959). Water production in the field ranged from 600,000 to 875,000 bbl per day in the 1930s, and the water-to-oil ratio for the producing wells increased from ~16:1 in 1930 to as much as 50:1 in 1934 (Carpenter and Hill, 1936). Operators disposed of the great quantities of water produced with oil in the early days in unlined natural and artificial earthen "evaporation" pits (Heithecker, 1932). In some places, dynamite was used to blast caliche or other hard rock units present in the floor of the pit. Pit berms for holding the water consisted of loose material scraped from the pit floor, covered with asphalt. Examination of aerial photographs taken in 1942, 1946, 1954, and 1968 showed that nearly 50 separate sites, ranging in size from 1 to 30 acres, were used at one time or another as disposal pits in the 4-mi$^2$ area embracing the Wink collapse and subsidence features (Johnson, 1986, 1987).

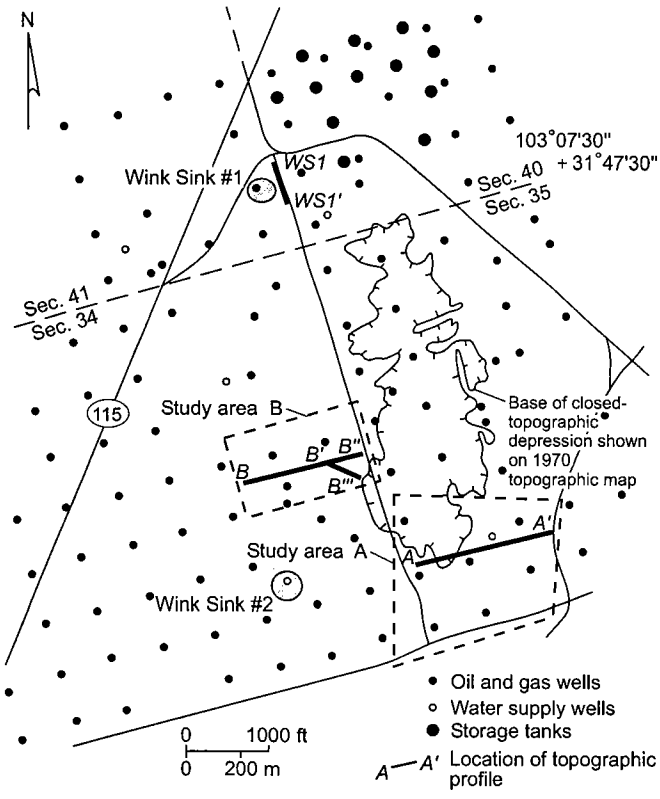


Figure 5. Map of part of Block B-5, Public School Land Survey, in the Hendrick oil field just northeast of Wink, Texas, showing wells and storage tanks from files of the Railroad Commission of Texas. Also shown are Wink Sinks nos. 1 and 2, study areas A and B (1999 study of fissures and subsidence), and lines of topographic profiles measured in 1999.

Within the Hendrick field area, the shallow freshwater aquifers have been recharged substantially by leakage of unsaturated wastewater from the disposal pits (Garza and Wesselman, 1959). Great volumes of water have seeped down through the permeable sandy soil in the central part of the field, including the Wink area, creating a large ground-water mound that in 1956 extended 8 mi north–south and 4 mi east–west (Garza and Wesselman, 1959). It appears that this surface recharge has raised the water table some 50–100 ft (Johnson, 1986). Garza and Wesselman (1959) reported that operators discharged ~150 million bbl of produced water in Winkler County during 1957. More recently, a number of water-supply wells have been drilled in parts of the Hendrick field to enable waterflooding of the petroleum reservoirs. In the Wink area these water-supply wells have been drilled into the Capitan Reef.

## WINK SINK NO. 1

Wink Sink no. 1 (Figs. 2, 5) formed ~2 mi north of Wink on June 3, 1980, and within 24 hr it had expanded to a maximum width of ~360 ft (Baumgardner and others, 1982). Two days later the maximum depth of the sinkhole was 110 ft, and the volume was estimated at about 5.6 million cubic ft. One abandoned oil well (the No. 10-A Hendrick, drilled in 1928) was incorporated within the sink itself, and another nearby oil well (the No. 3-A Hendrick) was later plugged and abandoned because of its proximity to the sinkhole.

Wink Sink no. 1 resulted from an underground cavity that migrated upward by successive roof failures, thereby producing a collapse chimney filled with brecciated rock (Fig. 6) (Baumgardner and others, 1982; Johnson, 1986, 1987). The cavity probably developed in salt beds of the Salado Formation by uncontrolled salt dissolution. The Salado is ~850 ft thick and at a depth of 1,300–2,150 ft beneath Wink Sink no. 1. Salt dissolution and collapse associated with Wink Sink no. 1 apparently resulted from, or at least was accelerated by, oil-field activity in the immediate vicinity of the sink. Baumgardner and others (1982, p. 33) concluded that "although the Wink Sink [no. 1] may be the result of natural processes, oil-field operations in the area may be related to its formation," and that

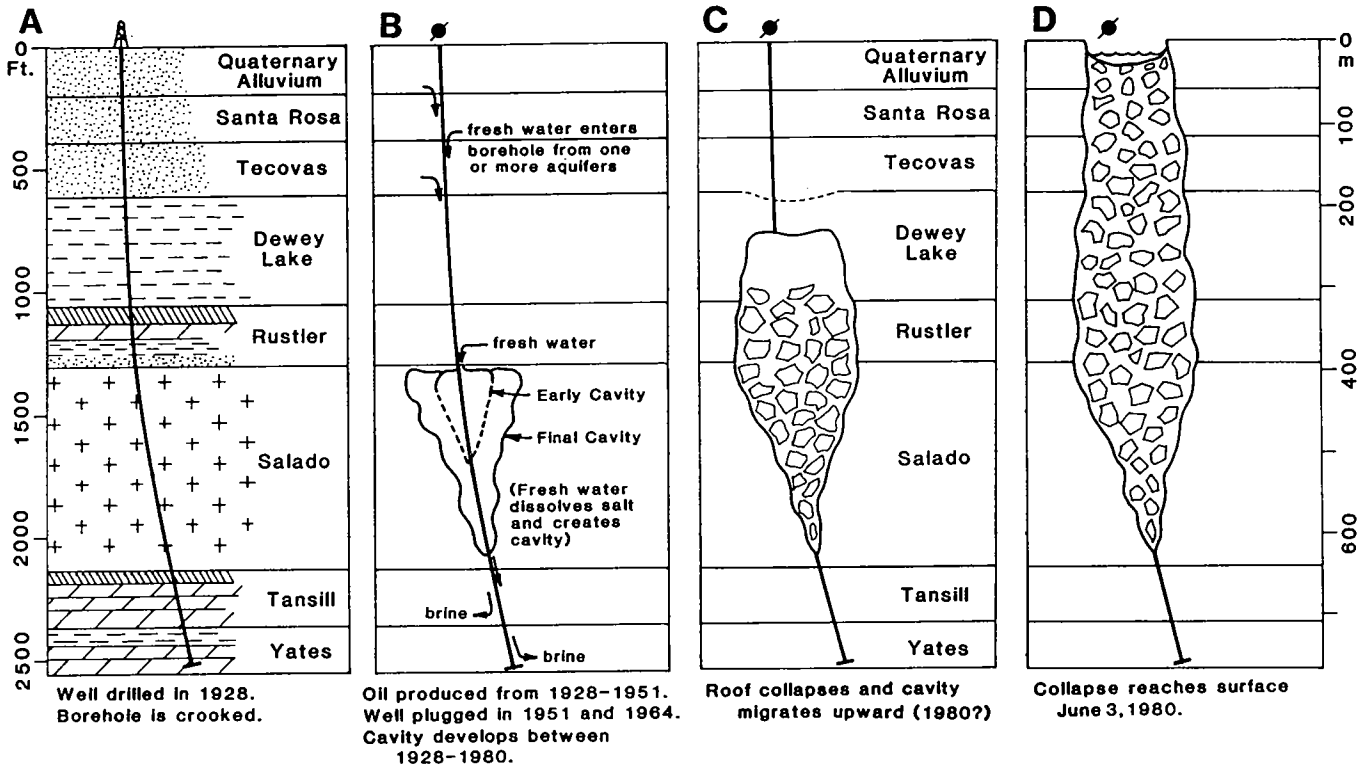


Figure 6. Schematic cross section through the No. 10-A Hendrick well, showing possible relationship of well to development of Wink Sink no. 1. Fresh water may have circulated down the borehole to dissolve the salt and create a cavity; by successive roof failures, the cavity migrated upward to the land surface.

the No. 10-A Hendrick well may have provided a conduit for water movement.

The No. 10-A Hendrick well was drilled at the site of the sinkhole, and it appears likely that it was a pathway for water to come in contact with the Salado salt (Johnson, 1986, 1987) (Fig. 6). In all likelihood, the well was drilled with a freshwater drilling fluid that enlarged or washed out the borehole within the salt sequence. Ineffective cement jobs, and possible fractures in the cement, may have opened pathways for water movement up or down the borehole outside of the casing. Because of probable salt dissolution and borehole enlargement during drilling through the Salado salts, the small amount of cement reportedly used (800 sacks) to set the casing in the hole probably was enough to cement only the lower part of the hole, thus leaving most of the salt section exposed behind the casing (Johnson, 1986, 1987).

Casing in the well probably was perforated by corrosion owing to production of great quantities of oilfield brine; this would parallel the casing corrosion that was observed in the nearby No. 3-A Hendrick well, which had a similar history of drilling, completion, and production. Explosives realigned well 10-A while drilling in the underlying Tansill Formation; this not only fractured the Tansill and increased its permeability locally but also may have fractured the cement farther up the borehole. In addition, final removal of casing from well 10-A in 1964 left an uncemented borehole in the interval from the base of the Santa Rosa aquifer to the top of the Rustler Formation for a period of 16 years, until formation of Wink Sink no. 1.

All of the above-mentioned activities, although consistent with standard industry practices during the life of the No. 10-A Hendrick well, could have aided in conducting fresh water from shallow aquifers down the borehole to the salt beds (Johnson, 1986, 1987) (Fig. 6B). Outlets for the high-salinity brine, formed by dissolution of salt in the borehole, may have included the porous and permeable strata underlying the Salado Formation as well as possible preexisting dissolution channels within the Salado. Thus, a dissolution cavity may well have been formed around well 10-A, probably in the upper part of the salt sequence (Fig. 6B), and this cavity eventually would have become sufficiently large to permit collapse of the roof (Fig. 6C). By successive roof failures, the cavity then migrated upward until it finally reached the land surface and created Wink Sink no. 1 (Fig. 6D).

Salt-dissolving waters may also have ascended from below, with the same end results. Baumgardner and others (1982) note that the hydraulic head of water in the Capitan Reef is above the elevation of the Salado at Wink Sink no. 1. Therefore, a brine-density-flow cycle could cause unsaturated water to rise along the borehole to the Salado under artesian pressure; and then denser brine, formed by salt dissolution, could move back down the borehole under gravity flow. Abandoned boreholes in which the salt section is unprotected could have provided a conduit to allow these

deep fluids to develop a dissolution cavity in the Salado salts.

### Subsidence at Wink Sink No. 1 Since 1980

Current conditions at Wink Sink no. 1, based upon a brief reconnaissance field study conducted in 1999, indicate that subsidence has continued to occur since 1980 in areas adjacent to the sinkhole (Collins, 2000). In addition, fissures (referred to as "tension fractures" by Baumgardner and others, 1982) and at least one fault have formed around the periphery of the sinkhole since 1980. On the east side of the sinkhole, a topographic profile was measured in 1999 using an Abney level, rod, measuring tape, and hip chain to determine approximate relative-elevation changes since 1970 (the date when the Wink North 7.5-minute quadrangle map was surveyed, with a 5-ft contour interval) (Fig. 7a). Differences between the 1970 topography and the elevations measured during 1999 were determined by tying the north end of the field-measured topographic profile to a location where the 1970 topography did not appear different from the 1999 elevations. In addition, an elevation measured at the east side of the sinkhole in 1980 was compared with the 1999 and 1970 data.

This methodology yields only approximate and relative-elevation differences, but they are accurate enough to identify large relative differences in elevation since 1970. Figure 7a, a composite profile of the 1970, 1980, and 1999 data, suggests that the ground elevations in 1970 and 1980 were almost the same, probably differing by less than 5 ft (i.e., the contour interval on the 1970 map) in the area studied at the east side of the sinkhole. Detailed re-leveling surveys conducted between July 1980 and December 1980 indicate that subsidence east of the sinkhole was only ~0.2 ft during that time (Baumgardner and others, 1982). The ground elevation in 1999 for the area east of the sinkhole is ~28 ft lower than it was in 1980, suggesting that ground subsidence in that area has continued, perhaps episodically (Fig. 7a).

In conjunction with the continued subsidence adjacent to Wink Sink no. 1 since 1980, fissures and small-displacement faults have also continued to form around the sinkhole's periphery. A paved road just west of Wink Sink no. 1 has been fractured and dis-

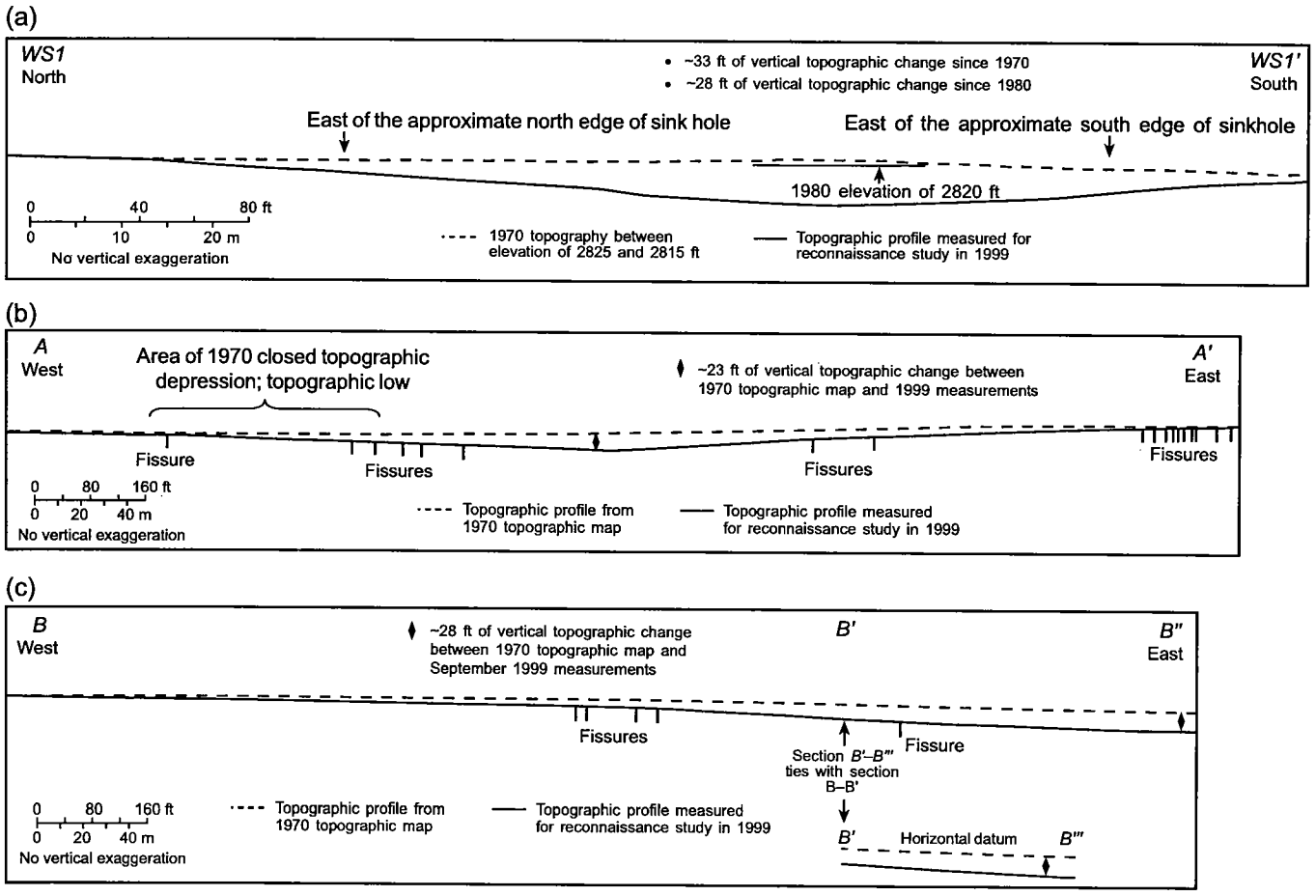


Figure 7. Profiles showing topography measured during 1999 compared with topography of 1970 (based upon Wink North 7.5-minute quadrangle map): (a) profile WS1–WS1′; (b) profile A–A′, in area A; and (c) profiles B–B″ and B′–B‴, in area B. Locations of profiles shown in Figure 5.

rupted, and is now abandoned; when the sinkhole formed in 1980 the road was still in use. Aerial photographs taken in 1980 do not indicate fissures or faults cutting this paved road, although very small fractures possibly would not be evident. A 1987 oblique aerial photograph of the area shows some fissures and faults cutting the paved road, although the fracture intensity does not appear to be great. During the field visit in 1999, fissures were observed as far as 280 ft west of the sinkhole's rim, and west (outside) of a fence that now surrounds the sinkhole area and prevents access.

## WINK SINK NO. 2

On May 21, 2002, Wink Sink no. 2 developed 1 mi south of Wink Sink no. 1 (Fig. 5). By the end of the first day, Wink Sink no. 2 was reported to be 450 ft long and 300 ft across. The water level was 100 ft below the ground surface, and the depth of the water in the sink was unknown. A fence was quickly constructed around the sink for safety purposes. The sink continued to enlarge by undercutting its vertical banks and sloughing material into the water-filled hole. Lateral expansion of the surface sink is continuing, as of March 2003, and the water-filled pool has not yet filled, in spite of the large volume of material that has sloughed into the hole. By March 2003, Wink Sink no. 2 was ~780 ft long and ~610 ft wide (Fig. 8). Therefore, the volume of Wink Sink no. 2 was then about 47.6 million cubic ft (780 × 610 ft × 100 ft), not including the unknown volume that is below water level in the sink.

Wink Sink no. 2 is centered on the site of a former water-supply well, the Gulf Oil Corporation No. WS-8 Grisham-Hunter Surface Fee. The Gulf WS-8 was drilled 1,320 ft from the south line and 1,320 ft from the east line of section 34, block B5, of PSL Survey. It was completed September 18, 1960, and was drilled into the Capitan Reef to a total depth of 3,583 ft. In the Gulf WS-8, the top and base of the Salado Formation are at depths of 1,353 and 2,252 ft, respectively; the thickness of the Salado is 899 ft. The Gulf WS-8 was plugged prior to formation of Wink Sink no. 2, but during its productive life it yielded about 800 million bbl of water for waterflood operations. The salinity of water produced from the Gulf WS-8 is not reported; however, Hiss (1975) reports that the chloride-ion concentration of water in the Capitan Reef is 1,100–3,600 mg/L (milligrams per liter, approximately equivalent to "ppm") in four wells drilled just 2–3.5 mi north of Wink.

There are insufficient data to assess how Wink Sink no. 2 formed, although it appears to be related to the Gulf WS-8 well. It is possible that unsaturated ground water in shallow aquifers—such as alluvium, the Santa Rosa aquifer, or the Rustler Formation—may have flowed down through the borehole against the salt. It is also possible that unsaturated water produced from the Capitan Reef may have escaped through the tubing and casing in the well (perhaps by corrosion of the metal, or failure at the joints), and thus encountered the salt. Or unsaturated waters in the Capitan Reef may have ascended under artesian pressure (after the well was abandoned) and created a brine-density-flow cycle. In any of these cases, a cavity may have developed in the Salado salt along the borehole, and this cavity may then have migrated upward by successive roof failures until it caused catastrophic collapse of the surface, in a manner similar to that postulated for Wink Sink no. 1 (Fig. 6). The underground cavity (or cavities) beneath Wink Sink no. 2 must be large enough to accommodate the collapse of nearly 48 million cubic ft of rock and earth at the sur-

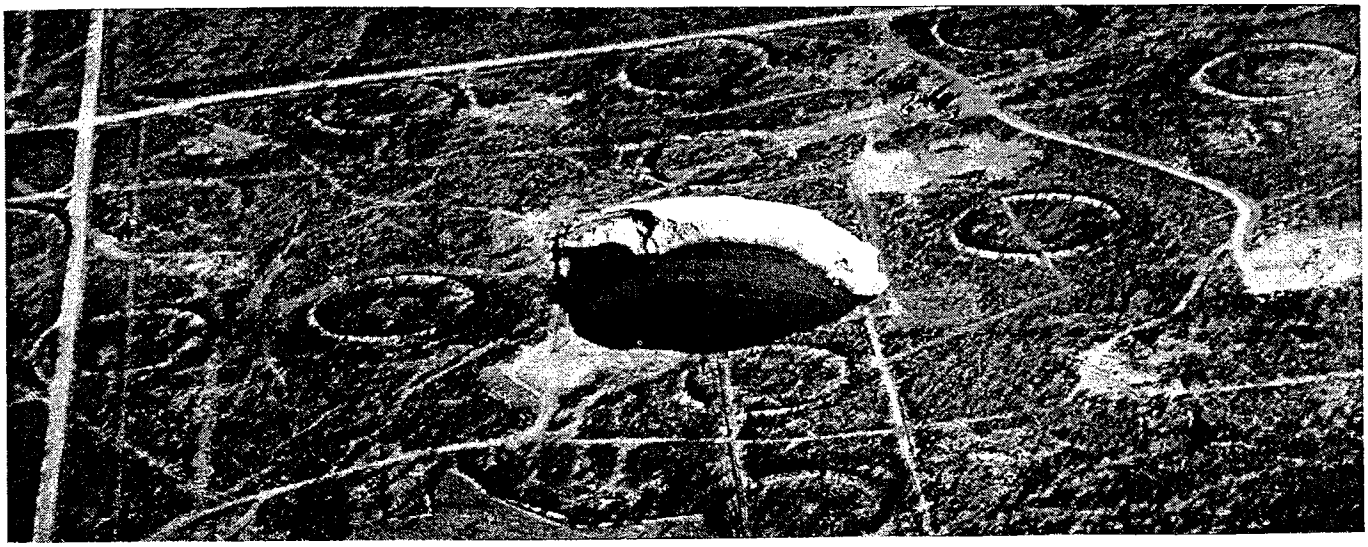

Figure 8. Aerial photograph of Wink Sink no. 2 in March 2003 (photograph by Jim Newman, Triple N Services, Midland, Texas). Sinkhole is ~780 ft by 610 ft. Viewed looking to the west, along the long axis of the sink (view shows 610-ft width). Each of the circular berms in the photo is ~300 ft in diameter.

face, as well as a "bulking factor" to accommodate the likely increase in void space of the collapsed material.

## ADDITIONAL FISSURES AND SUBSIDENCE NEAR WINK

In 1999, recently formed earth fissures, sagging power lines, tilted utility poles, and dip on the surface of a once-level well pad were first observed ~0.6 to 0.9 mi south-southeast of Wink Sink no. 1 by Winkler County residents Raleigh Morton and Donnie Harris. Their observations prompted a reconnaissance investigation by Collins (2000) to document the earth fissures and to search for any evidence of recent ground subsidence. The reconnaissance investigation focused on study areas A and B, at the southern end of a broad (~0.6-mi-wide), elongate (~1-mi-long), closed topographic depression, illustrated on the Wink North quadrangle map of 1970 (Figs. 5, 9). Fissures were noted, and the topography in parts of areas A and B appeared visibly different from that of the 1970 topographic map.

Field methods used for this reconnaissance study were intended to provide a preliminary interpretation of whether subsidence could have caused the newly formed fissures. Field methods were similar to those described previously (for Wink Sink no. 1 since 1980). Differences between the 1970 topographic map (contour interval, 5 ft) and the elevations measured in 1999 were determined by tying one end of each field-measured topographic profile to a location where the 1970 topography did not appear different from the 1999 elevation.

Results of this reconnaissance study indicate that ground subsidence has most likely occurred since 1970, and that a more detailed evaluation of the area, using precise techniques, is needed to evaluate and better quantify continuing subsidence. The principal lines of evidence for these ground disturbances are the fissures and subsidence observed in 1999. The cause(s) for the fissures and subsidence are unknown, but they probably are related to subsurface-cavity formation similar to the cause(s) for development of Wink Sinks nos. 1 and 2. Areas A and B are also within the Hendrick field, and they embrace several oil wells and a water-supply well (Fig. 5). We are concerned that the fissures and subsidence, whatever their cause(s), may presage the future development of large, catastrophic sinkholes similar to Wink Sinks nos. 1 and 2.

### Fissures

Fissures studied in areas A and B during 1999 (Fig. 9) are not peripheral to sinkholes, although they exhibit characteristics similar to the fissures that are common around the flanks of Wink Sink no. 1 (Baumgardner and others, 1982). It is not known whether the fissures peripheral to Wink Sink no. 1 preceded, or coincided with, the catastrophic collapse of the ground surface. The recent photographs of fissures cutting the road west of Wink Sink no. 1 (described above) indicate continued movement along the fissures. Fissures in areas A and B commonly have widths ranging from a few tenths of an inch to 1 ft. Local areas of surface collapse or soil pipes are aligned along some of the fissures. Fissures commonly display linked or en echelon patterns that extend >100 ft at some locations. The widths of fissures appear to narrow downward as they cut across the sand- and silt-rich surface and near-surface deposits. The fissures in areas A and B do not appear to have vertical or lateral slip, although it would be difficult to recognize very small amounts of slip in the relatively unconsolidated surficial sands and silts.

Trenches have not been dug to verify fissure depths, but open space in one fissure was measured to be at least 6.5 ft deep (Raleigh Morton, personal communication, 1999). Although individual fissures and fissure swarms are not precisely straight features, they generally exhibit linear to curvilinear orientations. Fis-

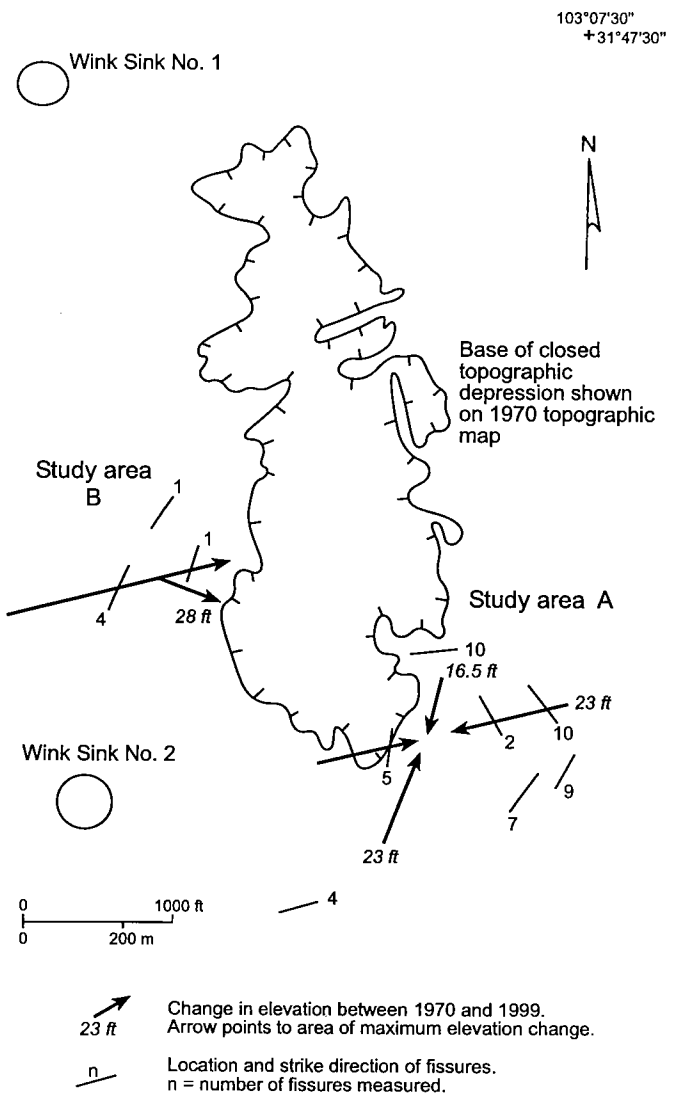


Figure 9. Map illustrating fissure locations and elevation changes in study areas A and B between 1970 and 1999.

sures in area A appear to roughly encircle a topographically low area; most of the fissures occur at the rim and flanks of the gentle topographic slopes (Fig. 9). The area encircled by fissures in area A is ~1,350 ft wide, which is similar to the size of subsidence areas around Wink Sinks nos. 1 and 2. Fissures in area B trend northeast and occur on the flank of the topographic slope at the southwest side of the 1970 closed topographic depression (Fig. 9).

### Subsidence

Topographic profiles were measured in areas A and B to compare relative-elevation differences between 1970 (topography on the Wink North quadrangle map) and the 1999 field visit by Collins (2000) (Figs. 5, 7, 9). Two profiles, trending approximately east to west across the study areas, are illustrated in Figure 7 (profiles b and c). In area A, the elevation differences indicate subsidence of as much as 23 ft between 1970 and 1999 (Figs. 7b, 9). The lowest elevation measured in 1999 is about 335 ft east of the 1970 closed topographic depression. Fissures roughly encircle this topographically low area. The Gulf Oil Corporation Grisham-Hunter Water-Supply Well No. WS-10 (Gulf WS-10) is within this area of maximum subsidence, and at least one oil well is adjacent to the subsided area (Fig. 5). No specific evidence, however, indicates a causative relationship between these boreholes and the subsidence.

In area B the relative-elevation differences between 1970 and 1999 indicate as much as 28 ft of subsidence (Figs. 7c, 9). Area B is at the southwestern flank of a broad, elongate, closed topographic depression illustrated on the Wink North quadrangle map of 1970. Fissures in this area strike north-northeast, similar to the orientation of the elongate closed topographic depression and approximately perpendicular to the topographic downslope direction toward the large closed topographic depression.

Although subsidence in areas A and B has occurred between 1970 and 1999, it is not known whether the subsidence rates were constant or if they varied episodically. Subsidence in area A appears to encircle an area that in 1970 flanked a large closed topographic depression, whereas subsidence in area B appears to occur at the edge of the large 1970 closed topographic depression.

## OTHER SINKHOLES IN WESTERN TEXAS AND NEW MEXICO

In addition to the sinkholes and subsidence features near Wink, four more sinkholes apparently have formed in association with salt-dissolution cavities and oil and gas activity in western Texas and New Mexico over the past 30 years (Fig. 10). One sinkhole is spatially associated with a water-supply well near Jal, New Mexico, and a second is associated with a salt-water-disposal well near McCamey, Texas. The other two sinkholes formed over relatively shallow brine-mining caverns near Borger, Texas.

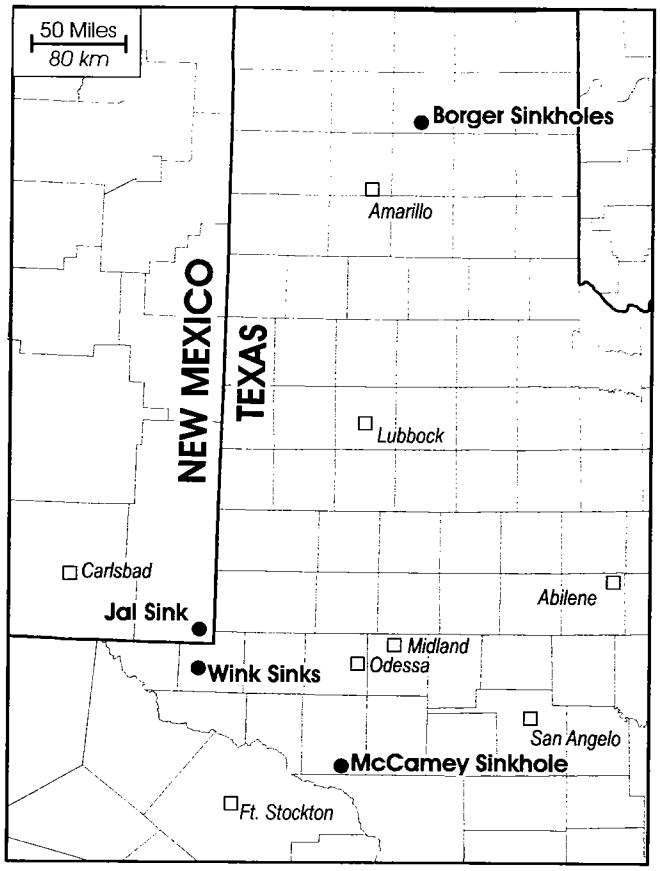


Figure 10. Map showing locations of sinkholes in western Texas and New Mexico that are discussed in this report.

### Jal Sink, Lea County, New Mexico

The Jal Sink formed on the Whitten Ranch sometime between August 31 and September 5, 1998, about 8 mi north-northwest of Jal, New Mexico (Powers, 2000, 2003) (Fig. 10). Rapid formation of the sinkhole is evidenced by displaced clasts of Ogallala caliche, up to 3 ft in diameter, extending in rays radiating away from the sinkhole. Aerial photographs taken in August 2002 reveal that the sinkhole retains relatively steep walls and a dry, rubble-strewn floor. Powers (2000, 2003) estimated that the sinkhole originally was 75 ft in diameter and 107 ft deep. He reported that the sinkhole likely resulted from circulation of fresh water and uncontrolled dissolution of evaporites in a nearby abandoned water-supply well, the Skelly No. 2 Jal Water System (Jal WS-2). The water-supply well is ~75 ft west of the sink.

The stratigraphy in the vicinity of the Jal Sink is similar to that at the Wink Sinks. In the Jal WS-2 well, the depth to the top of salt in the Rustler Formation is 1,530 ft, and the depth range of the salt-bearing Salado Formation is 1,944–3,310 ft (~1,366 ft of Salado salts). The Jal WS-2 produced relatively low-salinity water for waterflood operations from the Capitan Reef at depths from ~3,890 ft to a total depth of 4,500 ft. In 1979, a workover of the Jal WS-2 well

revealed collapsed casing in the Rustler interval at 1,642 ft. The well was plugged and abandoned, with cement plugs set in the casing at depths of 1,418–1,550 ft, 72–414 ft, and 0–10 ft. The casing was then perforated, and cement was emplaced at three levels: behind the casing at 1,250 ft, below a packer at 1,140 ft, and behind the casing at 400 ft.

Powers (2000, 2003) inferred that salt dissolution might have occurred after plugging of the well, because approximately 300 ft of the salt section was exposed behind the casing. However, the 1979 workover report indicates that the casing in the salt-bearing Rustler interval had collapsed prior to plugging. Salt also may have been dissolved during operation of the well, possibly as a result of a lack of integrity of the casing. No records indicate that the well underwent mechanical-integrity testing during its history of producing water.

### McCamey Sinkhole, Upton County, Texas

The McCamey Sinkhole formed in south-central Upton County, Texas (lat 102.0582370°W., long 31.1229507°N.), in 1977 (Fig. 10). The sinkhole formed around a salt-water-disposal well (RR Kennedy Production Well No. 17, in the Rodman–Noel field) that was permitted on May 17, 1967, to inject produced salt water at a depth of 1,800–2,000 ft into the Permian Grayburg Formation. Information submitted as part of the permit application indicated that 4,000–9,000 bbl/day of salt water was to be injected. Actual injection volumes are unknown. Approximately 620 ft of Salado Formation salt occurs at a depth interval of 850–1,470 ft. Although supporting evidence is scant, it is likely that injected fluids were not confined to the injection interval, thus allowing unsaturated brine to come in contact with, and dissolve, some of the Salado salts. Uncontrolled dissolution of salt in the borehole could have led to development of an enlarged cavity, and, with failure and collapse of its roof, the cavity could have migrated upward, eventually to form the sinkhole.

Plugging reports (W-3 dated Aug. 25, 1977) indicate that the sinkhole initially was ~70 ft across and 70 ft deep. Current estimates (Randall Ross, personal communication) indicate that the sinkhole is ~300 ft across and 80–100 ft deep. Bands of concentric fissures up to 3 ft wide extend out from the sinkhole.

### Borger Sinkholes, Hutchinson County, Texas

In most places where sinkholes develop unexpectedly, the formative mechanism, geometry, and location of the initial subsurface void are poorly understood. In contrast, the depth and geometry of the subsurface void that collapsed to form the Borger Sinkholes, near the town of Borger, in Hutchinson County, Texas (Fig. 10), are well known from Railroad Commission of Texas hearing files Docket 10-71,850.

From 1959 to 1961, Phillips Petroleum drilled five brine-mining boreholes to extract salt-water brines from the Permian Flowerpot salt at a depth of 600–610 ft. Hydraulic fracturing established communication between the wells to improve salt yields. The wells produced brine until 1964, when surface subsidence in the vicinity of the brine wells indicated that the cavern was unstable. By 1963, sonar surveys indicated that the cavern roof had migrated upward from a depth of 600 ft to 450 ft. By May 1964, sonar surveys indicated that the cavern volume was 2.225 million bbl. At that time the cavern extended ~1,250 ft east–west, paralleling the linear arrangement of the brine-mining wells. The maximum width of the cavern was ~400 ft.

Between 1964 and 1969, company personnel established a subsidence-monitoring program, and they measured surface subsidence of up to 6 ft, centered over the solution-mined cavern. On May 13, 1969, the first (west) sinkhole formed with a diameter of 150 ft, a depth of 50 ft, and a water level 15 ft below the ground surface. The first sinkhole developed just south of well no. 3, over the area of maximum surface subsidence, and was centered above the location where the volume of the cavern was at a maximum.

A second (east) sinkhole formed on July 27, 1978, about 300 ft east-northeast of the first; the second sink is just north of well no. 1, over the east end of the solution-mined cavern. Initially, the second sinkhole was 150 ft in diameter, and it increased to a diameter of 200 ft in August 1978. The operator filled and leveled the second sinkhole. The first sinkhole contained 166,000 bbl of water with a chloride content of 26,000–31,000 mg/L (RRC Docket 10-71,850). A sonar survey in August 1978 revealed that remnants of the collapsed cavern then had a roof 340 ft below ground surface, and a base 380 ft below ground surface. The maximum lateral span of the cavern had shrunk to 160 ft, and the minimum volume (based upon the sonar survey) was 54,217 bbl.

A second brine-mining cavern in the Flowerpot salt at the same Phillips Petroleum facility did not have a similar history of gentle surface subsidence or catastrophic collapse. The second cavern was created by hydraulic interconnection among brine-mining wells nos. 7, 8, 9, and 10. This cavern is 500–800 ft south-southeast of the collapsed cavern and was in operation from 1964 to 1966. The second cavern is within the same salt unit and originally was at the same depth as the collapsed cavern (600–610 ft). In 1966, a sonar survey determined the volume of this cavern to be 0.860 million bbl. At that time the cavern extended ~650 ft north–south and 150 ft east–west, and the top of the cavern had migrated upward and apparently stabilized at 530 ft below ground surface; 30–40 ft of intact salt was still above the cavern roof. The maximum roof span of this stable cavern was 200 ft.

The second cavern is inferred to owe its stability to its relatively small size and limited roof span: the volume of the second cavern is only 38% of the volume of the collapsed cavern, and the length of its roof span is about 50% that of the collapsed cavern. The relatively

large volume, excessive roof span, and shallow depth apparently all contributed to the collapse of the initial cavern and the formation of the Borger Sinkholes.

## OIL AND GAS REGULATIONS IN AREAS AT RISK OF SINKHOLES

Oil-field regulations typically are designed to prevent waste and pollution, and to protect public health and safety. The catastrophic formation of a sinkhole certainly represents a significant risk to public safety, and potentially to ground-water quality. The relative scarcity of sinkholes, in relation to the millions of existing oil and gas boreholes, indicates that typical oil and gas practices and regulations are reasonably protective against the risk of sinkholes. However, even though the risk of sinkhole formation is relatively low, the association between a few boreholes and sinkholes suggests at least a locally causative relationship. Modern completion and plugging practices must ensure that boreholes do not cause sinkholes to develop, or that they do not exacerbate natural sinkhole-forming processes.

### Completion and Plugging Practices in Texas

Historic completion and plugging practices have placed subsurface saline formations at risk of dissolution by promoting or allowing (1) shallow ground water to descend to the salt along the borehole, or (2) deep ground water with static fluid levels above the saline formations to ascend to the salt along the borehole. In the past, these practices included unlined wellbores, excessive use of downhole explosives, and ineffective plugging procedures. Modern State regulations that set requirements for drilling and completion are designed to ensure the integrity of the borehole. Statewide Rule 13 of the Railroad Commission (§3.13) identifies typical drilling and completion requirements for the oil and gas industry in Texas. Statewide Rule 14 of the Railroad Commission (§3.14) identifies typical plugging requirements for the oil and gas industry in Texas. Modern completion and plugging practices (since the 1930s) are designed to prevent communication between underground sources of drinking water and producing formations. However, because saline formations are not sources of drinking water or producing formations, they are not required to be isolated from fluids circulating across formation boundaries and behind uncemented pipe.

Surface casing typically is set to a depth that protects all usable-quality ground water, as defined by the Texas Commission on Environmental Quality (TCEQ), and cement is circulated behind casing until it rises to the surface. Intermediate and production casings must be cemented from the shoe to a point at least 600 ft above the shoe. Depending on the depth of the base of fresh water and production, the fluids from below the depth of usable-quality water and from >600 ft above the producing zones may be free to circulate behind casing.

Cement plugs ensure that all formations bearing usable-quality ground water, and oil, gas, and geothermal resources, are protected through isolation. A cement plug is set across the shoe of the surface casing, extending 50 ft above and 50 ft below the shoe. In some cases there is insufficient surface casing to protect all sources of usable-quality water, and the intermediate and production casings may have been pulled. In those cases, a cement plug must be spotted 50 ft below the base of the deepest usable-quality water and 50 ft above the top of the water-bearing stratum. If intermediate or production casing is left in the borehole, and is cemented through all usable-quality water strata and all productive zones, a cement plug meeting requirements similar to those in surface casing must be placed inside the casing and centered no less than 50 ft above and below the productive stratum.

For wells in which the intermediate or production casing has not been cemented through all usable-quality water strata and all productive zones, and if the casing is not to be pulled, the casing must be perforated at the required depths to place cement outside of the casing by squeeze cementing through casing perforations.

For wells in which the intermediate or production casings have been removed, cement plugs centered on the top and bottom of the formation must isolate any productive zone or any formation in which a pressure or formation-water problem is known to exist.

In Texas, district directors have the authority under §3.14 (d)(7) to require additional plugs to protect any productive zone, or to separate any water stratum from any other water stratum, if the water quantities or hydrostatic pressures differ sufficiently to justify separation. Beginning in October 2002, the Railroad Commission implemented new well-plugging procedures to prevent the development of dissolution caverns and sinkholes in Ward, Winkler, and Pecos Counties, Texas. The revised plugging requirements include the following: (1) any well that penetrates the top of the Capitan Reef, whether the Capitan is protected as usable-quality water or not, must have a plug placed at the top of the Capitan; the plug must be tagged and/or pressure tested; (2) any well drilled within the area of the Capitan Reef must have a plug placed at the top of the Salado or the base of the Rustler; the plug must be tagged and/or pressure tested.

### Other Oil-Field Practices That May Exacerbate Sinkhole Formation

The movement of fluids along boreholes is the most likely mechanism that has led to the series of sinkholes in West Texas and New Mexico. However, in most cases the specific source of the fluids is poorly understood. The transformational flow of unsaturated fluids behind casing is the most likely candidate; however, not all researchers agree whether the source is shallow, relatively fresh water, or deeper, brackish water or brine (such as from the Capitan Reef). At

least in Wink Sink no. 2, which developed around the Gulf WS-8 well, and the nearby subsidence area around the Gulf WS-10 well, Capitan Reef water may be implicated if corrosion allowed communication through the production tubing and intermediate casing. Production records indicate that the Gulf WS-8 produced approximately 800 million bbl of makeup water for waterflood operations. Records of integrity tests of the water-supply wells have not been identified. Corrosion of the production tubing and the intermediate casing is another possible mechanism that could bring large volumes of undersaturated water in contact with Salado salt.

The impact of producing 800 million bbl of water on the reservoir properties of the Capitan Reef has not been investigated. Reservoir compaction and the collapse of vugs and caverns in the Capitan Reef are a likely result of the withdrawal of support afforded by the reservoir water. The significance and magnitude of reservoir compaction on sinkhole formation in West Texas are poorly understood. In other regions of the United States, reservoir compaction owing to groundwater withdrawal has led to the development of many sinkholes (Newton, 1984). Most sinkholes in Florida, Alabama, and Georgia are ascribed to ground-water withdrawal in a karstic carbonate terrain (Newton, 1984).

Various aerial photographs and large-scale topographic maps clearly reveal circular surface-disposal pits across the Hendrick field (Fig. 8). The role of surface disposal of oil-field brines on the water quality of shallow aquifers is well known (Garza and Wesselman, 1959). The scale of such disposal in the Winkler County area is significant. Garza and Wesselman (1959) report that in one year (1957), operators discharged ~150 million bbl of oil-field fluids in surface pits. Such disposal may have played a poorly understood role in exacerbating the subsidence process. Large-scale surface disposal may have initiated downward mechanical transport of granular sediments in a process referred to as piping (Ege, 1984).

## SUMMARY

Subsurface cavity development, and partial or total collapse of the roof rock, have caused a series of sinkholes and subsidence features in western Texas and New Mexico. Although natural dissolution of salt is well documented in many parts of the two-state region, it appears that salt dissolution, cavity development, and resultant collapse or subsidence were influenced by oil-field or brine-well activities near Wink, McCamey, and Borger, Texas, and Jal, New Mexico. All these sinks and subsidence features embraced, or are near to, boreholes drilled into or through thick salt deposits. The probable origin for these sinks and subsidence features includes unsaturated water coming in contact with a thick salt deposit; dissolution of salt and creation of an uncontrolled cavity; an increase in the size of the cavity until the roof collapses; and the successive failure of overlying rock and earth materials, causing the cavity to migrate upward until it reaches the land surface. Proper drilling, completion, and plugging practices can prevent this scenario by keeping unsaturated water from coming in contact with the salt in boreholes, and by not allowing boreholes to be conduits for moving water to or from the salt deposit.

## REFERENCES CITED

Ackers, A. L.; DeChicchis, R.; and Smith, R. H., 1930, Hendrick field, Winkler County, Texas: American Association of Petroleum Geologists Bulletin, v. 14, p. 923–944.

Anderson, R. Y.; and Kirkland, K. W., 1980, Dissolution of salt deposits by brine density flow: Geology, v. 8, p. 66–69.

Baumgardner, R. W., Jr.; Hoadley, A. D.; and Goldstein, A. G., 1982, Formation of the Wink Sink, a salt dissolution and collapse feature, Winkler County, Texas: University of Texas at Austin, Bureau of Economic Geology, Report of Investigations 114, 38 p.

Bignell, L. E., 1929, Problems of Winkler County solved: Oil and Gas Journal, v. 28, no. 18, p. 39.

_____1930, Production problems in Winkler field: Oil and Gas Journal, v. 28, no. 49, p. 44, 82.

Carpenter, C. B.; and Hill, H. B., 1936, Petroleum engineering report, Big Spring field and other fields in West Texas and southeastern New Mexico: U.S. Bureau of Mines Report of Investigations 3316, 223 p.

Collins, E. W., 2000, Reconnaissance investigation of active subsidence and recent formation of earth fissures near the 1980 Wink Sink in the Hendrick oil field, Winkler County, Texas [abstract]: Geological Society of America, South-Central Section, Abstracts with Programs, v. 32, no. 3, p. A-6.

Dameron, J. H., 1928, Hendrick output cut to check water: Oil and Gas Journal, v. 27, no. 18, p. 37, 144.

Ege, J. R, 1984, Mechanisms of surface subsidence resulting from solution extraction of salt, *in* Holzer, T. L. (ed.), Man-induced land subsidence: Geological Society of America, Reviews in Engineering Geology, v. 6, p. 203–221.

Garza, S.; and Wesselman, J. B., 1959, Geology and groundwater resources of Winkler County, Texas: Texas Board of Water Engineers Bulletin 5916, Austin, 200 p.

Heithecker, R. E., 1932, Some methods of separating oil and water in West Texas fields, and the disposal of oil-field brines in the Hendrick oil field, Texas: U.S. Bureau of Mines Report of Investigations 3173, 16 p.

Hiss, W. L., 1975, Thickness of the Permian Guadalupian Capitan aquifer, southeast New Mexico and West Texas: New Mexico Bureau of Mines and Mineral Resources, Resource Map 5, scale 1:500,000.

Johnson, K. S., 1981, Dissolution of salt on the east flank of the Permian Basin in the southwestern USA: Journal of Hydrology, v. 54, p. 75–93.

_____1986, Salt dissolution and collapse at the Wink Sink in West Texas: Office of Nuclear Waste Isolation, Battelle Memorial Institute, Columbus, Ohio, BMI/ONWI-598, 83 p.

_____1987, Development of the Wink Sink in West Texas due to salt dissolution and collapse, *in* Beck, B. F.; and Wilson, W. L. (eds.), Karst hydrogeology: engineering and environmental implications: Balkema, Brookfield, Vermont, p. 127–136. (Also published in 1989 in Environmental Geology and Water Science, v. 14, p. 81–92.)

_____1993, Dissolution of Permian Salado salt during Salado time in the Wink area, Winkler County, Texas, *in* Love, D. W., and others (eds.), Carlsbad region, New Mexico and West Texas: New Mexico Geological Society Guide-

book, 44th Annual Field Conference (October 6–9, 1993), p. 211–218.

_____1998, Land subsidence above man-made salt-dissolution cavities, *in* Borchers, J. W. (ed.), Land subsidence; case studies and current research; proceedings of the Dr. Joseph F. Poland symposium on land subsidence: Association of Engineering Geologists Special Publication 8, p. 385–392.

Maley, V. L.; and Huffington, R. M., 1953, Cenozoic fill and evaporite solution in the Delaware Basin, Texas and New Mexico: Geological Society of America Bulletin, v. 64, p. 539–546.

Newton, J. G., 1984, Review of induced sinkhole development, *in* Beck, B. F. (ed.), Sinkholes: their geology, engineering and environmental impact: Balkema, Rotterdam, p. 3–8.

Powers, D. W., 2000, Evaporites, casing requirements, water-floods, and out-of-formation waters: potential for sinkhole developments: Solution Mining Research Institute, Technical Class presented during meeting in San Antonio, Texas, 11 p.

_____2003, Jal sinkhole in southeastern New Mexico: evaporite dissolution, drill holes, and the potential for sinkhole development, *in* Johnson, K. S.; and Neal, J. T. (eds.), Evaporite karst and engineering/environmental problems in the United States: Oklahoma Geological Survey Circular 109 [this volume], p. 219–226.

Railroad Commission, 2001, Railroad Commission annual report: Railroad Commission of Texas, 365 p.

Seni, S. J.; and Jackson, M. P. A., 1984, Sedimentary record of Cretaceous and Tertiary salt movement, East Texas Basin: times, rates, and volumes of salt flow and their implications for nuclear waste isolation and petroleum exploration: University of Texas at Austin, Bureau of Economic Geology, Report of Investigations 139, 89 p.

Vance, M., 1928, Development and production methods in West Texas: Oil Weekly (now World Oil), v. 50, no. 1, p. 34–44.

# Intrastratal Karst at the Waste Isolation Pilot Plant Site, Southeastern New Mexico

***Carol A. Hill***
University of New Mexico
Albuquerque, New Mexico

**ABSTRACT.**—The possibility of intrastratal karst at the Waste Isolation Pilot Plant (WIPP) site in southeastern New Mexico is evaluated in light of karst principles and processes and dissolution/hydrological studies. While little direct evidence exists for such karst at the site, many indirect lines of evidence suggest its possible presence: surface topographic depressions, negative gravity anomalies, lack of surface runoff, collapse breccias, insoluble-residue zones, WIPP-33 sinkholes and caves, anomalous drawdowns, and salinity variations within boreholes. Intrastratal karst, if it exists, would bypass slow matrix flow in the Culebra Dolomite aquifer and be subject to fast flow in cave conduits.

## INTRODUCTION

The Waste Isolation Pilot Plant (WIPP) is a U.S. Department of Energy (DOE) facility in southeastern New Mexico near Carlsbad (Fig. 1), which has been designed for the safe disposal of transuranic nuclear waste. To ensure that the WIPP site is safe in hydrological terms, two criteria need to be met according to DOE guidelines: (1) it must be shown that water will not invade the Salado Formation, where radioactive waste is interned in the WIPP repository; (2) it must be shown that radioactive waste cannot escape via some aquifer unit, should an accidental breach of the repository occur.

The Culebra Dolomite Member of the Rustler Formation is considered to be the principal aquifer stratum overlying the WIPP repository; thus, one of the primary objectives of past hydrologic studies has been to demonstrate that the Culebra will not discharge water to the surface within the regulatory time frame of 10,000 years.

Although the Culebra aquifer has been intensely studied over the past 20 years, another possible hydrologic route for radioactive-waste transport exists that has been only minimally investigated: intrastratal karst. Barrows and others (1983), and then Barrows (1985) and Barrows and Felt (1985), were the first to put forth what was dubbed "the karst proposition." This proposition was briefly reviewed by Chaturvedi and Channell (1985) and Lambert and Carter (1987), but after these reviews the topic of karst at the WIPP site seems to have been almost entirely dropped—except by Hill (1996), who cited karst as having been underestimated as a potential pathway for groundwater flow at the WIPP site.

This report is based on the unpublished study of Hill (1999), which was funded by DOE/Sandia Laboratories. The author is neither a proponent nor an opponent of WIPP.

## REGIONAL DISSOLUTION STUDIES

In order to understand dissolution at the WIPP site, past studies have focused on a number of dissolution features within and around the Delaware Basin (Fig. 1): (1) dissolution troughs, (2) breccia pipes, (3) solution and fill, (4) karst domes and mounds, (5) lateral dissolution, (6) vertical dissolution, and (7) surface evaporite karst. These features will only be briefly described here; for more detailed discussion, refer to Hill (1996, 1999) and references therein.

### Dissolution Troughs

Dissolution troughs are large-scale dissolution features in and around the Delaware Basin. First described by Maley and Huffington (1953), these troughs occur both along the eastern edge of the basin above the Capitan Reef (Fig. 1, *A, B, C*) and within the basin proper (*D, E, F, G*). The largest of these—the Belding–San Simon Trough, San Simon Swale/Sink, and Kermit Wink Sink—lie directly over the inner edge of the Capitan Reef and are related to dissolution caused by undersaturated artesian water leaching salts from overlying evaporite units. Because the WIPP site is not directly over the Capitan Reef, these dissolution troughs have no bearing on its integrity.

Within the basin proper are the Toyah (*D*), Balmorhea–Loving (*E* to *F*), and Big Sinks–Poker Lake (*G*) troughs. The origin of these features is debatable, but they are most likely related to vertical (upward) dissolution from sandstone channels in the Bell Canyon Formation (Anderson and others, 1978). No such

Hill, C. A., 2003, Intrastratal karst at the Waste Isolation Pilot Plant site, southeastern New Mexico, *in* Johnson, K. S.; and Neal, J. T. (eds.), Evaporite karst and engineering/environmental problems in the United States: Oklahoma Geological Survey Circular 109, p. 197–209.

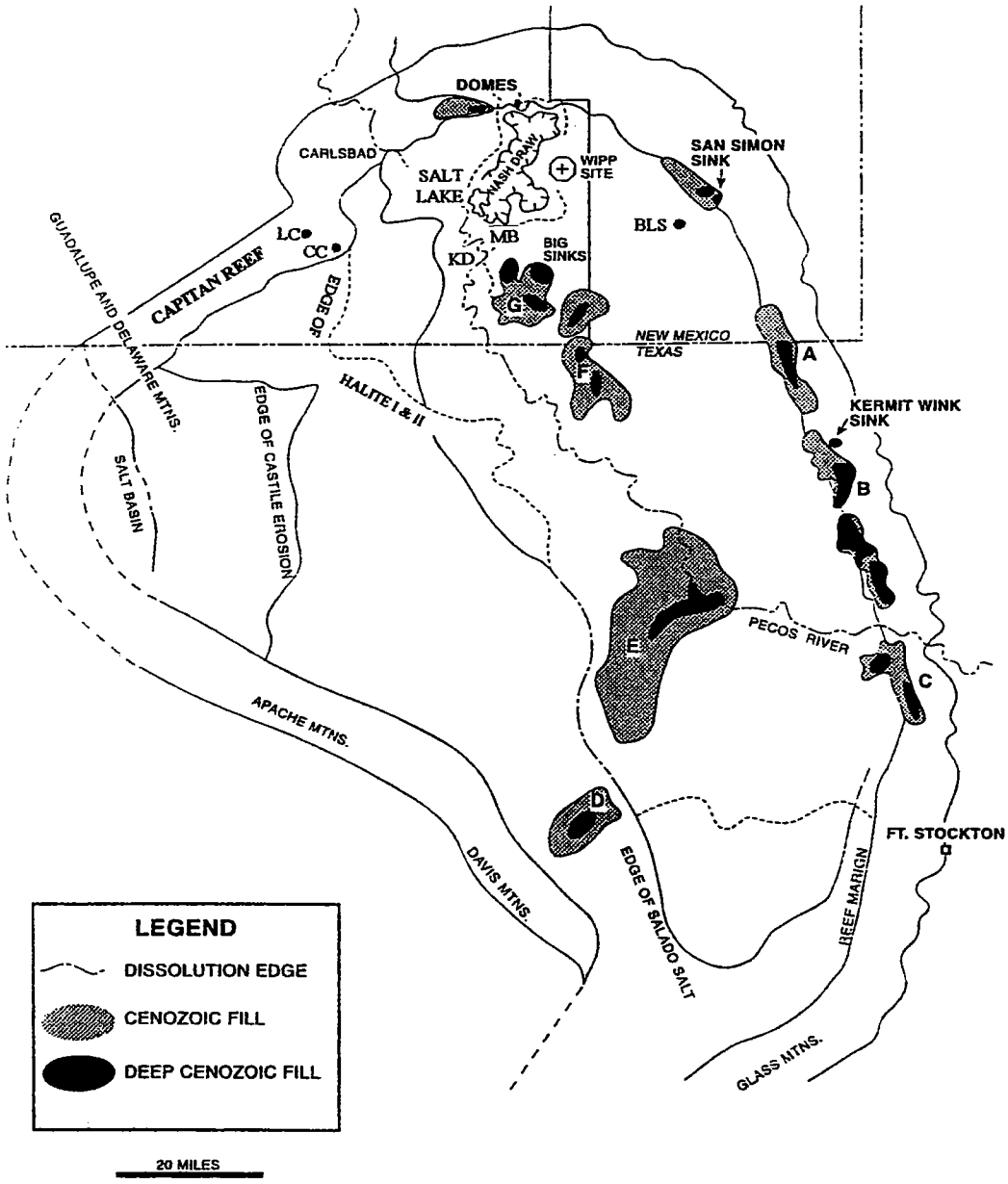


Figure 1. Map of Delaware Basin, showing Capitan Reef, major dissolution depressions (troughs), and western dissolution edge of evaporites. *A, B, C, D, E, F,* and *G* correspond to the dissolution troughs of Maley and Huffington (1953); *DOMES* are Vine's (1960) domes/breccia pipes; *CC* = Carlsbad Caverns; *LC* = Lechuguilla Cave; *BLS* = Bell Lake Sink; *MB* = Malaga Bend of Pecos River; *KD* = karst domes. Laguna Grande de la Sal (Salt Lake), Nash Draw, and WIPP site are also shown. From base map of Anderson (1981), modified by Hill (1996).

basinal troughs are known to exist at or near the WIPP site, although Bell Canyon sandstone channels are known to underlie sections of the site.

## BRECCIA PIPES

Breccia pipes are found in the Delaware Basin around its north side, directly over the Capitan Reef, and also within the basin proper. Vine (1960) was the first to describe a series of domes on the north side of the basin (Fig. 1, *DOMES*), which are the surface expression of breccia pipes. These formed when artesian water from the Capitan Limestone dissolved salt in the overlying Salado Formation, creating space (and collapse) by a brine-density flow mechanism (Davies, 1984; Hill, 1996). Vine's domes/breccia pipes are dissolution features related to the Capitan Reef and have no bearing on WIPP site integrity.

Breccia pipes identified within the basin proper are of two types: (1) paleokarst breccia pipes in the north-central part of the basin, and (2) breccia pipes near the WIPP site, which may still be actively forming. Paleokarst breccias are a key target of sulfur exploration (Crawford, 1990) and occur primarily along the halite margin of the Castile Formation (Fig. 1, *EDGE*

*OF HALITE I & II*). Such paleokarst has not been found near the WIPP site.

Closer to the WIPP site are breccia pipes that extend to the surface, an example of which is Bell Lake Sink (Fig.1, *BLS*). Hill (1993) performed sulfur, carbon, oxygen, and strontium isotope analyses on the selenite, celestite, barite, and calcite at Bell Lake Sink, and found that these values supported Anderson's (1980a) model of deep-seated dissolution originating in the Bell Canyon Formation. Bell Lake Sink is only about 20 km southeast of the WIPP site; however, no structures comparable to it have been detected at the WIPP site from geophysical or deep-drilling programs.

## Solution and Fill

The term *solution and fill* was first proposed by Lee (1924) for a process whereby "solution" from surface runoff and ground water penetrates rocks through joint and fracture systems, and "fill" occurs where rock collapses into solution voids. Nash Draw, just west of the WIPP site (Figs. 1, 2), is a karst valley formed by solution and fill. Solution-subsidence troughs are elongated depressions where solution and fill has formed along graben-boundary faults or fracture zones. These troughs are prevalent in the Castile Formation where it is exposed on the Gypsum Plain (Olive, 1957), but they are not known to occur near the WIPP site.

## Karst Domes and Mounds

Bachman (1980) introduced the terms *karst mounds* and *karst domes* for positive-relief features associated with the dissolution of evaporite rock in the Delaware Basin. Karst domes are circular to elongate, roughly symmetrical structures up to 200 m or more in diameter. They might represent the surface expressions of breccia pipes or salt anticlines (Hill, 1996). Karst

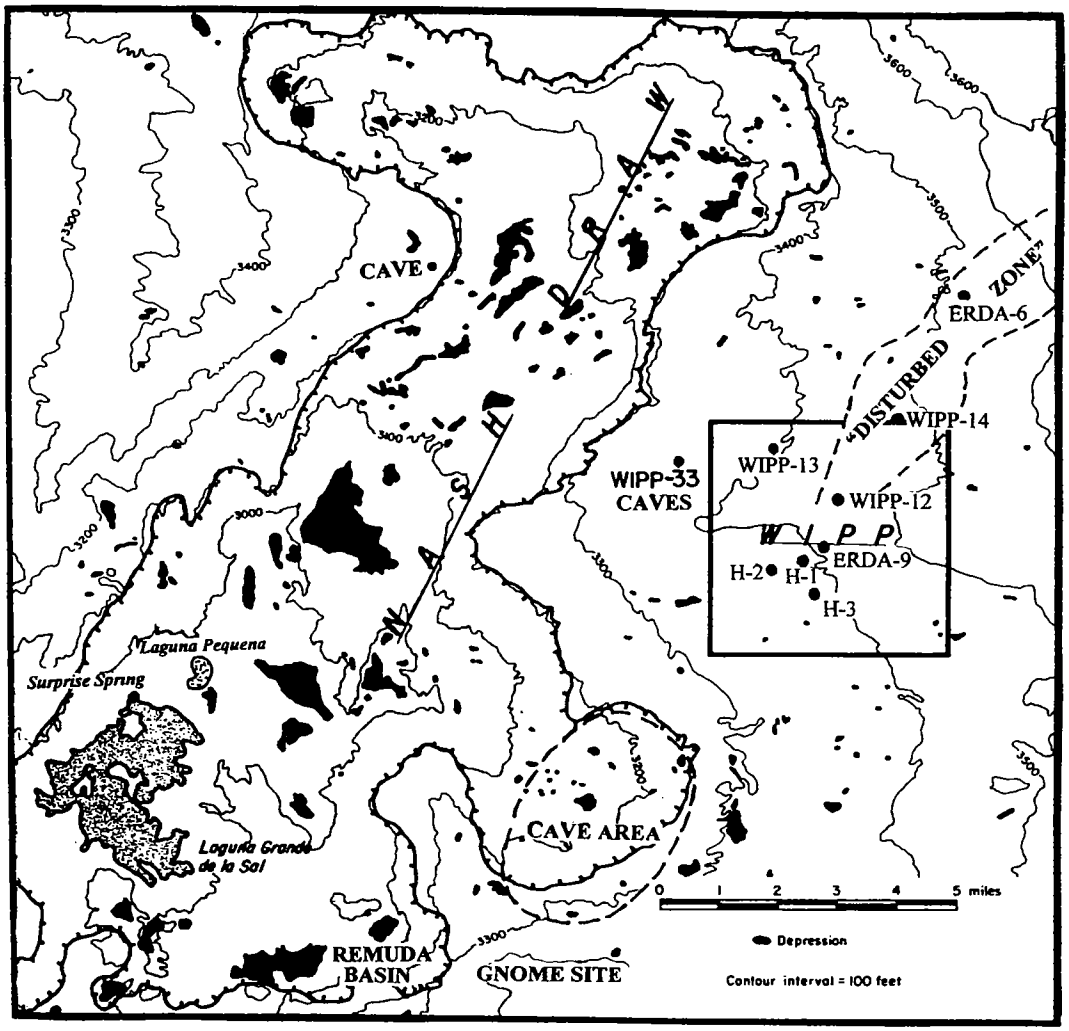


Figure 2. Map of karst valley, Nash Draw, showing location of WIPP site, Gnome site, and Laguna Grande de la Sal. Also shown are cave areas and the "disturbed zone." Black areas are closed depressions, interpreted to be collapse features. Nash Draw should be fed from all sides by smaller tributary karst channels. Topographic-contour interval, 30 m. From Chaturvedi and Channell (1985), modified by Hill (1996) .

domes seem to be concentrated in the Malaga Bend area (Fig. 1, *MB*); none have been identified at or near the WIPP site.

Karst mounds are circular, elongate to linear residual hills of dissolution breccia usually having a relief of about 3–10 m. These mounds appear to be related to shallow surface karst processes in which the surrounding strata weather faster than the collapse breccia. Karst mounds do not occur at the WIPP site because evaporite rock there is deeply buried (Fig. 3).

### Lateral Dissolution

Lateral dissolution (also called *salzhange, solution front, stratabound,* or *blanket* dissolution) is where water works its way down the dip slope of evaporite beds, dissolving soluble salt and gypsum along bedding planes. Blanket-dissolution breccias are typical of bedding-plane horizons that have undergone this type of dissolution. Calculations of Chaturvedi (1993) based on present dissolution rates have estimated that it should take ~225,000 years for the dissolution front in the Delaware Basin to reach the western edge of the WIPP site. However, Holt and Powers (1988) and Powers and Holt (2000) questioned the viability of this process at the site, and instead favored syndepositional dissolution in a salt-pan or hypersaline-lagoon, mud-flat environment in the Permian. In either case, this mechanism does not appear to be a threat to WIPP site integrity.

### Vertical Dissolution/Brine-Density Flow

Vertical dissolution can take place from above (the surface), or from below. Downward dissolution is not a problem at WIPP because it occurs much too slowly. However, the possibility of vertical dissolution from below has been a controversial subject. Anderson and Kirkland (1980) proposed a "brine-density-flow" mechanism whereby water under artesian pressure in the Bell Canyon Formation dissolves away salt in the overlying Salado Formation. This may be the mechanism by which the "disturbed zone" formed in the Castile and Salado Formations (Anderson, 1980b; Fig. 2) and by which "brine reservoirs" in the Castile Formation formed along the sides and crests of salt anticlinal structures. Brine reservoirs have been encountered in a number of boreholes in the northern, WIPP part, of the basin (e.g., WIPP-12 and ERDA-6; Fig. 2), and these brines have been of special concern because they are under anomalously high pressure (Neill and others, 1983). Reservoir brines appear to be in chemical equilibrium with the surrounding rock; i.e., they appear to be saturated with respect to most constituents. Thus, the brines appear to be static and not capable of actively dissolving more salt in a time frame that would affect the WIPP site.

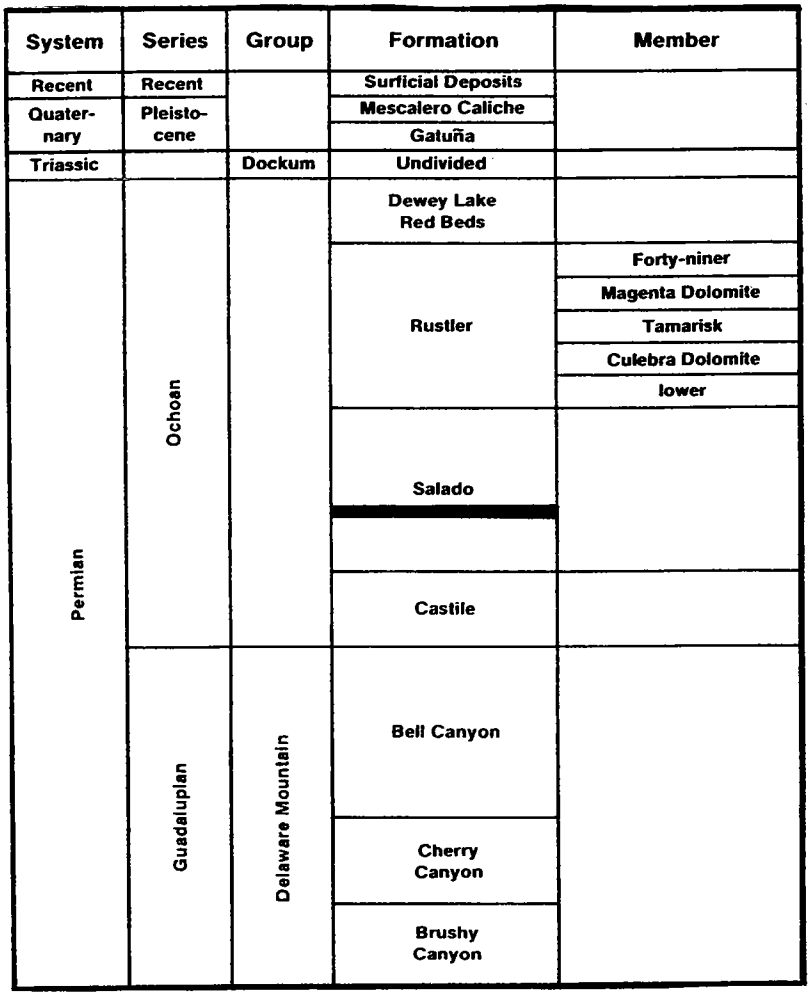


Figure 3. Diagrammatic representation of the stratigraphic column at the WIPP site, including members of the Rustler Formation. Black zone in the Salado represents the level of the WIPP repository. The distance from the surface down to the WIPP zone is 655 m.

### Surface Evaporite Karst

The Delaware Basin contains one of the most prominent gypsum karst areas in North America. Parks Ranch Cave (almost 8 km long) and Chosa Draw Sink are two prime examples of the many shallow surface-karst features present in this area. Such sinks and caves are conduits for flash-flood water that moves rapidly underground to the Pecos River. Velocities of 2–5 m/s have been measured for water discharging through these caves (Sares, 1984). Shallow caves and sinks are also known to exist in Nash Draw just west of the WIPP site, in the area of the Gnome site just south of WIPP, and in Remuda Basin (Fig. 2). Shallow evaporite karst does not occur directly over the WIPP site, because evaporite rocks in the Rustler and Salado Formations are deeply buried there (Fig. 3).

## INTRASTRATAL EVAPORITE KARST

All of the above studies relate to dissolution features that occur *around* the WIPP site, but none have been shown to affect fluid flow directly *at* the WIPP site. The one dissolution mechanism that has not been well studied—and the one with the highest potential for fluid transport—is intrastratal karst.

Intrastratal karst forms where solution processes occur beneath a layer or layers of non-karstic rock. The following characteristics are associated with intrastratal evaporite karst (Klimchouk, 2000): (1) it can form within the vadose zone, at or near the water table, or in the phreatic zone, as long as water is circulating and undersaturated with respect to gypsum and/or halite; (2) it is karst that usually does not have surface expression; i.e., it is concealed karst; (3) it can form at depth, even where evaporites are buried as deep as 4,000 m or more (at least 4 km in oil-drilling records in Canada; D. Ford, personal communication, 2003); (4) it is difficult to detect in the subsurface; it might be accidentally penetrated by boreholes or, where exhumed, might be exposed in the vadose zone and be overprinted by surface vadose karst; (5) it is widespread in evaporite rocks because of their high solubility.

### Principles and Processes Applicable to Intrastratal Karst

The following principles and processes of karst might be applicable to the WIPP site.

#### *Horton's Law of Stream Number*

Horton's law of stream number says that many smaller stream channels (first order, second order) feed fewer and fewer larger stream channels (third order) until a master trunk (fourth order) is reached. First-order to fourth-order streams and passages exist in caves, just as they do for surface streams, but the testing of Horton's law in caves has been difficult because of the incompleteness of information (some passages are impossible to follow) (Ford and Williams, 1989). Nash Draw is a major karst valley, and as such, smaller karst tributaries should feed it from all sides—including the eastern WIPP side (Fig. 2).

#### *Vertical Development of Intrastratal Karst*

The method of vertical development for intrastratal karst is shown in Figure 4. At first, water infiltration from the surface is by diffuse reflux, but with preferred flow and dissolution concentrated along fracture zones (A). Dissolution along these fracture zones by undersaturated water creates cavities and thus freer circulation downward (B). Rock then collapses into the cavities, creating stress in the surrounding rock (C). The stressed rock fractures, and so the area of the fracture zone is enlarged outward. As the fracture-zone area enlarges, the surface catchment area also enlarges, and a sinkhole is formed (D). This enlargement allows for a larger volume of water to pour down the sink in a self-perpetuating cycle.

The result of the above process in evaporite terrain is that, as more surface precipitation is funneled into a stream of "point source recharge," unsaturated water can dissolve its way into lower and lower levels of an evaporite-rock sequence. Once water reaches an evaporite horizon (Fig. 5), more material will be dissolved there than in overlying non-evaporite units, thus causing preferential solution and collapse at this horizon. Other consequences of this process are as follows: (1) as more surface-area water gets funneled into sinkholes, less surface area is available for diffuse reflux and evapotranspiration; and (2) surface runoff becomes predominantly subsurface drainage.

#### *Horizontal Development of Intrastratal Karst*

The process by which intrastratal karst develops horizontally in evaporite/dolomite rock (such as occurs at the WIPP site) is shown in Figure 5. Although a small amount of water may diffuse into the dolomite rock (wiggly arrows), most of the water point-sourced down a fracture zone begins to move along the contact of anhydrite–dolomite rock because it is easier and quicker to follow along this bedding plane in soluble evaporite rock than it is to enter the less soluble dolomite as matrix flow (i.e., the contact acts as a "perched aquifer" for preferred dissolution). Undersaturated water entering fractures dissolves the anhydrite at this contact and creates protocaves (A) and then first-order channels (B). If horizontally moving water meets with a vertical-fracture zone in the dolomite, it will transect the dolomite because this vertical fracture zone becomes the easiest route to follow (C). Caves may form either at the top or bottom of contacts, or a newer point source of water, created along the vertical fracture zone, can drill deeper into underlying evaporite rock (D).

#### *Integration of Cave Passages from Input to Output*

The development of a cave passage in salt or anhydrite at the contact between evaporite rock and more competent rock follows the principles of conduit propagation, which can apply to either the vadose or phreatic zone (Ford and Williams, 1989; Fig. 6). At first, the mode of flow is laminar within the plane and can be treated as Darcian (A). Distributary patterns of solutional micro-conduits develop that extend preferentially in the direction of the hydraulic gradient (B), their rates of extension being determined by the solvent-penetration distance and factors that control it. Courses are random and depend on micro-features of the bedding plane. A high resistance to flow is characteristic of the fracture at this initial stage of development.

As one principal conduit grows ahead of the others (B), it deforms the equipotential field, reducing the gradient at the solution front of its competitors ("sub-

sidiaries"), thus slowing their advance (C). When the principal conduit attains the output boundary (D), the high resistance to flow is destroyed, and a protocave now carries flow through the bedding-plane fissure from input to output (E). Darcian flow no longer applies, once the conduit expands to minimum (5–15-mm) cave (turbulent-flow) dimensions. Once this happens, cave enlargement can be comparatively rapid, especially in evaporite rock as long as undersaturated water is entering the system. Conduits can expand to diameters of 1–10 m in a few thousand years or less. An example of how fast this process can occur is the case of McMillan Dam, which was constructed in 1893 in gypsum/anhydrite rock along the Pecos River, just north of Carlsbad. No caves existed when the dam was built, but after only 12 years the reservoir had drained dry via caves formed in the surrounding evaporite rock.

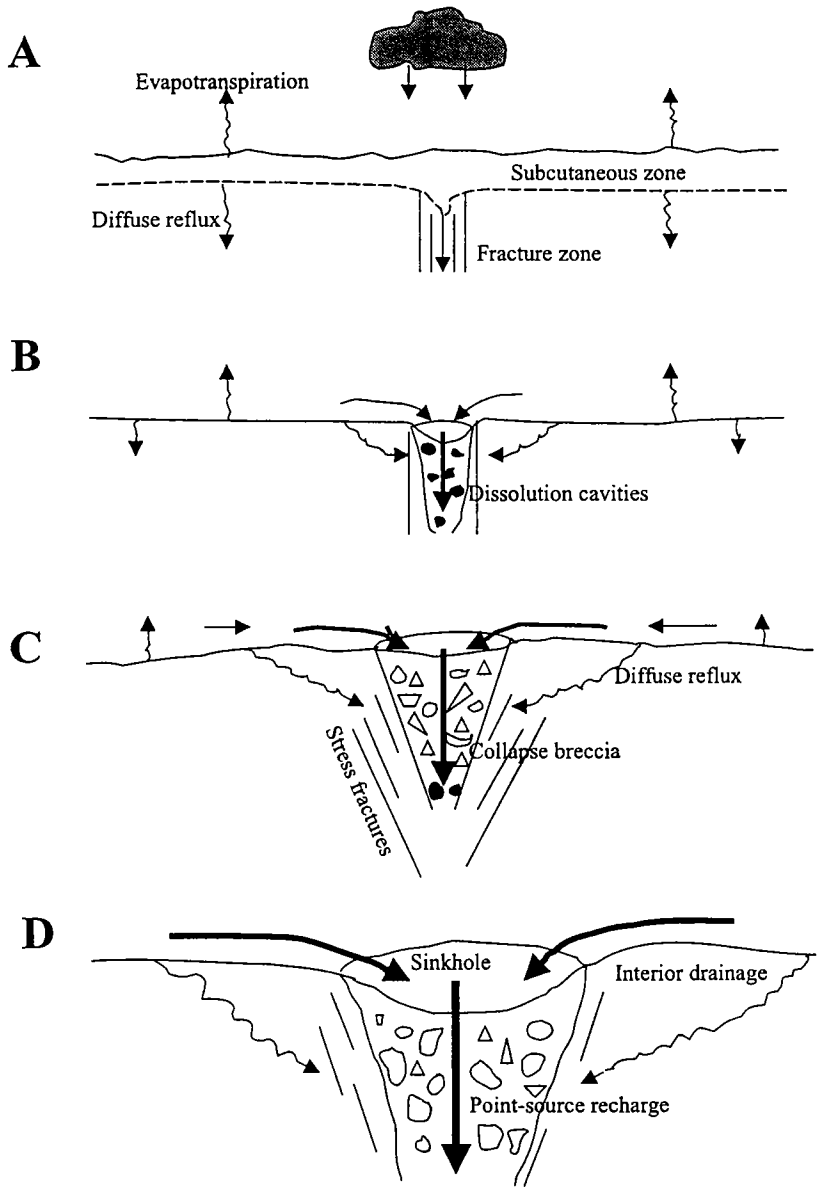


Figure 4. Diagrammatic model of the vertical input of water into intrastratal karst. (A) Preferred flow and dissolution along a fracture zone is initiated in the subcutaneous zone. (B) Dissolution creates cavities and freer circulation of water downward. (C) Rock collapses into cavities, thus enlarging the area of the fracture zone. (D) As the surface catchment area continually enlarges by collapse, even more water pours down the sinkhole. This creates a self-perpetuating cycle by which more and more water is point-sourced underground.

### *Conduit Flow*

As karstification proceeds from a protocave system to a cave system with large secondary cavities and channels, there is a further progressive decoupling of flow between that passing relatively rapidly through the cave conduits and that in subsidiary passages and in the surrounding porous and fissured rock matrix. As the principal conduits preferentially enlarge over the subsidiary branches, the branches might become disconnected from the flow path or become captured by the principal conduit. These branches might then be sealed by clay and/or collapse. The effect of this process is to produce only a few active principal underground passages that get progressively larger from input to output. Water movement might be rapid and turbulent in one (the cave passage), while slow and laminar in the other (the rock). In the phreatic zone, where water flows quickly into a conduit system from the surface during a heavy rain, a recharge wave causes a rise in the water table, and a pressure pulse ("piston flow") is forced through the phreatic conduits. If a cave system is large, the transmissivity of that system is so enormous that it operates only for a few days after a recharge event, and then becomes stagnant until the next major recharge event.

The progressive decoupling of subsidiary passages over time results in >95% of the flow being concentrated along only a few principal conduits. Water can recharge rapidly into this conduit system (in a matter of hours to days), while in the surrounding rock matrix recharge/discharge may take on the order of thousands to tens of thousands of years. If this rock is drilled—even right next to a principal karst conduit—"fossil" water can be found in the rock matrix (Fig. 7). The integration of cave passages over time into a few principal conduits also has another implication: 1–2% of the total rock volume (the cave passages) may carry >95% of the water through the system from input to output on a rapid time scale. This water may completely bypass aquifers having matrix or fracture flow.

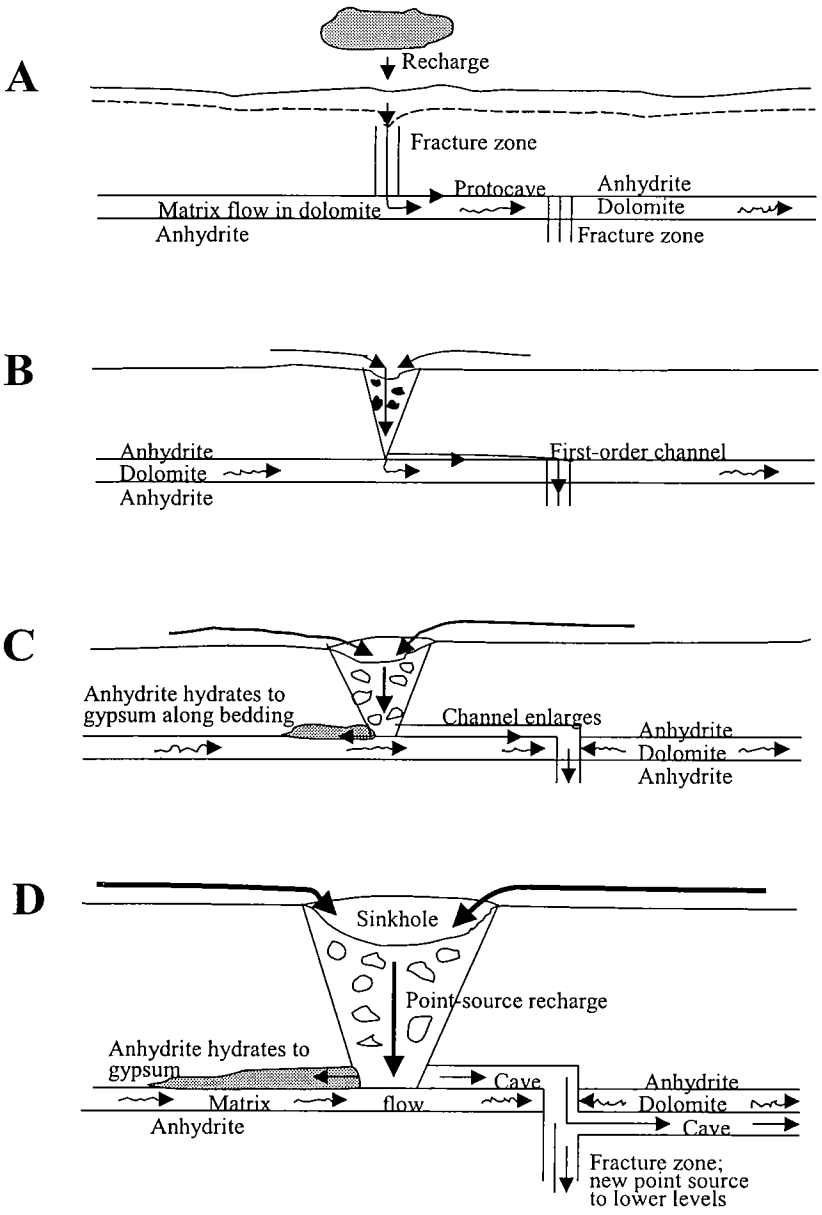


Figure 5. Diagrammatic model of the horizontal development of intrastratal karst, corresponding to the vertical development shown in Figure 4. As water progressively gets funneled more rapidly down sinkholes, it must find an equally rapid way of discharge. If this rate exceeds what matrix flow can accommodate, and if the water is unsaturated, then water will begin to form cave conduits in evaporite rock (e.g., anhydrite) at its contact with more competent rock (e.g., dolomite). (A) Water moves primarily along the anhydrite–dolomite contact because this is the easiest route to follow, and secondarily into the dolomite as matrix flow (wiggly arrows). (B) Undersaturated water entering fractures dissolves the anhydrite at this contact, creating protocaves and then first-order channels. (C) Where water meets with another vertical-fracture zone in the dolomite, it transects the dolomite. (D) Caves may form at the top or bottom of contacts, or a newer point source may drill deeper into underlying evaporite rock. As the first-order channels quickly enlarge to second-order and third-order cave conduits, water can move rapidly toward discharge.

For example, Worthington and others (2000) give data tables showing that the proportion of measured channel-flow permeability is 94–99.7% versus <0.02% for matrix permeability in karst systems.

### *Intersection of Karst*

Because the majority of flow can become concentrated along a few principal conduits and only about 1–2% of total rock volume becomes cavernous, this means that the chance for cave intersection by boreholes is slight. For example, at Mammoth Cave, Kentucky (the longest cave in the world; >480 km of passage), only 14 out of 1,000 randomly drilled boreholes have intercepted known cave passages (Worthington, 1999)—or a 1.4% chance of intersection. About 60 boreholes (including shafts) have been drilled on the WIPP site ridge, but only one (WIPP-33) is reported to have actually intersected caves—or a probability of 1.7%, greater than that for Mammoth Cave. If one also considers that the collapsed, displaced (from higher strata) breccias found in boreholes WIPP-13 and H-3 might indicate former cave passages, this would make three possible intersections of karst, or a probability of 5%—higher than for most known cave regions of the world. Most values lie between 0.5% and 2% for a chance interception of a borehole with a cave passage (Worthington and others, 2000). Therefore, the fact that most of the boreholes have not intersected intrastratal karst at the WIPP site is no reason for assuming it is not there.

### *Aggressiveness of Solutions and Annealing of Anhydrite*

The capacity of water to dissolve evaporite rock depends on how undersaturated it is. Even brines can be aggressive in most instances because the solubility of gypsum and halite is so great. This is true for both vadose and phreatic water: both have the potential for dissolving intrastratal evaporite karst. The aggressiveness of solutions can explain how deep intrastratal karst in anhydrite can "escape" annealing and clogging with gypsum (Fig. 8). If undersaturated solutions are continually widening cave passages at a rapid rate, there is not enough time for the anhydrite to anneal shut by a gypsum-conversion volume increase. The hydration of anhydrite to gypsum might take place with each surge of undersaturated water, but the gypsum will be carried away in solution so that a volume change will not affect closure of the cave passage.

This process was reported by Ferrall and Gibbons (1980) for borehole WIPP-19 in the Forty-Niner Mem-

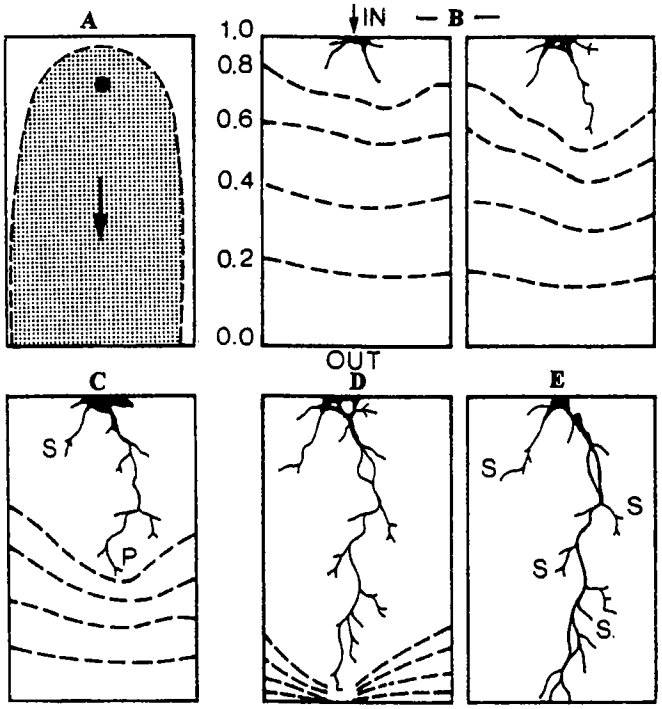


Figure 6. Diagrams showing propagation of a protocave from a single input to an output boundary in plane A. Shading shows the flow field or envelope at the start of dissolution. Black dot shows point-source vertical input. Dashed lines are equipotentials. *P* = principal (or victor) tube; *S* = subsidiary tubes. Scale: 1 m to 10 km. Pressure head: from thickness of a single bed to hundreds of meters. (A) The initial mode of flow is laminar within the plane (planar flow) and can be treated as Darcian. (B) Distributary patterns of solutional micro-conduits develop that extend preferentially in the direction of the hydraulic gradient. Their rates of extension are determined by the solvent-penetration distance and factors that control it (e.g., how undersaturated the incoming water is, solubility of the rock, etc.). Courses are random and depend on micro-features of the bedding plane. A high resistance to flow is characteristic of the fracture at this stage. (C, D) One principal conduit grows ahead of the others. It deforms the equipotential field, reducing the gradient at the solution front of its competitors ("subsidiaries"), thus slowing their advance. (E) When the principal or "victor" conduit attains the output boundary, the high resistance to flow is destroyed, and a protocave (whose diameter is 1 mm or more) now carries flow through the bedding-plane fissure. Darcian flow no longer applies, once the protocave conduit expands to minimum (5–15-mm) cave (turbulent-flow) dimensions. After this happens, cave enlargement can be comparatively rapid, especially in evaporite rock, as long as undersaturated water is entering the system. As the principal conduits preferentially enlarge over the subsidiary branches, the branches may become disconnected from the flow path or become captured by the principal conduit. These then may be sealed by clay and/or collapse. From Ewers (1982), modified by Ford and Williams (1989).

ber of the Rustler Formation, where leaching has created voids parallel to bedding as a result of ground water traveling along bedding laminae. Very little gypsification is found along these leached zones in the Forty-Niner, a situation that Ferrall and Gibbons attributed to water dissolving anhydrite along paleowaterways and then removing it by ground-water flow before the dissolved calcium sulfate could be redeposited as gypsum.

## Indirect Evidence for Intrastratal Karst

Because of the inherent concealed nature of intrastratal karst, such karst can be very difficult to detect. Whereas little direct evidence exists for intrastratal karst at the WIPP site, a number of indirect lines of evidence suggest the possibility of its existence. These indirect lines are briefly presented with respect to the karst principles and processes discussed above. Again, refer to Hill (1996, 1999) for a more detailed discussion.

### *Regional Considerations*

The Delaware Basin is one of the most prominent evaporite-karst areas in the world. As previously discussed, it contains a wide variety of dissolution features over its extent (Fig. 1). The WIPP site is just east of a major karst valley, Nash Draw, and lies adjacent to known cave areas (Fig. 2). Is it reasonable to assume that only the WIPP site section of the Delaware Basin is not influenced by karst processes?

### *Surface Topographic Depressions*

A number of closed topographic depressions occur at the surface of the WIPP site. The largest of these are at WIPP-14 and WIPP-33 (Fig. 2). The WIPP-14 depression is 210 m wide and 3 m deep; it is perfectly round and has interior drainage. The WIPP-33 depression is the largest of a linear chain of four surface depressions that trend eastward, toward the WIPP site. Barrows (1985) interpreted these and other topographic depressions at the WIPP site to be alluvial dolines (sinkholes).

### *Surface Runoff*

The WIPP site is a gently sloping, slightly hummocky plain blanketed with partly stabilized windblown sand and sand dunes. It displays almost no surface runoff—a primary characteristic of karst terrains. About 300 mm of precipitation falls annually on the WIPP site, mostly between May and October, with major rainstorms in the monsoon months of July, August, and September. The rain collects in the closed topographic depressions and then sinks into the subsurface.

Campbell and others (1996) used chloride mass-balance techniques to estimate infiltration and evaporation rates and ages of soil water in the sand dunes at the WIPP site. From their data it was concluded that diffuse recharge does not appear to be the major source of water to Rustler aquifers. Rather, the major source "must be water which has been recharged from surface runoff through karst features or other direct conduits that minimize evaporation" (Campbell and others, 1996, p. 164).

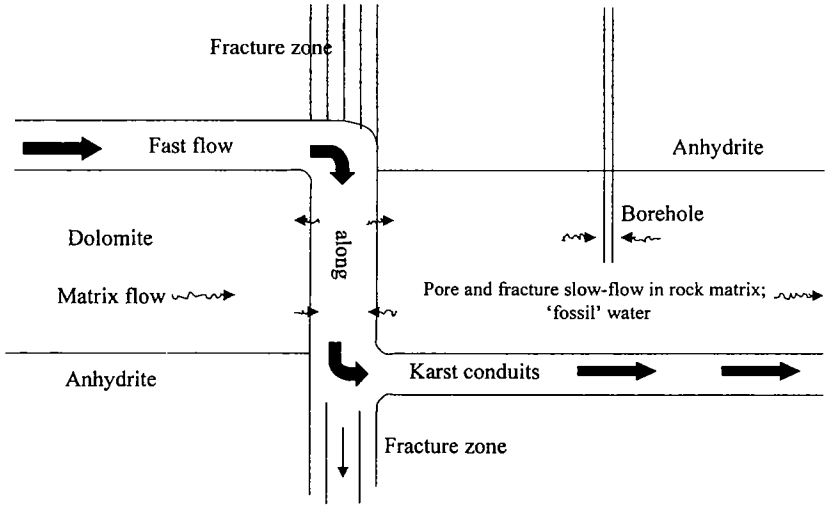


Figure 7. Diagram showing how karst conduits can discharge most of the water through a system, whereas a borehole right next to the cave passage might intersect "fossil" water in the rock matrix. Water might diffuse either into or out of the rock matrix, depending on flow conditions. During low flow, the conduits should receive water from the surrounding matrix, because they are zones of lower head. During high flow the conduits receive water more rapidly than the surrounding matrix, so water is temporarily forced into the surrounding matrix. This two-dimensional diagram shows water in the conduits moving either parallel or perpendicular to matrix flow in the dolomite, but in actuality karst-conduit water can move down-gradient in any direction toward a discharge point.

## Discharge

The discharge (outflow) point or points for water recharging the WIPP site has never been determined, even after more than 20 years of study. Corbet and Knupp (1996), in their computer model of flow within the Culebra, did not specify a discharge point—only that flow is toward the downstream parts of the Pecos River along the southern boundary of their model. However, Snow (2002, fig. 7) reported a karstic discharge into Laguna Pequena after a record rainfall event stimulated spring flow, and showed a person standing knee-deep in water from this discharge. This water then emptied from Laguna Pequena into Laguna Grande de la Sal (Salt Lake; Figs. 1, 2) at a measured rate of ~100,000 gallons/minute (~6.3 $m^3/s$). The most likely recharge source for this water was the Nash Draw watershed, perhaps including the area of the WIPP site. Flow into this discharge area was rapid but of very short duration—like it is in the Chosa Draw surface-karst region west of the Pecos River (Sares, 1984).

### *Negative Gravity Anomalies*

A gravity survey is a method used for establishing the maximum depth to the top of a causative density structure displaying a minimum amount of missing, or excess, mass. Barrows and others (1983) performed a gravity survey at the WIPP site, the results of which were found to be consistent with those reported from other gravity surveys in evaporite karstlands, where sharp negative anomalies are attributable to solution caverns in evaporite rock, hydration of anhydrite to gypsum, or low-density fill in local sinkholes. In a detailed traverse across the site, the WIPP gravity survey picked up four main negative anomalies: (1) WIPP-14 (–0.8 mGal), WIPP-13 (–0.15 mGal), H-3 (–0.45 mGal) (all three shown in Fig. 9), and WIPP-33 (–0.8 mGal) (location shown in Fig. 2). The WIPP-13 and H-3 anomalies correspond to collapse breccias in the subsurface, and the WIPP-33 anomaly to surface topographic depressions and subsurface caves. Because of these correlations, Barrows and others (1983) suggested that the WIPP-14 negative gravity anomaly also represents a karst-related feature caused by solution/removal and/or a rock-density decrease from gypsum hydration in the vicinity of karst conduits.

### *Collapse Breccias and Insoluble Residue*

Holt and Powers (1988) and Powers and Holt (2000) described facies variability and post-depositional alteration within the Rustler Formation from observing the rock in two shafts and many cores at or near the WIPP site. These authors interpreted many of the so-called "dissolution residues" of Anderson and others (1978) to be primary features owing to dissolution in the Permian, and considered only breccias to be key indicators of significant post-burial suberosion.

However, some collapse breccias and insoluble residues found in stratigraphic zones at WIPP may be the result of intrastratal karst processes where subsidiary passages become clogged with clay or breccia. For example, collapse, upward stoping, and mixing of breccia clasts derived from various stratigraphic zones occur in WIPP-13 and H-3, and both of these boreholes were drilled within the negative gravity features (sinkholes?) of Barrows and others (1983; Fig. 9), suggesting that karst processes may be responsible for these breccias. Ferrall and Gibbons (1980) reported 4.5 m of solution residue in the Tamarisk Member, directly overlying the Culebra Dolomite Member of the Rustler Formation. The upper 30 cm of this residue contains breccia clasts, and the lower 30 cm is layered, which caused these authors to speculate that the residue and clasts might have been deposited in the bottom of a solution cavity. Ferrall and Gibbons' description sounds similar to "trash zone" breccia deposits in paleokarst zones within Mississippi Valley–type ores (Sangster, 1988).

### *WIPP-33 Sinkholes and Caves*

Borehole WIPP-33 (Fig. 2) was drilled in the center of the largest (210 m in diameter, 4–9 m deep) of four topographic depressions (sinkholes) that trend east-

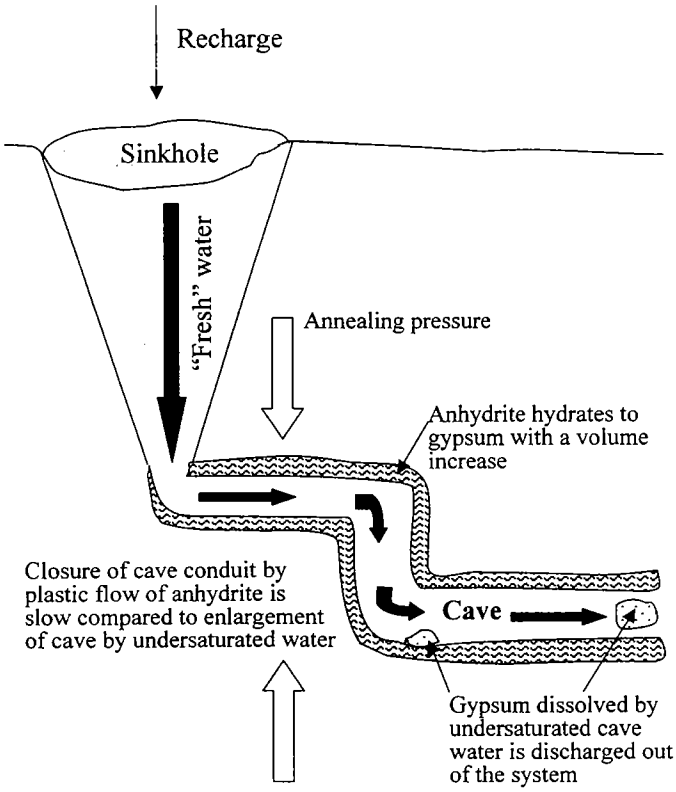


Figure 8. Diagram showing how circulating water causes cave passages to "escape" annealing and clogging with gypsum. Intrastratal evaporite karst can form very quickly; thus, the passage doesn't have time to anneal shut (opposing block arrows). Undersaturated water flowing into a phreatic intrastratal karst system at a time of heavy rain causes any dissolved anhydrite/gypsum to be discharged from the system.

ward toward the WIPP site. At the base of the Forty-Niner Member of the Rustler Formation (Fig. 3), the drill hole encountered a 2.9-m-high cave, a 1.8-m-high cave, and a 0.6-m-high cave above the Magenta Dolomite, all filled with water (i.e., the caves reside within the phreatic zone). These depressions and caves also correspond to the negative gravity anomaly of Barrows and others (1983). The caves intersected by WIPP-33 raise an important question: where does the water in these caves come from and go to? Caves cannot be isolated from a recharge/discharge system. Are these third-order channels draining into the fourth-order Nash Draw? Third-order channels, in turn, must be fed by first- and second-order channels (from farther east along the sinkhole trend, from beneath the WIPP site?).

### *Ages of Fossil Water*

The age of Rustler water was studied by Lambert (1987), who performed radiocarbon measurements on organic matter contained in it. Radiocarbon dates for water in the Culebra aquifer were found to vary between 12,000 and 16,000 Y.B.P., which suggested to Lambert that ground water in the Rustler is fossil water that was isolated from the atmosphere for at least 12,000 years, and that local recharge to the Culebra ceased before the present interglacial stage began about 10,000 Y.B.P.

However, if intrastratal karst is present at the WIPP site, these ages could be meaningless. As discussed earlier in the section on karst principles, if a borehole intersects slow matrix flow in the Culebra, fossil water can be obtained even though karst conduits might exist right next to this matrix flow (Fig. 7). Where karst channels provide rapid recharge/discharge through the subsurface, young water in conduits can be surrounded by older water in fractures and pores of the rock matrix (Worthington, 1999; Worthington and others, 2000). If intrastratal evaporite karst is present at the WIPP site, it could mean that two *separate* flow systems are operating simultaneously: (1) slow, lateral, matrix or fracture flow within the Culebra that is responsible for <5% of the total ground water discharging through the system; and (2) fast flow through intrastratal evaporite karst, which transects and bypasses the Culebra and which is responsible for >95% of the total ground water discharging through the system.

### *Anomalous Drawdowns*

Large-scale pumping tests of the Culebra Dolomite were performed at the WIPP site in early 1987. Among the results of these tests, Beauheim (1987) reported the following anomalous drawdowns: (1) an "apparent no-flow boundary," probably indicating a decrease in Culebra transmissivity fairly close to WIPP-13 (Beauheim, 1987, p. 39); (2) several anomalous responses of ERDA-9 (near the WIPP shaft), including a drawdown that was several hundred hours late, a recovery that, when it occurred, was sharp, and a drawdown in the middle of the recovery period that appeared to be a response to a separate event; (3) exhaust-shaft behavior that paralleled ERDA-9, as if a withdrawal of fluid from the Culebra at some locality temporarily caused drawdown at the exhaust shaft.

Anomalous pumping drawdowns and spatial or temporal changes in hydraulic heads are characteristic of karst, because karst channels/conduits permit leakage (Ford and Williams, 1989). Leakage might result in variable rates, time lags in recharge transfer, or short-period interruptions or delays in otherwise constant flow (Worthington and Ford, 1995).

Leakage into the WIPP exhaust shaft is known to be already occurring. When this shaft was first built in January 1984 and was mapped by D. Powers and R. Holt in July 1984–85, no leakage was observed (D. Powers, personal communication, 1999). Leakage was first detected in 1988 and has increased substantially since that time. The latest videos (1998 and 1999) show far more water leakage than the first video survey in 1995, demonstrating that in less than 15 years a new source of ground-water drainage had become focused in the subsurface by a point-source process (Fig. 6). Essentially, the WIPP exhaust shaft is acting as an

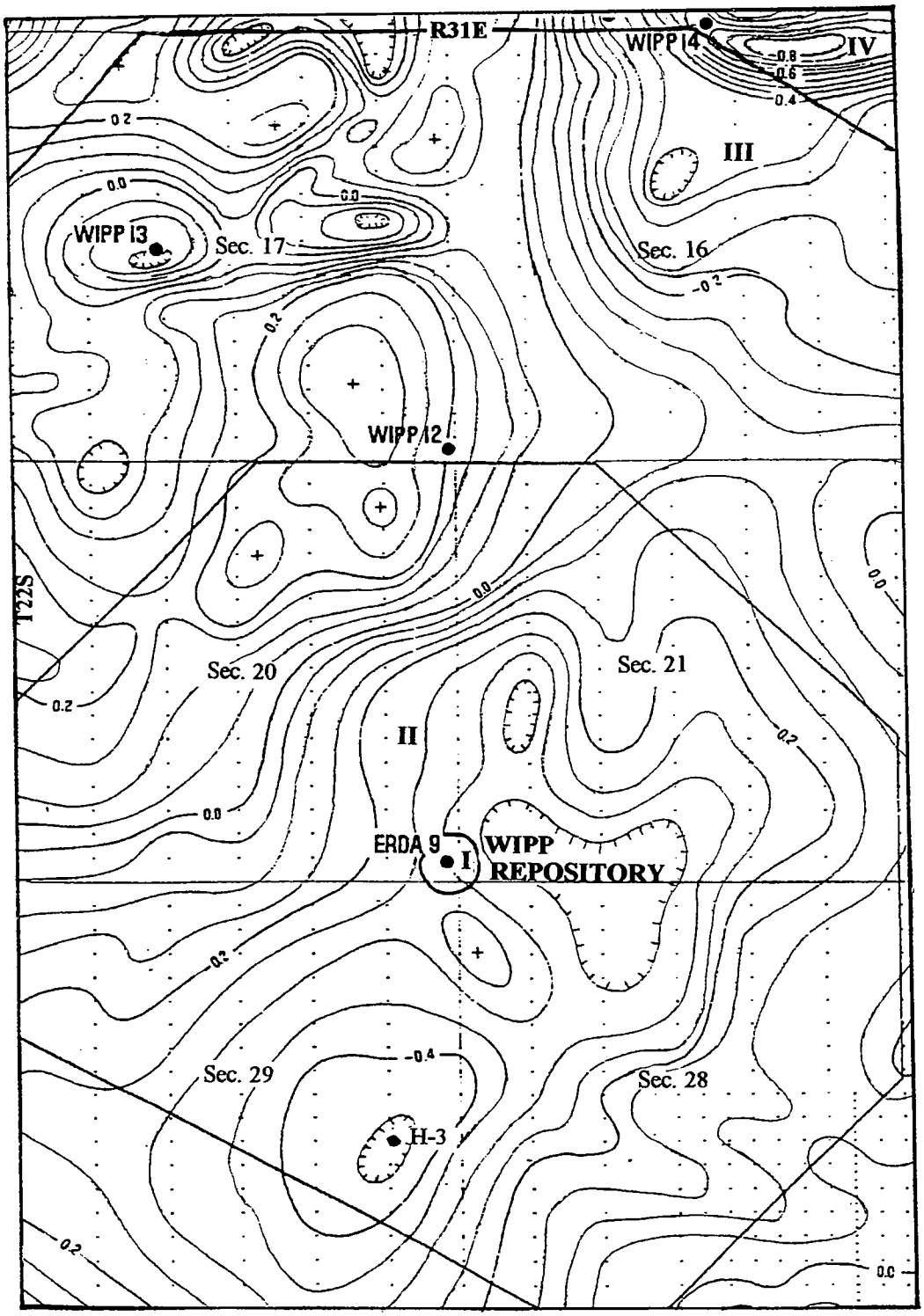


Figure 9. Map of a Bouguer gravity survey of the WIPP site, showing negative gravity anomalies at WIPP-14, WIPP-13, and H-3. (WIPP-33 is not shown in this figure.) WIPP-14 (and WIPP-33) correspond to topographic depressions. WIPP-13 and H-3 are known (by drilling) to correspond to collapse breccias and mixing of stratigraphic units in the subsurface. Contour interval, 0.05 mGal. Modified from Barrows and others (1983).

"output boundary" for cave dissolution whereby a high precipitation event could cause rapid enlargement of developing karst channels and water invasion of the WIPP repository via the exhaust shaft.

### *Salinity Variations*

Another characteristic of karst is spatial or temporal changes in water chemistry and salinity. Precipitation that rapidly infiltrates along channel networks

commonly has a much lower solute concentration than long residence-time matrix water. Total-dissolved-solids (TDS) anomalies may be related to karst because karst creates a complex system of freshwater/saline-water travel paths.

Chemical/salinity variations are characteristic of water collected in boreholes drilled at the WIPP site. For example, Ramey (1987, p. 11) stated:

> Considerable chemical variations exist between the wells H-1, H-2, and H-3, which are closest to the site. Total dissolved solids concentrations range from 9,700 to 62,000 mg/L between these wells, a difference of over 6×, and chloride ranges from 2,800 to 29,600 mg/L, an order of magnitude difference. The reasons for the abrupt chemical changes within the one square mile area surrounding wells H-1, H-2 and H-3 cannot be answered with the limited data currently available . . . large lateral variations exist between and within testholes (p. 13).

As discussed earlier, borehole H-3 contains what may be karst breccias, and undersaturated water coming into this system through a surface sinkhole (negative gravity anomaly; Fig. 9) could be causing the salinity variations described by Ramey. The values of 9,700 mg/L and 2,800 mg/L are exceptionally "fresh" to have been supplied by diffuse reflux from the surface. Instead, such undersaturated water is more typical of karst where water moves rapidly through the system.

Regions of low salinity are also known to exist hydraulically down-gradient from regions of intermediate salinity at the WIPP site, and a "facies" change is known to exist from NaCl to $CaSO_4$ over this same region (Chapman, 1988). Obviously there must be a flow of relatively undersaturated water to the down-gradient segment to produce this trend. Corbet and Knupp (1996) and Corbet (1998) modeled this undersaturated water into the system as diffuse, vertical reflux; however, relatively more dilute and oxidized water could be obtained by vertical flow along karst. Diffuse reflux should produce saturated water with an evaporative signature from the soil-subcutaneous zone, whereas karst water should be relatively undersaturated and have an isotopic signature characteristic of meteoric water, as has been demonstrated by Campbell and others (1996) to be the case for the WIPP site.

## SUMMARY

Karst aquifers pose more problems to the hydrologist than any other, because their characteristics are poorly defined and water flow within them is of a particular type. With direct observations limited to caves, boreholes, and recharge and discharge, the rest of the aquifer characteristics must necessarily be deduced from indirect evidence. One cannot treat the system as a "black box": such treatment can be far removed from physical reality and tell one little about the structure of the aquifer and how it really operates. This is especially true for intrastratal karst.

In the case of the WIPP site, documenting intrastratal karst by direct evidence is very difficult. The method of recharge is such that dye cannot easily be put into the system to trace water from input to output. The discharge point for WIPP is unknown, and possible discharge springs (e.g., Malaga Bend) have never been monitored hydrographically to correlate with rainfall on and around the WIPP site. And, without the parameters of recharge and discharge, water-balance studies are hypothetical at best. With deep, phreatic, intrastratal karst such as might possibly exist at the WIPP site, caves cannot be explored, and geophysical techniques cannot detect caves that deep. Many boreholes have been drilled at the WIPP site, but even their lack of intersection with caves is not a guarantee that instrastratal karst is not present.

It should be kept in mind that while well and drawdown tests have characterized fracture and matrix flow in the Culebra Dolomite aquifer, they have not characterized possible channel-network flow that may be occurring between wells. To quote Palmer (1995, p. 61):

> The laminar flow so commonly detected by well tests is tributary to conduits that convey water and contaminants at high velocities to spring outlets. Unless monitor wells happen to intercept these conduits, contaminants can pass right between them without the slightest chance of detection.

## ACKNOWLEDGMENTS

This project was funded by DOE/Sandia Laboratories under Contract no. BF-4551. I thank Derek Ford and Ken Johnson for reviewing the manuscript.

## REFERENCES CITED

Anderson, R. Y., 1980a, Field trip notes for salt dissolution features in the Delaware Basin, *in* Chaturvedi, L. (ed.), WIPP site and vicinity geological field trip: Environmental Evaluation Group, Albuquerque, New Mexico, EEG-7, p. 112–129.

_____1980b, Summary of session on deep dissolution and breccia pipes, *in* Geotechnical consideration for radiological hazard assessment of WIPP: Environmental Evaluation Group, Albuquerque, New Mexico, EEG-6, p. 13–15.

_____1981, Deep-seated salt dissolution in the Delaware Basin, Texas and New Mexico, *in* Wells, S. G.; and Lambert, W. (eds.), Environmental geology and hydrology in New Mexico: New Mexico Geological Society Special Publication 10, p. 133–145.

Anderson, R. Y.; and Kirkland, D. W., 1980, Dissolution of salt deposits by brine density flow: Geology, v. 8, p. 66–69.

Anderson, R. Y.; Kietzke, K. K.; and Rhodes, D. J., 1978, Development of dissolution breccias, northern Delaware Basin, New Mexico and Texas, *in* Austin, G. S. (compiler), Geology and mineral deposits of Ochoan rocks in Delaware Basin and adjacent areas: New Mexico Bureau of Mines and Mineral Resources Circular 159, p. 47–52.

Bachman, G. O., 1980, Regional geology and Cenozoic history of Pecos region, southeastern New Mexico: U.S. Geological Survey Open-file Report 80-1099, 116 p.

Barrows, L. J., 1985, WIPP geohydrology—the implication of karst, *in* Chaturvedi, L.; and Channell, J. K. (eds.), The Rustler Formation as a transport medium for contaminated groundwater: Environmental Evaluation Group, Albuquerque, New Mexico, EEG-32, 21 p.

Barrows, L. J.; and Felt, J. D., 1985, A high-precision gravity survey in the Delaware Basin of southeastern New

Mexico: Geophysics, v. 50, p. 825–833.
Barrows, L. J.; Shaffer, S. E.; Miller, W. B.; and Felt, J. D., 1983, Waste Isolation Pilot Plant (WIPP) site gravity survey and interpretation: Sandia National Laboratories, Albuquerque, New Mexico, SAND82-2922, 113 p.
Beauheim, R. L., 1987, Interpretation of the WIPP-13 multipad pumping test of the Culebra Dolomite at the Waste Isolation Pilot Plant (WIPP) site: Sandia National Laboratories, Albuquerque, New Mexico, SAND87-2456, 171 p.
Campbell, A. R.; Phillips, F. M.; and Van Landingham, J., 1996, Stable isotope study of soil water, WIPP site, New Mexico: estimation of recharge to Rustler aquifers: Radioactive Waste Management and Environmental Restoration, v. 20, p. 153–165.
Chapman, J. B., 1988, Chemical and radiochemical characteristics of groundwater in the Culebra Dolomite, southeastern New Mexico: Environmental Evaluation Group, Albuquerque, New Mexico, EEG-39, 63 p.
Chaturvedi, L., 1993, WIPP-related geological issues, *in* Love, D. W., and others (eds.), Carlsbad region, New Mexico and West Texas: New Mexico Geological Society Guidebook, 44th Annual Field Conference, p. 331–338.
Chaturvedi, L.; and Channell, J. K., 1985, The Rustler Formation as a transport medium for contaminated groundwater: Environmental Evaluation Group, Albuquerque, New Mexico, EEG-32, 84 p.
Corbet, T. F., 1998, Integration of hydrogeology and geochemistry of the Culebra Member of the Rustler Formaton in the vicinity of the Waste Isolation Pilot Plant (USA), *in* Use of hydrogeochemical information in testing groundwater flow models: NEA, Organization for economic cooperation and development, Workshop Proceedings, Börgholm, Sweden, Sept. 1–3, 1997, p. 135–149.
Corbet, T. F.; and Knupp, P. M., 1996, The role of regional groundwater flow in the hydrogeology of the Culebra Member of the Rustler Formation at the Waste Isolation Pilot Plant (WIPP), southeastern New Mexico: Sandia National Laboratories, Albuquerque, New Mexico, SAND96-2133, 148 p.
Crawford, J. E., 1990, Geology and Frasch-mining operations of the Culberson sulfur mine, Culberson County, West Texas, *in* Kyle, J. R. (ed.), Industrial mineral resources of the Delaware Basin, Texas and New Mexico: Society of Economic Geologists Guidebook, v. 8, p. 141–162.
Davies, P. B., 1984, Deep-seated dissolution and subsidence in bedded salt deposits: Stanford University unpublished Ph.D. dissertation, 379 p.
Ewers, R. O., 1982, Cavern development in the dimensions of length and breadth: McMaster University, Hamilton, Ontario, unpublished Ph.D. dissertation, 398 p.
Ferrall, C. C.; and Gibbons, J. F., 1980, Core study of Rustler Formation over the WIPP site: Sandia National Laboratories, Albuquerque, New Mexico, SAND79-7110, 80 p.
Ford, D. C.; and Williams, P. W., 1989, Karst geomorphology and hydrology: Unwin Hyman, London, 601 p.
Hill, C. A., 1993, Barite/celestite/selenite/calcite mineralization at Bell Lake Sink, Lea County, New Mexico, *in* Love, D. W., and others (eds.), Carlsbad region, New Mexico and West Texas: New Mexico Geological Society Guidebook, 44th Annual Field Conference, p. 117–128.
_____1996, Geology of the Delaware Basin—Guadalupe Mountains, Apache Mountains, Glass Mountains, New Mexico and West Texas: Society of Economic Paleontologists and Mineralogists, Permian Basin Section, Publication 96-39, 480 p.
_____1999, Intrastratal karst at the WIPP site: Unpublished report to DOE/Sandia National Laboratories, Contract no. BF-4451, Sept., 83 p.
Holt, R. M.; and Powers, D. W., 1988, Facies variability and post-depositional alteration within the Rustler Formation in the vicinity of the Waste Isolation Pilot Plant, southeastern New Mexico: Department of Energy, DOE/WIPP-88-004, inconseq. pages.
Klimchouk, A. B., 2000, Speleogenesis under deep-seated confined settings, *in* Klimchouk, A. B., and others (eds.), Speleogenesis: evolution of karst aquifers: National Speleological Society, Huntsville, Alabama, p. 244–260.
Lambert, S. J., 1987, Feasibility study: applicability of geochronologic methods involving radiocarbon and other nuclides to the groundwater hydrology of the Rustler Formation: Sandia National Laboratories, Albuquerque, New Mexico, SAND86-1054, 108 p.
Lambert, S. J.; and Carter, J. A., 1987, Uranium-isotope systematics in groundwaters of the Rustler Formaton, northern Delaware Basin, southeastern New Mexico—principles and preliminary results: Sandia National Laboratories, Albuquerque, New Mexico, SAND87-0388, 62 p.
Lee, W. T., 1924, Erosion by solution and fill: U.S. Geological Survey Bulletin 760-D, p. 107–121.
Maley, V. C.; and Huffington, R. M., 1953, Cenozoic fill and evaporite solution in the Delaware Basin, Texas and New Mexico: Geological Society of America Bulletin, v. 64, p. 539–546.
Neill, R. H.; Channell, J. K.; Chaturvedi, L.; Little, M. S.; Rehfeldt, K.; and Spiegler, P., 1983, Evaluation of the suitability of the WIPP site: Environmental Evaluation Group, Albuquerque, New Mexico, EEG-23, 157 p.
Olive, W. W., 1957, Solution-subsidence troughs, Castile Formation of the Gypsum Plain, Texas and New Mexico: Geological Society of America Bulletin, v. 68, p. 351–358.
Palmer, A. N., 1995, Presentation of the Kirk Bryan award to Arthur H. Palmer—a response: GSA Today, March, p. 61.
Powers, D. W.; and Holt, R. M., 2000, The salt that wasn't there: Mudflat facies equivalents to halite of the Permian Rustler Formation, southeastern New Mexico: Journal of Sedimentary Research, v. 70, p. 29–36.
Ramey, D. S., 1987, Chemistry of the Rustler fluids, *in* Chaturvedi, L. (ed.), The Rustler Formation at the WIPP site: Environmental Evaluation Group, Albuquerque, New Mexico, EEG-34, p. 8–13.
Sangster, D. F., 1988, Breccia-hosted lead–zinc deposits in carbonate rocks, *in* James, N. P.; and Choquette, P. W. (eds.), Paleokarst: Springer-Verlag, New York, p. 102–116.
Sares, S. W., 1984, Hydrologic and geomorphic development of a low-relief evaporite karst drainage basin, southeastern New Mexico: University of New Mexico unpublished M.S. thesis, 123 p.
Snow, D. T., 2002, Unsafe radwaste disposal at WIPP: Proceedings of Solution Mining Research Institute, Banff, Alberta, Canada, April 28–May 1, 22 p.
Vine, J. D., 1960, Recent domal structures in southeastern New Mexico: American Association of Petroleum Geologists Bulletin, v. 14, p. 765–788.
Worthington, S. R., 1999, A comprehensive strategy for understanding flow in carbonate aquifers, *in* Palmer, A. N.; Palmer, M. V.; and Sasowsky, I. D. (eds.), Karst modeling: Proceedings of Karst Water Institute, Special Publication 5, p. 30–37.
Worthington, S. R.; and Ford, D. C., 1995, Borehole tests for megascale channeling in carbonate aquifers: Proceedings of 26th Congress of International Association of Hydrogeologists, Edmonton, Alberta, Canada, June 5–9.
Worthington, S. R.; Ford, D. C.; and Beddows, P. A., 2000, Porosity and permeability enhancement in unconfined carbonate aquifers as a result of solution, *in* Klimchouk, A. B., and others (eds.), Speleogenesis: evolution of karst aquifers: National Speleological Society, Huntsville, Alabama, p. 463–472.

# Geological Factors Related to the Transmissivity of the Culebra Dolomite Member, Permian Rustler Formation, Delaware Basin, Southeastern New Mexico

***Dennis W. Powers***
Consulting Geologist
Anthony, Texas

***Robert M. Holt***
University of Mississippi
University, Mississippi

***Richard L. Beauheim and Sean A. McKenna***
Sandia National Laboratories
Carlsbad, New Mexico

**ABSTRACT.**—The Culebra Dolomite Member of the Permian Rustler Formation in southeastern New Mexico has been tested hydraulically at 42 sites, yielding reliable transmissivity (T) values. The T values show a strong relationship to depth with contributions from two additional factors: dissolution of halite from the upper part of the underlying Salado Formation, and distribution of halite in the Rustler.

Three maps related to these factors improve our understanding of the processes involved in creating the T distribution. An elevation map of the Culebra shows the general regional eastward dip, which contributes to the depth factor, and two northwest–southeast-trending anticlines. Along the eastern margin of Nash Draw (a closed depression formed by dissolution and erosion), elevation contours are disrupted where the Culebra subsided as halite was removed from the upper Salado Formation. A map of the thickness between the Culebra and an upper Salado unit reveals pronounced decreases identified as the margin of dissolution of upper Salado halite. The dissolution margin underlies, and is the apparent control for, the escarpment on the eastern margin of Nash Draw. Rustler halite margins on the third map mainly indicate limits to saline facies tracts; they are also the most likely location for any post-depositional dissolution.

The geologic data on these maps can be used to develop a quantitative model for predicting Culebra T. The data have also been used to select drilling and hydraulic-testing locations for an extensive field program, beginning in 2003.

## INTRODUCTION

The Culebra Dolomite Member of the Permian Rustler Formation (Fig. 1) in southeastern New Mexico has been intensively studied for nearly 30 years to determine its hydraulic properties. In the vicinity of the Waste Isolation Pilot Plant (WIPP) (Fig. 2), the Culebra has little significance for water production, but it is the dominant water-bearing unit above the Salado Formation, where radioactive waste is being stored for the WIPP. Its hydraulic properties are important parameters for estimating the probability of release of radionuclides from the WIPP to the boundaries of the controlled area over the next 10,000 years.

In the area of study (Fig. 2), Culebra transmissivity (T) varies over at least 6 orders of magnitude (e.g., Beauheim and Ruskauff, 1998). Across the study area, Culebra T values generally increase from east to west. Following several studies of Rustler geology as it relates to the hydrology of the Culebra (Holt and Powers, 1988, 2002; Beauheim and Holt, 1990; Powers and Holt, 1993; Holt, 1997), a detailed conceptual hydrogeological model for Culebra T has emerged. Unlike most geologic units, where heterogeneous hydraulic properties are attributable to depositional variations, spatial variability in Culebra T is primarily due to post-depositional processes (Holt, 1997).

The Culebra is a fractured dolomite (Holt and Powers, 1988), T in the Culebra is primarily due to fractures, and the amount of fracturing has been qualitatively shown to increase from east to west across the study area (Holt and Powers, 1988; Beauheim and Holt, 1990). Four regional-scale geologic processes have been postulated to account for the observed variations. Beauheim and Holt (1990) suggest that fracturing from erosion/unloading processes is a primary control on Culebra T, and Powers and Holt (1995) indicate that as much as 600 m of overburden might have been removed owing to Cenozoic erosion at the WIPP

Powers, D. W.; Holt, R. M.; Beauheim, R. L.; and McKenna, S. A., 2003, Geological factors related to the transmissivity of the Culebra Dolomite Member, Permian Rustler Formation, Delaware Basin, southeastern New Mexico, *in* Johnson, K. S.; and Neal, J. T. (eds.), Evaporite karst and engineering/environmental problems in the United States: Oklahoma Geological Survey Circular 109, p. 211–218.

| SYSTEM/ Series | | Formation | Members |
|---|---|---|---|
| CENOZOIC | | Mescalero caliche | |
| | | Gatuña | |
| TRIASSIC | | Santa Rosa | |
| | | Dewey Lake | |
| PERMIAN | Ochoan | Rustler | *Forty-niner*<br>*Magenta Dol.*<br>*Tamarisk*<br>***Culebra Dol.***<br>*Los Medaños* |
| | | Salado | *marker beds 100-116*<br>***Vaca Triste Ss.*** |
| | | Castile | |
| | Guadalupian | Bell Canyon | |

Figure 1. General stratigraphic column for the study area, showing formations described in the text. The Culebra Dolomite Member and the Vaca Triste Sandstone Member are emphasized because they are dominant features of later figures. The Los Medaños Member was named by Powers and Holt (1999) to replace the informal term "unnamed lower member" in common use. The scale of this figure does not represent unit thicknesses.

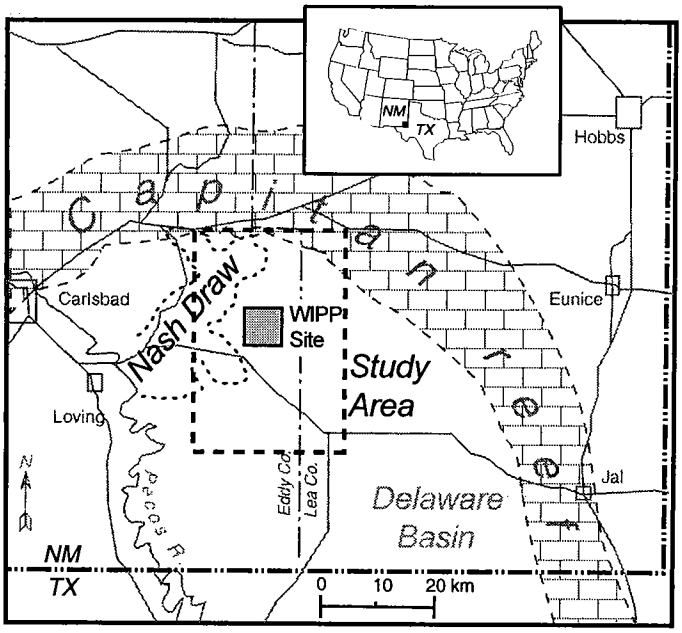


Figure 2. General location map of the study area, illustrating important features.

site. Structural deformation, including gravity foundering of the underlying Castile Formation and Cenozoic tilting of the Delaware Basin (Borns and others, 1983), also might have contributed to Culebra fracturing. In the western part of the study area (Nash Draw), halite from the Salado Formation has been dissolved, further fracturing the Culebra and, in some areas, resulting in collapse that lengthens the Culebra section (Holt and Powers, 1988; Beauheim and Holt, 1990; Powers and Holt, 1995; Holt, 1997). In the eastern part of the study area, halite directly underlies the Culebra (Holt and Powers, 1988). Holt (1997) suggests that halite cements in these areas may limit Culebra porosity and T; ground-water-chemistry data also show waters near halite saturation in these areas (e.g., Beauheim and Holt, 1990).

Here we develop the geological information and data for the Culebra necessary to create a geologically based quantitative model for predicting Culebra T. The principal geologic data necessary for this are elevations (structure-contour maps) of the top of the Culebra; thickness changes across an interval including the Rustler–Salado contact (as a means of determining the margin of dissolution of the upper Salado halite); and facies maps showing halite margins for various Rustler Formation members. Culebra overburden thickness can be obtained by subtracting interpolated Culebra elevations from topographic elevations (from digital elevation models) at grid points.

Weart and others (1998) introduce the location, function, broad setting, and some of the geological issues relevant to the WIPP for the interested reader. Part of our study area includes evaporite karst areas described by Lee (1925); we focus on more specific issues in this report.

## DATA AND SOURCES

In the study area or domain, there are three principal sources of geological data for the Culebra, Rustler halite units, and upper Salado. These sources are WIPP-sponsored work, oil and gas drilling, and drill holes for potash deposits. Within the WIPP site, most of the information comes from WIPP-sponsored drill holes and shafts (e.g., Holt and Powers, 1990). Cores, cuttings, and geophysical logs are important sources of information, but major insights into the geology of the Culebra and Rustler have come from shaft observations. Non-WIPP data sources have been interpreted on the basis of experience gained through more direct investigation of the rocks for WIPP. The second source of data is the oil and gas wells drilled in the study domain. Intensive exploration and development of previously overlooked resources, beginning in the late 1980s, have increased the number of wells with useful shallow geophysical logs, and this study includes

data from about 1,000 such drill holes. Geophysical logs from these more recent wells are commonly taken through the casing in the interval of interest to us, but the natural gamma log of the Rustler and upper Salado have distinctive signatures that are readily interpreted. The third source of geologic information for this study is the data recorded during drilling and coring to establish potash resources. Stratigraphic and lithologic data reported prior to the 1980s are sufficiently detailed to recognize consistently the important stratigraphic units. Recent potash drill-hole reports, however, commonly do not show the Culebra. To determine the margin of upper Salado dissolution, the interval from the top of Culebra to the base of the Vaca Triste Sandstone Member of the Salado Formation (Fig. 1) was most consistently reported across the various data sources. A narrower interval bounding the contact would have been preferable but was not practical. Rustler halite margins were interpreted on the basis of WIPP shafts, cores, and geophysical logs, and these margins were extended as possible, using open-hole geophysical logs from oil and gas wells and more detailed potash drill-hole descriptions.

Location data for the drill holes are most commonly the township, range, and section locations. For many drill holes, Dave Hughes (Washington TRU Solutions, LLC) provided an electronic data file of New Mexico State Plane (NAD27) locations. State Plane coordinates were converted to UTM metric using Corpscon for Windows (v. 5.11.08). As necessary, drill-hole locations were plotted on existing 7.5-minute quadrangle maps according to township, range, and section information. From these maps, UTM metric (NAD27) coordinates were obtained. Maps shown here in simplified form are based on 34- × 44-in. original maps.

## ELEVATION OF TOP OF CULEBRA

The relevant geological factor related to Culebra T is depth (Fig. 3), and the specific relationship is described elsewhere. The elevation (structure) of the Culebra can be used to estimate the depth to Culebra between drill holes by combining digitized maps of Culebra structure and digital surface-elevation maps. The Culebra elevation map (Fig. 4) reveals features that indicate dissolution as well as deformation of evaporites, and it is important to place the discussion of Culebra T in the context of these features.

The southeastern part of the study domain illustrates the general eastward regional dip of formations in the Delaware Basin (Fig. 4). Units below the evaporite beds (i.e., Guadalupian and older) tend to dip about 20 m/km eastward and show few variations. The Culebra shows distinctive features attributable to several processes.

Northeast of the WIPP site, the Culebra has been deformed by movement in the underlying evaporites of the Castile Formation and Salado Formation. The Culebra forms a northwest–southeast-trending anticline ("Divide anticline"), with structural relief ap-

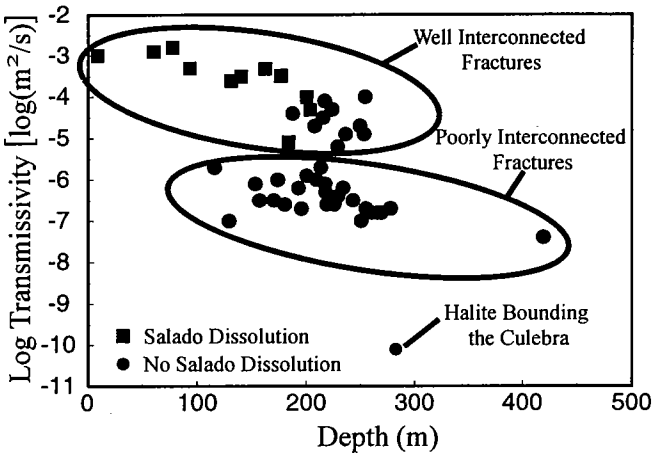


Figure 3. Log Culebra transmissivity (T) shows a strong relationship to depth. The lower field of T values is from test holes without well-interconnected fractures. The upper field is from drill holes with well-interconnected fractures and includes places where the upper Salado has been dissolved. The lowest value occurs in a location where the Culebra is underlain by halite in the Los Medaños Member and overlain by halite in the Tamarisk Member.

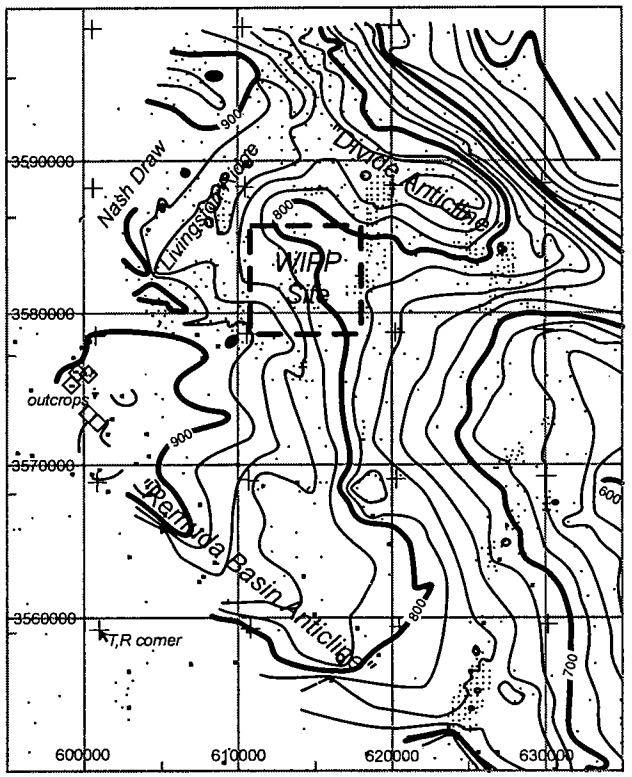


Figure 4. Elevation (structure-contour) map of the top of the Culebra Dolomite Member (in meters above mean sea level). The contour interval is 20 m. The grid lines represent the UTM (NAD27) coordinate system, in meters, for Zone 13. Small crosses show the corners for townships in the township, range system for New Mexico (see Fig. 5 to determine township numbers). Dots represent drill holes from which records were examined to obtain data. Some geophysical or geological logs were not interpretable for this datum. The data were originally plotted on large-format maps for data checking and contouring before producing this less detailed map.

proaching 100 m. Although the underlying evaporites are more significantly deformed, the structural relief diminishes upward.

In the southwestern part of the map, another northwest–southeast-trending anticline ("Remuda Basin anticline") is formed. The northern flank is a combination of eastward dip and some dissolution of Salado in the southeastern part of Nash Draw. The southern flank was created by substantial dissolution and possibly erosion associated with development of the Loving–Balmorhea trough (Maley and Huffington, 1953).

The structure map of the Culebra becomes more complicated in the vicinity of Nash Draw, marking the downdropped section where Salado dissolution has occurred (see below). Fewer reliable data points, and subsidence, indicate areas where contours are not likely to be very accurate, and therefore the structure contours haven't been extended into some of these areas.

Across the domain of interest, the Culebra structure contours are considered predictable and reliable; these are the conditions necessary for predicting the depth of the Culebra on a closely spaced (e.g., 50-m) grid by subtracting Culebra elevations from surface elevations (using digital elevation maps) at the grid points.

## DISSOLUTION OF UPPER SALADO HALITE

Across the east-central part of the study area, the interval between the top of the Culebra and the base of the Vaca Triste is about 200–220 m thick. As indicated by a broad arrow (Fig. 5), the interval tends to thin toward the northwest; in the vicinity of the WIPP site, it is about 190 m thick. From previous analysis of logs, part of this increase in thickness to the southeast is attributable to the presence of halite beds in the Los Medaños Member of the Rustler (see below). Core studies show that halite in the Los Medaños thins and disappears to the northwest owing to synsedimentary dissolution (Holt and Powers, 1988), and this process also occurred in other Rustler members (Powers and Holt, 2000).

To the north, west, and south of the WIPP site, the Culebra–Vaca Triste interval thins over a narrow band, as is shown in several areas where drill-hole control is very good. Along Livingston Ridge, the thickness of the interval drops from ~190 m to <150 m over a lateral distance ranging from about 200 to 400 m (Figs. 6, 7). The position of the dissolution margin corresponds directly to the Livingston Ridge escarpment (Fig. 8).

South of the WIPP, the interval thickness changes less dramatically. Geophysical logs reveal that halite beds of the upper Salado are thinner to the south. Cores are not available for the examination of textures, and we infer that thinning of this interval is due to dissolution rather than to depositional processes. The position of the dissolution margin (Fig. 5), placing WIPP drill hole H-9 in the zone of dissolution, is consistent with hydraulic-test results for this drill hole.

Dissolution reentrants (Fig. 5) have been interpreted west and north of the WIPP site where thickness changes occur, but these thickness changes generally are not as sharply defined as along Livingston Ridge. The reentrant to the west of the WIPP is controlled by a single datum. Data from other potash drill holes in the area did not include sufficient detail to calculate the interval thickness. The reentrant was extended from the trend of the dissolution margin along Livingston Ridge, because some connection to an outlet or inlet is required. The reentrant is extended to Livingston Ridge in an area where the Miocene–Pleistocene Gatuña Formation is thicker (Powers and Holt, 1993), possibly reflecting valley development over a dissolving trend (or a dissolving trend developing under a valley). The reentrant is also evident where a series of potash drill holes encountered water at depths where the Culebra is reasonably expected, though the drill-hole reports did not include data for Rustler stratigraphic units. Each of these reentrants will be tested by drilling and coring during FY03.

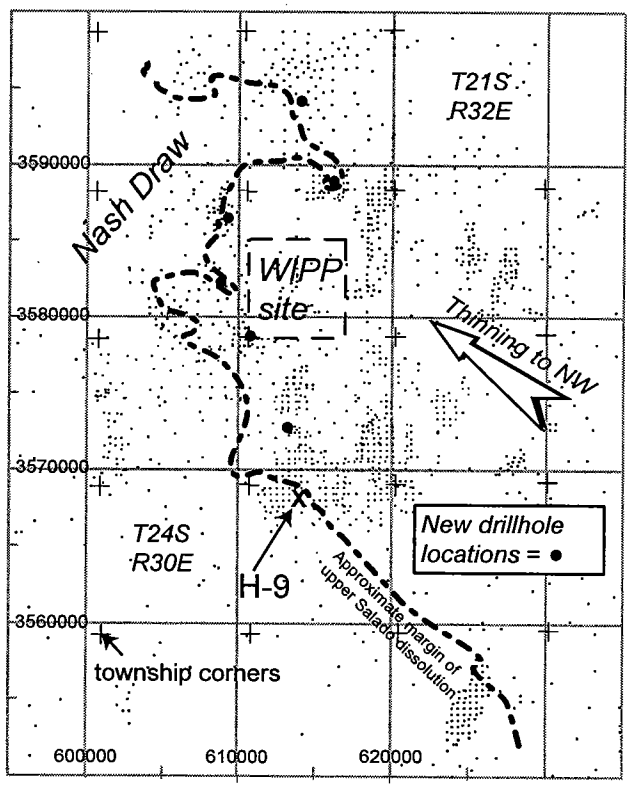


Figure 5. Map showing the dissolution margin of the upper Salado Formation. The margin is based on thickness changes for the interval between the top of the Culebra Dolomite Member and the base of the Vaca Triste Sandstone Member (see Fig. 1). Figure 6 shows a segment of the line along Livingston Ridge and the thickness data. The interval is thinner in general to the northwest, owing in part to depositional changes in the Los Medaños Member of the Rustler Formation (Fig. 1). A few township identifiers are included for reference. The data were originally plotted on large-format maps for data checking and contouring before production of this less detailed map.

## RUSTLER HALITE MARGINS

The database for determining Rustler halite margins (Fig. 9) is more restricted than for Salado dissolution or Culebra structure. Cores, shafts, and geophysical logs from uncased drill holes provide most of the data used to establish the margins. Some potash drill holes near the northern edge of the study area yielded sufficient detail to improve and extend the Rustler halite margins in those areas where other data sources are limited. Geophysical logs from recent oil and gas drill holes were more commonly taken through casing, and these logs have not been interpreted with respect to halite in the Rustler.

Rustler mudstone/halite facies tracts were interpreted by Holt and Powers (1988) and Powers and Holt (2000) as mainly the result of depositional processes, including syndepositional dissolution of halite. The margins of these halite tracts are the logical location for any post-depositional dissolution (Holt and Powers, 1988; Beauheim and Holt, 1990) that might affect the hydraulic properties of the Culebra. T values affected by such processes represent a small part of the field (Fig. 3). In addition, Culebra regions underlain or bounded by halite may have lower T.

The margin for halite (M-1/H-1) in the lower Los Medaños Member extends well west of most of the areas with halite in the remainder of the Rustler (Fig. 9). The M-1/H-1 margin very broadly parallels the margin of dissolution of the upper Salado (Fig. 5). Cores and shafts do not indicate alteration of the Culebra by late post-depositional dissolution of halite in M-1/H-1. M-2/H-2 directly underlies the Culebra, and it should be most relevant to changes in Culebra T from dissolution of Rustler halite. There is significant evidence of syndepositional and very early depositional adjustments in the basal Culebra from settling and probable dissolution of some halite from M-2/H-2 at that time (e.g., Holt and Powers, 1984, 1986, 1988, 1990; Holt, 1997). There is limited evidence of post-depositional dissolution of halite in M-3/H-3 in the vicinity of the site (Holt and Powers, 1988; Beauheim and Holt, 1990; Mercer and others, 1998). Some higher T values occur in these areas, but the exact relationship to dissolution in the Tamarisk Member is unclear. The M-4/H-4 margin generally follows the M-3/H-3 and M-2/H-2 margins except in the northeastern part of the site. It is not known to have any relationship to Culebra T.

The halite margins in the Rustler generally indicate that a saline pan environment existed to the east and that saline-mud-flat to mud-flat environments

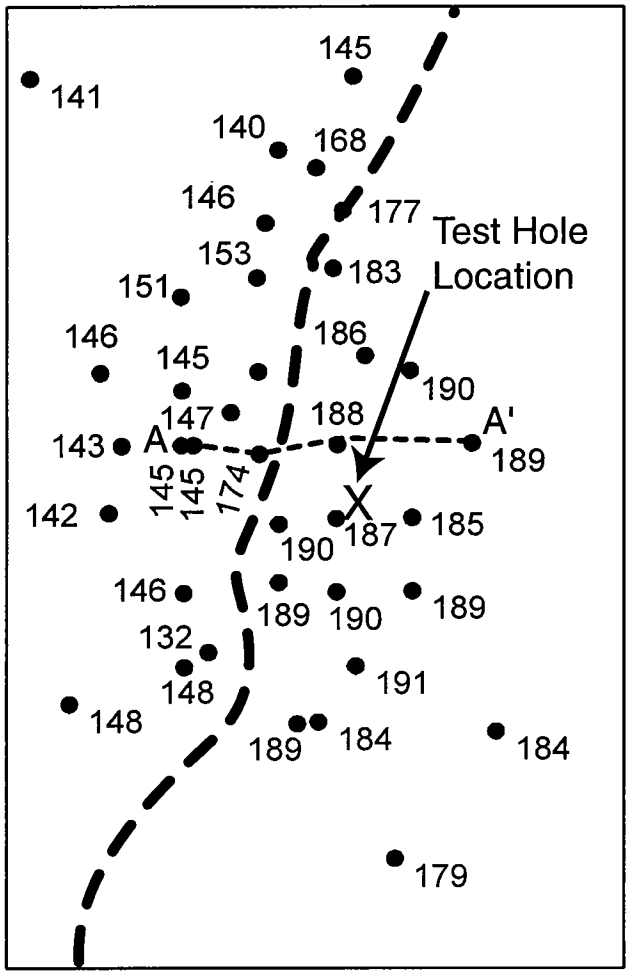


Figure 6. Thickness of upper Salado/lower Rustler strata, in meters. Along parts of Livingston Ridge, oil exploration and development drill holes are closely spaced, providing control for the margin of upper Salado dissolution based on thickness changes. The margin directly underlies the escarpment at Livingston Ridge, and the margin controls the location and development of the escarpment. The cross section (A–A') is shown in Figure 7. Livingston Ridge is shown in an oblique aerial photograph in Figure 8. A test hole (x) will be drilled during 2003 east of this margin and near the line of the cross section.

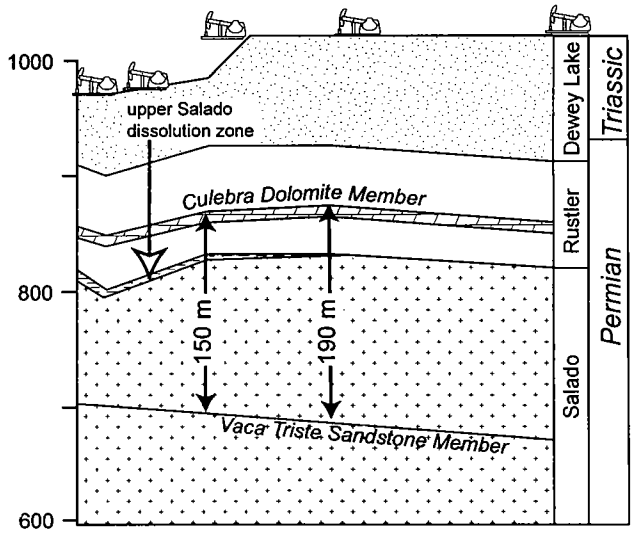


Figure 7. Cross section across Livingston Ridge, based on geophysical logs, shows the structural changes of the Culebra and the thickness changes of the interval between the Culebra and Vaca Triste. Drill holes are indicated by pump symbols; see Figure 6 for the cross-section position.

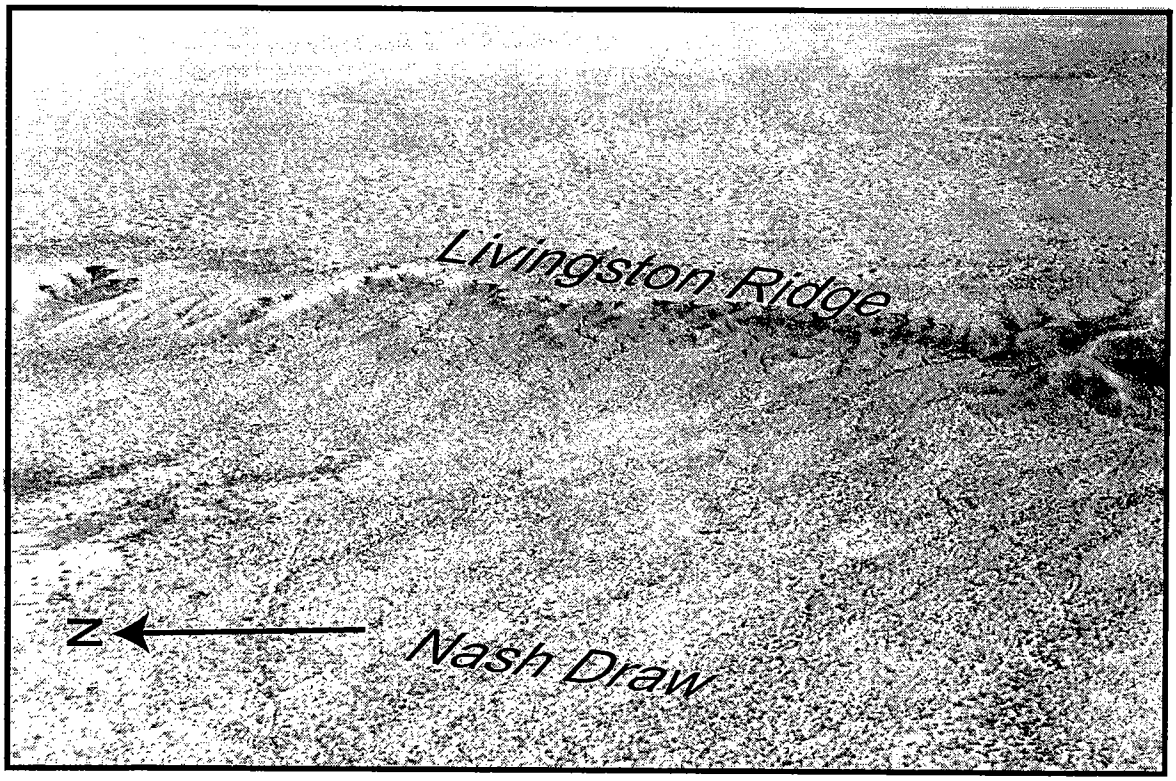


Figure 8. Low-angle aerial photograph of Livingston Ridge, just south of the area shown in Figure 6, displays downwarping across the dissolution margin and the escarpment eroded directly above the margin. The eastern part of Nash Draw is in the lower part of the photograph. The Mescalero caliche drapes the monocline, and internal textures suggest that subsidence occurred since the development of the caliche, starting about 570,000 years before present.

bordered the pan on the west. The general shapes of the depositional basins locally during these desiccating periods must have been similar.

## DISCUSSION

### Culebra Elevation

Within the study area, the Culebra generally dips to the east, and the surface topography generally rises to the east. The dip and topography combine to create a general increase in depth to the east, with a trend similar to structure contours. The general trend is for T values to decrease to the east because of depth, the presence of Rustler halite, and the lack of Salado dissolution. Drill holes with T values are sparse northeast of the WIPP site across the "Divide anticline" (Fig. 4). They do not constitute an adequate sample to determine if the structure created by deformation of deeper evaporites is a factor for estimating Culebra T.

### Upper Salado Dissolution

This study is the first effort in which the margin of upper Salado dissolution has been identified and bounded in any detail. This is a function mainly of a database that expanded greatly in the last 15 years because of oil and gas exploration and development in the area. Most of the potash exploration occurred earlier, but the drill holes are generally not as closely spaced as in developed oil or gas fields. Finding a relationship between Culebra T and Salado dissolution provided the impetus for delineating the margin of dissolution.

Two features of the upper Salado dissolution margin stand out. The first is that the margin underlies the escarpment (Livingston Ridge) on the east side of Nash Draw (Figs. 6–8). The second is that the margin appears to be relatively narrow; earlier interpretations suggested a much broader, thin wedge of dissolution penetrating significantly beyond Livingston Ridge (e.g., Mercer, 1983).

The escarpment at Livingston Ridge is believed to have been controlled by the dissolution of halite at the top of the Salado. The drill-hole evidence is now dense enough to support this conclusion. As overlying units subside above a relatively narrow dissolution margin, strain accumulates in fractures directly above the margin. These fractures would be expected to be parallel to the dissolution margin, which will be parallel to the escarpment. In parts of Nash Draw, such fractures are observable. The uneroded surface will form a monocline. Parts of Livingston Ridge (Fig. 8) also show such a monoclinal structure, in which the Mescalero caliche (which formed beginning about 570,000 ± 110,000 years before present; Rosholt and McKinney, 1980) has been deformed as well. This in-

dicates local movement (dissolution) since the Mescalero caliche was formed. The fracture system parallel to the escarpment likely contributes to infiltration and further dissolution.

Where drill-hole data are closely spaced because of oil and gas drilling, the thickness between the top of the Culebra and the base of the Vaca Triste is narrowly constrained (e.g., Fig. 6). Adjacent boreholes along Livingston Ridge are commonly spaced 200–400 m apart. They show that the thickness is reduced across about this distance. The interval in drill holes adjacent to, and east of, the margin is slightly thinner than in drill holes farther to the east. This narrow zone may be part of the dissolution margin, or it may be a continuation of the northwestward-thinning trend. It is probably the indicator of incipient dissolution.

Although the dissolution margin generally appears narrow, changes in thickness and direct borehole evidence suggest that dissolution may have advanced along two reentrants (Fig. 5), ahead of the migration of the general front and escarpment. A drill hole has been planned in each of these reentrants as a further test of the hypothesis linking Culebra T and upper Salado dissolution.

### Rustler Halite Facies

The present margins of halite in the Rustler in the study area are generally consistent among investigators, but our interpretation as dominantly depositional margins (based on intensive shaft, core, and geophysical-log studies) differs considerably from earlier interpretations of the margins as resulting from dissolution (based on changes in thickness) (see discussion in Powers and Holt, 2000).

The halite margin in the Tamarisk Member, for example, changes thickness across the depositional basin over many kilometers (e.g., Holt and Powers, 1988; Powers and Holt, 2000) rather than over the short width of the Salado dissolution margin demonstrated here. The margins expressed here are interpreted from the best information about where halite currently exists, but facies margins are commonly not so precise as to be defined by the width of a line on a map. The margins do represent well, however, the position where post-depositional dissolution might have occurred.

Textural features show that the saline mud flats were subaerially exposed and that halite was removed syndepositionally from the facies. Halite may also have survived locally in the saline-mud-flat facies and been removed later. An example is the minor disruption of the M-3 (Tamarisk) facies in the northwestern part of the WIPP site (Fig. 9). As a consequence, these facies tracts are considered to have local areas where Culebra T may have been affected by removal of Rustler halite.

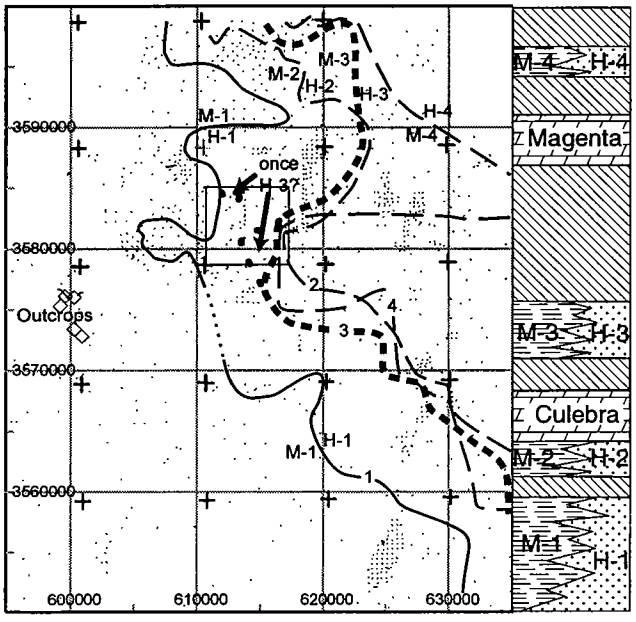


Figure 9. Rustler halite margins for four halite-bearing intervals (denoted M-x/H-x, as shown on the right side) are based on shaft and core descriptions and extrapolated to open-hole geophysical logs through the Rustler. The margins mark depositional facies changes (Holt and Powers, 1988; Powers and Holt, 2000), with some minor exceptions. The margin line for M-3/H-3 is thicker to distinguish it more easily, and the dotted lines near it are noted as areas of possible post-depositional dissolution of this halite margin or halite remnants after syndepositional dissolution.

## CONCLUSIONS

Culebra T values show a strong relationship to factors such as depth, dissolution of upper Salado halite, and distribution of Rustler halite facies. As a consequence, we acquired and interpreted data on Culebra structure, the thickness of an interval from the Culebra to the Vaca Triste, and distribution of halite in the Rustler. The data are the basis of further modeling studies (in progress). Drill holes have been located, partly on the basis of these data, to obtain additional data about Culebra hydraulic properties and geological factors contributing to these properties.

The structure of the Culebra differs from the regional structure of formations below the evaporites because of dissolution of the upper Salado and because of deformed evaporites of the Castile and Salado Formations. Over the study area, however, the structure appears well defined, and the maps will provide a basis for developing detailed estimates of depth to the Culebra as one of the factors for estimating Culebra T between test holes.

The map of the thickness of an interval, including the top of the Salado, provides details not previously reported, partly because drilling was not close-spaced in these areas until recently. We conclude that the upper Salado dissolution margin is commonly narrow (i.e., a few hundred meters wide) across much of the study area. The escarpment at Livingston Ridge overlies and is controlled by this narrow margin. Dissolution reentrants have been interpreted along Nash

Draw, based on much smaller changes in thickness. This interpretation will be directly tested by drilling, coring, and testing drill holes during 2003.

The map of Rustler halite margins is the most current representation of the distribution of halite in the Rustler. Although halite was syndepositionally dissolved from saline-mud-flat facies, there is evidence of local post-depositional dissolution of remnants in unpredictable locations. These are accounted for in modeling studies under way.

## ACKNOWLEDGMENTS

The authors acknowledge the support of the U.S. Department of Energy and Sandia National Laboratories for this work. Chris Mahoney assisted Powers in data acquisition and management. Craig Cranston (U.S. Bureau of Land Management, Carlsbad, New Mexico) facilitated access to stratigraphic records from potash drill holes and discussed the geology of the upper Salado. Helpful comments and reviews were provided by Mary Alena Martell, Mario Chavez, and Frank Hansen.

## REFERENCES CITED

Beauheim, R. L.; and Holt, R. M., 1990, Hydrogeology of the WIPP site, *in* Powers, D. W.; Holt, R. M.; Beauheim, R. L.; and Rempe, N. (eds.), Geological and hydrological studies of evaporites in the northern Delaware Basin for the Waste Isolation Pilot Plant (WIPP): Geological Society of America (Dallas Geological Society) Guidebook 14, p. 45–78.

Beauheim, R. L.; and Ruskauff, G. J., 1998, Analysis of hydraulic tests of the Culebra and Megenta Dolomites and Dewey Lake Redbeds conducted at the Waste Isolation Pilot Plant site: SAND98-0049, Sandia National Laboratories, Albuquerque, New Mexico.

Borns, D. J.; Barrows, L. J.; Powers, D. W.; and Snyder, R. P., 1983, Deformation of evaporites near the Waste Isolation Pilot Plant (WIPP) site: SAND82-1069, Sandia National Laboratories, Albuquerque, New Mexico.

Holt, R. M., 1997, Conceptual model for transport processes in the Culebra Dolomite Member, Rustler Formation, SAND97-0194: Sandia National Laboratories, Albuquerque, New Mexico.

Holt, R. M.; and Powers, D. W., 1984, Geotechnical activities in the waste handling shaft, Waste Isolation Pilot Plant (WIPP) project, southeastern New Mexico: WTSD-TME 038, U.S. Department of Energy, Carlsbad, New Mexico.

_____1986, Geotechnical activities in the exhaust shaft, Waste Isolation Pilot Plant: DOE-WIPP 86-008, U.S. Department of Energy, Carlsbad, New Mexico.

_____1988, Facies variability and post-depositional alteration within the Rustler Formation in the vicinity of the Waste Isolation Pilot Plant, southeastern New Mexico: WIPP-DOE-88-004, U.S. Department of Energy, Carlsbad, New Mexico.

_____1990, Geologic mapping of the air intake shaft at the Waste Isolation Pilot Plant: DOE/WIPP 90-051, U.S. Department of Energy, Carlsbad, New Mexico, 50 p., plus figures and appendixes.

_____2002, Impact of salt dissolution on the transmissivity of the Culebra Dolomite Member of the Rustler Formation, Delaware Basin, southeastern New Mexico [abstract]: Geological Society of America Abstracts with Programs, v. 34, no. 6, p. 215.

Lee, W. T., 1925, Erosion by solution and fill, *in* Contributions to geography in the United States: U.S. Geological Survey Bulletin 760-C, p. 107–121.

Maley, V. C.; and Huffington, R. M., 1953, Cenozoic fill and evaporite solution in Delaware Basin, Texas and New Mexico: Geological Society of America Bulletin, v. 64, p. 539–546.

Mercer, J. W., 1983, Geohydrology of the proposed Waste Isolation Pilot Plant site, Los Medaños area, southeastern New Mexico: U.S. Geological Survey Water-Resources Investigations Report 83-4016, 183 p.

Mercer, J. W.; Cole, D. L.; and Holt, R. M., 1998, Basic data report for drillholes on the H-019 hydropad (Waste Isolation Pilot Plant—WIPP): SAND98-0071, Sandia National Laboratories, Albuquerque, New Mexico.

Powers, D. W.; and Holt, R. M., 1993, The upper Cenozoic Gatuña Formation of southeastern New Mexico, *in* Hawley, J. W., and others (eds.), Geology of the Carlsbad Region, New Mexico and West Texas: 44th NMGS Fall Field Conference Guidebook, New Mexico Geological Society, Socorro, New Mexico, p. 271–282.

_____1995, Regional processes affecting Rustler hydrogeology: Prepared for Westinghouse Electric Corporation, Carlsbad, New Mexico.

_____1999, The Los Medaños Member of the Permian Rustler Formation: New Mexico Geology, v. 21, no. 4, p. 97–103.

_____2000, The salt that wasn't there: mudflat facies equivalents to halite of the Permian Rustler Formation, southeastern New Mexico: Journal of Sedimentary Research, v. 70, p. 29–36.

Rosholt, J. N.; and McKinney, C. R., 1980, Part II—Uranium trend dating of surficial deposits and gypsum spring deposit near WIPP site, New Mexico: U.S. Geological Survey Open-File Report 80-879, p. 7–20.

Weart, W. D.; Rempe, N. T.; and Powers, D. W., 1998, The Waste Isolation Pilot Plant: Geotimes, v. 43, no. 10, p. 14–19.

# Jal Sinkhole in Southeastern New Mexico: Evaporite Dissolution, Drill Holes, and the Potential for Sinkhole Development

***Dennis W. Powers***
Consulting Geologist
Anthony, Texas

**ABSTRACT.**—Sinkholes have developed rapidly where drill holes that penetrate shallow evaporites and beds with unsaturated (with respect to halite) water are uncased or inadequately cased and cemented. The recent (1998) Jal sinkhole (also known as the Whitten Ranch sinkhole) developed over deeper evaporites. In this area, modest casing requirements through the evaporites, and waterflooding operations with out-of-formation waters, may increase the possibilities of more such events.

The Jal sinkhole developed with little warning late in 1998. The uppermost halite, in the Permian Rustler Formation, is >1,500 ft below ground surface; the top of the Permian Salado Formation is ~2,000 ft deep. Although a natural origin cannot be ruled out, it is more likely that a nearby plugged and abandoned (P&A) water well to the Permian Capitan Reef permitted circulation of fresh water, the solution of overlying evaporites, and upward chimney collapse through the thick red-bed section and the Tertiary Ogallala Formation to the surface.

In part of southeastern New Mexico, surface casing is required to protect part of the red-bed sequence that locally bears ground water. The evaporite section may not be protected by cement in the production string to deeper units. Some areas show strong evidence of out-of-formation (high-pressure) waters from waterflooding operations in evaporite and red-bed sections. Producing wells and wells scheduled to be P&A get checked for evidence of casing integrity. Nevertheless, older wells that have been P&A, and some wells still in production, may be subject to the same process suspected for the Jal sinkhole. Will there be more such sinkholes?

A reasonable survey of conditions of out-of-formation waters, casing and cementing practices, casing integrity, and evaporite depths would be helpful in developing a better idea of the significance of these conditions and in indicating whether additional sinkholes are likely to develop. No doubt, liability concerns will make such a survey difficult.

## GENERAL BACKGROUND

The Jal sinkhole (Fig. 1), near Jal, New Mexico, developed sometime between August 31 and September 5, 1998. Although natural causes cannot be ruled out entirely, the most likely origin is through collapse after dissolution of evaporites in a nearby drill hole, the Skelly No. 2 Jal Water System. This is not the first example here or elsewhere of such collapse.

In 1980 the Wink Sink collapsed near Wink, Texas, about 30 mi (50 km) south of the Jal sinkhole. The geologic setting for the Wink Sink is similar to that of the Jal sinkhole. The initial collapse occurred adjacent to a drill hole (No. 10-A Hendrick); as the sinkhole widened, it engulfed the wellhead casing within the sinkhole perimeter. Baumgardner and others (1982) extensively examined the setting and history, concluding that dissolution of salt and upward migration of a cavity through collapse led to the surface sinkhole. The No. 10-A Hendrick drill hole is believed to have played a part in the solution and collapse, although Baumgardner and others (1982) also interpreted natural dissolution of salt in the Permian Salado Formation in the vicinity of the Wink Sink. Johnson (1989, 1993) further analyzed natural dissolution within the Salado in the vicinity, recognizing that some of the dissolution had occurred as early as Salado time. Johnson (1989) and Martinez and others (1998) also suggested that activities associated with drilling and drill holes may have contributed to the collapse. A more recent, second sinkhole in the Wink area (as well as some other collapse features in west Texas) is described elsewhere in this volume (Johnson and others, 2003).

Walters (1976) examined subsidence and collapse features in Kansas related to salt dissolution, and related eight features to dissolution in oil and gas drill holes. Collapse was most spectacular around the No. 11 W. M. Panning well, where a pit about 300 ft in

Powers, D. W., 2003, Jal sinkhole in southeastern New Mexico: evaporite dissolution, drill holes, and the potential for sinkhole development, *in* Johnson, K. S.; and Neal, J. T. (eds.), Evaporite karst and engineering/environmental problems in the United States: Oklahoma Geological Survey Circular 109, p. 219–226.

diameter developed within hours. Walters (1976) noted that these features were rare (with an estimated 80,000 drill holes in Kansas). Walters (1976) also noted that the known features involved old holes drilled before the State required cementing the casing opposite freshwater zones and that the drill holes were used for re-injection of undersaturated (with respect to sodium chloride) oil-field brines.

## JAL SINKHOLE

### Background

The Jal sinkhole is in the NW¼SW¼ sec. 9, T. 24 S., R. 36 E. (lat 32°13′48″N., long 103°16′ 34″W.), about 8 mi (13 km) north-northwest of Jal, New Mexico (Fig. 1).

Local residents Jimmy and Linda O'Rear noticed a small surface opening on August 31, 1998, at the site of the collapse. On the morning of September 5 they discovered the full-sized sinkhole (Fig. 2). In discussing the sinkhole, the O'Rears recalled that their dogs were particularly disturbed on the evening of September 4. In a newspaper interview, Mr. O'Rear also indicated he had seen unusual activity of rattlesnakes in the area. It is not clear whether these observations narrow the time frame for the sinkhole. A seismic network operated in southeastern New Mexico did not record any signal associated with this event (R. Aster, personal communication).

Some media reports of the sinkhole give dimensions of 170 ft (52 m) in diameter and 185 ft (56 m) in depth. I used dimensions provided for a fence placed at a distance around the sinkhole to estimate sinkhole diameter from low-angle aerial photographs that I took on September 15, 1998 (Fig. 3). The diameter appears to be ~75 ft (23 m) across. A similar low-angle aerial photograph (Fig. 4) taken October 23, 2001, shows that the surface diameter is about 50% larger. The approximate surface area in 2001 has been marked in Figure 2 (dashed white line) to show the difference. The collapse area appears to be offset somewhat to the west of the original sinkhole, closer to the No. 2 Jal Water System well.

High-angle aerial photographs I took in September 1998 allow an estimate of the depth (Fig. 5). The sun angle on September 15 is about 35° from vertical in this area around 1 p.m. (MDT) when the photograph was taken. As the shadow just covered the bottom, the depth can be estimated at ~107 ft (33 m). The sinkhole is reasonably cylindrical, permitting an estimate of the volume as ~$4.7 \times 10^5$ ft$^3$ ($1.4 \times 10^4$ m$^3$). By October 2001, debris in the sinkhole from collapse of the sides had filled the sinkhole to a depth estimated to be ~60 ft (18 m).

The sinkhole was not observed as it

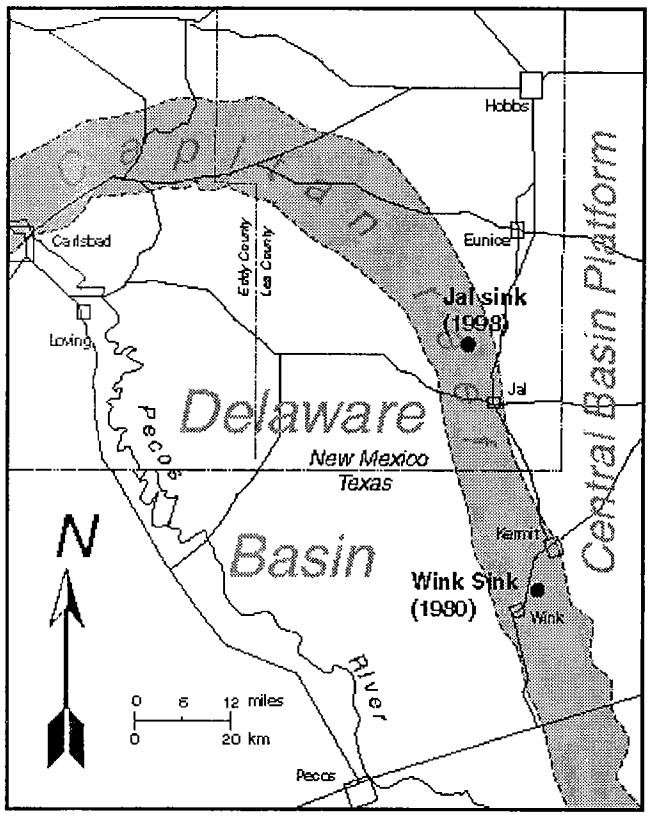


Figure 1. Location map showing the relationship of the Jal sinkhole to the Wink Sink and tectonic elements of the Permian Basin in west Texas and southeastern New Mexico. Modified from Hiss (1975).

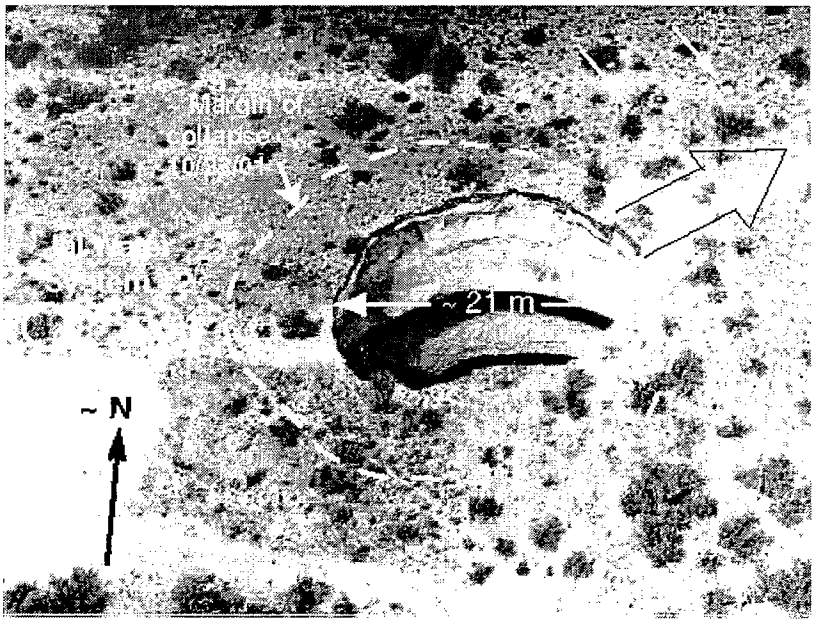


Figure 2. Low-angle aerial photograph of the Jal sinkhole, taken to the north. Small arrows show the location of some larger clasts of Ogallala caliche blown northeast (outline arrow) by the collapsing material. The drill pipe for the No. 2 Jal Water System well is circled. The dashed white line approximates the size and position of the surface collapse in October 2001 (see Fig. 4). Photo taken September 15, 1998, by D. W. Powers.

formed, but circumstantial evidence clearly indicates that at least part of it formed in seconds. Clasts of Ogallala Formation caliche are distributed along a lane northeast from the sinkhole, with some large clasts (about 3 ft [1 m] across) near the sinkhole (Figs. 2, 4) and clast sizes decreasing away from the hole. The aerial photograph also shows a lighter shading from caliche dust coating the surface of the light reddish brown sand. I suggest that the northeastern part of the sinkhole subsided first, whether by seconds or days, and that most or all of the southwestern part of the sinkhole then collapsed. As it collapsed into a void, it initially trapped and compressed air, which then released through a partially choked throat and blew Ogallala clasts from the collapsing mass and possibly from the northeastern lip of the sinkhole. The significance is that at least part of the sinkhole formed very quickly.

The O'Rears believe that there may have been water in the sinkhole on the morning of September 5, based on sounds from rocks tossed into the sinkhole. By the following day, they did not think they were hearing the same response. There was no evidence of water in aerial photographs taken September 15. The depth to Ogallala ground water in a nearby windmill was recently measured at about 189 ft (58 m) below the surface. The depth to Ogallala ground water at the Jal sinkhole would likely be ~175–180 ft (53–55 m), about the same as the greatest early estimate of depth of the Jal sinkhole.

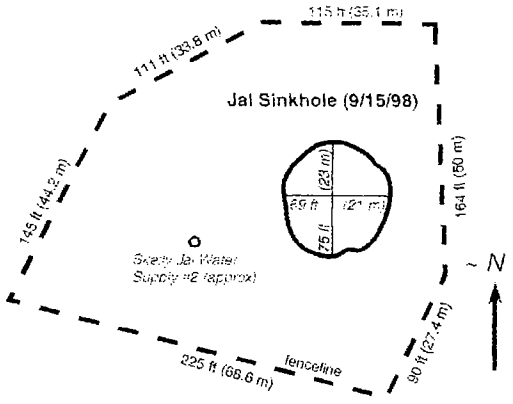


Figure 3. Fence dimensions used to estimate the diameter of the original Jal sinkhole from low-angle aerial photographs. These dimensions are smaller than some other early estimates.

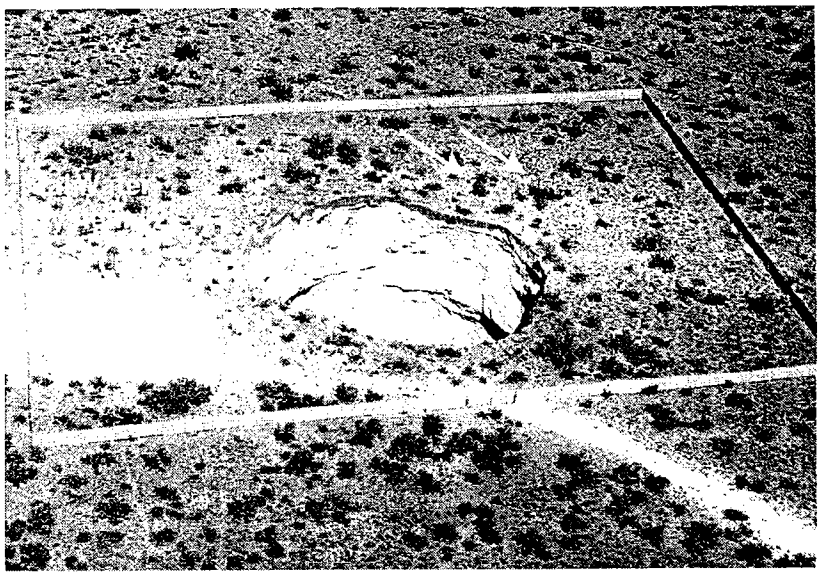

Figure 4. Low-angle aerial photograph of the Jal sinkhole, taken to the north, showing enlargement of the surface sinkhole with time. The approximate size and position are outlined on Figure 2 with a white dashed line. Arrows point to Ogallala caliche clasts, also shown in Figure 2. Photo taken October 23, 2001, by D. W. Powers.

## Geological Setting

The Jal sinkhole is on the Central Basin Platform near its margin with the Delaware Basin to the west. The well-known Capitan Reef of middle Permian age underlies the site; the hole (Skelly No. 2 Jal Water System) adjacent to the Jal sinkhole was drilled to this unit as a source of water in 1967 (Fig. 6). The Albert Gackle (Chambers & Kennedy) No. 1 Whitten well was also drilled in the SW¼ sec. 9, and the stratigraphy is believed to be similar to that at the Jal sinkhole. From drilling reports of the No. 2 Jal Water System and data from the No. 1 Whitten, depths to stratigraphic units at the Jal sinkhole have been estimated: the Capitan is at a depth of 3,600 ft (1,098 m), the Salado from 3,310 to 1,944 ft (1,009–593 m), the Rustler from 1,944 to 1,510 ft (593–460 m), and the Upper Permian Dewey Lake Formation from 1,510 to 910 ft (460–277 m). Triassic rocks of the Dockum Group overlie the Dewey Lake, and the late Tertiary Ogallala Formation is probably ~200 ft (61 m) thick. The casing in the No. 1 Whitten well obscures geophysical logs at a depth of 400 ft, and the exact depth of the Dockum–Ogallala contact is not known.

From analysis of geophysical logs, the middle Rustler (Tamarisk Member) includes the uppermost halite in the area, with a depth of about 1,700 ft (518 m). The lowest halite is at ~3,300 ft (1,006 m), in the basal Salado. Less soluble sulfates extend upward to 1,510 ft (460 m), to the top of the Rustler.

Like the Wink Sink area, both the Capitan and some of the red beds above the Rustler can be sources of relatively low-salinity water.

## Skelly No. 2 Jal Water System Well

This well is 1,980 ft (604 m) from the south line and 660 ft (201 m) from the west line of sec. 9. The well casing was about the diameter of the sinkhole (75 ft [23 m]) west of the margin of the Jal sinkhole when it formed in 1998 (Fig. 2). The

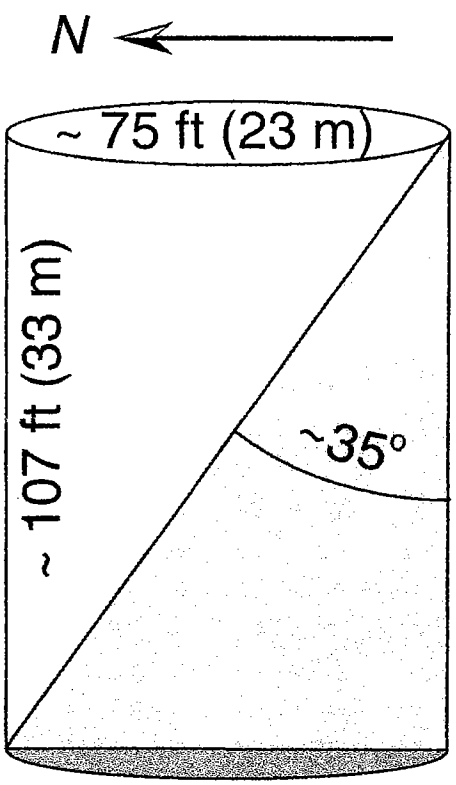


Figure 5. High-angle aerial photograph (Fig. 2) taken about 1 p.m. on September 15, 1998, showed shadow projecting to about the depth of fill on the north side of the Jal sinkhole, as shown in this diagram. Based on the sun angle and estimate of diameter, the depth to fill is estimated at ~107 ft (33 m).

well was spudded October 3, 1967. A string of 13.375-in. (34-cm) casing was set to 353-ft (108-m) depth and cemented, with circulation back to the surface (Fig. 6). The well was then drilled to a depth of 3,890 ft (1,186 m). New casing was set and cemented with 300 sacks of cement; a temperature survey indicated the top of cement at 2,772-ft (845-m) depth. The well was drilled to 4,500 ft (1,372 m) and left as an open hole from 3,890 ft (1,186 m) to total depth.

In 1979, work in the No. 2 well showed that the casing had collapsed at 1,642 ft (501 m). The P&A worksheet shows a cement plug from 1,550 to 1,418 ft (473–432 m), two perforations at 1,250 ft (381 m) with cement displaced below a packer at 1,140 ft (348 m), two perforations at 400 ft (122 m) with cement from 414 to 72 ft (126–22 m), and a surface plug from 0 to 10 ft (0–3 m).

From the original drilling, I estimate that ~300 ft (91 m) of the upper Salado remained open behind the casing, as did all of the Rustler and most of the Triassic clastics. After P&A work, the plugs in the casing are from about the top of the Rustler and above. The lower perforated and cemented zone is at about the middle of the Dewey Lake. The upper perforated zone is estimated to be in the upper Dockum. The plugs apparently do nothing to prevent circulation through the production casing into the Rustler, and possibly Salado, through the collapsed casing.

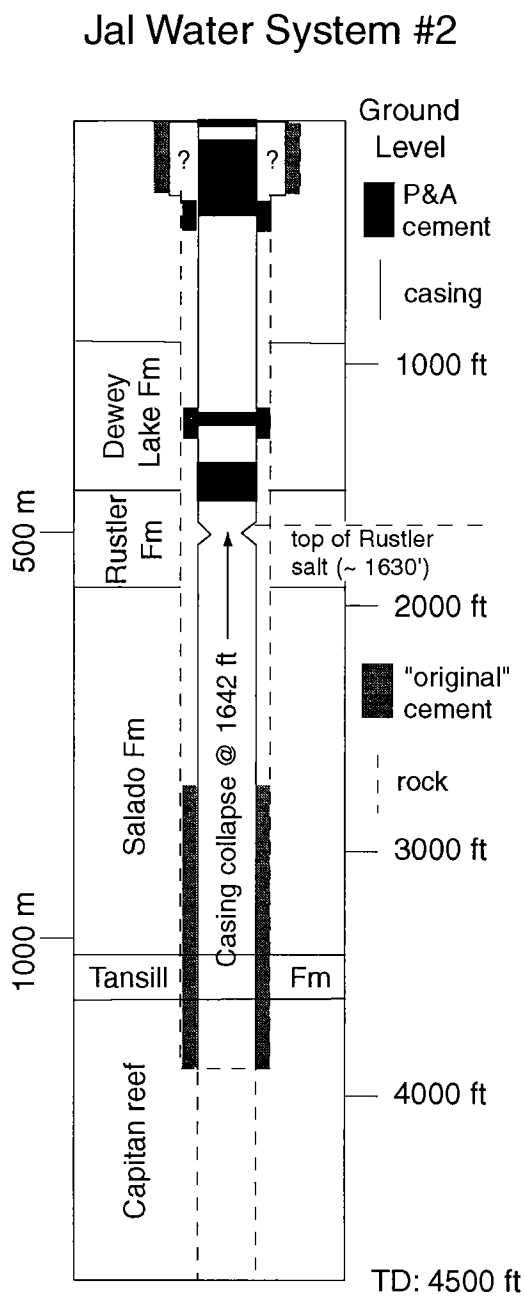


Figure 6. General stratigraphy and casing and cementing record for the Skelly No. 2 Jal Water System well, drilled adjacent to the Jal sinkhole.

### Hydrological Setting Around the Jal Sinkhole

At this time, I do not have enough local data to compare various sources of water in the vicinity of the Jal sinkhole. The water level of the Ogallala in a ranch well northwest of the Jal sinkhole was reported as 195 ft (59 m) (Nicholson and Clebsch, 1961) and as 189 ft (58 m) recently. Triassic units in the general area contain ground water, but they are not close enough to indicate comparable potentiometric surfaces. Water levels and salinities for the Capitan are still to be determined.

It is likely that the situation at the Jal sinkhole is

generally similar to that at the Wink Sink (Baumgardner and others, 1982). There, the potentiometric surface for the upper water-bearing units is higher than for the Capitan, indicating downward flow between connected units.

## BRECCIA PIPES AS POSSIBLE NATURAL ANALOGS

Baumgardner and others (1982) reviewed some of the natural analogs of collapse in evaporite settings where features formed similar to the Wink Sink. Over the Capitan Reef at the northern edge of the Delaware Basin, columnar collapse structures (breccia pipes) formed naturally that are at least 0.5 Ma (Snyder and Gard, 1982). At the surface, they are ~800–1,000 ft (244–305 m) across (Fig. 7), similar to the Wink Sink, but about an order of magnitude larger than the Jal sinkhole. One of these structures was encountered in a potash mine, showing that the breccia column is very close to vertical and maintains a similar size with depth. Drilling demonstrated that the "roots" must be at least as deep as the Capitan Reef. Surface domal structure contrasts with downturned strata adjacent to the collapse at depth. Regional dissolution of salt, probably at the top of the Salado, created the surface dome by lowering the area around the pipe. Tilted pedogenic nodules of the Mescalero caliche show that this structure was created after the caliche, which is ~0.5 Ma (Bachman, 1980). Gravity surveys showed little change in density, whereas electrical surveys showed a lower resistivity across the structure (see Powers, 1996, for a review of the program to investigate these features).

Snyder and Gard (1982) concluded that breccia pipes in the northern Delaware Basin developed by collapse within the Capitan Reef, followed by collapse to the surface. Based on Bachman's (1980) premise, the hydrological system of the Capitan changed when the Pecos River eroded to the reef near Carlsbad, New Mexico, and pressure was decreased. Bachman also inferred that collapse was before ~0.5 Ma.

Large features in the area include the San Simon Swale and the smaller San Simon Sink. The swale and sink are located over and adjacent to the Capitan to the northwest of the Jal sinkhole. The swale and sink are both much larger than the breccia pipes.

Near the Jal sinkhole, high-altitude aerial photographs (Fig. 8) do show circular features somewhat smaller (generally <300 ft in diameter) than known breccia pipes. Many of these features lie along lineations that trend about northwest–southeast. Bachman (1973) suggested that these features, which are observable over a much greater area, are aligned because they represent areas between long, linear dunes that are now gone or redeposited. Bachman believed that they represent areas where infiltrating water was concentrated between the dunes, which partially dissolved the near-surface Ogallala caliche. Based on soil surveys of Lea County, New Mexico, there is no evidence that these features are currently geologically active, though they do collect runoff. They are spread beyond the areal extent of the Capitan Reef, so they are not likely related to the deep-seated breccia pipes of the northern end of the Delaware Basin.

## WATERFLOODING AS A SOURCE OF DISSOLVING FLUIDS

There are large waterflooding operations in Lea County, New Mexico, for secondary recovery, espe-

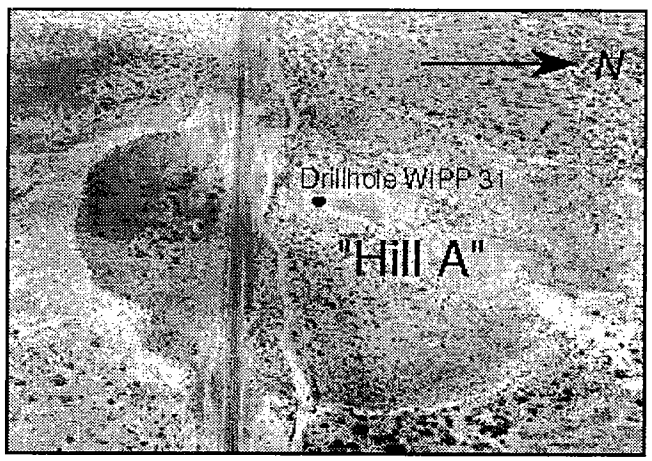


Figure 7. High-angle aerial photograph of the surface-collapsed dome structure of "Hill A," one of the breccia pipes over the Capitan Reef in the northern end of the Delaware Basin. Bachman (1980) and Snyder and Gard (1982) showed the relationship with the Capitan and showed that the doming was caused by lowering of the surrounding area by dissolution of upper Salado salt after collapse. Photo taken September 15, 1998, by D. W. Powers.

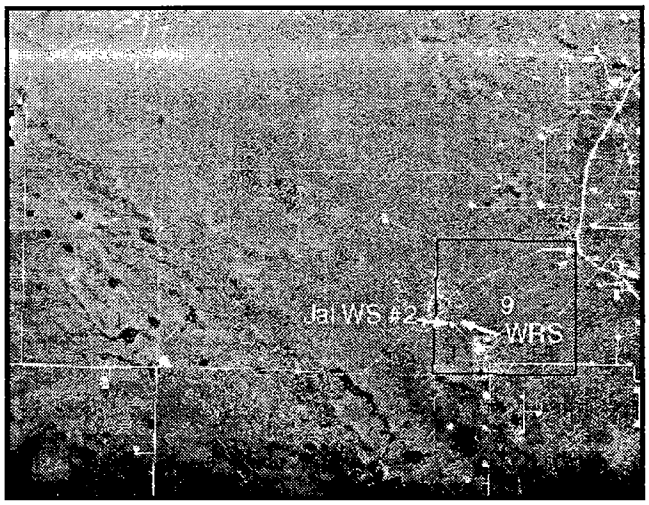


Figure 8. High-altitude aerial photograph of area around the Jal sinkhole prior to collapse. Outlined area is a square that is 1 mi (1.62 km) on a side. Note small, round, dark areas on the west (left) side of the photo along linear trends. Bachman (1973) attributed such features to caliche dissolution between paleodunes. Photo by National Aerial Photography Program, November 1977.

cially from the Permian Yates Formation. These operations are not implicated in the formation of the Jal sinkhole, but it seems clear that some injected waters have not been contained in the target formation. The New Mexico Oil Conservation Division (NMOCD) District 1 (Hobbs) has compiled some records of water flows in oil and gas holes within the district. Some of these flows are from the evaporites or formations above the red beds.

One example, from T. 23 S., R. 36 E., shows several wells drilled by different operators that had casing problems at depths of ~600–650 ft (183–198 m). In May 2000, Doyle Hartman tested the No. 6 Emery King "NW" well in sec. 1 for casing integrity, and reported holes in the casing between depths of 641 and 653 ft (195–199 m) (Hartman, 2000). After an initial-squeeze cement operation, pressure testing failed, and the casing was cemented again. A pressure test below the squeeze zone was successful. After the drill hole was shut in overnight, it flowed water. Wellhead pressures rose to 47 psi after 130 minutes of shut-in. The casing was squeeze-cemented a third time with different formulations, and the casing pressure tests showed that the shallow-water inflow was shut off.

The Emery King leases show casing problems at, and fluid under pressure from, a zone I interpret as a fine-grained unit ("shale") based on high natural gamma-ray deflections in the geophysical logs. The unit is well above the top of the Dewey Lake, and it should be considered the basal shale of the Triassic Chinle Formation (Dockum Group). Hartman (2000) considers the source of these pressurized waters to be out-of-formation water from a nearby waterflood operation. Earlier studies of water resources for Lea County (Nicholson and Clebsch, 1961) indicate no potential for flow to the surface from these units.

Another example comes from T. 25 S., R. 37 E., where Hartman encountered high-pressure flows from the lower Salado Formation in the No. 2 Bates well. After the flow was encountered, the NMOCD did not allow the well to be shut in because the upper casing string only reached 450 ft in depth and would not prevent the formations above evaporites from being charged with high-pressure saline waters. There is no history of natural high-pressure or high-volume brines from this formation or this setting. The other potential source of high-pressure, high-volume flows are nearby waterflooding operations, and it is clear that some waters are injected at pressures above the normal gradient. It is also noteworthy that the approved casing and cementing program was not considered sufficient to protect shallow units that may contain fresh water.

Other examples from NMOCD records indicate shallow waters in evaporite units and also in some of the overlying clastics. Where the pressures, chemistry, or presence of water is uncharacteristic of the formation, it is reasonable to consider waterfloods as a source. Various reports and documents indicate that regulatory agencies and industry groups recognize out-of-formation waters in the area.

## CASING REQUIREMENTS

NMOCD Rule 107 specifies casing and tubing requirements: "Any well drilled for oil or natural gas shall be equipped with such surface and intermediate casing strings and cement as may be necessary to effectively seal off and isolate all water-, oil-, and gas-bearing strata and other strata encountered in the well down to the casing point." In practice, wells in areas such as around the Jal sinkhole generally have a surface-casing string to a few hundred feet, cemented back to the surface. An intermediate string usually is cemented in the lower part, leaving part of the evaporite sequence, and possibly part of the overlying clastics, with an open annulus.

In the Delaware Basin, for drill holes in the area where potash mines and resources exist (NMOCD District 2), the requirements are more stringent for cementing intermediate strings to protect the evaporites.

## EVAPORITES, CASING REQUIREMENTS, WATERFLOODS, AND OUT-OF-FORMATION WATERS

The Jal sinkhole and the Wink Sink are closely associated with nearby drill holes that have casing problems and likely circulation of water that caused dissolution of evaporites prior to collapse. Although it is not possible to eliminate natural processes in either case, the circumstantial evidence favors the drill holes as the significant causal agent. The shallow water-bearing units and the deeper Capitan are both possible sources of undersaturated water for dissolution of the evaporites.

The annulus behind the casing was uncemented through a section of the evaporites in drill holes near both sinks. This appears to be a common situation for drill holes in the area; it is possible that tens of thousands of such drill holes exist. Although casings may be tested to show integrity, drill holes on the Emery King lease suggest that casings can be attacked from outside more easily when not protected by cement.

Although waterfloods and out-of-formation waters are not implicated in either the Jal sinkhole or the Wink Sink, a growing body of evidence indicates that waterfloods are leading to more occurrences of out-of-formation water. Most of these waters have potential to dissolve evaporites, once they reach such formations. In addition, natural and created oil-field brines have potential to corrode exposed casings and add to dissolution problems.

## THE BOTTOM LINE

The Jal sinkhole and the Wink Sink illustrate how dissolution of evaporites around or in association with drill holes that have casing problems can cause sudden collapse and sinkhole formation. Nevertheless, the potential for further collapse is unassessed; various

factors that may contribute to this potential have not been examined in detail.

It seems likely that a high proportion of drill holes in Lea County, for example, have an open annulus through significant parts of the evaporite section and through some of the overlying clastics. One line of investigation would be to assess the numbers and distribution of these drill holes. A pilot phase on a small scale (townships selected to represent certain kinds of problems, for example) would be helpful.

Another line of investigation would be to assess casing problems. A pilot phase in which areas are selected to show relationships in, near, and away from waterfloods might be appropriate.

It also would be appropriate to thoroughly review the history and effects of at least one older and one recent waterflood operation in association with a review of out-of-formation waters and the investigations of casing problems. Industry and regulators have cooperated in some previous studies, and these more limited ventures offer some basis for more thorough assessment.

The second Wink Sink (Johnson and others, 2003, this volume), which formed during May 2002, suggests that more such events are likely and that a more precise strategy for assessing the probability and patterns would be helpful.

Much of the area in New Mexico and west Texas where such events might occur is lightly populated. Nevertheless, drill holes are so numerous that many are near or in populated areas. As the casings in drill holes age, it seems that the likelihood of such events would increase. The drill hole adjacent to the Jal sinkhole was about 32 years old when the collapse occurred. The Hendrick well was 52 years old when the Wink Sink collapsed.

Although it may be appropriate to change the requirements for casing and cementing drill holes in the area discussed, this would not address the issue of existing drill holes completed according to current regulations.

For a useful evaluation, regulators and industry will need to have confidence in the group or agency conducting the study and be willing to cooperate. There is little reason for either to support such a study as long as there is perceived (or real) liability. Public records can provide considerable information for preliminary phases or possibly a pilot study, but useful conclusions may be beyond such a study without having more detailed data, which would be available largely through industry. Here we have the elements that make progress difficult: an industry operating under regulation, an unanticipated problem of undetermined significance, and unresolved liability concerns. Although a start can be made on assessing the significance of collapse around drill holes with existing information, some creative solution to the liability concern seems required before a thorough assessment can be made.

## ACKNOWLEDGMENTS

I thank Jimmy and Linda O'Rear for information and a tour, and Don Whitten for permission to inspect the Jal sinkhole. Dave ("Delaware Basin") Hughes and colleagues at the Waste Isolation Pilot Plant (WIPP) helped with background information. Personnel at the NMOCD District 1 Office (Hobbs) maintain invaluable records for the industry. Various industry oil and gas operators have provided useful information. Mary-Alena Martell and Marty Mitchell reviewed the revised manuscript for this volume.

Initial studies of the Jal sinkhole were supported by the Westinghouse Geotechnical Engineering group of WIPP. This particular article and all work on it have not been funded by any agency or company, and the conclusions reached are mine alone.

## REFERENCES CITED

Bachman, G. O., 1973, Surficial features and late Cenozoic history in southeastern New Mexico: U.S. Geological Survey Report USGS-4339-8, Denver, Colorado.

_____1980, Regional geology and Cenozoic history of Pecos region, southeastern New Mexico: U.S. Geological Survey Open-File Report 80-1099, Denver, Colorado.

Baumgardner, R. W., Jr.; Hoadley, A. D.; and Goldstein, A. G., 1982, Formation of the Wink Sink, a salt dissolution and collapse feature, Winkler County, Texas: Texas Bureau of Economic Geology Report of Investigations 114, Austin, 38 p.

Hartman, D., 2000, First notice and documentation of out-of-zone waterflood injection into fresh water strata in the vicinity of section 1, T-23S, R-36E, N.M.P.M.: Letter to L. Wrotenbery, New Mexico Oil Conservation Division, dated June 15.

Hiss, W. L., 1975, Thickness of the Permian Guadalupian Capitan aquifer, southeast New Mexico and West Texas: New Mexico Bureau of Mines and Mineral Resources Resource Map 5, Socorro, New Mexico.

Johnson, K. S., 1989, Development of the Wink Sink in West Texas, U.S.A., due to salt dissolution and collapse: Environmental Geology and Water Science, v. 14, p. 81–92.

_____1993, Dissolution of Permian Salado salt during Salado time in the Wink area, Winkler County, Texas, *in* Love, D. W., and others (eds.), Carlsbad Region, New Mexico and West Texas: New Mexico Geological Society 44th Annual Field Conference Guidebook, p. 211–218.

Johnson, K. S.; Collins, E. W.; and Seni, S., 2003, Sinkholes and land subsidence due to salt dissolution near Wink, west Texas, and other sites in west Texas and New Mexico, *in* Johnson, K. S.; and Neal, J. T. (eds.), Evaporite karst and engineering/environmental problems in the United States: Oklahoma Geological Survey Circular 109 [this volume], p. 183–195.

Martinez, J. D.; Johnson, K. S.; and Neal, J. T., 1988, Sinkholes in evaporite rocks: American Scientist, v. 86, no. 1 (Jan.–Feb.), p. 38–51.

Nicholson, A., Jr.; and Clebsch, A., Jr., 1961, Geology and ground-water conditions in southern Lea County, New Mexico: [New Mexico] State Bureau of Mines and Mineral Resources Ground-Water Report 6, Socorro, New Mexico, 123 p.

Powers, D. W., 1996, Tracing early breccia pipe studies, Waste Isolation Pilot Plant, southeastern New Mexico: a study of the documentation available and decision-

making during the early years of WIPP: Sandia National Laboratories Report SAND 94-0991, Albuquerque, New Mexico, 54 p. plus appendix.

_____2000, Evaporites, casing requirements, water-floods, and out-of-formation waters: potential for sinkhole developments: Technical Class, Solution Mining Research Institute, San Antonio, Texas, 11 p.

Snyder, R. P.; and Gard, L. M., Jr., 1982, Evaluation of breccia pipes in southeastern New Mexico and their relation to the Waste Isolation Pilot Plant (WIPP) site, with a section on drill-stem tests, WIPP 31, by J. W. Mercer: U.S. Geological Survey Open-File Report 82-968, Denver, Colorado, 73 p.

Walters, R. F., 1976, Land subsidence in central Kansas related to salt dissolution: Solution Mining Research Institute, Flossmoor, Illinois, 144 p.

# Evaporite Karst and Regional Ground-Water Circulation in the Lower Pecos Valley of Southeastern New Mexico

***Lewis A. Land***
New Mexico Bureau of Geology and Mineral Resources
New Mexico Institute of Mining and Technology
National Cave and Karst Research Institute
Carlsbad, New Mexico

**ABSTRACT.**—Natural ground-water discharge occurs from a series of cenotes, or sinkhole lakes, along the east side of the Pecos River flood plain at Bottomless Lakes State Park, southeastern New Mexico. The lakes are fed by underwater springs issuing from the underlying Permian San Andres artesian aquifer, which has caused subsurface dissolution and collapse of overlying gypsum and mudstones of the Permian Artesia Group. Lea Lake, the largest of the cenotes, has undergone an increase in spring discharge in recent years, reflecting the combined effects of rising water levels in the artesian aquifer and enhanced spring flow from mass-wasting processes along the steep eastern margin of the lake.

## INTRODUCTION

Sinkholes ranging from a few meters to ~100 m in diameter are common features of the lower Pecos River Valley and reflect the intimate relationship between karstification and ground-water circulation in the Roswell Artesian Basin. Many of the karst features along the lower Pecos are formed in interbedded gypsum and mudstone of the Permian Artesia Group and result from subsurface dissolution of gypsum units by upward leakage of ground water from the underlying Permian San Andres artesian aquifer (Martinez and others, 1998).

Bottomless Lakes State Park, 16 km east of Roswell in Chaves County (Fig. 1), is the site of several of the more spectacular gypsum sinkholes that are found in southeastern New Mexico. The Bottomless Lakes are unusual in that they occur in a semiarid setting, where annual evaporation rates exceed mean annual precipitation by a factor of 7 or more (Caran, 1988). The lakes are fed almost entirely by underwater springs and represent the discharge end of the regional hydrologic system in the Roswell Artesian Basin. Situated along the eastern edge of the Pecos River flood plain, the lakes also illustrate the fundamental role that karst processes have played in shaping the course of the Pecos River.

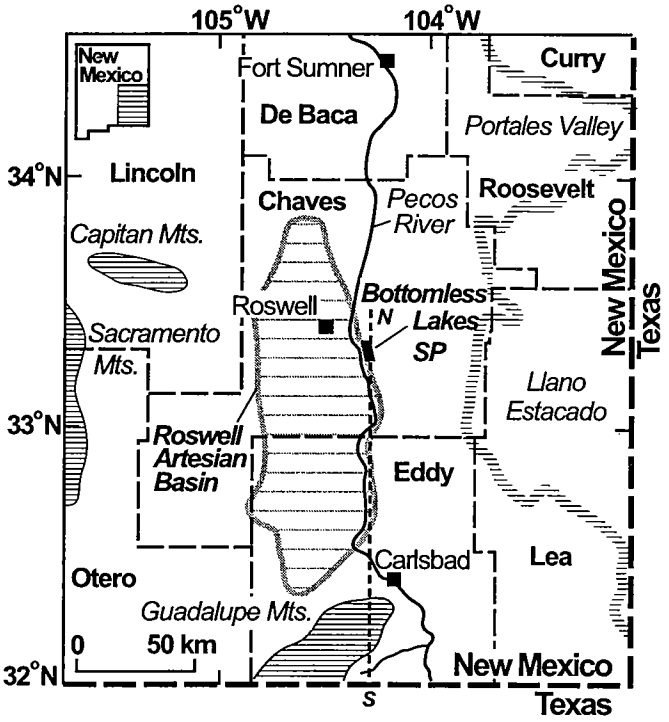


Figure 1. Regional map of southeastern New Mexico, showing lower Pecos River and approximate extent of Roswell Artesian Basin. Dashed line shows line of section in Figure 2.

## GEOLOGIC BACKGROUND

During late Miocene time, an ancestral lower Pecos Valley formed by solution-subsidence processes in carbonate and evaporite rocks of the Permian (Guadalupian) San Andres Formation and Artesia Group. At this time the upper Pecos River was a separate drainage system flowing southeast and east through the Portales Valley in central Roosevelt County (Fig. 1) (Bachman, 1987).

During the Pleistocene, the lower Pecos Valley extended farther to the north by continued karstification and headward erosion, progressively pirating streams

Land, L. A., 2003, Evaporite karst and regional ground-water circulation in the lower Pecos Valley of southeastern New Mexico, *in* Johnson, K. S.; and Neal, J. T. (eds.), Evaporite karst and engineering/environmental problems in the United States: Oklahoma Geological Survey Circular 109, p. 227–232.

flowing eastward from the Sacramento Mountains, and culminating in capture of the upper Pecos River near Fort Sumner, at which time the modern drainage system was established (Reeves, 1972).

The Pecos River originally flowed west of Roswell, but the channel has migrated eastward because of uplift of the Sacramento Mountains and downtilting of Permian strata to the east (McLemore, 1999). Bedrock along most of the lower Pecos River north of Carlsbad consists of limestones, dolomites, evaporites, and red beds of the Artesia Group, the back-reef equivalent of the Capitan Reef limestone that is exposed along the east flank of the Guadalupe Mountains to the south (Fig. 2) (Kelley, 1971). In the Carlsbad area the back-reef facies consists predominantly of carbonates, but in the area extending ~150 km north of the reef the section becomes increasingly evaporitic, and beyond that the rest of the shelf area consists of siliciclastics. In the vicinity of Roswell, the Artesia Group is made up of interbedded mudstone and gypsum at the surface, with thick, bedded salt and anhydrite in the subsurface. The presence of these highly soluble evaporitic rocks of the far back-reef facies has contributed to the formation of sinkholes and caves, which are abundant along the course of the lower Pecos River and adjacent areas. In addition, much of the topography along the valley margins has been influenced by local and regional subsidence from subsurface dissolution of evaporites (Bachman, 1984, 1987).

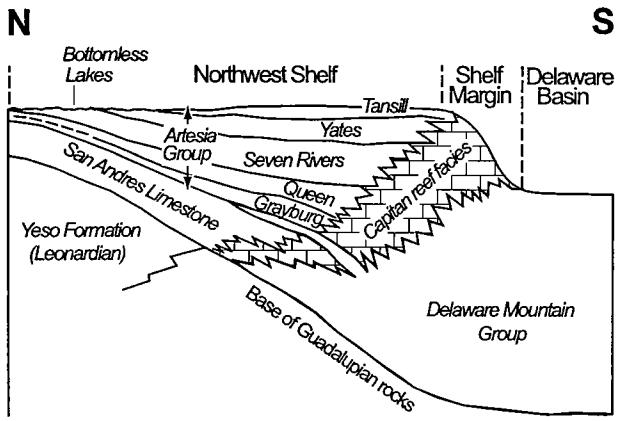


Figure 2. North–south diagrammatic stratigraphic section, showing facies relationships of Guadalupian rocks in southeastern New Mexico. Line of section shown in Figure 1.

## Regional Hydrology

The Roswell Artesian Basin (Fig. 1) consists of an eastward-dipping carbonate aquifer overlain by a leaky confining unit, which is in turn overlain by an unconfined alluvial aquifer (Fig. 3). The alluvial aquifer is hydraulically connected to the Pecos River. The carbonate aquifer is artesian to the east but is under water-table conditions in the western outcrop area. Ground water is stored in the carbonate aquifer in multiple highly porous and transmissive zones within the San Andres and Grayburg Formations. Secondary porosity in the artesian aquifer is represented by vuggy and cavernous limestones, solution breccias, and solution-enlarged fractures and bedding planes. Much of the porosity was formed by dissolution of evaporites within the San Andres Formation, probably in late Permian time when the formation was exposed to erosion prior to deposition of the Grayburg, and then subsequently extended by continued circulation of ground water (Welder, 1983).

The San Andres Limestone thickens downdip and is ~350 m thick in the subsurface east of the Pecos River. However, 120–185 m of evaporites has been removed from the upper part of the section by subsurface dissolution in the northwestern Artesian Basin, leaving an extensive solution breccia (Bachman, 1987). The San Andres aquifer is 80–140 m thick in the vicinity of the Pecos River. Although much of this dissolution probably occurred during the Permian, the resulting stratigraphic thinning seems to have influ-

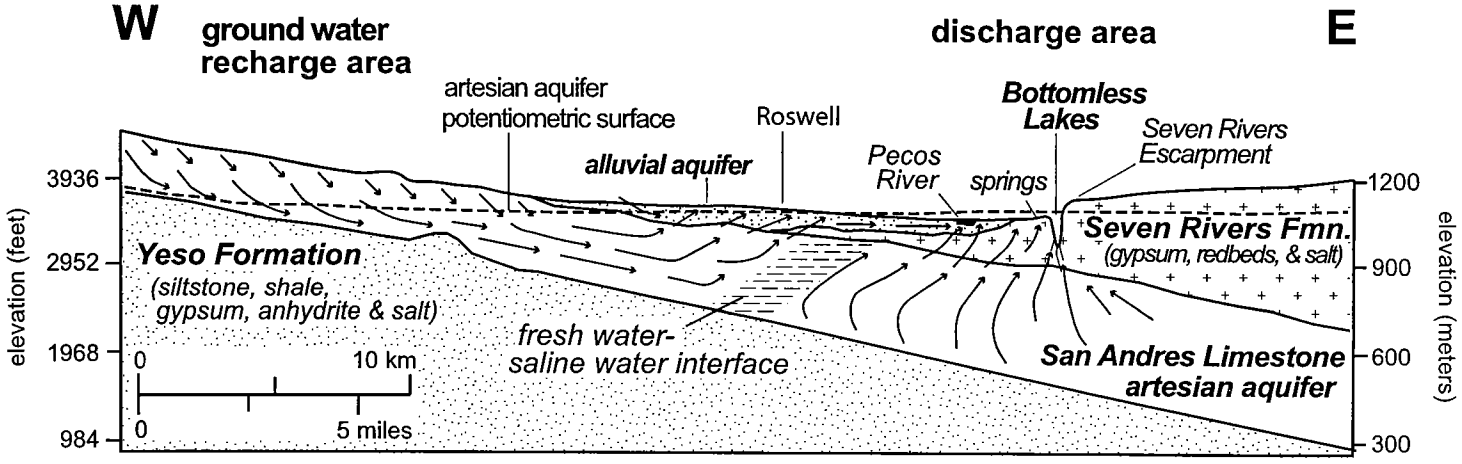


Figure 3. West–east cross section illustrating regional ground-water-flow patterns within the San Andres artesian aquifer. Arrows indicate general direction of ground-water flow. Modified from J. F. Quinlan (unpublished report, 1967).

enced the position of the present channel of the Pecos. In some cases, thinning and subsidence of the formation from gypsum dissolution has occurred gradually over many square kilometers, but there are also recent instances of sudden catastrophic collapse (Welder, 1983; Caran, 1988).

The confining unit consists of slightly to moderately permeable rocks of the upper Grayburg, Queen, and Seven Rivers Formations of the Artesia Group. The thickness of the confining unit varies from 0 to ~300 m, with thickening regionally downdip to the east. To the west the confining beds are truncated by erosion (Fig. 3). Local variations in thickness are caused by erosion and by dissolution of gypsum in the upper part of the section (Welder, 1983).

Recharge to the artesian aquifer occurs by direct infiltration from precipitation and by runoff from intermittent losing streams that flow eastward across the San Andres outcrop on the east slope of the Sacramento Mountains. Ground water flows east and south, downdip from the outcrop, then upward through leaky confining beds into the shallow aquifer, and ultimately to the Pecos River (Fig. 3). Since the inception of irrigated agriculture in the Roswell Artesian Basin more than a century ago, most of the discharge from both the artesian and alluvial aquifers has been from wells. Some natural discharge into the Pecos River still occurs by seepage from the alluvial aquifer and from the artesian aquifer through fractures and solution channels in the overlying confining beds (Welder, 1983).

In the early history of development of the artesian aquifer, many wells flowed to the surface, with yields as high as 21,500 liters/minute (~5,700 gpm). However, decades of intensive pumping have caused significant declines in hydrostatic head. By 1975 there were more than 800 irrigation wells in the Roswell Artesian Basin, and water levels in the artesian aquifer had declined in some areas by as much as 70 m. Nevertheless, it is not uncommon for some wells near the river to still exhibit artesian flow, particularly during the winter months when irrigation has decreased (Welder, 1983).

The salinity of ground water in the artesian aquifer is highly variable. Chloride concentrations range from 15 ppm in the unconfined, western part of the aquifer to 7,000 ppm in the confined, eastern part of the system, and they also increase with depth. Chloride content is lowest in the spring, and highest in the fall after the irrigation season is over. The largest annual fluctuations in mineral content occur in the area between Roswell and the Pecos River, where salt-water encroachment from the east is occurring (Welder, 1983).

## OBSERVATIONS

### Bottomless Lakes

The sinkholes at Bottomless Lakes State Park are formed in gypsum and mudstone of the Seven Rivers Formation (Artesia Group), part of the confining unit of the underlying San Andres artesian aquifer (Fig. 3). Eight sinkhole lakes lie within the park boundaries (Figs. 4, 5), but additional lakes and dry sinks are found in a similar geologic setting both north and south of the park (McLemore, 1999). The Bottomless Lakes occur along the east side of the Pecos River flood plain, adjacent to an abandoned former channel of the Pecos River that now flows ~2 km west of the park (Fig. 4). The lakes are joint-aligned and are formed within and at the base of the Seven Rivers Escarpment, which defines the eastern margin of the river

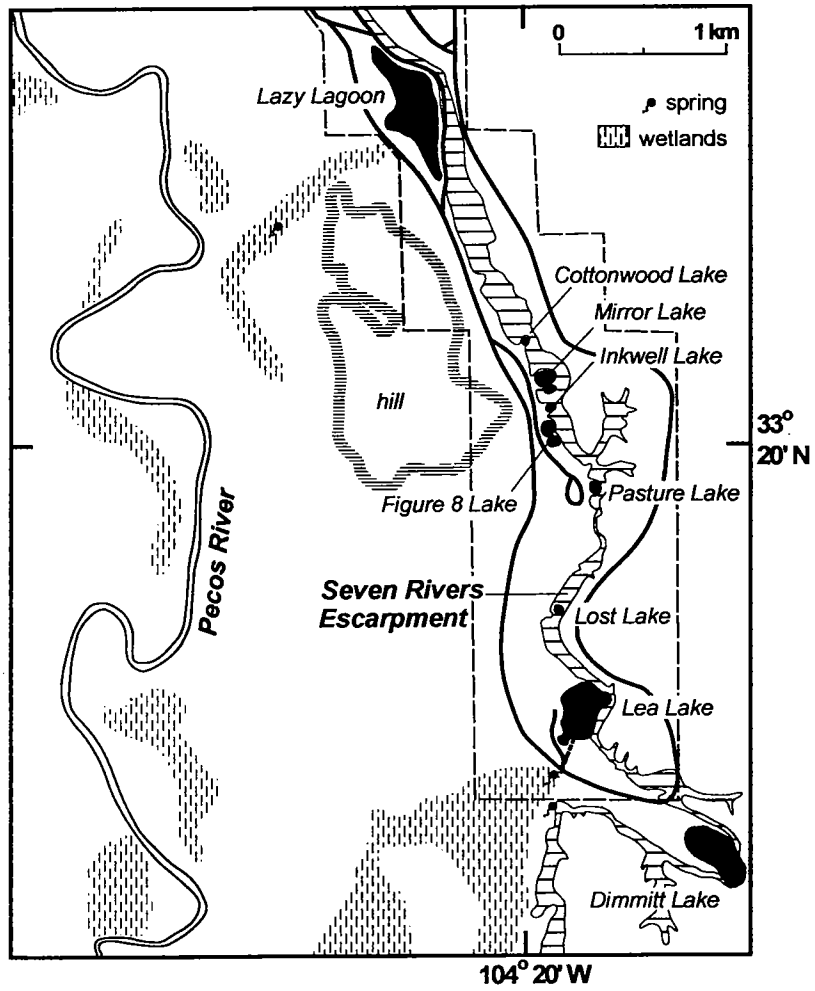


Figure 4. Map of Bottomless Lakes State Park, showing the Bottomless Lakes cenotes (in solid black) relative to the Seven Rivers Escarpment and the flood plain of the Pecos River. Park boundaries are shown by a light dashed line. The drainage canal issuing from Lea Lake is shown by a heavy dashed line.

valley. The gentle (~1°) eastward regional dip of the area is locally reversed along the escarpment, where strata in the Seven Rivers Formation dip steeply and abruptly to the southwest by as much as 40° (J. F. Quinlan, unpublished report, 1967). This local dip reversal was probably caused by subsurface dissolution of gypsum in the vicinity of the sinkholes and consequent slumping of overlying beds (Kottlowski, 1979).

The Bottomless Lakes sinkholes are more properly described as cenotes, similar to the deep, steep-walled, flooded sinks found on the Yucatan Peninsula in Mexico (Caran, 1988). Most of the Bottomless Lakes cenotes are circular, with steep to vertical walls, and are 50–100 m in diameter and 30–60 m deep (J. F. Quinlan, unpublished report, 1967). Several of the lakes are compound, consisting of multiple coalesced sinks. Lazy Lagoon, the northernmost of the lakes and the largest in areal extent, is actually three separate cenotes that occupy an abandoned channel of the Pecos River. Much of the lake is very shallow and dries up during the summer, with the exception of the three deep sinks. Lea Lake, the southernmost and largest of the cenotes within the park, is formed by the coalescence of three sinks (Fig. 5) and has a maximum water depth of 27 m (Navarre, 1959). All of the lakes are fed by discharge from underwater springs issuing from the underlying artesian aquifer. Discharge from the springs has caused subsurface dissolution of gypsum and halite within the Seven Rivers Formation, localized subsidence, and upward propagation of collapse chimneys, which ultimately formed the cenotes.

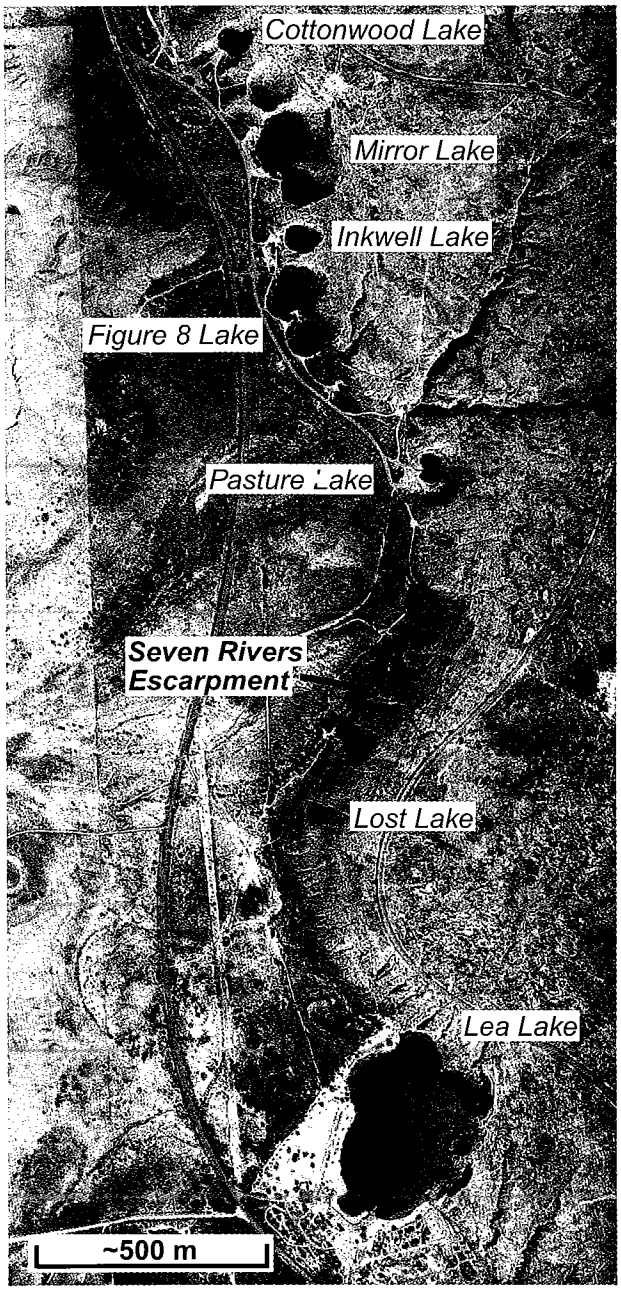


Figure 5. Orthophoto image of the Bottomless Lakes cenotes, the Seven Rivers Escarpment, and the adjacent flood plain of the Pecos River. Note the compound morphology of Lea Lake.

Water in all the lakes is brackish to saline, with high sulfate concentrations (Table 1), owing to passage of the discharging water through subsurface layers of gypsum and halite (Martinez and others, 1998). Water quality in the lakes is also affected by the original mineral content of ground water in the artesian aquifer, which is saline in the vicinity of the Bottomless Lakes. Total dissolved solids (TDS) in the lakes have progressively increased since 1927, when they were first measured. This increase in TDS may be related to westward migration of the fresh-water–salt-water interface in the underlying artesian aquifer (Welder, 1983; J. F. Quinlan, unpublished report, 1967).

Although the Bottomless Lakes sinks probably formed during the Pleistocene, catastrophic solution-collapse processes are still active along this part of the lower Pecos. For example, in 1998 a new sinkhole lake appeared ~32 km northeast of Roswell, on the west side of the Pecos River flood plain, in gypsum and red beds of the Artesia Group. The sinkhole is 35 m in diameter and 47 m deep, with a water depth of 27 m, similar in scale to the Bottomless Lakes cenotes.

### *Local Hydrology*

The mean annual evaporation deficit in the Roswell area is 2–2.5 m/year (i.e., evaporation exceeds precipitation), yet lake levels usually fluctuate by less than a meter, indicating that water levels in the Bottomless Lakes cenotes are not directly related to precipitation events (C. B. Hunt, unpublished report, 1976). Lake levels may differ from one another by as much as 11 m, but they roughly correspond to the irregular potentiometric surface of the artesian aquifer (Fig. 3). Only Dimmitt and Pasture Lakes have anomalously high lake levels because they also receive runoff from surface streams (J. F. Quinlan, unpublished report, 1967).

In the early 20th century, several of the lakes overflowed into wetlands along the east bank of the Pecos

**Table 1. — Maximum Water Depth, Areal Extent, and Selected Water-Quality Data for the Bottomless Lakes Cenotes**

| | Lazy Lagoon | Cottonwood Lake | Mirror Lake | Inkwell Lake | Figure 8 Lake | Pasture Lake | Lost Lake | Lea Lake |
|---|---|---|---|---|---|---|---|---|
| Max. water depth (m) | 27.4 | 9.1 | 15.2 | 9.8 | 11.3 | 5.5 | — | 27.4 |
| Areal extent (acres, $m^2$) | 26.1 acres (10,565 $m^2$) | 0.52 acre (2,105 $m^2$) | 3.44 acres (13,925 $m^2$) | 0.36 acre (1,457 $m^2$) | 2.22 acres (8,987 $m^2$) | 0.76 acre (3,076 $m^2$) | <1.0 acre (4,048 $m^2$) | 13.46 acres (54,486 $m^2$) |
| TDS (ppm) | 38,200 | 6,000 | 29,500 | — | — | — | — | 9,500 |
| Chloride (ppm) | 15,599 | 2,156 | 12,869 | — | — | — | — | 3,758 |
| Sulfate (ppm) | 8,934 | 2,139 | 5,860 | — | — | — | — | 2,113 |
| Total hardness (ppm) | — | 3,115 | 6,308 | — | — | — | — | 2,618 |
| pH | 7.9 | 7.2 | 8.3 | — | — | — | — | 7.6 |

Sources: Water depth and lake area are from McLemore (1999). Water-quality data for Lazy Lagoon, Mirror Lake, and Lea Lake are from Blinn (1993). Water-quality data for Cottonwood Lake, and total hardness data for all the lakes, are from an unpublished data sheet from the files of Bottomless Lakes State Park (1992). Dashes indicate no available data.

River, but the progressive decline in hydraulic head in the artesian aquifer caused lake levels to fall, so that now only Lea Lake overflows. A comparison of water levels in the artesian aquifer with discharge from Lea Lake over a 3-year period (Fig. 6) demonstrates the relationship of the Bottomless Lakes cenotes to ground-water circulation within the Roswell Artesian Basin. Seasonal variations in hydraulic head in the artesian aquifer reflect the irrigation cycle in the basin. Water levels are lowest in the summer when the aquifer is heavily pumped for irrigation, and they rise significantly in winter months when irrigation has decreased. Discharge from Lea Lake closely mimics the seasonal water-level cycle in the artesian aquifer. Longer term variations in artesian head are also shown by a gradual rise in water levels within the aquifer over the past 20 years, in part because of a systematic program by the State of New Mexico to purchase and retire irrigated farm land in the Roswell Artesian Basin. This long-term rise in water levels is also reflected by a gradual increase in discharge from Lea Lake (Fig. 7).

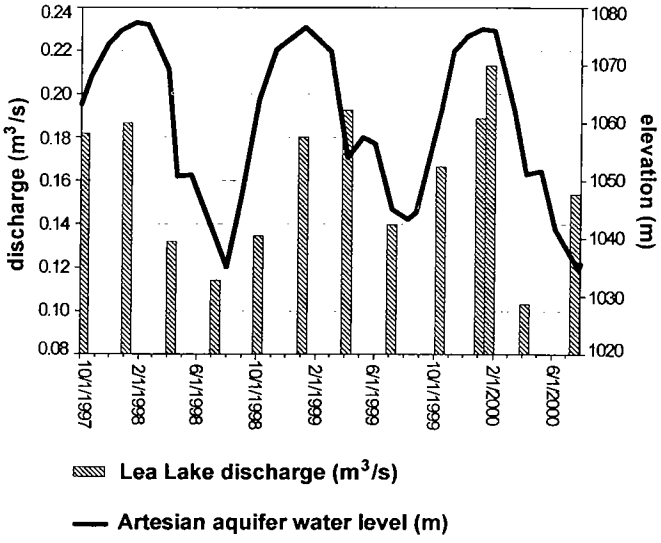


Figure 6. Discharge from Lea Lake and water levels in the San Andres artesian aquifer for water years 1998–2000. Water-level data for the artesian aquifer were measured in the U.S. Geological Survey Orchard Park monitoring well ~10 km southwest of Lea Lake at lat 33°15.417′N., long 104°24.867′W.

### *Effect of Mass Wasting*

Within the Bottomless Lakes cenotes, spring sapping at the base of the Seven Rivers Escarpment has resulted in localized oversteepening of the eastern walls of the sinks, causing occasional landslides and rockfalls. On May 30, 1975, a catastrophic rock slide occurred on the steep east wall of Lea Lake, and the resulting lake surge caused significant damage to a pavilion on the opposite shore. No measurements of lake discharge are available prior to 1976. However, the rock slide apparently opened new spring sources in the lake bed, as indicated by a significant increase in flow from the lake and flooding of adjacent grazing lands with several million gallons per day of saline and alkaline water (Brown, 1978). A culvert was installed to convey the increased flow to a wetland area west of the park, but the lake continued to flood an adjacent parking lot and campground during the winter. In January 2002, the Park Service completed con-

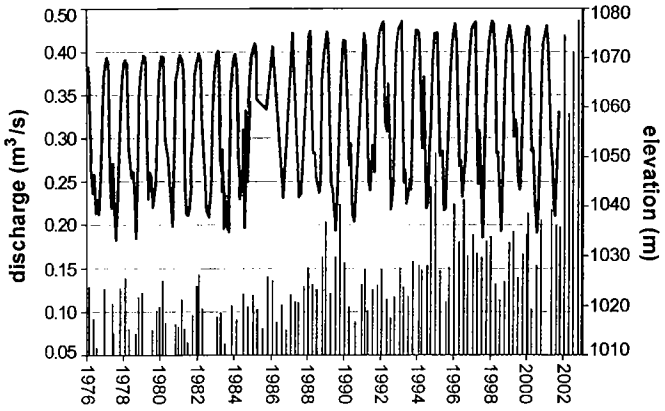


Figure 7. Lea Lake discharge (bar graph) and artesian-aquifer water levels (line graph), 1976–2002. The abrupt increase in discharge from Lea Lake in 2002 is due to completion of a drainage canal in January of that year. Prior to installation of the drainage canal, much of the lake discharge overflowed across a paved parking lot and thus was not measured.

struction of a more efficient drainage canal to capture all of the discharge, resulting in a substantial increase in measured flow volume from the lake (Fig. 7). On January 13, 2003, a discharge of 0.53 $m^3/s$ (18.8 cfs, or 8,460 gpm) was measured at the Lea Lake drain, the highest value since the U.S. Geological Survey began collecting data in 1976.

Because of the increase in flow from Lea Lake, the wetlands area to the west has expanded and is now hydraulically connected to the Pecos River, discharging into the river at five separate places along its east bank. The overflow wetland serves as a localized recharge area for the shallow alluvial aquifer, which also ultimately discharges into the river (M. McGee, 2003, written communication).

## DISCUSSION

The increase in discharge from Lea Lake appears to have resulted from a long-term rise in artesian head in the aquifer that feeds the lake, combined with enhanced spring flow caused by catastrophic solution-collapse processes along the steep eastern wall of the cenote. Diversion of the overflow to a wetland area west of the park has resulted in the growth of new wetlands and a net gain in water flow to the Pecos River, an interesting phenomenon in a semiarid region that is currently experiencing an extended drought. The broader implications of this local increase in water supply relate to the interstate use of surface-water resources in the lower Pecos Valley. New Mexico shares the water in the Pecos River with its downstream neighbor, the State of Texas, and is obligated by interstate compact to deliver a specific volume of water to Texas every year. The increase in flow from Lea Lake, amounting to roughly 8.5 million $m^3$/year (~7,000 acre-ft/year), will ultimately be used by the State of New Mexico to help meet its compact obligation.

## CONCLUSIONS

Although the Bottomless Lakes cenotes formed prior to the historic era in New Mexico, recent mass-wasting events indicate that catastrophic solution collapse is still active in this region and that karst phenomena are an integral part of the hydrologic system in the Roswell Artesian Basin. The cenotes at Bottomless Lakes State Park demonstrate the dynamic interaction of regional ground-water circulation, surface-water flow, and modern and ancient karst processes, and their relationship to the hydrostratigraphic framework of the lower Pecos Valley.

## ACKNOWLEDGMENTS

This paper benefited from critical reviews by Virginia McLemore and Peggy Johnson, New Mexico Bureau of Geology and Mineral Resources, and by Michael McGee, U.S. Bureau of Land Management. Steve Patterson, Superintendent at Bottomless Lakes State Park, generously provided access to park files and reports. The author wishes to acknowledge the work of the late James F. Quinlan, who very precisely summarized the geology and hydrology of Bottomless Lakes in the text and graphics of an unpublished Christmas card he circulated among friends in 1967.

## REFERENCES CITED

Bachman, G. O., 1984, Regional geology of Ochoan evaporites, northern part of Delaware Basin: New Mexico Bureau of Mines and Mineral Resources Circular 184, 22 p.

_____1987, Karst in evaporites in southeastern New Mexico: Sandia National Laboratories, Contractor Report SAND86-7078, 82 p.

Blinn, D. W., 1993, Diatom community structure along physicochemical gradients in saline lakes: Ecology, v. 74, p. 1246–1263.

Brown, J., 1978, Bottomless Lakes, report on alternative solutions [unpublished]: Kruger Lake Hutchinson Brown Inc., 20 p.

Caran, S., 1988, Bottomless Lakes, New Mexico—a model for the origin and development of ground water lakes [abstract]: Geological Society of America Abstracts with Programs, v. 20, no. 2, p. 93.

Kelley, V. C., 1971, Geology of the Pecos Country, southeastern New Mexico: New Mexico Bureau of Mines and Mineral Resources Memoir 24, 78 p.

Kottlowski, F. E., 1979, Bottomless Lakes: New Mexico Geology, v. 1, p. 57–58.

Martinez, J. D.; Johnson, K. S.; and Neal, J. T., 1998, Sinkholes in evaporite rocks: American Scientist, v. 86, p. 38–51.

McLemore, V. T., 1999, Bottomless Lakes: New Mexico Geology, v. 21, p. 51–55.

Navarre, R. J., 1959, Basic survey of the Bottomless Lakes: Fisheries Investigations of District no. 4, Job Completion Report, New Mexico Dept. of Game and Fish, 42 p.

Reeves, C. C., Jr., 1972, Tertiary–Quaternary stratigraphy and geomorphology of west Texas and southeastern New Mexico, *in* Kelley, V. C.; and Trauger, F. D. (eds.), Guidebook of east-central New Mexico: New Mexico Geological Society Guidebook 23, p. 108–117.

Welder, G. E., 1983, Geohydrologic framework of the Roswell ground-water basin, Chaves and Eddy Counties, New Mexico: New Mexico State Engineer Technical Report 42, 28 p.

# Field Survey of Evaporite Karst along New Mexico Highway 128 Realignment Routes

***Dennis W. Powers***
Consulting Geologist
Anthony, Texas

***David Owsley***
Larkin Group NM, Inc.
Albuquerque, New Mexico

**ABSTRACT.**—The phase 2 realignment study of alternate routes for State Highway 128 in Eddy County, New Mexico, considered the local effects of karst as well as other processes. Within parts of secs. 3–6 and 10, T. 22 S., R. 30 E., karst and related surficial features include caves, alluvial sinkholes, alluvial dolines, collapse valleys, springs, and lineaments. Cave features and alluvial sinkholes show that karst processes are active, and springs may be indicating some of the hydrological conditions within the karst system. Many of the alluvial dolines have relatively stable surfaces, based on soils and vegetation, indicating that internal drainage and sediment transport are relatively restricted and unable to cope with available sediments. Collapse valleys are interpreted as a consequence of coalescing sinkholes or dolines along relatively linear trends. Caves and alluvial sinkholes occur within collapse valleys, indicating that the karst system is still active within the valleys. Surface linear trends can be interpreted along these collapse valleys as well as between other features, such as alluvial dolines. Although not proven, we suggest that these lineaments are related to both bedding surfaces within the Permian Rustler Formation and fracturing trends created by subsidence after dissolution of salt from the upper Salado Formation.

Alluvial sinkholes appear to form in alluvial dolines where drainage concentrates runoff. As a consequence, some areas just north of the present right-of-way, particularly in sec. 4, should probably be avoided for highway construction. In addition, drainage from alluvial dolines and collapse valleys crossed by a new grade should be maintained or enhanced, whereas drainage into these same locations should be minimized or avoided. This should help avoid developing new alluvial sinkholes under a new grade.

## INTRODUCTION

The western end of State Highway 128 (NM 128) in southeastern New Mexico has been studied for possible realignment to avoid or lessen maintenance problems mainly from brine lakes along the current route (Fig. 1). Evaporite karst presents one possible construction and maintenance issue along alternate routes. Although Nash Draw (Fig. 1) is known as a locality where sinkholes and collapse features have formed (e.g., Bachman, 1981), areas along the current and proposed alternate rights-of-way weren't surveyed in any detail to identify specific features. For this study, a preliminary surface geological survey was conducted in 1999 along the more likely areas to identify specific features, assess the current level of karst activity, and suggest mitigating efforts. There have been no field geotechnical studies for the realignment since phase 2 was completed (1999).

For this geological survey, resources included reports on Nash Draw, standard topographic maps, contact prints from aerial photographs of October 1976, and printed images from digital records of aerial photographs taken in 1999. In the field, features were lo-

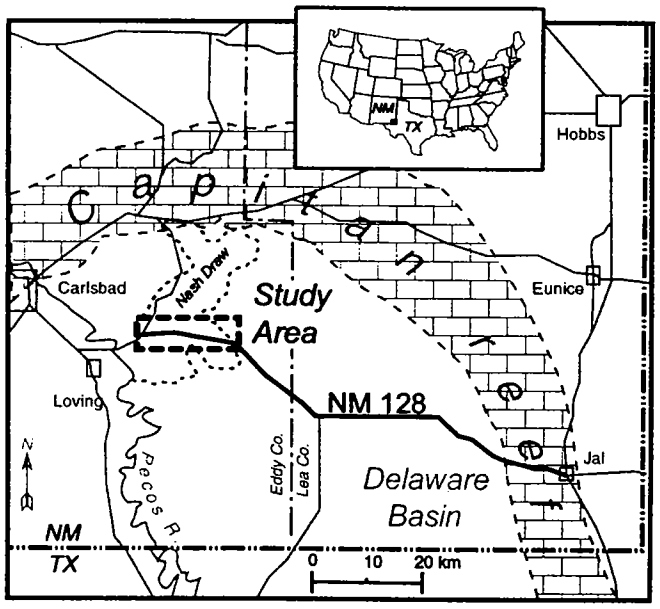


Figure 1. General location map of study area for realignment of western end of State Highway 128 (NM 128) in southeastern New Mexico.

Powers, D. W.; and Owsley, David, 2003, Field survey of evaporite karst along New Mexico Highway 128 realignment routes, *in* Johnson, K. S.; and Neal, J. T. (eds.), Evaporite karst and engineering/environmental problems in the United States: Oklahoma Geological Survey Circular 109, p. 233–240.

cated mainly through using the photographs; Dave Belski used his personal Global Positioning System (GPS) equipment for some of the field survey, which was quite helpful.

Based on previous field experience, most of the observable evaporite karst features of significance were expected to be east of Laguna Cuatro along outcrops and subcrops of the sulfate beds of the Tamarisk Member of the Permian Rustler Formation (Fig. 2). While the gypsites of the Tamarisk Flats area should also be susceptible to karst formation, surface features do not appear to have developed to the same degree. Trenching for the El Paso Energy pipeline across the Tamarisk Flats (Fig. 3) did not show significant features (Powers and others, 1997). Most of the field survey was conducted east of Laguna Cuatro and included areas both north and south of the present NM 128 right-of-way.

Field time focused on forming an overall impression of evaporite karst in this area and was limited. A detailed survey will no doubt yield additional features through this area, and this study by no means covers the extent of karst in Nash Draw. Nevertheless, it is possible to propose a course of action for geotechnical field activities to help in the final decision about the location and design of the realignment.

## BACKGROUND ON NASH DRAW EVAPORITE KARST

In 1925, Willis T. Lee examined this area as part of his broader studies of karst and caves in the region around Carlsbad Caverns. Sinkholes and small caves in central and northern Nash Draw (Fig. 1) were identified by Lee (1925), and he proposed a general theory of solution and fill to account for the development of the draw. Drilling in the late 1920s revealed potash minerals just north of Nash Draw, and further drilling resulted in development of the first potash mine in the early 1930s. Though this drilling focused on Nash Draw and the immediate surroundings, very shallow geology was not well studied. Robinson and Lang (1938) mapped some of the springs and the shallow hydrology, indicating that salt was being removed from the evaporites and that the overlying ground was subsiding in response. Vine (1963) also pieced together more of the geology and concluded that dissolution had affected the outcropping formations sufficiently so that it was difficult to make sense of the stratigraphic sequence. Vine also noted sinkholes in the central part of Nash Draw.

The most comprehensive theories of solution and fill or evaporite karst were developed by George Bachman (1974, 1976, 1980, 1981, 1985) for much of this area. Bachman (1981) mapped the Nash Draw area in more detail, identifying numerous areas of sinkholes or collapsed sinks. He also proposed (Bachman, 1980) that alluvial dolines observed just east of Livingston Ridge (well north of the NM 128 right-of-way) provided local catchment and feeders to

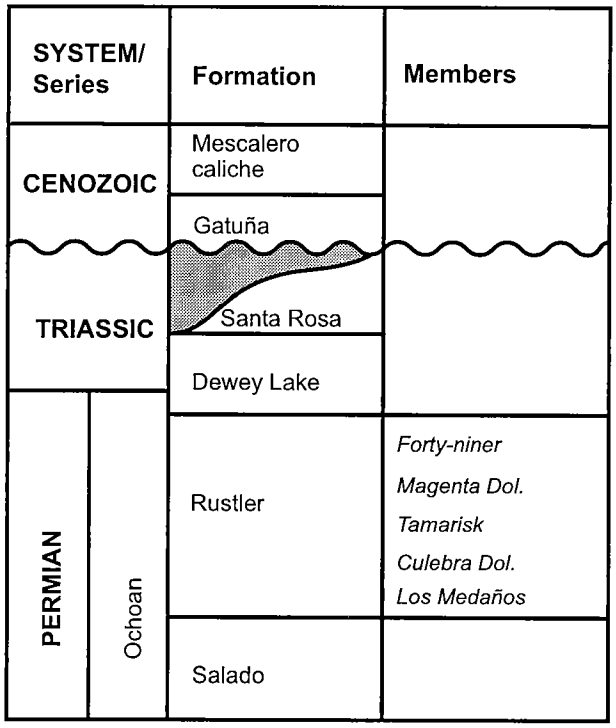


Figure 2. Simplified stratigraphic chart of the study area. Surficial deposits, including gypsite, dunes, and soils, are not shown.

Nash Draw at one time and developed local spring deposits on the eastern side slopes of Nash Draw. Bachman (1981) shows a few sinkholes in the general vicinity of proposed realignment routes for NM 128, but his studies were more general.

## SPECIFIC SURVEY FEATURES

Based on analysis of photos, topographic maps, and field surveys, features are grouped into six more-general categories that have utility for the realignment study:

1. Caves, which include a variety of shapes and sizes, but all are developed in gypsum rock or well-lithified gypsite.
2. Alluvial sinkholes, in which soft or unlithified alluvium has collapsed and should indicate a cave opening for drainage below the sinkhole.
3. Alluvial dolines, which are shallow depressions with alluvial fill in the depression. Cave or alluvial sinkholes may or may not be observable in an alluvial doline.
4. Collapse valleys or swales, postulated to develop as a series of dolines or caves connect and an area collapses after dissolution.
5. Springs, which feed some of the local lakes and may be fed by karst recharge.
6. Lineaments, which show apparent trends to a variety of features.

The first three features are individual and more objectively identified. The collapse valleys or swales

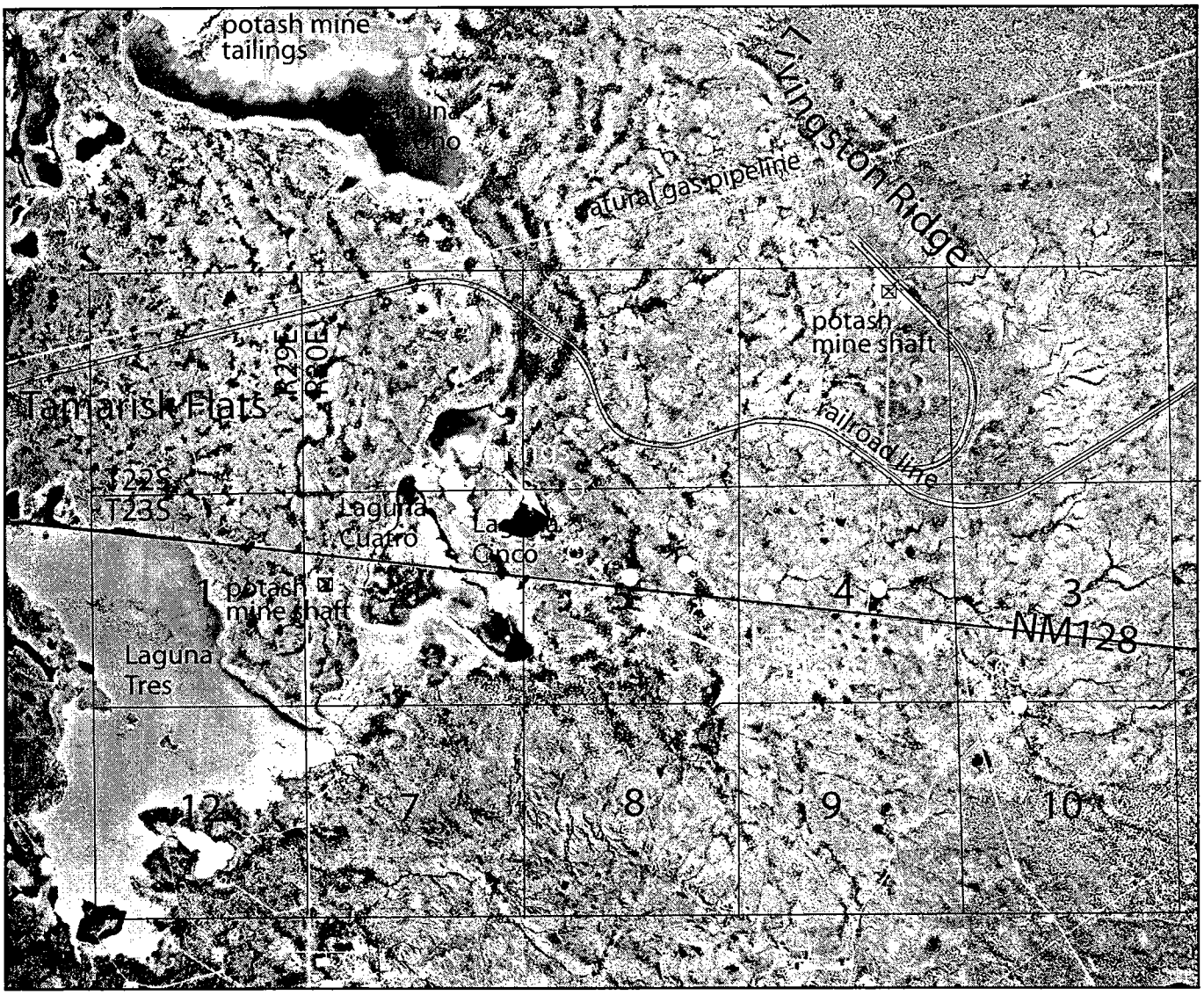


Figure 3. Aerial-photograph underlay of part of the study area, with NM 128, potash mines, brine lakes, and some township, range, and section lines. Open white circles show general locations of caves described in the text. Solid white circles show the general locations of sinkholes in alluvium or alluvial dolines. Small, round, dark areas in the photo commonly indicate alluvial dolines. Karst valleys probably developed from coalescing subsidence, and they may follow stratigraphic boundaries of gypsum beds in the Tamarisk and Forty-niner Members of the Rustler Formation. More linear trends are observable in this aerial photograph; no lines have been drawn that would obscure the features. The aerial-photograph source of the underlay is image NAPP 9611-51, dated 10/22/1996, from the EROS Data Center, Sioux Falls, South Dakota.

are identifiable as features, but their origin is more speculative in some cases. Although the springs are clearly identifiable, their relationship to karst is possible but speculative. Lineaments are yet more subjective groupings of features.

## Caves

At least five larger caves are within ~300 m of the existing or proposed rights-of-way that may be large enough to be entered (open white circles in Fig. 3). Around some of these caves are smaller drop holes or subsidiary entrances that are not separated for discussion.

*Los Medaños caves* (Zone 13: UTM ~606000 mE, 3577250 mN) are in a large area of caves and alluvial sinkholes developed in outcrops or over subcrops of the upper sulfate bed of the Tamarisk Member. This area is in the SW¼ sec. 3, T. 23 S., R. 30 E., just southeast of the intersection of NM 128 with Mobley Ranch Road (Fig. 3). The area is southwest of a vegetative-study plot adjacent to NM 128.

*Thornbush cave* (new name) is near the northern boundary of the NW¼ sec. 5, T. 23 S., R. 30 E. (UTM 602942 mE, 3578571 mN) (Fig. 3). A secondary cave is present near Thornbush cave. Thornbush cave (Fig. 4) is developed in surficial gypsite that likely overlies the upper sulfate bed of the Tamarisk Member.

*Saltbush cave* (new name) is near the center of the

NW¼ sec. 5, T. 23 S., R. 30 E. (UTM 602772 mE, 3578111 mN) (Fig. 3). It is in a large, heavily vegetated alluvial doline near the crest of a small hill. This cave entrance is relatively large (Figs. 5, 6), and it is also developed in gypsite. Although the Tamarisk Member likely underlies this site, there are no nearby outcrops to determine possible depth.

*Goldenrod cave* (new name) is in the SE¼ sec. 5, T. 23 S., R. 30 E. (UTM 603827 mE, 3577475 mN) (Fig. 3). The surficial deposits appear to be gypsite, but the Tamarisk sulfate beds must be shallow, as they are exposed at the mouth of nearby Acacia cave. The Goldenrod cave entrance is also relatively large (Fig. 7).

*Acacia cave* (new name) is in the SE¼ sec. 5, T. 23 S., R. 30 E. (UTM 603747 mE, 3577528 mN) (Fig. 3). It has the largest observed entrance (Fig. 8), and some notable rattlesnakes guarding the entrance. Acacia cave has nearby subsidiary unnamed caves, and it is in an area with several alluvial sinkholes in a broad collapse valley or swale.

Figure 4. The entrance to Thornbush cave is developed in surficial gypsite that likely overlies the upper sulfate bed (15+ m thick) of the Tamarisk Member. Dave Belski provides scale.

Figure 5. The entrance to Saltbush cave is in gypsite in a large, heavily vegetated alluvial doline near the crest of a small hill. The drainage into this cave is not very obvious on the surface.

A small, shallow series of caves occurs slightly west of the center of the NE¼ sec. 5, T. 23 S., R. 30 E. (UTM ~603350 mE, ~3578175 mN). These caves developed in gypsite along a north-northwest trend and show no significant drainage into them.

The rocks and lithified gypsite around cave entrances surveyed here commonly display some dip to bedding and fracturing. The dip is often at odds with the regional dip of about 1° to the east, no doubt caused by movement of the rocks after solution of underlying sulfate or Salado Formation halite (Powers and others, 2003). The fracture trends have not been mapped.

Exploration in the area of these caves will surely show additional caves and alluvial sinkholes. In view of the topography and drainage patterns, there should be additional caves to be found south and east of the localities given here. Though these caves and features would be of general interest in understanding the development and status of evaporite karst along the realignment routes, the survey of features was conducted in the more immediate vicinity of the routes.

## Alluvial Sinkholes

The term *sinkhole* generally refers to a small area of collapse at the surface in bedrock and soil. In this area, small cave openings occur in lithified gypsite or gypsum rock. Generally circular and local collapse of unlithified alluvium occurs within a larger alluvial doline. This collapse of alluvium is called here an *alluvial sinkhole*. For the most part, more lithified units that allow drainage are not observed in the bottom of an alluvial sinkhole. It is probable that, if the drainage is adequate, the alluvium is washed out, leaving an observable cave.

Six larger alluvial sinkholes were found in the area of the survey (solid white circles in Fig. 3). Numerous very shallow depressions in alluvial dolines or collapse valleys have been observed, but they were not documented if they appeared not to be active. Significant alluvial sinkholes are located as follows:

1. Near the center of sec. 5, T. 23 S., R. 30 E., at approximate UTM coordinates of 603250 mE, 3577925 mN. This alluvial sinkhole is near the current right-of-way, and it is within a major collapse valley or swale.

2. Near the southern boundary of the NE¼ sec. 5, T. 23 S., R. 30 E., at approximate UTM coordinates of 603625 mE, 3577975 mN. This alluvial sinkhole is developed along the edge of a major collapse valley or swale, and it also would be approximately on line from Thornbush cave through some other unnamed small caves.

3. North of the center of the SE¼ sec. 5, T. 23 S., R. 30 E., at approximate UTM coordinates of 603800 mE,

3577600 mN. There are at least two larger alluvial sinkholes and a number of small depressions. These alluvial sinkholes may have small areas of rock outcrop and may just be covering some cave entrances related to Acacia and Goldenrod caves.

4. Near NM 128 and the western boundary of sec. 4, T. 23 S., R. 30 E., at approximate UTM coordinates 604200 mE, 3577780 mN. This alluvial sinkhole (Fig. 9) developed in a large alluvial doline just up-drainage from a narrow arroyo cut through gypsite and into the top of the upper Tamarisk gypsum bed. Given the porosity observed in the gypsite in the arroyo, it seems likely that part of the drainage into the alluvial sinkhole feeds the arroyo at its head.

5. Slightly southeast of the center of sec. 4, T. 23 S., R. 30 E., and just east of the road to the former Western Ag Minerals surface facilities, at UTM coordinates 605139 mE, 3577814 mN. There are several major alluvial sinkholes here, at the north side of a large alluvial doline.

6. Near the northern edge of sec. 10, T. 23 S., R. 30 E., at UTM coordinates of 606160 mE, 3576964 mN. This alluvial sinkhole shows general evidence of a deep soil profile that likely indicates relatively rapid and uniform accumulation of alluvium before developing the soil profile from the surface down. The A and B horizons appear to be moderately developed (Fig. 10).

Several alluvial sinkholes are near the present right-of-way or preferred alternate routes. They indicate that these areas are still active in draining runoff through karst conduits that are of sufficient size to pass alluvium through without plugging.

### Alluvial Dolines

There are numerous alluvial dolines in the area, and they are commonly visible on the aerial photograph (Fig. 3) as small black dots owing to vegetation. Good examples occur at Saltbush cave in the NW¼ sec. 5, T. 23 S., R. 30 E., and at the alluvial sinkhole near the center of sec. 4, T. 23 S., R. 30 E. These alluvial dolines are relatively shallow depressions with a

Figure 6. Detail of the entrance to Saltbush cave shows debris indicating water inflow, and a packrat nest indicating that flow has not been too recent or deep. Rock hammer for scale.

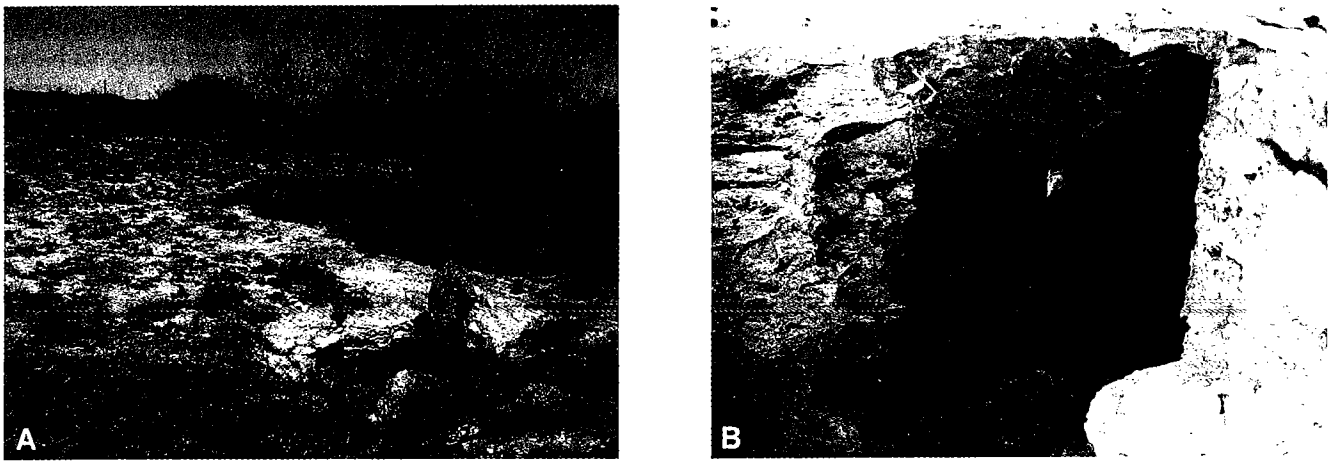


Figure 7. (A) Entrance to Goldenrod cave in gypsite deposits overlying Tamarisk Member gypsum. Goldenrod cave, like Acacia cave (Fig. 8), lies in the eastern of two apparent karst valleys (Fig. 3). Lewis Land provides scale. (B) Close-up of entrance to Goldenrod cave, showing some planar boundaries along fractures believed related to subsidence as Rustler gypsum, and possibly upper Salado halite, was dissolved.

Figure 8. Entrance to Acacia cave in Tamarisk Member gypsum. This cave has the largest entrance observed in the caves along the study area. Several subsidiary caves in the area are likely interconnected. Acacia cave lies in the eastern of two apparent karst valleys trending approximately north–south and crossing the NM 128 right-of-way (Fig. 3).

Figure 9. Large sinkhole developed in an alluvial doline south of Los Medaños caves. This sinkhole appears relatively stable, as grasses have developed, along with a few annuals.

fill of alluvium. There are many small alluvial dolines with no obvious alluvial sinkhole, cave, or other specific drainage points for water coming into the doline. Smaller alluvial dolines (~50–150 m across) tend to have limited arroyos or channels upslope, and they very commonly develop a single channel or arroyo somewhat downslope. Larger alluvial dolines are more likely to show a direct channel draining downslope.

The vegetation in many of the alluvial dolines consists of mesquite, creosote, and gramma grasses or sacaton. Because these species are perennial, these dolines would appear to have rather stable surfaces, not subject to significant sedimentation. It may also be that these dolines receive less inflow. Other alluvial dolines show a variety of annual species, including ragweed or other "weeds" that are characteristic colonizing species. This vegetation may be growing in fresh alluvium or in areas that appear to be subject to more recent flooding. It seems likely that these species indicate relative instability of the surface of the dolines they inhabit.

Alluvial dolines are important recharge points, as is obvious where an observable alluvial sinkhole or cave has developed within a doline. The dolines without specific drainage points are also likely to be important recharge points, but they may also provide some storage, allowing longer periods of steadier recharge to the system. This is speculative without some direct hydrological observations in this area. It may be helpful in some areas, however, to provide surface drainage for alluvial dolines to limit or avoid the possibility of unplugging an alluvial doline to create a large alluvial sinkhole under a right-of-way.

### Collapse Valleys or Swales

Two larger valleys or swales intersect the right-of-way in sec. 5, T. 23 S., R. 30 E. (Fig. 3). They tend to be 100–200 m wide and up to ~1 km long. Vegetation is heavy, consisting of larger mesquite, some creosote, and a variety of grasses. Local areas are covered with annuals, indicating surface instability owing to sedimentation or flooding or both.

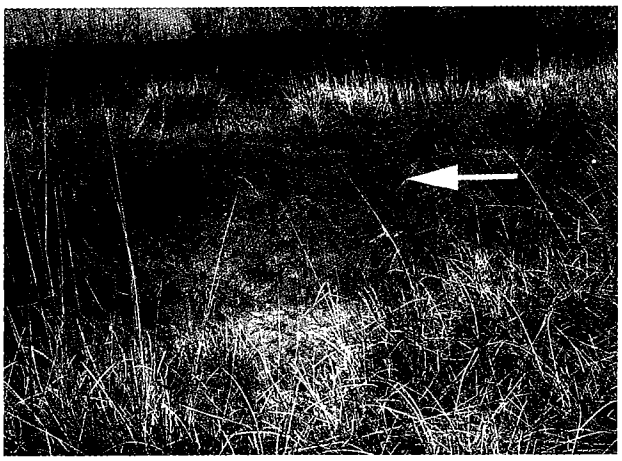

Figure 10. The soil profile developed in the alluvial doline (Fig. 9) is relatively thick for an arid climate, and it indicates a significant period of relative stability. The white arrow indicates the boundary between a grayish, more organic-rich A horizon above and a reddish-brown B horizon below it. Neither soil horizon appears well developed.

These valleys or swales include caves and alluvial sinkholes, showing that evaporite solution has occurred and is occurring. In addition, the outlines of these valleys tend to have small scallops or arcs, indicating that they were alluvial dolines. As a result, it appears most likely that these valleys or swales formed from coalescing alluvial dolines and collapse.

It is possible that Laguna Cuatro represents a larger version of a collapse valley or swale, but there is no direct evidence or obvious features that indicate this origin.

These collapse valleys or swales can't be avoided along the preferred routes for realigning NM 128 through this area. One of the important design and construction efforts should be to provide some reasonable surface drainage through the right-of-way across collapse valleys. Water has covered the highway at these points in the past, and debris caught in fences and vegetation show that surface-water flow has been considerable. There is no obvious means of diverting water that accumulates in the valleys or swales. It is preferable to make sure that the water doesn't accumulate at the right-of-way and possibly redevelop conduits under the right-of-way, causing alluvial sinks.

### Springs

There are several springs around the eastern and northeastern margin of the lake (Laguna Cinco) in the NW¼ sec. 5, T. 23 S., R. 30 E. (Fig. 3). Two smaller springs may be providing flow on the order of 10 liters/minute, while the larger spring on the northeastern edge may be flowing many tens of liters/minute.

This lake appears to be accumulating some subaqueous sulfate minerals but no subaqueous halite. Some of the water must seep from the brines in Laguna Cuatro, but the springs and runoff are probably more important. The water chemistry has not been tested, but it is likely that these springs are fed from karst-recharged zones in the area.

There is no apparent direct effect on the realignment from these springs. They likely indicate that the karst system is active and also that water may be encountered at rather shallow depths in some areas.

### Lineaments

In the area examined for karst features, the alluvial dolines and collapse valleys appear to be arranged along some persistent trends. Much of the drainage that has developed also tends to be linear and commonly about perpendicular to some of the trends of the dolines and collapse valleys.

A recent (1996) National Aerial Photography Program (NAPP) aerial photograph (Fig. 3) of this area illustrates these trends (photo is not marked, to avoid obscuring the trends). Some linear trends along the major collapse valleys trend about north–south. Most of the other linear trends of alluvial dolines and drainage trend between about east–west and about southeast–northwest. As might be expected, caves, alluvial sinkholes, and springs can also be related to these trends, though there are too few of these features mapped to develop the trends on that basis alone.

At this time it is not possible to demonstrate the source of the linear trends in this study area. There are, however, two likely contributors. A study of the underlying Salado thickness in this general area shows that the upper Salado thins rather abruptly owing to dissolution, and the thinning increases from northeast (edge of Nash Draw) to southwest (Powers and Holt, 1995; Powers and others, 2003). Subsidence of the overlying Rustler rocks as dissolution continues is likely to produce some fracturing oriented perpendicular to the thinning trend—i.e., in the range from about east–west to about southeast–northwest. In addition, the bedding within the Rustler tends to crop out along the same trend in part of the area and along a trend more nearly north–south in some parts of the study area. The Rustler is not exposed very well, however, so these general trends can't be related in a straightforward way to the surface lineaments. Although fractures caused by subsidence after dissolution and bedding are the most likely contributors to the lineaments, the relationship should be considered speculative at this time.

## GENERAL CONCLUSIONS REGARDING KARST

Several types of evaporite-karst features have developed mainly in the sulfate beds of the Rustler Formation or in the more recent gypsite that commonly blankets much of the Rustler gypsum outcrop. Caves and alluvial sinkholes clearly demonstrate that the karst is still active, whereas alluvial dolines and collapse valleys indicate that karst processes have continued for much longer, though the length of time is poorly bounded. Although it is likely that the hydrologic system that produces local springs is connected

to the local karst, the springs also indicate that the system has some storage capacity. Most karst conduits drain rapidly.

The principal concern with road construction and maintenance related to karst through this area is to avoid sudden collapse into either an unknown cave or from "unplugging" an alluvial doline to produce an alluvial sink. The potential for collapse is real and can be demonstrated by the past rerouting of the Mobley Ranch road, <0.5 mi south of NM 128, around a collapse in an area with alluvial dolines and caves. Although the date of the collapse is not clear, it occurred after 1976, on the basis of aerial-photo inspection.

In view of the collapse valleys and apparent trends to karst features, it is most likely that existing features and existing trends will be followed as karst continues to develop. Conduits that are already developed will most likely continue to develop over the lifetime of a road. Given that geologically short period of time, a "new" sinkhole or doline is less likely to develop from collapse into a cavernous system; it is more likely that an existing doline or collapse valley will be locally reactivated. Existing trends should be given priority during field investigations for final design.

The significant alluvial sinkholes found during this survey tend to be in alluvial dolines where surface drainage is connected over larger areas and appears to concentrate more runoff. This is most apparent in the drainage north of the current right-of-way through sec. 4, T. 23 S., R. 30 E. It is appropriate to avoid this drainage system, and it is also appropriate to minimize surface inflow to alluvial dolines intersected by the road grade.

## GENERAL DESIGN CONSIDERATIONS

Given the features already found in a basic field survey, it is highly probable that the existing NM 128 road grade was constructed across areas with active cave systems in evaporite rocks. The road grade has not failed because of karst processes. At least one localized collapse in this vicinity, however, caused the Mobley Ranch road to be rerouted in the last 24 years. Geologic inspection of the area suggests that the NM 128 route selection and design consider three recommendations.

The first is that the route through sec. 4 may be better if it stays on or slightly south of the existing road grade. The reason for this is that alluvial sinkholes appear to be developed in alluvial dolines along the drainage not far north of the existing right of way. This drainage apparently collects more water to flood the dolines, which may be the factor that develops the alluvial sinkholes. The sinkhole near the Western Ag Minerals access road is very large and is to be avoided. Some alluvial dolines south of the existing road grade may be aligned with this larger sinkhole and may be part of the same system, but they do not appear to be active at this time.

The second recommendation is to avoid concentrating road runoff and ditch drainage into alluvial dolines under the grade. At the same time, surface drainage out of any alluvial doline crossed by the grade should probably be enhanced or at least not hindered.

Third, grades crossing the larger alluvial valleys, especially in sec. 5, should provide adequate cross-grade drainage to eliminate unnecessary ponding in the low areas and possible activation of alluvial sinkholes. As practical, ditches may need to be designed to divert flow or minimize concentrations of flow into these areas.

## ACKNOWLEDGMENTS

Dave Belski, Mary-Alena Martell, Bruce Baker, and Lewis Land explored some of these areas and features and discussed them. Mary-Alena Martell reviewed the manuscript, and she provided technical comments that improved it.

## REFERENCES CITED

Bachman, G. O., 1974, Geologic processes and Cenozoic history related to salt dissolution in southeastern New Mexico: U.S. Geological Survey Open-File Report 74-194, 81 p.

_____1976, Cenozoic deposits of southeastern New Mexico and an outline of the history of evaporite dissolution: U.S. Geological Survey Journal of Research, v. 4, p. 135–149.

_____1980, Regional geology and Cenozoic history of Pecos region, southeastern New Mexico: U.S. Geological Survey Open-File Report 80-1099, 116 p.

_____1981, Geology of Nash Draw, Eddy County, New Mexico: U.S. Geological Survey Open-File Report 81-31, 8 p.

_____1985, Assessment of near-surface dissolution at and near the Waste Isolation Pilot Plant (WIPP), southeastern New Mexico: SAND84-7178, Sandia National Laboratories, Albuquerque, New Mexico.

Lee, W. T., 1925, Erosion by solution and fill [Pecos Valley, New Mexico]: U.S. Geological Survey Bulletin 760-C, p. 107–121.

Powers, D. W.; and Holt, R. M., 1995, Regional geological processes affecting Rustler hydrogeology: IT Corporation report prepared for Westinghouse Electric Corporation, 209 p.

Powers, D. W.; Martin, M. L.; and Terrill, L. J., 1997, Geology across Nash Draw as exposed in the El Paso Energy pipeline trench: Consultant report prepared for Westinghouse Electric Corporation, 27 p.

Powers, D. W.; Holt, R. M.; Beauheim, R. L.; and McKenna, S. A., 2003, Geological factors related to the transmissivity of the Culebra Dolomite Member, Permian Rustler Formation, Delaware Basin, southeastern New Mexico, *in* Johnson, K. S.; and Neal, J. T. (eds.), Evaporite karst and engineering/environmental problems in the United States: Oklahoma Geological Survey Circular 109 [this volume], p. 211–218.

Robinson, T. W.; and Lang, W. B., 1938, Geology and groundwater conditions of the Pecos River valley in the vicinity of Laguna Grande de la Sal, New Mexico, with special reference to the salt content of the river water: State Engineer of New Mexico, 12th and 13th Biennial Reports, p. 79–100.

Vine, J. D., 1963, Surface geology of the Nash Draw Quadrangle, Eddy County, New Mexico: U.S. Geological Survey Bulletin 1141-B, 46 p.

# Gypsum Karst in the Black Hills, South Dakota–Wyoming: Geomorphic Development, Hazards, and Hydrology

***Jack B. Epstein***
U.S. Geological Survey
Reston, Virginia

**ABSTRACT.**—Gypsum and anhydrite are found in four stratigraphic units in the Black Hills of South Dakota and Wyoming: in a large part of the Minnelusa Formation of Pennsylvanian and Permian age; in several zones in the red beds of the Opeche and Spearfish Formations of Permian and Triassic age; and in most of the Gypsum Spring Formation of Jurassic age. Dissolution of gypsum in the Spearfish and Gypsum Spring has resulted in collapse and formation of many sinkholes in several areas that are presently undergoing urban development in South Dakota, resulting in damage to houses and sewage-retention sites. Dissolution of anhydrite and some rock salt in the Minnelusa at depth has produced a regional collapse breccia, sinkholes, extensive disruption of bedding, and breccia pipes and pinnacles, some of which extend >1,000 ft into overlying strata. Removal of anhydrite in the Minnelusa probably began soon after the Black Hills were uplifted (early Tertiary) and continues today.

Recent subsidence is evidenced by sinkholes >60 ft deep that have opened up within the last several decades, collapse in water wells and natural springs that has resulted in sediment disruption and contamination, and fresh circular scarps surrounding shallow depressions. Some of the sinkholes in the Spearfish Formation might be too large to be accounted for by dissolution of the relatively thin gypsum beds within the lower 200 ft of that formation. They were more likely produced by the removal of much thicker anhydrite layers in the Minnelusa Formation, ~500 ft below. Some of the calcium sulfate in the lower part of the Spearfish has been dissolved, many of the beds are contorted because of expansion from hydration of anhydrite to gypsum, and many gypsum veinlets extend upward and downward from parent gypsum beds along random fractures. Thus, secondary porosity and permeability have developed in the lower part of the Spearfish Formation; it is an aquifer in at least the northern Black Hills.

Several sinkholes are sites of resurgent springs. These springs support fish hatcheries and are used for local agricultural water supply. As the anhydrite dissolution front in the subsurface Minnelusa moves downdip and radially away from the center of the Black Hills uplift, these resurgent springs will dry up and new ones will form as the geomorphology of the Black Hills evolves. Abandoned sinkholes and breccia pipes, preserved in cross section on canyon walls, attest to the former position of the dissolution front. Mirror Lake, which is expanding northwestward in a downdip direction, is a local analog of a migrating dissolution front.

Processes involved in the formation of gypsum karst should be considered in land-use planning in this increasingly developed part of the Black Hills.

## INTRODUCTION

The Black Hills of South Dakota are undergoing increased urban development, especially in the north, requiring a better understanding of geologic hazards and an assessment of ground-water-contamination potential. The study of gypsum karst in the Black Hills stems from two U.S. Geological Survey mapping projects: one in the southern Black Hills to evaluate uranium-resource potential during the 1960s (e.g., Brobst and Epstein, 1963), and the second recently in cooperation with the Lawrence County Planning Commission and the City of Spearfish, South Dakota, to help assess aquifer-contamination potential by describing major lithologic characteristics, delineating surface-recharge areas, and characterizing subsurface structural configuration (Epstein, 2001). The maps will also be useful for depicting areas of subsidence caused by solution of underground gypsum and anhydrite.

The Black Hills comprise an irregularly shaped uplift, elongated in a northwest direction, about 130 mi long and 60 mi wide (Fig. 1). Erosion has exposed a core of Precambrian metamorphic rocks that are in

Epstein, J. B., 2003, Gypsum karst in the Black Hills, South Dakota–Wyoming: geomorphic development, hazards, and hydrology, *in* Johnson, K. S.; and Neal, J. T. (eds.), Evaporite karst and engineering/environmental problems in the United States: Oklahoma Geological Survey Circular 109, p. 241–254.

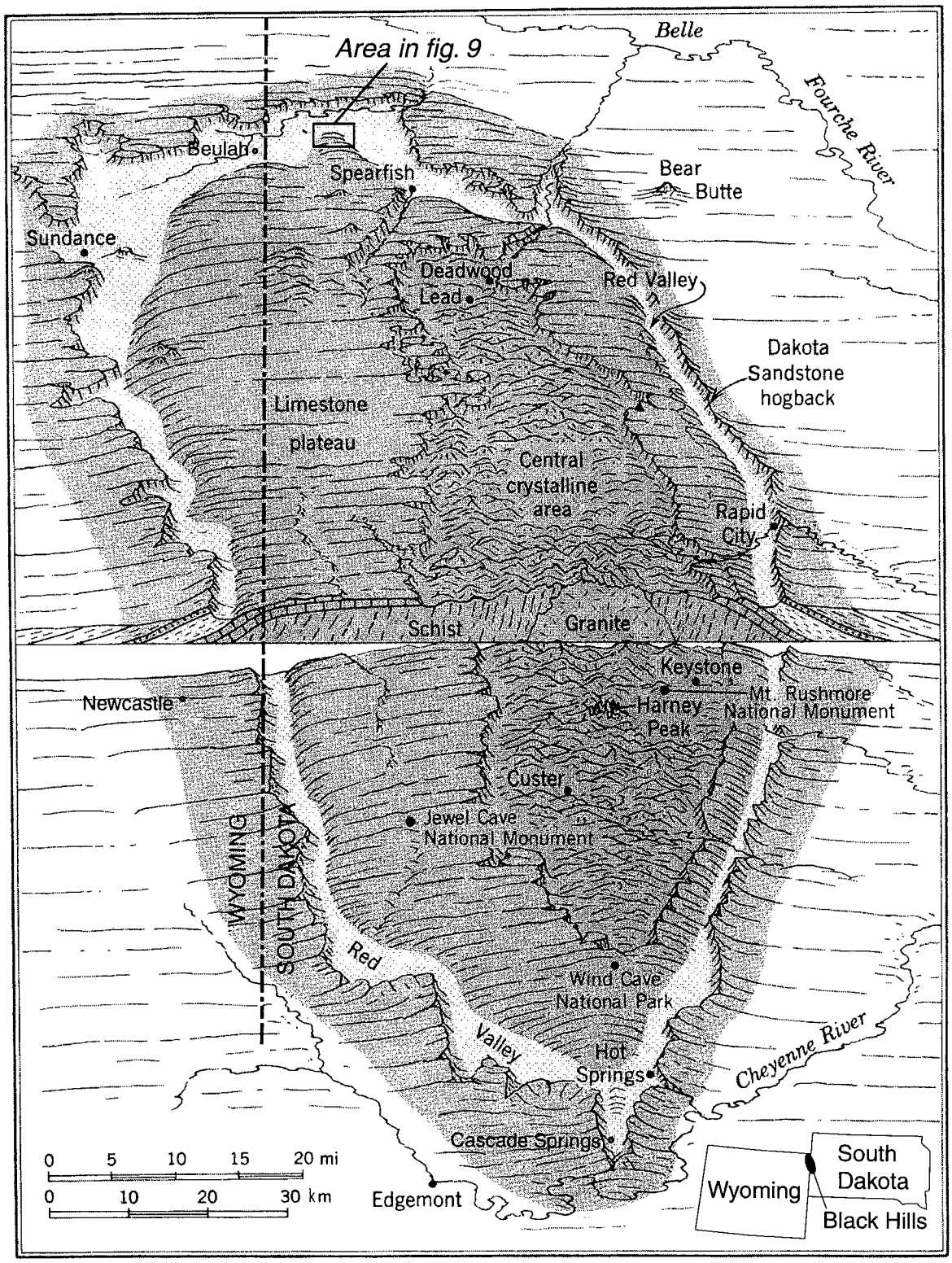


Figure 1. Generalized diagram showing the geology and geomorphology of the Black Hills. Most of the urban development and karst features are in the Red Valley, underlain by Triassic red beds and in the limestone plateau, underlain by a variety of Pennsylvanian and Permian rocks. Modified from Strahler and Strahler (1987), with permission.

turn rimmed by a series of sedimentary rocks of Paleozoic and Mesozoic age that generally dip away from the center of the uplift. These rocks are overlapped by Tertiary and Quaternary sediments and have been intruded by scattered Tertiary igneous rocks. The depositional environments of the Paleozoic and Mesozoic sedimentary rocks ranged from shallow marine to nearshore terrestrial. Study of the various sandstones, shales, siltstones, and limestones indicates that these rocks were deposited in shallow-marine environments, tidal flats, sand dunes, carbonate platforms, and by rivers. More than 300 ft of gypsum and anhydrite was deposited at various times in evaporite basins. At the end of the Cretaceous Period and into the beginning of the Tertiary these sediments were uplifted into an asymmetric dome, with the rocks dipping radially outward from the center. The homoclinal dips are locally interrupted by monoclines, structural terraces, low-amplitude folds, faults, and igneous intrusions.

Erosion of these uplifted rocks produced the landscape we see today. Rocks of the Mississippian Madison Limestone (Pahasapa of other reports), Minnelusa Formation, and older sediments form the "limestone plateau" that rims the central Precambrian metamorphic core. Erosion of red siltstones and shales of the Spearfish Formation has formed the "Red Valley," the main area of present and proposed future development. White gypsum caps many of the hills in the Spearfish and is a conspicuous landform in the overlying Gypsum Spring Formation. Resistant sandstones that are interbedded with other rocks lie outboard from the Red Valley and form the hogback that encircles the Black Hills and defines its outer physiographic perimeter.

## STRATIGRAPHY OF CALCIUM SULFATE–BEARING ROCKS

Whereas karstic features in limestone and dolomite, such as caves, sinkholes, and underground drainage, are abundant worldwide and notably in the Black Hills, similar solution features are also abundant in gypsum ($CaSO_4 \cdot 2H_2O$) and its anhydrous counterpart, anhydrite ($CaSO_4$), throughout the United States (Epstein and Johnson, 2003). Calcium sulfate rocks are much more soluble than carbonate rocks, especially where they are associated with dolomite undergoing dedolomitization, a process which results in ground water that is continuously undersaturated with respect to gypsum (Raines and Dewers, 1997), as it is in the Black Hills.

Gypsum and anhydrite are conspicuous evaporite deposits in four sedimentary-rock units in the Black Hills (Fig. 2). They compose as much as 30% of the Minnelusa Formation (generally present only in the subsurface), <5% of the Opeche Formation, >10% of the Spearfish Formation in places, and about half of the Gypsum Spring Formation.

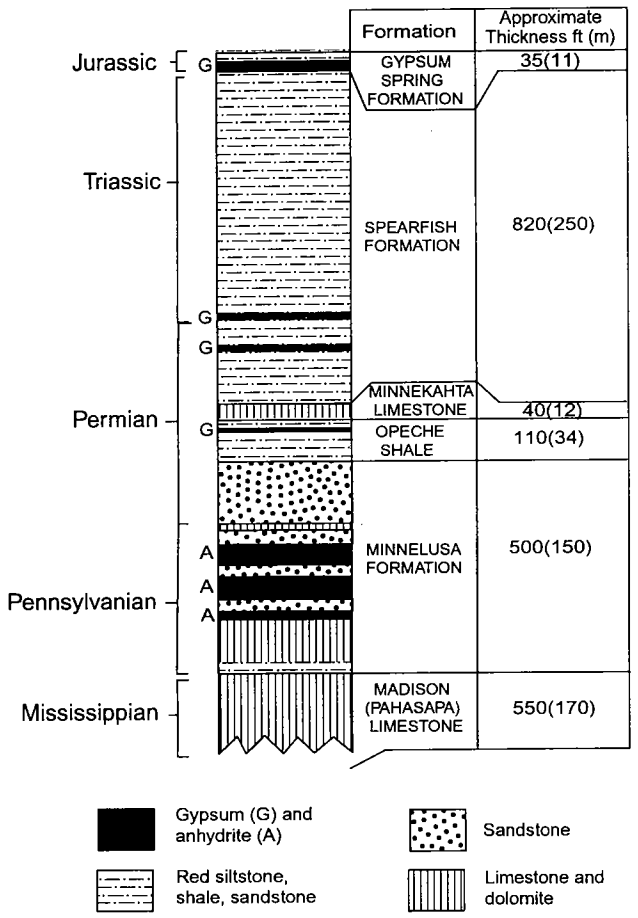


Figure 2. Stratigraphic column, showing formations containing gypsum and anhydrite in the Black Hills, South Dakota and Wyoming. Thicknesses are for the northern Black Hills.

### Minnelusa Formation

The Minnelusa ranges from 400 to 1,050 ft in thickness in the Black Hills and surrounding area. Conveniently for this report, Rahn and Gries (1973) divided the Minnelusa Formation in the northern Black Hills into three units: a lower sandstone and dolomite with basal shale, 0–300 ft thick; a middle dolomite, sandstone, and shale with anhydrite in the subsurface, 200–300 ft thick; and an upper sandstone, as much as 200 ft thick. Anhydrite is >200 ft thick in the subsurface in places but is mostly absent in surface outcrops, having been removed by solution. The dissolution of anhydrite and the consequent formation of voids in the Minnelusa at depth resulted in the foundering and fragmenting of overlying rocks, producing extensive disruption of bedding, a regional collapse breccia, many sinkholes, and breccia pipes and pinnacles (Fig. 3; Epstein, 1958a,b; Brobst and Epstein, 1963; Bowles and Braddock, 1963). Subsidence caused by anhydrite dissolution in the Minnelusa has extended >1,000 ft into overlying formations. For example, two sinkholes 30–60 ft deep, known locally as the "lost wells," are situated at an altitude of ~4,000 ft in the Seven Sisters Range, 2 mi south of the center of Hot Springs,

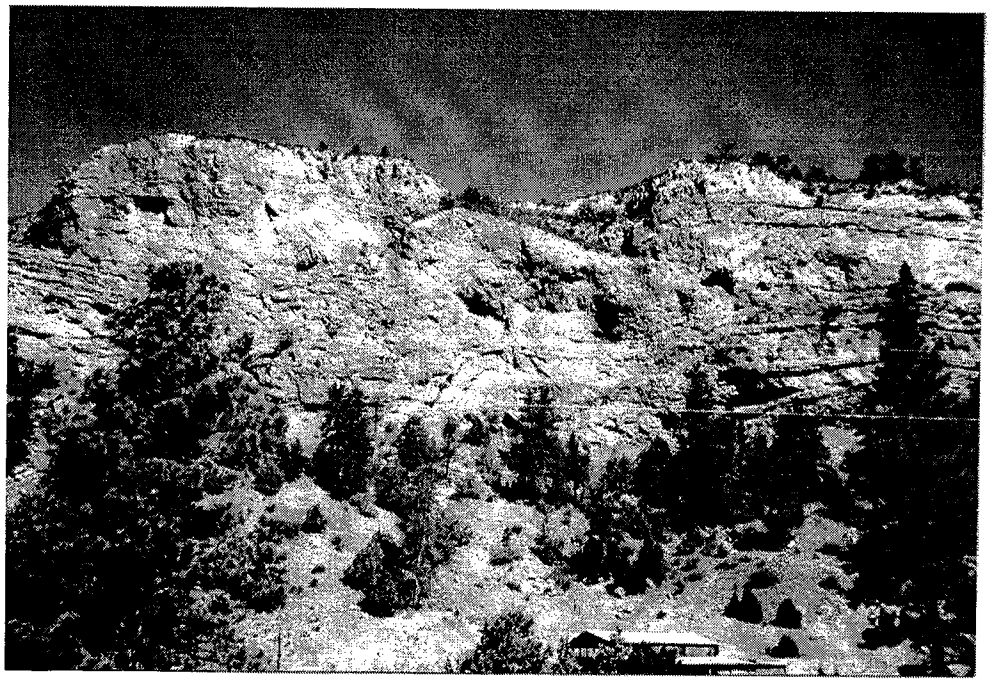

Figure 3. Sinkhole, disrupted bedding, and solution cavities in the Minnelusa Formation in 400-ft-high cliff face in Redbird Canyon, ~10 mi east of Newcastle, Wyoming. The collapse resulted from removal of anhydrite by artesian ground water prior to fluvial erosion, which exposed the sinkhole on the canyon wall.

South Dakota, in the Lakota Formation (Wolcott, 1967). The depth to the dissolved anhydrite in the Minnelusa Formation was ~1,300 ft.

The contrast between the brecciated rocks above the level at which the anhydrite has been removed and the undisturbed beds below is striking (Fig. 4). The breccia in the Minnelusa contains clasts that are slightly abraded, although some of the more friable rocks are partly rounded. These clasts consist of fragments from less than 1 in. long to clasts several tens of feet long. They consist of fine-grained, massive to cross-bedded sandstone, limestone, dolomite, and some shale. The matrix is principally fine-grained sand cemented by calcium carbonate. Many beds can be traced for distances of hundreds of feet, but the rocks are broken and may be displaced several tens of feet in a vertical direction. This crude bedding is a common feature throughout the upper part of the brecciated Minnelusa. At places the crude bedding gives way laterally to chaotic structure in which the rock fragments are randomly oriented and bedding layering is lost.

The breccia pipes are vertical cylindrical masses that transgress rocks having crude bedding and chaotic structure (Fig. 5A). They are up to 300 ft in diameter and extend upward from the upper part of the Minnelusa Formation more than 1,000 ft into overlying stratigraphic units (Bowles and Braddock, 1963). Braddock (1963) noted as much as 100 ft of downward movement of clasts in some breccia pipes that are found in the Minnekahta Limestone. The pipes stand out as protuberances on the canyon walls (Fig. 5B) or as chimney-like monoliths above the ground surface (Fig. 5C), depending on the stage of differential weathering and erosion between them and the less resistant enclosing rocks. Some are at an intermediate stage, forming a window on the canyon wall (Fig. 5D). The pipes developed where stoping was locally intense and probably formed along joints or at the intersection of joints, an ideal place for intense solution of intersected beds and lenses of subsurface anhydrite. The formation of solution chambers was followed by collapse of overlying and adjacent beds. No study has been carried out to determine the relationship between joint intensity and spacing with the occurrence of breccia pipes in the Black Hills. The brecciation has formed a vuggy secondary porosity, which, along with the porous sandstone, makes the upper half of the Minnelusa an important aquifer in the Black Hills. Whereas breccia pipes may extend upward through overlying formations, one of the most obvious effects is the production of undulations in the Minnekahta Limestone. The Minnekahta is a prominent resistant unit, ~40 ft thick, forming cliffs between the underlying soft rocks of the Opeche Shale and the overlying Spearfish Formation. In most places in the Black Hills the Minnekahta forms a widespread dip slope with variable domes and saddles that are undoubtedly due to settlement of the brecciated Minnelusa not far below. These undulations extend well beyond the area of breccia pipes that have been mapped in the southern Black Hills.

### Opeche Formation

The Opeche Formation, consisting of 25–150 ft of poorly exposed red shale, siltstone, and fine-grained

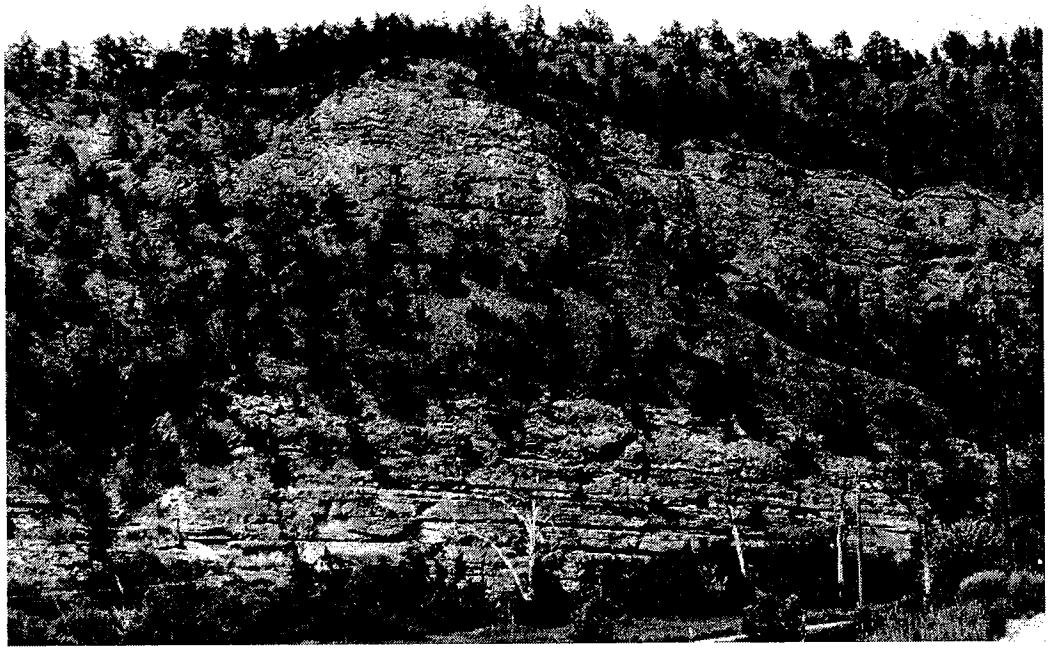

Figure 4. Lower non-brecciated rocks below tree-covered slope, and upper brecciated rocks in the Minnelusa Formation in Hot Brook Canyon, near Hot Springs, South Dakota. Many tens of meters of anhydrite have been removed in a zone above the non-brecciated beds.

sandstone, is a confining unit between the Minnelusa Formation and the Minnekahta Limestone. Gypsum is not abundant, aggregating no more than ~10 ft thick, and is absent in most places.

### Spearfish Formation

The Spearfish Formation consists of ~350–900 ft of fine red beds with several beds of gypsum, totaling between 50 and >80 ft in thickness. Anhydrite, which probably was the original form of calcium sulfate deposited in the Spearfish, undergoes about a 40% expansion when hydrated to form gypsum. As a result, beds of gypsum in the Spearfish Formation are commonly highly folded (Fig. 6). When gypsum dissolves, it may become mobile and is injected downward as thin veinlets into fractures in the confining red beds (Fig. 7). These veinlets are generally <2 in. wide, they occur along a multitude of variably oriented fractures above and beneath the parent gypsum bed, and they contain gypsum fibers lying perpendicular to the fracture walls. These fractures probably formed as the result of hydration expansion as well as by force of artesian pressure, similar to the "hydraulic fracturing" proposed by Shearman and others (1972). Thus, the lower 200 ft or so of the Spearfish has developed a secondary fracture porosity. This part of the formation has supplied water to wells, many sinkholes have developed in it, and resurgent springs are numerous. Ground water flows through the fractures and solution cavities in the gypsum. Although the entire Spearfish Formation is generally considered to be a confining formation, the lower 200 ft of the Spearfish is an aquifer, at least in the northern Black Hills. This is not surprising, since high ground-water flow has been reported in gypsum in many areas of the United States (Thordarson, 1989).

The upper part of the Spearfish, where gypsum beds are lacking, is >600 ft thick in places and consists of red siltstone, shale, and very fine grained sandstone. As in the northern Black Hills, bedding is regular, and the unit lacks the fractures seen in the lower part of the formation. This part of the Spearfish is a confining layer.

### Gypsum Spring Formation

The Gypsum Spring Formation consists of ~35 ft equally distributed between ledge-forming white gypsum at the bottom and shaly siltstone with thin gypsum at the top in the northern part of the Black Hills but absent in the southern part. Many sinkholes have developed in this unit, causing damage to several man-made structures.

## DISSOLUTION FRONT IN THE MINNELUSA FORMATION

The Minnelusa Formation contains abundant anhydrite in the subsurface; and except for a few areas near Beulah and Sundance, Wyoming (Brady, 1931), and in Hell Canyon in the southwestern Black Hills (Braddock, 1963), no anhydrite or gypsum crops out. A log of the upper part of the Minnelusa from Hell Canyon contains 235 ft of anhydrite and gypsum (Brobst and Epstein, 1963). Where anhydrite is present in the Minnelusa, both in the subsurface and in the few surface exposures, its rocks are not brecciated.

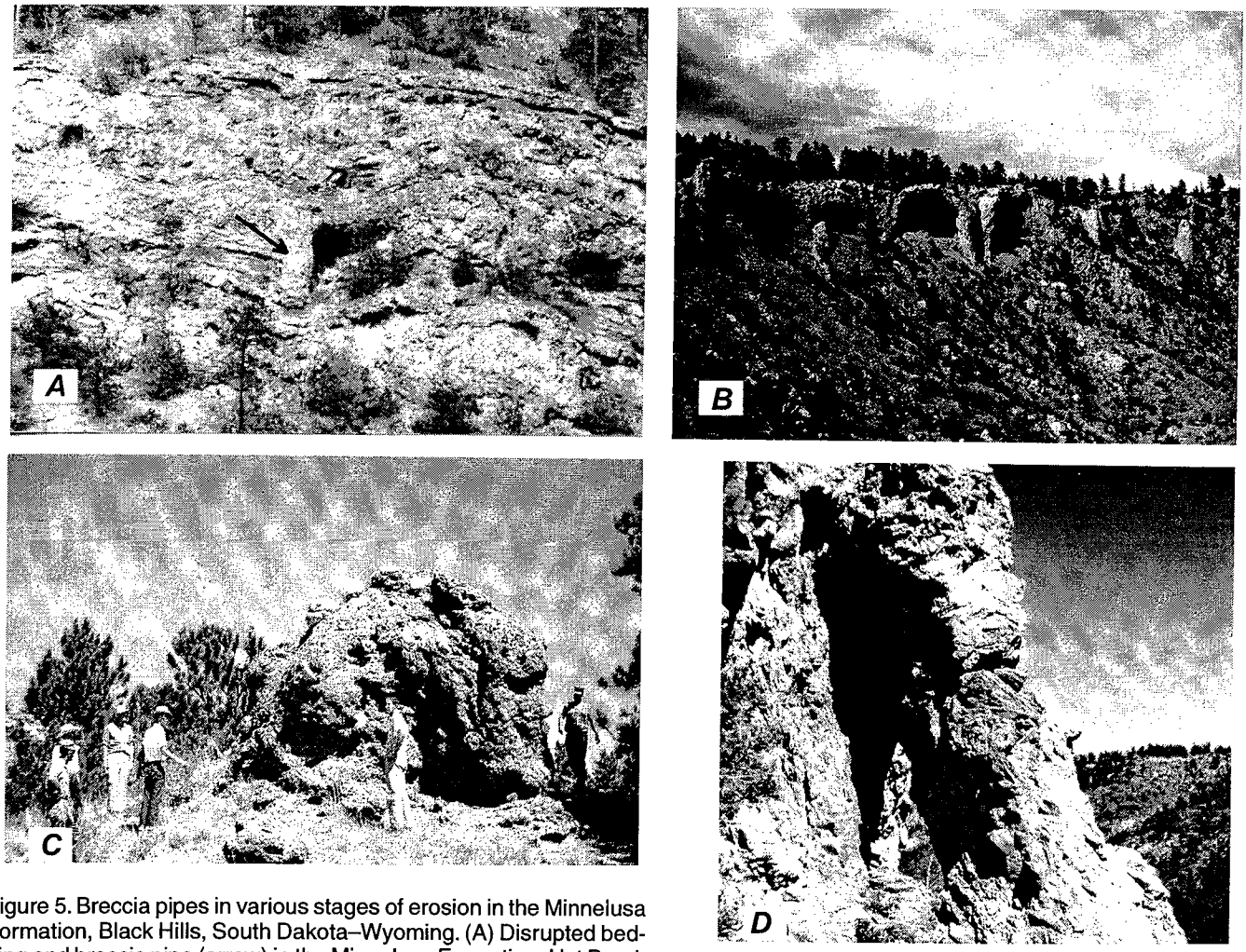


Figure 5. Breccia pipes in various stages of erosion in the Minnelusa Formation, Black Hills, South Dakota–Wyoming. (A) Disrupted bedding and breccia pipe (arrow) in the Minnelusa Formation, Hot Brook Canyon, 3 mi west of Hot Springs, South Dakota. (B) Calcite-cemented breccia pipes stand out in relief or are separated from the canyon wall as a pinnacle in the upper part of the Minnelusa Formation, Red Bird Canyon, ~10 mi east of Newcastle, Wyoming. (C) Resistant breccia pipe stands as a pinnacle in the Spearfish Formation, several hundred feet above the dissolved anhydrite in the Minnelusa Formation, ~15 mi west of Hot Springs, South Dakota. Some sandstone clasts were derived from the overlying Sundance Formation, >100 ft above. (D) Breccia pipe still connected to canyon wall. Progressive erosion will isolate it, forming a pinnacle similar to the one in Fig. 5C.

Where the rocks are brecciated in outcrop, anhydrite is absent. Clearly, the brecciation is the result of collapse following subsurface dissolution of anhydrite.

Because ground water has dissolved the anhydrite in the Minnelusa in most areas of exposure, and because anhydrite is present in the subsurface, a transition zone should be present where dissolution of anhydrite is currently taking place. A model of this zone has been presented by Brobst and Epstein (1963, p. 335) and Gott and others (1974, p. 45) and is shown here in Figure 8. Consequences of this model include the following: (1) the updip part of the Minnelusa is thinner than the downdip part because of removal of significant thicknesses of anhydrite; (2) the upper part of the Minnelusa should be continually collapsing, even today; and (3) the properties of the water in this transition zone may be different than elsewhere. Total subsidence in the Minnelusa did not equal the total thickness of anhydrite removed, the difference being due to the development of voids ranging from intergranular in size to several tens of feet long and resulting in development of a secondary porosity that has made the Minnelusa an important aquifer in the Black Hills.

Numerous water-well logs, on file at the U.S. Geological Survey Water Resources Office in Rapid City, South Dakota, document the thickness variations in the Minnelusa to be expected by this model. Recent removal of calcium sulfate is borne out by chemical analyses of water from numerous springs throughout the Black Hills (e.g., Brobst and Epstein, 1963; Post, 1967; Gott and others, 1974). The presence of salt (sodium chloride) in the Minnelusa is confirmed by more than 5% NaCl in the water of Salt Spring, 8.5 mi north of Newcastle, Wyoming, reported by Darton (1904), and by about 4% salt reported by Brobst and Epstein (1963). The salt was commercially extracted after evaporation during the late 19th century. Calcium,

Figure. 6. Contorted gypsum is a common feature in the Spearfish Formation in the Red Valley of the southwestern Black Hills, southeast of Newcastle, Wyoming.

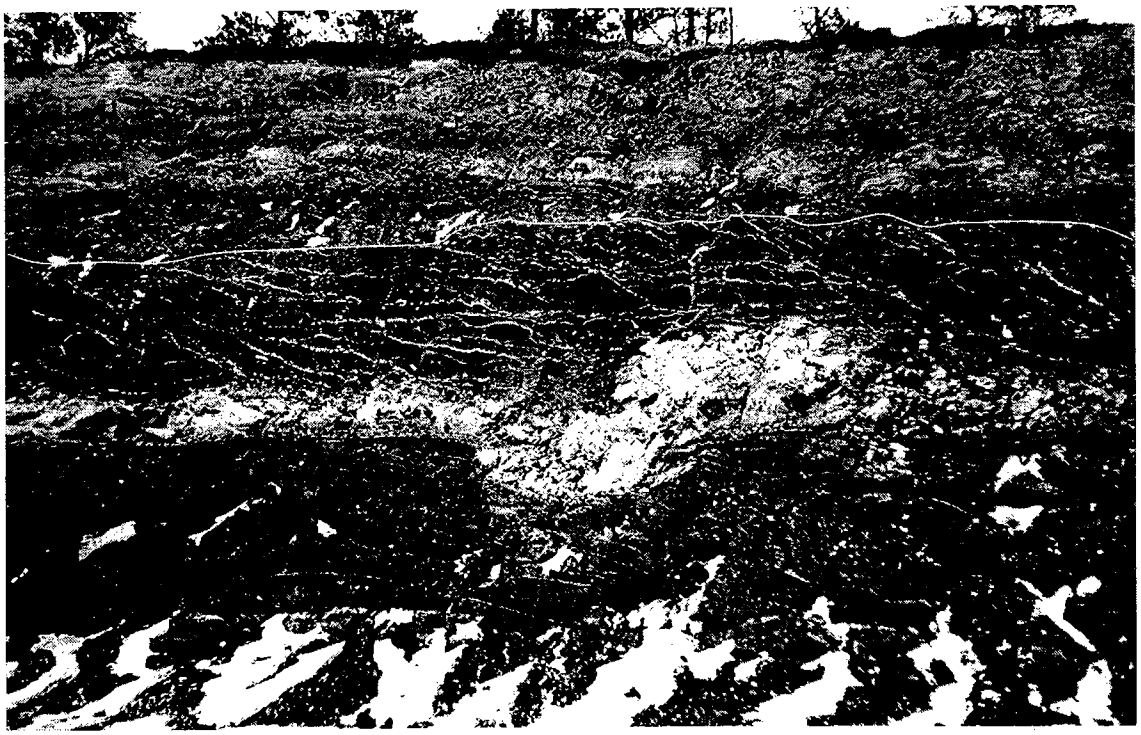

Figure 7. Thin gypsum veinlets, extending upward from a contorted parent gypsum bed in the Spearfish Formation, which has altered from anhydrite, into green shale of the Sundance Formation (above line), at Cascade Springs, South Dakota, along State Highway 71, 13 mi southwest of Hot Springs, South Dakota.

sodium, and potassium sulfate are abundant in the water at Hot Springs, as reported on a sign at Evans Plunge, a popular spa in the area. Present-day collapse in the Minnelusa from anhydrite removal is evidenced by sediment disruption in water wells and springs (Hayes, 1996).

Klemp (1995) characterized the spring and aquifer geochemistry of five springs in the northern Black Hills and noted an irregular northward increase in specific conductance, which indicates the line of anhydrite dissolution in the Minnelusa aquifer (Fig. 9). The McNenny Springs are near the crest of a prominent

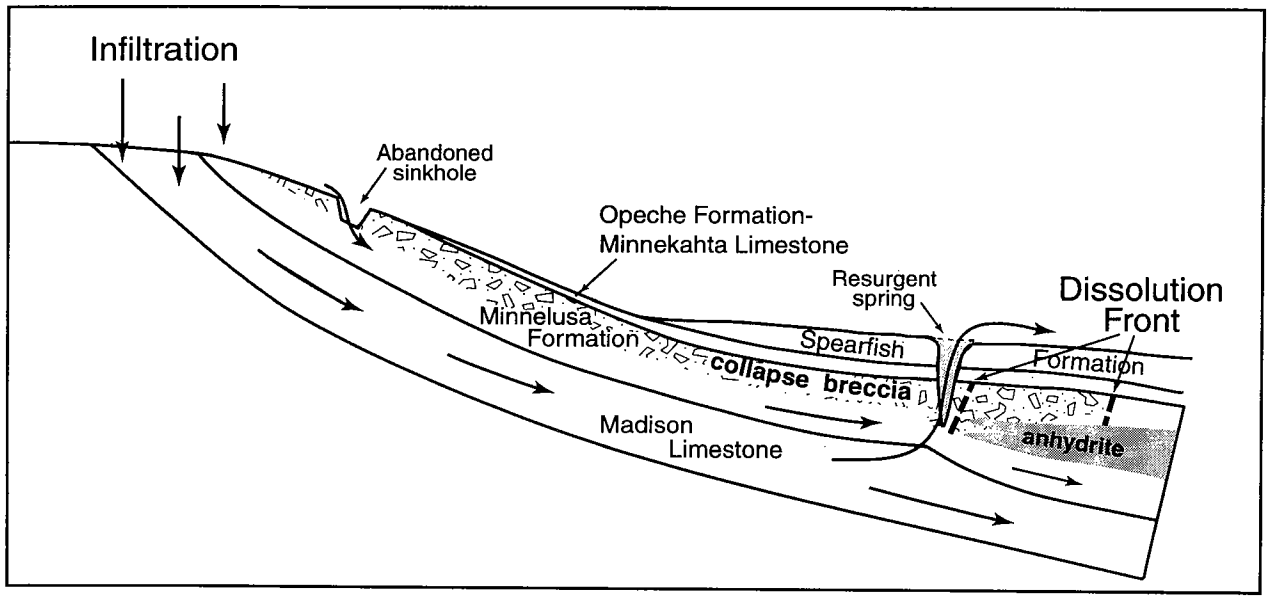


Figure 8. Generalized diagram showing dissolution of anhydrite in the Minnelusa Formation and downdip migration of the dissolution front. Cox Lake, and other resurgent springs (see Fig. 9), are near the position of the dissolution front. As the front moves downdip with continued solution of the anhydrite, and as the Black Hills are slowly lowered by erosion, these sinkholes and related collapse structures are left abandoned on canyon walls (see Fig. 3).

structure west of Spearfish, South Dakota, the La-Flamme Anticline. It plunges to the northwest, is at least 10 mi long and ~8 mi wide, has a structural relief in places of >600 ft, and its flanks dip as much as 20°. The sources for the springs are mainly the Madison (Pahasapa) Limestone and the Minnelusa Formation, the major aquifers in the Black Hills. They are recharged by rainfall on and by streams flowing across their updip outcrop area. In the Minnelusa, removal of anhydrite progresses downdip with continued solution of the anhydrite (Fig. 8), collapse breccia is formed, breccia pipes extend upward, and resurgent springs develop at the sites of sinkholes. Cox Lake (Fig. 10), Mud and Mirror Lakes, and McNenny Springs, ~300 ft above the base of the Spearfish Formation, are near the position of the dissolution front. As the Black Hills are slowly lowered by erosion, the anhydrite-dissolution front in the subsurface Minnelusa moves downdip and radially away from the center of the uplift. The resurgent springs will dry up, and new ones will form downdip, as the geomorphology of the Black Hills evolves. Abandoned sinkholes that remain high on canyon walls (Fig. 3) attest to the former position of the dissolution front.

If this process is correct, then present resurgent springs should be eventually abandoned, and new springs should develop down the regional hydraulic gradient of the Black Hills. One example might be along Crow Creek where a cloud of sediment from an upwelling spring lies 1,000 ft north of McNenny Springs (Fig. 9). This circular area, ~200 ft across, might eventually replace McNenny Springs.

Breccia pipes have been mapped in some detail in the southern Black Hills (Braddock, 1963; Brobst and Epstein, 1963). Braddock (1963) used the location of the breccia pipes to show the probable limit of collapse breccia in the Minnelusa Formation, the dissolution front. However, the front may be more extensive than he depicted, because undulations in the overlying Minnekahta Limestone are probably due to settling in the underlying Minnelusa, and those undulations extend well beyond the breccia-pipe locations.

Solution of anhydrite in the Minnelusa probably began soon after the Black Hills were uplifted in the early Tertiary and continues today. Recent subsidence is evidenced by sinkholes >60 ft deep opening up within the last 50 years (Fig. 11), collapse in water wells and natural springs resulting in sediment disruption and contamination (Hayes, 1996), and fresh circular scarps surrounding shallow depressions.

The Plains Indians that inhabited the area 300 years ago trapped and slaughtered thousands of buffalo for their primary food by stampeding the animals over the steep rim of one of the large sinkholes near Beulah, Wyoming (the Vore Buffalo Jump; Epstein, 2000, fig. 17). The site is now a major archeological dig by the University of Wyoming. Another large sinkhole in the Spearfish Formation that was the site of a breccia pipe extending down into the Minnelusa Formation near Hot Springs, South Dakota, was an active trap for large mammals at least 26,000 years ago (Laury, 1980; Agenbroad and Mead, 1994).

A series of springs that apparently occupy sinkholes as well as dry sinkholes emanate from the lower half of the Spearfish Formation, generally within 200 ft of the base of the formation, and at or near where several beds of gypsum are exposed. Several lines of reasoning suggest that these sinkholes are not the result

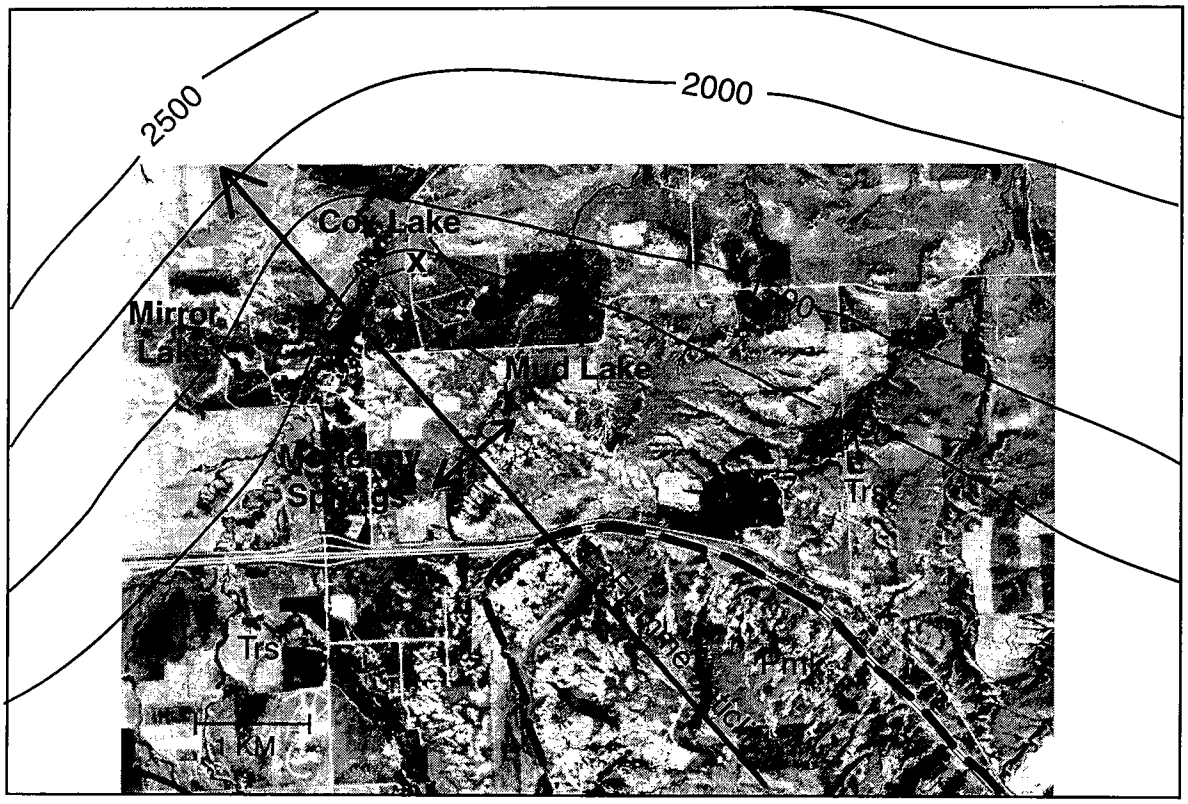


Figure 9. Air photograph showing location of resurgent springs in the Spearfish Formation and rapid increase of specific conductance in the Minnelusa aquifer (contours in microsiemens per centimeter at 25°C; from Klemp, 1995) adjacent to the LaFlamme Anticline. *Pmk,* Minnekahta Limestone; *Trs,* Spearfish Formation. X, location of upwelling water that may replace McNenny Springs in the future.

of solution of gypsum in the Spearfish, even though there is some collapse from removal of gypsum in that formation: (1) the gypsum beds in the lower Spearfish aggregate no more than ~25 ft in thickness, whereas the sinkholes are >50 ft deep in places; (2) several of the sinkholes lie below many of the gypsum beds; and (3) the waters of some of the lakes occupying the sinkholes are derived from underlying formations (Klemp, 1995).

## SINKHOLES IN THE LOWER PART OF THE SPEARFISH FORMATION— HYDROLOGIC IMPLICATIONS

The Spearfish Formation comprises red shale, siltstone, and fine sandstone with scattered beds of gypsum. In the area of Spearfish, South Dakota, and west to the Wyoming–South Dakota border, the lower part of the formation has different structural and lithologic characteristics than the upper part that affect its hydrologic behavior. The lower 200 ft or so is an aquifer. The overlying rocks are a confining layer. The lower part yields abundant water to wells and springs. It contains gypsum beds, many of which are contorted, and gypsum veinlets that are intruded into fractures at variable angles. The sinkhole shown in Figure 11 was examined by local ranchers, and running water was heard beneath. A cavern extended horizontally beyond the limits of their flashlight beam (Ted Vore, personal communication, 1999). Cox (1962, p. 11 ) reported a well 2.8 mi east-northeast of Cox Lake that bottomed in a cavern in the Spearfish. A working hypothesis is that the lower Spearfish contains abundant, interconnected caves and solution fractures along which water flows rapidly, supplying wells, Cox Lake, and surrounding resurgent springs. This unit is a fractured rock aquifer in which ground water travels by conduit flow.

Where the potentiometric surface lies above the ground surface in this zone, the sinkholes are sites of resurgent springs. Where the potentiometric surface lies below the ground surface within this zone, dry sinkholes have developed (Fig. 12). It is possible that the aquifer rocks are more intensely fractured in the LaFlamme anticlinal area, allowing for greater secondary porosity and permeability, and accounting for the location of these springs (Fig. 8). In places the gypsum beds and associated fractured red beds that contain gypsum veinlets are sites of perched water above impermeable beds (Fig. 13). Dissolution along joints in near-surface gypsum, such as shown in Figure 13, has resulted in numerous small sinkholes in the northern Black Hills that have damaged houses and parking areas (Fig. 14).

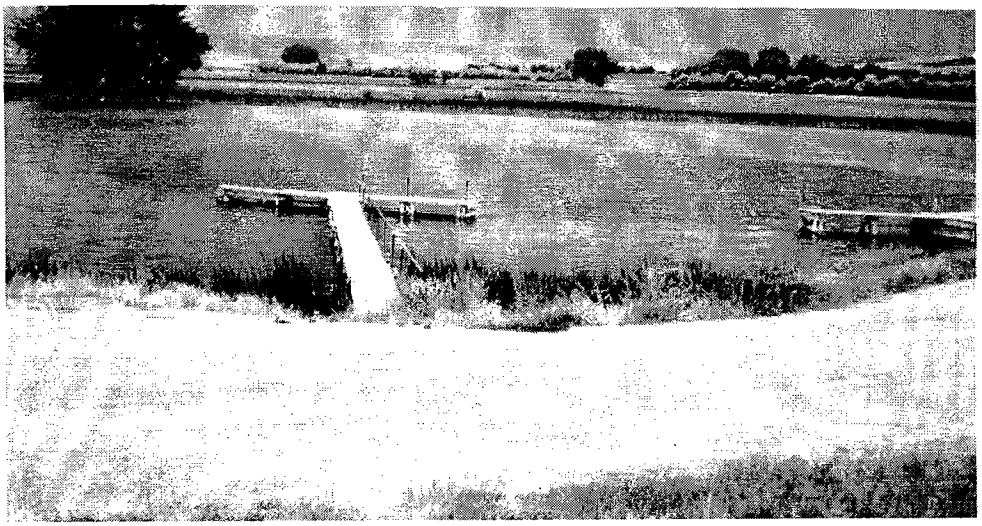

Figure 10. Cox Lake, a resurgent (artesian) spring with a flow of nearly 5 ft³/s in the Spearfish Formation in the northern Black Hills. It occupies a sinkhole that is >60 ft deep (outlined by the darker water just beyond the edge of the dock). The chemical signature of the water indicates that the Minnelusa Formation and underlying Madison Limestone are the contributing aquifers (Klemp, 1995). Its position is near the anhydrite-dissolution front shown in Figure 8.

Figure 11. Sinkhole that formed about 1950 near Beulah, Wyoming, in the red beds of the Spearfish Formation. It developed in a larger and shallower 1,000-ft-wide depression. Abundant gypsum veinlets are present in the walls of the hole.

Many of the sinkholes in the Spearfish Formation are too large to be accounted for by solution of the relatively thin gypsum beds within that formation. They were more likely produced by the removal of much thicker gypsum in the Minnelusa Formation, ~500 ft below. Many sinkholes that extend down through the Spearfish into the Minnelusa are sites of resurgent springs (Fig. 12), resulting from fairly recent dissolution of anhydrite in the Minnelusa. These springs are important for recharging surface streams

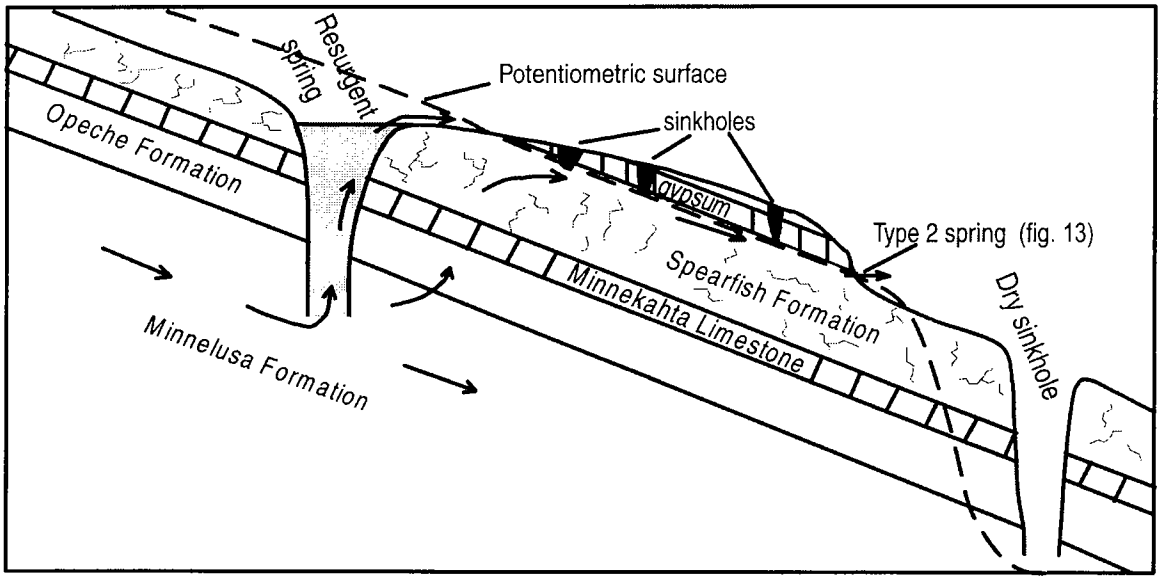


Figure 12. Generalized diagram showing hypothetical flow path of ground water in resurgent spring and in spring emerging from beneath gypsum in Spearfish Formation (type 2 spring of Rahn and Gries, 1973), and sinkholes developed by solution of anhydrite in the Minnelusa Formation. Dry sinkhole lies above potentiometric surface. Gypsum veinlets in fractured rocks of the lower part of the Spearfish are shown by jagged lines.

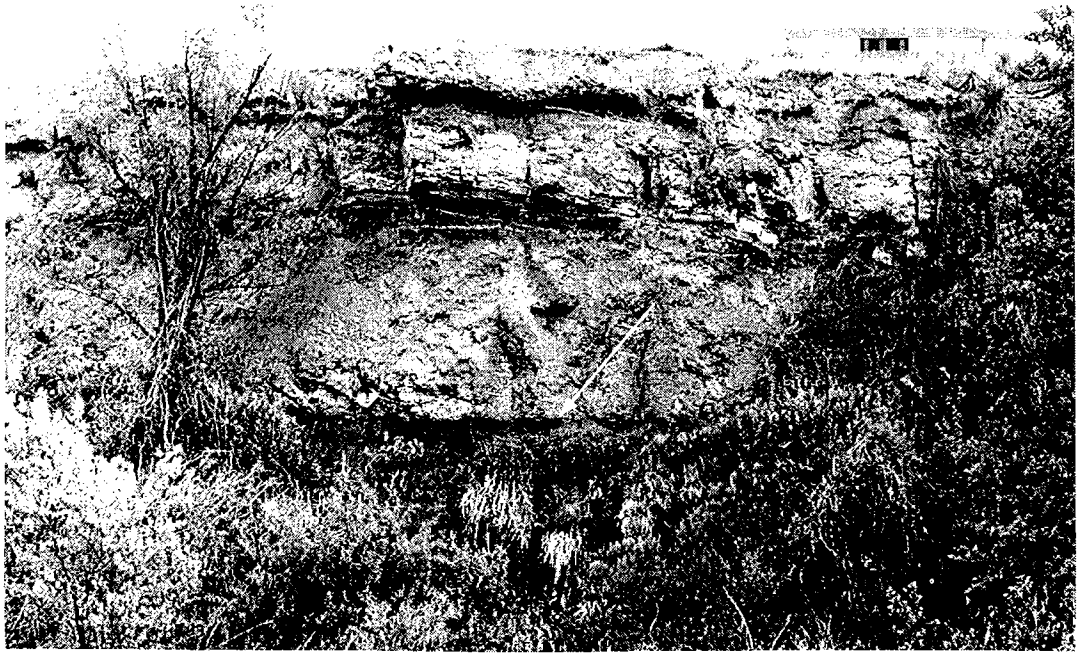

Figure 13. Perched water table with springs below zone of gypsum and fractured red beds with intruded gypsum veinlets. The water emits at the top of impermeable red shale and siltstone (arrow) and supports lush vegetation. McNenny Fish Hatchery, 4 mi east-northeast of Beulah, Wyoming.

in the Black Hills. Rainfall recharges aquifers higher up near the core of the Black Hills. The ground water discharges along the flanks of the hills, mainly in or near the Spearfish aquiclude, where the potentiometric surface is higher than the ground surface. Much of the water in these springs is partly derived from the Madison Limestone, which underlies the Minnelusa.

## ENLARGEMENT OF MIRROR LAKE VIA "HEADWARD COLLAPSE"

Mirror Lake, in the South Dakota State Wildlife Management Area (see Fig. 9), has a dogleg shape. The eastward-trending section is artificial, formed by a dam at the east end. The northwest-trending, 900-ft-long alcove is cut into a 50-ft-high ridge of the

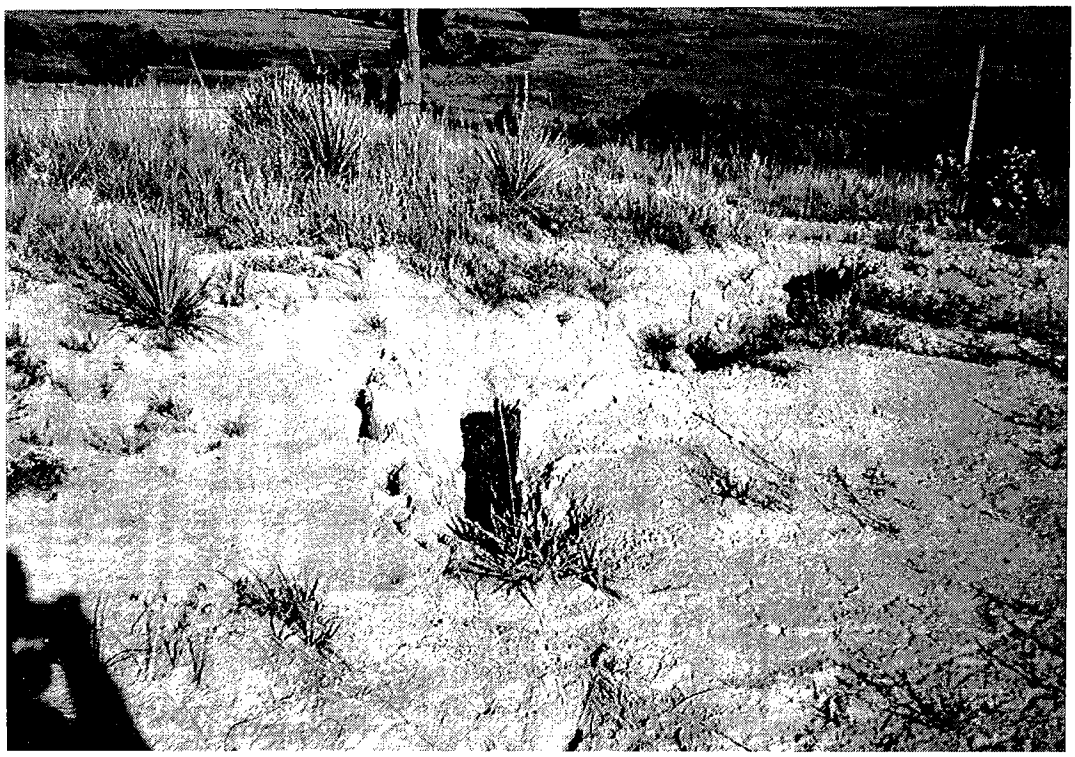

Figure 14. Solution widening of joint and soil collapse in gypsum in the lower part of the Spearfish Formation in parking area near McNenny Fish Hatchery. Gypsum bed is the same as the one in Figure 13.

Spearfish Formation (Fig. 15). The lake, similar to other lakes in the area, occupies a depression formed by dissolution of calcium sulfate at depth, probably in the Minnelusa, although gypsum underlies the lake in the Spearfish, as shown by outcrops nearby. A deposit of calcareous tufa, as much as 4 ft thick, consisting of light brown, porous limestone with abundant plant impressions ("moss rock" of local ranchers) is found 1,000 ft southeast of the lake. The deposit dips gently to the east, away from Mirror Lake, and presumably was deposited earlier by spring water that emerged from the lake. Numerous sinkholes several feet deep are found at the north end of the alcove. These presently are active and indicate that the lake is expanding to the northwest by continued collapse from solution of gypsum. The fine sediment derived from the Spearfish is presumably removed by the emerging spring water. The lake was once probably higher at the time the tufa was deposited (Fig. 15). Continued downcutting and northwest migration of the headwall have produced the present landform, a pocket valley that has been termed a *steephead* (Jennings,

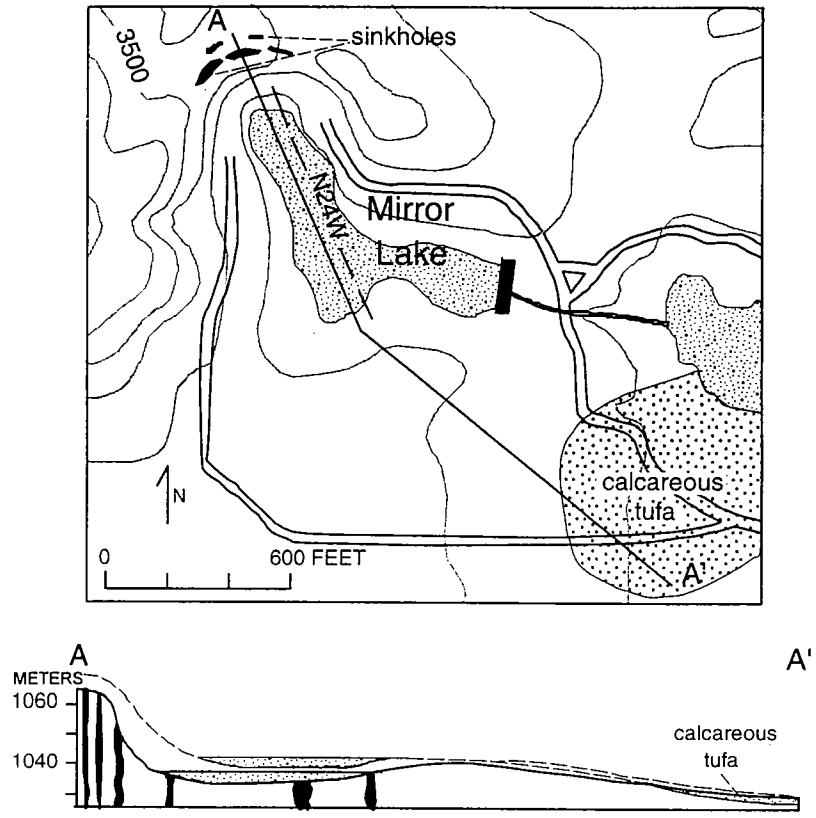


Figure 15. Map and cross section showing sinkholes at the northwest end of Mirror Lake, 3.5 mi east-northeast of Beulah, Wyoming, and the inferred earlier topography on which calcareous tufa was deposited. Contour interval, 20 ft.

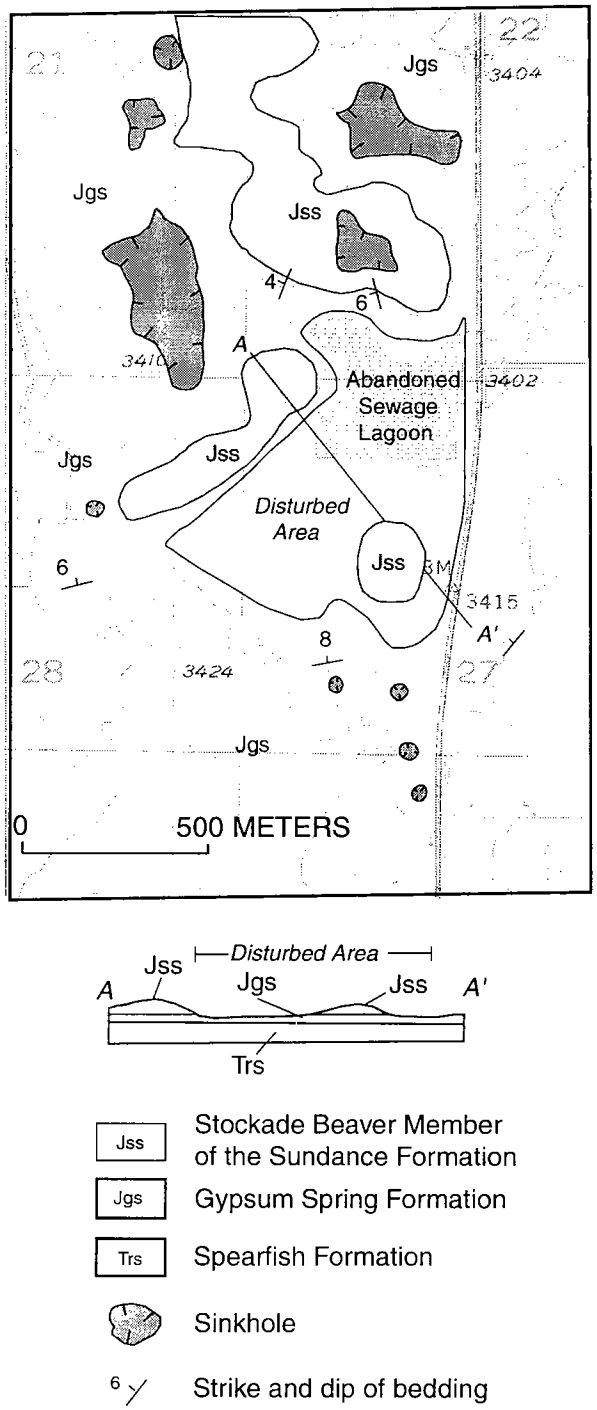


Figure 16. Geologic map of the abandoned sewage-lagoon area west of U.S. Highway 85, 2 mi north of I-90, Spearfish, South Dakota. Base from Jolly 7.5-minute quadrangle, South Dakota. Contour interval, 10 ft.

1971). Dating the sediments in the bottom of the lake may yield the rate of headward erosion of the steep-head.

## ENVIRONMENTAL CONCERNS

Karstic collapse owing to dissolution of gypsum and anhydrite is an active process in the Black Hills. Dissolution of gypsum in the Spearfish and Gypsum Spring has resulted in collapse and formation of many sinkholes in several areas that are presently undergoing rapid development between Rapid City and Spearfish, South Dakota (Rahn and Davis, 1996; Davis and Rahn, 1997; Davis and others, 2003). Some gypsum beds form terraces that are attractive as housing sites (see Epstein and Johnson, 2003, fig. 10). Foundation stability should be a concern at such sites. In 1972 the City of Spearfish constructed a sewage lagoon on the Gypsum Spring Formation. The lagoon leaked into sinkholes, and the lagoon was abandoned in favor of an expensive water-treatment plant. Recently, the city entertained plans to convert the lagoon site into a recreation area with construction of buildings and light towers. The Public Works Administrator requested the USGS for a judgment on the potential for subsidence at the site. A geologic map was prepared, similar to one prepared by Davis (1979, fig. 3), showing that at least 10 sinkholes, one of which is ~1,000 ft long, had developed in the gypsum (Fig. 16). This information was subsequently used by the city planners in their decision to abandon the project.

The lower part of the Spearfish Formation is also undergoing active collapse and is demonstrated to be an aquifer. This zone is more susceptible to rapid infiltration of contaminants than the upper part of the Spearfish, which should be considered in future land-use planning. Collapse resulting from dissolution of soluble rocks can be exacerbated by removal of ground water by pumping. If areas in the Red Valley of the northern Black Hills are extensively developed, and water supplies derived from pumping, then a possible concern might be the increase in frequency of such collapse in the Spearfish Formation.

## SUMMARY AND CONCLUSIONS

Dissolution of gypsum and anhydrite in the Minnelusa and Spearfish Formations in the northern Black Hills has led to subsidence and collapse, resulting in the development of disrupted bedding, breccia pipes and pinnacles in the Minnelusa, and sinkholes and breccia pipes extending up into the Spearfish and higher formations. Many of these sinkholes in the Spearfish are sites of resurgent springs, where the piezometric surface is above the land surface. Dry, steep-walled sinkholes have been formed where the piezometric surface lies below the bottom of the sinkholes. The largest sinkholes are the result of dissolution of the thick anhydrite in the subsurface Minnelusa, and consequent stoping to the surface. As the dissolution front of the Minnelusa anhydrite moves radially outward from the center of the Black Hills, and as the piezometric surface falls to lower stratigraphic levels while the land surface is lowered by erosion, the present springs will dry up, and new ones will develop down the regional dip. Abandoned sinkholes attest to the former position of these springs. The downdip migration of these springs is exemplified by Mirror Lake, where headward spring migra-

tion resulted from continued sinkhole collapse of the headwall of this steephead valley. The presence of many of the sinkholes within the lower part of the Spearfish may be related to the greater fracturing of that part of the Spearfish owing to downward intrusion of gypsum veinlets. The springs emerge at or near a prominent gypsum horizon. Above that horizon siltstone and shale are highly impermeable, restricting the upward movement of ground water. Appreciation of the processes involved in the formation of gypsum karst should be considered in land-use planning in this increasingly developed part of the northern Black Hills.

## REFERENCES CITED


Agenbroad, L. D.; and Mead, J. I. (eds.), 1994, The Hot Springs Mammoth Site: a decade of field and laboratory research in paleontology, geology, and paleoecology: Mammoth Site of South Dakota, Hot Springs, South Dakota, 457 p.

Bowles, C. G.; and Braddock, W. A., 1963, Solution breccia of the Minnelusa Formation in the Black Hills, South Dakota and Wyoming, *in* Short papers in geology and hydrology: U.S. Geological Survey Professional Paper 475-C, p. C91–C95.

Braddock, W. A., 1963, Geology of the Jewel Cave SW quadrangle, Custer County, South Dakota: U.S. Geological Survey Bulletin 1063-G, p. 217–268.

Brady, F. H., 1931, Minnelusa formation of Beulah district, northwestern Black Hills, Wyoming: American Association of Petroleum Geologists Bulletin, v. 15, p. 183–188.

Brobst, D. A.; and Epstein, J. B., 1963, Geology of the Fanny Peak quadrangle, Wyoming–South Dakota: U.S. Geological Survey Bulletin 1063-I, p. 323–377.

Cox, E. J., 1962, Artesian water, Minnelusa and Pahasapa Formations, Spearfish–Belle Fourche area: South Dakota Geological Survey Special Report 19, 23 p.

Darton, N. H., 1904, Description of the Newcastle quadrangle, Wyoming and South Dakota: U.S. Geological Survey Geologic Atlas, Folio 107, 9 p.

Davis, A. D., 1979, Hydrogeology of the Belle Fourche, South Dakota, water infiltration gallery area: Proceedings of the South Dakota Academy of Science, v. 58, p. 122–143.

Davis, A. D.; and Rahn, P. H., 1997, Karstic gypsum problems at wastewater stabilization sites in the Black Hills of South Dakota: Carbonates and Evaporites, v. 12, p. 73–80.

Davis, A. D.; Beaver, F. W.; and Stetler, L. D., 2003, Engineering problems of gypsum karst along the Interstate 90 development corridor in the Black Hills of South Dakota, *in* Johnson, K. S.; and Neal, J. T. (eds.), Evaporite karst and engineering/environmental problems in the United States: Oklahoma Geological Survey Circular 109 [this volume], p. 255–261.

Epstein, J. B., 1958a, Gravity sliding, brecciation, and structure, Fanny Peak quadrangle, Wyoming–South Dakota [abstract]: Geological Society of America Annual Meeting, 1958, St. Louis, Missouri, p. 56.

_____1958b, Geology of part of the Fanny Peak quadrangle, Wyoming–South Dakota: University of Wyoming unpublished M.A. thesis, and U.S. Geological Survey Open-File Report 454, 90 p.

_____2000, Gypsum-karst collapse in the Black Hills, South Dakota–Wyoming, USA: Acta Carsologica, v. 29, p. 103–122.

_____2001, Hydrology, hazards, and geomorphic development of gypsum karst in the northern Black Hills, South Dakota and Wyoming, *in* Kuniansky, E. L. (ed.), U.S. Geological Survey Karst Interest Group Proceedings, St. Petersburg, Florida, February 13–16, 2001: U.S. Geological Survey Water-Resources Investigations Report 01-4011, p. 30–37.

Epstein, J. B.; and Johnson, K. S., 2003, The need for a national evaporite karst map, *in* Johnson, K. S.; and Neal, J. T. (eds.), Evaporite karst and engineering/environmental problems in the United States: Oklahoma Geological Survey Circular 109 [this volume], p. 21–30.

Gott, G. B.; Wolcott, D. E.; and Bowles, C. G., 1974, Stratigraphy of the Inyan Kara Group and localization of uranium deposits, southern Black Hills, South Dakota and Wyoming: U.S. Geological Survey Professional Paper 763, 57 p.

Hayes, T. S., 1996, Suspended-sediment "reddening" in Cascade Springs, southern Black Hills, South Dakota [abstract]: Geological Society of America Abstracts with Programs, v. 28, no. 4, p. 11.

Jennings, J. N., 1971: Karst: M.I.T. Press, Cambridge, Massachusetts, 252 p.

Klemp, J. A., 1995, Source aquifers for large springs in northwestern Lawrence County, South Dakota: South Dakota School of Mines and Technology, Rapid City, unpublished M.S. thesis, 175 p.

Laury, R. L., 1980, Paleoenvironment of a late Quaternary mammoth-bearing sinkhole deposit, Hot Springs, South Dakota: Geological Society of America Bulletin, v. 91, p. 465–475.

Post, E. V., 1967, Geology of the Cascade Springs quadrangle, Fall River County, South Dakota: U.S. Geological Survey Bulletin 1063-L, p. 443–504.

Rahn, P. H.; and Davis, A. D., 1996, Gypsum foundation problems in the Black Hills area, South Dakota: Environmental and Engineering Geoscience, v. 2, p. 213–223.

Rahn, P. H.; and Gries, J. P., 1973, Large springs in the Black Hills, South Dakota and Wyoming: South Dakota Geological Survey Report of Investigations 107, 46 p.

Raines, M. A.; and Dewers, T. A., 1997, Dedolomitization as a driving mechanism for karst generation in Permian Blaine Formation, southwestern Oklahoma, USA: Carbonates and Evaporites, v. 12, p. 24–31.

Shearman, D. J.; Mossop, G.; Dunsmore, H.; and Martin, M., 1972, Origin of gypsum veins by hydraulic fracture: Transactions of Institution of Mining and Metallurgy, v. 81, p. B149–B155.

Strahler, A. N.; and Strahler, A. H., 1987, Modern physical geography: Wiley & Sons, New York, 544 p.

Thordarson, William, 1989, Hydrogeology of anhydrite, *in* Dean, W. E.; and Johnson, K. S. (eds.), Anhydrite deposits of the United States and characteristics of anhydrite important for storage of radioactive wastes: U.S. Geological Survey Bulletin 1794, p. 95–105.

Wolcott, D. E., 1967, Geology of the Hot Springs quadrangle, Fall River and Custer Counties, South Dakota: U.S. Geological Survey Bulletin 1063-K, p. 427–442.

# Engineering Problems of Gypsum Karst along the Interstate 90 Development Corridor in the Black Hills of South Dakota

***Arden D. Davis***
South Dakota School of Mines and Technology
Rapid City, South Dakota

***Frank W. Beaver***
University of North Dakota
Grand Forks, North Dakota

***Larry D. Stetler***
South Dakota School of Mines and Technology
Rapid City, South Dakota

**ABSTRACT.**—Approximately 80 km of Interstate 90 extends along outcrops of the Triassic Spearfish Formation between Rapid City and Spearfish, South Dakota. The Gypsum Spring Member is near the top of the Spearfish Formation and consists of up to 10 m of massive gypsum. This member has formation status in Wyoming and forms a prominent ridge that is continuous from the Wyoming–South Dakota border southeastward for more than 50 km along I-90. Other scattered gypsum layers are present throughout the 100- to 200-m thickness of the Spearfish Formation in the Black Hills.

Residential and industrial development is accelerating along the I-90 development corridor in the Black Hills, and much of the area is becoming urban or suburban. Although the white gypsum layers typically are prominent and recognizable, new housing and other construction often is built on or near unstable gypsum in the Spearfish Formation, including the Gypsum Spring Member.

Because of increasing development pressure, it is critical that geological engineers and geologists participate in land-use decisions where karstic gypsum is involved. Current initiatives have proposed mapping engineering hazards for the entire I-90 development corridor in the Black Hills to inform the public and local government about potential problems.

## INTRODUCTION AND BACKGROUND

Geological engineering is concerned with the conservation and optimal development of natural resources. In its service to society, this branch of the engineering profession can provide information to elected officials, planners, managers, and regulators for the wise use of resources and the avoidance of geologic hazards. This paper discusses hazards associated with gypsum karst in the context of expanding development in a mixed urban and rural environment.

Engineering problems of gypsum karst can be described in two broad categories: (1) vulnerability of ground water and surface water to contamination, as well as related drainage and water-quality problems; and (2) geotechnical concerns and associated problems, including land subsidence, foundation settlement, soil suitability, and geologic hazards.

Gypsum in the Black Hills area occurs mainly in the Spearfish Formation (Triassic), but it is also present in the Madison (Pahasapa) Limestone (Mississippian), the Minnelusa Formation (Pennsylvanian and Permian), and the Opeche Shale (Permian). The Spearfish Formation forms the "Red Valley" (Fig. 1) and contains numerous gypsum beds in which karstic conditions have developed. The gypsum karst has caused severe engineering problems for foundations, roads, water-treatment lagoons, and other construction.

The Gypsum Spring Member is near the top of the Spearfish Formation and contains up to 10 m of massive gypsum. This member is considered a formation in Wyoming. In the Black Hills, the Gypsum Spring Member forms a prominent ridge that is continuous from the Wyoming–South Dakota border southeastward for more than 50 km. Other, scattered outcrops of gypsum also are prominent in the Spearfish Forma-

Davis, A. D.; Beaver, F. W.; and Stetler, L. D., 2003, Engineering problems of gypsum karst along the Interstate 90 development corridor in the Black Hills of South Dakota, *in* Johnson, K. S.; and Neal, J. T. (eds.), Evaporite karst and engineering/environmental problems in the United States: Oklahoma Geological Survey Circular 109, p. 255–261.

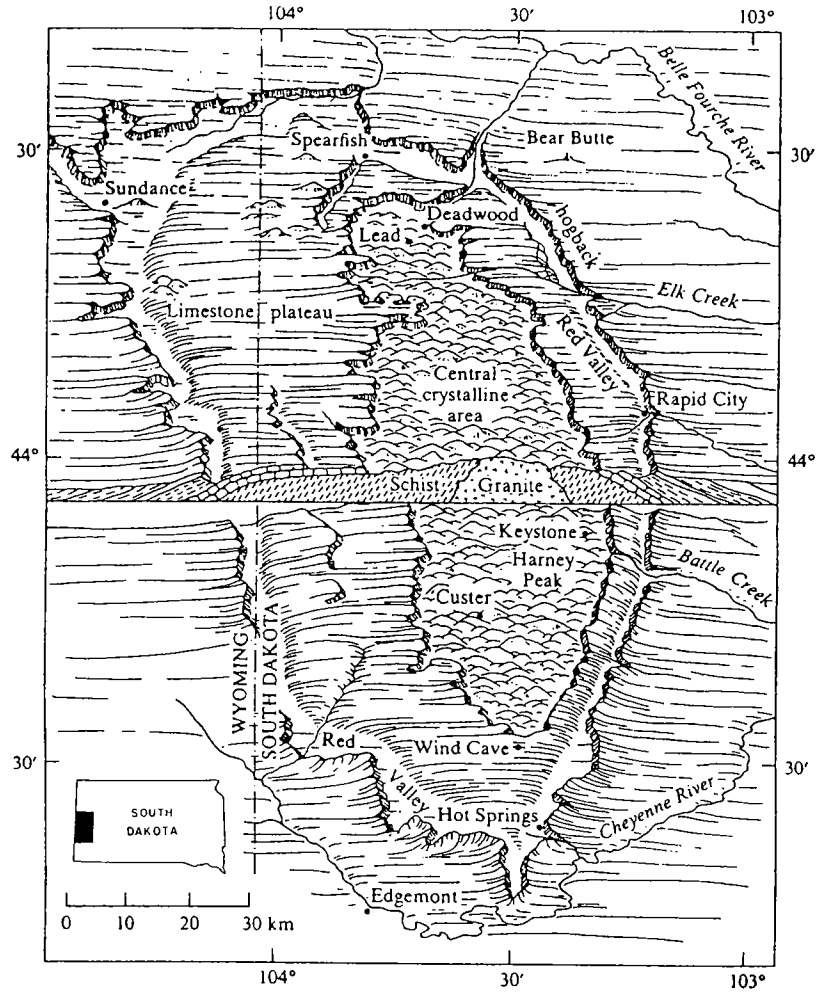


Figure 1. Physiographic diagram of the Black Hills. Note location of Red Valley between Rapid City and Spearfish. Interstate 90 was built predominantly on the Spearfish Formation, which forms the Red Valley (from Strahler, 1960).

tion. In some places, gypsum crops out as small buttes; in other places, sinkholes and caves are common.

The Interstate 90 development corridor, in the Black Hills of western South Dakota, extends along the eastern and northern flanks of the Laramide Black Hills Uplift (Fig. 2). Anchored by Rapid City at its southeastern end and by Spearfish at its northwestern end near the border of South Dakota and Wyoming, this corridor includes the bulk of western South Dakota's population, mainly in Pennington, Meade, and Lawrence Counties. Approximately 80 km of I-90 was built on outcrops of the Triassic Spearfish Formation between Rapid City and Spearfish.

Since the disastrous flood of 1972, development of residential and commercial areas in the eastern Black Hills has expanded from flood plains onto higher ground, including the outcrop of the Spearfish Formation. Almost the entire I-90 corridor between Rapid City and Spearfish, South Dakota, is on outcrops of the Spearfish Formation. Residential and industrial development is accelerating along the I-90 corridor in the Black Hills, and much of the area is becoming urban or suburban. Currently there are no special regulations for construction in these areas, and many contractors view the gypsum as an annoyance because of the difficulty of excavation for foundations, roads, and utility lines.

## ENGINEERING PROBLEMS OF GYPSUM KARST IN THE BLACK HILLS

This paper includes examples of gypsum-karst problems along the I-90 development corridor in the Black Hills. Instances of subsidence in karstic-gypsum areas are occurring with increasing frequency. Typically, sinkholes open suddenly, with collapse of driveways, roads, or yards. Gradual differential settlement of houses and infiltration of water into basements are causes of severe distress to some homeowners.

### Vulnerability of Ground Water and Surface Water

#### *Spearfish Sewage Lagoons*

A dramatic engineering failure on karstic gypsum occurred during the 1970s near Spearfish, South Dakota (Rahn and Davis, 1996; Davis and Rahn, 1997). Sewage lagoons were built above the Gypsum Spring Member of the Spearfish Formation, but they could not retain wastewater. Sewage piped through caverns in the gypsum, pouring into a nearby drainage. The failed lagoons were near the gallery intake of the Belle Fourche water supply, in alluvium along Spearfish Creek. The lagoon site eventually was abandoned. Figure 3 shows a cross section from the water-supply intake to the failed lagoons. Figure 4 is a photograph, looking northeast, along the line of the cross section.

#### *Proposed Whitewood Sewage Lagoon and Artificial Wetlands*

A sewage lagoon and artificial wetlands were proposed in 1988 for the City of Whitewood, South Dakota (see Fig. 2 for location of Whitewood along the I-90 development corridor). The proposed site's geology was similar to the failed Spearfish lagoon site. After an engineering report was submitted, the Lawrence County commissioners tabled the proposal, and the facilities were not built at this site. Figure 5 is a map of geological-engineering hazards at the proposed site. A recent sinkhole is shown in Figure 6.

#### *Western Rapid City*

The western half of Rapid City, South Dakota, lies predominantly on the Spearfish Formation, much within areas of gypsum outcrops. A focus of concern

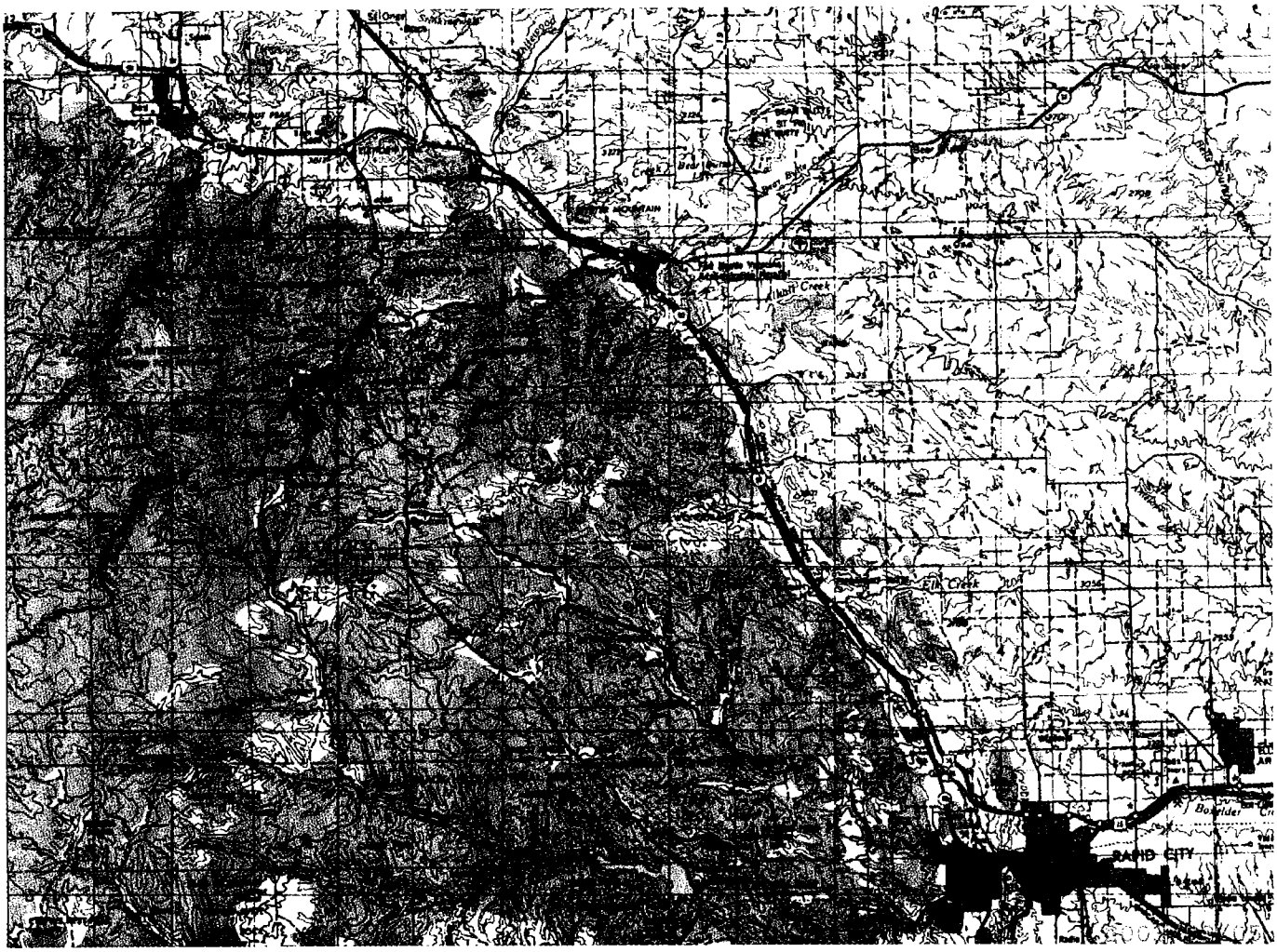


Figure 2. Interstate 90 development corridor between Rapid City and Spearfish, South Dakota (modified from U.S. Geological Survey's 1:250,000-scale Rapid City sheet).

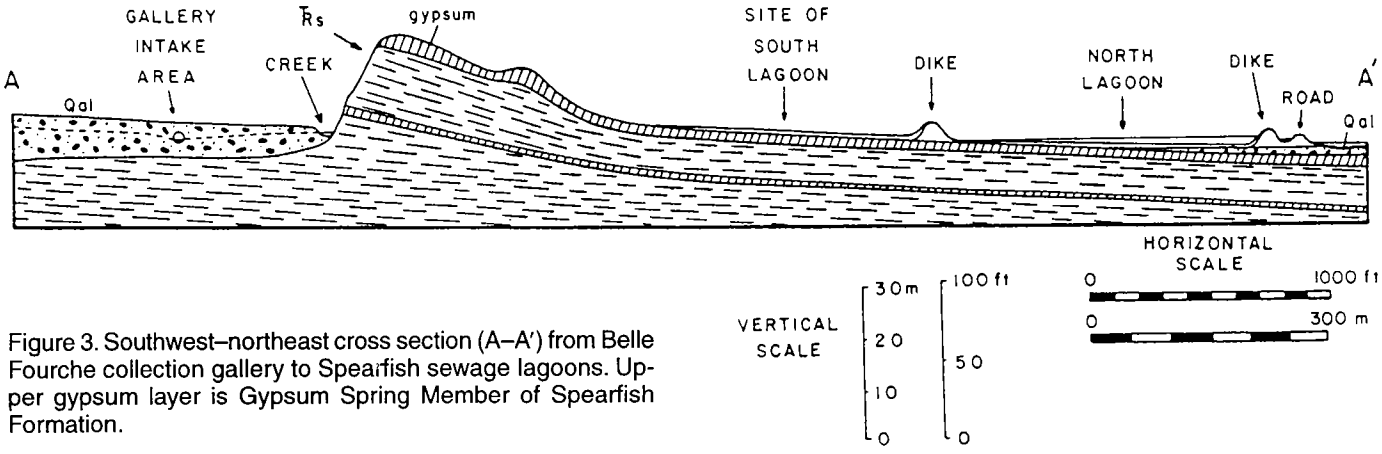


Figure 3. Southwest–northeast cross section (A–A') from Belle Fourche collection gallery to Spearfish sewage lagoons. Upper gypsum layer is Gypsum Spring Member of Spearfish Formation.

in western Rapid City is on-site wastewater-treatment facilities (primarily septic tanks and drain fields) in areas that formerly were outside the city limits. The hydraulic-conductivity contrast between karstic gypsum and the low-permeability shale of the Spearfish Formation can cause problems for treatment of domestic wastewater by soils. In water samples from at least one drainage, DNA ribotyping has confirmed that fecal coliform bacteria were from human sources. Thus, surface water and ground water are vulnerable

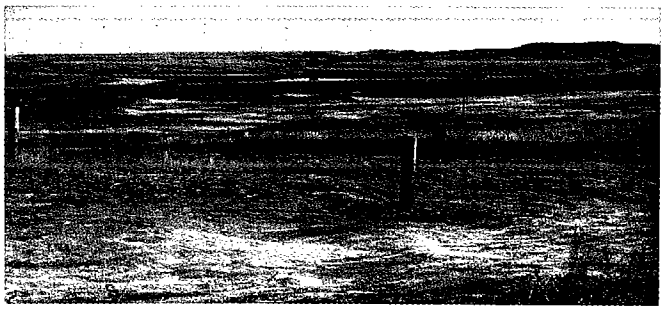

Figure 4. Photograph looking northeast along line of cross section in Figure 3. Note gypsum in foreground and north Spearfish sewage lagoon in middle distance.

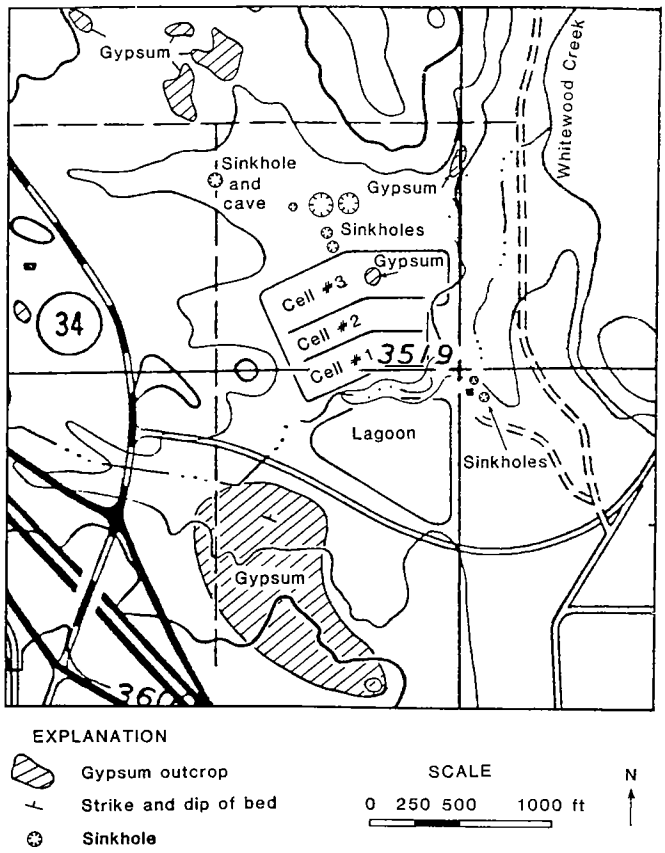


Figure 5. Map of proposed Whitewood sewage lagoon and artificial wetland cells (from Davis and Rahn, 1997).

to wastewater contamination in this geologic setting. Figure 7 shows an example of surface-water drainage near a gypsum outcrop in the basin mentioned above.

### *Piedmont Valley*

Piedmont Valley lies north of the Rapid City limits and is an area of urban expansion along the I-90 development corridor. During the past 25 years, much of the Spearfish Formation's outcrop area in the Piedmont Valley has become urban. In the late 1990s a water-quality-assessment study was undertaken, including an inventory of wells and septic tanks (Royse,

Figure 6. Recent sinkhole near proposed Whitewood sewage lagoon (see Fig. 5). Sinkhole's surface expression is in alluvium above gypsum.

Figure 7. Gypsum outcrop and associated surface-water drainage in western Rapid City.

2000). Analysis by Bartlett and West Engineering (Royse and Matkins, 1998) showed nitrate concerns for 13% of all tested wells, total coliform bacteria in 28% of tested wells, and fecal coliform bacteria in 4% of tested wells. The most likely source of the contaminants appears to be septic tanks and drain fields in the Spearfish Formation.

## Geotechnical Problems and Geologic Hazards

### *Residential and Industrial Development*

The western half of Rapid City during the past 40 years has developed mainly on the Spearfish Formation. Although the white gypsum layers of the Spearfish are prominent and recognizable, new housing and other construction often is built on or near unstable gypsum outcrops (see, e.g., Fig. 8). The areas of greatest damage appear to be associated with natural-cave-fill areas (Rahn and Davis, 1996) where piping and dissolution occur within gypsum. Ouyang (1983) mapped areas of gypsum outcrops in western Rapid City and identified approximately 10 $km^2$ of areas that

Figure 8. House built on gypsum outcrop in western Rapid City.

he classified as either "hazardous," "very hazardous," or "most hazardous." Hazardous areas were defined as higher ground with gypsum outcrops. Very hazardous and most hazardous areas were those with high water tables and great infiltration rates.

Ouyang (1983) identified collapses, piping failure, and sag failures in the Rapid City area. He also developed a conceptual model of subsidence in gypsum in the western part of Rapid City, shown in a west–east cross section in Figure 9.

One of the most instructive examples of what might be anticipated in the future for the I-90 development corridor is urbanization on areas of gypsum of the Spearfish Formation in western Rapid City. As mentioned earlier, Ouyang (1983) identified about 10 $km^2$ of hazardous gypsum areas in western Rapid City. In the 20 years since his work, more than half of that area has been developed. As an example, extensive gypsum outcrops have been mapped in the Spearfish Formation within the area of the southern half of Figure 2. Virtually the entire outcrop of the Spearfish Formation in that area has been developed.

Other areas of concern include differential settling of houses, slope failures, and collapses in streets, driveways, and yards. During the past 25 years, examples of these failures have been documented in most of the communities along the development corridor, including Rapid City, Black Hawk, Piedmont Valley, Sturgis, Whitewood, and Spearfish.

## BLACK HILLS MAPPING INITIATIVE

Residential and industrial development is expanding rapidly along the entire I-90 corridor in the Black Hills. Increased population and simultaneous industrial growth have driven a substantial increase in housing development within Pennington, Meade, and Lawrence Counties. This development has placed increased stress on natural resources, including availability of surface water and ground water, soil and water contamination from improperly designed and sited septic systems, and problems of slope stability and sinkhole development. Development can have a magnified impact on gypsum-bearing formations where increased drainage and runoff exacerbate dissolution. In an era of accelerated growth, it is paramount to identify and protect natural resources and to define potential geologic hazards. Thus, the Department of Geology and Geological Engineering at South

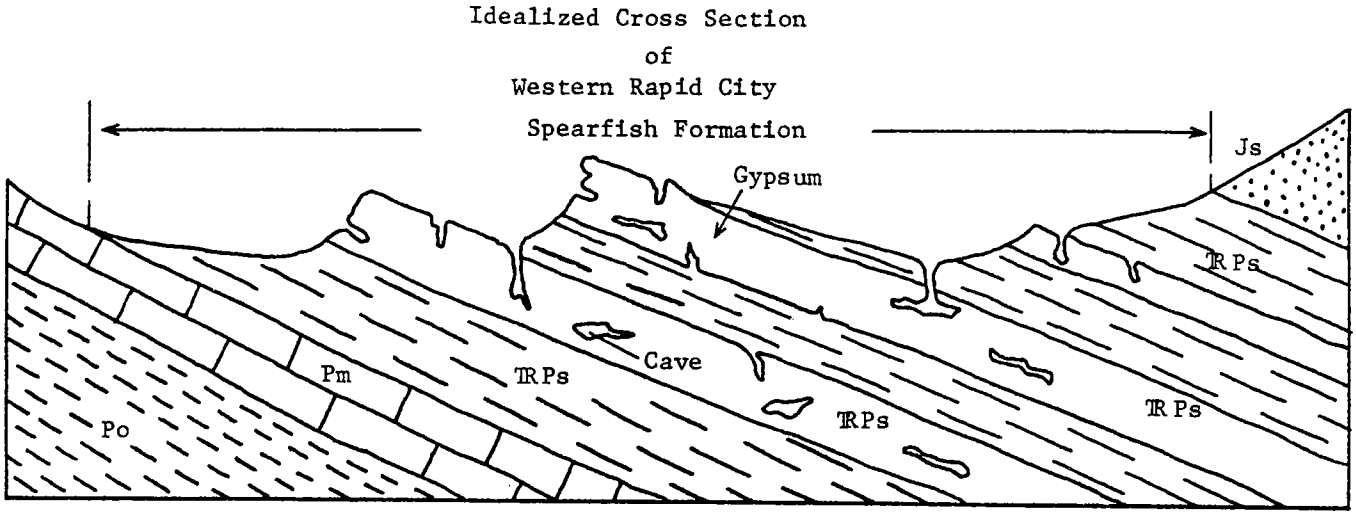


Figure 9. West–east cross section of Spearfish Formation (TRPs) in western Rapid City. Gypsum beds are shown thicker than true dimensions for ease of visualization (from Ouyang, 1983).

Dakota School of Mines and Technology is cooperating with the South Dakota Department of Environment and Natural Resources and the West Dakota Water Development District (a local government entity) in developing the Black Hills Mapping Initiative, an effort to quantify the natural-resource base and identify geologic hazards along the I-90 development corridor.

The primary objective of the Black Hills Mapping Initiative is to compile digital geologic maps for each 7.5-minute quadrangle within the development corridor, showing the natural resources and geological-engineering hazards. Each quadrangle map in the series will consist of a geologic base map of bedrock and surficial deposits. Digital overlay maps will include geologic hazards and numerous other layers as described below.

- Geologic-hazard map series that will ultimately include:

(1) Engineering properties of bedrock and soils;

(2) Slope-stability evaluation of landslide, slump, sinkhole, and earth-movement potential for each geologic formation and soil class as a function of composition, slope, climate, and land use;

(3) Dissolution potential, indicating areas where geologic conditions support or promote dissolution or karstification;

(4) Flood-analysis potential, using established U.S. Geological Survey methods for streams with and without flow records.

- Map of current septic-tank locations for use in identifying susceptible underlying formations and potential for contamination of surface water and ground water.
- Aquifer-sensitivity map, indicating areas where harmful contaminants could most readily enter ground water.
- Potential recharge areas and identification of favorable sites for construction of retention dams.
- Structural-contour maps of major aquifers, using water-elevation data from water wells and structural-contour information.
- Depth-to-water maps, based on the elevation difference between the top of an aquifer and the ground elevation directly above it (from a topographic map). For confined aquifers the top of the aquifer is shown on structural-contour maps; for unconfined aquifers the top of the aquifer is shown by water-table contour maps.
- Economic-resources map, delineating surface distribution of mineral resources of potential economic importance. Identification will be based on distribution of mineralization within formations, field observations, aerial photographs, and remote sensing. The subsurface occurrence of these resources within limits of open-pit mining will also be identified, and the inventories of amounts of each resource in the quadrangle will be estimated.
- Surface-water-resource analysis for each watershed will include drainage-composition studies, demarcation of physical watershed characteristics (morphology), and preparation of regional curves assessing flow characteristics of the watersheds. Many of these parameters are important to, and will be included in, the engineering-hazards analysis described above.

The main outcome from these initiatives will be in the form of residential-development-suitability maps that use all of the above information to assess the suitability of proposed building sites. To ensure protection of natural resources and maintain human occupation of the landscape in a fashion consistent with natural properties, all analyses will focus on variations in material properties and characteristics in spatial and temporal terms. The final products, represented in digital format with a geographic information system, will allow zoning commissioners, planners, engineers, builders, and the general population

to quickly define the physical character of any occupied or proposed building site.

## SUMMARY

The best way to cope with a geological-engineering hazard is to avoid it. There is no substitute for an acceptable site. However, it is unrealistic to expect local planning agencies to completely avoid areas of gypsum in the Spearfish Formation. Much of this land along the I-90 development corridor is prime real estate, and local government agencies are under pressure from developers to keep regulations to a minimum.

South Dakota School of Mines and Technology, along with the South Dakota Geological Survey and the West Dakota Water Development District, has proposed engineering-hazards mapping along the entire I-90 development corridor from Rapid City to Spearfish in the Black Hills. The goals include educating the public and local planning agencies about potential hazards of gypsum, and, where necessary, to point out areas that should be avoided if possible.

## REFERENCES CITED

Davis, A. D.; and Rahn, P. H., 1997, Karstic gypsum problems at wastewater stabilization sites in the Black Hills of South Dakota: Carbonates and Evaporites, v. 12, p. 73–80.

Ouyang, S., 1983, Land subsidence due to gypsum solution in the western part of Rapid City, South Dakota: South Dakota School of Mines and Technology unpublished M.S. thesis, Rapid City, 67 p.

Rahn, P. H.; and Davis, A. D., 1996, Gypsum foundation problems in the Black Hills area, South Dakota: Environmental and Engineering Geoscience, v. 2, p. 213–223.

Royse, K. W., 2000, Piedmont Valley water quality assessment study [abstract], *in* Strobel, M. L.; and Davis, A. D. (eds.), Hydrology of the Black Hills: South Dakota School of Mines and Technology Bulletin 20, p. 213.

Royse, K. W.; and Matkins, C., 1998, Piedmont Valley water quality assessment study: project background, procedures, and vulnerability determinations: Bartlett and West Engineers, Inc., final technical report, Bismarck, North Dakota, 114 p.

Strahler, A. N., 1960, Physical geography: Wiley & Sons, New York, 534 p.

# A Stinking Lake and Perpetual Potholes: Living with Gypsite Karst in Laramie, Wyoming

**Todd Jarvis**
Oregon State University,
Corvallis, Oregon

**Peter Huntoon**
Consultant
Boulder City, Nevada

**ABSTRACT.**—Much of Laramie, Wyoming, is built over gypsite, an earthy weathering product derived from gypsum bedrock in the underlying red beds of the Permian and Triassic formations in the area. Both the gypsum bedrock and gypsite have been mined in the area for >100 years, first for plaster and recently for cement. The gypsite deposits range from 10 to 20 ft thick.

Dissolution of gypsite has produced subsidence features that contain ponds. One of these, LaBonte Lake, has been incorporated into a city park. Soil instabilities under streets, gutters, sidewalks, and foundations are caused by freeze–thaw swelling and dissolution of wetted gypsite. Sinkhole collapses in roads are caused by piping associated with leaking water and sewer lines.

Networks of horizontal conduits dissolved in the gypsite allow for the rapid lateral migration of contaminants. The State of Wyoming has been forced to grant technical impracticability waivers for the remediation of contaminated karst networks, because isolating and removing the pollutants is infeasible owing to the complex permeability and storage characteristics of the karst.

## LOCATION AND HYDROGEOLOGIC SETTING

Laramie is in southeastern Wyoming (Fig. 1), on the eastern side of the Laramie Basin adjacent to the Laramie River. The town occupies the lower part of the gently sloping west flank of the Laramie Range. Elevations in the area climb from about 7,125 ft at the Laramie River to 8,500 ft along Interstate Highway 80 at the crest of the range.

The climate is temperate and semiarid, with wide variations in temperature and precipitation between the summer and winter seasons. The mean annual temperature at the Laramie weather station is 40.7°F; annual precipitation averages 10.17 in. (Martner, 1986).

The Laramie Basin is an intermontane structural basin bounded on the east, south, and west by Laramide foreland uplifts. A Paleozoic through Tertiary section measuring 2.5 mi in thickness occurs within the basin. Those rocks ramp up on the Laramie Range in broad hogbacks, where, as shown in Figure 2, most of the section has been beveled by erosion. The lower part of the section subcropping under Laramie dips to the west at about 3–4°. The hogbacks are held up by resistant limestones that form subdued north–south-trending ridges throughout the area.

The Permian Satanka and Triassic Chugwater red beds contain thick layers up to 60 ft of bedded gypsum and anhydrite, which subcrop below gypsite layers and white gypsum earth soils under much of Laramie. The gypsite is the focus of this article. Ten- to 20-ft-thick deposits of it are the norm. The gypsite is readily mapped in undisturbed areas on the basis of the presence of greasewood (*Sarcobatus remiculatus*), which has an affinity for alkaline soils (Slosson and Moudy, 1900).

Laramie was sited by Union Pacific Railroad surveyors to take advantage of large springs that discharge from the Casper aquifer. These springs are localized along prominent fracture zones (Huntoon and Lundy, 1979). Lesser springs discharge from all the permeable strata exposed low along the flanks of the Laramie Range, including small amounts of water from the red-bed sequences and even from the gypsum itself. Much of that spring and seep flow is derived from circulation of ground water, parallel to the strike of the strata, to gulches eroded perpendicular to strike that dissect the saturated zones. The origin of the water is locally derived recharge along the flank of the Laramie Range, and a minor component of artesian discharge from the Laramie Basin.

## GYPSUM IN THE LARAMIE BASIN

Darton and Siebenthal (1909) identified two classes of gypsum that were quarried in the Laramie Basin: gypsite and rock gypsum. Quarrying commenced in the late 1800s and peaked after the turn of the cen-

Jarvis, Todd; and Huntoon, Peter, 2003, A stinking lake and perpetual potholes: living with gypsite karst in Laramie, Wyoming, *in* Johnson, K. S.; and Neal, J. T. (eds.), Evaporite karst and engineering/environmental problems in the United States: Oklahoma Geological Survey Circular 109, p. 263–269.

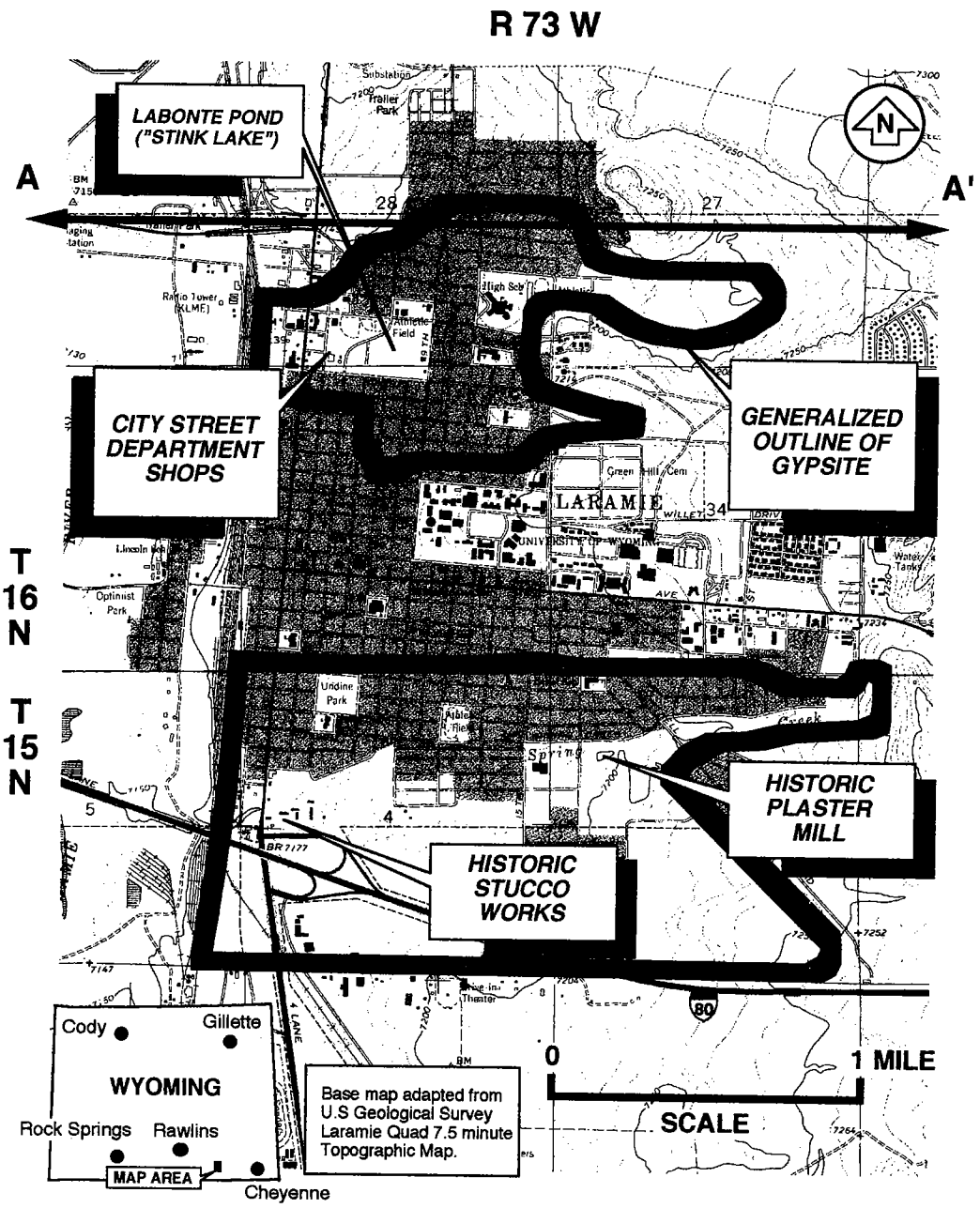


Figure 1. Map showing gypsite deposits and localities in Laramie, Wyoming, mentioned in the text. Line A–A′ is the location of the geologic profile in Figure 2.

tury (Fig. 3). The gypsum was initially used in plaster and stucco mills; today it is used in the manufacture of cement. Active quarrying within the Laramie city limits ceased decades ago.

## Gypsite Occurrence

The Laramie gypsite occurs in the two deposits shown in Figure 1. The northern gypsite bed is <10 ft thick. Most quarrying took place in the southern deposit, which is ~20 ft thick. The turn-of-the-century stucco works shown in Figure 4 was located at what is now the junction of Interstate Highway 80 and U.S. Highway 287. The feedstock for that plant was the high-purity, thick southern deposit. Similarly, a long-gone plaster mill was also located in south Laramie (Fig. 5), where Slosson and Moudy (1900) reported that the gypsite was found "fine as flour," which could be harrowed and scraped up by horse-drawn scrapers and calcined with little to no grinding or sifting.

## Origin of the Gypsite

Sonnenfeld (1984) developed a three-part classification for gypsite deposits, based on modes of emplacement: (1) spring deposits, representing precipitates from gypsum-rich ground-water seeps where the gypsite accumulates in shallow depressions through

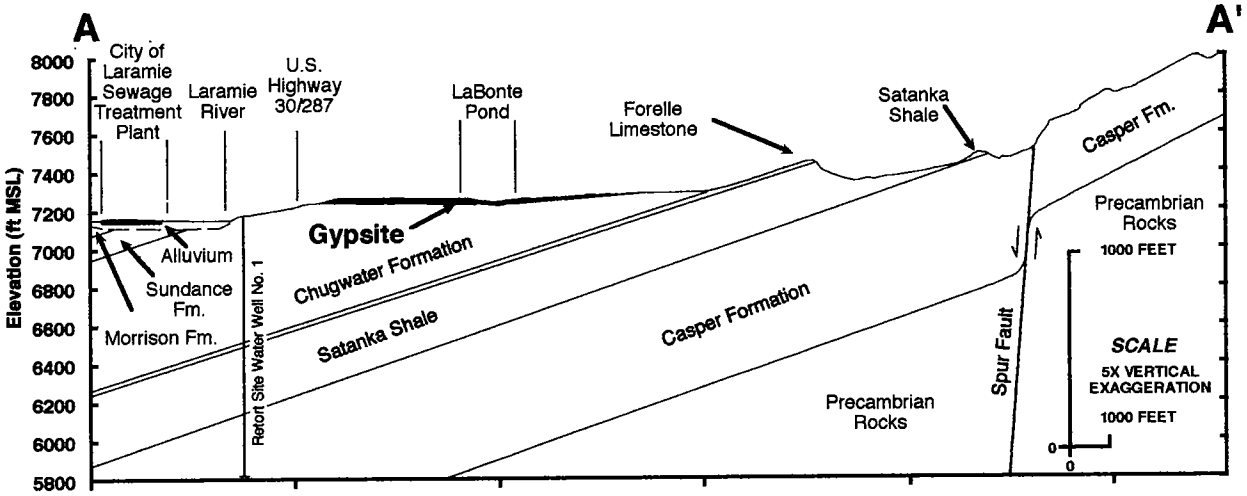


Figure 2. Geologic cross section through Laramie, showing west-dipping Paleozoic and Mesozoic strata, and surficial gypsite deposits. Line of section shown in Figure 1.

Figure 3. May 1891 photograph of a gypsum quarry in bedded gypsum 8 mi south of Laramie. Photo courtesy of University of Wyoming American Heritage Center.

evaporation; (2) blanket deposits, resulting from the downward leaching of gypsum in soils, ultimately forming crusts within the soil; and (3) eolian deposits, formed where wind carries gypsum dust derived from eroding soil crusts or playa deposits to gypsum dune fields. Slosson and Moudy (1900) favored a spring-deposit origin for the Laramie gypsite wherein they proposed that the gypsum was derived from weathering of the red beds and deposited in local depressions.

We tend to favor a spring–eolian origin in which the gypsum is derived from gypsum-rich ground water that was evaporated in low-lying, intermittently dry playas to the west. In this scenario, the gypsum dust was mobilized by prevailing westerly winds during drier, colder climatic intervals and carried eastward to dune fields in hollows along the west flank of the Laramie Range. The gypsum dunes in the White Sands National Monument west of Alamogordo, New Mexico, are a modern analog. The appeal of this model is that it explains the purity and homogeneity of the Laramie gypsites, the spatial distribution of the deposits in what were shallow valleys, and the absence of significant percentages of other detritus.

## LABONTE PARK AND KARSTIFICATION

LaBonte Lake (Fig. 1) fills a large subsidence structure caused by dissolution of the gypsite substrate. The pond, locally called "Stink Lake" because of a sulfurous odor emanating from it during the summer months, is situated on the northern Laramie gypsite deposit.

Local myth attributes the origin of LaBonte Lake to quarrying of the gypsite. However, old topographic and city-planning maps dating back to the early 1900s document that two natural ponds existed in the LaBonte Park area. Aerial photographs dating to the 1940s revealed no ground disturbances near the ponds consistent with past mining, but rather the opposite. One of the lakes, and surrounding low swampy ground,

Figure 4. Turn-of-the-20th-century photograph of the stucco works, Laramie. Photo courtesy of University of Wyoming American Heritage Center.

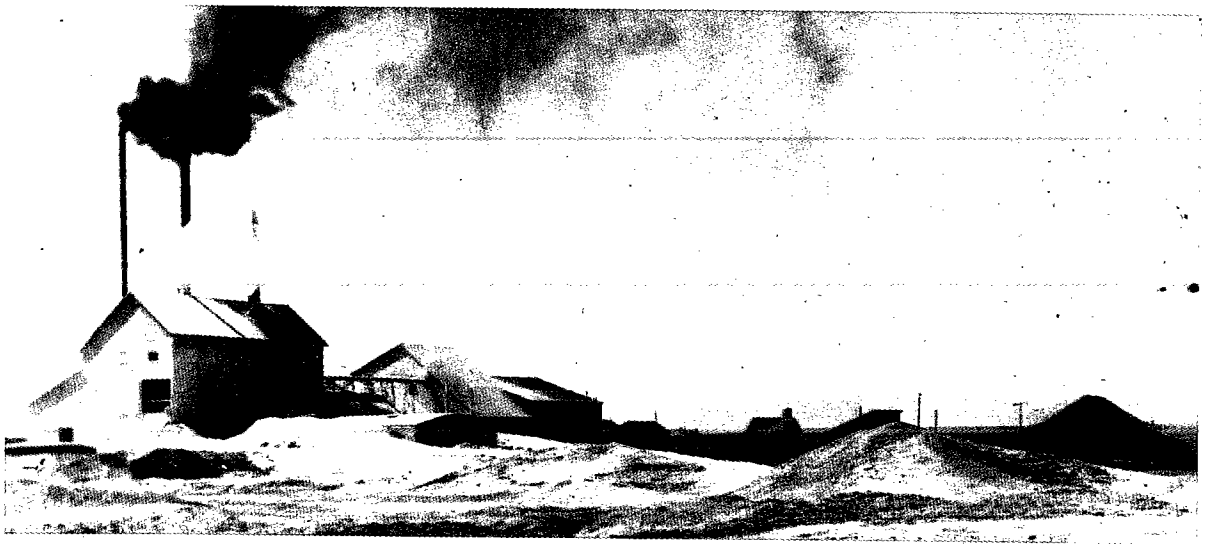

Figure 5. Photograph (1906) of the Overland Cement Plaster Company mill, Laramie. Photo courtesy of University of Wyoming American Heritage Center.

were being actively infilled with trash and fill. Ultimately, the westerly pond was infilled under the area that is now part of the city street department shops and commercial areas to the west along Third and Fourth Streets, and the easterly pond was developed as the center of LaBonte Park.

The subsidence origin for the ponds can be deduced from two complementary suites of borings. The first were made by personnel of Empire Laboratories, Inc. (1983), to evaluate the stability of the lake bottom to allow for construction of an island in the center of the pond complete with picnic facilities. These imaginative workers drilled a transect across the lake by boring through the ice in the dead of winter to reach the lake floor. More recently, borings made by JMM (James M. Montgomery Consulting Engineers, Inc., 1989) were for the purpose of delineating hydrocarbon plumes thought to have originated in the vicinity of the street department shops, thus extending the line of boring data appreciably to the west of the lake.

The results are summarized in Figure 6. Notice how the black organic clay and overlying sediments are downfolded into the depression under the pond. This profile is consistent with dissolution of the underlying gypsite and subsidence of the overburden, not with quarrying.

The character of the cavities in a dissolving section of the gypsite was revealed in trenches in the vicinity of the street department shops dug in the course of utility repairs (Fig. 7). A two-dimensional maze of interconnected, small, saturated, horizontal dissolution conduits and cavities was exposed near the top of the gypsite deposit. Water flowed freely from some of the tubes, which were demonstrated to be laterally extensive from ground-penetrating-radar profiles (Fig. 8). Thus the trench provided a view into an area that will eventually subside as the cavities continue to enlarge and collapse, the mechanism we believe operated to create the subsidence zone now occupied by LaBonte Lake.

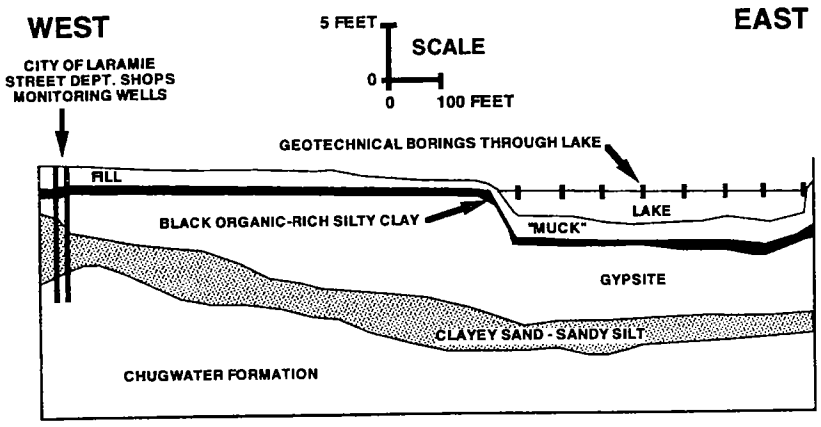


Figure 6. Cross section through LaBonte Lake, Laramie, showing subsidence of surficial strata under the lake. The infolding of the surficial strata is interpreted as evidence for dissolution of the upper part of the gypsite and subsidence of the overburden during development of the basin.

## ENVIRONMENTAL AND ENGINEERING PROBLEMS

### Perpetual Potholes

Slosson and Moudy (1900) reported that the water content in the gypsite approaches 30%. Instabilities under streets, gutters, sidewalks, and foundations are caused by freeze–thaw swelling and dissolution of the wetted gypsite. The cold temperatures during prolonged winters, coupled with the large water content, lead to blistering of road pavement. Similarly, gutters and sidewalks are heaved, buckled, and cracked. Most houses built on the Laramie gypsite deposits are constructed without basements because of past problems with aggressive alkali rot and buckling of the cement foundations.

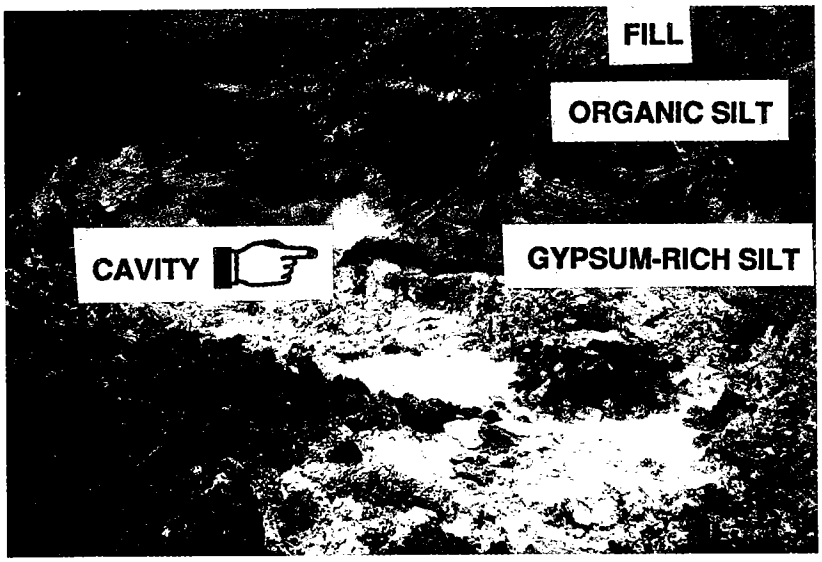


Figure 7. Small water-bearing conduit in the upper part of the gypsite exposed by a utility trench in the vicinity of the street department shops, Laramie.

Sinkhole collapses (Figs. 9, 10) develop rapidly, and are usually caused by piping in the gypsite attending leaking water and sewer lines. Sewer lines composed of unsealed jointed pipes are a particular nuisance. Leakage from the unsealed joints dissolves shafts below the joints that progressively capture larger percentages of the flow. Soon, insufficient fluid remains within the sewer lines to transport the solids, and they settle out and clog the lines. The clearing of such plugs does not solve the problem, so repeated calls to plumbers prove futile.

### Contaminant Distribution in Gypsite Deposits

Extensive underground-storage-tank (UST) investigations were undertaken at the City of Laramie Street Department Shops in response to ground-water contamination identified by Delta Environmental Consultants, Inc. (1989), and JMM (1989). The Wyoming Department of Environmental Quality (DEQ) determined that no further action regarding the UST site investigations was required in October 1991, because residual-contamination concentrations of fuel-related volatile organic compounds and petroleum hydrocarbons did not exceed U.S. Environmental Protection Agency (EPA) drinking-water standards and DEQ's standards for the class of ground water at the site.

DEQ personnel detected trace concentrations of tetrachloroethene (PCE) in two of the four site-monitoring wells. The source for the PCE at the site is unknown, but it may have been related to past landfilling in the area. Exhumed bottles were clearly labeled dry-cleaning fluid, a common source of PCE. Another potential source was PCE in fire-extinguishing compounds used to suppress a fire that destroyed buildings on the site in the 1940s.

Pumping tests of wells drilled in the gypsite spaced 50 ft apart exhibited yields that varied from 1 to 10 gallons per minute. Such variability is consistent with

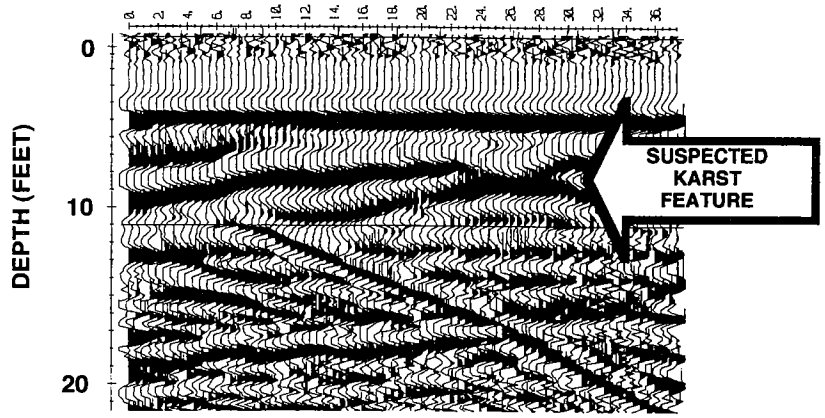


Figure 8. Ground-penetrating-radar profile near the street department shops, Laramie, showing a suspected dissolution zone in the gypsite. Profile courtesy of Scott Smithson, University of Wyoming Department of Geology and Geophysics.

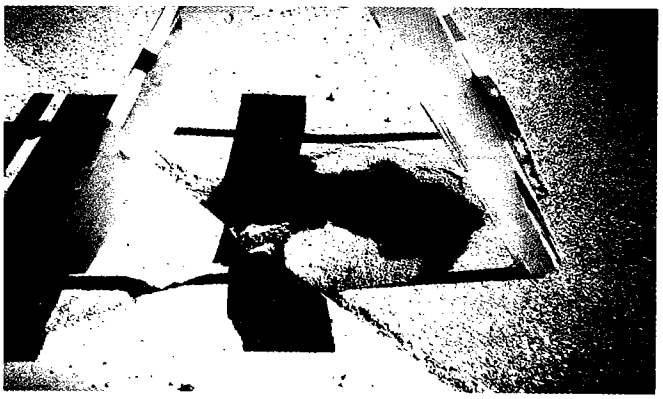

Figure 9. Collapse of asphalt next to a seam between a concrete gutter and the asphalt pavement owing to dissolution of the underlying gypsite, Laramie. Foster White photo.

Figure 10. Sudden collapse in alley caused by piping in the underlying gypsite, Laramie. Foster White photo.

the karstic-permeability distribution observed in the utility trench. PCE concentrations varied from nondetectable in the high-yield wells to 30 micrograms per liter in a low-yield well. The water extracted from the interconnected high-yielding karst features carried the smallest concentrations of contaminants. In contrast, wells drawing from zones having small permeabilities yielded elevated levels of contamination derived from local storage. Flushing contaminants from the zones of small permeability was deemed infeasible, because circulation in the surrounding karst conduits would bypass the contaminated zones.

Experience gained during the past few decades at both Superfund and Resource Conservation and Recovery Act Corrective Action sites with heterogeneous and anisotropic karstified rocks, such as those described here, has demonstrated that restoration to drinking-water standards using available technologies usually is futile. This has led EPA personnel to develop criteria for issuing Technical Impracticability Waivers for such sites.

The Wyoming Department of Environmental Quality has no formal regulations that parallel the EPA Technical Impracticability Waiver process. However, using the impracticability philosophy, State officials deemed that cleanup at the street department shops was impractical on the basis of the heterogeneous character of the gypsite karst and the presence of naturally occurring highly mineralized water at the site. They ruled "no further action at this time" with respect to PCE contamination in the gypsite karst.

## CONCLUSIONS

Gypsum and gypsite have been a historic resource for the Laramie economy; however, ongoing costs are associated with living on these rocks. Freeze–thaw blisters in pavement become potholes in short order. Heaving of concrete structures of all types is costly. The only cost-effective remedy is to excavate the upper couple of feet of the gypsite and replace it with geotextiles that promote drainage, and to cover those with an imported road base. Piping associated with water- and sewer-line leaks is a continuing maintenance challenge, costly both for the utilities operators and landowners. What appears to be a simple plugged sewer pipe turns into an expensive excavation project as carefully laid pipes with well-sealed connections replace the old.

The capture and containment of pollutants released into the gypsite aquifer are technically impracticable. Although it is sometimes possible to detect conduits within the gypsite with surface geophysical methods, it is virtually impossible to recover the contaminants once the conduits are drilled. The problem is, as in all karst, the removal of contaminants from a so-called dual-porosity aquifer, one in which large-capacity, interconnected conduits allow higher quality water on its way to recovery wells to bypass contaminants in storage in the intervening zones of low permeability. As soon as

pumping ceases, contaminant concentrations begin to rise as the bypassed fluids leak into the conduits.

Dissolution and piping of the Laramie gypsite are rapid. Water-line leaks and storm water migrating along cracks in gutters or openings around tree roots facilitate the dissolution of the gypsite. Collapses can be sudden.

## ACKNOWLEDGMENTS

Harold Colby, City of Laramie Street Department Superintendent, provided historic documents on contamination investigations and allowed us to study the gypsite karst at the Street Department Shops using trenching and various geophysical techniques. Scott Smithson, of the Department of Geology and Geophysics at the University of Wyoming, led efforts to detect shallow karst features with ground-penetrating-radar equipment. Foster White, of the South Laramie Water and Sewer District, provided photographs of sinkholes in the Laramie area. The City of Laramie Engineering Department made available geotechnical reports pertaining to LaBonte Lake. Historic photographs of the gypsum quarry, stucco works, and plaster mill are courtesy of the University of Wyoming American Heritage Center. Jon King, Utah Geological Survey, critiqued the manuscript.

## REFERENCES CITED

Darton, N. H.; and Siebenthal, C. E., 1909, Geology and mineral resources of the Laramie Basin, Wyoming: U.S. Geological Survey Bulletin 364, 81 p.

Delta Environmental Consultants, Inc., 1989, Laramie technical investigation, vols. 1 and 2: Consultant's report prepared for Wyoming Department of Environmental Quality, Cheyenne.

Empire Laboratories, Inc., 1983, Report of a geotechnical investigation for renovation of LaBonte Lake, Laramie, Wyoming: Consultant's report prepared for City of Laramie, Wyoming.

Huntoon, P. W.; and Lundy, D. A., 1979, Fracture controlled ground-water circulation in the vicinity of Laramie, Wyoming: Ground Water, v. 17, p. 463–469.

James M. Montgomery Consulting Engineers, Inc. (JMM), 1989, Report of contamination investigations at the Street Department Shops: Consultant's report prepared for City of Laramie, Wyoming.

Martner, B. E., 1986, Wyoming climate atlas: University of Nebraska Press, Lincoln, 432 p.

Slosson, E. E.; and Moudy, R. B., 1900, The Laramie cement plaster: Published as part of Tenth Annual Report of Wyoming College of Agriculture and Mechanics.

Sonnenfeld, P., 1984, Brines and evaporites: Academic Press, New York, 580 p.

U.S. Geological Survey, 1976, Laramie, Wyoming, 7.5-minute topographic-quadrangle map, scale 1:24,000.

# The Money Pit: Karst Failure of Anchor Dam, Wyoming

***Todd Jarvis***
Oregon State University
Corvallis, Oregon

**ABSTRACT.**—Anchor Dam, a 200-ft-high thin-arch concrete dam, ~35 mi west of Thermopolis, Wyoming, was constructed by the U.S. Bureau of Reclamation at a cost of >$7 million during the dam-building boom of the 1950s and 1960s. Sinkholes and earth fissures within the reservoir area allowed drainage of the reservoir to karstic gypsum units in the underlying Triassic Chugwater and Dinwoody Formations, and in the Permian Park City Limestone, Phosphoria Formation, and Goose Egg Formation before, during, and after construction. In addition, caverns encountered in carbonate strata within the Pennsylvanian Tensleep Formation, which forms the abutments, required grouting during construction at significant additional cost. The reservoir and dam were doomed from the beginning by these two karst systems. The irony is that both the gypsum- and the carbonate-karst systems were identified prior to and during dam construction by U.S. Bureau of Reclamation personnel.

## INTRODUCTION

Anchor Dam was constructed by the U.S. Bureau of Reclamation during the dam boom of the late 1950s and early 1960s. Frequently referred to as a "boondoggle" and a textbook example of where not to build a dam, the notoriety of Anchor Dam has served as an example of the value of geologic investigations prior to constructing engineering projects. However, the conventional explanation for failure of the reservoir to hold water is that the dam and reservoir area are located on the Mississippian Madison Limestone, a recognized karstified limestone with numerous caves.

A review of the earliest mapping of the area, coupled with the technical records of design and construction, reveals that the dam was constructed on the carbonates and sandstones of the Pennsylvanian Tensleep Formation. These same maps show the reservoir area being underlain by the red beds and gypsum units of the Triassic Chugwater and Dinwoody Formations, as well as by the Permian Phosphoria Formation. Explanations for the more than 50 sinkholes documented in the reservoir area, as provided by U.S. Bureau of Reclamation and U.S. Geological Survey personnel, included (1) piping of fine-grained material in the alluvial overburden that led to development of a cavity within the overburden, the roof of which subsequently collapsed to form the sinkhole; (2) collapse and sluicing of alluvium into solution-widened joints and fractures in the underlying Tensleep sandstone and carbonate bedrock; and (3) dissolution of gypsum in the red beds (U.S. Bureau of Reclamation, 1962).

Dam construction proceeded despite sinkholes forming before and during construction, and even after caves were found during excavation of the dam abutments. The U.S. Bureau of Reclamation invested 4 years in construction and nearly 30 years in attempts to repair a reservoir that failed to ever store water, no matter the remedy attempted. Perhaps the story behind the continued efforts to salvage Anchor Dam was based less on need and more on politics. The political tale of Anchor Dam is documented by Lindholm (1997).

## LOCATION AND GEOGRAPHIC SETTING

Anchor Dam is in the southwestern part of the Bighorn Basin of Wyoming, along the South Fork of Owl Creek (Fig. 1). The topography of the basin is dominated by plains and badlands ranging in elevation from 4,000 to 6,500 ft above sea level that are drained by the Bighorn River. Owl Creek is a prominent tributary of the Bighorn River, and the Bighorn River in turn is a tributary of the Missouri River.

## OVERVIEW OF ANCHOR DAM

The U.S. Bureau of Reclamation (1962) designed Anchor Dam to provide supplemental irrigation water for the Owl Creek Irrigation District, and also to provide for recreation and for fish and wildlife conservation. The active capacity was 17,254 acre-ft of water stored behind a thin-arch concrete dam with a structural height of 208 ft. The dam widens downward from 13.7 ft at the top to 54.2 ft at the base. The crest length spans 660 ft in a graceful, concave-downstream arch. An uncontrolled overflow weir in the center with a ski-jump–type bucket constitutes the spillway (U.S. Bureau of Reclamation, 1962).

Proposals for a dam at the Anchor Dam site have a long history, dating back to the early 1900s (Lindholm, 1997). According to Milek (1986), "water problems

Jarvis, Todd, 2003, The money pit: karst failure of Anchor Dam, Wyoming, *in* Johnson, K. S.; and Neal, J. T. (eds.), Evaporite karst and engineering/environmental problems in the United States: Oklahoma Geological Survey Circular 109, p. 271–278.

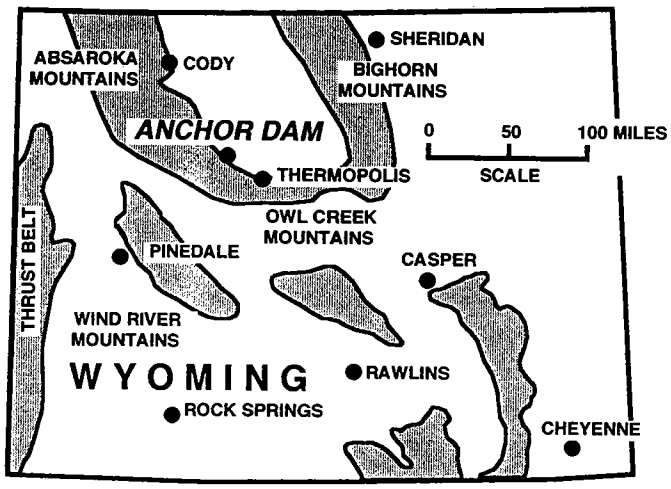


Figure 1. Map showing location of Anchor Dam in the Bighorn Basin of Wyoming.

developed early on Owl Creek . . . ." A local newspaper in 1897 reported that "during the dry season water completely disappears in spots (on Owl Creek) . . . ." The loss of water during low-flow conditions apparently caused no second thoughts about building the Anchor Dam site, and in 1910 several local dignitaries visited the site and had preliminary plans drawn up. Geologic studies were conducted by S. H. Knight, State Geologist and Chair of the University of Wyoming Geology Department, during the 1930s (Knight and Hurwitz, 1935). In 1944, passage of the Flood Control Act authorized the Pick–Sloan plan for the Missouri River Basin, which included Anchor Dam.

Anchor Dam was selected not because of water-storage or flood-control needs (the project was regularly rejected for funding prior to 1944), but rather because the Flood Control Act "resuscitated the Anchor Dam proposal as well as many other questionable water projects in the Missouri River's upper basin" (Lindholm, 1997). The project was funded in 1956, and construction commenced in 1957 (U.S. Bureau of Reclamation, 1962). The outlet gates were closed in late 1960, but the reservoir never held more than a small pond.

The U.S. Bureau of Reclamation reported a total project cost of $5.2 million, nearly $1.8 million more than the $3.4 million originally budgeted for the project in 1962. By 1997, the total costs exceeded $7.0 million, which, if adjusted for inflation, would approach $25 to $30 million in 2000 dollars. The majority of the identified extra expenditures were change orders associated with grouting the abutments and attempts since the 1960s to plug or isolate sinkholes in the reservoir area.

Excavation of rubble from a solution cavity in the north abutment had to be done by hand and added almost a year to the construction of the dam. Sometime in the 1970s the dam was made a government research installation, so the continued costs associated with remediation could not be accurately tracked (Lindholm, 1997). Because the reservoir still could not be made to hold water, drastic cures were proposed in 1984, including lining the reservoir floor with plastic or concrete for a cost estimated at $20 to $70 million (Lindholm, 1997).

## REGIONAL GEOLOGIC SETTING

The 8,000-mi$^2$ Bighorn Basin is a typical structural basin in the Rocky Mountain foreland province (Fig. 1). Such basins are broad, north–south-elongated, asymmetric synclinal downwarps, terminated on the west by mountain ranges—in this case the Absaroka and Beartooth Ranges—that have overridden the basins along huge west-dipping thrust faults. The eastern basin parameters commonly are characterized by grand, west-dipping hogbacks falling away from mountain uplifts that in turn are thrust over the next basin to the east: in this case the Bighorn Mountains crowding into the Powder River Basin. The structural relief of the Paleozoic rocks between the crest of the Bighorn Mountains and the basin interior is ~6 mi. This grand structural framework was the result of east–west crustal shortening during the Late Cretaceous–late Eocene Laramide orogeny.

A Paleozoic and younger sedimentary section measuring 4 mi thick fills the interior of the basin, resting on a deeply down-bowed Precambrian crystalline basement. The sedimentary rocks ramp up along some of the mountain uplifts, where they have been beveled by erosion. The result is grand, basinward-tilted hogbacks with long, linear ridges that parallel the mountain ranges which are held up by the more resistant strata.

If you drive into the Bighorn Basin on U.S. Highway 20, you pass though the spectacular Wind River Canyon south of Thermopolis. Each of the Paleozoic and Mesozoic units along the way is labeled by highway department signs, which list the formation names and ages. Immediately upon exiting the canyon, broad expanses of Goose Egg and Chugwater red beds come into view. Each contains conspicuous solution-collapse features (Cooley and Head, 1979). Most of the basin interior is mantled by Tertiary and younger gravels and silt, the flat-lying surficial materials that dominate the vistas north of Thermopolis.

Smaller scale but laterally extensive folds and faults are superimposed on the rocks along, and interior to, the margins of the Bighorn Basin. These, too, are a series of asymmetric anticlines and synclines. Typically, the anticlines are sharply folded Paleozoic and Mesozoic strata cored by west-dipping reverse faults, some with several thousands of feet of displacement. The strata to the west of the anticlines dip gently into the adjacent syncline to the west. To the east, the beds dip steeply or are even overturned into the syncline to the east.

Long, north–south-trending ridges commonly demark the anticlines, their crests held up by particu-

larly resistant strata. One such is Anchor Anticline. A gap eroded through the ridge by Owl Creek was selected as the perfect site for Anchor Dam.

## GEOLOGY OF THE RESERVOIR SITE

Knight and Hurwitz (1935) prepared the first geologic map of the Anchor Dam site and reservoir area. The reservoir area is in a syncline. The floor of the reservoir rests on the red beds and gypsum deposits of the Triassic Chugwater Formation (Fig. 2). The abutments for the dam were placed on the resistant sandstones and carbonates of the Tensleep Formation on the west limb of Anchor Anticline (Fig. 3), and the reservoir was developed west of the resistant strata.

The dam site was ideal in terms of geometry. The gap eroded by Owl Creek through Anchor Anticline was a narrow, deep canyon. Its width minimized the length of the dam. The west-dipping resistant strata exposed in both canyon walls seemed perfect for anchoring the abutments of the structure.

While Knight and Hurwitz (1935) recognized that gypsum beds were characteristic of the Chugwater Formation, they reported that no gypsum beds were found in the Chugwater Formation underlying the proposed reservoir. They concluded: "No avenues of escape are known whereby large water losses would be encountered within the enclosing contour of the reservoir site." They failed to heed the observation of local rancher Henry Freudenthal, who stated in 1931 "that there would be a significant loss of water where it crossed the redbeds" (Milek, 1986). According to Lindholm (1997), Knight later developed reservations about the geologic suitability of the site for the reservoir, in the 1950s.

## GYPSUM KARST UNDER THE RESERVOIR

In 1955, U.S. Bureau of Reclamation personnel discovered a sinkhole on the north side of the proposed reservoir area that apparently had formed in 1952. The sinkhole was 30 ft in diameter and 35 ft deep (Fig. 4). Exploratory drilling revealed no evidence of gypsum except for a 0.25-in. seam in one hole; other drill holes revealed several gypsum seams up to 1 in. thick elsewhere in the reservoir area. Absent evidence that the sinkhole was related to rock gypsum, the U.S. Bureau of Reclamation (1962) suggested that fluctuating ground water had "piped out the fines from the

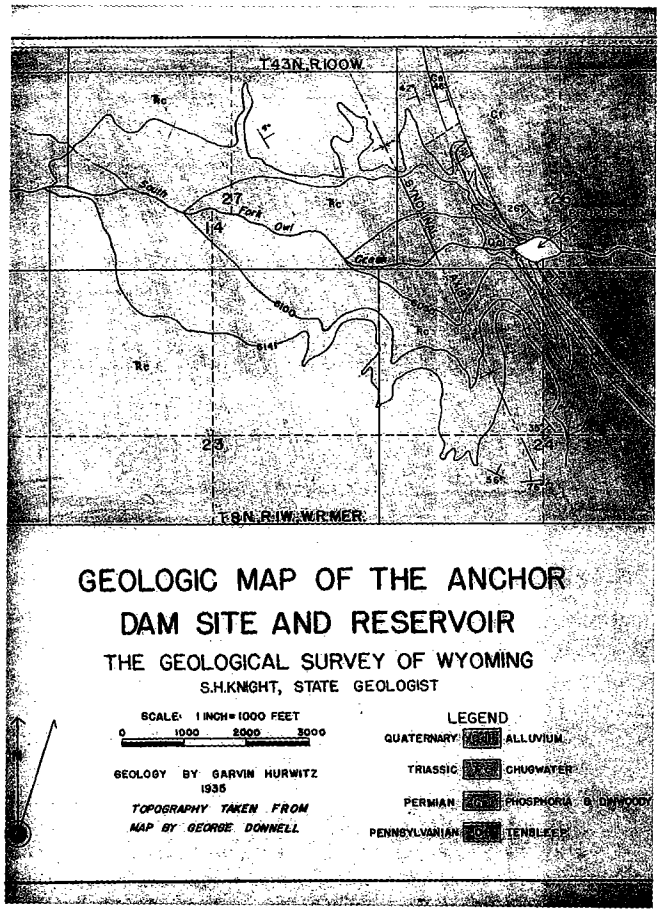


Figure 2. Geologic map of the Anchor Dam site prepared by Knight and Hurwitz (1935).

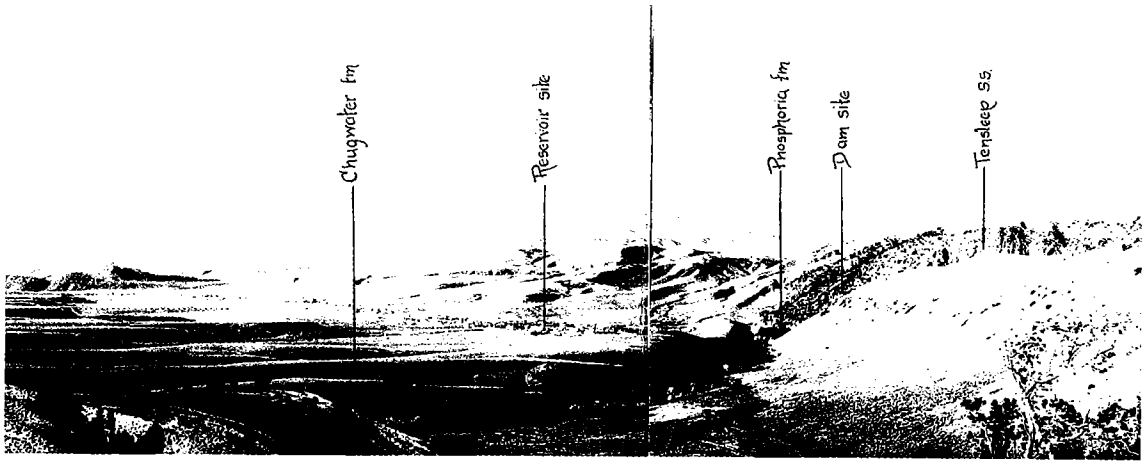


Figure 3. Historic photograph of Anchor Dam reservoir and dam site from Knight and Hurwitz (1935). View is toward north. Wyoming Geological Survey photograph.

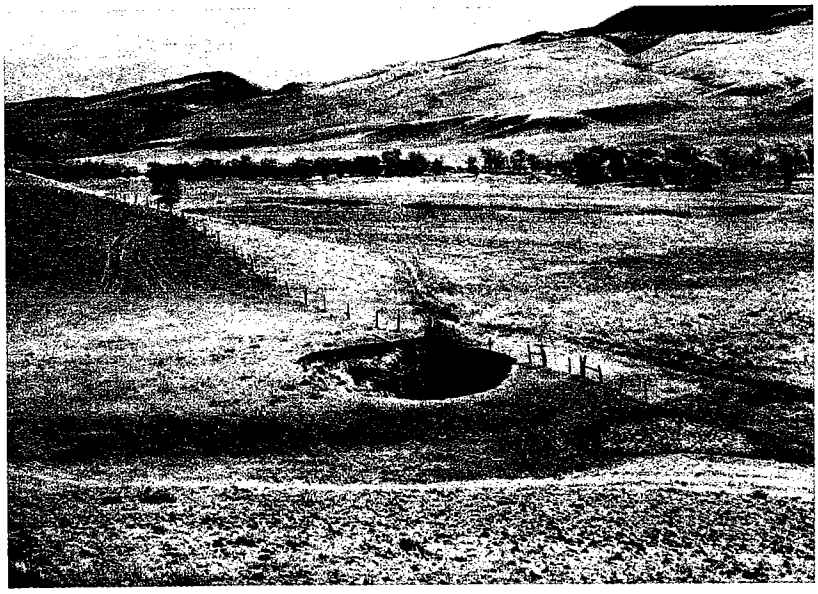

Figure 4. Contemporary photograph of the 1952 sinkhole. Reproduced from U.S. Bureau of Reclamation (1962).

overburden and so developed a cavity within the overburden the roof of which collapsed in 1952 to form the sinkhole."

Other sinkholes and earth fissures formed in the reservoir area early during dam construction and were subsequently backfilled with "selected material and settled by saturation with water." Later field studies by U.S. Bureau of Reclamation geologists during construction discovered "an outcrop of a thin bed of gypsum at the base of the Chugwater shale and overlying the Dinwoody shale . . . upstream from the reservoir . . . and that backfill of the sinkholes with suitable impervious material was all that was necessary to prevent reservoir leakage" (U.S. Bureau of Reclamation, 1962).

The closing of the outlet gates of Anchor Dam in late 1960 should have heralded filling of the reservoir. However, a large "crack" formed in 1961, and almost 90,000 $yd^3$ of material was missing 1,000 ft upstream from the dam (Lindholm, 1997). The associated sinkhole (no. 3) had a reported diameter of nearly 300 ft and a depth of 40–60 ft (Fig. 5). U.S. Bureau of Reclamation geologists speculated that the sinkhole developed by sluicing of material from the Chugwater, Dinwoody, and Phosphoria (Goose Egg) Formations into the deeper Tensleep Formation (see Fig. 6). The observation that cores retrieved by the Bureau from the bedrock underlying other sinkholes were undisturbed indicates that local dissolution of gypsum in the red beds is a more plausible explanation for the sinkholes.

An earthen dike was constructed around sinkhole no. 3, but the height of the dike was below the crest of the dam (Fig. 7). When the dike was completed in 1976, the reservoir volume lost to the diked-off area, and the reduced pool depth exceeded 50% of the original design volume. Specifically, the design capacity had been reduced from 17,254 to 7,910 acre-ft. Lindholm (1997) noted that U.S. Bureau of Reclamation reports pertaining to the Anchor Dam project began to dwindle in the late 1970s, and the sinkhole count was up to 54 in the reservoir area.

Voight (circa 1968) indicated that gravimetric and standing-wave geophysical surveys were successful in determining the locations of other potential sinkholes (Fig. 8) in the reservoir area. In a study along the Nowood River, floored by the same rocks 60 mi to the northwest, Cooley and Head (1979) used surface resistivity surveys to identify above-average thicknesses of alluvial deposits. They concluded that these excess thicknesses were the result of solution cavities up to 75 ft in diameter and 45 ft in depth in the Goose Egg Formation.

## GEOLOGY AT THE DAM SITE

Mapping by Knight and Hurwitz (1935) placed the dam site within the Tensleep Formation in the west-dipping limb of Anchor Anticline (Figs. 2, 3). They noted that the sandstones at the site were extensively jointed, with three sets of joints: two sets in vertical to near-vertical orientation, and a third irregular set cutting the other two sets at high angles. They considered that the movement of water through these cracks would "not be sufficient to permit piping through the bed rock, thereby entailing large water loss."

The permeability architecture within a typical anticline in the Bighorn Basin is unfavorable for anchoring dams. Field and subsurface data compiled by Jarvis (1986) reveal that extensional fractures and small-scale normal faults tend to parallel the strike of the folds. Fracture density is greatest along the axes of the anticlines, and the fractures occur as near-vertical sets of joints like those noted by Knight and Hurwitz (1935) at Anchor Anticline. Such extended fractures greatly increase the permeabilities of rocks in the hanging walls of the anticlines, especially parallel to strike. The permeability problem is particularly onerous where ground-water circulation has further enhanced permeabilities by dissolution along the fractures (Huntoon, 1993). These findings are summarized in Figure 9.

## CARBONATE KARST AT THE DAM SITE

Solution cavities in the dolomite beds of the Tensleep Formation were encountered during excavation of the north abutment for the dam in 1957 (U.S. Bureau of Reclamation, 1962). As shown in Figure 10, dissolution channels were well developed along near-vertical fractures. The troublesome size of the caves is shown in Figure 11. Their permeability was revealed

by the fact that the entire flow of Owl Creek was diverted into one of the cavities for a period of 8 days with "no indication that the cavity was being filled or that the streamflow reappeared at any point on the stream below the dam" (U.S. Bureau of Reclamation, 1962). Furthermore, historic discharge data for Owl Creek in Cooley and Head (1982) revealed streamflow losses to the fractured and karstified rocks near the dam site that were on the order of 25,000 to 30,000 gallons per minute.

## SUMMARY AND CONCLUSIONS

Anchor Reservoir has barely stored enough water to be considered much more than a small lake during the past 40 years. The most recent temporary filling of the reservoir apparently occurred in 1991, when heavy spring rains raised the pool to within 3 ft of the spillway. The dam "serves wonderfully as a flood water retention facility," according to the U.S. Bureau of Reclamation Bighorn Basin Project Office (*Casper Star Tribune,* 1991).

Examination of the available technical records for design and construction reveal that the U.S. Bureau of Reclamation scientists and engineers carefully documented the geotechnical problems found at Anchor Dam before, during, and after the dam was built. The reasons that construction moved forward, and subsequent extensive remedial efforts have been undertaken, have little to do with geotechnical realities.

The available information indicates that two karst systems led to the failure of Anchor Reservoir. Gypsum karst in the Chugwater and Goose Egg Formations served to ruin the hydraulic integrity of the reservoir. Carbonate karst in the solution-enhanced fractures of the Tensleep Formation in the dam abutments, particularly the north side, caused additional serious problems.

Anchor Dam serves as an example of geologic reality getting in the way of a neat engineering project. Sometimes the political momentum of developing water in the arid west cannot control nature, regardless of how much money is thrown at a project. The architectural grace and beauty of Anchor Dam stand as a monument to human humility.

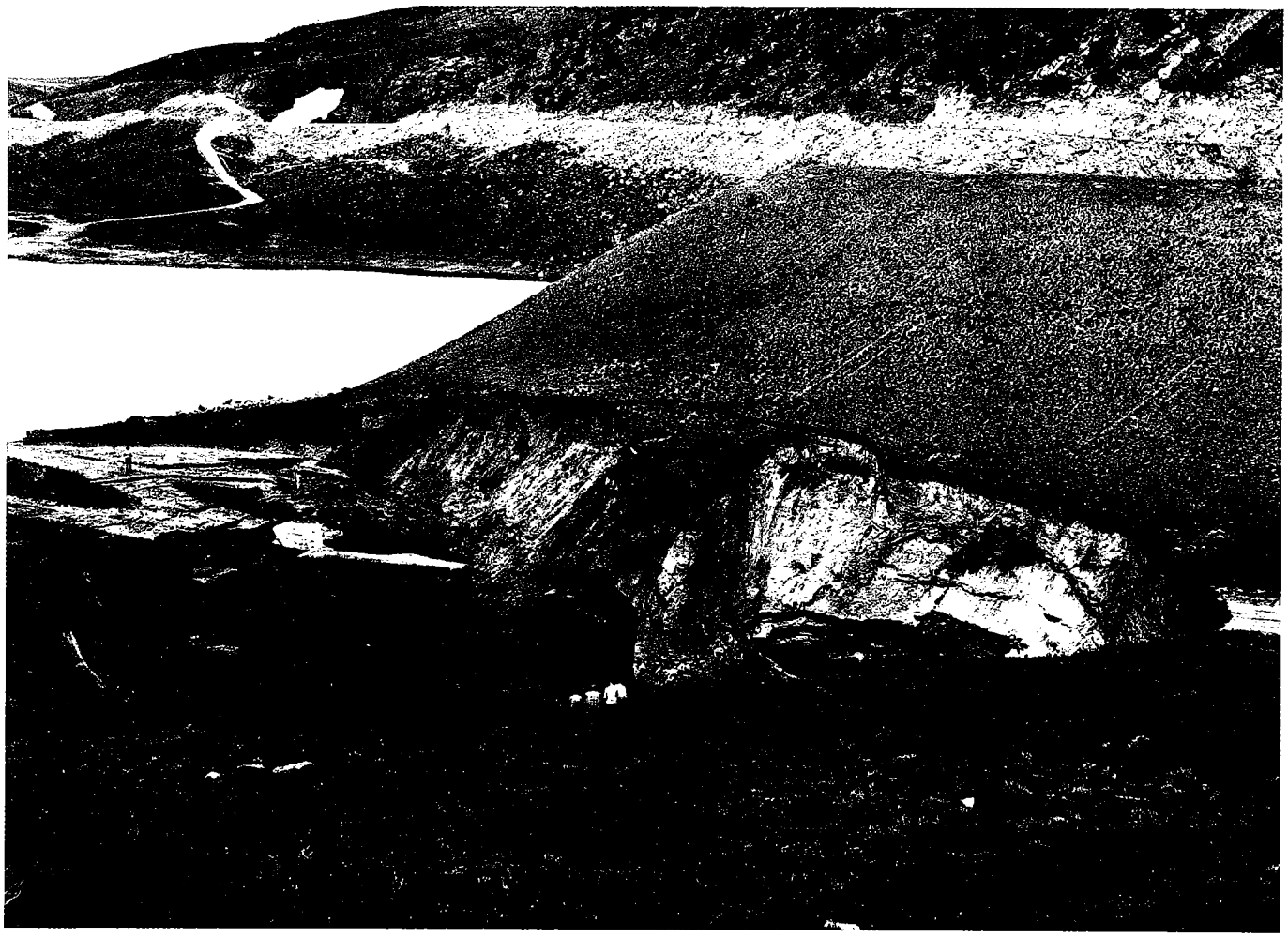

Figure 5. West part of sinkhole no. 3, with people for scale in the foreground and left center. Reproduced from a photograph in the files of the U.S. Bureau of Reclamation, Billings, Montana.

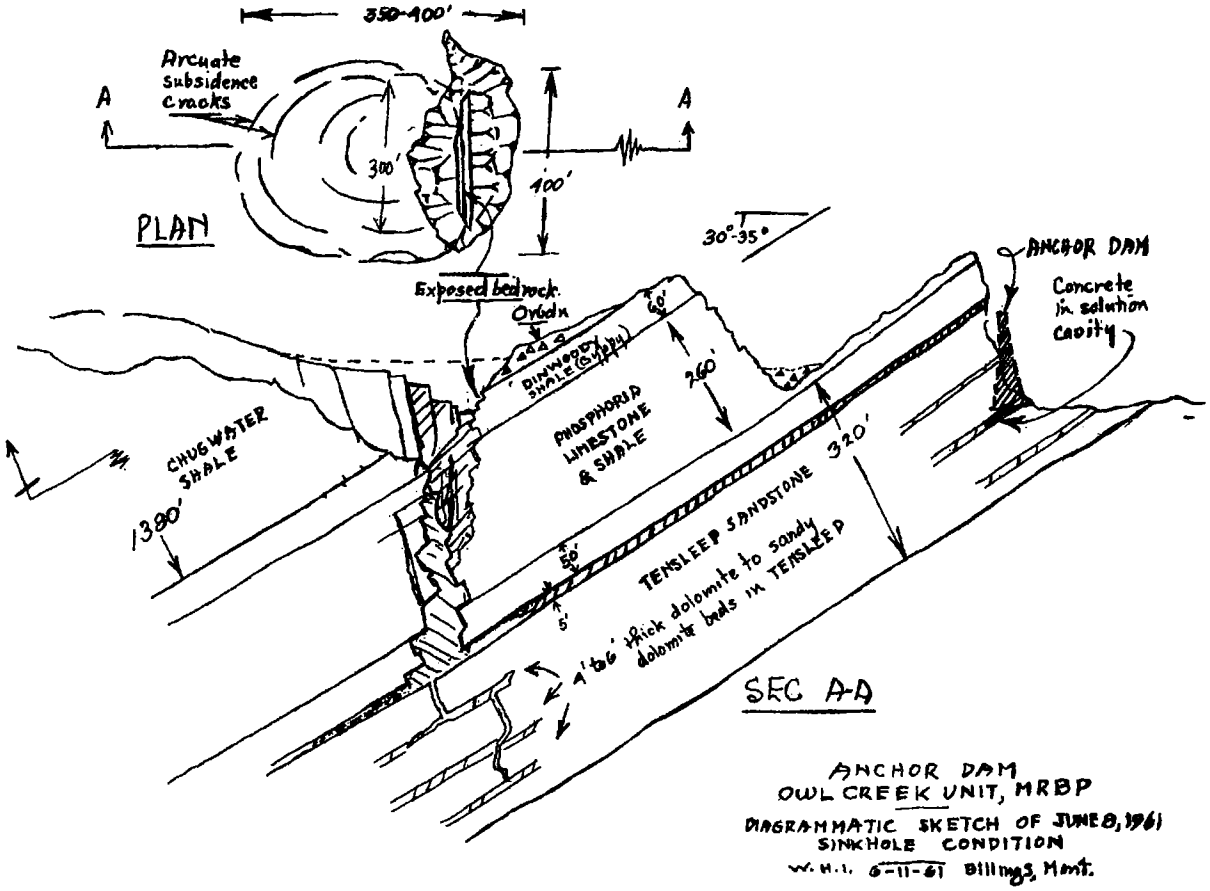


Figure 6. Diagrammatic sketch of sinkhole no. 3 by U.S. Bureau of Reclamation geologists. Reproduced from the files of the U.S. Bureau of Reclamation, Denver, Colorado.

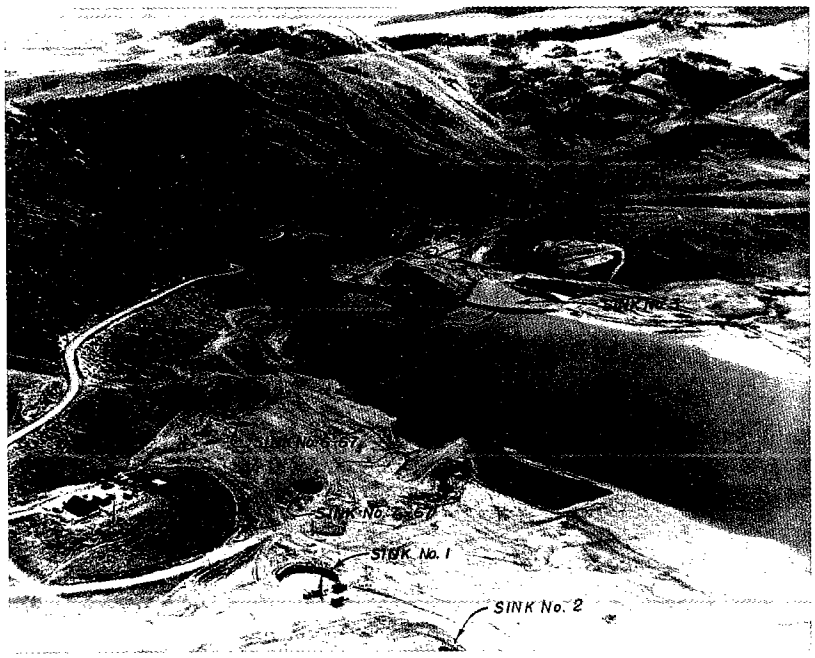


Figure 7. A 1976-vintage oblique aerial photograph of the dike constructed around sinkhole no. 3. Note that the crest of the dike is below the crest of the dam. Recent sinkholes 6-67 and 7-67 in the reservoir floor are out of view. Reproduced from a photograph in the files of the U.S. Bureau of Reclamation, Billings, Montana.

## ACKNOWLEDGMENTS

U.S. Bureau of Reclamation personnel gave access to their archives and historic photographs pertaining to the Anchor Reservoir project to Kathy Lindholm, who provided copies for this paper. B. S. Hinckley of Laramie, Wyoming, provided a copy of the important Voight reference. Peter Huntoon (University of Wyoming, retired), Kimberly Jensen (Western Oregon University), and Jon King (Utah Geological Survey) reviewed the manuscript and made valuable suggestions for its improvement.

## REFERENCES CITED

Cooley, M. E.; and Head, H. J., 1979, Hydrogeologic features of the alluvial deposits in the Nowood River drainage area, Bighorn Basin, Wyoming: U.S. Geological Survey Water Resources Investigation [Open-File] Report 79-1291, 55 p.

_____1982, Hydrogeologic features of the alluvial deposits in the Owl Creek valley, Bighorn Basin, Wyoming: U.S. Geological Survey Water Resources Investigation [Open-File] Report 82-4007, 33 p.

Huntoon, P. W., 1993, The influence of Laramide foreland structures on modern ground-water circulation in Wyoming artesian basins, *in* Snoke, A. W.; Steidtmann, J. R.; and Roberts, S. M. (eds.), Geology of Wyoming: Geological Survey of Wyoming Memoir 5, p. 756–789.

Jarvis, W. T., 1986, Regional hydrogeology of the Paleozoic Aquifer System, southeastern Bighorn Basin, Wyoming, with an impact analysis on Hot Springs State Park: University of Wyoming unpublished M.S. thesis, 227 p.

Knight, S. H.; and Hurwitz, G., 1935, Preliminary report on the geology of the Anchor Dam and Reservoir sites, Hot Springs County, Wyoming: Geological Survey of Wyoming unpublished report, 10 p.

Lindholm, K. H., 1997, Wyoming's Anchor Dam: a study in Bureau of Reclamation mistakes, community influence, political pork and sinkholes: University of Colorado, Boulder, unpublished M.S. thesis, 172 p.

Milek, D. B., 1986, Hot Springs—a Wyoming county history: Saddlebag Books, Thermopolis, Wyoming, p. 121–127.

U.S. Bureau of Reclamation, 1962, Technical record of design and construction, Anchor Dam: U.S. Government Printing Office, Washington, D.C., variously paginated.

Voight, B., circa 1968, Anchor Dam and Reservoir—the unsolved problem of sealing a sieve, *in* Rock Mechanics; The American Northwest, Third Congress Expedition Guide: Pennsylvania State University, College of Earth and Mineral Sciences Experiment Station Special Publication, University Park, Pennsylvania, p. 56–58.

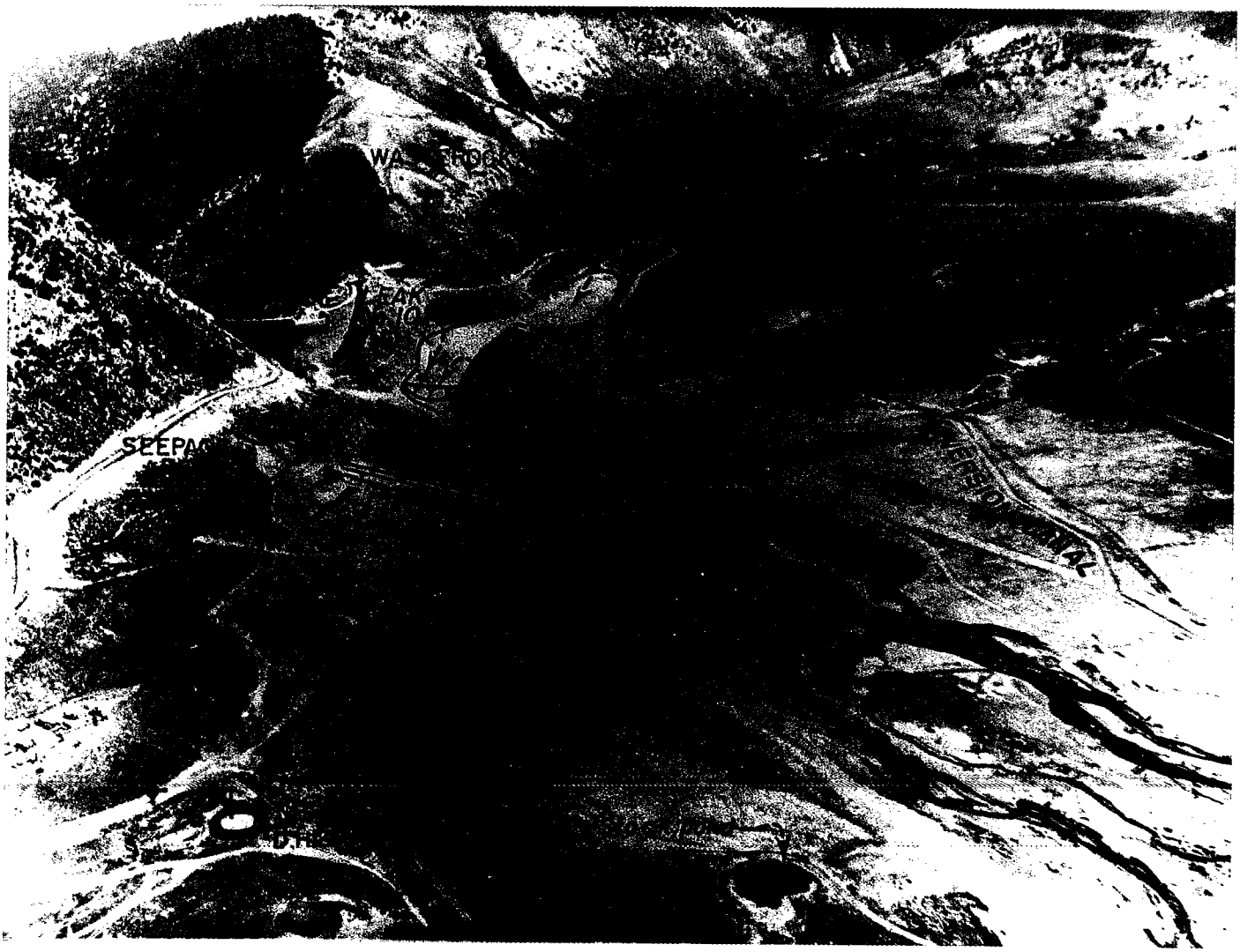

Figure 8. Mid-1960s oblique aerial photograph of Anchor Dam reservoir as viewed toward the southeast. Note the various sinkholes in the floor of the reservoir and the cavernous area detected by the geophysical surveys. Reproduced from a photograph in the files of the U.S. Bureau of Reclamation, Billings, Montana.

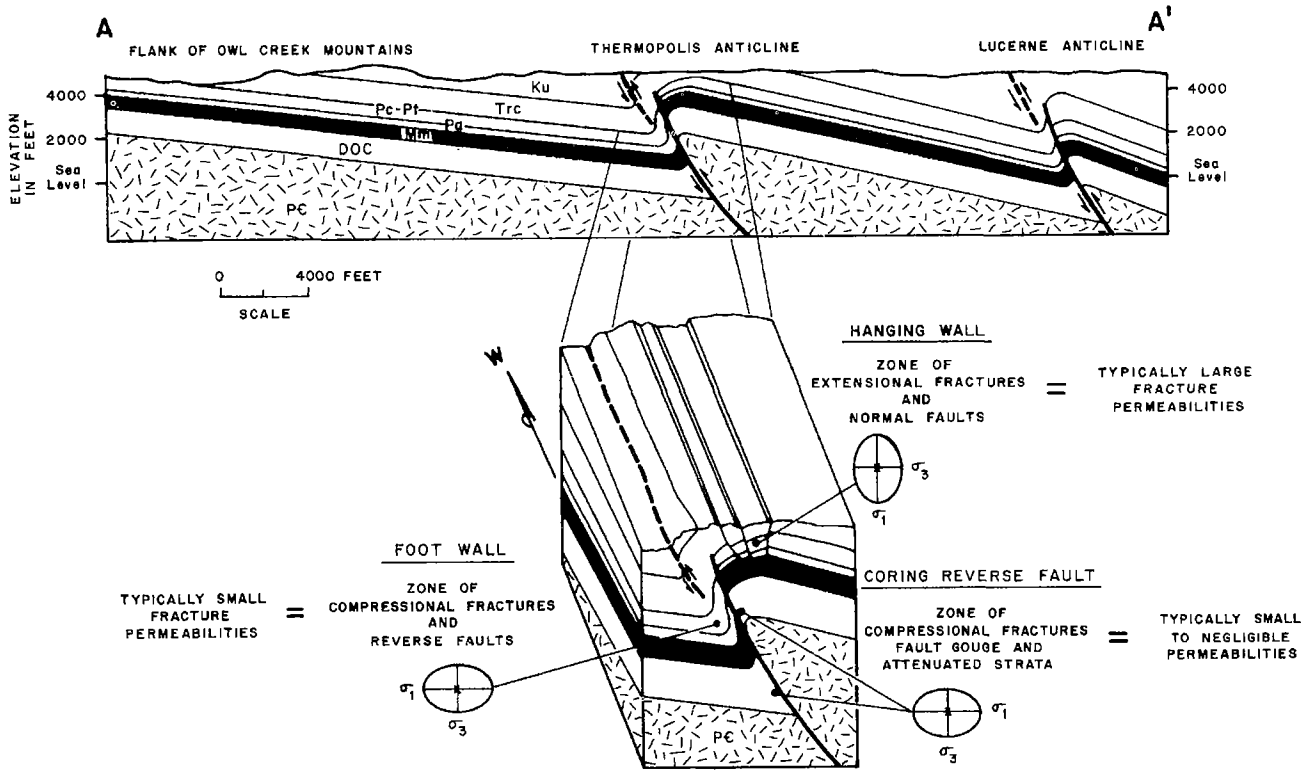


Figure 9. Schematic geologic cross section through a typical anticline in Bighorn Basin. Modified from Jarvis (1986).

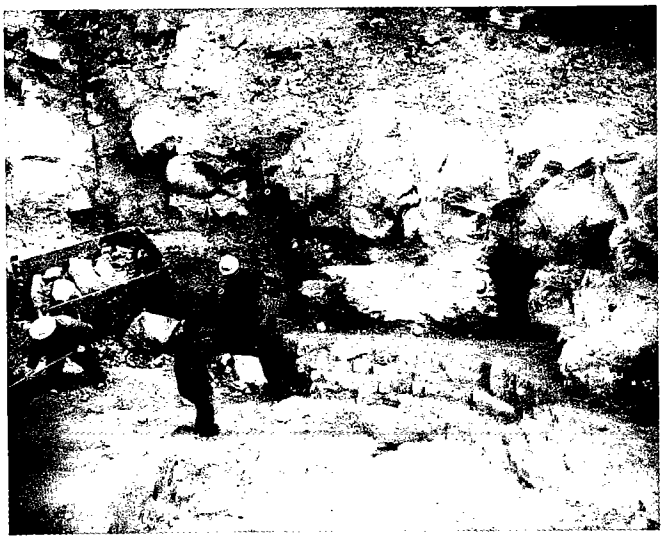

Figure 10. Solution-enhanced fractures in dolomite of the Tensleep Formation in the north abutment of Anchor Dam. Reproduced from U.S. Bureau of Reclamation (1962).

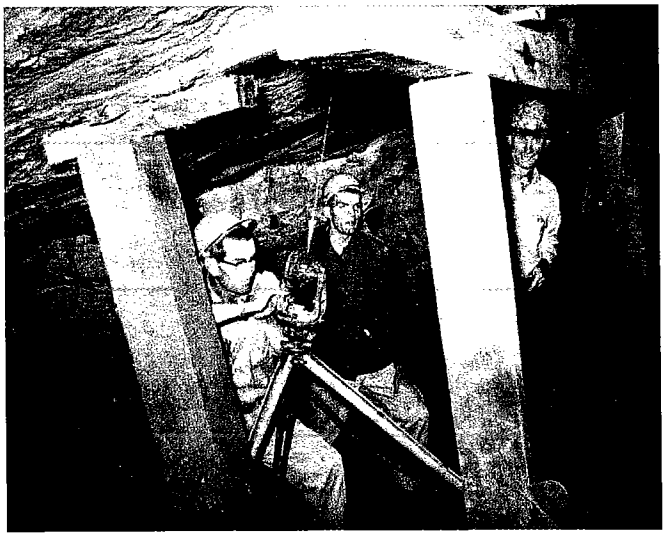

Figure 11. Workers surveying the cavern shown in Figure 10. The flow of Owl Creek was diverted into this cavity for 8 days without filling it or reappearing downstream in Owl Creek. Reproduced from U.S. Bureau of Reclamation (1962).

# Engineering and Environmental Aspects of Evaporite Karst in West-Central Colorado

**R. M. Kirkham**
Consulting Geologist
Alamosa, Colorado

**J. L. White and M. A. Sares**
Colorado Geological Survey
Denver, Colorado

**R. G. Mock**
HP Geotechnical, Inc.
Golden, Colorado

**D. J. Lidke**
U.S. Geological Survey
Denver, Colorado

**ABSTRACT.**—Impressive evaporite karst in west-central Colorado formed in response to dissolution and flow of Pennsylvanian evaporite on both regional and local scales. Regional subsidence affects an area of at least 3,600 km$^2$ in two adjacent collapsed areas, the Carbondale and Eagle collapse centers. Much of the collapse occurred during the past 3 m.y., a time when river incision greatly accelerated, and the collapse process is still active. Where present, Neogene volcanic rocks clearly define the margins of the collapse centers. The volcanic rocks are downdropped as much as 1,200 m within collapsed areas, and locally they are complexly deformed. Broad subsidence troughs are common in Pleistocene outwash terraces; these depressions probably resulted from accelerated local dissolution. In spite of this regional collapse, upward flow of evaporite beneath valleys has created valley-centered anticlines in bedrock and upwarped surficial deposits at least as young as middle Pleistocene.

Sinkholes are the principal engineering problem associated with evaporite collapse in west-central Colorado. Sinkholes of varying ages have formed throughout the Carbondale and Eagle collapse centers, but historic ones are most abundant where human activities surcharge fresh water to the soil column and underlying bedrock. Irrigation ditches and irrigated land, especially those that cross broad subsidence troughs on outwash terraces, are favorable environments for sinkhole formation. Surface water that drains into sinkholes may enhance evaporite dissolution at shallow depths.

Modern rates of regional collapse and diapirism are poorly constrained. It is unknown if the present rates of vertical deformation related to regional evaporite tectonism are sufficiently high to pose hazards to structures with anticipated life spans of 100 years or less.

Dissolved halite, gypsum, and anhydrite from the collapse areas enter the surface-water system of the Colorado River and cause the primary environmental concern associated with evaporite karst. These dissolved minerals constitute the first major salt loads to a river well known for its high salinity. Thermal springs that flow directly into the streams are responsible for much of the loading, but subsurface seepage of saline ground water into alluvial aquifers also is an important component. Most of the thermal springs discharge sodium chloride waters, whereas calcium and sulfate are the dominant constituents in shallow ground water. An estimated 0.8 million metric tons of dissolved evaporite enters the Colorado River from the collapse areas each year (Chafin and Butler, 2002).

## INTRODUCTION

This paper is based on three studies presented at the Geological Society of America's 2002 Annual Meeting held in Denver, Colorado (Kirkham and others, 2002c; White and others, 2002; Lidke and others, 2002b). These presentations described widespread collapse of the earth's surface in west-central Colorado, a process that resulted from the combined effects of dissolution and flow of Pennsylvanian evaporite (Fig. 1), and the engineering and environmental factors related to this collapse. Halite, gypsum, and anhydrite, which are the primary evaporite minerals in the study area, have well-known physical and chemical properties that facilitate the collapse process. They are soluble in fresh water, are about 10% less dense than most clastic sedimentary rocks, and readily change shape by recrystallizing and flowing. Relatively minor differences in confining pressures will cause evaporites to flow from high confining pressures toward lower confining pressures. Processes that cre-

Kirkham, R. M.; White, J. L.; Sares, M. A.; Mock, R. G.; and Lidke, D. J., 2003, Engineering and environmental aspects of evaporite karst in west-central Colorado, *in* Johnson, K. S.; and Neal, J. T. (eds.), Evaporite karst and engineering/environmental problems in the United States: Oklahoma Geological Survey Circular 109, p. 279–292.

ate sufficient differential confining pressures can induce deformation. They include (1) deposition of differential loads of relatively dense and thick overburden above an evaporite layer, (2) compressional or extensional tectonic stresses on a rock package that contains thick layers of evaporite between relatively rigid strata, and (3) deep incision of relatively narrow stream valleys into strata overlying evaporite layers.

Flow can cause local thinning or thickening of evaporite sequences. As evaporite flows laterally away from an area, the evaporite strata are thinned, and overlying rocks subside or collapse to lower elevations. Thickening of evaporite sequences occurs in areas into which evaporite flows. The low-density evaporite can flow vertically upward, sometimes as diapirs, beneath valleys where lithostatic loading on the evaporite is less than beneath adjoining upland areas. Valley-centered anticlines and upwarped Pleistocene terraces document upward flow of evaporite beneath the valleys. In contrast, dissolution causes volume losses in the evaporite strata, which induces subsidence or collapse of overlying strata. Dissolution occurs beneath both upland areas and valleys.

Evidence of regional evaporite collapse in west-central Colorado was discovered and evaluated during recent collaborative studies by the Colorado Geological Survey and the U.S. Geological Survey. Their investigations involved geologic mapping of 21 7.5-minute quadrangles and supporting investigations (Kirkham and Scott, 2002). The regional extent; the timing, geometry, and mechanism of collapse; the amount of vertical collapse; and the volume of evaporite removed from the collapse area are described in Kirkham and others (2002a). Other significant prior reports relating to evaporite collapse in the area include those by Murray (1966, 1969), Mallory (1966, 1971), Stover (1986), Unruh and others (1993), Kirkham and Widmann (1997), Scott and others (1998, 1999), and Kirkham and others (2001b). We herein summarize the information presented in those publications and briefly discuss the environmental and engineering problems related to evaporite karst in west-central Colorado.

Early during the collaborative investigations of the Colorado Geological Survey and the U.S. Geological Survey, it was recognized that mapping provided the geologic framework needed to recognize collapsed areas, but the key to understanding many aspects of the collapse involved a thorough knowledge of late Cenozoic volcanic stratigraphy. These geologically young volcanic flows are widespread across the region and are especially abundant within the lower Roaring Fork River valley (Fig. 1). The collaborative studies of the volcanic stratigraphy included geochronologic, geochemical, petrographic, and paleomagnetic investigations.

More than 130 samples of basaltic rocks were dated using the $^{40}Ar/^{39}Ar$ method; their ages range from 0.3 to 35.2 Ma, but most are Miocene in age (Kunk and others, 2002). Significant pulses of lava were erupted between 24 and 22 Ma, 16 and 13 Ma, 11 and 9 Ma, and 8 and 7 Ma. Smaller eruptions, widely separated in time and space, occurred during the past 4 m.y. More than 220 samples of basaltic rocks were geochemically analyzed for major, minor, and trace elements (Unruh and others, 2001; Budahn and others, 2002). Selected samples were also analyzed for Pb, Sr, and Nd isotopes. Petrologic studies included phenocryst and aphyric groundmass modal analyses of polished thin sections. These data led Budahn and others (2002) to define 44 geochemical rock groups that were correlated across the collapse areas by Kirkham and others (2001b, 2002b) and Lidke and others (2002a).

Paleomagnetic data from 57 sites supported the volcanic correlations that were based on flow geochemistry and geochronology (Hudson and others, 2002). These data also demonstrated that the modern tilts of flows were a result of deformation and were not representative of original emplacement attitudes. In some outcrops, paleomagnetic data indicate that the flows are sharply tilted and may be overturned.

Using these geochemical, geochronologic, and paleomagnetic data in conjunction with available geologic mapping, Kirkham and Scott (2002) concluded that many volcanic vents, each with a distinct geochemical composition, erupted between 24 and 10 Ma. These flows blanketed large parts of a low-relief erosion surface that extended across west-central Colorado from the east side of the Eagle collapse center nearly to the Colorado–Utah border. Outside the collapse areas, these flows stand at elevations of 2.9–3.4 km, whereas within the collapse areas they are as low as 2.1 km.

## EVAPORITE TECTONISM

The collaborative investigations promptly led to the recognition of two contiguous evaporite-collapse areas (Fig. 1). General attributes of the collapse areas are summarized by Kirkham and Scott (2002), whereas detailed characteristics are described by Kirkham and others (2002b), Lidke and others (2002a), and Scott and others (2002). The Carbondale collapse center includes much of the lower Roaring Fork River valley between Mount Sopris and the town of Glenwood Springs; it also has an elongate arm that follows the Grand Hogback Monocline northwestward from Glenwood Springs. The topographically low area between Minturn, Yarmony Mountain, the White River Uplift, Dotsero, Basalt Mountain, and the Sawatch Uplift, except for a small topographic high near Castle Peak, is within the Eagle Collapse Center. The combined area of the Carbondale and Eagle collapse centers is at least 3,600 $km^2$, and it may exceed 5,000 $km^2$ (Kirkham and Scott, 2002). Late Cenozoic volcanic rocks are downdropped as much as 1,200 m, and an estimated 2,300 $km^3$ of evaporite has been removed from the collapsed areas. Since dissolution is a driv-

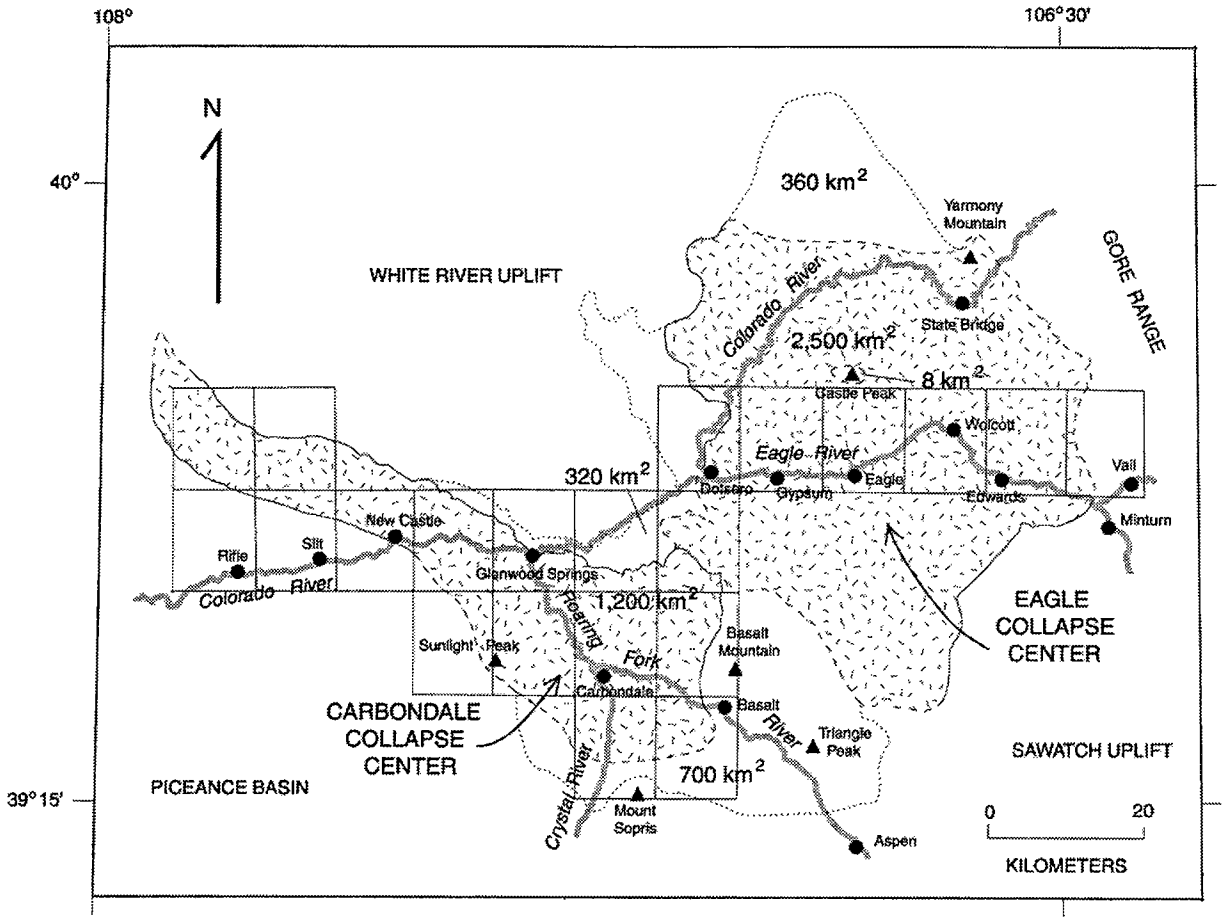


Figure 1. Map showing areas of known and suspected collapse in the Carbondale and Eagle collapse centers in west-central Colorado (from Kirkham and Scott, 2002; reproduced with permission of the publisher, the Geological Society of America, Boulder, Colorado, USA; copyright© 2002, Geological Society of America). Areas with strong evidence of collapse are patterned. The limits of collapse are outlined by solid lines where well constrained and by dashed lines where less certain. Dotted lines denote limits of suspected areas of collapse. Boxes outline quadrangles recently mapped in collapse areas by the Colorado Geological Survey and the U.S. Geological Survey.

ing force responsible for the collapse, the topography that resulted from collapse is a form of karst. Several factors lead us to conclude that the evaporite deformation in west-central Colorado is a type of tectonism. These factors include (1) the large areal extent of collapse (3,600–5,000 km²), (2) the great amount of vertical collapse (1,200 m), (3) the long time span during which collapse has occurred (several million years), and (4) the synchronous diapiric upwelling of evaporite that locally accompanies regional collapse.

Collapse is still active, as shown by (1) the occurrence of historic sinkholes within collapsed areas (Mock, 2002; White, 2002; White and others, 2002), (2) deformed Holocene deposits, and (3) high loads of dissolved sodium, chloride, calcium, and sulfate in springs and rivers (Barrett and Pearl, 1976; URS Corporation, 1981; Warner and others, 1984; Chafin and Butler, 2002). Available data from well logs (Kirkham and others, 2002b) and interpretations of seismic-reflection lines (Perry and others, 2002) indicate that hundreds of meters of evaporite remain in the subsurface beneath the collapse centers. Therefore, evaporite tectonism in west-central Colorado will continue into the foreseeable future.

## Conceptual Model

A broad undulatory, low-relief erosion surface with maximum local relief of ~500 m characterized west-central Colorado ~25 Ma. Between ~25 and 10 Ma, lavas erupted onto the erosion surface. Widespread, large-scale late Cenozoic evaporite collapse in west-central Colorado was triggered sometime after ~10 Ma by the incision of rivers through the basalt-mantled erosion surface (Kirkham and Scott, 2002). As the rivers cut ever-deepening valleys, the thickness of strata between the valley floor and the top of the evaporite sequence was diminished. Lithostatic loads on evaporite under the river valleys was reduced relative to the loads on evaporite beneath adjacent highlands. This differential lithostatic load enabled evaporite to laterally flow from under the highlands toward river valleys.

Withdrawal of evaporite from beneath the highlands induced collapse there. Upward flow of evaporite beneath river valleys formed evaporite-cored valley anticlines and local diapirs (Benson and Bass, 1955; Mallory, 1966; Perry and others, 2002). Dissolution of evaporite minerals created occasional irregular cavities and interconnective pipes. The closure and collapse of these features further induced collapse of the evaporite and overlying strata. As these processes of flow and dissolution continued, overlying basaltic flows, along with other strata between the flows and evaporite sequences, gradually collapsed to increasingly lower elevations. Dissolution and collapse rates must have equaled or exceeded the rates at which evaporite flowed upward beneath the valleys, because there is no evidence that rivers and streams were ever blocked by upwelled evaporite.

## Collapse in Roaring Fork River Valley

Of the two collapse centers in west-central Colorado, the evidence of evaporite collapse is best preserved in the southern part of the Carbondale collapse center, which lies between the towns of Basalt and Glenwood Springs in the lower Roaring Fork River valley (Fig. 2). The widespread distribution of Neogene volcanic rocks in and adjacent to the southern part of the Carbondale collapse center provides abundant opportunities to characterize and quantify the timing, rates, and amounts of evaporite collapse (Kirkham and others, 2001b, 2002b). A structure-contour map of the top of late Miocene lava flows (Fig. 3) depicts the general character and amount of collapse in the lower Roaring Fork River valley. Much of the structural lowering occurs along the margins of the collapse center, but major structures within the interior parts of the collapse center also have as much as 300 m of structural relief across relatively narrow zones of deformation.

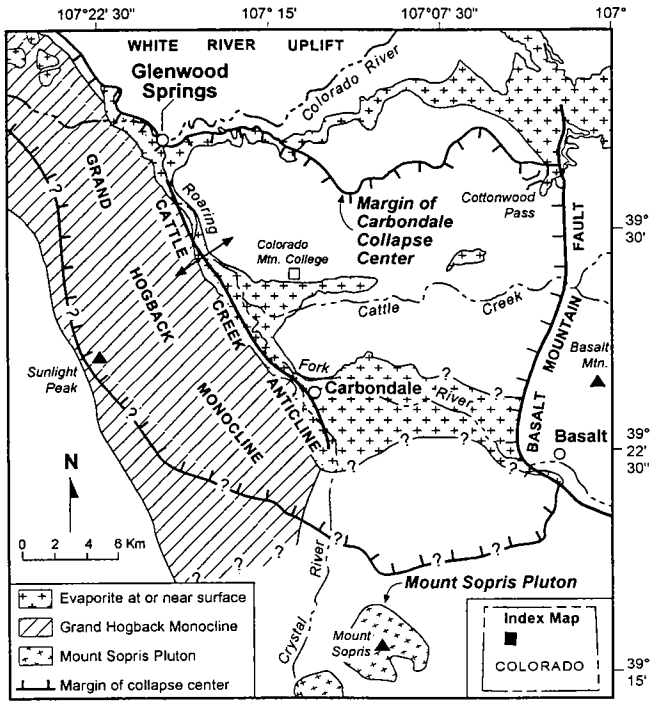


Figure 2. Location map of the southern part of the Carbondale collapse center, lower Roaring Fork River valley (from Kirkham and others, 2002b; reproduced with permission of the publisher, the Geological Society of America, Boulder, Colorado, USA; copyright© 2002, Geological Society of America). Queries indicate locations where collapse margin is poorly constrained.

A distinctive topographic low within an otherwise mountainous region marks the southern part of the Carbondale collapse center. This topographic depression is readily apparent in an oblique shaded-relief image (Fig. 4). The land surface within this collapse area is as much as 1,220 m lower than surrounding upland areas.

Conspicuous escarpments mark the northern and eastern margins of the collapse center (Fig. 4). Structural deformation along the eastern margin of the Carbondale collapse center is controlled by the Basalt Mountain Fault, a high-angle Laramide (Late Cretaceous to Eocene) reverse fault with down-to-east displacement (Kirkham and others, 2002b, fig. 13). Today, evaporite beds lie at shallow depths on the west side of the fault and are readily subject to flow and dissolution, but the evaporite is buried by as much as 2,500 m of strata east of the fault. Strong evidence of collapse is widespread west of the fault but is absent or weak east of the fault where evaporite is deep in the subsurface. Basalt flows that erupted from a shield volcano at Basalt Mountain ~10 Ma are monoclinally folded in a zone along the eastern margin of the collapse area and were lowered ~580 m. A small eruptive center and flow, dated at 2.90 ± 0.01 Ma (Kunk and others, 2002), crop out within the eastern hinge zone. These rocks are tilted about the same amount as are the ~10-Ma flows (Kirkham and others, 2001b, 2002b). Stacked sequences of basaltic flows cap Little Grand Mesa (Fig. 4) near the northern margin of the Carbondale collapse area. These 7.75-Ma flows (Kunk and others, 2002) are monoclinally folded in a style similar to that on the eastern margin of the collapse center.

Another Laramide structure, the Grand Hogback Monocline, controls the western margin of the Carbondale collapse center. Evaporite beneath this west-dipping monocline has withdrawn, causing the monocline to collapse (Unruh and others, 1993; Perry and others, 2002; Kirkham and others, 2001b, 2002a; Scott and others, 2002). As the monocline collapsed, down-to-west flexural slip occurred along bedding planes in the west-dipping sedimentary strata within the monocline (Murray, 1969).

Parallel, northwest-trending valleys and ridges west of the confluence of the Roaring Fork and Crystal Rivers (Fig. 4) are related to differential erosion of Mesozoic and Paleozoic sedimentary rocks within the

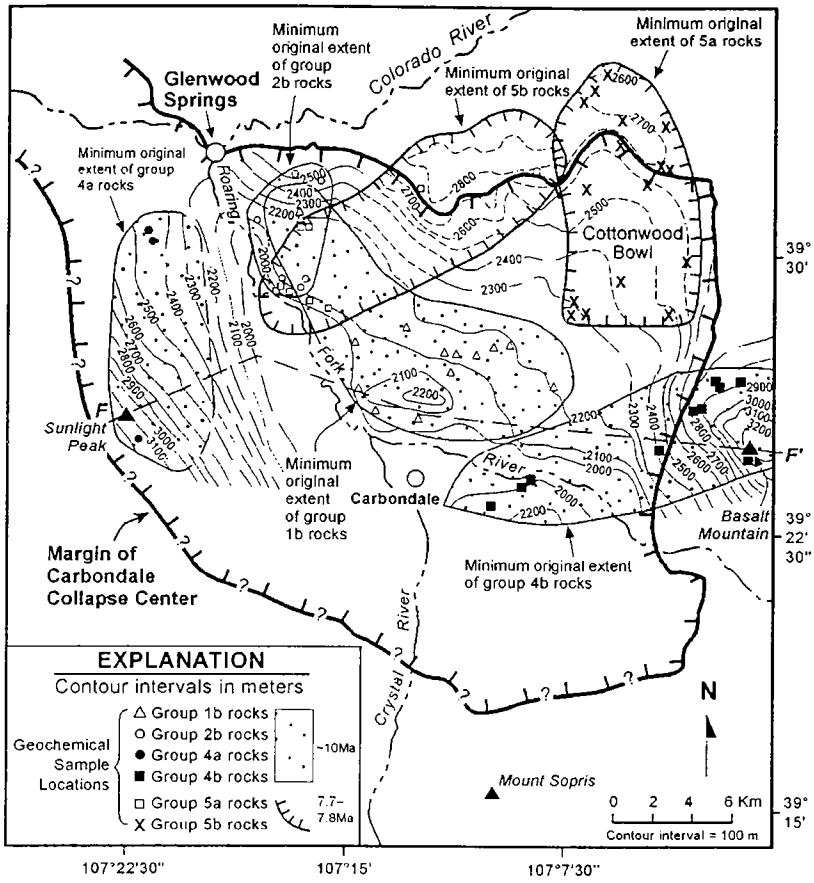


Figure 3. Structure-contour map depicting the top of late Miocene volcanic flows (from Kirkham and others, 2002b; reproduced with permission of the publisher, the Geological Society of America, Boulder, Colorado, USA; copyright© 2002, Geological Society of America). Geochemical groups are those of Budahn and others (2002): groups 5a and 5b are 7.75 Ma; groups 1b, 2b, 4a, and 4b, whose present approximate distribution is depicted by the open stipple pattern, are ~10 Ma.

Grand Hogback Monocline. Note the eastward bend in the prominent hogback ridge where it crosses the boundary of the collapse area; the bend occurs where the collapsing strata within the monocline transition to strata that escaped collapse. Gently east-sloping, basalt-capped Sunlight Mesa (Fig. 4) is north-northwest of the hogback ridges associated with the monocline. The late Miocene (~10-Ma) flows that cap the mesa were originally erupted onto a low-relief erosion surface or angular unconformity that was cut across the sedimentary strata folded by the monocline during the Laramide orogeny. A broad, bowl-like depression superposed on the mesa is probably a result of differential collapse of the monocline. Several northwest-trending, parallel, relatively shallow valleys and low ridges cross basalt-capped Sunlight Mesa. The valleys are underlain by flexural-slip faults related to collapse of the Grand Hogback Monocline. These faults parallel bedding planes in the sedimentary strata within the monocline, and they cut the ~10-Ma basaltic flows that cap Sunlight Mesa. Each of the ridges is underlain by east-tilted late Miocene flows.

Broad, flat valleys such as Spring Valley, gently sloping basalt-capped mesas like Los Amigos Mesa, and the rolling hills of Missouri Heights typify the interior parts of the collapse area (Fig. 4). Los Amigos Mesa and the block of rock northeast of the confluence of the Crystal and Roaring Fork Rivers protrude onto the valley floor. These blocks may be sliding or rafting into the valley as the underlying evaporite flows toward the river, a model that requires a pull-apart structure at the release zone of the rafted block. The rolling hills of Missouri Heights are underlain by heterogeneous jumbled blocks of sedimentary and volcanic rock of varying sizes that are intermixed with or overlain by sporadic, locally thick surficial deposits (Kirkham and Widmann, 1997).

Sinkholes are common within the collapse area (Mock, 2002; White, 2002; White and others, 2002). Several closed or nearly closed topographic depressions lie within the collapse area in the Roaring Fork River valley; they include broad, downwarped river terraces and shallow synclines formed in volcanic rocks. Syn-collapse sediments accumulated in many of the subsiding depressions. The interfluve between the Roaring Fork and Crystal Rivers is underlain by syn-collapse sediments that locally exceed 450 m in thickness (Kirkham and others, 2002b). These sediments were deposited between ~35 and 13 Ma during a period of collapse that preceded most other collapse in the region. This early collapse may have been influenced by thermal heating of ground water by emplacement of the Mount Sopris intrusive stock (Kirkham and others, 2002b). Lacustrine sediments crop out on and near the ridge tops in Missouri Heights, denoting the positions of former closed depressions that have been breached by more recent erosion.

### Collapse in and Adjacent to Eagle River Valley

In the region of the Eagle collapse center (Fig. 1), previous studies conducted during the middle of the 20th century documented late Cenozoic evaporite-related deformation, as evidenced by such features as the Eagle River Anticline near Gypsum (Benson and Bass, 1955) and the sag of basaltic flows south of Wolcott (Hubert, 1954). Recent geologic mapping, isotopic dating, sparse geochemical analyses, and paleomagnetic studies of Miocene basaltic flows, as well as evaluation of seismic data, provide evidence of more widespread late Cenozoic evaporite-related tectonism (Scott and others, 1998, 1999; Lidke and others, 2002a, 2002b; Hudson and others, 2002; Perry and others,

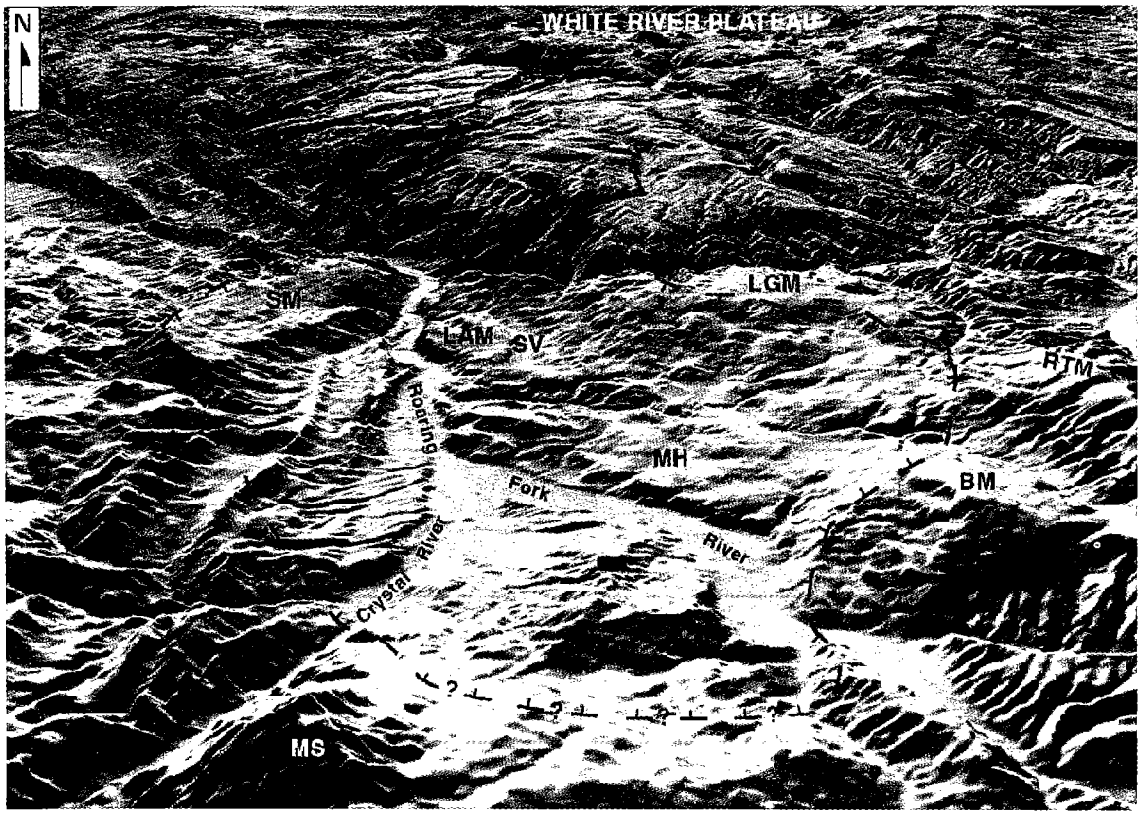


Figure 4. Oblique shaded-relief digital elevation model of the lower Roaring Fork River valley (from Kirkham and others, 2002b; reproduced with permission of the publisher, the Geological Society of America, Boulder, Colorado, USA; copyright© 2002, Geological Society of America). View is to north. Boundary of Carbondale collapse center marked by dashed line with hachures. Major geographic features include Basalt Mountain (*BM*); Los Amigos Mesa (*LAM*); Little Grand Mesa (*LGM*); Missouri Heights (*MH*); Mount Sopris (*MS*); Red Table Mountain (*RTM*); Sunlight Mesa (*SM*); and Spring Valley (*SV*). The collapse margin drops down into Glenwood Canyon at the west edge of Little Grand Mesa and is not visible in this perspective.

2002). Deformed early Miocene (24–22-Ma) basaltic flows provide a time constraint and obvious evidence for late Cenozoic deformation in this collapse area. Basaltic flows younger than ~22 Ma, however, are sparse to absent in the region of the Eagle collapse center. Consequently, constraints on the timing of late Cenozoic collapse deformation, such as those provided by the widespread post–22-Ma basaltic flows in the Carbondale collapse center, are lacking in the Eagle collapse center. However, tephra-capped terrace gravels suggest post-middle Pleistocene evaporite-related collapse in the central part of the Eagle collapse center (Lidke and others, 2002a, 2002b).

At Castle Peak (Fig. 1), the highest point within the Eagle collapse center, 23–22-Ma basaltic flows lie at altitudes of about 3.0–3.5 km, similar to altitudes of more extensive flows that cap the White River Uplift, to the west of this collapse region. The high-standing Castle Peak basaltic cap apparently has not collapsed, or collapsed only little, suggesting that evaporite-related collapse was not ubiquitous, nor equally distributed, throughout the Eagle collapse area. High-level basaltic flows at Castle Peak apparently represent a small erosional remnant of a previously more extensive basaltic plateau that provides a high-level datum, as described earlier in this paper and in Kirkham and Scott (2002).

Elsewhere in the Eagle collapse center—to the south, southwest, southeast, and northeast of Castle Peak—deformed early Miocene (24–22-Ma) basaltic flows are present at elevations about 1 km lower than the flows at Castle Peak. Relatively low-elevation basaltic flows near Gypsum, Eagle, and Wolcott (Fig. 1) are cut by discontinuous, linear to arcuate normal faults and show evidence of having sagged downward to form synclinal sags above underlying Pennsylvanian evaporite (Lidke and others, 2002a, 2002b). These deformed, low-lying basaltic flows appear to define a northwest-trending synclinal sag that extends about 25 km, from south of Wolcott through the Eagle area and into the area north of Gypsum (Fig. 1).

Early Miocene (24–22-Ma) basaltic flows near State Bridge (Fig. 1) are similarly deformed in a northwest-trending syncline. Although this deformation is obviously late Cenozoic in age, evidence to indicate that it is evaporite-related is inconclusive. On the basis of available data and the similarity of this syncline to the sag in the Wolcott-Gypsum area, Lidke and others (2002a, 2002b) suggested that late Cenozoic flow and dissolution may have removed evaporite be-

neath the State Bridge area and created a synclinal sag.

Evaporite-cored anticlines are present in several localities along the Eagle River valley. Some or all of these anticlines are late Cenozoic in age and are probably related to incision of the Eagle River and the rise of evaporite beneath the river valley. Benson and Bass (1955) documented the Eagle River anticline near Gypsum, which deforms early Miocene basaltic flows. They concluded that this anticline reflects a diapiric rise of evaporite beneath the erosionally unloaded valley of the Eagle River. Between Eagle and Wolcott (Fig. 1), the Horn Ranch Anticline follows the Eagle River valley, and it may also reflect the rise of evaporite beneath the valley (Lidke, 2002a). Near Eagle, and farther east near Edwards (Fig. 1), west-trending, evaporite-cored anticlinal features along the Eagle River valley appear to deform older north-trending folds that probably are related to the north-trending Laramide Sawatch Anticline south of Minturn (Fig. 1). Like the Eagle River Anticline, these other anticlinal features appear to be related to upwelling of evaporite that probably rose in response to erosional unloading of the valley area during late Cenozoic incision by the Eagle River.

Sparse remnants of tephra, which correlate chemically with the 0.64-Ma Lava Creek B ash (Izett and Wilcox, 1982; Andrei Sarna-Wojcicki, written communication, 1998), overlie Pleistocene terrace gravels near Dotsero and east of Eagle. The difference in elevation of ash-capped terrace deposits at these localities implies post–0.64-Ma deformation (Lidke and others, 2002a, 2002b). The terrace deposits capped by Lava Creek B ash near Eagle, in the central part of this collapse center, appear to be lowered by post–0.64-Ma collapse. Although correlation of these fluvial deposits overlain by the Lava Creek B ash is not well established, the correlation presented in Lidke and others (2002a) implies at least 25 m of post–0.64-Ma collapse near Eagle that may be related to dissolution or flow of underlying evaporite.

Historic evaporite-related collapse, as indicated by modern sinkholes, also occurs in the Eagle collapse center. For the most part, these recent sinkholes have not been systematically studied in detail. They are, however, similar to sinkholes better documented in the region of the Carbondale collapse center. The Eagle River valley, which is largely within the Eagle collapse center, is a popular and rapidly growing part of the Interstate Highway 70 corridor. It seems likely that continued urban growth in this corridor and future development of sinkholes may mix in costly and unpleasant ways.

## RELATIONSHIP TO RIVER-INCISION RATES

As described in a prior section, incision by the Colorado River and its tributaries after ~10 Ma was the triggering mechanism for widespread, large-scale, late Cenozoic evaporite tectonism. Bryant and others (2002), Kunk and others (2002), and Kirkham and others (2001a) summarized the incision history of the Colorado River in west-central Colorado, largely on the basis of the geochronology and mapped relationships of basaltic flows. These interpretations built upon prior data published by Larson and others (1975) and also utilized new data from basaltic flows outside known areas of evaporite collapse that were collected during the collaborative Colorado Geological Survey and U.S Geological Survey investigations.

All of the 24–22-Ma and 16–13-Ma flows beyond the limits of collapse lie at similar elevations, which suggests that little or no incision occurred prior to 13 Ma. The ~10-Ma flows on the north flank of the Basalt Mountain shield volcano flowed into and filled a paleovalley; these rocks are ~300 m closer to modern river level than are all other ~10-Ma flows in the region. This suggests, but does not prove, that by ~10 Ma the rivers may have cut perhaps as deep as a few hundred meters. The low-elevation flows north of Basalt Mountain are underlain at depth by evaporite, so this area could potentially have been lowered by evaporite collapse. Between 7.8 and 7.7 Ma, basaltic lava flows filled a different paleovalley. This paleovalley was south of the southern rim of Glenwood Canyon, which is the deep gorge east of Glenwood Springs. Kirkham and others (2001a) postulated that an ancestral Colorado River flowed through this paleovalley, and that the river was diverted into modern Glenwood Canyon ~7.8–7.7 m.y. ago.

An isolated remnant of a 3.0-Ma flow found high on the south wall of Glenwood Canyon suggests only minor river incision between 7.7 Ma and 3.0 Ma, and an accelerated incision post-3 Ma. During the past 3 m.y the Colorado River has had an average incision rate of 0.24 m/k.y., and it has cut more than half the total vertical distance between the base of the Miocene basalts that cap the White River Plateau and the modern floor of Glenwood Canyon. This high rate of late Pliocene and Quaternary incision is supported by data from Triangle Peak along the Roaring Fork River between the towns of Basalt and Aspen and from Rock Creek northeast of the town of McCoy. The basal flow from a basaltic volcano at Triangle Peak is 1.36 Ma (Kunk and others, 2002), overlies river gravels (V. Freeman, personal communication, cited in Larson and others, 1975), and is about 396 m above the Roaring Fork River. The height of the Triangle Peak flows above the Roaring Fork River indicates a post–1.36-Ma incision rate of 0.29 m/k.y. A flow about 150 m above Rock Creek has a K-Ar age of 0.64 ± 0.2 Ma, suggesting a post–middle Quaternary incision rate of ~0.24 m/k.y. for this tributary to the Colorado River (Larson and others, 1975). These data document a post–late Pliocene incision rate for the Colorado River that is about one order of magnitude greater than the average incision rate for the preceding part of the late Cenozoic.

As the incision rate accelerated, so did the rate of evaporite collapse. Flows from a 2.90-Ma volcano

within the hinge zone along the eastern margin of the Carbondale collapse center are tilted about the same as are ~10-Ma flows from the Basalt Mountain shield volcano, which means that much of the collapse at this locality happened since 2.90 Ma. Relationships between two small Pliocene eruptive centers south of Little Grand Mesa and the late Miocene flows that cap Little Grand Mesa also support a major, post–3-Ma collapse (Kirkham and others, 2002b). Remnants of 3.17-Ma and 3.97-Ma Pliocene eruptive centers are within the collapse area, yet they lie at about the same elevations as the 7.75-Ma flows on Little Grand Mesa, which are beyond the limits of the collapse area. If significant collapse occurred between 7.75 and ~3 Ma, then the younger vents would have formed on a landscape that was topographically lower than Little Grand Mesa. Flows from these Pliocene volcanoes are lowered about the same amount as are the late Miocene lavas, a relationship that also supports major post–3-Ma collapse. Slip rates calculated for flexural-slip faults associated with collapse of the Grand Hogback Monocline attest to moderately accelerated, post–late Pliocene collapse.

## ENGINEERING ASPECTS

Subsidence of the earth's surface is the primary geologic hazard associated with evaporite collapse in west-central Colorado. The dissolution of evaporite minerals creates subsurface voids, dissolution breccia zones, and fissures. Sinkholes, caverns, open fissures, closed depressions, and swallow holes, all of which can be problematic for development, are common in the Carbondale and Eagle collapse centers, as well as in other areas where evaporite is at or near the ground surface.

Many sinkholes form in surficial deposits that overlie the evaporite, but some occur directly in outcrops of evaporite or in bedrock that overlies the evaporite. Mock (2002) described three basic forms of sinkholes in the area (Fig. 5). Type A sinkholes are deep, rubble-pipe sinkholes that disturb the entire column of surficial deposits above the evaporite. Type B sinkholes, or shallow fissure-piping sinkholes, involve shallow surface collapse by piping of fine-grained soil deposits through fissures or small pipes into underlying bedrock voids. Cavity-roof-collapse sinkholes are classified as type C sinkholes. They are characterized by spontaneous roof collapse and rubble filling of existing, near-surface dissolution cavities or caverns. Several time-dependent stages of sinkhole development have been described (Mock, 2002). Most known sinkholes are on flat-lying river terraces or on the sloping valley sides, but some are fissures and caverns directly in evaporite bedrock. Occasionally, sinkholes form in lava flows and in soil and debris that have collapsed into and filled voids within the underlying evaporite; examples of these types of sinkholes include those near Colorado Mountain College, which is at the south end of Spring Valley.

Subsurface borings in the vicinity of sinkholes on river terraces indicate that the underlying bedrock surface can be highly irregular. While the ground surface of the terrace is relatively flat, the underlying bedrock surface is commonly more typical of karst topography. This relationship also is exposed in the walls of a tributary to the Roaring Fork River west of Carbondale, where middle Pleistocene outwash gravels overlie an irregularly shaped surface cut on underlying evaporite. The highest sinkhole densities occur along the Roaring Fork River valley between the

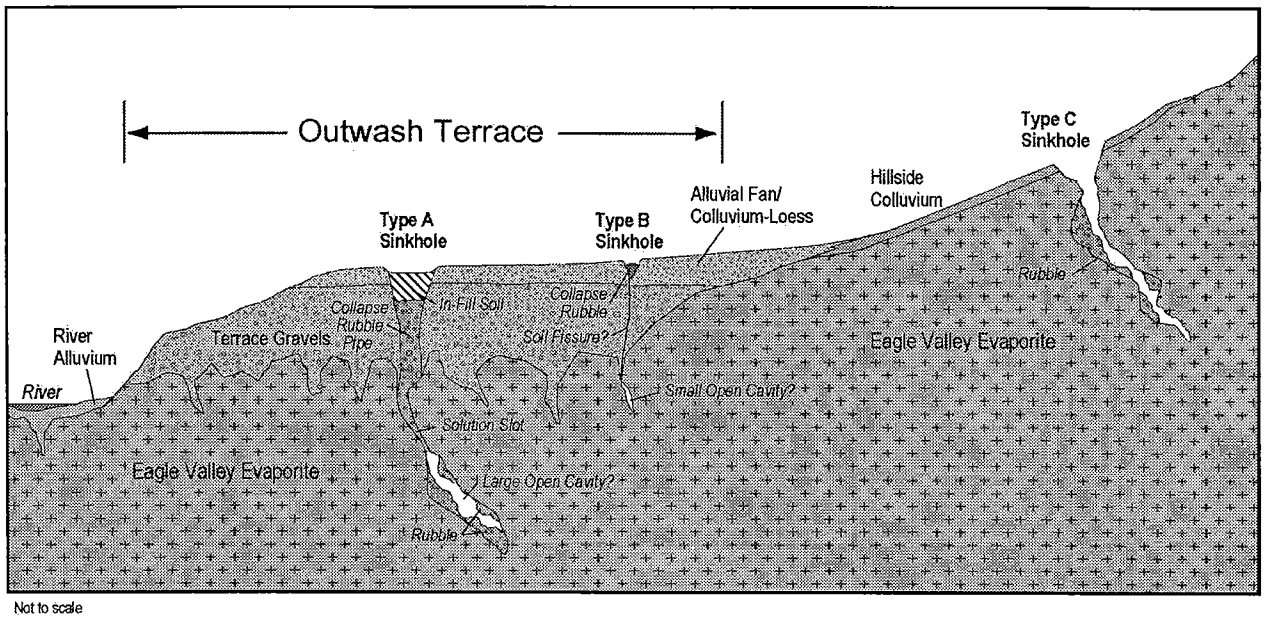


Figure 5. Schematic cross section showing types of sinkholes (modified from Mock, 2002; reproduced with permission of the publisher, the Geological Society of America, Boulder, Colorado, USA; copyright© 2002, Geological Society of America).

towns of Carbondale and Glenwood Springs (Fig. 6), where diapirism associated with the Cattle Creek anticline has exposed evaporite and deformed late Quaternary glacial-outwash terraces (Mock, 2002; White, 2002; White and others, 2002; Kirkham and others, 2002b). In addition to isolated sinkholes, large, shallow subsidence troughs up to several tens of acres in size commonly occur on the flood plain and on outwash terraces of the Roaring Fork River valley from Carbondale to El Jebel (Kirkham and others, 2002b).

### Considerations for Proposed and Existing Development

Geologic and geotechnical investigations for land-use planning and development should address evaporite hazards in areas where evaporite crops out or exists at shallow depths in the subsurface. Subsidence and sinkhole hazards are probably greater in areas with higher sinkhole densities; however, future sinkholes may not be restricted to these areas. Spontaneous collapse of the ground surface can be dangerous and life threatening, but such occurrences are relatively rare in this region. Nonetheless, they do occur. For example, in February 2003 a sinkhole spontaneously opened in a soccer field at the Colorado Mountain College near the south end of Spring Valley (Fig. 7). A more common problem is gradual settlement from subsidence or removal of fine-grained soils by piping, which causes differential stress and strain to rigid structures. This can damage facilities that are unknowingly constructed over or near a sinkhole, subsidence trough, or near-surface underground void.

Avoidance of known subsidence features is the preferred mitigation alternative, but this is not always feasible. Many areas in west-central Colorado that are susceptible to sinkhole formation are experiencing rapid growth, and pressure to develop is high (Fig. 8). Ground-modification and structural solutions can mitigate the threat of subsidence if avoidance is not an option. Some of those measures include backfilling with reinforced fill, compaction grouting, chemical or polyurethane grouting, and structural bridging. Landowners and developers who are planning projects in these areas should consult with and contract the services of knowledgeable geotechnical and structural engineering firms.

Many sinkholes at advanced stages have been infilled with naturally deposited sediments or historically filled by humans and forgotten. Filled sinkholes often are completely concealed at the surface. Near-surface voids that have not yet broken through to the surface are also concealed. Subsurface inspections, either by investigative trenching, a series of investigative borings, and observations made during overlot grading or utility installation can ascertain whether filled sinkholes and near-surface voids exist within a

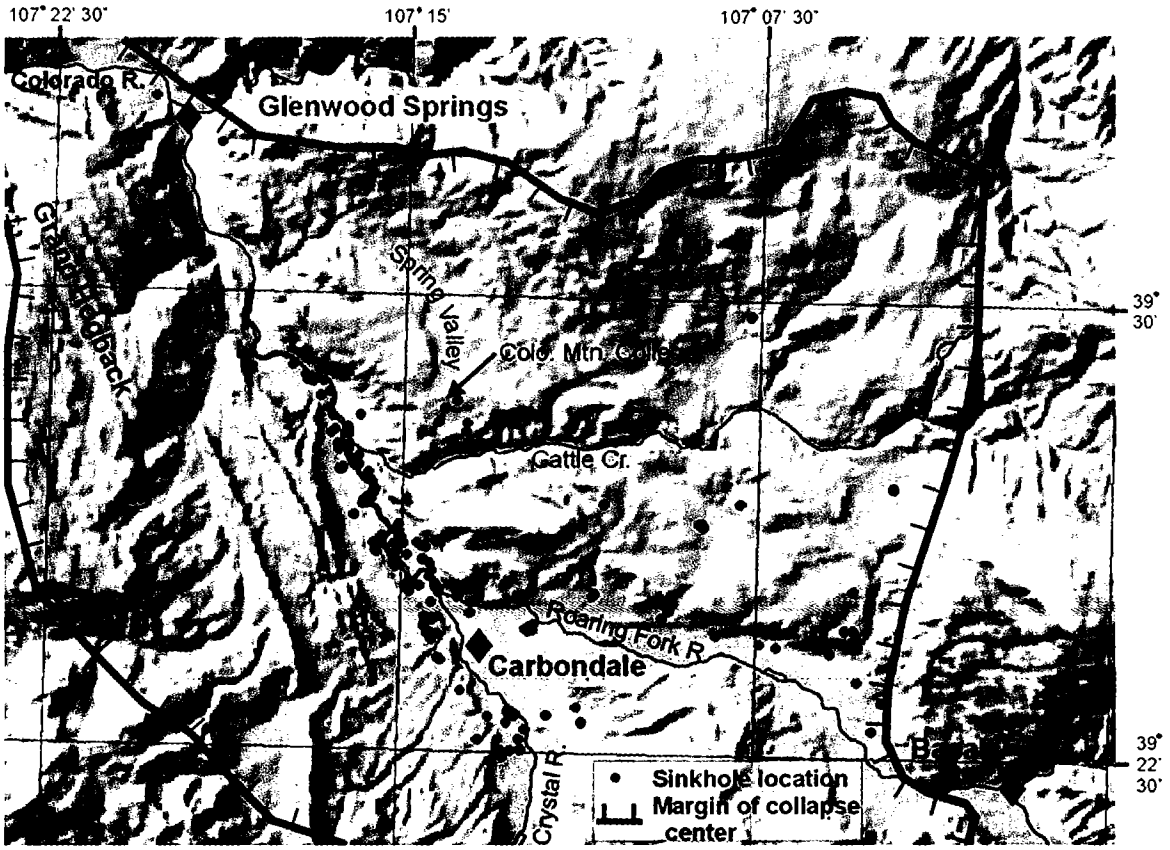


Figure 6. Locations of sinkholes in the lower Roaring Fork River valley in the vicinity of Carbondale and Glenwood Springs.

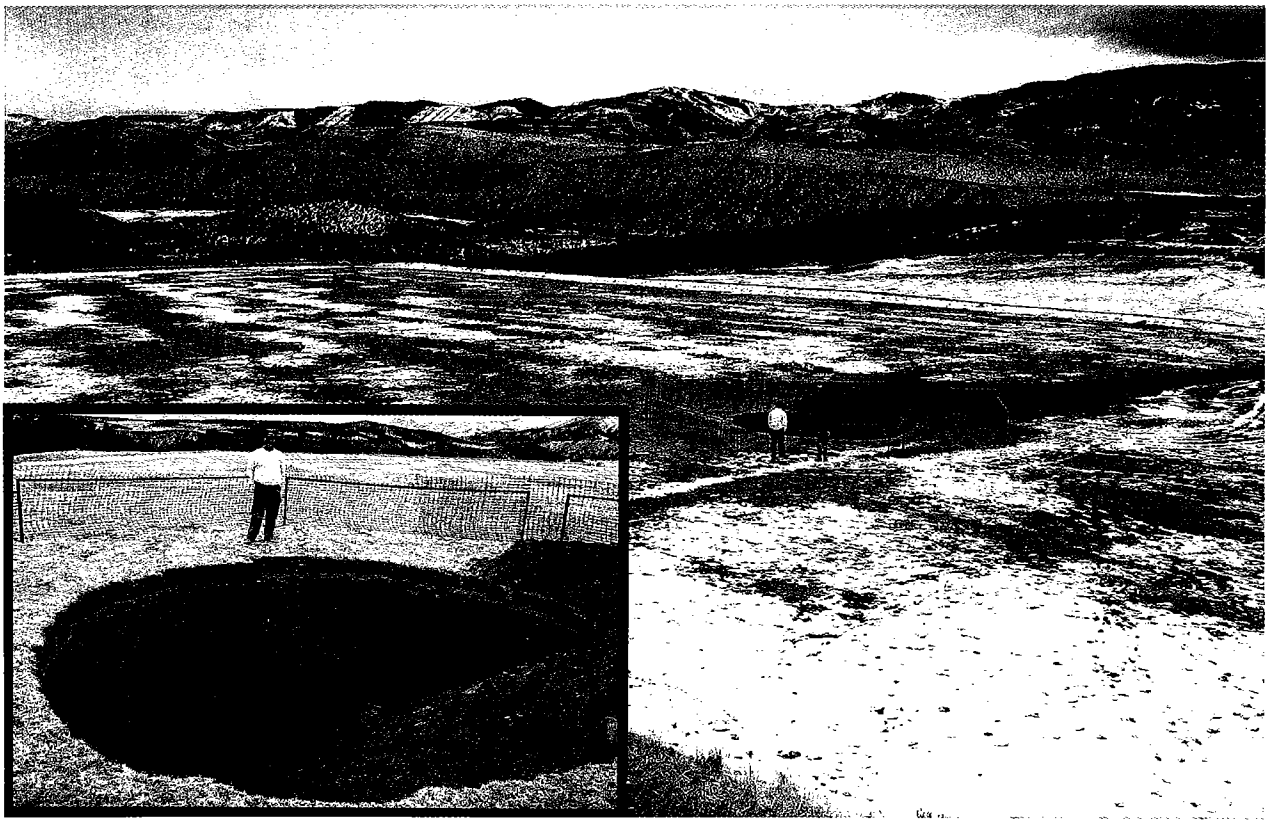

Figure 7. Overview photograph of a sinkhole that suddenly formed in a soccer field at Colorado Mountain College during February 2003. View is to southwest. Roaring Fork River valley is in middle background. Inset photograph is a close-up view of the sinkhole. Photos by J. L. White.

development area. Low-altitude aerial photography (stereo pairs and oblique), eyewitness reports, and historical records also may be helpful for identifying filled sinkholes. Geophysical-investigation methods can also detect voids and soil/rock property changes in the shallow subsurface.

Another engineering concern with evaporite rocks in the semiarid climates of west-central Colorado is that the low-density, gypsiferous soils derived from them—including those deposited in alluvial or debris-flow fans, sheetwash aprons, and colluvial wedges at the base of hillslopes—are especially susceptible to hydrocompaction (White, 2002). Hydrocompaction involves the densification or compaction of low-density deposits upon wetting and saturation, which induces ground settlement and corresponding distress to any structure founded on them.

Drainage issues and proper water management are important in evaporite-karst terrains. Because the bedrock and the gypsiferous soils derived from them are soluble, changed hydrologic conditions and the introduction of surcharges of fresh water to the soil column may destabilize certain subsidence areas, rejuvenate older sinkholes, or cause new dissolution to occur. Most historical reactivations of sinkholes in the study area were in flood-irrigated fields and irrigation ditches.

Ground movements are not just a concern near existing sinkholes or other karst-type subsidence features. New geologic evidence presented earlier in this paper indicates that evaporite tectonism is still active in west-central Colorado. However, the rates of this modern crustal deformation and the hazards of associated ground movements are presently unknown. The potential risks posed by evaporite tectonism to current or planned developments with structures having 50- to 100-year life spans are unknown but are believed to be low. Rates of evaporite deformation may be sufficiently high to pose hazards in the following areas: (1) structural margins of the collapse centers; (2) along late Quaternary faults related to evaporite deformation; (3) hinge zones of structural troughs, subsidence depressions, and synclinal sags; (4) areas of diapiric uplift; and (5) areas underlain by collapse debris.

## ENVIRONMENTAL ASPECTS

As streams incised through the low-relief, basalt-capped surface during the past several million years, topographic relief increased in the stream valleys. This allowed ground water to discharge at progressively lower elevations and altered hydrologic flow paths. Fresh meteoric waters circulated to greater depths, which enhanced evaporite dissolution where it encountered highly to moderately soluble evaporite miner-

Figure 8. Oblique aerial photograph of a large, trash-filled sinkhole on a middle Pleistocene outwash terrace along the Roaring Fork River (at center of photograph). Small, circular features on the terrace surface are smaller sinkholes. Note housing development being built on the valley floor in a similar geologic setting. Photo by J. L. White.

als such as halite, gypsum, and anhydrite. Dissolution of these solid minerals adds sodium, chloride, calcium, and sulfate ions to the ground water. This saline ground water is subsequently discharged to the Colorado River and its tributaries as springs and as seepage into alluvial aquifers (URS Corporation, 1982; Warner and others, 1984; Kirkham and others, 1999), effectively increasing salt loads in the surface-water system. These combined sources constitute the largest natural point-source contribution of dissolved solids to the upper Colorado River Basin (URS Corporation, 1981).

Thermal springs in the area, such as Yampah and Dotsero hot springs, discharge large volumes of dissolved halite and gypsum directly to the Colorado River (URS Corporation, 1981; Eisenhauer, 1986). Yampah hot spring, which supplies water for the Glenwood Hot Springs Pool in the town of Glenwood Springs, flows at about 151 L/s and contains 11 g/L of chloride, 6.9 g/L of sodium, 1.1 g/L of sulfate, and 0.5 g/L of calcium (Barrett and Pearl, 1976). This one single source adds about 240 metric tons of dissolved halite and gypsum each day to the Colorado River. The amount of dissolved halite and gypsum that discharges from this hot spring is roughly equivalent to the creation of one new sinkhole with a volume of about 108 $m^3$ every day, assuming a specific gravity of 2.23 $g/cm^3$. Geothermal heat in the ground-water system greatly increases the solubility of evaporite, which may in part explain the high salt concentrations in the thermal springs. Within the collapse centers, subsurface seepage of saline ground water into the alluvial aquifers and direct discharge of saline cold springs are locally significant sources of salts, as has been documented in the Roaring Fork River valley (Warner and others, 1984; Kirkham and others, 1999).

Gypsum, which is moderately soluble, is the primary evaporite mineral in outcrops of the Eagle Valley Evaporite. Highly soluble halite has been reported in oil-test wells in the area but is not observed at the surface. The halite apparently is dissolved by ground water well below the earth's surface. Similarly, anhydrite has been reported in deep wells and is rare or absent in outcrops, probably because it is hydrated to gypsum prior to exposure in outcrops. Within the southern part of the Carbondale collapse center, surface-water tributaries that are underlain by gypsum-rich outcrops have moderately high specific conductance (Kirkham and others, 1999), which is an indirect measure of salinity. For example, the specific conductance of Cattle Creek near its mouth was 766 µS/cm (microsiemens per centimeter). Cold-water springs that discharged from gypsiferous outcrops in the area exhibited specific-conductance values up to 1,134 µS/cm.

Recent investigations along the lower Roaring Fork

River discovered local occurrences of non-thermal ground water with much higher specific conductance (Kirkham and others, 1999). These waters seep from alluvial material adjacent to and beneath the Roaring Fork River and have specific-conductance values as high as 7,860 µS/cm. Laboratory analyses indicate that they are a sodium chloride type of water. In contrast, waters with only moderate conductance are calcium bicarbonate or calcium sulfate bicarbonate waters. The higher conductivity, sodium chloride–type waters occur along the valley-centered Cattle Creek Anticline, which is a salt diapir. This indicates that (1) halite is closest to the surface along the valley-centered anticlines; (2) meteoric ground water circulates to significant depths and encounters and dissolves halite along its flow path, but does not circulate to depths sufficient to be geothermally heated; or (3) both situations are true.

Upstream of the Eagle and Carbondale collapse centers, the Colorado, Eagle, and Roaring Fork Rivers have relatively low dissolved-solids loads (Warner and others, 1984; Bauch and Spahr, 1998). The loads in the Colorado and Eagle Rivers greatly increase as the rivers cross the Eagle collapse center (Bauch and Spahr, 1998); the load in the Roaring Fork River increases by a factor of 4 as it crosses the Carbondale collapse center (Warner and others, 1984). Chafin and Butler (2002) estimated that the Colorado River removes about 0.8 million metric tons of dissolved evaporite from the collapsed areas each year.

## SUMMARY

Dissolution and flow of evaporite during the late Cenozoic has caused major collapse of the earth's surface in west-central Colorado. Collapse affects an area of at least 3,600 km$^2$ in the contiguous Carbondale and Eagle collapse centers. Detailed studies of Miocene and Pliocene volcanic rocks, which are well preserved in the lower Roaring Fork River valley, constrain the timing, rates, and style of collapse. These volcanic rocks are downdropped as much as 1,200 m in collapse areas.

Widespread regional collapse initiated sometime after ~10 Ma. Several lines of evidence suggest that collapse rates accelerated during the past 3 m.y., a time period when rates of river incision also increased. As rivers cut to progressively greater depths, lithostatic loads on the evaporite sequence beneath the valleys diminished relative to the loads beneath adjacent uplands. These differential lithostatic loads encouraged flow of evaporite toward the valleys and allowed fresh ground water to discharge to the surface from increasing depths. Diapiric flow of evaporite beneath the valleys locally formed valley-centered anticlines in bedrock and tilted Pleistocene outwash terraces along the valley floor.

Subsurface dissolution of evaporite created voids, complex dissolution cavities, and fissures. Where these propagate to the ground surface, broad depressions and sinkholes, which constitute the primary engineering problem associated with evaporite collapse, may develop. Sinkholes are found throughout much of the collapse area but are especially abundant on the floor of the Roaring Fork valley in areas of diapirism. Many of the historic sinkholes occurred in areas where human activities, including irrigation, add surcharges of water to the soil column and underlying bedrock. Both the sudden and gradual subsidence associated with sinkholes poses significant engineering challenges. No historical problems have been attributed to regional evaporite tectonism. However, a regional mechanism should not be overlooked as a potential cause of subsidence or ground deformation along the margins of the collapse centers, along late Quaternary faults, in hinge zones of subsidence structures, and in areas of diapirism or collapse debris.

Dissolution of evaporite increases concentrations of dissolved salts in ground water. The saline ground water subsequently discharges to the Colorado River and its tributaries through springs, both hot and cold, and through subsurface seepage into alluvial aquifers. Salt loading in the collapse areas constitutes the largest natural source of dissolved salts to the upper Colorado River.

The high-salinity loads of springs and rivers, along with the historic occurrence of sinkholes and deformed late Quaternary deposits, indicate that evaporite dissolution and collapse are still active. Since hundreds of meters of evaporite remain in the subsurface beneath the collapse centers, the environmental and engineering concerns related to evaporite in west-central Colorado will continue into the foreseeable future.

## ACKNOWLEDGMENTS

Funding for this project was provided by the National Cooperative Geologic Mapping Program, State of Colorado General Funds, and Colorado Department of Natural Resources Severance Tax Operational Funds. The manuscript benefited from the reviews of David Noe, Colorado Geological Survey, and Karl Kellogg, U.S. Geological Survey.

## REFERENCES CITED

Barrett, J. K.; and Pearl, R. H., 1976, Hydrogeologic data of thermal springs and wells in Colorado: Colorado Geological Survey Information Series 6, 124 p.

Bauch, N. J.; and Spahr, N. E., 1998, Salinity trends in surface waters of the upper Colorado River Basin, Colorado: Journal of Environmental Quality, v. 27, p. 640–655.

Benson, J. C.; and Bass, N. W., 1955, Eagle River anticline, Eagle County, Colorado: American Association of Petroleum Geologists Bulletin, v. 39, p. 103–106.

Bryant, B.; Kunk, M. J.; and Kirkham, R. M., 2002, Timing and rates of late Cenozoic incision by the Colorado River in Glenwood Canyon, Colorado [abstract]: Geological Society of America Abstracts with Programs, v. 34, no. 6, p. 320–321.

Budahn, J. R.; Unruh, D. M.; Kunk, M. J.; Byers, F. M., Jr.; Kirkham, R. M.; and Streufert, R. K., 2002, Correlation of late Cenozoic basaltic lava flows in the Carbondale and Eagle collapse centers in west-central Colorado based

on geochemical, isotopic, age, and petrologic data, *in* Kirkham, R. M.; Scott, R. B.; and Judkins, T. W. (eds.), Late Cenozoic evaporite tectonism and volcanism in west-central Colorado: Geological Society of America Special Paper 366, p. 167–196.

Chafin, D. T.; and Butler, D. L., 2002, Dissolved-solids-load contribution of the Pennsylvanian Eagle Valley Evaporite to the Colorado River, west-central Colorado, *in* Kirkham, R. M.; Scott, R. B.; and Judkins, T. W. (eds.), Late Cenozoic evaporite tectonism and volcanism in west-central Colorado: Geological Society of America Special Paper 366, p. 149–155.

Eisenhauer, R. J., 1986, Characterization of Glenwood springs and Dotsero springs source aquifers: U.S. Bureau of Reclamation Report REC-ERC-86-1, 35 p.

Hubert, J. F., 1954, Structure and stratigraphy of an area east of Brush Creek, Eagle County, Colorado: Harvard University unpublished M.S. thesis, Cambridge, Massachusetts, 104 p.

Hudson, M. R.; Harlan, S. S.; and Kirkham, R. M., 2002, Paleomagnetic investigation of the structural deformation and magnetostratigraphy of Neogene basalts in western Colorado, *in* Kirkham, R. M.; Scott, R. B.; and Judkins, T. W. (eds.), Late Cenozoic evaporite tectonism and volcanism in west-central Colorado: Geological Society of America Special Paper 366, p. 197–212.

Izett, G. A.; and Wilcox, R. E., 1982, Map showing localities and inferred distributions of the Huckleberry Ridge, Mesa Falls, and Lava Creek ash beds (Pearlette family ash beds) of Pliocene and Pleistocene age in the western United States and southern Canada: U.S. Geological Survey Miscellaneous Investigations Series Map I-1325, scale 1:4,000,000.

Kirkham, R. M.; and Scott, R. B., 2002, Introduction to late Cenozoic evaporite tectonism and volcanism in west-central Colorado, *in* Kirkham, R. M.; Scott, R. B.; and Judkins, T. W. (eds.), Late Cenozoic evaporite tectonism and volcanism in west-central Colorado: Geological Society of America Special Paper 366, p. 1–14.

Kirkham, R. M.; and Widmann, B. L., 1997, Geologic map of the Carbondale quadrangle, Garfield County, Colorado: Colorado Geological Survey Open-File Report 97-3, scale 1:24,000.

Kirkham, R. M.; Zook, J. M.; and Sares, M. A., 1999, Reconnaissance field investigation of surface-water conductance in the Snowmass–Glenwood Springs area, west-central Colorado: Colorado Geological Survey Information Series 49, 21 p.

Kirkham, R. M.; Kunk, M. J.; Bryant, Bruce; and Streufert, R. K., 2001a, Constraints on timing and rates of late Cenozoic incision by the Colorado River in Glenwood Canyon, Colorado: a preliminary synopsis, *in* Young, R. A.; and Spamm, E. E. (eds.), The Colorado River: origin and evolution: Grand Canyon Association Monograph 12, Arizona, in press.

Kirkham, R. M.; Streufert, R. K.; Budahn, J. R.; Kunk, M. J.; and Perry, W. J., 2001b, Late Cenozoic regional collapse due to evaporite flow and dissolution in the Carbondale collapse center, west-central Colorado: The Mountain Geologist, v. 38, p. 193–210.

Kirkham, R. M.; Scott, R. B.; and Judkins, T. W. (eds.), 2002a, Late Cenozoic evaporite tectonism and volcanism in west-central Colorado: Geological Society of America Special Paper 366, 234 p.

Kirkham, R. M.; Streufert, R. K.; Kunk, M. J.; Budahn, J. R.; Hudson, M. R.; and Perry, W. J., 2002b, Evaporite tectonism in the lower Roaring Fork River valley, west-central Colorado, *in* Kirkham, R. M.; Scott, R. B.; and Judkins, T. W. (eds.), Late Cenozoic evaporite tectonism and volcanism in west-central Colorado: Geological Society of America Special Paper 366, p. 73–99.

Kirkham, R. M.; White, J. L.; and Sares, M. A., 2002c, Environmental and engineering aspects of evaporite tectonism, west-central Colorado [abstract]: Geological Society of America Abstracts with Programs, v. 34, no. 6, p. 215.

Kunk, M. J.; Budahn, J. R.; Unruh, D. M.; Stanley, J. O.; Kirkham, R. M.; Bryant, Bruce; Scott, R. B.; Lidke, D. J.; and Streufert, R. K., 2002, $^{40}Ar/^{39}Ar$ ages of late Cenozoic volcanic rocks within and around the Carbondale and Eagle collapse centers, Colorado: constraints on the timing of evaporite related collapse and incision of the Colorado River, *in* Kirkham, R. M.; Scott, R. B.; and Judkins, T. W. (eds.), Late Cenozoic evaporite tectonism and volcanism in west-central Colorado: Geological Society of America Special Paper 366, p. 213–234.

Larson, E. E.; Ozima, Minoru; and Bradley, W. C., 1975, Late Cenozoic basic volcanism in northwest Colorado and its implications concerning tectonism and origin of the Colorado River system, *in* Curtis, Bruce (ed.), Cenozoic history of the southern Rocky Mountains: Geological Society of America Memoir 144, p. 155–178.

Lidke, D. J.; Hudson, M. R.; Scott, R. B.; Shroba, R. R.; Kunk, M. J.; Perry, W. J., Jr.; Kirkham, R. M.; Budahn, J. R.; Streufert, R. K.; Stanley, J. O.; and Widmann, B. L., 2002a, Eagle collapse center: interpretation of evidence for late Cenozoic evaporite-related deformation in the Eagle River basin, Colorado, *in* Kirkham, R. M.; Scott, R. B.; and Judkins, T. W. (eds.), Late Cenozoic evaporite tectonism and volcanism in west-central Colorado: Geological Society of America Special Paper 366, p. 101–120.

_____2002b, Eagle collapse center: interpretation of evidence for late Cenozoic evaporite-related deformation in the Eagle River basin, Colorado [abstract]: Geological Society of America Abstracts with Programs, v. 34, no. 6, p. 288.

Mallory, W. W., 1966, Cattle Creek anticline, a salt diapir near Glenwood Springs, Colorado: U.S. Geological Survey Professional Paper 550-B, p. B12–B15.

_____1971, The Eagle Valley Evaporite, northwest Colorado—a regional synthesis: U.S. Geological Survey Bulletin 1311-E, 37 p.

Mock, R. G., 2002, Geologic setting, character, and potential hazards for evaporite-related sinkholes in Eagle and Garfield Counties, northwest Colorado, *in* Kirkham, R. M.; Scott, R. B.; and Judkins, T. W. (eds.), Late Cenozoic evaporite tectonism and volcanism in west-central Colorado: Geological Society of America Special Paper 366, p. 157–166.

Murray, F. N., 1966, Stratigraphy and structural geology of the Grand Hogback monocline, Colorado: University of Colorado unpublished Ph.D. dissertation, Boulder, 219 p.

_____1969, Flexural slip as indicated by faulted lava flows along the Grand Hogback monocline, Colorado: Journal of Geology, v. 77, p. 333–339.

Perry, W. J.; Miller, J. J.; and Scott, R. B., 2002, Implications for evaporite tectonism in the Carbondale and Eagle collapse centers of west-central Colorado, based on reprocessed seismic reflection data, *in* Kirkham, R. M.; Scott, R. B.; and Judkins, T. W. (eds.), Late Cenozoic evaporite tectonism and volcanism in west-central Colorado: Geological Society of America Special Paper 366, p. 55–72.

Scott, R. B.; Lidke, D. J.; Shroba, R. R.; Hudson, M. R.; Kunk, M. J.; Perry, W. J., Jr.; and Bryant, Bruce, 1998, Large-scale active collapse in western Colorado: interaction of salt tectonism and dissolution, *in* Brahana, J. V.;

Eckstein, Yoram; Ongley, L. K.; Schneider, Robert; and Moore, J. E. (eds.), Gambling with groundwater—physical, chemical, and biological aspects of aquifer–stream relations: Proceedings of joint meeting of 28th Congress of International Association of Hydrologists and annual meeting of American Institute of Hydrologists, Las Vegas, September 28–October 2, 1998, p. 195–204.

Scott, R. B.; Lidke, D. J.; Hudson, M. R.; Perry, W. J.; Bryant, Bruce; Kunk, M. J.; Budahn, J. R.; and Byers, F. M., Jr., 1999, Active evaporite tectonism and collapse in the Eagle River valley and the southwestern flank of the White River uplift, Colorado, *in* Lageson, D. R.; Lester, A. P.; and Trudgill, B. D. (eds.), Colorado and adjacent areas: Geological Society of America Field Guide 1, p. 97–114.

Scott, R. B.; Bryant, B.; and Perry, W. J., Jr., 2002, Late Cenozoic deformation by evaporite tectonism in the Grand Hogback monocline, southwest of the White River uplift, Colorado, *in* Kirkham, R. M.; Scott, R. B.; and Judkins, T. W. (eds.), Late Cenozoic evaporite tectonism and volcanism in west-central Colorado: Geological Society of America Special Paper 366, p. 121–147.

Stover, B. K., 1986, Geologic evidence of Quaternary faulting near Carbondale, Colorado, with possible associations to the 1984 Carbondale earthquake swarm, *in* Rogers, W. P.; and Kirkham, R. M. (eds.), Contributions to Colorado seismicity and tectonics—a 1986 update: Colorado Geological Survey Special Publication 28, p. 295–301.

Unruh, D. M.; Budahn, J. R.; Siems, D. F.; and Byers, F. M., Jr., 2001, Major- and trace-element geochemistry; lead, strontium, and neodymium isotopic compositions; and petrography of late Cenozoic basaltic rocks from west central Colorado: U.S. Geological Survey Open-File Report 01-477, 90 p.

Unruh, J. R.; Wong, I. G.; Bott, J. D.; Silva, W. J.; and Lettis, W. R., 1993, Seismotectonic evaluation, Rifle Gap Dam, Silt Project, Ruedi Dam, Fryingpan–Arkansas Project: Unpublished report prepared by William A. Lettis & Associates and Woodward-Clyde Consultants for U.S. Bureau of Reclamation, Denver, Colorado, 154 p.

URS Corporation, 1981, Salinity investigations of Glenwood–Dotsero Springs unit: Report prepared for U.S. Department of Interior, Water and Power Resources Services, 98 p.

Warner, J. W.; Heimes, F. J.; and Middelburg, R. F., 1984, Ground-water contribution to the salinity of the upper Colorado River Basin: U.S. Geological Survey Water-Resources Investigation Report 84-4198, 113 p.

White, J. L., 2002, Collapsible soils and evaporite karst hazards of the Roaring Fork River corridor, Garfield, Eagle, and Pitkin Counties, Colorado: Colorado Geological Survey Map Series MS-34, scale 1:50,000.

White, J. L.; Kirkham, R. M.; and Mock, R. G., 2002, Evaporite karst hazards of the lower Roaring Fork River valley, west-central Colorado [abstract]: Geological Society of America Abstracts with Programs, v. 34, no. 6, p. 288.

# Gypsum Karst in Southwestern Utah: Failure and Reconstruction of Quail Creek Dike

***C. Charles Payton***
AMEC Earth & Environmental, Inc.
Salt Lake City, Utah

***Michael N. Hansen***
RB&G Engineering, Inc.
Provo, Utah

**ABSTRACT.**—Quail Creek Dam and Reservoir are owned and operated by the Washington County Water Conservancy District (WCWCD) in St. George, Utah. The reservoir is ~15 mi northeast of St. George. The 40,000-acre-ft, off-stream reservoir was formed by two dams. Originally, both dams were zoned earth-fill-embankment dams, with the lower dam on the southwest being called the dike. Construction of the dike was completed in April 1984; reservoir filling began in April 1985, after the main dam was completed. The dike had severe leakage problems, and three foundation-grouting programs were undertaken at different times in an attempt to control seepage. However, on January 1, 1989, the dike failed.

Morrison Knudsen Engineers of San Francisco (now part of Washington Group International, Inc., Boise, Idaho) and James M. Montgomery Consulting Engineers of Salt Lake City (now Montgomery Watson Harza) were retained to design a replacement dike. Geotechnical investigations began in June 1989 for the purpose of evaluating foundation conditions and borrow materials. The foundation bedrock consists of thinly bedded sedimentary rocks, including silty dolomicrite, gypsiferous siltstone, gypsum, and sandstone. The sequence is in the upper part of the Moenkopi Formation of Triassic age. Seventeen rock units were identified.

Rock quality, the amount of gypsum, hydraulic-conductivity data, rock-core recovery, and previous grouting records were evaluated to aid in the selection of the type and depth of cutoff. A positive concrete cutoff was selected; it has a maximum depth of ~75 ft in the breach area, tapering to 50 ft at the left abutment, and 25 ft at the right abutment. The rebuilt dike is a concrete gravity dam constructed by the roller-compacted-concrete (RCC) method. The dike has a maximum height of 80 ft and a crest length of ~2,000 ft. It was completed in June 1990.

Since the second reservoir filling in 1990–91, the dike has performed well. However, seepage has increased slowly over the years since construction, exceeding 12 cubic feet per second by the spring of 2002. By the spring of 2003, the WCWCD had completed a foundation-grouting program from within the drainage gallery of the dike and had placed a partial clay blanket upstream of the dike, which is overlain with a geomembrane liner topped with compacted fill. The seepage is due to continued dissolution of gypsum within the foundation bedrock. Dam safety, while always a concern, is not in question at this time.

## INTRODUCTION

The Quail Creek Project was planned as an off-stream water-storage project in Washington County, southwestern Utah. The Quail Creek dams and reservoir are owned and operated by the Washington County Water Conservancy District (WCWCD). The project location is shown in Figure 1, and a more detailed location map of the dam, dike, and reservoir is shown in Figure 2. The project provides for the storage of ~40,000 acre-ft of irrigation, municipal, and industrial water. Water is supplied to the off-stream reservoir by a 66-in. pipeline from a diversion dam on the Virgin River ~2 mi upstream from Hurricane, Utah. The reservoir is formed by Quail Creek Dam, which is a zoned embankment with a maximum height of 200 ft and length of 900 ft, and Quail Creek Dike, which was a zoned embankment with a maximum height of 78 ft and length of 1,980 ft. The crest elevation for dam and dike is 2,995 ft.

The project design was started in 1982, and construction began in 1983; the project was completed in January 1985. Reservoir filling was started in April 1985.

## GEOLOGIC SETTING

Quail Creek Reservoir lies within a northeast–southwest-trending valley between hills that are the eroded remnants of a portion of the Harrisburg Dome known as the Virgin Anticline. The anticline is a dou-

Payton, C. C.; and Hansen, M. N., 2003, Gypsum karst in southwestern Utah: failure and reconstruction of Quail Creek Dike, *in* Johnson, K. S.; and Neal, J. T. (eds.), Evaporite karst and engineering/environmental problems in the United States: Oklahoma Geological Survey Circular 109, p. 293–303.

bly-plunging dome, which exposes beds of the Shnabkaib Member of the Triassic Moenkopi Formation in the area of the dike (O'Neill and Gourley, 1991). The axis of the Virgin Anticline is approximately at the right (west) abutment of the Quail Creek Dike. The Shnabkaib Member is overlain by the Upper Red Member, which is prominent in the hills southeast of the site. A buff-colored sandstone unit, known as the Purgatory Sandstone, lies between these two Moenkopi members locally and is the predominant rock unit in the left abutment of the dike.

The thin-bedded sediments at the site were most likely deposited in a complex mixture of environments, which may have included streams, lagoons, salt flats, flood plains, tidal flats, and shallow sea floors. During deposition, the climate was probably semiarid to arid, as evidenced by the abundance of gypsum, an evaporite mineral. Regional geologic studies, completed many years before construction of the reservoir, reported the Shnabkaib Member to be composed of 65% siltstone, 10% limestone and dolomite, and 25% gypsum (Gourley, 1992). This sedimentary sequence was later tilted, uplifted, and eroded. The sedimentary beds exposed at the dike strike northeast–southwest and dip 5–25° to the southeast.

Locally, the Shnabkaib Member is thinly bedded to laminated, and hardness ranges from moderately hard to very soft (where the cementing, which is mostly gypsum, has been removed) (Gourley, 1992). Differential erosion and weathering of the sedimentary beds

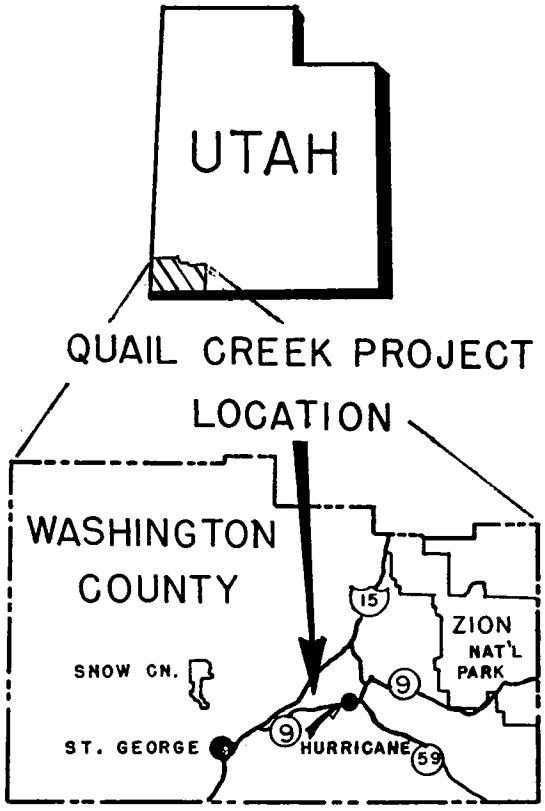


Figure 1. Map showing location of Quail Creek Reservoir in Washington County, southwestern Utah (modified from Gourley, 1992).

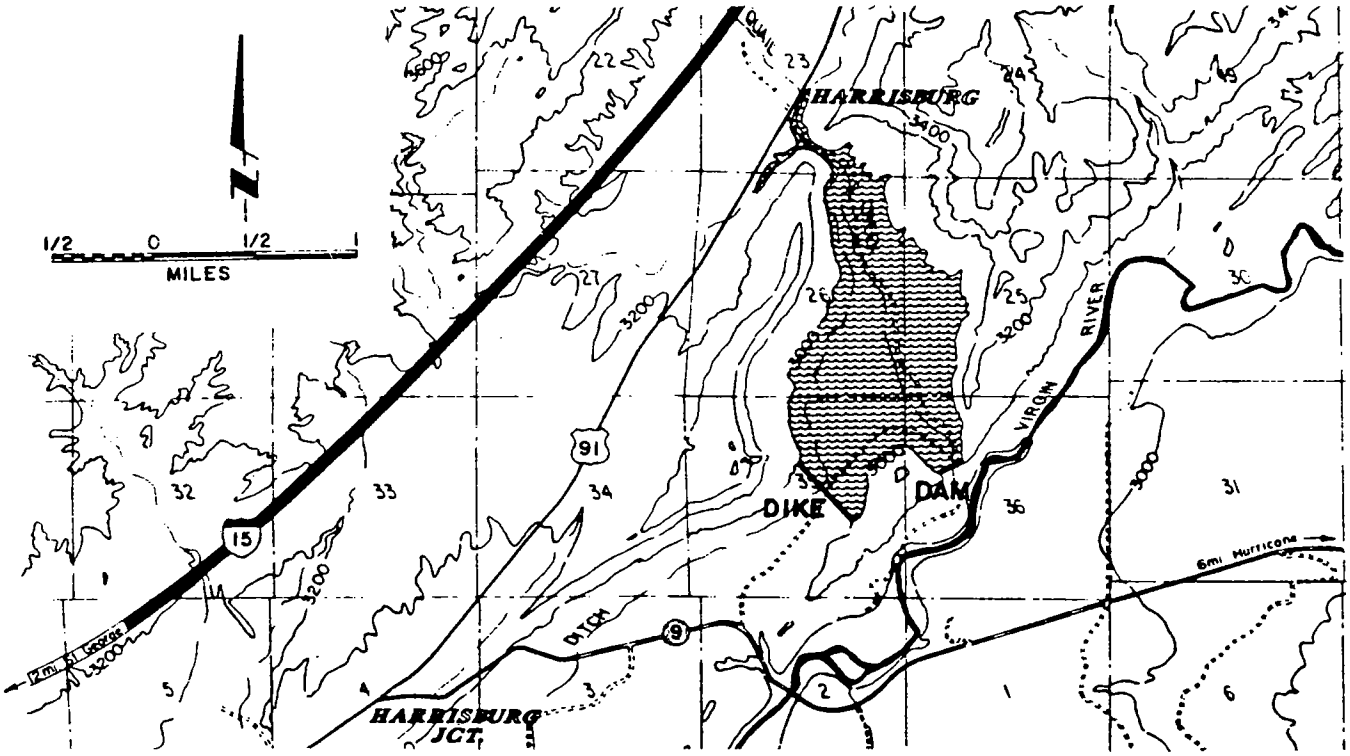


Figure 2. Map showing details of Quail Creek Dam, Dike, and Reservoir in southwestern Utah (modified from James and others, 1989).

have resulted in a topography that reflects the dipping nature of alternating strata with varying resistance to weathering and erosion. The topography consists of a series of small hogbacks aligned in a northeast–southwest direction, with the steep side toward the northwest and the more gentle dip slope toward the southeast. The formation of hogbacks may also be related to joint density and gypsum content. Within the upper 10 ft of the weathered zone, thin beds of gypsum expand up to several times their original thickness. This expansion and subsequent heave often fracture the surrounding or overlying rock in a brittle manner. The reformed or recrystallized gypsum exists as thin pillars or filaments, surrounded by void space, which support the overlying rock (O'Neill and Gourley, 1991).

## DIKE CONSTRUCTION

The original Quail Creek Dike had a maximum height of 78 ft, a crest width of 20 ft, and a length of 1,980 ft. Foundation treatment consisted of a 30-ft-wide centerline cutoff trench through weathered bedrock to an average depth of 10 ft and nominal stripping to a depth of 1 ft. Exposed rock contacts were not treated, and grouting was limited to a sandstone section in the left abutment. A zoned embankment was placed over the cutoff trench, which consisted of a centrally located zone I of generally low-plasticity silty and clayey sands, with a 1-ft blanket of medium-plasticity weathered shale (zone II) at the bottom of the cutoff trench and a 10-ft-thick, vertical processed-sand filter downstream of zone I. The upstream shell was pit-run sand and gravel (zone III), and the downstream shell was random fill (zone IV) enveloped by zone III gravels. Upstream slope protection consisted of 18 in. of dumped basalt riprap.

During construction, zone I material was used to level the stripped foundation, and because bedrock topography consists of a series of hogback ridges and valleys oriented perpendicular to the dike axis, at some locations more than 10 ft of zone I material was placed over the foundation from the upstream toe to the downstream toe. Construction of the dike was completed in April 1984.

## DIKE PERFORMANCE

Reservoir filling began in April 1985, after the main Quail Creek Dam was completed in January 1985. As the reservoir rose to an elevation of ~2,935 ft, seepage appeared along the downstream toe of the dike and from the hillside downstream of the left abutment. Figure 3 is an aerial photograph showing the many seepage rivulets, which developed downstream of the dike. In March 1986, initial actions to mitigate this seepage included placing a weighted filter blanket of concrete sand, pea gravel, and coarse gravel along the downstream toe in the seepage area, and drilling 18 inclined drain holes along the downstream toe from station 6+40 to station 10+00.

In May 1986, with the reservoir at elevation 2,969 ft, seepage flow was estimated at 6.3 cubic feet per second (cfs), with major seepage concentrations downstream of the toe at stations 3+00 and 6+50. Grouting had been initiated in April 1986 and was completed in September 1986. Seepage had been reduced to ~0.3 cfs, with the reservoir at an elevation of 2,949 ft. In October 1986, a contract was let to install an upstream cutoff trench to partially blanket the reservoir for 500 ft upstream of the upstream toe. In June 1987, seepage started to increase downstream near station 6+00. Grouting resumed in July 1987 and continued to April 1988, when seepage was reduced to ~1 cfs at a reservoir elevation of 2,985 ft. During the summer of 1988, seepage increased again to ~5 cfs, primarily at station 4+30. Grouting was resumed in September 1988 and stopped in November 1988, with seepage reduced to 0.1 cfs, at a reservoir elevation of 2,976 ft.

## DIKE FAILURE

On December 31, 1988, discolored water was observed flowing upward around an observation well near station 5+90. Equipment and materials were mobilized to place a gravel filter over the seep area. Despite continued efforts to control the seepage, the flow increased to an estimated 70 cfs at ~10:30 p.m., when the flow changed from vertical to horizontal from a rapidly growing cavity at the toe. At ~11:30 p.m., a wedge of the downstream slope, ~50 ft wide and extending about one-third of the way up the slope, dropped down. Continuing embankment caving toward the reservoir crossed the dike crest and breached the dike, releasing the reservoir water at ~12:30 a.m. on January 1, 1989. By 1:00 p.m. on January 1, ~25,000 acre-ft of water had drained from the reservoir, resulting in a breach ~300 ft wide and 80 to 90 ft deep. An aerial photograph of the dike breach is presented

Figure 3. Aerial view of dike seepage, 1986 (from Utah Division of Water Resources).

in Figure 4. A photograph taken from the scoured area downstream of the dike is shown in Figure 5. A plan view of the original Quail Creek Dike embankment showing the area of the breach is given in Figure 6.

Water flowed from the reservoir, through the breached dike, and then to the highway between St. George and Hurricane, Utah, resulting in extensive erosion of the highway embankment, pipelines, bridge abutments at the Virgin River, and flooding downstream along the Virgin River. No loss of human life occurred, and the estimated cost of damages amounted to ~$15 million.

As a result of the breach failure of the Quail Creek Dike, the State of Utah Engineer appointed an independent review team to investigate the failure. Team investigations began on January 11, 1989. The initial objective was to determine the mechanism that caused failure of the dike, including how the design or remedial work undertaken may have contributed to the failure. The team completed a report (James and others, 1989) on the cause of the failure in March 1989. They concluded that the failure resulted because embankment materials placed on the foundation, including the overburden left in place, were not protected from erosion by seepage moving along the foundation contact. While proper defensive design measures would have prevented failure, the dissolution of gypsum by continuing foundation seepage might eventually have led to unacceptable volumes of seepage from an economic standpoint.

Figure 4. Aerial view of the dike breach, January 1989 (from Utah Division of Water Resources).

## DESIGN AND RECONSTRUCTION OF QUAIL CREEK DIKE

### Dike Foundation Conditions

Geotechnical investigations for the design of a new dam at the Quail Creek Dike site were begun in June

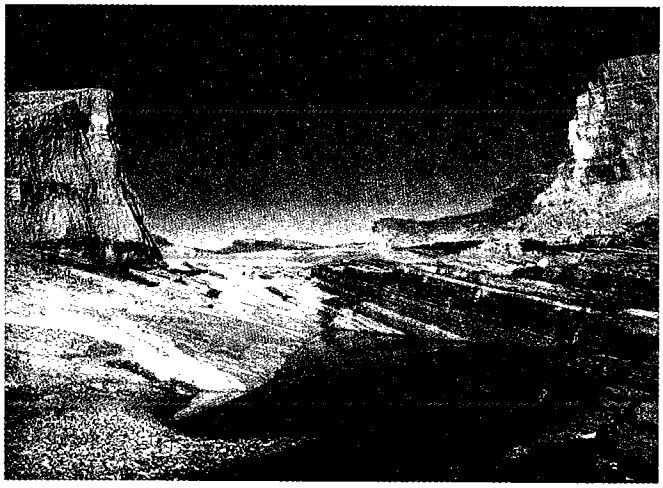

Figure 5. View of breach area from downstream, showing scoured area, January 1989 (from Utah Division of Water Resources).

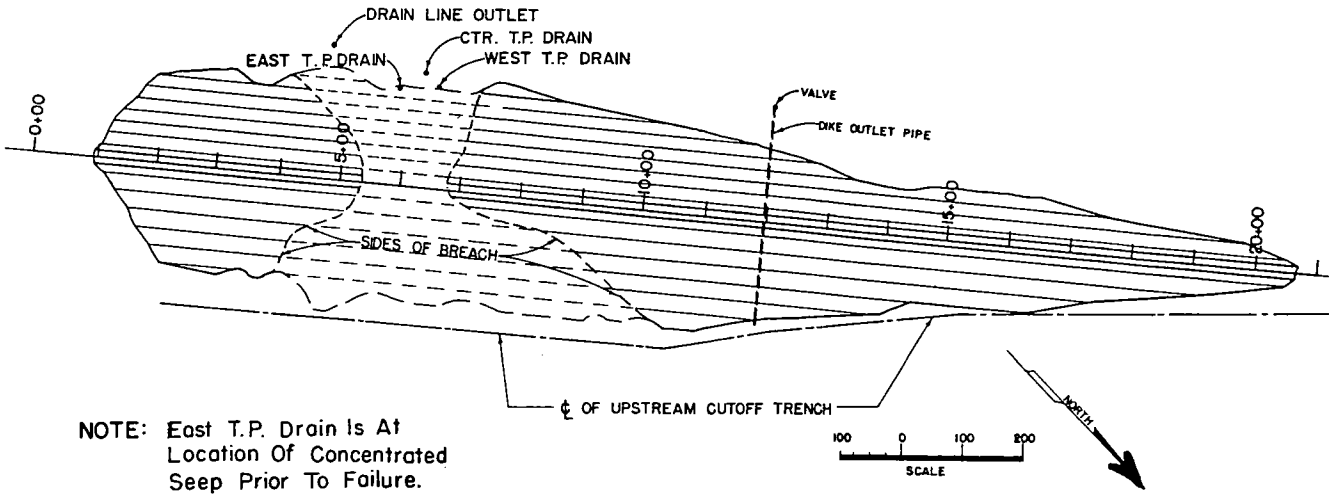


Figure 6. Plan view of original Quail Creek Dike, showing the area breached on January 1, 1989 (from James and others, 1989). View looking to the southwest.

1989. The purpose of these investigations was to determine rock conditions and to determine foundation treatment and cutoff depth for the new dike. The scope of work for the geotechnical studies included the following: (1) exploration of the rock foundation by angled drill holes and two vertical holes for piezometer installation; (2) geologic mapping of the exposed rock within the breach, and upstream and downstream of the dike embankment; (3) evaluation of potential borrow sources for embankment and aggregate materials; (4) laboratory testing of soil and rock samples to determine engineering and chemical properties; and (5) seismicity studies to determine design ground-motion parameters.

Drilling through the dike embankment began in July 1989, together with the mapping of exposed bedrock in the breach area. A geologic map of the bedrock exposed in the breach was prepared and is shown in Figure 7. The foundation rock was divided into several rock units and numbered, based on exploratory drilling and bedrock exposures in the breach area. The rock units within the breach area were measured, and a stratigraphic section (Fig. 8) was developed by James and others (1989).

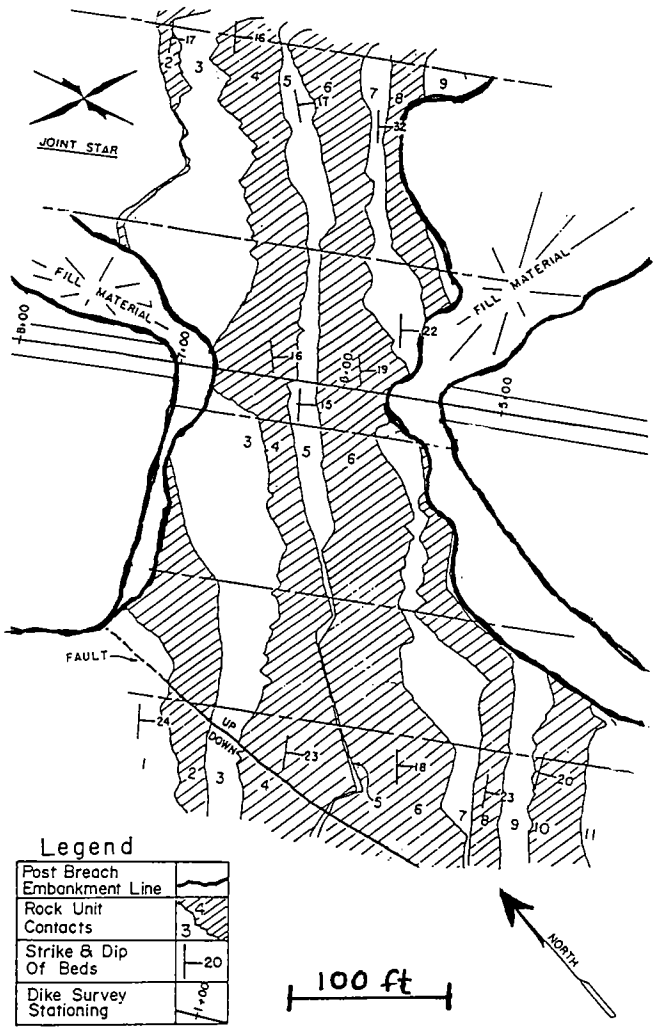


Figure 7. Geologic map of bedrock units exposed in the Quail Creek Dike breach (from James and others, 1989). View looking to the northeast.

Gypsiferous siltstone is the principal rock type exposed in the breach on the basis of an examination of the various rock types in outcrop and in core samples. Results of a petrographic and X-ray-diffraction study of the rock units and joint-filling materials indicate that many of the rock units are actually a fine-grained silty dolomite, more appropriately called dolomicrite. During geotechnical investigations, the softer, reddish-brown beds were identified as siltstone, and the moderately hard, light-greenish-gray beds were designated as dolomicrite. Some of the siltstone beds were also light gray. It was postulated that the red color was imparted to the rocks during diagenesis as iron-rich silicate and ferrous oxide changed to ferric oxide.

The hogback topography in the area of the dam foundation has developed because of differential weathering and erosion of the soft to moderately hard, reddish-brown siltstone, and the moderately hard to hard, light-gray dolomicrite beds. Other soft-rock conditions are associated with seepage areas along open joints and fractures. Weathering has occurred along the flow paths and into the adjacent rock. Flow paths and erosion of the softer bedrock were noticeable in the breach area. The thin-bedded siltstone and dolomicrite of rock units 4, 5, and 6 are shown in Figure 9.

Joint systems in some of the rock units were clearly exposed in the breach area. Through joint mapping by geologists from the Utah State Division of Water Resources, and additional work by the authors, three principal joint sets were identified. The joint sets average N. 25° E., N. 20° W., and N. 80° W., all with near-vertical dips. The spacing between individual joints ranges from a few feet to >20 ft, with an average spacing of ~10 ft. The more competent beds (rock units 2, 4, 5, and 7) show stronger joint patterns. A photograph of the joints within rock unit 4 is given in Figure 10. The average spacing of open joints within rock units 4 and 5 is 2 ft, whereas the spacing within rock units 2 and 7 is 10 ft or more. Widths of some of the open joints average 2 in. The filling materials observed are gypsum, calcite, and quartz, and the clay minerals illite, kaolinite, and smectite. Joint fillings are usually pale red, grayish red, and light greenish gray.

Gypsum is a common constituent in all the rock units stratigraphically below the yellow-brown Purgatory Sandstone in the left abutment. Gypsum laminae parallel to bedding planes range in thickness from one-thirty-secondth of an inch to three-fourths of an inch, with an average thickness of one-eighth of an inch. Gypsum is present as a cementing agent in many of the beds, ranging from <10% to >50% of the rock. It occurs as nodules in some beds, particularly within rock units P, 0, 6, and 8. Unit P was added, during exploration, to include a thick sequence of thin beds below unit 0. Within unit P were local small voids and

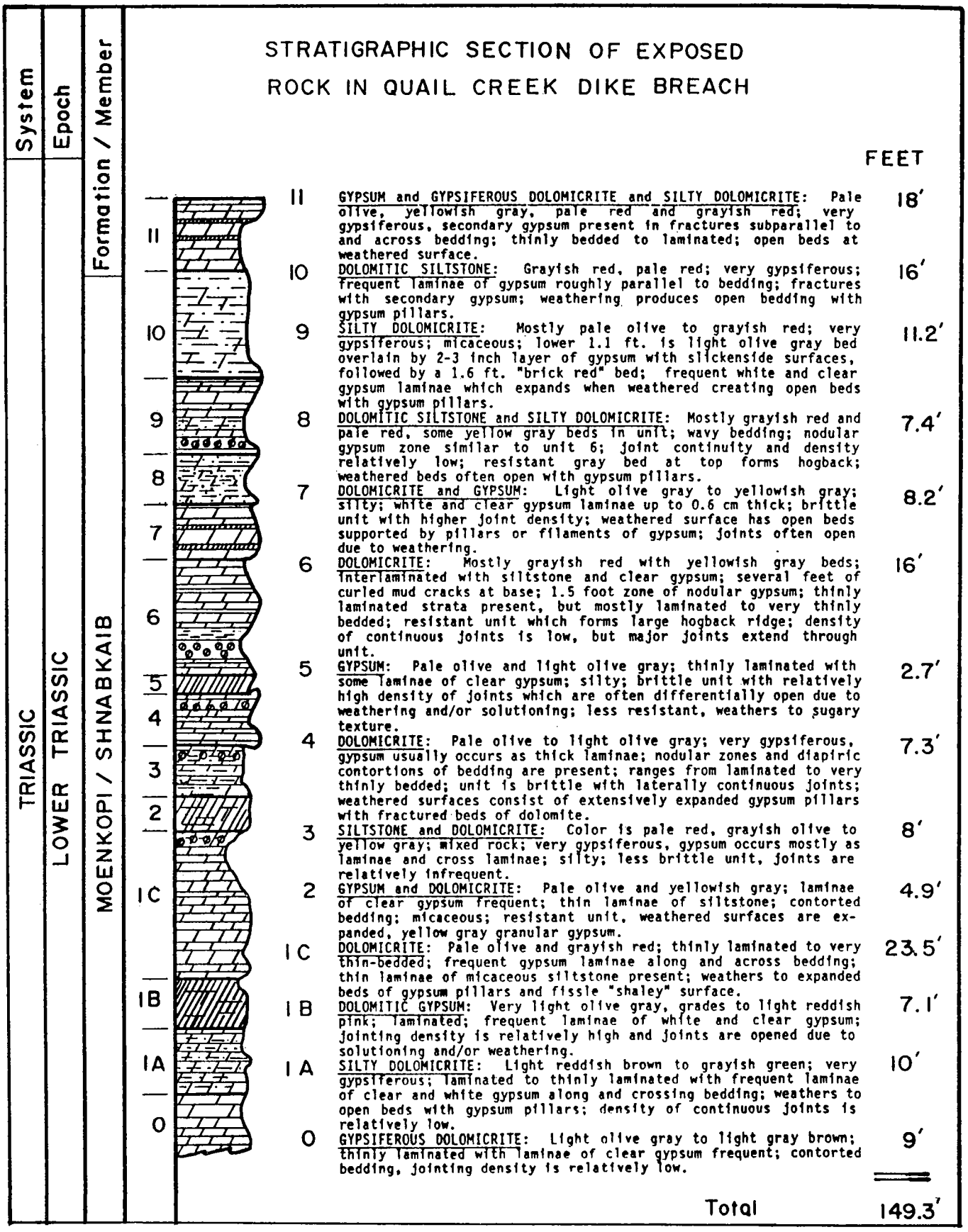


Figure 8. Stratigraphic section of rocks exposed in the Quail Creek Dike breach (from James and others, 1989).

open joints filled with crude oil. Unit P extended to the right abutment and is along the axis of the Virgin Anticline. Unit 0 apparently forms a stratigraphic trap, and small amounts of the crude oil have accumulated along the center of the anticline. Table 1 (from Payton, 1992) presents a brief description of each rock unit identified throughout the Quail Creek Dike foundation.

Gypsum fills a large variety of the mud cracks; this is particularly noticeable in rock unit 4. Gypsum is also present as a secondary mineral in thin layers nearly parallel to bedding as lenticular seams, as cross-cutting veins, and as the filling material in joints. A geologic cross section along the dike axis was developed to show the general attitude of the interbedded rock units and the dip of the beds toward the left abutment (Fig. 11).

## Geochemical Analyses

Gypsum and other soluble evaporite minerals within the bedrock units, and other salt samples collected near the breached dike, were evaluated for the purpose of providing quantitative information on the total amount and rate of gypsum dissolution that could be expected.

Chemical analyses and X-ray-diffraction studies were performed on rock-core samples and samples of soluble minerals taken from rock core. The studies showed that gypsum (hydrated calcium sulfate) is the predominant evaporite mineral, with subordinate amounts of kieserite (hydrated magnesium sulfate), calcite (calcium carbonate), halite (sodium chloride), and thenardite (sodium sulfate). Gypsum is also the dominant cementing mineral in most of the rock units, exceeding 50% in rock unit 5.

The rate of gypsum dissolution or retreat is proportional to seepage velocity, which in turn is proportional to the permeability of joints and other rock discontinuities. The results of the dissolution study indicated

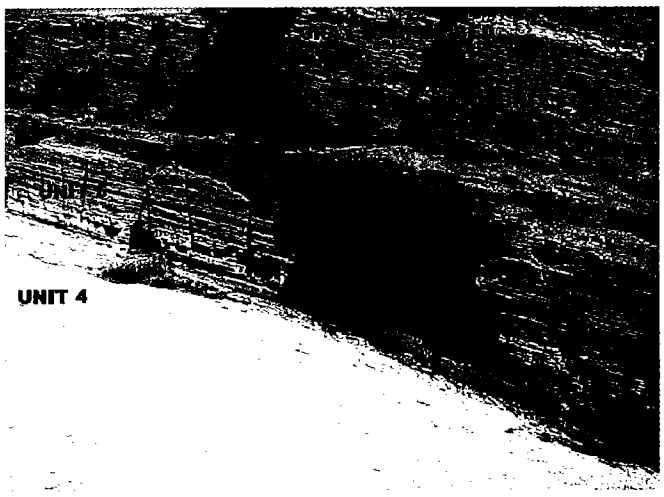


Figure 9. View of rock units 4, 5, and 6. Note dissolution of gypsum along joints in unit 5 (from Utah Division of Water Resources).

Figure 10. Dissolution of joints in rock unit 4 (from Utah Division of Water Resources).

that for seepage velocities on the order of $1.0 \times 10^{-4}$ cm/s, an 0.8-in.-thick gypsum vein could dissolve at the rate of a few inches per year. For seepage velocities of $\sim 1.0 \times 10^{-2}$ cm/s, the gypsum vein could dissolve at the rate of ~30 ft per year. Dissolution of gypsum from joints will proceed until the concentration of calcium sulfate in the seepage water becomes saturated (~2,000 ppm calcium sulfate).

Chemical analyses were made of reservoir water, as well as of water from seeps downstream of the dam axis. Significant differences in the results suggest that gypsum, calcite, and sodium and magnesium sulfates are dissolving within the reservoir basin.

## Dike-Foundation Preparation

Approximately 10 ft of weathered and fractured bedrock was removed to expose unweathered bedrock below the footprint of the dike. Hogbacks were removed so that a relatively flat rock foundation was formed. Excavation of the weathered rock was accomplished with large dozers equipped with single-shank hydraulic rippers. The hogbacks required drilling and blasting.

A positive cutoff was designed, and the depth was based on the following considerations: (1) the cutoff should intercept as many zones as economically feasible of poor-quality rock, rock with a high gypsum content, and rock with high hydraulic conductivities and water loss; (2) the cutoff should extend below the existing grout curtain of the dike, which generally had a depth of ~50 ft; evidence indicated that the grout curtain, consisting of type II cement, may have deteriorated from sulfate attack; (3) the cutoff should reduce the hydraulic gradient within the foundation as much as economically practical; reducing the hydraulic gradient reduces seepage velocities and the rate of gypsum dissolution.

The cutoff could be constructed to intercept only a

## Table 1. — Rock Unit Stratigraphic Descriptions

| Rock Unit Designation/Rock Type | Thickness (feet) | Macroscopic Properties: Color | Bedding | Hardness | Visible Gypsum: Percent, Distribution | Discontinuities, Other: Nature, density, spacing, interbeds, etc. |
|---|---|---|---|---|---|---|
| Purgatory Sandstone SANDSTONE | 60 to 70 | Light brownish yellow to yellowish brown | Bedded, some cross-bedding N 40-45°E, 20-23°SE | Moderately hard, slightly friable | None Reported | Fine- to medium- grained slightly weathered. Joint set N20°W, 80°SW, 7-foot spacing |
| 12 SILTSTONE AND DOLOMICRITE | 60 to 70 | Alternating reddish brown and light greenish gray | Thinly bedded | Soft to moderately hard | 20-30% along bedding planes, as modules, in healed fractures | Fractures to 1 inch wide healed with gypsum. |
| 11 GYPSIFEROUS DOLOMITE | 18 | Light greenish gray and light reddish gray | Thinly bedded, some cross-bedding | Soft to moderately hard | 20%, along bedding planes and in healed fractures | Healed fractures |
| 10 SILTSTONE | 16 | Reddish brown | Thinly bedded | Soft to moderately hard | 15-25% in laminae parallel to bedding | |
| 9 SILTY DOLOMICRITE | 11.2 | Light greenish gray to reddish gray | Thinly bedded | Moderately hard | 10% in laminae parallel to bedding | |
| 8 DOLOMITIC SILTSTONE | 7.4 | Reddish brown | Thinly bedded, with ripple marks | Soft to moderately hard | 20%, along bedding planes, healing fractures, and as modules | Low joint density |
| 7 DOLOMICRITE | 8.2 | Light greenish gray | Thinly bedded | Moderately hard to hard | 10%, white and clear, along bedding planes | Open joints, high joint density |
| 6 DOLOMITIC SILTSTONE | 16 | Brownish gray to reddish brown | Thinly bedded | Soft to moderately hard fractures | 20-25%, along bedding planes and in irregular fractures and nodules | Open joints; low joint density |
| DOLOMICRITE Marker Bed | 1 | Light greenish gray | | | | Marker bed 8 feet above contact with Rock Unit 5 |
| 5 DOLOMICRITE | 2.7 | Light greenish gray | Thinly bedded | Moderately hard to hard | 20%, along bedding planes | Open vertical joints, high joint density |
| 4 DOLOMICRITE | 7.3 | Light greenish gray | Thinly bedded; some warped beds | Moderately hard to hard | 20%, along bedding planes | Open, vertical joints; high joint density; fossil mud cracks and warped bedding |
| 3 DOLOMITIC SILTSTONE | 8.0 | Brownish gray to light reddish gray | Thinly bedded | Moderately hard | 15%, along bedding planes | Open joints, low joint density; some interbedded DOLOMICRITE |
| 2 DOLOMICRITE | 4.9 | Light greenish gray to brownish gray | Thinly bedded; smooth bedding | Moderately hard | 10-15%, along bedding planes | Open, near vertical joints; moderate joint density; some interbedded SILTSTONE |
| 1C SILTSTONE | 23.5 | Reddish brown | Thinly bedded | Soft to moderately hard | 25-30%, along bedding planes and in healed, irregular fractures | Open joints; low joint density; occasional thin beds of light greenish greenish gray DOLOMICRITE |
| 1B DOLOMICRITE | 7.1 | Light greenish | Thinly bedded | Moderately hard to hard | White and clean, along bedding planes | Open joints; high joint density |
| 1A SILTSTONE | 10 | Reddish brown to light reddish gray | Thinly bedded | Soft to moderately hard | 10-15%, as laminae along bedding planes | Low joint density |
| 0 DOLOMICRITE and SILTSTONE Interbeds | Approx. 70 | Light greenish gray; Brown to reddish brown | Thinly bedded; contorted beds at bottom; Thinly bedded | Moderately hard to hard; Soft, slightly friable | 5-10%, as laminae along bedding planes | Moderate joint density; some pyrite healing of fractures, and along bedding, near bottom of unit |
| P Interbedded SILTSTONE, DOLOMICRITE and SANDSTONE | Over 100 | Light brown and light bluish gray | Reddish; some contorted bedding | Moderately hard | Nodules | Open joints; moderate joint density; blebs of crude oil in sandstone beds, some sulfur |

small fraction of the gypsiferous foundation rock. The cutoff depth selected was 75 ft in the breach area. The depth was ~50 ft at the left abutment and 25 ft at the right abutment, with transitional areas up to 400 ft in length between the maximum depth and the abutment sections. A typical cross section of the cutoff at maximum depth (~sta. 6+00) in relation to the dike cross section is shown in Figure 12. Also shown in Figure 12 is the configuration of the cutoff near the right abutment at station 11+50. Note that the upstream foundation area of the RCC dike is placed on bedrock and not on the cutoff concrete. This area became a problem area later, which is discussed in the section Quail Creek Dike Performance. The cutoff configuration consisted of a 32-in.-wide saw-cut slot extending below the trench. To permit sufficient working space for construction equipment, the bottom width of the trench was designed to be 20 ft.

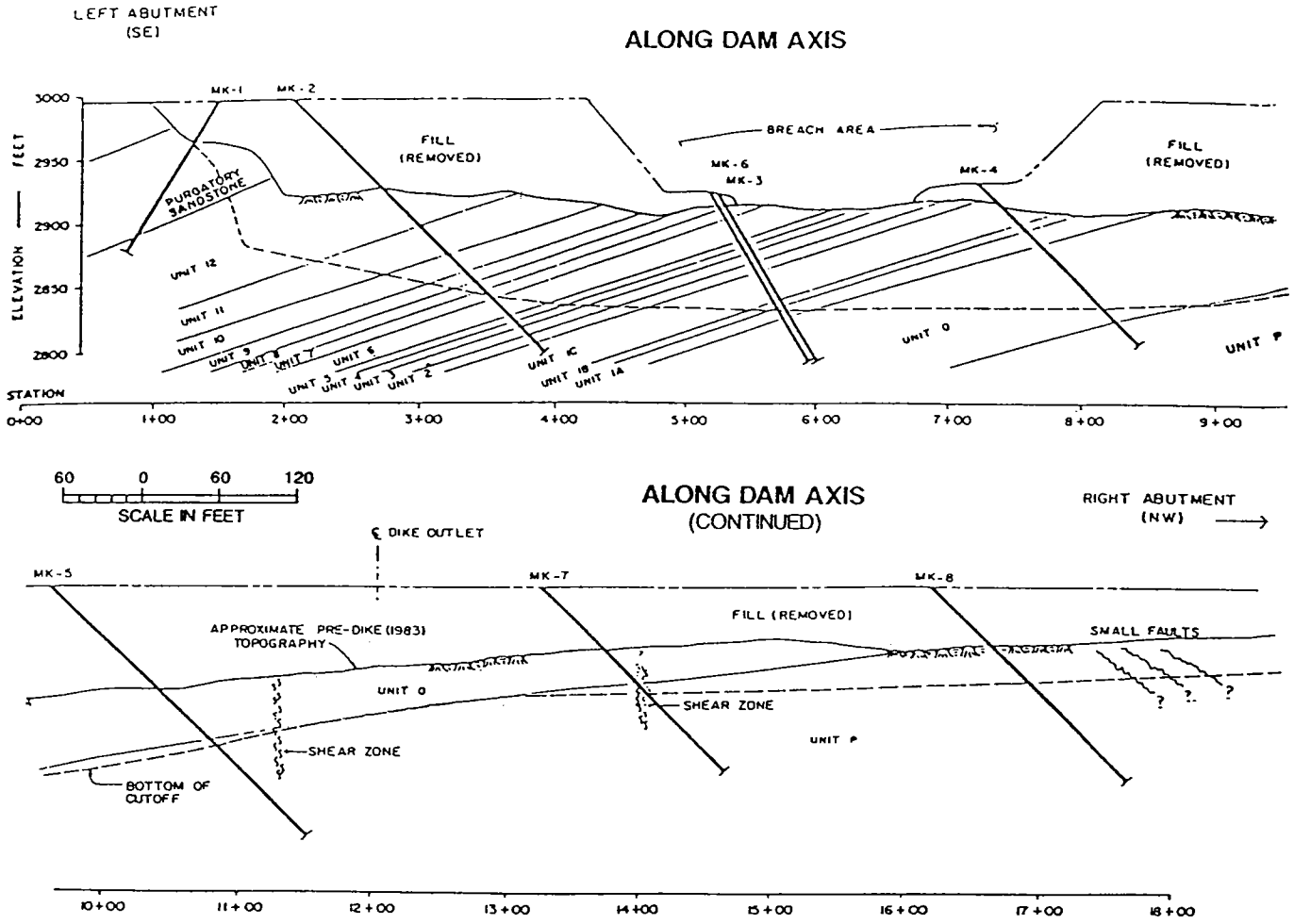


Figure 11. Geologic cross section along the axis of the Quail Creek Dike, looking to the southwest (modified from Payton, 1992). Strata dip to the southeast, toward the left abutment.

The cutoff was excavated with the use of a rock trencher, because drilling and blasting, even with controlled pre-splitting techniques, was considered to have the potential to damage the rock beyond the excavation limits. Excavation of the Quail Creek South Dike cutoff began in December 1989 and was completed in February 1990. Approximately 62,000 cubic yards of rock was excavated from the cutoff trench. The lowest 32-in.-wide, 19-ft-deep slot was backfilled with a conventional concrete mix using type V cement. At the 20-ft-wide bench level, a 12-in. PVC water stop was placed in the top of the slot concrete at the contact between the RCC and the conventional concrete. Detailed geologic mapping of the cutoff trench walls was accomplished prior to the placement of any concrete.

### Dike Construction

The Quail Creek Dike construction began as the placement of the RCC backfill in the cutoff trench reached the level of the dike foundation. RCC placement was continuous from the cutoff trench to the dike section. The volume of the RCC dike is ~123,500 cubic yards. The crest length is 2,050 ft, with a crest width of 16 ft. The upstream face is vertical, and the downstream face slopes at 0.85:1. The base elevation at the maximum section is ~2,908 ft, with a dam width of ~72 ft, and a crest elevation of the non-overflow section of 2,993 ft. The overflow section is at an elevation of 2,988 ft, with a crest length of 1,800 ft. The maximum normal full-pool elevation is 2,985 ft, with a gross reservoir capacity of 40,325 acre-ft. The new Quail Creek Dike was completed in June 1990.

## QUAIL CREEK DIKE PERFORMANCE

The Quail Creek Dike is currently referred to as the Quail Creek South Dam. Since the completion of the RCC structure, and the refilling of the reservoir in the spring of 1991, the dam has performed very well. Upon completion of the dam it was anticipated that a grouting program might be needed within 5 years. Seepage beneath the structure had gradually increased during the past 11 years. Seepage had originally been most noticeable along the right (west) side of the dam, leading to the installation of a toe drain system by RB&G Engineering. During the past few years, subsidence features had been noted downstream of this area. Since January 2002, seepage beneath the left (east) side of the dam had increased significantly.

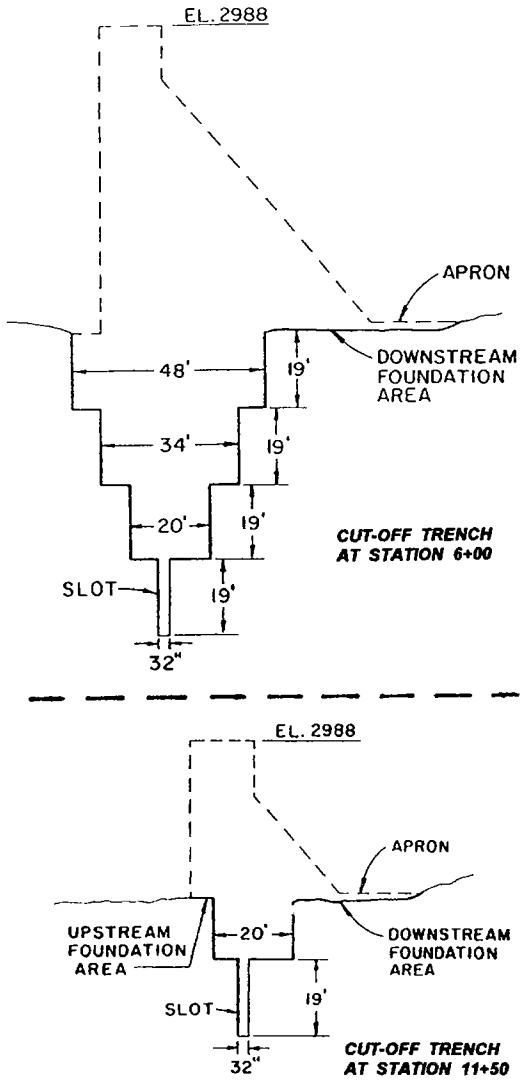


Figure 12. Configuration of the cutoff trench in the main part of the new Quail Creek Dike (from Payton, 1992). Station 6+00 (above) shows the maximum depth of the trench (76 ft) in the vicinity of the breach that occurred in 1989. Station 11+50 (below) shows the cutoff-trench configuration near the right abutment. Reservoir is on the left.

About 400 ft downstream of station 5+00, water began flowing out of several closely grouped, open eroded fractures in a highly fractured, highly gypsiferous light-greenish-gray dolomicrite layer, identified as unit 5 (see Figs. 8, 13). As shown in Figures 8 and 13, this unit is only 2.7 ft thick, but it contains >20% visible gypsum, with a chemical analysis showing ~50% gypsum. During the spring of 2002, seepage had reached the point of overflowing a 12-in. flume downstream. To measure the increasing flow more accurately, RB&G Engineering had two V-notch weirs installed downstream of the main spring. Overall seepage had increased to ~12 cfs, with flows from the main spring reaching ~5 cfs. Flows from the spring were discolored and cloudy. Analysis showed water from the spring to be carrying up to 1.4 tons of sediment per day on March 23, 2002, then dropping to ~760 lb per day 9 days later (Hansen, 2002). While the high flows were of concern, the safety of the RCC dam was not in question. The high velocity of the flows at this source indicates that the dissolution of gypsum had been replaced by more rapid erosion and piping of bedrock foundation material.

Plans were made to lower the reservoir to perform some general maintenance and address the seepage problems. On the basis of a review of the previous grouting programs for the original dike, and the logs from the new cutoff trench, RB&G Engineering designed an extensive grouting program to intersect open fractures beneath the cutoff trench. An emphasis was placed on the most susceptible zones, including units 4 and 5, where grout-hole spacings were designed as close as 2.5 ft apart and extending >50 ft below the contact between the RCC cutoff trench and bedrock. Grout holes were drilled from within the drainage gallery of the dam. Holes were drilled with a predominant dip of 45°, and toward the left abutment (bedrock dipping ~15–23° toward the left abutment). The majority of the beds were drilled parallel to the axis of the dam, with some angled 10–20° upstream, for wider coverage.

The second grout hole drilled encountered a large water take a few feet below unit 5. Dye placed in the hole was noted downstream at the main spring 7 minutes later. As water levels in the reservoir were dropping, the basin area was monitored for sinkholes. Dye placed in sinkholes was also noted downstream within ~15 minutes. Figure 14 shows a whirlpool associated with one of the sinkholes. As water levels in the reservoir dropped, flows downstream remained about the same, indicating that fractures were likely eroding as fast as the water level was dropping. Seepage downstream did not drop off until a cofferdam had been built and water levels within 600 ft of the dam had drained off. After water levels had dropped, >200 sinkholes were documented within 400 ft upstream of the dam (see Fig. 15). The highest concentration of sinkholes was noted along the left side of the basin.

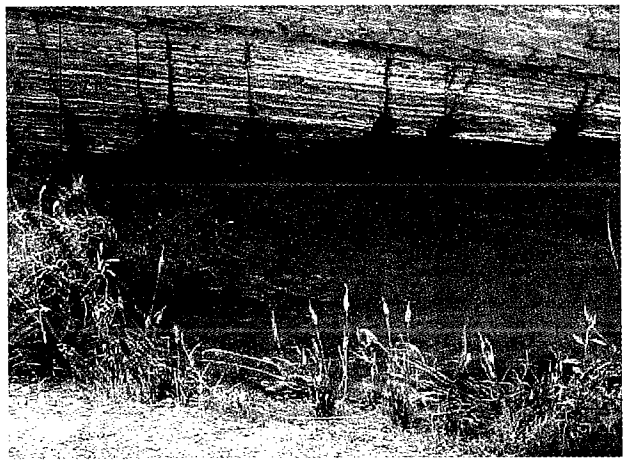

Figure 13. Major spring flowing from channels in highly fractured gypsiferous dolomicrite (unit 5).

During May 2003, the grouting project was completed, with a total of 177 holes drilled and grouted with a combined footage of ~28,540 ft. Many of the grout holes have been relatively tight with only minor grout takes. Holes that have taken grout are generally within very narrow zones. Several holes encountered open voids ~1–2 ft wide. Six holes had relatively large grout takes, ranging from 210 to 565 bags of type V (sulfate-resistant) portland cement. For this project, ~4,825 bags of cement and ultrafine and microfine grout were used. The total cost of the grouting program was ~$750,000.

An examination along the upstream contact of the dam and bedrock revealed evidence of widespread dissolution of gypsum along the right side of the dam. The dissolution of gypsum has caused up to 5 in. of subsidence, creating a gap between the dam and the underlying softened bedrock, as shown in Figure 16. In this area the softened bedrock was excavated from beneath and along the heel of the dam and replaced with concrete, along with a concrete apron ~10 ft wide out in front of the dam.

In an effort to increase the length of time before a second grouting program is needed, a partial basin lining was placed along a part of the upstream basin next to the dam. The basin lining consists of compacted subgrade and a clay lining overlain with a geomembrane liner and topped with compacted fill. The partial basin lining covers ~139,000 square yards of the basin, extending along the upstream heel of the dam and tapering out ~1,200 ft upstream of the dam on the left side. The cost for the partial basin lining was ~$1.5 million.

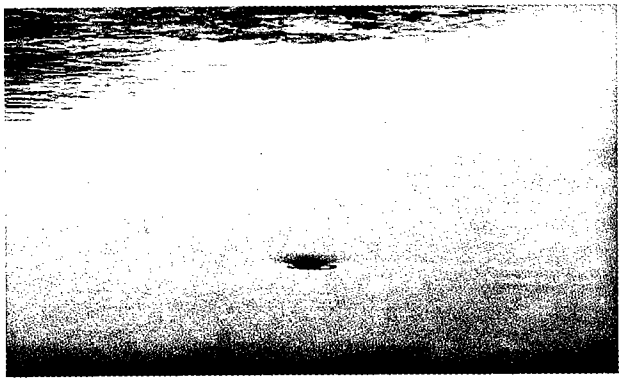

Figure 14. Whirlpool going down into a sinkhole. Diameter of whirlpool is ~4 in.

Figure 15. Dark spots are ~50 of the more than 200 sinkholes upstream of dam. Field of view is ~300 ft wide.

Figure 16. Weathered bedrock just below RCC (roller-compacted concrete), showing open voids and collapse features caused by the dissolution of gypsum (pencil for scale).

While the grouting program and partial basin lining will slow the dissolution and erosion of gypsum and soluble materials within the foundation of the dam, it is expected that these processes will continue. Because of the ever-growing need for additional water and water storage in southwestern Utah, the WCWCD will be faced with the recurring expense of maintaining the bedrock foundation of the South Dam during the life of the structure. Quail Creek Reservoir also serves as a Utah State Park and provides valuable recreational facilities for the region. It is anticipated that the remediation measures taken during the past year will prolong the time before a second grouting program is needed.

## REFERENCES CITED

Gourley, C., 1992, Geological aspects of the Quail Creek Dike failure, *in* Harty, K. M. (ed.), Engineering and environmental geology of southwestern Utah: Utah Geological Association Publication 21, p. 17–38.

Hansen, M. N., 2002, Seepge evaluation of the Quail Creek South Dam in southwest Utah [abstract]: Geological Society of America Abstracts with Programs, v. 34, no. 6, p. 216.

James, R. L.; Catanach, R. B.; O'Neill, A. L.; and Von Thun, J. L., 1989, Investigation of the cause of Quail Creek Dike failure: Unpublished report of the Independent Review Team to Norman H. Bangerter, Governor of Utah, 155 p.

O'Neill, A. L.; and Gourley, C., 1991, Geologic perspectives and cause of the Quail Creek Dike failure: Bulletin of Association of Engineering Geologists, v. 27, no. 2, p. 127–145.

Payton, C. C., 1992, Geotechnical investigation and foundation design for the reconstruction of Quail Creek Dike, *in* Harty, K. M. (ed.), Engineering and environmental geology of southwestern Utah: Utah Geological Association Publication 21, p. 39–51.

# A Compound Breccia Pipe in Evaporite Karst: McCauley Sinks, Arizona

***James T. Neal***
Sharlot Hall Museum
Prescott, Arizona

***Kenneth S. Johnson***
Oklahoma Geological Survey
Norman, Oklahoma

**ABSTRACT.**—The McCauley Sinks, in the Holbrook Basin of northeastern Arizona, are composed of some 50 individual sinkholes within a 3-km-wide depression. The sinks are grouped concentrically in three nested rings, although the pattern is imperfect. The outer and least conspicuous ring contains ring fractures and is an apparent tension zone. The two inner rings are semicircular chains of large sinkholes, ranging up to 100 m across and 50 m deep. Several sub-basins within the larger depression show local downwarping and potential incipient sinkholes.

Limestone of the Permian Kaibab Formation, <15 m thick, is the principal surface lithology and is near its easternmost outcropping. Although surface rillenkarren are present, and the sinks occur within the Kaibab limestone outcrops, the Kaibab is a passive rock unit that has collapsed into solution cavities developed in underlying salt. Beneath the Kaibab is the Coconino Sandstone, which overlies the Permian Schnebly Hill Formation, the unit containing the evaporite rocks—principally halite in the Corduroy Member. Evaporite karst in this part of the basin is different from that in the eastern part, probably because of the disappearance of the Holbrook Anticline, a structure with major joint systems that help channel water to the salt beds below. The McCauley Sinks area also is near the western edge of the evaporite basin.

The structure at McCauley Sinks suggests a compound breccia pipe, with multiple sinks contributing to the inward-dipping major depression. The depression at Richards Lake, 5 km southeast of McCauley Sinks, is similar in form and size with a single, central sinkhole, and one along the periphery. An apparent hydrologic difference at McCauley Sinks is its proximity to the deeply incised Chevelon Canyon drainage.

The 3-km-wide karst depression at McCauley Sinks, along with five other depressions nearby, provides substantial hydrologic catchment. Because of widespread piping into karst features and jointed bedrock at shallow depth, runoff seldom ponds at the surface. There appears to be greater recharge efficiency here than in adjacent alluvial areas; thus concern exists for ground-water users downgradient from the karst area, specifically from pollutants that might enter the karst openings.

Sinkholes and open fissures should not be used for waste disposal. Although this is a remote area, collapse of karst features around engineered structures is also possible.

## INTRODUCTION

McCauley Sinks are a unique and conspicuous feature of the northern Arizona landscape. This group of some 50 sinkholes in the westernmost part of the Holbrook Basin, adjacent to Chevelon Canyon, forms a saucer-shaped depression that is unlike any other known sinkhole cluster. The 3-km diameter of the depression at McCauley Sinks is similar in size to Meteor Crater and its ejecta field, just 45 km to the northwest, but there is no genetic relationship between the two. McCauley Sinks resulted from dissolution in the underlying salt; Meteor Crater was caused by meteorite impact—beyond any reasonable doubt.

Kaibab Formation limestone crops out extensively around the sinks, and therefore some early observers believed that the features were limestone karst. But individual sinks transect the entire 12–15-m thickness of the Kaibab at this locale, and the collapse extends through the underlying Coconino Sandstone. Well records show that evaporites in the Corduroy Member of the Schnebly Hill Formation beneath the Coconino have thinned markedly, suggesting that evaporite dissolution and collapse are responsible for the karst. The area adjacent to McCauley Sinks contains five other subsidence depressions, three of which have associated sinkholes. Richards Lake, the largest

Neal, J. T.; and Johnson, K. S., 2003, A compound breccia pipe in evaporite karst: McCauley Sinks, Arizona, *in* Johnson, K. S.; and Neal, J. T. (eds.), Evaporite karst and engineering/environmental problems in the United States: Oklahoma Geological Survey Circular 109, p. 305–314.

of the five depressions, is smaller than McCauley Sinks and contains one central and one peripheral sinkhole. The saucer-like attributes of Richards Lake and McCauley Sinks are similar to some breccia-pipe structures on the Colorado Plateau that are ascribed to dissolution in the Mississippian Redwall Limestone.

The evidence for an origin similar to the Colorado Plateau breccia pipes (by dissolution of limestones) is examined here, along with hydrogeologic implications in this environment. LPG (liquefied petroleum gas) is currently stored in the eastern part of the Holbrook Basin, in solution caverns formed in salts of the Corduroy Member, and potential space exists for more caverns. Geologic site characterization that is required for the permitting of additional storage caverns must evaluate the varieties of karst expression in the basin.

## GEOLOGY AND HYDROLOGY

McCauley Sinks and five adjacent depressions occur in west-central Navajo County, 28 km southeast of Winslow, Arizona (Figs. 1–3). The Holbrook Anticline, if extended westward from its more conspicuous expression to the southeast, would pass through a point near the Richards Lake/McCauley Sinks area. But its surface manifestation has virtually disappeared, except for en-echelon swarms of buckle folds and open fissures in bedrock, aligned along the same northwesterly structural trend as the Holbrook Anticline (Wilson and others, 1960; Neal and others, 1998; Rauzi, 2000). The western edge of Permian salt in the Holbrook Basin is only a few kilometers beyond McCauley Sinks (Fig. 2). Dissolution at this edge of the salt body is occurring but is less straightforward than in Dry Lake Valley to the southeast. The area around McCauley Sinks displays totally different features as compared with those along the collapsing crest of the Holbrook Anticline to the southeast, which is coincident with the dissolution front and karst occurrence (Bahr, 1962; Peirce and Gerrard, 1966; Neal and others, 1998).

The Permian evaporite sequence in the Holbrook Basin originally was termed *Supai salt* and was thought to be equivalent to Supai red beds in the Grand Canyon (Bahr, 1962; Peirce and Gerrard, 1966). The Permian Grand Canyon sequence is traceable to the area of Sedona, Arizona, but has been renamed there for the type locality at Schnebly Hill (Blakey, 1990). The members of the Schnebly Hill Formation are, in ascending order, Bell Rock, Big A Butte, Fort Apache, Corduroy (the 400-m-thick evaporites of the Holbrook Basin, isolated by the Sedona Arch), and Sycamore Pass (Fig. 3). The oldest Bell Rock Member rests conformably on the Permian Hermit Shale, which is underlain by the Naco Group and the Mississippian Redwall Limestone. The Redwall displays widespread dissolution in northern Arizona. It has produced at least six sinkholes in the Sedona area (Lindberg, 1998) and hundreds of breccia pipes and sinkholes elsewhere on the Colorado Plateau (Wenrich and Billingsley, 1986). The Redwall in the Holbrook Basin is generally <30 m thick and is ~1,200 m below land surface; it is not thought to be a factor in karst development at McCauley Sinks.

### Hydrogeology

The principal aquifer in southern Navajo County is the Coconino Sandstone (Mann, 1976), but the overlying Kaibab Limestone and the uppermost beds of the underlying Schnebly Hill Formation are hydraulically connected as part of the aquifer. The Coconino Sandstone is fine- to medium-grained quartz sand, light yellowish gray to tan, and is weakly cemented by quartz, iron oxide, and calcite. The sandstone is conspicuously cross-bedded. It thickens from 120 to 250 m toward the northwest across southern Navajo County and is ~200 m thick in the vicinity of the Holbrook Anticline.

Recharge of the aquifer occurs from precipitation and streamflow (Mann, 1976). Most recharge occurs along the Mogollon Rim, some 50 km to the south, where the average precipitation is 50–75 cm/yr. Some recharge also occurs along the Holbrook Anticline as a result of precipitation (which averages 25–35 cm/yr) and from consequent piping of surface waters downward through Dry Lake, sinkholes, and other karst-induced fractures in the area. Ground water flows to the north, toward the Little Colorado River, with a hydraulic gradient of about 6 m/km (30 ft/mi) in the vicinity of the Holbrook Anticline (Fig. 4). The Coconino aquifer is unconfined in most of southern Navajo County but is confined by the overlying Moenkopi Formation to the north and near the Little Colorado River (Mann, 1976).

The water table of the Coconino aquifer typically is 120–200 m below land surface in most areas along, or adjacent to, the Holbrook Anticline (Mann, 1976). In several areas near the crest of the anticline the Coconino Sandstone is dry, or nearly dry, and the water table is in the uppermost layers of the underlying Schnebly Hills Formation, which does not yield much water. The Coconino typically yields 200–2,000 L/min, whereas the Schnebly Hill, along the Holbrook Anticline, yields <200 L/min.

In most of southern Navajo County the quality of water in the Coconino aquifer is good, typically with 200–400 mg/L TDS (total dissolved solids). The principal constituents are calcium, magnesium, and bicarbonate (Mann, 1976). However, in the vicinity of the Holbrook Anticline the water is much less desirable, with 500–4,410 mg/L TDS. This water is high in sodium chloride and is present mainly in the lower part of the aquifer: undoubtedly it is part of the brine formed by dissolution of salt in the directly underlying Corduroy Member of the Schnebly Hill Formation. A plume of this brine extends northward from the Holbrook Anticline, following the hydraulic gradient (Fig. 4).

Karst activity in the area involves lateral and down-

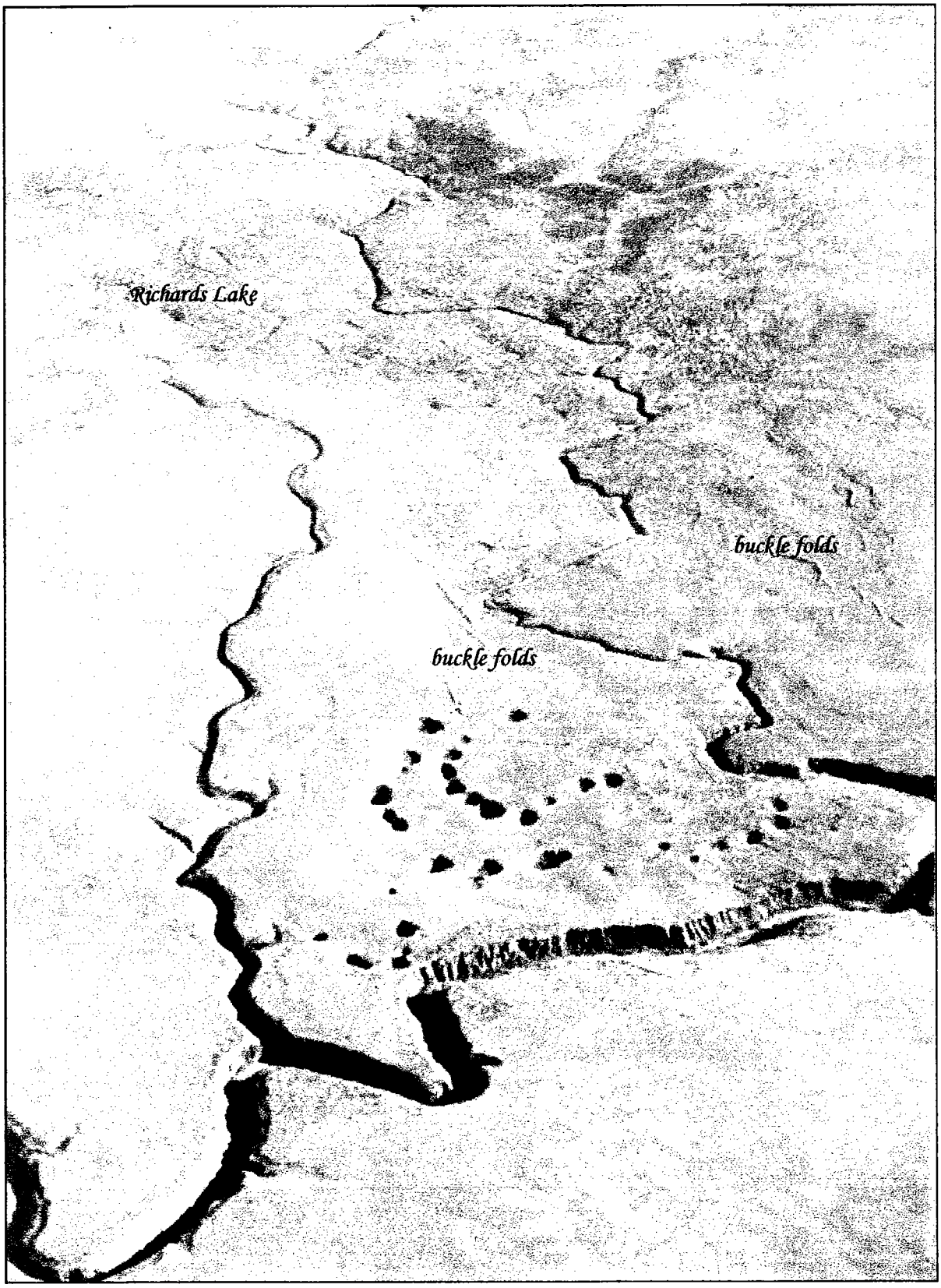


Figure 1. McCauley Sinks, in the western part of the Holbrook Basin, displays entirely different karst characteristics from those seen in the eastern part of the basin, where graben sinks and fracture-induced sinkhole patterns predominate. Some 50 sinks occur here in a semi-concentric pattern, consisting of three separate "rings." The outer ring is indistinct in this photograph but is marked by fractures at the surface. Chevelon Canyon (foreground) and its two tributary canyons are all 80+ m deep and might influence the local hydrologic flow pattern. Richards Lake is 5 km southeast of McCauley Sinks. View looking to the south.

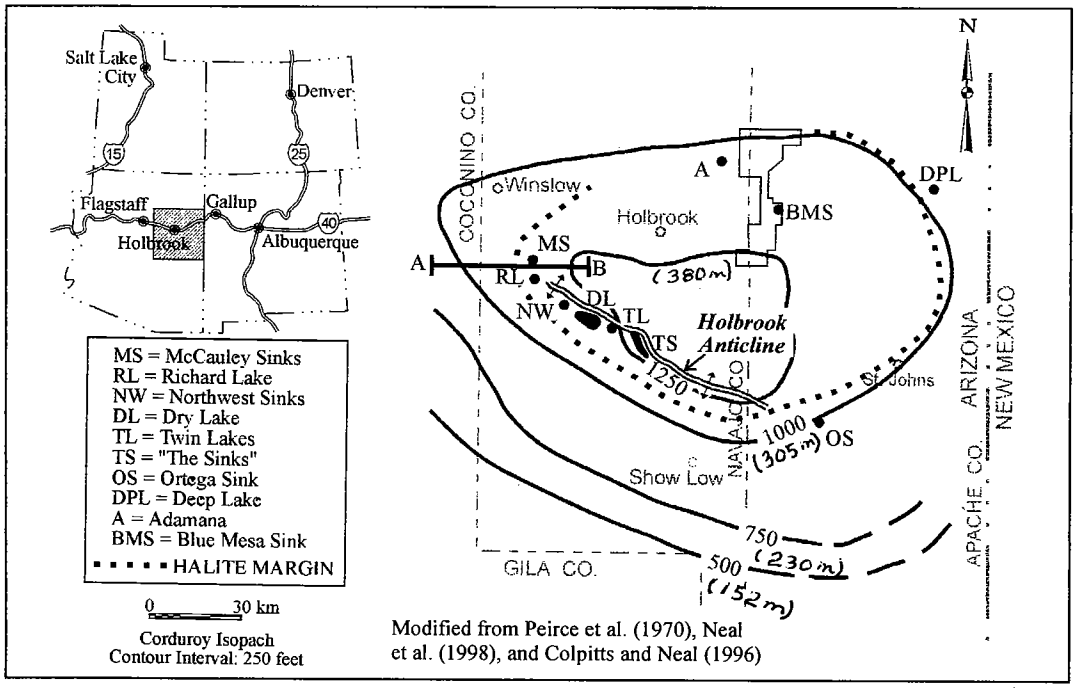


Figure 2. Holbrook Basin, in northeastern Arizona, showing thickness of the Corduroy Member of the Schnebly Hill Formation, and the more limited distribution of its salt (dotted line). McCauley Sinks are in the west side of the basin, near the edge of halite deposits and the end of the surface anticline. Line A–B marks cross section shown in Figure 3.

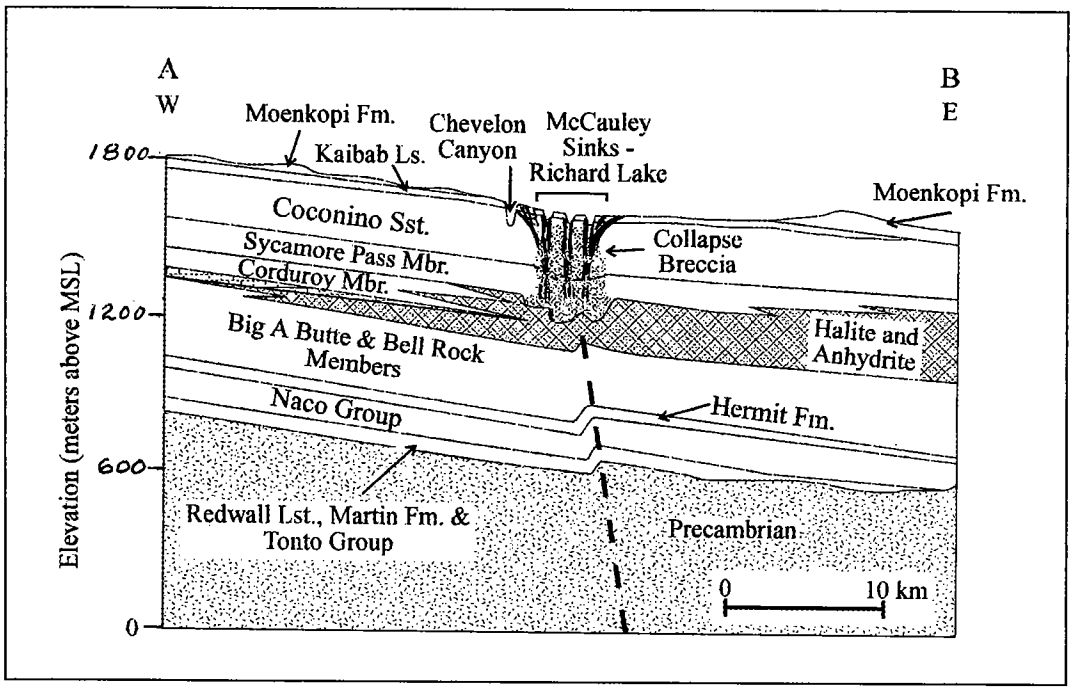


Figure 3. Cross section A–B (see Fig. 2), showing collapse area (diagrammatic) at McCauley Sinks, caused by dissolution of evaporites in the Corduroy Member. Fault offset in units beneath the salt is unproven but is thought likely by some geologists.

ward percolation of fresh water through the Coconino aquifer until it encounters the uppermost salt layers in the Corduroy Member, about 215–250 m below the land surface. Salt dissolution is accompanied by development of sinkholes and collapse structures in overlying strata (Fig. 3) that enhance further flow of fresh water to the dissolution zone. Therefore, karst development is self-perpetuating.

Figure 4 reveals a substantially lower TDS range for the McCauley Sinks/Richard Lake area, suggest-

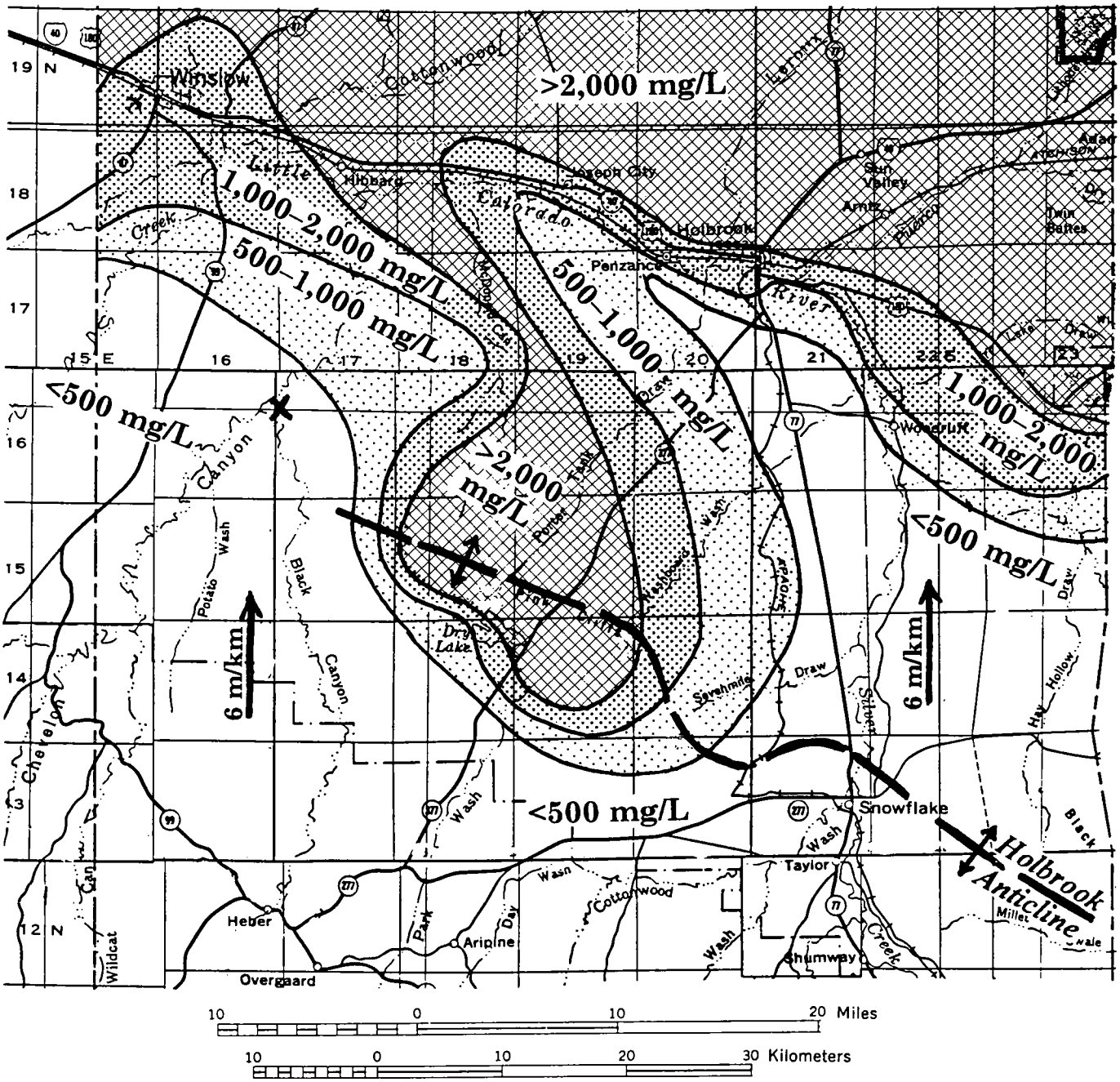


Figure 4. Water quality of Coconino Sandstone aquifer in southern Navajo County, Arizona (from Mann, 1976). Map shows total dissolved solids of ground water in mg/L. Also shown are Holbrook Anticline, arrows showing direction of the hydraulic gradient (6m/km), and McCauley Sinks (**x**) in west-central part of map area.

ing either that (1) dissolution processes are less active now than in the past, and that the karst may be in a more mature stage of development; or that (2) wells have not been drilled deep enough to encounter higher salinity waters in the area.

### Collapse Processes at McCauley Sinks and Richards Lake

McCauley Sinks comprise a group of 50 sinks covering ~5 km$^2$ in a generally low-relief area adjacent to Chevelon Canyon, 29 km southeast of Winslow (Figs. 1, 2, 4, 5). A cursory look at the overall grouping of the McCauley Sinks shows a roughly nested arrangement of two arcuate rows of coalesced sinkholes. A third and less distinct outer arc is marked by several disconnected surface fractures. Field inspection of the topographic setting suggests that the sinkhole and fracture arcs may be the concentric stress-field expression of a larger subsidence basin.

Nearby Chevelon Canyon, a losing stream at this locale most of the time because of a dam upstream, probably contributes less ground-water recharge than

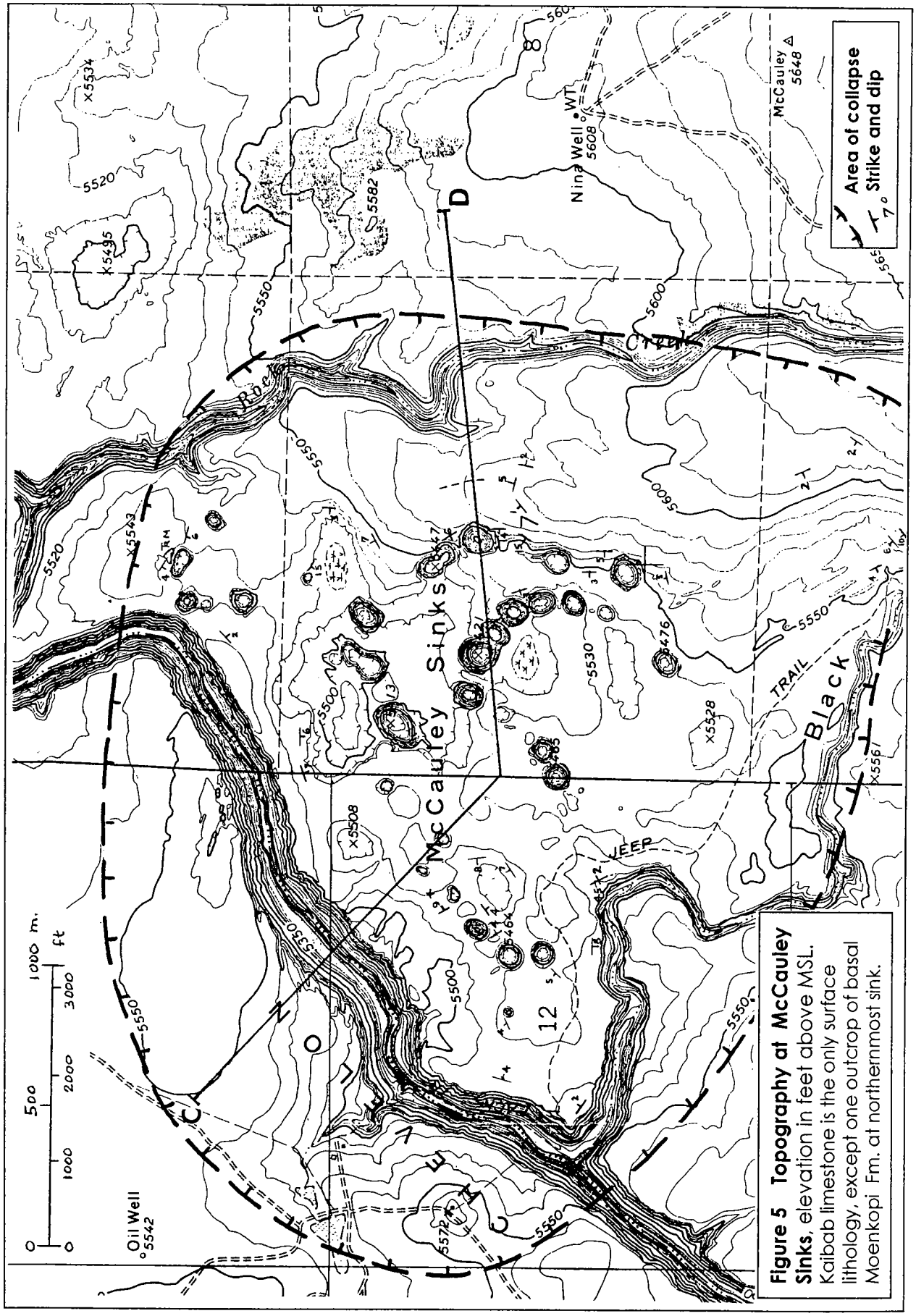


Figure 5. Topographic map of an area around McCauley Sinks. Kaibab limestone is the only surface lithology, except for one outcrop of basal Moenkopi Formation at northernmost sink. Line C–D marks cross section shown in Figure 7.

in the past. Substantially greater infiltration in the past, especially during pluvial stages of the Pleistocene, may have accelerated the sinkhole patterns that exist today.

Conjugate joints in the Kaibab Formation (limestone) and Cononino Sandstone have an important bearing on the expression and development of individual sinks. Steep sidewalls commonly are aligned along near-vertical joint planes parallel to regional structure, and some sinks have nearly square corners. Several sinks are as wide as 100 m and as deep as 30–35 m; the largest is a compound sink that is 185 m in its long dimension. Some depressions appear to be either older (filled) sinks or possibly the loci of future collapse.

Distinctive pressure ridges, or local buckle folds, seen principally in the nearly horizontal Kaibab Formation limestone beds are identical to similar features within the Richards Lake depression and occur in association with other sinkholes along the Holbrook Anticline. The pressure ridges within the area of karst expression are compression features that originated from subsidence caused by evaporite dissolution. The ridges are 2–10 m high, with beds dipping away at low angles and forming sinuous linear hills about 15–25 m wide. The ridges are parallel and are commonly >100 m long (Fig. 1), trending generally N. 30° W., which is subparallel to the trend of the probable northward-bending and waning Holbrook Anticline. Similar buckle folds are interpreted as stress-relief features in some geologic environments undergoing compression (Sanford, 1959; Ramsey, 1967).

### Richards Lake Similarities

Richards Lake is a 2-km-wide natural depression 5 km southeast of the McCauley Sinks (Figs. 1, 2, 6). The Richards Lake depression contained water for short periods after heavy rains and after the diversion of Black Creek in 1902, but it has been generally dry since the 1940s, according to local residents. It is situated within the Moenkopi/Kaibab outcrop belt, with the Coconino Sandstone at shallow depths. Richards Lake is near the western end of the Holbrook Anticline and is interpreted as a large collapse depression with concentric faults and pressure ridges, with a 170-m-wide sinkhole near the center (Neal and Colpitts, 1997). A second set of pressure ridges parallels the waning Holbrook Anticline, trending N. 30° W. In the alluvium at the bottom of the sinkhole, two secondary piping features were forming in early 1996, suggesting continuing dissolution at depth. A northwest-trending fissure was also observed, essentially parallel to the regional structure.

The presence of Richards Lake amidst numerous salt-karst features suggests a similar dissolution origin but with unique characteristics. A similar collapse origin for Richards Lake and the McCauley Sinks is likely because of their close proximity and their comparable geological setting, size, and appearance. Two less well-developed depressions occur 1 and 3 km to the northwest, on an azimuth of ~N. 62° W. (Fig. 6), in tandem with Richards Lake. Secondary sinkholes occur within each of these depressions, as at Richards Lake. A similar, 1-km-wide depression, 2 km northeast of McCauley Sinks (at Rattlesnake Bend), contains buckle folds but no central sinkholes (Fig. 6). Similar processes appear likely for all of these smaller depressions, although their development is much less advanced than either Richards Lake or McCauley Sinks.

The shallow depressions adjacent to Richards Lake and south of McCauley Sinks are near the suspected western limit of salt in the Corduroy Member (Figs. 2, 3). They also are near the western terminus of the Holbrook Anticline, although the precise locations of the salt margin and the anticline are not known. Unlike the sinkholes in Dry Lake Valley and other sites farther east, these westernmost depressions (including Richard Lake and McCauley Sinks) appear to have a unique karst style, with collapse related more to the dissolution front along the margin of the salt basin than to collapse along the Holbrook Anticline. All six depressions in the study area are in the Kaibab Formation outcrop belt, and all have local basinward dips of 0–10°. The pattern and geometry are similar to many breccia pipes in northwestern Arizona that are attributed to dissolution in the Redwall Limestone, but clearly the structures in this study result from salt dissolution and collapse.

The topographic map and cross section at McCauley Sinks (Figs. 5, 7) reveal the imperfect, nested arrangement of three concentric rings. The area involved in the collapse extends well beyond the sinkhole cluster, as shown by the local disruption of the regional dip of Kaibab outcrops, the topographic depression, and fractures in rocks on the north side of Chevelon Canyon.

The regional structural alignment of depressions and major surface fractures is shown in Figure 6. McCauley Sinks and Rattlesnake Bend depressions are aligned N. 45° E., along with the major trend of Chevelon Canyon. Richards Lake and the adjacent two depressions trend N. 62° W., somewhat offset from the N. 45° W. trend of major fractures and Chevelon Canyon tributary channels, which are fracture controlled.

## COMPARISON WITH OTHER BRECCIA PIPES AND COLLAPSE FEATURES

The depressions at McCauley Sinks and Richards Lake are perennially dry, karst-subsidence basins. They may have a counterpart at Deep Lake in the eastern Holbrook Basin, and they also resemble the breccia pipe in evaporites at San Simon Sink in the Delaware Basin of southeastern New Mexico, as well as some breccia pipes in northern Arizona attributed to dissolution in the Redwall Limestone.

San Simon Sink is the lowest point in the San Simon Swale, a 260-km$^2$ depression along the eastern margin of the Delaware Basin, above the Capitan Reef,

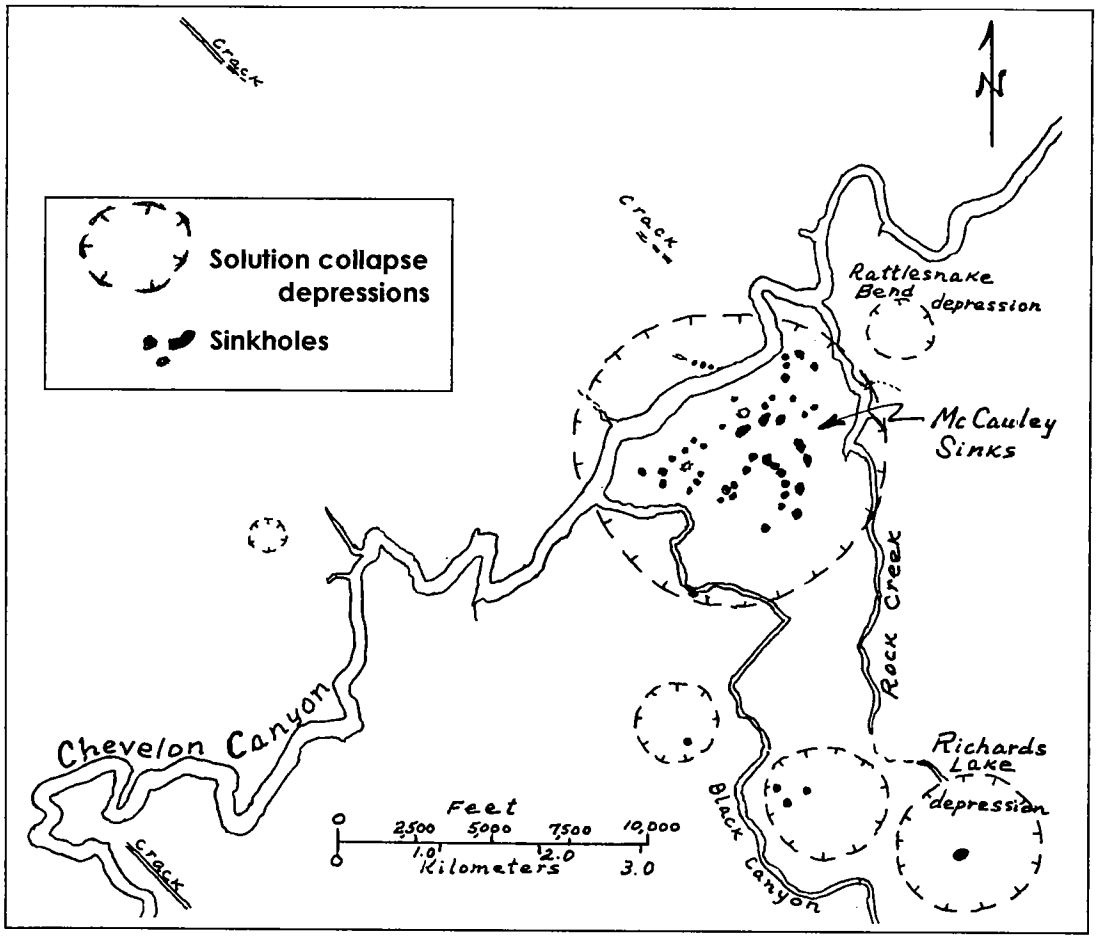


Figure 6. Structural features, surface hydrology, and related depressions associated with McCauley Sinks. N. 45° W. trend is predominant; orthogonal trend is ~N. 45° E.

which outlines the basin. It has formed as a result of evaporite removal by dissolution of salt in the underlying Rustler and Salado Formations. The San Simon Sink forms a generally oval depression ~30 m deep, covering ~1.3 km$^2$. It contains a secondary collapse sink, ~100 m across and some 8–10 m deep, which subsided abruptly in 1927. Annular rings that cut the surface around the sink suggest continuing subsidence and readjustment to the earlier collapse. The position of the sink over the reef led to the suggestion by Lambert (1983) and Bachman (1984, 1987) that the collapse originated in a ground-water cavity in the Capitan Reef, and that the sink may be a modern analog of a breccia pipe that is actively forming.

Breccia chimneys typically are features of positive relief, originating by the gravity collapse of flanking materials into sinkholes and forming indurated "chimneys" in the throat leading to the void below. Subsequent erosion and subsidence of the surrounding and more soluble country rock leads to topographic inversion. While not nearly as common as sinkholes and other collapse features, breccia chimneys may be locally significant, such as at the northern border of the Capitan Reef, where they have been observed in potash mines. "Karst domes" may resemble breccia chimneys, as features of positive relief, but their cores contain older, as well as younger, rocks than their flanks (Davies, 1984; Hill, 1996).

Solution-subsidence structures are well known in the Devonian Prairie Formation of southern Saskatchewan, Canada. The Rosetown Low and the Regina Hummingbird Trough show formation thinning of several hundred feet, which has been attributed to interstratal dissolution of evaporites at depth (DeMille and others, 1964). Underlying reefs and bedrock fractures possibly supply the necessary circulation channels for additional localized evaporite dissolution, similar perhaps to the Capitan Reef features. Surface expression of this dissolution is obscured by the presence of glacial drift.

Breccia pipes on the Colorado Plateau, some of which are aligned with northwest-trending structural lineaments, are commonly marked by surface depressions having dimensions and structural geometry similar to McCauley Sinks. They are believed to have been caused by dissolution in the Mississippian Redwall Limestone and concomitant stoping to the surface (Wenrich and Billingsley, 1986; Sutphin and Wenrich, 1989). The karst openings in the Redwall are along solution-widened fractures and joint-controlled caves.

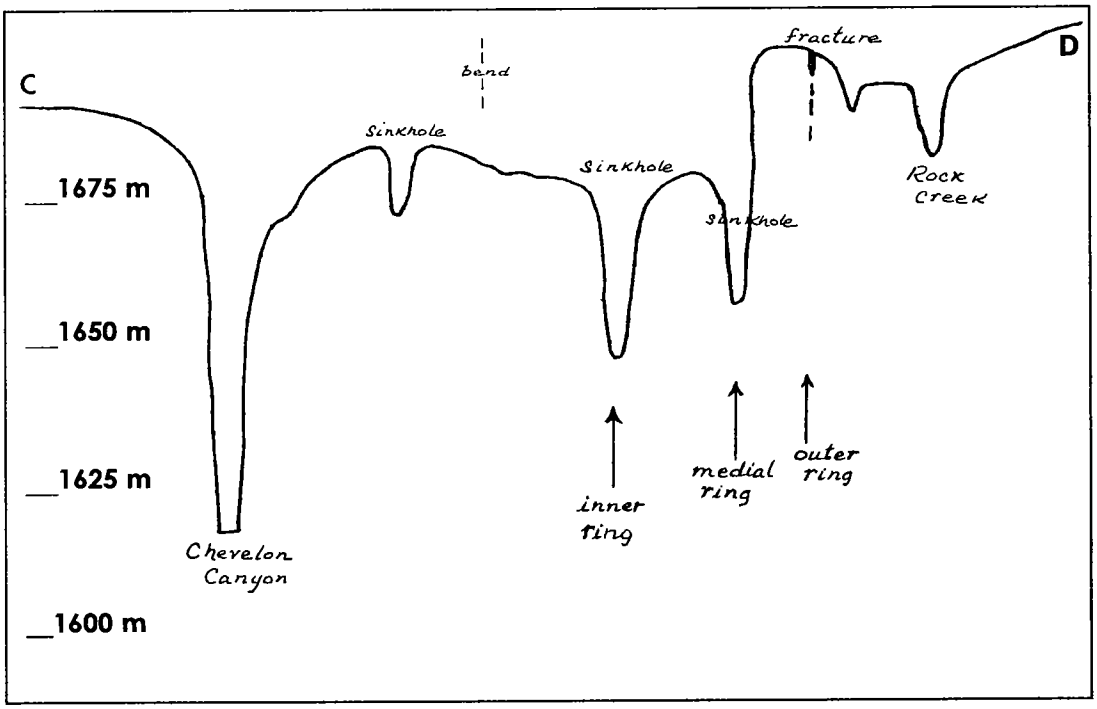


Figure 7. Cross section C–D (see Fig. 5) across McCauley Sinks, showing arrangement and relative elevations of the three concentric rings. Upper limit of collapse structure is at ~1,690 m.

Breccia pipes in evaporites have been described in the Paradox Basin (Sugiura and Kitcho, 1981), but their dimensions are not at all similar to either San Simon Sink or McCauley Sinks and Richards Lake.

The similarity of structural alignment in the McCauley Sinks area with other Colorado Plateau breccia pipes is perhaps not surprising, given the relative short separation and similar hydrogeologic controls. The mechanism of deep hydrologic drainage and evaporite transport, such as occurs into the fractured Capitan Reef beneath San Simon Sink, is speculative at McCauley Sinks, as the deepest water wells have penetrated only the uppermost Schnebly Hill strata. Hydrologic connections with the deeper Redwall are speculative, as logs are unavailable for the one nearby oil-well penetration.

## CONSIDERATIONS OF GEOLOGIC SITE CHARACTERIZATION

Further development of this area for storage caverns, or for other industrial, agricultural, or commercial and residential purposes, must address the presence of active karst formation. Hundreds of square kilometers are potentially hazardous to some degree, but land-use classification that categorizes the elements of relative potential risk is achievable so that limited industrial, agrarian, or residential use can continue safely. Such categorization may be useful in simplifying procedures for licensing new cavern fields for underground storage, or in updating and validating locations of existing caverns.

The 3-km-wide karst depression manifested in McCauley Sinks, along with the five adjacent depressions, forms a hydrologic catchment area that provides substantial hydrologic recharge. Because of widespread piping into karst features and jointed bedrock at shallow depth, it is difficult to pond water for either industrial or agricultural purposes, and recharge is greater than in alluvial areas. Assuming that moderately high recharge efficiency exists, a condition of possible concern exists for ground-water users downgradient from the karst area. For this reason, sinkholes and open fissures should not be used as trash and garbage repositories, in contrast with previous widespread disposal practices.

Probable solution-induced subsidence features occur in the eastern and northern margins of the Holbrook Basin—at Deep Lake south of Sanders, and at Blue Mesa Sink in Petrified Forest National Park (Colpitts and Neal, 1996). The latter depression is ~8 km from the LPG storage-cavern facility at Adamana, and presumably outside of its influence. Blue Mesa Sink was not identified at the time the underground storage facility in salt was established.

As land-use requirements expand beyond existing boundaries, more detailed understanding and geologic mapping will be required. New interpretations of karst features continue to modify land-use concepts (Martinez and others, 1998).

## SUMMARY AND CONCLUSIONS

The collapse structure at McCauley Sinks is suggestive of a compound breccia pipe, with multiple sinks contributing to the major depression. The Richards

Lake depression, 5 km south of McCauley Sinks, is similar in form and size but contains only a single central sinkhole. The only apparent difference in the hydrologic setting at McCauley Sinks is the adjacent Chevelon Canyon drainage, but any cause and effect relationship is speculative.

Kaibab Formation limestone is the principal surface lithology, occurring here near its easternmost limit and with thicknesses <15 m. Other than displaying surface rillenkarren and forming the topmost unit in sinkhole walls, the Kaibab is not a causal factor in karst development. The underlying Coconino Sandstone overlies the Schnebly Hill Formation, the unit containing the evaporite rocks, principally halite; all these rocks are of Permian age. The karst manifestation in this part of the Holbrook Basin is quite different from that in the eastern part, possibly because of the gradual disappearance of the Holbrook Anticline, combined with its location near the western limit of known salt occurrence.

Karst and fracture development constitute a potentially significant hazard to ground-water quality, land use, and structural integrity.

## ACKNOWLEDGMENTS

We thank Professor Dick Young at the State University of New York at Geneseo for his review comments, and George Billingsley of the U.S. Geological Survey for his review of an earlier version.

## REFERENCES CITED

Bachman, G. O., 1984, Regional geology of Ochoan evaporites, northern part of Delaware Basin: New Mexico Bureau of Mines and Mineral Resources Circular 184, 24 p.

_____ 1987, Karst in evaporites in southeastern New Mexico: Sandia National Laboratories Report SAND87-7078, Albuquerque, New Mexico, 82 p.

Bahr, C. W., 1962, The Holbrook Anticline, Navajo County, Arizona, *in* Weber, R. H.; and Peirce, H. W. (eds.), Guidebook of the Mogollon Rim region, east-central Arizona: 13th New Mexico Geological Society Guidebook, p. 118–122.

Blakey, R. C., 1990, Stratigraphy and geologic history of Pennsylvanian and Permian rocks, Mogollon Rim region, central Arizona and vicinity: Geological Society of America Bulletin, v. 102, p. 1189–1217.

Colpitts, R.; and Neal, J. T., 1996, Blue Mesa Sink, a possible solution depression in Petrified Forest National Park, Arizona [abstract]: Geological Society of America Abstracts with Programs, v. 28, no. 7, p. A-392.

Davies, P. B., 1984, Deep-seated dissolution and subsidence in bedded salt deposits: Stanford University unpublished Ph.D. dissertation, 379 p.

DeMille, G.; Shouldice, J. R.; and Nelson H. W., 1964, Collapse structures related to evaporites of the Prairie Formation, Saskatchewan, Canada: Geological Society of America Bulletin, v. 74, p. 307–316.

Hill, C. A., 1996, Geology of the Delaware Basin—Guadalupe Mountains, Apache Mountains, and Glass Mountains, New Mexico and West Texas: Society of Economic Paleontologists and Mineralogists, Permian Basin Section, Publication 96-39, 480 p.

Lambert, S. J., 1983, Dissolution of evaporites in and around the Delaware Basin, southeastern New Mexico and West Texas: Sandia National Laboratories Report SAND82-0461, Albuquerque, New Mexico, 96 p.

Lindberg, P. A., 1998, Structural controls of Devils Kitchen sinkhole, Sedona, Arizona: 49th Highway Geology Symposium Proceedings, Sept. 11–14, 1998, Prescott, Arizona, p. 256–265.

Mann, L. J., 1976, Ground-water resources and water use in southern Navajo County, Arizona: Arizona Water Commission Bulletin 10, Phoenix, 106 p.

Martinez, J. D.; Johnson, K. S.; and Neal, J. T., 1998, Sinkholes in evaporite rocks: American Scientist, v. 86, p. 38–51.

Neal, J. T.; and Colpitts, R. M., 1997, Evaporite karst in the western part of the Holbrook Basin, Arizona, *in* Beck, B. F.; and Stephenson, J. B. (eds.), The engineering geology and hydrogeology of karst terranes: Balkema, Rotterdam, p. 107–115.

Neal, J. T.; Colpitts, R.; and Johnson, K. S., 1998, Evaporite karst in the Holbrook Basin, Arizona, *in* Borchers, J. (ed.), J. F. Poland Symposium on Land Subsidence: Association of Engineering Geologists Special Publication 8, Sudbury, Massachusetts, p. 373–384.

Peirce, H. W.; and Gerrard, T. A., 1966, Evaporite deposits of the Permian Holbrook Basin, Arizona, *in* Rau, J. L. (ed.), Second Symposium on Salt: Northern Ohio Geological Society, Cleveland, v. 1, p. 1–10.

Peirce, H. W.; Keith, S. B.; and Wilt, J. C., 1970, Coal, oil, natural gas, helium, and uranium in Arizona: Arizona Bureau of Mines Bulletin 182, 289 p.

Ramsey, J. G., 1967, Folding and fracturing of rocks: McGraw-Hill, New York, 568 p.

Rauzi, S. L., 2000, Permian salt in the Holbrook Basin, Arizona: Arizona Geological Survey Open-File Report 00-03, 20 p.

Sanford, A. R., 1959, Analytical and experimental study of simple geologic structures: Geological Society of America Bulletin, v. 70, p. 19–52.

Sugiura, R.; and Kitcho, C. A., 1981, Collapse structures in the Paradox Basin, *in* Weigand, D. L. (ed.), Geology of the Paradox Basin: Rocky Mountain Association of Geologists Field Conference Guidebook, p. 33–45.

Sutphin, H. B.; and Wenrich, K. J., 1989, Map showing structural control of breccia pipes on the southern Marble Plateau, north-central Arizona: U.S. Geological Survey Miscellaneous Investigations Map I-778.

Wenrich, K. J.; and Billingsley, G. H., 1986, Breccia pipes in northern Arizona, *in* Nations, J. D.; Conway, C. M.; and Swann, G. A. (eds.), Geology of central and northern Arizona: Geological Society of America and University of Northern Arizona, Rocky Mountain Section Meeting Guidebook, p. 43–58.

Wilson, E. D.; Moore, R. T.; and O'Haire, R. T., 1960, Geologic map of Navajo and Apache Counties: Arizona Bureau of Mines, Tucson, fig. 1.

# Evaporite Karst in Michigan

***Tyrone J. Black***
Michigan Department of Environmental Quality
Geological and Land Management Division
Gaylord, Michigan

**ABSTRACT.**—The restrictive depositional history of the Michigan Basin resulted in three major and several minor evaporite sequences in Michigan's Paleozoic record. Solution of the thick halite and gypsum Silurian sequences resulted in a widespread but largely unmapped collapse breccia, the Mackinac Breccia of Devonian age. The areal extent of this breccia subcrop is poorly defined under the glacial till and its adjacent extent under overlying formations. Footings for the Mackinac Bridge, at the northern edge of Michigan's Southern Peninsula, were designed to sit on this breccia. The breccia might also merge into another widespread breccia of the second major evaporite sequence of Devonian age. Glacial scouring of the basins for Lakes Huron and Michigan during the Pleistocene was influenced by the structurally weakened formations.

The second sequence is in the Detroit River Group in which the evaporite facies is and was thickest at the northern edge of the basin. Evaporites have been dissolved at least 14 mi from the subcrop edge downdip into the basin under >900 ft of overlying bedrock. Ground water penetrates through tectonic and structural adjustment faults developed in overlying layers. Surface geomorphic expressions include soil and stream swallows, extension fractures, subsidence grabens, collapse sinkholes 50–800 ft in diameter and floors 6–120 ft from the surface. Major sinkholes occur along fault linears. Numerous swallows are identified; but only three sinkhole resurgences have been located so far, and they are in Lake Huron.

The Michigan Formation is the third major evaporate sequence. The subcrop of this Mississippian formation is completely within the landmass of Michigan's Southern Peninsula except where it crosses Saginaw Bay. The thickness of glacial drift at the collapse areas is 8–80 ft. Roadways, foundations, utilities, and open-field collapse have occurred dozens of times over the past 40 years in four counties. However, the reporting of such incidents to geologists is rare. The greatest impact has been within Grandville, Kent County, with street, yard, sidewalk, foundation, and utility right-of-way collapses.

## INTRODUCTION

The Michigan Basin developed in Early Cambrian time. A restricted flow of marine waters through the basin at various times resulted in several complex cycles of clastic, carbonate, and evaporite deposits. Evaporite karst features and potential for them exist in (1) nearly 2,400 ft of total salt, plus additional thinner layers of anhydrite, in four central basin Silurian deposits (Sonnenfeld and Al-Aasm, 1991); (2) >450 ft of salt, thinning on the margins to anhydrite, in the Devonian Detroit River Group (Gardner, 1974); (3) ~100 ft of gypsum, thinning to 40 ft along outcrop margins in the Mississippian Michigan Formation (Harrell and others, 1991); and (4) several minor evaporite deposits in various facies of these and other formations (Fig. 1). Pleistocene glaciers scraped across the bedrock of Michigan, removing most ancient surficial karst features. The last glacier began its retreat from southern Michigan 15,000 years B.P., and by 9,000 years B.P. had left northern Michigan. Most shallow and near-surface karst features have developed since then, but the large sinkhole and graben features in the northern Lower Peninsula have changed little since their development shortly after the glaciers retreated.

## MACKINAC BRECCIA

The thick Salina Group salts thin and grade laterally into anhydrite along the basin margins. Additional evaporites had also existed into the northern margin of the basin in the Mackinac Straits area. The dissolution of these Silurian evaporites has resulted in the largest area of karst influence (Fig. 1). The basin underwent an emergent phase after deposition of the Early Devonian Detroit River Group and before deposition of the Dundee Limestone (Landes and others, 1945). Ground water gradually dissolved evaporites at the basin margin, causing collapse of the sequence from the Salina Group to the Detroit River Group into a breccia.

Black, T. J., 2003, Evaporite karst in Michigan, *in* Johnson, K. S.; and Neal, J. T. (eds.), Evaporite karst and engineering/environmental problems in the united States: Oklahoma Geological Survey Circular 109, p. 315–320.

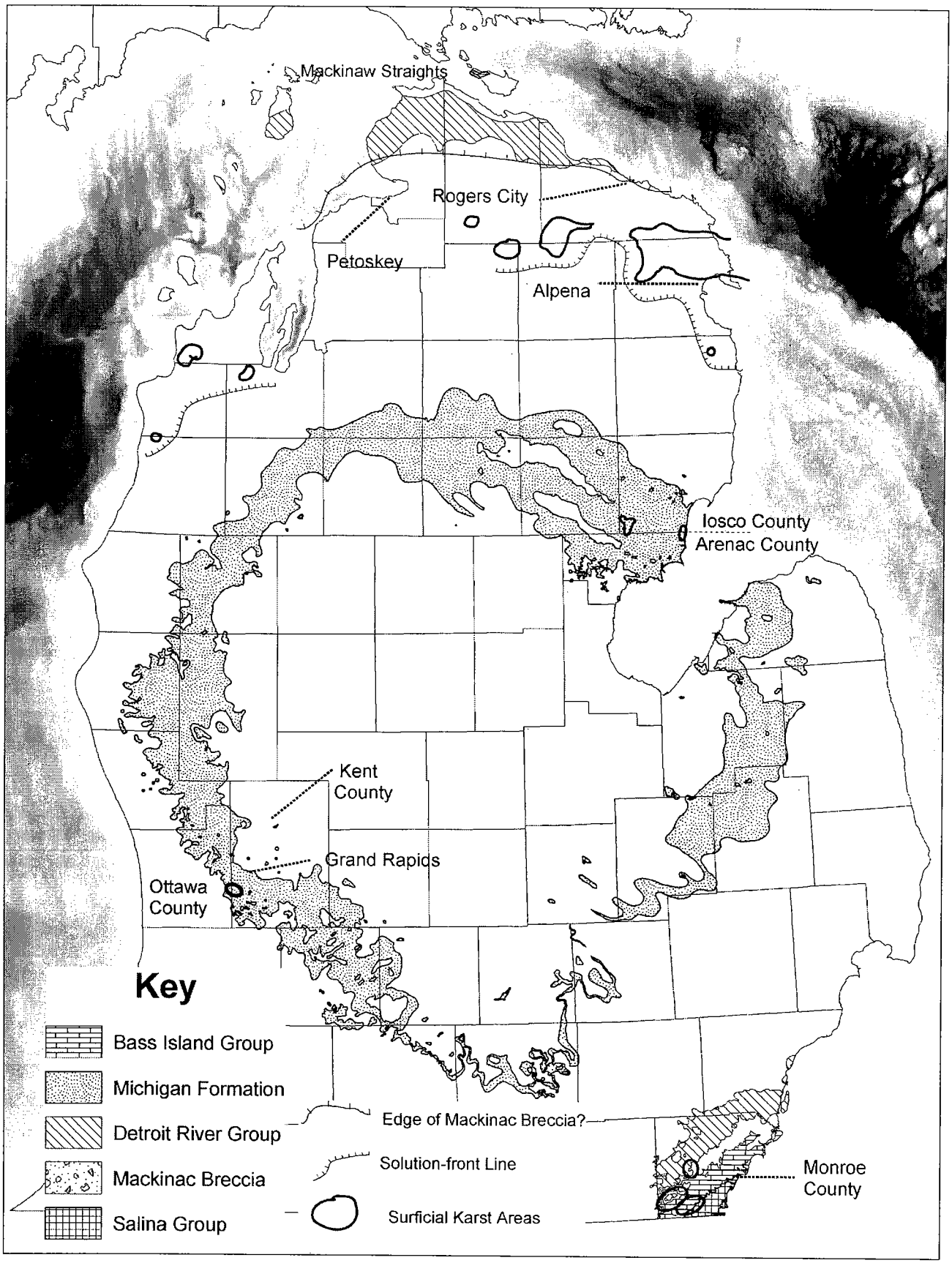


Figure 1. Map showing Michigan evaporite-karst areas, with digital-elevation models of Lakes Michigan and Huron (MDNR, 2001).

The northern parts of Lakes Michigan and Huron were deeply scoured by glaciation where these weakened strata would have existed. Additional dissolution of remaining evaporites continues to the present day. Breccia still remains in outcrop at the Mackinac Straits area. Following a geological-engineering study of the Straits, engineers designed oversized footings for the Mackinac Bridge to assure stability. Cemented breccia stacks and arches, and poorly indurated breccia, exist throughout the area and constitute a productive freshwater aquifer.

## KARST OF THE DETROIT RIVER GROUP

Basinward in higher stratigraphy, and possibly merging with or overlapping part of the Mackinac Breccia, is another (unnamed) breccia. It extends southward from the northern tip of southern Michigan to an approximate collapse limit line shown in Figure 1. It lies wholly within the Detroit River. Central basin halite deposits of this group total >450 ft, but they also thin abruptly toward pinch-out near the margins (Gardner, 1974). Gypsum and anhydrite deposits thicken toward the margins to the point at which they have been removed by dissolution. This zone of evaporite karst and breccia is marked by lost circulation in drilling for oil and gas, localized areas of data-acquisition difficulties in seismic exploration, areas of disappearing streams and internal drainage, rock-walled sinkholes up to 400 ft in diameter and 120 ft deep, and sinkholes expressed through as much as 300 ft of glacial mantle and >1,000 ft in diameter across the northern Lower Peninsula of Michigan. Glacial drift is 0–250 ft thick and overlies formations of an additional 700–1,300 ft in thickness (Fig. 2).

### Development

Sonnenfeld and Al-Aasm (1991) state that the basin had an emergent phase during Early Pennsylvanian time and that some Devonian evaporites might have been recycled from the Salina deposits. Gardner (1974, p. 39) states, "No solution effects could be confirmed although salt solution is known to be present, and marker anhydrites may be traced without disruption across most of the [central basin] study area." The accidental recovery of a vuggy limestone with residual gypsum from within the Detroit River Group of Early Devonian strata from a well at a depth of ~1,560 ft in southwestern Alpena County (Fig. 3), and lost circulation commonly encountered by oil- and gas-well drilling in this zone even into the central basin, both indicate that a significant dissolution event occurred before overlying strata were deposited.

Current ground-water penetration to the evaporites is possible, owing to hydrologically open tectonic faults and subsidence fractures. The flow of water into the paleokarst referred to above through fractures could then readily reactivate paleo-flow paths or establish a new gradient. The U.S. Geological Survey datum for the surface of Lake Huron is 580 ft. During

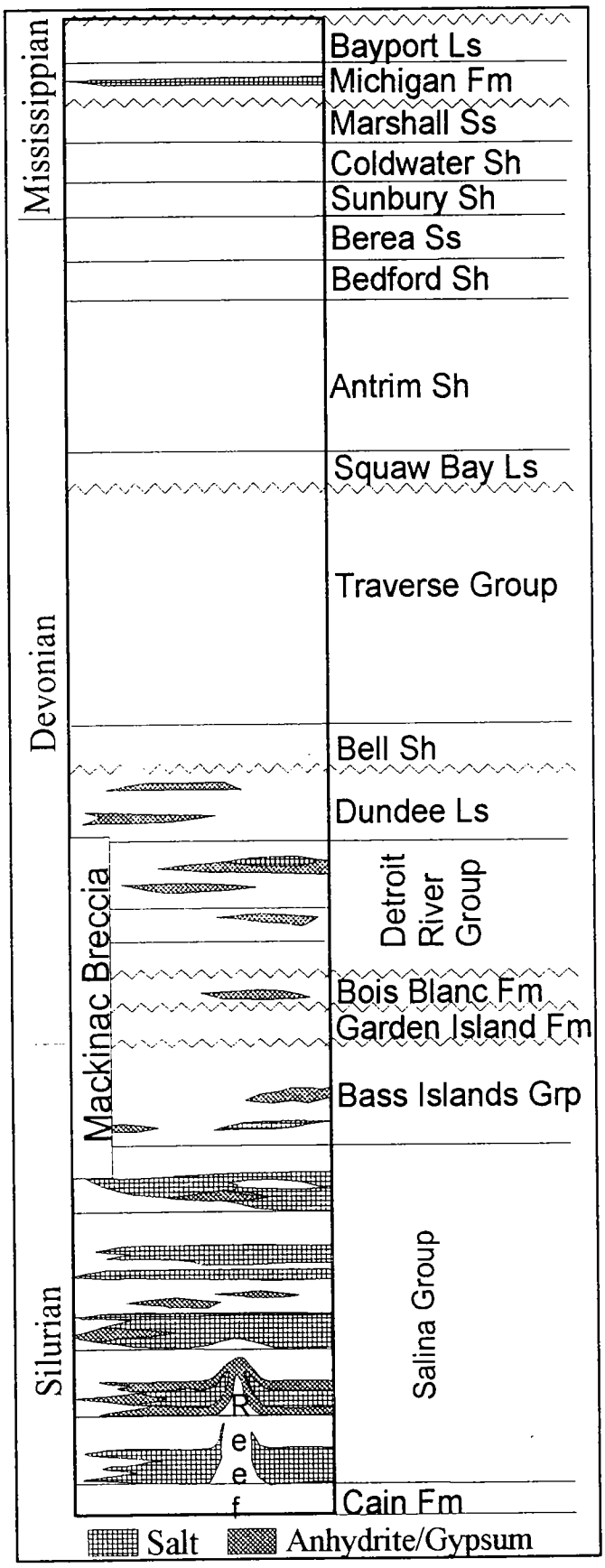


Figure 2. Part of Michigan's stratigraphic succession, covering Devonian rocks (Michigan Geological Survey, 2000).

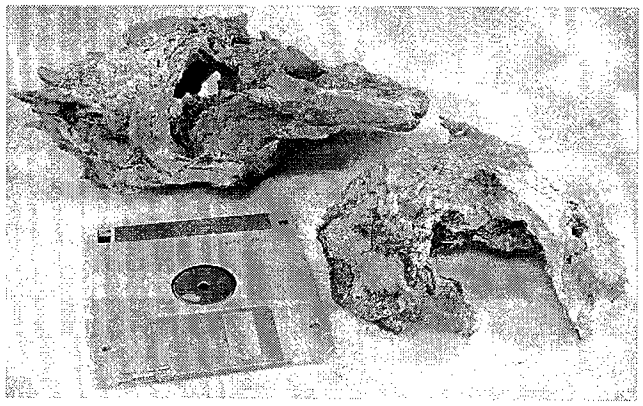

Figure 3. Detroit River Group fragments, showing residual limestone karst from dissolution of gypsum. The specimens were accidentally retrieved in the caliper arm of an electric-logging tool in a gas-test well, the Broad 1-10, Wolverine Environmental Production and Grace Petroleum, Michigan permit no. 40496, sec. 10, T. 29 N., R. 5 E., Alpena County.

Figure 4. Oblique aerial photograph, looking southeast over El Cajon Bay and its sinkholes toward the city of Alpena, Michigan.

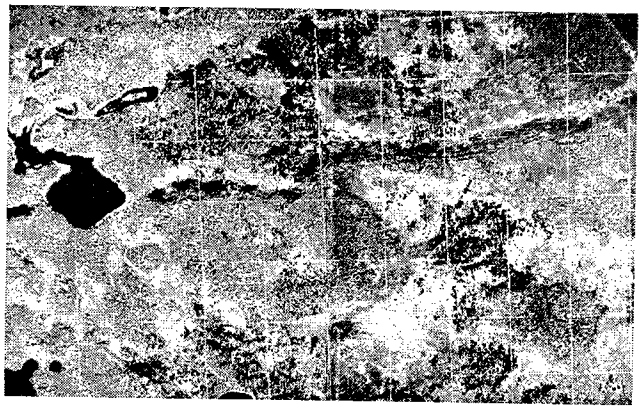

Figure 5. Aerial photograph showing the geomorphic expression of karst collapse along a fault line and post-glacial block subsidence, Shoepac Lake area, Presque Isle County, Michigan. Note the slump scars along the south side of the east end of the collapse valley (U.S. Department of Agriculture, 1932).

the post-glacial Lake Stanley stage, this elevation was ~180 ft (Farrand, 1987).

No outflow from this system to the land surface has been discovered. All outflow emerges within Lakes Huron and Michigan, as evidenced by a blue hole and springs within the edges of El Cajon Bay by Alpena (Fig. 4), a sinkhole in Lake Huron off the northeast side of Middle Island, and another sinkhole several miles farther into the lake. Steven Ruburg, National Oceanic and Atmospheric Administration, provided information from 2002 research in Lake Huron of water with high conductivity and contrasting temperature in the remote sinkhole. The research discovered several sinkholes in the area that will be examined further in 2003 by Ruburg and the Thunder Bay National Marine Sanctuary and Underwater Preserve/IFE.

Water is sinking into the system from hundreds of locations onshore. Water exiting the blue hole in El Cajon Bay nearly equals the volume sinking into only one sink, Rainy Lake. The water chemistry tested from the known outflows show the water to be saturated with respect to gypsum (Morrow, 1983).

Reports of collapses since European settlement of the area are rare, and such reports are usually further development of existing sinkholes or their redevelopment since being plugged with glacial deposits. On the northeast side of the Southern Peninsula, the sinkholes follow a strong trend, with a fault scarp visible in places. Outflow chemistry, a lack of significant evaporites in oil and gas wells north of the trend line, the strong geomorphic expression of a fault/karst line, and post-glacial block subsidence (Fig. 5) suggest an active solution front within the Detroit River Group. North of this active zone, stagnant sinkholes have been discovered in limestone quarries at Charlevoix and Rogers City. They had no surficial expression in the glacial drift. At Charlevoix they were filled with fine sand and silt of glacial outwash. Radial fractures from sinkhole walls leak water into the quarry, which is below the surface elevation of Lake Michigan. At Rogers City these fractures were filled with breccia that had collapsed from formations and clay above the Dundee Formation (Black, 1983). Those formations were no longer present at the site, and the layers of coarse glacial sediments above were undisturbed. This indicates that a number of sinkholes had collapsed before the final retreat of Wisconsinan glaciation from the area about 11,000 years ago. These sinkholes probably have active hydrological impact but are structurally plugged and do not swallow the glacial drift.

## MICHIGAN FORMATION

The Michigan Formation subcrops in a circular pattern in southern Michigan (Fig. 1). It contains beds of shale, gypsum, anhydrite, limestone, and dolostone. Karst reported in this formation is limited to the Kent and Ottawa county and the Iosco and Arenac county subcrops. The drift mantle is <20 ft deep but is as deep as 100 ft where sinkholes are reported in these counties.

### Kent and Ottawa Counties

In Jenison, Grandville, and the southwest part of Grand Rapids, gypsum karst sinkholes are visible through a glacial-drift mantle 40–100 ft thick. The sinkholes are visible as drift sinks and collapses. They are from a few tens to a few hundreds of feet in diameter and from several feet to 60 ft deep. Workers in the Grand Rapids Gypsum Mine encountered a 330-ft cave in the gypsum (Elowski and Ostrander, 1977). Some area sinkholes are over mine workings and are thought to be due to some mine collapse. Numerous other sinkholes and recent collapses are in areas where no mining is known to have taken place.

The following is a typical scenario for sinkhole collapse and treatment in the area. An initial soil failure occurs at the surface; the landowner fills the sinkhole with sand or gravel; the site continues to settle over many years; the landowner continues to restore the contour with more coarse fill. The use of coarse fill exacerbates the remediation attempts by focusing more drainage into the already active zone. Impacted land use includes streets, sidewalks, driveways, building foundations, and yards in the communities of Jenison and Grandville.

In the case of the house-foundation damage, a Jenison homeowner contracted to have the house jacked up, leveled, and a reinforced foundation placed under the house. A homeowner one block away has a driveway with an 8-ft-diameter soil sink. He had replaced his concrete driveway twice but finally used red brick on a sand bed. Now every 2 years he moves the bricks, lays down additional sand, and replaces the brick. In Grand Rapids at the U.S. Highway 131 bridge over the Grand River, one end of the bridge gradually settled several inches. The river enhanced dissolution of the gypsum bedrock under the concrete foundation. The Michigan Department of Transportation replaced the bridge in 2001, using a deeper foundation.

### Eastern Michigan

The Michigan Formation also subcrops beneath shallow overburden in southern Iosco and northern Arenac Counties. Sinkholes and small sink valleys are found in Burleigh Township of Iosco County. There have been few cases of new collapses reported; however, anecdotal information suggests that collapses occur annually. The writer was informed of only one "recent" collapse. The landowner described it as ~12 ft across and 15–20 ft deep, in a field. It involved the collapse of a shale or hardpan roof, and occurred between winter and late spring. The surface owner had filled it in with gravel by the time the writer was notified.

Benson and Kaufmann (2001) reported their investigation into a small sinkhole that had occurred in a lane of U.S. Highway 23 in Iosco County. Their work revealed several potential collapse areas along a part of the highway that was built over a thin sand and clay cover above gypsum beds. They concluded that dewatering from a nearby quarry or nearby residential water wells may have been a trigger factor.

## MINOR EVAPORITE FACIES

In southeastern Michigan, Monroe County karst (Fig. 1) occurs in the same formation as northeastern Michigan's deep system. But here the formation is directly under shallow soil cover (<50 ft), and the formation contains no documented evaporite beds. A shallow ground-water flow system (<100 ft) appears to have developed . The sinkholes are drift sinks, although a few show rock walls. They are typically 10–30 ft deep at the area of greatest expression. Groundwater quality varies, with some waters being high in sulfate. The depositional facies of the Detroit River Group in southeastern Michigan is characterized by scattered inclusions and nodules of gypsum, except where ground-water flow has dissolved the gypsum. Small voids and high permeability exist in the shallower parts of the formation, where the acidity of the dissolved mineral assisted in dissolving the host limestone. Limestone karst has developed in this area, resulting in some internal drainage and discharge into Lake Erie from springs (Hart, 1975). Hart (1975) also reports that in deepening some rock wells in this area to increase water supply, existing water supplies were lost upon penetration of deeper rock strata, indicating cavernous conditions.

Monroe County established a karst study committee to understand the ground-water system. The county also began an initiative to filter waters drained into the system by ditch and farm-field sinkholes and drainage wells. Monroe County has a nearly level topography, with few hills. The only known springs are near the shore of Lake Erie. Dye-tracing under these difficult conditions was begun in 2000 to determine if water wells were impacted.

A limestone fragment was recovered from Lake Erie off the shore of Monroe County by a commercial fishing boat. The nets of the boats frequently catch on the sharp scallops and hooks of the limestone, tearing the nets and occasionally breaking off a fragment of limestone. This form of limestone karst suggests dissolved-gypsum inclusions and associated acidity.

## REFERENCES CITED

Benson, R. C.; and Kaufmann, R. D., 2001, Characterization of a highway sinkhole within the gypsum karst of Michigan, *in* Environmental applications of karst geology and hydrology: Balkema, Lisse, Netherlands, p. 103–112.

Black, T. J., 1983, Selected views of tectonics, structure, and karst of northern Lower Michigan, *in* Tectonics, structure, and karst in northern Lower Michigan: Michigan Basin Geological Society, 1983 field conference, p. 22, 23.

Elowski, R. C.; and Ostrander, A. G., 1977, Gypsum karst and related features in the Michigan Basin, *in* Fritz, Carol (ed.), Official 1977 guidebook, Alpena, Michigan: National Speleological Society, Huntsville, Alabama, p. 37.

Farrand, W. R., 1987, The glacial lakes around Michigan, revised: Geological Survey Divsion, Michigan Depart-

ment of Natural Resources, Bulletin 4, chart inside back cover.

Gardner, W. C., 1974, Middle Devonian stratigraphy and depositional environments in the Michigan Basin: Michigan Basin Geological Society Special Papers no. 1, p. 39.

Harrell, J. A.; Hatfield, C. B.; and Gunn, G. R., 1991, Mississippian System of the Michigan Basin, *in* Catacosinos, P. A.; and Daniels, P. A., Jr. (eds.), Early sedimentary evolution of the Michigan Basin: Geological Society of America Special Paper 256, p. 215.

Hart, D. N., 1975, Report of geophysical and boring survey, US-223 (Old 151) from existing US233 to US-23, Whiteford Township–Monroe County; Control Section 58021, Job Number 00783A: Michigan Department of State Highways and Transportation, Testing Laboratory Section, Ann Arbor, Michigan, p. 2.

Landes, K. K.; Ehlers, G. M.; and Stanley, G. M., 1945, Geology of the Mackinac Straits Region and sub-surface geology of Northern Southern Peninsula: State of Michigan Department of Conservation, Geological Survey Division, Publication 44, Geological Series 37, p. 116.

Michigan Department of Natural Resources, 2001, Great Lakes Bathymetry Geographic Theme, MiGDL–Center for Geographic Information, http://www.state.mi.us/webapp/cgi/mgdl/.

Michigan Geological Survey Division and Michigan Basin Geological Society, 2000, Stratigraphic nomenclature for Michigan (chart).

Morrow, R., 1983, A review of the limnological characteristics of Alpena Michigan, area flowing wells and sinkholes, *in* Tectonics, structure, and karst in northern Lower Michigan: Michigan Basin Geological Society, 1983 Field Conference, p. 91-118.

Sonnenfeld, Peter; and Al-Aasm, Ihsar, 1991, The Salina evaporites in the Michigan Basin, *in* Catacosinos, P. A.; and Daniels, P. A., Jr. (eds.), Early sedimentary evolution of the Michigan Basin: Geological Society of America Special Paper 256, p. 148–151.

# Mechanism of Sinkhole Formation in Glacial Sediments above the Retsof Salt Mine, Western New York

***Samuel W. Gowan and Steven M. Trader***
Alpha Geoscience
Clifton Park, New York

**ABSTRACT.**—The Retsof Salt Mine in Livingston County, New York, was successfully operated for 109 years by extracting ~12 ft of salt from a gently dipping layer within the Vernon Formation of Silurian age. A collapse and inrush of brine occurred at mine level on March 12, 1994. The brine gradually changed to fresh water and flowed in at a sufficiently high rate to result in the complete flooding of the 6,500-acre mine in 21 months. Although the initial collapse occurred into a room with a nominal height of 12 ft, a 15-ft-deep sinkhole eventually developed at the land surface 1,100 ft above the mine. This initial sinkhole destroyed part of a U.S. highway and bridge. A second sinkhole formed over an adjacent panel and resulted in nearly 70 ft of surface subsidence. These sinkholes penetrated geologic materials consisting of 600 ft of rock overlain by 500 ft of glacial sediments.

Two distinct theories were postulated for the mechanism of sinkhole formation: (1) piping of glacial sediments through open fractures in the bedrock without actual loss of bedrock support, and (2) loss of support for the glacial sediments by undermining and downdropping of the bedrock. The resolution of these theories was important in order to assess whether similar sinkholes were possible over other parts of the mine, or whether the existing sinkholes would stabilize sufficiently to allow reconstruction of the U.S. highway and bridge. Drill-hole data, seismic-activity records, subsidence measurements, and seismic-reflection data were analyzed. The data indicate that the sinkholes formed by the downdropping of the bedrock and glacial sediments into voids created by the dissolution of salt and the slaking of salt-bearing shale upon exposure to fresh water.

## INTRODUCTION

Operations at the Retsof Salt Mine in western New York were initiated in 1885 by excavating a 1,140-ft shaft through shale and limestone of the Upper and Middle Devonian and through shale and dolomite of the Upper Silurian to reach a bedded salt layer in the Salina Group. Extraction at the Retsof Salt Mine was conducted using room-and-pillar methods that involved removing 12 ft from the middle of a salt bed that has an average thickness of 20 ft (Dunn Corp., 1992). Mining progressed eastward and southward (Gowan and Trader, 2000) down the dip of bedding, which is to the southeast at ~0.65° (Dunn Corp., 1992). The mine, which had become the largest salt mine in the Western Hemisphere (Yager and others, 2001), occupied ~6,500 acres and extended under parts of three townships in Livingston County, New York (Fig. 1). A roof fall occurred, and brine began flowing into the mine in March 1994. The inflowing brine gradually changed to fresh water, and two large sinkholes developed at the land surface directly above the collapse during the 2.5-month period following the collapse. Water inflow continued unabated and resulted in closure of the mine in September 1995.

The roof fall occurred on March 12, 1994, in a small-yield-pillar mining panel near the southernmost limit of the mine. The collapse caused an earthquake with a magnitude of 3.6 ($M_{bLg}$) (Kelly, 1999) and formed a shallow circular depression with concentric fractures at the land surface. The mine-level collapse was coincident with a release of gas (methane) and brine into the mine. The brine inflow initially entered at a rate of 5,400 gallons per minute (gpm) and eventually became fresh and increased to a rate of 20,000 gpm. The mine was completely inundated in 21 months.

The observable collapse occurred in the roof over a mine panel identified as 2 Yard South (2YS). Panel 2YS is near the southern end of the mine (Fig. 2) and is ~1,100 ft beneath a deeply scoured glacial valley presently occupied by the Genesee River. Panel 2YS and neighboring panel 11 Yard West (11YW) were mined using a small-yielding-pillar method, which was adopted to solve problems with the large-pillar method that had been the normal practice in the adjacent areas of the mine (Gowan and Trader, 2000; Gowan and others, 1999).

The fractures and gentle circular subsidence that developed above 2YS at the time of the collapse re-

Gowan, S. W.; and Trader, S. M., Mechanism of sinkhole formation in glacial sediments above the Retsof Salt Mine, western New York, *in* Johnson, K. S.; and Neal, J. T. (eds.), Evaporite karst and engineering/environmental problems in the United States: Oklahoma Geological Survey Circular 109, p. 321–336.

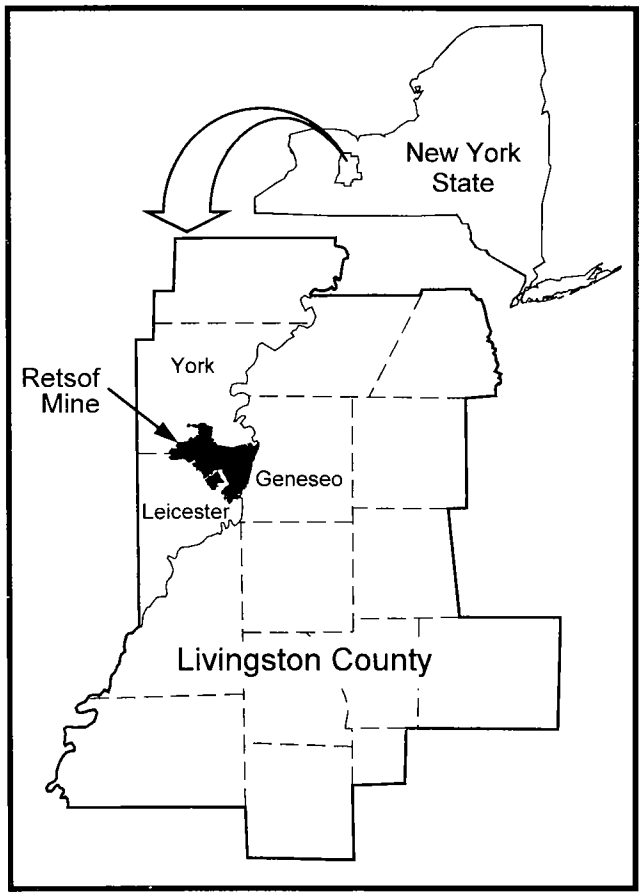


Figure 1. Map showing the Retsof Salt Mine in Livingston County, New York State.

sulted in structural damage to a highway bridge that forced the closure of U.S. Highway 20A (Fig. 2). The depression over 2YS subsided gradually during the first month after the collapse, and then the land surface dropped suddenly and formed a sinkhole with an approximate depth of 15 ft and a diameter of 600 ft. This sinkhole filled with water from Beards Creek, which passed directly over the panel. The land surface over the adjacent small-yield-pillar panel (11YS) appeared stable during the first month, and then began to subside gently with periods of sudden drops that resulted in a sinkhole with a depth of 70 ft and a nominal diameter of 640 ft. The sudden drops over both panels were associated with seismic events and changes in the rate of ground-water inflow to the mine. The sinkhole over 11YW also filled with water from Beards Creek.

The need to understand the process of sinkhole formation became important during the first few weeks following the collapse when the mine operator, Akzo Nobel Salt, Inc., was evaluating various methods for stopping the inflow and saving the mine. Attention was refocused on the process of sinkhole development during the later stages of mine flooding after it had become apparent that the inflow could not be controlled and the mine would be lost. Issues were raised, during the final stages of mine flooding, as to whether the sinkholes would expand laterally or vertically, change shape, stabilize, or form elsewhere over the mine.

Knowledge of sinkhole formation was applied specifically toward the development of a safe design for the new Route 20A bridge, to the determination of when the ground had stabilized sufficiently to reconstruct the bridge, and for the assessment of whether infrastructure or property elsewhere over the mine was prone to damage by new sinkholes.

## Postulated Sinkhole Mechanisms

Two mechanisms for sinkhole formation were postulated by the consultants to Akzo Nobel Salt, Inc. One of the these consisted of the formation of sinkholes by piping of unconsolidated glacial sediments downward through open fractures in the rock above the mine. The other scenario called for the downdropping of the rock and overlying glacial sediments into a void created by the dissolution of salt.

### *Piping Model*

The piping model assumed that the primary source of water entering the mine was coming from a prolific aquifer in the glacial sediment above the rock. The focus on a ground-water source was predicated on streamflow measurements in Beards Creek and the Genesee River by the U.S. Geological Survey that demonstrated that surface water was not the source of water inflow (Yager and others, 2001). Ground water was interpreted to be flowing vertically from the glacial aquifer down through open fractures in the carbonate and shale between the glacial aquifer and the mine. This water needed sufficient velocity and fracture width to transport glacial sediment down through the rock interval and into the mine. The episodic expansion of the sinkholes at the land surface was presumed to be due to the collapse of voids near the base of the unconsolidated glacial sediments. These voids were believed to be forming as the sediments were removed by piping.

The primary evidence for the piping scenario was the discovery of glacial sediments at great depths below the top of bedrock within the exploration and grouting holes drilled above and near the collapse area. Substances, such as cellophane fragments that were added to control fluid loss while drilling through the glacial sediments, were encountered at great depths in the rock at a few places despite the fact that these materials were not being utilized during bedrock drilling. The sediment-piping model was also supported by the fact that 11YS subsided approximately 70 ft, which was far greater than the subsidence that could be accounted for by the 12-ft mine height or the 20-ft maximum thickness of the salt bed that was being mined. The possibility that piping was the acting sinkhole mechanism raised the concern that unstable voids could persist in the glacial sediments, the sinkhole

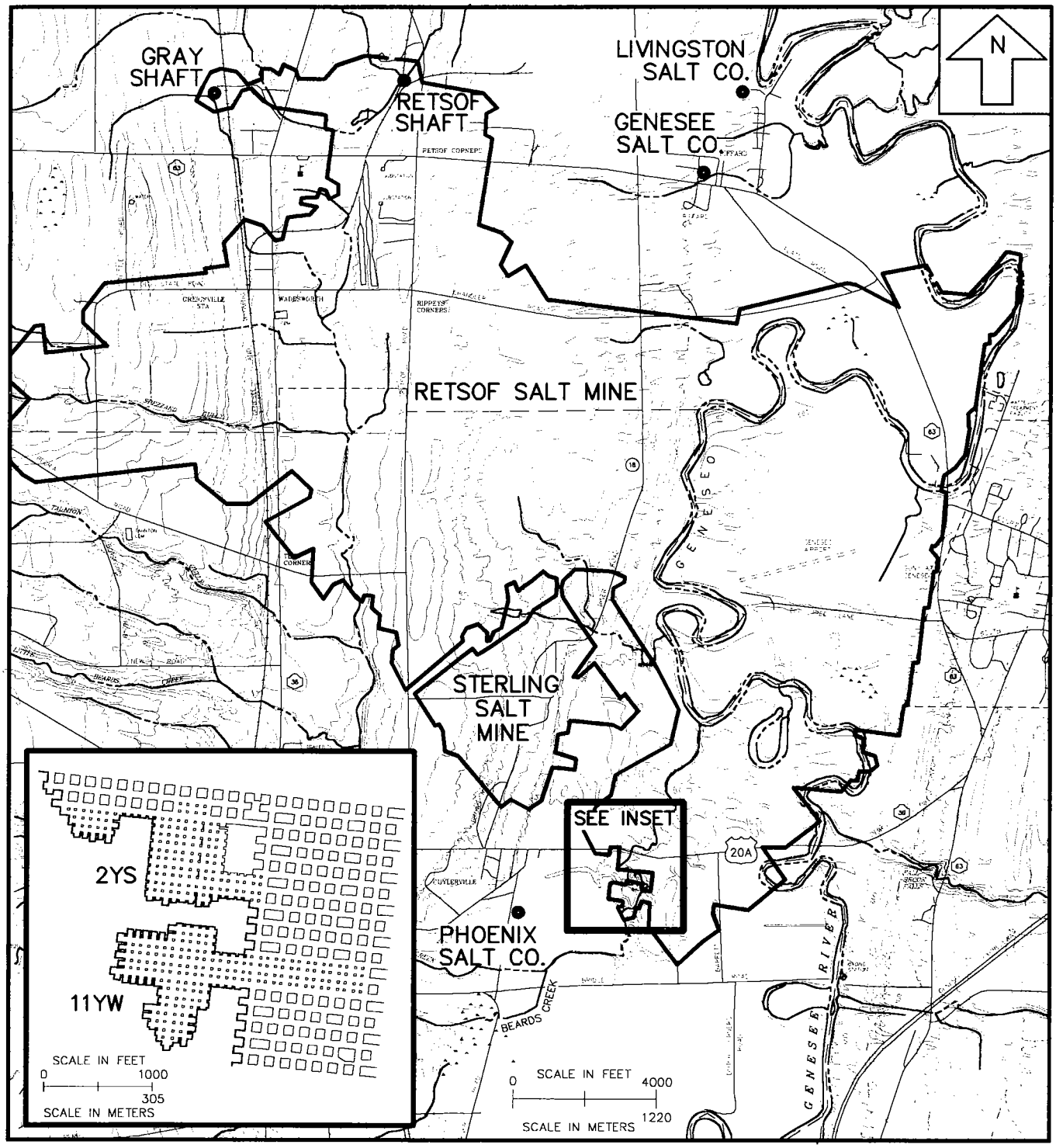


Figure 2. Map showing the footprint of the Retsof Salt Mine and the small-pillar panels 2YS and 11YW.

could expand laterally, or new sinkholes could form at locations beyond the footprint of 2YS and 11YW.

### *Dissolution Model*

The dissolution model assumed that a void was created by dissolution of salt beds and disaggregation of salt-bearing shales. The loss of support for the rocks above the void would have resulted in the dropping of the carbonates and slumping of the overlying glacial sediments. The initial evidence for the dissolution scenario was based primarily on the fact that the sudden drops in the sinkholes were associated with seismic events, the shale above the mine level was known to contain salt, and the sinkholes appeared to remain above the footprints of panels 2YS and 11YW.

If dissolution was the mechanism operating at the

site, it was anticipated that the resulting sinkholes would tend to stabilize more quickly than they would for the piping scenario. The sinkholes were expected to stabilize when all soluble materials were removed from the contact area within the water-entry zone. It was also anticipated that the sinkholes would remain directly above the panels where inflowing fresh water had the greatest opportunity for dissolving soluble materials.

## Data Evaluation and Interpretation

The sinkhole mechanism remained unresolved until 1996, when the available data were analyzed for insurance claims and the subsurface stability was assessed for the Route 20A highway and bridge reconstruction (Gowan and others, 1996). The analysis of the sinkhole mechanism involved establishing the geology, correlating sinkhole development with seismic events and inflow rates, determining whether the rock had dropped beneath the glacial sediments during sinkhole formation, assessing how glacial sediment and fluid-control materials had reached significant depths in the rock, evaluating the geotechnical and hydrogeologic characteristics of the glacial sediments, and quantifying the thickness of soluble materials at and above the mine level. These analyses were conducted from logs of holes drilled around the collapse; elevation data measured from drill holes and subsidence markers; regional core-hole data; recorded chronology of seismic events, inflow rates, and sinkhole progression following the collapse; and seismic-reflection data.

## Geology

The bedrock geology of the Retsof Mine area consists of a thick sequence of salt-bearing shale and dolomite of the Vernon and Syracuse Formations, overlain by shale, dolomite, and limestone (Fig. 3). The bedrock geologic units near the collapse were identified by correlating descriptions of cuttings and geophysical logs from hole 9401 with geophysical logs and continuous rock-core data from hole 9441/9441A, which was drilled on the valley margin southeast of the collapse (Fig. 4). The unit that was being mined, known locally as the B6 or Retsof salt bed, appears at the base of the section in Figure 3. This bed (B6 salt) was mapped in the Retsof Mine area by Rickard (1969) as being the top bed in the Unit B member of the Vernon Formation. The Vernon is in the Upper Silurian Salina Group, which also includes the Syracuse Formation, the Camillus Formation, and dolomitic shale and limestone beds known variously as the Bertie Formation (Rickard, 1969) or the Bertie Group (Ciurca and Hamell, 1994).

Unit C of the Vernon Formation begins at the top of the B6 salt bed. Unit C is predominantly a shale/mudstone with beds of shaly dolomite. Salt and anhydrite are present throughout Unit C. The salt is reddish brown and occurs as hoppers, lenses, and fill in

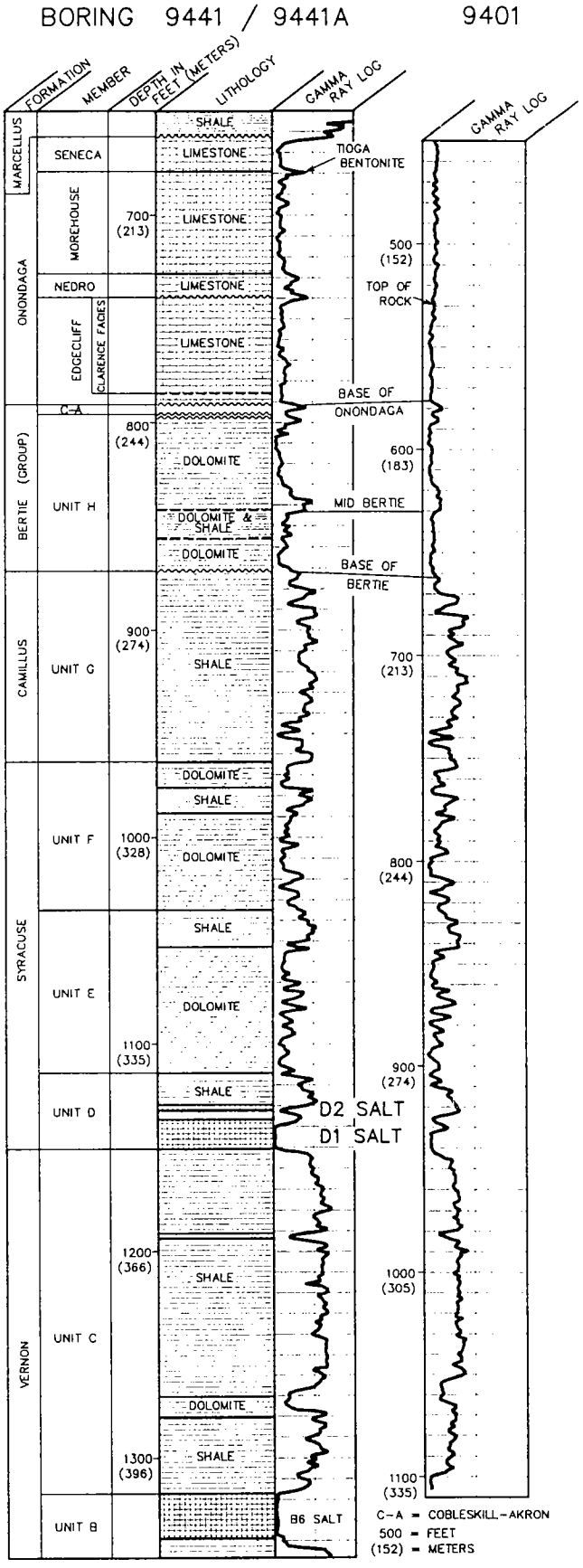


Figure 3. Stratigraphic correlation of the collapse area to regional core-hole and geophysical data.

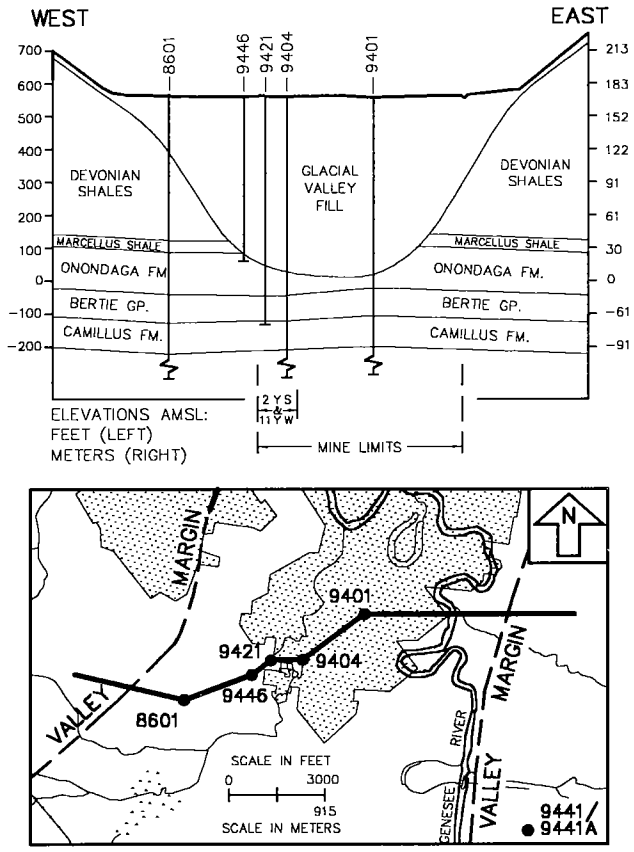


Figure 4. Cross section and map showing relative position of the glacially scoured Genesee River Valley over the mine and collapsed panels.

fractures, which have a variety of orientations relative to vertical. The salt-filled fractures form a polygonal pattern where observable in the shale of the mine roof.

Salt is also present at the base of the Unit D member of the Syracuse Formation. Two salt layers, known locally as the D2 and D1 salts (Fig. 3), occur at the base of the Unit D member ~160 ft above the B6 salt. The D salts apparently were dissolved and replaced by an overpressured brine zone in the area above the collapsed panels well before mining commenced in the valley (Gowan and others, 1999; Gowan and Trader, 2000).

A regional, angular unconformity defines the boundary between the Upper Silurian beds at the top of the Bertie Group and the overlying Middle Devonian Onondaga Formation (Fig. 3) (Rickard, 1989). The Onondaga Formation is a 120-ft-thick limestone that is overlain by shale and thin limestone beds of the Hamilton Group throughout most of the area above the mine west of the Genesee River Valley. All of the overlying Hamilton Group and most of the Onondaga were removed from the Genesee River Valley and backfilled with unconsolidated sediments (Fig. 4) by Pleistocene glacial processes. The glacial deposits were investigated in the area around the collapse using a dual rotary-drilling system that yielded samples of cuttings and provided access for the collection of Shelby-tube and split-spoon samples of the fine-grained zones (Alpha Geoscience, 1996). Geologic-investigation hole 9446, which was drilled close to the 11YW collapse, revealed that the valley fill consists of 200 ft of interlayered glaciolacustrine, glaciofluvial, and glacial-till deposits, overlain by 200 ft of glaciolacustrine sediments, which are capped by 50 ft of recent river alluvium (Fig. 5). The interlayered unit rests on top of rock, and the specific layer within that unit that is in contact with the rock varies throughout the collapse area and the valley. The glacial till consists of loose to densely compacted sand, gravel, silt, and clay. The glaciofluvial sediment is composed of silt, sand, and gravel, and the glaciolacustrine deposit is predominantly silt and clay. The river alluvium is primarily a clay with minor amounts of sand and gravel.

## History of Sinkhole Development

The initial collapse in panel 2YS occurred at 5:40 a.m. on March 12, 1994. The mine-level collapse and resulting 3.6-$M_{bLg}$ seismic event created concentric fractures that were visible in the snow at the land surface. These cracks were surveyed as shown in Figure 6. Although no survey datum was available to measure subsidence immediately after the collapse, the amount of the initial drop did not appear significant.

Brine began entering 2YS about the time of the collapse at an estimated rate of 5,400 gpm. This brine had a measured salt saturation of 98% when access to the panel was finally allowed the day after the collapse (March 13). No water was observed entering the adjacent 11YW panel as of March 13.

A baseline elevation datum was established from survey monuments and drill casings during the period between March 12 and March 18. The locations of these survey data points appear in Figure 7. The land surface above 2YS subsided an unknown amount between March 12 and March 18, and >1.0 ft was measured between March 18 and March 28 after the elevation datum was established (Fig. 7). The center of the subsiding area had an estimated total drop of >3.0 ft as of March 28 on the basis of visual observation. No measurable subsidence occurred over most of the adjacent 11YW panel from March 18 to April 1, 1994. The salt concentration of the brine entering the mine began to decrease a couple of days after the initial 2YS collapse but was still at slightly more than 60% (Table 1) when the last sample was collected and analyzed by mine personnel on March 21. The inflow rate had increased to an estimated 13,000 gpm by April 2, 1994.

A large seismic event, with a drop of the land surface to a depth of 15 ft above 2YS and a drop of 0.17 ft above 11YW, was recorded on April 6, 1994 (Fig. 8). Although the 11YW subsidence was directly above the panel, the maximum subsidence appeared to be

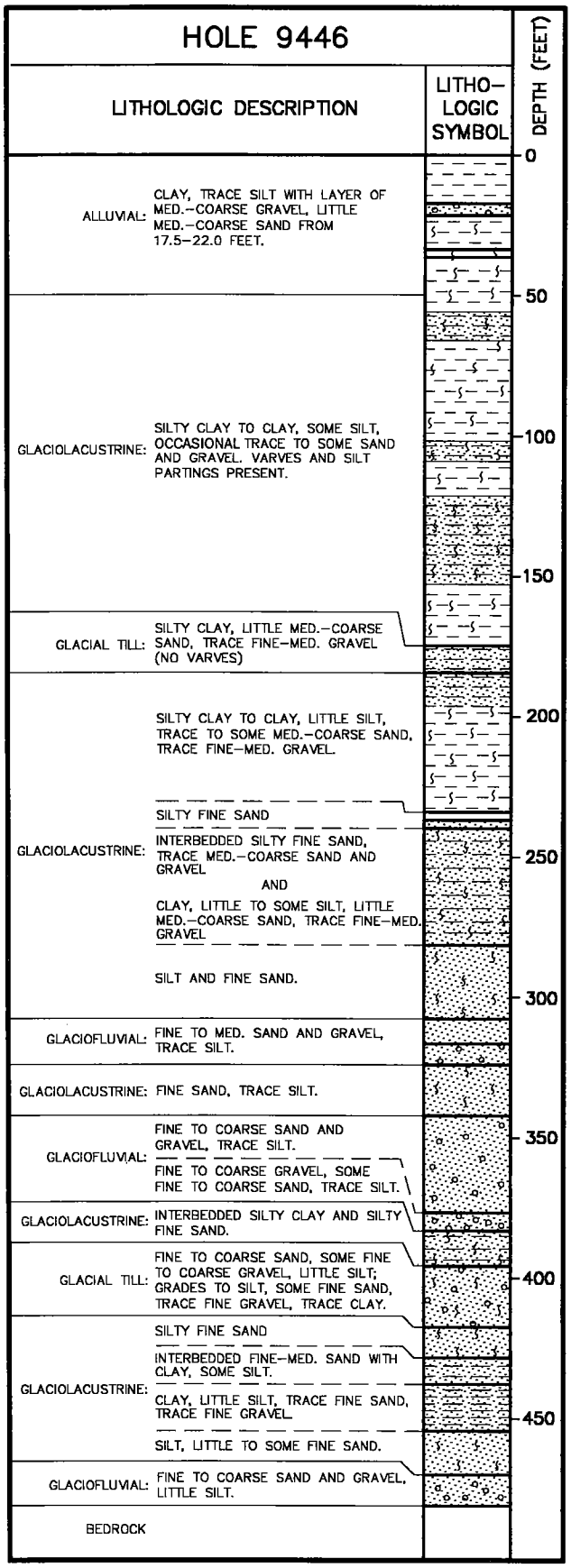


Figure 5. Geologic log of the valley-fill sediments near the collapse area.

skewed somewhat to the south and east of the panel's center. The center of the 2YS subsidence was not observable owing to flooding of the surface (Fig. 8) by Beards Creek.

Another large seismic event was recorded on April 8, 1994. This event appears to correlate with a measured drop of 4.0 ft near the center of 11YW between April 6 and April 14 (Fig. 9) and an increase of water inflow to an estimated rate of 15,000–20,000 gpm. Although the total subsidence and inflow estimate were not recorded until April 14, 1994, it is believed that most of the change occurred as the result of the April 8 event, based on the shearing of the drill casing on April 7 in well 9407, which was being used to pump cement into 11YW, and an anecdotal report of a 5-ft drop in the land surface over 11YW by April 12. The inflow rates remained in the range of 18,000–20,000 gpm throughout the rest of the period of sinkhole development and full inundation of the mine.

The sinkholes continued to subside gently from April 14 through May 25, 1994. A major seismic event occurred on May 25 at 2:15 a.m., followed by the formation of a large sinkhole over 11YW at 4:00 a.m. that same morning. The center of the sinkhole achieved a total drop of more than 60 ft, but the sinkhole perimeter was still within the footprint of the underlying panel. Another large seismic event occurred on May 31, and the sinkhole over 11YW collapsed further on June 3. The approximate dimensions of the sinkhole are represented by the survey data recorded as of June 13 and 15, 1994 (Fig. 10).

The sinkhole continued to subside gently from June 1994 until full inundation in late 1995. The post–June 1994 subsidence was focused primarily in the eastern entries of both panels and the northern entry to 2YS, where water was moving out of the panels into the rest of the mine (Gowan and others, 1996).

## Depth to Rock beneath the Sinkholes

The depth to rock in the center of each sinkhole was interpreted from seismic-reflection data and drillhole logs. The seismic-reflection studies, which were conducted at three different stages of sinkhole development, were designed specifically to determine whether and how much the top of the rock had dropped, and to assess the conditions of the rock and glacial sediments. Most of the borings in the collapse, which were drilled for a variety of reasons, record the depth to the top of the rock.

### *Seismic-Reflection Results*

The first seismic investigation was conducted over 2YS on March 22 and 23, 1994. This survey interpreted a sag in the Onondaga (top bedrock unit beneath the glacial sediments) and a zone of broken rock (Fig. 11) (Dobecki, 1994a). The second investigation was conducted above both panels during the period April 21–27, which was after the sinkhole had formed above 2YS and 4 ft of subsidence had occurred above 11YW.

**Table 1. — Results of Chemical Analyses of Water-Inflow Samples from Retsof Mine**

| Sample location | Date | Saturation with salt (%) | Chloride (mg/L) | pH | Specific gravity |
|---|---|---|---|---|---|
| 2YS/3 Room | 3/13/94 | 98 | 193,050 | 6.7 | 1.19 |
| Unknown (outflow from 2YS) | 3/15/94 | 86 | 169,100 | 6.8 | 1.162 |
| 11YS/Fan (outflow from 2YS | 3/17/94 | 68 | 130,250 | 6.9 | 1.134 |
| 2YS/61 Room | 3/20/94 | 63 | 115,500 | 7.1 | 1.119 |
| 2YS/61 Room | 3/21/94 | 62 | 110,000 | 6.9 | 1.116 |

The second survey was not definitive relative to a possible drop in the rock over 2YS, but it did show a sag and fracturing of the rock over 11YW (Dobecki, 1994b).

A third seismic survey was focused strictly on assessing whether the rock had dropped over 11YW and on the magnitude of drop, if present. This final survey was undertaken during the period July 6–10, 1994, after the large sinkhole had formed above 11YW. Dobecki (1994c) interpreted that the rock had dropped an estimated 45 ft in the center of the area above 11YW (Fig. 12).

The seismic interpretations did not resolve whether dissolution or piping was the principal factor in sinkhole formation. The results were inconclusive as to whether the rock had dropped over 2YS, and many investigators were skeptical of the interpreted drop of 45 ft at 11YW. The drill-hole data were analyzed 2 years later in an attempt to resolve some of the questions.

### *Drilling Results*

The drill-hole data were used to assess the rock drop only over 2YS, because an insufficient number of holes were available to evaluate 11YW. The analysis was conducted by first representing the elevation of the rock surface as it existed prior to the collapse. The surface was then interpreted for the period immediately following the collapse but before the sinkhole had formed above 2YS on April 6. The final surface represented conditions after formation of the 2YS sinkhole. Each respective surface model required selecting only well data that were appropriate for a given time frame or had a reasonable chance of not being affected to a significant extent by subsidence throughout the period of collapse and sinkhole development.

The rock surface as it existed prior to March 12, 1994, was interpreted from holes over unmined salt, over large buttress-pillar areas, and over areas that had not experienced significant subsidence at the time the holes were drilled and surveyed (Fig. 13). The resulting map represents a generalized surface that indicates that the 2YS and 11YW panels lie to the west of the axis of the deeply scoured glacial valley that is illustrated in Figure 4. The original rock surface sloped eastward and had many low irregularities, as can be seen where the drill-hole density is greatest. This gen-

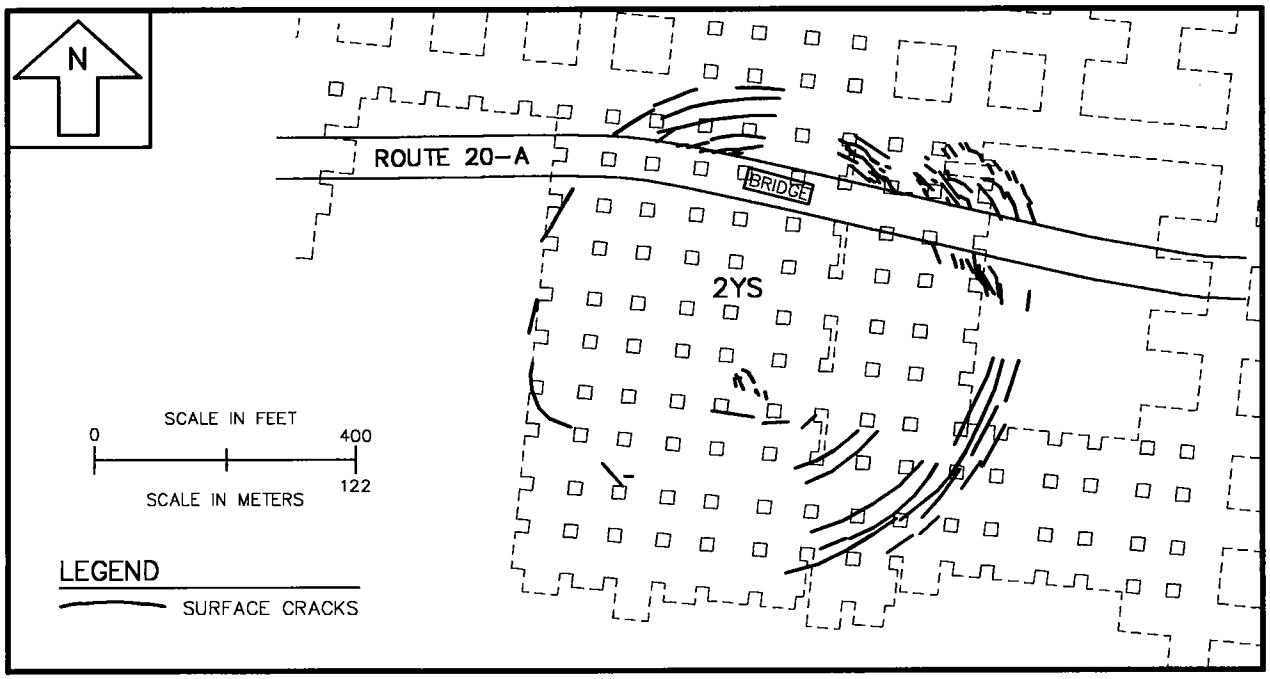


Figure 6. Map showing ground-surface cracks observed above 2YS on March 12, 1994.

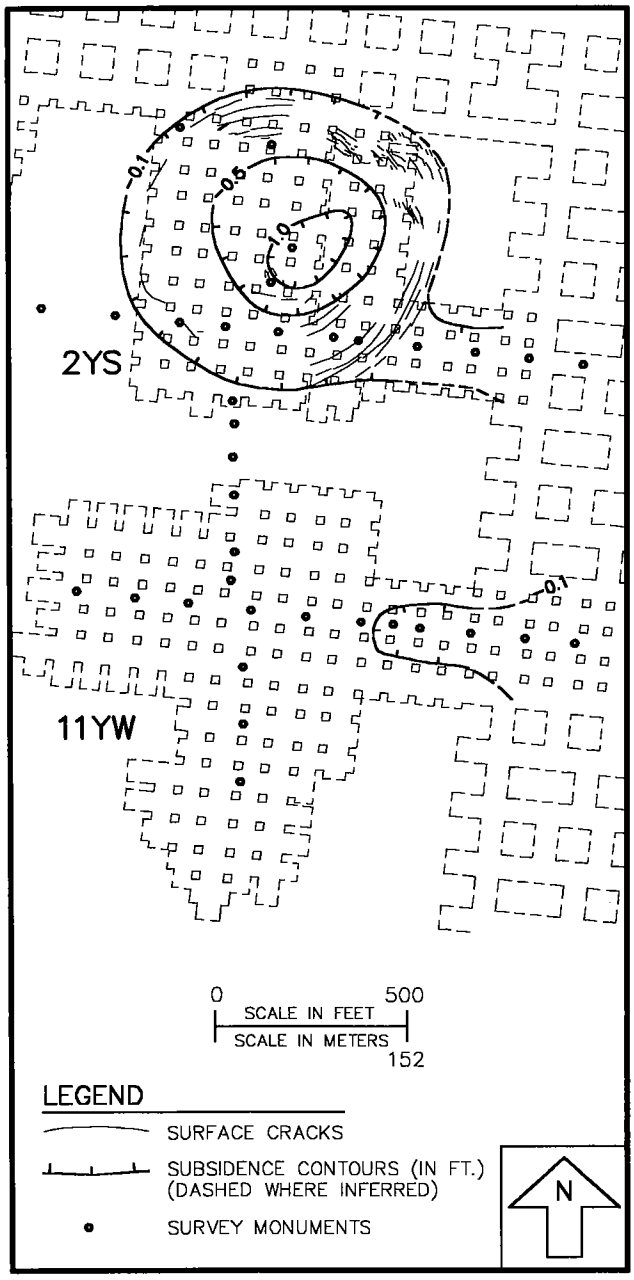


Figure 7. Map showing surface subsidence as of March 28, 1994.

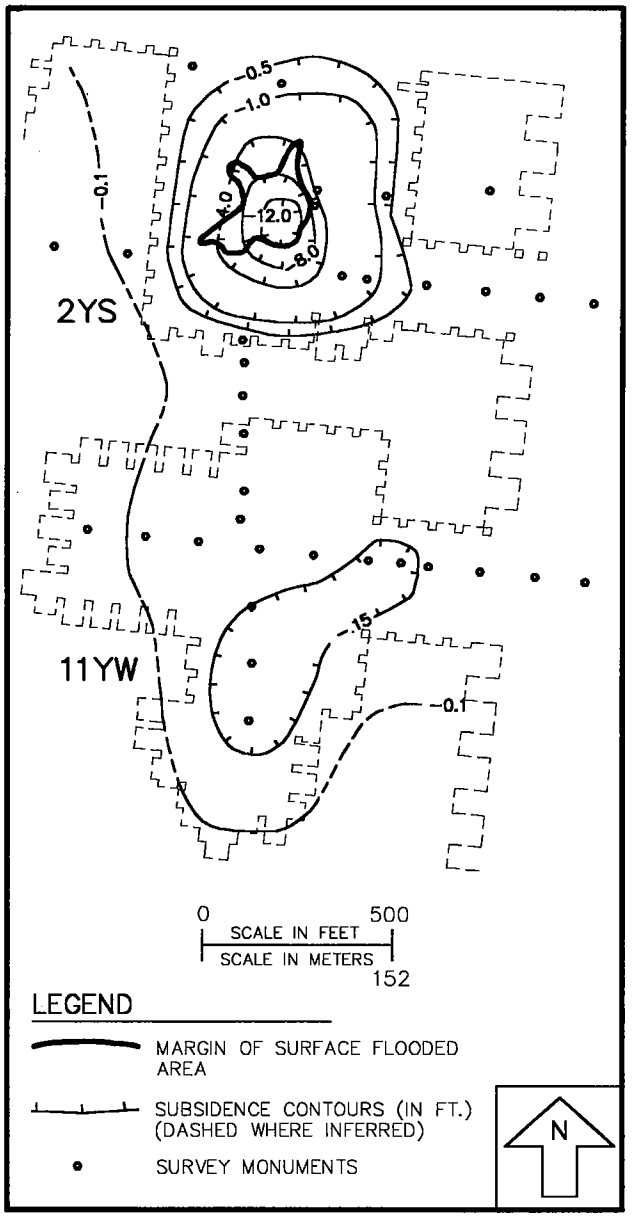


Figure 8. Map showing surface subsidence as of April 6, 1994.

eralized contour map of the original rock surface provided the datum for assessing relative changes in the surface through time.

A second contour map was drawn to represent the subsiding rock surface as it existed after the March 12 event but prior to the formation of the sinkhole over 2YS on April 6 (Fig. 14). The primary data adjustment relative to the preexisting condition was the addition of hole 9412, which was drilled near the center of the subsiding panel, and hole 9411. Hole 9411 was actually drilled after April 6, but it was in an area of minimal subsidence beyond the sinkhole.

The post-collapse contour-map surface (Fig. 14) was subtracted from the pre-collapse surface (Fig. 13) to create a subsidence-contour map for the top of rock (Fig. 15). The subsidence map suggests that the rock had dropped >8 ft before formation of the sinkhole on April 6, 1994. This apparent sag in the rock is consistent with the seismic-reflection survey and anecdotal reports from visual observation that the land surface above 2YS had dropped within the first few days after the collapse. The full extent of surface subsidence could not be documented by measurement of the subsidence markers, because the markers were not established until after the collapse on March 12.

The process was repeated for the post-sinkhole period by eliminating hole 9412 and adding holes 9413, 9415, 9416, 9418, and 9420, which were drilled after April 6 (Fig. 16). The map shows a significant depression over the eastern parts of 2YS. The exact shape

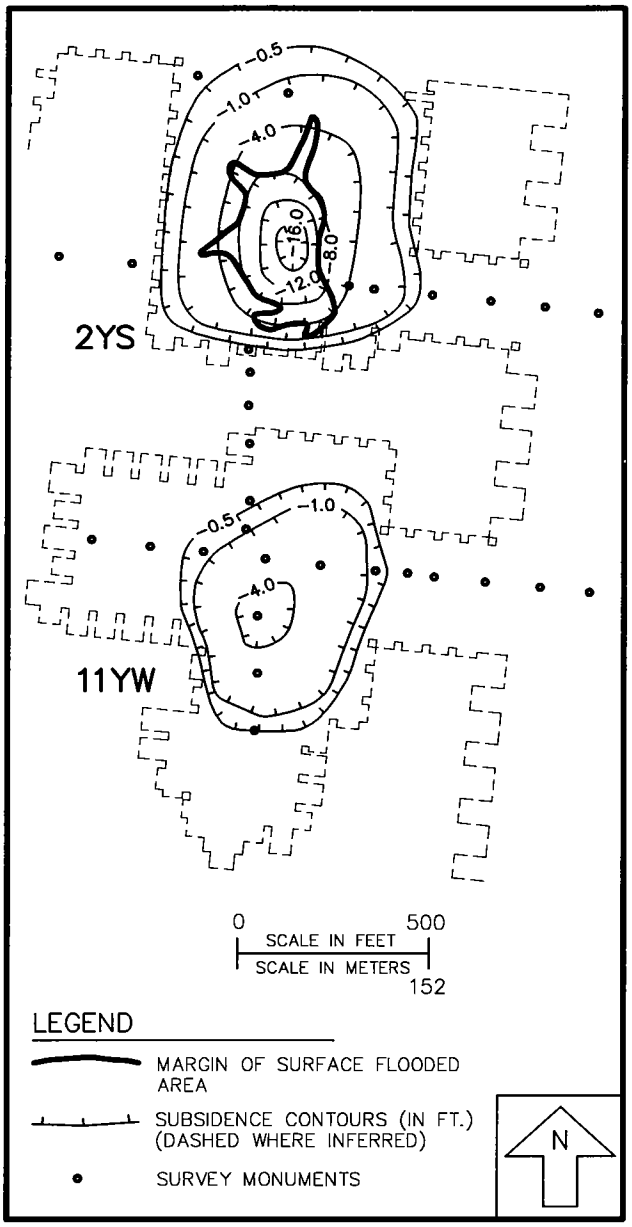


Figure 9. Map showing surface subsidence as of April 14, 1994.

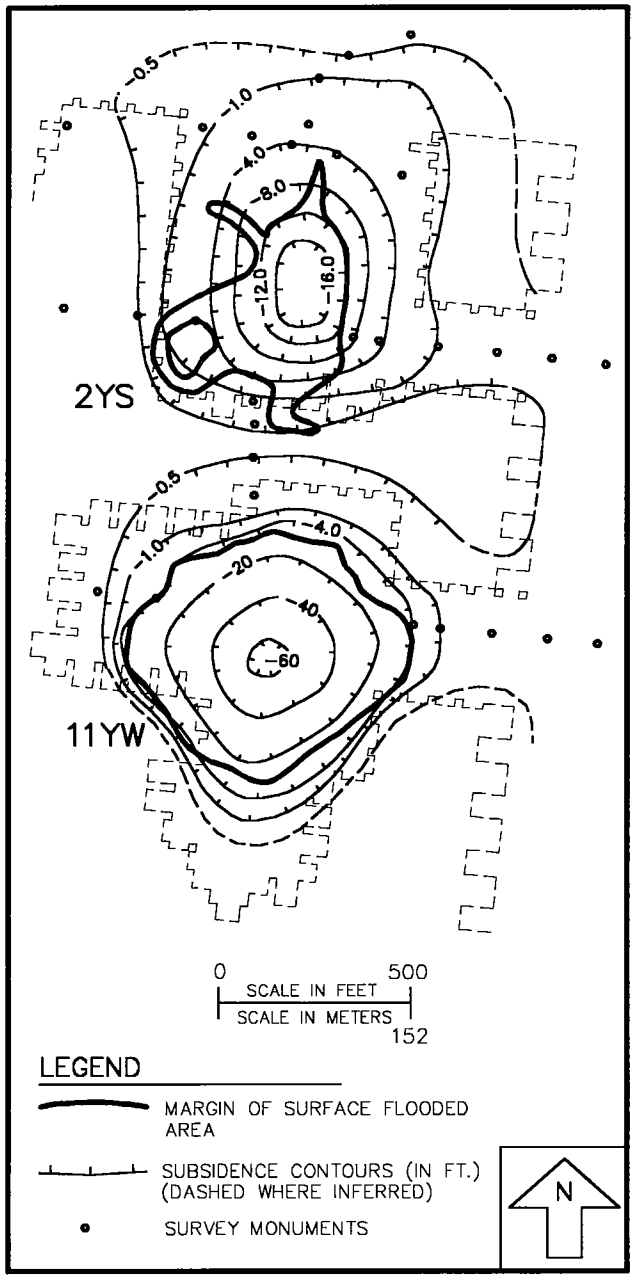


Figure 10. Map showing surface subsidence as of June 13 and 15, 1994.

and position indicated by the map are likely skewed by the loci of the data. A clearer representation of the post-sinkhole depth of rock is shown by subtracting the post-sinkhole surface from the pre-collapse surface (Fig. 17). The map shows that the rock surface had dropped >16 ft after the April 6 seismic event.

### Occurrence of Glacial Sand and Gravel in Bedrock

The existence of glacial sediments in the bedrock fractures above 11YW and above the barrier pillar between the two panels was provided by some investigators as key evidence for the piping mechanism. Nine borings (9408, 9413, 9415, 9417, 9418, 9419, 9425, 9426, and 9428) encountered glacial sand and gravel in the bedrock below the surface casing. The drilling logs for these wells were evaluated carefully to assess whether a reason other than piping could account for glacial materials being encountered well below their natural position.

The borehole logs show that the surface casings in seven of the holes (9408, 9417, 9418, 9419, 9425, 9426, and 9428) were not seated deep enough into bedrock to prevent glacial overburden from moving around the end of the casing and dropping into the hole. The most obvious evidence of poor casing seats is from the logs of 9419 and 9428, which were set 3.0 ft and 0.5 ft above rock, respectively. Four of the seven holes (9408, 9417, 9425, and 9426) were set a foot or less into the top of rock. The geologic logs for these four holes all describe the top of rock as being fractured and highly incompe-

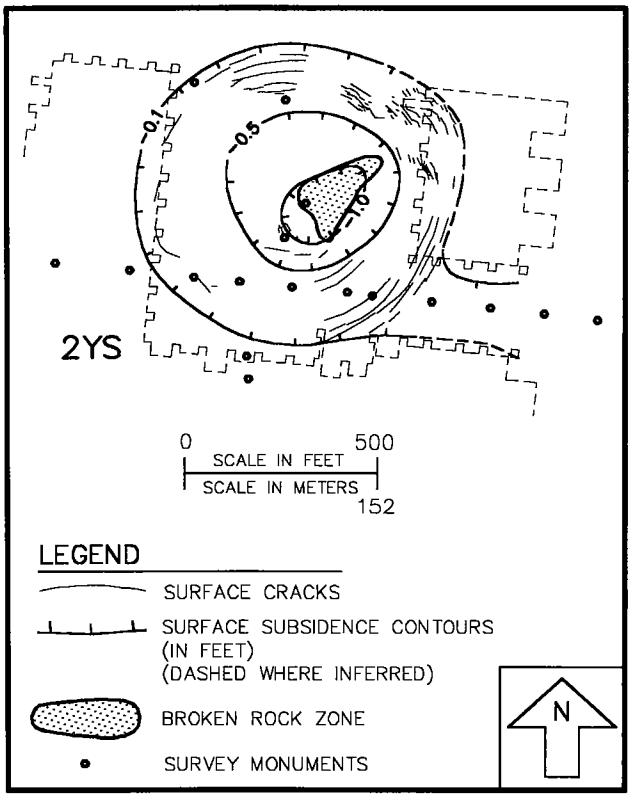


Figure 11. Map showing zone of broken rock from seismic-reflection data collected (March 22 and 23, 1994) and interpreted by Dobecki (1994a).

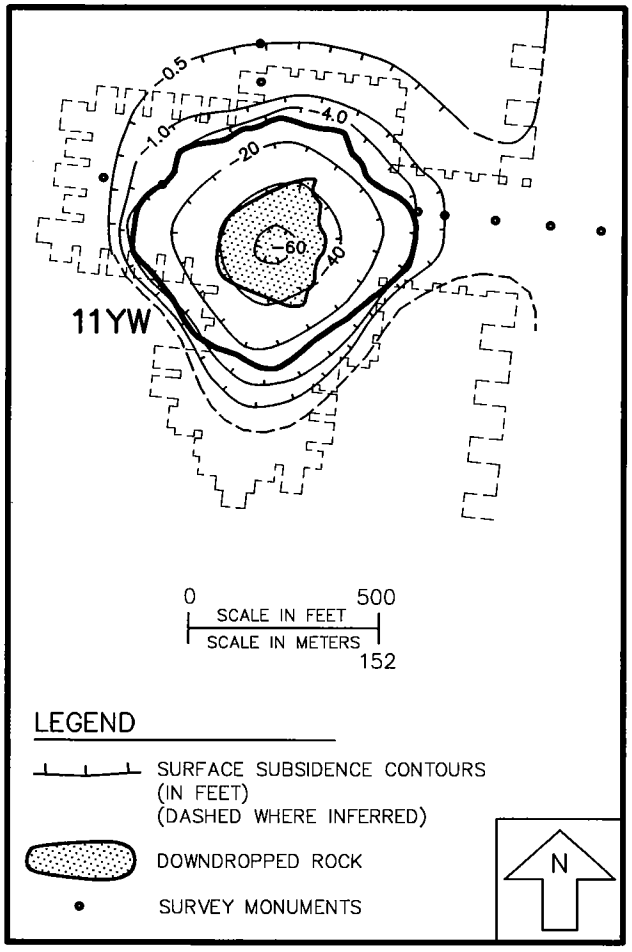


Figure 12. Map showing area of downdropped rock from seismic-reflection data collected (July 6–10, 1994) and interpreted by Dobecki (1994c).

tent. These broken zones may well have been cobble/boulder zones within glacial till rather than rock. Hole 9418 was set 2.7 ft into rock, but the borehole log notes that sand and gravel were entering the bore from around the casing.

Only two of the nine rock holes that encountered glacial sediments in the rock received those sediments from sources other than improper casing seals. Holes 9413 and 9415 may have encountered gravel that was introduced to the rock through a natural or a mine-collapse-related process. Borehole 9413 was an angle hole drilled 23° from vertical, with casing set 10.0 ft into rock. No glacial sand or gravel or LCM (lost-circulation material introduced while drilling the glacial overburden) was detected in the rock below the surface casing until the base of the Syracuse Formation was reached, where numerous pieces of sand and gravel were encountered. This hole was extended well out into the 2YS collapse and was drilled after the sinkhole formed at the surface. It is very likely that the glacial sediments dropped vertically into the broken rock when the sinkhole formed.

Borehole 9415 was drilled above 2YS at the edge of the sinkhole after the sinkhole had formed. The casing was set 173 ft into rock. The description of the cuttings suggests that glacial sediments were encountered throughout the hole and specifically mentions glacial gravel and a pebble wedged in the bit at the final drilling depth of 776 ft. It is likely that these sediments dropped vertically as the glacial valley fill slumped into the broken-rock zone when the rock fell.

## Geotechnical and Hydrogeologic Conditions

Two important requirements were necessary to facilitate the formation of the observed sinkholes by the piping mechanism. First, most of the water inflow had to enter the rock from the glacial overburden directly above the collapse. Second, the glacial overburden had to have sufficient cohesive strength to sustain voids that would periodically collapse. These requirements were necessary for the sediment to be piped, and for the resultant episodic development of the sinkhole directly above the collapsed panels. The data necessary to address these conditions were collected from a series of wells drilled to investigate the geologic, geotechnical, and hydrologic characteristics of the overburden and the top few feet of the underlying rock.

Hole 9446, which was drilled west of the collapse (see plan view in Fig. 4), was one of the holes drilled to investigate and monitor the glacial overburden and the top of the rock (Alpha Geoscience, 1996). The hole

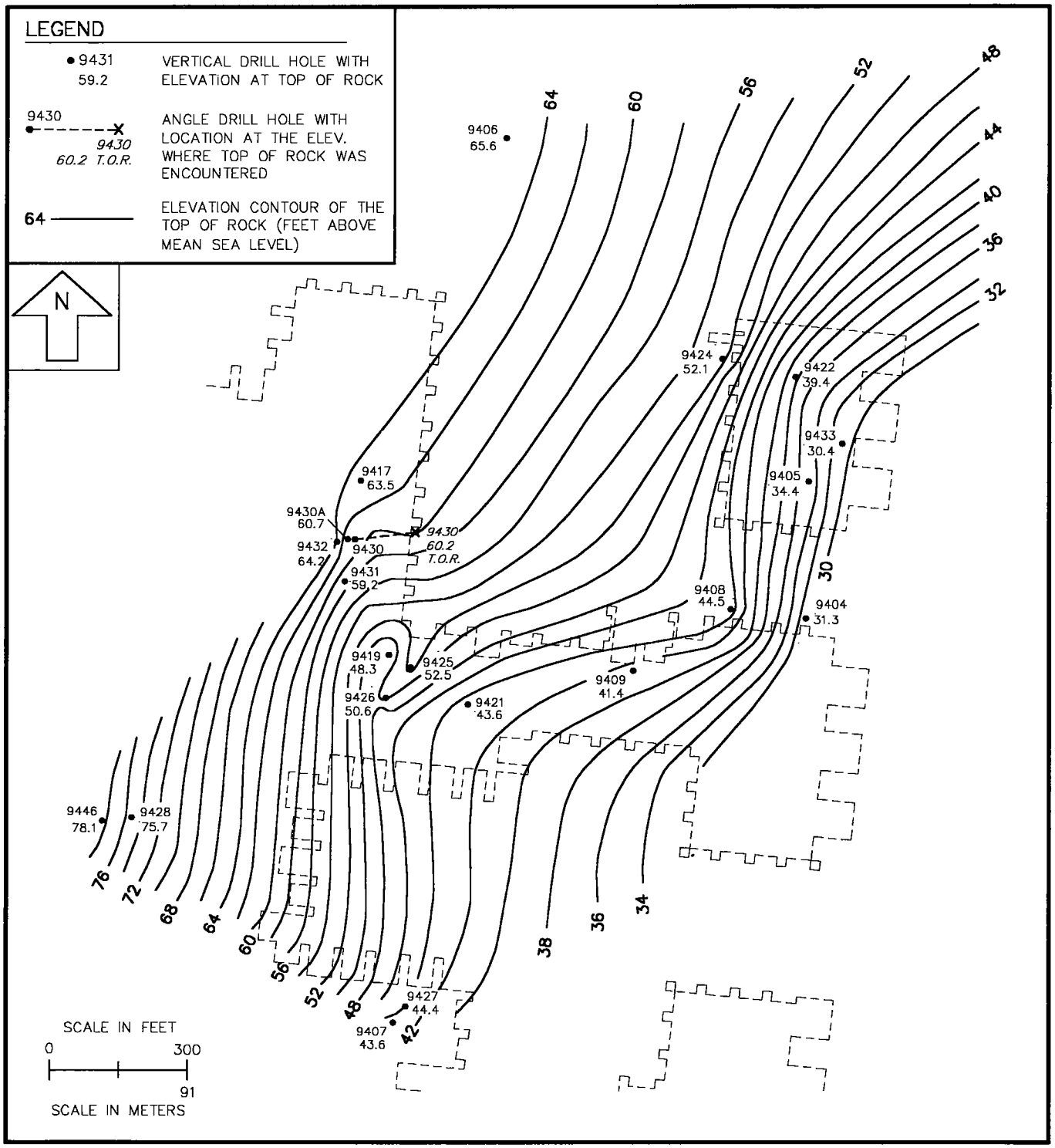


Figure 13. Map showing contours of the bedrock surface as it likely appeared prior to the collapse of 2YS on March 12, 1994.

was drilled using air and a dual rotary system that advances a large-diameter outer casing while drilling with smaller diameter inner casing. Sampling of the glacial sediments was accomplished by removing the inner drill casing and driving a split-spoon sampler or Shelby tube through the open end of the outer casing. The sampling was very difficult owing to the high content of fine-grained material and overpressured conditions throughout the glacial fill. These conditions often resulted in the heaving of glacial materials up inside the casing when the drill bit was pulled out for sampling. The lack of cohesive strength in the overpressured glacial sediments would have precluded the development of voids if glacial sediments were being removed.

Three wells were drilled at the 9446 location. One

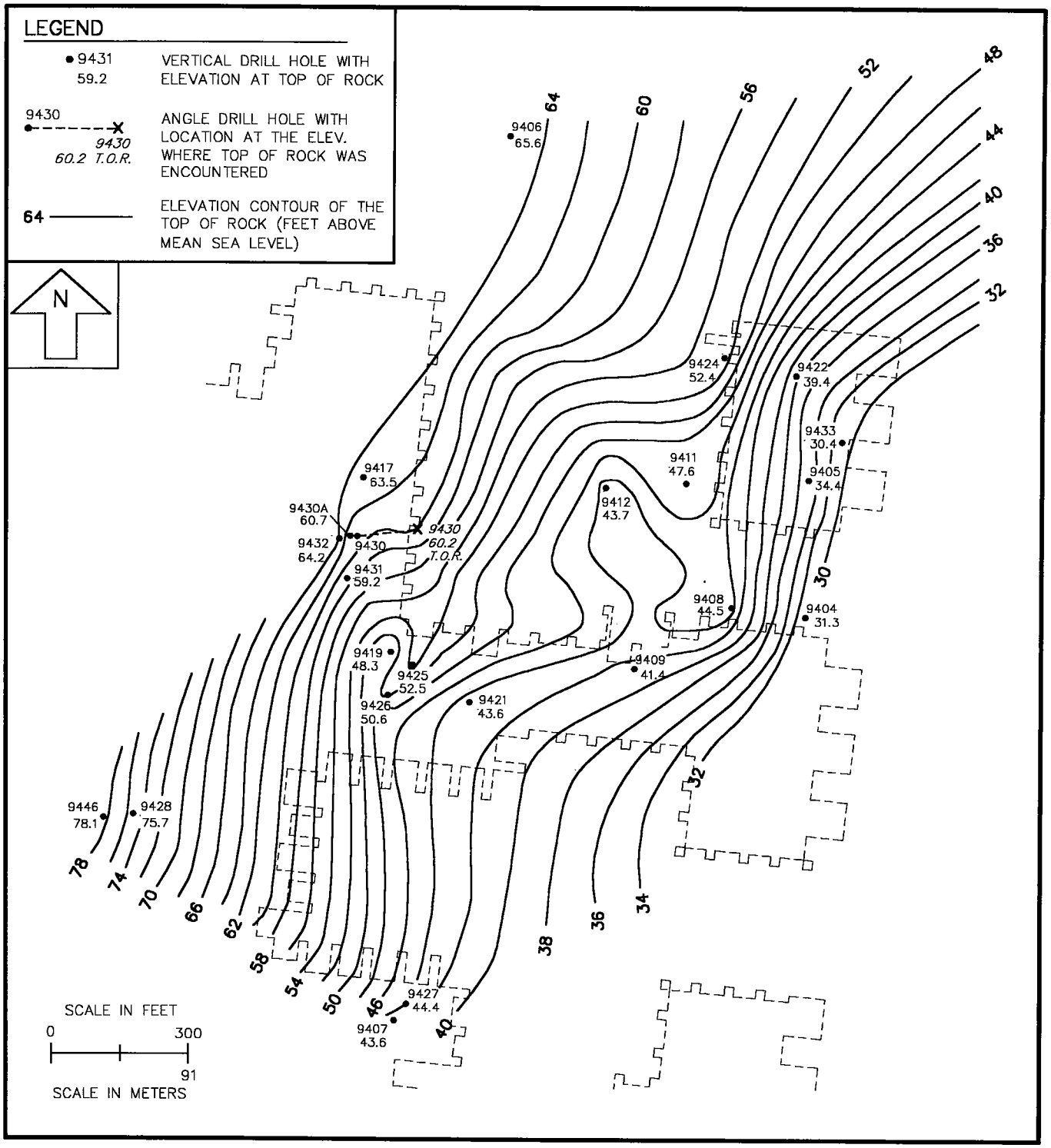


Figure 14. Map showing contours of the bedrock surface after March 12, 1994, but before sinkhole development above 2YS.

of these wells was drilled in a glaciofluvial sand and gravel directly above the bedrock surface. A second well was drilled in the glacial sediments farther up in the section. The third well was drilled within the top 10 ft of the Onondaga Formation (Alpha Geoscience, 1996). Testing of the basal sand and gravel unit indicated a moderate to low permeability, and the well yielded 10 gpm. The fractured top 10 ft of the bedrock was much more prolific. The pump yielded >90 gpm, which was the maximum capacity of the pump. The high-yielding fracture zone encountered in the top of the rock at site 9446 is consistent with other holes and test wells drilled in the Genesee River Valley (Eyermann, 1979; Alpha Geoscience, 2000).

The hydrogeologic data indicate that the more transmissive zones, at least within the collapse area,

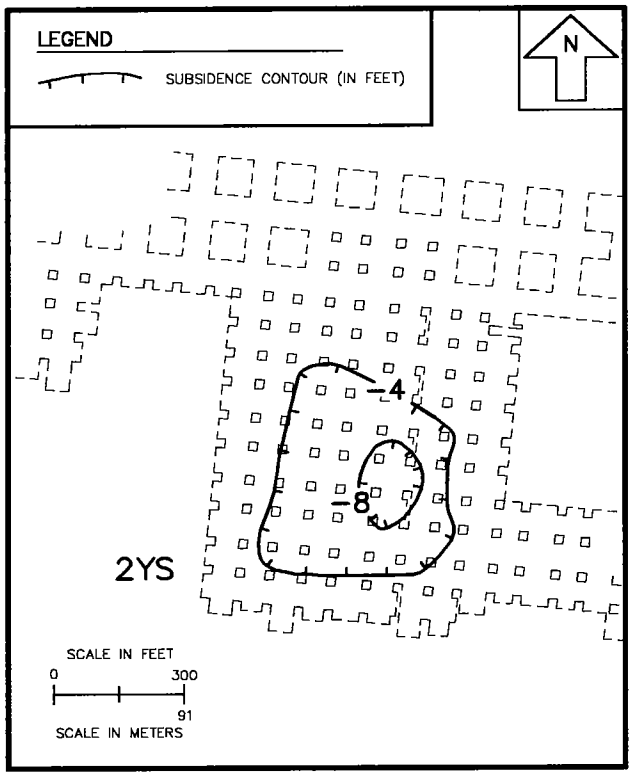


Figure 15. Map showing subsidence contours that represent the drop in the bedrock surface, interpreted from the difference between the pre-collapse surface (Fig. 13) and the post-collapse surface (Fig. 14).

were within the top of the rock. The higher permeability of the rock relative to the glacial overburden in the collapse area and beyond indicates that the water entering the mine was being transmitted through the rock from a much larger area than just the glacial sediments above the mine-level collapse. The observed hydrogeologic condition would not be favorable to the formation of sinkholes confined to the area directly above the collapsed panels.

### Thickness of Soluble Materials and Voids

The large drop of >60 ft in the 11YW sinkhole required a large volume of open space at depth to accommodate the volume of the sinkhole. This space may have been derived from the preexisting brine cavity in the D unit, the dissolution of salt, and the slaking of salt-bearing shales. An analysis was conducted of the space that could have been derived from these sources.

An estimate of the size of the preexisting brine cavity above the panels was made, based on comparison of natural gamma logs from holes 9411, 9426, and 9427 in the collapse area with that from hole 8601, which was 2,500 ft west of the collapse (Gowan and Trader, 2000). The geophysical log from 8601 has a signature that corresponds to voids that were measured while drilling through the Syracuse brine pocket in 1986 (Langill, 1987). The analysis resulted in an estimated total thickness of 5 ft for the preexisting brine cavities at the D1 and D2 levels of the Syracuse Formation.

The total salt thickness in the Vernon C shale was estimated to be 8 ft, based on an examination of rock core from core holes southeast of the collapse. The combination of this 8 ft with 20 ft of salt at mine level (12 ft from the room height and 8 ft of salt left in the roof and floor) yielded 28 ft of soluble salt. The total salt thickness of 28 ft, combined with the 5 ft of brine-filled cavities, could have resulted in 33 ft of the observed sinkhole depth.

The slaking or disaggregation of the shale intervals that do not contain obvious megascopic salt inclusions also may have been a significant factor in the creation of available space. The apparent susceptibility of the Vernon to disintegration was first reported by Miller (1909), who noted that the rock crumbles to a fine dust soon after exposure to the weather. The potential for roof slaking was also tested in the laboratory by immersing single pieces of roof shale in fresh water and also brine. Neither sample was agitated during the test. Both samples exhibited slaking and had broken down within 48 hours to particle sizes ranging from clay to gravel. An X-ray-diffraction analysis of a part of the roof sample, which did not exhibit megascopic salt inclusions, revealed that the rock is composed of anhydrite, dolomite, quartz, and halite. It is apparent that the rock contains halite in the matrix. These findings indicate that the 160 ft of Vernon C shale, between the mine level and the brine cavity in the overlying Syracuse, would have been susceptible to salt dissolution, slaking of the shale, and erosion by the ground water entering from overlying aquifers.

## DISCUSSION OF RESULTS

The data provide strong support for the dissolution mechanism of sinkhole formation. The initial 2YS collapse at mine level on March 12, 1994, apparently did not result in an immediate failure of the carbonates in the upper sections of the overlying rock; however, the rock column and overlying glacial sediments began to subside immediately after collapse. The seismic-reflection data indicate that fractures propagated to the upper sections of the rock (top of the Onondaga Formation), which was already fractured and contained a prolific aquifer.

The prolific rock aquifer at the top of the Onondaga Formation had a direct link with large quantities of ground water from scattered prolific aquifers in the glacial overburden. The fresh water in the Onondaga Formation and the glacial fill apparently had a preexisting link with the salt in the D unit of the Syracuse Formation that resulted in the development of the brine zone 160 ft above the 2YS and 11YW panels prior to mining in the valley (Gowan and others, 1999; Gowan and Trader, 2000). The collapse and 3.6-$M_{bLg}$ seismic event of March 12, and the subsequent sagging, certainly enhanced that vertical connection to the aquifer system.

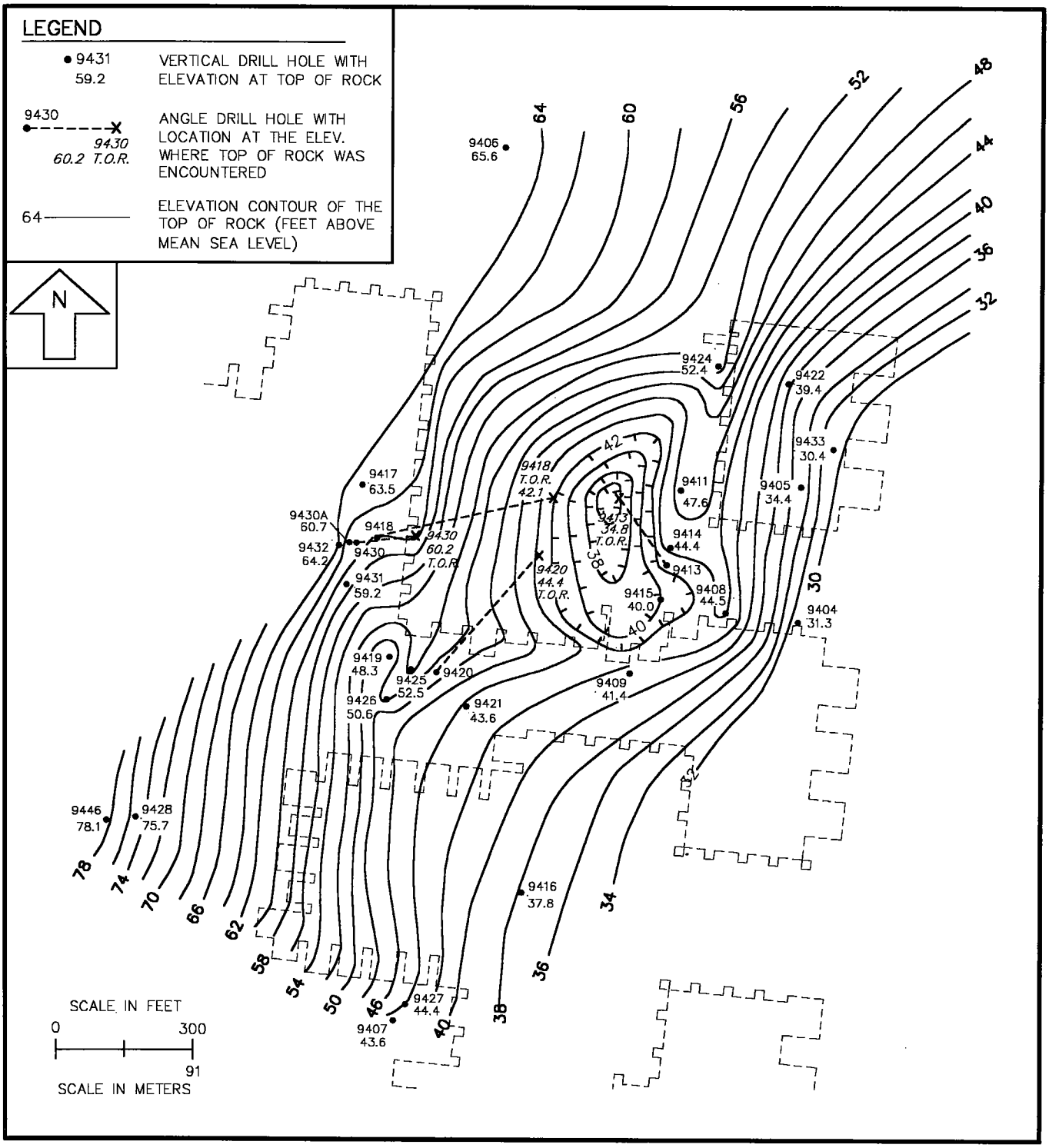


Figure 16. Contour map of the bedrock surface following formation of a sinkhole over 2YS.

The movement of fresh water down through fractures in the roof shale and into the mine created voids in the salt and shale within the Vernon Formation. Subsequent rock breakage and rock collapse into the voids created the large seismic events that correlated with visible sinkhole development, drops in the rock surface, and some of the early increases of water inflow. The overpressured glacial sediments did not have sufficient strength to maintain a void over the failing rock support; consequently, the sediments slumped with the rock. The limited cohesive strength in the glacial material also would have been reduced by the vibratory loading from the initial earthquake that produced the surface cracks above 2YS on March 12.

The evidence indicates that the sand and gravel encountered in holes 9413 and 9415 would have en-

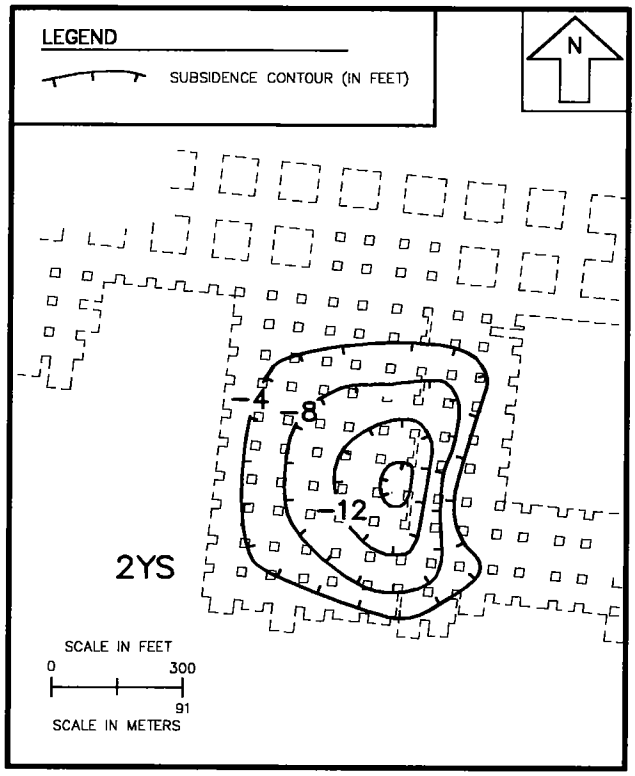


Figure 17. Map showing subsidence contours that represent the drop in the bedrock surface, interpreted from the difference between the pre-collapse surface (Fig. 13) and the post-sinkhole surface (Fig. 16).

tered the open spaces deep in the rubble zones after the glacial sediments had dropped with the collapsing rock. Coarse gravel could have entered the large open spaces created by the separation and rotation of rock blocks as they dropped to fill the underlying void. The breakage of the rock also may have allowed some piping of glacial sediments during this later stage of sinkhole development.

The dissolution model derived from the data is represented by Figure 18. This model is similar in some respects to the mechanism interpreted for the large sinkhole that developed in the Verchnekamsky Potash Basin in the Urals in July 1986 (Andreichuk and others, 2000). The Verchnekamsky example, like Retsof, was associated with pressurized brine that entered from above the mine. The inflow created large voids by dissolving overlying evaporites and eroding the disaggregated shale. These voids eventually collapsed to form a large sinkhole.

The primary differences between the Verchnekamsky and Retsof models are that the subsurface progression of the voids at Verchnekamsky followed a very irregular pathway that was not necessarily directly beneath the collapse, and the ultimate sinkhole shape was more elongate and slightly irregular. The Verchnekamsky voids and sinkhole development were guided by irregular fault planes and folded structures. The Retsof sinkholes were relatively uniform in surface expression and aligned directly above the collapsed panels. The morphology of the Retsof sinkholes was apparently a function of the mine pattern and the uniform dip and thickness of geologic units above the mine.

## SUMMARY AND CONCLUSIONS

The seismic and drill-hole data, along with the subsidence and collapse history, indicate that the dissolution mechanism was the primary process acting to create the sinkholes above 2YS and 11YW. Piping of

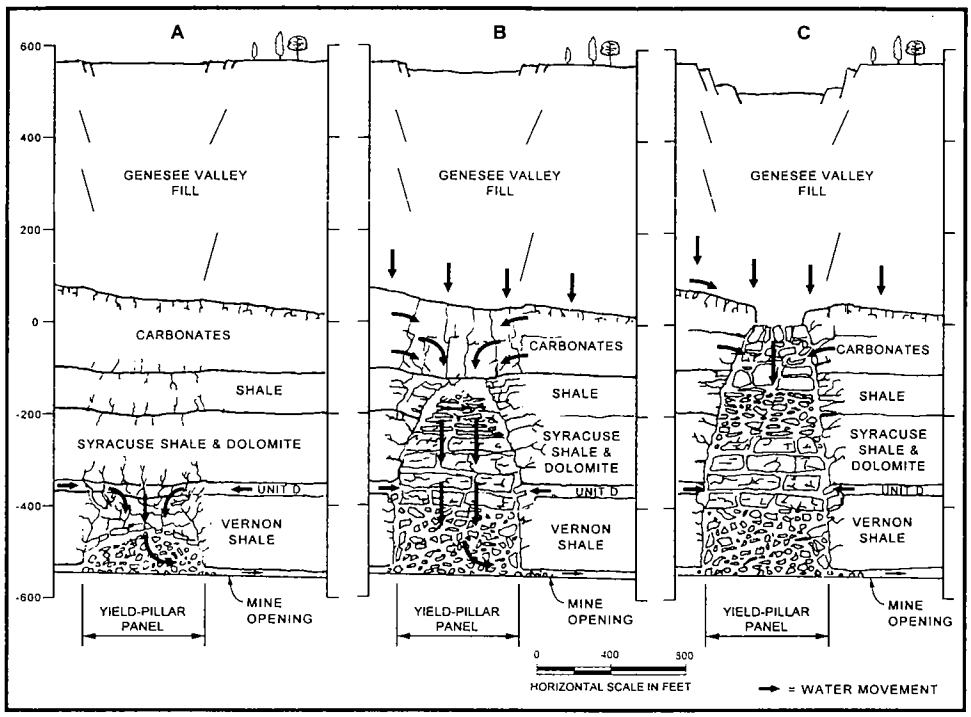


Figure 18. Cross section showing general sequence of collapse and sinkhole formation. (A) Initial collapse at mine level. (B) Progression of the rubble zone to the base of the Bertie and Onondaga carbonates. (C) Downdropping of carbonates and sinkhole formation.

glacial sediments likely occurred to a minor extent after the rock column collapsed and dropped the glacial sediments into the voids of the rubble zone. The dropping of sediments into the rubble zone would have placed them in direct contact with water coming in from the fractured Onondaga at the top of the rock. This water could have carried the dropped sediment farther down into the rubble zone and into the open fractures, where the sediments were encountered by the two properly cased holes (9413 and 9415).

The active formation of the sinkhole diminished after most of the soluble salts and shales had dissolved or were no longer in direct contact with the inflowing water. The sinkhole area stabilized when the mine was completely inundated in late 1995.

The relatively uniform sinkhole shapes, and the direct alignment above the collapsed panels, appear to be a function of geologic conditions characterized by uniform dip and thickness of the rock units. Vertical fractures above the collapsed panels allowed vertical connection to the overlying Syracuse D brine zone and the fresh water at the top of the Onondaga and in the basal valley-fill aquifers.

## ACKNOWLEDGMENTS

The authors would like to thank Akzo Nobel Salt, Inc., for the opportunity to publish the data contained in this paper. We greatly appreciate the critical review and helpful comments from Dr. William Kelly of the New York State Geological Survey and Cynthia L. Cason of Alpha Georesources in Castlerock, Colorado. We also appreciate the talent of Terry Broiles in the preparation of the figures and are grateful for William S. Neubeck's mineralogical analysis of the roof rock.

## REFERENCES CITED

Alpha Geoscience, 1996, Geologic and hydrogeologic investigation of the Genesee River Valley: Unpublished consulting report prepared by Alpha Geoscience, Albany, New York, for Akzo Nobel Salt, Inc., Retsof, New York, 31 p.

_____2000, Summary and hydrogeologic interpretations of data from Akzo cluster wells and residential wells near Fowlerville, New York: Unpublished consulting report prepared by Alpha Geoscience, Latham, New York, for Akzo Nobel Salt, Inc., and Zurich American Insurance Company, 23 p.

Andreichuk, V.; Eraso, A.; and Dominguez, M. C., 2000, A large sinkhole in the Verchnekamsky Potash Basin in the Urals: Mine Water and the Environment, Journal of International Mine Water Association, v. 19, no. 1, p. 2–18.

Ciurca, S. J., Jr.; and Hamell, R. D., 1994, Late Silurian sedimentation, sedimentary structures and paleoenvironmental settings within an Euripterid-bearing sequence [Salina and Bertie Groups], western New York State and southwestern Ontario, Canada, *in* Brett, C. E.; and Scatterday, James (eds.), Field Trip Guidebook: New York State Geological Association, 66th Annual Meeting, p. 457–488.

Dobecki, T. L., 1994a, Report, seismic survey above collapsed salt mine section, Akzo Retsof Mine, Cuylerville, New York area: Unpublished consulting report prepared by Dobecki Earth Sciences, Inc., Houston, Texas, for Akzo Nobel Salt, Inc., Retsof, New York, 14 p.

_____1994b, Report, Phase II, seismic survey above collapsed salt mine section and 11 West Panel, Akzo Retsof Mine, Cuylerville, New York area: Unpublished consulting report prepared by Dobeski Earth Sciences Inc., Houston, Texas, for Akzo Nobel Salt, Inc., Retsof, New York, 16 p.

_____1994c, Report, Phase III, seismic survey above 11 West Panel, Akzo Nobel Retsof Mine, Cuylerville, New York area: Unpublished consulting report prepared by Dobecki Earth Sciences, Inc., Houston, Texas, for Akzo Nobel Salt, Inc., Retsof, New York, 20 p.

Dunn Corporation, 1992, Hydrogeologic report for the Akzo Ash Processing Plant: Unpublished consulting report prepared by Dunn Corporation, Albany, New York, for Akzo Salt, Inc., 35 p.

Eyermann, T. J., 1979, Drilling report for well 7901, power borehole–Retsof Mine: Unpublished internal document for International Salt Company, Inc., Retsof, New York, 10 p.

Gowan, S. W.; and Trader, S. M., 2000, Mine failure associated with a pressurized brine horizon: Retsof Salt Mine, western New York: Environmental and Engineering Geoscience, v. 6, no. 1, p. 57–70.

Gowan, S. W.; Van Sambeek, L. L.; and Brekken, G. A., 1996, Anticipated conditions for the Route 20A highway and bridge reconstruction at Cuylerville, New York: Unpublished consulting report RSI-0918, prepared by RE/SPEC, Inc., Rapid City, South Dakota, and Alpha Geoscience, Albany, New York, for Akzo Nobel Salt, Inc., Retsof, New York, 36 p.

Gowan, S. W.; Van Sambeek, L. L.; and Trader, S. M., 1999, The discovery of an apparent brine pool associated with anomalous closure patterns and the eventual failure of the Retsof Salt Mine: Proceedings, Meeting of Solution Mining Research Institute, Washington, D.C., U.S.A., p. 241–272.

Kelly, W., 1999, New York State Geological Survey investigation of the March 12, 1994, seismic event in the vicinity of Cuylerville, New York: Unpublished report by New York State Geological Survey, Albany, 2 p.

Langill, R. F., 1987, Investigations of the Phoenix Dairy Company site near Cuylerville, New York: Unpublished consulting report, prepared by Richard F. Langill and Associates, Germantown, Maryland, for International Salt Co., Inc., Retsof, New York, 7 p.

Miller, W. J., 1909, Origin of color in the Vernon shale: New York State Museum Bulletin 140, University of the State of New York, Albany, p. 150–156.

Rickard, L. V., 1969, Stratigraphy of the Upper Silurian Salina Group, New York, Pennsylvania, Ohio, Ontario: Map and Chart Series 12, New York State Museum and Science Service, University of the State of New York, State Education Department, Albany, 57 p.

_____1975, Correlation of the Silurian and Devonian rocks of New York State: Map and Chart Series 24, University of the State of New York, State Education Department, Albany, 16 p.

_____1989, Stratigraphy of the subsurface Lower and Middle Devonian of New York, Pennsylvania, Ohio, and Ontario: Map and Chart Series 39, University of the State of New York, State Education Department, Albany, 59 p.

Yager, R. M.; Miller, T. S.; Kappel, W. M., 2001, Simulated effects of salt-mine collapse on ground-water flow and land subsidence in a glacial aquifer system, Livingston County, New York: U.S. Geological Survey Professional Paper 1611, 85 p.

# Development History and Subsidence Resulting from Salt Extraction at Saltville, Virginia

***Charles S. Bartlett***
Bartlett Geological Consultants
Abingdon, Virginia

**ABSTRACT.**—Saltville, Virginia—The name is obvious, but it gives only a hint of the fascinating story to be found there, extending from ~350 m.y. ago during Early Mississippian time to the present. This 2-mi$^2$ spot in southwestern Virginia's Valley and Ridge Province was once a highly saline embayment created shortly after the spread of the multiple-river-formed sandy delta (the Lower Mississippian Price Formation). Into this sabkha-like basin was deposited a mixed set of maroon and greenish-gray muds, beds of halite and gypsum, and rare layers of limestone now composing the Maccrady Formation. Much later, the region was subjected to intense compression, resulting in a series of steep folds and a southeast-dipping, low-angle thrust fault. The Saltville thrust may be the most lengthy (410 mi) and have the largest displacement (17,000 ft vertically) of any in the eastern United States. During Pleistocene time, a river traversed the Saltville Valley, drawing mastodons, mammoths, and other mammals to drink, graze, and browse. When early settlers attempted to dig wells for fresh water, they found saline brine.

By 1790, the salt deposit was being commercially developed. Ultimately, ~181 brine wells were drilled to depths of 450–2,280 ft in the valley. Additionally, between 1931 and 1963, Olin-Mathieson Chemical Corporation drilled 28 wells to depths of 1,580–3,969 ft on the bounding southern ridge and the valley slopes. The precise amount of salt production is unknown, but conservative estimates list nearly 27 million total tons extracted before operations ceased in 1972. During the Civil War, this resource provided the Confederate States with their primary source of salt.

It is estimated that the salt removal created more than 55 million cubic feet of cavities. As salt was slowly removed beneath the Saltville Valley, the plastic mudstones of the Maccrady Formation yielded to hydrostatic and lithostatic pressure, resulting in small cave-ins, undulating roads, and tilting structures with foundation and interior damage. Engineering studies estimate a maximum average subsidence of 34 ft in the developed field area. On the south-valley rim, a major collapse occurred in 1960 owing to a coalesced four-well cavern. The resulting crater is ~600 ft across and 310 ft deep.

In 1994, Virginia Gas Company began development of some of the deepest salt caverns for use in storage of natural gas. Much additional salt brine has been removed and processed by a modern evaporation plant. Once again, salt is being marketed from Saltville.

## INTRODUCTION

Saltville, Virginia, is in Smyth and Washington Counties in southwestern Virginia's Valley and Ridge Province, and ~30 mi northeast of Bristol (Fig. 1). Saltville can, probably without challenge, claim to be the most fascinating 2 square miles in Virginia, or possibly the eastern United States, owing to its geology, paleontology, history, and past industrial production. Verifying this apparently preposterous claim is quite easy but complex.

Entering the Saltville town limits, you will notice the elaborate sign "Saltville, Salt Capital of the Confederacy." Actually, utilization of the salt deposit found beneath the town began much earlier than what some locals have referred to as the "recent unpleasantness." Some believe that mammals, including extinct mammoths and mastodons, were attracted to brine springs in prehistoric times. Today, only one significant spring, Palmer Spring, flows into the town basin. An analysis by Environmental Monitoring, Inc., in 1996 found a sodium content of 6.55 ppm and a chloride content of 16 ppm; this is only slightly higher than other area springs issuing from carbonate-rock exposures. Palmer Spring exits at the outcrop trace of the Saltville Fault, where Cambrian dolomite of the Honaker Formation is thrust over the evaporite-bearing Maccrady shale of Early Mississippian age.

In Colonial times, settlers arriving in the mid-1700s

Bartlett, C. S., 2003, Development history and subsidence resulting from salt extraction at Saltville, Virginia, *in* Johnson, K. S.; and Neal, J. T. (eds.), Evaporite karst and engineering/environmental problems in the United States: Oklahoma Geological Survey Circular 109, p. 337–345.

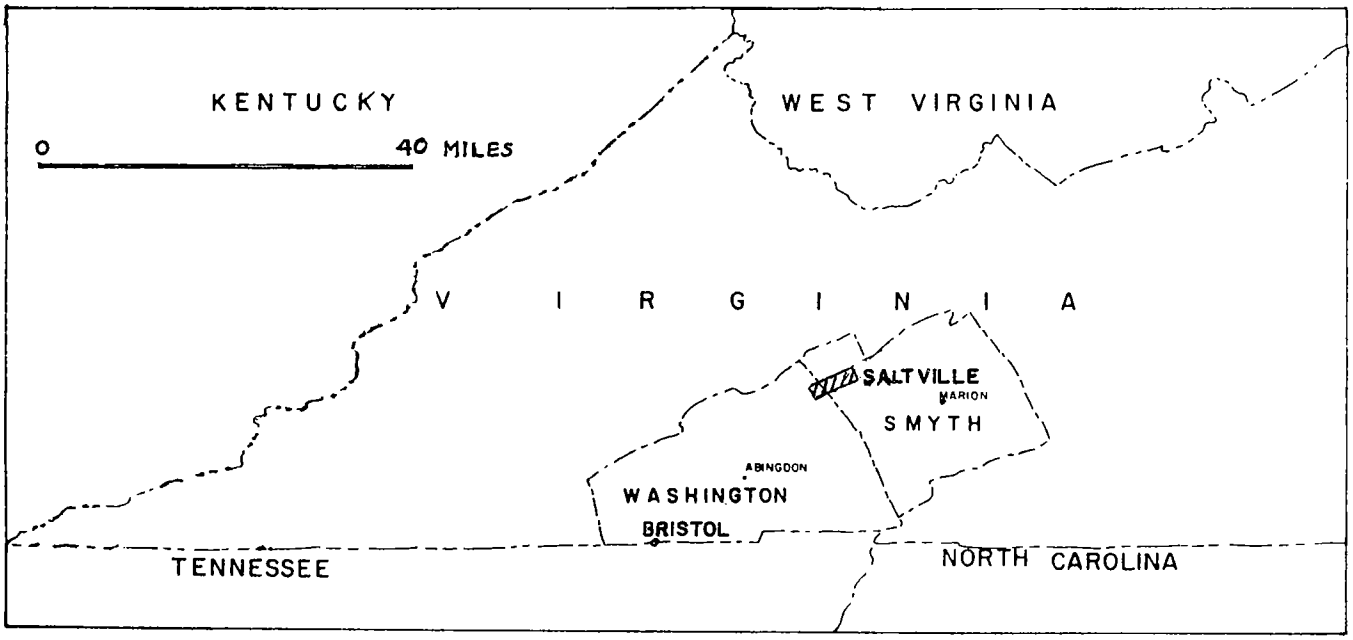


Figure 1. Location map of Saltville, Smyth and Washington Counties, Virginia (modified from Cooper, 1966).

attempted to sink hand-dug freshwater wells in the valley but discovered that water seeping in was an unpalatable brine. Thus, by 1790 the deposit was being commercially developed by pumping the natural brine and heating it to evaporate the water. During the Civil War this locality provided the primary salt source for the Southern States. Inevitably, nearly 200 years of extensive salt extraction resulted in significant subsidence throughout the Saltville Valley, and one spectacular cave-in near the northern lip of the carbonate-capped cliff on the southern uplands and near the trace of the Saltville Fault.

This paper documents the history of this mineral production and subsequent environmental effects.

## GEOLOGY

### Structure and Stratigraphy

#### *Structure*

A geologic cross section (Fig. 2) illustrates the principal structural features of the Saltville area. This is highlighted by the Saltville Fault, which may be the largest displacement thrust fault in the eastern United States. This rupture can be traced from west-central Virginia to northeastern Alabama, a distance of roughly 410 mi. Several well borings near Saltville, and as much as a mile south of the fault outcrop trace, revealed an undulating low-angle fault plane dipping to the southeast at an average of 21°. Proprietary seismic data later confirmed the interpretation shown.

At Saltville, the thrust fault has a stratigraphic displacement of ~15,000 ft, which placed the Middle Cambrian Honaker Formation against the overturned Lower Mississippian evaporite-bearing Maccrady Formation. The maximum known stratigraphic shift was mapped ~20 mi west of Saltville at the western edge of adjacent Washington County, where an approximate 17,000-ft shift places shale of the Lower Cambrian Rome Formation against steeply inclined limestone and shale of the Upper Mississippian Pennington Formation.

The lateral northwest shift of the Saltville Fault has been postulated to be on the order of >20 mi. Since this author is a native "Tar Heel" from North Carolina living in "exile" for the last 35 years in Virginia, and at a point above the Saltville thrust fault, I frequently remind my local neighbors and visitors that we still live on lands that originated in North Carolina only ~280 million years ago.

The stack of Devonian to Cambrian shales, sandstones, limestones, and dolomites composing the Saltville plate dip south-southeast at 47° to 19°, declining southward. Northwestward-directed compression created the Saltville Fault and several associated back-splays such as the smaller displacement Pulaski thrust fault, which likely joins the Saltville décollement at an unknown depth. The enormous compressional pressures created an overturned south limb of the Greendale Syncline, formed in the Mississippian limestone and shale directly north of the Saltville Fault trace. Numerous overturned slices (horses) of Mississippian, Devonian, and Silurian rocks appear erratically along the trace of the Saltville Fault wedged between the Cambrian rocks of the hanging wall and Mississippian rocks of the footwall. North of the Greendale Syncline the Paleozoic sequence is unbroken for 6 mi into adjacent Russell County and resumes a regional southerly dip of 15° to 25°.

#### *Stratigraphy*

The region bounded by the Saltville Fault on the south and the Copper Creek thrust fault 10.5 mi north

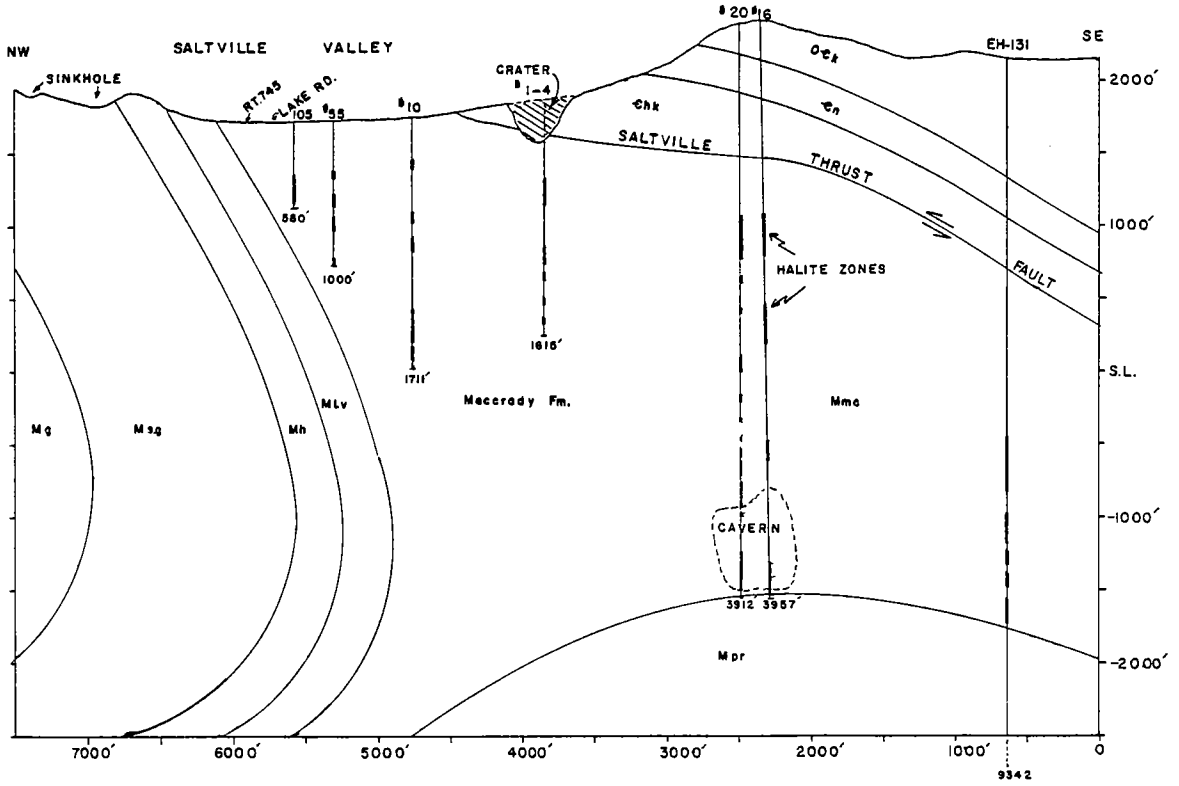


Figure 2. Northwest to southeast geologic cross section across the Saltville well fields. See Figure 3 for formation names, symbols, and location of cross section.

(in central Russell County, Virginia) contains an unbroken and nearly complete Paleozoic depositional series. In the Greendale Syncline (Fig. 3), along the northern limits of Saltville and south of the North Fork of the Holston River, the land surface is underlain by Mississippian limestone, shale, and sandstone subdivided into 10 formations capped by the partially preserved Pennington Formation. A detailed description of those units is published in Bartlett and Webb (1971).

The unit of primary concern for this report is the Maccrady Formation, which underlies the Saltville Valley and is mostly hidden by a few feet of Quaternary lacustrine clays and some recent colluvium that occurs mainly along the valley margins. The Maccrady Formation beneath the Saltville Valley is mostly overturned to the north from the compressional action prior to and after the Saltville Fault rupture. The Maccrady Formation has a known thickness of at least 3,019 ft in the 1999 Olin-Mathieson Chemical Corporation no. 16 salt-brine well (Fig. 2). This formation is folded underneath the Greendale Syncline and reappears in a narrow exposure belt near the North Fork of the Holston River, where the author measured a southward-inclined exposure of only 131 ft. This great difference in thickness in a distance of ~1.7 mi is due to the salt well having been drilled through a very steep to overturned section of Maccrady strata, and also to a combination of southward depositional thickening and tectonically caused flowage of this incompetent unit (Bartlett, 1997).

The Maccrady Formation consists of maroon and pale-green mudstones, siltstones, and minor amounts of light-gray limestone and dolomite interbeds. In the Saltville area, and extending for at least 20 mi along a northeasterly trace between Plasterco (northeast Washington County) and Locust Cove (north-central Smyth County), the Maccrady Formation also contains variable amounts of gypsum pods and stringers. Gypsum was mined from the mid-1800s until 2000 at two mines. Commercial quantities of salt are known only beneath the Saltville Valley and under the adjacent hills below the Saltville Fault.

In 1996, Virginia Gas Company drilled a deep well (EH-131) in search of porous rock for brine disposal ~3,500 ft south of the Saltville Fault. This well crossed the fault at a depth of ~1,300 ft (Fig. 2) and penetrated ~2,600 ft of mudstone, halite, and anhydrite of the Maccrady Formation. The well drilled an interval from 2,540 to 2,972 ft (432 ft net) of nearly pure halite. In Washington County, ~3 mi west of the EH-131 well, Westinghouse Electric Corporation drilled the No. 1 Morton Salt Company wildcat well in 1976, which encountered the Saltville Fault at 2,000 ft. The well penetrated 2,100 ft of the Maccrady Formation, composed of mostly light-gray and maroon mudstone and interbedded anhydrite, some limestone, and a predominantly halite-bearing interval from 3,350 to 3,430 ft.

The hills and ridges in the area south of the Saltville Fault are underlain by generally more competent Cambrian and Ordovician limestone, dolomite, and

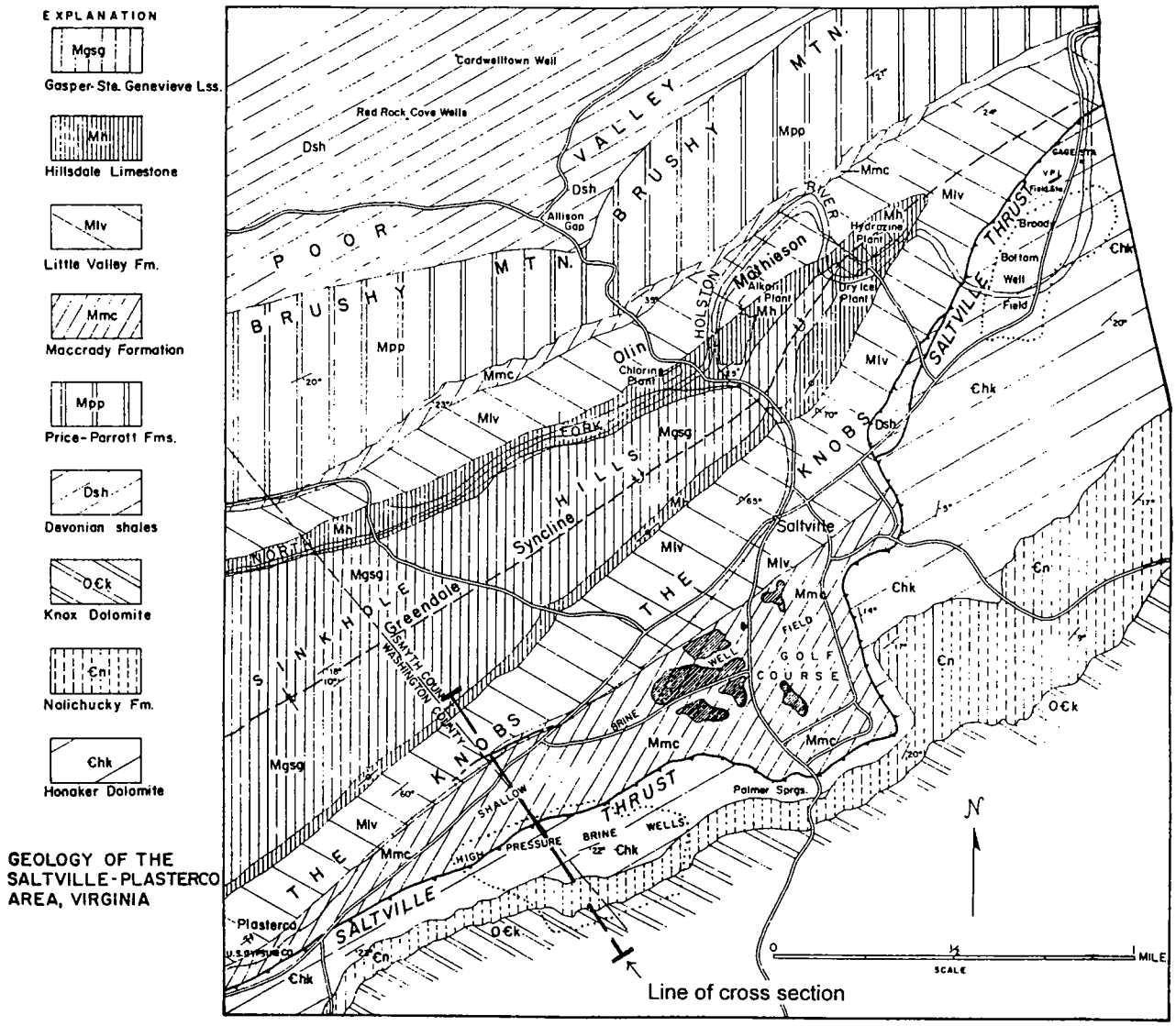


Figure 3. Geologic map of Saltville, Virginia, and environs (from Cooper, 1966, fig. 1). Cross section shown in Figure 2.

compact shale. Directly bordering the fault is a belt of highly fractured and partially silicified dolomite of the Honaker Formation, with a thickness of 450–500 ft. In western Washington County I measured 1,140 ft of the Honaker Formation, consisting of chert-bearing dolomite, above the fault (Bartlett and Webb, 1971, p. 81). This does not imply a thickening of the unit but shows that the fault plane cuts into higher parts of this formation at Saltville.

## SALT-MINING HISTORY

Saltville's natural resources were used by wild animals and Indians before settlers came to the area in the late 17th century. Evidence of Indian occupation, dating back at least 12,000 years, has been found in this valley and adjacent river terraces and caves. McDonald (2000) presented additional evidence of probable pre-Clovis, tool-using Native Americans dating to 14,510 years B.P.

Pleistocene stream gravels and lake deposits (Bartlett, 1979, 1981) containing remains of extinct mastodon, mammoth, musk ox (McDonald and Bartlett, 1983), ground sloth, turtle, fish, shellfish, and plant remains are found beneath much of the Saltville Valley. Arthur Campbell, in a 1782 letter to Thomas Jefferson, reported "bones of an uncommon size of which the jaw tooth now offered you is one" (Boyd, 1952). This is the earliest known mention of fossils from Saltville. The tooth probably belonged to a mastodon (Jefferson, 1787). Excavation-recovery reports by Peterson (1917), Virginia Polytechnical Institute/Smithsonian Institution (Ray and others, 1967), Bartlett (1979, 1981), McDonald and Bartlett (1983), and McDonald (2000) have added to the faunal and floral listing of this site. Excavation tests conducted each summer have led to the institution and development of the Museum of the Middle Appalachians in Saltville, which displays and stores many of these recovered remains.

Early settlers dug wells in a search for potable water and were surprised to find instead quantities of salt brine. Upon finding the unanticipated brine, the salt was recovered by natural evaporation or by boiling off the water in small iron pots (Stose, 1913). A patent covering 330 acres of the valley was issued to Charles Campbell in 1753. Thomas Jefferson made reference to the occurrence of salt brines at Saltville (Jefferson, 1787), and the first brine well was in production by 1750 (Lonn, 1965).

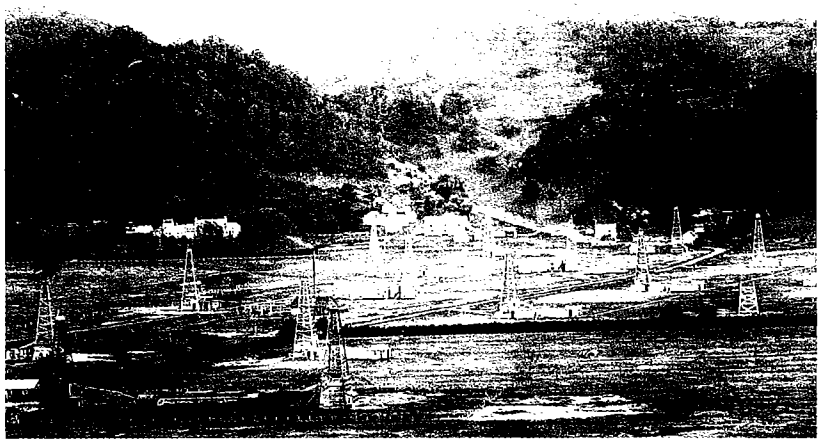

Figure 4. View to the south, showing the Saltville Valley and the salt wells in the southeastern part of the "low-pressure" field drilled ~1901 to 1904. The "high-pressure" wells were drilled after 1931 on the high ridge to the south. The Saltville Fault trace is mapped about halfway up on this ridge. Photo courtesy of the Museum of the Middle Appalachians, from the Totten collection.

In 1840, a shaft was drilled to intercept the "brine stream"; however, at a depth of 210 ft, rock salt was encountered (Watson, 1907). The boring continued deeper through at least 166 ft of halite. The Reverend Steven Taylor of Abingdon, Virginia, described this discovery in 1841, noting that gypsum occurred at a depth of 30 ft and that the rock salt also contained interbeds of "slate and blue clay." This was the first discovery of a bed of rock salt drilled in the then-established states of the United States, although some bedded salt outcrops were previously known from western areas that later became states (Cox and Edgerton, 1968).

Commercial production, by brine-extraction methods, began in the late 1700s, according to Withington (1965). Saltville Valley marshes were drained in the early 1800s by cutting channels to the North Fork of the Holston River to permit expansion of this early extraction area of the valley. The valley well field was later designated the "low-pressure" and relatively shallow part of the field (Figs. 3, 4) as distinct from the much deeper "high-pressure" wells later drilled on the southern highlands, mainly on the overthrust sheet above the Saltville thrust fault (Fig. 3).

By 1842, annual salt production from six wells in the "low-pressure" field reached 200,000 bushels (~14,412 short tons). During the Civil War, this deposit was the principal source of salt for the Confederate States, and production soared to 10,000 bushels (721 tons) per day (Eckel, 1902). Owing to a lack of refrigeration at that time, per capita salt consumption, primarily utilized for meat preservation, was estimated at 100 pounds per year (Dietrich, 1970). Ultimately, many of the Southern States set up their own brine-extraction sheds at Saltville, hauling in wagons loaded with wood to fire the simple furnaces.

The Confederacy recognized the strategic importance of this deposit and stationed as many as 4,000 troops at Saltville. Union forces made cavalry probes in 1863, which were repulsed. On October 2, 1864, the Saltville defenders soundly defeated a Union force of about 5,000 soldiers led by Brigadier General Stephen G. Burbridge. This only delayed the inevitable, for on December 21, 1864, a Union army under Major General George Stoneman overran the by-then-undermanned Confederate defenses and proceeded to demolish the furnaces, burn the storage buildings, and dump debris into the wells before moving on to other regional targets. With frantic effort the wells were quickly cleared, and production was resumed at a reduced level (Rachal, 1953). (Note: A well pump and reconstructed furnace is displayed at a small park near the western edge of Saltville [Figs. 5, 6].)

In 1907, Watson reported brine recovery from 24 producing wells with a maximum depth of 2,280 ft. Records and well-field maps note 13 salt wells drilled from 1812 to 1889, and 147 more from 1894 to 1930. Of the early wells drilled from 1812 to 1889, four were hand dug to depths of 200–270 ft; they were mostly ~10 ft square and timbered. In well 8, which was taken

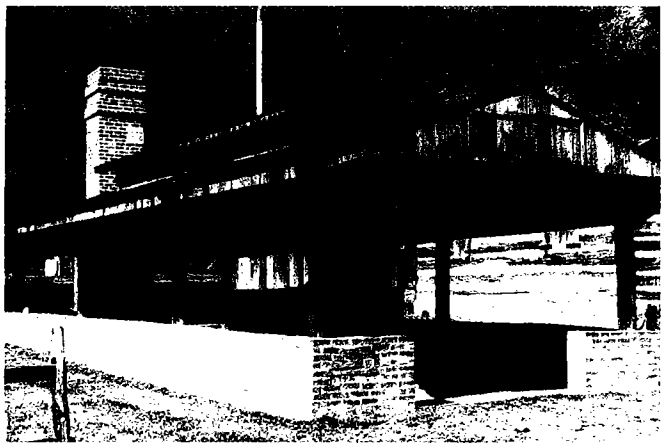

Figure 5. Reconstructed salt furnace at the salt park near the Smyth–Washington county line, containing several large original iron kettles on a long wood-fired chamber. Photo supplied by Robert C. Whisonant, retired Radford University geology professor.

to 270 ft, the bottom 55 ft was drilled in salt rock. It was also recorded that "3 negroes drowned in this well" (Low, 1894). These wells were all drilled in a small 400-ft-wide area astride the Washington–Smyth county line. For unknown reasons, a deep tunnel connected wells 8 and 9. Nine of these early wells were drilled with 4–6-in.-diameter pipe.

The Mathieson Alkali Works began production in July 1895 and drilled most of the low-pressure, shallow wells. They next drilled 28 high-pressure, deep wells from 1931 to 1963. These wells ranged from 1,580 to 3,957 ft in depth. Mathieson merged with Olin Industries in 1954 and produced brine until 1972 for the manufacture of soda ash, chlorine, and hydrozine rocket fuel. Production ceased in 1972 owing to changing economics and state and federal regulations related to mercury leakage from the chlorine plant and residue-storage ponds adjacent to the north bank of the North Fork of the Holston River. Elevated mercury levels were discovered in fish and shellfish. The complex of industry facilities was closed, and hundreds of employees were phased out, plunging the town into severe economic disruption from which it is still recovering.

## SALT EXTRACTION AND RESERVES

### Production

Studies by Fenix and Scisson (1972a) tabulated 13,384,150 tons of salt extracted from 1900 to 1972, with no record for 31 wells, and incomplete records for another 150 wells in the valley "low-pressure" brine field (Craig, 1973). This extraction was conservatively calculated to have created 277,050,000 $ft^3$ of cavities, beneath an area of ~177 acres (Fig. 3). For the "high-pressure" brine wells, more complete records list extraction from these 28 wells at a nearly identical 13,384,160 tons of salt, creating 279,620,000 $ft^3$ of cavities, with a surface area of ~209 acres (Fig. 3).

### Reserves

The true vertical and lateral distribution of the salt-bearing area is poorly defined. According to Craig (1973), the well descriptions in the "low-pressure" field document a salt thickness up to 1,000 ft in the southeastern sector. In the "high-pressure" field, log data reveal total salt thickness varying from 170 to 1,020 ft. Nevertheless, Craig (1973) presents a conservative estimate of the salt reserves of 8 billion cubic feet. Thus, in >150 years of salt production, only about 7% of the reserves have been extracted.

## SUBSIDENCE REVIEW

### "Low-Pressure" Field

The Saltville Valley was the location for about 181 "low- pressure" wells, meaning relatively shallow wells that could be pumped of natural brine, or after salt solution following injection of water. The author has examined drillers' logs for 150 of these wells, which range from 450 to 2,280 ft deep and average 840 ft deep. Only seven of these brine wells exceed a depth of 1,250 ft. Thirteen wells are recorded as having been "bored" or "dug" between 1812 and 1894. Records for these wells are brief. The other 168 wells are listed on a 1936 map prepared by Olin-Mathieson Chemical Corporation for the wells drilled from 1884 to 1933.

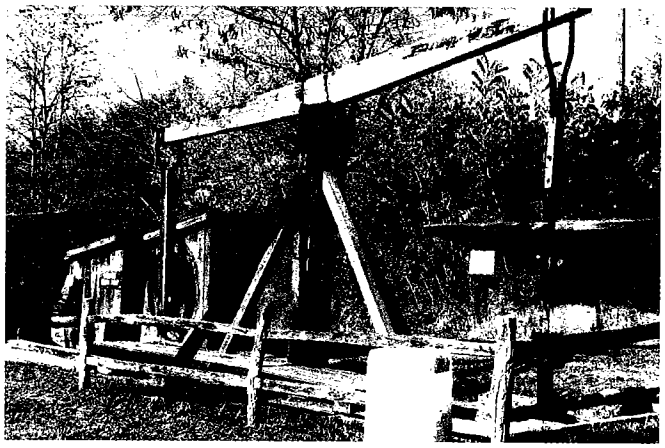

Figure 6. Walking-beam-style brine pump at the salt park. Photo courtesy of Robert C. Whisonant.

The drillers' logs range from very incomplete to quite detailed. Logs for 143 of the wells provide details about the salt and salt–mudstone mixed intervals in the Maccrady Formation. Commonly, the upper few hundred feet of "red" and "gray" mudstones contain a small amount of "gypsum" inclusions before penetrating the halite-rich middle and lower Maccrady beds. Some of the better logs show the percentage of salt by intervals, and some describe salt of white or red hues. The total thickness of salt-bearing beds noted varies from 15 to 617 ft, which is partly related to well depth and to the part of the Maccrady Formation that was penetrated; the latter is related to where the well was drilled in the Saltville Valley and to the steep dip of the Maccrady. The average thickness of saline rock tallied in these well records is 186 ft. There is a high variability in the thickness of the high-purity salt intervals even between adjacent wells. This fact supports a tectonic-related flow of the salt, creating thick pods and localized thinning.

The well records also reveal a strong variability in the depth to the first salt, which ranges from 192 to 820 ft and averages 350 ft below the surface. The deepest salt occurs along the northern part of the valley close to the outcrop of the Mississippian Little Valley Formation, and thus the area underlain by the upper part of the Maccrady Formation. Here, the first salt was found at a depth of 400–800 ft. Southward, the salt is reached at mostly shallower depths.

During the more than 160 years of salt extraction, there has been a consequent, mostly slow subsidence of the valley land surface. Forty-three of the drillers' logs note caving while drilling, or ground settlement following a period of production. A cave-in occurred in well 104, which required 821 tons of fill rock to correct. Most wells required workovers for repair of bro-

ken or bent casing caused by shifting ground as salt was extracted. Sixty-eight well records that list an abandonment date show individual well production ranging from <1 year to a maximum of 34 years. The average productive life of a well was only 8.5 years.

One of the early accounts of ground collapse was published in a report by O. A. Peterson (1917), a paleontologist with the Carnegie Museum in Philadelphia. Apparently, there had been a cave-in around well 69 near the Norfolk and Western Rail Line on the northern limits of the field development. This well was drilled in 1915 to a depth of 867 ft and encountered 440 ft of salt-bearing beds, beginning at a depth of 325 ft. The cave-in opened a pit >8 ft in depth that exposed a bone-bearing layer of coarse gravel, "indicating the conditions usually found in the beds of streams" (Peterson, 1917, p. 471). Mastodon, ground sloth, moose, elk, and horse bones, and shells of freshwater mollusks, were recovered. This gravel deposit is present beneath much of the Saltville Valley, where no river now exists owing to multiple stream piracy that dates to the late Pleistocene (Stocking and others, 1979). This ancient river is now referred to as the *Saltville River*.

Precise data that define the general subsidence of the well field are apparently unknown owing to a lack of surveyed monuments for reference points. However, Craig (1973, p. 22–24), utilizing engineering figures generated by Fenix and Scisson, estimated an ultimate maximum subsidence of 34 ft. The Olin Corporation apparently monitored the field between 1929 and 1953. Their records indicated an annual subsidence rate of 3.9 in. per year. Furthermore, an extrapolation back to 1900 indicates that 23 ft of subsidence developed from 1900 to 1972.

Salt extraction was at a decreased rate from 1953 to the cessation of operations in 1972. Craig (1973, p. 23) records examples of subsidence-related structural damage to company buildings, the old Union Church, and an old hotel on Main Street (State Route 91). Local citizens claim that Route 91, in a section in the western part of Saltville known as Smoky Row, was once a gentle, uniform grade. Now, that part of the road undulates in a manner similar to a subdued roller coaster.

In November 2000 I was asked to inspect a few of the houses and properties on Smoky Row. These were mainly simple, inexpensive dwellings that had been built by the salt companies for their employees. My brief inspection noted significant foundation cracks. Most of the claimed ground effects proved to be settling of fill over an abandoned septic tank and root decay where large trees had been cut down. One linear earth crack, however, beside a cinderblock garage had recently been filled with soil. I was able to easily push a 5-ft-long auger to its full length without encountering substantial resistance. I concluded that this was a crack probably related to lingering earth adjustments near several brine wells ~300 ft north of these houses or, less likely, from the northernmost high-pressure wells on the north slope of the ridge to the south of these houses.

Another example of subsidence-related damage is associated with the historic Stuart house, constructed in the mid-1950s (Worsham, 2001) and occupied by William A. Stuart, one of the founding owners of the Holston Salt and Plaster Company. In 1993, I examined the house for evidence of subsidence damage. The structure is within 300 ft of three valley wells on the north and within 400 ft of two salt caverns created by the high-pressure wells to the south. The building suffers from some architectural deficiencies but has an easily noted tilt to the north. For example, a ball placed on the south edge of the dining room floor will readily and independently roll across to the north wall.

The owner of the Hartwood Building Supply store, on the north side of the valley, measured a 16-in., southward tilt of the 60-ft north–south length of the building. About 12 shallow, "low-pressure" brine wells were drilled within 400–600 ft south and west of his store.

The best defined subsidence evidence I have viewed was near the southwest corner of the Saltville Golf Course. During an examination in 1973 of landslip on the slope south of the golf course, I observed a well pipe protruding >10 ft near a tee box. Recently, Charles Norris (now retired from the position of property manager with Olin-Mathieson Chemical Corporation) stated that the top of this pipe for well 28 was 14 ft above ground level before it was cut off.

As salt was slowly extracted from the Saltville Valley, the remaining plastic mudstones of the Maccrady Formation yielded to hydrostatic and lithostatic pressure. The result has been a fairly uniform, slow subsidence. This effect has not only been in the proximity of the wells but has also reached out differentially owing to the unknown area of salt removal from each well. Even if this were accurately known, the potential area of subsidence effect is not only above the salt extraction area but may also extend outward for as much as a few hundred feet owing to the tendency of the rock layers to sag toward the cavity at angles of draw of 10° or more. This effect would be expected to be more pronounced in the soft, semi-plastic mudstones of the Maccrady Formation.

## "High-Pressure" Field

Finally, we focus on the interesting conditions in the part of the brine field that was last developed on the elevated terrain to the south of the Saltville Valley. From 1931 to 1963, Olin-Mathieson drilled 28 wells that ranged in depth from 1,580 to 3,969 ft. Eleven of these wells were drilled on the north-facing slope of this rugged terrain very near or north of the Saltville Fault trace. The remaining 17 wells were drilled higher on this north slope at 400–2,050 ft south of the fault. This part of the field was produced by pumping fresh water into the salt beds and then pumping the saline water up to the surface; hence, this area was designated the "high-pressure" field.

Salt-bearing intervals ranged from 496 to 1,603 ft thick in the 20 well records that were examined. Also, the first salt recorded ranged greatly in depth from 299 to 1,309 ft, but this is directly related to the well-site position; i.e., the farther south the location, the deeper the salt occurs.

The 17 wells drilled south of the Saltville Fault outcrop trace penetrated an increased thickness of Cambrian carbonates and stiff shales, as the sites were farther southward. Several wells near the base of the overthrust sheet encountered crevices and caving problems. The basal part of the overthrust hanging wall is underlain by thick-bedded competent, but brittle, dolomite of the Honaker Formation. Near wells 13, 14, and 15, huge blocks of dolomite are exposed at the cliff edge with deep, open fractures subparallel to the north lip of the ridge. It is possible that these dangerous crevasses are only related to soil creep in the underlying plastic Maccrady shales, but "low-pressure" wells were drilled only ~500 ft northward, and three of the early and relatively shallow "high-pressure" wells are as close as 500 ft to the northwest.

"High-pressure" wells 1–4 were drilled from 1931 to 1939 and were closely spaced at intervals of 50–75 ft. Salt extraction eventually joined these four wells into a single, large, void cavern. The driller's log for well 4 shows that the wellbore penetrated only 200 ft of the fractured Honaker dolomite before crossing the Saltville Fault. The well then was drilled into the Maccrady Formation, where salt was encountered at a depth of 521 ft; a total of 496 ft of salt-bearing beds was present from 532 to 1,576 ft.

After 21–28 years of salt extraction, the area beneath wells 1–4 underwent a spectacular collapse on April 18, 1960 (Fig. 7). The initial crater was ~400 ft across (Craig, 1973, p. 25) but had enlarged to ~600 ft across by 1972 (Fenix and Scisson, Inc., 1972a, fig. 4a). This chasm is now ~310 ft deep and has a clear pool of water at its bottom.

Sometime shortly before 1972, unknown amounts of diesel oil were pumped into some of the "high-pressure" field well cavities (Craig, 1973, p. 29). The diesel oil would float on any unrecovered brines and would help reduce shale hydration and sloughing in the caverns. No additional subsidence has been documented in the "high-pressure" field to date. Fourteen caverns were mapped with downhole devices in 1972 (Fenix and Scisson, Inc., 1972b, fig. 4b). The tops of these cavities are described below (east to west). Where two or more wells are shown on one line, their caverns are believed to have coalesced.

| *Well no.* | *Depth to top of cavity (feet)* | *Well no.* | *Depth to top of cavity (feet)* |
|---|---|---|---|
| 15 | 1,640 | 11, 12 | 1,673 |
| 13, 14 | 1,550 | 28 | 3,023 |
| 9, 17 | unknown | 27 | 3,118 |
| 1, 2, 3, 4 | collapsed | 18, 19, 20 | 2,640 |
| 8 | 1,448 | 25, 26 | 3,170 |
| 5, 6, 7 | 336 | 24 | 3,200 |
| 10 | 1,308 | 22, 23 | 3,900 |

Thus, we can surmise that the shallow cavern beneath wells 5–7 would pose the greatest danger for a future collapse, and that all the other 12 caverns are sufficiently deep to have a low potential for collapse.

## AN UNUSUAL COMMERCIAL REVIVAL

In 1994, Virginia Gas Company began permit applications to build a pipeline and other site facilities to utilize the cavern below "high-pressure" field wells 16 and 20 for the storage of natural gas. This gas was to be drawn from the major gas line owned by East Tennessee Gas Company, which passes north of Chilhowie, about 9 mi from the brine field. The existing cavern was created by two wells drilled by Olin-Mathieson in 1959 and 1962 to depths of 3,957 ft and 3,912 ft, respectively. An estimated 2.8 million "barrels" (1,386,000 tons, approximately, assuming 55 gal per bbl) of salt was removed by 1972, when the wells were plugged and the company ceased its Saltville operations. The cavern top was 1,601 ft below well 15, and 3,609 ft below well 20 (Fenix and Scisson, 1972b, fig. 4b). The project was approved and has been successfully operated for several years. The company is currently testing the feasibility of using other existing caverns and possibly creating new caverns. Brine in the cavern at wells 16 and 20 has been temporarily stored in two large, lined ponds. An evaporation

Figure 7. View to the south shortly after the April 1960 cavern collapse at "high-pressure" field wells 1–4. The crater, the white area in the background, is now ~600 ft in diameter and >300 ft deep, exposing, from top to bottom, parts of the Honaker dolomite, the Saltville Fault, and the Maccrady shale. Photo courtesy of the Museum of the Middle Appalachians, from the Totten collection.

plant was built, and recovered salt is again being sold to available agricultural markets.

A network of ~250 survey monuments was installed in 1997 to monitor potential subsidence. According to a Virginia Gas Company spokesman, regular surveys have shown only minor elevation changes. These variations are only on the order of a few tenths of a foot and may be related to temperature and moisture changes.

## SUMMARY

The reader should now understand how Saltville got its name. The discovery of this vast mineral resource beneath the Saltville area was an accidental but inevitable event. The development of this resource led to the recovery of extinct Pleistocene mammal remains, which has spawned continuing valley-floor scientific excavations and an excellent museum. The salt deposit was vital to the Confederacy, and this area was twice attacked by Union forces. The salt also has been used to make baking powder, chlorine gas to purify water, hydrozine fuel to send rockets into Earth's orbit and beyond, and many other useful products.

Often, mineral extraction and manufacturing come with an environmental price. At Saltville, this has resulted in widespread, slow subsidence and damage to surface structures. The manufacture of chlorine caused mercury pollution of the North Fork of the Holston River, which has necessitated a warning against eating fish caught along several miles of the river. This problem is still being worked on 30 years after Olin-Mathieson closed their plants. On the positive side, Virginia Gas Company is using the "high-pressure" field's deep cavities to store natural gas for peak-demand use and is again recovering salt from brine. With only an estimated 7% extraction of the salt reserves to date, it is likely that Saltville could continue to provide a part of U.S. salt needs for several additional centuries.

## ACKNOWLEDGMENTS

I thank Roger Sharpe, geologist at U.S. Gypsum Company, and Samuel Gowan of Alpha Geoscience for a very thorough review of this paper. Many of their suggestions were incorporated, greatly enhancing the clarity of my intended narrative. Their time and timeliness are sincerely appreciated.

## REFERENCES CITED

Bartlett, C. S., Jr., 1979, Saltville well field recreation project, archeological and geological impact report: Letter to Mayor Lewis and members of the Saltville Town Council, 4 p.

_____1981, Saltville Recreation Park, archeological testing, preliminary results: Letter to Town of Saltville, June 26, 3 p.

_____1997, The rock salt deposit at Saltville, Virginia, *in* Bartlett, C. S., Jr.; and Whisonant, R. C., A geological sample of Saltville and vicinity, Smyth and Washington Counties, Virginia: Field-trip guidebook, Southern Appalachian Geological Association, 14 p.

Bartlett, C. S., Jr.; and Webb, H. W., 1971, Geology of the Bristol and Wallace quadrangles, Virginia: Virginia Division of Mineral Resources, Charlottesville, Report of Investigations 25, 93 p.

Boyd, J. P. (ed.), 1952, The papers of Thomas Jefferson: Princeton University Press, Princeton, New Jersey, v. 6, 668 p.

Cooper, B. N., 1966, Geology of the salt and gypsum deposits in the Saltville area, Smyth and Washington Counties, Virginia, *in* Ray, J. L. (ed.), Second symposium on salt, v. 1, Geology, geochemistry, and mining: Northern Ohio Geological Society, Cleveland, p. 11–34.

Cox, D. P.; and Edgerton, C. D., Jr., 1968, Salines, *in* Mineral resources of the Appalachian Region: U.S. Geological Survey Professional Paper 580, p. 206–210, 327–336.

Craig, J. R., 1973, Geologic evaluation of the Saltville area, Smyth County, Virginia: Saltville Planning Commission, 49 p.

Dietrich, R. V., 1970, Geology and Virginia: University Press of Virginia, Charlottesville, p. 24, 146–153.

Eckel, E. C., 1902, Salt and gypsum deposits of southwestern Virginia, *in* Contributions to economic geology, 1902: U.S. Geological Survey Bulletin 213, p. 406–417.

Fenix and Scisson, Inc., 1972a, Evaluation of abandonment procedures for the Olin brine field, Saltville, Virginia, *in* Craig, J. R., Geologic evaluation of the Saltville area, Smyth County, Virginia: Saltville Planning Commission, fig. 4a.

_____1972b, Programs for abandonment of the high-pressure brine field, Saltville, Virginia, *in* Craig, J. R., Geologic evaluation of the Saltville area, Smyth County, Virginia: Saltville Planning Commission, fig. 4b.

Jefferson, Thomas, 1787, Notes on the State of Virginia: John Stockdale, London, 382 p.

Lonn, Ella, 1965, Salt as a factor in the Confederacy: University of Alabama Press, University, Alabama, 324 p.

Low, Emile, 1894, Data concerning salt wells, obtained from Mr. Musselwhite: Museum of the Middle Appalachians, Saltville, file records, 3 p.

McDonald, J. N., 2000, An outline of the pre-Clovis archeology of SV-2, Saltville, Virginia, with special attention to a bone tool dated 14,510 yr B.P.: Jeffersoniana, no. 9, Nov. 30, 2000, Virginia Museum of Natural History, 60 p.

McDonald, J. N.; and Bartlett, C. S., Jr., 1983, An associated musk ox skeleton from Saltville, Virginia: Journal of Vertebrate Paleontology, v. 2, p. 453–470.

Peterson, O. A., 1917, A fossil-bearing alluvial deposit in Saltville Valley, Virginia: Annals of the Carnegie Museum, v. 11, nos. 3–4, p. 469–474.

Rachal, W. M. E., 1953, Salt the South could not savor: Virginia Cavalcade, v. 3, no. 2, p. 4–7.

Ray, C. E.; Cooper, B. N.; and Benninghoff, W. S, 1967, Fossil mammals and pollen in a late Pleistocene deposit at Saltville, Virginia: Journal of Paleontology, v. 41, p. 608–622.

Stocking, Jan; Thompson, John; and Bartlett, C. S., Jr., 1979, Preliminary reports of the Saltville Pleistocene bone beds: regional geology and geomorphology [abstract]: Virginia Journal of Science, Richmond, v. 30, no. 2, p. 81.

Stose, G. W., 1913, Geology of the salt and gypsum deposits of southwestern Virginia, *in* Mineral production of Virginia: Virginia Geological Survey Bulletin 8, p. 51–73.

Taylor, S. E., 1841, Discovery in Virginia of the regular mineral salt formation: American Journal of Science, v. 41, p. 214–215.

Watson, T. L., 1907, Mineral resources of Virginia: Virginia–Jamestown Exposition Commission, Lynchburg, Virginia, p. 211–215, 327–335.

Withington, C. F., 1965, Suggestions for prospecting for evaporite deposits in southwestern Virginia, *in* Geological Survey research, 1965: U.S. Geological Survey Professional Paper 525-B, p. B29–B33.

Worsham, Gibson, 2001, Conservation assessment report for the Stuart house: Museum of the Middle Appalachians, Saltville, Virginia, 35 p.

# Sinkholes above the U.S. Strategic Petroleum Reserve Storage Site at Weeks Island Salt Dome, Louisiana: Recognition, Diagnostics, and Remediation

***James T. Neal***
Sharlot Hall Museum
Prescott, Arizona

**ABSTRACT.**—A sinkhole formed circa 1991 over the outer edge of the two-tiered former salt mine that was converted in 1980 for oil storage by the U.S. Strategic Petroleum Reserve; the site was at the Weeks Island salt dome in coastal Louisiana. Diagnostic studies included geophysical, geochemical, drilling, and hydrological methods and suggested that a direct connection existed between the surface-collapse area and the underground mine. The connection was confirmed by correlative measurements of sediment-slump rates, piezometric-surface deflection, and brine-influx rates into the mine. The dissolution of salt below the sinkhole that initiated the leak into the mine was likely caused by several confluent geologic processes, and exacerbated by mining-induced stresses that created fractures that subsequently became hydrologic flow paths. A second, smaller sinkhole was noted in early 1995, but it showed negligible activity, unlike the much larger initial sinkhole.

Modeling of mine stresses showed that years of accumulated tensional stress was required before cracking began, but once started, it continued to develop and to relieve the stress in that specific regime. The crack regime created an avenue for incursion of ground water, very slowly initially, but the cracks gradually enlarged as undersaturated ground water mixed with brine at the top of salt.

Remediation included increasing the mine pressurization, slowing the dissolution by injecting brine into the sinkhole throat, and construction of a freeze curtain around the principal sinkhole. Because the remediation was successful by stopping active enlargement, the oil was safely withdrawn and transferred to other sites, and the mine was backfilled with saturated brine.

## INTRODUCTION

Weeks Island, a salt-dome island in the coastal marshland of south Louisiana, was one of six original storage sites selected for the U.S. Strategic Petroleum Reserve (SPR), which was established after the Middle East oil embargo of 1973–74. It was the only site that used a room-and-pillar mine as the storage method; the other five used leached caverns in domal salt, and four of them are still used for storage.

Congress approved the SPR in 1975 to ensure that the nation would not again be faced with inventory shortages, inflated prices, and gasoline lines at the pump, all of which occurred following the embargo. The SPR was designed, sited, engineered, and constructed between 1975 and 1981 in a major peacetime effort that was comparable to other major construction projects, such as the Panama Canal. During the Persian Gulf War of 1990–91, the SPR's usefulness was demonstrated after Kuwait and Iraq stopped producing oil. Through the withdrawal of just 30 million barrels (5% of the SPR inventory), world oil prices were stabilized. The SPR was not drawn down during the Iraq War of 2003, but often was the subject of political discourse.

In May 1992, only a year after the first Gulf War, a sinkhole was noted over the edge of the mine, but the initial reaction was largely one of surprise rather than alarm (Neal and Myers, 1995). The sinkhole, when first observed, was 11 m across and 9 m deep, and an obvious hazard—it was just 25 m from the main access road to the adjacent salt mine operated by Morton Salt Co. The contractor charged with operating the Reserve stated that they believed the sinkhole had formed around a root cellar at a former residence. In hindsight, an element of denial was probably involved, as it appears that personnel hoped the problem would just go away: root cellars were not even part of the former company houses. After considerable discussion, an unofficial policy of "wait and watch" was adopted, regardless of geological or engineering opinion. It appeared that as long as the hole was not enlarging and that nothing serious was happening, there was no real danger.

But knowledge of the feature spread, and local experts and miners suggested not only the exact cause of the sinkhole but that more occurrences could be expected. Only a dozen years earlier, a major penetration of the salt mine at Jefferson Island, Louisiana,

Neal, J. T., 2003, Sinkholes above the U.S. Strategic Petroleum Reserve storage site at Weeks Island salt dome, Louisiana: recognition, diagnostics, and remediation, *in* Johnson, K. S.; and Neal, J. T. (eds.), Evaporite karst and engineering/environmental problems in the United States: Oklahoma Geological Survey Circular 109, p. 347–353.

occurred, leading to its being flooded with water and its eventual closing (Martinez and others, 1998). The information presented by the experts was based on many years of experience in Gulf Coast salt mining and could not be ignored. Further, the sinkhole gradually deepened and was actively enlarging. The U.S. Department of Energy recognized that the storage site should be closed, and the oil transferred to another site. Actions to decommission the site began in 1994, but a second, smaller sinkhole was noticed soon thereafter, and anxiety over the threat of an oil spill from the mine accelerated, even though it was considered to be unlikely.

## SINKHOLE OCCURRENCE AND LOCATION

The Weeks Island salt dome is 23 km south of New Iberia, Louisiana, and is the central dome in the Five Island chain, along with Belle Isle, Cote Blanche, Avery, and Jefferson Island. All five have been mined because of their near-surface salt and their logistical advantage near the Gulf of Mexico and the Intracoastal Waterway. Belle Isle and Jefferson Island are now closed to room-and-pillar mining because of deliberate and inadvertent flooding, respectively.

The Weeks Island sinkhole occurred over the southern perimeter of the upper level of the two-tiered SPR mine (Figs. 1–3), which held 73 million barrels of crude

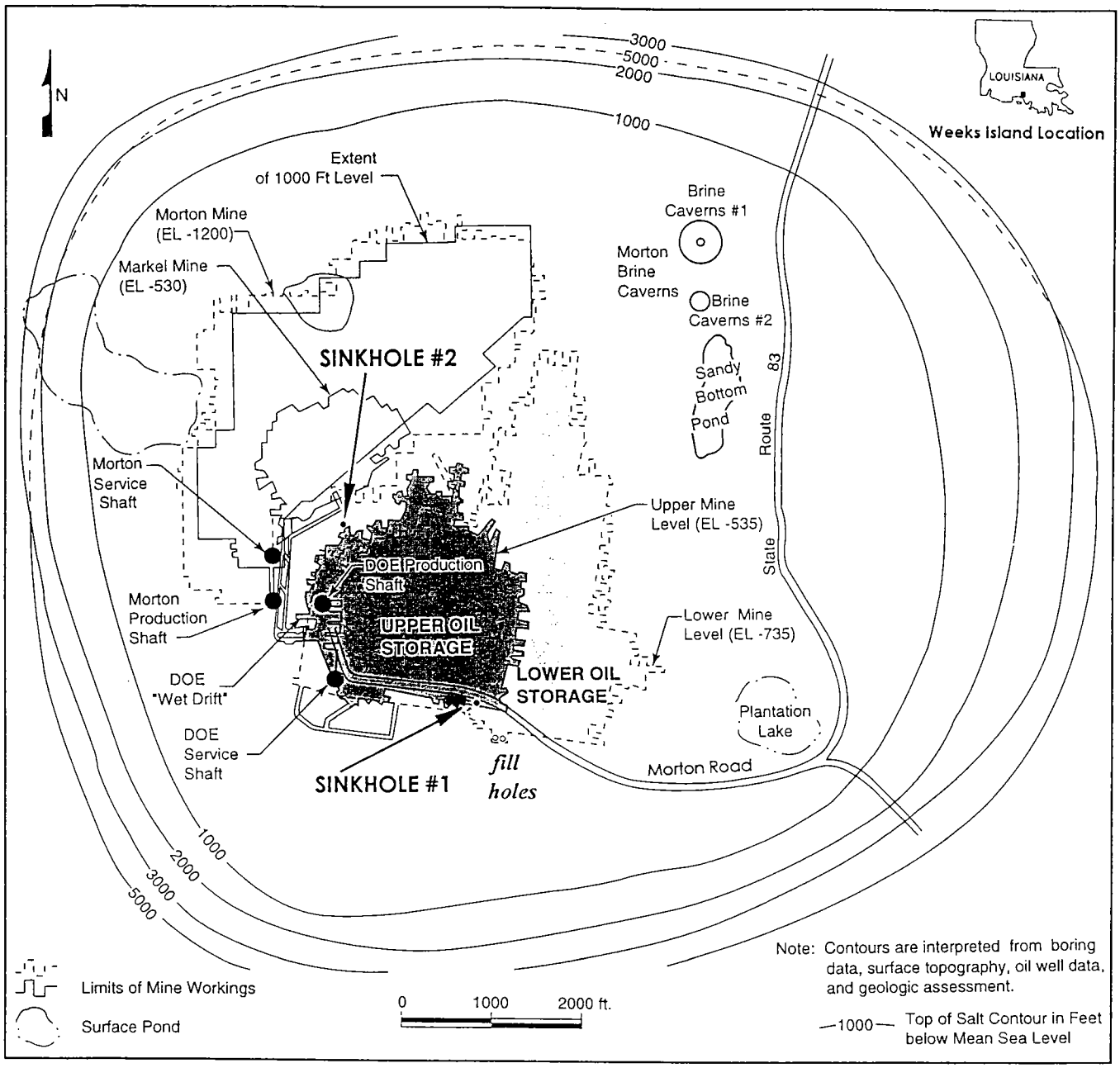


Figure 1. Map of Weeks Island, Louisiana, showing the two sinkholes over the edges of the upper level of the SPR oil-storage mine, near the point of superposition of the lower level. Contours define outer edge of dome.

oil from 1981 through 1995. The mine originally opened in 1902, and salt was extracted commercially until 1977, at which time Morton Salt Co. developed a new mine directly adjacent, to the northwest, while the older workings were converted for oil storage. Minor leaks of water had been noted at various times during the 75 years of active mining, but in-mine grouting controlled inflow (Acres International Corp., 1987). At the time of initial study to convert the mine to oil storage, an indication of anomalous geochemical composition was noted in brine seeps but did not seem to preclude use of the mine for oil storage. Reexamination (after the fact) showed that the anomaly was in the vicinity of the sinkhole, and also near an earlier

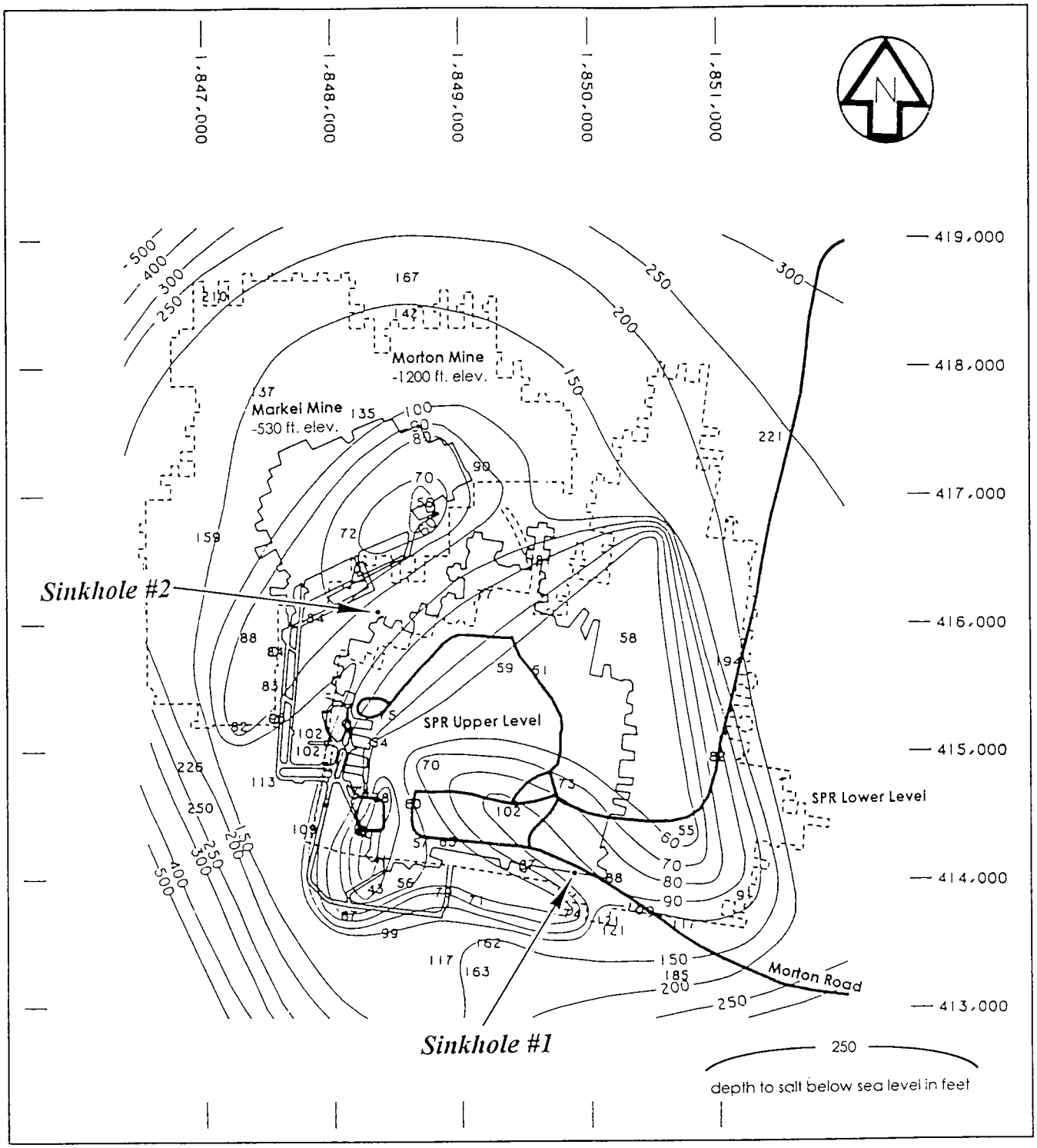


Figure 2. Contour map showing top of salt and outlines of mine openings. Sinkholes 1 and 2 are in apparent troughs, possibly separating individual lobes or "spines" in the salt (from Acres International Corp., 1987).

exploratory penetration by the mining company. Records that might have revealed causal factors associated with the earlier penetration were apparently unavailable, so little information existed that might explain how this failure occurred. All attention then focused on remediation and removal of stored oil.

The nearly vertical sidewalls in the surface sediments surrounding the sinkhole caused some confusion initially, but were readily explained geologically as typical of Pleistocene loess that caps the island. The sinkhole was directly beneath a former residence of the dismantled Morton company townsite, but the residence had no apparent relationship to the origin of the sinkhole.

## SINKHOLE DIAGNOSTICS

Unlike other mines where underground leaks are observed directly (and grouted), the SPR mine was sealed and had to rely on indirect evidence, such as increased pressure or changes in isotopic composition of the contained water, which was ~1% of the total volume. Pressure diagnostics were complicated by salt-creep closure, which gradually reduced the storage volume by one-fifth of 1% per year, a very small amount overall, but a *very large* amount with respect to the few-gallons-per-minute leaks, which could explain the sinkhole.

*Ground-water inflow* into the mine was suggested by increasing amounts of brine seen in the fill-hole sumps, used initially during oil-fill operations. The trend began increasing from 1 to nearly 3 gallons per minute by early 1994, enough to establish a distinct, ongoing change. At the same time these increases were noticed, the sinkhole was filled with sand because it deepened to >13 m and became increasingly more hazardous. As soon as the fill was placed, slumping continued at a rate of about 2 $m^3$ per day and required new fill weekly. This showed that dissolution was ongoing, and there was a rough correlation with the amount of increasing brine that was observed in the fill holes and the amount of unsaturated water required to leach an equivalent volume of salt. Sinkhole 2 did not deepen or change and was never considered a threat.

*Brine hydrochemistry* in salt mines can distinguish meteoric water from connate water. At Weeks Island, a decided change in isotopic composition was evident when 1994 analyses were compared with brine obtained in late 1991, about the same time postulated for the sinkhole origin (Knauth, 1994). Comparative earlier data suggested that the leak may have existed as early as 1987, but these data were inconclusive.

*Rock-mechanics modeling* by Ehgartner (Neal and others, 1998) showed that the mine perimeter would have been in tension and that fractures in salt could have formed as early as 1970. Such cracks could have been exposed to undersaturated ground water and gradually could have enlarged at the same time the crack was propagating. The modeling results were substantiated by survey data showing subsidence over the mine, which agreed closely with Ehgartner's modeling.

*Seismic-reflection profiles* around the sinkhole were obtained in early 1994; it was an expedient method for obtaining subsurface information (Miller and others, 1994). A prominent reflector first thought to be top of salt was noted throughout the area at shallow depth. Subsequent drilling, measurement, and geophysics showed that the reflector was the piezometric surface, and that a localized 4-m deflection at the sinkhole was likely from drawdown created by the inflow of ground water into the presumed point of leakage. A secondary anomalous step deflection was noted north of the main sinkhole and caused some concern, as sinkholes often progress and occur in multiples.

*Cross-well seismic tomography* was conducted by placing sources and receivers in diagonal cased boreholes on four sides of the sinkhole (Fig. 4). The bore-

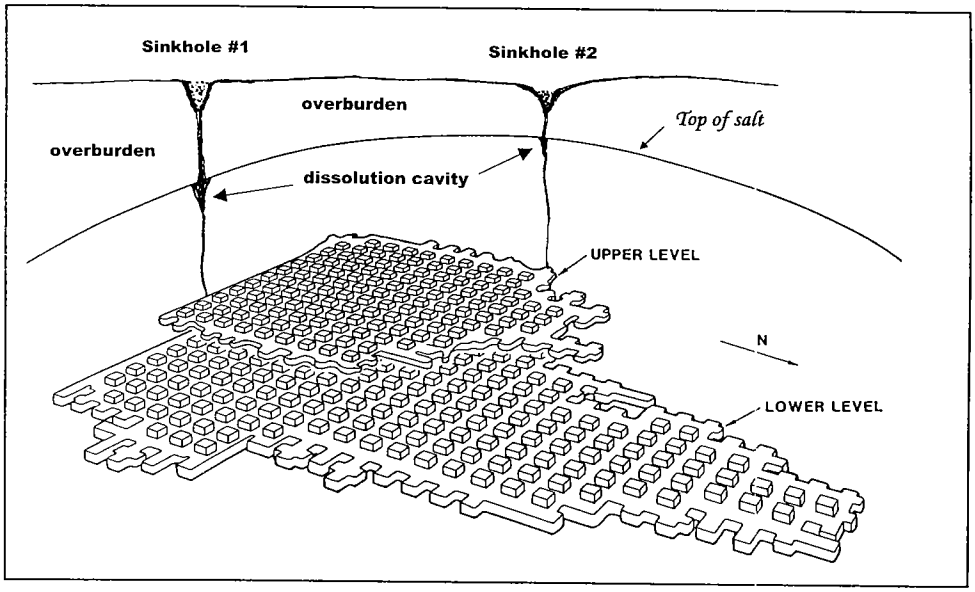


Figure 3. Diagrammatic sketch showing the two sinkholes along the edge of the upper mine, in the zone of maximum stretching and bending of salt.

holes also provided direct information on sediment and salt geometry and the hydrologic environment. The steep deflection in the water table was observed on neutron logs from borehole BH-4 and was measured directly on electrotape. The tomograms showed clear evidence of low-velocity material below the top of salt, verifying that a sediment-filled void had occurred between the much higher velocity salt on either side. The graphical displays did not show the high-quality imaging that some people had anticipated, but the nature of the method is inherently limited in mapping seismic-velocity distribution—but not necessarily the geometry. The graphics did show, however, that the area of dissolution below the sinkhole was laterally limited, and with a strongly vertical dimension. Such information was useful when grouting options were considered.

*Slant-hole drilling* directly into and below the sinkhole provided the most direct confirmation of dissolution geometry (Fig. 4). BH-9, adjacent to the sinkhole, drilled a high-angle approach directly over the top of the subsurface extension of the surface expression. It extended below the top-of-salt elevation encountered in the tomography holes. This hole provided the opportunity for injection of Rhodamine dye into the apparent throat of the sinkhole. The dye, if detected in the fill holes, would provide unequivocal evidence of hydrologic connection with the mine; otherwise, the evidence would be circumstantial.

BH-7A started at a less steep angle and was aimed at the "plumbing" at depth, penetrating the top of salt at the normal depth and then continuing on through the salt into a major void at least 22 m deep. Fear of disrupting the channel stopped the drilling at this point, but not without first having a *3-D hydrologic flowmeter* installed, which provided data for 2 weeks (Sandia National Laboratories/DynMcDermott, 1994). The data indicate essentially vertical flow down the throat, at a rate of >1 m per day. The 2.5-cm-per-day downward movement of the flowmeter (alone) also indicated that sediment was moving down the throat, presumably in response to dissolution of salt by undersaturated ground water at some point below. The discovery of this channel also provided the opportunity for additional injection of tracer dye.

## REMEDIATION

Once the geometry of a deep void or crevasse was identified, with direct measurement of downward flow of water, a suggestion was made by Diamond and Mills (1994) to inject saturated brine directly down the throat. Approximately 12 L/minute was consumed under gravity feed, and continuous injection continued from August 1994 until the stored oil was removed. The startling result was that subsidence at the sinkhole was arrested, and virtually no downward movement was measurable. In addition, the ground-water depression at the sinkhole had recovered to a normal position. Evidently the brine had stopped the dissolution of salt, but whether this could be a longer term fix was problematic. The near-saturated brine was particularly sensitive to temperature fluctuation, and halite crystallization often led to line clogging and flow cessation.

The internal mine pressure was raised from 7 to 30 psi in mid-1994 as a means of reducing inflow of brine. Although this increase was only a small amount, raising the pressure reduced the external pressure gradient and slowed salt-creep closure (Sandia National Laboratories/DynMcDermott, 1994).

*Grouting* was considered early but was not instituted because of the lack of urgency and because of uncertainty about how and where to place grout. Grout is normally injected under pressure, and this process caused a real fear of doing more harm than good, as openings could easily be enlarged.

An engineered *freeze curtain* was constructed around the sinkhole in 1995 as a further control mea-

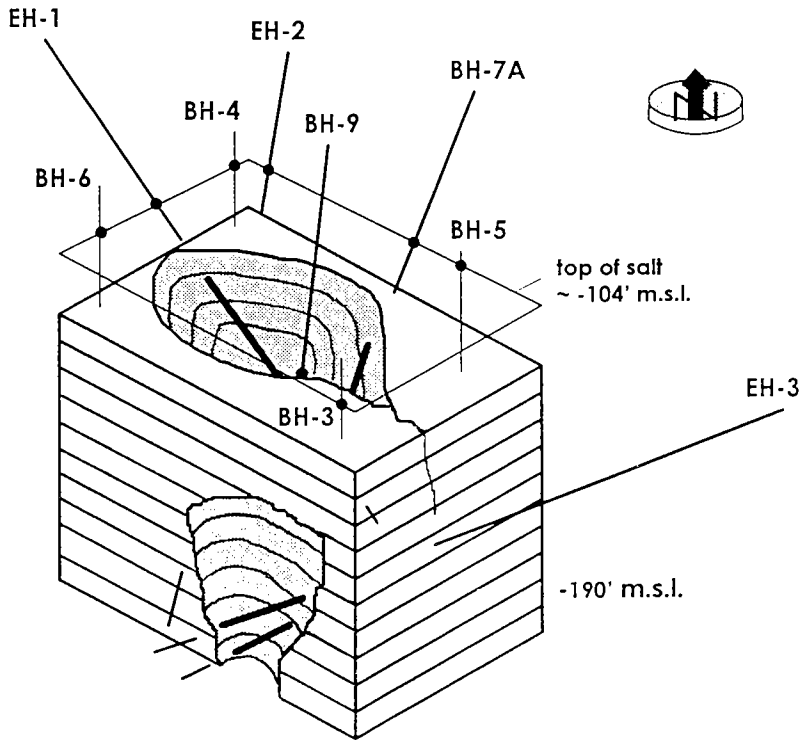


Figure 4. Diagrammatic representation of exploratory drilling and geometry of Sinkhole 1 throat. Boreholes BH-3, 4, 5, and 6 were drilled for cross-well tomography and helped define the geological configuration beneath the surface sinkhole. Angled exploratory boreholes BH-7 and 9 determined the actual geometry and enabled a hydrologic flowmeter to be inserted 22 m below the top of salt and into the throat. Exploratory holes EH-1, 2, and 3 further defined the throat and provided decisive information regarding grouting potential. Accentuated portions of boreholes define throat geometry.

sure that would ensure additional containment during withdrawal of oil from the mine. This was accomplished by installing 56 wells in the overburden around the sinkhole, which isolated the sinkhole to a depth of 67 m into the salt (Fig. 5). The boreholes that penetrated the dissolution cavity were used to position a hydrologic flowmeter, and to inject brine, which effectively stopped further salt dissolution during the time it took to freeze the overburden solid.

Once the freeze wall around the sinkhole was solid and the flowmeter indicated that ground-water inflow had stopped, oil was evacuated and transferred to other SPR sites in Louisiana and Texas. The mine was subsequently filled with 85%-saturated brine so that stabilization would be achieved rapidly and subsidence would be reduced. A complete accounting of the sinkhole occurrence and causes, and the decommissioning process, are found in reports by Neal (1996) and Molecke (2000).

## LESSONS LEARNED FROM THE SPR EXPERIENCE AT WEEKS ISLAND

The sinkhole at Weeks Island formed over the edge of the SPR mine as a result of geological, hydrological, and mine-induced factors, most of which were poorly understood at the time the repository was established. The location near the edge of the dome, astride a possible anomalous zone and along a valley in the top of salt, set the stage for the initial mine configuration and boundaries. Underground openings in the mine placed the salt along the periphery in tension, probably favoring crack development as early as 1970. Eventual incursion of undersaturated ground water traversed the 107-m salt back over the mine, allowing entry of brine into the SPR mine. Gradually increasing dissolution enlarged a void at the top of salt, creating the collapse environment for the sinkhole that formed circa 1991.

Exploratory drilling and geophysics defined the void or crevasse beneath the sinkhole, enabling the introduction of saturated brine directly into the throat. The brine completely arrested the continuing subsidence at the sinkhole, apparently as a result of controlling ongoing dissolution. The construction of a freeze curtain around the sinkhole enabled the oil to be evacuated and transferred to other sites with the maximum degree of environmental safety.

The SPR experience at Weeks Island could not have been foreseen, but undesirable environmental consequences were avoided because of attentiveness on the part of the operators. The knowledge gained here effectively negates future use of a salt mine for crude-oil storage. In addition, storage of any kind in a salt mine is ill-advised when internal access to grouting is denied.

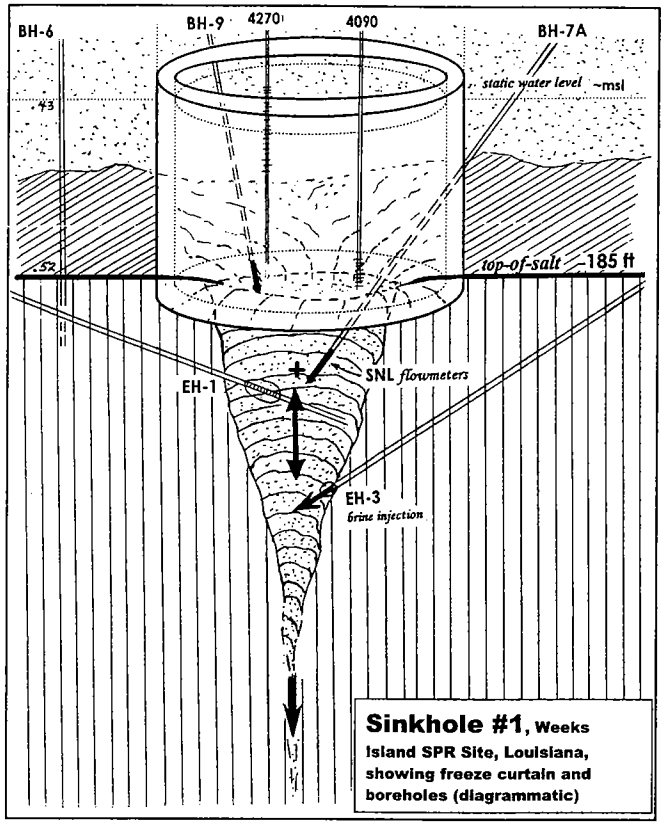


Figure 5. Diagrammatic sketch showing configuration of the cylindrical freeze curtain and the sinkhole that it surrounded.

## ACKNOWLEDGMENTS

The events and actions described here occurred while the author was employed at Sandia National Laboratories, Albuquerque, New Mexico, 1980–97. I am indebted to the many individuals who contributed to this effort, thus enabling the safe resolution of a potentially serious condition. I thank Ken Johnson for his review of the paper.

## REFERENCES CITED

Acres International Corporation, 1987, Weeks Island Strategic Petroleum Reserve geological site characterization report: Sandia National Laboratories, Report SAND87-7111, Albuquerque, New Mexico, 175 p.

Diamond, H. W.; and Mills, K. E., 1994, Informal communication at a meeting of SPR participants and Morton Salt Company, July 1994. The idea of injecting brine evidently was a collective, spontaneous decision arrived at by several individuals, but most conspicuously by Diamond and Mills.

Knauth, L. P., 1994, Stable isotope constraints on the origin of brine in the Weeks Island Strategic Petroleum Reserve: Arizona State University contract report to DynMcDermott Petroleum Operations Company, New Orleans, Louisiana, 10 p.

Martinez, J. D.; Johnson, K. S.; and Neal, J. T.,1998, Sinkholes in evaporite rocks: American Scientist, v. 86, no. 1, p. 38–51.

Miller, R. D., and others, 1994, High resolution seismic survey near SPR surface collapse feature at Weeks Island, Louisiana: Contract letter report, Kansas Geological Survey to Sandia National Laboratories, Albuquerque, New Mexico, 29 p.

Molecke, M. A. (ed.), 2000, Final status of the Strategic Pe-

troleum Reserve (SPR) Weeks Island Mine: Sandia National Laboratories Report SAND2000-0400, Albuquerque, New Mexico, 56 p.

Neal, J. T. (ed.), 1996, Summary of events and geotechnical factors leading to decommissioning of the Strategic Petroleum Reserve (SPR) facility at Weeks Island, Louisiana: Sandia National Laboratories Report SAND96-2263, Albuquerque, New Mexico, 38 p.

Neal, J. T.; and Myers, R. E., 1995, Origin, diagnostics, and mitigation of a salt dissolution sinkhole at the U.S. Strategic Petroleum Reserve Storage Site, Weeks Island, Louisiana: Proceedings, 5th International Symposium on Land Subsidence, International Association of Scientific Hydrology, p. 187–195.

Neal, J. T.; Bauer, S. J.; and Ehgartner, B. L., 1998, Mine-induced sinkholes over the U.S. Strategic Petroleum Reserve (SPR) storage facility at Weeks Island, Louisiana; geologic causes and effects, *in* Borchers, J. W. (ed.), Land subsidence case studies and current research; Joseph F. Poland Symposium on Land Subsidence: Association of Engineering Geologists Special Publication 8, p. 327–336.

Sandia National Laboratories/DynMcDermott, 1994, Internal memorandum to U.S. Department of Energy, New Orleans, Louisiana, ~27 p.